

Handbook of
Hydrocarbon and Lipid Microbiology

SPRINGER
REFERENCE

Series Editors: Kenneth N. Timmis (Editor-in-Chief)

Matthias Boll · Otto Geiger · Howard Goldfine · Tino Krell

Sang Yup Lee · Terry J. McGenity · Fernando Rojo

Diana Z. Sousa · Alfons J. M. Stams · Robert J. Steffan · Heinz Wilkes

Heinz Wilkes *Editor*

Hydrocarbons, Oils and Lipids: Diversity, Origin, Chemistry and Fate

 Springer

Handbook of Hydrocarbon and Lipid Microbiology

Series Editors

Kenneth N. Timmis (Editor-in-Chief)
Emeritus Professor
Institute of Microbiology
Technical University Braunschweig
Braunschweig, Germany

Matthias Boll
Microbiology, Faculty of Biology
Albert-Ludwigs-Universität Freiburg
Freiburg, Germany

Institute of Biology II, Microbiology
Albert-Ludwigs-Universität Freiburg
Freiburg, Germany

Otto Geiger
Centro de Ciencias Genómicas
Universidad Nacional Autónoma de
México
Cuernavaca, Morelos, Mexico

Howard Goldfine
Department of Microbiology
Perelman School of Medicine
University of Pennsylvania
Philadelphia, PA, USA

Tino Krell
Department of Environmental
Protection
Estación Experimental del Zaidín
Consejo Superior de Investigaciones
Científicas, Granada, Granada, Spain

Sang Yup Lee
Dept. Chem. Engineer. and BioProcess
Korea Adv. Inst. Science and Techn.
Taejon, Korea (Republic of)

Terry J. McGenity
School of Life Sciences
University of Essex
Colchester, UK

Fernando Rojo
CSIC
Centro Nacional de Biotecnología
Madrid, Spain

Diana Z. Sousa
Laboratory of Microbiology
Wageningen University and Research
Wageningen, The Netherlands

Alfons J. M. Stams
Laboratory of Microbiology
Wageningen University and Research
Wageningen, The Netherlands

Robert J. Steffan
Blue Crab Lure Company
Cape Coral, FL, USA

Centre of Biological Engineering
University of Minho
Braga, Portugal

Heinz Wilkes
Organic Geochemistry, Institute for
Chemistry and Biology of the Marine
Environment (ICBM)
Carl von Ossietzky University
Oldenburg, Germany

This handbook is the unique and definitive resource of current knowledge on the diverse and multifaceted aspects of microbial interactions with hydrocarbons and lipids, the microbial players, the physiological mechanisms and adaptive strategies underlying microbial life and activities at hydrophobic material:aqueous liquid interfaces, and the multitude of health, environmental and biotechnological consequences of these activities.

Scientific Advisory Board

Victor de Lorenzo, Eduardo Diaz, Otto Geiger, Ian Head, Sang Yup Lee, Terry J. McGenity, Colin Murrell, Balbina Nogales, Roger Prince, Juan Luis Ramos, Wilfred Röling, Eliora Ron, Burkhard Tümmler, Jan Roelof van der Meer, Willy Verstraete, Friedrich Widdel, Heinz Wilkes and Michail Yakimov.

More information about this series at <http://www.springer.com/series/13884>

Heinz Wilkes
Editor

Hydrocarbons, Oils and Lipids: Diversity, Origin, Chemistry and Fate

With 227 Figures and 42 Tables

 Springer

Editor

Heinz Wilkes

Organic Geochemistry

Institute for Chemistry and Biology of the Marine

Environment (ICBM), Carl von Ossietzky University

Oldenburg, Germany

ISBN 978-3-319-90568-6

ISBN 978-3-319-90569-3 (eBook)

ISBN 978-3-319-90570-9 (print and electronic bundle)

<https://doi.org/10.1007/978-3-319-90569-3>

© Springer Nature Switzerland AG 2020

This work is subject to copyright. All rights are reserved by the Publisher, whether the whole or part of the material is concerned, specifically the rights of translation, reprinting, reuse of illustrations, recitation, broadcasting, reproduction on microfilms or in any other physical way, and transmission or information storage and retrieval, electronic adaptation, computer software, or by similar or dissimilar methodology now known or hereafter developed.

The use of general descriptive names, registered names, trademarks, service marks, etc. in this publication does not imply, even in the absence of a specific statement, that such names are exempt from the relevant protective laws and regulations and therefore free for general use.

The publisher, the authors, and the editors are safe to assume that the advice and information in this book are believed to be true and accurate at the date of publication. Neither the publisher nor the authors or the editors give a warranty, expressed or implied, with respect to the material contained herein or for any errors or omissions that may have been made. The publisher remains neutral with regard to jurisdictional claims in published maps and institutional affiliations.

This Springer imprint is published by the registered company Springer Nature Switzerland AG.

The registered company address is: Gewerbestrasse 11, 6330 Cham, Switzerland

This book is dedicated to my partner Susanne.

Preface

Hydrocarbons and lipids comprise extremely diverse organic compounds that play fundamental roles in biosphere and geosphere. They constitute important functional components in all living organisms as well as a major fraction of fossil organic matter in sedimentary systems. Representing the most reduced forms of carbon, they are essential for human food and energy supply. However, both agriculture and the exploitation of fossil fuels have a profound influence on climate and thus on the ecosystems of our planet. In all these contexts, interactions of microorganisms with hydrocarbons and lipids play an integral role. With this in mind, this volume of the *Handbook of Hydrocarbon and Lipid Microbiology* introduces the structural diversity and properties as well as the origin and fate of hydrocarbons and lipids in nature. It discusses their environmental context both from a bio- as well as a geoscience perspective and thus provides a system framework for the subsequent volumes dealing with specific aspects of their microbiology.

This volume is subdivided into four parts. Part 1 treats the structural diversity of hydrocarbons and lipids occurring naturally which is directly associated with the great variability of their physical and chemical properties and their multi-faceted biological activity. In Part 2, the diversity of hydrocarbons and lipids occurring in different biota including autotrophs and heterotrophs as well as eukaryotes and prokaryotes is covered. This includes aspects of biosynthesis and degradation but also biological functions. Part 3 examines the distribution of hydrocarbons and lipids in the geosphere and fundamental processes controlling the fate of fossil organic matter, the formation of petroleum, and the various manifestations of hydrocarbon accumulations. Part 4 addresses important aspects of the environmental biogeochemistry of hydrocarbons and lipids as well as transfer processes between different compartments of bio- and geosphere. Various chapters in this volume describe the use of hydrocarbons and lipids as marker compounds of natural processes in time and space including microbiologically relevant aspects. The assignment of chapters to the one or other part of this volume may certainly appear arbitrary to some extent as it is obvious that the topics addressed are often not exclusively related to one of the overall themes only, that is, biosphere, geosphere, or environment. This, however, also illustrates nicely that there are no strict boundaries between environmental compartments which are often studied by relatively enclosed disciplinary communities. In this sense, this volume hopefully will contribute to overcoming artificial

walls between scientific work areas and thus foster interdisciplinary research on the microbiology of lipids and hydrocarbons.

This volume would not have been possible without the excellent contributions by the authors – thanks a lot to all of you! I am very grateful to the Editor-in-Chief, Kenneth Timmis, who gave me the opportunity to participate in this exciting journey. Finally, I would like to thank the people at Springer, in particular Sylvia Blago, for great support and patience.

Oldenburg
September 2020

Heinz Wilkes

Contents

Part I Structures and Properties of Hydrocarbons and Lipids	1
1 Hydrocarbons and Lipids: An Introduction to Structure, Physicochemical Properties, and Natural Occurrence	3
Heinz Wilkes, René Jarling, and Jan Schwarzbauer	
2 Introduction to Oil Chemistry and Properties Related to Oil Spills	49
Merv Fingas	
3 Gas Hydrates: Formation, Structures, and Properties	81
Judith Maria Schicks	
Part II Hydrocarbons and Lipids in the Biosphere	97
4 Factors Controlling Carbon and Hydrogen Isotope Fractionation During Biosynthesis of Lipids by Phototrophic Organisms	99
Nikolai Pedentchouk and Youping Zhou	
5 Plant Cuticular Waxes: Composition, Function, and Interactions with Microorganisms	123
Viktoria Valeska Zeisler-Diehl, Wilhelm Barthlott, and Lukas Schreiber	
6 Biosynthesis of the Plant Cuticle	139
Jérôme Joubès and Frédéric Domergue	
7 Lipids of Geochemical Interest in Microalgae	159
John K. Volkman	
8 Abiotic Transformation of Unsaturated Lipids and Hydrocarbons in Senescent Phytoplanktonic Cells	193
Jean-François Rontani	

9	Cuticular Hydrocarbons and Pheromones of Arthropods	213
	Gary J. Blomquist, Claus Tittiger, and Russell Jurenka	
10	Lipidomic Analysis of Lower Organisms	245
	Tomáš Řezanka, Irena Kolouchová, Lucia Gharwalová, Andrea Palyzová, and Karel Sigler	
Part III	Hydrocabons and Lipids in the Geosphere	267
11	Composition and Properties of Petroleum	269
	R. Paul Philp	
12	Petroleomics	311
	Clifford C. Walters and Meytal B. Higgins	
13	Stable Isotopes in Understanding Origin and Degradation Processes of Hydrocarbons and Petroleum	339
	A. Vieth-Hillebrand and Heinz Wilkes	
14	The Origin of Organic Sulphur Compounds and Their Impact on the Paleoenvironmental Record	355
	Ilya Kutuzov, Yoav O. Rosenberg, Andrew Bishop, and Alon Amrani	
15	History of Life from the Hydrocarbon Fossil Record	409
	Clifford C. Walters, Kenneth E. Peters, and J. Michael Moldowan	
16	Phospholipids as Life Markers in Geological Habitats	445
	Kai Mangelsdorf, Cornelia Karger, and Klaus-G. Zink	
17	Formation of Organic-Rich Sediments and Sedimentary Rocks	475
	Ralf Littke and Laura Zieger	
18	Thermogenic Formation of Hydrocarbons in Sedimentary Basins	493
	Nicolaj Mahlstedt	
19	Oil and Gas Shales	523
	Brian Horsfield, Hans-Martin Schulz, Sylvain Bernard, Nicolaj Mahlstedt, Yuanjia Han, and Sascha Kuske	
20	Hydrothermal Petroleum	557
	Bernd R. T. Simoneit	
21	Environmental and Economic Implications of the Biogeochemistry of Oil Sands Bitumen	593
	H. Huang, R. C. Silva, J. R. Radović, and S. R. Larter	
22	Secondary Microbial Gas	613
	Alexei V. Milkov	

23 Geological, Geochemical, and Microbial Factors Affecting Coalbed Methane	623
Curtis Evans, Karen Budwill, and Michael J. Whiticar	
24 Gas Hydrates as an Unconventional Hydrocarbon Resource	651
Klaus Wallmann and Judith Maria Schicks	
Part IV Hydrocarbons and Lipids in the Environment	667
25 The Biogeochemical Methane Cycle	669
Michael J. Whiticar	
26 Marine Cold Seeps: Background and Recent Advances	747
Erwin Suess	
27 Mud Volcano Biogeochemistry	769
Helge Niemann	
28 Methane Carbon Cycling in the Past: Insights from Hydrocarbon and Lipid Biomarkers	781
Volker Thiel	
29 Chemistry of Volatile Organic Compounds in the Atmosphere ...	811
Ralf Koppmann	
30 Organic Matter in the Hydrosphere	823
Jan Schwarzbauer	
31 Lessons from the 2010 <i>Deepwater Horizon</i> Accident in the Gulf of Mexico	847
Terry C. Hazen	
Index	865

About the Series Editor-in-Chief



Kenneth N. Timmis

Emeritus Professor
Institute of Microbiology
Technical University Braunschweig
Braunschweig, Germany

Kenneth Timmis studied microbiology and obtained his Ph.D. at Bristol University. He undertook postdoctoral training at the Ruhr-University Bochum, Yale and Stanford, at the latter two as a Fellow of the Helen Hay Whitney Foundation. He was then appointed Head of an independent research group at the Max Planck Institute for Molecular Genetics in Berlin and subsequently Professor of Biochemistry in the University of Geneva, Faculty of Medicine. Thereafter, for almost 20 years, he was Director of the Division of Microbiology at the National Research Centre for Biotechnology (GBF)/now the Helmholtz Centre for Infection Research (HZI), and concomitantly Professor of Microbiology in the Institute of Microbiology of the Technical University Braunschweig. He is currently Emeritus Professor in this institute.

The Editor-in-Chief has worked for more than 30 years in the area of environmental microbiology and biotechnology, has published over 400 papers in international journals, and is an ISI Highly Cited Microbiology-100 researcher. His group has worked for many years, inter alia, on the biodegradation of oil hydrocarbons, especially the genetics and regulation of toluene degradation, and on the ecology of hydrocarbon-degrading microbial communities, discovered the new group of marine oil-degrading hydrocarbonoclastic bacteria, initiated genome sequencing

projects on bacteria that are paradigms of microbes that degrade organic compounds (*Pseudomonas putida* and *Alcanivorax borkumensis*), and pioneered the topic of experimental evolution of novel catabolic activities.

He is Fellow of the Royal Society, Member of the European Molecular Biology Organisation, Fellow of the American Academy of Microbiology, Member of the European Academy of Microbiology, and Recipient of the Erwin Schrödinger Prize. He is the founder and Editor-in-Chief of the journals *Environmental Microbiology*, *Environmental Microbiology Reports*, and *Microbial Biotechnology*.

About the Volume Editor



Heinz Wilkes

Organic Geochemistry
Institute for Chemistry and Biology of the
Marine Environment (ICBM),
Carl von Ossietzky University
Oldenburg, Germany

Heinz Wilkes studied chemistry at the University of Hamburg. During his Ph.D., he investigated the bacterial degradation of dibenzo-*p*-dioxins, dibenzofurans, and other aromatic compounds. He was a Research Scientist in the Institute of Petroleum and Organic Geochemistry at the Research Centre Jülich and in the Organic Geochemistry Section at the German Research Centre for Geosciences in Potsdam. Since 2015, he is a Full Professor of Organic Geochemistry at Carl von Ossietzky University of Oldenburg in the Institute for Chemistry and Biology of the Marine Environment where he is responsible for the B.Sc. program in Environmental Sciences. His research has focused on molecular mechanisms of biogeochemical key reactions and metabolic pathways in microorganisms; the origin, fate, and transformation of hydrocarbons and petroleum in the environment and in the geosphere; and the reconstruction of past environments and climates using organic-geochemical proxy parameters. For many years he has been particularly interested in elucidating degradation pathways of hydrocarbons in anaerobic bacteria. He has published more than 120 articles in peer-reviewed journals and books. Since 2015, he is a Member of the Board of the European Association of Organic Geochemists.

Contributors

Alon Amrani The Hebrew University of Jerusalem, Jerusalem, Israel

Wilhelm Barthlott Nees Institut for Biodiversity of Plants, University of Bonn, Bonn, Germany

Sylvain Bernard Muséum National d'Histoire Naturelle, Sorbonne Université, CNRS UMR 7590, IRD, Institut de Minéralogie, de Physique des Matériaux et de Cosmochimie, IMPMC, Paris, France

Andrew Bishop Power, Environmental and Energy Research Institute, Covina, CA, USA

Gary J. Blomquist Department of Biochemistry and Molecular Biology, University of Nevada, Reno, NV, USA

Karen Budwill Processing Technologies, InnoTech Alberta, Edmonton, AB, Canada

Frédéric Domergue Laboratoire de Biogenèse Membranaire, UMR5200, Université de Bordeaux, Bordeaux, France

Laboratoire de Biogenèse Membranaire, UMR5200, CNRS, Bordeaux, France

Curtis Evans School of Earth and Ocean Sciences, University of Victoria, Victoria, BC, Canada

Merv Fingas Spill Science, Edmonton, AB, Canada

Lucia Gharwalová Department of Biotechnology, University of Chemical Technology Prague, Prague, Czech Republic

Yuanjia Han GFZ German Research Centre for Geosciences, Organic Geochemistry, Potsdam, Germany

Terry C. Hazen Department of Civil and Environmental Engineering, Department of Earth and Planetary Sciences, Department of Microbiology, Institute for Secure and Sustainable Environment, Methane Center, University of Tennessee, Knoxville, TN, USA

Biosciences Division, Oak Ridge National Laboratory, Oak Ridge, TN, USA

Meytal B. Higgins Corporate Strategic Research, ExxonMobil Research and Engineering Company, Annandale, NJ, USA

Brian Horsfield GFZ German Research Centre for Geosciences, Organic Geochemistry, Potsdam, Germany

H. Huang PRG, Department of Geoscience, University of Calgary, Calgary, AB, Canada

René Jarling Organic Geochemistry, Institute for Chemistry and Biology of the Marine Environment (ICBM), Carl von Ossietzky University of Oldenburg, Oldenburg, Germany

Jérôme Joubès Laboratoire de Biogénèse Membranaire, UMR5200, Université de Bordeaux, Bordeaux, France

Laboratoire de Biogénèse Membranaire, UMR5200, CNRS, Bordeaux, France

Laboratoire de Biogénèse Membranaire, UMR5200, CNRS-Université de Bordeaux, Bâtiment A3 – INRA Bordeaux Aquitaine, Villenave d’Ornon, France

Russell Jurenka Department of Entomology, Iowa State University, Ames, IA, USA

Cornelia Karger GFZ German Research Centre for Geosciences – Helmholtz Centre Potsdam, Organic Geochemistry, Potsdam, Germany

Irena Kolouchová Department of Biotechnology, University of Chemical Technology Prague, Prague, Czech Republic

Ralf Koppmann Institute for Atmospheric and Environmental Research, University of Wuppertal, Wuppertal, Germany

Sascha Kuske GFZ German Research Centre for Geosciences, Organic Geochemistry, Potsdam, Germany

Ilya Kutuzov The Hebrew University of Jerusalem, Jerusalem, Israel

S. R. Larter PRG, Department of Geoscience, University of Calgary, Calgary, AB, Canada

Ralf Littke Institute of Geology and Geochemistry of Petroleum and Coal, Energy and Mineral Resources Group, RWTH Aachen University, Aachen, Germany

Nicolaj Mahlstedt GFZ German Research Centre for Geosciences, Organic Geochemistry, Potsdam, Germany

Kai Mangelsdorf GFZ German Research Centre for Geosciences – Helmholtz Centre Potsdam, Organic Geochemistry, Potsdam, Germany

Alexei V. Milkov Department of Geology and Geological Engineering, Colorado School of Mines, Golden, CO, USA

J. Michael Moldowan Biomarker Technology, Rohnert Park, CA, USA

Department of Geological Sciences, Stanford University, Stanford, CA, USA

Helge Niemann Department of Marine Microbiology and Biogeochemistry, and Utrecht University, NIOZ Royal Netherlands Institute for Sea Research, 't Horntje, the Netherlands

CAGE – Centre for Arctic Gas Hydrate, Environment and Climate, Department of Geology, UiT the Arctic University of Norway, Tromsø, Norway

Andrea Palyzová Institute of Microbiology, Academy of Sciences of the Czech Republic, Prague, Czech Republic

Nikolai Pedentchouk School of Environmental Sciences, University of East Anglia, Norwich, UK

Institute of Plant Physiology, Russian Academy of Sciences, Moscow, Russia

Kenneth E. Peters Schlumberger, Mill Valley, CA, USA

R. Paul Philp School of Geosciences, University of Oklahoma, Norman, OK, USA

J. R. Radović PRG, Department of Geoscience, University of Calgary, Calgary, AB, Canada

Tomáš Řezanka Institute of Microbiology, Academy of Sciences of the Czech Republic, Prague, Czech Republic

Jean-François Rontani Aix Marseille Université, Mediterranean Institute of Oceanography (MIO), Université de Toulon, CNRS/INSU/IRD, Marseille, France

Yoav O. Rosenberg The Hebrew University of Jerusalem, Jerusalem, Israel
Geological Survey of Israel, Jerusalem, Israel

Judith Maria Schicks GFZ German Research Centre for Geosciences, Potsdam, Germany

Lukas Schreiber Institute of Cellular and Molecular Botany (IZMB), University of Bonn, Bonn, Germany

Hans-Martin Schulz GFZ German Research Centre for Geosciences, Organic Geochemistry, Potsdam, Germany

Jan Schwarzbauer Institute of Geology and Geochemistry of Petroleum and Coal, Energy and Mineral Resources Group (EMR), School of Geosciences, RWTH Aachen University, Aachen, Germany

Karel Sigler Institute of Microbiology, Academy of Sciences of the Czech Republic, Prague, Czech Republic

R. C. Silva PRG, Department of Geoscience, University of Calgary, Calgary, AB, Canada

Bernd R. T. Simoneit BRT Simoneit, Department of Chemistry, College of Science, Oregon State University, Corvallis, OR, USA

Erwin Suess Marine Biogeochemistry, GEOMAR Helmholtz Centre for Ocean Research Kiel, Kiel, Germany

College of Earth, Ocean, and Atmospheric Sciences, Oregon State University, Corvallis, OR, USA

Volker Thiel Geobiology, Geoscience Centre, Georg-August University of Göttingen, Göttingen, Germany

Claus Tittiger Department of Biochemistry and Molecular Biology, University of Nevada, Reno, NV, USA

A. Vieth-Hillebrand Organic Geochemistry, GFZ German Research Centre for Geosciences, Potsdam, Germany

John K. Volkman CSIRO Oceans and Atmosphere, Hobart, TAS, Australia

Klaus Wallmann GEOMAR – Helmholtz Centre for Ocean Research Kiel, Kiel, Germany

Clifford C. Walters Corporate Strategic Research, ExxonMobil Research and Engineering Company, Annandale, NJ, USA

Michael J. Whiticar Biogeochemistry Facility (BF-SEOS), School of Earth and Ocean Sciences, University of Victoria, Victoria, BC, Canada

Hanse-Wissenschaftskolleg, HWK (Institute for Advanced Study), Delmenthorst, Germany

Heinz Wilkes Organic Geochemistry, Institute for Chemistry and Biology of the Marine Environment (ICBM), Carl von Ossietzky University, Oldenburg, Germany

Viktoria Valeska Zeisler-Diehl Institute of Cellular and Molecular Botany (IZMB), University of Bonn, Bonn, Germany

Youping Zhou School of Chemistry and Chemical Engineering, Shaanxi University of Science & Technology, Xi'an, China

Laura Zieger Institute of Geology and Geochemistry of Petroleum and Coal, Energy and Mineral Resources Group, RWTH Aachen University, Aachen, Germany

Klaus-G. Zink GFZ German Research Centre for Geosciences – Helmholtz Centre Potsdam, Organic Geochemistry, Potsdam, Germany

Part I

**Structures and Properties of Hydrocarbons
and Lipids**



Hydrocarbons and Lipids: An Introduction to Structure, Physicochemical Properties, and Natural Occurrence

1

Heinz Wilkes, René Jarling, and Jan Schwarzbauer

Contents

1	Introduction	4
2	Covalent Bonding	5
3	Hydrocarbons	7
3.1	Saturated Hydrocarbons	7
3.2	Unsaturated Hydrocarbons	12
3.3	Aromatic Hydrocarbons	15
4	Functionalized Organic Compounds and Lipids	18
4.1	Oxygen- and Sulfur-containing Compounds	18
4.2	Nitrogen-containing Compounds	26
4.3	Halogenated Compounds	28
5	Physical Properties	31
6	Reactions	38
6.1	Reactions of Saturated Hydrocarbons	38
6.2	Reactions of Unsaturated Hydrocarbons	40
6.3	Reactions of Aromatic Hydrocarbons	42
6.4	Specific Reactions of Functionalized Organic Compounds	45
	References	46

H. Wilkes (✉)

Organic Geochemistry, Institute for Chemistry and Biology of the Marine Environment (ICBM),
Carl von Ossietzky University, Oldenburg, Germany
e-mail: heinz.wilkes@uni-oldenburg.de

R. Jarling

Organic Geochemistry, Institute for Chemistry and Biology of the Marine Environment (ICBM),
Carl von Ossietzky University of Oldenburg, Oldenburg, Germany
e-mail: rene.jarling1@uni-oldenburg.de

J. Schwarzbauer

Institute of Geology and Geochemistry of Petroleum and Coal, Energy and Mineral Resources
Group (EMR), School of Geosciences, RWTH Aachen University, Aachen, Germany
e-mail: jan.schwarzbauer@emr.rwth-aachen.de

© Springer Nature Switzerland AG 2020

H. Wilkes (ed.), *Hydrocarbons, Oils and Lipids: Diversity, Origin, Chemistry and Fate*,
Handbook of Hydrocarbon and Lipid Microbiology,
https://doi.org/10.1007/978-3-319-90569-3_34

3

Abstract

Hydrocarbons and lipids are among the most abundant organic compound classes in the biogeosphere. They are formed directly by living organisms as biosynthetic products or through geological transformation of biomass in sedimentary systems. This chapter provides an introduction to the structural diversity of hydrocarbons and lipids and their occurrence in natural environments. Besides saturated, unsaturated, and aromatic hydrocarbons, also selected types of functionalized organic compounds including lipids which play key roles in biogeochemical processes are presented. Important physicochemical parameters are discussed in relation to the structural characteristics of the presented compound classes. For each compound type, reactivity and important reaction types with a special focus on mechanisms relevant to biochemical transformations are presented.

1 Introduction

Hydrocarbons occur in great structural diversity as biosynthetic products of living organisms in the biosphere or as abiotic transformation products of biogenic organic matter in the geosphere. They are the main constituents of petroleum and thus are extremely abundant in geological systems. Increasing exploitation of hydrocarbon-based energy resources was one of the driving forces of the industrial revolution with dramatic impact on the evolution of human culture (e.g., Hall et al. 2003) but has also led to the ongoing anthropogenic perturbation of the Earth's climate system with still not foreseeable consequences for societies worldwide. The presence of hydrocarbons already on the early Earth has promoted the evolution of metabolic pathways which allow microorganisms to exploit them as energy sources as well. The interactions of microorganisms and hydrocarbons are manifold.

Hydrocarbons by definition contain exclusively the elements carbon and hydrogen. This chapter attempts to provide a compact introduction to fundamental aspects of hydrocarbon structure, properties, and occurrence which are most relevant for environmental and microbiological processes. Hydrocarbons are divided into three main compound classes, namely, saturated, unsaturated, and aromatic hydrocarbons which are discussed separately in subsequent sections of this chapter. In addition to hydrocarbons *sensu stricto*, this chapter also provides an introduction to naturally occurring lipids and technical lipid-like compounds. In contrast to hydrocarbons, lipids are not defined by their elemental composition but rather by their solubility. In strict terms, a lipid is a natural product which is well soluble in nonpolar organic solvents (lipophilic) but almost insoluble in water (hydrophobic). Beside unfunctionalized hydrocarbons, this definition may include all important types of functionalized natural organic compounds containing the halogens fluorine, chlorine, bromine, or iodine or the hetero elements nitrogen, sulfur, and oxygen (NSO compounds). Halogenated organic compounds occurring in the environment are mainly released by anthropogenic activity although numerous natural products containing halogen atoms are known. NSO compounds may occur in natural environments along with complex assemblages of hydrocarbons, e.g., crude oils always

contain non-hydrocarbons in highly variable but often significant amounts. Moreover, functionalized organic compounds, particularly oxygen compounds, represent important biological transformation products of hydrocarbons and play a crucial role as intermediates/products of biodegradation pathways. The discussion will consider both natural products and xenobiotics, i.e., compounds found in organisms which are not produced by these organisms or expected to occur in them.

We will not give any introduction to the nomenclature of organic compounds. The common rules of organic nomenclature as defined by the International Union of Pure and Applied Chemistry (IUPAC) are accessible via suitable resources (Favre and Powell, Nomenclature of Organic Chemistry – IUPAC Recommendations and Preferred Names 2013; see also <http://www.acdlabs.com/iupac/nomenclature/>). Furthermore, software packages are available that generate the correct names of organic compounds from drawn structures (e.g., http://www.acdlabs.com/products/name_lab/).

2 Covalent Bonding

A characteristic feature of hydrocarbons is that they contain covalent bonds exclusively. In covalent bonds, pairs of electrons are shared between atoms. Covalent bonds are typically formed between elements which do not differ too strongly in electronegativity (see below). The quantum mechanical valence bond model describes the nature of covalent bonds based on *orbitals* which are regions around a single atom or in a molecule in which electrons may be found with a certain probability. Covalent bonding is explained based on the assumption that two or more atomic orbitals from two atoms overlap to form the same number of molecular orbitals but with different energies (higher and lower than the parent atomic orbitals). The electrons of the former atomic orbitals can now occupy the molecular orbitals with lower energy (binding orbitals) and leave the higher-energy orbitals (anti-binding) unoccupied. This leads to an energy gain, which stabilizes the system, i.e., the covalent bond.

In atoms of elements of the second period of the periodic table of the chemical elements, such as carbon, nitrogen, oxygen, and fluorine, only atomic orbitals of the first and second shell, i.e., the $1s$, $2s$, $2p_x$, $2p_y$, and $2p_z$ orbitals, may be occupied by electrons. $1s$, $2s$, and $2p$ orbitals correspond to particular increasing energy levels of the electrons. Central to the understanding of covalent bonding is the concept of orbital hybridization, which assumes that mixing of energetically different atomic orbitals forms the same number of energetically equivalent hybrid orbitals. The three modes of orbital hybridization that may occur in carbon form four sp^3 , three sp^2 , or two sp orbitals by mixing of three, two, or one $2p$ orbital(s) with the $2s$ orbital, respectively.

Covalent bonds formed by overlapping of a sp^3 , sp^2 , or sp hybrid orbital with the $1s$ orbital of a hydrogen atom or a hybrid orbital of another carbon atom (or an atom of another element) are termed σ -bonds. Carbon atoms with sp^3 hybridization form four single bonds along the connecting lines to the bonding partners. Methane, the simplest organic molecule, is built up by four equivalent C–H σ -bonds. The structure of methane is that of a regular tetrahedron in which all bond lengths (110 pm) and bond angles (109.5°) are identical (Fig. 1). The length of a C–C σ -bond between two sp^3 hybridized carbon atoms as in ethane is 154 pm (Fig. 1). The A–C–B

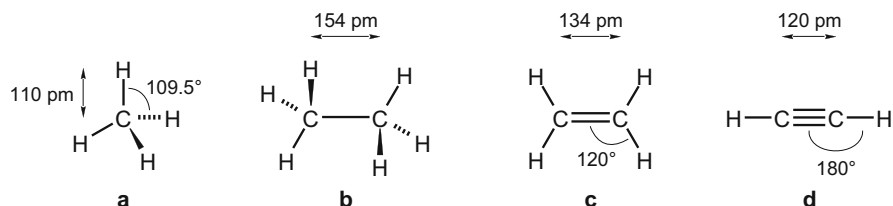


Fig. 1 Structures of simple hydrocarbons; (a) methane CH₄, (b) ethane C₂H₆, (c) ethene C₂H₄, (d) ethyne C₂H₂

bond angles in tetrahedral carbon atoms may deviate from 109.5° depending on the electronic and steric properties of the bonding partners. Varying lengths (150–120 pm) are found for σ -bonds between differently hybridized carbon atoms.

Three or two σ -bonds are formed by sp^2 and sp hybridized carbon atoms, respectively. The remaining non-hybridized $2p$ orbital(s) overlap(s) with (a) non-hybridized $2p$ orbital(s) of other atoms to form π -bonds in addition to the σ -bond. In π -bonds the molecular orbital is located above and below the connecting line between the atoms. Bonding between two sp^2 and two sp hybridized carbon atoms thus leads to C–C double or triple bonds, respectively. Simple examples are ethene (H₂C=CH₂) with a C–C double bond length of 134 pm and ethyne (HC≡CH) with a C–C triple bond length of 120 pm (Fig. 1). The bonding angles at sp^2 and sp hybridized carbon atoms are 120° and 180°, respectively.

Carbon atoms may also form covalent bonds to atoms of elements other than carbon and hydrogen. Most relevant in naturally occurring organic compounds are halogens, nitrogen, sulfur, and oxygen (Table 1). As the halogens are monovalent elements, only single bonds are possible between carbon and halogen atoms. In contrast, oxygen and sulfur are divalent elements and nitrogen is a trivalent element. Therefore, C–O and C–S single and double bonds as well as C–N single, double, and triple bonds are possible.

The chemical reactivity of organic compounds depends directly on the properties of the individual bonds within their molecules. The strength of a bond is measured by the bond dissociation energy which is directly related to the bond distance. In chemical reactions, bond cleavage may occur by homolytic or heterolytic mechanisms. An example of a homolytic mechanism would be the cleavage of an alkane into an alkyl radical and a hydrogen radical, i.e., both cleavage products retain one of the shared electrons. By contrast, the dissociation of a carboxylic acid into a carboxylate anion and a proton represents a heterolytic mechanism. Here, both electrons are retained in one of the cleavage products, viz., the carboxylate ion. The most important control on the bond energy is the electronegativity of the atoms bonding together. Electronegativity denominates the ability of an atom in a covalent bond to attract the shared electrons to itself (Table 1). This will result in an asymmetric charge distribution, whose magnitude depends on the electronegativity difference between the bonding atoms. In the periodic table of the chemical elements, electronegativity increases from left to right within periods and from bottom

Table 1 Elements most relevant to organic chemistry and biochemistry ordered by atomic number

Element	H	C	N	O	F	P	S	Cl	Br	I
Atomic number	1	6	7	8	9	15	16	17	35	53
Electronegativity ^a	2.20	2.55	3.04	3.44	3.98	2.19	2.58	3.16	2.96	2.66

^aAllred (1961)

to top within groups. As a general rule, reactivity of covalent bonds increases with increasing polarity. Therefore, compounds containing exclusively nonpolar σ -bonds such as saturated hydrocarbons are rather unreactive or inert (see below).

3 Hydrocarbons

3.1 Saturated Hydrocarbons

3.1.1 *n*-Alkanes

The term *n*-alkane refers to linear hydrocarbons with the general formula C_nH_{2n+2} . The prefix *n* stands for *normal* indicating that the molecule does not contain branches so that it represents a straight chain of carbon atoms (Fig. 2). Each carbon atom (except the two terminal ones) is bound via σ -bonds to two other carbon atoms. The two remaining free valences are occupied by hydrogen atoms, respectively; only the terminal carbon atoms have three hydrogen atoms as bonding partners. The structurally simplest organic molecule, methane (Fig. 1), can be regarded as the lower end member of the homologues series of *n*-alkanes. There is no principal upper limit as to the chain length of *n*-alkanes. Polyethylene is a synthetic polymer consisting of extremely long carbon chains principally representing *n*-alkanes (up to about 400.000 carbon atoms per molecule).

A characteristic structural feature of *n*-alkanes is the existence of conformers. Conformers are isomers which are transformed into each other by rotation about individual C–C bonds without breaking chemical bonds. The stability of different conformers depends on (a) *hyperconjugation*, i.e., the energy gained by overlapping of a fully occupied binding molecular orbital (e.g., from a C–H bond) with an unoccupied anti-binding orbital on an adjacent bond, which is possible only when the conformation is staggered, and (b) steric repulsion, whose extent is determined by the size of the substituents. In *n*-alkanes the rotation barrier (= the activation energy required to transform one conformer to another) is relatively low, thus the rotatability about C–C σ -bonds can be regarded as relatively unrestricted under conditions relevant to most natural environments.

Methane, likely the most abundant low-molecular-weight organic compound on the planet Earth, is formed by both biological and geological processes. Biogenic and thermogenic methane are easily discriminated by their stable carbon isotopic compositions (for review, see ► Chap. 13, “Stable Isotopes in Understanding Origin and Degradation Processes of Hydrocarbons and Petroleum”, this volume). Isotopically light methane in deep natural gas reservoirs may be regarded as an indication

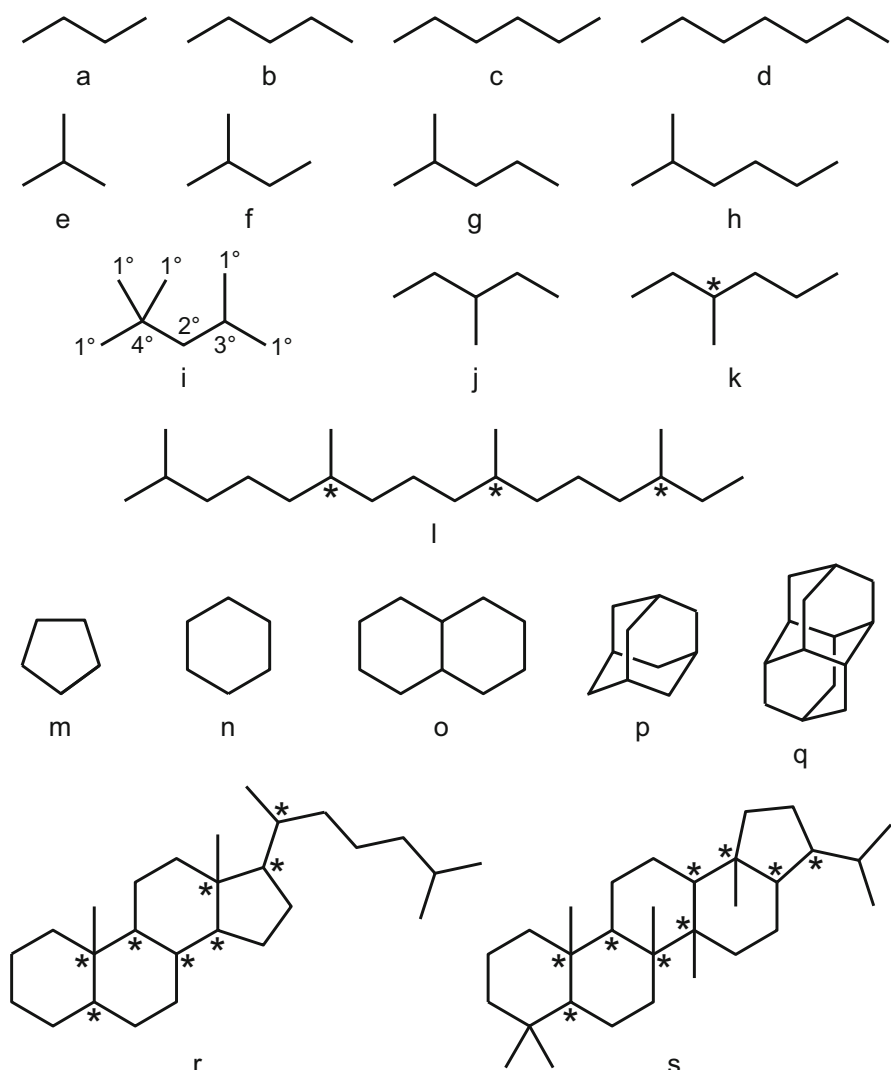


Fig. 2 Structures of selected saturated hydrocarbons. *n*-Alkanes, (a) *n*-butane C_4H_{10} , (b) *n*-pentane C_5H_{12} , (c) *n*-hexane C_6H_{14} , (d) *n*-heptane C_7H_{16} ; **branched alkanes**, (e) 2-methylpropane (isobutane) C_4H_{10} , (f) 2-methylbutane (isopentane) C_5H_{12} , (g) 2-methylpentane C_6H_{14} , (h) 2-methylhexane C_7H_{16} , (i) 2,2,4-trimethylpentane (isooctane) C_8H_{18} , (j) 3-methylpentane C_6H_{14} , (k) 3-methylhexane C_7H_{16} , (l) 2,6,10,14-tetramethylhexadecane (phytane) $C_{20}H_{42}$; **cycloalkanes**, (m) cyclopentane C_5H_{10} , (n) cyclohexane C_6H_{12} , (o) decalin $C_{10}H_{18}$, (p) adamantane $C_{10}H_{16}$, (q) diamantane $C_{14}H_{20}$, (r) cholestane $C_{27}H_{42}$, (s) hopane $C_{30}H_{42}$. Isooctane, a branched saturated hydrocarbon which defines the 100 point on the octane rating scale, contains primary (1°), secondary (2°), tertiary (3°), and quaternary (4°) carbon atoms. Stereogenic centers are present in 3-methylhexane, phytane, cholestane, and hopane as indicated by asterisks

for the existence of a deep subterranean biosphere (e.g., Schoell 1980). Conventional and unconventional (clathrate hydrates, shale gas, coal seams) gas resources represent the by far largest pool of hydrocarbons in the geosphere (e.g., ► Chaps. 19, “Oil and Gas Shales”, ► 22, “Secondary Microbial Gas”, ► 23, “Geological, Geochemical, and Microbial Factors Affecting Coalbed Methane”, and ► 24, “Gas Hydrates as an Unconventional Hydrocarbon Resource”, this volume. Moreover, evidence has been provided that higher natural gas hydrocarbons, i.e., ethane and propane, are not exclusively formed by thermal processes but may also be produced biologically in the deep marine subsurface (Hinrichs et al. 2006; Xie et al. 2013). Higher *n*-alkanes occur as major constituents of leaf waxes of macrophytes and land plants, which can be distinguished chemotaxonomically according to the carbon number range of the homologues (e.g., Ficken et al. 2000). Due to the biosynthesis from fatty aldehydes with even-numbered carbon chains via decarbonylation (e.g., Schneider-Belhaddad and Kolattukudy 2000), carbon numbers of biogenic alkanes typically show a significant odd-over-even predominance. *n*-Alkanes are also the main constituents of crude oils which have not been affected by biodegradation. Here, typically no clear carbon number predominance is observed due to the unspecific formation via thermally controlled reactions. It is important to note that the majority of the global oil reserves is more or less significantly biodegraded and thus may lack *n*-alkanes.

3.1.2 Branched Alkanes

For hydrocarbons represented by the general formula C_nH_{2n+2} , more than one constitutional isomer is possible if $n \geq 4$. In these structural isomers, the atoms are connected in different ways; thus interconversion is not possible without breaking chemical bonds. These alkanes do not possess straight chains of carbon atoms and therefore, in contrast to the *normal* alkanes, are termed *branched* alkanes (Fig. 2). The number of possible constitutional isomers increases exponentially with increasing number of carbon atoms in the molecule. In general, the higher the degree of substitution is, the more will the molecule have a spherical rather than a rodlike shape. This has a significant influence on the physical properties of isomers with implications for features such as bioavailability.

Carbon atoms in these molecules are classified according to the number of 1, 2, 3, or 4 other carbon atoms to which they are connected as primary, secondary, tertiary, and quaternary carbon atoms, respectively, as illustrated for isooctane in Fig. 2. Tertiary and quaternary carbon atoms which are connected to four different substituents are termed chiral or stereogenic centers. Molecules containing chiral carbon atoms may exist as configurational isomers (or stereoisomers) which cannot be converted into each other without breaking of chemical bonds, although the connectivity of the atoms is identical. This class of isomers is subdivided into enantiomers, which are nonsuperimposable mirror images of each other, and diastereoisomers, which are not. A structurally simple example of the former is 3-methylhexane (Fig. 2), a common constituent of fossil fuels, which exists as two enantiomers, while 2,6,10,14-tetramethylhexadecane (phytane, Fig. 2), another ubiquitous constituent of fossil fuels, contains three stereogenic centers and therefore

exists as eight different stereoisomers (four pairs of diastereoisomeric enantiomers). In general, diastereoisomers possess different physical properties, while enantiomers do not. However, in biological systems the two enantiomers of a molecule may behave different if chiral components (e.g., enzymes) are involved in a process.

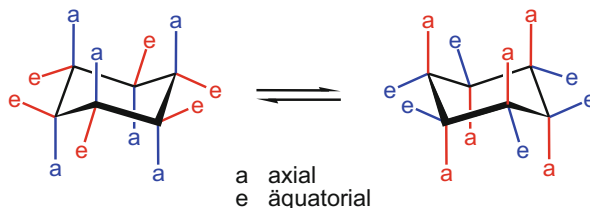
In fossil fuels some branched alkanes (Fig. 2, e.g., isobutane, isopentane, 2-methylpentane, 3-methylpentane, 2-methylhexane, 3-methylhexane) are relatively abundant in the molecular range up to approximately $C_{10}H_{22}$. With increasing molecular weight, individual isomers become less pronounced in comparison to the prevailing *n*-alkanes; however, the mixtures become more complex. It appears that biodegradability generally decreases with increasing degree of branching which is often observed as the relative enrichment of an unresolved complex mixture (UCM, also called the “hump”) during biodegradation of crude oil and related petroleum products. The lower biodegradability of highly branched alkanes might be related to the low natural abundance of individual isomers having not favored the evolution of appropriate degradation pathways.

3.1.3 Cycloalkanes

Formally, cycloalkanes are generated by (homolytic) removal of two hydrogen atoms from two different carbon atoms in *n*-alkanes or branched alkanes; formation of a σ -bond between these carbon atoms (which have to be interrupted by at least one carbon atom) will then result in a cycloalkane. The minimum number of carbon atoms in a cyclic hydrocarbon is three (cyclopropane derivatives), while there is no principal upper limit as to the ring size. Cycloalkanes are also called naphthenes, a term which particularly refers to a petroleum-related origin. Cycloalkanes with alkyl substituents may be called alkylcycloalkanes or cycloalkylalkanes. The structural diversity becomes even greater if the various types of polycyclic hydrocarbons are taken into account. Among these, annulated structures which formally are built up from side-on condensed cyclic segments are most prominent in naturally occurring hydrocarbon assemblages of fossil fuels. A simple example is decalin (Fig. 2) which consists of two annulated cyclohexane rings. Cycloalkanes can be represented by the general formula $C_nH_{2(n+1-r)}$ where *n* is the number of carbon atoms and *r* the number of rings in the molecule.

Ring carbon atoms in cycloalkanes, as in *n*-alkanes and branched alkanes, are sp^3 hybridized and therefore ideally should have tetrahedral bond angles of 109.5° . However, depending on the ring size, the actual structure will deviate more or less from a tetrahedral arrangement which will result in more or less pronounced ring strain. Cyclohexane (Fig. 2) in the chair conformation allows almost ideal tetrahedral angles; therefore ring strain is negligible. Similarly, no strong deviation from the tetrahedron will occur for the C–C–C bond angles in cyclopentane (Fig. 2). Cyclopropane with C–C–C bond angles of 60° and, to a lesser extent, cyclobutane with C–C–C bond angles of 90° deviate most from the tetrahedral angle. They therefore are highly strained and significantly less stable than larger rings. The strain of rings with more than six carbon atoms varies irregularly but in general decreases with increasing ring size and is negligible in larger ring systems.

Fig. 3 Ring flipping of cyclohexane



In cyclohexane, the two hydrogen atoms attached to each carbon atom are chemically not equivalent. The torsional strain is lowest if the molecule adopts the so-called chair conformation in which 6 of the 12 hydrogen atoms are in the plane of the ring (*equatorial*) while the other 6 are perpendicular to it (*axial*). Ring flipping leads to the interchange of equatorially and axially attached substituents (Fig. 3). For spatial reasons, axial substituents interact more strongly with each other than equatorial substituents. Therefore, substituted cyclohexane conformers will be generally more stable if more of the larger substituents are in the equatorial position.

The natural occurrence of rings of different sizes reflects their different stability. Cyclohexane and, to a lesser extent, cyclopentane moieties are by far predominating in natural products and naphthenic petroleum constituents. A broad variety of lipids in eukaryotes and prokaryotes, such as steroids, hopanoids, and other triterpenoids, possess carbon skeletons which are based on annulated cyclohexane and cyclopentane rings. These important constituents of biomass are a relevant source of the structurally diverse mixtures of naphthenes found in fossil fuels. During diagenetic and catagenetic transformation of sedimentary organic matter, biogenic lipids lose functional groups and structural elements such as C–C double bonds (see below) but usually retain the original carbon skeleton. In geochemistry, hydrocarbons such as phytane, cholestane, and hopane (Fig. 2), which can be regarded as chemical fossils, are called biomarkers as their carbon skeletons can directly be related to those of the respective biological precursors (for a detailed introduction to biomarkers, see Peters et al. 2005).

Cyclopropyl moieties occur, for example, in certain fatty acids and steroid derivatives. They are also a structural element of pyrethrins such as chrysanthemic acid, a natural insecticide from *Tanacetum cinerariifolium* (Trev.) Sch. Bip. and *T. coccineum* (Willd.) Grierson (Staudinger and Ruzicka 1924). Ladderane lipids produced by anammox bacteria are an interesting example of natural products containing annulated cyclobutane rings (Sinninghe Damsté et al. 2002). Such three- and four-membered rings normally will not survive diagenetic and catagenetic transformation of biogenic organic compounds deposited in the geosphere. Therefore, cyclopropane and cyclobutane derivatives are not relevant as constituents of fossil fuels. Likewise, there is only very limited evidence that larger rings with more than six carbon atoms play a significant role.

If the fusion occurs across a sequence of atoms rather than at two mutually bonded atoms, bi- and polycyclic hydrocarbons may form bridged structures. α -Pinene (2,6,6-trimethyl[3.1.1]hept-2-ene) (Fig. 5), a widely distributed constituent of plants and in particular of conifer resins, represents a typical example of a bridged

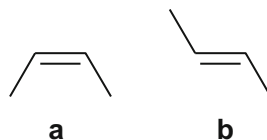
hydrocarbon (additionally containing a double bond; see below). In general, bridged hydrocarbons are of subordinate relevance as constituents of fossil fuels. However, the so-called diamondoids are a class of petroleum constituents with bridged structures which apparently are generated at higher levels of thermal maturity (possibly from annulated hydrocarbons such as steranes or hopanes) (Dahl et al. 1999). These cage-like structures (e.g., adamantane, diamantane, Fig. 2) can be regarded as representing the building blocks of diamonds (in contrast to polycyclic aromatic hydrocarbons which represent the building blocks of graphite). Polymantanes containing up to 11 diamond-crystal cages (undecamantane) have been isolated from natural gas condensates (Dahl et al. 2003a,b). These constituents of fossil fuels appear to be highly resistant to biodegradation (Grice et al. 2000) and therefore may represent major constituents of severely altered crude oils.

3.2 Unsaturated Hydrocarbons

Unsaturated hydrocarbons are molecules that contain at least one C–C double bond or one C–C triple bond. These types of compounds are termed alkenes (resp. cycloalkenes) or olefins (resp. cycloolefins), if the structure contains one or more double bonds, and alkynes (resp. cycloalkynes), if it contains one or more triple bonds. Unsaturated hydrocarbons can be represented by the general formula $C_nH_{2(n+1-r-d-2t)}$ where n is the number of carbon atoms, r the number of rings, d the number of C–C double bonds, and t the number of C–C triple bonds in the molecule. The simplest alkene is ethene (ethylene); the simplest alkyne is ethyne (acetylene) as depicted in Fig. 1. The term *conjugated double bond* denominates two or more double bonds in a molecule which are not separated by CH_2 groups or other structural moieties, i.e., alternating double and single bonds. This is a significant structural element of naturally occurring hydrocarbons such as the carotenes lycopene, β -carotene, or isorenieratene (Figs. 5 and 7).

As it requires significant amount of energy to break a C–C π -bond, free rotation about C–C double bonds is essentially impossible. (This is in contrast to the saturated hydrocarbons where rotation about C–C σ -single bonds is relatively unrestricted as pointed out.) As a consequence, asymmetrically substituted alkenes such as but-2-ene may occur as two distinct constitutional isomers, which are classified according to the *cis*-/*trans*- or *Z*-/*E*-nomenclature (Fig. 4). No *cis*-/*trans*-isomerism can occur in alkenes in which at least one of the two carbon atoms forming the C–C double bond is connected to two identical substituents. In general, *cis*- and *trans*-isomers of a given alkene (or, more generally, of an unsaturated

Fig. 4 Structures of (a) *Z*-but-2-ene (*cis*-isomer) and (b) *E*-but-2-ene (*trans*-isomer) C_4H_8



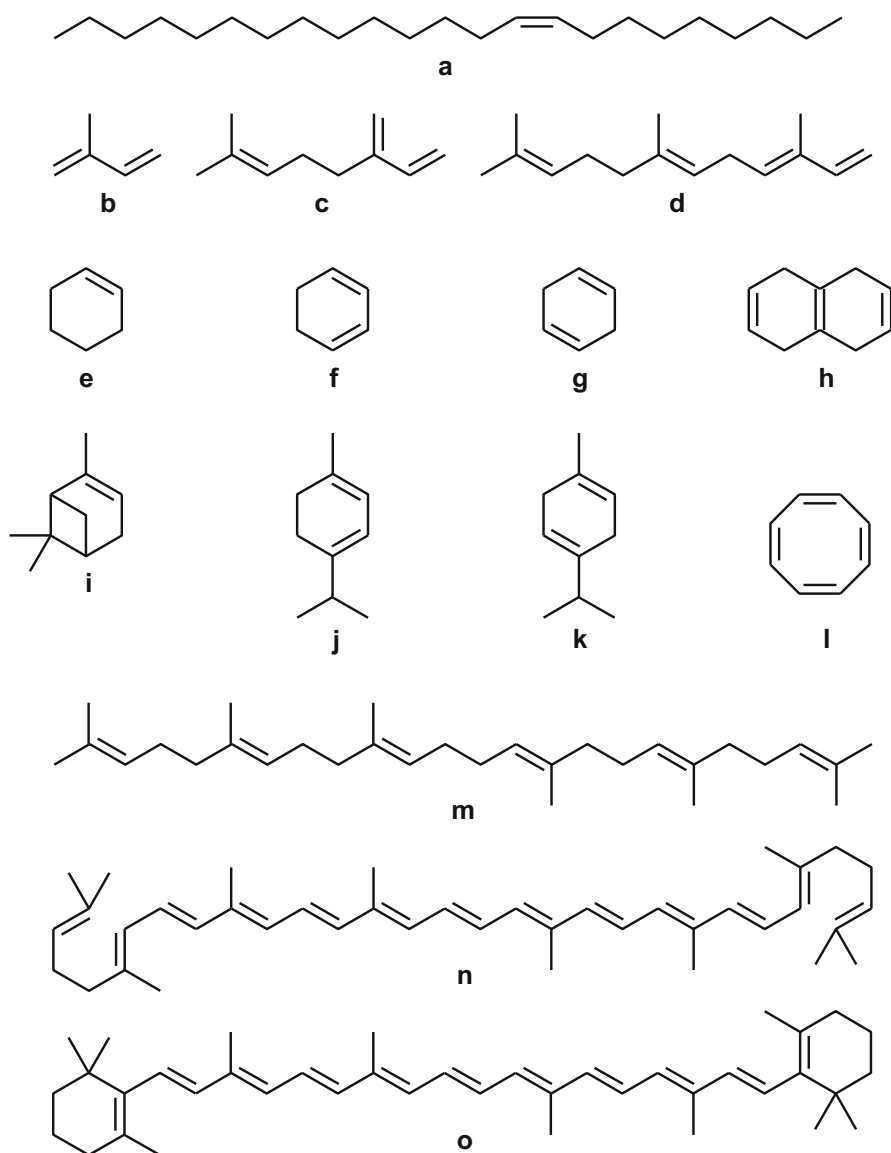


Fig. 5 Structures of selected unsaturated hydrocarbons. **Linear and branched alkenes**, (a) (*Z*)-tricos-9-ene $C_{23}H_{46}$ (muscalure, sex pheromone of the housefly *Musca domestica*), (b) 2-methylbuta-1,3-diene C_5H_8 (isoprene), (c) 7-methyl-3-methylenocta-1,6-diene $C_{10}H_{16}$ (myrcene, constituent of essential oils), (d) (3*E*,6*E*)-3,7,11-trimethyldodeca-1,3,6,10-tetraene $C_{15}H_{24}$ (α -farnesene, natural coating of apples and other fruits); **cycloalkenes and monoterpenes**, (e) cyclohexene C_6H_{10} , (f) cyclohexa-1,3-diene C_6H_8 , (g) cyclohexa-1,4-diene C_6H_8 , (h) 1,4,5,8-tetrahydronaphthalene $C_{10}H_{12}$, (i) 2,6,6-trimethylbicyclo[3.1.1]hept-2-ene $C_{10}H_{16}$ (α -pinene, monoterpene from conifer resins), (j) 1-isopropyl-4-methylcyclohexa-1,3-diene $C_{10}H_{16}$ (α -terpinene, monoterpene from cardamom and marjoram oils), (k) 1-isopropyl-4-

organic compound) exhibit different physical properties. Isomerization of *cis*- to *trans*-double bonds and vice versa is a physiologically significant process, e.g., the transformation of 11-*cis*-retinal to all-*trans*-retinal (and the recycling of the latter to the former) is an integral element of the vision cycle.

Alkenes (and cycloalkenes) of great structural diversity occur as natural products in numerous living organisms (Fig. 5). Even the simplest alkene, ethene, occurs as a biosynthetic product and acts as a hormone on various stages in the life cycle of plants. Many alkenes and cycloalkenes with one or more double bonds act as insect pheromones (Francke and Schulz 1998). Carotenoids (both carotenes = hydrocarbons and xanthophylls = non-hydrocarbons) are pigments, which may be involved in energy transfer in photosynthetic organisms or act as antioxidants in living organisms in general, due to their system of conjugated double bonds. Moreover, C–C double bonds play an important role in many types of heteroatom-containing natural products, such as unsaturated fatty acids, steroids, and other triterpenoids. Examples of natural products containing C–C triple bonds are tridec-1-ene-3,5,7,9,11-pentayne, a polyene hydrocarbon isolated from *Echinacea* spp.; (*Z*)-13-hexadecen-11-yn-1-yl acetate, a pheromone of processionary moths (*Thaumetopoea* spp.); and histrionicotoxin, a toxin of the harlequin poison-dart frog *Oophaga histrionica*.

Unsaturated hydrocarbons, in contrast to saturated and aromatic hydrocarbons, appear to play a minor role in fossil fuels. C–C double (and triple) bonds in most biogenic compounds are too reactive to survive the diagenetic and catagenetic transformations occurring in geological systems over geological timescales. For example, hydrogenation processes with reduced sulfur species such as H₂S (generated by microbial activity, i.e., bacterial sulfate reduction) as hydrogen donors may be responsible for the loss of double bonds (Hebting et al. 2006). An example is the diagenetic transformation of the already mentioned carotenoidal hydrocarbon isorenieratene to isorenieratane (Fig. 7) which may lose all conjugated double bonds on the aliphatic chain connecting the two benzene rings, while the aromatic systems survive even elevated thermal stress due to their high stability (see below). Concentrations of olefins in crude oils are generally low (mostly below 1% by weight), although significantly higher concentrations have been reported in some instances. Curiale and Frolov (1998) reviewed various possible origins of olefins in crude oil. These compounds may migrate with other soluble organic compounds directly from the source rock or get into oils through the process of migration-contamination, wherein light oils act as solvents for syndepositional olefins that occur along the migration route or within the reservoir section. Olefins in crude oils may also derive from “cold” radiolytic dehydrogenation of saturated hydrocarbons, introduced as a by-product of decay of uranium, thorium, and other radioactive elements among the



Fig. 5 (continued) methylcyclohexa-1,4-diene C₁₀H₁₆ (γ -terpinene, various plant sources), (l) cycloocta-1,3,5,7-tetraene C₈H₈; **tri- and tetraterpenes**, (m) (6*E*,10*E*,14*E*,18*E*)-2,6,14,19,23,27-hexamethyltetracosane-2,6,10,14,18,22-hexaene C₃₀H₅₀ (squalene, shark liver oil), (n) lycopene C₄₀H₅₆, (o) β -carotene C₄₀H₅₆

reservoir minerals, or from pyrolysis due to thermal impact from igneous intrusions that occur close to the reservoired oil.

3.3 Aromatic Hydrocarbons

3.3.1 Aromaticity

Aromaticity denominates a chemical property which is found in certain (but not all) cyclic molecules containing conjugated double bonds. Due to resonance stabilization, aromatic compounds are more stable than would be expected from the conjugation of the double bonds alone. The basic example of an aromatic hydrocarbon is benzene (Fig. 7), for which two indistinguishable resonance structures exist (Fig. 6). In benzene all six carbon atoms forming the six-membered ring are sp^2 hybridized; therefore all C–C–C bond angles must be 120° , which is only possible if all carbon atoms lie in the same plane. The six unhybridized p -orbitals which are out of the plane of the atoms can freely overlap and are thought to form conjugated molecular orbitals above and below the ring plane in which the six π -electrons are delocalized. As a consequence, all six C–C bonds in the benzene ring have the same length (140 pm). In general, aromatic compounds are planar cyclic molecules with a fully conjugated double bond system which obeys the Hückel rule, i.e., it must contain $4n + 2$ delocalized π -electrons ($n = 0, 1, 2, 3$, and so on; please note that the Hückel rule is strictly applicable to monocyclic aromatic compounds only). Accordingly, cycloocta-1,3,5,7-tetraene (Fig. 5), a molecule with eight π -electrons which does exist, is *not* aromatic and also not planar. Any (bio)chemical reaction leading to a breakdown of the aromatic system has to overcome the resonance stabilization ($\sim 151 \text{ kJ mol}^{-1}$ for benzene).

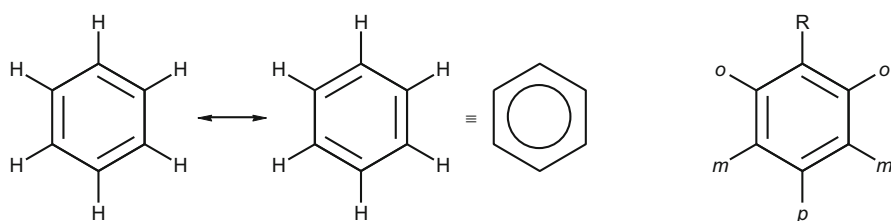


Fig. 6 Resonance structures of benzene (resonance between two structures is indicated by a double arrow). Aromaticity in benzene rings may also be depicted by an inner circle. (Note: Inner circles often are used in a misleading way to depict aromaticity in PAHs. Each circle represents 6 delocalized π -electrons; thus in the case of, e.g., naphthalene, two inner circles would represent 12 delocalized π -electrons, although naphthalene has only 10 delocalized π -electrons; a system with 12 delocalized π -electrons would even not obey the Hückel rule. This is best avoided if one of the possible resonance structures with its alternating double and single bonds is depicted.) Mono-substituted benzene derivatives possess three distinguishable hydrogen atoms on the aromatic ring, two in *ortho*- (*o*-; 1,2-) and *meta*- (*m*-; 1,3-) and one in *para*- (*p*-; 1,4-) position to the substituent, respectively

3.3.2 Benzene Derivatives

All six hydrogen atoms in benzene, which are chemically equivalent, may be substituted by alkyl and aryl groups resulting in two principal classes of aromatic hydrocarbons, alkylbenzenes and polyphenyls. Mixed types are also possible. Three different isomers of disubstituted benzene derivatives are possible which are classified according to their substitution pattern as *ortho*-, *meta*-, or *para*-isomers (Fig. 6). Environmentally most significant are benzene, toluene, ethylbenzene, and the three xylene isomers (BTEX, Fig. 7), which occur in relatively high amounts in fossil fuels, are rather bioavailable due to their physicochemical properties (see below) and have significant health effects. Fossil fuels contain complex mixtures of alkylbenzenes. Linear alkylbenzenes are produced industrially as intermediates in the fabrication of tensides. Biphenyl is the structurally simplest representative among the polyphenyls (Fig. 7). Especially *ortho*-substituted biphenyls may exhibit restricted rotatability about the C–C single bond between the two aromatic rings which can result in atropisomers in which the individual C₂-isomers are optically stable. More complex polyphenyls such as *o*-, *m*-, and *p*-terphenyl (Fig. 7) may occur in small amounts in fossil fuels (Marynowski et al. 2001).

3.3.3 Polycyclic Aromatic Hydrocarbons

Polycyclic aromatic hydrocarbons (PAHs) are fused aromatic hydrocarbons consisting of two or more aromatic rings. The structurally simplest representative of this class of compounds is naphthalene (Fig. 7). The number of condensed aromatic rings is essentially unlimited; larger PAHs can be regarded as structural subunits of graphite. Main environmental sources of PAHs are fossil fuels and incomplete combustion of organic materials. Thermogenic (origin from fossil fuels) and pyrogenic PAHs typically can be distinguished by the relative amounts of alkyl-substituted derivatives versus the parent (unsubstituted) carbon skeleton with the former being enriched in petroleum-related products and depleted in combustion-derived products. More specific PAH ratios are used to distinguish pyrogenic or petrogenic PAHs (Yunker et al. 2002). Certain PAHs are carcinogenic, mutagenic, and/or teratogenic.

While all hydrogen atoms are chemically equivalent in benzene, this is typically not the case in PAHs, with few exceptions such as in coronene (Fig. 7). Naphthalene contains two sets of four chemically equivalent hydrogen atoms, which are classified as α - and β -positions. Therefore two isomers of monosubstituted naphthalene derivatives exist, e.g., 1- and 2-methylnaphthalene (Fig. 7). Anthracene and phenanthrene have three and five chemically nonequivalent hydrogen atoms and may thus form the corresponding number of monosubstituted derivatives, respectively. Chemically nonequivalent carbon and hydrogen atoms may behave different in (bio)chemical reactions which may result in certain regioselectivities. Furthermore, the degree of aromaticity may be different for each ring segment; e.g., in phenanthrene the central ring is less aromatic and therefore more reactive than the outer rings according to Clar's rule (Portella et al. 2005; Randić 2003).

Based on an operational definition, the term "aromatic hydrocarbon" is often used for certain heterocyclic aromatic compound types, such as dibenzofurans and

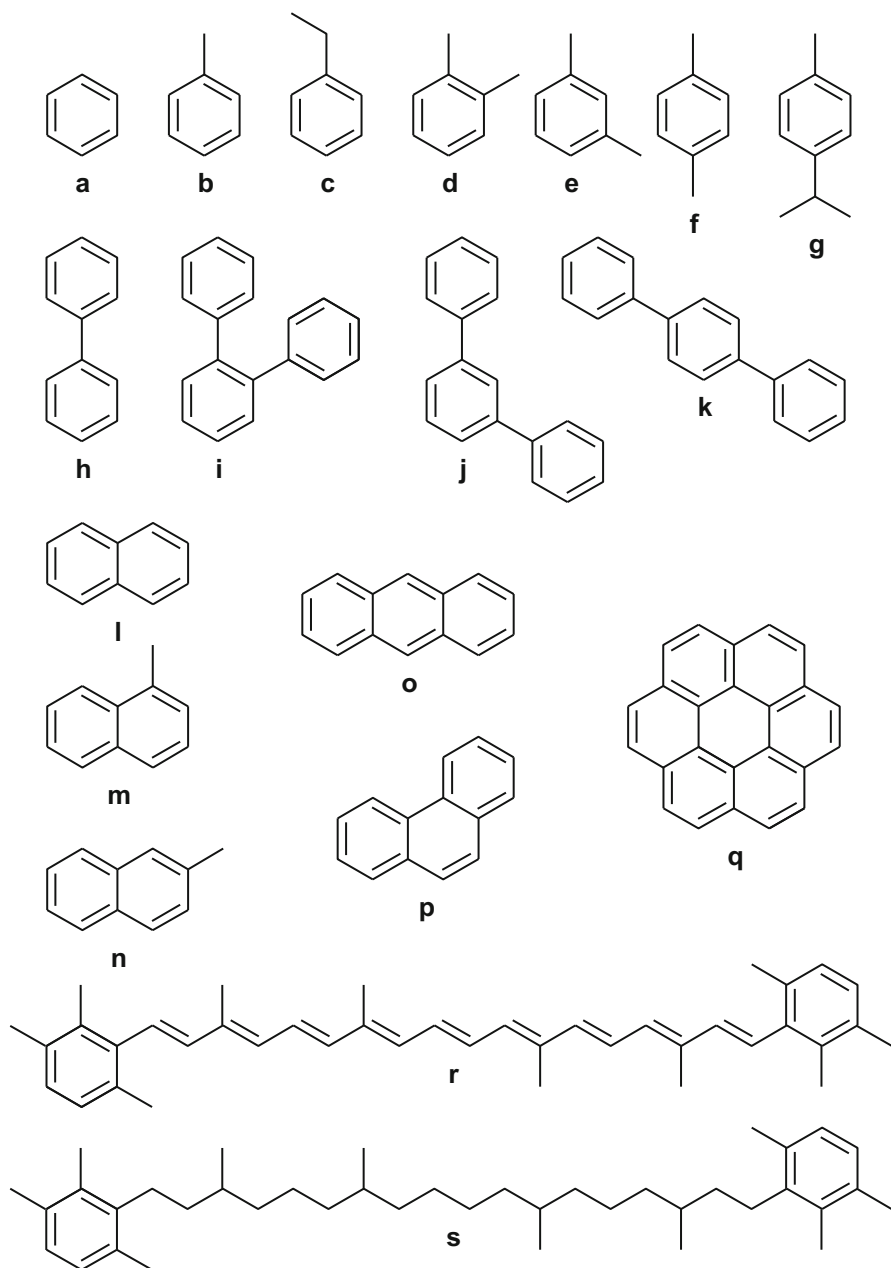


Fig. 7 Structures of selected aromatic hydrocarbons. **Monocyclic aromatic hydrocarbons**, (a) benzene C_6H_6 , (b) toluene, C_7H_8 , (c) ethylbenzene C_8H_{10} , (d) *o*-xylene C_8H_{10} , (e) *m*-xylene C_8H_{10} , (f) *p*-xylene C_8H_{10} , (g) 1-isopropyl-4-methylbenzene $C_{10}H_{14}$ (*p*-cymene, constituent of essential oils); **polyphenyls**, (h) biphenyl $C_{12}H_{10}$, (i) *o*-terphenyl $C_{18}H_{14}$, (j) *m*-terphenyl $C_{18}H_{14}$, (k) *p*-terphenyl $C_{18}H_{14}$; **polycyclic aromatic hydrocarbons**, (l) naphthalene $C_{10}H_8$, (m)

dibenzothiophenes, in environmental and petroleum geochemistry. As these compounds contain heteroatoms, they do not represent hydrocarbons *sensu stricto*. Therefore, these compound classes will be discussed in the appropriate parts of the next chapters.

4 Functionalized Organic Compounds and Lipids

In contrast to hydrocarbons, lipids are natural products defined by their property to be soluble in nonpolar organic solvents like *n*-hexane (McNaught and Wilkinson 1997) but insoluble in water, i.e., they are hydrophobic. This implies that biosynthetic hydrocarbons can be considered as lipids, too. However, except for hydrocarbons, many biogenic lipids are amphiphilic, i.e., they contain both lipophilic and hydrophilic groups, and therefore are able to form vesicles or membranes in an aqueous environment. Thus, any heteroatom-containing compound, like alcohols, aldehydes, ketones, carboxylic acids, esters, sulfur compounds, amines, amides, and halides, of biogenic origin can be a lipid, as long as its hydrocarbon backbone is adequate to achieve a sufficient lipophilicity (see also chapter 5 Physical Properties). In the following, basic information on functionalized organic compounds with a special emphasis on lipids and lipid-like compounds is given in the order of their main heteroatom. Rules for the “nomenclature of lipids” are provided by the IUPAC-IUB Commission on Biochemical Nomenclature (see, e.g., the World Wide Web version prepared by G. P. Moss at “www.qmul.ac.uk/sbcs/iupac/lipid/” and updated references therein).

4.1 Oxygen- and Sulfur-containing Compounds

Since chalcogens (group 16 of the periodic table) are divalent elements, they are able to form either single or double bonds with carbon atoms. Inserting oxygen or sulfur into C–H bonds leads to alcohols in the case of aliphatic moieties as well as the sulfur-analog thiols. The corresponding oxygen containing functional group is called hydroxy group, whereas for S–H it is called sulfanyl group. Since sulfur has a lower electronegativity than oxygen (Table 1), a higher polarity and bond strength of the C–O single bond and, correspondingly, different bond length of C–O (ca. 143 pm) and C–S (ca. 180 pm) single bonds as well as differing reactivities are evident. Based on their high polarity, hydroxy groups are forming strong so-called hydrogen bonds, special intermolecular forces between partially positively charged hydrogen atoms



Fig. 7 (continued) 1-methylnaphthalene $C_{11}H_{10}$, (**n**) 2-methylnaphthalene $C_{11}H_{10}$, (**o**) anthracene $C_{14}H_{10}$, (**p**) phenanthrene $C_{14}H_{10}$, (**q**) coronene $C_{24}H_{12}$; **carotenoids**, (**r**) isorenieratene $C_{40}H_{48}$ (carotenoid of green sulfur bacteria *Chlorobiaceae*), (**s**) isorenieratane $C_{40}H_{60}$ (diagenetic product of isorenieratene)

and partially negatively charged heteroatoms (like oxygen) of neighbored molecules (see also Chapter 5). Such strong intermolecular interactions do not exist between thiols, but on the contrary thiols exhibit a higher acidity in comparison to alcohols as the result of lower bond strength of S–H as compared to O–H bonds.

Hydroxy and sulfanyl groups can also be attached to aromatic moieties, representing the phenols (resp. thiophenols) named according to the simplest representative of this compound class, phenol. Noteworthy, a direct linkage of hydroxy groups to aromatic rings strongly influences the acidity of the functional group. Aliphatic alcohols exhibit only a weak acidity and, consequently, strong bases like alkali metal hydrides are needed to generate the corresponding salts, viz., the alkoxides. The acidity depends dominantly on the inductive effects of further substituents. Thus, perfluorination of the methyl group in ethanol (high negative inductive effect as the result of the high electronegativity of fluorine) shifts the pK_a value from 16 (ethanol) to 12.5 (2,2,2-trifluoroethanol). On the contrary, the pK_a value of 10 of phenol indicates a relatively high acidity as the result of resonance stabilization; hence, phenols react principally as weak acids. However, their acidity is also influenced by inductive effects of further substituents (e.g., halogens) attached to the aromatic ring.

The reactivity of aliphatic alcohols is also influenced by the structural properties of the hydroxylated carbon atoms. Three different types, namely, *primary*, *secondary*, and *tertiary* alcohols, are differentiated according to the number of 1, 2, or 3 carbon atoms to which the hydroxylated carbon atom is bonded (e.g., ethanol, isopropanol, and *tert*-butanol in Fig. 9). Due to differences in resonance stabilization, the reactivity of these different alcohols varies. For example, the type of elimination reactions shifts from a more unimolecular mechanism (E1) in tertiary alcohols to a more bimolecular mechanism (E2) in primary alcohols. The latter are commonly found in nature, e.g., ethanol as the main product of alcoholic fermentation. Primary alcohols with long hydrocarbon chains occur as lipids, for example, in plant waxes, and can result from the enzymatic reduction of respective fatty acids or during metabolic activation of *n*-alkanes in aerobic organisms.

More than one hydroxy group may be attached to aliphatic and aromatic moieties in diverse compound classes. In case of two hydroxy groups bound to adjacent carbon atoms, the term vicinal substitution (*vic*-) has been established. Polyhydroxybenzene derivatives are well-known metabolic intermediates, and mono- or dihydroxylation of aromatic rings is a key reaction in degradation pathways of aromatic hydrocarbons. However, aliphatic polyols play a more prominent role in biochemistry. 1,2,3-Propanetriol (Fig. 9), named glycerol, being the backbone of many lipid compounds, is itself fully mixable with water due to the high degree of hydroxylation. This is also the case in carbohydrates, where most of the carbon atoms carry a hydroxy group leading to a high relative oxygen content. In geminal (*gem*-) diols, two hydroxy groups are bonded to the same carbon atom. Typically, these compounds are unstable and form carbonyl compounds (see below) by elimination of water. Only very few *gem*-diols such as formalin and chloral hydrate (Fig. 9) are stable under normal conditions.

Alkylated phenols are common constituents of crude oil; likewise, phenolic moieties occur widespread in biogeomacromolecules (lignin, humic substances,

kerogen). In contrast, aliphatic alcohols are less represented in geologic organic matter. However, alcohols are a fundamental compound class in the chemical industry. Methanol, the simplest aliphatic alcohol, is one of the most important industrial chemicals with an annual production rate of around 30 million tons. Further specific alcohols used in plasticizers and additives are 2-ethylhexanol and *tert*-butanol (Fig. 9).

An exchange of the hydrogen atom in hydroxy groups by aliphatic or aromatic moieties leads to the compound classes of ethers (R–O–R'). The sulfur analogues are named thioethers. Principally, alkyl/alkyl-, aryl/aryl-, and alkyl/aryl ethers exist in cyclic (e.g., tetrahydrofuran, 1,4-dioxan, polychlorinated dibenzo-*p*-dioxins and dibenzofurans PCDD/F) or acyclic constitution (e.g., diethyl ether, diphenyl ether, anisole, Fig. 9). The smallest cyclic ether, oxirane, consists of a three-membered ring and is highly reactive due to high ring strain; it also occurs as a functional group, the epoxy group, in larger molecules. The generation of epoxides by insertion of oxygen in C=C double bonds is an important reaction to form reactive intermediates in biochemistry. For example, epoxidation is the starting reaction for the cyclization of steroids from squalene or for the initial activation of aromatic hydrocarbons as a part of their degradation pathways. Cyclic ether moieties of higher stability occur in numerous xenobiotics (e.g., crown ethers) and natural products such as α -tocopherol. As the ether group is no hydrogen bond donor, ethers are poorly soluble in water and, therefore, can be considered as lipids or lipid-like compounds. A prominent group of ether lipids found in archaeal cell membranes are the GDGTs (glycerol dialkyl glycerol tetraethers).

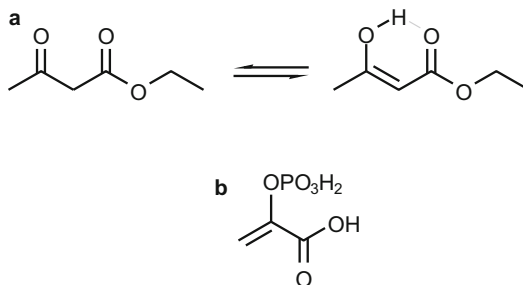
The chemical behavior of ethers differs significantly from that of alcohols. Most ethers are less reactive and, consequently, are often used as solvents in the chemical industry or inert additives in commercial products (e.g., methyl-*tert*-butyl ether MTBE, Fig. 9, as antiknocking agent in gasoline). Polyether synthesis using ethylene oxide leads to the polymer groups of polyethylene glycols or polyethylene oxides with molecular weights of up to 10.000.000 g/mol. This compound class is used widespread in industrial, pharmaceutical, medicinal, and personal care products, in detergents, and as additives in other polymers. Thioether moieties are also present in natural products (e.g., dimethyl sulfide, methionine) as well as in xenobiotic compounds (e.g., the chemical warfare agent bis(2-chloroethyl)sulfide known as mustard gas or S-Lost, Fig. 9).

Linkages between carbon and oxygen atoms are not restricted to single bonds but may also occur as C=O double bonds forming the carbonyl group which is an important moiety in organic compounds. The formation of C=O double bonds needs the reorganization of the sp^3 hybridization of the carbon and oxygen atoms in C–O single bonds to sp^2 hybrid orbitals for generating the C–O σ -bond as well as the π -bond by interaction of the remaining *p*-orbitals. As a result the geometry of this functional group is planar. In case of asymmetrically substituted carbonyl groups, both plains (below and beyond the planar group) are enantiotopic. Thus, the direction of addition of a nucleophilic reaction partner to the carbon atom determines the resulting stereochemical properties of the generated enantiomer.

Carbonyl groups occur in two different compound types, the aldehydes in case of terminal attachment, and ketones, in which the C=O double bond is located at secondary carbon atoms. The conversion of primary alcohols to aldehydes or secondary alcohols to ketones is an oxidation reaction. Aldehyde lipids deriving from long-chain fatty acids are constituents of plant waxes as well as intermediates in the enzymatic formation of *n*-alkanes in plants, while unsaturated long-chain ketones (alken-2-ones) are found in the cosmopolitan marine coccolithophore *Emiliania huxleyi*. Carbonyl groups may also be incorporated into cyclic structures, for example, in cyclohexanone. The need of two free valences prohibits the formation of C=O double bonds directly at aromatic carbon atoms. However, the specific cyclic structure of *p*-quinone (cyclohexa-2,5-diene-1,4-dione) is a building block of many natural products, especially in plant pigments or vitamins (vitamin K), but is also a known moiety in abiotically formed oxidation products of PAHs (e.g., anthra-9,10-quinone derived from photooxidation of anthracene, Fig. 9).

As a result of the high polarity of the carbonyl group, addition and condensation reactions dominate the chemical behavior of aldehydes and ketones. The primary reaction step is the attack of the carbon atom by a nucleophilic reagent. However, for several ketones and to a minor extent for aldehydes, two different reaction characteristics exist in parallel. Carbonyl groups can undergo a so-called keto-enol tautomerism, where two different forms (tautomers) of one molecule, the carbonyl form and an unsaturated alcohol, coexist in a rapid equilibrium (Fig. 8). The interconversion of tautomers requires the shift of σ - and π -bonds as well as the transfer of one hydrogen atom via the enolate anion. For most of the ketones and nearly all aldehydes, the keto tautomer is energetically favorable and thus much more abundant (enol tautomer of acetone approx. 0.00025%). However, in β -dicarbonyl compounds, an extended resonance and the additional inductive effect of the second C=O bond induce a higher stability of the enol tautomers highly influenced by the solvent (e.g., enol tautomer of ethyl acetoacetate in water approx. 0.4%, in hexane approx. 46.4%). Furthermore, the α -hydrogen atom can be easily abstracted as a proton, because of the mesomeric stabilization of the corresponding anion. This effect leads to an increasing acidity of β -dicarbonyl compounds. An interesting example for a “frozen” keto-enol tautomerism is the biochemically important

Fig. 8 Keto-enol tautomerism as exemplified for (a) ethyl acetoacetate $C_6H_{10}O_3$ whose enol form is stabilized by an intramolecular hydrogen bond and (b) a “frozen” example, phosphoenolpyruvic acid $C_3H_5O_6P$



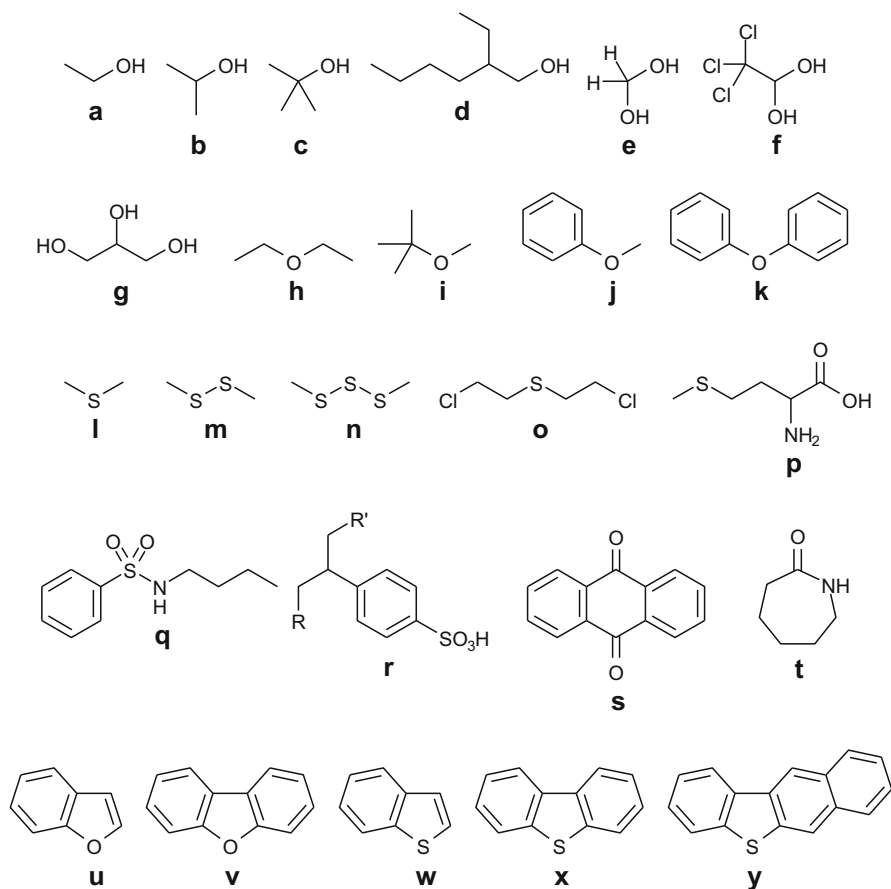


Fig. 9 Structures of selected oxygen- and sulfur-containing compounds. **Alcohols**, (a) ethanol C_2H_6O , (b) isopropanol C_3H_8O (2-propanol), (c) *tert*-butanol $C_4H_{10}O$ (2-methyl-2-propanol), (d) 2-ethylhexanol $C_8H_{18}O$; **polyols**, (e) formalin CH_4O_2 (methanediol), (f) chloral hydrate $C_2H_3Cl_3O_2$ (2,2,2-trichloroethane-1,1-diol), (g) glycerol $C_3H_8O_3$ (1,2,3-trihydroxypropane); **ethers**, (h) diethyl ether $C_4H_{10}O$, (i) methyl-*tert*-butyl ether MTBE $C_5H_{12}O$, (j) anisole C_7H_8O (methoxybenzene), (k) diphenyl ether $C_{12}H_{10}O$; **sulfur compounds**, (l) dimethyl sulfide C_2H_6S ; (m) dimethyl disulfide $C_2H_6S_2$, (n) dimethyl trisulfide $C_2H_6S_3$, (o) bis(2-chloroethyl)sulfide $C_4H_8Cl_2S$ (S-Lost), (p) methionine $C_5H_{11}NO_2S$ (2-amino-4-(methylthio)butanoic acid), (q) *N*-butylbenzenesulfonamide NBBS $C_{10}H_{15}NO_2S$, (r) linear alkylbenzenesulfonates LAS; **further oxygen compounds**, (s) anthra-9,10-quinone $C_{14}H_8O_2$, (t) ϵ -caprolactam $C_6H_{11}NO$ (azepan-2-one); **heterocyclic aromatic compounds**, (u) benzofuran C_8H_6O , (v) dibenzofuran $C_{12}H_8O$, (w) benzothiophene C_8H_6S , (x) dibenzothiophene $C_{12}H_8S$, (y) naphthobenzothiophene $C_{16}H_{10}S$

phosphoenolpyruvic acid (PEP, Fig. 8), which, from a formal point of view, is the ester of phosphoric acid and pyruvic acid in its enol form.

Acetals and hemiacetals are compounds with two C–O single bonds at one carbon atom but without a double bond. These derivatives of aldehydes and ketones are

formally two ether groups or one ether and one hydroxy group attached to one carbon atom and, therefore, represent mono- or dialkylated *gem*-diols. In contrast to the unstable *gem*-diols, acetals exhibit a higher stability, whereas hemiacetals are also of minor stability. However, the most important natural products exhibiting hemiacetal groups are carbohydrates in their cyclic form, in which one hydroxy group is added intramolecularly to the double bond of the keto or aldehyde group. Further intermolecular reactions of these hemiacetals with hydroxy groups of other carbohydrate molecules form acetals, and the frequent repetition of this intermolecular reaction by numerous monomers builds up oligo- and polysaccharides. Such oligosaccharides can also be part of lipid molecules, e.g., glycolipids.

A C–O single and a C=O double bond at one carbon atom are present in carboxylic acids, the oxidation products of aldehydes, and certain of their derivatives. Carboxylic acids with long carbon chain lengths (more than six carbon atoms) are lipophilic and termed fatty acids. These lipids are also prominent building blocks of many other lipid classes and responsible for their low aqueous solubility. Abstraction of a proton from the carboxy group results in an anion highly stabilized by resonance which explains the high acidity of this compound class. Beside acid/base reactions, carboxylic acid derivatives are known in which the hydroxy group is replaced by other functional moieties like amines, alkoxy groups, or halogen atoms resulting in amides, esters, and acyl halides, respectively. In particular amides and esters are important biologic and anthropogenic compounds. Esters can be also formed from inorganic acids (sulfuric acid, phosphoric acid, nitric acid, etc.) and alcohols. Phosphoric acid and carbohydrate derivatives are the monomers building up the backbone of the nucleic acids DNA and RNA.

Ester groups are the central structural feature of many lipid classes (see Fig. 10 for structures of selected examples). As they, like the ether group, do not represent a hydrogen bond donor, esters are quite hydrophobic. Wax esters are esters of long-chain fatty acids with long-chain fatty alcohols and found in different insects (e.g., ants, honey bees) but also in plant epicuticular impregnation (e.g., carnauba wax). Triglycerides (fats) are triesters of glycerol and fatty acids, used by mammals and plants as storage compounds. Lipids of biological membranes need to have an amphiphilic character, i.e., one side of their molecules is hydrophilic, while the other is hydrophobic. In glycolipids fatty acids are bond across ester linkages with glycerol (glyceroglycolipids) or across amide bonds with sphingosine (glycosphingolipids) which are themselves bond to mono- or oligosaccharides, to achieve the amphiphilicity. Phospholipids (also termed glycerophospholipids) are the most important membrane components in eukaryotes and bacteria and comprise a phosphate residue carrying a further small molecule (e.g., ethanolamine, choline, inositol) instead of the sugar moiety in glyceroglycolipids. Sphingolipids (also termed phosphosphingolipids) are the respective compounds containing sphingosine instead of glycerol.

Cyclic esters, referred to as lactones, are realized in numerous natural products. Remarkable examples are the so-called macrolides, cyclic biomolecules with rings of usually 14 to 16 atoms (maximum variation of ring size 6 to 62) frequently used as antibiotics. Cyclic amides, the so-called lactams, are of lesser importance, and their

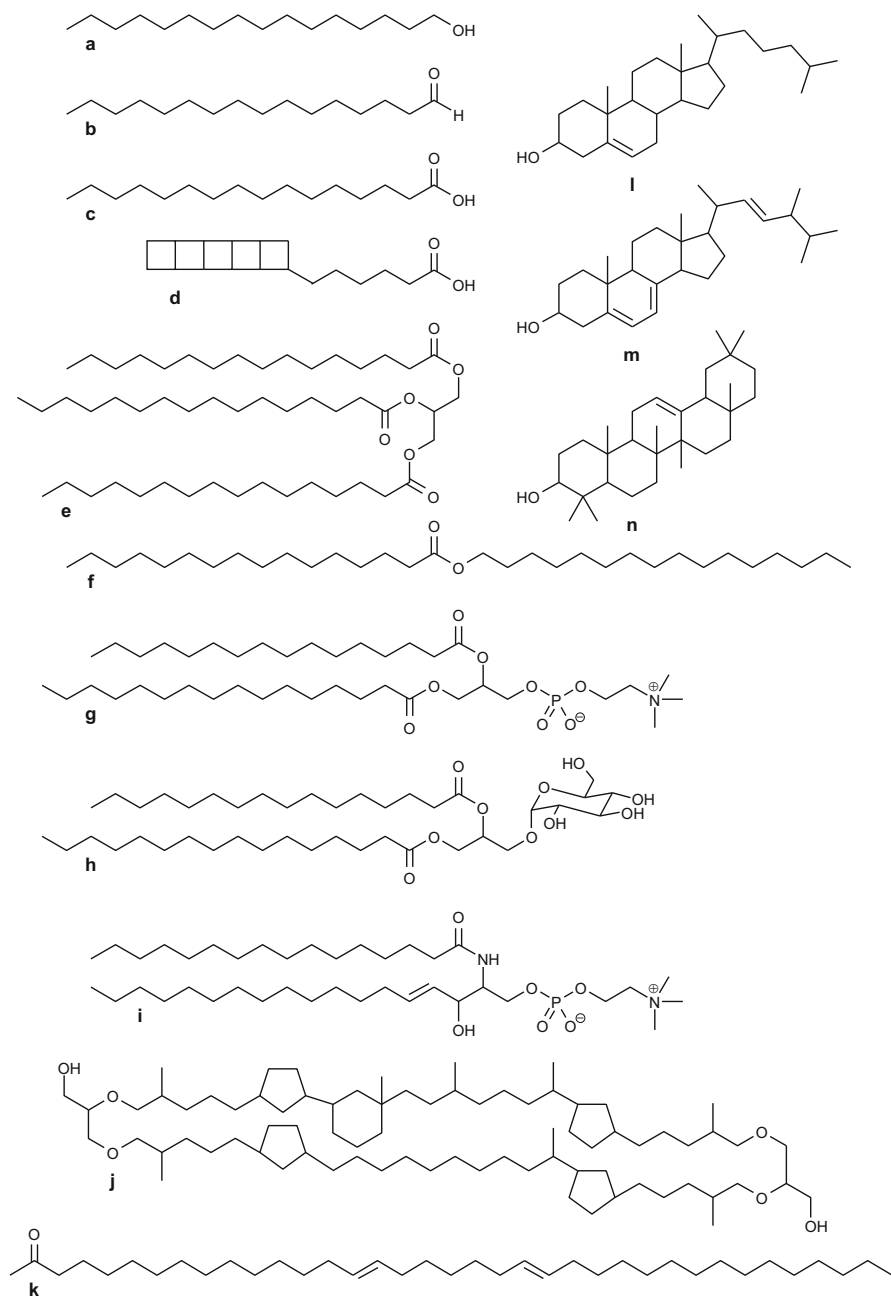


Fig. 10 Structures of selected biogenic lipids. (a) 1-hexadecanol $C_{16}H_{34}O$ (a fatty alcohol), (b) hexadecanal $C_{16}H_{32}O$ (a fatty aldehyde); (c) hexadecanoic acid $C_{16}H_{32}O_2$ (a fatty acid); (d) pentacycloanammoxic acid $C_{18}H_{26}O_2$ (a ladderane fatty acid), (e) tripalmitin $C_{51}H_{98}O_6$ (a triglyceride), (f) hexadecanoyl hexadecanoate $C_{32}H_{64}O_2$ (a wax ester), (g)

structural properties are less diverse as compared to lactones. However, the core structure of penicillin consists of a four-membered lactam ring, and five to seven ring lactams are useful starting materials for technical polyamide synthesis (e.g., ϵ -caprolactam, Fig. 9). Macrocyclic compounds comprising ester as well as amide (peptide) bonds are represented by the depsipeptides – a diverse group of pharmaceutically active substances.

Beside sulfur analogues of alcohols and ethers, sulfur is also involved in other more specific functional groups. One special structural feature of sulfur is the possibility to form oligosulfides by insertion of sulfur atoms into S–S, S–H, or S–C bonds of thioethers or thiols. This reaction is the result of a weak oxidation, during which the oxidation state of the sulfur atoms increases with ongoing rate of insertion. Disulfides are also formed by oxidative coupling of two thiols. Since this reaction is reversible, the thiol/disulfide redox reaction system plays a particular role in the three-dimensional arrangement of various biomacromolecules (e.g., enzymes and hormones). Naturally occurring polysulfides with a very simple molecular structure are dimethyl disulfide and dimethyl trisulfide (Fig. 9).

In organic molecules sulfur can be present also in higher oxidation states than in thiols and thioethers. Formal oxidation of the latter results in the formation of sulfoxides (R–SO–R') and sulfones (R–SO₂–R'). Exchanging an alkyl or aryl substituent in sulfones by a hydroxy group or amines leads to the compound classes of sulfonic acids and sulfonamides, which are frequently found in technical products, e.g., plasticizers, pharmaceuticals, or detergents, like *N*-butylbenzenesulfonamide (NBBS) or linear alkylbenzenesulfonates (LAS, Fig. 9).

Special molecular structures, in which oxygen and sulfur atoms are involved in aromatic systems with sp^2 -hybridization, are five-membered rings containing heteroatoms. The conjugated C=C double bonds form together with the remaining *p*-orbital of the heteroatom the delocalized aromatic π -system. Basic compounds of this group of so-called heterocyclic aromatic compounds are furan and thiophene. Their aromaticity is lower (lowest for furan) when compared to aromatic hydrocarbons *sensu stricto*, but they exhibit typical aromatic properties with respect to their reactivity, spectroscopic behavior, and thermodynamic stability. Higher ring systems are built up by fusion of further benzene moieties leading to benzofuran, dibenzofuran, or benzothiophene, dibenzothiophene, or benzonaphthothiophenes (Fig. 9), respectively. Furan and thiophene derivatives are common constituents of coals, tar, and petroleum. Furthermore, one of the most prominent groups of anthropogenic pollutants, the dioxins or PCDD/PCDFs, consist to a major part of chlorinated congeners of dibenzofuran (Fig. 9).



Fig. 10 (continued) dihexadecanoylphosphatidylcholine C₄₀H₈₀NO₈P (a phosphatidylcholine), (h) dihexadecanoyl glyceroglucopyranose C₄₁H₇₈O₁₀ (a glycolipid), (i) hexadecanoylsphingomyelin C₃₉H₇₉N₂O₆P (a sphingolipid), (j) crenarchaeol C₈₂H₁₅₄O₆ (an ether lipid), (k) (15*E*,22*E*)-heptatriaconta-15,22-dien-2-one C₃₇H₇₀O, (l) cholesterol C₂₇H₄₆O (a sterol), (m) ergosterol C₂₈H₄₄O (a sterol), (n) β -amyrin C₃₀H₅₀O (a triterpenol)

4.2 Nitrogen-containing Compounds

The elements of group 15 of the periodic table of the chemical elements, viz., the pnictogens, that are involved significantly in organic chemistry, are nitrogen and to a much lower extent phosphorus. The latter element appears in biogenic organic compounds dominantly as phosphoric acid coupled to organic moieties via ester bonds. Although the structural diversity of organically bound phosphorus is limited, certain of these compounds are of essential relevance in biochemical processes. Well-known examples highlighting this importance are adenosine tri- and diphosphate (ATP, ADP), the nucleic acids (RNA, DNA), phospholipids, or phosphoglycerates.

The structural diversity of nitrogen-containing organic compounds is much higher and comparable to those of oxygen- and sulfur-containing compounds. A group of simple nitrogen-containing compounds can be obtained by sequential alkylation of ammonia forming the amines which, depending on the degree of alkylation, are classified as primary, secondary, and tertiary amines. Compared with the ammonium cation, quaternary alkylation results in the formation of quaternary ammonium cations and corresponding salts. Aliphatic ring systems involving secondary or tertiary amines are common structural moieties (e.g., pyrrolidine, piperidine, Fig. 11). Furthermore, the functional group of amines, the amino group, can be attached manifold to carbon backbones leading to diamines, triamines, etc. such as spermidine (Fig. 11), a biogenic compound involved in cellular metabolism. In analogy to the corresponding oxygen compounds (alcohols, phenols), also amines form intermolecular hydrogen bonds and are therefore well soluble in water. However, amines are prominent parts of membrane lipids, especially of the polar head groups, like ethanolamine, choline, and sphingosine (Fig. 11).

Under physiological conditions, amines are usually protonated due to their strong basicity. The replacement of hydrogen atoms in ammonia by alkyl groups enhances the basicity by a positive inductive effect, which can partially be compensated by an opposite direction of the inductive impact or by steric hindrance. Therefore, first and second alkylation leads to a slightly elevated basicity, whereas tertiary amines exhibit similar pK_b values when compared to ammonia. On the contrary, amines with aromatic substituents exhibit a lesser alkalinity as a result of the strong negative mesomeric effect of the aromatic substituent. This compound class refers to anilines denominated according to its simplest member, aniline (Fig. 11).

Amines are widespread constituents of the biosphere. Amino substitution is a basic structural feature of amino acids and enables this group of essential compounds to build up peptides and proteins by polycondensation. Further important biogenic nitrogen compounds act as neurotransmitters, like serotonin and dopamine, or as hormones, like histamine and adrenalin (Fig. 11). Volatile aliphatic amines exhibit bad odor and represent degradation products of more complex nitrogen-containing compounds. Industrially, amines are frequently used directly or act as raw material for the synthesis of dyes, in particular azo dyes (e.g., methyl orange), and drugs (e.g., amphetamine and derivatives, Fig. 11).

As introduced in Sect. 4.1 Oxygen- and Sulfur-containing Compounds, amines as well as anilines react readily with carboxylic acids to form amides or anilides,

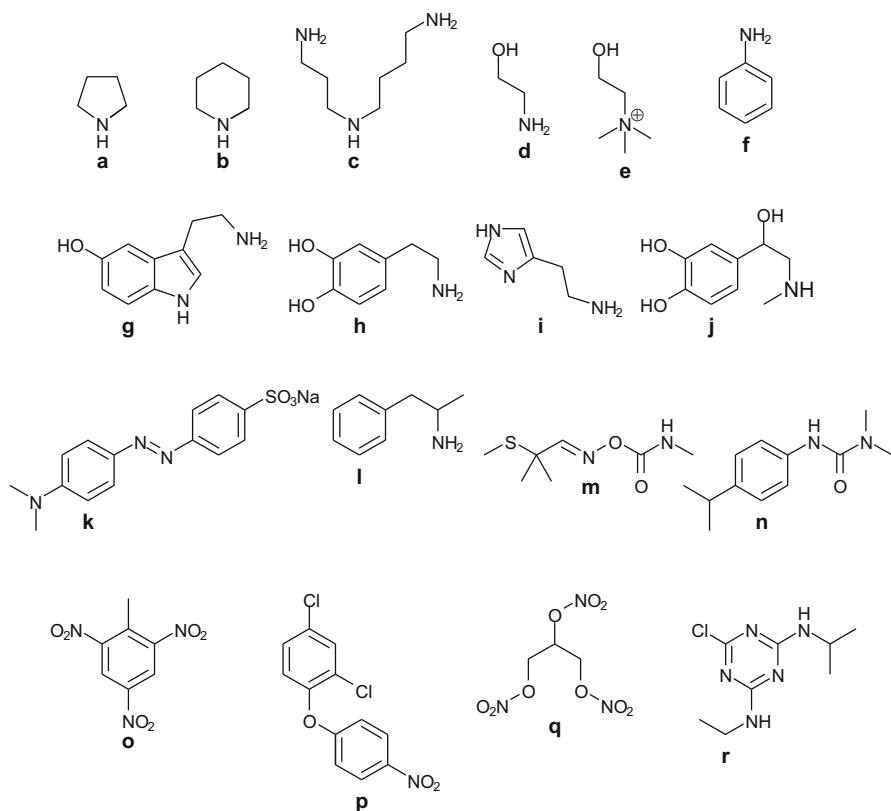


Fig. 11 Structures of selected nitrogen-containing compounds. **Amines**, (a) pyrrolidine C_4H_9N , (b) piperidine $C_5H_{11}N$, (c) spermidine $C_7H_{19}N_3$ (*N*-(3-aminopropyl)butane-1,4-diamine), (d) ethanolamine C_2H_7NO (2-aminoethanol), (e) choline $C_5H_{14}NO$ (2-(trimethylammonium)ethanol), (f) aniline C_6H_7N ; **biogenic nitrogen compounds**, (g) serotonin $C_{10}H_{12}N_2O$ (3-(2-aminoethyl)-1*H*-indol-5-ol), (h) dopamine $C_8H_{11}NO_2$ (4-(2-aminoethyl)benzene-1,2-diol), (i) histamine $C_5H_9N_3$ (2-(1*H*-imidazol-4-yl)ethanamine), (j) adrenaline $C_9H_{13}NO_3$ (4-[1-hydroxy-2-(methylamino)ethyl]benzene-1,2-diol); **synthetic nitrogen compounds**, (k) methyl orange $C_{14}H_{14}N_3O_3SNa$ (4-[(*E*)-[4-(dimethylamino)phenyl]diazenyl]-2-methylbenzenesulfonic acid), (l) amphetamine $C_9H_{13}N$ (1-methyl-2-phenylethylamine), (m) aldicarb $C_7H_{14}N_2O_2S$ ((*E*)-2-methyl-2-(methylthio)propanal *O*-[(methylamino)carbonyl]oxime), (n) isoprotrurone $C_{12}H_{18}N_2O$ (*N'*-(4-isopropylphenyl)-*N,N*-dimethylurea), (o) 2,4,6-trinitrotoluene (TNT) $C_7H_5N_3O_6$, (p) nitrofen $C_{12}H_7Cl_2NO_6$ (1-(4-nitrophenoxy)-2,4-dichlorobenzene), (q) nitroglycerine $C_3H_5N_3O_9$, (r) atrazine $C_8H_{14}ClN_5$ (6-chloro-*N*-ethyl-*N'*-isopropyl-1,3,5-triazine-2,4-diamine)

respectively. In accordance with the nomenclature of substituted amines, also amides are differentiated by their degree of substitution forming primary, secondary, and tertiary amides. Of particular interest is the stabilization of carbonic acid by the formation of its mono- or diamide resulting in carbamate or urea derivatives. Beside its natural occurrence, these structural moieties are building up important classes of pesticides, e.g., aldicarb and isoprotrurone with carbamate or urea structures,

respectively (Fig. 11). Noteworthy, the formation of amides is not limited to carboxylic acids but also possible with sulfonic acids (sulfonamides) and phosphoric acid (phosphoramides).

Carbon-nitrogen bonds are also realized as double or triple bonds. Imines, which exhibit a C–N double bond, are usually easily hydrolyzed in aqueous system and, thus, play a minor role with respect to structural diversity in the environment. However, imine formation is known as an initial reaction in the nonenzymatic browning reaction between amino acids and carbohydrates, the so-called Maillard reaction. The C≡N triple bond, the functional group of nitriles, is mainly found in anthropogenic products; for example, acetonitrile is an important solvent, and the polymerization of nitriles, especially acrylonitrile, forms resistant polymers. However, various nitrile-containing natural products have been described (Fleming 1999). From a chemical point of view, nitriles are classified as carboxylic acid derivatives, since reductive hydrolysis of nitriles yields carboxylic acids.

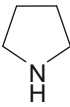
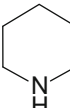
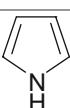
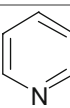
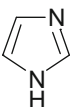
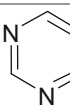
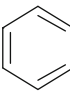
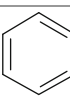
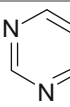
The nitrogen atom in amino groups is amenable to oxidation forming the nitro group. Principally, nitro groups can be attached to aliphatic and aromatic moieties. However, in terms of environmental occurrence, only the nitro arenes are of greater importance. The nitro group exhibits an elevated relative oxygen content, which is the reason for the highly explosive properties of polynitro arene derivatives. Best known nitro-containing explosives are 2,4,6-trinitrotoluene (TNT), tetryl (2,4,6-trinitrophenyl-*N*-methylnitramine), and picric acid (2,4,6-trinitrophenol). Nitro substitution can also be found in selected personal care products, especially as fragrances like musk xylene or musk ketone, and pesticides (e.g., nitrofen). Nitro compounds should not be confused with organic nitrates, which represent the esters of nitric acid with alcohols also forming explosives (e.g., nitroglycerin) and are used as pharmaceuticals, like isosorbide mononitrate. Some structural examples are given in Fig. 11.

Nitrogen atoms are often incorporated in aromatic systems. With respect to sulfur and oxygen, heterocyclic aromatic compounds are dominated by five-membered ring systems containing one heteroatom. However, the possibility to form heterocyclic aromatic systems is not restricted to five-membered rings or to one heteroatom. In particular, nitrogen is forming a more complex family of heterocyclic aromatic compounds including different ring sizes with one (e.g., pyrrole, pyridine, azepine cation) or more (e.g., imidazole, pyrazine, triazine) nitrogen atoms. Bicyclic structures include nitrogen atoms in one or both ring systems, like in quinoline and purine. Despite their aromatic character, many of these compounds exhibit weak basicity. These structural moieties appear widespread in natural products comprising alkaloids, amino acids, nucleic acids, various coenzymes, and chlorophylls (Table 2). Xenobiotics with nitrogen containing heteroaromatic moieties are, for example, the triazine pesticides including atrazine (Fig. 11), simazine, and terbuthylazine.

4.3 Halogenated Compounds

Halogen atoms are attached to aliphatic as well as aromatic moieties. From a formal point of view, halogen atoms substitute hydrogen atoms in C–H bonds resulting in

Table 2 Selected nitrogen containing heterocyclic systems and corresponding biogenic compounds exhibiting these moieties

Pyrrolidine		Proline, nicotine
Piperidine		Tropane alkaloids
Pyrrole		Hemoglobin, chlorophyll
Pyridine		Nicotine, NAD, NADP, PLP
Imidazole		Caffeine, histidine
Pyrimidine		Cytosine, thymine
Indole		Serotonin, tryptophan
Quinoline		Quinine
Purine		Adenine, guanine

alkyl and aryl halides. Chemical reactions leading to halogenated organic compounds include radical, nucleophilic, or electrophilic substitutions of hydrogen atoms in hydrocarbons or functional groups in functionalized compounds (primarily alcohols) as well as electrophilic additions to unsaturated compounds. Dominantly chlorine and bromine are organically bound halogens, whereas fluorinated and iodinated compounds are less represented, especially in natural products (prominent exceptions are sodium fluoroacetate, an antiherbivore poison in various plants, or the iodine-containing thyroid hormones thyroxine and triiodothyronine). However, fluorine-containing compounds are still important xenobiotics with partially high environmental impact, e.g., chlorofluorocarbons (CFC) or perfluorinated detergents

(PFAS, PFCA). Even for iodine-organic compounds, some very special applications are known, e.g., the iodine-containing X-ray contrast medium iopromide, leading also to an environmental occurrence of these compounds.

The high structural diversity of halogenated organic compounds is based on three independent factors. Firstly, the degree of halogenation may cover a wide range from monohalogenated to perhalogenated compounds. Secondly, the location of halogen substituents at different carbon atoms of aliphatic or aromatic moieties leads to numerous constitutional isomers. Finally, mixed halogenation strongly expands the compositional variability. Thus, halogenated compounds with a given carbon skeleton exist as large sets of so-called congeners, as exemplified for chlorinated/brominated benzenes in Table 3.

Numerous congener groups of xenobiotic halogenated organic compounds represent important environmental contaminants featuring the described structural diversity. Polychlorinated dibenzo-*p*-dioxins and dibenzofurans (usually summarized as “dioxins”) exhibit specific congener patterns allowing to differentiate their typical emission sources (e.g., Fiedler 1996). Also polychlorinated biphenyls (PCBs) or polybrominated diphenyl ethers, which are widespread used flame retardants, appear with characteristic patterns of congeners (Ballschmiter et al. 1987; de Boer et al. 2000). Due to the moderate polarity of the C–halogen bond and their inability to form hydrogen bonds, organic halogen compounds are often quite lipophilic and thus behave like lipids.

Over decades it has been assumed that halogenated compounds can be found only infrequently in living organisms. However, over the last 20 years, the information on natural chlorinated and brominated compounds increased dramatically and disclosed a high diversity of halogenated natural products in fungi, algae, terrestrial plants, mammals, and further biota (Gribble 1994, 2000; Ballschmiter 2003). The molecular structures range from simple haloalkanes to complex and highly functionalized compounds as partially illustrated in Fig. 12. It is also shown that a high degree of halogenation is not restricted to xenobiotic compounds but can be also observed in natural products.

Table 3 Structural diversity of halogenated benzenes

Degree of halogenation	Number of distinct substitution patterns for chlorine only	Number of distinct substitution patterns for chlorine + bromine
1	Cl ₁ : 1	Cl ₁ + Br ₁ : 2
2	Cl ₂ : 3	Cl ₂ + ClBr + Br ₂ : 9
3	Cl ₃ : 3	Cl ₃ + BrCl ₂ + Br ₂ Cl + Br ₃ : 17
4	Cl ₄ : 3	Cl ₄ + BrCl ₃ + Br ₂ Cl ₂ + Br ₃ Cl + Br ₄ : 40
5	Cl ₅ : 1	Cl ₅ + BrCl ₄ + Br ₂ Cl ₃ + Br ₃ Cl ₂ + Br ₄ Cl + Br ₅ : 20
6	Cl ₆ : 1	Cl ₆ + BrCl ₅ + Br ₂ Cl ₄ + Br ₃ Cl ₃ + Br ₄ Cl ₂ + Br ₅ Cl + Br ₆ : 13
Resulting number of congeners	12	101

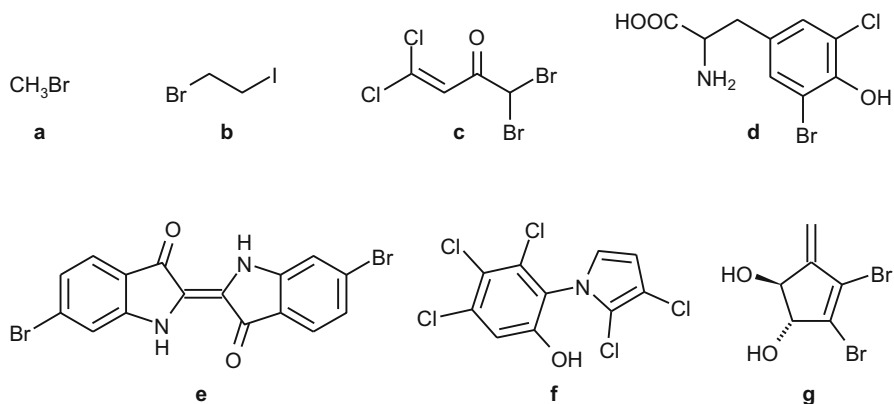


Fig. 12 Halogenated organic compounds naturally produced by living organisms. (a) Bromomethane CH_3Br (marine algae), (b) 1-bromo-2-iodoethane $\text{C}_2\text{H}_4\text{BrI}$ (marine algae), (c) 1,1-dibromo-4,4-dichlorobut-3-en-2-one $\text{C}_4\text{H}_2\text{Br}_2\text{Cl}_2\text{O}$ (red alga *Asparagopsis taxiformis*), (d) 2-amino-3-(3-bromo-5-chloro-4-hydroxyphenyl)propanoic acid $\text{C}_9\text{H}_9\text{BrClNO}_3$ (mollusk *Buccinum undatum*), (e) (2E)-6-bromo-2-(6-bromo-2-oxo-1H-indol-2-ylidene)-1H-indol-3-one $\text{C}_{16}\text{H}_8\text{Br}_2\text{N}_2\text{O}_2$ (tyrian purple from marine snail), (f) 3,4,5-trichloro-2-(2,3-dichloro-1H-pyrrol-1-yl)phenol $\text{C}_{10}\text{H}_4\text{Cl}_5\text{NO}$ (*Streptomyces* sp.), (g) (1S,2R)-3,4-dibromo-5-methylenecyclopent-3-ene-1,2-diol $\text{C}_6\text{H}_6\text{Br}_2\text{O}_2$ (red alga *Vidalia spirala*)

5 Physical Properties

The environmental behavior of an organic compound, like its bioavailability or its tendency to accumulate in certain compartments, is controlled by its macroscopic physicochemical properties, such as melting and boiling point, density, viscosity, vapor pressure, or aqueous solubility. These properties show systematic variations directly related to the molecular structure of a compound which determines the ability of its molecules to interact with other molecules (or other components of their direct environment such as the surfaces of solids). Relevant structural features are the presence or absence (as in hydrocarbons) of certain functional groups, intramolecular interactions of different substituents (e.g., shielding effects), or molecular size and shape.

The most important intermolecular forces in order of increasing strength are van der Waals interactions, dipole-dipole interactions, and hydrogen bonding. Van der Waals interactions depend on weak forces between molecules and/or ions, whose energy decreases by the sixth power of the distance between the involved species. Asymmetric distribution of electron density or electronic charge in molecular or ionic species generates permanent dipole moments. A comparison of dipole moments of selected hydrocarbons and functionalized organic compounds illustrates the influence of heteroatoms and functional groups (Table 4). Dipole moments are typically weak in hydrocarbons. Due to the high degree of structural symmetry, certain hydrocarbons such as methane, 2,2-dimethylpropane, or benzene do not even

Table 4 Dipole moments of selected organic compounds

Aliphatic compounds			Aromatic compounds		
<i>Formula</i>	<i>Name</i>	μ [D]	<i>Formula</i>	<i>Name</i>	μ [D]
CH(CH ₃) ₃	Isobutane	0.13	C ₆ H ₅ -CH ₃	Toluene	0.38
CH ₃ -CH ₂ -CH(CH ₃) ₂	Isopentane	0.13	C ₆ H ₅ -CH ₂ -CH ₃	Ethylbenzene	0.59
C ₅ H ₈	Cyclopentene	0.20	<i>o</i> -C ₆ H ₄ (CH ₃) ₂	<i>o</i> -Xylene	0.64
CH ₂ =CH-CH ₃	Propene	0.37	C ₆ H ₅ -CH(CH ₃) ₂	Isopropylbenzene	0.79
CH ₂ =CH-CH ₂ -CH ₃	1-Butene	0.44	C ₆ H ₅ -C(CH ₃) ₃	<i>tert</i> -Butylbenzene	0.83
CH ₂ =CH-CH ₂ -CH ₂ -CH ₃	1-Pentene	0.50	C ₁₂ H ₁₀	Acenaphthene	0.85
CH ₃ -CH ₂ -O-CH ₃	Ethylmethyl ether	1.17	C ₆ H ₅ -O-CH ₃	Anisole	1.38
CH ₃ -CH ₂ -NH ₂	Ethylamine	1.22	C ₆ H ₅ -NH ₂	Aniline	1.13
CH ₃ -CH ₂ -SH	Ethanethiol	1.61	C ₆ H ₅ -SH	Benzenethiol	1.23
CH ₃ -CH ₂ -OH	Ethanol	1.69	C ₆ H ₅ -OH	Phenol	1.22
CH ₃ -(C=O)-O-CH ₃	Methyl acetate	1.72	C ₆ H ₅ -(CO)-O-CH ₃	Methyl benzoate	1.94
CH ₃ -CH ₂ -Cl	Chloroethane	2.05	C ₆ H ₅ -Cl	Chlorobenzene	1.69
CH ₃ -CH ₂ -CHO	Propanal	2.72	C ₆ H ₅ -CHO	Benzaldehyde	3.00
CH ₃ -CH ₂ -(C=O)-CH ₃	2-Butanone	2.78	C ₆ H ₅ -(CO)-CH ₃	Acetophenone	3.02
CH ₃ -CH ₂ -NO ₂	Nitroethane	3.23	C ₆ H ₅ -NO ₂	Nitrobenzene	4.22
CH ₃ -CH ₂ -CN	Propionitrile	4.05	C ₆ H ₅ -CN	Benzonitrile	4.18

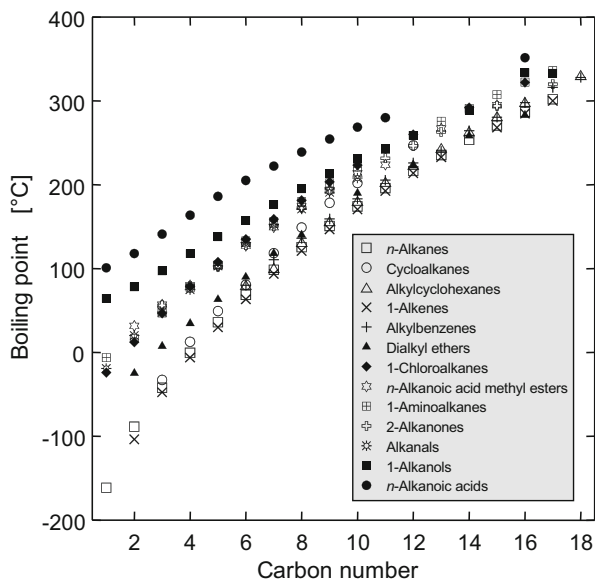
possess a permanent dipole moment. Notably, carbonyl compounds (aldehydes and ketones) possess rather elevated dipole moments which contribute to their relatively high melting and boiling points and aqueous solubilities.

Hydrogen bonding requires the presence of functional groups in which hydrogen is covalently bound to a heteroatom such as nitrogen or oxygen. Carboxylic acids, alcohols, phenols, or amines are typical compound classes which exhibit the ability to form hydrogen bonds. A negative partial charge is at the more electronegative heteroatom, whereas carbon and hydrogen atoms carry a positive partial charge in these structural moieties. The resulting dipole moments induce electrostatic forces between functional groups of two different molecules leading to intermolecular interactions or of the same molecule, resulting in intramolecular interactions. Importantly, functional groups, without hydrogen being bound to a heteroatom such as carbonyl groups, may be involved in hydrogen bonding by interacting with heteroatom-bound hydrogen atoms of functional groups in the same or another molecule. The bond strength ranges from <5 to 155 kJ mol⁻¹; the average bond length of hydrogen bridges in water is approximately 180 pm. Such intra- and intermolecular interactions of low energy play an important role in secondary and tertiary structures of biogenic macromolecules such as proteins or nucleic acids.

In homologous series of various compound classes, there is a systematic increase in melting and boiling points (Fig. 13). The difference in boiling points of the most (methane) and least (formic acid) volatile C_1 compound is as high as $262.5\text{ }^\circ\text{C}$. The total range of boiling points for representatives of different compound classes at a given carbon number decreases with increasing carbon number and is below $100\text{ }^\circ\text{C}$ at C_{16} for the compound classes depicted in Fig. 13. Hydrocarbons generally show the lowest, and compound classes such as carboxylic acids and 1-alkanols, which are able to form strong hydrogen bonds, the highest melting and boiling points. According to Carnelley's rule, high molecular symmetry is associated with high melting points, for example, the melting point of benzene ($5.5\text{ }^\circ\text{C}$) is significantly higher than that of toluene ($-94.9\text{ }^\circ\text{C}$) despite the lower molecular weight (Brown and Brown 2000).

Differences in density between members of different compound classes are large for the lower homologues and become systematically smaller with increasing molecular size (Fig. 14a). As for the boiling points, the largest overall difference among the compound classes depicted in Fig. 14a is observed between methane and formic acid. The plot also reveals that the density increases with increasing carbon number for hydrocarbons, while it decreases for n -alkanoic acids and their methyl esters. Some compound classes such as 1-alkanols, alkanals, and 2-alkanones do not show significant variations of density in relation to the carbon number. At a given carbon number, the densities of n -alkanes and 1-alkenes are relatively similar, while those of alkylbenzenes and alkylcyclohexanes are significantly higher. An increasing degree of halogenation of organic compounds leads to a significant increase in

Fig. 13 Boiling points at atmospheric pressure versus carbon number for selected compound classes. (All data are from Lide 2002)



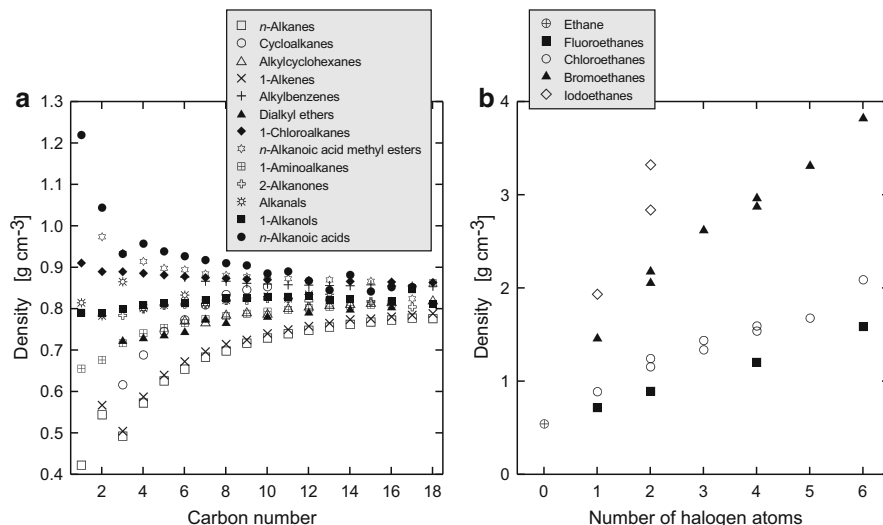


Fig. 14 (a) Density versus carbon number for selected compound classes. (b) Density versus number of halogen atoms for ethane and its halogenated derivatives (for di-, tri-, and tetra-haloethanes, data for both isomers were included if available). If available, density data determined at 20 °C were used; otherwise data obtained at different temperatures were included as well (total range -162 °C to 100 °C). (All data are from Lide 2002)

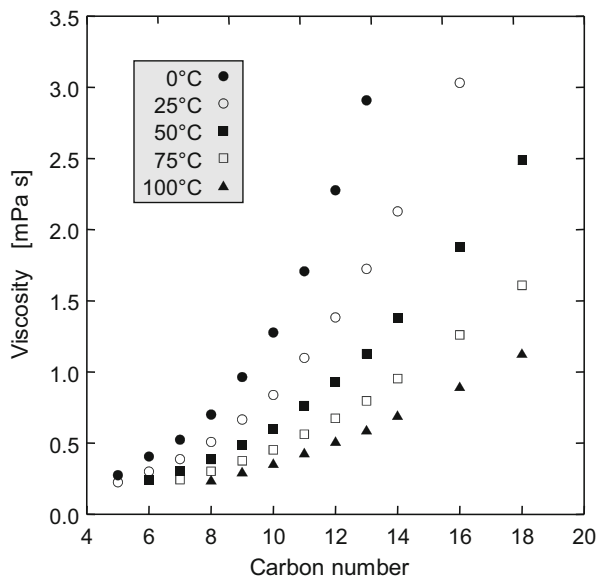
density as illustrated for haloethanes in Fig. 14b; the effect increases in the order fluorine < chlorine < bromine < iodine. Density should not be confused with specific gravity which is calculated as the ratio of the density of a given compound to that of water. In the petroleum industry, the API gravity (= American Petroleum Institute gravity) is the most important measure for the quality of crude oils. It is calculated according to the formula

$$\text{API gravity} = (141.5/\text{specific gravity at } 15.5^{\circ}\text{C}) - 131.5;$$

thus API gravity is inversely proportional to density. In-reservoir biodegradation is one of the most important processes leading to a decrease of API gravity and thus a quality deterioration of crude oils. The increase of density in such oils is due to the specific loss of hydrocarbons of relatively low density and a resulting relative enrichment of functionalized organic compounds of higher density.

Viscosity is an important physicochemical property which characterizes the resistance of a fluid being deformed and may be applied to pure organic compounds or mixtures. Within homologous series of compounds, it increases exponentially with increasing carbon number as illustrated for selected *n*-alkanes in Fig. 15. As a consequence crude oils containing high proportions of long-chain *n*-alkanes may be highly viscous and therefore difficult to produce. Viscosity decreases with increasing temperature (Fig. 15); therefore, some crude oils which are produced as a liquid from

Fig. 15 Viscosity at different temperatures versus carbon number for selected *n*-alkanes. (All data are from Lide 2002)



their deep hot subsurface reservoirs become solid under surface conditions. For crude oils, a rough positive correlation of API gravity and viscosity is observed.

The interaction with different phases in multiphase systems is crucial for the environmental behavior of organic compounds. In natural environments, various gaseous (air, natural gas, gas condensates), liquid (aqueous phases, nonaqueous phase liquids (NAPL)) and solid (inorganic sediment particles and rock matrices, organic particles, and amorphous kerogen) phases have to be considered. Very important with respect to the effects of organic compounds on biota is their transport behavior in mobile gaseous and liquid phases. Boiling point and vapor pressure are relevant properties controlling the abundance of hydrocarbons and other organic compounds in air, while aqueous solubility represents a key parameter with respect to their occurrence and distribution in the hydrosphere.

Only certain organic compounds are miscible with water. Typically, these consist of rather polar molecules containing functional groups that may form hydrogen bonds. For a broad range of organic compound classes including all known types of hydrocarbons, aqueous solubility shows a systematic relationship to specific structural features. In homologous series of various compound classes, the aqueous solubility decreases with increasing carbon number (Fig. 16a). It is evident from Fig. 16a, that the aqueous solubility of hydrocarbons is typically lower than that of functionalized organic compounds with the same number of carbon atoms. Among the hydrocarbons, acyclic saturated compounds are 1–3 orders of magnitude less water soluble than aromatic hydrocarbons of similar molecular weight (Fig. 16b). As a consequence, compounds structurally as different as *n*-dodecane ($C_{12}H_{26}$, molecular weight 170) and picene ($C_{22}H_{14}$, molecular weight 278) have very similar

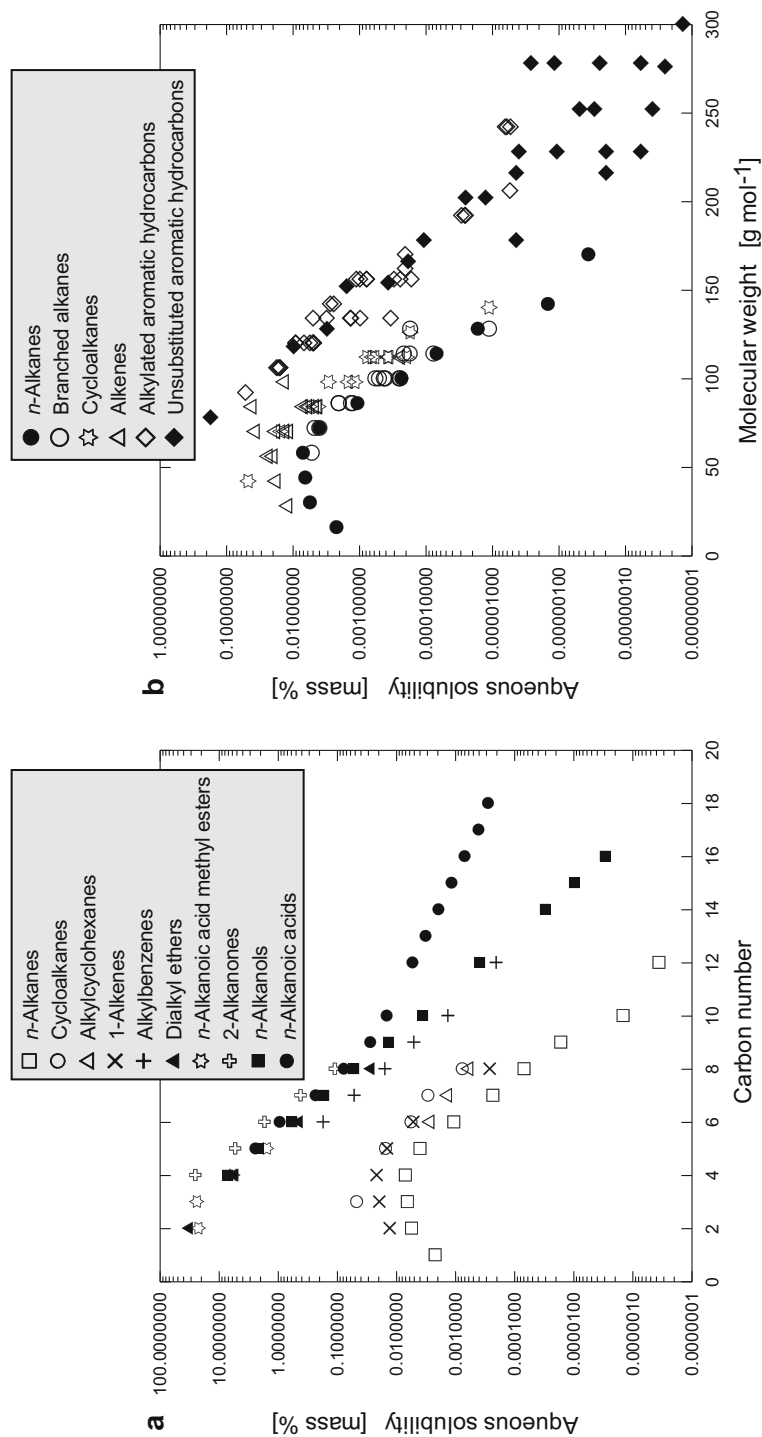


Fig. 16 (a) Aqueous solubility versus carbon number for different compound classes. Formic, acetic, propionic, and butanoic acid as well as methanol, ethanol, and 1-propanol are fully miscible with water and therefore do not occur in this plot. (b) Aqueous solubility versus molecular weight for different types of hydrocarbons. With very few exceptions, solubility data determined at 25 °C were used. (All data are from Lide 2002). Please note the logarithmic scale of the y-axes

aqueous solubilities at 25 °C (*n*-dodecane 0.00000037 mass %, picene 0.00000025 mass %). The aqueous solubility of cycloalkanes, alkenes, and cycloalkenes is typically slightly higher than that of saturated hydrocarbons of similar molecular weight reflecting their slightly higher polarity.

Importantly, some of the mentioned physicochemical properties show a significant dependence on environmental parameters which have to be taken into account when evaluating the behavior of a specific compound. For example, boiling points show a strong pressure dependence, while viscosities strongly depend on temperature (Fig. 15). The phase behavior of hydrocarbon fluids (exclusive occurrence as gas or liquid or co-occurrence of both phases) in subsurface petroleum systems is governed by the given temperature-pressure regime. The aqueous solubility of hydrocarbons typically increases with increasing temperature but decreases with increasing salinity.

An environmentally highly relevant parameter of organic compounds is their octanol-water partition coefficient, which characterizes the distribution of a compound between 1-octanol (as a model phase for lipophilic compartments) and water phases which are in equilibrium. Increasing octanol-water partition coefficients as typically seen in homologous series of organic compounds (Fig. 17) indicate the increasingly lipophilic nature of these compounds. However, there is no specific threshold value for the octanol-water coefficient above which a compound is classified as a lipid. At a given carbon number, hydrocarbons but also halogenated

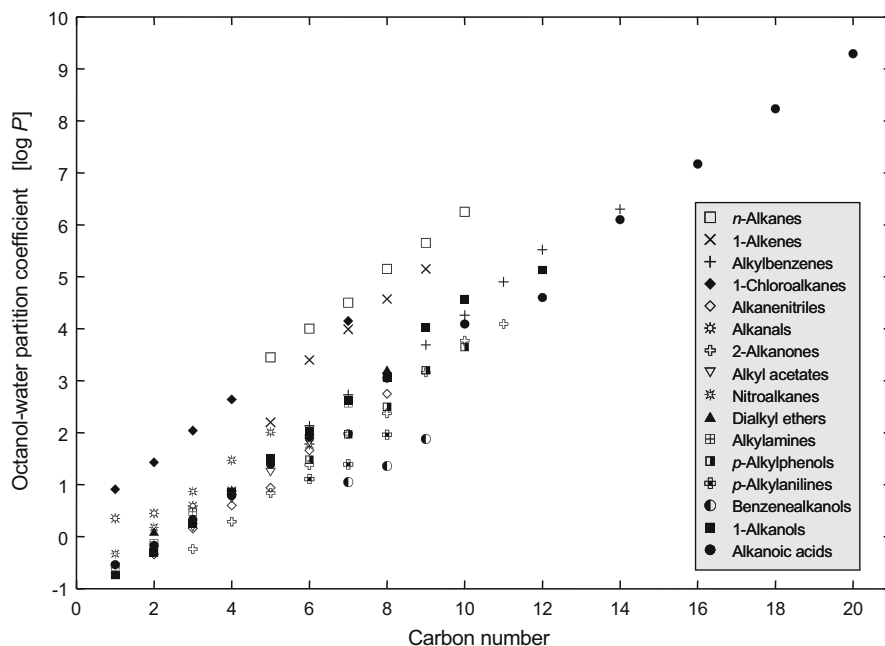


Fig. 17 Octanol-water partition coefficients versus carbon number for selected compound classes. Please note that log *P* is used in this plot. (All data are from Lide 2002)

organic compounds typically show higher octanol-water partition coefficients than (other) functionalized compounds. Octanol-water partition coefficients should be used cautiously when assessing the behavior of a compound in a natural environment. For example, crude oil-water partition coefficients determined for alkyl phenols (Taylor et al. 1997) differ significantly from the octanol-water partition coefficients of these compounds with respect to the differences between isomers. Analogously, Henry's law constant may be used to characterize the behavior of gases. According to Henry's law, the amount of a given gas dissolved in a given type and volume of liquid is directly proportional to the partial pressure of that gas in equilibrium with that liquid.

All physicochemical data used in this chapter were taken from the *Handbook of Chemistry and Physics* (Lide 2002) which represents a very useful source of information. In its Appendix B, it also provides a comprehensive compilation of sources of physical and chemical data including web-based resources. It should be noted that in addition to experimental determination of such data, modern tools of molecular modeling provide a complementary approach toward an improved understanding of the environmental behavior of hydrocarbons and other organic compounds.

6 Reactions

6.1 Reactions of Saturated Hydrocarbons

Saturated hydrocarbons (*n*-alkanes, branched alkanes, and cycloalkanes) contain exclusively σ -bonds but no (polar) functional groups. The difference in electronegativity of carbon (2.55) and hydrogen (2.20) is small; therefore C–H bonds are rather nonpolar. As a consequence, saturated hydrocarbons are quite unreactive or inert. The term *paraffin* in fact describes this lack of affinity in chemical reactions. Efficient, specific, and selective methods for C–H bond activation in nonreactive substrates can continuously be regarded as one of the great challenges in synthetic organic chemistry. Despite the enormous progress within the last decades in understanding the biochemical (enzymatic) mechanisms of C–H bond activation (e.g., Rabus et al. 2016) – as an integral component of any hydrocarbon oxidation pathway – new still undiscovered modes of C–H bond activation can potentially contribute to an forward-looking use of fossil fuel hydrocarbons beyond combustion.

Due to the lack of polar bonds in saturated hydrocarbons, reactions with polar species via heterolytic mechanisms are relatively unimportant. In fact, the main reactions of saturated hydrocarbons proceed via (free) radical species (= atomic or molecular species with unpaired electrons). Alkyl radicals may be generated from saturated hydrocarbons by a homolytic cleavage of a C–H or a C–C bond. This process requires significant amounts of energy, known as the homolytic bond dissociation energy (see Table 5 for homolytic C–H bond dissociation energies of saturated hydrocarbons). The amount of energy required is related to the stability of the formed radical which increases in the order primary < secondary < tertiary due

Table 5 Homolytic C–H bond dissociation energies of saturated hydrocarbons. (Data from McMillen and Golden 1982)

Hydrocarbon	Product radical	kJ mol^{-1}
Cyclopropane	Cyclopropyl-	445
Methane	Methyl-	440
2,2-Dimethylpropane	Neopentyl-	419
Ethane	Ethyl-	411
Propane	Propyl-	410
Methylcyclopropane	Cyclopropylmethyl-	408
Cyclobutane	Cyclobutyl-	404
<i>n</i> -Butane	<i>sec</i> -Butyl-	400
Cyclohexane	Cyclohexyl-	400
Propane	Isopropyl-	398
Cyclopentane	Cyclopentyl-	396
Isobutane	<i>tert</i> -Butyl-	390
Cycloheptane	Cycloheptyl-	387

to hyperconjugation. In other words, the homolytic cleavage of a terminal C–H bond in alkanes requires more energy than the homolytic cleavage of a subterminal C–H bond. This is a possible reason for the observation that *n*-alkane activation in anaerobic bacteria (via radical addition to the double bond of fumarate) takes place at the subterminal but not at the terminal carbon atom, despite the unfavorable fact that this introduces an additional branch into the initial activation product (Rabus et al. 2001).

Radicals may undergo a number of reaction types, including substitution, addition to double bonds, intramolecular rearrangement, and fragmentation. Radical halogenation is an important process in synthetic chemistry, in which haloalkanes are formed from alkanes and molecular halogen by substitution of a hydrogen atom by a halogen atom via radical intermediates. In the production of synthetic polymers (e.g., of polyethylene from ethene), the multiple steps of chain elongation can proceed via radical addition to the double bond of the respective unsaturated monomers. Addition of hydrocarbons to fumarate during their activation in anaerobic metabolism is thought to involve alkyl and arylalkyl radicals which can be formed from their parent hydrocarbon via homolytic cleavage of a C–H bond by glyceryl radical enzymes (e.g., Buckel and Golding 2006; Heider 2007). However, Jarling et al. (2012) identified the stereoisomers of (1-methylpentyl)succinate formed from anaerobic activation of *n*-hexane by an anaerobically cultivated bacterial strain, leading to the assumption that no alkyl radical intermediate but rather a concerted mechanism is involved in that reaction. Activation of toluene might still proceed via a benzyl radical (Szaleniec and Heider 2016; Seyhan et al. 2016).

Combustion denominates the complete oxidation of saturated hydrocarbons to carbon dioxide and water with oxygen being the other reactant. The overall process is a complex interplay of numerous types of chemical reactions in which diverse radical species are key players. Activated oxygen itself is a diradical, which forms various reactive intermediates such as hydroperoxide or hydroxyl radicals. Again homolytic cleavage yielding alkyl or aryl radicals is a key step in the activation of the

inert hydrocarbons to be converted to functionalized (oxygenated) species that can be further oxidized in subsequent reactions. Likewise, highly reactive oxygen species play a crucial role as co-substrates in the activation of hydrocarbons for aerobic biodegradation.

Radical reactions are also of major importance in the formation of fossil fuels, especially natural gas and crude oil. It is generally accepted that these petroleum fluids are formed via thermal breakdown of a geomacromolecule termed kerogen during deep burial of biogenic organic matter in sedimentary basins. As temperatures increase with burial depth, pyrolytic reactions, i.e., radical reactions, will lead to the fragmentation of larger structural moieties and the formation of low molecular weight organic compounds, predominantly hydrocarbons. Depending on the temperature-pressure regime and the geological history, secondary cracking through radical reactions leads to further processing of the original petroleum fluids, e.g., oil-to-gas cracking is a significant process in many petroleum systems (Schenk et al. 1997). There are controversial discussions as to which extent these processes are controlled by thermal or catalytic mechanisms (e.g., Mango 2000). Similar reactions are employed in the industrial reformation of crude oil.

6.2 Reactions of Unsaturated Hydrocarbons

Due to the minor relevance of alkynes as natural products or constituents of fossil fuels, only the reactivity of C–C double bonds is considered in this section. Alkenes undergo three main types of reactions, namely, addition to the double bond, oxidation, and polymerization. Polymerization of unsaturated hydrocarbons occurs in some plants, i.e., formation of natural rubber and gutta-percha from isoprene (Fig. 5). Polymerization of a wide range of unsaturated organic compounds (both hydrocarbons and non-hydrocarbons) via ionic or radical mechanisms is a key industrial process in the production of synthetic polymers.

Due to the π -electrons, C–C double bonds are characterized by an elevated electron density and act as nucleophiles in chemical reactions. Therefore, their most important reaction type is electrophilic addition in which the C–C double bond is converted to a C–C single bond by removal of the π -bond under concomitant formation of two new covalent σ -bonds (Fig. 18). In the first step a suitable

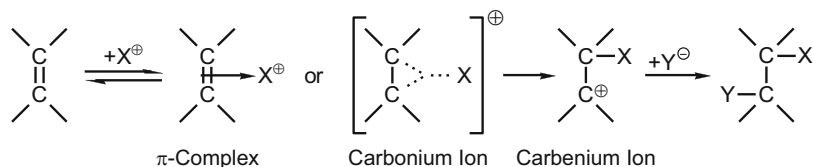


Fig. 18 General mechanism of electrophilic addition to C–C double bonds. Typical reactants X–Y that may be added to C–C double bonds in electrophilic addition reactions are molecular hydrogen (H–H), molecular halogen (F–F, Cl–Cl, Br–Br), hydrogen halide (H–Cl, H–Br, H–I), and water (H–OH)

electrophile, i.e., a species with an electron deficiency, typically a cation, forms a covalent bond with one of the two carbon atoms of the double bond, while the positive charge is located on the other carbon atom. In a second step, a neutral molecule is formed by connection of the originally formed cation to a nucleophile, i.e., a species with an electron surplus, typically an anion. A specific situation occurs if both reactants are unsymmetrical, e.g., two different products are possible from the addition of HCl to propene, namely, 1- and 2-chloropropane. In such cases the Markovnikov rule helps to predict the expected product distribution. According to the Markovnikov rule, the addition of the electrophile in the first step of the reaction occurs in a mode that the more stable carbenium ion (= trivalent carbocation) is formed preferentially. The stability of carbenium ions depends mainly on the extent of hyperconjugation of the unoccupied *p*-orbital with binding molecular orbitals of the substituents. As a general rule of thumb, in alkenes the electrophile will be connected to the carbon atom of the double bond with the higher number of hydrogen atoms because the stability of the formed carbenium ions decreases in the order tertiary > secondary > primary due to the stabilization by hyperconjugation with C–H or C–C bonds of the adjacent alkyl groups. Many electrophilic additions are reversible, i.e., alkenes (or unsaturated organic compounds) may be formed by suitable elimination reactions.

Beside combustion which completely oxidizes unsaturated hydrocarbons (in analogy to saturated hydrocarbons) to carbon dioxide and water, various reactions with different types of oxygenating reagents are known that yield specific products. Catalytic oxidation with oxygen or the reaction with percarboxylic acids yields epoxides which can be ring-opened to vicinal *trans*-diols by acid-catalyzed hydrolysis. The reaction of alkenes with osmium tetroxide on the other hand yields vicinal *cis*-diols. Ozonolysis, i.e., the reaction of alkenes with ozone, produces either ketones/aldehydes upon reductive work-up or ketones/carboxylic acids upon oxidative work-up depending on the structure of the alkene. In the case of cycloalkenes with a double bond in the ring system, diketones, dialdehydes, or oxoaldehydes are formed.

It should be noted that these reactions of double bonds do not form new C–C bonds and therefore are not directly useful for (bio)synthesis of more complex carbon skeletons. However, they are very suitable for introducing functional groups. Thus, most of the synthetic reactions have enzymatic analogues which play important roles in many metabolic pathways. Hydrogenation of C=C double bonds is a step in the biosynthesis of fatty acids. Hydration of C=C double bonds occurs in the TCA cycle (transformation of *cis*-aconitate to isocitrate and of fumarate to malate) and in β -oxidation of fatty acids.

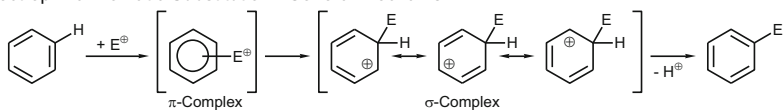
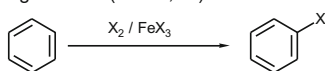
Various examples illustrate the relevance of oxidation of C=C double bonds for activation and further metabolism of alkenes and aromatic hydrocarbons. Alkene monooxygenase catalyzes the transformation of propene to 1,2-epoxypropane, the first step in the aerobic metabolism of this hydrocarbon. Epoxidation of C=C double bonds plays a key role in biosynthetic pathways, e.g., squalene-2,3-epoxide formed from the hydrocarbon squalene (Fig. 5) is a central intermediate in biosynthesis of steroids and triterpenoids.

Similar monooxygenase-catalyzed reactions may also be involved in the aerobic transformation/activation of aromatic hydrocarbons. Such transformations formally are epoxidations of one specific double bond in a “cyclohexa-1,3,5-triene” moiety (rather than a reaction of an aromatic system) although the reaction has to overcome the aromatic resonance stabilization. The resulting arene oxides may be rearranged to phenols (NIH-shift) or attacked by nucleophiles; an example of the latter is the stereospecific ring opening of arene oxides to *trans*-cyclohexa-3,5-diene-1,2-diol moieties. Likewise, the activation of aromatic hydrocarbons by dioxygenases resembles the synthesis of vicinal *cis*-diols from alkenes using osmium tetroxide. The assumed initial step is the addition of dioxygen to one specific double bond of a “cyclohexa-1,3,5-triene” moiety; the resulting 1,2-dioxetane is hydrogenated in a NADH-dependent reaction to form a *cis*-cyclohexa-3,5-diene-1,2-diol moiety. Intra- and extra-diol (*ortho*- and *meta*-) ring cleavage in the further aerobic metabolism of catechols oxidize double bonds in a way which to a certain extent is similar to the reaction of alkenes with ozone.

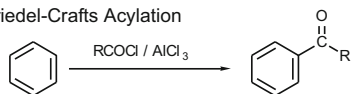
6.3 Reactions of Aromatic Hydrocarbons

The most important reaction of aromatic hydrocarbons is electrophilic aromatic substitution, where the hydrocarbon reacts as a nucleophile due to the high electron density on the aromatic ring. In electrophilic aromatic substitution, one hydrogen atom of the aromatic hydrocarbon is substituted by a functional group (Fig. 19a). The first step in the reaction mechanism is the formation of a π -complex through the interaction of an electrophile with the π -electron system. The π -complex is then converted to a σ -complex in which the σ -bond between the electrophile and a carbon atom of the aromatic ring already exists. The reaction is completed by removal of the hydrogen that is substituted as a proton. Classical electrophilic aromatic substitutions are halogenation, nitration, sulfonation, and Friedel-Crafts acylation and alkylation (Fig. 19b).

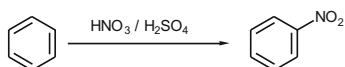
It is important to note that substituents in aromatic molecules have a significant effect on the course of electrophilic aromatic substitutions in a twofold manner. Firstly, they may either activate or deactivate the aromatic system for subsequent reactions (Fig. 19c, Table 6). The ability of substituents to activate or deactivate an aromatic compound with respect to an electrophilic attack depends on their ability to increase or decrease the electron density on the aromatic ring by inductive or resonance effects. Benzene derivatives containing deactivating substituents such as chlorobenzene or nitrobenzene react significantly slower in electrophilic substitutions than benzene, while derivatives containing activating substituents such as toluene or phenol react significantly faster. Therefore, the introduction of oxygen substituents is an important mechanism of biological activation of aromatic hydrocarbons for further metabolism. Secondly, substituents have a directing influence on the regioselectivity of subsequent reactions (Table 6). *Ortho*-/*para*-directors typically are substituents with unshared electron pairs such as the hydroxy group in phenol which support the attack of electrophiles in the *o*- and *p*-position by

a Electrophilic Aromatic Substitution: General Mechanism**b** Halogenation (X = Cl, Br)

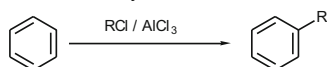
Friedel-Crafts Acylation



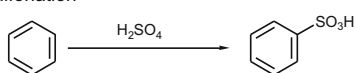
Nitration



Friedel-Crafts Alkylation



Sulfonation



Alkylation with Alkenes

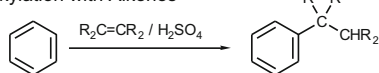
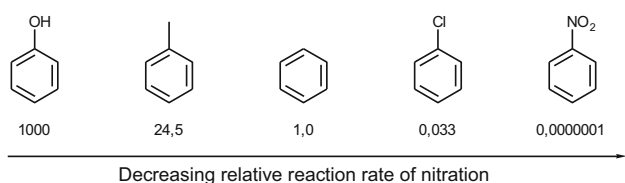
**c** Reactivity

Fig. 19 (a) General mechanism of electrophilic aromatic substitution. (b) Selected examples. (c) The activating or deactivating influence of substituents on the reactivity compared to that of benzene is illustrated for nitration of different benzene derivatives

Table 6 Classification of substituents with respect to their effects on electrophilic aromatic substitution

	<i>o</i> -/ <i>p</i> -directing		<i>m</i> -directing	
Activating	-NH ₂ , -NHR, -NR ₂	Amino-		
	-OH, -OR	Hydroxy-, Alkoxy-		
	-NHCOR	Acylamino-		
	-R	Alkyl-		
Deactivating	-F, -Cl, -Br, -I	Halogen-	-COR, CO ₂ H	Acyl-, carboxy-
			-CONH ₂ , -CO ₂ R	Carboxamido-, carboalkoxy-
			-SO ₃ H	Sulfonic acid
			-CN	Cyano-
			-NO ₂	Nitro-

resonance stabilization of the intermediate σ -complexes. The *o*-/*p*-directing effect of alkyl substituents is best explained by hyperconjugation. Sterical effects are most important for observed deviations from the statistical distribution (2:1) of *o*- and *p*-products. *Meta*-directors such as the nitro group destabilize the σ -complexes formed by attack of an electrophile in *o*- and *p*-position due to resonance structures with positive (partial) charges on adjacent atoms; therefore, the reaction in *meta* position is favored.

Aromatic molecules may also react with nucleophiles; however, such reactions are not typical for aromatic hydrocarbons, i.e., the nucleophilic substitution of hydrogen in aromatic compounds is uncommon. Important mechanisms of reactions with nucleophiles are the substitution of suitable leaving groups such as chloride, bromide, or sulfite via an addition-elimination mechanism (similar to electrophilic aromatic substitution) or the attack of the nucleophile on a free aryl cation that has been generated by elimination of nitrogen from an aryl diazonium salt. Some substitution reactions proceed via addition of nucleophiles to arynes (e.g., 1,2-dehydrobenzene) generated from suitable aromatic substrates by the removal of two *o*-substituents. Nucleophilic substitution plays a role in coupling reactions such as the Ullmann reaction used to synthesize biaryls.

Homolytic cleavage of aromatic C–H bonds is energetically unfavorable (the homolytic C–H bond dissociation energy to form the phenyl radical from benzene is as high as 464 kJ mol⁻¹; McMillen and Golden 1982). Therefore reactions of aromatic molecules via free aryl radical intermediates are not very common. An interesting reaction involving aryl radicals is the hydroxylation of benzene to phenol by Fenton's reagent. Fenton's reagent, a solution of hydrogen peroxide and an iron catalyst which generates hydroxyl and hydroperoxide radicals as reactive species, is used to oxidize contaminants and wastewater.

Aromatic hydrocarbons may be catalytically hydrogenated to the corresponding cycloalkanes at high temperature and pressure. Reactions of aromatic hydrocarbons leading to a partial reduction of the aromatic ring are rare because of the high resonance energy. In fact, cyclohexa-1,3-diene and cyclohexa-1,4-diene (Fig. 5) are excellent hydrogen donors in transfer hydrogenation as they readily oxidize to benzene. The reduction of benzene to cyclohexa-1,4-diene with sodium and an alcohol in liquid ammonia is known as the Birch reduction. Likewise, naphthalene may be reduced under these conditions to 1,4,5,8-tetrahydronaphthalene (Fig. 5). The Birch reaction proceeds via alternating single electron- and proton-transfer steps to the aromatic ring. It is assumed that the enzymatic reduction of benzoyl-CoA, a key step in anaerobic metabolism of aromatic compounds, proceeds via a Birch-like mechanism, although the product is a conjugated 1,3-diene but not a nonconjugated 1,4-diene (Boll et al. 2002; Thiele et al. 2008). It is worth mentioning that hydrocarbons with a cyclohexa-1,3- or -1,4-diene moiety occur as natural products, e.g., α - and γ -terpinene (Fig. 5); however, biosynthesis does *not* proceed via reduction of the corresponding aromatic hydrocarbon *p*-cymene which is a common constituent of essential oils.

6.4 Specific Reactions of Functionalized Organic Compounds

Since functional groups influence dramatically the polarity in organic molecules, these moieties are likewise primary regions of chemical reactivity. Reactions leading to their exchange are predominantly substitution reactions. Nucleophilic substitution is of great relevance for functional groups in which more electronegative heteroatoms shift off negative electronic charge from the attached carbon atoms; in nucleophilic substitution reactions, the nucleophilic agents primarily attack these carbon atoms. Typical nucleophiles are anions or agents with atoms exhibiting free electron pairs such as ammonium and amines, halides, hydroxide ions, alkoxylates, and sulfur analogues. Important nucleophilic substitution reactions are, for example, the conversion of alcohols to halides, the methylation of alcohols generating methyl ethers or the alkylation of primary amines to form secondary or tertiary derivatives. Depending on the number of reactants involved in the rate determining step of substitution reactions (one or two), a mono- and bimolecular reaction mechanism has to be distinguished. Beside kinetic effects these mechanistic differences have implications for the stereochemistry of the substitution product. In monomolecular substitutions (S_N1), a triplanar ionic transition state is attacked in the second reaction step from two sides or directions leading to racemization in the case of prochiral compounds. On the contrary, a bimolecular reaction (S_N2) proceeds via a fixed bipyramidal structure of the intermediate and thus results in the inversion of the stereochemistry.

Note that nucleophilic substitutions are not restricted to the exchange of functional groups but are also useful tools to link individual molecules via heteroatoms. For example, ether bridges are generated by the nucleophilic attack of alkoxy ions on appropriate substrates; they are key structural elements in archaeal and bacterial lipids (isoprenoidal and non-isoprenoidal glycerol diethers). The inverse reaction in which the ether bond cleavage is typically initiated by strong Lewis acids also ranks among nucleophilic substitutions. A specific reaction type, in which solely functionalized molecules are involved is the condensation. This important reaction type is characterized by the linkage of two functional groups leading to a larger product molecule accompanied by the release of a second small-sized molecule. This second product is typically a thermodynamically highly stable compound (H_2O , HCl , or similar), whose generation represents the propulsion of the reaction. Basically, condensation reactions are a subcategory of substitution reactions. Essential condensation reactions are performed by carboxylic groups with alcohols and amines forming esters and amides. These condensation reactions are used not only to build up dimers (e.g., aspartame) but also (in case of polyfunctionalized molecules) to form oligomers (e.g., valinomycin) or natural as well as xenobiotic polymers (e.g., proteins, suberins, nylon). Beside intermolecular reactions, also intramolecular substitution and condensation are realized abundantly. In particular, for oxygen-containing compounds, the formation of (a) cyclic ethers via nucleophilic substitution, (b) cyclic acetals and hemiacetals via addition/condensation, or (c) esters via condensation are important modes of transformation.

As a result of heteroatom functionalization, the state of oxidation at the affected carbon atoms may change. By introducing a more electronegative binding partner or more bonds to heteroatoms, the oxidation state shifts to a more positive value as the result of depleted electron density at the carbon atom. Reactions leading to increasing oxidation states are oxidation reactions; the inverse reactions are reduction reactions. Oxidation and reduction are not limited to carbon atoms since heteroatoms also exhibit different oxidation states. Essential oxidation reactions are the sequential transformation of primary alcohols to carboxylic acids via aldehydes as exemplified in the initial steps of the aerobic degradation pathway of citronellol forming citronellic acid. In this reaction sequence, two new carbon-oxygen bonds are introduced shifting the oxidation state of the involved carbon atom.

References

- Allred AL (1961) Electronegativity values from thermochemical data. *J Inorg Nucl Chem* 17:215–221
- Ballschmiter K (2003) Pattern and sources of naturally produced organohalogens in the marine environment: biogenic formation of organohalogens. *Chemosphere* 52:313–324
- Ballschmiter K, Schäfer W, Buchert H (1987) Isomer-specific identification of PCB congeners in technical mixtures and environmental samples by HRGC-ECD and HRGC-MSD. *Fresenius J Anal Chem* 326:253–257
- Boll M, Fuchs G, Heider J (2002) Anaerobic oxidation of aromatic compounds and hydrocarbons. *Curr Opin Chem Biol* 6:604–611
- Brown RJC, Brown RFC (2000) Melting point and molecular symmetry. *J Chem Educ* 77:724–731
- Buckel W, Golding BT (2006) Radical enzymes in anaerobes. *Annu Rev Microbiol* 60:27–49
- Curiale JA, Frolov EB (1998) Occurrence and origin of olefins in crude oils. A critical review. *Org Geochem* 29:397–408
- Dahl JE, Moldowan JM, Peters KE, Claypool GE, Rooney MA, Michael GE, Mello MR, Kohnen ML (1999) Diamondoid hydrocarbons as indicators of natural oil cracking. *Nature* 399:54–57
- Dahl JE, Liu SG, Carlson RMK (2003a) Isolation and structure of higher diamondoids, nanometer-sized diamond molecules. *Science* 299:96–99
- Dahl JEP, Moldowan JM, Peakman TM, Clardy JC, Lobovsky E, Olmstead MM, May PW, Davis TJ, Steeds JW, Peters KE, Pepper A, Ehkuan A, Carlson RMK (2003b) Isolation and structural proof of the large diamond molecule, cyclohexamantane (C₂₆H₃₀). *Angew Chem* 115:2086–2090
- de Boer J, de Boer K, Boon JP (2000) Polybrominated biphenyls and diphenyl ethers. In: Paasivirta J (ed) *The handbook of environmental chemistry, vol 3. Anthropogenic compounds, Part K*. Springer, Berlin, pp 61–96
- Favre HA, Powell WH (2013) *Nomenclature of organic chemistry. IUPAC recommendations and preferred name 2013*. The Royal Society of Chemistry, Cambridge
- Ficken KJ, Li B, Swain DL, Eglinton G (2000) An n-alkane proxy for the sedimentary input of submerged/floating freshwater aquatic macrophytes. *Org Geochem* 31:745–749
- Fiedler H (1996) Sources of PCDD/PCDF and impact on the environment. *Chemosphere* 32:55–64
- Fleming FF (1999) Nitrile-containing natural products. *Nat Prod Rep* 16:597–606
- Francke W, Schulz S (1998) Pheromones. In: Mori K (ed) *Comprehensive natural products chemistry, vol 8*. Pergamon, Oxford, pp 197–261
- Gribble GW (1994) The natural production of chlorinated compounds. *Environ Sci Technol* 28:310A–319A
- Gribble GW (2000) The natural production of organobromine compounds. *Environ Sci Pollut Res* 7:37–49

- Grice K, Alexander R, Kagi RI (2000) Diamondoid hydrocarbon ratios as indicators of biodegradation in Australian crude oils. *Org Geochem* 31:67–73
- Hall C, Tharakan P, Hallock J, Cleveland C, Jefferson M (2003) Hydrocarbons and the evolution of human culture. *Nature* 426:318–322
- Hebting Y, Schaeffer P, Behrens A, Adam P, Schmitt G, Schneckenburger P, Bernasconi SM, Albrecht P (2006) Biomarker evidence for a major preservation pathway of sedimentary organic carbon. *Science* 312:1627–1631
- Heider J (2007) Adding handles to unhandy substrates: anaerobic hydrocarbon activation mechanisms. *Curr Opin Chem Biol* 11:188–194
- Hinrichs K-U, Hayes JM, Bach W, Spivack AJ, Hmelo LR, Holm NG, Johnson CG, Sylva SP (2006) Biological formation of ethane and propane in the deep marine subsurface. *Proc Natl Acad Sci U S A* 103:14684–14689
- Jarling R, Sadeghi M, Drozdowska M, Lahme S, Buckel W, Rabus R, Widdel F, Golding BT, Wilkes H (2012) Stereochemical investigations reveal the mechanism of the bacterial activation of n-alkanes without oxygen. *Angew Chem Int Ed* 51:1334–1338
- Lide DR (2002) CRC handbook of chemistry and physics, 83rd edn. CRC Press, Boca Raton. 2002–2003
- Mango FD (2000) The origin of light hydrocarbons. *Geochim Cosmochim Acta* 64:1265–1277
- Marynowski L, Czechowski F, Simoneit BRT (2001) Phenylanthracenes and polyphenyls in Palaeozoic source rocks of the Holy Cross Mountains, Poland. *Org Geochem* 32:69–85
- McMillen DF, Golden DM (1982) Hydrocarbon bond dissociation energies. *Annu Rev Phys Chem* 33:493–532
- McNaught AD, Wilkinson A (1997) Compendium of chemical terminology, 2nd ed. (the “Gold Book”). Blackwell Scientific Publications, Oxford
- Peters KE, Walters CC, Moldowan JM (2005) The biomarker guide. Cambridge University Press, Cambridge/New York
- Portella G, Poater J, Solà M (2005) Assessment of Clar’s aromatic pi-sextet rule by means of PDI, NICS and HOMA indicators of local aromaticity. *J Phys Org Chem* 18:785–791
- Rabus R, Wilkes H, Behrens A, Armstroff A, Fischer T, Pierik AJ, Widdel F (2001) Anaerobic initial reaction of n-alkanes in a denitrifying bacterium: evidence for (1-methylpentyl)succinate as initial product and for involvement of an organic radical in n-hexane metabolism. *J Bacteriol* 183:1707–1715
- Rabus R, Boll M, Heider J, Meckenstock RU, Buckel W, Einsle O, Ermler U, Golding BT, Gunsalus RP, Kroneck PMH, Krüger M, Lueders T, Martins BM, Musat F, Richnow HH, Schink B, Seifert J, Szaleniec M, Treude T, Ullmann GM, Vogt C, von Bergen M, Wilkes H (2016) Anaerobic microbial degradation of hydrocarbons: from enzymatic reactions to the environment. *J Mol Microbiol Biotechnol* 26:5–28
- Randic M (2003) Aromaticity of polycyclic conjugated hydrocarbons. *Chem Rev* 103:3449–3606
- Schenk HJ, Horsfield B, Krooss B, Schaefer RG, Schwochau K (1997) Kinetics of petroleum formation and cracking. In: Welte DH, Horsfield B, Baker DR (eds) Petroleum and basin evolution. Springer, Berlin, pp 231–269
- Schneider-Belhaddad F, Kolattukudy P (2000) Solubilization, partial purification, and characterization of a fatty aldehyde decarboxylase from a higher plant, *Pisum sativum*. *Arch Biochem Biophys* 377:341–349
- Schoell M (1980) The hydrogen and carbon isotopic composition of methane from natural gases of various origins. *Geochim Cosmochim Acta* 44:649–661
- Seyhan D, Friedrich P, Szaleniec M, Hilberg M, Buckel W, Golding BT, Heider J (2016) Elucidating the stereochemistry of enzymatic benzylsuccinate synthesis with chirally labeled toluene. *Angew Chem Int Ed* 55:11664–11667
- Sinninghe Damsté JS, Strous M, Rijpstra WIC, Hopmans EC, Geenevasen JAJ, van Duin ACT, van Niftrik LA, Jetten MSM (2002) Linearly concatenated cyclobutane lipids form a dense bacterial membrane. *Nature* 419:708–712
- Staudinger H, Ruzicka L (1924) Insektentötende Stoffe I. Über Isolierung und Konstitution des wirksamen Teiles des dalmatinischen Insektenpulvers. *Helv Chim Acta* 7:177–201

- Szaleniec M, Heider J (2016) Modeling of the reaction mechanism of enzymatic radical C-C coupling by benzylsuccinate synthase. *Int J Mol Sci* 17:514
- Taylor P, Larter S, Jones M, Dale J, Horstad I (1997) The effect of oil-water-rock partitioning on the occurrence of alkylphenols in petroleum systems. *Geochim Cosmochim Acta* 61:1899–1910
- Thiele B, Rieder O, Golding BT, Müller M, Boll M (2008) Mechanism of enzymatic birch reduction: stereochemical course and exchange reactions of benzoyl-CoA reductase. *J Am Chem Soc* 130:14050–14051
- Xie S, Lazar CS, Lin Y-S, Teske A, Hinrichs K-U (2013) Ethane- and propane-producing potential and molecular characterization of an ethanogenic enrichment in an anoxic estuarine sediment. *Org Geochem* 59:37–48
- Yunker MB, MacDonald RW, Vingarzan R, Mitchell RH, Goyette D, Sylvestre S (2002) PAHs in the Fraser River basin: a critical appraisal of PAH ratios as indicators of PAH source and composition. *Org Geochem* 33:489–515



Introduction to Oil Chemistry and Properties Related to Oil Spills

2

Merv Fingas

Contents

1	Introduction	50
2	The Composition of Oil	50
2.1	SARA	51
2.2	Sulfur Compounds	58
2.3	Oxygen Compounds	66
2.4	Nitrogen Compounds	69
2.5	Metals	70
2.6	Resins	73
2.7	Asphaltenes	73
3	Properties of Oil	74
3.1	Oils with High Densities Have Low API Gravities and Vice Versa	76
4	Research Needs	77
	References	78

Abstract

This chapter is a review of petroleum chemistry particularly as it relates to oil spills. The traditional separation of saturates, aromatics, resins, and asphaltenes (SARA) oil components is summarized. Details on these groupings and many compounds within the groupings and, where available, the typical amounts found in some oils are given. A detailed look at compounds found in oil and the amount of these is presented. The compounds are related to the overall composition and the SARA composition. Details of more than 500 compounds will be given in the chapter.

M. Fingas (✉)
Spill Science, Edmonton, AB, Canada
e-mail: fingasmerv@shaw.ca

© Springer Nature Switzerland AG 2020
H. Wilkes (ed.), *Hydrocarbons, Oils and Lipids: Diversity, Origin, Chemistry and Fate*,
Handbook of Hydrocarbon and Lipid Microbiology,
https://doi.org/10.1007/978-3-319-90569-3_29

The composition can be related to bulk properties and bulk composition. Examples of bulk composition and relation to properties are given.

1 Introduction

Oil is a general term that describes a wide variety of natural substances of plant, animal, or mineral origin and a range of synthetic compounds. This chapter covers crude oil and petroleum products derived from such oils. Crude oils are made up of hundreds of major constituents and thousands of minor ones. As their composition varies, each type of oil or petroleum product has certain unique characteristics or properties. These properties influence how the oil behaves when it is spilled and subsequently determines the fate and effects of the oil in the environment. Oil properties strongly influence the efficiency of cleanup operations.

2 The Composition of Oil

Crude oils are complex mixtures of hydrocarbons and organic compounds containing other elements ranging from smaller, volatile compounds to very large, nonvolatile compounds (Fingas 2011). The mixture of compounds varies with the geological formation of the area in which the crude oil is found. Crude oils are often similar in a given region and when drawn from a similar reservoir. Petroleum products such as gasoline and diesel fuel are mixtures of fewer compounds and are refined to specific standards. Thus, their properties are more specific and less variable. Crude oil contains many compounds of different sizes and different classes. In fact, there are so many that, as time goes by, more and more compounds are identified in oil. Analysts have preliminarily identified up to 17,500 compounds in an oil (Kinghorn 1983). At this time, about 100,000 are identified.

Hydrocarbon compounds are composed of hydrogen and carbon, which are the main elements in oils. Oils also contain varying amounts of sulfur, nitrogen, oxygen, and trace metals such as nickel, vanadium, and chromium. This section will detail some of these compounds. In general, the hydrocarbons found in oils are characterized by their structures.

A common and older method of classification is by SARA – saturates, aromatics, resins, and asphaltenes. Table 1 illustrates the SARA classification along with classes of compounds typically found in this overall classification. The saturate group of components in oils consists primarily of alkanes, which are compounds of hydrogen and carbon with the maximum number of hydrogen atoms around each carbon atom. Thus, the term saturate is used because the carbon atoms are saturated with hydrogen atoms. The saturate group includes straight-chain alkanes and branched-chain alkanes and also includes cycloalkanes, which are compounds made up of the same carbon and hydrogen constituents, but with the carbon atoms

Table 1 Illustration of SARA and compound classes in oils

Groupings	Chemical class	Alternate name	Description	Example compound
Saturates	Alkanes	Paraffins	C ₁₈ -C ₈₀ <i>n</i> -alkanes are designated as waxes	Dodecane
	Cycloalkanes	Naphthenes		Decalin
Aromatics	BTEX		Benzene, toluene, ethylbenzene, <i>o</i> -, <i>m</i> - and <i>p</i> -xylene	Benzene
	PAHs			Anthracene
	Naphthenoaromatics		Combinations of aromatics and cycloalkanes	Tetralin
Resins			Class of mostly polar compounds typically containing nitrogen, sulfur, oxygen, or metals	Carbazole
Asphaltenes			Class of large non-hydrocarbon compounds containing nitrogen, sulfur, oxygen, or metals	Exact structures Not known

Table 2 Elemental composition of oil

Element	Contents (%)
Carbon	83–87
Hydrogen	10–14
Nitrogen	0.05–6
Sulfur	0.1–2
Oxygen	0.05–1.5

bonded to each other in rings. Straight-chain saturate compounds from C₁₈ and up are often referred to as waxes.

The elemental composition of oil is sometimes of interest. Crude oils have a typical composition as shown in Table 2 (Speight 2015).

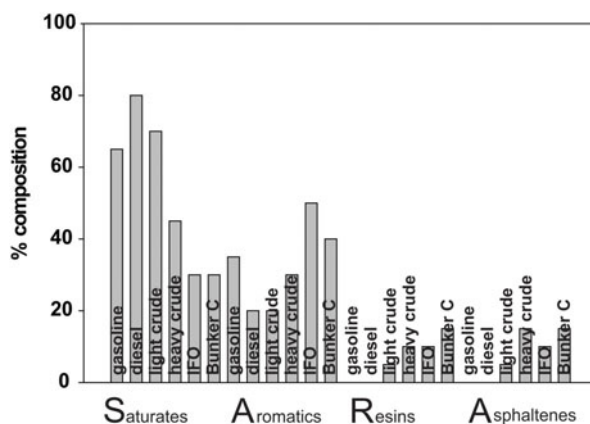
2.1 SARA

The saturates, aromatics, resins, and asphaltenes (SARA) composition of oil is a more general analytical method which defines oils by precipitation and then by weight. Newer methods now employ thin-layer chromatography, and the values from both methods vary somewhat. This method is still useful however, and it provides useful data both to the refiner and to the environmentalist. Table 1 illustrates the typical compositions designated by SARA and some example compounds. Table 3 shows the gross composition of some typical oils and petroleum products. It is noted that the ranges of these compositions vary widely. Saturates are hydrocarbon compounds with the maximum number of hydrogen atoms. Aromatics are hydrocarbon compounds with at least one benzene ring. Resins and asphaltenes are

Table 3 Typical composition of some oils and petroleum products in % except for metals which are given in ppm

Group	Compound class	Gasoline	Diesel	Light crude	Heavy crude	IFO ^a	Bunker C
Saturates		50–60	65–95	55–90	25–80	25–35	20–30
	Alkanes	45–55	35–45	40–85	20–60	10–25	10–20
	Cycloalkanes	5	25–50	5–35	0–10	0–5	0–5
Olefins		5–10	0–10				
Aromatics		25–40	5–25	10–35	15–40	40–60	30–50
	BTEX	15–25	0.5–2.0	0.1–2.5	0.01–2.0	0.05–1.0	0.00–1.0
	PAHs		0–5	10–35	15–40	30–50	30–50
Polar compounds			0–2	1–15	5–40	15–25	10–30
	Resins		0–2	0–10	2–25	10–15	10–20
	Asphaltenes			0–10	0–20	5–10	5–20
Sulfur		0.02	0.1–0.5	0–2	0–5	0.5–20	2–4
Metals				30–250	100–500	100–1000	100–2000

^aIFO is intermediate fuel oil which is residual fraction diluted by diesel fractions

Fig. 1 An illustration of the typical amounts of SARA in various oils and fuel

larger compounds containing mostly carbon and hydrogen, but containing other elements such as oxygen, sulfur, nitrogen, and metals.

Figure 1 shows the SARA composition of some typical oils and petroleum products. It can be seen that SARA content varies widely for the various products. The products illustrated in Fig. 1 are gasoline, diesel fuel, a light crude oil, a heavy crude oil, IFO (intermediate fuel oil), and Bunker C. These represent a large cross section of oils and petroleum products and serve to illustrate the broad spectrum of hydrocarbon liquids.

2.1.1 Saturates

As noted in the general discussion on SARA, saturates are important economical constituents of oils. Saturates are often the most abundant compounds in any oil or petroleum product. Saturates are so-called because they are compounds containing the maximum number of hydrogen atoms and thus are saturated with hydrogen.

2.1.2 Alkanes

Alkanes, an important part of saturate composition, are hydrocarbons with a chain-like structure and without double bonds or atoms of other elements such as sulfur, nitrogen, or oxygen attached (Neumann et al. 1981). Alkanes, sometimes called paraffins, are typically the most abundant compounds in crude oils as well as in most fuels such as diesel fuel and gasoline. Most crude oils have anywhere between a few percent up to 30% alkanes. Alkanes are typically the target compounds sought by petroleum producers. It should be noted, however, that larger alkanes are also called waxes, and these are sometimes less desirable from a petroleum producer's point of view.

Normal alkanes are those which are unbranched. All normal and branched alkanes have the generalized molecular formula of C_nH_{n+2} where n is the number of carbon atoms present. All alkanes are saturated, that is, they contain the most hydrogen that the configuration can have. The branching potential for alkanes increases as the size of the alkane increases. Table 4 shows the typical alkanes contained in crude oils and some fuels (Wang et al. 1993; 2003; CRC 2016–2017; Yalkowsky et al. 2010; Mackay et al. 1992; Verchueren 2001; Faksness et al. 2010; Wang and Brown 2008). Some properties and content of n -alkanes in some crude oils are also shown in this table. Figure 2 shows the structural isomers possible for C_6H_{14} (n -hexane, 2- and 3-methylpentane, 2,2- and 2,3-dimethylbutane), as an example of the diversity of branched alkanes. The column in Table 4 indicating the number of isomers shows the possible number of branched compounds. As can be seen in this table, the number of possible branched compounds rises to over one million by the time that carbon atom number 22 is reached. In fact, it is impossible to separate most branched compounds during chemical analysis. Thus, the specific nature of branched compounds in crude oils may be unknown for some time to come.

Table 5 shows the known subdivisions of the SARA contents. Table 5 shows that the n -alkanes typically account for about 10% of the saturates. It is suspected that the branched alkanes account for about two to five times that amount and that the cycloalkanes may account for about the same amount as the n -alkanes. Much more analytical work is required to adequately describe the detailed composition of oil.

2.1.3 Cycloalkanes

Cycloalkanes, compounds containing rings or cyclic structural moieties, are also saturated alkanes. These are sometimes called naphthenes. Monocyclic alkanes have the general formula C_nH_{2n} . Typical base structures for cycloalkanes are shown in Fig. 2 (cyclopentane, cyclohexane, decalin). These base structures contribute to the

Table 4 *n*-Alkanes found in oils and petroleum

Carbon number	Number of isomers	Formula	IUPAC name	Molecular weight	CAS number	Solubility in water ^a g/L	Ref.
5	3	C ₅ H ₁₂	Pentane	72.149	109-66-0	3.9E ⁻²	1
6	5	C ₆ H ₁₄	Hexane	86.175	110-54-3	~0.01	2
7	9	C ₇ H ₁₆	Heptane	100.202	142-82-5	~0.003	2
8	18	C ₈ H ₁₈	Octane	114.229	111-65-9	0.7E ⁻³	2
9	35	C ₉ H ₂₀	Nonane	128.255	111-84.2	1.2E ⁻⁴	1
10	75	C ₁₀ H ₂₂	Decane	142.282	124-18-5	~5E ⁻⁵	1
11	159	C ₁₁ H ₂₄	Undecane	156.309	1120-21-4	~6E ⁻⁶	1
12	355	C ₁₂ H ₂₆	Dodecane	170.334	112-40-3	~2E ⁻⁶	1
13	802	C ₁₃ H ₂₈	Tridecane	184.361	629-50-5	~4E ⁻⁷	1
14	1858	C ₁₄ H ₃₀	Tetradecane	198.388	629-59-4	~3E ⁻⁷	1
15	4347	C ₁₅ H ₃₂	Pentadecane	212.415	629-62-9	~4E ⁻⁸	1
16	1.04E+04	C ₁₆ H ₃₄	Hexadecane	226.441	544-76-3	<6E ⁻⁶	1
17	2.49E+04	C ₁₇ H ₃₆	Heptadecane	240.468	629-78-7		
18	6.05E+04	C ₁₈ H ₃₈	Octadecane	254.495	593-45-3	5.8E ⁻⁶	1
19	1.48E+05	C ₁₉ H ₄₀	Nonadecane	268.521	629-92-5		
20	3.66E+05	C ₂₀ H ₄₂	Icosane	282.547	112-95-8		
21	9.11E+05	C ₂₁ H ₄₄	Henicosane	296.574	629-94-7		
22	2.28E+06	C ₂₂ H ₄₆	Docosane	310.600	629-97-0		
23	5.73E+06	C ₂₃ H ₄₈	Tricosane	324.627	638-67-5		
24	1.45E+07	C ₂₄ H ₅₀	Tetracosane	338.654	646-31-1		
25	3.68E+07	C ₂₅ H ₅₂	Pentacosane	352.681	629-99-2		
26	9.38E+07	C ₂₆ H ₅₄	Hexacosane	366.707	630-01-3		

(continued)

Table 4 (continued)

Carbon number	Number of isomers	Formula	IUPAC name	Molecular weight	CAS number	Solubility in water ^a g/L	Ref.
27	2.40E+08	C ₂₇ H ₅₆	Heptacosane	380.734	593-49-7		
28	6.17E+08	C ₂₈ H ₅₈	Octacosane	394.761	630-02-4		
29	1.59E+09	C ₂₉ H ₆₀	Nonacosane	408.786	630-03-5		
30	4.11E+09	C ₃₀ H ₆₂	Triacotane	422.813	638-68-6		

^aApproximate sign ~ indicates solubility values are variable

1 Yalkowsky et al. (2010)

2 Verschuere (2001)

majority of the cycloalkanes found in oil. The smaller cycloalkanes such as cyclopropane and cyclobutane are not common because they are not as stable as the smaller-ring carbon bonds which have considerable ring strain, being stretched above the normal carbon-carbon tetrahedral angle of 109°. Cycloalkanes with more than one side chain may exist as stereoisomers (e.g., *cis*- and *trans*-isomers). Some cycloalkanes found in oils are shown in Table 6. Because cycloalkanes are low in abundance and may be difficult to separate in chromatographic analysis, there is not much data on their abundance in oils.

2.1.4 Alkenes or Olefins

The olefins, or unsaturated compounds, are another group of compounds that contain less hydrogen atoms than the maximum possible. Olefins have at least one carbon-to-carbon double bond which displaces two hydrogen atoms. Significant amounts of olefins are found only in refined products; however, some cyclic alkenes have been observed in crude oils. It should be noted that SARA analysis does not include alkenes in the analysis and does not specifically provide a method to separate them from many other hydrocarbons.

2.1.5 Aromatic Compounds

The aromatic compounds include at least one benzene ring of six carbon atoms. Three carbon-to-carbon double bonds float around the ring, and all six carbon atoms are equivalent, thus providing high stability to the ring. Because of this stability, benzene rings are very persistent and can have toxic effects on the environment. The most common smaller aromatic compounds found in oil are often referred to as BTEX, or benzene, toluene, ethylbenzene, and xylenes. BTEX compounds and data on them are shown in Table 7. Polycyclic aromatic hydrocarbons or PAHs are compounds consisting of at least two benzene rings. PAHs make up between 0 and 60% of the composition of crude oil. Common PAHs and their substituted counterparts are shown in Table 8. As these are easily separated, there are much data

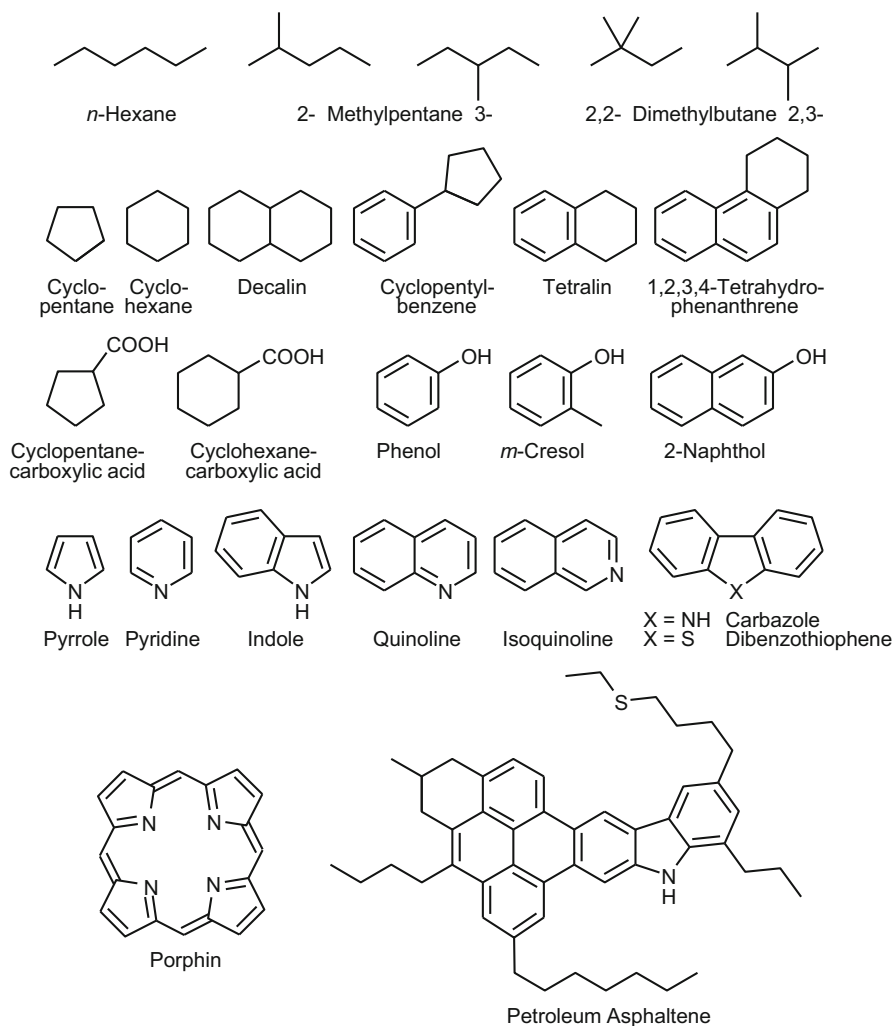


Fig. 2 Structures of selected compounds mentioned in the text or the tables

on their presence in oils. These compounds have also been used somewhat as indicators of presence of certain types of oils. There exists a set of compounds designated by the US EPA as priority PAHs (Wang et al. 1993). The list of 34 EPA priority PHAs is given in Table 9, and the structures of 16 EPA priority PAHs are shown in Fig. 3. The concern with these compounds is that many of them are known to be relatively toxic and some to be carcinogenic as indicated in Table 9.

Aromatic compounds have the general formula C_nH_{2n-6r} , where r is the number of rings. The amounts of aromatics in crude oils vary, but range from 0 to 15%. Aromatics are frequently concentrated by distillation in the refining processes into the heavier or residual fractions. Diesel fuel typically contains 5 to 25% aromatics,

Table 5 Gross composition of some crude oils and petroleum products (all values in %)

	ANS	Arabian heavy	Arabian light	ASMB	Cook inlet	Diesel fuel	Fuel #5	Heavy fuel	Mars TLP	Maya Orimulsion	Platform Elly	Prudhoe Bay	Sockeye	South Louisiana	South Louisiana	Troll	West Delta Block 143	West Texas
Saturates	75.0	60.1	75.5	77.3	66.7	88.2	44.2	42.5	58.4	46.5	34.6	60.8	49.2	80.8	79.4	66.9	61.0	78.5
<i>n</i> -Alkanes	6.3	7.3	8.5	7.9	7.9	12.0	3.7	2.8	4.9	6.2	2.2	6.3	2.6	5.9	7.4	3.6	5.5	9.5
Aromatics	15.0	24.6	15.2	16.8	25.2	10.2	39.5	29.0	27.5	27.3	32.4	28.3	17.2	12.6	16.9	26.6	26.6	14.8
BTEX and C ₃	2.2	0.1	1.1	3.1	0.2	1.9	0.3	0.2	0.2	0.1	0.1	0.2	0.8	1.2	0.3	0.2	0.2	3.4
PAHs	1.1	0.9	0.8	1.1	1.2	3.0	5.6	2.8	1.0	0.9	0.4	1.8	0.5	0.9	1.3	1.7	0.9	7.8
Estimated UCM ^a		65.7			69.1						58.3				76.3	78.9		
Estimated remainder		10.7			13.5						6.0				11.0	9.1		
Resins	6.1	6.3	5.7	4.2	5.1	1.7	8.0	15.5	9.5	12.7	13.3	7.7	15.1	5.9	3.4	5.8	8.9	6.0
Asphaltenes	4.0	9.0	3.6	1.7	3.1	0.0	8.4	13.0	4.7	15.5	13.6	3.2	18.5	0.8	0.4	0.7	3.6	0.7

^aUCM is the GC unresolved complex mixture as calculated from Wang and Brown (2008) by estimating that total petroleum hydrocarbons consist of the total saturates and aromatics

Table 6 Cycloalkanes found in oils and petroleum

Carbon number	Formula	IUPAC name	Molecular weight	CAS number	Solubility in water ^{a,1} g/L
5	C ₅ H ₁₀	Cyclopentane	70.133	287-92-3	0.16
6	C ₆ H ₁₂	Methylcyclopentane	84.159	96-37-7	4.1E ⁻²
7	C ₇ H ₁₄	Dimethylcyclopentane	98.186	A	
8	C ₈ H ₁₆	Trimethylcyclopentane	112.213	B	~3.7E ⁻³
6	C ₆ H ₁₂	Cyclohexane	84.159	110-82-7	5.5E ⁻²
7	C ₇ H ₁₄	Methylcyclohexane	98.186	108-87-2	~1.6E ⁻²
8	C ₈ H ₁₆	Dimethylcyclohexane	112.213	C	6E ⁻³
8	C ₈ H ₁₆	Ethylcyclohexane	112.213	1678-91-7	<6E ⁻³
9	C ₉ H ₁₈	Trimethylcyclohexane	126.239	D	1.7E ⁻³
10	C ₁₀ H ₁₈	<i>cis</i> -Decahydronaphthalene	138.254	493-01-6	~8.5E ⁻⁴
10	C ₁₀ H ₁₈	<i>trans</i> -Decahydronaphthalene	138.254	493-02-7	~8.5E ⁻⁴

A, 1,1- 1638-26-2; *cis*-1,2- 1192-18-3; *trans*-1,2- 822-50-4; *cis*-1,3- 2532-58-3; *trans*-1,3- 1759-58-6

B, 1,1,2- 4259-00-1; 1,1,3- 4516-69-2; 1 α ,2 α ,4 β -1,2,4- 4850-28-6; 1 α ,2 β ,4 α ,-1,2,4- 16883-48-0

C, 1,1- 590-66-9; *cis*-1,2- 2207-01-4; *trans*-1,2 - 6876-23-9; *cis*-1,3- 638-04-0; *trans*-1,3- 2207-03-6; *cis*-1,4- 624-29-3; *trans*-1,4- 2207-04-7

D, 1,1,2- 7094-26-0; 1,1,3- 3073-66-3; 1 α ,2 β ,4 β ,-1,2,4- 7667-60-9; 1 α ,3 α ,5 β -1,3,5- 1795-26-2

^aApproximate sign ~ indicates solubility values are variable

¹Yalkowsky et al. (2010)

while gasoline contains 25 to 40% aromatics, mostly BTEX compounds. In crude oils, the alkylated compounds occur more frequently than the parent un-alkylated rings. This can be of use in identifying the source of contamination as many PAH pollution sources have more abundant parent compounds than alkylated ones.

2.1.6 Naphthoenaromatic Compounds

There exists a series of compounds which contain aromatic and cycloalkane rings. These are not typically analyzed for either petroleum or environmental purposes, and thus there is not a large amount of data on their contents in crude oils or in petroleum products. Table 10 shows some of the naphthoenaromatic compounds found in crude oils and petroleum products.

2.2 Sulfur Compounds

Sulfur compounds constitute a significant percentage of some crude oils and are also found in petroleum products as an unwanted contaminant (Neumann et al. 1981). The sulfur compounds found in oils and petroleum are generally found as one of four groups:

Table 7 Alkylbenzenes found in oils and petroleum

Carbon number	Name	Formula	Molecular weight	CAS number	Solubility in water ^{a,1} g/L
6	Benzene	C ₆ H ₆	78.112	71-43-2	~1.8
7	Toluene	C ₇ H ₈	92.139	108-88-3	0.5 to 0.6
8	Ethylbenzene	C ₈ H ₁₀	106.165	100-41-4	0.15 to 0.2
8	<i>m</i> -Xylene	C ₈ H ₁₀	106.165	108-38-3	0.14 to 0.16
8	<i>o</i> -Xylene	C ₈ H ₁₀	106.165	95-47-6	0.17 to 0.2
8	<i>p</i> -Xylene	C ₈ H ₁₀	106.165	106-42-3	~0.16
9	1,2,3-Trimethylbenzene	C ₉ H ₁₂	120.191	526-73-8	~7E ⁻²
9	1,2,4-Trimethylbenzene	C ₉ H ₁₂	120.191	95-63-6	5.9E ⁻²
9	1,3,5-Trimethylbenzene	C ₉ H ₁₂	120.191	108-67-8	~5E ⁻²
9	1-Ethyl-2-methylbenzene	C ₉ H ₁₂	120.191	611-14-3	~7.5E ⁻²
9	1-Ethyl-3-methylbenzene	C ₉ H ₁₂	120.191		
9	1-Ethyl-4-methylbenzene	C ₉ H ₁₂	120.191	622-96-8	
9	Isopropylbenzene	C ₉ H ₁₂	120.191	98-82-8	5 to 6E ⁻²
9	Propylbenzene	C ₉ H ₁₂	120.191	103-65-1	~5E ⁻²
10	1,2,3,4-Tetramethylbenzene	C ₁₀ H ₁₄	134.218	488-23-3	
10	1,2,3,5-Tetramethylbenzene	C ₁₀ H ₁₄	134.218	537-53-7	
10	1,2,4,5-Tetramethylbenzene	C ₁₀ H ₁₄	134.218	95-93-2	3.5E ⁻³
10	1,2-Diethylbenzene	C ₁₀ H ₁₄	134.218	135-01-3	~7E ⁻²
10	1,3-Diethylbenzene	C ₁₀ H ₁₄	134.218	141-93-5	
10	1,4-Diethylbenzene	C ₁₀ H ₁₄	134.218	105-5-5	~2.5E ⁻²
10	1-Ethyl-2,4-dimethylbenzene	C ₁₀ H ₁₄	134.218	874-41-9	
10	1-Ethyl-3,5-dimethylbenzene	C ₁₀ H ₁₄	134.218	934-74-7	
10	1-Methyl-2-propylbenzene	C ₁₀ H ₁₄	134.218	1074-17-5	~1E ⁻²
10	1-Methyl-3-propylbenzene	C ₁₀ H ₁₄	134.218	1074-43-7	~1E ⁻²
10	1-Methyl-4-propylbenzene	C ₁₀ H ₁₄	134.218	1074-55-1	~1E ⁻²
10	2-Ethyl-1,3-dimethylbenzene	C ₁₀ H ₁₄	134.218	2870-04-4	
10	2-Ethyl-1,4-dimethylbenzene	C ₁₀ H ₁₄	134.218	1758-88-9	
10	3-Ethyl-1,2-dimethylbenzene	C ₁₀ H ₁₄	134.218	933-98-2	
10	4-Ethyl-1,2-dimethylbenzene	C ₁₀ H ₁₄	134.218	934-80-5	

(continued)

Table 7 (continued)

Carbon number	Name	Formula	Molecular weight	CAS number	Solubility in water ^{a,1} g/L
10	Butylbenzene	C ₁₀ H ₁₄	134.218	104-51-8	1.2 to 1.4E ⁻²
10	<i>sec</i> -Butylbenzene	C ₁₀ H ₁₄	134.218	135-98-8	1.1 to 1.8E ⁻²
10	Isobutylbenzene	C ₁₀ H ₁₄	134.218	538-93-2	
10	<i>m</i> -Cymene	C ₁₀ H ₁₄	134.218	535-77-3	
10	<i>p</i> -Cymene	C ₁₀ H ₁₄	134.218	99-87-6	~3E ⁻²
10	<i>tert</i> -Butylbenzene	C ₁₀ H ₁₄	134.218	98-06-6	1.8 to 3E ⁻²
11	Pentylbenzene	C ₁₁ H ₁₆	148.245	538-68-1	
11	Isopentylbenzene	C ₁₁ H ₁₆	148.245	2049-94-7	~3.5E ⁻³
11	Diethyltrimethylbenzene	C ₁₁ H ₁₆	148.245		
11	Ethyltetramethylbenzene	C ₁₁ H ₁₆	148.245		
11	Diethylmethylbenzene	C ₁₁ H ₁₆	148.245		
11	Butylmethylbenzene	C ₁₁ H ₁₆	148.245		
11	Pentamethylbenzene	C ₁₁ H ₁₆	148.245	700-12-9	~1.5E ⁻²
12	C ₆ -Benzenes	C ₁₂ H ₁₈	162.271		
13	C ₇ -Benzenes	C ₁₄ H ₂₀	176.298		
14	C ₈ -Benzenes	C ₁₆ H ₂₂	190.325		

^aApproximate sign ~ indicates solubility values are variable; a range indicates the range of values

¹Yalkowsky et al. (2010)

1. Mercaptans or thiols with the general structure H–S–R where R is an alkyl or aryl group
2. Sulfides with the general structure R–S–R
3. Thiophenes with the general structure of five-membered rings containing a sulfur atom and with two double bonds
4. As part of asphaltene constituents, whose structures are unknown

Dibenzothiophenes, as shown in Table 11, are often used as forensic markers to track oil spills (Wang et al. 2003). Table 11 also shows the typical sulfur compounds found in oils.

Gaudalupe analyzed oils for total sulfur and for sulfides (Gaudalupe et al. 1991). Sulfides and asphaltenes correlate with the total sulfur found in the oil. Nishioka and Tomisch developed a method for analyzing oils for thiols noting that many thiols had not yet been identified (Nishioka and Tomisch 1993).

Most sulfur compounds in oil are foul-smelling and corrosive. The presence of these compounds lowers the price of the crude oils, as sulfur compounds have to be removed before or during refining. In recent years, the standards for the sulfur content of fuels have been lowered, increasing the expense of refining.

Table 8 PAHs and alkylated PAHs found in oils and petroleum

Carbon number	Number of rings	Name	Formula	Molecular weight	CAS number	Solubility in water ^{a,1,2} g/L	ASMB ³ µg/g oil	ANS ⁴ µg/g oil	Diesel fuel ⁴ µg/g oil	Heavy fuel oil ⁴ µg/g oil
10	2	Naphthalene	C ₁₀ H ₈	128.171	91-20-3	30–30E ⁻³	680	260	820	140
11	2	Methyl-naphthalenes	C ₁₁ H ₁₀	142.197	A	26–28E ⁻³	1180	1000	3700	1300
12	2	Dimethyl-naphthalenes	C ₁₂ H ₁₂	156.233	B	~2.4E ⁻³	1600	1800	7000	2900
12	2	Ethyl-naphthalenes	C ₁₂ H ₁₂	156.233	C	~1E ⁻²	1600	1800	7000	2900
13	2	C ₃ -Naphthalenes	C ₁₃ H ₁₄	170.255	D	~1.6E ⁻³	1560	1700	6600	2900
14	2	C ₄ -Naphthalenes	C ₁₄ H ₁₆	184.282			450	820	2800	1400
14	3	Phenanthrene	C ₁₄ H ₁₀	178.229	85-01-8	~1E ⁻³	170	210	440	420
15	3	C ₁ -Phenanthrenes	C ₁₅ H ₁₂	192.256	E	~7E ⁻⁵	400	670	1000	1900
16	3	C ₂ -Phenanthrenes	C ₁₆ H ₁₄	206.288			400	710	620	2900
17	3	C ₃ -Phenanthrenes	C ₁₇ H ₁₆	220.315			160	490	190	3100
18	3	C ₄ -Phenanthrenes	C ₁₈ H ₁₈	234.342			60	300	50	2200
12	3	Dibenzothiophene	C ₁₂ H ₈ S	184.257	132-65-0	5E ⁻⁴	200	120	70	100
13	3	C ₁ -Dibenzothiophenes	C ₁₃ H ₁₀ S	198.283			370	230	110	320
14	3	C ₂ -Dibenzothiophenes	C ₁₄ H ₁₂ S	212.310			450	320	100	620
15	3	C ₃ -Dibenzothiophenes	C ₁₅ H ₁₄ S	226.337			220	270	40	700
13	3	Fluorene	C ₁₃ H ₁₀	166.218	86-73-7	~8E ⁻⁵	50	140	570	220
14	3	C ₁ -Fluorenes	C ₁₄ H ₁₂	180.245	F		110	330	800	570
15	3	C ₂ -Fluorenes	C ₁₅ H ₁₄	194.277			150	450	760	1000
16	3	C ₃ -Fluorenes	C ₁₆ H ₁₆	208.304			85	380	360	940
18	4	Chrysene	C ₁₈ H ₁₂	228.288	218-01-9	~1.5E ⁻⁶	25	50	<1	380
19	4	C ₁ -Chrysenes	C ₁₉ H ₁₄	242.314	G		70	70	<1	1200

(continued)

Table 8 (continued)

Carbon number	Number of rings	Name	Formula	Molecular weight	CAS number	Solubility in water ^{a,1,2} g/L	ASMB ³ µg/g oil	ANS ⁴ µg/g oil	Diesel fuel ⁴ µg/g oil	Heavy fuel oil ⁴ µg/g oil
20	4	C ₂ -Chrysenes	C ₂₀ H ₁₆	256.348				100	<1	1800
21	4	C ₃ -Chrysenes	C ₂₁ H ₁₈	270.375				80		1400
20	5	Perylene	C ₂₀ H ₁₂	252.309	198-55-0	~4E ⁻⁷				

A, 1-90-12-0; 2-91-57-6

B, 1,2-573-98-8; 1,3-575-41-7; 1,4-571-61-9; 1,5-571-61-9; 1,6-575-43-9; 1,7-575-37-1; 1,8-569-41-5; 2,3-581-40-8; 2,6-581-42-0; 2,7-582-16-1

C, 1-1127-76-0; 2-939-27-5

D, 1,4,5-2131-41-1

E, 1-832-69-9; 3-832-71-3; 4-832-64-4

F, 1-1730-37-6; 9-2523-37-7

G, 3-3351-31-3; 5-3697-24-3; 6-1705-85-7

^aApproximate sign ~ indicates solubility values are variable; a range indicates the range of values

¹Yalkowsky et al. (2010)

²Verschuere (2001)

³Wang et al. (1993)

⁴Wang et al. (2003)

Table 9 EPA 34 priority PAHs found in oils and petroleum

Carbon number	Number of rings	Name	EPA 16 priority PAH	Formula	Molecular weight	CAS number	Solubility in water ^{a,1} g/L	US. EPA Toxicity value ^b	ASMB ^{2,3} µg/g oil	ANS ³ µg/g oil	Diesel fuel ³ µg/g oil	Heavy fuel oil ⁴ µg/g oil
10	2	Naphthalene	x	C ₁₀ H ₈	128.717	91-20-3	~3.5E ⁻²	193.47	6802	260	820	140
11	2	1-Methylnaphthalene		C ₁₁ H ₁₀	142.197	90-12-0	~2.8E ⁻²	72.16				
11	2	2-Methylnaphthalene		C ₁₁ H ₁₀	142.197	91-57-6	~1.8E ⁻²	75.37				
12	2	C ₂ -Naphthalenes		C ₁₂ H ₁₂	156.233	A	1 to 8E ⁻³	30.24	16002	1800	7000	2900
13	2	C ₃ -Naphthalenes		C ₁₃ H ₁₄	170.255	B	~2E ⁻³	11.10	15602	1700	6600	2900
14	2	C ₄ -Naphthalenes		C ₁₄ H ₁₆	184.282			4.05	4502	820	2800	1400
12	3	Acenaphthene	x	C ₁₂ H ₁₀	154.207	83-32-9	3.4E ⁻³	306.85				
12	3	Acenaphthylene	x	C ₁₂ H ₈	152.192	208-96-8	~4E ⁻³	55.85				
13	3	Fluorene	x	C ₁₃ H ₁₀	166.218	86-73-7	~2E ⁻³	39.30	50	140	570	220
14	3	C ₁ -Fluorenes		C ₁₄ H ₁₂	180.245	C	~1E ⁻³	13.99	110	330	800	570
15	3	C ₂ -Fluorenes		C ₁₅ H ₁₄	194.277			5.30	150	450	760	1000
16	3	C ₃ -Fluorenes		C ₁₆ H ₁₆	208.304			1.92	85	380	360	940
14	3	Anthracene	x	C ₁₄ H ₁₀	178.229	120-12-7	~1E ⁻³	19.13	2	3	13	95
14	3	Phenanthrene	x	C ₁₄ H ₁₀	178.229	85-01-8	2.7E ⁻⁴	20.72	170	210	440	420
15	3	C ₁ -Phenanthrenes		C ₁₅ H ₁₂	192.256	D	~2.7E ⁻⁴	7.44	400	670	1000	1900
16	3	C ₂ -Phenanthrenes		C ₁₆ H ₁₄	206.288			3.20	400	710	620	2900

(continued)

Table 9 (continued)

Carbon number	Number of rings	Name	EPA 16 priority PAH	Formula	Molecular weight	CAS number	Solubility in water ^{a,1} g/L	US. EPA Toxicity value ^b	ASMB ^{2,3} µg/g oil	ANS ³ µg/g oil	Diesel fuel ³ µg/g oil	Heavy fuel oil ⁴ µg/g oil
17	3	C ₃ -Phenanthrenes		C ₁₇ H ₁₆	220.315			1.26	160	490	190	3100
18	3	C ₄ -Phenanthrenes		C ₁₈ H ₁₆	232.326			0.56	60	300	50	2200
16	4	Fluoranthene	x	C ₁₆ H ₁₀	202.256	206-44-0	2.7 ⁻⁴	711	2	3	7	40
16	4	Pyrene	x	C ₁₆ H ₁₀	202.256	129-00-0	0.9 to 1.4E ⁻⁴	10.11	18	8	31	230
17	4	C ₁ -Fluoranthenes/ Pyrenes		C ₁₇ H ₁₂	216.277	E		4.89				
18	4	Chrysene	x	C ₁₈ H ₁₂	228.288	218-01-9	2 to 1.6E ⁻⁶	2.04	25	50	<1	380
19	4	C ₁ -Chrysenes		C ₁₉ H ₁₄	242.314	F	~6E ⁻⁵	0.86		70	<1	1200
20	4	C ₂ -Chrysenes		C ₂₀ H ₁₆	256.348		~3E ⁻⁵	0.48		100	<1	1800
21	4	C ₃ -Chrysenes		C ₂₁ H ₁₈	270.375			0.17		80		1400
18	4	Benz[<i>a</i>]anthracene	x	C ₁₈ H ₁₂	228.288	56-55-3	0.9 to 1.3E ⁻⁵	2.23	3	5	0.3	200
20	5	Perylene		C ₂₀ H ₁₂	252.309	198-55-0	4E ⁻⁷	0.90				
20	5	Benzo[<i>a</i>]pyrene	x	C ₂₀ H ₁₂	252.309	50-32-8	1.4 to 3.8E ⁻⁶	0.65	1	2	0	150
20	5	Benzo[<i>c</i>]pyrene		C ₂₀ H ₁₂	252.309	192-97-2		0.90				
20	5	Benzo[<i>k</i>]fluoranthene ^e	x	C ₂₀ H ₁₂	252.309	205-99-2	~1.5E ⁻⁶	0.96	3	5	0	50
20	5	Benzo[<i>k</i>]fluoranthene ^e	x	C ₂₀ H ₁₂	252.309	207-08-9	~1E ⁻⁶	0.96	3	1	0	10

22	5	Dibenz[<i>a,h</i>]anthracene	x	C ₂₂ H ₁₄	278.346	53-70-3	~1E ⁻⁶	0.27	1	1	0	20
22	6	Indeno[1,2,3- <i>cd</i>]pyrene	x	C ₂₂ H ₁₂	276.338	193-39-5	~2E ⁻⁷	0.28	1	0.1	0	10
22	6	Benzo[<i>g,h,i</i>]perylene	x	C ₂₂ H ₁₂	276.338	191-24-2	1.8 to 2.6E ⁻⁷	0.44	3	3	0	30

^aApproximate sign ~ indicates solubility values are variable; a range indicates the range of values

^bUS EPA chronic toxicity value taken from EPA, 2003 – smaller numbers indicate higher toxicity

^cThese two compounds are combined for EPA-34 considerations

A, Dimethylnaphthalenes 1,2- 573-98-8; 1,3- 575-41-7; 1,4- 571-58-4; 1,5- 571-61-9; 1,6- 575-43-9; 1,7- 575-37-1; 1,8- 569-41-5; 2,3- 581-40-8; 2,6- 581-42-0; 2,7- 582-16-1; ethylnaphthalenes 1- 1127-76-0; 2- 939-27-5

B, 1,4,5- 2131-41-1

C, 1- 1730-37-6; 9- 2523-37-7

D, 1- 832-69-9; 3- 832-71-3; 4- 832-64-4

E, 1- 2381-21-7; 2- 3442-78-2

F, 3- 3351-31-3; 5- 3697-24-3; 6- 1705-85-7

¹Yalkowsky et al. (2010)

²Verschueren (2001)

³Wang et al. (1993)

⁴Wang et al. (2003)

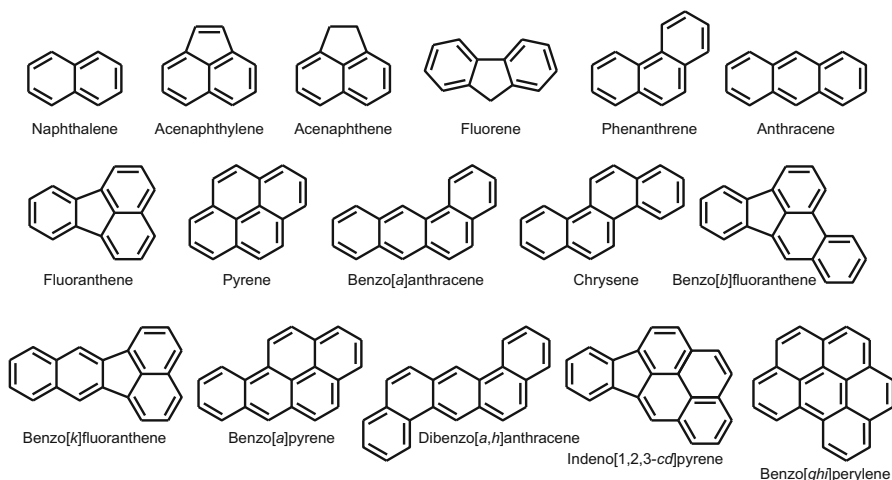


Fig. 3 Structures of 16 EPA priority PAHs

Table 10 Naphthenoaromatic compounds found in oils and petroleum

Compound	Formula	Molecular weight	CAS No.
Cyclopropylbenzene	C ₉ H ₁₀	118.175	873-49-4
Cyclopentylbenzene	C ₁₁ H ₁₄	146.229	700-88-9
1,2,3,4-Tetrahydronaphthalene (Tetralin)	C ₁₀ H ₁₂	132.202	119-64-2
Methyl-1,2,3,4-tetrahydronaphthalene	C ₁₁ H ₁₄	146.229	A
Dimethyl-1,2,3,4-tetrahydronaphthalene	C ₁₁ H ₁₄	160.255	B
Trimethyl-1,2,3,4-tetrahydronaphthalene	C ₁₁ H ₁₄	174.282	C
1,2,3,4-Tetrahydrophenanthrene	C ₁₄ H ₁₄	182.261	1013-08-7
Cyclopentanephenanthrene	C ₁₇ H ₁₄	218.299	

A, 1-methyl - 1559-81-5; 5-methyl - 2809-64-5; 6-methyl - 1680-561-9

B, 1,5-dimethyl - 21564-91-0

C, 1,1,6-trimethyl - 475-03-6

2.3 Oxygen Compounds

Oxygen compounds are found in oils and petroleum. Measurement of these compounds is not frequent because they do not have known forensic potential and because they may be relatively well soluble in water. They are more difficult to measure than many hydrocarbons. The common groups of oxygen compounds found in oils are:

1. Naphthenic acids or their salts
2. Phenols and phenolic compounds
3. Fatty acids
4. Inclusions in asphaltenes

Table 11 Sulfur compounds found in oils and petroleum

Carbon number	Name	Formula	Molecular weight	CAS number	Solubility in water g/L	Reference
	Sulfides					
2	Dimethyl sulfide	C ₂ H ₆ S	62.134	75-18-3	6.3E ⁻³	1
4	Diethyl sulfide	C ₄ H ₁₀ S	90.187	352-93-2	3.1E ⁻³	1
4	Diethyl disulfide	C ₄ H ₁₀ S ₂	122.252	110-81-6		
6	Dipropyl sulfide	C ₆ H ₁₄ S	118.238	111-47-7		
8	Dibutyl sulfide	C ₈ H ₁₈ S	146.294	544-40-1	3.4E ⁻²	1
8	Di- <i>sec</i> -butyl sulfide	C ₈ H ₁₈ S	146.294	626-26-6		
8	Di- <i>tert</i> -butyl sulfide	C ₈ H ₁₈ S	146.294	107-47-1		
8	Dibutyl disulfide	C ₈ H ₁₈ S ₂	178.359	629-45-8		
8	Di- <i>tert</i> -butyl disulfide	C ₈ H ₁₈ S ₂	178.359	110-06-5	2E ⁻³	1
12	Dihexyl sulfide	C ₁₂ H ₂₆ S	202.399	6294-31-1		
14	Dioctyl sulfide	C ₁₄ H ₃₀ S	230.453	629-65-2		
16	Dioctyl sulfide	C ₁₆ H ₃₄ S	258.506	2690-08-6		
	Thiols (Mercaptans)					
2	Ethanethiol	C ₂ H ₆ S	62.134	75-08-1	15	1
2	1,2-Ethanedithiol	C ₂ H ₆ S ₂	94.199	540-63-6		
3	1-Propanethiol	C ₃ H ₈ S	76.161	107-03-9		
3	2-Propanethiol	C ₃ H ₈ S	76.161	75-33-2		
3	1,2-Propanedithiol	C ₃ H ₈ S ₂	108.226	814-67-5		
3	1,3-Propanedithiol	C ₃ H ₈ S ₂	108.226	109-80-8		
4	1-Butanethiol	C ₄ H ₁₀ S	90.187	109-79-5	0.59	1
4	2-Butanethiol	C ₄ H ₁₀ S	90.187	91840-99-2		
4	1,4-Butanedithiol	C ₄ H ₁₀ S ₂	122.252	1191-08-8		
5	1-Pentanethiol	C ₅ H ₁₂ S	104.214	110-66-7		
5	2-Pentanethiol	C ₅ H ₁₂ S	104.214	2084-19-7		
5	3-Pentanethiol	C ₅ H ₁₂ S	104.214	616-31-9		

(continued)

Table 11 (continued)

Carbon number	Name	Formula	Molecular weight	CAS number	Solubility in water g/L	Reference
6	1-Hexanethiol	C ₆ H ₁₄ S	118.238	111-31-9		
6	2-Hexanethiol	C ₆ H ₁₄ S	118.238	1679-06-7		
6	1,6-Hexanedithiol	C ₆ H ₁₄ S ₂	150.305	1191-43-1		
6	1,2-Benzenedithiol	C ₆ H ₆ S ₂	142.242	17534-15-5		
6	1,3-Benzenedithiol	C ₆ H ₆ S ₂	142.242	626-04-0		
7	Benzenemethanethiol	C ₇ H ₈ S	124.204	100-53-8		
7	1-Heptanethiol	C ₇ H ₁₆ S	132.267	1639-09-4		
	Dibenzothiophenes					
12	Dibenzothiophene	C ₁₂ H ₈ S	184.257	132-65-0	1.4E ⁻³	2
13	C ₁ -Dibenzothiophenes	C ₁₃ H ₁₀ S	198.283			
14	C ₂ -Dibenzothiophenes	C ₁₄ H ₁₂ S	212.310			
15	C ₃ -Dibenzothiophenes	C ₁₄ H ₁₂ S	212.310			

Table 12 Oxygenated compounds sometimes found in oils and petroleum

Compound	Molecular formula	CAS No.	Molecular weight	Reference	Solubility in water ¹ g/L
Naphthenic acids					
Cyclopentanecarboxylic acid	C ₆ H ₁₀ O ₂	3400-45-1	114.142	1	
Cyclohexanecarboxylic acid	C ₇ H ₁₂ O ₂	98-89-5	128.169	1	2
Cyclohexaneacetic acid	C ₈ H ₁₄ O ₂	5292-21-7	142.196	1	
Phenols					
Phenol	C ₆ H ₆ O	108-95-2	94.111	1	80
Resorcinol	C ₆ H ₆ O ₂	108-46-3	110.111	1	700
<i>o</i> -Cresol	C ₇ H ₈ O	95-48-7	108.138	1	25
<i>m</i> -Cresol	C ₇ H ₈ O	108-39-4	108.138	1	20
<i>p</i> -Cresol	C ₇ H ₈ O	106-44-5	108.138	1	20
Xylenol	C ₈ H ₁₀ O	A	122.164	1	4 to 8
1-Naphthol	C ₁₀ H ₈ O	90-15-3	144.173	1	0.9
2-Naphthol	C ₁₀ H ₈ O	135-19-3	144.173	1	0.7
Fatty acids	CH ₃ -(CH ₂) _n -COOH	many	different		

¹Yalkowsky et al. (2010)

A, 2,3- 526-75-0; 2,4- 105-67-9; 2,5- 95-87-4; 2,6- 576-26-1; 3,4- 95-65-8; 3,5- 108-69-9

Some of the compounds that have been found in oils are shown in Table 12. Analysis has shown that some of the acid species include complex compounds with two to six aromatic rings and often including sulfur and nitrogen compounds (Tomczyk et al. 2001). Porter et al. analyzed several resins and determined the presence of carbazole and similar compounds in these oils (Porter et al. 2004).

2.4 Nitrogen Compounds

Nitrogen compounds are abundant in most crude oils and constitute about 0.1 to 2 wt.% of the total. Several workers have carried out qualitative and quantitative analysis on nitrogen compounds in oils (Oliveira et al. 2006; Li et al. 2010; Von Muehlen et al. 2010; Zhang et al. 2010). Nitrogen compounds in oils are often divided into two groups of basic or nonbasic compounds. This division is also useful for separation schemes. Most compounds are present as cyclic compounds as shown

Table 13 Nitrogen compounds sometimes found in oils and petroleum

Compound	Molecular formula	CAS No.	Molecular weight	Solubility in water ^{a,1} g/L
Pyrrole	C ₄ H ₅ N	109-97-7	67.091	48
Pyridine	C ₅ H ₅ N	110-86-1	79.101	
Indole	C ₈ H ₇ N	120-72-9	117.149	3.6 to 10
Methylindole	C ₉ H ₉ N	A	131.174	~0.5
Quinoline	C ₉ H ₇ N	91-22-5	129.159	~6
Isoquinoline	C ₉ H ₇ N	119-65-3	129.159	
Methylquinoline	C ₁₀ H ₉ N	B	143.185	
Methylisoquinoline	C ₁₀ H ₉ N	C	143.185	~1
Dimethylquinoline	C ₁₁ H ₁₁ N	D	157.212	1.8
Carbazole	C ₁₂ H ₉ N	86-74-8	167.206	1.2 E ⁻³
Methylcarbazole	C ₁₃ H ₁₁ N	E	181.238	
Dimethylcarbazole	C ₁₄ H ₁₃ N		195.265	
Trimethylcarbazole	C ₁₅ H ₁₅ N		209.292	

^aApproximate sign ~ indicates solubility values are variable, a range indicates the range of values, many of these values are the average of several determinations

¹Yalkowsky et al. (2010)

A, 1- 603-76-9; 2- 95-20-5; 3- 83-34-1; 5- 614-96-0; 7- 933-67-5

B, 2- 91-63-4; 3- 612-58-8; 4- 491-35-0; 5- 7661-55-4; 6- 91-62-3; 7- 612-60-2; 8- 611-32-5

C, 1- 1721-93-3; 3- 1125-80-0

D 2,4- 1198-37-4; 2,6- 877-43-0; 2,7- 93-37-8

E, 3- 4630-20-0; 9- 1484-12-4

in Table 13. Furthermore, there is significant nitrogen content in the asphaltenes and in metal-binding compounds such as porphyrins.

2.5 Metals

Crude oils and their heavy refined petroleum products often contain significant amounts of metals. Metals are found in oils as:

1. Inorganic salts
2. Metal soaps
3. Organic metal-complex compounds
4. Attached to asphaltenes

Table 14 shows the metal content in several oils. The metals shown here are the most common metals identified in oils. In the past some metals, notably chromium, vanadium, and nickel, were used for crude oil identification. The ratios of these metals have a tendency to remain constant. Further, the ratios of these metals can be used to identify tanks from which the oils may have come, as there is exchange of metals with the tank bodies. At the present time, there is little use of this type of identification as the use of biomarkers is easier and better understood.

Table 14 Metal content in oils in ppm

Metal	Light fuels		Aviation gas 100	Jet A	Jet B	Diesel	Heavy fuel oils		IFO – marine	Refinery intermediates	
	Aviation gas 80						Bunker C			FCC heavy cycle	Heavy reformate
Chromium	<		1.4	<	<	<	<	<	<	<	<
Copper	1.1		<	<	<	<	<	<	<	<	<
Iron	<		39	13	4.6	3.5	29.5	29.5	<	<	<
Lead	175		795	<	<	<	<	<	<	<	<
Magnesium	8.2		7.5	9.8	3.6	12.3	23.9	10.2	3.8	10.6	<
Molybdenum	0.6		<	1.9	<	<	<	<	<	<	<
Nickel	<		<	<	<	<	8.6	29.5	<	<	<
Titanium	<		<	2.7	<	<	<	0.6	<	1.2	<
Vanadium	<		<	<	<	<	42	76.4	<	<	<
Zinc	<		<	2.4	0.6	1.2	1.6	1.1	0.4	<	<
Metal	Light crude oils										
	Brent		Panuke	Norman Wells	Pitas Point	Oseberg	Ninian	Empire	Iranian heavy	Maya	
Country of origin	UK		Canada	Canada	USA – Cal	Norway	UK	USA – Cal	Iran	Mexico	
Chromium		<	<	<	<	<	<	<	<	<	<
Copper		<	<	<	<	<	<	<	0.6	<	<
Iron		<	<	<	10.3	4.2	4.2	39.5	6	<	<
Lead		<	<	<	<	<	<	<	<	<	<
Magnesium		<	<	<	<	1	<	17.4	8.8	16.7	<
Molybdenum		<	<	<	<	<	<	<	<	1.2	<
Nickel	1	<	3.3	<	<	3.8	<	<	22.6	46.5	<
Titanium		<	<	<	0.6	<	<	105	<	<	<

(continued)

Table 14 (continued)

Metal	Light fuels		Aviation gas 100	Jet A	Jet B	Diesel	Heavy fuel oils		IFO – marine	Refinery intermediates	
	Aviation gas 80	Heavy crudes					Bunker C	FCC heavy cycle		Heavy reformate	
Vanadium	6		<	8.7	<	2.7	4	<	<	81	257
Zinc			<	<	3.3	<	<	<	<	<	<
Metal											Bitumen
	Lago Medio	Platform Irene	Port Hueneme	Hondo	Dos Cuadras	Carpinteria	California 11	California 15	Cold Lake bitumen		
Country of origin	Venezuela	USA – Cal	USA – Cal	USA – Cal	USA – Cal	USA – Cal	USA – Cal	USA – Cal	Canada		
Chromium	<	2.3	<	<	<	>	1.5	1.7	<	<	<
Copper	<	0.8	<	<	<	<	<	<	<	<	<
Iron	<	44	16	30.5	42.1	29.5	21.5	9.1	15.2		
Lead	<	<	<	<	<	<	3	3	<		<
Magnesium	3.8	237	3.1	5.4	16	<	237	8	9		
Molybdenum	<	<	0.6	2.3	<	<	4	5.1	3.7		
Nickel	5.6	60.5	68	75	62	48.9	106	111	69		
Titanium	<	1.1	0.6	1.6	<	<	2.2	2	<		
Vanadium	163	238	253	196	70.5	112	245	266	190		
Zinc	<	5.1	0.6	0.5	<	4.3	<	<	4.3		

Quadros et al. studied the simultaneous measurement of nickel and vanadium in Brazilian and Venezuelan crude oils (Quadros et al. 2010). They found that the total nickel in three Brazilian crudes ranged from 9 to 25 $\mu\text{g g}^{-1}$ and from 29 to 69 $\mu\text{g g}^{-1}$ in three Venezuelan crudes. The total vanadium in the same Brazilian crudes ranged from 13 to 32.7 $\mu\text{g g}^{-1}$ and in the Venezuelan crudes ranged from 224.7 to 277.0 $\mu\text{g g}^{-1}$.

The bonding of metals, particularly nickel, vanadium, iron, and cobalt into porphyrins, is a known source of metal stability in oils. Figure 2 shows the porphyrin skeleton. These compounds are residuals of chlorophyll which has a similar structure.

Metals are concentrated into petroleum residuals and often in the asphalt fractions of the oil. Metals are very low in the diesel fraction and absent in gasoline.

2.6 Resins

Resins are polar compounds that are defined by precipitation or by open-column chromatography. The composition of resins is largely unknown. The nitrogen compounds noted above may be present in resins, largely as alkylated variants of the basic compounds.

Porter et al. (2004) analyzed several resins and determined the presence of carbazole and similar compounds in these oils. They also looked at the average molecular weight of resins using electrospray tandem mass spectrometry and found that the residual resins in diesel are of smaller molecular weight than in crude oils.

2.7 Asphaltenes

The important fact concerning asphaltenes is that currently the structure and composition of this broad class of compounds is unknown (Mullins et al. 2007). Currently asphaltenes are defined by their precipitation from oil in pentane, hexane, or heptane. The mass of asphaltenes, typically defined as percentage by weight, increases as one uses smaller compounds as solvents. As Mullins points out in his recent volume on the topic, that until a number of structures of asphaltenes have been identified, asphaltenes will remain a mystery such as the whole field of genetics before Watson and Crick identified the structure of DNA (Groenzin and Mullins 2007). Despite recent progress in the field, not one single compound has been positively characterized in the asphaltene mix.

Recent progress on the study of asphaltenes will be summarized below, but includes the fact that for the first time the molecular weight has been found to be about 760, ranging from 500 to 1000 (Rodgers and Marshall 2007). The aromatic ring system is felt to contain about seven fused rings, a range of four to ten rings, and that these rings are fused and thus the asphaltene is felt to have a “hand shape” with the aliphatic chains (fingers) radiating outward from the central fused ring (palm). Further, analysis has been problematic because asphaltene molecules aggregate at

low concentrations, typically about 150 mg/L in toluene. These nano-aggregates can range up to ten or more individual molecules and do not easily lend themselves to analysis or separation.

Studies up to about 2006 concluded that the molecular weight of asphaltenes varied from about 500 to about 70,000 amu or Daltons (Mullins et al. 2007). More recent studies, using more refined techniques, show that the molecular weight of asphaltenes is smaller than previously thought. One of the problems of determining the molecular weight is the aggregation tendency of asphaltenes. As noted above, this is a severe problem for any analysis of asphaltenes. Vapor pressure osmometry (VPO), gel permeation chromatography (GPC), and certain introduction methods for mass spectrometry such as laser desorption methods can result in asphaltene aggregation and therefore high molecular weight values. Electrospray ionization Fourier transform ion cyclotron resonance spectroscopy (ESI-FT-ICR) has been successful in studying asphaltenes and other heavy oil components (Rodgers and Marshall 2007). Electrospray ionization (ESI) is a useful introduction method for heavy oil components as the analyte molecule is not evaporated, rather the solvent is. The molecules do not reaggregate as they are charged in the process, and electrostatic repulsion keeps them separated. All these methods do not result in separation of the asphaltene mixture, rather just enable a bulk analysis which can lead to some structure indications and idea of the molecular weight. Further details on the information that mass spectrometry can in the characterization of such complicated mixtures are provided by Walters and Higgins (► Chap. 12, “Petroleomics”).

Groenzin and Mullins (2007) report on the use of time-resolved fluorescence depolarization (TRFD) to assess the molecular weight of asphaltenes. This method is basically a look at the decay of fluorescent molecules. Molecular weight is estimated by comparison to the decay rate of molecules of known molecular weight. The results of this analysis show the typical molecular weight is 750 g/mol and that this varies from about 500 to 1000 g/mol. Interestingly, coal asphaltenes displayed an average molecular weight of about 500 g/mol.

Dr. Yen proposed that asphaltene molecule aggregates are like micelles and will behave like stacks of fused aromatic ring systems (Rodgers and Marshall 2007). This is now known as the “Yen” model. The micelles will grow to a limiting size and reaggregate into “aggregates” until there is again a limiting size. So, there is a double mode of aggregation. Groenzin and Mullins used the sum total of information found to date to propose a structure for one oil asphaltene as shown in Fig. 2.

3 Properties of Oil

The properties of oil discussed here are viscosity, density, specific gravity, solubility, flash point, pour point, distillation fractions, interfacial tension, and vapor pressure. These properties for the oils noted as examples above are listed in Table 15 (Wang et al. 2004).

Viscosity is the resistance to flow at a given shear rate. The lower the viscosity, the more readily the liquid flows. For example, water has a low viscosity and flows

Table 15 Typical oil properties

Property	Units	Gasoline	Diesel	Light crude	Heavy crude	Intermediate fuel oil	Bunker C
Viscosity	mPa·s at 15°C	0.5	2	5–50	50–50,000	1000–15,000	10,000–50,000
Density	g/mL at 15°C	0.72	0.84	0.78–0.88	0.88–1.00	0.94–0.99	0.96–1.04
Flash point	°C	–35	45	–30–30	–30–60	80–100	>100
Solubility in water	ppm	200	40	10–50	5–30	10–30	1–5
Pour point	°C	NR	–35– –10	–40– 30	–40– 30	–10–10	5–20
API gravity		65	35	30–50	7–15	10–20	5–15
Interfacial tension	mN/m at 15°C	27	27	10–30	15–30	25–30	25–35
Distillation fractions	% distilled at						
	100°C	70	1	2–15	1–10	–	–
	200°C	100	30	15–40	2–25	2–5	2–5
	300°C		85	30–60	15–45	15–25	5–15
	400°C		100	45–85	25–75	3–40	15–25
	Residual			15–55	25–75	60–70	75–85

NR not relevant

readily. Molasses with a high viscosity flow slowly. The viscosity of the oil is largely determined by the amount of lighter and heavier fractions that it contains. The greater the percentage of light components such as small saturates and the lesser the amount of asphaltenes, the lower the viscosity. Conversely, oils with a high asphaltene content have high viscosities. Viscosity is affected by temperature, with a lower temperature giving a higher viscosity. For most oils, the viscosity varies as the logarithm of the temperature. Oils that flow readily at high temperatures can become a slow-moving, viscous mass at low temperatures. In terms of oil spill cleanup, viscosity is important. Viscous oils do not spread rapidly, do not penetrate soil as readily, but are difficult to pump and skim.

Density is the mass of a unit volume of oil and is typically expressed in grams per cubic centimeter (g/cm^3). It is the property often used by the petroleum industry to define light or heavy crude oils. The density of fresh water is $1.0 \text{ g}/\text{cm}^3$ at 15°C , and the density of most oils ranges from 0.7 to $0.99 \text{ g}/\text{cm}^3$; thus most oils will float on water. As the density of seawater is $1.03 \text{ g}/\text{cm}^3$, even heavier oils will usually float on seawater. The density of oil increases with time, as the light fractions evaporate. When the density of an oil becomes greater than the density of freshwater or seawater, the oil will sink. Sinking is rare and happens only with a few oils, usually residual fuels such as Bunker C or raw products such as bitumen. Significant amounts of oil have sunk in only about 50 incidents out of thousands. However, as

heavier and heavier oils are being used more frequently, sinking may become more common in the future.

Specific gravity is another measure of density and is an oil's relative density compared to that of water. If the oil specific gravity is greater than 1, it sinks; if less than 1, it floats. Another gravity scale is that of the American Petroleum Institute (API). The API gravity is based on the density of pure water which has an arbitrarily assigned API gravity value of 10° (10 degrees). Oils with progressively lower specific gravities have higher API gravities. The following is the formula for calculating API gravity:

$$\text{API gravity} = [141.5 \div (\text{oil density at } 15.5^\circ\text{C})] - 131.5$$

3.1 Oils with High Densities Have Low API Gravities and Vice Versa

Oil solubility in water is the measure of how much will dissolve in water on a molecular basis. Solubility is important in that the soluble fractions of the oil are sometimes toxic to aquatic life, especially at higher concentrations. As the amount of oil lost to solubility is always small, this is not a large loss mechanism and is typically ignored in mass balance calculations. In fact, the solubility of oil in water is so low (generally less than 100 parts per million) that it would be the equivalent of approximately one grain of sugar dissolving in a cup of water. This small amount is important to the environment as even small amounts may be toxic to certain biota.

The flash point of an oil is the temperature at which the liquid oil yields sufficient vapors to ignite upon exposure to an open flame. A liquid is considered to be flammable if its flash point is less than 60°C . There is a broad range of flash points for oils and petroleum products, many of which are considered flammable, especially when fresh. Gasoline, which is flammable under all ambient conditions, poses a serious fire hazard when spilled. Many fresh crude oils have an abundance of volatile components and may be flammable for as long as 1 day until the more volatile components have evaporated. On the other hand, Bunker C and heavy crude oils generally are not flammable even when freshly spilled.

The pour point of an oil is the temperature at which it takes longer than a specified time to pour from a standard measuring vessel. It is important to note that pour point is not the solidification temperature. As oils are made up of hundreds of compounds, some of which may still be liquid at the pour point, the pour point is not the temperature at which the oil will no longer pour. The pour point represents a consistent temperature at which an oil will pour very slowly from a standard container. Therefore, pour point has limited use as an indicator of the state of the oil. In fact, pour point has been overused in the past to predict how oils will behave in the environment. For example, waxy oils can have very low pour points, but may

continue to spread slowly at low temperatures and can evaporate to a significant degree. As produced crude oils become heavier, pour point becomes less relevant.

Distillation fractions of an oil represent the fraction (generally measured by volume) of an oil that is boiled off at a given temperature. This data is obtained on crude oils so that oil refineries can adjust parameters to handle the oil. This data also provides environmentalists with useful insights into the chemical composition of oils. For example, while 70% of gasoline will boil off at 100 °C, only about 5% of one selected crude oil will boil off at that temperature and an even smaller amount of a typical Bunker C. The distillation fractions correlate to the composition as well as to other physical properties of the oil. Distillation fraction data is sometimes used for estimation equations of evaporation.

The oil-water interfacial tension, sometimes called surface tension, is the force of attraction or repulsion between the surface molecules of oil and water. Together with viscosity, surface tension is one indication of how rapidly and to what extent an oil will spread on water. The lower the interfacial tension with water, the greater the extent of spreading. In actual practice, the interfacial tension must be considered along with the viscosity because it has been found that interfacial tension alone does not account for spreading behavior.

The vapor pressure of an oil is a measure of how the oil partitions between the liquid and gas phases or how much vapor is in the space above a given amount of liquid oil at a fixed temperature. Because oils are a mixture of many compounds, the vapor pressure changes as the oil weathers. Vapor pressure is difficult to measure and is not frequently used to assess oil spills. Oil is a mixture of hundreds of compounds; therefore vapor pressure is not entirely relevant to spill control.

While there is a high correlation between the various properties of an oil, these correlations should be used cautiously as oils vary so much in composition. For example, the density of many oils can be predicted using their viscosity values. For other oils, however, this could result in errors. For example, waxy oils have much higher viscosities than would be predicted from their densities. There are several mathematical equations for predicting one property of an oil from another property, but these must be used carefully as there are many exceptions

4 Research Needs

The issues around oil composition and properties certainly are complex, and therefore the research needs are very diverse. The foremost need is the continuance of existing efforts along the various research lines to define and clarify oil composition. The second need is to correlate and compile the various findings to ascertain if there are patterns or relationships between the various data. The measurement of both oil composition and properties needs to follow international standards. Finally, there needs to be central or readily available sources of data. Data needs to be available to potential users.

References

- CRC (2016–2017) Handbook of chemistry and physics. CRC Press, Boca Raton
- Faksness L-G, Daae RL, Brandvik PJ, Leivik F, Borseth JF (2010) Oil distribution and bioavailability field experiment – FEX 2009, Sintef Report A 16584, Trondheim
- Fingas M (2011) Introduction to oil chemistry and properties, Chapter 3. In: Oil spill science and technology. Elsevier Publishers, New York, pp 51–70
- Gaudalupe MFM, Castello Branco VA, Schmid JC (1991) Isolation of sulfides in oils. *Org Geochem* 17:355
- Groenzin H, Mullins OC (2007) Asphaltene molecular size and weight by time-resolved fluorescence depolarization, Chapter 2. In: *Asphaltenes, heavy oils and petroleomics*. Springer Publications, New York, pp 17–40
- Kinghorn RRF (1983) An introduction to the physics and chemistry of petroleum. Wiley, New York
- Li N, Ma X, Zha Q, Song C (2010) Analysis and comparison of nitrogen compounds in different liquid hydrocarbon streams derived from petroleum and coal. *Energy Fuel* 5539. <https://doi.org/10.1021/ef1007598>
- Mackay D, Shiu WY, Ma KC (1992) Illustrated handbook of physical-chemical properties and environmental fate for organic chemicals, vol 1–5. Lewis Publishers, Boca Raton
- Mullins OC, Sheu EY, Hammami A, Marshall AG (eds) (2007) *Asphaltenes, heavy oils and petroleomics*. Springer Publications, New York
- Neumann H-J, Paczynska-Lahme B, Severin D (1981) Composition and properties of petroleum. Halsted Press, New York
- Nishioka M, Tomisch RS (1993) Isolation of aliphatic sulfur compounds in a crude oil by a non-reactive Procedure. *Fuel* 72:1007–1016. [https://doi.org/10.1016/0016-2361\(93\)90301-H](https://doi.org/10.1016/0016-2361(93)90301-H)
- Oliveira EC, Vaz de Campos MC, Rorigues MR, Perez VF, Melecchi MIS, Vale MGR, Zini CA, Caramao EB (2006) Identification of alkyl carbazoles and alkyl benzocarbazoles in Brazilian petroleum derivatives. *J Chromatogr* 186. <https://doi.org/10.1016/j.chroma.2005.11.001>
- Porter DJ, Mayer PM, Fingas MF (2004) Analysis of petroleum resins using electrospray ionization tandem mass spectrometry. *Energy Fuel*:987–996. <https://doi.org/10.1021/ef0340099>
- Quadros DPC, Chaves ES, Lepri FG, Borges DLG, Welz B, Becker-Ross H, Curtius AJ (2010) Evaluation of Brazilian and Venezuelan Crude oil samples by means of the simultaneous determination of Ni and V as their total and non-volatile fractions using high-resolution continuum source graphite furnace atomic absorption spectrometry. *Energy Fuel*:5907–5916. <https://doi.org/10.1021/ef100148d>
- Rodgers RP, Marshall AG (2007) *Petroleomics: advanced characterization of petroleum-derived materials by Fourier transform ion cyclotron resonance mass spectrometry (FT-ICR MS)*, Chapter 3. In: *Asphaltenes, heavy oils and petroleomics*. Springer Publications, New York, pp 63–78
- Speight JG (2015) *The chemistry and technology of petroleum*, 5th edn. CRC Press, Boca Raton
- Tomczyk NA, Winans RE, Shinn JH, Robinson RC (2001) On the nature and origin of acidic species in petroleum. 1. Detailed acid type distribution in a California crude oil. *Energy Fuel*:1498–1506. <https://doi.org/10.1021/ef010106v>
- Verchueren K (2001) *Handbook of environmental data on organic chemicals*. Wiley, New York
- Von Muehlen C, de Oliveria EC, Zini CE, Caramao EB, Mariott PJ (2010) Characterization of nitrogen-containing compounds in heavy gas oil petroleum fractions using comprehensive two-dimensional gas chromatography coupled to time-of-flight mass spectrometry. *Energy Fuel* 3572. <https://doi.org/10.1021/ef1002364>
- Wang Z, Brown C (2008) Chemical fingerprinting of petroleum hydrocarbons, Chapter 3. In: *Environmental forensic investigation*. CRC Press, New York, pp 43–115
- Wang Z, Fingas M, Li K (1993) Fractionation of ASMB oil and identification and quantitation of aliphatic, aromatic and biomarker compounds by GC/FID and GC/MS. In: *Proceedings of the Arctic and Marine oilspill program technical seminar*, pp 11–30.

- Wang Z, Hollebone BP, Fingas M, Fieldhouse B, Sigouin L, Landriault M, Smith P, Noonan J, Thouin G (2003) Characteristics of spilled oils, fuels and petroleum products: 1. Composition and properties of selected oils. Environment Canada, Ottawa
- Wang Z, Hollebone BP, Yang C, Fieldhouse B, Fingas M, Landriault M (2004) Oil composition and properties for oil spill modelling. Environment Canada, Ottawa
- Yalkowsky SH, He Y, Jain P (2010) Handbook of aqueous solubility data. CRC Press, Boca Raton
- Zhang Y, Xu C, Shi Q, Zhao S, Chung KH, Hou D (2010) Tracking neutral nitrogen compounds in subfractions of crude oil obtained by liquid chromatography separation using negative-ion electrospray ionization Fourier transform ion cyclotron resonance mass spectrometry. Energy Fuel:6321–6330. <https://doi.org/10.1021/ef1011512>



Gas Hydrates: Formation, Structures, and Properties

3

Judith Maria Schicks

Contents

1	Introduction	82
2	Structure and Composition	83
3	Hydrate Formation Processes	85
3.1	Hypothesis of the Nucleation at the Interface	85
3.2	Labile Cluster Nucleation Hypothesis	85
3.3	Local Structuring Nucleation Hypothesis	87
3.4	Hydrate Growth	87
3.5	Hydrate Formation in Nature: Effects of Sediments	89
4	Thermodynamic Properties of Simple and Mixed Hydrates	90
5	Research Needs	92
	References	93

Abstract

In this chapter, the characteristics of clathrate hydrates of natural gases, generally called gas hydrates, will be presented. After an introduction to hydrate structures, which have been verified in nature as well as the associated hydrate formers, the phase diagrams exhibiting the stability fields and thermodynamic properties of these natural systems depending on their composition will be discussed. Natural gas hydrates are methane-rich but may also contain CO₂, H₂S, and other hydrocarbons and hence vary in their thermodynamic properties.

Different models regarding the formation and growth processes, including kinetics with respect to heat and mass transfer effects, experimental observations

J. M. Schicks (✉)

GFZ German Research Centre for Geosciences, Potsdam, Germany

e-mail: schick@gfz-potsdam.de; judith.schicks@gfz-potsdam.de

© Springer Nature Switzerland AG 2020

H. Wilkes (ed.), *Hydrocarbons, Oils and Lipids: Diversity, Origin, Chemistry and Fate*, Handbook of Hydrocarbon and Lipid Microbiology,

https://doi.org/10.1007/978-3-319-90569-3_2

81

regarding the cage occupancy during the formation process as well as the influence of sediments and pore water salinity will be presented and discussed.

1 Introduction

Gas hydrates are ice-like, nonstoichiometric, crystalline solids composed of a three-dimensional network of hydrogen-bonded water molecules enclosing gas molecules in defined cavities of different sizes. The (nonpolar) gas molecules in turn prevent the water cages from collapsing (e.g., von Stackelberg 1949, Sloan 1998, and literature within). From a chemical point of view, gas hydrates are assigned to inclusion compounds or clathrates. The required conditions for hydrate formation are elevated pressures, low temperatures, and sufficient amounts of gas and water. In general, these conditions are given at the seafloor and in permafrost regions, but they may also occur in pipelines. In nature, gas hydrate deposits could be verified worldwide (e.g. Cherskiy et al. 1985; Dallimore et al. 1999; Kvenvolden and Lorenson 2001; Suess et al. 2001 – see also ► [Chap. 24, “Gas Hydrates as an Unconventional Hydrocarbon Resource”](#)).

Natural gas hydrates encase predominantly methane, but also higher hydrocarbons as well as CO_2 and H_2S . Depending on the source of the feed gas, the amount of additional gases besides methane varies from less than 1 mol% to more than 40 mol% (Kvenvolden and Lorenson 2001; Lu et al. 2011). Investigations on hydrocarbon gases in natural gas hydrates with respect to the carbon-isotopic ($\delta^{13}\text{C}$) composition provide data for the interpretation of the origin of these gases. Analyses of marine gas hydrates show that most of these samples have a carbon-isotopic composition of methane lighter than -60% (relative to the PeeDee Belemnite standard), indicating a microbial methane origin. It is very likely that this microbial methane is a product of CO_2 reduction from organic matter to methane as a result of methanogenic processes occurring in shallow sediments (Kvenvolden 1995; Kvenvolden and Lorenson 2001). A carbon-isotopic composition above -50% and the occurrence of higher hydrocarbons such as ethane or propane in the hydrate indicate a predominantly thermogenic gas origin (Bernard et al. 1976; Schoell 1988). These gases result from thermal decomposition of organic matter in sediment depths generally greater than 1000 m. H_2S , which is occasionally incorporated in marine gas hydrates occurring in shallow sediments above the SMI (sulfate-methane interface), is locally produced here by the reduction of sulfate via anaerobic oxidation of methane (AOM) as a result of a complex interaction of microbes which use the sulfate to oxidize the methane anaerobically (Kastner et al. 1998; Barnes and Goldberg 1976; Zehnder and Brock 1979; Boetius et al. 2000).

The composition of the feed gas determines the structure and composition and thus the thermodynamic properties of the resulting hydrate phase. The feed gas composition also influences the hydrate formation process and its kinetics. This will be discussed in detail in the following paragraphs.

2 Structure and Composition

Simple methane hydrates as well as complex mixed hydrates alone or as coexisting phases with different composition and structures have been recovered from natural samples (Sloan and Koh 2008, and literature within). Three hydrate structures have been confirmed in these natural gas hydrate samples: the cubic structures I (sI) and II (sII) and the hexagonal structure H (sH). Structures I and II were already described in 1951 and 1952 by von Stackelberg and Müller, whereas structure H was identified 35 years later by Ripmeester and co-workers (von Stackelberg and Müller 1951; Müller and von Stackelberg 1952; Ripmeester et al. 1987). All structures are composed of various kinds of cages as shown in Table 1.

In structure I, two small pentagonal dodecahedrons (5^{12}) are combined with six tetrakaidecahedrons ($5^{12}6^2$) into a unit cell. The pentagonal dodecahedron consists of 20 water molecules forming a 12-sided cavity which has pentagonal faces with equal angles and edge length. It is the smallest cavity type with an average radius of 0.39 nm and part of all hydrate structures. The tetrakaidecahedron combines 12 pentagons with 2 hexagons, and, therefore, the radius of these cavities increases to 0.433 nm (McMullan and Jeffrey 1965; Sloan 1998).

A unit cell of structure II consists of 16 pentagonal dodecahedrons (5^{12}) and 8 hexakaidecahedrons ($5^{12}6^4$). The latter cage combines 12 pentagonal faces with 4 hexagonal faces and has a radius of about 0.473 nm (Mak and McMullan 1965; Sloan 1998) (see also Fig. 1).

Structure H is the only structure containing a cavity with three square faces in addition to pentagonal and hexagonal faces ($4^35^66^3$). The combination of three pentagonal dodecahedrons (5^{12}), two irregular dodecahedrons ($4^35^66^3$), and one icosahedron $5^{12}6^8$, which is the largest cavity (average radius 0.579 nm), forms the characteristic unit cell of structure H (Ripmeester et al. 1987; Sloan 1998).

The formed structure depends – among others – on the composition of the feed gas, namely, the size of the enclathrated gas molecules: small guest molecules, such as nitrogen or oxygen, form structure II hydrates with both large and small cavities being filled. Slightly larger guest molecules such as methane, CO₂, or H₂S form structure I hydrates, with partial filling of the small cavities, whereas larger molecules such as propane form structure II hydrates with small cavities being empty. Even larger molecules such as 2,2-dimethylbutane (neohexane) form structure H hydrates in the presence of a supporting gas that fills smaller cavities of the structure (e.g., methane). However, in the presence of a gas mixture, the relationship between

Table 1 Number of cavities per unit cell for different gas hydrate structures (Sloan 1998)

	Cavities				
	5^{12}	$5^{12}6^2$	$5^{12}6^4$	$4^35^66^3$	$5^{12}6^8$
Structure I	2	6	–	–	–
Structure II	16	–	8	–	–
Structure H	3	–	–	2	1

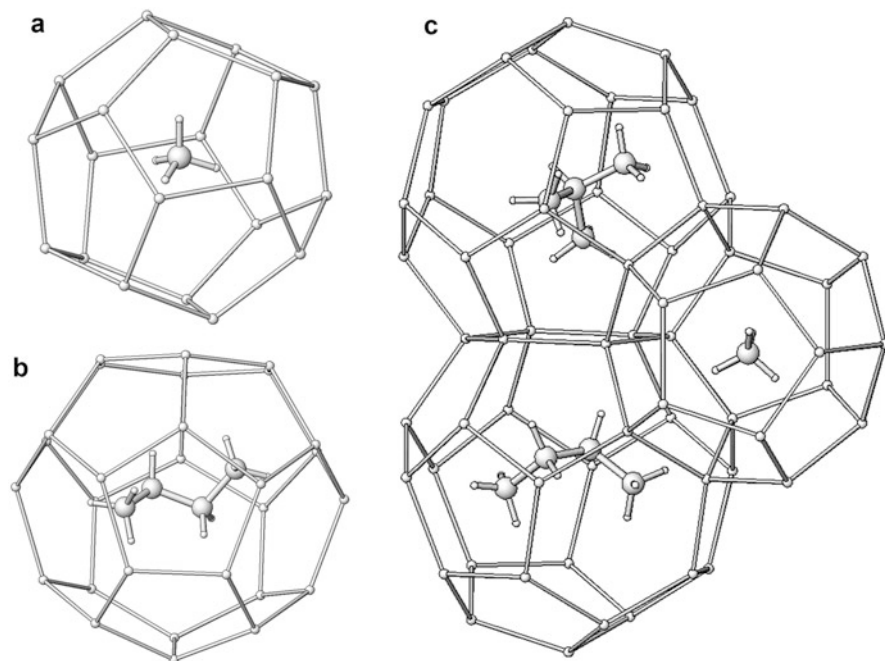


Fig. 1 Variety of hydrate cavities; (a) Pentagonal dodecahedron 5^{12} occupied with a methane molecule. (b) Hexakaidecahedron $5^{12}6^4$ occupied with a *n*-butane molecule. (c) Combination of two hexakaidecahedron $5^{12}6^4$ occupied with *n*-butane and *iso*-butane molecules, respectively, and a pentagonal dodecahedron 5^{12} occupied with a methane molecule. (Modified from Luzi et al. 2008)

structure and size is not always straightforward. Gas molecules which individually form structure I hydrates may form structure II in a mixture, as has been demonstrated for methane-ethane hydrates in certain proportions (Subramanian et al. 2000).

All three structures have been confirmed on natural hydrate samples (Sloan and Koh 2008, and literature within). Structure I CH₄ hydrates with very little amounts of additional gases such as CO₂ or H₂S are the most common species. In 2007, oceanic gas hydrates on the Cascadian margin were investigated for the first time in situ using Raman spectroscopy. They have also been identified as structure I hydrates containing predominately methane (Hester et al. 2007). A more complex hydrate, composed of coexisting structure II and structure H hydrate, has been identified in a sample from the Barkley Canyon on the northern Cascadian margin. Surprisingly, the samples contain, besides methane and other lighter hydrocarbons, some molecules which were not known as hydrate formers before, such as *n*-pentane and *n*-hexane. For the first time, these hydrate structures and compositions could be verified directly using powder X-ray diffraction and solid-state ¹³C NMR (Lu et al. 2007). The coexistence of hydrate phases with different structures and compositions could also be confirmed at the Chapopote Knoll, southern Gulf of Mexico. Raman spectroscopic and X-ray diffraction measurements on the recovered gas hydrate indicated the coexistence of a structure I CH₄-C₂H₆ hydrate in addition to a

complex structure II hydrate containing C₂ through C₄ hydrocarbons besides CH₄ (Klapp et al. 2010).

3 Hydrate Formation Processes

Hydrate formation can be specified as hydrate nucleation as the first step and hydrate growth as the second step. The nucleation process can be defined as a microscopic process involving tens of thousands of molecules which first form small clusters and then further develop into hydrate nuclei. By the time these small nuclei obtain a critical size, a continuous hydrate growth process starts. Three different hypotheses for hydrate nucleation are discussed here: the labile cluster nucleation hypothesis, the nucleation at the interface hypothesis, and the local structuring hypothesis.

3.1 Hypothesis of the Nucleation at the Interface

The *hypothesis of the nucleation at the interface* was presented by Rodger (1990) and Kvamme (1996). It suggests the transportation of the gas molecules to the water-gas interface, where the gas molecules are adsorbed at the aqueous surface and diffuse to a suitable location. At this location, the gas molecules will be enclathrated into the cavity, formed from water molecules. These cavities either agglomerate or grow by the addition of gas and water molecules into the vapor side of the interface. The general observation of the formation of a hydrate film at the interface between gas and an aqueous phase, for example, during a methane hydrate formation process, may support this hypothesis on the one hand. On the other hand, it is probably not a satisfying concept for those hydrates with a higher density compared to the density of water. Those hydrates show a preferential nucleation and growth on the subsurface which could be observed, for example, for CO₂ – SO₂ hydrates (Beeskow-Strauch et al. 2011). The labile cluster model presented in the following shows a higher universal validity since it can be applied for hydrate nucleation processes with or without a free gas or liquid phase of the guest molecule.

3.2 Labile Cluster Nucleation Hypothesis

The *labile cluster nucleation hypothesis* was first presented by Sloan and Fleyfel (1991) for the formation of hydrates from gas and ice and modified and extended by Christiansen and Sloan (1994): It starts with the presumption that the molecules of pure water without any dissolved gas molecules form labile ring structures of pentamers and hexamers. This assumption is supported by Ludwig who could show by means of ab initio calculations that besides tetrahedrally coordinated water molecules, ring structures in the pure liquid water phase are very likely (Ludwig 2007). According to Christiansen and Sloan, these labile water rings will construct labile clusters around gas molecules after gas is dissolved in the water phase. The

coordination number of the water molecules depends on the size of the guest molecules, e.g., 20 water molecules surrounding 1 CH₄ molecule, whereas 24 water molecules surround 1 C₂H₆ molecule, and 28 water molecules cover 1 C₃H₈ molecule. The clusters of the dissolved species combine to form unit cells. For the formation of a unit cell, the coordination number of the water molecules surrounding the dissolved gas molecules has to be changed. This transformation of the cluster coordination number of the water molecules needs activation energy, and therefore this step becomes a barrier in the formation process (Christiansen and Sloan 1994). The approach of the labile cluster nucleation hypothesis was developed further by Walsh et al. (2009) who modeled with direct molecular dynamics simulations the spontaneous nucleation and growth of CH₄ hydrate. Walsh and co-workers could show nucleation steps similar to the labile cluster hypothesis: pentagonal faces of water molecules exist in the water phase and arrange close to a dissolved CH₄ molecule and partial cages form around the CH₄ molecule. Small cavities (coordination number of water molecules is 20) form around a methane molecule, and additional CH₄ molecules and partial water cages try to attach. The early cages are mostly face-sharing partial small cages, favoring structure II. An extended growth of these partial cavities into face-sharing pentagonal dodecahedrons around the central pentagonal dodecahedron is now hindered by steric constraints. Therefore, the coordination number of the water molecules has to be changed to build a unit cell of structure I with well-defined cavities. An interesting outcome of this study is the formation of uncommon 5¹²6³ cavities during the formation process, which was already suggested by Vatamanu and Kusalik (2006). This cavity type is not part of any final hydrate structure but may act as some kind of transition state toward the formation of large cavities of structure I (5¹²6²) and structure II (5¹²6⁴), respectively. The 5¹²6³ cavity seems to form as a link to promote the growth of the thermodynamically preferred structure I hydrate phase from the kinetically preferred structure II hydrate phase which was formed initially (Walsh et al. 2009; Vatamanu and Kusalik 2006). Jacobson et al. described the nucleation of clathrate hydrates from various guest molecules also using molecular dynamics simulations as a multistep mechanism. They observed the formation of so-called “blobs” which can be understood as large analogues of the labile clusters proposed by Christiansen and Sloan (Jacobson et al. 2010a; Christiansen and Sloan 1994). These “blobs” persist in the aqueous solution and consist of gas molecules separated by half-cages of water molecules. After becoming a critical nucleus, the water molecules of the “blob” order to hydrate cavities. The nucleus recruits more gas and water molecules from the solution, resulting in an amorphous clathrate hydrate nucleus. Within the amorphous nucleus, the water molecules are locally ordered, but the gas molecules do not show the necessary order for a crystalline hydrate structure. In a third step, the amorphous clathrate nuclei rearrange to form a crystalline hydrate with elements of both, structure I and structure II (Jacobson et al. 2010b). In situ Raman spectroscopic investigations on CH₄ hydrate and mixed hydrates during the formation process may support the labile cluster hypothesis in general and in particular the formation of an amorphous hydrate phase (e.g., Subramanian and Sloan 1999; Uchida et al. 2000; Schicks and Luzi-Helbing 2013). Even though the nucleation process itself is very short comprising a few micro seconds and thus

cannot be detected by Raman spectroscopy, it could be shown that during the initial stages of hydrate formation pentagonal dodecahedrons 5^{12} of structure I are formed preferentially and that the formation of tetrakaidecahedrons $5^{12}6^2$ may be the rate-limiting factor (Subramanian and Sloan 1999; Uchida et al. 2000). Time-resolved Raman spectroscopic investigations on the formation of mixed hydrates also clearly show the incorporation of CH_4 into pentagonal dodecahedrons 5^{12} as a first step during the initial hydrate formation process, whereas the formation of all other cavity types occurs later. This could also be observed for all investigated systems, regardless of these cavities being occupied with CH_4 or larger molecules, such as CO_2 , H_2S , C_3H_8 , 2-methylpropane, or 2-methylbutane (Schicks and Luzzi-Helbing 2015).

3.3 Local Structuring Nucleation Hypothesis

The *local structuring nucleation hypothesis* is based on the Landau free energy calculations performed by Radhakrishnan and Trout (2002). These calculations for carbon dioxide hydrate nucleation at the water-liquid carbon dioxide interface lead to the assumption that a group of CO_2 molecules arrange in a configuration similar to that in the hydrate phase. This causes a local order of the surrounding water molecules which is different from that in the bulk water phase. If the number of CO_2 molecules in this arrangement with a local order exceeds that of a critical hydrate nucleus, the formation of a hydrate nucleus starts.

3.4 Hydrate Growth

After the small hydrate nuclei obtain a critical size, a continuous hydrate growth starts. Regarding the hydrate growth, three important aspects have to be considered: the transportation of gas and water molecules (mass transfer), the kinetics of the hydrate growth process, and – due to the fact that hydrate formation is an exothermic process – the heat transfer away from the reaction (growth) site. The clathrate hydrate growth model presented by Englezos et al. (1987) is based on mass transfer theories. It describes the growth of the hydrate as a three-step process. The first step is the transport of the gas molecule into the liquid phase, the second step is the diffusion of the gas molecule through a stagnant liquid diffusion layer which surrounds the hydrate particle, and the last step is the incorporation of the gas molecule into the structured water framework of the hydrate particle, in the so-called “reaction” layer. Due to the fact that a concentration gradient of the gas molecules in the stagnant liquid layer is not allowed, the diffusion rate of the gas molecule through the stagnant liquid layer and the incorporation rate of the gas molecule into the hydrate structure are equal at steady state. In this context, it should be noted that the solubility of gases varies. CO_2 and H_2S , for example, show a much better solubility in water than CH_4 , resulting in a higher concentration of these gases in the liquid phase. A higher concentration of CO_2 or H_2S in the aqueous phase again results in an

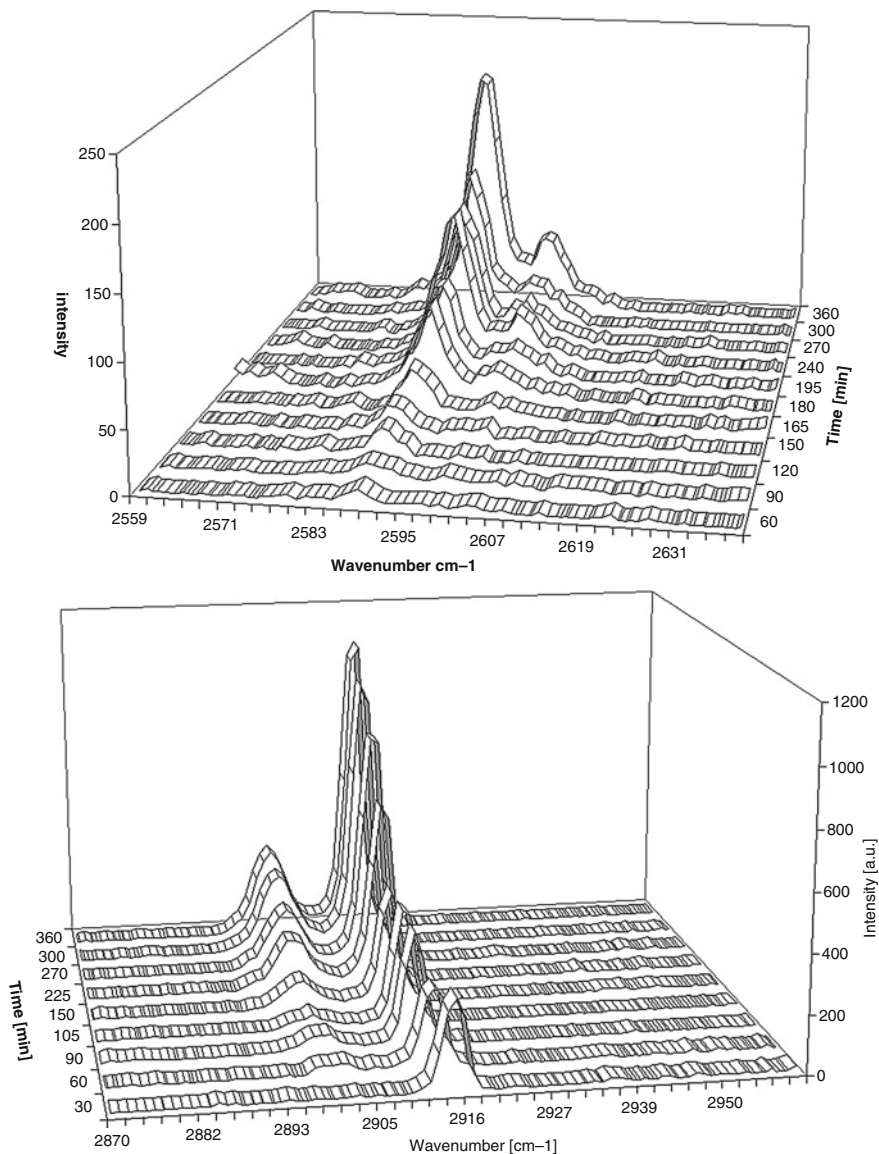


Fig. 2 Above: Real-time Raman spectra monitoring the incorporation of H₂S in large 5¹²6² (2592 cm⁻¹) and small 5¹² (2602 cm⁻¹) cavities of structure I H₂S-CH₄ hydrate. Below: Real-time Raman spectra monitoring the incorporation of CH₄ in large 5¹²6² (2903 cm⁻¹) and small 5¹² (2916 cm⁻¹) cavities of a mixed structure I H₂S-CH₄ hydrate

enrichment of these gases in the hydrate phase (Schicks and Luzi-Helbing 2015). In this context, a clear preference of the guest molecules regarding formation and occupancy of cavities could also be shown. The Raman spectra in Fig. 2 indicate a preferred incorporation of H₂S into tetrakaidecahedrons 5¹²6² during the initial

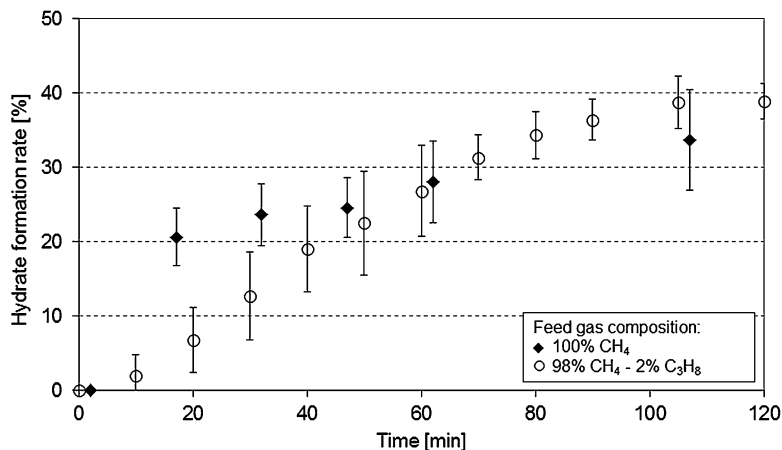


Fig. 3 Transformation rates of ice into hydrate over time. The results indicate that the formation of CH₄ hydrate is faster during the first 40 min compared to the formation rate of CH₄-C₃H₈ hydrate

stages of hydrate formation, whereas CH₄ is preferentially incorporated into dodecahedrons 5¹² of structure I (Schicks et al. 2008). The observed cage occupancies with methane or H₂S during the initial stages of hydrate formation do not correspond to those of the hydrate phase at equilibrium conditions.

The presence of additional gases besides CH₄ in the feed gas affects the hydrate formation kinetics. The formation of a simple CH₄ hydrate seems to be preferred compared to the formation of a mixed hydrate. This could be shown for mixed hydrate containing C₃H₈ or *iso*-C₄H₁₀ besides CH₄. Figure 3 shows the transformation rates of ice into simple CH₄ or a mixed CH₄-C₃H₈ hydrate over time. The results indicate that the formation of CH₄ hydrate is faster during the first 40 min compared to the formation rate of CH₄-C₃H₈ hydrate (Schicks and Luzi-Helbing 2015).

Uchida et al. (1999) presented a model focusing on heat transfer which describes the formation of a hydrate film at the water-liquid carbon dioxide interface. They observed the primary nucleation at the interface and occasionally a secondary nucleation on the primary film. However, the propagation rate was temperature-dependent which indicates that the heat diffusion is a restrictive factor. The model was recently modified and generalized by Mochizuki and Mori (2006) describing a heat-transfer-controlled lateral growth of a hydrate film at the interface between liquid water and an immiscible hydrate-forming fluid.

3.5 Hydrate Formation in Nature: Effects of Sediments

Regarding gas hydrate formation in nature, it is questionable if a hydrate-forming fluid phase – e.g., a free gas phase – is available. In the absence of a free gas phase, the formation of gas hydrates is limited to the availability of dissolved gas molecules. Furthermore, the presence of sediments and their influence on the hydrate formation

process has to be considered when modeling hydrate formation processes. Recent studies show that not only the presence of particles is favorable for gas hydrate formation but that the particle size has an effect on the gas hydrate formation kinetics: A high concentration of fine grains ($<125\ \mu\text{m}$) led to an explicitly faster gas hydrate formation compared to medium or coarse sands (Heeschen et al. 2016).

For the estimation of stabilization effects of gas hydrates on continental slopes, it is necessary to know how and where hydrate forms in the sediments. In the case of hydrate particle formation in contact with sediment grains, the hydrate phase may interact as cement, and a hydrate saturation of less than 3% may already result in a stabilizing effect (Bernabé et al. 1992). Recent studies showed that the formation process of hydrates in sediments strongly depends on the water content and the absence or presence of a free gas phase. Klapproth et al. (2007) showed that hydrates between sediment (quartz) grains behave like cement in the presence of a free gas phase and with a water content of 10–17 wt%. However, other authors describe hydrate growth without any contact to the sediment grains (pore filling) when the water content is high both in presence of a free gas phase (Tohidi et al. 2001) and in absence of a free gas phase (Schicks et al. 2007; Spangenberg et al. 2015).

4 Thermodynamic Properties of Simple and Mixed Hydrates

The thermodynamic properties of a hydrate phase describe the phase behavior including stability fields and decomposition conditions as well as metastable states and transition processes. In particular, the stability field of a hydrate phase depends on its composition. Gas hydrates, containing N_2 besides CH_4 , are less stable than pure CH_4 hydrates: the stability field of these hydrates is shifted to higher pressures and lower temperatures compared to the stability conditions of pure methane hydrates (Jhaveri and Robinson 1965). In contrast, mixed gas hydrates containing H_2S , CO_2 , or higher hydrocarbons such as C_3H_8 besides CH_4 show a larger stability field compared to simple CH_4 hydrates. An optimal interaction between the size and shape of the guest molecule on the one hand and the size and form of the cavity on the other hand seems to enhance the stability of the resulting hydrate phase. Experimental data presented in Fig. 4 show that the stability fields of these mixed hydrates are shifted to lower pressures and higher temperatures. The experimental data are in good agreement with calculated data (e.g., using CSMGem, Sloan and Koh 2008).

Investigations on mixed gas hydrates containing small amounts of C_3H_8 (less than 5 vol% C_3H_8 besides CH_4 in the feed gas) reveal an interesting phase behavior in the course of a transformation process as pressure and temperature conditions approach the decomposition line of pure CH_4 hydrate (Schicks et al. 2006). During this transformation process, a simultaneous formation and decomposition of hydrate crystals was observed. Additionally, the morphology of the system changed from larger euhedral crystals to a foamy fine crystal mass. Raman

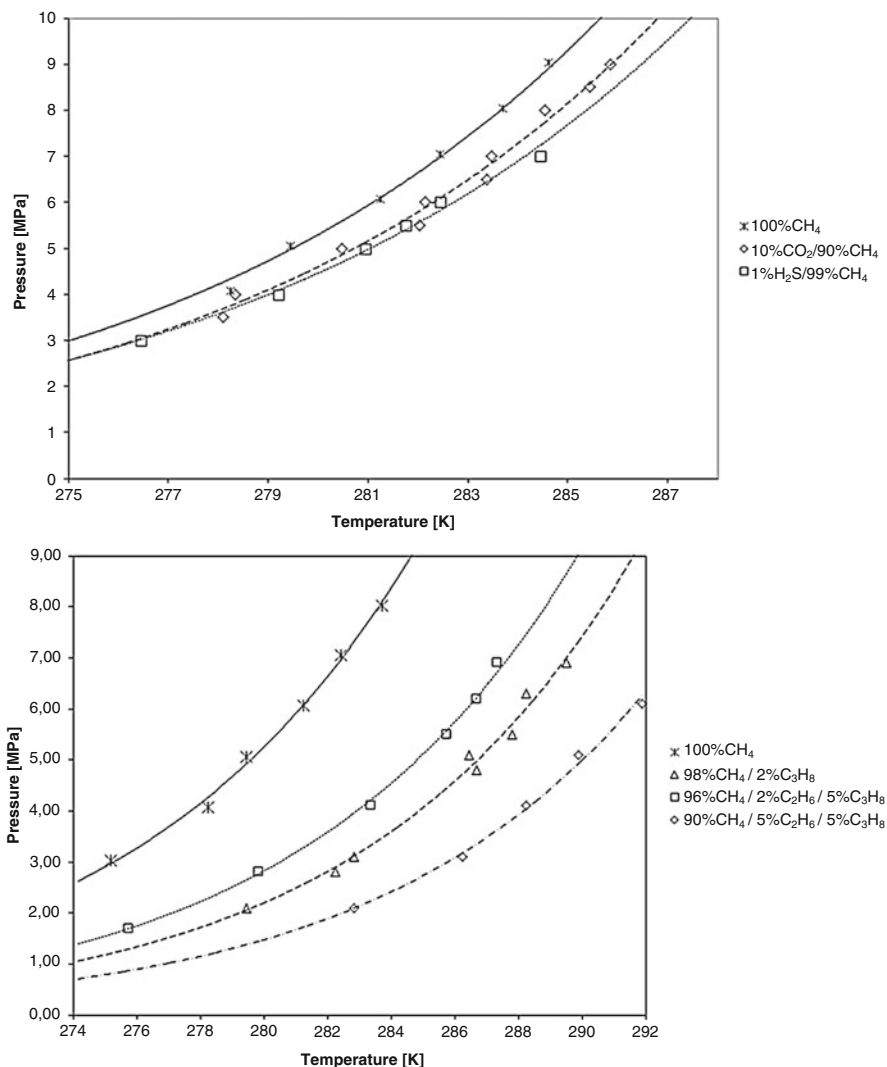


Fig. 4 P-T diagrams based on experimental data presenting the stability fields of methane hydrate and mixed hydrates. The diagram above shows the stability fields for pure methane hydrate versus CO₂-CH₄ and H₂S-CH₄ hydrates. The diagram below shows the stability fields of pure methane hydrate versus CH₄-C₃H₈ and CH₄-C₂H₆-C₃H₈ hydrates. Independent from structure I or structure II formers, the decomposition conditions for the mixed hydrates are shifted to lower pressures and higher temperatures compared to pure methane hydrate

spectroscopic and X-ray diffraction measurements indicate that the formation and decomposition of structure I hydrate in coexistence with structure II CH₄-C₃H₈ hydrate are characteristic. The process could be observed by passing over the defined pressure and temperature conditions (transformation conditions) in both

directions. This observation does not describe an equilibrium state but indicates kinetic preference versus thermodynamic factors. The excess supply of CH_4 compared to C_3H_8 in the aqueous solution on the one hand and the kinetic preference of CH_4 hydrate formation compared to the mixed hydrate formation on the other hand may result in the formation of a CH_4 hydrate phase besides the mixed hydrate phase, although the mixed hydrate phase should be thermodynamically preferred. In case formation of CH_4 hydrate starts at temperature and pressure conditions close to (but out of) the CH_4 hydrate stability field, the formed crystals are unstable and decompose immediately. If the CH_4 hydrate formation occurs at temperature and pressure conditions within the CH_4 hydrate stability field, this metastable structure I CH_4 hydrate phase coexists besides the structure II mixed hydrate phase (Schicks et al. 2006). A coexistence of structure I CH_4 hydrate and structure H CH_4 -iso- C_5H_{12} mixed hydrate could also be observed when studying the hydrate formation from a gas mixture containing 1% 2-methylbutane in CH_4 (Schicks and Luzi-Helbing 2015). As mentioned before, the coexistence of hydrates with different structures and compositions could also be proven in nature, e.g., in gas hydrate samples from the Cascadia margin with coexisting structure II and structure H hydrate phases (Lu et al. 2007).

In addition to the composition of the gas hydrate, the presence of sediment may also affect their stability conditions. Several experiments show a shift of gas hydrate equilibrium toward higher pressure and lower temperature in the presence of small particles, such as clays, silica sand, and glass beads, and in accordance with the salinity of the pore water (e.g., Uchida et al. 2004; Østergaard et al. 2002). However, the interaction between the sediment and the hydrate seems to be quite complex and does not only depend on the grain size but also on the mineral composition (Heeschen et al. 2016).

5 Research Needs

Before gas hydrates were discovered in natural environments, they were recognized as a problem in natural gas pipelines due to the formation of undesirable hydrate plugs. Therefore, laboratory investigations on hydrate formation and decomposition conditions were performed before the first hydrate deposit in the Messoyakha field was discovered in 1967 (Sloan 1998). However, the results of laboratory and field studies are documented in a huge amount of publications. Nevertheless, there are still open questions in many areas of gas hydrate research, beginning at molecular level with the understanding of hydrate nucleation and growth processes. The formation of coexisting hydrate phases with different structures and compositions in a natural environment is not yet understood. Furthermore, as already mentioned the influence of sediments on gas hydrates and vice versa is still not sufficiently clarified. The formation of gas hydrates in nature is a very complex process and involves many aspects which have to be investigated systematically.

References

- Barnes RO, Goldberg ED (1976) Methane production and consumption in anoxic marine sediments. *Geology* 4:297–300
- Beeskow-Strauch B, Schicks JM, Naumann R, Erzinger J (2011) The influence of SO₂ and NO₂ impurities on CO₂ gas hydrate formation and stability. *Chem Eur J* 17:4376–4384
- Bernabé Y, Fryer DT, Hayes JA (1992) The effect of cements on the strength of granular rocks. *Geophys Res Lett* 19:1511–1514
- Bernard BB, Brooks JM, Sackett WM (1976) Natural gas seepage in the Gulf of Mexico. *Earth Planet Sci Lett* 31:48–54
- Boetius A, Ravensschlag K, Schubert CJ, Rickert D, Widdel F, Giesecke A, Amman R, Jørgensen BB, Witte U, Pfannkuche O (2000) A marine microbial consortium apparently mediating anaerobic oxidation of methane. *Nature* 407:623–626
- Cherskiy NV, Tsarev VP, Nikitin SP (1985) Investigations and predictions of conditions of accumulation of gas resources in gas-hydrate pools. *Pet Geol* 21:65–89
- Christiansen RL, Sloan ED (1994) Mechanisms and kinetics of hydrate formation. In: Sloan ED, Happel J, Hnatow MA (eds) International conference on natural gas hydrates, vol 715. New York Academy of Science, New Paltz, pp 283–305
- Dallimore SR, Uchida T, Collett TS (1999) Scientific results from JAPAX/JNOC/GSC Mallik 2L-38 gas hydrate research well, Mackenzie Delta, Northwest Territories, Canada. *Geol Surv Canada Bull* 544:295–311
- Englezos P, Kalogerakis N, Dholabhai PD, Bishnoi PR (1987) Kinetics of formation of methane and ethane gas hydrates. *Chem Eng Sci* 42:2647–2658
- Heeschen K, Schicks JM, Oeltzschner G (2016) The promoting effect of natural sand on methane hydrate formation: grain sizes and mineral composition. *Fuel* 181:139–147
- Hester KC, Dunk RM, White SN, Brewer PG, Peltzer ET, Sloan ED (2007) Gas hydrate measurements at hydrate ridge using Raman spectroscopy. *Geochim Cosmochim Acta* 71:2947–2959
- Jacobson LC, Hujo W, Molinero V (2010a) Amorphous precursors in the nucleation of clathrate hydrates. *J Am Chem Soc* 132:11806–11811
- Jacobson LC, Hujo W, Molinero V (2010b) Nucleation pathways of clathrate hydrates: effects of guest size and solubility. *J Phys Chem B* 114:13796–13807
- Jhaveri J, Robinson DB (1965) Hydrates in the methane-nitrogen system. *Can J Chem Eng* 43:75–78
- Kastner M, Kvenvolden KA, Lorenson TD (1998) Chemistry, isotopic composition, and origin of a methane-hydrogen sulfide hydrate at the Cascadia subduction zone. *Earth Planet Sci Lett* 156:173–183
- Klapp SA, Murshed MM, Pape T, Klein H, Bohrmann G, Brewer PG, Kuhs WF (2010) Mixed gas hydrate structures at the Chapopote Knoll, southern Gulf of Mexico. *Earth Planet Sci Lett* 299:207–217
- Klapproth A, Techmer KS, Klapp SA, Murshed MM, Kuhs WF (2007) Microstructure of gas hydrates in porous media. In: Kuhs WF (ed) *Physics and chemistry of ice*. RSC Publishing, Cambridge, UK, pp 321–328
- Kvamme B (1996) A new theory for kinetics of hydrate formation. In: *Proceedings of the 2nd international conference on natural gas hydrates*, June 2–6, Toulouse, pp 139–146
- Kvenvolden KA (1995) A review of the geochemistry of methane in natural gas hydrate. *Org Geochem* 23:997–1008
- Kvenvolden KA, Lorenson TD (2001) The global occurrence of natural gas hydrate. In: Paull CK, Dillon WP (eds) *Natural gas hydrates: occurrence, distribution, and detection*. American Geophysical Union, Washington, DC, pp 3–18
- Lu H, Seo Y, Lee J, Moudrakovski I, Ripmeester JA, Chapman NR, Coffin RB, Gardner G, Pohlman J (2007) Complex gas hydrate from Cascadia margin. *Nature* 445:303–306
- Lu Z, Zhu Y, Zhang Y, Wen H, Li Y, Liu C (2011) Gas hydrate occurrences in the Qilian Mountain permafrost, Qinghai province, China. *Cold Reg Sci Technol* 66(2):93–104

- Ludwig R (2007) The importance of tetrahedrally coordinated molecules for the explanation of liquid water properties. *ChemPhysChem* 8:938–943
- Luzi M, Schicks JM, Naumann R, Erzinger J, Udachin K, Moudrakowski I, Ripmeester JA, Ludwig R (2008) Investigations on the influence of guest molecule characteristics and the presence of multicomponent gas mixtures on gas hydrate properties. In: Proceedings of the 6th international conference on gas hydrates, Vancouver
- Mak TCW, McMullan RK (1965) Polyhedral clathrate hydrates. X. Structure of the double hydrate of tetrahydrofuran and hydrogen sulfide. *J Chem Phys* 42:2732–2737
- McMullan RK, Jeffrey GA (1965) Polyhedral clathrate hydrates. IX. Structure of ethylene oxide hydrate. *J Chem Phys* 42:2725–2732
- Mochizuki T, Mori YH (2006) Clathrate-hydrate film growth along water/hydrate-former phase boundaries – numerical heat-transfer study. *J Cryst Growth* 290:642–652
- Müller HR, von Stackelberg M (1952) Zur Struktur der Gashydrate – 2. *Mitt Naturwissenschaften* 39:20–21
- Østergaard KK, Anderson R, Llamedo M, Tohidi B (2002) Hydrate phase equilibria in porous media: effect of pore size and salinity. *Terra Nova* 14:307–312
- Radhakrishnan R, Trout BL (2002) A new approach for studying nucleation phenomena using molecular simulations: application to CO₂ hydrate clathrates. *J Phys Chem* 117:1786–1796
- Ripmeester JA, Tse JS, Ratcliffe CI, Powell BM (1987) A new clathrate hydrate structure. *Nature* 325:135–136
- Rodger PM (1990) Stability of gas hydrates. *J Phys Chem* 94:6080–6089
- Schicks JM, Luzi-Helbing M (2013) Cage occupancy and structural changes during hydrate formation from initial stages to resulting hydrate phase. *Spectrochim Acta, Part A* 115:528–536
- Schicks JM, Luzi-Helbing M (2015) Kinetic and thermodynamic aspects of clathrate hydrate nucleation and growth. *J Chem Eng Data* 60:269–277
- Schicks JM, Naumann R, Erzinger J, Hester K, Koh CA, Sloan ED (2006) Phase transitions in mixed gas hydrates: experimental observations versus calculated data. *J Phys Chem B* 110:11468–11474
- Schicks JM, Luzi M, Erzinger J, Spangenberg E (2007) Clathrate hydrate formation and growth: experimental data versus predicted behaviour. In: Kuhs WF (ed) *Physics and chemistry of ice*. RSC Publishing, Cambridge, UK, pp 537–544
- Schicks JM, Luzi M, Spangenberg E, Naumann R, Erzinger J (2008) Hydrate formation investigations and kinetic studies under various defined conditions. In: Proceedings of the 6th international conference on gas hydrates, Vancouver
- Schoell M (1988) Multiple origins of methane in the Earth. *Chem Geol* 71:1–10
- Sloan ED Jr (1998) *Clathrate hydrates of natural gases*. Marcel Dekker, New York
- Sloan ED Jr, Fleyfel F (1991) A molecular mechanism for gas hydrate nucleation from ice. *AIChE* 37:1281–1292
- Sloan ED Jr, Koh CA (2008) *Clathrate hydrates of natural gases*, 3rd edn. CRC Press Taylor and Francis Group, Boca Raton
- Spangenberg E, Priegnitz M, Heeschen K, Schicks JM (2015) Are laboratory-formed hydrate-bearing systems analogous to those in nature? *J Chem Eng Data* 60(2):258–268
- Subramanian S, Sloan ED (1999) Molecular measurements of methane hydrate formation. *Fluid Phase Equilibra* 158–160:813–820
- Subramanian S, Kini RA, Dec SF, Sloan ED (2000) Evidence of structure II hydrate formation from ethane + methane mixtures. *Chem Eng Sci* 55:1981–1999
- Suess E, Torres ME, Bohrmann G, Collier RW, Rickert D, Goldfinger C, Linke P, Heuser A, Sahling H, Heeschen K, Jung C, Nakamura K, Greinert J, Pfannkuche O, Trehu A, Klinkhammer G, Whiticar MJ, Eisenhauer A, Teichert B, Elvert M (2001) Sea floor methane hydrates at hydrate ridge, Cascadia margin. In: Paull CK, Dillon WP (eds) *Natural gas hydrates: occurrence, distribution, and detection*. American Geophysical Union, Washington, DC

- Tohidi B, Anderson R, Clennell MB, Burgass RW, Biderkab AB (2001) Visual observation of gas-hydrate formation and dissociation in synthetic porous media by means of glass micromodels. *Geology* 29:867–870
- Uchida T, Ebinuma T, Kawabata J, Narita H (1999) Microscopic observations of formation processes of clathrate-hydrate films at an interface between water and carbon dioxide. *J Cryst Growth* 204:348–356
- Uchida T, Okabe R, Mae S, Ebinuma T, Narita H (2000) In situ observation of methane hydrate formation mechanism by Raman spectroscopy. *Ann N Y Acad Sci* 912:593–601
- Uchida T, Takeya S, Chuvilin EM, Ohmura R, Nagao J, Yakushev VS et al (2004) Decomposition of methane hydrates in sand, sandstone, clays, and glass beads. *J Geophys Res Solid Earth* 109: B05206
- Vatamanu J, Kusalik PG (2006) Unusual crystalline and polycrystalline structures in methane hydrates. *J Am Chem Soc* 128:15588–15589
- von Stackelberg M (1949) Feste Gashydrate. *Naturwissenschaften* 36(11):327–333
- von Stackelberg M, Müller HR (1951) Zur Struktur der Gashydrate. *Naturwissenschaften* 38:456
- Walsh MR, Koh CA, Sloan ED, Sum AK, Wu DT (2009) Microsecond simulations of spontaneous methane hydrate nucleation and growth. *Science* 326:1095–1098
- Zehnder AJB, Brock TD (1979) Methane formation and methane oxidation by methanogenic bacteria. *J Bacteriol* 137:420–432

Part II

Hydrocarbons and Lipids in the Biosphere



Factors Controlling Carbon and Hydrogen Isotope Fractionation During Biosynthesis of Lipids by Phototrophic Organisms

Nikolai Pedentchouk and Youping Zhou

Contents

1	Introduction	100
2	Controls on Isotopic Fractionation	101
3	Algae	103
3.1	Algal Lipids	103
3.2	Carbon Isotopes in Algal Lipids	104
3.3	Hydrogen Isotopes in Algal Lipids	107
4	Higher Plants	109
4.1	Higher Plant Lipids	109
4.2	Carbon Isotopes in Higher Plant Lipids	110
4.3	Hydrogen Isotopes in Higher Plant Lipids	112
5	Research Needs	114
	References	116

Abstract

The analysis of carbon and hydrogen stable isotope ratios of lipids from natural products is an integral component of research in Earth sciences. The isotopic composition of lipids from algae and higher plants can be linked with various environmental parameters, which makes lipid biomarkers a rich source of information about biological, chemical, and physical processes in the environment. This chapter reviews the key external and internal factors that affect C and H isotopic fractionation during biosynthesis of lipids. Significant advances need to

N. Pedentchouk (✉)

School of Environmental Sciences, University of East Anglia, Norwich, UK

Institute of Plant Physiology, Russian Academy of Sciences, Moscow, Russia

e-mail: n.pedentchouk@uea.ac.uk

Y. Zhou

School of Chemistry and Chemical Engineering, Shaanxi University of Science & Technology, Xi'an, China

© Springer Nature Switzerland AG 2020

H. Wilkes (ed.), *Hydrocarbons, Oils and Lipids: Diversity, Origin, Chemistry and Fate*, Handbook of Hydrocarbon and Lipid Microbiology,

https://doi.org/10.1007/978-3-319-90569-3_37

be made to increase our level of understanding of the processes that control fractionation in different lipid groups and within individual lipid molecules.

1 Introduction

Over the past several decades, the analysis of carbon and hydrogen stable isotope compositions of lipids from natural products has become an integral component of research in biogeochemistry, Earth history, and petroleum exploration. The pioneering studies using compound-specific $^{13}\text{C}/^{12}\text{C}$ (Freeman et al. 1990; Hayes et al. 1990) and $^2\text{H}/^1\text{H}$ (Sessions et al. 1999; Sauer et al. 2001) analyses have shown the potential of this methodology to address a broad spectrum of research questions in various branches of Earth sciences (Evershed et al. 2007; Sachse et al. 2012; Sachs 2014; Sessions 2016; Diefendorf and Freimuth 2017; Pedentchouk and Turich 2017).

Lipids produced by photosynthesizing organisms serve several key metabolic and structural functions including the storage of energy and protection against dehydration and pathogens. Because of their recalcitrant nature, lipid biomarkers are among the most widely used geomolecules in organic geochemistry (Peters et al. 2005a, b). Lipids differ greatly in their chemical structure and complexity within and between terrestrial and aquatic organisms. In spite of these differences, however, ultimately, all lipids are generated from biosynthetic precursors that require inorganic sources of carbon and hydrogen, i.e., CO_2 and H_2O . The fact that the isotopic composition of lipids can incorporate information about various environmental parameters (e.g., the concentration and $^{13}\text{C}/^{12}\text{C}$ ratios of atmospheric CO_2 , $^2\text{H}/^1\text{H}$ ratios of meteoric H_2O , etc.) makes lipid biomarkers a rich source of information about present and past biological, chemical, and physical processes operating in the environment.

To get this information, the researcher needs to evaluate various pathways and mechanisms that affect carbon and hydrogen isotopes during assimilation, biosynthesis, and subsequent burial and transformation of an organic compound. The pathways and mechanisms will vary depending on the nature of investigation. For instance, studies dealing with biogeochemical and paleoclimatic investigations focus on extracting an environmental signal and disentangling it from physiological and metabolic processes that impact isotopic composition of lipids during biosynthesis (Fig. 1). The evaluation of $\delta^{13}\text{C}$ and $\delta^2\text{H}$ data of lipid biomarkers in petroleum exploration, however, has to take into account additional physicochemical processes that affect the isotopic composition of these compounds in the source rocks and petroleum during diagenesis and catagenesis (Fig. 1). In both cases, however, the initial isotopic composition of inorganic C and H sources, environmental conditions during biological assimilation, and biosynthetic and metabolic isotope effects are key factors that influence the isotopic composition of lipid biomarkers.

This chapter reviews the role of these factors on C and H isotopic compositions of lipids derived from phototrophic sources. A full description of the current state of knowledge regarding individual pathways and mechanisms that affect stable isotope

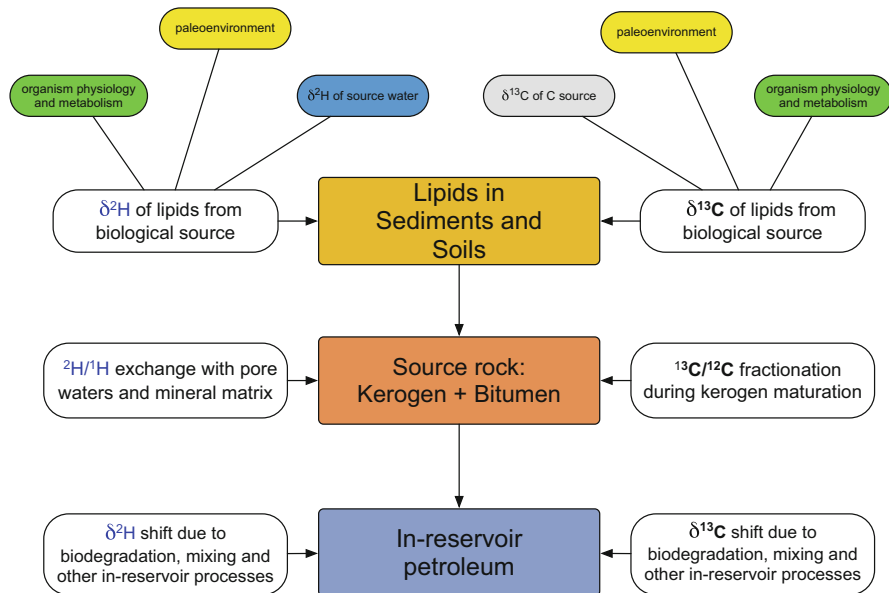


Fig. 1 The main factors controlling the carbon and hydrogen isotope composition of lipid biomarkers in sediments and petroleum systems

signatures of lipid biomarkers and their precursors is beyond the scope of this chapter. (Interested readers will be guided to key original and review publications.) Rather, the focus is on the broad picture that shows the hierarchy of controls on the isotopic composition of lipids derived from algal and higher plant sources.

2 Controls on Isotopic Fractionation

Depending on the nature of the depositional environment, sedimentary lipids can originate either from aquatic or terrestrial biota, or both. Algae exist in an aqueous environment and rely on CO_2 (aq) and/or HCO_3^- as their source of carbon. Higher plants, however, obtain water mainly from the soil and use atmospheric CO_2 . Additionally, while algae depend primarily on the availability of light and nutrients, higher terrestrial plants are very sensitive to water availability and ambient temperature. These different life habits result in significant differences in the nature of controls that affect the $\delta^{13}\text{C}$ and $\delta^2\text{H}$ values of lipid biomarkers during biosynthesis.

Broadly speaking, these controls can be classified as “external” and “internal” to the organism in which isotope fractionation takes place. Even if somewhat subjective, this division provides a framework for discussing these controls as well as for clarifying the link between the $\delta^{13}\text{C}$ and $\delta^2\text{H}$ values of lipids and biochemical, physicochemical, and environmental information that can be gleaned from these data.

Carbon and hydrogen compositions of plants have been the subject of research since the 1950s (Wickman 1952; Craig 1954) and 1970s (Smith and Epstein 1970), respectively. Numerous reviews of $^{13}\text{C}/^{12}\text{C}$ (Deines 1980; O'Leary 1981; Farquhar et al. 1989; Fogel and Cifuentes 1993; Hobbie and Werner 2004; Diefendorf et al. 2010; Tcherkez et al. 2011; Cernusak et al. 2013) and $^2\text{H}/^1\text{H}$ (Estep and Hoering 1980; White 1988; Ziegler 1988; Fogel and Cifuentes 1993) isotope systematics at the bulk plant level provide an excellent starting point for evaluating the role of *external* and *internal* controls. Further insight regarding the role of internal factors – particularly the role of compound type as well as biosynthetic and metabolic pathways – requires investigation of the processes that take place at the compound-specific level. The reviews of $^{13}\text{C}/^{12}\text{C}$ (Hayes 2001; Pancost and Pagani 2006; Chikaraishi 2014; Freeman and Pancost 2014; Diefendorf and Freimuth 2017) and $^2\text{H}/^1\text{H}$ (Hayes 2001; Schmidt et al. 2003; Sachse et al. 2012; Sachs 2014; Sessions 2016) provide state-of-the-art coverage of pathways and processes operating on lipids and their precursors. What follows is a discussion of the key external and internal controls on $^{13}\text{C}/^{12}\text{C}$ and $^2\text{H}/^1\text{H}$ fractionation in the most common lipid biomarkers in algae (Fig. 2) and higher plants (Fig. 3).

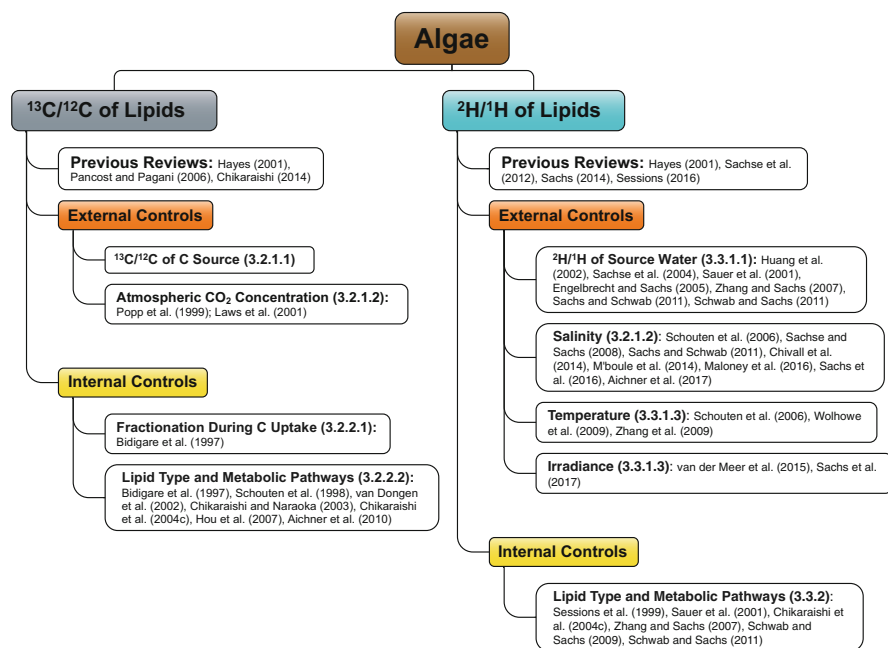


Fig. 2 External and internal controls on $^{13}\text{C}/^{12}\text{C}$ and $^2\text{H}/^1\text{H}$ compositions of algal lipids. Numbers in bold refer to the sections that cover the topic. Representative references (not all of them are discussed in the text) are given as well

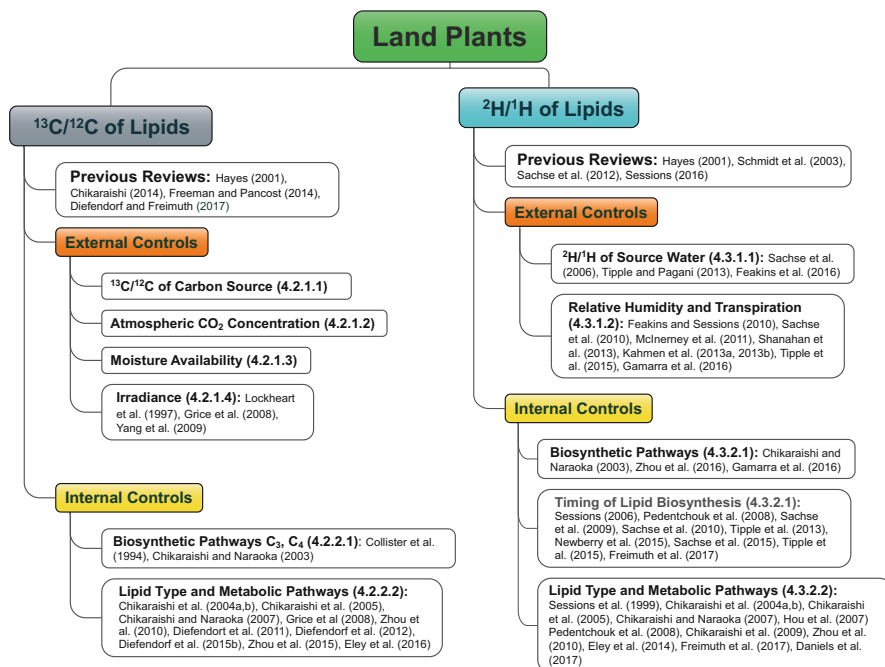


Fig. 3 External and internal controls on $^{13}\text{C}/^{12}\text{C}$ and $^2\text{H}/^1\text{H}$ compositions of higher plant lipids. Numbers in bold refer to the sections that cover the topic. Representative references (not all of them are discussed in the text) are given as well

3 Algae

3.1 Algal Lipids

Alkenones, long-chain (C_{37} – C_{39}) polyunsaturated alkyl ketones, are by far the most commonly used algal lipids in paleoenvironmental studies. They are synthesized by only a small number of haptophyte species (Volkman et al. 1980; Marlowe et al. 1984) and are used as a proxy for sea surface temperature (Brassell et al. 1986) and paleo- $p\text{CO}_2$ levels (Pancost and Pagani 2006). They are diagenetically robust and relatively easy to prepare for GC separation and can be readily analyzed by GC-IRMS. They are one of the main targets for investigating the role of various external and internal factors controlling $^{13}\text{C}/^{12}\text{C}$ and $^2\text{H}/^1\text{H}$ compositions of algal lipids.

Steroids are another group of algal lipids that have been investigated for their isotopic composition. Even though they can be diagnostic of specific taxa, e.g., dinosterol as a biomarker for dinoflagellates (Robinson et al. 1984), and are well preserved in the sedimentary record, they are easily isomerized and can create complex chromatographic patterns making precise $\delta^{13}\text{C}$ measurements difficult.

Sterol $\delta^{13}\text{C}$ values have been used previously to determine their sources (Pancost et al. 1999), but because of the complexity of their patterns during chromatographic separation and potentially multiple sources in sedimentary mixtures, deriving a particular environmental signal from their $\delta^{13}\text{C}$ or $\delta^2\text{H}$ values remains a challenge.

Even though they lack species or taxon specificity, short- and long-chain *n*-alkanes can be used as an indicator of contribution from aquatic sources. Short-chain *n*-alkanes (C_{15} , C_{17} , and C_{19}) are typical of phytoplankton (Cranwell 1982). However, the longer *n*-alkanes maximizing at C_{21} , C_{23} , and C_{25} are characteristic of submerged and floating aquatic macrophytes (Ficken et al. 2000). Previous studies have shown that the $\delta^{13}\text{C}$ values of *n*-alkanes from algae can help delineate sources of vegetation (Mead et al. 2005). Algal $\delta^2\text{H}$ values, on the other hand, can provide information about the $\delta^2\text{H}$ values of source water (Pagani et al. 2006) and changes in moisture availability (Rach et al. 2014).

Another group of algal lipid biomarkers are C_{20} , C_{25} , and C_{30} highly branched isoprenoid (HBI) alkenes, which are thought to be derived from a limited number of diatom genera (Rowland and Robson 1990; Volkman et al. 1994). Even though the diagenetic stability and pathways of these compounds and the extent to which they can be used back in time are uncertain (Belt and Müller 2013), recent research has shown that these compounds can be used as a proxy for seasonal Arctic and Antarctic sea ice extent (Belt and Müller 2013; Belt et al. 2016). Though potentially promising, the ability of the $\delta^{13}\text{C}$ and $\delta^2\text{H}$ values of these biomarkers to provide information about more specific biogeochemical (carbon cycling, photooxidation of organic matter) and physical parameters (ice thickness and/or snow cover) has not yet been explored.

3.2 Carbon Isotopes in Algal Lipids

The systematics of carbon isotopes of lipid biomarkers from algae has been the focus of intensive research by biogeochemists and paleoclimatologists primarily because of the use of $\delta^{13}\text{C}$ values of alkenones as a proxy for paleo- $p\text{CO}_2$ (Pagani 2014). Hence, the major focus of previous investigations on algal lipids has been on understanding the influence of both external and internal factors on the link between these parameters.

3.2.1 External Controls

$\delta^{13}\text{C}$ of Carbon Source

It is well established that the carbon isotopic composition of algal lipids depends on that of dissolved inorganic carbon (DIC). The chemical equilibrium of the carbonate system is linked with temperature-dependent isotopic fractionation of carbon resulting in distinct carbon isotope compositions of the CO_2 (aq), CO_3^{2-} , and HCO_3^- species. Thus, CO_2 (aq) is typically ^{13}C -depleted in comparison to CO_3^{2-} and HCO_3^- relative to gaseous CO_2 (Mook et al. 1974). Additionally, due to shifts in the global sources and sinks of carbon, there can be variations in the $\delta^{13}\text{C}$ values of

CO₂ in the entire atmosphere-ocean reservoir, e.g., the $\delta^{13}\text{C}$ values of DIC increased by 2–3‰ during the Mesozoic oceanic anoxic events (Scholle and Arthur 1980). Both possible shifts in the concentration/ $\delta^{13}\text{C}$ of aqueous carbon species and changes in the $\delta^{13}\text{C}$ values of CO₂ over geologic time need to be considered when investigating the role of external variables on the $\delta^{13}\text{C}$ values of algal lipids.

Concentration of CO₂

The link between CO₂ concentration and the $\delta^{13}\text{C}$ values of marine algae has been explored in detail since the 1990s (Rau et al. 1992). The link exists because the magnitude of $^{13}\text{C}/^{12}\text{C}$ fractionation during carbon transport and fixation in algae depends on the concentration of extra- and intracellular CO₂. Theoretical calculations, laboratory experiments, and field studies have shown that growth rate, algal shell geometry, and the availability of trace elements (Se, Co, and Ni) can also influence the $\delta^{13}\text{C}$ values of the algal biomass (Bidigare et al. 1997; Laws et al. 2001). Using the concentration of soluble phosphate as a proxy for these physiological variables, it then becomes possible to relate alkenone $\delta^{13}\text{C}$ values to CO₂ levels. The success of this approach has been clearly demonstrated by multiple studies (Pagani 2014).

3.2.2 Internal Controls

Fractionation During Carbon Uptake

The uptake of carbon in the aqueous environment can proceed either (a) passively when CO₂ (aq) diffuses across the cell membrane or (b) actively when CO₂ (aq) and/or HCO₃⁻ is enzymatically transported across the cell membrane. In both cases, a large $^{13}\text{C}/^{12}\text{C}$ fractionation takes place during photosynthesis because of the role of ribulose-1,5-bisphosphate carboxylase/oxygenase (RuBisCO) which fixes carbon as part of the Calvin cycle. Laboratory experiments have shown that $^{13}\text{C}/^{12}\text{C}$ fractionation by RuBisCO is approximately 29‰ in comparison with aqueous CO₂ (Bidigare et al. 1997).

Lipid Type and Metabolic Pathways

Following carbon assimilation, the process of post-photosynthetic processes biosynthesis leads to additional $^{13}\text{C}/^{12}\text{C}$ fractionation and significant variation in the $\delta^{13}\text{C}$ values among algal lipids (Table 1). The isotopic heterogeneity results from different sets of reactions that take place during the biosynthesis of acetogenic (*n*-alkanoic acids, *n*-alkanes, *n*-alkanols) and isoprenoid (sterols, hopanols, phytol) lipids. (A further detailed review of these reasons for differences can be found in Hayes 2001 and Chikaraishi 2014.) Generally, the acetogenic lipids are expected to be ca. 4‰ ^{13}C -depleted relative to bulk tissue (Hayes 1993). The magnitude of ^{13}C -depletion of isoprenoid lipids, however, is less clear. While isoprenoids synthesized by the mevalonic acid pathway are thought to be ^{13}C -depleted by ca. 2‰ relative to biomass, the magnitude of ^{13}C -depletion in isoprenoids synthesized via glyceraldehyde phosphate/pyruvate pathway is quite variable. The data in Table 1 clearly shows that the general patterns predicted for acetogenic and

Table 1 Differences in the isotopic composition (net isotopic fractionation) of lipids relative to biomass carbon; the units are in per mil. Extracted, expanded, and redrawn from Chikaraishi (2014)

	C3 angiosperms	C3 gymnosperms	C4 plants	CAM plants	Algae	Cyanobacteria	References
<i>n</i> -alkanoic acids	3.1–6.5	5.8	10.1–10.3	9.4	4.6–5.4	7.6	van Dongen et al. (2002), Sakata et al. (1997), Ballentine et al. (1998), Schouten et al. (1998), Conte et al. (2003), Chikaraishi et al. (2004a, b, c), Chikaraishi and Naraoka (2007)
<i>n</i> -alkanes	3.1–10.0	2.5–4.6	8.9–13.0	7.7	9.6		Conte et al. (2003), Chikaraishi et al. (2004a), Collister et al. (1994), Chikaraishi and Naraoka (2003), Bi et al. (2005), Diefendorf et al. (2011), Eley et al. (2016)
<i>n</i> -alkanols	4.0–5.4	4.7	8.9–9.5	8.1		9.8	Sakata et al. (1997), Chikaraishi et al. (2004a, b), Chikaraishi and Naraoka (2007)
sterols	1.3	2.0	5.0	3.8	1.3–6.5		van Dongen et al. (2002), Schouten et al. (1998), Chikaraishi et al. (2004a, b), Chikaraishi (2006)
phytol	4.1	5.3	9.2	8.6	2.5–3.8	6.4	van Dongen et al. (2002), Sakata et al. (1997), Chikaraishi et al. (2004a, b)
alkenone					3.1–4.5		van Dongen et al. (2002), Schouten et al. (1998), Bidigare et al. (1997)
hopanoids						08.5	Sakata et al. (1997)

isoprenoid lipids by theoretical and controlled laboratory studies are only a crude approximation of the natural variability of ^{13}C -discrimination in algal (and higher plant) lipids. For example, even though algal *n*-alkanes show a ^{13}C -depletion by 9.6‰, there is a significant overlap between *n*-alkanoic acids with 4.6–5.4‰ depletion and sterols, which are depleted by 1.3–6.5‰.

3.3 Hydrogen Isotopes in Algal Lipids

Several paleohydrological studies have used the $\delta^2\text{H}$ values of algal lipids to reconstruct changes in the $\delta^2\text{H}$ values of environmental water (Pagani et al. 2006; Pahnke et al. 2007) as well as shifts in moisture availability (Rach et al. 2014). Both approaches rely on the assumption that – because water is the only source of H for plants – the $\delta^2\text{H}$ values of lipid biomarkers are tightly linked with the $\delta^2\text{H}$ values of source water (external factor) and thus they can be used to track changes of this environmental parameter over time. Thus, a significant research effort has focused on demonstrating this link. Other studies have also focused on several other external factors, such as water salinity, temperature, and irradiance, which can potentially modify or override the above link.

3.3.1 External Controls on H Isotopes

$^2\text{H}/^1\text{H}$ of Source Water

Since the first study to demonstrate it (Sauer et al. 2001), the link between $\delta^2\text{H}$ of lipids and environmental water has been explored both in the field and laboratory settings. Hydrogen isotope data for *n*-heptadecane (*n*- C_{17} alkane; Sachse et al. 2004) and palmitic acid (Huang et al. 2002) showed correlation with the $\delta^2\text{H}$ values of source water across climatic gradients in western Europe and the eastern USA, respectively. Research on alkenone and dinosterol biomarkers in the Chesapeake Bay estuary, USA, has further demonstrated the link between lipid and source water $\delta^2\text{H}$ values (Sachs and Schwab 2011, Schwab and Sachs 2011). Tightly controlled culture growth experiments, using several freshwater and marine algal species, have provided a solid confirmation for the relationship (Englebrecht and Sachs 2005; Zhang and Sachs 2007).

Salinity

Demonstrating and quantifying the link between the $\delta^2\text{H}$ values of lipid biomarkers from algae and salinity has significant implications not only for understanding what drives $^2\text{H}/^1\text{H}$ fractionation in algae but would also provide a new research tool for algal physiologists and paleoclimatologists. Schouten et al. (2006) were the first to show that the $^2\text{H}/^1\text{H}$ fractionation in alkenones decreases as salinity increases. Research on algal and cyanobacterial lipids in environmental samples from Christmas Island in the Pacific has supported this earlier result (Sachse and Sachs 2008). More recent studies that focused on alkenones significantly expanded the applicability of this potential proxy by demonstrating the same effect of salinity on $^2\text{H}/^1\text{H}$

fractionation in coastal and open ocean haptophyte algae (Chivall et al. 2014; M'boule et al. 2014).

Sachs (2014) offered three mechanisms – in the form of hypotheses to be tested – that could explain the observed relationship between salinity and $^2\text{H}/^1\text{H}$ fractionation in algal lipids. First, greater salinities could reduce water transport through the cell membrane and lead to greater recycling of internal water, thus increasing the pool of ^2H -enriched water. Second, higher salinities could reduce growth rates leading to a reduction of $^2\text{H}/^1\text{H}$ fractionation between extracellular water and biosynthates. Third, greater salinities would increase the rate of production of osmolytes, which would attract ^2H -depleted water molecules, thus resulting in a ^2H -enriched pool of water for biosynthesis. These hypotheses provide a fertile ground for further research into the effect of salinity on hydrogen isotopes in algal lipids.

Temperature and Irradiance

Even though they could potentially modify the link between the $\delta^2\text{H}$ values of environmental water and algal lipids, these two external variables have not yet been explored in detail. Several studies on the effect of temperature have suggested an increase in $^2\text{H}/^1\text{H}$ fractionation at higher temperatures in fatty acids (Zhang et al. 2009) and alkenones (Schouten et al. 2006; Wolhowe et al. 2009). Because only a few different temperatures (2 to 3), species, and algal lipids were investigated in these studies, it is too early to make any definitive conclusions about the robustness of temperature effects.

Investigation of the effect of light intensity on $^2\text{H}/^1\text{H}$ fractionation has shown that the direction of response might depend on the type of algal lipids. While an increase in light intensity was observed to decrease fractionation in alkenones from the haptophyte *Emiliania huxleyi* (van der Meer et al. 2015) and phytol and tetradecanoic acid (C14:0 fatty acid), an opposite effect was found in a sterol biomarker from a marine diatom (Sachs et al. 2017). The discrepancy in the lipid response from the diatom was explained as a result of shifts toward a greater contribution of ^2H -enriched biosynthates to phytol and the C14:0 fatty acid and ^2H -depleted compounds to the sterol. If confirmed, the proposed mechanism is an excellent example of the interaction between the roles of both external and internal controls on $^2\text{H}/^1\text{H}$ in algal lipids. Further research is certainly needed to confirm lipid- (and species-?) specific trends and mechanisms proposed by these initial investigations.

3.3.2 Internal Controls on H Isotopes

Lipid Type and Metabolic Pathways

The photolysis of water during biosynthesis leads to the formation of NADP(H) which is thought to have $\delta^2\text{H}$ values between ca. -250‰ and -600‰ (Luo et al. 1991; Schmidt et al. 2003). Further biochemical steps lead to a progressive ^2H -enrichment, the magnitude of which will depend on the biosynthetic pathway, i.e., whether the compound is synthesized using the acetogenic or isoprenoid

pathways. Field and laboratory studies investigating the differences in the $\delta^2\text{H}$ values of various algal biomarker lipids have shown that the acetogenic lipids (fatty acids, alkenones, alkadienes) are ^2H -enriched relative to isoprenoidal lipids (sterols, phytol, botryococcones, and phytadienes) by ca. 100–200‰ (Sessions et al. 1999; Sauer et al. 2001; Zhang and Sachs 2007). The magnitude and the details of these differences between and within individual algal lipid classes in relation to the external environmental parameters ($\delta^2\text{H}$ of source water, salinity, temperature, and irradiance) require further research.

4 Higher Plants

4.1 Higher Plant Lipids

Long-chain *n*-alkanes, *n*-alkanols, *n*-alkanoic acids, and wax esters are a major group of leaf wax biochemicals in vascular plants (Eglinton et al. 1962). These *n*-alkyl compounds are among the most resistant lipid structures and are considered to be diagnostic geochemical biomarkers for higher plants (Brassell et al. 1978). Leaf wax *n*-alkanes are characterized by carbon chain lengths ranging from C_{25} to C_{35} (Kolattukudy 1976) and by a strong predominance of odd-carbon-number homologues. *n*-Alkanoic acids and *n*-alkanols range from C_{26} to C_{34} with a strong even-over-odd predominance (Kolattukudy 1976, Eglinton and Hamilton 1967). Even though these compounds cannot be readily assigned to a particular higher plant species or taxonomic group, they have been used extensively for paleoclimatic and paleoecological reconstructions based on their molecular distribution and stable isotopic compositions. These compounds are very abundant in the sedimentary record, are mostly resistant to degradation (particularly *n*-alkanes), and require only relatively simple cleanup and derivatization procedures to make them amenable to GC-IRMS analysis. These characteristics make sedimentary *n*-alkanes and *n*-alkanoic acids key targets for $\delta^{13}\text{C}$ and $\delta^2\text{H}$ measurements in paleoecological (e.g., leaf wax lipids from C_3 vs. C_4 vegetation) and paleohydrological (changes in $^2\text{H}/^1\text{H}$ composition of meteoric water and/or humidity) studies, respectively.

Terpenoids are another common group of lipids in higher plants. The fact that some diterpenoids and triterpenoids can be assigned to particular taxa, e.g., oleanoids to angiosperms (Moldowan et al. 1994) and taraxeroids to mangroves (Versteegh et al. 2004), makes them diagnostic biomarkers for certain groups of terrestrial plants. They can be used to investigate shifts in plant paleocommunities (Diefendorf et al. 2014) and for identifying differences in the values of $\delta^{13}\text{C}$ of angiosperm vs. gymnosperm plants (Schouten et al. 2007) during periods of climate change. Even though significant advances have been made in understanding the role of salinity on $\delta^{13}\text{C}$ and $\delta^2\text{H}$ of *n*-alkanes in mangroves (Ladd and Sachs 2012; Ladd and Sachs 2013; Ladd and Sachs 2017), little is currently known about the effect of this environmental parameter on the isotopic composition of taraxerol.

4.2 Carbon Isotopes in Higher Plant Lipids

The carbon isotope composition of lipid biomarkers from higher plants is a rich source of information for plant biochemists, plant ecologists, and paleoclimatologists. The $\delta^{13}\text{C}$ values of leaf wax lipids provide information about plant ecology and evolution, e.g., the origin and expansion of C_4 vegetation (Tippel and Pagani 2007; Tippel and Pagani 2010), and for tracking changes in the $\delta^{13}\text{C}$ values of atm. CO_2 during periods of dramatic climate change, e.g., the Paleocene-Eocene Thermal Maximum (Pagani et al. 2006; Schouten et al. 2007; McInerney and Wing 2011). When dealing with these types of applications, a thorough understanding of the contribution of key internal factors (i.e., C_3 or C_4 biosynthetic pathway) vs. those that operate externally (e.g., $\delta^{13}\text{C}$ values of CO_2 , moisture availability, etc.), particularly on C_3 plants, is required when interpreting the carbon isotope record of leaf wax lipid biomarkers.

4.2.1 External Controls on C Isotopes

$\delta^{13}\text{C}$ of Carbon Source

Carbon dioxide is the sole source of carbon for higher plants; therefore, the $\delta^{13}\text{C}$ value of atmospheric CO_2 is a key variable that influences the $\delta^{13}\text{C}$ values of leaf wax lipids. Depending on the scale of investigation and the nature of sample material, this factor can operate at two different levels. First, there could be changes in the global patterns of $\delta^{13}\text{C}$ values of atmospheric CO_2 over decadal, millennial, and longer timescales. For instance, changes over the Cenozoic on the order of ca. 2‰ (Tippel et al. 2010) and certain dramatic changes during climatic events like the Paleocene-Eocene Thermal Maximum with leaf wax *n*-alkane records showing excursions of up to ca. 5‰ (McInerney and Wing 2011) could take place. Second, on a more local, short-term scale, the contribution of ^{13}C -depleted CO_2 from soil respiration in the closed canopy could play a role. The extent of this effect on plant $\delta^{13}\text{C}$ values varies substantially among different types of forests but can lead to ca. 1.5 to 5.0‰ differences between lower and upper canopy leaves (Broadmeadow and Griffiths 1993).

Atmospheric Concentration of CO_2

Changes in the concentration of atmospheric CO_2 will shift the ratio between intra- and extracellular concentrations of CO_2 leading to a shift in the $\delta^{13}\text{C}$ values of plant tissues (Farquhar et al. 1982). Even though the effect is clearly seen on relatively short timescales, e.g., up to a month (Schubert and Jahren 2012), the response is not as obvious on the geological timescales (Diefendorf et al. 2015a). Diefendorf and Freimuth (2017) provided an up-to-date review on the subject including short- and long-term studies and concluded that on geological timescales, $^{13}\text{C}/^{12}\text{C}$ discrimination in higher plants is not sensitive to $p\text{CO}_2$.

Moisture Availability

Low soil moisture and low relative humidity restrict evapotranspiration, which results in a decrease in the ratio of inter- and extracellular CO₂. Multiple studies have shown that wetter conditions are characterized by lower $\delta^{13}\text{C}$ values of plant biomass. Globally, plant $\delta^{13}\text{C}$ values are linked with mean annual precipitation (Pataki et al. 2003; Diefendorf et al. 2010) and with a vapor pressure deficit (Bowling et al. 2001) suggesting that differences in $^{13}\text{C}/^{12}\text{C}$ fractionation in C₃ plants correlate with the availability of moisture.

Irradiance

A greater exposure to sunlight will increase the rate of carbon assimilation and plant's growth rate. Higher assimilation rates would in turn lower the ratio between inter- and extracellular concentration of CO₂. This correlation between light intensity and plant $\delta^{13}\text{C}$ values has been observed not only at the bulk plant level (Ehleringer et al. 1987; Zimmerman and Ehleringer 1990) but also in leaf wax *n*-alkanes (Lockheart et al. 1997; Grice et al. 2008). These studies have shown that the leaves that had greater exposure to light were ^{13}C -enriched in comparison with those at low light levels.

4.2.2 Internal Controls on C Isotopes

Biosynthetic Pathways

The key factor that controls the carbon isotope composition of higher plants is the type of carbon assimilation mechanism used by the plant. The difference in the $\delta^{13}\text{C}$ values of C₃ and C₄ plants arises from different carbon isotope fractionations associated with different mechanisms of carbon assimilation. In C₃ plants, CO₂ diffusion through stomata leads to 4.4‰ fractionation (O'Leary 1981) followed up by a much greater fractionation – in the range of ca. 27–29‰ (Farquhar et al. 1989; Lloyd and Farquhar 1994) – during CO₂ fixation catalyzed by RuBisCO. In C₄ plants, however, the $^{13}\text{C}/^{12}\text{C}$ fractionation is much smaller because the additional CO₂-concentrating mechanism, which involves phosphoenolpyruvate (PEP) carboxylase, and structural and biochemical modifications of the carbon assimilation process reduce the realized isotope effect associated with RuBisCO (Farquhar et al. 1989).

Global compilations have shown that C₃ plants employing the Calvin-Benson-Bassham (CBB) cycle are typically characterized by bulk $\delta^{13}\text{C}$ values of ca. –25‰ to –27‰, though they can range from ca. –20 to –36‰. However, $\delta^{13}\text{C}$ values of C₄ plants which employ the Hatch-Slack pathway have a less ^{13}C -depleted and overall less broad range of –9‰ to –15‰, with the most common values around –11‰ to –12‰ (Tippie and Pagani 2007). Differences of similar magnitude are observed between *n*-alkanes from leaf waxes of C₃ and C₄ plants (Collister et al. 1994; Chikaraishi and Naraoka 2003; Eley et al. 2016) though they are significantly ^{13}C -depleted relative to leaf tissue (Table 1). It is of interest that even within the same group of C₃ plants, there is a considerable difference with regard to the extent of the

net isotope fractionation (relative to biomass) between and within each group of C₃ angiosperm and C₃ gymnosperm plants (3.1–10.0‰ vs. 2.5–4.6‰, respectively). Recent work by Diefendorf and colleagues has linked these differences to phylogenetic variability among the plants (Diefendorf et al. 2011, 2015a).

Lipid Type and Metabolic Pathways

Similar to the patterns observed in algae, the process of photosynthesis imposes significant isotopic heterogeneity among acetogenic and isoprenoid lipids in higher plants (Table 1). For example, within both C₃ and C₄ plant groups, net fractionation between *n*-alkane and biomass carbon is noticeably greater than that in sterols. In C₃ plant angiosperms, *n*-alkanes differ from biomass by 3.1–10.0‰, while sterols differ by 1.3‰. In C₄ plants, *n*-alkanes differ by 8.9–13.0‰ and sterols by 5.0‰.

Differences in ¹³C/¹²C fractionation can also be observed within individual compound classes in a single organism. For instance, Grice et al. (2008) found that due to different biosynthetic precursors, the anteiso- and isoalkanes were ¹³C-enriched by ca. 3.0–4.5‰ in comparison with *n*-alkanes in tobacco leaves.

4.3 Hydrogen Isotopes in Higher Plant Lipids

Since the advent of the hydrogen isotope compound-specific methodology, the use of δ²H values of lipids from leaf waxes is one of the fastest-growing research areas in paleoclimatology. The methodology provides an opportunity to investigate the link between the global carbon and hydrological cycles in the past and thus project how the distribution and amount of precipitation might respond to increasing levels of atmospheric CO₂ in the future. The focus of current research into the systematics of hydrogen isotopes in leaf waxes is to provide a better understanding and to quantify the link between the δ²H values of leaf wax lipids and those of the source water used by plants. Of great additional interest is the role of relative humidity and transpiration (external factors) as well as several internal factors, such as the biosynthetic pathway and the lipid type, which have a strong additional effect on leaf wax hydrogen isotope composition.

4.3.1 External Controls on H Isotopes

²H/¹H of Source Water

Similar to the case with algal lipids, the use of the δ²H values of leaf wax lipids as proxy for paleohydrology requires demonstrating that these values are closely linked with those of source water. The link is shown best when looking at large environmental gradients in the δ²H of meteoric precipitation. Field studies in western Europe (Sachse et al. 2006), eastern North America (Tipple and Pagani 2013), and South America (Feakins et al. 2016) have clearly demonstrated that *n*-alkyl lipids from different C₃ species generally track the δ²H values of meteoric water across climatic zones in those regions. The global and/or regional pattern of this relationship can however be modified locally by the timing of lipid synthesis.

Currently, there is no agreement as to whether leaf wax $\delta^2\text{H}$ values reflect $\delta^2\text{H}$ values of source water during leaf flush only and are then essentially “locked in” for the rest of the growth season (Sachse et al. 2010; Tipple et al. 2013) or whether they continue to respond to environmental changes over the rest of the season (Sessions 2006; Sachse et al. 2009; Newberry et al. 2015; Freimuth et al. 2017). This potential complication certainly needs to be considered when interpreting sedimentary $\delta^2\text{H}$ record of higher plant lipid biomarkers.

Relative Humidity and Transpiration

In addition to the uncertainty of the effect of timing of leaf wax synthesis, another external variable has the potential to significantly modify the link with the $\delta^2\text{H}$ values of meteoric precipitation. The isotopic composition of water taken by the plant can be substantially altered by the evaporation of water from the leaf through stomata. While several studies have claimed that transpiration has no significant effect on lipid $\delta^2\text{H}$ values (Feakins and Sessions 2010; McInerney et al. 2011), other studies involving both theoretical considerations and empirical data have reported a major effect (Sachse et al. 2010; Shanahan et al. 2013; Kahmen et al. 2013a, b; Tipple et al. 2015; Gamara et al. 2016). A compilation of multiple studies used to investigate the dependence of $^2\text{H}/^1\text{H}$ fractionation on relative humidity (RH) suggests that at $\text{RH} < 70\%$, leaf waxes are ca. 50–60‰ ^2H -enriched in comparison with those at $> 70\%$ RH (Sachse et al. 2012). Even though the compilation uses multiple plant types with different physiologies, it does show a general trend of increasing $^2\text{H}/^1\text{H}$ fractionation between lipids and source water when RH decreases.

4.3.2 Internal Controls on H Isotopes

Biosynthetic Pathways

Unlike the case with carbon isotope systematics, where there is a clear understanding of the effect of the C_3 versus C_4 photosynthetic pathways on the $\delta^{13}\text{C}$ values of leaf wax lipids, the role of this factor on $^2\text{H}/^1\text{H}$ fractionation between leaf wax lipids and source water is still not very clear. An early study that investigated a broad range of C_3 and C_4 plants in Japan and Thailand did not show any appreciable difference in fractionation between leaf wax *n*-alkanes and source water (Chikaraishi and Naraoka 2003). On the one hand, a compilation of multiple studies that included various growth forms showed that the median value of $^2\text{H}/^1\text{H}$ fractionation between *n*-nonacosane (*n*- C_{29} alkane) and mean annual precipitation in C_3 graminoids is ca. 10‰ greater than that in C_4 graminoids, though there is a considerable overlap when all the reported data are considered (Sachse et al. 2012). A more recent study reported a significantly greater difference between these two groups: ca. 200‰ in C_3 grasses and ca. 160‰ in C_4 grasses. On the other hand, another recent study has shown an opposite trend, whereby $^2\text{H}/^1\text{H}$ fractionation is greater in C_4 grasses – by ca. 30‰ when acetogenic lipids are considered. The situation is complicated by the fact that the trend is reversed in isoprenoid lipids, with fractionation in C_4 grass smaller by ca. 200‰ in phytol and ca. 50‰ in sterols (Zhou et al. 2016).

Another way of looking at the patterns observed in higher plant leaf wax $\delta^2\text{H}$ values is to consider phylogenetic relationships as suggested by several recent studies that investigated *n*-alkanes and *n*-fatty acids grouped by phylogeny. For instance, monocots were found to be 30–70‰ more ^2H -depleted in comparison with dicots (Gao et al. 2014; Liu et al. 2016).

Lipid Type and Metabolic Pathways

Early investigations of lipid biomarkers from higher plants highlighted major differences between *n*-alkyl and isoprenoid compounds, with isoprenoid lipids being ^2H -depleted by more than 100‰, within a single organism (Sessions et al. 1999; Chikaraishi et al. 2004a, b, 2009). Further research has shown that significant variability can also be observed within *n*-alkyl lipids, e.g., by 20–30‰ among *n*-alkanes, *n*-alkanols, and *n*-fatty acids (Hou et al. 2007; Chikaraishi and Naraoka 2007; Freimuth et al. 2017; Daniels et al. 2017) and even different types of alkanes, e.g., *n*-alkanes, isoalkanes, and anteisoalkanes, may vary in their $\delta^2\text{H}$ values by ca. 50–60‰ (Zhou et al. 2010). The biochemical mechanisms responsible for these differences are currently not well understood, and further research is certainly needed to get fundamental understanding of what drives the observed differences in $^2\text{H}/^1\text{H}$ fractionation between and within individual lipid groups in higher plants.

5 Research Needs

Previous research has demonstrated that the isotopic composition of lipids from algae and higher plants can provide a wealth of information about current and past biological, chemical, and physical processes operating in the environment. To increase the level of our understanding of the link between the $\delta^{13}\text{C}$ and $\delta^2\text{H}$ values of lipids and environmental signals and to get a better grasp of the fundamental processes controlling carbon and hydrogen fractionation during photosynthesis, the following research issues should be addressed (Fig. 4):

Internal factors. The exact pathways and mechanisms controlling carbon and hydrogen isotopic composition of lipids are still poorly known. Even though general trends concerning key fractionation steps have been described (e.g., Hayes 2001; Schmidt et al. 2003; Chikaraishi 2014), there is little empirical data about the biochemical precursors of algal and higher plant lipids. Information about precursor $\delta^{13}\text{C}$ and $\delta^2\text{H}$ values – both at intra- and intermolecular levels – of acetogenic and isoprenoid lipids is needed to narrow this gap.

Paleoclimatic and paleoecological studies would benefit from an improved understanding of isotopic differences within and between lipid groups. Thus, future research should explore the extent of $^{13}\text{C}/^{12}\text{C}$ and $^2\text{H}/^1\text{H}$ fractionation in lipids from individual plants and plant groups. More attention should also be given to exploring a possible role of phylogeny that might provide key insights into the isotopic differences among different plant groups.

Algal response to different levels of salinity has been described previously; however, a mechanistic understanding of the internal biochemical processes that

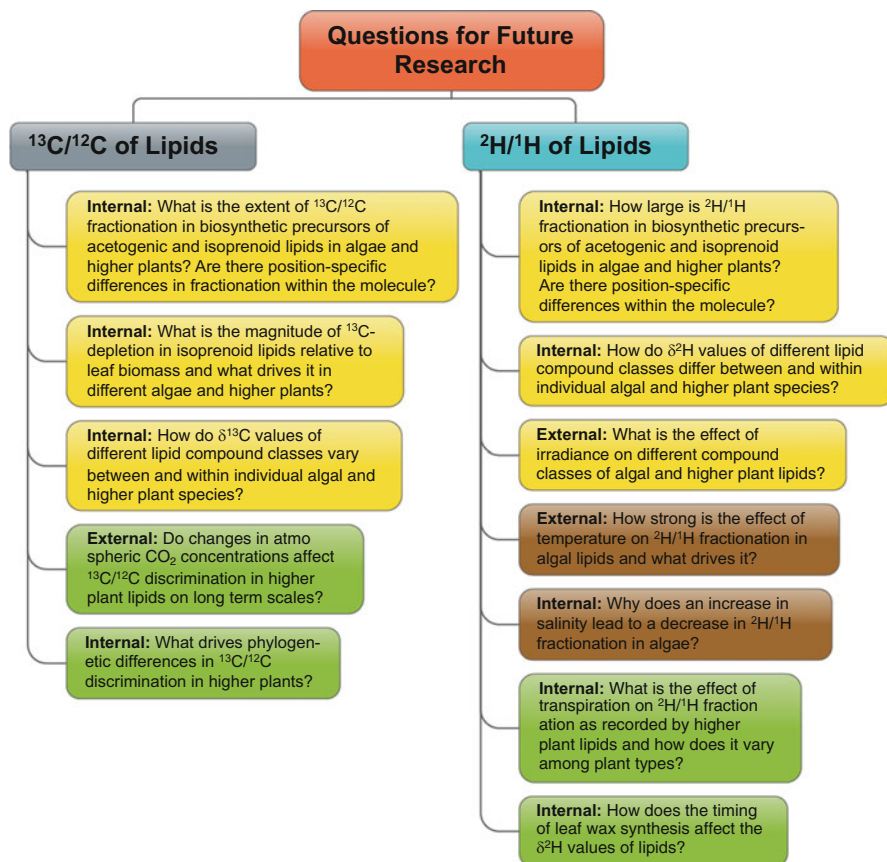


Fig. 4 Research questions to be addressed in the future. This is not an exhaustive list of questions that need to be addressed – mainly a compilation of the key issues based on the reviewed literature. Yellow color indicates questions that refer to both algae and higher plants, brown to algae, and green to higher plants

are responsible for $^2\text{H}/^1\text{H}$ fractionation is still lacking. Further research using both culture and field studies will increase our level of confidence about this promising proxy.

The effect of leaf transpiration on the $\delta^2\text{H}$ values of lipids is one of the key factors that need to be better understood and quantified to make the leaf wax hydrogen isotope paleohydrology proxy more robust. Studies focusing on individual higher plant species as well as plant groups will provide further insight into the link between moisture availability and hydrogen isotope response in lipids.

External factors. The role of some of the external factors on the $\delta^{13}\text{C}$ and $\delta^2\text{H}$ values of algae and higher plants is still not clear. Conflicting data dealing with short- and long-term scales about the effect of CO_2 concentration on $^{13}\text{C}/^{12}\text{C}$ fractionation in higher plants precludes an effective use of carbon isotope composition of lipid

biomarkers in paleoclimatology. Studies integrating data from other proxies (e.g., $\delta^{13}\text{C}$ values of cellulose and lignin from tree rings) on longer-term scales (hundreds to thousands of years) would provide more clarity about the effect of this external variable.

The effect of temperature on the $\delta^2\text{H}$ values of algal lipids needs further research. The link is unlikely to be robust enough to provide a new proxy for water paleotemperature. However, a possible effect of this parameter needs to be better understood to use the $\delta^2\text{H}$ values as a proxy for paleosalinity with more confidence.

The effect of irradiance on $^2\text{H}/^1\text{H}$ fractionation in algal lipids is barely known, particularly with regard to how different lipid groups respond to this variable. The great diversity of microalgae that occupy various ecological niches with different light levels, e.g., in the polar regions with different amounts and types of ice, provides an exciting opportunity for future research. Future studies using both culture and environmental studies could explore whether the link between light intensity and $^2\text{H}/^1\text{H}$ fractionation of algal lipids is robust enough to make $\delta^2\text{H}$ of algal lipids a new proxy for ice/snow pack thickness.

References

- Ballentine DC, Macko SA, Turekian VC (1998) Variability of stable carbon isotopic compositions in individual fatty acids from combustion of C4 and C3 plants: implications for biomass burning. *Chem Geol* 152:151–161
- Belt ST, Müller J (2013) The Arctic Sea ice biomarker IP25: a review of current understanding, recommendations for future research and applications in palaeo sea ice reconstructions. *Quaternary Sci Rev* 79:9–25
- Belt ST, Smik L, Brown TA et al (2016) Source identification and distribution reveals the potential of the geochemical Antarctic Sea ice proxy IPSO25. *Nat Commun* 7:12655
- Bi X, Sheng G, Liu X, Li C, Fu J (2005) Molecular and carbon and hydrogen isotopic composition of *n*-alkanes in plant leaf waxes. *Org Geochem* 36:1405–1417
- Bidigare R, Fluegge A, Freeman KH et al (1997) Consistent fractionation of ^{13}C in nature and in the laboratory: growth-rate effects in some haptophyte algae. *Global Biogeochem C* 11:279–292
- Bowling DR, Tans PP, Monson RK (2001) Partitioning net ecosystem carbon exchange with isotopic fluxes of CO_2 . *Glob Chang Biol* 7:127–145
- Brassell SC, Eglinton G, Maxwell JR et al (1978) Natural background of alkanes in the aquatic environment. In: Hutzinger O, van Lelyveld LH, Zoeteman BCJ (eds) *Aquatic pollutants, transformation and biological effects*. Pergamon Press, Oxford, pp 69–86
- Brassell SC, Eglinton G, Marlowe IT et al (1986) Molecular stratigraphy: a new tool for climatic assessment. *Nature* 320:129–133
- Broadmeadow MSJ, Griffiths H (1993) Carbon isotope discrimination and the coupling of CO_2 fluxes within forest canopies. In: Ehleringer JR, Hall AE, Farquhar GD (eds) *Stable isotope and plant carbon-water relationships*. Academic, San Diego, pp 109–129
- Cernusak LA, Ubierna N, Winter K et al (2013) Environmental and physiological determinants of carbon isotope discrimination in terrestrial plants. *New Phytol* 200:950–965
- Chikaraishi Y (2006) Carbon and hydrogen isotopic composition of sterols in natural marine brown and red macroalgae and associated shellfish. *Org Geochem* 37:428–436
- Chikaraishi Y (2014) $^{13}\text{C}/^{12}\text{C}$ signatures in plants and algae. In: *Treatise on geochemistry*, 2nd edn. Elsevier, London, pp 95–123
- Chikaraishi J, Naraoka H (2003) Compound-specific δD – $\delta^{13}\text{C}$ analyses of *n*-alkanes extracted from terrestrial and aquatic plants. *Phytochemistry* 63:361–371

- Chikaraishi Y, Naraoka H (2007) $\delta^{13}\text{C}$ and δD relationships among three *n*-alkyl compound classes (*n*-alkanoic acid, *n*-alkane and *n*-alcohol) of terrestrial higher plants. *Org Geochem* 38:198–215
- Chikaraishi Y, Naraoka H, Poulson SR (2004a) Carbon and hydrogen isotopic fractionation during lipid biosynthesis in a higher plant (*Cryptomeria japonica*). *Phytochemistry* 65:323–330
- Chikaraishi Y, Naraoka H, Poulson SR (2004b) Hydrogen and carbon isotopic fractionations of lipid biosynthesis among terrestrial (C₃, C₄ and CAM) and aquatic plants. *Phytochemistry* 65:1369–1381
- Chikaraishi Y, Suzuki Y, Naraoka H (2004c) Hydrogen isotopic fractionations during desaturation and elongation associated with polyunsaturated fatty acid biosynthesis in marine macroalgae. *Phytochemistry* 65:2293–2300
- Chikaraishi Y, Matsumoto K, Ogawa NO et al (2005) Hydrogen, carbon and nitrogen isotopic fractionations during chlorophyll biosynthesis in C₃ higher plants. *Phytochemistry* 66:911–920
- Chikaraishi Y, Tanaka R, Tanaka A et al (2009) Fractionation of hydrogen isotopes during phytol biosynthesis. *Org Geochem* 40:569–573
- Chivall D, M'Boule D, Sinke-Schoen D et al (2014) The effects of growth phase and salinity on the hydrogen isotopic composition of alkenones produced by coastal haptophyte algae. *Geochim Cosmochim Acta* 140:381–390
- Collister JW, Rieley G, Stern B et al (1994) Compound-specific $\delta^{13}\text{C}$ analyses of leaf lipids from plants with differing carbon dioxide metabolisms. *Org Geochem* 21:619–627
- Conte MH, Weber JC, Carlson PJ, Flanagan LB (2003) Molecular and carbon isotopic composition of leaf wax in vegetation and aerosols in a northern prairie ecosystem. *Oecologia* 135:67–77
- Craig H (1954) Carbon-13 in plants and the relationships between carbon-13 and carbon-14 variations in nature. *J Geol* 62:115–149
- Cranwell PA (1982) Lipids of aquatic sediments from Upton broad, a small productive lake. *Prog Lipid Res* 21:271–308
- Daniels WC, Russell JM, Giblin AE et al (2017) Hydrogen isotope fractionation in leaf waxes in the Alaskan Arctic tundra. *Geochim Cosmochim Acta* 213:216–236
- Deines P (1980) The isotopic composition of reduced organic carbon. In: Fritz P, Fontes JC (eds) *Handbook of environmental geochemistry*, vol 1. Elsevier, New York/Amsterdam, pp 239–406
- Diefendorf AF, Freimuth EJ (2017) Extracting the most from terrestrial plant-derived *n*-alkyl lipids and their carbon isotopes from the sedimentary record: a review. *Org Geochem* 103:1–21
- Diefendorf AF, Mueller KE, Wing SL et al (2010) Global patterns in leaf ^{13}C discrimination and implications for studies of past and future climate. *P Natl Acad Sci USA* 107:5738–5743
- Diefendorf AF, Freeman KH, Wing SL et al (2011) Production of *n*-alkyl lipids in living plants and implications for the geologic past. *Geochim Cosmochim Acta* 75:7472–7485
- Diefendorf AF, Freeman KH, Wing SL (2014) A comparison of terpenoid and leaf fossil vegetation proxies in Paleocene and Eocene Bighorn Basin sediments. *Org Geochem* 71:30–42
- Diefendorf AF, Freeman KH, Wing SL, Curran ED, Mueller KE (2015a) Paleogene plants fractionated carbon isotopes similar to modern plants. *Earth Planet Sc Lett* 429:33–44
- Diefendorf AF, Leslie AB, Wing SL (2015b) Leaf wax composition and carbon isotopes vary among major conifer groups. *Geochim Cosmochim Acta* 170:145–156
- Eglinton G, Hamilton RJ (1967) Leaf epicuticular waxes. *Science* 156:1322–1335
- Eglinton G, Gonzalez AG, Hamilton RJ et al (1962) Hydrocarbon constituents of the wax coatings of plant waxes: a taxonomic survey. *Phytochemistry* 1:89–102
- Ehleringer JR, Lin ZF, Field CB, Sun GC, Kuo CY (1987) Leaf carbon isotope ratios of plants from a subtropical monsoon forest. *Oecologia* 72:109–114
- Eley Y, Dawson L, Black S et al (2014) Understanding $^2\text{H}/^1\text{H}$ systematics of leaf wax *n*-alkanes in coastal plants at Stiffkey saltmarsh, Norfolk, UK. *Geochim Cosmochim Acta* 128:13–28
- Eley Y, Dawson L, Pedentchouk N (2016) Investigating the carbon isotope composition and leaf wax *n*-alkane concentration of C₃ and C₄ plants in Stiffkey saltmarsh, Norfolk, UK. *Org Geochem* 96:28–42
- Englebrecht AC, Sachs JP (2005) Determination of sediment provenance at drift sites using hydrogen isotopes and unsaturation ratios in alkenones. *Geochim Cosmochim Acta* 69:4253–4265

- Estep MF, Hoering TC (1980) Biogeochemistry of the stable hydrogen isotopes. *Geochim Cosmochim Acta* 44:1197–1206
- Evershed RP, Bull ID, Corr LT et al (2007) Compound-specific stable isotope analysis in ecology and paleoecology. In: Michener R, Lajtha K (eds) *Stable isotopes in ecology and environmental science*. Blackwell, Malden, pp 480–540
- Farquhar GD, O’Leary MH, Berry JA (1982) On the relationship between carbon isotope discrimination and the intercellular carbon dioxide concentration in leaves. *Aust J Plant Physiol* 9:121–137
- Farquhar GD, Ehleringer JR, Hubick KT (1989) Carbon isotope discrimination and photosynthesis. *Annu Rev Plant Phys* 40:503–537
- Feakins SJ, Sessions AL (2010) Controls on the D/H ratios of plant leaf waxes in an arid ecosystem. *Geochim Cosmochim Acta* 74:2128–2141
- Feakins SJ, Bentley LP, Salinas N et al (2016) Plant leaf wax biomarkers capture gradients in hydrogen isotopes of precipitation from the Andes and Amazon. *Geochim Cosmochim Acta* 182:155–172
- Ficken KJ, Li B, Swain DL, Eglinton G (2000) An *n*-alkane proxy for the sedimentary input of submerged/floating freshwater aquatic macrophytes. *Org Geochem* 31:745–749
- Fogel ML, Cifuentes LA (1993) Isotope fractionation during primary production. In: Engel MH, Macko SA (eds) *Organic geochemistry*. Plenum Press, New York, pp 73–98
- Freeman KH, Pancost RD (2014) Biomarkers for terrestrial plants and climate. In: *Treatise on geochemistry*, 2nd edn. Elsevier, London, pp 79–94
- Freeman KH, Hayes JM, Trendel JM et al (1990) Evidence from carbon isotope measurements for diverse origins of sedimentary hydrocarbons. *Nature* 343:254–256
- Freimuth EJ, Diefendorf AF, Lowell TV (2017) Hydrogen isotopes of *n*-alkanes and *n*-alkanoic acids as tracers of precipitation in a temperate forest and implications for paleorecords. *Geochim Cosmochim Acta* 206:166–183
- Gamarra B, Sachse D, Kahmen A (2016) Effects of leaf water evaporative ^2H -enrichment and biosynthetic fractionation on leaf wax *n*-alkane $\delta^2\text{H}$ values in C_3 and C_4 grasses. *Plant Cell Environ* 39:2390–2403
- Gao L, Edwards EJ, Zeng Y, Huang Y (2014) Major evolutionary trends in hydrogen isotope fractionation of vascular plant leaf waxes. *PLoS One* 9:e112610
- Grice K, Lu H, Zhou Y et al (2008) Biosynthetic and environmental effects on the stable carbon isotopic compositions of anteiso- (3-methyl) and iso- (2-methyl) alkanes in tobacco leaves. *Phytochemistry* 69:2807–2814
- Hayes JM (1993) Factors controlling ^{13}C contents of sedimentary organic compounds: principles and evidence. *Mar Geol* 113:111–125
- Hayes JM (2001) Fractionation of carbon and hydrogen isotopes in biosynthetic processes. In: Valley JW, Cole DR (eds) *Stable isotope geochemistry, Reviews in Mineralogy & Geochemistry*, vol 43. The Mineralogical Society of America, Washington, DC, pp 225–277
- Hayes JM, Freeman KH, Popp BN et al (1990) Compound-specific isotopic analysis: a novel tool for the reconstruction of ancient biogeochemical processes. In: Durand B, Behar F (eds) *Advances in organic geochemistry*. Pergamon, Oxford, pp 1115–1128
- Hobbie E, Werner RA (2004) Intramolecular, compound-specific, and bulk carbon isotope patterns in C_3 and C_4 plants: a review and synthesis. *New Phytol* 161:371–385
- Hou J, D’Andrea WJ, MacDonald D, Huang Y (2007) Hydrogen isotopic variability in leaf waxes among terrestrial and aquatic plants around blood pond, Massachusetts (USA). *Org Geochem* 38:977–984
- Huang Y, Shuman B, Wang Y et al (2002) Hydrogen isotope ratios of palmitic acid in lacustrine sediments record late quaternary climate variations. *Geology* 30:1103–1106
- Kahmen A, Schefuß E, Sachse D (2013a) Leaf water deuterium enrichment shapes leaf wax *n*-alkane δD values of angiosperm plants I: experimental evidence and mechanistic insights. *Geochim Cosmochim Acta* 111:39–49

- Kahmen A, Hoffmann B, Schefuß E et al (2013b) Leaf water deuterium enrichment shapes leaf wax *n*-alkane δD values of angiosperm plants II: observational evidence and global implications. *Geochim Cosmochim Acta* 111:50–63
- Kolattukudy PE (1976) The chemistry and biochemistry of natural waxes. Elsevier, Amsterdam
- Ladd SN, Sachs JP (2012) Inverse relationship between salinity and *n*-alkane δD values in the mangrove *Avicennia marina*. *Org Geochem* 48:25–36
- Ladd SN, Sachs JP (2013) Positive correlation between salinity and *n*-alkane $\delta^{13}C$ values in the mangrove *Avicennia marina*. *Org Geochem* 64:1–8
- Ladd SN, Sachs JP (2017) $^2H/^1H$ fractionation in lipids of the mangrove *Bruguiera gymnorhiza* increases with salinity in marine lakes of Palau. *Geochim Cosmochim Acta* 204:300–312
- Laws EA, Popp BN, Bidigare RR et al (2001) Controls on the molecular distribution and carbon isotopic composition of alkenones in certain haptophyte algae. *Geochem Geophys Geosys* 2. <https://doi.org/10.1029/2000GC000057>
- Liu J, Liu W, An Z, Yang H (2016) Different hydrogen isotope fractionations during lipid formation in higher plants: implications for paleohydrology reconstruction at a global scale. *Sci Rep-UK* 6:19711
- Lloyd J, Farquhar GD (1994) ^{13}C discrimination during CO_2 assimilation by the terrestrial biosphere. *Oecologia* 99:201–215
- Lockheart MJ, Van Bergen PF, Evershed RP (1997) Variations in the stable carbon isotope compositions of individual lipids from the leaves of modern angiosperms: implications for the study of higher land plant-derived sedimentary organic matter. *Org Geochem* 26:137–153
- Luo Y-H, Steinberg L, Suda S, Kumazawa S, Mitsui A (1991) Extremely low D/H ratios of photoproduced hydrogen by cyanobacteria. *Plant Cell Physiol* 32:897–900
- M'boule D, Chivall D, Sinke-Schoen D et al (2014) Salinity dependent hydrogen isotope fractionation in alkenones produced by coastal and open ocean haptophyte algae. *Geochim Cosmochim Acta* 130:126–135
- Maloney AE, Shinneman ALC, Hemeon K et al (2016) Exploring lipid $^2H/^1H$ fractionation mechanisms in response to salinity with continuous cultures of the diatom *Thalassiosira pseudonana*. *Org Geochem* 101:154–165
- Marlowe IT, Brassell SC, Eglinton G et al (1984) Long chain unsaturated ketones and esters in living algae and marine sediments. *Org Geochem* 6:135–141
- McInerney FA, Wing SL (2011) The Paleocene-Eocene Thermal Maximum: A Perturbation of carbon cycle, climate, and biosphere with implications for the future. *Annu Rev Earth Pl Sc* 39:489–516
- McInerney FA, Helliker BR, Freeman KH (2011) Hydrogen isotope ratios of leaf wax *n*-alkanes in grasses are insensitive to transpiration. *Geochim Cosmochim Acta* 75:541–554
- Mead R, Xu Y, Chong J, Jaffè R (2005) Sediment and soil organic matter source assessment as revealed by the molecular distribution and carbon isotopic composition of *n*-alkanes. *Org Geochem* 36:363–370
- Moldowan JM, Dahl J, Huizinga BJ et al (1994) The molecular fossil record of oleanane and its relation to angiosperms. *Science* 265:768–771
- Mook WG, Bommerson JC, Staverman WH (1974) Carbon isotope fractionation between dissolved bicarbonate and gaseous carbon dioxide. *Earth Planet Sc Lett* 22:169–176
- Newberry SL, Kahmen A, Dennis P et al (2015) *n*-alkane biosynthetic hydrogen isotope fractionation is not constant throughout the growing season in the riparian tree *Salix viminalis*. *Geochim Cosmochim Acta* 165:75–85
- O'Leary MH (1981) Carbon isotope fractionation in plants. *Phytochemistry* 20:553–567
- Pagani M (2014) Biomarker-based inferences of past climate: the alkenone *pCO2* proxy. In: *Treatise on geochemistry*, 2nd edn. Elsevier, London, pp 361–378
- Pagani M, Pedentchouk N, Huber M et al (2006) Arctic's hydrology during global warming at the Palaeocene-Eocene thermal maximum. *Nature* 442:671–675

- Pahnke K, Sachs JP, Keigwin LD, Timmermann A, Xie S-P (2007) Eastern tropical Pacific hydrological changes during the past 27,000 years from D/H ratios in alkenones. *Paleoceanography* 22. <https://doi.org/10.1029/2007PA001468>
- Pancost R, Pagani M (2006) Controls on the carbon isotopic composition of lipids in marine environments. In: Volkman J (ed) *Marine organic matter: biomarkers, isotopes and DNA*. Springer, Berlin/Heidelberg, pp 209–249
- Pancost RD, Freeman KH, Wakeham SG (1999) Controls on the carbon-isotope compositions of compounds in Peru surface waters. *Org Geochem* 30:319–340
- Pataki DE, Ehleringer JR, Flanagan LB, Yakir D (2003) The application and interpretation of Keeling plots in terrestrial carbon cycle research. *Global Biogeochem Cycles* 17. <https://doi.org/10.1029/2001GB001850>
- Pedentchouk N, Turich C (2017) Carbon and hydrogen isotopic compositions of *n*-alkanes as a tool in petroleum exploration. In: Lawson M, Formolo MJ, Eiler JM (eds) *From source to seep: geochemical applications in hydrocarbon systems*, Geological society, special publications, vol 468. Geological Society, London. <https://doi.org/10.1144/SP468.1>
- Peters KE, Walters CC, Moldowan JM (2005a) *The biomarker guide*, volume 1, biomarkers and isotopes in environment and human history, 2nd edn. Cambridge University Press, Cambridge
- Peters KE, Walters CC, Moldowan JM (2005b) *The biomarker guide: volume 2, biomarkers and isotopes in petroleum exploration and earth history*, 2nd edn. Cambridge University Press, Cambridge
- Rach O, Brauer A, Wilkes H, Sachse D (2014) Delayed hydrological response to Greenland cooling at the onset of the younger Dryas in western Europe. *Nat Geosci* 7:109–112
- Rau G, Takahashi T, Des Marais D, Repeta D, Martin J (1992) The relationship between $\delta^{13}\text{C}$ of organic matter and $[\text{CO}_2\text{aq}]$ in ocean surface water: data from a JGOFS site in the northeastern Atlantic Ocean and a model. *Geochim Cosmochim Acta* 56:1413–1419
- Robinson N, Eglinton G, Brassell SC, Cranwell PA (1984) Dinoflagellate origin for sedimentary 4α -methylsteroids and $5\alpha(H)$ -stanols. *Nature* 308:439–442
- Rowland SJ, Robson JN (1990) The widespread occurrence of highly branched acyclic C₂₀, C₂₅ and C₃₀ hydrocarbons in recent sediments and biota – a review. *Mar Environ Res* 30:191–216
- Sachs JP (2014) Hydrogen isotope signatures in the lipids of phytoplankton. In: *Treatise on geochemistry*, 2nd edn. Elsevier, Oxford, pp 79–94
- Sachs JP, Schwab VF (2011) Hydrogen isotopes in dinosterol from the Chesapeake Bay estuary. *Geochim Cosmochim Acta* 75:444–459
- Sachs JP, Maloney AE, Gregersen J et al (2016) Effect of salinity on $^2\text{H}/^1\text{H}$ fractionation in lipids from continuous cultures of the coccolithophorid *Emiliania huxleyi*. *Geochim Cosmochim Acta* 189:96–109
- Sachs JP, Maloney AE, Gregersen J (2017) Effect of light on $^2\text{H}/^1\text{H}$ fractionation in lipids from continuous cultures of the diatom *Thalassiosira pseudonana*. *Geochim Cosmochim Acta* 209:204–215
- Sachse D, Sachs JP (2008) Inverse relationship between D/H fractionation in cyanobacterial lipids and salinity in Christmas Island saline ponds. *Geochim Cosmochim Acta* 72:793–806
- Sachse D, Radke J, Gleixner G (2004) Hydrogen isotope ratios of recent lacustrine sedimentary *n*-alkanes record modern climate variability. *Geochim Cosmochim Acta* 68:4877–4889
- Sachse D, Radke J, Gleixner G (2006) δD values of individual *n*-alkanes from terrestrial plants along a climatic gradient – implications for the sedimentary biomarker record. *Org Geochem* 37:469–483
- Sachse D, Kahmen A, Gleixner G (2009) Significant seasonal variation in the hydrogen isotopic composition of leaf-wax lipids for two deciduous tree ecosystems (*Fagus sylvatica* and *Acer pseudoplatanus*). *Org Geochem* 40:732–742
- Sachse D, Gleixner G, Wilkes H et al (2010) Leaf wax *n*-alkane δD values of field-grown barley reflect leaf water δD values at the time of leaf formation. *Geochim Cosmochim Acta* 74:6741–6750

- Sachse D, Billault I, Bowen GJ et al (2012) Molecular palaeohydrology: interpreting the hydrogen-isotopic composition of lipid biomarkers from photosynthesizing organisms. *Annu Rev Earth Pl Sc* 40:221–249
- Sachse D, Dawson TE, Kahmen A (2015) Seasonal variation of leaf wax *n*-alkane production and $\delta^2\text{H}$ values from the evergreen oak tree, *Quercus agrifolia*. *Isot Environ Healt S* 51:124–142
- Sakata S, Hayes JM, McTaggart AR, Evans RA et al (1997) Carbon isotopic fractionation associated with lipid biosynthesis by a cyanobacterium: relevance for interpretation of biomarker records. *Geochim Cosmochim Acta* 61:5379–5389
- Sauer PE, Eglinton TI, Hayes JM et al (2001) Compound-specific D/H ratios of lipid biomarkers from sediments as a proxy for environmental and climatic conditions. *Geochim Cosmochim Acta* 65:213–222
- Schmidt H-L, Werner RA, Eisenreich W (2003) Systematics of ^2H patterns in natural compounds and its importance for the elucidation of biosynthetic pathways. *Phytochem Rev* 2:61–85
- Scholle PA, Arthur MA (1980) Carbon isotope fluctuations in cretaceous pelagic limestones: potential stratigraphic and petroleum exploration tool. *AAPG Bull* 64:67–87
- Schouten S, Klein Breteler WCM, Blokker P et al (1998) Biosynthetic effects on the stable carbon isotopic compositions of algal lipids: implications for deciphering the carbon isotopic biomarker record. *Geochim Cosmochim Acta* 62:1397–1406
- Schouten S, Ossebaar J, Schreiber K et al (2006) The effect of temperature, salinity and growth rate on the stable hydrogen isotopic composition of long chain alkenones produced by *Emiliania huxleyi* and *Gephyrocapsa oceanica*. *Biogeosciences* 3:113–119
- Schouten S, Woltering M, Rijpstra WIC et al (2007) The Paleocene–Eocene carbon isotope excursion in higher plant organic matter: differential fractionation of angiosperms and conifers in the Arctic. *Earth Planet Lett* 258:581–592
- Schubert BA, Jahren AH (2012) The effect of atmospheric CO_2 concentration on carbon isotope fractionation in C_3 land plants. *Geochim Cosmochim Acta* 96:29–43
- Schwab VF, Sachs JP (2009) The measurement of D/H ratio in alkenones and their isotopic heterogeneity. *Org Geochem* 40:111–118
- Schwab VRF, Sachs JP (2011) Hydrogen isotopes in individual alkenones from the Chesapeake Bay estuary. *Geochim Cosmochim Acta* 75:7552–7565
- Sessions AL (2006) Seasonal changes in D/H fractionation accompanying lipid biosynthesis in *Spartina alterniflora*. *Geochim Cosmochim Acta* 70:2153–2162
- Sessions A (2016) Factors controlling the deuterium contents of sedimentary hydrocarbons. *Org Geochem* 96:43–64
- Sessions AL, Burgoyne TW, Schimmelmann A (1999) Fractionation of hydrogen isotopes in lipid biosynthesis. *Org Geochem* 30:1193–1200
- Shanahan TM, Hughen KA, Ampel L et al (2013) Environmental controls on the 2H/1H values of terrestrial leaf waxes in the eastern Canadian Arctic. *Geochim Cosmochim Acta* 119:286–301
- Smith BN, Epstein S (1970) Biogeochemistry of the stable isotopes of hydrogen and carbon in salt marsh biota. *Plant Physiol* 46:738–742
- Tcherkez G, Mahé A, Hodges M (2011) $^{12}\text{C}/^{13}\text{C}$ fractionations in plant primary metabolism. *Trends Plant Sci* 16:499–506
- Tipple BJ, Pagani M (2007) The early origins of terrestrial C_4 photosynthesis. *Annu Rev Earth Pl Sc* 35:435–461
- Tipple BJ, Pagani M (2010) A 35 Myr north American leaf-wax compound-specific carbon and hydrogen isotope record: implications for C_4 grasslands and hydrologic cycle dynamics. *Earth Planet Sc Lett* 299:250–262
- Tipple BJ, Pagani M (2013) Environmental control on eastern broadleaf forest species' leaf wax distributions and D/H ratios. *Geochim Cosmochim Acta* 111:64–77
- Tipple BJ, Meyers SR, Pagani M (2010) Carbon isotope ratio of Cenozoic CO_2 : a comparative evaluation of available geochemical proxies. *Paleoceanography* 25:PA3202
- Tipple BJ, Berke MA, Doman CE et al (2013) Leaf-wax *n*-alkanes record the plant-water environment at leaf flush. *P Natl Acad Sci USA* 110:2659–2664

- Tipple BJ, Berke MA, Hambach B et al (2015) Predicting leaf wax *n*-alkane $^2\text{H}/^1\text{H}$ ratios: controlled water source and humidity experiments with hydroponically grown trees confirm predictions of Craig-Gordon model. *Plant Cell Environ* 38:1035–1047
- van der Meer MTJ, Benthien A, French KL et al (2015) Large effect of irradiance on hydrogen isotope fractionation of alkenones in *Emiliania huxleyi*. *Geochim Cosmochim Acta* 160:16–24
- van Dongen BE, Schouten S, Sinninghe Damsté JS (2002) Carbon isotope variability in monosaccharides and lipids of aquatic algae and terrestrial plants. *Mar Ecol Prog Ser* 232:83–92
- Versteegh GJM, Schefuß E, Dupont L et al (2004) Taraxerol and Rhizophora pollen as proxies for tracking past mangrove ecosystems. *Geochim Cosmochim Acta* 68:411–422
- Volkman JK, Eglinton G, Corner EDS et al (1980) Long-chain alkenes and alkenones in the marine coccolithophorid *Emiliania huxleyi*. *Phytochemistry* 19:2619–2622
- Volkman JK, Barrett SM, Dunstan GA (1994) C25 and C30 highly branched isoprenoid alkenes in laboratory cultures of two marine diatoms. *Org Geochem* 21:407–414
- White JWC (1988) Stable hydrogen isotope ratios in plants: a review of current theory and some potential applications. In: Rundel PW, Ehleringer JR, Nagy KA (eds) *Stable isotopes in ecological research*. Springer, New York, pp 142–162
- Wickman FE (1952) Variations in the relative abundance of the carbon isotopes in plants. *Geochim Cosmochim Acta* 2:243–254
- Wolhowe MD, Prahl FG, Probert I et al (2009) Growth phase dependent hydrogen isotopic fractionation in alkenone-producing haptophytes. *Biogeosciences* 6:1681–1694
- Zhang Z, Sachs JP (2007) Hydrogen isotope fractionation in freshwater algae: I. Variations among lipids and species. *Org Geochem* 38:582–608
- Zhang Z, Sachs JP, Marchetti A (2009) Hydrogen isotope fractionation in freshwater and marine algae: II. Temperature and nitrogen limited growth rate effects. *Org Geochem* 40:428–439
- Zhou Y, Grice K, Stuart-Williams H et al (2010) Biosynthetic origin of the saw-toothed profile in $\delta^{13}\text{C}$ and $\delta^2\text{H}$ of *n*-alkanes and systematic isotopic differences between *n*-, *iso*- and *anteiso*-alkanes in leaf waxes of land plants. *Phytochemistry* 71:388–403
- Zhou Y, Stuart-Williams H, Grice K et al (2015) Allocate carbon for a reason: priorities are reflected in the $^{13}\text{C}/^{12}\text{C}$ ratios of plant lipids synthesized via three independent biosynthetic pathways. *Phytochemistry* 111:14–20
- Zhou Y, Grice K, Stuart-Williams H et al (2016) Hydrogen isotopic differences between C₃ and C₄ land plant lipids: consequences of compartmentation in C₄ photosynthetic chemistry and C₃ photorespiration. *Plant Cell Environ* 39:2676–2690
- Ziegler H (1988) Hydrogen isotope fractionation in plant tissues. In: Rundel PW, Ehleringer JR, Nagy KA (eds) *Stable isotopes in ecological research*. Springer, New York, pp 105–123
- Zimmerman JK, Ehleringer JR (1990) Carbon isotope ratios are correlated with irradiance levels in the Panamanian orchid *Catasetum viridiflavum*. *Oecologia* 83:247–249



Plant Cuticular Waxes: Composition, Function, and Interactions with Microorganisms

5

Viktoria Valeska Zeisler-Diehl, Wilhelm Barthlott, and
Lukas Schreiber

Contents

1	Introduction	124
2	Composition of Plant Cuticular Waxes	125
3	Function of Plant Cuticular Waxes	126
4	Interactions of Microorganisms with Plant Cuticular Waxes	128
5	Research Needs	134
	References	135

Abstract

The interface between leaves and the surrounding environment is formed by the wax-covered plant cuticle, which is hydrophobic and highly impermeable to water and dissolved solutes. The surface itself may become superhydrophobic by complex three-dimensional wax crystals. There is evidence that this system evolved already early with the colonization of land some 450 million years ago. Although the leaf surface represents a hostile environment, because water and nutrient availability is very limited and variations in temperature and light intensity can be quite large, it forms the habitat for specialized epiphyllic microorganisms successfully colonizing the leaf surface which is also called phyllosphere. Certain strategies improving living conditions within the phyllosphere have been developed by epiphyllic microorganisms. They can significantly enhance leaf surface wetting and water permeability of the hydrophobic cuticle. This interaction

V. V. Zeisler-Diehl · L. Schreiber (✉)

Institute of Cellular and Molecular Botany (IZMB), University of Bonn, Bonn, Germany

e-mail: vzeisler@uni-bonn.de; lukas.schreiber@uni-bonn.de

W. Barthlott

Nees Institut for Biodiversity of Plants, University of Bonn, Bonn, Germany

e-mail: barthlott@uni-bonn.de

© Springer Nature Switzerland AG 2020

H. Wilkes (ed.), *Hydrocarbons, Oils and Lipids: Diversity, Origin, Chemistry and Fate*,
Handbook of Hydrocarbon and Lipid Microbiology,

https://doi.org/10.1007/978-3-319-90569-3_7

123

significantly increases the abundance of water on the leaf surface, and as a consequence, leaching of nutrients to the leaf surface should be increased, thus becoming available for epiphyllic microorganisms. This strategy is supported by the ability of biosurfactant production, which represents a common and important adaptation of epiphyllic microorganisms.

1 Introduction

Outer epidermal cell walls of leaves and fruits are covered by the plant cuticle (Riederer and Müller 2006). It represents an extracellular lipid polymer of hydroxy fatty acids, which are esterified and in addition often linked by ether bonds and direct carbon/carbon bonds between the monomers (Pollard et al. 2009; Villena et al. 1999). Furthermore, the cuticle contains cell wall carbohydrates extending from the epidermal cell into the cutin polymer (Guzman et al. 2014; Segado et al. 2016). Cuticular waxes are deposited on the outer surface (epicuticular wax) and within (intracuticular wax) the cutin polymer (Samuels et al. 2009). Cuticular waxes, which are diverse in their chemical composition (Buschhaus and Jetter 2011), are solid and partially crystalline at room temperature (Reynhardt and Riederer 1994). Due to this highly ordered structure of cuticular waxes on the molecular level, they seal the plant cuticle and make it highly impermeable to water and dissolved organic and inorganic solutes (Schreiber and Schönherr 2009). The evolutionary invention of cuticles sealing aboveground parts of higher land living plants represented an important adaptation for successfully colonizing the mainland about 450 to 500 million years ago (Kenrick and Crane 1997). There is good evidence that superhydrophobicity caused by epicuticular wax crystals already evolved in the late Ordovician or Silurian (Barthlott et al. 2016). Apoplastic hydrophobic barriers were a key innovation in plants for life outside of water (Niklas et al. 2017).

The largest fraction of the terrestrial biomass is formed by plants representing the main primary producers by photosynthesis (Groombridge and Jenkins 2002). Leaves as the sites of photosynthesis are designed as two-dimensional organs with larger surface area/volume ratios for efficiently absorbing sun light. Consequently, leaf surfaces form a large surface area which amounts to 1 billion square kilometers, thus being 6.8-times larger than the surface of the mainland on earth (Vorholt 2012). All leaf surfaces are covered by a waxy cuticle forming the habitat for microorganisms which has been named phyllosphere (Ruinen 1961). Since more than half a century, the microbial ecology of the phyllosphere represents interdisciplinary research conducted by a small but diverse group of scientists mostly from either microbial ecology or plant sciences (Bailey et al. 2006). They are interested in studying and understanding the hydrophobic leaf surfaces as habitats for microorganisms (Fig. 1) investigating basic ecological questions such as abiotic and biotic factors in this habitat (Meyer and Leveau 2012), microbial diversity (Whipps et al. 2008), interactions between microorganisms (Hunter et al. 2010) and between microorganisms and waxy leaf surfaces (Knoll and Schreiber 2004), and immigration and emigration of microorganisms (Kinkel 1997). It has been estimated that 10^6 to 10^7 bacteria per square

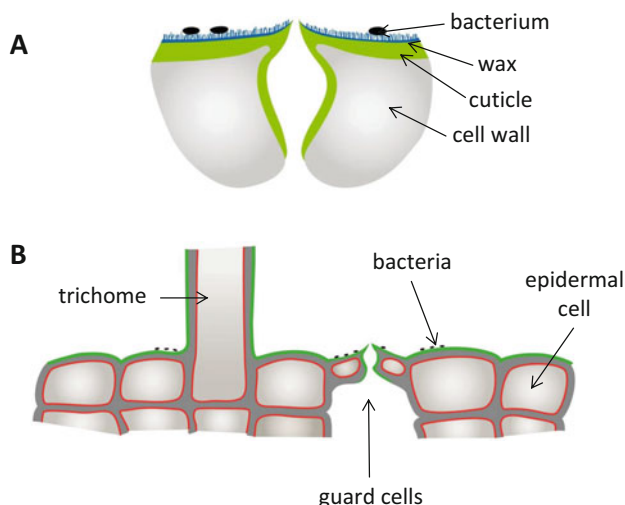


Fig. 1 Schematic cross section through the outer leaf surface with a trichome and guard cells. (a) detail, (b) overview. Epidermal cells surrounded by the cell membrane (red), the cell wall (gray), the cuticle (green), epi- and intracuticular waxes (blue), and bacterial cells (black) sitting on the waxy cuticle surface

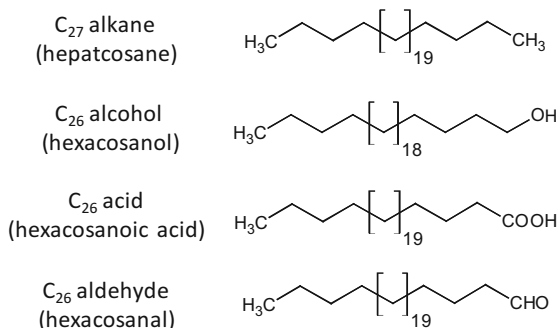
centimeter can live on the surface of an individual leaf (Lindow and Brandl 2003). Compared to bacteria, fungi as further important group of microorganisms have been less studied.

In this review, we will focus on leaf surfaces from a plant scientist's view. We will shortly describe the chemical composition of epicuticular waxes, forming the chemical basis of this habitat, and we will discuss the function of cuticular waxes essentially establishing the barrier properties of the leaf surface. Finally, modifications of the waxy leaf surface by microorganisms and interactions between microorganisms (mainly bacteria) and waxy leaf surfaces will be discussed. The focus will be mostly, but not exclusively, on epiphyllic nonpathogenic bacteria. However, pathogenic as well as nonpathogenic microorganisms (bacteria and fungi) face the same conditions and problems when arriving on the leaf surface and trying to establish there; thus, examples given here could also apply to pathogenic microorganisms.

2 Composition of Plant Cuticular Waxes

Plant cuticular waxes represent a highly diverse mixture of aliphatic compounds (Jetter et al. 2006). They can be extracted with organic solvents from the surfaces of leaves, fruits, and shoots in their primary developmental state (Riederer and Schneider 1989). The chemical composition of cuticular wax can best be analyzed using gas chromatography and mass spectroscopy (Kolattukudy and Walton 1973).

Fig. 2 Examples of the chemical structure of the four most abundant classes (alkanes, alcohols, acids, and aldehydes) of linear long-chain aliphatic wax constituents. Chain lengths of the molecules can vary between C_{16} and C_{35}



Two major fractions have been described: linear long-chain aliphatics and pentacyclic triterpenoids (Jetter et al. 2006). Biosynthesis of cuticular wax is described in a separate article of this volume (► [Chap. 6, “Biosynthesis of the Plant Cuticle”](#)); thus, it will not be discussed in detail here. Linear long-chain aliphatic compounds are essentially derivatives of C_{16} and C_{18} fatty acids, which are elongated and in addition functionally modified (Kunst and Samuels 2003). Pentacyclic triterpenoids are derived from the terpenoid pathway composed of 6 C_5 units finally leading to C_{30} molecules (Wang et al. 2011).

The fraction of linear, long-chain aliphatic molecules mainly consists of fatty acids, alcohols, aldehydes, and alkanes with chain lengths varying between C_{16} and C_{35} (Fig. 2). Esters formed between fatty acids and alcohols are consequently characterized by extraordinarily long chain lengths between C_{32} and C_{64} . Besides these most common compound classes, a large number of additional more specialized compound classes (ketones, secondary alcohols, diols, etc.) have been described and characterized as more specific wax constituents occurring within certain taxonomic groups (Jetter et al. 2006). Whereas linear long-chain aliphatic compounds occur as a relevant fraction in all samples of cuticular wax analyzed so far, pentacyclic triterpenoids can form a significant or even the major wax fraction in certain taxonomic groups (Jetter et al. 2006), whereas they are almost or completely absent in other species. This chemical diversity of plant waxes is visualized by the high complexity and diversity of the three-dimensional crystalline epicuticular wax covers, which is determined by their chemistry (Barthlott et al. 1998).

3 Function of Plant Cuticular Waxes

Cuticular waxes, which are deposited within the outer fraction of the cutin polymer and on the outer surface of the cutin polymer, form the interface between the plant and the surrounding atmosphere. Depending on the plant species, the organ and the developmental state wax coverage can significantly vary (Wang et al. 2015). Most leaves are characterized by a wax coverage varying between 10 and 100 μg per square centimeter (Schreiber and Riederer 1996). When assuming a wax density of 1 g per cm^3 , this leads to a thickness of the wax layer on leaf surfaces between 10 and

100 nm. This very thin wax layer in fact forms the actual interface between the leaf and the environment.

Making leaf surfaces non-wettable or even superhydrophobic represents one of the main functions of epicuticular waxes. This phenomenon is best known as Lotus effect (Barthlott and Neinhuis 1997). Wax molecules, which are mostly composed of methyl and methylene groups, are hydrophobic and thus water-repellent leading to contact angles of 90 degree (Holmes-Farley et al. 1988). However, with the formation of three-dimensional epicuticular wax crystallites, contact angles can be significantly increased reaching values of 140 to 175 degrees, which is also of considerable interest for biomimetic technical applications (Barthlott et al. 2017). This renders leaf surfaces essentially non-wettable. This effect prevents guard cells from infiltration with water, which would inhibit gas exchange, and it would offer microorganisms, colonizing the leaf surface, a route into the leaf interior (apoplastic space), which must be avoided.

Besides rendering leaf surfaces non-wettable, cuticular waxes have to seal the cuticle, making it highly impermeable to water and dissolved molecules (Schönherr and Riederer 1989). The cutin polymer itself is highly permeable since upon wax extraction with organic solvents, permeability of plant cuticles increases by 2 to 3 orders of magnitude (Fig. 3; Schönherr 1976; Schönherr and Lenzian 1981). Thus, only with cuticular waxes, which are solid and partially crystalline at room temperature, cuticles represent efficient transport barriers. It is still a matter of debate whether intracuticular or both epi- and intracuticular waxes establish the transport barrier of cuticles. Epicuticular waxes can selectively be removed from the cuticle surface by mechanical stripping (Jetter et al. 2000). Thus, cuticular permeability can be measured before and after removal of epicuticular wax. Whereas in some experiments it was found that the cuticular transport barrier is essentially established

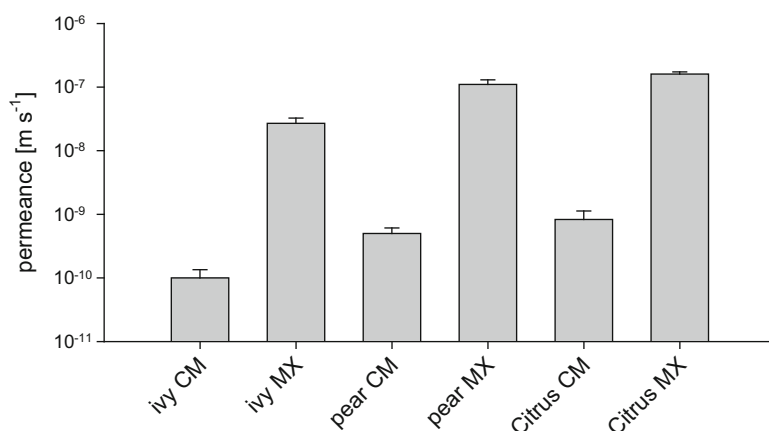


Fig. 3 Effect of cuticular wax extraction on permeability of leaf cuticles. Permeances for water [m s^{-1}] were measured for intact cuticular membranes (CM) and wax-free cuticular membranes (MX). Upon wax extraction with organic solvent, permeances increased by factors between 100 and 1000. (Data from Schönherr and Lenzian 1981)

by the intracuticular wax fraction (Zeisler and Schreiber 2016), in other experiments, a contribution of both epi- and intracuticular waxes to total barrier properties was described for some species (Jetter and Riederer 2016).

Since it is the cuticular wax establishing the transport barrier, methods have been developed studying transport properties of isolated cuticular wax. Chloroform-extracted wax can be re-crystallized as thin layers, and sorption and diffusion of organic molecules in these wax layers using radiolabeled probes can be measured (Schreiber and Schönherr 1993). These experiments confirmed that it is the cuticular wax layer sealing the cutin polymer and thus establishing the cuticular transport barrier. Diffusion coefficients of solutes, which were sufficiently soluble in re-crystallized wax, e.g., benzoic acid or salicylic acid, was as low as $10^{-17} \text{ m}^2 \text{ s}^{-1}$ (Kirsch et al. 1997). These are diffusion coefficients which are several orders of magnitude lower compared to diffusion of comparable molecules in water, where diffusion coefficients are in the range of 10^{-10} to $10^{-12} \text{ m}^2 \text{ s}^{-1}$ (Cussler 1984).

It was described within the last decades that polar compounds, e.g., ions and charged organic molecules, which are basically insoluble in the lipophilic cutin and wax phase, can diffuse along a polar path of transport across the cuticle (Schönherr 2006). It is postulated that these polar paths of transport are formed at sites in the cuticle where carbohydrates from the outer epidermal cell wall extend into the cutin polymer and thus form these polar regions within the hydrophobic cutin polymer. The occurrence of these polar paths of transport, which are preferentially observed in the cuticle covering guard cells, trichomes, and anticlinal cell walls (Schreiber 2005), should be of special relevance for microorganisms sitting on the leaf surfaces. At these sites of the leaves, higher amounts of essential nutrients diffuse from the leaf interior to the leaf surface, where they could be metabolized by epiphyllic microorganisms. It was in fact described that epiphyllic microorganisms preferentially colonized these niches (base of trichomes, surrounding of guard cells, and anticlinal cell walls) of the leaf surfaces (Krimm et al. 2005; Leveau and Lindow 2001).

4 Interactions of Microorganisms with Plant Cuticular Waxes

The leaf surface represents a very harsh habitat with unfavorable environmental conditions. Light conditions, including UV light, temperature, and humidity can vary extremely on a diurnal and annual scale (Lindow and Brandl 2003; Vorholt 2012). Due to the high impermeability and the pronounced lipophilicity of the cuticle, nutrient and water availability is very limited, because (1) wetting of the leaf surface is poor if not impossible (Koch et al. 2008) and (2) the diffusion resistance of the cuticle is very high, although the outer epidermal cell wall below the cuticle is fully saturated with water and the apoplast (plant cell wall space) contains ions, sugars, and amino acids (Lohaus et al. 2001; Ruan et al. 1996). Nevertheless, leaf surfaces are frequently colonized by microorganisms, although depending on the corresponding environmental conditions, colonization can vary largely (Kinkel 1997). Consequently, any strategy of microorganisms changing physicochemical properties of leaf surface, e.g., increasing leaf surface wettability

or cuticular permeability for water and dissolved nutrients, should be beneficial for survival in the phyllosphere.

It has been shown that leaf (Knoll and Schreiber 1998) and needle surface wettability (Schreiber 1996), quantified by contact angles of water, significantly increased with the intensity of colonization by microorganisms. With conifer needles, it was observed by scanning electron microscopy that colonization of the wax-covered needle surfaces with microorganisms significantly increased with needle age increasing from the current year to the fourth year (Fig. 4). Artificial colonization of silanized, hydrophobic glass surfaces with specific bacteria (*Pseudomonas fluorescens*) confirmed these observations. The degree of the contact angle of water was highly correlated and decreased with increasing relative fractions of the glass surface covered by bacteria (Fig. 5). Obviously, the droplet of water used for measuring the contact angle is in contact with the polar outer surface of the bacterial cell wall instead of the lipophilic waxy leaf surface, and depending on the intensity of bacterial colonization, this leads to a continuous decrease in contact angles.

In addition, it has been described that epiphyllic bacteria living on the hydrophobic leaf surface can form an extracellular matrix (EPS: extracellular polymeric substances), which protects microorganisms from rapid dehydration and direct exposure to UV light (Morris and Monier 2003). Since EPS are composed of carbohydrates, which by nature are polar compared to the lipophilic water-repellent wax molecules, consequently this also leads to enhanced leaf surface wettability. The occurrence of biosurfactants can be considered as a further efficient strategy increasing leaf surface wetting. Many epiphyllic bacteria (Burch et al. 2016) and also some epiphyllic fungi (Bhardwaj et al. 2013) are characterized by the ability to synthesize biosurfactants and export them to the leaf surface. Biosurfactants, as synthetic surfactants, are amphiphilic and thus can efficiently mediate between the hydrophobic water-repellent waxy leaf surface and polar water. Biosurfactants covering a

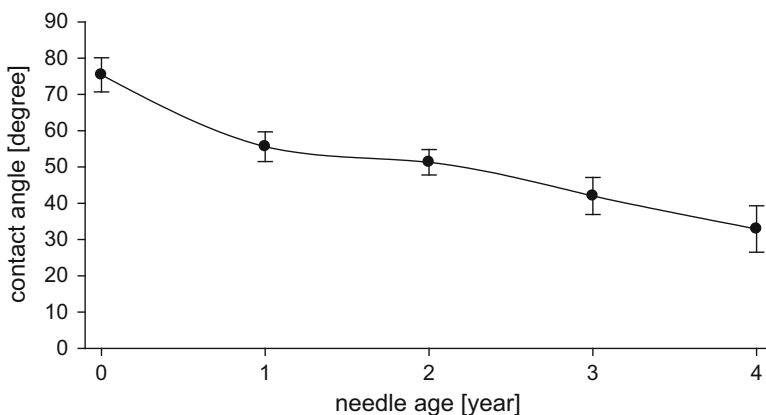


Fig. 4 Contact angles of water droplets measured on *Abies grandis* needle surfaces. Contact angles decreased with increasing needle age between the current year (0) and the fourth year (4). Data from Schreiber (1996)

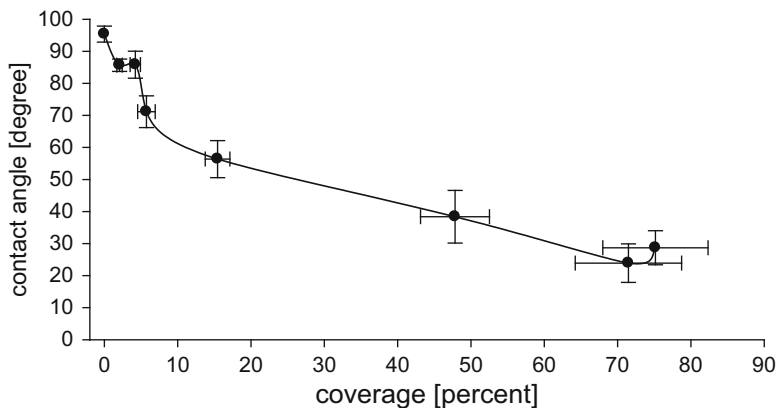


Fig. 5 Contact angles of water droplets measured on silanized glass surfaces colonized with bacterial cells (*Pseudomonas fluorescens*). Contact angles decreased with increasing density of surface colonization by bacterial cells from 95 to about 30 degree. (Data from Knoll and Schreiber 1998)

hydrophobic leaf surface can lead to significantly improved wetting of the water-repellent hydrophobic waxy leaf surface (Bunster et al. 1989).

In addition, biosurfactants will also significantly increase overall water availability in the phyllosphere since they are hygroscopic and tend to efficiently bind water to the leaf surface at a given humidity normally much lower than 100%, at which water would not tend to bind to a clean bacteria- and biosurfactant-free lipophilic leaf surface. Since water is very limited in the phyllosphere and biosurfactants can increase water availability, they also enhance survival of epiphyllic bacteria. Biosurfactant-deficient mutants showed a significantly decreased survival rate in the phyllosphere with varying humidity compared to the biosurfactant-producing wildtype (Burch et al. 2014). Bacterial population densities significantly decreased in periods of reduced humidity, and recovery of bacterial population density of the biosurfactant-producing strain compared to the biosurfactant-deficient mutant was much higher.

Bacteria living on the outer hydrophobic leaf surface could use three different sources of nutrients. (1) They can use nutrients deposited via rain and fog droplets or dust from the atmosphere to the leaf surface (Lindberg et al. 1986). (2) The living leaf interior below the cuticle represents a nutrient-rich source which contains essentially all inorganic (ions) and organic (C-, N-sources, etc.) nutrients needed by microorganisms. (3) Finally, the leaf surface itself composed of wax and cutin monomers could represent a carbon and energy source. Concerning the leaf interior as a potential nutrient source, it must be kept in mind that the outer leaf surface is highly isolated from the leaf interior (symplastic as well as apoplastic space) by the fairly impermeable plant cuticle. Especially permeability of charged ions and polar organic compounds, e.g., sugars and amino acids, across the lipophilic plant cuticle is very low (Schönherr 2006). In the past model calculations predicted that the plant

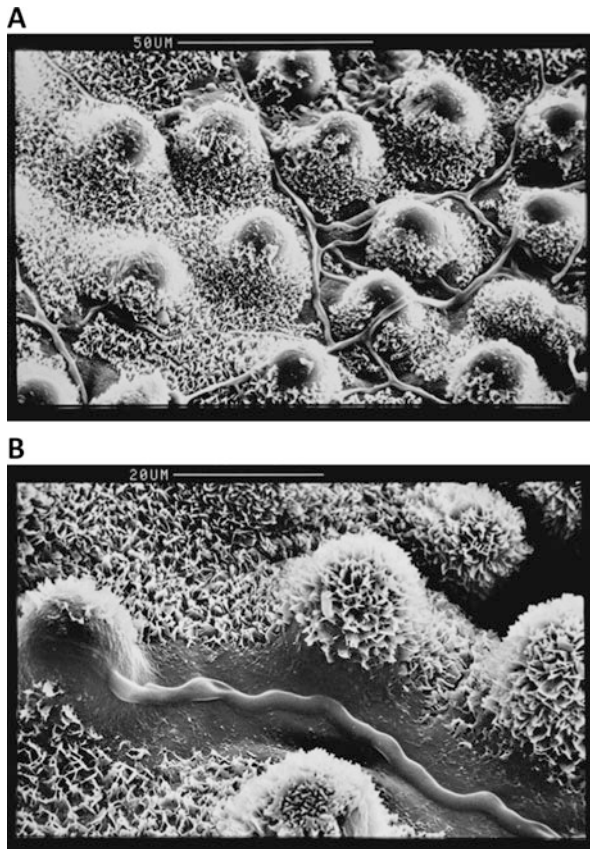
cuticle would not allow diffusion of significant amounts of ions and polar organic solutes across cuticles to be used by epiphyllic bacteria as nutrient sources (Schönherr and Baur 1996).

These model calculations however were based on a very specialized experimental system exclusively using isolated cuticular membranes which were free of guard cells and trichomes. In following transport and permeability studies using intact leaves, which had guard cells and trichomes, it became evident that the cuticle-covering guard cells, trichomes, and also anticlinal cell walls represented sites where polar compounds obviously could more efficiently leach through the cuticle to the leaf surface (Schlegel et al. 2005; Schreiber 2005; Schönherr 2006). Microscopic observations studying the distribution of epiphyllic bacteria on the leaf surface in fact found that trichomes, guard cells, and anticlinal cell walls represented niches preferentially colonized by epiphyllic microorganisms (Krimm et al. 2005; Leveau and Lindow 2001). Obviously, epiphyllic microorganisms select these specific sites in the phyllosphere because of increased nutrient availability. Thus, this lateral heterogeneity within the leaf surface, which is very common with many leaf surfaces, should not be ignored when studying the interaction between leaf surfaces and microorganisms. It was also observed that lower leaf sides are often more densely colonized by epiphyllic microorganisms compared to the upper leaf side (Krimm et al. 2005). The reasons for this are probably the protection of microorganisms from direct irradiation and the higher abundance or exclusive occurrence of guard cells on the lower leaf side, which will lead to higher ambient humidity at the leaf surface due to the stomatal transpiration. Thus, exposure of microorganisms to various environmental conditions is less harsh on the lower compared to the upper leaf side.

Utilization of wax (and potentially cutin) constituents as carbon and energy sources could also represent a nutrition strategy of epiphyllic microorganisms. However, up to now, direct experimental results verifying that wax (and cutin) could be used as carbon and energy source are still missing. There are observations that epiphyllic microorganisms can lead to significant visual changes in the appearance of the leaf surface (Ueda et al. 2015). This has been interpreted as a potential enzymatic degradation of cutin and/or wax; however, direct chemical or biochemical evidence for the metabolism of cutin or wax constituents is not yet available. Scanning electron microscopic investigations of a fungus growing on the leaf surface of a Euphorbiaceae (*Euphorbia myrsinites*), characterized by a dense coverage with epicuticular wax platelets, show for the first time impressively that wax platelets along the growing hyphae disappear (Fig. 6). The underlying mechanism, whether it is “wax melting,” eventually induced by biosurfactants, or enzymatic wax degradation by extracellular enzymes, or the presence of an extracellular fungal substance similar to EPS just covering the wax platelets is not yet solved. Nevertheless, these dramatic changes of the highly ordered leaf surface waxes should lead to significant changes in the physicochemical properties of the waxy leaf surface, e.g., enhanced wetting, and thus be advantageous for the epiphyllic fungus.

It is remarkable that epiphyllic microorganisms are often characterized by the ability of biosurfactant production (Bhardwaj et al. 2013; Burch et al. 2016). Besides

Fig. 6 Fungal hyphae growing on the leaf surface of *Euphorbia myrsinites* densely covered with epicuticular wax platelets. (a) Overview, (b) detail. Wax platelets completely disappeared in the vicinity of the fungal hyphae



enhancing leaf surface wetting and increasing water availability, biosurfactants might be essential for microbial wax degradation. It is well known that certain environmental strains of bacteria are capable of degrading petroleum constituents (Ron and Rosenberg 2002). An essential prerequisite for degrading these lipophilic compounds represents the ability of these bacteria to synthesize biosurfactants, which solubilize the petroleum molecules in water and thus make them available to bacteria for the enzymatic degradation. Different from plant waxes, which are solid and partially crystalline at room temperature (Reynhardt and Riederer 1994) due to their chain lengths between C_{20} and C_{64} , chain lengths of petroleum start at C_1 and can extend to C_{70} and even higher. The liquid petroleum fraction with chain lengths between C_1 and C_{20} is characterized by higher water solubilities and lower octanol-water partition coefficients compared to the solid fraction with chain lengths higher than C_{20} . Thus, this petroleum fraction with short chain lengths is more accessible to biosurfactant-mediated degradation by extracellular microbial enzymes. Bacterial degradation of very lipophilic and highly water-insoluble plant waxes, where chain lengths start at C_{20} , will be a lot more challenging.

With the production of biosurfactants, enhancing leaf surface wetting and water availability, living conditions in the leaf surface habitats are already changed in favor of epiphyllic microorganisms. As a further strategy, it should also be of major advantage to enhance leaf surface permeability and thus potentially increase nutrient leaching from inside of the leaf to the leaf surface. It is well known that synthetic surfactants used in spray solutions in agrochemistry not only enhance leaf surface wetting of the spray droplets (Kirkwood 1999) but also act as plasticizers within the transport-limiting barrier of the plant cuticle made of wax (Schreiber 2006). As a consequence, diffusion rates of agrochemicals across the transport-limiting plant cuticle into the leaf are significantly enhanced (Shi et al. 2005).

It has been described that epiphyllic bacteria when inoculated to the surface of isolated cuticles could increase cuticular water permeability by two-fold (Fig. 7; Burch et al. 2014; Schreiber et al. 2005). This effect was most pronounced with bacteria-producing biosurfactants. Although water itself does not represent a nutrient, this enhanced cuticular permeability of water increases water availability for epiphyllic microorganisms living in the phyllosphere. Furthermore, increased amounts of water present on the leaf surface, especially in the presence of biosurfactants, should form a sink for ions and organic solutes and enhance the leaching of these compounds through the cuticle to the leaf surface, which will not occur on a dry water-free leaf surface.

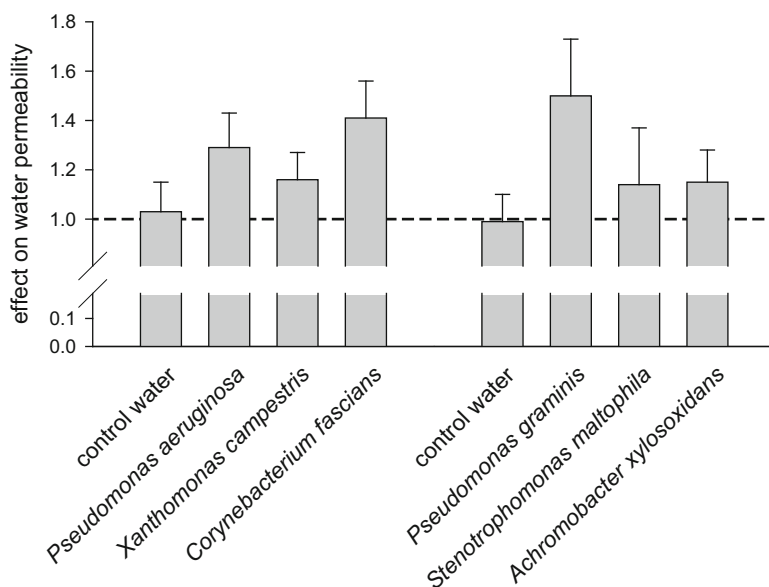


Fig. 7 Effect of bacteria colonizing the surface of cuticles isolated from cherry laurel (bars 1 to 4) and ivy (bars 5 to 8) on cuticular water permeability. Water permeability increased by factors up to 1.5-fold in the presence of the bacteria compared to the control (treatment of the cuticle surface with water). (Data from Schreiber et al. 2005)

The exact mechanism how this increase in rates of cuticular water permeability is achieved is not yet known. However, it is unlikely that the mechanism increasing cuticular permeability, which has been described for technical surfactants used in agrochemistry (Schreiber 2006), is the same here. These technical surfactants reducing barrier properties of plant cuticles are on average much smaller (molecular weights around 300–500) compared to biosurfactants (molecular weights around 1000), and they are generally uncharged and fairly lipophilic. These technical surfactants, which enhance cuticular permeability by one order of magnitude or even more, are sorbed in significant amounts in the transport-limiting wax layer and thus cause this described plasticizing effect (Burghardt et al. 1998). With much larger, polar, and charged biosurfactants (Parra et al. 1989), such a mode of action seems to be less probable. Nevertheless, this effect of biosurfactants enhancing rates of cuticular water permeability, although the mode of action remains to be solved, represents an important strategy improving living conditions within the phyllosphere.

A very specific type of recognition between a fungal pathogen (*Blumeria*) and its host (barley) based on the chemical composition of the epicuticular wax fraction has been discovered recently (Hansjakob et al. 2010; Zabka et al. 2008). It was found that specifically linear-long chain aldehydes, with *n*-hexacosanal being the most effective compound, were strongly inducing germination and further differentiation of conidia on both the surface of barley leaves and on artificial model surfaces which were spiked with the corresponding aldehydes varying in chain length. Other linear long-chain aliphatic compounds also occurring in barely wax, including primary fatty acids, *n*-alkanes, primary alcohols, or esters, were obviously not sensed by the conidia since germination was affected.

Within the last years, genomic and proteomic approaches and the smart combination of both approaches (proteogenomics) revealed that there is also sensing across the cuticle between epiphyllic bacteria and the plant leading to specific gene expression and protein synthesis in bacteria (Delmotte et al. 2009). In adaptation to the availability of specific nutrients available on the leaf surface, characteristic patterns of proteins were detectable, which were synthesized by bacteria. This included enzymes utilizing methanol, which is evolving from the leaf interior reaching the leaf surface via diffusion through guard cells and thus can be utilized by epiphyllic bacteria. Furthermore, expression and synthesis of transporters involved in bacterial transport of carbohydrates, originating from the leaf interior and being available in the phyllosphere, has been described. Using this approach in future, specific interactions between leaves and epiphyllic microorganisms on the molecular level can be studied in more detail.

5 Research Needs

Future research questions regarding leaf surfaces and the interaction with microorganisms should address specific questions related to the three areas: (i) diversity of wax chemistry, (ii) function of the cuticular transport barrier, and (iii) active modification of the leaf surface by microorganisms.

Wax chemistry: Why is there such a tremendous diversity in wax chemistry (chain lengths, compound classes, and functionalities) between different plant organs but also between different plant species? Each species has its unique wax composition, but to date, there is no convincing answer why this is needed. Is it the specific “wax flavor” at the outer surface of the leaf, which regulates the interaction of every individual species with the surrounding abiotic and biotic environment including epiphyllic microorganisms? Can an individual species-specific wax composition be recognized by a specific microorganism thus allowing the identification of its host?

Cuticular transport barrier: Further research is needed to clarify why certain regions of the leaf surface (guard cells, trichomes, anticlinal cell walls) are characterized by an enhanced diffusion of polar compounds through the cuticle to the leaf surface. Guard cells, trichomes, cuticular permeability? However, since trichomes and guard cells represent structures which are abundant on many leaf surfaces, future studies in phyllosphere microbiology should focus on intact leaves characterized by these structures, which seem to be of major significance for nutrient availability for epiphyllic microorganisms living on leaves.

Leaf surface/microorganism interactions: Besides increasing leaf surface wetting, there is good evidence that epiphyllic microorganisms can increase cuticular water permeability to some extent. However, the mechanism how this is achieved still remains unknown. The questions to be solved are whether biosurfactants themselves could cause this effect or if there is any activity of wax- and/or cutin-degrading enzymes contributing to this effect of enhanced cuticular water permeability? If there would be any active microbial metabolisms involved, this also raises the question whether cuticular wax and/or cutin could be used as a carbon and energy source? There is convincing microscopical evidence that epiphyllic fungi can significantly change the three-dimensional epicuticular wax structure (Fig. 6), but the underlying mechanisms causing this observation are not known to date. It is also not known in detail what signals can be exchanged across the cuticle between epiphyllic microorganisms and the living leaf tissue below and whether this could lead to mutual responses in both plants and epiphyllic microorganisms?

Acknowledgments Long-lasting financial support by the DFG (Deutsche Forschungsgemeinschaft) to LS is gratefully acknowledged.

References

- Bailey MJ, Lilley AK, Timms-Wilson TM, Spencer-Phillips PTN (2006) Microbial ecology of aerial plant surfaces. CABI, Wallingford
- Barthlott W, Mail M, Bhushan B, Koch K (2017) Plant surfaces: structures and functions for biomimetic innovations. *Nano-Micro Letters* 9:23
- Barthlott W, Mail M, Neinhuis C (2016) Superhydrophobic hierarchically structured surfaces in biology: evolution, structural principles and biomimetic applications. *Philos Trans R Soc Lond A* 374:20160–20191
- Barthlott W, Neinhuis C (1997) Purity of the sacred lotus, or escape from contamination in biological surfaces. *Planta* 202:1–8

- Barthlott W, Neinhuis C, Cutler D, Ditsch F, Meusel I, Theisen I, Wilhelmi H (1998) Classification and terminology of plant epicuticular waxes. *Bot J Linn Soc* 126:237–260
- Bhardwaj G, Cameotra SS, Chopra HK (2013) Biosurfactants from fungi: a review. *J Pet Environ Biotechnol* 4:1–6
- Bunster L, Fokkema NJ, Schippers B (1989) Effect of surface-active *Pseudomonas* spp. on leaf wettability. *Appl Environ Microbiol* 55:1340–1345
- Burch AY, Do PT, Sbodio A, Suslow TV, Lindow SE (2016) High-level culturability of epiphytic bacteria and frequency of biosurfactant producers on leaves. *Appl Environ Microbiol* 82:5997–6009
- Burch AY, Zeisler V, Yokota K, Schreiber L, Lindow SE (2014) The hygroscopic biosurfactant syringafactin produced by *Pseudomonas syringae* enhances fitness on leaf surfaces during fluctuating humidity. *Environ Microbiol* 16:2086–2098
- Burghardt M, Schreiber L, Riederer M (1998) Enhancement of the diffusion of active ingredients in barley leaf cuticular wax by monodisperse alcohol ethoxylates. *J Agric Food Chem* 46:1593–1602
- Buschhaus C, Jetter R (2011) Composition differences between epicuticular and intracuticular wax substructures: how do plants seal their epidermal surfaces? *J Exp Bot* 62:841–853
- Cussler EL (1984) Diffusion. Mass transfer in fluid systems. Cambridge University Press, Cambridge
- Delmotte N, Knief C, Chaffron S, Innerebner G, Roschitzki B, Schlappbach R, von Mering C, Vorholt JA (2009) Community proteogenomics reveals insights into the physiology of phyllosphere bacteria. *Proc Natl Acad Sci U S A* 106:16428–16433
- Groombridge B, Jenkins M (2002) World atlas of biodiversity: Earth's living resources in the 21st century. University of California Press, Berkeley
- Guzman P, Fernandez V, Graca J, Cabral V, Kayali N, Khayet M, Gil L (2014) Chemical and structural analysis of *Eucalyptus globulus* and *E. camaldulensis* leaf cuticles: a lipidized cell wall region. *Front Plant Sci*. <https://doi.org/10.3389/fpls.2014.00481>
- Hansjakob A, Bischof S, Bringmann G, Riederer M, Hildebrandt U (2010) Very-long-chain aldehydes promote in vitro prepenetration processes of *Blumeria graminis* in a dose- and chain length-dependent manner. *New Phytol* 188:1039–1054
- Holmes-Farley SR, Bain CD, Whitesides GM (1988) Wetting of functionalized polyethylene film having ionizable organic acids and bases at the polymer-water interface: relations between functional group polarity, extent of ionisation, and contact angle with water. *Langmuir* 4:921–937
- Hunter PJ, Hand P, Pink D, Whipps JM, Bending GD (2010) Both leaf properties and microbe-microbe interactions influence within-species variation in bacterial population diversity and structure in the lettuce (*Lactuca* species) phyllosphere. *Appl Environ Microbiol* 76:8117–8125
- Jetter R, Kunst L, Samuels AL (2006) Composition of plant cuticular waxes. In: Riederer M, Müller C (eds) *Biology of the plant cuticle*. Blackwell, Oxford, pp 145–181
- Jetter R, Riederer M (2016) Localization of the transpiration barrier in the epi- and intracuticular waxes of eight plant species: water transport resistances are associated with fatty acyl rather than alicyclic components. *Plant Physiol* 170:921–934
- Jetter R, Schäffer S, Riederer M (2000) Leaf cuticular waxes are arranged in chemically and mechanically distinct layers: evidence from *Prunus laurocerasus* L. *Plant Cell Environ* 23:619–628
- Kenrick P, Crane PR (1997) The origin and early evolution of plants on land. *Nature* 389:33–39
- Kinkel LL (1997) Microbial population dynamics on leaves. *Annu Rev Phytopathol* 35:327–347
- Kirkwood RC (1999) Recent developments in our understanding of the plant cuticle as a barrier to the foliar uptake of pesticides. *Pestic Sci* 55:69–77
- Kirsch T, Kaffarnik F, Riederer M, Schreiber L (1997) Cuticular permeability of the three tree species *Prunus laurocerasus* L., *Ginkgo biloba* L. and *Juglans regia* L. - comparative investigation of the transport properties of intact leaves, isolated cuticles and reconstituted cuticular waxes. *J Exp Bot* 48:1035–1045

- Knoll D, Schreiber L (1998) Influence of epiphytic micro-organisms on leaf wettability: wetting of the upper leaf surface of *Juglans regia* L. and of model surfaces in relation to colonisation by micro-organisms. *New Phytol* 140:271–282
- Knoll D, Schreiber L (2004) Methods for analysing the interactions between epiphytic micro-organisms and leaf cuticles. In: Varma A, Abbott L, Werner D, Hampp R (eds) *Plant surface microbiology*. Springer, Heidelberg, pp 471–487
- Koch K, Bhushan B, Barthlott W (2008) Diversity of structure, morphology and wetting of plant surfaces. *Soft Matter* 4:1943–1963
- Kolattukudy PE, Walton TJ (1973) The biochemistry of plant cuticular lipids. *Prog Chem Fats Other Lipids* 13:119–175
- Krimm U, Abanda-Nkpaw D, Schwab W, Schreiber L (2005) Epiphytic microorganisms on strawberry plants (*Fragaria ananassa* cv. Elsanta): identification of bacterial isolates and analysis of their interaction with leaf surfaces. *FEMS Microbiol Ecol* 53:483–492
- Kunst L, Samuels AL (2003) Biosynthesis and secretion of plant cuticular wax. *Prog Lipid Res* 42:51–80
- Leveau JHJ, Lindow SE (2001) Appetite of an epiphyte: quantitative monitoring of bacterial sugar consumption in the phyllosphere. *Proc Natl Acad Sci U S A* 98:3446–3453
- Lindberg SE, Lovett GM, Richter DD, Johnson DW (1986) Atmospheric deposition and canopy interactions of major ions in a forest. *Science* 231:141–146
- Lindow SE, Brandl MT (2003) Microbiology of the phyllosphere. *Appl Environ Microbiol* 69:1875–1883
- Lohaus G, Pennewiss K, Sattelmacher B, Hussmann M, Mühlhling KH (2001) Is the infiltration-centrifugation technique appropriate for the isolation of apoplastic fluid? A critical evaluation with different plant species. *Physiol Plant* 111:457–465
- Meyer KM, Leveau JHJ (2012) Microbiology of the phyllosphere: a playground for testing ecological concepts. *Oecologia* 168:621–629
- Morris CE, Monier JM (2003) The ecological significance of biofilm formation by plant-associated bacteria. *Annu Rev Phytopathol* 41:429–453
- Niklas KJ, Cobb ED, Matas AJ (2017) The evolution of hydrophobic cell wall biopolymers: from algae to angiosperms. *J Experiment Botany*. <https://doi.org/10.1093/jxb/erx215>
- Parra JL, Guinea J, Manresa MA, Robert M, Mercadé ME, Comelles F, Bosch MP (1989) Chemical characterization and physicochemical behavior of biosurfactants. *J Am Oil Chem Soc* 66:141–145
- Pollard M, Beisson F, Li YH, Ohlrogge JB (2009) Building lipid barriers: biosynthesis of cutin and suberin. *Trends Plant Sci* 13:236–246
- Reynhardt EC, Riederer M (1994) Structures and molecular dynamics of plant waxes. II Cuticular waxes from leaves of *Fagus sylvatica* L. and *Hordeum vulgare* L. *Eur Biophys J* 23:59–70
- Riederer M, Müller C (2006) *Biology of the plant cuticle*. Blackwell Publishing, Oxford
- Riederer M, Schneider G (1989) Comparative study of the composition of waxes extracted from isolated leaf cuticles and from whole leaves of *Citrus*: evidence for selective extraction. *Physiol Plant* 77:373–384
- Ron EZ, Rosenberg E (2002) Biosurfactants and oil bioremediation. *Curr Opin Biotechnol* 13:249–252
- Ruan YL, Patrick JW, Brady CJ (1996) The composition of apoplast fluid recovered from intact developing tomato fruit. *Aust J Plant Physiol* 23:9–13
- Ruinen J (1961) The phyllosphere: 1. An ecologically neglected milieu. *Plant Soil* 15:81–109
- Samuels L, Kunst L, Jetter R (2009) Sealing plant surfaces: cuticular wax formation by epidermal cells. *Annu Rev Plant Biol* 59:683–707
- Schlegel TK, Schönherr J, Schreiber L (2005) Size selectivity of aqueous pores in stomatous cuticles of *Vicia faba* leaves. *Planta* 221:648–655
- Schönherr J (1976) Water permeability of isolated cuticular membranes: the effect of cuticular waxes on diffusion of water. *Planta* 131:159–164

- Schönherr J (2006) Characterization of aqueous pores in plant cuticles and permeation of ionic solutes. *J Exp Bot* 57:2471–2491
- Schönherr J, Baur P (1996) Cuticle permeability studies - a model for estimating leaching of plant metabolites to leaf surfaces. In: Morris CE, Nicot PC, Nguyen-The C (eds) *Aerial plant surface microbiology*. Plenum Press, New York, pp 1–23
- Schönherr J, Lenzian K (1981) A simple and inexpensive method of measuring water permeability of isolated plant cuticular membranes. *Z Pflanzenphysiol* 102:321–327
- Schönherr J, Riederer M (1989) Foliar penetration and accumulation of organic chemicals in plant cuticles. *Rev Environ Contam Toxicol* 108:1–70
- Schreiber L (1996) Wetting of the upper needle surface of *Abies grandis*: influence of pH, wax chemistry and epiphyllic microflora on contact angles. *Plant Cell Environ* 19:455–463
- Schreiber L (2005) Polar paths of diffusion across plant cuticles: new evidence for an old hypothesis. *Ann Bot* 95:1069–1073
- Schreiber L (2006) Review of sorption and diffusion of lipophilic molecules in cuticular waxes and the effects of accelerators on solute mobilities. *J Exp Bot* 57:2515–2523
- Schreiber L, Krimm U, Knoll D, Sayed M, Auling G, Kroppenstedt RM (2005) Plant-microbe interactions: identification of epiphytic bacteria and their ability to alter leaf surface permeability. *New Phytol* 166:589–594
- Schreiber L, Riederer M (1996) Ecophysiology of cuticular transpiration: comparative investigation of cuticular water permeability of plant species from different habitats. *Oecologia* 107:426–432
- Schreiber L, Schönherr J (1993) Mobilities of organic compounds in reconstituted cuticular wax of barley leaves: determination of diffusion coefficients. *Pestic Sci* 38:353–361
- Schreiber L, Schönherr J (2009) *Water and solute permeability of plant cuticles*. Springer, Heidelberg
- Segado P, Dominguez E, Heredia A (2016) Ultrastructure of the epidermal cell wall and cuticle of tomato fruit (*Solanum lycopersicum* L.) during development. *Plant Physiol* 170:935–946
- Shi T, Simanova E, Schönherr J, Schreiber L (2005) Effects of accelerators on mobility of ^{14}C -2,4-dichlorophenoxy butyric acid in plant cuticles depends on type and concentration of accelerator. *J Agric Food Chem* 53:2207–2212
- Ueda H, Mitsuhashi I, Tabata J, Kugimiya S, Watanabe T, Suzuki K, Yoshida S, Kitamoto H (2015) Extracellular esterases of phylloplane yeast *Pseudozyma antarctica* induce defect on cuticle layer structure and water-holding ability of plant leaves. *Appl Microbiol Biotechnol* 99:6405–6415
- Villena JF, Dominguez E, Stewart D, Heredia A (1999) Characterization and biosynthesis of non-degradable polymers in plant cuticles. *Planta* 208:181–187
- Vorholt JA (2012) Microbial life in the phyllosphere. *Nat Rev Microbiol* 10:828–840
- Wang ZH, Guhling O, Yao RN, Li FL, Yeats TH, Rose JKC, Jetter R (2011) Two oxidosqualene cyclases responsible for biosynthesis of tomato fruit cuticular triterpenoids. *Plant Physiol* 155:540–552
- Wang Y, Wang JH, Chai GQ, Li CL, Hu YG, Chen XH, Wang ZH (2015) Developmental changes in composition and morphology of cuticular waxes on leaves and spikes of glossy and glaucous wheat (*Triticum aestivum* L.). *PLoS One* 10(11):e0143671
- Whipps JM, Hand P, Pink D, Bending GD (2008) Phyllosphere microbiology with special reference to diversity and plant genotype. *J Appl Microbiol* 105:1744–1755
- Zabka V, Stangl M, Bringmann G, Vogg G, Riederer M, Hildebrandt U (2008) Host surface properties affect prepenetration processes in the barley powdery mildew fungus. *New Phytol* 177:251–263
- Zeisler V, Schreiber L (2016) Epicuticular wax on cherry laurel (*Prunus laurocerasus*) leaves does not constitute the cuticular transpiration barrier. *Planta* 243:65–81



Biosynthesis of the Plant Cuticle

6

Jérôme Joubès and Frédéric Domergue

Contents

1	Introduction	140
2	Cutin Biosynthesis	141
2.1	Cutin Monomer Synthesis	142
2.2	Cutin Polymerization	144
3	Pathways for Cuticular Wax Biosynthesis	145
3.1	Fatty Acid Elongases Produce Very-Long-Chain Fatty Acids	145
3.2	Alcohol-Forming Pathway	147
3.3	Alkane-Forming Pathway	148
3.4	Other Compounds	150
4	Export of Cutin Monomers and Wax Compounds	150
5	Research Needs	151
	References	152

Abstract

Cuticular waxes and cutin form the cuticle, a hydrophobic layer covering the aerial surfaces of land plants, mainly preventing non-stomatal water loss and acting as a protective barrier against environmental stresses. Fatty acid-derived

J. Joubès (✉)

Laboratoire de Biogenèse Membranaire, UMR5200, Université de Bordeaux, Bordeaux, France

Laboratoire de Biogenèse Membranaire, UMR5200, CNRS, Bordeaux, France

Laboratoire de Biogenèse Membranaire, UMR5200, CNRS-Université de Bordeaux,

Bâtiment A3 – INRA Bordeaux Aquitaine, Villenave d’Ornon, France

e-mail: jerome.joubes@u-bordeaux.fr

F. Domergue

Laboratoire de Biogenèse Membranaire, UMR5200, Université de Bordeaux, Bordeaux, France

Laboratoire de Biogenèse Membranaire, UMR5200, CNRS, Bordeaux, France

e-mail: frederic.domergue@u-bordeaux.fr

© Springer Nature Switzerland AG 2020

H. Wilkes (ed.), *Hydrocarbons, Oils and Lipids: Diversity, Origin, Chemistry and Fate*,
Handbook of Hydrocarbon and Lipid Microbiology,

https://doi.org/10.1007/978-3-319-90569-3_8

139

compounds that compose the building blocks of the cuticle are produced in the endoplasmic reticulum of epidermal cells before being exported to the environmental face of the epidermis. Thirty years of plant genetic studies and the recent development of analytical tools for lipid identification have led to the molecular and biochemical characterization of the enzymes catalyzing the major steps in cuticular compound biosynthesis.

1 Introduction

Four hundred and fifty million years ago, the development of the cuticle, a thin translucent waterproof barrier, represented an important adaptation of plants for colonizing the terrestrial environment. Covering the surface of all aerial organs, the cuticle is strategically located at the plant/air interface, thereby, playing essential functions in plant interactions with the environment mainly by limiting water loss. The protective capacities of the cuticle are based on the physical and biochemical properties of its two highly hydrophobic components, cutin and cuticular waxes, which are assembled ultrastructurally in several layers (Nawrath et al. 2013). The cutin polymer, with embedded intracuticular waxes, constitutes the cuticle proper that is connected to the cell wall by a cuticular layer made of cutin and polysaccharides. Covering the cutin matrix, the outermost layer of the cuticle is composed of epicuticular waxes that can form wax crystal microstructures. Cuticle synthesis starts in early stages of embryo development and is tightly co-regulated with plant growth to provide constant cuticle deposition (Delude et al. 2016). Although the biochemical composition and the thickness of the cuticle vary among different plant species and/or among organs and developmental stages, a set of primary compounds is ubiquitously found in plant cuticles. Cutin, a three-dimensional biopolyester of long-chain polyhydroxy- and epoxyhydroxy-fatty acids cross-esterified to each other or via glycerol backbones, provides the main mechanical strength of the cuticle (Dominguez et al. 2015). Cuticular waxes consist of a complex mixture of homologue series of very-long-chain (VLC) aliphatic compounds, as well as non-acyl lipid cyclic components including terpenoids and flavonoids (Buschhaus and Jetter 2011; Bernard and Joubès 2013). In the past 30 years, the development of sensitive quantitative and qualitative technologies to accurately analyze cuticle composition, coupled with plant reverse genetic analyses, has yielded significant advances toward unraveling the many aspects of plant cuticle metabolism.

Cuticle biosynthetic pathway can be divided into several metabolic blocks (Fig. 1). Initially, the C16:0, C18:0, or C18:1 fatty acids resulting from *de novo* fatty acid synthesis in the plastids are transferred to the acyl-coenzyme A (CoA) pool, which will be used as precursor for the synthesis of cutin monomers and wax components. The subsequent generation of the cutin polymer can be divided in three successive steps, fatty acyl-chain oxidation, esterification of oxygenated fatty acyl

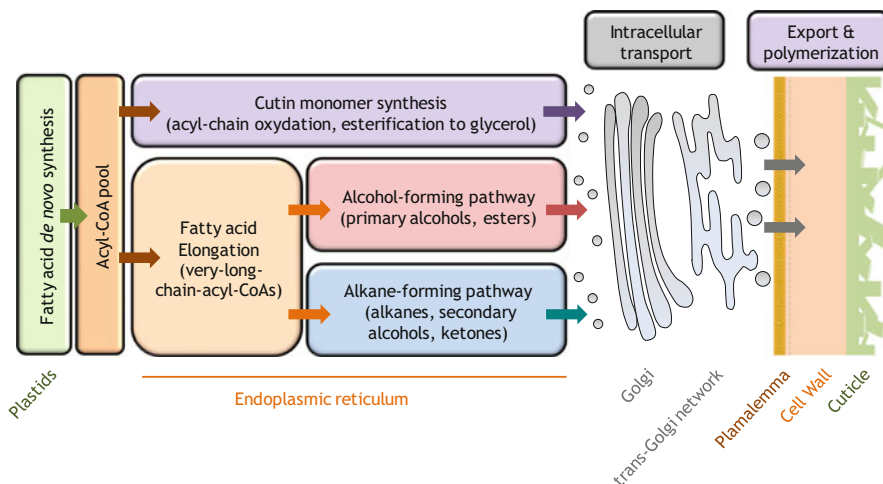


Fig. 1 Cuticle biosynthetic pathway

chains to glycerol, and their export and extracellular polymerization. During wax biosynthesis, VLC acyl-CoAs derived from fatty acid elongation may be converted into primary alcohols and alkyl esters by the alcohol-forming pathway or into aldehydes, alkanes, secondary alcohols, and ketones by the alkane-forming pathway. Cuticle precursors synthesized within the endoplasmic reticulum (ER) are then transported in a directional manner through the Golgi apparatus and trans-Golgi network (TGN) to reach the plasma membrane before being secreted to cover the cell wall of epidermal cells facing the external environment.

2 Cutin Biosynthesis

Although the cutin monomer acyl composition is now well characterized, its macromolecular structure, as well as its association with the outermost cell wall layer of epidermal cells, remains poorly described (Yeats and Rose 2013). Through the use of particular plants and organs for which the physical isolation of cuticle by chemical and/or hydrolytic enzyme treatments had been achieved, the first analyses of cutin composition revealed that long-chain polyhydroxy- and epoxyhydroxy-fatty acids represent the major components of the polymer (Kolattukudy 1980). In the early twenty-first century, the adaption of isolation procedures to the plant model *Arabidopsis thaliana* (Franke et al. 2005), as well as the establishment of protocols based on extensive delipidation of plant tissues to eliminate all soluble lipids (Bonaventure et al. 2004), resulted in rapid progress toward elucidation of the major biochemical pathways generating cutin.

2.1 Cutin Monomer Synthesis

The most recent discoveries concerning cutin synthesis suggest that the basic building block of the cutin polymer is *sn*-2 mono(oxygenated)acyl-glycerol (2MAG; Yeats et al. 2014). In most plants, the major oxidized acyl chains are long-chain ω -hydroxy- and polyhydroxy-fatty acids, of which the latter are hydroxylated at positions 9 and/or 10 as well as at the ω -position (Fig. 2). In that respect, the cutin of *Arabidopsis* leaves and stems, which is richer in dicarboxylic acids (DCA) than in hydroxy-fatty acids, may represent a unique composition. If it is highly likely that fatty acids produced in the plastids are first activated, then oxidized, and finally transferred to glycerol in the ER, the sequential order of the different enzymatic reactions yielding 2MAGs has not been unambiguously determined.

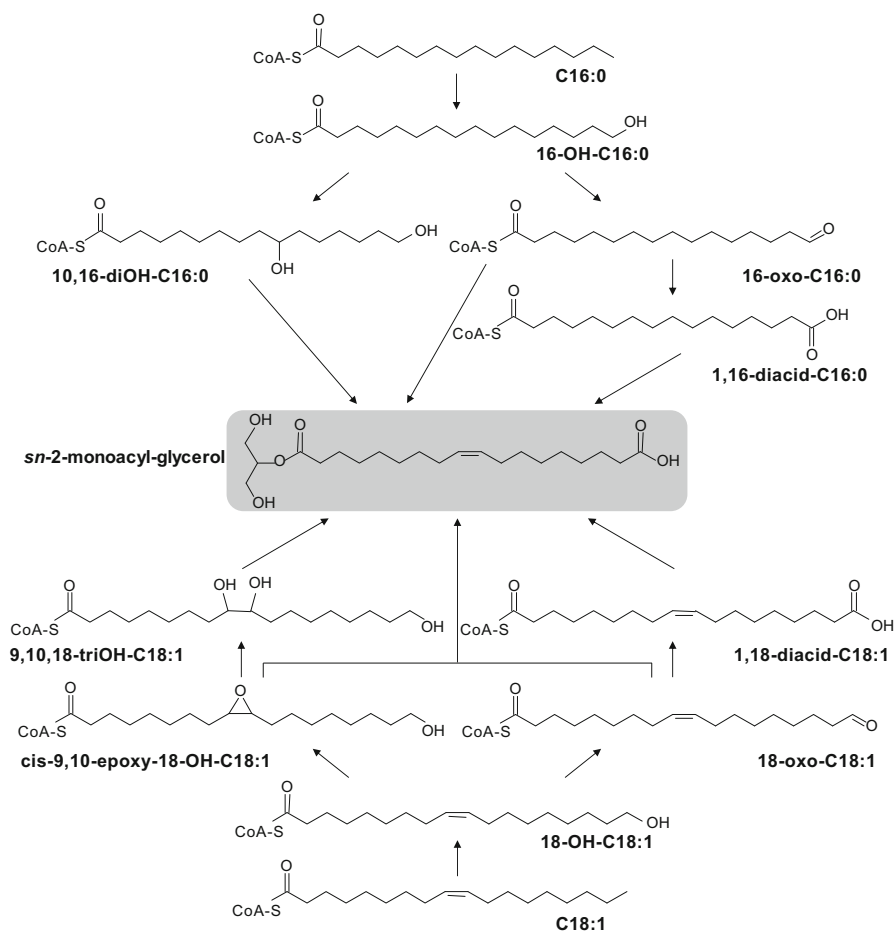


Fig. 2 Cutin monomer biosynthetic pathways

In *Arabidopsis*, the C16:0, C18:0, and C18:1 free fatty acids derived from the de novo synthesis within plastids are activated in the form of acyl-CoAs by two ER-resident, long-chain acyl-CoA acyltransferases, LACS1 and LACS2 (Weng et al. 2010). Mutations in *LACS2* globally impact cuticle development and especially wax content (Schnurr et al. 2004), whereas mutations in *LACS1* affect both cutin and wax loads (Lü et al. 2009). The double *lacs1lacs2* mutant is more afflicted than either single mutant, and the many pleiotropic effects, including the fusion of organs, suggest that LACS1 and LACS2 have overlapping activities that are obligatory for normal cuticle establishment (Weng et al. 2010; Lü et al. 2009). However, the exact role of these enzymes remains elusive as the type of acyl chains activated in *planta* remains unknown. In addition, the observation that LACS2 displays more activity toward 16-hydroxy-palmitic acid than to palmitic acid in vitro (Schnurr et al. 2004) raises further questions about the exact position of these enzymes within the metabolic pathway.

Oxidation of the acyl chains is catalyzed by various cytochrome P450 enzymes (Fig. 2). First, members of the *Arabidopsis* CYP86 subfamily produce ω -hydroxy-fatty acids. In *Arabidopsis* leaves and stems, CYP86A8 (LCR) and CYP86A2 (ATT1) were shown to be the major cytochrome P450s involved in the acyl oxidation of cutin precursors (Wellesen et al. 2001; Xiao et al. 2004). Although the cutin composition of these tissues contains substantial amounts of 16:0, 18:1, and 18:2 ω -hydroxy-fatty acids, it is strongly dominated by the corresponding DCA (Li-Beisson et al. 2013). Nevertheless, the enzymes responsible for the conversion of ω -hydroxy-fatty acids to DCA remain uncharacterized. Since cytochrome P450 enzymes that are able to oxidize the terminal methyl group of a fatty acid to a carboxyl group have been previously characterized, at least in vitro (Le Bouquin et al. 2001), it is possible that CYP86A8 (LCR), CYP86A2 (ATT1), or another cytochrome P450 enzyme produces DCA from ω -hydroxy-fatty acids and/or generates oxo-fatty acids. Oxidoreductases, such as HOTHEAD (HTH), might also be involved in this process, since the corresponding mutants have reduced levels of DCAs (Krolkowski et al. 2003; Kurdyukov et al. 2006). In *Arabidopsis* flowers, CYP86A4 converts palmitic acid to 16-hydroxy-palmitic acid. Another cytochrome P450 enzyme, CYP77A6, catalyzes the in-chain hydroxylation to produce 10,16-dihydroxypalmitate, which represents 80% of acyl monomers in floral cutin (Li-Beisson et al. 2009). The cytochrome P450 enzymes from this subfamily might also produce epoxy-fatty acids, since microsomes from yeast expressing CYP77A4 are able to catalyze the epoxidation of monounsaturated fatty acids (Sauveplane et al. 2009).

The generation of 2MAGs relies on a specific family of glycerol-3-phosphate: acyl-CoA acyltransferases (GPAT) that are only present in land plants and that are specifically involved in lipid polyester synthesis (Yang et al. 2012). GPATs involved in cutin biosynthesis differ from the classical acyltransferases involved in membrane and storage lipid biosynthesis by specifically acylating the *sn*-2 position of glycerol-3-phosphate instead of the *sn*-1 position for classical GPATs. Additionally, they carry a phosphatase activity allowing subsequent conversion of 2-acyl-lysophosphatidic acids into 2MAGs. In addition, in vitro assays using yeast microsomes from cells

expressing these GPATs showed a clear preference for ω -hydroxy-fatty acids and DCAs. These special features most probably allow the epidermis to separate the glycerolipid precursors of cutin from those of membrane glycerolipids (Yang et al. 2010, 2012). In *Arabidopsis*, the *gpat4 gpat8* double mutant has strongly reduced cutin loads in both leaves and stems (Li et al. 2007), whereas the *gpat6* mutant is affected in the cutin load of flowers (Li-Beisson et al. 2009), thus indicating that this small clade of GPATs is specifically devoted to cutin biosynthesis. It should be noted that these acyltransferases are not responsible for the incorporation of phenylpropanoids into the cutin polyester; instead, this reaction is carried out by the BAHD acyltransferases. In particular, DCF (for Deficient in Cutin Ferulate) was shown in *Arabidopsis* to control cutin ferulate content and, in vitro, to transfer ferulic acid to ω -hydroxyacids (Rautengarten et al. 2012). Another BAHD, DCR (for Deficient in Cuticular Ridges), was shown to strongly affect flower cutin content (Panikashvili et al. 2009), although its principal activity remains unknown (Molina and Kosma 2015).

2.2 Cutin Polymerization

Whereas all the reactions yielding 2MAGs have been shown to occur in the endoplasmic reticulum, the enzymes responsible for the polymerization process of cutin have been localized within the cell wall (Girard et al. 2012; Yeats et al. 2012). Therefore, cutin precursors must be transported within the epidermal cell and, then, through both the plasmalemma and the cell wall to reach their final location. Some components of these steps have been characterized, but the entire transport of cutin monomers remains poorly described as discussed in Sect. 4.

The long-running mystery of cutin polymerization was recently solved by two groups, both of which simultaneously reported the identification of an extracellular enzyme that strongly influences cutin cross-linking in tomato, and which is capable of polymerizing 2MAGs in vitro (Girard et al. 2012; Yeats et al. 2012). This enzyme, now referred to as cutin synthase, belongs to the Gly-Asp-Ser-Leu family of esterases/acylhydrolases, commonly called GDSL-lipases. Fruits from *GDSL1*-silenced tomato lines have a much thinner cuticle with strongly reduced amounts of cutin monomers and display increased brightness, permeability, and post-harvested water loss, as well as significant decreases in cutin polymerization according to FTIR (Fourier transform infrared spectroscopy) analyses (Girard et al. 2012). At the same time, the *cd1* mutant (for *cutin deficient 1*), with a point mutation resulting in an early stop codon in the same gene, shows a similar fruit phenotype with cutin load being reduced by 90 to 95% (Yeats et al. 2012). Most importantly, these authors also reported that the CD1 protein, upon heterologous expression in *Nicotiana benthamiana* and purification, was able to polymerize 2-mono(10,16-dihydroxyhexadecanoyl)glycerol in vitro, confirming its acyltransferase activity and fundamental role in cutin polymerization (Yeats et al. 2012). A putative *Arabidopsis* orthologue, AtCUS1/LTL1, was shown to have similarly strong polyester synthase activity but displayed negligible hydrolytic activity (Yeats et al. 2014).

In addition, plants expressing an artificial microRNA that silences *LTL1* show flowers with fused petals devoid of adaxial nanoridges (Shi et al. 2011). The fact that the oligomers synthesized *in vitro* by cutin synthases are linear may, nevertheless, suggest that other enzymes are responsible for the branching and cross-linking of the polymer.

3 Pathways for Cuticular Wax Biosynthesis

Cuticular wax aliphatic compounds consist of a mixture of VLC molecules ranging from 22 to 38 carbon atoms. Produced by the elongase complexes, VLC acyl-CoAs can be transformed into free VLC fatty acids (VLCFAs) and/or processed through two distinct pathways. The alcohol-forming pathway produces even-numbered primary alcohols and alkyl esters, and the alkane-forming pathway yields aldehydes as well as odd-chain-numbered alkanes, secondary alcohols, and ketones (Fig. 1).

In the last 30 years, visual screens of ethyl methanesulfonate (EMS) mutant libraries identified wax-deficient mutants such as *eceriferum* (*cer*, waxless), *glossy* (*gl*), *bloomless* (*bm*), or *wax crystal-sparse leaf* (*wsl*) in *Arabidopsis*, barley, maize, sorghum, or rice. In *Arabidopsis thaliana*, 89 *cer* mutants were isolated and shown to be affected on 21 independent loci, defining a set of 21 genes with potential function in wax biosynthesis, transport, or regulation (Koorneef et al. 1989). Moreover, new candidate genes with a role in the wax pathways were identified based on gene co-regulation data and gene expression enrichment in the epidermis of young developing organs as compared to the entire organs, a typical expression pattern of wax associated genes, allowing the characterization of the major steps in wax biosynthetic pathways (Lee and Suh 2015).

3.1 Fatty Acid Elongases Produce Very-Long-Chain Fatty Acids

Fatty acid elongation initially uses C16:0 and C18:0 fatty acids resulting from the plastidial *de novo* synthesis that are esterified to coenzyme A before entering the ER-bound, multienzyme fatty acid elongase (FAE) complexes (Fig. 3). Each FAE cycle catalyzes four successive reactions generating an acyl chain extended by two carbon atoms: formation of β -ketoacyl-CoA by condensation of malonyl-CoA with an acyl-CoA catalyzed by a β -ketoacyl-CoA synthase (KCS), reduction of β -ketoacyl-CoA to β -hydroxyacyl-CoA by a β -ketoacyl-CoA reductase (KCR), dehydration of β -hydroxyacyl-CoA to enoyl-CoA by a β -hydroxyacyl-CoA dehydratase (HCD), and reduction of enoyl-CoA by an enoyl-CoA reductase (ECR).

Studies, including photoperiod and chemical inhibition of elongase activities, initially raised the idea for existence of multiple elongase complexes, each with a distinct chain-length specificity that perform sequential and/or parallel reactions to produce the broad chain-length range of VLCFAs found in plants (von Weisstein-Knowles 1982). The KCR, HCD, and ECR enzymes are thought to have broad substrate specificity and may be shared by all FAE complexes (Kunst and Samuels 2009).

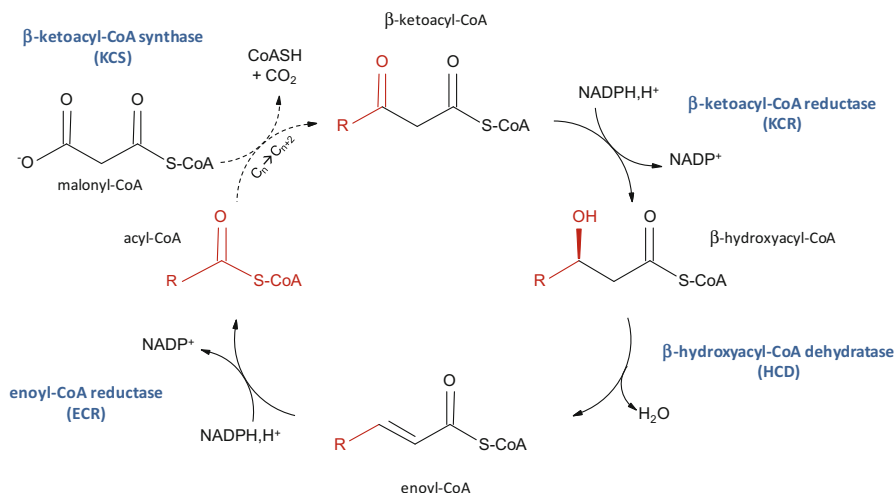


Fig. 3 Fatty acid elongation

In contrast, KCS enzymes determine the chain-length substrate specificity of each elongation reaction.

Consistent with the coexistence of multiple FAE complexes, approximately 20 KCS members have been annotated in several angiosperm genomes (Guo et al. 2016). Expression pattern analyses and heterologous expression in yeast of a subset of the 21 *Arabidopsis* KCS indicated that some of them have overlapping functions, or they are specialized to particular environmental conditions (Joubès et al. 2008; Haslam and Kunst 2013). To date, several KCS have been shown to be involved in cuticle precursor synthesis (KCS1, KCS2, KCS5/CER60, KCS6/CER6, KCS9, KCS10/FDH, KCS13/HIC, KCS16, and KCS20) (Haslam and Kunst 2013; Hegebarth et al. 2017). Nevertheless, based on expression patterns and mutant phenotypes, KCS5/CER60 and KCS6/CER6 appear as major actors involved in the elongation of fatty acids longer than C₂₆ for the production of cuticular waxes (Haslam et al. 2015). However, KCS are not the only factors that dictate elongation of VLCFAs, as the functional characterization of the *Arabidopsis* and rice CER2-LIKE proteins has suggested a role of these proteins in the regulation of FAE activities for the elongation of VLCFAs (Haslam et al. 2012, 2015; Pascal et al. 2013; Wang et al. 2017). As such, they could facilitate the formation of VLC acyl-CoAs by stabilizing the FAE complexes, by enhancing their activity, or by allowing the newly elongated acyl-CoA to be presented back to the KCS enzyme after an elongation cycle. However, further work is needed to determine the mode of action of these proteins. The *Arabidopsis* PAS1 protein is another example of a FAE complex regulator (Roudier et al. 2010). PAS1 is a member of the immunophilin family of chaperones that are known to target protein complexes and regulate their

assembly or activity. Similar to a loss of one of the elongase core components, a defect in PAS1 was shown to reduce the amounts of all VLCFA-containing lipids.

In the last decade, major findings on VLCFA synthesis in yeast allowed the identification of the corresponding KCR, HCD, and ECR enzymes in *Arabidopsis*. Complementation assays of yeast mutants revealed that *KCR1* and *PASTICCINO2* (*PAS2*) encode a functional KCR and HCD, respectively (Bach et al. 2008; Beaudoin et al. 2009). Complementation of the *Arabidopsis cer10* mutant and the yeast *tsc13-lelo2Δ* mutant by expression of *AtECR* demonstrated that *CER10* encodes a functional ECR (Zheng et al. 2005). Consistent with the assumption that the three enzymes are common to all FAE complexes, the total loss of KCR1 or PAS2 is embryo lethal, whereas the loss of CER10 and partial loss of KCR1 or PAS2 activity result in a severe reduction of all major classes of VLCFA-containing lipids (waxes, triacylglycerols, and sphingolipids) causing major developmental impairment (Zheng et al. 2005; Bach et al. 2008; Beaudoin et al. 2009).

3.2 Alcohol-Forming Pathway

The alcohol-forming pathway, also called reduction pathway, produces even-numbered primary alcohols and alkyl esters (Fig. 4).

The first biochemical studies of primary alcohol formation suggested a two-step reaction in which fatty acyl-CoA reductase (FAR) reduces VLC acyl-CoAs to aldehydes, which are further reduced to primary alcohols by an aldehyde reductase (Kolattukudy 1971). However, biochemical studies on jojoba seeds and pea leaves, as well as expression of genes encoding alcohol-forming activities in heterologous systems, revealed that a single enzyme produced fatty alcohols, with the intermediate aldehyde remaining bound to the enzyme (Rowland and Domergue 2012). In *Arabidopsis*, the *cer4* mutant shows a severe reduction of primary alcohols and wax esters, suggesting that CER4 (also called FAR3) could play a role in this biosynthetic pathway (Jenks et al. 1995). Expression of CER4 in yeast results in the production of VLC primary alcohols confirming the FAR activity of CER4 (Rowland et al. 2006).

Detailed analysis of wax ester chain lengths from the stems of *Arabidopsis cer4* mutants indicated that primary alcohols formed by CER4 are substrates for subsequent alkyl ester formation (Lai et al. 2007). Wax synthase (WS) enzymes catalyze the esterification of primary alcohols to acyl-CoAs in higher plants, mammals, and bacteria (Lardizabal et al. 2000; Cheng and Russell 2004; Stoveken et al. 2005). In *Arabidopsis*, the search for sequences similar to the jojoba WS and bifunctional WS/diacylglycerol acyltransferases (DGATs) from *Acinetobacter calcoaceticus* revealed 12 and 11 sequences, respectively. Analysis of a WS/DGAT-encoding gene (*WSD1*), which is highly expressed in the epidermis, subsequently confirmed its involvement as the major WS in cuticular wax synthesis (Li et al. 2008).

3.3 Alkane-Forming Pathway

The alkane-forming pathway, also called the decarbonylation pathway, produces aldehydes and odd-numbered alkanes, secondary alcohols, and ketones (Fig. 4).

Analyses of *Arabidopsis cer* mutants and complementary biochemical experiments proposed an alkane-forming pathway in which VLC acyl-CoAs are used as precursors to form alkanes through aldehydes (Bernard and Joubès 2013). However, how even-numbered VLCFAs are transformed into odd-numbered alkanes remains an intriguing question, although significant advances have been made recently in the characterization of the alkane-forming complex (Bernard et al. 2012). Initially, biochemical analyses led to the proposal that alkanes could be produced from VLCFAs through the formation of an intermediate aldehyde (Cheesbrough and Kolattukudy 1984; Dennis and Kolattukudy 1991; Vioque and Kolattukudy 1997; Schneider-Belhaddad and Kolattukudy 2000). Although this hypothesis has never been demonstrated for plants, it is the only one that has been experimentally tested in microsomal fractions from pea leaves (Vioque and Kolattukudy 1997) and from the green alga *Botryococcus braunii* (Cheesbrough and Kolattukudy 1984; Dennis and Kolattukudy 1991; Schneider-Belhaddad and Kolattukudy 2000). Contrary to the NADPH-cytochrome P450 reductase mechanism of hydrocarbon synthesis in insects, in which aldehydes are converted to alkanes by a decarboxylation mechanism that releases a CO₂ molecule (Reed et al. 1994; Qiu et al. 2012), the coproduct of the aldehyde conversion in pea and *Botryococcus braunii* was a CO molecule

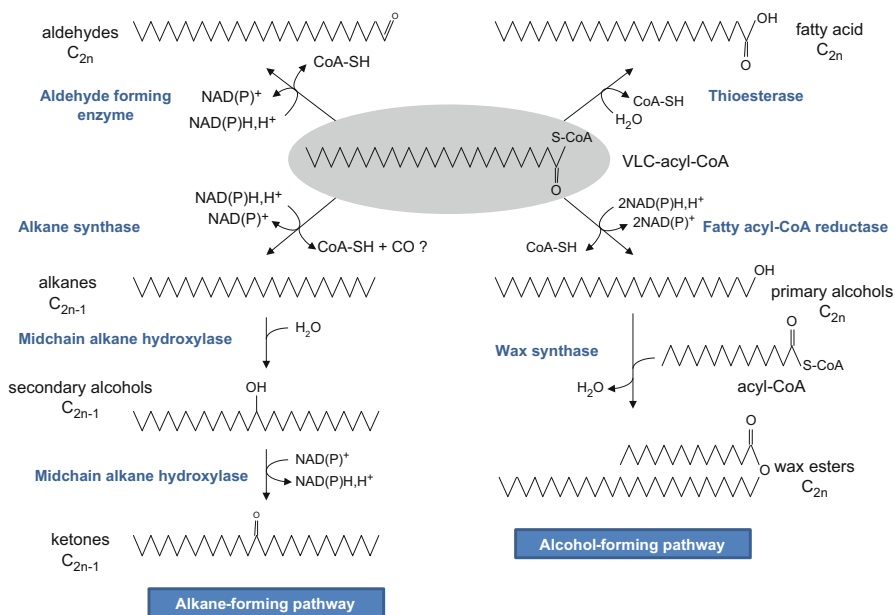


Fig. 4 Cuticular wax compounds biosynthetic pathways

suggesting a decarbonylation mechanism. Therefore, it was proposed for plants that VLC acyl-CoAs are reduced by a fatty acyl-CoA reductase into corresponding even-numbered aldehydes, which are converted by an aldehyde decarbonylase into alkanes with the loss of one carbon atom.

Several *Arabidopsis cer* mutants with a decreased alkane load have been biochemically characterized. The *cer3* mutant shows a dramatic reduction in aldehydes, alkanes, secondary alcohols, and ketones. The *cer1* mutant exhibits a dramatic decrease in alkanes and a near abolition of secondary alcohol and ketone production, accompanied by a slight increase in aldehyde content (Aarts et al. 1995; Chen et al. 2003; Kurata et al. 2003; Bourdenx et al. 2011). It has been proposed from these phenotypes that CER3 may encode the VLC-acyl-CoA reductase that produces aldehydes, whereas CER1 may encode the alkane-forming enzyme that catalyzes the presumed decarbonylation of aldehydes to alkanes. Wax analyses of CER1 over-expressors have revealed a specific increase in alkanes with chain lengths of between 27 and 33 carbon atoms, which is consistent with CER1 encoding an alkane-forming activity with a strict substrate specificity for compounds containing more than 27 carbon atoms (Bourdenx et al. 2011). Recently, the proof that CER1 and CER3 act synergistically as a heterodimer complex that catalyzes the conversion of VLC-acyls-CoAs to alkanes, with the intermediate aldehyde remaining bound to the complex, was provided by co-expression of the two proteins in yeast (Bernard et al. 2012).

Early characterization of the aldehyde decarbonylase partially purified from pea leaves indicated that this activity requires metal ions and is inhibited by O_2 and reducing powers, suggesting that the reaction would be redox independent (Schneider-Belhaddad and Kolattukudy 2000). Nevertheless, CER1 was shown to interact with the ER-localized cytochrome b_5 (CYTB5), and co-expression of CYTB5-B with the CER1/CER3 complex in yeast was shown to increase VLC-alkane production. This suggests that CYTB5 is a redox cofactor of the CER1/CER3 alkane-forming activity (Bernard et al. 2012). The observation that CER1 contains catalytic histidine-clusters typical of a di-iron-binding site and that CYTB5 physically interacts with CER1 highlights the analogy between CER1 and the cyanobacterial aldehyde decarbonylase. This latter is structurally related to nonheme di-iron enzymes, uses iron as the only active metal for its activity, and appears to catalyze a redox-neutral aldehyde decarbonylase reaction even though a reducing system is strictly required (Warui et al. 2011; Das et al. 2011). Experimental evidence and functional analogy to cyanobacterial aldehyde decarbonylase strongly suggest that CER1 serves as the alkane-forming enzyme even though the enzymatic activity of the protein is still unknown. On the other hand, as neither aldehydes nor other potential intermediates were detected in yeast expressing CER3 alone, or co-expressed with CER1, the role of CER3 in VLC-alkane synthesis remains unknown.

As mentioned above, alkanes can be further modified, for instance, in *Arabidopsis* stems, by consecutive oxidation to produce secondary alcohols and, subsequently, ketones (Fig. 4). Evidence for alkanes as precursors of these compounds has been provided by the following experiments. Feeding experiments have

demonstrated that alkanes and secondary alcohols can be transformed into ketones in *Brassica oleracea* (Kolattukudy et al. 1973). There exists an apparent correlation between secondary alcohols, ketones, and alkane chain lengths in *Arabidopsis*, as well as mutant phenotypes showing a deficit in alkanes accompanied by a similar deficit in these compounds (Aarts et al. 1995; Chen et al. 2003). By looking for genes upregulated in the *Arabidopsis* stem epidermis, and which encode proteins potentially involved in lipid oxidation, a cytochrome P450 encoding gene, *CYP96A15*, was identified as a candidate for a catalytic role in secondary alcohol and ketone formation (Greer et al. 2007). Ectopic expression of *CYP96A15* in *Arabidopsis* leaves yielded the production of secondary alcohols and ketones demonstrating that *CYP96A15* functions as a mid-chain alkane hydroxylase (MAH1) that can produce secondary alcohols and catalyze their subsequent oxidation into ketones (Greer et al. 2007).

3.4 Other Compounds

Wax mixtures typically contain homologous series of VLC saturated alkanes or alcohols derived from the alkane- and alcohol-forming pathways, but VLC acyl-CoAs that are produced by the FAE complexes can be also converted to free VLCFAs or aldehydes (Fig. 4). Indeed, detection of significant amounts of homologous series of these compounds in extracellular lipids in almost all plant wax mixtures indicated that at least a proportion of VLC acyl-CoAs can be converted to VLCFAs by an unknown, ER-localized VLC-acyl-CoA thioesterase. The other possibility is that they are reduced to aldehydes, potentially independently, from the alcohol- or alkane-forming pathway, by an unknown aldehyde-forming enzyme (Fig. 4).

Furthermore, wax compounds with modified carbon chains have been reported in many species. Iso- and anteiso-alkanes or alcohols have been found in several *Brassicaceae* or *Solanaceae* species (Busta and Jetter 2017), alkanes with within-chain methyl branches or cyclopropyl rings have been identified in barley (von Wettstein-Knowles 2007), and β -diketones have been found in waxes of many *Gramineae* species (von Wettstein-Knowles 2012). However, the biochemical reactions yielding these unusual wax components and the sequence of the corresponding metabolic steps are not fully understood, and the enzymes involved in these biosynthetic pathways remain uncharacterized.

4 Export of Cutin Monomers and Wax Compounds

As indicated by the subcellular localization of the cuticular biosynthetic pathway enzymes, it is now well established that the biosynthesis of the different cuticular compounds occurs in the endoplasmic reticulum (Fig. 1). The recent use of *Arabidopsis* mutants defective in vesicle trafficking and protein secretion suggests that the transfer of these hydrophobic molecules through the hydrophilic cytoplasm

involves vesicles that transit through the ER-Golgi interface and the trans-Golgi network to deliver cargo to the plasma membrane (Fig. 1) (McFarlane et al. 2014).

Once the cuticle compounds have reached the plasmalemma, their export is carried out by ABC transporters (ATP-binding cassette transporters). The gene encoding the first ABC transporter identified in *Arabidopsis* facilitating wax transport was ABCG12/CER5 (Pighin et al. 2004). A search for ABC protein-encoding genes with an expression pattern similar to ABCG12 revealed ABCG11 as a candidate for wax export (Bird et al. 2007; Panikashvili et al. 2007). The *abcg11* mutant and the double mutant *abcg11 abcg12* show similar wax composition, suggesting that both transporters act in the same pathway or ABC transporter unit. Furthermore, *abcg11* showed organ fusions, defects in cuticle permeability, and a reduced cutin load, indicating that ABCG11 is also involved in cutin monomer export (Panikashvili et al. 2007, 2010). ABCG11 and ABCG12 are half-transporters, and, whereas ABCG11/ABCG12 heterodimers have a function in wax export, ABCG11 may also homodimerize or heterodimerize with unknown component (s) to transport cutin monomers (McFarlane et al. 2010). However, residual export of waxes and cutin monomers onto the plant surface in the absence of ABCG11 and ABCG12 indicates that other ABC transporters might also export these compounds. Recently, several other ABCG transporters have been characterized in *Arabidopsis*. ABCG13, which is closely related to ABCG11 and ABCG12, contributes to cutin formation in flowers (Panikashvili et al. 2011). ABCG9 and ABCG14 can also form dimers with ABCG11, and these, as well as ABCG31, affect sterol ester levels in vegetative tissues or pollen grains (Le Hir et al. 2013; Choi et al. 2014). In contrast, ABCG32/PEC1, which is a full-length transporter, is required for hydroxy-fatty acid transport in leaves and flowers (Bessire et al. 2011).

Based on transcriptome analysis of *Arabidopsis* stems and stem epidermal cells, seven candidate LTPs (lipid transfer proteins), which could play a role in cuticular precursor transport, were isolated (Suh et al. 2005). The cuticle phenotype of *ltpg1* and *ltpg2* mutants suggests that both of these glycosylphosphatidylinositol-anchored LTPs (LTPGs) could be involved in cuticle formation (DeBono et al. 2009; Lee et al. 2009; Kim et al. 2012). However, the subtle changes in wax composition observed in *ltpg1* or *ltpg2* mutants have given rise to the proposition that multiple, specialized LTPs, but with overlapping functions, are required to deliver the entire diversity of cuticle compounds to the epidermal surface.

5 Research Needs

Over the last years, significant progress has been made in the understanding of the molecular and biochemical mechanisms underlying cuticle biosynthesis. These advances have greatly benefitted from the development of molecular reverse and forward genetic tools in different species and the simultaneous development of analytical methods for detailed lipid characterization. However, several processes still remain to be clarified, especially those following:

1. The exact order of the reactions involved in cutin monomer synthesis needs to be unambiguously established. For this purpose, it will be important to establish when LACS activity is exactly required, to determine the substrates of the different cytochrome P450 enzymes identified thus far, and to discover the enzymes responsible for the other reactions of the proposed pathways.
2. The processes whereby VLC acyl-CoAs are generated and subsequently converted to the VLC aliphatic wax compounds found on the surfaces of many plant species are now well understood. However, the catalytic activities of several enzymes involved in these metabolic pathways have to be characterized in more detail. The activities of the KCS subunits of the different FAE complexes and the regulation of these activities, for example, by the CER2-LIKE proteins, have to be puzzled out. Similarly, the exact enzymatic activity of the alkane-forming complex remains to be solved. Furthermore, the enzymes involved in the biosynthesis of free VLCFAs and aldehydes must be identified and characterized.
3. As many unusual compounds are found in the plant wax mixtures, the biosynthetic pathways and the related genes or enzymes involved in their generation have to be discovered. The development of molecular and biochemical tools to characterize the synthesis of these components in species that accumulate them will be a major challenge for the next few years.
4. If some information concerning the transport of cuticular compounds across the plasma membrane are now available, future reporting must take into account the intra- and extracellular transport of the cuticular components to provide a cell-wide understanding of these processes.

References

- Aarts MGM, Keijzer CJ, Stiekema WJ, Pereira A (1995) Molecular characterization of the *CER1* gene of *Arabidopsis* involved in epicuticular wax biosynthesis and pollen fertility. *Plant Cell* 7:2115–2127
- Bach L, Michaelson LV, Haslam R, Bellec Y, Gissot L, Marion J, Da Costa M, Boutin JP, Miquel M, Tellier F, Domergue F, Markham JE, Beaudoin F, Napier JA, Faure JD (2008) The very-long-chain hydroxy fatty acyl-CoA dehydratase PASTICCINO2 is essential and limiting for plant development. *Proc Natl Acad Sci U S A* 105:14727–14731
- Beaudoin F, Wu X, Li F, Haslam RP, Markham JE, Zheng H, Napier JA, Kunst L (2009) Functional characterization of the *Arabidopsis* β -ketoacyl-Coenzyme A reductase candidates of the fatty acid elongase. *Plant Physiol* 150:1174–1191
- Bernard A, Joubès J (2013) *Arabidopsis* cuticular waxes: advances in regulation, synthesis, export and functions. *Prog Lipid Res* 52:110–129
- Bernard A, Domergue F, Pascal S, Jetter R, Renne C, Faure JD, Haslam RP, Napier JA, Lessire R, Joubès J (2012) Reconstitution of plant alkane biosynthesis in yeast demonstrates that *Arabidopsis* ECERIFERUM1 and ECERIFERUM3 are core components of a very-long-chain alkane synthesis complex. *Plant Cell* 24:3106–3118
- Bessire M, Borel S, Fabre G, Carraça L, Efremova N, Yephremov A, Cao Y, Jetter R, Jacquat AC, Métraux JP, Nawrath C (2011) A member of the PLEIOTROPIC DRUG RESISTANCE family of ATP binding cassette transporters is required for the formation of a functional cuticle in *Arabidopsis*. *Plant Cell* 23:1958–1970

- Bird D, Beisson F, Brigham A, Shin J, Greer S, Jetter R, Kunst L, Wu X, Yephremov A, Samuels L (2007) Characterization of *Arabidopsis* ABCG11/WBC11, an ATP binding cassette (ABC) transporter that is required for cuticular lipid secretion. *Plant J* 52:485–498
- Bonaventure G, Beisson F, Ohlrogge J, Pollard M (2004) Analysis of the aliphatic monomer composition of polyesters associated with *Arabidopsis* epidermis: occurrence of octadeca-cis-6, cis-9-diene-1, 18-dioate as the major component. *Plant J* 40:920–930
- Bourdenx B, Bernard A, Domergue F, Pascal S, Léger A, Roby D, Pervent M, Vile D, Haslam RP, Napier JA, Lessire R, Joubès J (2011) Overexpression of *Arabidopsis* *ECERIFERUM1* promotes wax very-long-chain alkane biosynthesis and influences plant response to biotic and abiotic stresses. *Plant Physiol* 156:29–45
- Buschhaus C, Jetter R (2011) Composition differences between epicuticular and intracuticular wax substructures: how do plants seal their epidermal surfaces? *J Exp Bot* 62:841–853
- Busta L, Jetter R (2017) Structure and biosynthesis of branched wax compounds on wild type and wax biosynthesis mutants of *Arabidopsis thaliana*. *Plant Cell Physiol* 58:1059. <https://doi.org/10.1093/pcp/pcx051>
- Cheesbrough TM, Kolattukudy PE (1984) Alkane biosynthesis by decarbonylation of aldehydes catalyzed by a particulate preparation from *Pisum sativum*. *Proc Natl Acad Sci U S A* 81:6613–6617
- Chen X, Goodwin SM, Boroff VL, Liu X, Jenks MA (2003) Cloning and characterization of the *WAX2* gene of *Arabidopsis* involved in cuticle membrane and wax production. *Plant Cell* 15:1170–1185
- Cheng JB, Russell DW (2004) Mammalian wax biosynthesis. *J Biol Chem* 279:37789–37797
- Choi H, Ohyama K, Kim YY, Jin JY, Lee SB, Yamaoka Y, Muranaka T, Suh MC, Fujioka S, Lee Y (2014) The role of *Arabidopsis* ABCG9 and ABCG31 ATP binding cassette transporters in pollen fitness and the deposition of steryl glycosides on the pollen coat. *Plant Cell* 26:310–324
- Das D, Eser BE, Han J, Sciore A, Marsh EN (2011) Oxygen-independent decarbonylation of aldehydes by cyanobacterial aldehyde decarbonylase: a new reaction of diiron enzymes. *Angew Chem Int Ed Eng* 50:7148–7152
- DeBono A, Yeats TH, Rose JKC, Bird D, Jetter R, Kunst L, Samuels L (2009) *Arabidopsis* LTPG is a glycosylphosphatidylinositol-anchored lipid transfer protein required for export of lipids to the plant surface. *Plant Cell* 21:1230–1238
- Delude C, Moussu S, Joubès J, Ingram G, Domergue F (2016) Plant surface lipids and epidermis development. *Subcell Biochem* 86:287–313
- Dennis MW, Kolattukudy PE (1991) Alkane biosynthesis by decarbonylation of aldehyde catalyzed by a microsomal preparation from *Botryococcus braunii*. *Arch Biochem Biophys* 287:268–275
- Domínguez E, Heredia-Guerrero JA, Heredia A (2015) Plant cutin genesis: unanswered questions. *Trends Plant Sci* 20:551–558
- Franke R, Briesen I, Wojciechowski T, Faust A, Yephremov A, Nawrath C, Schreiber L (2005) Apoplastic polyesters in *Arabidopsis* surface tissues – a typical suberin and a particular cutin. *Phytochemistry* 66:2643–2658
- Girard AL, Mounet F, Lemaire-Chamley M, Gaillard C, Elmorjani K, Vivancos J, Runavot JL, Quemener B, Petit J, Germain V, Rothan C, Marion D, Bakan B (2012) Tomato GDSL1 is required for cutin deposition in the fruit cuticle. *Plant Cell* 24:3119–3134
- Greer S, Wen M, Bird D, Wu X, Samuels L, Kunst L, Jetter R (2007) The cytochrome P450 enzyme CYP96A15 is the midchain alkane hydroxylase responsible for formation of secondary alcohols and ketones in stem cuticular wax of *Arabidopsis*. *Plant Physiol* 145:653–667
- Guo HS, Zhang YM, Sun XQ, Li MM, Hang YY, Xue JY (2016) Evolution of the KCS gene family in plants: the history of gene duplication, sub/neofunctionalization and redundancy. *Mol Gen Genomics* 291:739–752
- Haslam TM, Kunst L (2013) Extending the story of very-long-chain fatty acid elongation. *Plant Sci* 210:93–107
- Haslam TM, Manas-Fernandez A, Zhao L, Kunst L (2012) *Arabidopsis* *ECERIFERUM2* is a component of the fatty acid elongation machinery required for fatty acid extension to exceptional lengths. *Plant Physiol* 160:1164–1174

- Haslam TM, Haslam R, Thoraval D, Pascal S, Delude C, Domergue F, Fernández AM, Beaudoin F, Napiet JA, Kunst L, Joubès J (2015) ECERIFERUM2-LIKE proteins have unique biochemical and physiological functions in very-long-chain fatty acid elongation. *Plant Physiol* 167:682–692
- Hegebarth D, Buschhaus C, Joubès J, Thoraval D, Bird D, Jetter R (2017) Arabidopsis ketoacyl-CoA synthase 16 forms C₃₆/C₃₈ acyl precursors for leaf trichome and pavement surface wax. *Plant Cell Environ* 40:1761. <https://doi.org/10.1111/pce.12981>
- Jenks MA, Tuttle HA, Eigenbrode SD, Feldmann KA (1995) Leaf epicuticular waxes of the *eceriferum* mutants in *Arabidopsis*. *Plant Physiol* 108:369–377
- Joubès J, Raffaele S, Bourdenx B, Garcia C, Laroche-Traineau J, Moreau P, Domergue F, Lessire R (2008) The VLCFA elongase gene family in *Arabidopsis thaliana*: phylogenetic analysis, 3D modelling and expression profiling. *Plant Mol Biol* 67:547–566
- Kim H, Lee SB, Kim HJ, Min MK, Hwang I, Suh MC (2012) Characterization of glycosylphosphatidylinositol-anchored lipid transfer protein 2 (LTPG2) and overlapping function between LTPG/LTPG1 and LTPG2 in cuticular wax export or accumulation in *Arabidopsis thaliana*. *Plant Cell Physiol* 53:1391–1403
- Kolattukudy PE (1971) Enzymatic synthesis of fatty alcohols in *Brassica oleracea*. *Arch Biochem Biophys* 142:701–709
- Kolattukudy PE (1980) Cutin, suberin and waxes. In: Stumpf PK (ed) *The biochemistry of plants*. Academic, London, pp 571–645
- Kolattukudy PE, Buckner JS, Liu T-Y (1973) Biosynthesis of secondary alcohols and ketones from alkanes. *Arch Biochem Biophys* 156:613–620
- Koornneef M, Hanhart CJ, Thiel F (1989) A genetic and phenotypic description of *eceriferum* (*cer*) mutants in *Arabidopsis thaliana*. *J Hered* 80:118–122
- Krolukowski KA, Victor JL, Wagler TN, Lolle SJ, Pruitt RE (2003) Isolation and characterization of the *Arabidopsis* organ fusion gene *HOTHEAD*. *Plant J* 35:501–511
- Kunst L, Samuels L (2009) Plant cuticles shine: advances in wax biosynthesis and export. *Curr Opin Plant Biol* 12:721–727
- Kurata T, Kawabata-Awai C, Sakuradani E, Shimizu S, Okada K, Wada T (2003) The *YOPE-YOPE* gene regulates multiple aspects of epidermal cell differentiation in *Arabidopsis*. *Plant J* 36:55–66
- Kurdyukov S, Faust A, Trenkamp S, Bär S, Franke R, Efremova N, Tietjen K, Schreiber L, Saedler H, Yephremov A (2006) Genetic and biochemical evidence for involvement of *HOTHEAD* in the biosynthesis of long-chain α -, ω -dicarboxylic fatty acids and formation of extracellular matrix. *Planta* 224:315–329
- Lai C, Kunst L, Jetter R (2007) Composition of alkyl esters in the cuticular wax on inflorescence stems of *Arabidopsis thaliana cer* mutants. *Plant J* 50:189–196
- Lardizabal KD, Metz JG, Sakamoto T, Hutton WC, Pollard MR, Lassner MW (2000) Purification of a jojoba embryo wax synthase, cloning of its cDNA, and production of high levels of wax in seeds of transgenic *Arabidopsis*. *Plant Physiol* 122:645–656
- Le Bouquin R, Skrabs M, Kahn R, Benveniste I, Salaün JP, Schreiber L, Durst F, Pinot F (2001) CYP94A5, a new cytochrome P450 from *Nicotiana tabacum* is able to catalyze the oxidation of fatty acids to the omega-alcohol and to the corresponding diacid. *Eur J Biochem* 268:3083–3090
- Le Hir R, Sorin C, Chakraborti D, Moritz T, Schaller H, Tellier F, Robert S, Morin H, Bako L, Bellini C (2013) ABCG9, ABCG11 and ABCG14 ABC transporters are required for vascular development in *Arabidopsis*. *Plant J* 76:811–824
- Lee SB, Suh MC (2015) Advances in the understanding of cuticular waxes in *Arabidopsis thaliana* and crop species. *Plant Cell Rep* 34:557–572
- Lee SB, Go YS, Bae H-J, Park JH, Cho SH, Cho HJ, Lee DS, Park OK, Hwang I, Suh MC (2009) Disruption of glycosylphosphatidylinositol-anchored lipid transfer protein gene altered cuticular lipid composition, increased plastoglobules, and enhanced susceptibility to infection by the fungal pathogen *Alternaria brassicicola*. *Plant Physiol* 150:42–54
- Li Y, Beisson F, Koo AJ, Molina I, Pollard M, Ohlogge J (2007) Identification of acyltransferases required for cutin biosynthesis and production of cutin with suberin-like monomers. *Proc Natl Acad Sci U S A* 104:18339–18344

- Li F, Wu X, Lam P, Bird D, Zheng H, Samuels L, Jetter R, Kunst L (2008) Identification of the wax ester synthase/acyl-CoenzymeA: diacylglycerol acyltransferase WSD1 required for stem wax ester biosynthesis in *Arabidopsis*. *Plant Physiol* 148:97–107
- Li-Beisson Y, Pollard M, Sauveplane V, Pinot F, Ohlrogge J, Beisson F (2009) Nanoridges that characterize the surface morphology of flowers require the synthesis of cutin polyester. *Proc Natl Acad Sci U S A* 106:22008–22013
- Li-Beisson Y, Shorrosh B, Beisson F, Andersson MX, Arondel V, Bates PD, Baud S, Bird D, Debono A, Durrett TP, Franke RB, Graham IA, Katayama K, Kelly AA, Larson T, Markham JE, Miquel M, Molina I, Nishida I, Rowland O, Samuels L, Schmid KM, Wada H, Welti R, Xu C, Zallot R, Ohlrogge J (2013) Acyl-lipid metabolism. *Arabidopsis Book* 11:e0161
- Lü S, Song T, Kosma DK, Parsons EP, Rowland O, Jenks MA (2009) *Arabidopsis CER8* encodes LONG-CHAIN ACYL-COA SYNTHETASE 1 (LACS1) that has overlapping functions with LACS2 in plant wax and cutin synthesis. *Plant J* 59:553–564
- McFarlane HE, Shin JJH, Bird DA, Samuels AL (2010) *Arabidopsis* ABCG transporters, which are required for export of diverse cuticular lipids, dimerize in different combinations. *Plant Cell* 22:3066–3075
- McFarlane HE, Watanabe Y, Yang W, Huang Y, Ohlrogge J, Samuels AL (2014) Golgi- and trans-Golgi network-mediated vesicle trafficking is required for wax secretion from epidermal cells. *Plant Physiol* 164:1250–1260
- Molina I, Kosma D (2015) Role of HXXXD-motif/BAHD acyltransferases in the biosynthesis of extracellular lipids. *Plant Cell Rep* 34:587–601
- Nawrath C, Schreiber L, Franke RB, Geldner N, Reina-Pinto JJ, Kunst L (2013) Apoplastic diffusion barriers in *Arabidopsis*. *Arabidopsis Book* 11:e0167
- Panikashvili D, Savaldi-Goldstein S, Mandel T, Yifhar T, Franke RB, Höfer R, Schreiber L, Chory J, Aharoni A (2007) The *Arabidopsis* DESPERADO/AtWBC11 transporter is required for cutin and wax secretion. *Plant Physiol* 145:1345–1360
- Panikashvili D, Shi JX, Schreiber L, Aharoni A (2009) The *Arabidopsis* DCR encoding a soluble BAHD acyltransferase is required for cutin polyester formation and seed hydration properties. *Plant Physiol* 151:1773–1789
- Panikashvili D, Shi JX, Bocobza S, Franke RB, Schreiber L, Aharoni A (2010) The *Arabidopsis* DSO/ABCG11 transporter affects cutin metabolism in reproductive organs and suberin in roots. *Mol Plant* 3:563–575
- Panikashvili D, Shi JX, Schreiber L, Aharoni A (2011) The *Arabidopsis* ABCG13 transporter is required for flower cuticle secretion and patterning of the petal epidermis. *New Phytol* 190:113–124
- Pascal S, Bernard A, Sorel M, Pervent M, Vile D, Haslam RP, Napier JA, Lessire R, Domergue F, Joubès J (2013) The *Arabidopsis cer26* mutant, like the *cer2* mutant, is specifically affected in the very-long-chain fatty acid elongation process. *Plant J* 73:733–746
- Pighin JA, Zheng H, Balakshin LJ, Goodman IP, Western TL, Jetter R, Kunst L, Samuels AL (2004) Plant cuticular lipid export requires an ABC transporter. *Science* 306:702–704
- Qiu Y, Tittiger C, Wicker-Thomas C, Le Goff G, Young S, Wajnberg E, Fricaux T, Taquet N, Blomquist GJ, Feyereisen R (2012) An insect-specific P450 oxidative decarbonylase for cuticular hydrocarbon biosynthesis. *Proc Natl Acad Sci U S A* 109:14858–14863
- Rautengarten C, Ebert B, Ouellet M, Nafisi M, Baidoo EE, Benke P, Stranne M, Mukhopadhyay A, Keasling JD, Sakuragi Y, Scheller HV (2012) *Arabidopsis deficient in cutin ferulate* encodes a transferase required for feruloylation of ω -hydroxy fatty acids in cutin polyester. *Plant Physiol* 158:654–665
- Reed JR, Vanderwel D, Choi S, Pomonis JG, Reitz RC, Blomquist GJ (1994) Unusual mechanism of hydrocarbon formation in the housefly: cytochrome P450 converts aldehyde to the sex pheromone component (Z)-9-tricosene and CO₂. *Proc Natl Acad Sci U S A* 91:10000–10004
- Roudier F, Gissot L, Beaudoin F, Haslam R, Michaelson L, Marion J, Molino D, Lima A, Bach L, Morin H, Tellier F, Palauqui JC, Bellec Y, Renne C, Miquel M, Dacosta M, Vignard J, Rochat C, Markham JE, Moreau P, Napier J, Faure JD (2010) Very-long-chain fatty acids are involved in polar auxin transport and developmental patterning in *Arabidopsis*. *Plant Cell* 22:364–375

- Rowland O, Domergue F (2012) Plant fatty acyl reductases: enzymes generating fatty alcohols for protective layers with potential for industrial applications. *Plant Sci* 193–194:28–38
- Rowland O, Zheng H, Hepworth SR, Lam P, Jetter R, Kunst L (2006) *CER4* encodes an alcohol-forming fatty acyl-coenzyme A reductase involved in cuticular wax production in *Arabidopsis*. *Plant Physiol* 142:866–877
- Sauveplane V, Kandel S, Kastner PE, Ehlting J, Compagnon V, Werck-Reichhart D, Pinot F (2009) *Arabidopsis thaliana* CYP77A4 is the first cytochrome P450 able to catalyze the epoxidation of free fatty acids in plants. *FEBS J* 276:719–735
- Schneider-Belhaddad F, Kolattukudy PE (2000) Solubilization, partial purification, and characterization of a fatty aldehyde decarboxylase from a higher plant, *Pisum sativum*. *Arch Biochem Biophys* 377:341–349
- Schnurr J, Shockey J, Browse J (2004) The acyl-CoA synthetase encoded by *LACS2* is essential for normal cuticle development in *Arabidopsis*. *Plant Cell* 16:629–642
- Shi JX, Malitsky S, De Oliveira S, Branigan C, Franke RB, Schreiber L, Aharoni A (2011) SHINE transcription factors act redundantly to pattern the archetypal surface of *Arabidopsis* flower organs. *PLoS Genet* 7:e1001388
- Stoveken T, Kalscheuer R, Malkus U, Reichelt R, Steinbuechel A (2005) The wax ester synthase/acyl coenzyme A:diacylglycerol acyltransferase from *Acinetobacter* sp. strain ADP1: characterization of a novel type of acyltransferase. *J Bacteriol* 187:1369–1376
- Suh MC, Samuels AL, Jetter R, Kunst L, Pollard M, Ohlrogge J, Beisson F (2005) Cuticular lipid composition, surface structure, and gene expression in *Arabidopsis* stem epidermis. *Plant Physiol* 139:1649–1665
- Vioque J, Kolattukudy PE (1997) Resolution and purification of an aldehyde-generating and an alcohol-generating fatty acyl-CoA reductase from pea leaves (*Pisum sativum* L.). *Arch Biochem Biophys* 340:64–72
- von Wettstein-Knowles P (1982) Elongase and epicuticular wax biosynthesis. *Physiol Vég* 20:797–809
- von Wettstein-Knowles P (2007) Analyses of barley spike mutant waxes identify alkenes, cyclopropanes and internally branched alkanes with dominating isomers at carbon 9. *Plant J* 49:250–264
- von Wettstein-Knowles P (2012) Plant waxes. In: John Wiley & Sons (eds) *eLS*, Ltd, Chichester, pp 1–12
- Wang X, Guan Y, Zhang D, Dong X, Tian L, Qu LQ (2017) A β -ketoacyl-CoA synthase is involved in rice leaf cuticular wax synthesis and requires a CER2-LIKE protein as a cofactor. *Plant Physiol* 173:944–955
- Warui DM, Li N, Nørgaard H, Krebs C, Bollinger JM, Booker SJ (2011) Detection of formate, rather than carbon monoxide, as the stoichiometric coproduct in conversion of fatty aldehydes to alkanes by a cyanobacterial aldehyde decarboxylase. *J Am Chem Soc* 133:3316–3319
- Wellesen K, Durst F, Pinot F, Benveniste I, Nettekheim K, Wisman E, Steiner-Lange S, Saedler H, Yephremov A (2001) Functional analysis of the *LACERATA* gene of *Arabidopsis* provides evidence for different roles of fatty acid ω -hydroxylation in development. *Proc Natl Acad Sci U S A* 98:9694–9699
- Weng H, Molina I, Shockey J, Browse J (2010) Organ fusion and defective cuticle function in a *lacs1lacs2* double mutant of *Arabidopsis*. *Planta* 231:1089–1100
- Xiao F, Goodwin SM, Xiao Y, Sun Z, Baker D, Tang X, Jenks MA, Zhou J-M (2004) *Arabidopsis* CYP86A2 represses *Pseudomonas syringae* type III genes and is required for cuticle development. *EMBO J* 23:2903–2913
- Yang W, Pollard M, Li-Beisson Y, Beisson F, Feig M, Ohlrogge J (2010) A distinct type of glycerol-3-phosphate acyltransferase with sn-2 preference and phosphatase activity producing 2-monoacylglycerol. *Proc Natl Acad Sci U S A* 107:12040–12045
- Yang W, Simpson JP, Li-Beisson Y, Beisson F, Pollard M, Ohlrogge JB (2012) A land-plant-specific glycerol-3-phosphate acyltransferase family in *Arabidopsis*: substrate specificity, sn-2 preference, and evolution. *Plant Physiol* 160:638–652

- Yeats TH, Rose JK (2013) The formation and function of plant cuticles. *Plant Physiol* 163:5–20
- Yeats TH, Martin LB, Viart HM, Isaacson T, He Y, Zhao L, Matas AJ, Buda GJ, Domozych DS, Clausen MH, Rose JK (2012) The identification of cutin synthase: formation of the plant polyester cutin. *Nat Chem Biol* 8:609–611
- Yeats TH, Huang W, Chatterjee S, Viart HM, Clausen MH, Stark RE, Rose JK (2014) Tomato cutin deficient 1 (CD1) and putative orthologs comprise an ancient family of cutin synthase-like (CUS) proteins that are conserved among land plants. *Plant J* 77:667–675
- Zheng H, Rowland O, Kunst L (2005) Disruptions of the Arabidopsis enoyl-CoA reductase gene reveal an essential role for very-long-chain fatty acid synthesis in cell expansion during plant morphogenesis. *Plant Cell* 17:1467–1481



Lipids of Geochemical Interest in Microalgae

7

John K. Volkman

Contents

1	Introduction	160
2	Hydrocarbons	161
2.1	<i>n</i> -Alkanes and <i>n</i> -Alkenes	161
2.2	Isoprenoid Alkanes and Alkenes	163
2.3	Highly Branched Isoprenoid (HBI) Alkenes in Diatoms	163
2.4	Cyclic Hydrocarbons	166
3	Fatty Acids	166
3.1	Hydroxy Fatty Acids	167
4	Fatty Alcohols	168
5	Alkenones and Alkyl Alkenoates	169
6	Alkyl Diols	173
7	Algaenan	175
8	Sterols	177
9	Other Biochemical Constituents	180
10	Research Needs	180
	References	182

Abstract

Microalgae have a long geological history and a diversity of biochemical constituents which vary systematically between algal classes. This review provides an update on those lipid constituents that have proven useful in organic geochemical studies as biomarkers for assigning sources of organic matter in seawater and sediments. These functionalized biomarkers are degraded in sediments by well-established pathways ultimately yielding hydrocarbons which can also be used to assign organic matter sources in ancient sediments and crude oils. Compound classes covered here include hydrocarbons, fatty acids, hydroxy fatty acids, fatty

J. K. Volkman (✉)
CSIRO Oceans and Atmosphere, Hobart, TAS, Australia
e-mail: john.volkman@csiro.au

© Springer Nature Switzerland AG 2020
H. Wilkes (ed.), *Hydrocarbons, Oils and Lipids: Diversity, Origin, Chemistry and Fate*,
Handbook of Hydrocarbon and Lipid Microbiology,
https://doi.org/10.1007/978-3-319-90569-3_10

159

alcohols, alkyl diols, alkenones, alkenoates, and sterols. Information on biopolymeric substances called algaenans found in just a few algal classes is also provided.

1 Introduction

Microalgae are often the major primary source of organic matter in aquatic ecosystems and hence they are a significant source of the lipids in sediments, together with contributions from bacteria, archaea, higher plants, and animals such as zooplankton and benthic species. Microalgae have a long geological history and have evolved into numerous different classes since the first appearance of red algae at least 1.6 billion years ago (Bengtson et al. 2017). These eukaryotes share many common features in their lipid biochemistry, but with evolutionary change some have developed specific biochemical characteristics. For example, some diatoms developed the ability to synthesize unusual highly branched isoprenoid (HBI) alkenes about 92 million years ago (Sinninghe Damsté et al. 2004), while the unusual branched isoprenoidal botryococenes made by the green alga *Botryococcus braunii* may only have evolved in the Eocene less than 50 million years ago (Volkman 2014).

Comprehensive studies of microalgal lipids are unfortunately fairly sparse, but a sufficiently large number of species have now been studied to formulate some of the more important features. Much of this literature is spread over many journals reflecting the different areas where such data are of interest. For example, with the growing interest in growing microalgae for biodiesel production, there has been an upsurge in algal lipid analyses although many of these simply focus on the fatty acid distributions.

Traditionally recognized phyla in microalgae include Rhodophyta (red algae), Euglenophyta (euglenoids), Cryptophyta (cryptomonads), Pyrrophyta (dinoflagellates), Raphidophyta (raphidophytes), Chrysophyta (chrysophytes, golden-brown algae), Xanthophyta (= Tribophyta, yellow-green algae), Chlorophyta (green algae), Eustigmatophyta (eustigmatophytes), Prasinophyta (green algae, prasinophytes), Phaeophyta (brown algae), Bacillariophyta (diatoms), and Glaucophyta (glaucophytes). Cyanophyta are referred to as blue-green algae in the older literature, but they are actually prokaryotic cyanobacteria and thus not microalgae at all. I have chosen not to cover their lipids in this review. Unfortunately, many of these algal classifications are in a state of flux, and some of the early identifications have been modified with some species reassigned to other classes as more information from molecular biology becomes available. This can make assessment of some of the earlier literature problematic, and so modern assignments are used where possible in this review.

Lipid biomarkers are often used to assign sources of organic matter in aquatic systems and sediments and, with appropriate calibration and knowledge of diagenetic effects, can be used as a proxy for contributions of organic matter from different organisms, even in ancient sediments (Briggs and Summons 2014). Microalgae contain a number of distinctive biomarkers not found in other organisms which

affords an opportunity to use them as palaeoproxies. For example, the contents of C_{37} alkenones, dinosterol, “brassicasterol” (strictly epi-brassicasterol, since diatoms usually make sterols with 24α -alkyl stereochemistry), and C_{30} alkyl diols in sediments have been used as productivity proxies for haptophytes, dinoflagellates, diatoms, and eustigmatophytes, respectively (He et al. 2008). This approach can only be semi-quantitative since these compounds have very different susceptibility to the effects of biodegradation and diagenesis. Moreover, the abundance of these biomarkers per unit biomass is very different in the different algae and can be quite variable due to a range of environmental factors.

This review mainly focuses on new developments in our understanding of lipid biochemistry in microalgae with an emphasis on data that are relevant to the field of organic geochemistry. For a summary of the earlier literature, the reader is referred to Volkman et al. (1998) and other reviews mentioned in each section.

2 Hydrocarbons

Hydrocarbons are rarely significant components of the lipids in microalgae. Perhaps the most common is the hexa-unsaturated alkene n - $C_{21:6}$ which is formed by decarboxylation of the polyunsaturated fatty acid 22:6n-3 (Lee and Loeblich 1971). For convenience, a shorthand nomenclature is used for hydrocarbons (n - $C_{x,y}$) where x is the number of carbon atoms and y is the number of double bonds. For fatty acids, the nomenclature used here is X:Yn-Z where X is the number of carbon atoms, Y is the number of double bonds, and Z is the position of the closest methylene-interrupted double bond to the methyl (ω) end of the molecule. High contents of n - $C_{21:6}$ can be found in diatoms due to efficient conversion of the fatty acid 22:6n-3 which, as a consequence, is not abundant in diatoms. In a few species, n - $C_{21:6}$ is accompanied by small amounts of n - $C_{21:5}$ (e.g., Cranwell et al. 1988; Volkman et al. 1994a).

2.1 n -Alkanes and n -Alkenes

Shorter-chain n - C_{15} , n - C_{17} , and n - C_{19} alkanes and monounsaturated alkenes occur in some microalgae (e.g., Gelpi et al. 1970; Weete 1976) and are particularly common in chlorophytes (Cranwell et al. 1990). However, the amounts of hydrocarbons are typically low compared to other lipid classes. Recent work has confirmed that alkanes are likely to be formed by decarboxylation of the corresponding fatty acids (Sorigué et al. 2016). Some alkenes with longer chain lengths have been reported. For example, the freshwater chlorophyte *Scenedesmus* spp. contain C_{21} , C_{23} , and C_{25} n -alk-1-enes (Cranwell et al. 1990), and *Scenedesmus quadricauda* contains high amounts of the C_{27} monoene (Gelpi et al. 1970). Polyunsaturated C_{25} and C_{27} n -alkenes have also been found in a strain of the diatom *Rhizosolenia setigera* (Schouten et al. 1998; Sinninghe Damsté et al. 1999a). From these data, it is clear that some microalgae are able to biosynthesize long-chain alkenes although

reliable reports of long-chain *n*-alkanes are rare. For example, Nagashima et al. (1986) reported *n*-alkanes (*n*-C₁₄–*n*-C₃₀) with a predominance of *n*-C₁₇ (46.3%) and a diene C_{19:2} in *Cyanidium caldarium* (RK-1 strain), while *Cyanidium* (M-8 strain) contained *n*-alkanes (*n*-C₁₅ to *n*-C₂₅) and alkenes (C_{19:1} and smaller amounts of C_{21:1}).

Allard and Templier (2000) studied the lipids in nine species of freshwater and marine green microalgae from the class Chlorophyceae that make distinctive thin trilaminar outer walls. C₂₃–C₂₉ straight-chain hydrocarbons were identified in most of the algaenan-producing *Chlorella* and in the algaenan-devoid *Chlorella minutissima marina*, whereas only low molecular weight hydrocarbons were detected in algaenan-producing *Scenedesmus subspicatus* and in algaenan-devoid *C. marina*. The hydrocarbon compositions of different races of the geochemically important green alga *Botryococcus braunii* (Trebouxiophyceae) are of particular interest. Early work established the presence of odd-chain C₂₇–C₃₃ *n*-alkadienes (Brown et al. 1969; Gelpi et al. 1970) in Race A as well as isoprenoid alkenes (see next section).

Some eustigmatophytes also contain significant amounts of long-chain hydrocarbons. Odd-chain saturated and polyunsaturated C₁₄–C₃₁ hydrocarbons have been isolated from two marine *Nannochloropsis* species and show a predominance of C₂₅, C₂₇, and C₂₉ *n*-alkenes which vary in abundance in the different species (Gelin et al. 1997b). Indeed, Zhang et al. (2015) showed a correlation between long-chain alkyl diols in sediments of Lake Lugu and long-chain alkenes. Chlorophytes, on the other hand, cannot be excluded as a possible contributor of the long-chain *n*-alkenes because these algae are common in Lake Lugu and they are known to biosynthesize an *n*-C_{27:1} alkene.

Alkenone-producing haptophytes such as *Emiliania*, *Chrysolita*, and *Isochrysis* contain high amounts of two classes of long-chain alkenes (Volkman et al. 1980a, b; Marlowe et al. 1984a, b; Patterson et al. 1994a; Conte et al. 1995; Grossi et al. 2000; Rontani et al. 2004; Theroux et al. 2013; Nakamura et al. 2015). Volkman et al. (1980b) first showed that *E. huxleyi* contains high amounts of very-long-chain C_{31:2} (3 isomers), C_{33:3} (2 isomers), C_{33:4} (2 isomers), C_{37:3}, and C_{38:3} *n*-alkenes. Rontani et al. (2004) showed that *Chrysolita lamellosa* contained a mixture of C₂₉–C₃₃ *n*-alkenes, dominated by the C_{31:1} monoene, although previous analysis of other strains reported only the presence of a C_{31:2} diene (Marlowe et al. 1984a). These variations can reflect biochemical differences between strains and the effects of differing culturing conditions such as temperature (Grossi et al. 2004). The hydrocarbons in cultures of *E. huxleyi* NIES837 and *G. oceanica* NIES1315 were analyzed by Nakamura et al. (2015) who found C_{29:2} and C_{31:2} dienes as major constituents together with smaller amounts of C_{29:1} and C_{31:1} monoenes and di-, tri-, and tetra-unsaturated C₃₃ alkenes. Rather surprisingly, C₃₇ and C₃₈ alkenes were not detected.

The major alkenes of *I. galbana* CCAP 927/14 and *E. huxleyi* (strains CCAP 920/2 and VAN 556) were identified by Rieley et al. (1998) using NMR and GC–MS analysis of DMDS adducts. The dominant alkene in *I. galbana* is (*Z*)-hentriaconta-1,22-diene, with hentriaconta-1,24-diene and tritriaconta-1,24-diene present in much lower abundance; (*Z*)-hentriaconta-1,22-diene also occurs in *E. huxleyi* (strain

CCAP 920/2), together with (2*Z*,22*Z*)-hentriaconta-2,22-diene (the major hydrocarbon) and (3*Z*,22*Z*)-hentriaconta-3,22-diene. Minor amounts of hentriaconta-2,24-diene and hentritriaconta-2,24-diene are also present in this strain. Nakamura et al. (2015) also used DMDS adducts to show that the C₂₉ alkenes in *E. huxleyi* NIES837 and *G. oceanica* NIES1315 included nonacosa-2,20-diene (most abundant), as well as nonacosa-1,20-diene, nonacosa-3,20-diene (both novel reports) and nonacos-9-ene.

The work of Rieley et al. (1998) and Grossi et al. (2000) clearly showed the presence of two biochemically different groups of hydrocarbons in haptophytes, each with a different biosynthesis and presumably biological function. The C₃₁–C₃₃ alkenes with *cis* (*Z*) double bonds are likely derived from chain extension and decarboxylation of (*Z*)-octadec-9-enoic acid or (*Z*)-hexadec-7-enoic acid, using a pathway analogous to that in *B. braunii* (Rieley et al. 1998; Nakamura et al. 2015). In contrast to the C₂₉–C₃₃ alkenes, the C₃₇–C₃₉ alkenes have *trans* (*E*) double bonds indicating that their biosynthesis is closely related to the alkenones.

Hydrocarbon contents and compositions can be affected by growth conditions, but there have been few systematic studies. Dodson and Leblond (2015) examined the hydrocarbons made by the common diatom *Phaeodactylum tricoratum* at different temperatures. At 20 °C, the diatom made C₈, C₁₁, C₁₉, and C₂₁ *n*-alkanes, but at 30 °C it produced C₁₇, C_{17:1}, C_{18:1}, C₁₉, C_{19:1}, and C₂₀ *n*-alkanes and *n*-alkenes. The alkenes were not present at the lower temperature.

2.2 Isoprenoid Alkanes and Alkenes

It is now known that *B. braunii* exists in four distinct races (A, B, L, and S) based on their hydrocarbon compositions and DNA profiles (Metzger and Largeau 2005; Kawachi et al. 2012; Volkman 2014). Race A contains C₂₅–C₃₃ *n*-alkadienes and *n*-alkatrienes derived from fatty acids (Templier et al. 1992). Race B contains C₃₀–C₃₇ isoprenoid-based hydrocarbons called botryococcenes (Metzger et al. 1985) (Fig. 1) as well as squalene and methylated squalenes as minor components (Huang and Poulter 1989; Achitouv et al. 2004) (Fig. 1). Strains of Race L contain the C₄₀ isoprenoid alkene lycopadiene [(6*R*,10*R*,14*E*,18*E*,23*R*,27*R*)-2,6,10,14,19,23,27,31-octamethyldotriaconta-14,18-diene] (Metzger and Casadevall 1987; Metzger et al. 1990) (Fig. 1). The newly defined S Race produces C₁₈ and C₂₀ *n*-alkanes and epoxy alkanes, but lacks botryococcenes and lycopadiene (Kawachi et al. 2012) and thus is closer to race A.

2.3 Highly Branched Isoprenoid (HBI) Alkenes in Diatoms

This unusual class of C₂₀, C₂₅, and C₃₀ “T-shaped” highly branched isoprenoid (HBI) alkanes and alkenes was first recognized by the identification of an unusual C₂₀ alkane 2,6,10-trimethyl-7-(3-methylbutyl)dodecane (termed Gx) in the Rozel Point oil (Yon et al. 1982). A biological source was not known until Nichols et al. (1988) found high amounts of a C₂₅ HBI diene in Antarctic sea ice samples.

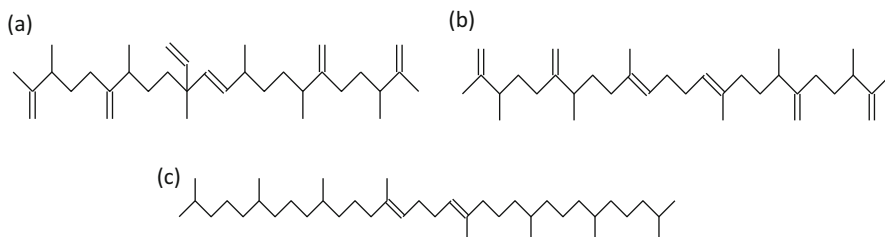


Fig. 1 Structures of some of the unusual isoprenoid alkenes found in the green alga *Botryococcus braunii* (Trebouxiophyceae): (a) C₃₄ botryococcene; (b) C₃₄ tetramethylsqualene; (c) C₄₀ isoprenoid lycopadiene. Compounds (a) and (b) are found in the B race while (c) is found in the L race

Volkman et al. (1994a) confirmed a diatom source by demonstrating the occurrence of C₂₅ HBI alkenes with 3, 4, and 5 double bonds in cultured cells of the diatom *Haslea ostrearia* and C₃₀ HBI alkenes with 4, 5, and 6 double bonds in the diatom *R. setigera*. Once an algal source had been identified, it was possible to isolate sufficient material for full structures of the C₂₅ HBIs to be elucidated using NMR, epoxide derivatization and mass spectrometry by researchers at Plymouth University (Rowland et al. 1995; Belt et al. 1996; Wraige et al. 1997). A few representative structures are shown in Fig. 2. HBIs are widespread in sediments, but to date the only natural source identified is diatoms. Intriguingly, a biological source for C₂₀ HBIs has not yet been found. The early literature is summarized by Rowland and Robson (1990) and Volkman et al. (1998).

C₂₅ HBIs (sometimes called haslenes – examples are shown in Fig. 2a–e) have now been found in laboratory cultures of species within the genera *Haslea* (Volkman et al. 1994a; Belt et al. 1996, 2007; Wraige et al. 1997; Allard et al. 2001; Poulin et al. 2004), *Rhizosolenia* (Volkman et al. 1994a; Sinninghe Damsté et al. 1999a,b; Belt et al. 2001a, 2002; Rowland et al. 2001), *Navicula* (Belt et al. 2001c, d), *Pleurosigma* (Belt et al. 2000a, 2001b; Grossi et al. 2004), and *Berkeleya* (Brown et al. 2014). Recent work by Kaiser et al. (2016) has shown that the marine planktonic diatom *Pseudosolenia calcar-avis* (Schultze) isolated from near surface waters in Mecklenburg Bay in the southwestern Baltic Sea biosynthesizes one C_{25:2} and two C_{25:3} HBI alkenes as previously reported in some benthic diatoms. C₃₀ HBIs (rhizenes; e.g., Fig. 2f and g) have only been identified in laboratory cultures of *R. setigera* (Volkman et al. 1994a; Belt et al. 2001a, 2002; Rowland et al. 2001; Massé et al. 2004b).

This taxonomic specificity has practical application in taxonomy. For example, Poulin et al. (2004) proposed the transfer of *Gyrosigma nipkowii* Meister to *Haslea nipkowii* (Meister) Poulin & Massé based on morphology, SEM, molecular analyses, and the presence of characteristic HBIs.

A mono-unsaturated C₂₅ highly branched isoprenoid (HBI) alkene termed IP₂₅ (Belt and Müller 2013; Belt et al. 2007; Fig. 2d) is produced by sea ice diatoms including *Haslea crucigeroides*, *H. spicula*, *H. kjellmanii*, and *Pleurosigma stuxbergii* var. *rhomboides* that bloom in the underside of seasonal sea ice (Brown

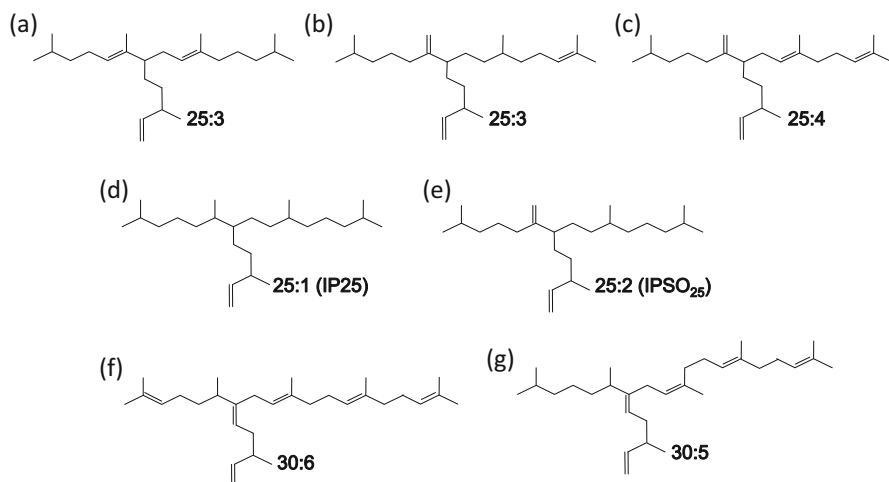


Fig. 2 Structures of some of the C₂₅ and C₃₀ highly branched isoprenoid (HBI) alkenes (haslenes and rhizenes) found in some diatoms

et al. 2014). Since IP₂₅ is deposited in underlying sediment following ice melt in the late spring, this HBI alkene has been used as a proxy for the extent of Arctic sea ice (Belt and Müller 2013; Smik and Belt 2017). Another 25:2 HBI termed IPSO₂₅ (Fig. 2e) may be a comparable sea ice marker for the Antarctic (Belt et al. 2016). Brown et al. (2014) have also shown that not all species within the *Haslea*, *Pleurosigma*, and *Navicula* genera produce HBI alkenes. For example, species such as *H. ostrearia* and *P. intermedium* produce HBIs, but *H. wawriake* and *P. angulatum* do not. Also, note that IP₂₅ was identified in *H. kjellmanii* but was absent in *H. vitrea*.

Within the genus *Rhizosolenia*, strains of *R. setigera* have been reported that contain only the C₃₀ HBIs (strain CS-62: Volkman et al. 1994a; strain Nante 99: Belt et al. 2001a). In contrast, Rowland et al. (2001) detected both C₂₅ and C₃₀ HBIs in *R. setigera* (strain CS 389/A); Belt et al. (2017) found C₂₅ HBIs but not C₃₀ HBIs in *R. polydactyla f. polydactyla* and *R. hebetata f. semispina*. C₃₀ HBIs were also absent in cultures of *R. setigera* isolated from the east coast of the USA (Sinninghe Damsté et al. 1999b). Different distributions of HBIs have also been identified in *R. fallax*, *R. shrubshrolei*₂ and *R. pungens* (Sinninghe Damsté et al. 2004).

Some of the factors affecting HBI distributions have been elucidated, but a complete picture is yet to emerge. Rowland et al. (2001) showed that there was an increase in the degree of unsaturation in the haslenes and *E* to *Z* isomerization in the C₂₅ triene as well as an increase in unsaturation in the rhizenes, with hexaenes dominant over the pentaenes, in strain CS 389/A of *R. setigera* with increasing growth temperature from 18 to 25 °C, which is opposite the behavior usually seen in membrane lipids with temperature. Increased salinity from 15 to 35 ppt increased cell growth and rhizene production but decreased haslene production. Belt et al. (2002) showed that HBI distributions are strongly influenced by stages within the

life cycle, with the biosynthesis of C₂₅ HBIs stimulated during sexual reproduction (i.e., the auxosporulation stage).

Recent work has shown that HBIs in sediments and extracts can degrade on storage with significant changes to the compositions (Sanz et al. 2016), so it is preferable to work on fresh or frozen material. This also indicates that the analytical window in sediment studies needs to be widened to include HBI degradation products, particularly since HBIs undergo facile acid-catalyzed isomerization and cyclization reactions in sediments (Belt et al. 2000b).

2.4 Cyclic Hydrocarbons

The HBI-synthesizing diatom *R. setigera* also contains unusual C₃₀ monocyclic alkenes (Belt et al. 2003; Massé et al. 2004a). These have an isoprenoid structure and a single 6-membered ring but are apparently unrelated to the HBI alkenes. It is thought that they are biosynthesized by coupling of a geranyl (C₁₀) moiety to either a farnesyl (C₁₅) or geranylgeranyl unit (C₂₀) at C-7 to yield C₂₅ and C₃₀ compounds, respectively.

3 Fatty Acids

Monocarboxylic fatty acids with 0–6 double bonds are the most abundant lipids in microalgae. These occur in a variety of different lipid types including triacylglycerols, phospholipids, glycolipids, and other less common forms such as betaine lipids (e.g., Pedro Canavate et al. 2016). For a detailed recent review of the various polar lipids in microalgae, their biosynthesis, and genetic aspects see Khozin-Goldberg (2016). The proportions of these lipids can vary significantly under different environmental and physiological conditions (e.g., Li et al. 2016 and references therein). For example, Dodson et al. (2014) examined the effects of growth temperature on galactolipids, the primary component of chloroplast membranes, in two pennate diatoms. At 20 °C, both *P. tricornutum* and *H. ostrearia* possessed different galactolipid profiles, with the former possessing mostly C₂₀/C₁₆ (sn-1/sn-2) forms of mono- and digalactosyldiacylglycerol (MGDG and DGDG, respectively) and the latter possessing mostly C₁₈/C₁₆ forms of MGDG and DGDG. However, both diatoms had similar lipid profiles when grown at 30 °C and were characterized by a higher proportion of more saturated lipids, an increase in C₁₈ fatty acids at the sn-1 position of the lipid, and an absence of C₂₀ fatty acids.

Polar lipids are rapidly hydrolyzed on cell death or senescence and so the major form of fatty acids found in sediments is typically as free fatty acids. Intact polar lipids such as phospholipids have been used as a measure of living cells (both prokaryotic and eukaryotic) in sediments (e.g., Lipp and Hinrichs 2009).

Fatty acid distributions vary systematically between algal classes (reviewed by Lang et al. 2011; Khozin-Goldberg 2016) and so can often be used to assign organic matter sources in sediments. For example, diatoms often have simple distributions

dominated by 16:0 (palmitic acid), 16:1n-7 (palmitoleic acid), 20:5n-3 (icosapentaenoic acid), and sometimes 14:0 (e.g., Dunstan et al. 1994). Eustigmatophytes can have similar distributions dominated by 14:0, 16:0, 16:1n-7, and 20:5n-3 (Volkman et al. 1993, 1999b; Olofsson et al. 2012, 2014; Mitra et al. 2015). In contrast, the fatty acids in green algae are typically dominated by unsaturated C₁₈ fatty acids such as 18:1n-9 (oleic acid), 18:2n-6 (linoleic acid), and 18:3n-3 (linolenic acid), much like higher plants, although some green algae also have appreciable amounts of 18:4n-3 (Cranwell et al. 1990). Dinoflagellates have quite different distributions with high contents of 16:0 and 18:0 (stearic acid), together with unsaturated C₁₈ fatty acids (including uncommon 18:5n-3) and 22:6n-3 (docosahexaenoic acid), the latter being common in marine zooplankton. A few species of dinoflagellates make small amounts (< 2.3%) of very-long-chain C₂₈ highly unsaturated fatty acids (HUFAs) including 28:7n-6 and 28:8n-3 by chain elongation and further desaturation (Mansour et al. 1999; Rezanka et al. 2017). Several fatty acid patterns are found in haptophytes with 14:0, 16:0, 16:1n-7, 18:1n-9, and 22:6n-3 abundant in many species together with low contents of C₁₈ PUFA other than 18:4 (e.g., Wang et al. 2015). *Pavlova* species also show high contents of 20:5n-3, but this is not the case for *E. huxleyi* (Jeffrey et al. 1994; Lang et al. 2011).

The double bond positions of some PUFA can be distinctive if chain shortening or elongation of preformed unsaturated fatty acids is involved in their biosynthesis. For example, Volkman and Johns (1977) were able to distinguish fatty acid sources in intertidal sediments from elucidation of double bond positions in the C₁₆ polyunsaturated fatty acids. The 16:2 fatty acids consisted mainly of the n-4 and n-7 isomers, and 16:3n-4 was the only 16:3 isomer detected. These are typical of diatoms (Ackman et al. 1968), whereas in green microalgae the main isomers are n-3 and n-6 fatty acids (Cranwell et al. 1990).

Fatty acid contents and distributions can be strongly affected by environmental conditions such as differing nutrient, irradiance, and salinity conditions as well as growth stage (exponential vs. stationary phase) as shown by many culture studies (e.g., Dunstan et al. 1993; Xu et al. 2008; Pal et al. 2011; Martinez-Roldan et al. 2014; Pan et al. 2017). Under nitrogen-deficient conditions, phytoplankton cells typically accumulate storage lipids such as triacylglycerols (Dunstan et al. 1993; Jia et al. 2015). Green algae *Chlorella kessleri* and *Chlamydomonas reinhardtii* substantially increase their fatty acid content upon desiccation (Shiratake et al. 2013).

3.1 Hydroxy Fatty Acids

Mono- and dihydroxy fatty acids have been reported in very few microalgae, but comprehensive studies have not been carried out. Matsumoto and Nagashima (1984) reported 3-hydroxy fatty acids (β -hydroxy acids) in cultured microalgae from the Chlorophyta (*Chlamydomonas reinhardtii* and *Chlorella pyrenoidosa*) and Rhodophyta (two strains of the rhodophyte *Cyanidium caldarium*) and cyanobacteria. Matsumoto et al. (1984) found C₁₆–C₂₆ 2-hydroxy acids (α -hydroxy acids) in the green algae *C. reinhardtii* and *C. pyrenoidosa*, *C. caldarium*, and

various cyanobacteria ranging in concentrations from 40 to 320 pg/g dry alga. Volkman et al. (1999b) detected a series of 2- and 3-hydroxy fatty acids ranging from C₂₆ to C₃₀ (with traces of C₁₈ but no intermediate chain-lengths) in the freshwater eustigmatophytes *Vischeria punctata*, *Vischeria helvetica*, and *Eustigmatos vischeri*. C₂₇ and C₂₉ 12-hydroxy methyl alkanooates have been identified in the rhizosolenid diatoms *Proboscia indica* and *Proboscia alata* (Sinninghe Damsté et al. 2003).

Hydroxylated fatty acids in green algae and eustigmatophytes appear to be involved in the structure of the algaenan made by these species. For example, Blokker et al. (1998a) identified ester-bound C₃₀, C₃₂, and C₃₄ mono- and C₃₀ and C₃₂ diunsaturated ω-hydroxy fatty acids in some freshwater green microalgae *Tetraedron minimum*, *Scenedesmus communis*, and *Pediastrum boryanum*. These compounds were not identified in the cytosol of the algae but were released by saponification of the cell implying that they were a main building block of the highly cross-linked algaenan present in the cell walls.

C₃₀–C₃₄ mid-chain hydroxy fatty acids were identified in hydrolyzed extracts from marine eustigmatophytes of the genus *Nannochloropsis* (Gelin et al. 1997b). These all contained a hydroxy group at the ω18 position suggesting that the series is produced by chain-shortening or elongation (at the carboxyl end) from a single major precursor. Two dihydroxy fatty acids identified as 15,16-dihydroxydotriacontanoic acid and 16,17-dihydroxytritacontanoic acid were also found. Balzano et al. (2017) also suggested that long-chain hydroxy fatty acids (LCHFAs) could originate from 14:0 and 16:0 fatty acids via hydroxylation and chain elongation. LCHFAs were previously suggested to share the same biosynthetic pathways as the long-chain alkenones (LCAs) and the long-chain n-alkyl diols (LCDs) in *Nannochloropsis* spp. because compounds from these three classes exhibit the same carbon number range and are functionalized at the same position (Volkman et al. 1992; Gelin et al. 1997b). However, LCHFAs, C_{14:0}, and C_{16:0} fatty acids did not cluster with LCDs as well as LCAs abundance in the PCA, suggesting that not all the LCHFAs biosynthesized by *Nannochloropsis* spp. were converted to LCDs and LCAs (Balzano et al. 2017).

4 Fatty Alcohols

Fatty alcohols other than phytol are rarely reported in microalgae. A summary of reported occurrences can be found in Volkman et al. (1999a). These include 18:1 and 34:4 alcohols in two diatoms, C₁₀–C₂₀ saturated and monounsaturated n-alcohols in the green alga *Chlorella*, C₁₂–C₂₀ n-alkanols (as esters) in various freshwater green algae, and saturated C₁₂–C₂₀ and monoenes 20:1, 22:1 (as esters) in some freshwater chrysophytes.

Acid hydrolysis of the lipids extracted from marine eustigmatophytes of the genus *Nannochloropsis* liberated mainly even-chain C₃₀–C₃₂ mono and diunsaturated straight-chain alcohols with C₃₂ the dominant chain-length. The distributions of the alcohols were very similar to the long-chain alkyl diols in the

same species suggesting that both compound classes are formed by the same biosynthetic pathway (Volkman et al. 1999a). Base hydrolysis of lipids from *Nannochloropsis gaditana* yielded *n*-alkenols in which C_{29:2} and C_{30:1} predominated (Méjanelle et al. 2003). This species also contained novel C₂₈–C₃₂ hydroxy ketones.

Freshwater eustigmatophytes *Eustigmator vischeri*, *Vischeria helvetica* and *Vischeria punctata* have been found to contain long-chain *n*-alcohols. C₁₆–C₃₀ monounsaturated alcohols were abundant with 26:1 and 28:1 as the major constituents. Saturated *n*-alcohols ranged from 14:0 to 28:0 (both present in trace amounts), with 22:0 as the major alkanol (Volkman et al. 1999a). The latter has been reported as the major *n*-alkanol in some lacustrine sediments. The distributions of long-chain *n*-alkanols and *n*-alkenols were very similar in all species.

Allard and Templier (2000) observed that fatty alcohols were the major constituents of the polar fraction of the neutral lipids of each of the nine species of chlorophytes these authors investigated. High molecular weight saturated or mono-unsaturated alcohols were detected in *Chlorella emersonii* and in all the microalgae belonging to the genus *Scenedesmus*. Monoesters were composed predominantly of saturated C₁₆ or C₁₈ fatty acids and saturated C₈, C₁₆, or C₁₈ alcohols. Interestingly, long-chain methyl ketones from C₂₅ to C₃₁ were detected in several species.

Rontani et al. (2001) developed a new technique based on NaBH₄ reduction of alkenones to the corresponding alkenols as a useful tool for characterizing alkenones in natural samples. The TMSi-ethers of these alcohols provide very useful EI mass spectra, which show strong fragment ions at *m/z* 117 or *m/z* 131 due to cleavage at the functional group, allowing methyl and ethyl alkenols (and hence the parent alkenones) to be readily differentiated. This technique provided a suite of standard long-chain *n*-alkenols that could be used to confirm that small amounts (< 1% of alkenone abundance) of these compounds do occur in *G. oceanica* and *I. galbana*.

5 Alkenones and Alkyl Alkenoates

Long-chain alkenones is a term coined by Volkman et al. (1980b) for an unusual class of unsaturated C₃₇–C₃₉ straight-chain methyl ketones (MK: alken-2-ones; Fig. 3) and ethyl ketones (EK: alken-3-ones) found widely in sediments (de Leeuw et al. 1980; Volkman et al. 1980a) and synthesized by the cosmopolitan marine haptophyte *E. huxleyi* (Volkman et al. 1980a, b). The double bond positions in the diunsaturated 37:2 MK and 36:2 EK were established as ω15 and ω22 by de Leeuw et al. (1980) using GC–MS analysis of DMDS adducts of the double bonds. The triunsaturated compounds have double bonds at ω15, ω22, and ω29 and the tetra-unsaturated ketones at ω7, ω15, ω22, and ω29 (Zheng et al. 2016; Fig. 3) and *trans* (*E*) geometry (Rechka and Maxwell 1988; Volkman et al. 1988). It had been thought that the double bonds were a fixed number of carbon atoms from the methyl end of the molecule (e.g., ω15 and ω22), but Rontani et al. (2006b) were able to show from double bond analysis of a wider range of compounds that it is actually the number of carbon atoms from the carbonyl group that is fixed (see Fig. 3). For this reason, Zheng et al. (2016) adopted a Δ nomenclature where the double bond is measured



Fig. 3 Structures of (a) 37:3 methyl alkenone (MK) and (b) 37:3 ethyl alkenones (EK) found in haptophytes such as *Emiliania* and *Gephyrocapsa* (pictured). Note the unusual *trans* (*E*) geometry of the double bonds and ω 15,22,29 double bond positions. By contrast, (c), (d), and (e) show unusual shorter chain 35:2 ω 15,22 MK; 35:2 ω 16,23 MK; and 36:2 ω 15,22 EK found in *E. huxleyi* by Prahl et al. (2006). The latter structure can be compared to the unusual 36:2 ω 15,20 EK (f) found in Black Sea sediments by Xu et al. (2001)

from the carbonyl group, rather than the IUPAC-preferred nomenclature which numbers the longest alkyl chain. Both Rontani et al. (2006b) and Zheng et al. (2016) have speculated on possible modes of biosynthesis, but to date, the actual enzymes and genes involved in alkenone biosynthesis have not been elucidated.

The proportions of the various isomers having two, three, or four double bonds, expressed as $U_{37}^{K'}$ where $U_{37}^{K'} = [37:2]/([37:2] + [37:3])$, respond approximately linearly to growth temperatures from 5 °C to 25 °C (Brassell et al. 1986; Prahl and Wakeham 1987; Prahl et al. 1988; Conte et al. 1998) and exhibit a nonlinear response at more extreme temperatures (Prahl et al. 1988; Sikes and Volkman 1993; Conte et al. 1998). The occurrence of alkenones in modern and ancient sediments has been reviewed by Brassell (2014).

Marlowe et al. (1984a, b) carried out the first extensive survey for alkenones in haptophytes. They examined 13 species from 9 genera and established that alkenones and alkenoates (methyl and ethyl esters of a 36:2 fatty acid; Volkman et al. 1980a) occur in *Chrysolita lamellosa* (now *Ruttnella*) and three species of *Isochrysis* as well as in *E. huxleyi*. They were absent from five other members of the order Isochrysidales and from representatives of the orders Coccosphaerales, Prymnesiales, and Pavlovales. Indeed, only a few genera of haptophytes have been reported to contain alkenones (Volkman et al. 1980a, b, 1995; Marlowe et al. 1984a, b, Conte et al. 1994; Versteegh et al. 2001; Zink et al. 2001; Andersen et al. 2014; Pelusi et al. 2016; Zheng et al. 2016; Longo et al. 2016 and references therein). These include the fully marine species *E. huxleyi* (Volkman et al. 1980a, b; Conte et al. 1994) and *G. oceanica* (Volkman et al. 1995), both belonging to the family Noëlaerhabdaceae (formerly known as the Gephyrocapsaceae). Brackish water species include

Tisochrysis (formerly *Isochrysis* sp., strain T.iso), *Isochrysis galbana*, and *Ruttnera lamellosa* (formerly *Chrysofila lamellosa*), all belonging to the family Isochrysidaceae. The phylogenetic relationships between the Isochrysidaceae and Noëlaerhabdaceae have not been fully elucidated, but 18S rRNA sequence data confirm that the genera *Emiliana*, *Gephyrocapsa*, and *Isochrysis* are monophyletic (Pelusi et al. 2016).

Sufficient data are now available to recognize distinct patterns of alkenone compositions in different groups of haptophytes. Various groups have been proposed based on alkenone/alkenoate compositions, but Theroux et al. (2010) noted from DNA data from sediments that a simple marine/coastal vs. lacustrine separation does not adequately represent the extent of variation. Similarly, Coolen et al. (2004) had noted from 18S rRNA data that changes in the abundance of six phylotypes, all related to *Isochrysis*, in an Antarctic lake data accounted for the subtle changes in alkenone distributions with sediment depth.

Based on their work on a number of lakes, particularly those from Greenland, Theroux et al. (2010) proposed three groups of haptophytes. Group I comprised representative sequences from operational taxonomic units (OTUs) 1, 2, 3, 4, and 5 and occurred in a number of lake sediments including published sequences from the Greenland lakes (D'Andrea et al. 2006). Group II comprised of OTU 6, OTU 7, and OTU 8 sequences and occurred in various *Isochrysis* species; *C. lamellosa*, *I. litoralis*, and *Dicrateria* sp. sequences; and sequences from Ace Lake, Antarctica (Coolen et al. 2004). Group III consisted of marine species *E. huxleyi* and *G. oceanica* and an unidentified marine coccoid haptophyte (U40924). D'Andrea and Huang (2005) have shown that the presence of C₃₈ methyl ketones distinguishes Greenland LCA distributions from those found in other saline lakes in cold regimes and D'Andrea et al. (2016) have demonstrated that the “Greenland strain” of alkenone-producing haptophytes, as represented by OTU5, is able to occupy a wide range of environmental conditions. Isomeric tri-unsaturated alkenones seem to be unique to Group I haptophytes and are not found in other phylogenetic groups (Longo et al. 2013). The marine non-calcifying Isochrysidales *Tisochrysis lutea* apparently does not produce tetraunsaturated alkenones (Bendif et al. 2013; Nakamura et al. 2016).

In a recent review, Ho et al. (2013) constructed two alkenone distributions as type A (*Emiliana*-like) and type B (*Chrysofila*-like). While all the above-mentioned alkenone producers belong to the order Isochrysidales – a coccolithophorid order thought to be composed exclusively of marine to brackish haptophytes – recent studies based on molecular phylogenetic analyses of a variety of freshwater ecosystems have revealed the presence of monophyletic groups without described close relatives that branch within the order Isochrysidales (Theroux et al. 2010; Toney et al. 2012).

In addition to the three main alkenone distribution patterns discussed above, a number of usual alkenones have been found in cultures or in sediments indicating additional alkenone-producers. For example, Rontani et al. (2001) were also able to show the presence of small amounts of a 35:1 MK and two isomers of a 35:2 alkenone in *G. oceanica* and monounsaturated C₃₅–C₃₈ alkenones in *E. huxleyi* by

analysis of alcohols produced by reduction of alkenones. Prah et al. (2006) reported that the benchmark strain (CCMP1742) of *E. huxleyi* used for temperature calibrations had started producing, for reasons not yet clear, major amounts of three new alkenones identified as ω 15,22-C₃₅ MK, ω 15,22-C₃₆ EK, and ω 16,23-C₃₆ MK (see Fig. 3 for structures) when cultured at 15 °C. Prah et al. (2006), and Rontani et al. (2006a) showed the presence of unusual long-chain, diunsaturated alkenones and alkyl alkenoates exhibiting double bonds separated by three methylene units in Holocene Black Sea sediments. The positions of the double bonds were confirmed after OsO₄ treatment and silylation resulting in tetra(trimethylsilyloxy) derivatives. Xu et al. (2001) had previously shown that (16*E*,21*E*)-hexatriaconta-16,21-dien-3-one (i.e., the ω 15,20-C₃₆ EK isomer; Fig. 3) is particularly abundant in Holocene Black Sea Unit II sediments. Zheng et al. (2016) surmised that it and related alkenones were produced by certain mutant Group II brackish haptophytes (i.e., related to *R. lamellosa* or *I. galbana*).

Zheng et al. (2016) found that *E. huxleyi* CCMP2758 had abundant ω 15,22-C₃₅ MK when cultured at 15 °C, but when this strain was cultured at 4–10 °C it produces abundant C_{35:3} MK, C_{36:3} MK, and small amounts of C_{36:3} EK alkenones with unusual double bond positions at Δ^7 , Δ^{12} , and Δ^{19} (as measured from the carbonyl group). Zhao et al. (2014) have noted very long-chain C₄₁ and C₄₂ alkenones in the surface sediments of hypersaline lakes from China suggesting that they may be produced by an unknown haptophyte species living in these hypersaline environments. Ho et al. (2013) found novel pentaunsaturated C₃₈ and C₃₉ alkenones in the surface sediments of a perennially ice-covered Lake Fryxell in the Antarctica, which they suggest were synthesized by *Isochrysis* and/or *R. lamellosa* based on a previous genetics study.

There have been a number of studies with cultured microalgae of possible non-temperature effects on alkenone distributions that might lead to erroneous palaeotemperature estimations (e.g., Volkman 2000; Prah et al. 2003; Ho et al. 2013). These include nutrient and light availability as shown by culture studies (e.g., Epstein et al. 1998, 2001; Prah et al. 2003; Versteegh et al. 2001; Pan et al. 2017), as well as the effects of microbial degradation (Rontani et al. 2008; Zabeti et al. 2010). Conte et al. (1998) examined physiological effects on alkenone and alkenoate distributions in *E. huxleyi* and *G. oceanica*. Cells in late logarithmic and stationary growth had significantly increased abundance of alkenoates and C₃₈ EKs relative to C₃₈ MKs. The unsaturation ratios of both C₃₇ and C₃₈ alkenones also significantly decreased when cells entered the late log phase. They concluded that the average physiological state of alkenone-synthesizers in the open ocean differs from cultured cells growing under exponential growth and appears to be more similar to cells in late log or stationary growth phases. Prah et al. (2006) showed that anomalously warm alkenone-derived SSTs are obtained under light-deprived conditions, while the opposite is true for nutrient-depleted conditions. They also showed that the alkenone/alkenoate composition responds to these physiological stresses.

There has been considerable interest in the possibility that high contents of the 37:4 MK in sediments might be an indicator of higher salinity conditions (Rosell-Melé 1998). The robustness of this proxy was questioned by Sikes and

Sicre (2002) based on alkenone distributions in 106 surface water and sediment trap samples from the Atlantic, Pacific, and Southern oceans. Of interest is their finding that $U_{37}^{K'}$ showed a correlation with salinity in the Atlantic, but not in other oceans. Recently, Chivall et al. (2014) showed that while salinity does have a direct effect on alkenone distributions, the effects of growth phase and species composition also have a marked impact complicating the use of alkenone distributions as a salinity proxy. They found that 37:4 was much more abundant in *C. lamellosa* (30–44%) than in *I. galbana* (4–12%). $U_{37}^{K'}$ values decreased slightly with salinity for *C. lamellosa* but were largely unaffected for *I. galbana*. The values decreased with incubation time in both species. The proportion of 37:4 increased in both species (0.16–0.20% per salinity unit), except during the stationary phase for *I. galbana*.

A number of studies have shown that the hydrogen isotope composition ($^2\text{H}/^1\text{H}$ or $\delta^2\text{H}$) of microalgal lipids increases systematically with salinity opening the way for development of lipid-based paleosalinity proxy. Sachs et al. (2016) showed that $\delta^2\text{H}$ values in *E. huxleyi* grown in chemostats increased by 1.6 ± 0.3 per unit ppt in eight individual alkenones and by 2.0 ± 0.1 per unit ppt in three individual fatty acids over the salinity range 20–42 ppt. Hydrogen isotope ratios of phytol and the sterol 24-methylcholesta-5,22E-dien-3 β -ol also increased with salinity, but the correlations were weaker.

Zheng et al. (2017) have examined various capillary columns for alkenone and alkenoate analysis and found that the Rtx-200 column (105 m \times 250 μm \times 0.25 μm film thickness) provides the best resolution allowing simultaneous analysis of alkenones and alkenoates and baseline resolution of closely eluting double bond positional isomers. They also used DMDS adducts to show that the double bond positions in two isomers of triunsaturated $\text{C}_{36:3}$ EKs in *Ruttnera lamellosa* isolated from a brackish lacustrine environment and the Group III marine strain *E. huxleyi* Van556 isolated from northeast Pacific, both cultured at 9 $^\circ\text{C}$, were $\Delta^{7,14,21}$ and $\Delta^{14,21,28}$ (measured from the carbonyl group). Group I haptophytes produce little alkenoates as shown by Braya S ϕ sample, whereas both the Group II Lake George *R. lamellosa* and Group III Van 556 *E. huxleyi* produce large amounts of alkenoates (C_{36}OMe and C_{36}OEt) (Longo et al. 2013, 2016). Group II haptophytes produce C_{38} EK, but not (or only trace amounts of) C_{38} MK, whereas both C_{38} EK and C_{38} MK are produced by Group I and III haptophytes (e.g., Conte et al. 1998; Nakamura et al. 2014; Longo et al. 2016).

6 Alkyl Diols

Long-chain *n*-alkyl diols (LCDs) of algal origin (Fig. 4) have been found in a wide range of marine and lacustrine environments (de Leeuw et al. 1981; Villanueva et al. 2014a; De Bar et al. 2016 and references therein). C_{30} – C_{32} alkyl diols with hydroxyl groups mainly at positions C-1 and C-15 with small amounts of the 1,13 isomers and a monounsaturated C_{32} 1,15-diol were first identified in acid hydrolyzed lipids from cultures of the marine eustigmatophyte *Nannochloropsis oculata*

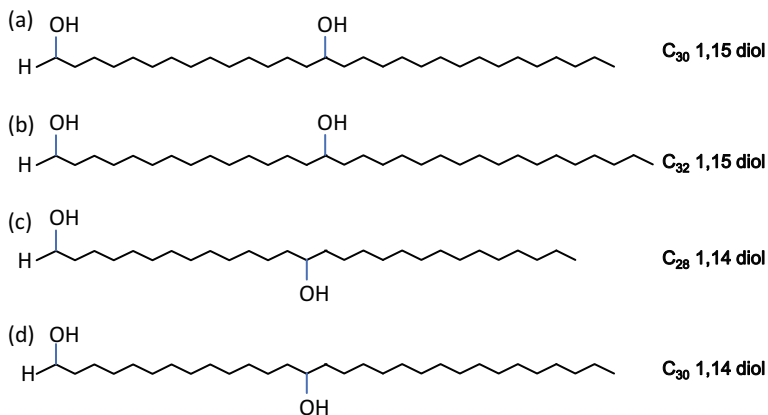


Fig. 4 Structures of some alkyl diols found in microalgae. (a) C_{30} 1,15- and C_{32} 1,15-diols found in eustigmatophytes; (c) C_{28} 1,14- and C_{30} 1,14-diols found in some diatoms

(Volkman et al. 1992). More recent work by Méjanelle et al. (2003) found saturated and monounsaturated C_{28} to C_{36} *n*-alkyl diols in *Nannochloropsis gaditana*. These occurred as a mixture of hydroxyl positional isomers with $\omega 16$ predominating in the C_{28} alkyl diols, $\omega 18$ among the C_{30} , C_{32} , C_{34} and C_{36} alkyl diols and $\omega 17$ for the odd chain alkyl diols. This species also contained C_{28} – C_{32} hydroxy ketones with a similar chain-length distribution to the alkyl diols suggesting a biosynthetic relationship between the two lipid classes. C_{28} – C_{32} LCDs have also been isolated from freshwater eustigmatophytes (Volkman et al. 1999a).

An additional algal source for alkyl diols was identified when Sinninghe Damsté et al. (2003) found C_{28} , $\text{C}_{28:1}$, C_{30} , and $\text{C}_{30:1}$ 1,14-LCDs in the rhizosolenid diatoms *Proboscia indica* and *Proboscia alata* (Fig. 4). Notably, *Proboscia* diatoms can contribute 20–35% of the total lipid flux in the Arabian Sea during the start of the upwelling season (Sinninghe Damsté et al. 2003) giving rise to the idea that these compounds could be used as upwelling indicators. However, this idea is challenged by the observation by Rampen et al. (2011) of saturated C_{28} , C_{30} , and C_{32} 1,14-LCDs in the marine heterokont alga *Apedinella radians* (Class Dictyochophyceae, order Pedinellales). *Apedinella* spp. occur globally and are particularly found in estuarine waters.

Compositional changes in LCDs with growth temperature have been reported by Rampen et al. (2014) for *N. gaditana*.

Long-chain alkyl diols occur in some freshwater microalgae such as species of *Ochromonas* (Mercer and Davies 1974, 1979). In both *O. danica* and *O. malhamensis*, the major alkyl diol is the C_{22} compound docosane-1,14-diol disulfate. *O. danica* also contained small amounts of the C_{24} tetracosane-1,15-diol disulfate and *O. malhamensis* contained some tetracosane-1,14-diol disulfate (Mercer and Davies, 1979). These chain lengths are much shorter than those commonly found in sediments, but the 1,14- and 1,15-dihydroxylation pattern is the same as that found in diatoms and *Nannochloropsis*, respectively.

Application of a 18S rRNA gene-based method has revealed the presence of both known and novel groups of Eustigmatophyceae in Lake Challa (Villanueva et al. 2014a). The maximum abundance of Eustigmatophyceae gene sequences coincided with maximum LCD abundance at 9 m water depth, suggesting an important role of eustigmatophytes as LCD-producers. Seasonal variation in LCD distributions suggested that successive LCD-producing blooms were due to different eustigmatophyte algae or changes in the LCDs produced by a unique algal population as environmental conditions changed.

7 Algaenan

A number of studies have now shown that an aliphatic, solvent-insoluble, cross-linked and chemically resistant biopolymeric material termed “algaenan” occurs in some species of microalgae (e.g., Tegelaar et al. 1989; Derenne et al. 1990; de Leeuw and Largeau, 1993; Gelin et al., 1999). It is a significant component of the outer cell wall in *B. braunii* (e.g., Berkaloﬀ et al. 1983; Templier et al. 1993; Derenne et al. 1989, 1990; Gatellier et al. 1993; Gelin et al. 1994); in other green algae including *Tetradron minimum*, *Scenedesmus communis*, and *Pediastrum boryanum* (e.g., Blokker et al., 1998b); in eustigmatophytes of the genus *Nannochloropsis* (Gelin et al. 1996, 1997a,b, 1999); and the dinoflagellate *Gymnodinium catenatum* (Gelin et al. 1999).

In *Nannochloropsis* species, LCAs, LCDs, and LCHFAs are thought to be bound together via ether or ester bonds to form algaenans (Gelin et al. 1996, 1997a, 1999; Volkman et al. 1998; Zhang and Volkman, 2017). A partial structure of the algaenan in *N. oculata* is shown in Fig. 5 (Gelin et al. 1996; Zhang and Volkman, 2017). Algaenans are thought to be highly resistant to degradation (Tegelaar et al. 1989; Volkman et al. 1998) and are likely to be present in the outer layers of the cell walls, forming a trilaminar structure (Gelin et al. 1999). Fourier transform infrared spectroscopy on the cell wall of *N. gaditana* confirmed the ether-linked aliphatic structures of algaenans and revealed also the presence of C=O bonds (Scholz et al. 2014), which likely correspond to ketone or carboxylic functional groups of long-chain keto-ols, LCHFAs, and dihydroxy fatty acids, respectively, which were previously reported to occur in *Nannochloropsis* spp. (Volkman et al. 1992; Gelin et al. 1997a; Versteegh et al. 1997).

Algaenans have also been described in several genera of Chlorophyta (Derenne et al. 1988, 1990; Gelin et al. 1997b; Blokker et al. 1998b; Allard and Templier 2001). Allard and Templier (2001) showed using flash pyrolysis with in situ methylation using tetramethylammonium hydroxide (TMAH) and alkaline hydrolysis that the high molecular weight lipids isolated from *Chlorella emersonii* and *Scenedesmus communis* are mainly composed of saturated *n*-C₂₆ and *n*-C₂₈ fatty acids and alcohols and of saturated *n*-C₃₀ and *n*-C₃₂ α,ω -diols and ω -hydroxy acids. In contrast, the high molecular weight lipids isolated from *T. minimum* are predominantly composed of long-chain fatty acids and ω -hydroxy acids.

Algaenan is found in the A, B, and L races of *Botryococcus* and is thought to have a similar structure based on an ether-linked highly aliphatic structure.

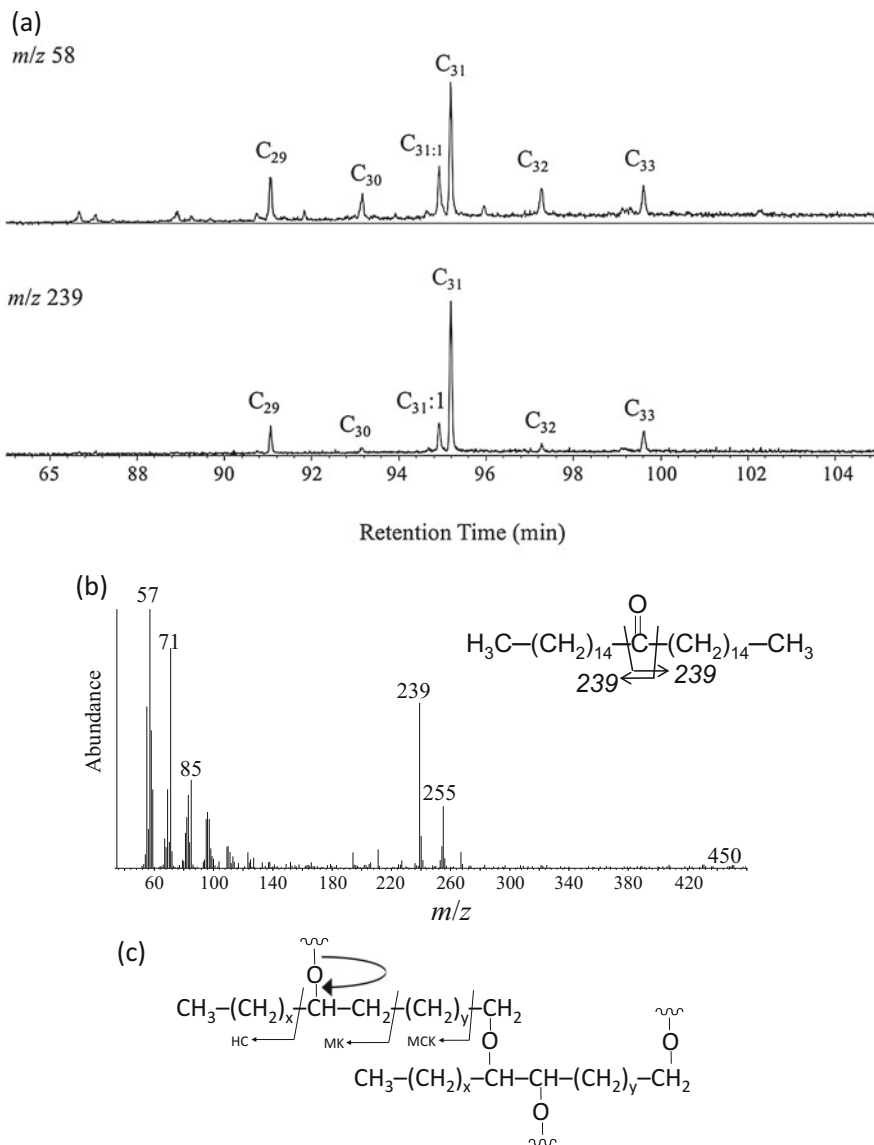


Fig. 5 (a) Mass fragmentograms showing distribution of mid-chain ketones from stepwise pyrolysis of the algaenan from *N. oculata* (after Zhang and Volkman 2017). Note that this species is now known as *N. oceanica*. (b) Mass spectrum of the major component showing cleavage at either side of the carbonyl group to produce the m/z 239 ion. (c) Structural element of the algaenan in *N. oceanica* (after Gelin et al. 1996) showing how a repeating C_{32} 1,17-diol can account for the major pyrolysis products (HC = alkenes; MK = methyl ketones, MCK = mid-chain ketones). For a C_{32} diol, $x + y = 28$, the major alkan-2-one is C_{17} (Zhang and Volkman 2017), so $x = 14$, and hence $y = 14$. The C_{31} *n*-alkan-16-one also has $x = 14$ and $y = 14$, so the basic repeating unit is the C_{32} alkyl-1,17-diol precursor

Bertheas et al. (1999) showed the presence of a high molecular weight poly-aldehyde in the L race and proposed that it is derived from the condensation-polymerization of a n -C₃₂ diunsaturated dialdehyde, involving an aldolization-dehydration mechanism similar to that in the A race. However, it differed by the multi-incorporation of 14,15-dihydroxylycopa-18-ene, derived from lycopadiene, by acetalization of ca. seven aldehyde functions out of ten. This study demonstrated that ether functions are not the major cross-linking groups in the algaenan of the L race, as had been previously proposed (Derenne et al. 1989; Gelin et al. 1994). The polymeric nature of the algaenan results from the formation of C=C bonds (conjugated to the formyl groups), during the condensation-polymerization reaction.

8 Sterols

Sterols are tetracyclic triterpenoids biosynthesized by all eukaryotic organisms although a few bacteria contain simple sterol distributions. A generalized structure with numbered carbon atoms is shown in Fig. 6 together with structures of some common algal sterols. The occurrence of sterols alkylated in the side-chain appears to be a diagnostic feature of eukaryote sterol biosynthesis (e.g., Volkman, 2016). In sediments, sterols are converted to sterenes and then steranes which thus provide a valuable biomarker for studying the first appearance of eukaryotes. Molecular clock calculations by Gold et al. (2017) show that simple sterol biosynthesis probably existed well before the diversification of living eukaryotes and predates the oldest detected sterane biomarkers in sediments deposited in the Barney Creek Formation about 1.64 Gyr ago (Brocks et al. 2005). This new work by Gold et al. (2017) implies that sterol biosynthesis is tied to the first widespread availability of molecular oxygen in the ocean-atmosphere system.

Microalgae display a wide range of structures reflecting differences in the sterol biosynthetic pathway used by different organisms (e.g., Volkman, 1986, 2003, 2016; Volkman et al. 1998; Nes, 2011; Villanueva et al. 2014b, Ahmed et al. 2015). Some algal classes show characteristic distributions, but in others a wide range of structures can be found either because the taxonomic grouping is polyphyletic or the different algae accumulate sterols produced at different stages in the biosynthetic pathway – perhaps due to evolutionary changes in some of the biosynthetic steps.

A comprehensive overview of the sterols in microalgae was recently published by Volkman (2016) so only the salient features will be discussed here. A sufficiently large number of species of green microalgae, diatoms, dinoflagellates, and haptophytes have been studied (over 100 species in the case of diatoms) that reasonable generalizations can be made about their typical sterol patterns.

Diatoms contain a surprising diversity of sterol distributions, and over 40 different sterols have been identified (Rampen et al. 2010). Common sterols include (22*E*)-24-methylcholesta-5,22-dien-3 β -ol (epi-brassicasterol since the C-24 stereochemistry is alpha; Fig. 6), 24-methylcholesta-5,24(28)-dien-3 β -ol (24-methylenecholesterol), and cholesterol (Fig. 6). A few diatom species display

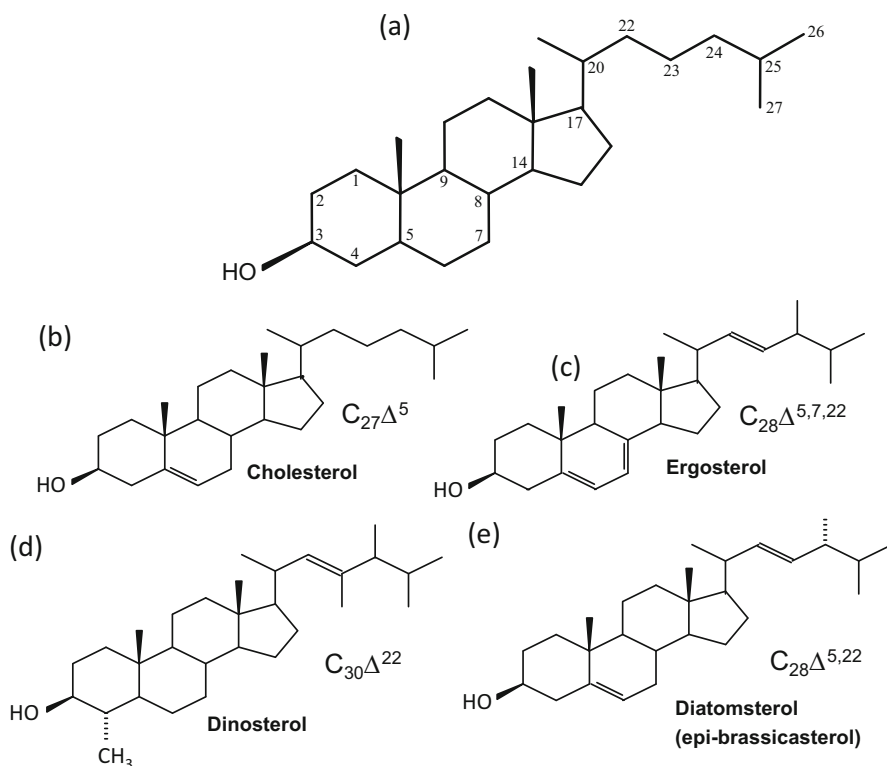


Fig. 6 (a) Basic sterol skeleton with numbering system and shorthand nomenclature as well as structures of some common sterols found in microalgae. Methyl groups can be found at positions C-4 (mainly dinoflagellates and rarely in some haptophytes and diatoms), C-24 (common), sometimes at C-23 (some diatoms and dinoflagellates), and rarely at C-26. Ethyl and propyl groups can also be found at position C-24. Double bonds in the ring system can be found at positions 5, 7, 8(9), and 8 (11); double bonds in the side chain typically occur at C-22, C-24(25), and C-24(28). The stereochemistry of the alkyl group at C-24 can be either α (typical of diatoms and haptophytes, as in (e)) or β (typical of some green microalgae and dinoflagellates); (b) structure of cholesterol which is found in many microalgae despite being considered a sterol characteristic of animals; (c) ergosterol found in yeasts and some green algae; (d) dinosterol found in some, but not all, dinoflagellates; (e) epi-brassicasterol (diatomsterol) with C-24 α stereochemistry for the methyl group as found in diatoms and haptophytes

distinctive distributions such as *Amphora* which contains high contents of the C_{29} sterol (22*E*)-24-ethylcholesta-5,22-dien-3 β -ol (stigmasterol). Belt et al. (2017) identified desmosterol (cholesta-5,24-dien-3 β -ol) as the major sterol in the sample from West Svalbard, containing >90% diatoms assigned as *R. setigera*. 4-Methylsterols are rare in diatoms, but a species of *Navicula* contains dinosterol or its isomer (Volkman et al. 1993). Indeed, sterols with a methyl group at C-23 in the side-chain (Fig. 6) are also surprisingly common in diatoms (Volkman et al. 1993; Volkman 2003; Rampen et al. 2009a, 2010) showing that this feature is not unique to dinoflagellate sterols. One of the more unusual findings is the identification of the

C₃₀ sterol gorgosterol (22,23-methylene-23,24-dimethylcholest-5-en-3 β -ol) in diatoms of the genus *Delphineus* (Rampen et al. 2009b); this sterol is more commonly found in some corals. *Delphineus* species also contain (22*E*)-24-methylcholesta-5,22-dien-3 β -ol and (22*E*)-cholesta-5,22-dien-3 β -ol, both often present in diatoms, and (22*E*)-23,24-dimethylcholesta-5,22-dien-3 β -ol.

Green microalgae (chlorophytes, prasinophytes, and trebouxiphytes) display a wide variety of compositions including some with simple distributions of sterols dominated by the C₂₉ sterol 24-ethylcholest-5-en-3 β -ol (sitosterol or more likely its 24(*S*)-epimer) more commonly associated with higher plants. In some chlorophytes, a predominance of Δ^7 -unsaturated sterols is found dominated by (22*E*)-24-methylcholesta-5,7,22-trien-3 β -ol (ergosterol; Fig. 6) (Patterson, 1969; Ahmed et al. 2015) which is commonly found in yeast. Some prasinophytes such as *Pyramimonas cordata* and *Pycnococcus provasolii* contain simple distributions of Δ^5 -sterols including 24-methylenecholesterol, 24-methylcholesterol (campesterol, also found in higher plants), and [24(28)*Z*]-24-ethylcholesta-5,24(28)-dien-3 β -ol (28-isofucosterol) (Volkman et al. 1994b). *Tetraselmis* spp. also contain high contents of 24-methylcholesterol (e.g., Ahmed et al. 2015). In marked contrast, *Pyramimonas grossii* contains a complex mixture of C₂₈ and C₂₉ sterols with Δ^7 , $\Delta^{5,7}$, and $\Delta^{5,7,9(11)}$ nuclear double bond systems (Patterson et al. 1992) and the freshwater *Scenedesmus quadricauda* contains only Δ^7 sterols including 24-methyl-5 α -cholest-7-en-3 β -ol, (22*E*)-24-ethyl-5 α -cholesta-7,22-dien-3 β -ol, and 24-ethyl-5 α -cholest-7-en-3 β -ol (Cranwell et al. 1990).

Many dinoflagellates contain mixtures of 4-methylsterols including the C₃₀ sterol (22*E*)-4 α ,23,24-trimethyl-5 α -cholest-22-en-3 β -ol (dinosterol; Fig. 6), as well as related 5 α (H)-stanols. It is important to recognize that not all dinoflagellates contain dinosterol (Volkman, 1986). A few genera contain unusual sterols such as *Amphidinium* and *Karenia* species which contain $\Delta^{8(14)}$ -unsaturated sterols (e.g., Leblond et al., 2011).

Haptophytes, in contrast, usually have simple sterol distributions of one to five compounds, often dominated by either cholesterol or (22*E*)-24-methylcholesta-5,22-dien-3 β -ol (as also found in diatoms). Moderate amounts of the C₂₉ sterols 24-ethylcholesterol and (22*E*)-24-ethylcholesta-5,22-dien-3 β -ol are found in several species (Conte et al. 1994). For example, the geochemically important coccolithophorids *E. huxleyi* and *G. oceanica* have simple sterol distributions dominated (> 90%) by (22*E*)-24-methylcholesta-5,22-dien-3 β -ol. Species of the genus *Pavlova* also contain 5 α (H)-stanols lacking a Δ^5 double bond and unusual dihydroxylated 4-methylsterols called pavlovols including 4 α ,24-dimethylcholestan-3 β ,4 β -diol (Volkman et al., 1997; Xu et al., 2008; Ahmed et al., 2015).

Compositional data for eustigmatophytes are rather limited. Volkman et al. (1999a) showed that three freshwater species contained simple distributions consisting predominantly of the C₂₉ sterol 24-ethylcholesterol (more typical of plants) with small amounts of cholesterol, 24-methylcholesterol, (22*E*)-24-ethylcholesta-5,22-dien-3 β -ol and isofucosterol. In contrast, marine species from the genus *Nannochloropsis* contain mainly cholesterol (>75%) together with small amounts of the C₂₉ sterols [24(28)*E*]-24-ethylcholesta-5,24(28)-dien-3 β -ol

(fucosterol) and [24(28)Z]-24-ethylcholesta-5,24(28)-dien-3 β -ol (isofucosterol) (Volkman et al. 1992; Patterson et al. 1994b). The sterol composition of *Nannochloropsis gaditana* is similar with a predominance of cholesterol and small amounts of 24-ethylcholesterol (Méjanelle et al. 2003) as also found in *N. salina*.

Only a few microalgal species from the Rhodophyta (red algae) have been examined and some contain unusual compositions (Volkman, 2016). For example, *Porphyridium cruentum* contains 24-methylcholesta-5,7,22-trien-3 β -ol (ergosterol) and cholesta-5,22-dien-3 β -ol, whereas other species of *Porphyridium* contain unusual 4-methyl Δ^8 -unsaturated sterols including 4 α -methyl-5 α -cholesta-8,22-dien-3 β -ol, 4 α ,24-dimethyl-5 α -cholesta-8,22-dien-3 β -ol, 4-methylcholest-8-en-3 β -ol, and 4,24-dimethylcholest-8-en-3 β -ol (Beastall et al. 1974).

9 Other Biochemical Constituents

In addition to lipids, microalgae contain a diverse range of other biochemicals making them useful substrates for nutritional feeds used in aquaculture, as health supplements, food additives, and a source of bioactives (e.g., Volkman and Brown, 2005; Gouveia et al. 2010; Shukla and Dhar, 2013; Stonik and Stonik, 2015; D'Alessandro and Antoniosi Filho, 2016). Some species also produce toxins which can cause food poisoning when people consume mollusks or fish that have accumulated the toxin. Microalgae are known for their variety of colors – and were initially classified on that basis – due to a wide range of chlorophylls and phaeopigments present in their cells. The distributions of these can be taxonomically distinct (e.g., Serive et al. 2017) and have been used to assign microalgal sources to organic matter in seawater and sediments (see review by Bianchi and Canuel, 2011). Microalgae contain abundant amino acids and sugars although abundances can vary with growth conditions (Volkman and Brown, 2005). They also contain several important vitamins (Volkman and Brown, 2005) including tocopherols (vitamin E) which after degradation can be an important source of isoprenoids in sediments (Goossens et al. 1984).

10 Research Needs

One of the recurring problems with algal lipid research is the use of poorly defined algal strains compounded by the fact that phycologists are now redefining the taxonomic position of many species as new information becomes available from molecular biology. There are examples in the early literature where the origins of a sample are unclear and the results can't be duplicated. The use of properly defined and curated unialgal strains, preferably grown under axenic conditions, is essential. DNA data are vital for correct identification and there is a growing interest in genes associated with lipid biosynthesis. There is also a need for careful attention to strain designation since it is now clear that there can be significant differences in lipid

composition between strains of the same species (e.g., Conte et al. 1994) and even of changes when a strain is cultured for long periods (e.g., Prahel et al. 2006).

As pointed out throughout the text, there are still many algal groups for which data are limited and additional species need to be analyzed. Unfortunately, this is often because only a limited number of species are held in culture collections and it is expensive to isolate, identify, and culture new species. Even where a reasonable number of species are available, there are still only a few cases, such as the diatoms, where more than 100 species have been analyzed for lipids. In the case of the haptophytes, there is a clear need for a comprehensive survey of alkenone producers that includes DNA typing to firmly establish which genera synthesize these compounds and to relate the data to the geological record of haptophytes. Identification of the genes involved in alkenone and alkenoate biosynthesis would also be valuable.

Given the many thousands of microalgal species, and difficulties in culturing many of them, more rapid methods for screening of novel lipids in microalgae are needed. Pyrolysis techniques have rarely been applied to algae, but recently Zhang and Volkman (2017) showed that stepwise pyrolysis could be used to provide structural information about the constituents of algaenan made by a marine eustigmatophyte (Fig. 5). The technique uses initial low pyrolysis temperatures which can yield distributions of lipids similar to those obtained by extraction, although some breakdown of labile compounds does of course occur. This technique does not require prior extraction of the cells and so could be used to rapidly screen algal biomass for novel components.

Most lipid studies of microalgae have used GC–MS with non-polar GC stationary phases. While these columns are useful for analyzing a wide range of lipids they lack selectivity and more targeted analyses (such as polar columns for polyunsaturated fatty acid esters) can be useful. New methods using different capillary GC columns have been developed for high resolution separation of alkenones and alkenoates (Zheng et al. 2017), which provides an indication of what can be achieved. GC–MS analysis is not well suited for highly polar or higher molecular weight lipids which are better studied using HPLC–MS. New methods are needed here in an analogous way to which better methods have been developed for GDGT analysis in archaea. Stranska-Zachariasova et al. (2016) have studied microalgae using a range of solvent extraction methods to fractionate lipid constituents. In their work, they examined compounds with a broad range of polarities using ultra-high-performance liquid chromatography coupled with high resolution tandem mass spectrometric detection (UHPLC–MS–MS). While this methodology was designed for bioactives, it could be modified to look for compounds of geochemical interest.

Culture studies that can elucidate the effects of environmental conditions on lipid compositions and isotope ($\delta^{13}\text{C}$, $\delta^2\text{H}$) values continue to provide much valuable data and should be expanded particularly for microalgal species which synthesize compounds being used as palaeoproxies for temperature, salinity, CO_2 , etc. Continuous cultures are preferred here since individual environmental parameters can be isolated, whereas in batch culture there is the added complication of varying growth stage and growth rate. Studies of natural populations of microalgae would also be

useful, even though it is difficult to obtain pure samples, since many algal species have not been cultured and few data are available for microalgae living under natural conditions. In favorable cases, flow cytometry or other concentrating methods can yield samples sufficiently pure for lipid analysis.

References

- Achitouv E, Metzger P, Rager M-N, Largeau C (2004) C₃₁–C₃₄ methylated squalenes from a Bolivian strain of *Botryococcus braunii*. *Phytochemistry* 65:3159–3165
- Ackman RG, Tocher CS, McLachlan J (1968) Marine phytoplankton fatty acids. *J Fish Res Bd Canada* 25:1603–1620
- Ahmed F, Zhou WX, Schenk PM (2015) *Pavlova lutheri* is a high-level producer of phytosterols. *Algal Res Biomass Biofuels Bioprods* 10:210–217
- Allard B, Templier J (2000) Comparison of neutral lipid profile of various trilaminar outer cell wall (TLS)-containing microalgae with emphasis on algaenan occurrence. *Phytochemistry* 54:369–380
- Allard B, Templier J (2001) High molecular weight lipids from the trilaminar outer wall (TLS)-containing microalgae *Chlorella emersonii*, *Scenedesmus communis* and *Tetraedron minimum*. *Phytochemistry* 57:459–467
- Allard WG, Belt ST, Massé G, Naumann R, Robert J-M, Rowland S (2001) Tetra-unsaturated sesterterpenoids (Haslenes) from *Haslea ostrearia* and related species. *Phytochemistry* 56:795–800
- Balzano S, Villanueva L, de Bar M, Sinninghe Damsté JS, Schouten S (2017) Impact of culturing conditions on the abundance and composition of long chain alkyl diols in species of the genus *Nannochloropsis*. *Org Geochem* 108:9–17
- Beastall GH, Tyndall AM, Rees HH, Goodwin TW (1974) Sterols in *Porphyridium* series. 4 α -Methyl-5 α -cholesta-8,22-dien-3 β -ol and 4 α ,24-dimethyl-5 α -cholesta-8,22-dien-3 β -ol: two novel sterols from *Porphyridium cruentum*. *Eur J Biochem* 41:301–309
- Belt ST, Cooke DA, Robert J-M, Rowland S (1996) Structural characterisation of widespread polyunsaturated isoprenoid biomarkers: a C₂₅ triene, tetraene and pentaene from the diatom *Haslea ostrearia* Simonsen. *Tetrahedron Lett* 37:4755–4758
- Belt ST, Allard G, Massé G, Robert J-M, Rowland S (2000a) Important sedimentary sesterterpenoids from the diatom *Pleurosigma intermedium*. *Chem Comm* 6:501–502
- Belt ST, Allard WG, Rintatalo J, Johns LA, van Duin ACT, Rowland SJ (2000b) Clay and acid catalysed isomerisation and cyclisation reactions of highly branched isoprenoid (HBI) alkenes: implications for sedimentary reactions and distributions. *Geochim Cosmochim Acta* 64:3337–3345
- Belt ST, Allard WG, Johns L, Konig WA, Massé G, Robert J-M, Rowland S (2001a) Variable stereochemistry in highly branched isoprenoids from diatoms. *Chirality* 13:415–419
- Belt ST, Allard WG, Massé G, Robert J-M, Rowland SJ (2001b) Structural characterisation of C₃₀ highly branched isoprenoid alkenes (rhizenes) in the marine diatom *Rhizosolenia setigera*. *Tetrahedron Lett* 42:5583–5585
- Belt ST, Massé G, Allard WG, Robert J-M, Rowland SJ (2001c) C₂₅ highly branched isoprenoid alkenes in planktonic diatoms of the *Pleurosigma* genus. *Org Geochem* 32:1271–1275
- Belt ST, Massé G, Allard WG, Robert J-M, Rowland SJ (2001d) Identification of a C₂₅ highly branched isoprenoid triene in the freshwater diatom *Navicula sclesvicensis*. *Org Geochem* 32:1169–1172
- Belt ST, Massé G, Allard WG, Robert JM, Rowland SJ (2002) Effects of auxosporulation on distributions of C₂₅ and C₃₀ isoprenoid alkenes in *Rhizosolenia setigera*. *Phytochemistry* 59:141–148

- Belt ST, Massé G, Allard WG, Robert JM, Rowland SJ (2003) Novel monocyclic sester- and triterpenoids from the marine diatom, *Rhizosolenia setigera*. *Tetrahedron Lett* 44:9103–9106
- Belt ST, Massé G, Rowland SJ, Poulin M, Michel C, LeBlanc B (2007) A novel chemical fossil of palaeo sea ice: IP₂₅. *Org Geochem* 38:16–27
- Belt ST, Müller J (2013) The Arctic sea ice biomarker IP₂₅: a review of current understanding, recommendations for future research and applications in palaeo sea ice reconstructions. *Quat Sci Rev* 79:9–25
- Belt ST, Smik L, Brown TA, Kim J-H, Rowland SJ, Allen CS, Gal J-K, Shin K-H, Lee JI, Taylor KWR (2016) Source identification and distribution reveals the potential of the geochemical Antarctic sea ice proxy IP_{SO}₂₅. *Nature Comms* 7:12655. <https://doi.org/10.1038/ncomms12655>
- Belt ST, Brown TA, Smik L, Tatarek A, Wiktor J, Stowasser G, Assmy P, Allen C, Husum K (2017) Identification of C₂₅ highly branched isoprenoid (HBI) alkenes in diatoms of the genus *Rhizosolenia* in polar and sub-polar marine phytoplankton. *Org Geochem* 110:65–72
- Bendif EM, Probert I, Schroeder DC, de Vargas C (2013) On the description of *Tisochrysis lutea* gen. nov. sp. nov. and *Isochrysis nuda* sp. nov. in the Isochrysidales, and the transfer of *Dicrateria* to the Prymnesiales (Haptophyta). *J Appl Phycol* 25:1763–1776
- Bengtson S, Sallstedt T, Belivanova V, Whitehouse M (2017) Three-dimensional preservation of cellular and subcellular structures suggests 1.6 billion-year-old crown-group red algae. *PLoS Biol.* <https://doi.org/10.1371/journal.pbio.2000735>
- Berkaloff C, Casadevall E, Largeau C, Metzger P, Peracca S, Virlet J (1983) Hydrocarbon formation in the green alga *Botryococcus braunii*. 3. The resistant polymer of the walls of the hydrocarbon-rich alga *Botryococcus braunii*. *Phytochemistry* 22:389–397
- Bertheas O, Metzger P, Largeau C (1999) A high molecular weight complex lipid, aliphatic polyaldehyde tetraterpenediol polyacetal from *Botryococcus braunii* (L. race). *Phytochemistry* 50:85–96
- Bianchi TS, Canuel EA (2011) Chemical biomarkers in aquatic ecosystems. Princeton University Press, Princeton
- Blokker P, Schouten S, van den Ende H, de Leeuw JW, Sinninghe Damsté JS (1998a) Cell wall-specific ω-hydroxy fatty acids in some freshwater green microalgae. *Phytochemistry* 49:691–695
- Blokker P, Schouten S, van den Ende H, de Leeuw JW, Hatcher PG, Sinninghe Damsté JS (1998b) Chemical structure of algaenans from the fresh water algae *Tetraedron minimum*, *Scenedesmus communis* and *Pediastrum boryanum*. *Org Geochem* 29:1453–1468
- Brassell SC, Eglinton G, Marlowe IT, Pflaumann U, Sarnthein M (1986) Molecular stratigraphy: a new tool for climatic assessment. *Nature* 320:129–133
- Brassell SC (2014) Climatic influences on the Paleogene evolution of alkenones. *Paleoceanography* 29:255–272
- Briggs DEG, Summons RE (2014) Ancient biomolecules: their origins, fossilization, and role in revealing the history of life. *BioEssays* 36:482–490
- Brocks JJ, Love GD, Summons RE, Knoll AH, Logan GA, Bowden SA (2005) Biomarker evidence for green and purple sulphur bacteria in a stratified Palaeoproterozoic sea. *Nature* 437:866–870
- Brown AC, Knights PA, Conway E (1969) Hydrocarbon content and its relationship to physiological state in the green alga *Botryococcus braunii*. *Phytochemistry* 8:543–547
- Brown TA, Belt ST, Tatarek A, Mundy CJ (2014) Source identification of the Arctic sea ice proxy IP₂₅. *Nature Comms* 5:Article 4197. <https://doi.org/10.1038/ncomms5197>
- Chivall D, M'Boule D, Sinke-Schoen D, Sinninghe Damsté JS, Schouten S, van der Meer MT (2014) Impact of salinity and growth phase on alkenone distributions in coastal haptophytes. *Org Geochem* 67:31–34
- Conte MH, Volkman JK, Eglinton G (1994) Lipid biomarkers of the Haptophyta. In: Green JC, Leadbeater BSC (eds) *The haptophyte algae*. Clarendon Press, Oxford, pp 351–377
- Conte MH, Thompson A, Eglinton G, Green JC (1995) Lipid biomarker diversity in the coccolithophorid *Emiliania huxleyi* (Prymnesiophyceae) and the related species *Gephyrocapsa oceanica*. *J Phycol* 31:272–282

- Conte MH, Thompson A, Lesley D, Harris RP (1998) Genetic and physiological influences on the alkenone/alkenoate versus growth temperature relationship in *Emiliania huxleyi* and *Gephyrocapsa oceanica*. *Geochim Cosmochim Acta* 62:51–68
- Coolen MJL, Muyzer G, Rijpstra WIC, Schouten S, Volkman JK, Sinninghe Damsté JS (2004) Combined DNA and lipid analyses of sediments reveal changes in Holocene haptophyte and diatom populations in an Antarctic Lake. *Earth Planet Sci Lett* 223:225–239
- Cranwell PA, Creighton ME, Jaworski GHM (1988) Lipids of four species of freshwater chrysophytes. *Phytochemistry* 27:1053–1059
- Cranwell PA, Jaworski GHM, Bickley HM (1990) Hydrocarbons, sterols, esters and fatty acids in six freshwater chlorophytes. *Phytochemistry* 29:145–151
- De Bar MW, Dorhout DJC, Hopmans EC, Rampen SW, Sinninghe Damsté JS, Schouten S (2016) Constraints on the application of long chain diol proxies in the Iberian Atlantic margin. *Org Geochem* 101:184–195
- D'Alessandro EB, Antoniosi Filho NR (2016) Concepts and studies on lipid and pigments of microalgae: a review. *Renew Sust Energ Rev* 58:832–841
- D'Andrea WJ, Huang Y (2005) Long chain alkenones in Greenland lake sediments: Low $\delta^{13}\text{C}$ values and exceptional abundance. *Org Geochem* 36:1234–1241
- D'Andrea WJ, Lage M, Martiny JBH, Laatsch AD, Amaral-Zettler LA, Sogin ML, Huang YS (2006) Alkenone producers inferred from well-preserved 18S rDNA in Greenland lake sediments. *J Geophys Res Biogeosci* 111(G3). <https://doi.org/10.1029/2005JG000121>
- D'Andrea WJ, Theroux S, Bradley RS, Huang XH (2016) Does phylogeny control U_{37}^K temperature sensitivity? Implications for lacustrine alkenone paleothermometry. *Geochim Cosmochim Acta* 175:168–180
- de Leeuw JW, Largeau C (1993) A review of macromolecular organic compounds that comprise living organisms and their role in kerogen, coal and petroleum formation. In: Engel MH, Macko SA (eds) *Organic geochemistry*. Plenum Press, New York, pp 23–72
- de Leeuw JW, van der Meer JW, Rijpstra WIC, Schenck PA (1980) On the occurrence and structural identification of long chain ketones and hydrocarbons in sediments. In: Douglas AG, Maxwell JR (eds) *Advances in organic geochemistry 1979*. Pergamon Press, Oxford, pp 211–217
- de Leeuw JW, Rijpstra WIC, Schenck PA (1981) The occurrence and identification of C_{30} , C_{31} and C_{32} alkan-1,15-diols and alkan-15-one-1-ols in Unit I and Unit II Black Sea sediments. *Geochim Cosmochim Acta* 45:2281–2285
- Derenne S, Largeau C, Casadevall E, Tegelaar E, de Leeuw JW (1988) Relationships between algal coals and resistant cell wall biopolymers of extant algae as revealed by Py-GC-MS. *Fuel Process Tech* 20:93–101
- Derenne S, Largeau C, Casadevall E, Berkaloﬀ C (1989) Occurrence of a resistant biopolymer in the L race of *Botryococcus braunii*. *Phytochemistry* 28:1137–1142
- Derenne S, Largeau C, Casadevall E, Sellier N (1990) Direct relationship between the resistant biopolymer and the tetraterpene hydrocarbon in the lycopadiene race of *Botryococcus braunii*. *Phytochemistry* 29:2187–2192
- Dodson VJ, Mouget JL, Dahmen JL, Leblond JD (2014) The long and short of it: temperature-dependent modifications of fatty acid chain length and unsaturation in the galactolipid profiles of the diatoms *Haslea ostrearia* and *Phaeodactylum tricorutum*. *Hydrobiologia* 727:95–107
- Dodson VJ, Leblond JD (2015) Now you see it, now you don't: differences in hydrocarbon production in the diatom *Phaeodactylum tricorutum* due to growth temperature. *J Appl Phycol* 27:1463–1472
- Dunstan GA, Volkman JK, Barrett SM, Garland CD (1993) Changes in the lipid composition and maximisation of the polyunsaturated fatty acid content of three microalgae grown in mass culture. *J Appl Phycol* 5:71–83
- Dunstan GA, Volkman JK, Barrett SM, Leroi JM, Jeffrey SW (1994) Essential polyunsaturated fatty acids from 14 species of diatom (Bacillariophyceae). *Phytochemistry* 35:155–161
- Epstein BL, D'Hondt S, Quinn JG, Zhang J, Hargraves PE (1998) An effect of dissolved nutrient concentrations on alkenone-based temperature estimates. *Paleoceanography* 13:122–126

- Epstein BL, D'Hondt S, Hargraves PE (2001) The possible metabolic role of C₃₇ alkenones in *Emiliania huxleyi*. *Org Geochem* 32:867–875
- Gatellier J-PLA, de Leeuw JW, Sinninghe Damsté JS, Derenne S, Largeau C, Metzger PA (1993) A comparative study of macromolecular substances of a coorongite and cell walls of the extant alga *Botryococcus braunii*. *Geochim Cosmochim Acta* 57:2053–2068
- Gelin F, de Leeuw JW, Sinninghe Damsté JS, Derenne S, Largeau C, Metzger P (1994) The similarity of chemical structures of soluble aliphatic polyaldehyde and insoluble algaenan in the green microalga *Botryococcus braunii* race A as revealed by analytical pyrolysis. *Org Geochem* 21:423–435
- Gelin F, Boogers I, Noordeloos AAM, Sinninghe Damsté JS, Hatcher PG, de Leeuw JW (1996) Novel, resistant microalgal polyethers: an important sink of organic carbon in the marine environment? *Geochim Cosmochim Acta* 60:1275–1280
- Gelin F, Volkman JK, de Leeuw JW, Sinninghe Damsté JS (1997a) Mid-chain hydroxy long-chain fatty acids in microalgae from the genus *Nannochloropsis*. *Phytochemistry* 45: 641–646
- Gelin F, Boogers I, Noordeloos AAM, Sinninghe Damsté JS, Riegman R, de Leeuw JW (1997b) Resistant biomacromolecules in marine microalgae of the classes Eustigmatophyceae and Chlorophyceae: geochemical implications. *Org Geochem* 26:659–675
- Gelin F, Volkman JK, Largeau C, Derenne S, Sinninghe Damsté JS, de Leeuw JW (1999) Distribution of aliphatic, non-hydrolysable biopolymers in marine microalgae. *Org Geochem* 30:147–159
- Gelpi E, Schneider H, Mann J, Oró J (1970) Hydrocarbons of geochemical significance in microscopic algae. *Phytochemistry* 9:603–612
- Gold DA, Caron A, Fournier GP, Summons RE (2017) Paleoproterozoic sterol biosynthesis and the rise of oxygen. *Nature*. <https://doi.org/10.1038/nature21412>
- Goossens H, de Leeuw JW, Schenck PA, Brassell SC (1984) Tocopherols as likely precursors of pristane in ancient sediments and crude oils. *Nature* 312:440–442
- Gouveia L, Marques AE, Sousa JM, Moura P, Bandarra NM (2010) Microalgae – source of natural bioactive molecules as functional ingredients. *Food Sci Technol Bull Funct Foods* 7:21–37
- Grossi V, Raphel D, Aubert C, Rontani J-F (2000) The effect of growth temperature on the long-chain alkenes composition in the marine coccolithophorid *Emiliania huxleyi*. *Phytochemistry* 54:393–399
- Grossi V, Beker B, Geenevasen JAJ, Schouten S, Raphel D, Fontaine M-F, Sinninghe Damsté JS (2004) C₂₅ highly branched isoprenoid alkenes from the marine benthic diatom *Pleurosigma strigosum*. *Phytochemistry* 65:3049–3055
- He J, Zhao MX, Li L, Wang H, Wang PX (2008) Biomarker evidence of relatively stable community structure in the northern South China Sea during the last glacial and Holocene. *Terr Atmos Ocean Sci* 19:377–387
- Ho SL, Naafs BDA, Lamy F (2013) Alkenone paleothermometry based on the haptophyte algae. In: Elias SA (ed) *The Encyclopedia of quaternary science*. Elsevier, Amsterdam, pp 755–764
- Huang Z, Poulter CD (1989) Tetramethylsqualene, a triterpene from *Botryococcus braunii* var Showa. *Phytochemistry* 28:1467–1470
- Jeffrey SW, Brown MR, Volkman JK (1994) Haptophytes as feedstocks in mariculture. In: Green JC, Leadbeater BSC (eds) *The haptophyte algae*, Systematics Association special volume no. 51. Clarendon Press, Oxford
- Jia J, Han DX, Gerken HG, Li YT, Sommerfeld M, Hu Q, Xu J (2015) Molecular mechanisms for photosynthetic carbon partitioning into storage neutral lipids in *Nannochloropsis oceanica* under nitrogen-depletion conditions. *Algal Res Biomass Biofuels Bioprod* 7:66–77
- Kaiser J, Belt ST, Tomczak M, Brown TA, Wasmund N, Arz HW (2016) C₂₅ highly branched isoprenoid alkenes in the Baltic Sea produced by the marine planktonic diatom *Pseudosolenia calcar-avis*. *Org Geochem* 93:51–58
- Kawachi M, Tanoi T, Demura M, Kaya K, Watanabe MM (2012) Relationship between hydrocarbons and molecular phylogeny of *Botryococcus braunii*. *Algal Res* 1:114–119

- Khozin-Goldberg I (2016) Lipid metabolism in microalgae. In: Borowitzka M, Beardall J, Raven JA (eds) *The physiology of microalgae*, Developments in applied phycology series 6. Springer, Cham, pp 413–484
- Lang I, Hodac L, Friedl T, Feussner I (2011) Fatty acid profiles and their distribution patterns in microalgae: a comprehensive analysis of more than 2000 strains from the SAG culture collection. *BMC Plant Biol* 11:124. <https://doi.org/10.1186/1471-2229-11-124>
- Leblond JD, Roche SA, Porter NM, Howard JC, Dunlap NK (2011) Sterol biosynthesis in the harmful marine dinoflagellate, *Karenia brevis*: identification of biosynthetic intermediates produced during exposure to the fungicide fenpropidine. *Phycol Res* 59:54–63
- Lee RF, Loeblich AR III (1971) Distribution of 21:6 hydrocarbon and its relationship to 22:6 fatty acid in algae. *Phytochemistry* 10:593–602
- Li YR, Ye MW, Zhang RT, Xu JL, Zhou CX, Yan XJ (2016) Lipid compositions in diatom *Conticribra weissflogii* under static and aerated culture conditions. *Phycol Res* 64:281–290
- Lipp JS, Hinrichs K-U (2009) Structural diversity and fate of intact polar lipids in marine sediments. *Geochim Cosmochim Acta* 73:6816–6833
- Longo WM, Dillon JT, Tarozo R, Salacup JM, Huang Y (2013) Unprecedented separation of long chain alkenones from gas chromatography with a poly(trifluoropropylmethylsiloxane) stationary phase. *Org Geochem* 65:94–102
- Longo WM, Theroux S, Giblin AE, Zheng YS, Dillon JT, Huang YS (2016) Temperature calibration and phylogenetically distinct distributions for freshwater alkenones: evidence from northern Alaskan lakes. *Geochim Cosmochim Acta* 180:177–196
- Mansour MP, Volkman JK, Holdsworth DG, Jackson AE, Blackburn SI (1999) Very-long-chain (C₂₈) highly unsaturated fatty acids in marine dinoflagellates. *Phytochemistry* 50:541–548
- Marlowe IT, Green JC, Neal AC, Brassell SC, Eglinton G, Course PA (1984a) Long chain (*n*-C₃₇–C₃₉) alkenones in the Prymnesiophyceae. Distribution of alkenones and other lipids and their taxonomic significance. *Br Phycol J* 19:203–216
- Marlowe IT, Brassell SC, Eglinton G, Green JC (1984b) Long chain unsaturated ketones and esters in living algae and marine sediments. *Org Geochem* 6:135–141
- Martinez-Roldan AJ, Perales-Vela HV, Canizares-Villanueva RO, Torzillo G (2014) Physiological response of *Nannochloropsis* sp. to saline stress in laboratory batch cultures. *J Appl Phycol* 26:115–121
- Massé G, Belt ST, Rowland SJ (2004a) Biosynthesis of unusual monocyclic alkenes by the diatom *Rhizosolenia setigera* (Brightwell). *Phytochemistry* 65:1101–1106
- Massé G, Belt ST, Rowland SJ, Rohmer M (2004b) Isoprenoid biosynthesis in the diatoms *Rhizosolenia setigera* (Brightwell) and *Haslea ostrearia* (Simonsen). *Proc Nat Acad Sci USA* 101:4413–4418
- Matsumoto GI, Nagashima H (1984) Occurrence of 3-hydroxy acids in microalgae and cyanobacteria and their geochemical significance. *Geochim Cosmochim Acta* 48:1683–1687
- Matsumoto GI, Shioya M, Nagashima H (1984) Occurrence of 2-hydroxy acids in microalgae. *Phytochemistry* 23:1421–1423
- Méjanelle L, Sanchez-Gargallo A, Bentaleb I, Grimalt JO (2003) Long chain *n*-alkyl diols, hydroxy ketones and sterols in a marine eustigmatophyte, *Nannochloropsis gaditana*, and in *Brachionus plicatilis* feeding on the algae. *Org Geochem* 34:527–538
- Mercer EI, Davies CL (1974) Chlorosulfolipids of *Tribonema aequale*. *Phytochemistry* 13:1607–1610
- Mercer EI, Davies CL (1979) Distribution of chlorosulfolipids in algae. *Phytochemistry* 18:457–462
- Metzger P, Casadevall E, Pouet MJ, Pouet Y (1985) Structures of some botryococenes: branched hydrocarbons from the B-race of the green alga *Botryococcus braunii*. *Phytochemistry* 24:2995–3002
- Metzger P, Casadevall E (1987) Lycopadiene, a tetraterpenoid hydrocarbon from new strains of the green alga *Botryococcus braunii*. *Tetrahedron Lett* 28:3931–3934

- Metzger P, Allard B, Casadevall E, Berkaloff C, Cout A (1990) Structure and chemistry of a new race of *Botryococcus braunii* (Chlorophyceae) that produces lycopadiene, a tetraterpenoid hydrocarbon. *J Phycol* 26:258–266
- Metzger P, Largeau C (2005) *Botryococcus braunii*: a rich source for hydrocarbons and related ether lipids. *Appl Microbiol Biotechnol* 66:486–496
- Mitra M, Patidar SK, George B, Shaha F, Mishra SA (2015) A euryhaline *Nannochloropsis gaditana* with potential for nutraceutical (EPA) and biodiesel production. *Algal Res Biomass Biofuels Bioprod* 8:161–167
- Nagashima H, Matsumoto GI, Fukuda I (1986) Hydrocarbons and fatty acids in two strains of the hot spring alga *Cyanidium caldarium*. *Phytochemistry* 25:2339–2341
- Nakamura H, Sawada K, Araie H, Suzuki I, Shiraiwa Y (2014) Long chain alkenes, alkenones and alkenoates produced by the haptophyte alga *Chrysothila lamellosa* CCMP1307 isolated from a salt marsh. *Org Geochem* 66:90–97
- Nakamura H, Sawada K, Araie H, Suzuki I, Shiraiwa Y (2015) *n*-Nonacosadienes from the marine haptophytes *Emiliania huxleyi* and *Gephyrocapsa oceanica*. *Phytochemistry* 111:107–113
- Nakamura H, Sawada K, Araie H, Shiratori T, Ishida K-I, Suzuki I, Shiraiwa Y (2016) Composition of long chain alkenones and alkenoates as a function of growth temperature in marine haptophyte *Tisochrysis lutea*. *Org Geochem* 99:78–89
- Nes WD (2011) Biosynthesis of cholesterol and other sterols. *Chem Rev* 111:6423–6451
- Nichols PD, Volkman JK, Palmisano AC, Smith GA, White DC (1988) Occurrence of an isoprenoid C₂₅ diunsaturated alkene and high neutral lipid content in Antarctic sea-ice diatom communities. *J Phycol* 24:90–96
- Olofsson M, Lamela T, Nilsson E, Berge JP, Del Pino V, Uronen P, Legrand C (2012) Seasonal variation of lipids and fatty acids of the microalgae *Nannochloropsis oculata* grown in outdoor large-scale photobioreactors. *Energies* 5:1577–1592
- Olofsson M, Lamela T, Nilsson E, Berge JP, Del Pino V, Uronen P, Legrand C (2014) Combined effects of nitrogen concentration and seasonal changes on the production of lipids in *Nannochloropsis oculata*. *Mar Drugs* 12:1891–1910
- Pal D, Khozin-Goldberg I, Cohen Z, Boussiba S (2011) The effect of light, salinity, and nitrogen availability on lipid production by *Nannochloropsis* sp. *Appl Microbiol Biotechnol* 90:1429–1441
- Pan H, Culp RA, Sun MY (2017) Influence of physiological states of *Emiliania huxleyi* cells on their lipids and associated molecular isotopic compositions during microbial degradation. *J Exp Mar Biol Ecol* 488:1–9
- Patterson GW (1969) Sterols of *Chlorella*. III. Species containing ergosterol. *Comp Biochem Physiol* 31:391–394
- Patterson GW, Gladu PK, Wikfors GH, Lusby WR (1992) Unusual tetraene sterols in some phytoplankton. *Lipids* 27:154–156
- Patterson GW, Tsitsa-Tzardis E, Wikfors GH, Gladu PK, Chitwood DJ, Harrison D (1994a) Sterols and alkenones of *Isochrysis*. *Phytochemistry* 35:1233–1236
- Patterson GW, Tsitsa-Tzardis E, Wikfors GH, Ghosh P, Smith BC, Gladu PK (1994b) Sterols of eustigmatophytes. *Lipids* 29:661–664
- Pedro Canavate J, Armada I, Luis Rios J, Hachero-Cruzado I (2016) Exploring occurrence and molecular diversity of betaine lipids across taxonomy of marine microalgae. *Phytochemistry* 124:68–78
- Pelusi A, Hanawa Y, Araie H, Suzuki I, Giordano M, Shiraiwa Y (2016) Rapid detection and quantification of haptophyte alkenones by Fourier transform infrared spectroscopy (FTIR). *Algal Res Biomass Biofuels Bioprod* 19:48–56
- Poulin M, Massé G, Belt ST, Delavault P, Rousseau F, Robert JM, Rowland SJ (2004) Morphological, biochemical and molecular evidence for the transfer of *Gyrosigma nipkowii* Meister to the genus *Haslea* (Bacillariophyta). *Eur J Phycol* 39:181–195
- Prahl FG, Wakeham SG (1987) Calibration of unsaturation patterns in long-chain ketone compositions for palaeotemperature assessment. *Nature* 330:367–369

- Prahl FG, Muehlhausen LA, Zahnle DL (1988) Further evaluation of long-chain alkenones as indicators of paleoceanographic conditions. *Geochim Cosmochim Acta* 52:2303–2310
- Prahl FG, Wolfe GV, Sparrow MA (2003) Physiological impacts on alkenone paleothermometry. *Paleoceanography* 18(2), art. no.-1025. <https://doi.org/10.1029/2002PA000803>
- Prahl FG, Rontani J-F, Volkman JK, Sparrow MA, Royer IM (2006) Unusual C₃₅ and C₃₆ alkenones in a paleoceanographic benchmark strain of *Emiliania huxleyi*. *Geochim Cosmochim Acta* 70:2856–2867
- Rampen SW, Schouten S, Hopmans EC, Abbas B, Noorderloos AAM, Geenevasen JAJ, Moldowan JM, Denisevich P, Sinninghe Damsté JS (2009a) Occurrence and biomarker potential of 23-methyl steroids in diatoms and sediments. *Org Geochem* 40:219–228
- Rampen SW, Volkman JK, Hur SB, Abbas BA, Schouten S, Jameson ID, Holdsworth DG, Bae JH, Sinninghe Damsté JS (2009b) Occurrence of gorgosterol in diatoms of the genus *Delphineis*. *Org Geochem* 40:144–147
- Rampen SW, Abbas BA, Schouten S, Sinninghe Damsté JS (2010) A comprehensive study of sterols in marine diatoms (Bacillariophyta): implications for their use as tracers for diatom productivity. *Limnol Oceanogr* 55:91–105
- Rampen SW, Schouten S, Sinninghe Damsté JS (2011) Occurrence of long chain 1,14-diols in *Apedinella radians*. *Org Geochem* 42:572–574
- Rampen SW, Datema M, Rodrigo-Gamiz M, Schouten S, Reichart G-J, Sinninghe Damsté JS (2014) Sources and proxy potential of longchain alkyl diols in lacustrine environments. *Geochim Cosmochim Acta* 144:59–71
- Rechka JA, Maxwell JR (1988) Unusual long chain ketones of algal origin. *Tetrahedron Lett* 29:2599–2600
- Rezanka T, Lukaysky J, Nedbalova L, Sigler K (2017) Lipidomic profile in three species of dinoflagellates (*Amphidinium carterae*, *Cystodinium* sp., and *Peridinium aciculiferum*) containing very long chain polyunsaturated fatty acids. *Phytochemistry* 139:88–97
- Rieley G, Teece MA, Peakman TM, Raven AM, Greene KJ, Clarke TP, Murray M, Leftley JW, Campbell CN, Harris RP, Parkes RJ, Maxwell JR (1998) Long-chain alkenes of the haptophytes *Isochrysis galbana* and *Emiliania huxleyi*. *Lipids* 33:617–625
- Rontani J-F, Marchand D, Volkman JK (2001) NaBH₄ reduction of alkenones to the corresponding alkenols: a useful tool for their characterisation in natural samples. *Org Geochem* 32:1329–1341
- Rontani J-F, Beker B, Volkman JK (2004) Long-chain alkenones and related compounds in the benthic haptophyte *Chrysothila lamellosa* Anand HAP 17. *Phytochemistry* 65:117–126
- Rontani J-F, Prahl FG, Volkman JK (2006a) Characterization of unusual alkenones and alkyl alkenoates by electron ionization gas chromatography/mass spectrometry. *Rapid Comm Mass Spectrom* 20:583–588
- Rontani J-F, Prahl FG, Volkman JK (2006b) Re-examination of the double bond positions of alkenones and derivatives: biosynthetic implications. *J Phycol* 42:800–813
- Rontani J-F, Harji R, Guasco S, Prahl FG, Volkman JK, Bhosle NB, Bonin P (2008) Degradation of alkenones by aerobic heterotrophic bacteria: selective or not? *Org Geochem* 39:34–51
- Rosell-Melé A (1998) Interhemispheric appraisal of the value of alkenone indices as temperature and salinity proxies in high-latitude locations. *Paleoceanography* 13:694–703
- Rowland SJ, Robson JN (1990) The widespread occurrence of highly branched acyclic C₂₀, C₂₅ and C₃₀ hydrocarbons in recent sediments and biota – a review. *Mar Env Res* 30:191–216
- Rowland SJ, Belt ST, Cooke DA, Hird SJ, Neeley S, Robert J-M (1995) Structural characterisation of saturated through heptaunsaturated highly branched isoprenoids. In: Grimalt J, Dorronsoro C (eds) *Organic geochemistry: developments and applications to energy, climate, environment and human history*. A.I.G.O.A. Donostia-San Sebastian, Spain, pp 580–582
- Rowland SJ, Allard WG, Belt ST, Massé G, Robert J-M, Blackburn S, Frampton D, Revill AT, Volkman JK (2001) Factors influencing the distributions of polyunsaturated terpenoids in the diatom, *Rhizosolenia setigera*. *Phytochemistry* 58:717–728
- Sachs JP, Maloney AE, Gregersen J, Paschall C (2016) Effect of salinity on ²H/¹H fractionation in lipids from continuous cultures of the coccolithophorid *Emiliania huxleyi*. *Geochim Cosmochim Acta* 189:96–109

- Sanz PC, Smik L, Belt ST (2016) On the stability of various highly branched isoprenoid (HBI) lipids in stored sediments and sediment extracts. *Org Geochem* 97:74–77
- Scholz MJ, Weiss TL, Jinkerson RE, Jing J, Roth R, Goodenough U, Posewitz MC, Gerken HG (2014) Ultrastructure and composition of the *Nannochloropsis gaditana* cell wall. *Eukaryot Cell* 13:1450–1464
- Schouten S, Klein Breteler WCM, Blokker P, Rijpstra WIC, Grice K, Baas M, Sinninghe Damsté JS (1998) Biosynthetic effects on the stable carbon isotopic compositions of algal lipids: implications for deciphering the carbon isotopic biomarker record. *Geochim Cosmochim Acta* 62:1397–1406
- Serive B, Nicolau E, Bérard JB, Kaas R, Pasquet V, Picot L, Cadoret JP (2017) Community analysis of pigment patterns from 37 microalgae strains reveals new carotenoids and porphyrins characteristic of distinct strains and taxonomic groups. *PLoS One* 12(2). <https://doi.org/10.1371/journal.pone.0171872>
- Shiratake T, Sato A, Minoda A, Tsuzuki M, Sato N (2013) Air-drying of cells, the novel conditions for stimulated synthesis of triacylglycerol in a green alga, *Chlorella kessleri*. *PLoS One* 8(11). <https://doi.org/10.1371/journal.pone.0079630>
- Shukla M, Dhar DW (2013) Biotechnological potentials of microalgae: past and present scenario. *Vegetos* 26:229–237
- Sikes EL, Volkman JK (1993) Calibration of alkenone unsaturation ratios ($U_{37}^{K'}$) for paleotemperature estimation in cold polar waters. *Geochim Cosmochim Acta* 57:1883–1889
- Sikes EL, Sicre MA (2002) Relationship of the tetra-unsaturated C_{37} alkenone to salinity and temperature: implications for paleoproxy applications. *Geochem Geophys Geosyst* 3:Article 1063. <https://doi.org/10.1029/2002GC000345>
- Sinninghe Damsté JS, Rijpstra WIC, Schouten S, Peletier H, van der Maarel MJEC, Gieskes WWC (1999a) A C_{25} highly branched isoprenoid alkene and C_{25} and C_{27} *n*-polyenes in the marine diatom *Rhizosolenia setigera*. *Org Geochem* 30:95–100
- Sinninghe Damsté JS, Schouten S, Rijpstra WIC, Hopmans EC, Peletier H, Gieskes WWC, Geenevasen JAJ (1999b) Structural identification of the C_{25} highly branched isoprenoid pentene in the marine diatom *Rhizosolenia setigera*. *Org Geochem* 30:1581–1583
- Sinninghe Damsté JS, Rampen S, Rijpstra WIC, Abbas B, Muyzer G, Schouten S (2003) A diatomaceous origin for long-chain diols and mid-chain hydroxy methyl alkanooates widely occurring in Quaternary marine sediments: indicators for high-nutrient conditions. *Geochim Cosmochim Acta* 67:1339–1348
- Sinninghe Damsté JS, Muyzer G, Abbas B, Rampen SW, Massé G, Allard WG, Belt ST, Robert JM, Rowland SJ, Moldowan JM, Barbanti SM, Fago FJ, Denisevich P, Dahl J, Trindade LAF, Schouten S (2004) The rise of the rhizosolenid diatoms. *Science* 304:584–587
- Smik L, Belt ST (2017) Distributions of the Arctic sea ice biomarker proxy IP_{25} and two phytoplanktonic biomarkers in surface sediments from West Svalbard. *Org Geochem* 105:39–41
- Sorigué D, Légeret B, Cuiné S, Morales P, Mirabella B, Guédeney G, Li-Beisson Y, Jetter R, Peltier G, Beisson F (2016) Microalgae synthesize hydrocarbons from long-chain fatty acids via a light-dependent pathway. *Plant Physiol* 171:2393–2405
- Stonik V, Stonik I (2015) Low-molecular-weight metabolites from diatoms: structures, biological roles and biosynthesis. *Mar Drugs* 13:3672–3709
- Stranska-Zachariasova M, Kastanek P, Dzuman Z, Rubert J, Godula M, Hajslova J (2016) Bioprospecting of microalgae: proper extraction followed by high performance liquid chromatographic-high resolution mass spectrometric fingerprinting as key tools for successful metabolome characterization. *J Chrom B Analyt Technol Biomed Life Sci* 1015:22–33
- Tegelaar EW, de Leeuw JW, Derenne S, Largeau CA (1989) A reappraisal of kerogen formation. *Geochim Cosmochim Acta* 53:3103–3106
- Templier J, Diesendorf C, Largeau C, Casadevall E (1992) Metabolism of normal-alkadienes in the A Race of *Botryococcus braunii*. *Phytochemistry* 31:113–120
- Templier J, Largeau C, Casadevall E (1993) Variations in external and internal lipids associated with inhibition of the resistant biopolymer from the a race of *Botryococcus braunii*. *Phytochemistry* 33:1079–1086

- Theroux S, D'Andrea WJ, Toney J, Amaral-Zettler L, Huang Y (2010) Phylogenetic diversity and evolutionary relatedness of alkenone-producing haptophyte algae in lakes: implications for continental paleotemperature reconstructions. *Earth Planet Sci Lett* 300:311–320
- Theroux S, Toney J, Amaral-Zettler L, Huang Y (2013) Production and temperature sensitivity of long chain alkenones in the cultured haptophyte *Pseudoisochrysis paradoxa*. *Org Geochem* 62:68–73
- Toney JL, Theroux S, Andersen RA, Coleman A, Amaral-Zettler L, Huang YS (2012) Culturing of the first 37:4 predominant lacustrine haptophyte: geochemical, biochemical, and genetic implications. *Geochim Cosmochim Acta* 78:51–64
- Versteegh GJM, Bosch HJ, de Leeuw JW (1997) Potential palaeoenvironmental information of C₂₄ to C₃₆ mid-chain diols, keto-ols and mid-chain hydroxy fatty acids: a critical review. *Org Geochem* 27:1–13
- Versteegh GJM, Riegman R, de Leeuw JW, Jansen JHF (2001) U₃₇^{K'} values for *Isochrysis galbana* as a function of culture temperature, light intensity and nutrient concentrations. *Org Geochem* 32:785–794
- Villanueva L, Besseling M, Rodrigo-Gamiz M, Rampen SW, Verschuren D, Sinninghe Damsté JS (2014a) Potential biological sources of long chain alkyl diols in a lacustrine system. *Org Geochem* 68:27–30
- Villanueva L, Rijpstra WIC, Schouten S, Sinninghe Damsté JS (2014b) Genetic biomarkers of the sterol-biosynthetic pathway in microalgae. *Env Microbiol Rep* 6:35–44
- Volkman JK, Johns RB (1977) The geochemical significance of positional isomers of unsaturated fatty acids from an intertidal zone sediment. *Nature* 267:693–694
- Volkman JK, Eglinton G, Corner EDS, Sargent JR (1980a) Novel unsaturated straight-chain C₃₇–C₃₉ methyl and ethyl ketones in marine sediments and a coccolithophorid *Emiliana huxleyi*. In: Douglas AG, Maxwell JR (eds) *Advances in organic geochemistry 1979*. Pergamon Press, Oxford, pp 219–227
- Volkman JK, Eglinton G, Corner EDS, Forsberg TEV (1980b) Long chain alkenes and alkenones in the marine coccolithophorid *Emiliana huxleyi*. *Phytochemistry* 19:2619–2622
- Volkman JK (1986) A review of sterol markers for marine and terrigenous organic matter. *Org Geochem* 9:83–99
- Volkman JK, Burton HR, Everitt DA, Allen DI (1988) Pigment and lipid compositions of algal and bacterial communities in Ace Lake, Vestfold Hills, Antarctica. *Hydrobiologia* 165:41–57
- Volkman JK, Barrett SM, Dunstan GA, Jeffrey SW (1992) C₃₀–C₃₂ alkyl diols and unsaturated alcohols in microalgae of the class Eustigmatophyceae. *Org Geochem* 18:131–138
- Volkman JK, Barrett SM, Dunstan GA, Jeffrey SW (1993) Geochemical significance of the occurrence of dinosterol and other 4-methyl sterols in a marine diatom. *Org Geochem* 20:7–15
- Volkman JK, Barrett SM, Dunstan GA (1994a) C₂₅ and C₃₀ highly branched isoprenoid alkenes in laboratory cultures of two marine diatoms. *Org Geochem* 21:407–413
- Volkman JK, Barrett SM, Dunstan GA, Jeffrey SW (1994b) Sterol biomarkers for microalgae from the green algal class Prasinophyceae. *Org Geochem* 21:1211–1218
- Volkman JK, Barrett SM, Blackburn SI, Sikes EL (1995) Alkenones in *Gephyrocapsa oceanica*: implications for studies of paleoclimate. *Geochim Cosmochim Acta* 59:513–520
- Volkman JK, Farmer CL, Barrett SM, Sikes EL (1997) Unusual dihydroxysterols as chemotaxonomic markers for microalgae from the order Pavlovaales (Haptophyceae). *J Phycol* 33:1016–1023
- Volkman JK, Barrett SM, Blackburn SI, Mansour MP, Sikes EL, Gelin F (1998) Microalgal biomarkers: a review of recent research developments. *Org Geochem* 29:1163–1179
- Volkman JK, Barrett SM, Blackburn SI (1999a) Eustigmatophyte microalgae are potential sources of C₂₉ sterols, C₂₂–C₂₈ *n*-alcohols and C₂₈–C₃₂ *n*-alkyl diols in freshwater environments. *Org Geochem* 30:307–318
- Volkman JK, Barrett SM, Blackburn SI (1999b) Fatty acids and hydroxy fatty acids in three species of freshwater eustigmatophytes. *J Phycol* 35:1005–1012

- Volkman JK (2000) Ecological and environmental factors affecting alkenone distributions in seawater and sediments. *Geochem Geophys Geosyst* 1: Paper number 2000GC000061
- Volkman JK (2003) Sterols in microorganisms. *Appl Microbiol Biotechnol* 60:495–506
- Volkman JK, Brown MR (2005) Nutritional value of microalgae and applications. In: Subba Rao DV (ed) *Algal cultures, analogues of blooms and applications*, vol 1. Science Publishers, Enfield, pp 407–457
- Volkman JK (2014) Acyclic isoprenoid biomarkers and evolution of biosynthetic pathways in green microalgae of the genus *Botryococcus*. *Org Geochem* 75:36–47
- Volkman JK (2016) Sterols in microalgae. In: Borowitzka M, Beardall J, Raven JA (eds) *The physiology of microalgae*, Developments in applied phycology series 6. Springer, Cham, pp 485–505
- Wang HT, Yao CH, Liu YN, Meng YY, Wang WL, Cao XP, Xue S (2015) Identification of fatty acid biomarkers for quantification of neutral lipids in marine microalgae *Isochrysis zhangjiangensis*. *J Appl Phycol* 27:249–255
- Weete JD (1976) Algal and fungal waxes. In: Kolattukudy PE (ed) *Chemistry and biochemistry of natural waxes*. Elsevier, Amsterdam, pp 349–418
- Wraige EJ, Belt ST, Lewis CA, Cooke DA, Robert J-M, Massé G, Rowland SJ (1997) Variations in structures and distributions of C₂₅ highly branched isoprenoid (HBI) alkenes in cultures of the diatom, *Haslea ostrearia* (Simonsen). *Org Geochem* 27:497–505
- Xu L, Reddy CM, Farrington JW, Frysiner GS, Gaines RB, Johnson CG, Nelson RK, Eglinton TI (2001) Identification of a novel alkenone in Black Sea sediments. *Org Geochem* 32:633–645
- Xu ZB, Yan XJ, Pei LQ, Luo QJ, Xu JL (2008) Changes in fatty acids and sterols during batch growth of *Pavlova viridis* in photobioreactor. *J Appl Phycol* 20:237–243
- Yon DA, Maxwell JR, Ryback G (1982) 2,6,10-Trimethyl-7-(3-methylbutyl)-dodecane, a novel sedimentary biological marker compound. *Tetrahedron Lett* 23:2143–2146
- Zabeti N, Bonin P, Volkman JK, Jameson ID, Guasco S, Rontani J-F (2010) Potential alteration of $U_{37}^{K'}$ paleothermometer due to selective degradation of alkenones by marine bacteria isolated from the haptophyte *Emiliania huxleyi*. *FEMS Microbiol Ecol* 73:83–94
- Zhao JJ, An CB, Longo WM, Dillon JT, Zhao YT, Shi C, Chen YF, Huang Y (2014) Occurrence of extended chain length C₄₁ and C₄₂ alkenones in hypersaline lakes. *Org Geochem* 75:48–53
- Zhang YD, Su YL, Liu ZW, Chen XC, Yu JL, Di XD, Jin M (2015) Long-chain *n*-alkenes in recent sediment of Lake Lugu (SW China) and their ecological implications. *Limnologia* 52:30–40
- Zhang ZR, Volkman JK (2017) Algaenan structure in the microalga *Nannochloropsis oculata* characterized by stepwise pyrolysis. *Org Geochem* 104:1–7
- Zheng YS, Dillon JT, Zhang YF, Huang YS (2016) Discovery of alkenones with variable methylene-interrupted double bonds: implications for the biosynthetic pathway. *J Phycol* 52:1037–1050
- Zheng YS, Tarozo R, Huang YS (2017) Optimizing chromatographic resolution for simultaneous quantification of long chain alkenones, alkenoates and their double bond positional isomers. *Org Geochem* 111:136–143
- Zink K-G, Leythaeuser D, Melkonian M, Schwark L (2001) Temperature dependency of long-chain alkenone distributions in recent to fossil limnic sediments and in lake waters. *Geochim Cosmochim Acta* 65:253–265



Abiotic Transformation of Unsaturated Lipids and Hydrocarbons in Senescent Phytoplanktonic Cells

8

Jean-François Rontani

Contents

1	Introduction	194
2	Photo- and Autoxidation during the Senescence of Phytoplankton	194
2.1	Photosensitized Oxidation	194
2.2	Free Radical Oxidation (Autoxidation)	196
3	Photo- and Autoxidation of the Main Unsaturated Lipid Components of Algae	197
3.1	Chlorophyll Phytyl Side-Chain	197
3.2	Alkenes	199
3.3	Alkenones	202
3.4	Unsaturated Fatty Acids	205
3.5	Δ^5 -Sterols	205
4	Conclusion	208
	References	209

Abstract

The present paper reviews the effects of photooxidation and autoxidation (free radical oxidation) processes on the main unsaturated lipid components (branched and linear alkenes, chlorophyll phytyl side-chain, alkenones, unsaturated fatty acids, and Δ^5 -sterols) of phytoplankton. A particular attention is given to the mechanisms of these degradation processes and to the potential role of tracers of the products formed. With these specific lipid tracers of abiotic degradation in hand, a more precise estimation of the behavior of particulate organic matter during sedimentation is expected.

J.-F. Rontani (✉)

Aix Marseille Université, Mediterranean Institute of Oceanography (MIO), Université de Toulon, CNRS/INSU/IRD, Marseille, France

e-mail: jean-francois.rontani@mio.osupytheas.fr

© Springer Nature Switzerland AG 2020

H. Wilkes (ed.), *Hydrocarbons, Oils and Lipids: Diversity, Origin, Chemistry and Fate*, Handbook of Hydrocarbon and Lipid Microbiology,

https://doi.org/10.1007/978-3-319-90569-3_23

193

1 Introduction

Although less widely studied than its biologically mediated (heterotrophic) counterpart, abiotic degradation by processes such as photooxidation and autoxidation (spontaneous free radical reaction of organic compounds with oxygen) is now understood to play a non-negligible role in the fate of particulate organic matter in the ocean (Rontani 2005). During the two last decades, a particular attention was given to the role played by photochemical and free radical-mediated processes in the degradation of most unsaturated lipid components: *n*-alkenes (Mouzdahir et al. 2001), highly branched isoprenoid (HBI) alkenes (Rontani et al. 2011, 2014), alkenones (Rontani et al. 1997, 2006), chlorophyll phytyl side-chain (Rontani et al. 1994, 2003; Rontani and Aubert 2005), unsaturated fatty acids (Marchand and Rontani 2001), and Δ^5 -sterols (Christodoulou et al. 2009), during the senescence of phytoplankton. The present paper reviews the results obtained in the course of these different studies.

2 Photo- and Autoxidation during the Senescence of Phytoplankton

2.1 Photosensitized Oxidation

Photochemical damages in phytodetritus are not a monopoly of UV radiation (Christodoulou et al. 2010). In fact, numerous organic components of phytoplankton are susceptible to being photodegraded during senescence by photosynthetically active radiation (PAR) (Rontani 2012). During the last years, it was demonstrated that irradiation of senescent phytoplanktonic cells by the PAR light employed for their growth resulted in fact in the photodegradation of most of their unsaturated lipid components (Rontani 2012).

Due to the presence of chlorophyll, a very efficient photosensitizer (Foote 1976; Knox and Dodge 1985), visible light-induced photosensitized processes act intensively during phytoplankton senescence. When chlorophyll absorbs a quantum of light energy, an excited singlet state (^1Chl) is formed which, in healthy cells, leads predominantly to the fast reactions of photosynthesis (Foote 1976). However, a small proportion (<0.1%) undergoes intersystem crossing (ISC) to form the longer lived triplet state (^3Chl ; Knox and Dodge 1985). ^3Chl is not only in itself potentially damaging in type I reactions (hydrogen atom or electron abstraction) (Knox and Dodge 1985) but can also generate singlet oxygen ($^1\text{O}_2$), by reaction with ground state oxygen ($^3\text{O}_2$) via type II processes (Fig. 1). In order to avoid oxidative damage, there are many antioxidant protective mechanisms that operate in chloroplasts. For example, carotenoids quench ^3Chl and $^1\text{O}_2$ by energy transfer mechanisms (Foote 1976), while tocopherols (e.g., vitamin E) can remove $^1\text{O}_2$ by acting as sacrificial scavengers (Halliwell 1987).

The stopping of photosynthetic reactions in senescent phytoplanktonic organisms results in an accelerated rate of formation of ^3Chl and $^1\text{O}_2$ (Nelson 1993). The rate of

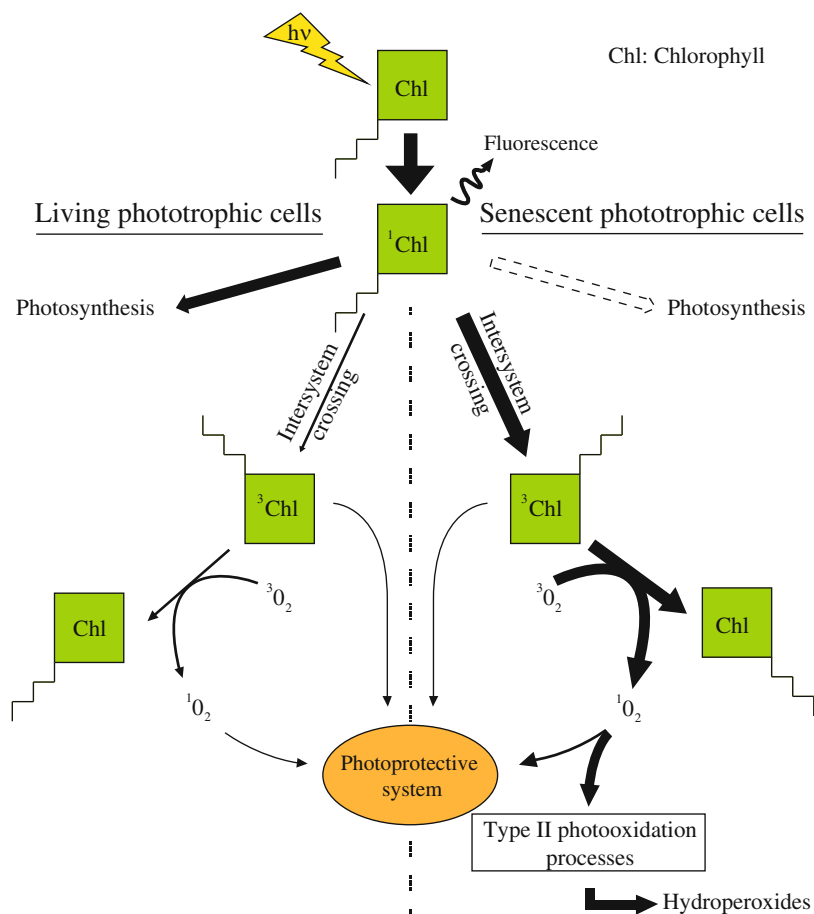


Fig. 1 Potential pathways for chlorophyll excitation energy in healthy and senescent phytoplanktonic cells (simplified scheme taking into account only the involvement of $^1\text{O}_2$)

formation of these potentially damaging species can then exceed the quenching capacity of the photoprotective system, and photodegradation can occur (photodynamic effect; Merzlyak and Hendry 1994) (Fig. 1). In phytodetritus, when the ordered structure of the thylakoid membranes has been disrupted, pigments tend to remain associated with other hydrophobic cellular components such as membrane lipids (Nelson 1993). The photooxidative effect of chlorophyll sensitization is strongly amplified within such a hydrophobic microenvironment. Moreover, the lifetime of $^1\text{O}_2$ produced from sensitizers in a lipid-rich hydrophobic environment could be longer, and its potential diffusive distance greater, than in aqueous solution (Suwa et al. 1977). Consequently, it is not surprising that photodegradation processes act on the majority of unsaturated lipid components of senescent phytoplankton.

Type II photosensitized oxidation of phytoplankton lipids appeared to be strongly enhanced at high latitudes (Rontani et al. 2012a). This apparent paradox (i.e., increased photooxidation despite relatively low temperature and solar irradiance) has been attributed recently by Amiraux et al. (2016) to (i) the relative preservation of the sensitizer (chlorophyll) at low irradiance allowing a longer production time for $^1\text{O}_2$ and (ii) the slower diffusion rate of $^1\text{O}_2$ through the cell membranes at low temperature (Ehrenberg et al. 1998), thereby favoring the intracellular involvement of type II photosensitized reactions.

2.2 Free Radical Oxidation (Autoxidation)

Autoxidation has long been recognized as a free radical chain reaction (Schaich 2005). It thus includes an initiation, a propagation, and a termination phase. In senescent algae, homolytic cleavage (catalyzed by some metal ions, temperature, or UV radiations) (Schaich 2005) of hydroperoxides resulting from type II photosensitized oxidation (Fig. 1) seems to be at the origin of the initiation of this process (Girotti 1998; Rontani et al. 2003). Redox-active metal ions play a very important role in this homolysis as they are ubiquitous, active in many forms, and only needed in trace quantities for effective catalysis. Only metals undergoing one electron transfers appear to be active catalysts; they may direct the cleavage of hydroperoxides either through alkoxy or peroxy radicals (Schaich 2005). The driving force in this chain reaction is the repeated abstraction of hydrogen atoms by peroxy radicals to form hydroperoxides plus free radicals on new substrate molecules (Fig. 2). The process continues indefinitely (propagation phase) until no hydrogen source is available or the chain is intercepted. The radical reaction stops when radicals recombine and produce non-radical species (termination phase).

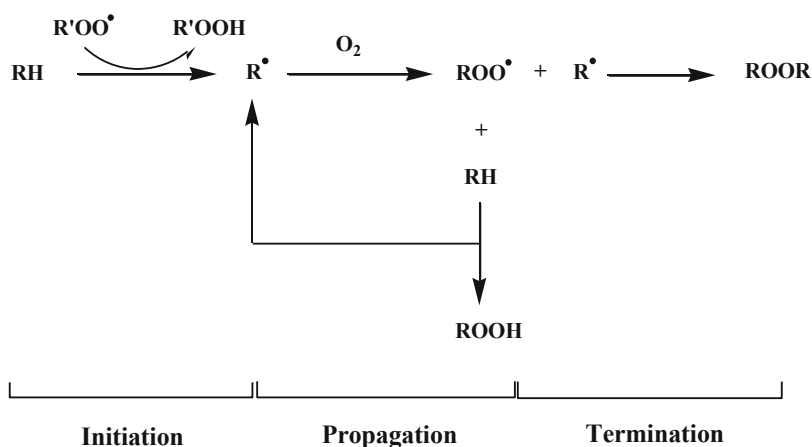


Fig. 2 Free radical oxidation reaction

Until now, autoxidative degradation in the marine environment has been largely ignored. Specific markers of these reactions have been highlighted by *in vitro* studies (Frankel 1998; Rontani et al. 2003; Rontani and Aubert 2005). Using these markers, it was demonstrated *in situ* that autoxidation processes play an important role in the degradation of phytoplankton (Marchand et al. 2005; Rontani et al. 2009; Christodoulou et al. 2009). It was also demonstrated that viral infection (Evans et al. 2006) and autocatalytic programmed cell death (Bidle and Falkowski 2004) of phytoplanktonic cells could also lead to elevated production of reactive oxygen species (ROS) able to induce the degradation of cell components.

The importance of autoxidative damages in phytodetritus depends on several parameters, among them: their hydroperoxide content, the temperature, the solar irradiance and the concentration of some metal ions. Hydroperoxides are mainly formed photochemically during the senescence of phytoplankton (see previous chapter), and their homolytic cleavage is likely at the origin of the involvement of autoxidative processes (Girotti 1998; Rontani et al. 2003). This cleavage being favored by high temperatures and strong solar irradiance (Foote et al. 1995), an intense autoxidative degradation of phytodetritus at low latitudes could be expected. However, it was recently demonstrated that high temperatures and strong solar irradiance can limit photooxidative damages in senescent phytoplanktonic cells (Amiraux et al. 2016) and thus their hydroperoxide content. It is thus very difficult to predict the zones where autoxidation of phytoplankton should be favored.

3 Photo- and Autoxidation of the Main Unsaturated Lipid Components of Algae

3.1 Chlorophyll Phytyl Side-Chain

It was previously demonstrated in phytodetritus that the photodegradation rates were only three to five times higher for the chlorophyll tetrapyrrolic structure than for its phytyl side-chain (Cuny et al. 1999; Christodoulou et al. 2010). Photodegradation of the chlorophyll phytyl side-chain involved mainly $^1\text{O}_2$ and leads to the production of photoproducts of structures *a* and *b* (Fig. 3), quantifiable after NaBH_4 -reduction and alkaline hydrolysis, respectively, in the form of 6,10,14-trimethylpentadecan-2-one (phytone) (1) and 3-methylidene-7,11,15-trimethyl-hexadecan-1,2-diol (phytyldiol) (2) (Fig. 3) (Rontani et al. 1994). Phytyldiol is ubiquitous in the marine environment and has been proposed as specific tracer for photodegradation of the chlorophyll phytyl side-chain (Rontani et al. 1994, 1996; Cuny and Rontani 1999). Further, the molar ratio phytyldiol/phytol (Chlorophyll Phytyl side-chain Photodegradation Index, CPPI) was employed to estimate the extent of chlorophyll photodegraded in natural marine samples by the empirical equation (Eq. 1) (Cuny et al. 2002).

$$\text{Chlorophyll photodegradation}\% = \left(1 - (\text{CPPI} + 1)^{-18.5}\right) \times 100 \quad (1)$$

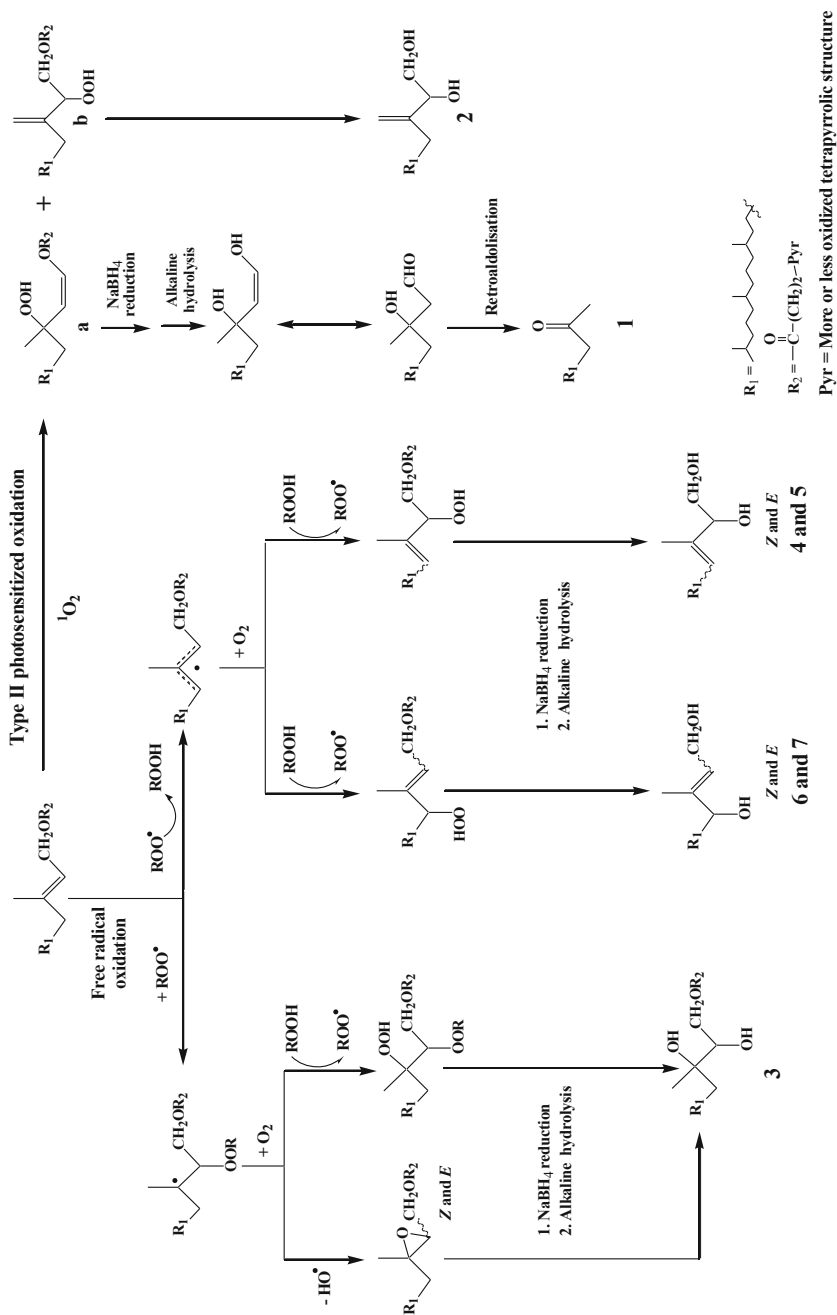


Fig. 3 Type II photosensitized and free radical oxidation of the chlorophyll phytyl side-chain

Autoxidation of the chlorophyll phytyl side-chain involves either addition of peroxy radicals to the double bond or hydrogen atom abstraction at the allylic carbon atom 4 (Rontani and Aubert 1994, 2005). Addition of a peroxy radical to the double bond gives a tertiary radical (Fig. 3). This radical can then (i) lead to *Z* and *E* epoxides by fast intramolecular homolytic substitution (Fossey et al. 1995) or (ii) react with molecular oxygen affording (after hydrogen atom abstraction on another molecule of substrate) a diperoxide (Fig. 3). Subsequent NaBH₄-reduction and alkaline hydrolysis of these compounds gives 3,7,11,15-tetramethylhexadecan-1,2,3-triol (**3**) (Fig. 3). In contrast, abstraction of a hydrogen atom at the allylic carbon atom 4 of the phytyl chain and subsequent oxidation of the allylic radicals thus formed affords (after NaBH₄-reduction and alkaline hydrolysis) *Z* and *E* 3,7,11,15-tetramethylhexadec-3-en-1,2-diols (**4,5**) and *Z* and *E* 3,7,11,15-tetramethylhexadec-2-en-1,4-diols (**6,7**) (Fig. 3). These isomeric compounds, which are widespread in the marine environment, were proposed as specific tracers of autoxidation processes in phytodetritus (Rontani and Aubert 2005).

It is interesting to note that free radical oxidation of the chlorophyll phytyl side-chain appeared to be different in senescent cells of the diatom *Skeletonema costatum* (Rontani et al. 2003). The differences observed were attributed to the well-documented high chlorophyllase activity of this strain (Jeffrey and Hallegraeff 1987) catalyzing the hydrolysis of chlorophyll to free phytol and chlorophyllide. Indeed, it is well known that in the case of free allylic alcohols hydrogen atom abstraction at carbon atom 1 is strongly favored to the detriment of addition reactions (Huyser and Johnson 1968).

3.2 Alkenes

The reactivity of alkenes toward ¹O₂ increases logically with their number of unsaturations (Frankel 1998) but also with the substitution degree of their double bonds (Hurst et al. 1985). Indeed, the order of photoreactivity of the double bonds in alkenes follows the order: tetrasubstituted > trisubstituted > disubstituted > monosubstituted.

The type II photosensitized oxidation of *n*-alkenes was previously studied in killed cells of *Emiliania huxleyi* and *Nannochloropsis salina* (Mouzdahir et al. 2001). In the case of *E. huxleyi*, minor C₃₁ and C₃₃ *n*-alkenes were strongly photo-degraded, while the major C₃₇ and C₃₈ *n*-alkenes appeared particularly recalcitrant toward photochemical processes. The photochemical recalcitrance of C₃₇ and C₃₈ *n*-alkenes was partly attributed to the *E* geometry of their internal double bonds known to be five- to sevenfold less reactive toward ¹O₂ than the *Z* geometry (Hurst et al. 1985) but also to a localization of these compounds elsewhere than in cellular membranes. This last hypothesis is in good agreement with the results of Eltgroth et al. (2005), who showed that C₃₇ *n*-alkenes were localized mainly in chloroplasts or cytoplasmic vesicles of *E. huxleyi* cells. In the case of *N. salina* killed cells, the authors failed to detect significant photo-degradation of monounsaturated hydrocarbons (Mouzdahir et al. 2001); this result

was attributed to the terminal position of the double bond in these compounds, which is poorly reactive toward $^1\text{O}_2$ (Hurst et al. 1985). In contrast, di-, tri-, and tetraenes were strongly photodegraded during irradiation. The photodegradation of phytoplanktonic alkenes showed apparent second-order kinetics with respect to light exposure, and the half-life doses obtained logically decrease with increasing number of double bonds in these compounds.

Photoreactivity of HBI alkenes was studied in dead cells of the diatom *Haslea ostrearia* (Rontani et al. 2011). Despite their believed localization in the cytoplasm (Massé 2003), HBI alkenes with at least one trisubstituted double bond appeared to be photodegraded at similar or higher rates compared to other highly reactive membrane lipids (e.g., polyunsaturated fatty acids, vitamin E, and chlorophyll-a). In contrast, HBIs with only di- and monosubstituted double bonds were relatively inert with respect to type II photoprocesses. In polyolefinic systems, attack by $^1\text{O}_2$ occurs preferentially at the more highly substituted double bond, which also has the lowest ionization potential (Frimer 1983). The reaction of $^1\text{O}_2$ with such a double bond results in the formation of two allylic hydroperoxides, which after homolytic cleavage and subsequent hydrogen atom abstraction mainly afford the corresponding alcohols (Fig. 4).

A kinetic study of several HBI alkenes in solution allowed to propose the following order of reactivity toward autoxidation: HBI with one *bis*-allylic position \gg HBI with two trisubstituted double bonds $>$ HBI with one trisubstituted double bond \gg HBI with only di- or monosubstituted double bonds (Rontani et al. 2014). HBI trienes possessing one *bis*-allylic position (where hydrogen atom abstraction is highly favored) were found to be particularly reactive toward autoxidation and degraded at similar rates compared to polyunsaturated fatty acids (PUFA) in dead diatom cells. Epoxidation of olefins under autoxidation conditions is well known and arises from the addition of peroxy radicals ($\text{ROO}\cdot$) to the $\text{C}=\text{C}$ bond, followed by a unimolecular ring-closure and elimination of an alkoxy radical ($\text{RO}\cdot$) (Fossey et al. 1995). The $\text{ROO}\cdot$ addition to the $\text{C}=\text{C}$ bond competes with allylic hydrogen atom abstraction when there is a double bond that is either conjugated or 1,1-disubstituted (Schaich 2005). In the case of HBIs possessing one trisubstituted double bond such as 2,6,10,14-tetramethyl-7-(3-methylpent-4-enyl)-pentadeca-6(17),9*E*-diene, the majority (more than 90%) of autoxidation products thus appeared to result from the initial addition of a peroxy radical to the nine to ten double bond (Fig. 5). The very low amounts of autoxidation products detected in the case of HBIs possessing two trisubstituted double bonds (Rontani et al. 2014) resulted likely from the secondary oxidation of primary oxidation products to polar and oligomeric compounds, which were not detectable using the GC-MS methods employed.

The very low reactivity of the monounsaturated HBI IP₂₅ (2,6,10,14-tetramethyl-7-(3-methylpent-4-enyl)-pentadecane) (**9**) toward autoxidative (Rontani et al. 2014) and photooxidative (Rontani et al. 2011) degradation processes, both support the proposed use of this compound as a proxy for paleo sea ice by Belt et al. (2007). However, it may be noted that the stay of ice algal material within the oxic zone of some Arctic sediments may be >100 years (Belt, unpublished results). Despite its very low autoxidative reactivity, IP₂₅ could thus be strongly

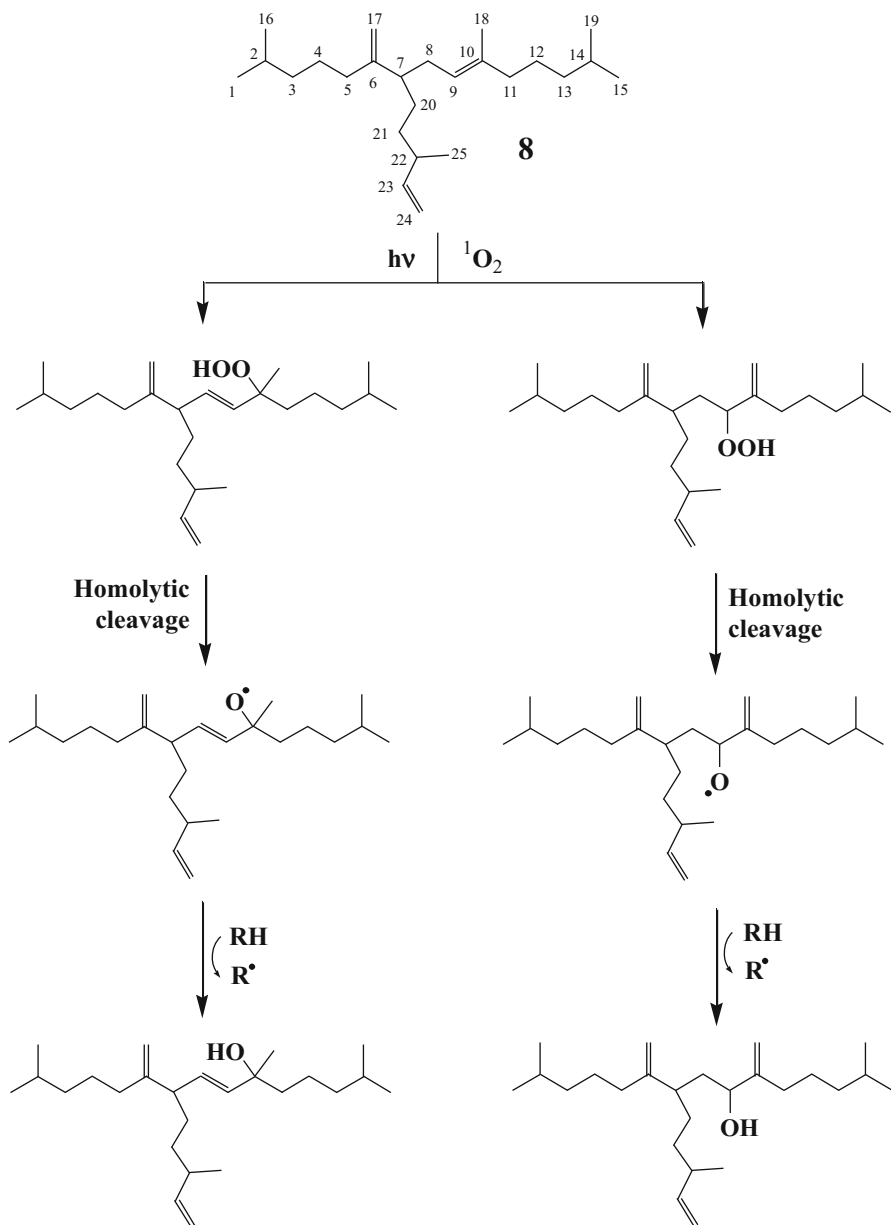


Fig. 4 Type II photosensitized oxidation of the HBI alkene 2,6,10,14-tetramethyl-7-(3-methylpent-4-enyl)-pentadeca-6(17),9*E*-diene (**8**) (RH = hydrogen donors)

autoxidized during the crossing of the oxic zone of such sediments (Rontani et al. 2018). A greater understanding of the factors that influence the sedimentary environments is clearly required before more detailed and quantitative assessments based on IP₂₅ can be made

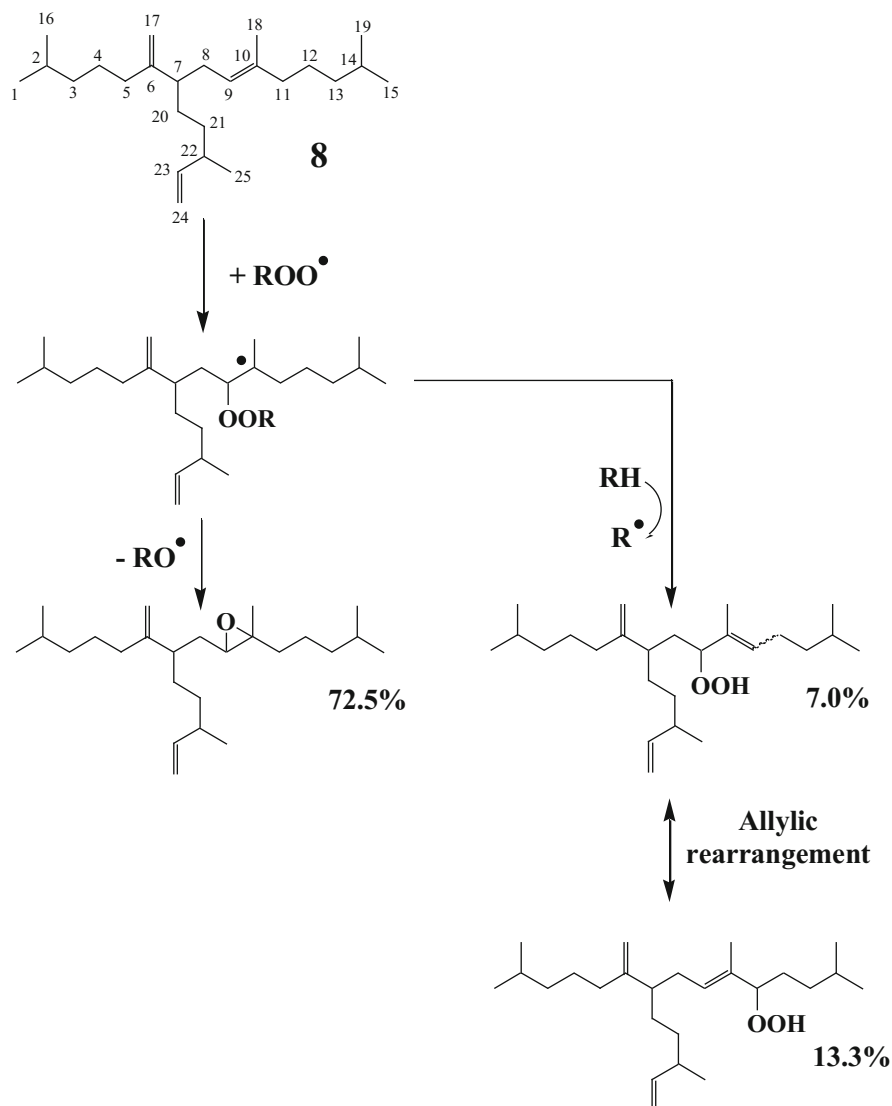


Fig. 5 Free radical oxidation of the HBI alkene 2,6,10,14-tetramethyl-7-(3-methylpent-4-enyl)-pentadeca-6(17),9*E*-diene (**8**) (RH = hydrogen donors)

3.3 Alkenones

Alkenones are a class of mono-, di-, tri-, tetra-, and pentaunsaturated C_{35} – C_{40} methyl and ethyl ketones (De Leeuw et al. 1980; Volkman et al. 1980; Marlowe et al. 1984; Prahl et al. 2006; Jaraula et al. 2010) produced by certain haptophytes (*E. huxleyi*, *Gephyrocapsa oceanica*, *Isochrysis galbana*, and *Chrysolita lamellosa*)

(Volkman et al. 1995; Conte et al. 1994; Versteegh et al. 2001; Rontani et al. 2004). The unsaturation ratio of C_{37} alkenones, defined as $U_{37}^{K'} = [C_{37:2}] / ([C_{37:2}] + [C_{37:3}])$, where $[C_{37:2}]$ and $[C_{37:3}]$ are the concentrations of di- and triunsaturated C_{37} alkenones, respectively, varies positively with the growth temperature of the alga (Prahl and Wakeham 1987; Prahl et al. 1988). This index is now routinely used for paleotemperature reconstruction. For alkenones to be useful as measures of sea surface temperature in the geological record, it is essential that any effects of degradation in the water column and in sediments do not affect the temperature signal established during their initial biosynthesis by the alga (Harvey 2000; Grimalt et al. 2000).

Photochemical degradation of alkenones is not sufficiently fast enough in dead cells of *E. huxleyi* to induce strong modification of the $U_{37}^{K'}$ ratio before the photodestruction of the photosensitizing substances (the increase in $U_{37}^{K'}$ ranges from 0 to +0.04; Rontani et al. 1997; Mouzdahir et al. 2001). This poor photo-reactivity was attributed not only to the *E* geometry of the double bonds of alkenones poorly reactive toward 1O_2 (Hurst et al. 1985) but also to the compartmentalization effects. Indeed, these compounds occur in parts of the cell (chloroplasts or cytoplasmic vesicles; Elgroth et al. 2005), which are less accessible for 1O_2 than cell membranes. It may be expected that if the geometry of their double bonds had been *Z* (as for usual lipids), then selective photolysis of di- and triunsaturated alkenones would occur intensively during the senescence of haptophytes, thus confounding the use of the alkenone unsaturation index for paleotemperature estimation.

The autoxidative reactivity of alkenones in the laboratory has been studied (Rontani et al. 2006). They appeared to be more sensitive toward oxidative free radical processes than analogues of other common marine lipids such as phytyl acetate (model for the chlorophyll phytyl side-chain), methyl oleate (model for esterified FAs), and cholesteryl acetate (model for esterified sterols), and their oxidation rates increase in proportion to the number of double bonds. As a result of this increasing reactivity with degree of unsaturation, $U_{37}^{K'}$ values increased significantly (up to 0.20) during the incubation. Free radical oxidation of isolated 1,2-disubstituted double bonds generally involves allylic hydrogen atom abstraction (Schaich 2005). Effectively, the autoxidation of alkenones appears to involve mainly allylic hydrogen atom abstraction and subsequent oxidation of the allylic radical thus formed (Fig. 6). Alkenone autoxidation, measured indirectly as alkenediols produced from post-extraction $NaBH_4$ -reduction of the corresponding allylic hydroperoxyalkenones (Fig. 6), has been observed in cultures of *E. huxleyi* strain CS-57 that exhibited anomalously high $U_{37}^{K'}$ values (Rontani et al. 2007) and in surface sediments from the SE Alaska (Rontani et al. 2013). Autoxidation of alkenones may thus be significant in some marine areas and could explain some discrepancies between sea surface temperatures (SST) and alkenone-based temperature estimates for marine particles (Freeman and Wakeham 1992) and oxic sediments (Hoefs et al. 1998; Gong and Hollander 1999).

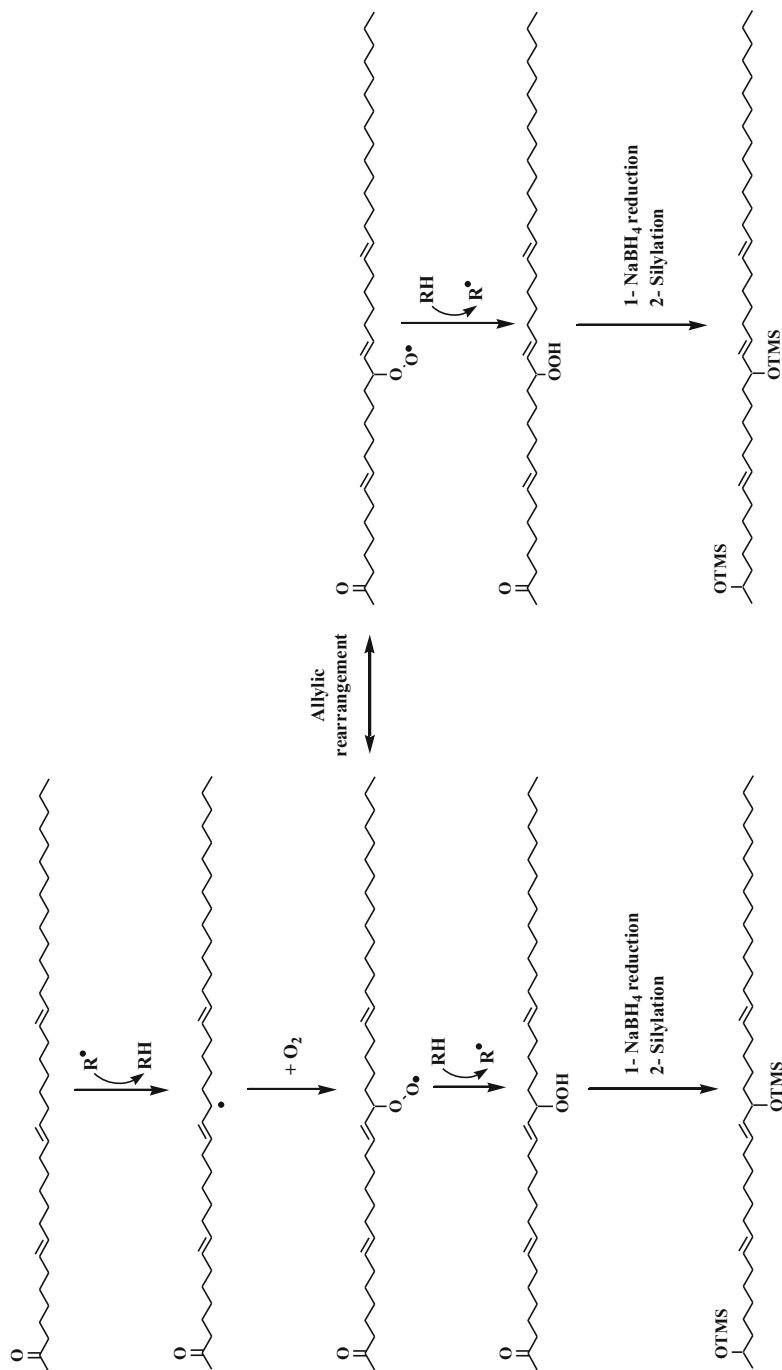


Fig. 6 Free radical oxidation of the C_{37:3} alkenone involving allylic hydrogen atom abstraction (only the attack of the allylic carbon atom 17 is shown) (*RH* hydrogen donors)

3.4 Unsaturated Fatty Acids

Algal unsaturated fatty acids, which generally predominate in the photosynthetic membranes (Woods 1974), are particularly susceptible to type II photooxidation (Heath and Packer 1968) and free radical oxidation (Girotti 1990). In killed phytoplanktonic cells, the photo- (Rontani et al. 1998) and autoxidation (Rontani et al. 2014) rates of unsaturated fatty acids logically increase with their unsaturation degree. Despite the very high reactivity of their parent compounds with $^1\text{O}_2$ and radicals, oxidation products of polyunsaturated fatty acids (PUFAs) could not be detected in natural samples. This is possibly due to (i) the instability of the hydroperoxides formed or (ii) the involvement of cross-linking reactions leading to the formation of macromolecular structures (Neff et al. 1988) non-amenable to gas chromatography. In contrast, high proportions of oxidation products of monounsaturated fatty acids (MUFAs) are often present in particulate matter (Marchand and Rontani 2001; Christodoulou et al. 2009) and sediment (Rontani et al. 2012b) samples. The quantification of these compounds involved NaBH_4 -reduction of the labile hydroperoxides yielding the corresponding alcohols, which are more amenable to analysis using gas chromatography-mass spectrometry (GC-MS) and subsequent saponification.

Singlet oxygen-mediated photooxidation of MUFAs involves a direct reaction of $^1\text{O}_2$ with the carbon-carbon double bond by a concerted “ene” addition (Frimer 1979) and leads to formation of hydroperoxides at each carbon atom of the original double bond. Thus, photooxidation of oleic acid produces a mixture of 9- and 10-hydroperoxides with an allylic *E*-double bond (Frankel et al. 1979; Frankel 1998), which can subsequently undergo stereoselective radical allylic rearrangement to 11-*E* and 8-*E* hydroperoxides, respectively (Porter et al. 1995) (Fig. 7).

Autoxidation of MUFAs mainly involves allylic hydrogen atom abstraction and subsequent oxidation of the allylic radicals thus formed. For example, autoxidation of oleic acid mainly results in the formation of a mixture of 9-*E*, 10-*E*, 11-*E*, 11-*Z*, 8-*E*, and 8-*Z* hydroperoxides (Frankel 1998) (Fig. 7). Free radical oxidative processes can be easily characterized based on the presence of *Z* allylic hydroperoxyacids, which cannot be produced photochemically (Fig. 7) and are specific products of these degradation processes (Porter et al. 1995; Frankel 1998).

During early diagenesis, photo- and autoxidative isomeric hydroperoxyacids undergo allylic rearrangement, heterolytic cleavage to aldehydes and ω -oxocarboxylic acids (Frimer 1979), or homolytic cleavage and subsequent transformation to the corresponding alcohols or ketones (Fig. 8).

3.5 Δ^5 -Sterols

As important unsaturated components of biological membranes, Δ^5 -sterols are highly susceptible to photooxidative degradation during the senescence of phytoplankton. Type II photosensitized oxidation of Δ^5 -sterols produces mainly Δ^6 -5 α -hydroperoxides with smaller amounts of Δ^4 -6 α /6 β -hydroperoxides (Kulig and Smith 1973)

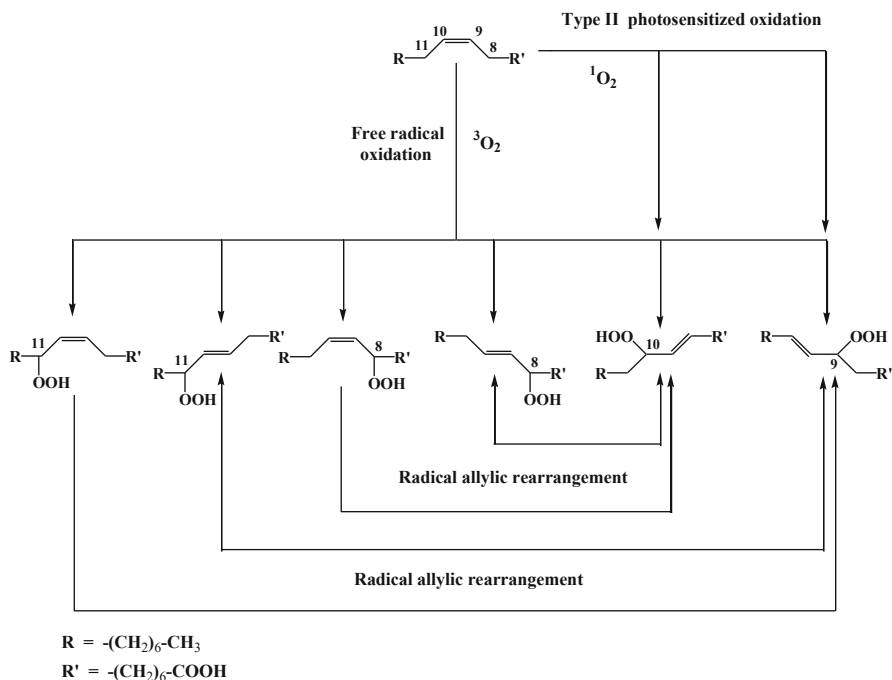


Fig. 7 Type II photosensitized and free radical oxidation of oleic acid

(Fig. 9). The latter were selected as tracers of photooxidation of Δ^5 -sterols due to their high specificity and relative stability (Christodoulou et al. 2009; Rontani et al. 2009). As Δ^4 -6 α /6 β -hydroperoxides could not be analyzed directly by GC-MS techniques, they are generally quantified after NaBH_4 -reduction to the corresponding diols (Rontani and Marchand, 2000). On the basis of the ratio Δ^4 -6 α /6 β -hydroperoxides/ Δ^6 -5 α -hydroperoxides observed in biological membranes (0.30) (Korytowski et al. 1992), equation (Eq. 2) was previously proposed for sterol photooxidation proportion estimates (Christodoulou et al. 2009).

$$\text{Sterol photooxidation}\% = \left(\Delta^4 - 3\beta, 6\alpha/\beta\text{-dihydroxysterol}\% \right) \times (1 + 0.3)/0.3 \quad (2)$$

Due to the trisubstitution of the Δ^5 double bond, free radical autoxidation of Δ^5 -sterols involves both allylic hydrogen atom abstraction and epoxidation reactions and yields 7 α - and 7 β -hydroperoxides, 5 α / β ,6 α / β -epoxysterols, and 3 β ,5 α ,6 β -trihydroxysterols (Smith 1981) (Fig. 9). 3 β ,5 α ,6 β -trihydroxysterols were selected as specific tracers of sterol autoxidation. 7-hydroperoxides were ruled out as possible markers due to their lack of specificity and instability (Christodoulou et al. 2009; Rontani et al. 2009), and 5 α / β ,6 α / β -epoxysterols could not be used since they are

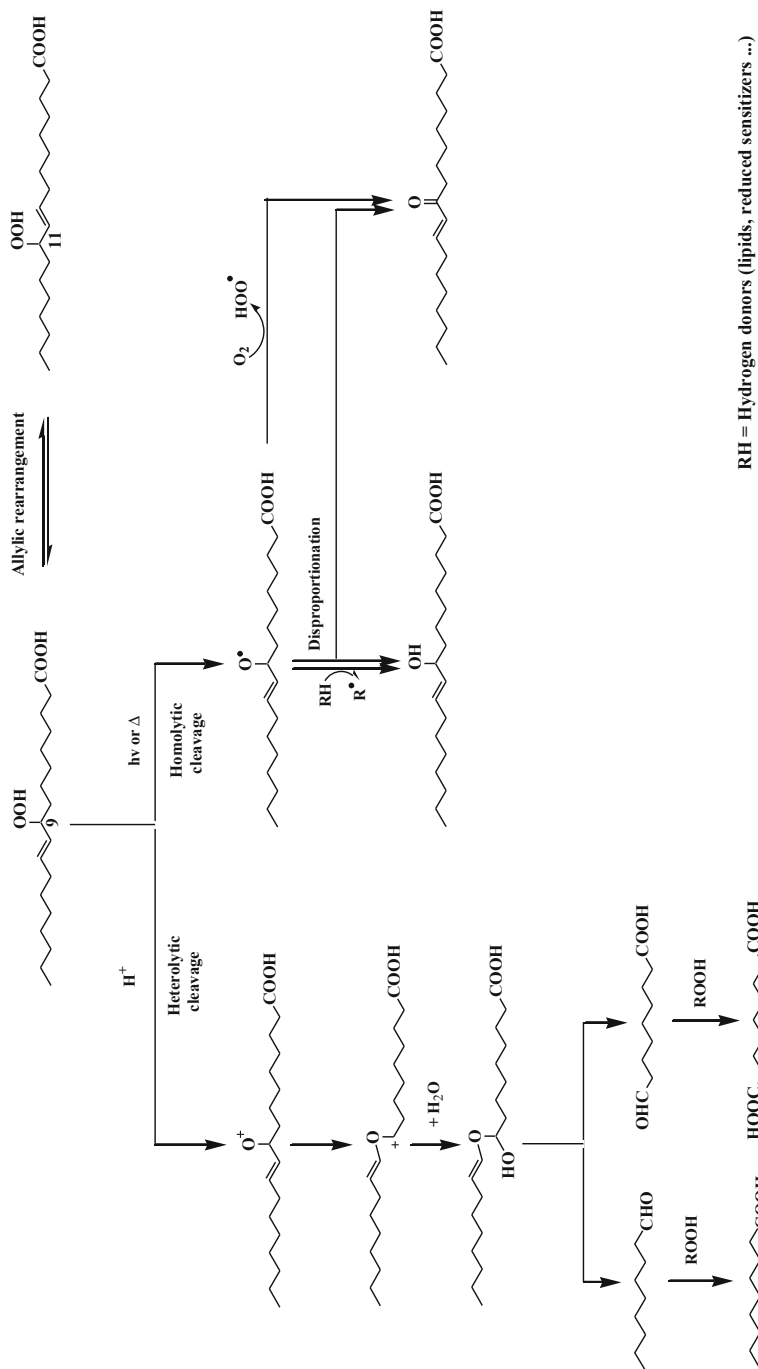


Fig. 8 Degradation of allylic hydroperoxides resulting from type II photosensitized or free radical oxidation of monounsaturated fatty acids (the example given is that of 9-hydroperoxyoctadec-10-enoic acid) (10)

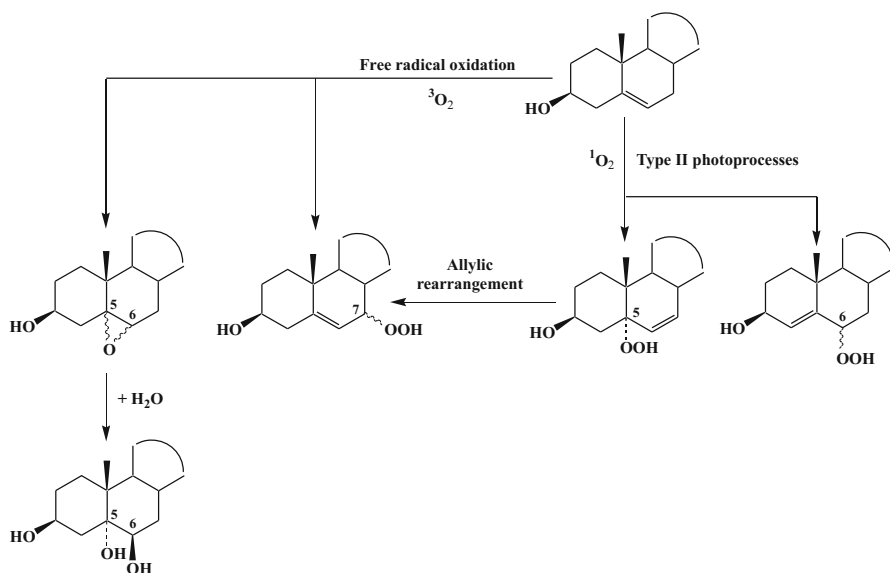


Fig. 9 Type II photosensitized and free radical oxidation of Δ^5 -sterols

converted to the corresponding triol during saponification. The extent of sterol autoxidation was estimated using Eq. (3) based on autoxidation rate constants previously obtained (Christodoulou et al. 2009; Rontani et al. 2009; Morrissey and Kiely 2006) (averaged value of $k_{\text{epoxidation}}/k_{\text{allylic abstraction}} = 0.725$).

$$\text{Sterol autoxidation}\% = (\text{3}\beta, \text{5}\alpha, \text{6}\beta - \text{trihydroxysterols}\%) \times (1 + 0.725)/0.725 \quad (3)$$

4 Conclusion

Numerous works summarized in the present review demonstrated that most of the unsaturated lipid components of phytoplankton could be degraded intensively by visible light-induced photochemical and free radical-mediated (autoxidative) processes during senescence. Some lipid oxidation products sufficiently specific of these two kinds of abiotic degradative processes have been proposed as tracers. These compounds could be very useful for the monitoring of the abiotic degradation of particulate organic matter in the marine realm.

On the basis of the different photodegradation rate constants measured after irradiation of dead phytoplanktonic cells (Christodoulou et al. 2010; Rontani et al. 2011), the following order of photoreactivity of phytoplanktonic lipids may be proposed: HBIs with three trisubstituted double bonds > HBIs with two trisubstituted double bonds > HBIs with one trisubstituted double bond \approx PUFAs \approx vitamin

E > MUFAs > chlorophyll phytyl side-chain > Δ^5 -sterols > HBI with zero trisubstituted double bonds > alkenones.

Concerning autoxidation, dark incubations of dead phytoplanktonic cells in the presence of Fe^{2+} ions (Rontani et al. 2014) allow to propose the following order of reactivity: HBIs with *bis*-allylic position \approx alkenones \approx PUFAs > HBIs with one trisubstituted double bond \approx chlorophyll phytyl side-chain > MUFAs > Δ^5 -sterols \approx HBI with zero trisubstituted double bonds.

Acknowledgments Financial support over many years from the Centre National de la Recherche Scientifique (CNRS) and the Aix-Marseille University is gratefully acknowledged.

References

- Amiraux R, Jeanthon C, Vaultier F, Rontani J-F (2016) Paradoxical effects of temperature and solar irradiance on the photodegradation state of killed phytoplankton. *J Phycol* 52:475–485
- Belt ST, Massé G, Rowland SJ, Poulin M, Michel C, LeBlanc B (2007) A novel chemical fossil of palaeo sea ice: IP₂₅. *Org Geochem* 38:16–27
- Bidle KD, Falkowski PG (2004) Cell death in planktonic photosynthetic microorganisms. *Nat Rev Microbiol* 2:643–655
- Christodoulou S, Marty J-C, Miquel J-C, Volkman JK, Rontani J-F (2009) Use of lipids and their degradation products as biomarkers for carbon cycling in the northwestern Mediterranean Sea. *Mar Chem* 113:25–40
- Christodoulou S, Joux F, Marty J-C, Sempéré R, Rontani J-F (2010) Comparative study of UV and visible light induced degradation of lipids in non-axenic senescent cells of *Emiliania huxleyi*. *Mar Chem* 119:139–152
- Conte MH, Volkman JK, Eglinton G (1994) Lipid biomarkers of the Haptophyta. In: Green JC, Leadbeater BSC (eds) The haptophyte algae. Systematics Association special volume, vol 51. Clarendon Press, Oxford, pp 351–377
- Cuny P, Rontani J-F (1999) On the widespread occurrence of 3-methylidene-7,11,15-trimethylhexadecan-1,2-diol in the marine environment: a specific isoprenoid marker of chlorophyll photodegradation. *Mar Chem* 65:155–165
- Cuny P, Romano J-C, Beker B, Rontani J-F (1999) Comparison of the photo-degradation rates of chlorophyll chlorin ring and phytol side chain in phytodetritus: is the phytyldiol versus phytol ratio (CPPI) a new biogeochemical index? *J Exp Mar Biol Ecol* 237:271–290
- Cuny P, Marty J-C, Chiaverini J, Vescovali I, Raphael D, Rontani J-F (2002) One-year seasonal survey of the chlorophyll photodegradation process in the Northwestern Mediterranean Sea. *Deep-Sea Res II* 49:1987–2005
- De Leeuw JW, van der Meer JW, Rijpstra WIC, Schenck PA (1980) On the occurrence and structural identification of long chain ketones and hydrocarbons in sediments. In: Douglas AG, Maxwell JR (eds) *Advances in organic geochemistry 1979*. Pergamon Press, Oxford, pp 211–217
- Ehrenberg B, Anderson J, Foote CS (1998) Kinetics and yield of singlet oxygen photosensitized by hypericin in organic and biological media. *Photochem Photobiol* 68:135–140
- Eltgroth ML, Watwood RL, Wolfe GV (2005) Production and cellular localization of neutral long-chain lipids in the haptophyte algae *Isochrysis galbana* and *Emiliania huxleyi*. *J Phycol* 41:1000–1009
- Evans C, Malin G, Mills GP (2006) Viral infection of *Emiliania huxleyi* (Prymnesiophyceae) leads to elevated production of reactive oxygen species. *J Phycol* 42:1040–1047
- Foote CS (1976) Photosensitized oxidation and singlet oxygen: consequences in biological systems. In: Pryor WA (ed) *Free radicals in biology*. Academic, New York, pp 85–133

- Foote CS, Valentine JS, Greenberg A, Liebman JF (1995) Active oxygen in chemistry. Chapman & Hall, New York
- Fossey J, Lefort D, Sorba J (1995) Free radicals in organic chemistry. Masson, Paris, pp 1–307
- Frankel EN (1998) Lipid oxidation. The Oily Press, Dundee
- Frankel EN, Neff WE, Bessler TR (1979) Analysis of autoxidized fats by gas chromatography-mass spectrometry: V. Photosensitized oxidation. *Lipids* 14:961–967
- Freeman KH, Wakeham SG (1992) Variations in the distributions and isotopic compositions of alkenones in Black Sea particles and sediments. *Org Geochem* 19:277–285
- Frimer AA (1979) The reaction of singlet oxygen with olefins: the question of mechanism. *Chem Rev* 79:359–387
- Frimer AA (1983) Singlet oxygen in peroxide chemistry. In: Patai S (ed), *The chemistry of functional groups, peroxides*. Wiley, Chichester, pp 202–229
- Girotti AW (1990) Photodynamic lipid peroxidation in biological systems. *Photochem Photobiol* 51:497–509
- Girotti AW (1998) Lipid hydroperoxide generation, turnover and effector action in biological systems. *J Lipid Res* 39:1529–1542
- Gong C, Hollander DJ (1999) Evidence for differential degradation of alkenones under contrasting bottom water oxygen conditions: implication for paleotemperature reconstruction. *Geochim Cosmochim Acta* 63:405–411
- Grimalt JO, Rullkötter J, Sicre M-A, Summons R, Farrington J, Harvey HR, Goñi M, Sawada K (2000) Modifications of the C₃₇ alkenone and alkenoate composition in the water column and sediment: possible implications for sea surface temperature estimates in paleoceanography. *Geochem Geophys Geosyst* 1. <https://doi.org/10.1029/2000G000053>
- Halliwell B (1987) Oxidative damage, lipid peroxidation and antioxidant protection in chloroplasts. *Chem Phys Lipids* 44:327–340
- Harvey HR (2000) Alteration processes of alkenones and related lipids in water columns and sediments. *Geochem Geophys Geosyst* 1. <https://doi.org/10.1029/2000GC000054>
- Heath RL, Packer L (1968) Photoperoxidation in isolated chloroplasts. II Role of electron transfer. *Arch Biochem Biophys* 125:850–857
- Hoefs MJL, Versteegh GJM, Rijpstra WIC, de Leeuw JS, Sinninghe Damste JS (1998) Post-depositional oxic degradation of alkenones: implications for the measurement of palaeo sea surface temperatures. *Paleoceanography* 13:42–49
- Hurst JR, Wilson SL, Schuster GB (1985) The ene reaction of singlet oxygen: kinetic and product evidence in support of a peroxide intermediate. *Tetrahedron* 41:2191–2197
- Huysen ES, Johnson KL (1968) Concerning the nature of the polar effect in hydrogen atom abstractions from alcohols, ethers and esters. *J Organomet Chem* 33:3972–3974
- Jaraula CMB, Brassell SC, Morgan-Kiss R, Doran PT, Kenig F (2010) Origin and distribution of tri- to pentaunsaturated alkenones in Lake Fryxell, East Antarctica. *Org Geochem* 41:386–397
- Jeffrey SW, Hallegraeff GM (1987) Chlorophyllase distribution in ten classes of phytoplankton: a problem for chlorophyll analysis. *Mar Ecol Prog Ser* 35:293–304
- Knox JP, Dodge AD (1985) Singlet oxygen and plants. *Phytochemistry* 24:889–896
- Korytowski W, Bachowski GJ, Girotti AW (1992) Photoperoxidation of cholesterol in homogeneous solution, isolated membranes, and cells: comparison of the 5 α - and 6 β -hydroperoxides as indicators of singlet oxygen intermediacy. *Photochem Photobiol* 56:1–8
- Kulig MJ, Smith LL (1973) Sterol metabolism. XXV. Cholesterol oxidation by singlet molecular oxygen. *J Organomet Chem* 38:3639–3642
- Marchand D, Rontani J-F (2001) Characterization of photooxidation and autoxidation products of phytoplanktonic monounsaturated fatty acids in marine particulate matter and recent sediments. *Org Geochem* 32:287–304
- Marchand D, Marty J-C, Miquel J-C, Rontani J-F (2005) Lipids and their oxidation products as biomarkers for carbon cycling in the northwestern Mediterranean Sea: results from a sediment trap study. *Mar Chem* 95:129–147

- Marlowe IT, Green JC, Neal AC, Brassell SC, Eglinton G, Course PA (1984) Long chain (n -C₃₇–C₃₉) alkenones in the Prymnesiophyceae. Distribution of alkenones and other lipids and their taxonomic significance. *British Phycol J* 19:203–216
- Massé G (2003) Highly branched isoprenoid alkenes from diatoms: a biosynthetic and life cycle study. PhD thesis, University of Plymouth
- Merzlyak MN, Hendry GAF (1994) Free radical metabolism, pigment degradation and lipid peroxidation in leaves during senescence. *Proc Roy Soc Edinb* 102B:459–471
- Morrissey PA, Kiely M (2006) Oxysterols: formation and biological function. In: Fox PF, McSweeney PLH (eds) *Advanced dairy chemistry*, 3rd edn. Lipids, vol 2. Springer, New York, pp 641–674
- Mouzdahir A, Grossi V, Bakkas S, Rontani J-F (2001) Photodegradation of long-chain alkenes in senescent cells of *Emiliana huxleyi* and *Nannochloropsis salina*. *Phytochemistry* 56: 677–684
- Neff WE, Frankel EN, Fujimoto K (1988) Autoxidative dimerization of methyl linolenate and its monohydroperoxides, hydroperoxy epidioxides and dihydroperoxides. *J Am Oil Chem Soc* 65:616–623
- Nelson JR (1993) Rates and possible mechanism of light-dependent degradation of pigments in detritus derived from phytoplankton. *J Mar Res* 51:155–179
- Porter NA, Caldwell SE, Mills KA (1995) Mechanisms of free radical oxidation of unsaturated lipids. *Lipids* 30:277–290
- Prahl FG, Wakeham SG (1987) Calibration of unsaturation patterns in long-chain ketone compositions for palaeotemperature assessment. *Nature* 330:367–369
- Prahl FG, Muehlhausen L, Zahnle DL (1988) Further evaluation of long-chain alkenones as indicators of paleoceanographic conditions. *Geochim Cosmochim Acta* 52:2303–2310
- Prahl FG, Rontani J-F, Volkman JK, Sparrow MA, Royer IM (2006) Unusual C₃₅ and C₃₆ alkenones in a paleoceanographic benchmark strain of *Emiliana huxleyi*. *Geochim Cosmochim Acta* 70:2856–2867
- Rontani J-F (2005) Importance of visible light-induced photodegradation processes in the north western Mediterranean Sea. In: Salot A (ed) *The handbook of environmental chemistry, water pollution*, vol 5. Springer, Heidelberg, pp 297–317
- Rontani J-F (2012) Photo- and free radical-mediated oxidation of lipid components during the senescence of phototrophic organisms. In: Nagata T (ed) *Senescence*. Intech, Rijeka, pp 3–31
- Rontani J-F, Aubert C (1994) Effect of oxy-free radicals upon the phytol chain during chlorophyll-a photodegradation. *J Photochem Photobiol A* 79:167–172
- Rontani J-F, Aubert C (2005) Characterization of isomeric allylic diols resulting from chlorophyll phytol side-chain photo- and autoxidation by electron ionization gas chromatography/mass spectrometry. *Rapid Commun Mass Spectrom* 19:637–646
- Rontani J-F, Marchand D (2000) Δ^5 -Stenol photoproducts of phytoplanktonic origin: a potential source of hydroperoxides in marine sediments? *Org Geochem* 31:169–180
- Rontani J-F, Grossi V, Faure R, Aubert C (1994) “Bound” 3-methylidene-7,11,15-trimethylhexadecan-1,2-diol: a new isoprenoid marker for the photodegradation of chlorophyll-a in seawater. *Org Geochem* 21:135–142
- Rontani J-F, Raphael D, Cuny P (1996) Early diagenesis of the intact and photooxidized chlorophyll phytol chain in a recent temperate sediment. *Org Geochem* 24:825–832
- Rontani J-F, Cuny P, Grossi V, Beker B (1997) Stability of long-chain alkenones in senescing cells of *Emiliana huxleyi*: effect of photochemical and aerobic microbial degradation on the alkenone unsaturation ratio (U_{37}^K). *Org Geochem* 26:503–509
- Rontani J-F, Cuny P, Grossi V (1998) Identification of a pool of lipid photoproducts in senescent phytoplanktonic cells. *Org Geochem* 29:1215–1225
- Rontani J-F, Rabourdin A, Marchand D, Aubert C (2003) Photochemical oxidation and autoxidation of chlorophyll phytol side chain in senescent phytoplanktonic cells: potential sources of several acyclic isoprenoid compounds in the marine environment. *Lipids* 38:241–253

- Rontani J-F, Beker B, Volkman JK (2004) Regiospecific enzymatic oxygenation of alkenones in the benthic haptophyte *Chrysothila lamellosa* Anand HAP 17. *Phytochemistry* 65:3269–3278
- Rontani J-F, Marty J-C, Miquel J-C, Volkman JK (2006) Free radical oxidation (autoxidation) of alkenones and other microalgal lipids in seawater. *Org Geochem* 37:354–368
- Rontani J-F, Jameson I, Christodoulou S, Volkman JK (2007) Free radical oxidation (autoxidation) of alkenones and other lipids in cells of *Emiliania huxleyi*. *Phytochemistry* 68:913–924
- Rontani J-F, Zabeti N, Wakeham SG (2009) The fate of marine lipids: biotic vs. abiotic degradation of particulate sterols and alkenones in the Northwestern Mediterranean Sea. *Mar Chem* 113:9–18
- Rontani J-F, Belt ST, Vaultier F, Brown TA (2011) Visible light-induced photo-oxidation of highly branched isoprenoid (HBI) alkenes: a significant dependence on the number and nature of the double bonds. *Org Geochem* 42:812–822
- Rontani J-F, Charriere B, Forest A, Heussner S, Vaultier F, Petit M, Delsaut N, Fortier L, Sempéré R (2012a) Intense photooxidative degradation of planktonic and bacterial lipids in sinking particles collected with sediment traps across the Canadian Beaufort Shelf (Arctic Ocean). *Biogeosciences* 9:4787–4802
- Rontani J-F, Charriere B, Petit M, Vaultier F, Heipieper H, Link H, Chailloux G, Sempéré R (2012b) Degradation state of organic matter in surface sediments from the Southern Beaufort Sea: a lipid approach. *Biogeosciences* 9:3513–3530
- Rontani J-F, Volkman JK, Prahl FG, Wakeham SG (2013) Biotic and abiotic degradation of alkenones and implications for paleoproxy applications: a review. *Org Geochem* 59:93–113
- Rontani J-F, Belt ST, Brown TA, Vaultier F, Mundy CJ (2014) Sequential photo- and autoxidation of diatom lipids in Arctic sea ice. *Org Geochem* 77:59–71
- Rontani J-F, Belt ST, Amiraux R (2018) Biotic and abiotic degradation of the sea ice diatom biomarker IP₂₅ and selected algal sterols in near-surface Arctic sediments. *Org Geochem* 118:73–88
- Schaich KM (2005) Lipid oxidation: theoretical aspects. In: Shahidi F (ed) *Bailey's industrial oil and fat products*, 6th edn. Wiley, Hoboken, pp 269–355
- Smith LL (1981) *The autoxidation of cholesterol*. Plenum Press, New York
- Suwa K, Kimura T, Schaap AP (1977) Reactivity of singlet molecular oxygen with cholesterol in a phospholipidic membrane matrix: a model for oxidative damage of membranes. *Biochem Biophys Res Commun* 75:785–792
- Versteegh GJM, Riegman R, De Leeuw JW, Jansen JHF (2001) $U_{37}^{K'}$ values for *Isochrysis galbana* as a function of culture temperature, light intensity and nutrient concentrations. *Org Geochem* 32:785–794
- Volkman JK, Eglinton G, Corner EDS, Forsberg TEV (1980) Long chain alkenes and alkenones in the marine coccolithophorid *Emiliania huxleyi*. *Phytochemistry* 19:2619–2622
- Volkman JK, Barrett SM, Blackburn SI, Sikes EL (1995) Alkenones in *Gephyrocapsa oceanica* – implications for studies of paleoclimate. *Geochim Cosmochim Acta* 59:513–520
- Wood BJB (1974). Fatty acids and saponifiable lipids. In: Steward WD (ed) *Algal Physiology and Biochemistry*. University of California Press, Berkeley, pp 236–265



Cuticular Hydrocarbons and Pheromones of Arthropods

9

Gary J. Blomquist, Claus Tittiger, and Russell Jurenka

Contents

1	Introduction: Cuticular Hydrocarbons and Pheromones	214
2	Insect Cuticular Hydrocarbons	217
3	Insect Pheromones	218
3.1	Lepidopteran Fatty Acid Derived (Type I Pheromones)	219
3.2	Polyene Hydrocarbons (Type II) Pheromones	219
3.3	Terpenoid Pheromones	219
3.4	Other Pheromones	220
4	Hydrocarbon Biosynthesis	220
5	Pheromone Biosynthesis	224
5.1	Alcohol, Aldehyde, and Acetate Ester Pheromones	224
5.2	Polyene Hydrocarbons	229
5.3	Terpenoid Pheromones	230
5.4	Other Pheromones	232
6	Research Needs	235
	References	235

Abstract

Cuticular hydrocarbons and pheromones of insects are often derived from fatty acids and terpenoid lipid components. This chapter describes the chemistry and biochemistry of insect hydrocarbons and pheromones and emphasizes recent work. Cuticular hydrocarbons consist of complex mixtures of straight chain, unsaturated, and methyl-branched components with 21 to 40+ carbon atoms. They function both to restrict water loss to prevent a lethal rate of desiccation

G. J. Blomquist (✉) · C. Tittiger
Department of Biochemistry and Molecular Biology, University of Nevada, Reno, NV, USA
e-mail: garyb@cabnr.unr.edu; crt@unr.edu

R. Jurenka
Department of Entomology, Iowa State University, Ames, IA, USA
e-mail: rjurenka@iastate.edu

© Springer Nature Switzerland AG 2020

H. Wilkes (ed.), *Hydrocarbons, Oils and Lipids: Diversity, Origin, Chemistry and Fate*,
Handbook of Hydrocarbon and Lipid Microbiology,
https://doi.org/10.1007/978-3-319-90569-3_11

213

and serve in chemical communication in many species. The major volatile insect pheromones consist of modified fatty acids and terpenoids. Many of the lepidopteran pheromones arise from fatty acid precursors, are modified with desaturases, and undergo limited chain shortening or elongation followed by modification of the carboxyl group to produce acetate esters, aldehydes, alcohols, and hydrocarbons. Many coleopteran pheromones are terpenoids, while still other insects use a variety of other compounds. The volatile, long range pheromones produced by insects are often produced in specific glands, and pheromone glands on the abdomen of many lepidopterans produce 10–21 carbon atom pheromone components. In some coleopterans, midgut tissue produces terpenoid pheromones. Recent work on hydrocarbon and pheromone production is taking advantage of the tools of molecular biology to better understand hydrocarbon and pheromone biosynthesis, and this information is summarized.

1 Introduction: Cuticular Hydrocarbons and Pheromones

Due to their small size, insects have large surface area to volume ratios and are therefore susceptible to water loss and desiccation. Cuticular lipids on the surface of insects are essential to prevent desiccation and death of insects. They are often comprised primarily of long-chain hydrocarbon components of 21 to 40+ carbon atoms. The ability of insects to withstand desiccation was recognized in the 1930s to be due in part to the epicuticular wax layer on the cuticle. The presence of hydrocarbons in this wax layer was suggested by Chibnall et al. (1934) and Blount et al. (1937). Over the next few decades, the importance of hydrocarbons in the cuticular wax of insects was established and the first components were identified by Baker et al. (1963) from the American cockroach, *Periplaneta americana*, as *n*-pentacosane, 3-methylpentacosane, and (*Z,Z*)-6,9-heptacosadiene. The development and application of combined gas-liquid chromatography and mass spectrometry was key to the rapid and efficient analyses of insect hydrocarbons. In the late 1960s and during the next few decades, GC-MS analyses of insect hydrocarbons were established (Nelson and Sukkestad 1970), and since that time the hydrocarbons of thousands of insect species were analyzed, first on packed columns and then much more efficiently on capillary columns. It became recognized that for many insect species, very complex mixtures of normal (straight-chain), methyl-branched, and unsaturated components exist (Howard and Blomquist 2005; Blomquist 2010; Ginzl and Blomquist 2016). In many insect species, cuticular hydrocarbons function in chemical communication where relatively nonvolatile pheromones are needed. Thus, it appears that many species have evolved unique blends of hydrocarbon components that serve both to prevent a lethal rate of water loss and to provide informational cues.

The biosynthetic pathways for insect hydrocarbons were examined with radioactive and stable isotopes in the 1970s and 1980s, and it was established that fatty acids are elongated and converted to hydrocarbons by the loss of the carboxyl carbon

atom. More recent studies have examined the origin of the fatty acyl precursors by selective desaturation and incorporation of methyl-branch groups, the subsequent elongation of the fatty acyl-CoAs to very-long-chain fatty acids, and their reduction and oxidative decarbonylation by insect-specific cytochromes P450 (Ginzel and Blomquist 2016).

The elucidation of the structure of the first insect sex pheromone, bombykol ((*E*, *Z*)-10,12-hexadecadien-1-ol) (Butenandt et al. 1959) (Fig. 1), from the silkworm moth, *Bombyx mori*, spanned more than 20 years and required a half million female abdomens. A few years later, (*Z*)-7-dodecenyl acetate (Fig. 1) was identified as the sex pheromone of the cabbage looper, *Trichoplusia ni* (Berger 1966). At about the same time, Silverstein et al. (1966) identified three terpenoid alcohols, ipsenol, ipsdienol, and verbenol (Fig. 1), as the aggregation pheromone of the bark beetle, *Ips paraconfusus*. This latter finding led to the recognition that most insect pheromones consisted of multicomponent blends. This has since been shown to be true for most insects, and single component pheromones are rare. Rapid improvements in analytical instrumentation and techniques reduced the number of insects needed for pheromone analysis from a half million or more to where now individual insects can sometimes provide sufficient material for chemical analysis. Over the last half century, extensive research on insect pheromones has resulted in the chemical and/or behavioral elucidation of pheromone components from well over 3000 insect species, with much of the work concentrating on sex pheromones from economically important pests with the aim of using this knowledge in insect control.

An early issue addressed in pheromone production was the origin of pheromone components. A question asked in several systems was whether pheromone components were derived from dietary components that were altered only minimally or whether they were synthesized de novo. This simple question proved surprisingly difficult to answer, and different answers were obtained for different groups of insects. It is now clear that most insect pheromone components are synthesized de novo by insect tissue (Tillman et al. 1999; Jurenka et al. 2017), with a number of notable exceptions that include several bark beetle pheromones (Tittiger and Blomquist 2016) and polyunsaturated hydrocarbons (Millar 2010).

By the mid-1980s, it had become apparent that the products of normal metabolism, particularly those of the fatty acid and isoprenoid pathways, were modified by a few pheromone-tissue-specific enzymes to produce the myriad of pheromone molecules. The elegant work of the Roelofs laboratory (Bjostad et al. 1987) demonstrated that many lepidopteran pheromones could be formed by the appropriate interplay of unique $\Delta 11$ and other desaturases and highly selective chain shortening followed by modification of the carboxyl group. This work has been extended, and there now exists a clear understanding of the biosynthetic pathways for many of the lepidopteran pheromones (Jurenka et al. 2017). The honeybee also uses highly specific chain shortening of fatty acids to produce the major components of the queen pheromone (Plettner et al. 1996, 1998). In some insects, the elongation of polyunsaturated dietary fatty acids followed by loss of the carboxyl carbon atom produces hydrocarbon and hydrocarbon-derived pheromones (Tillman et al. 1999; Millar 2010; Ginzel and Blomquist 2016). *Ips* and *Dendroctonus* spp. produce their

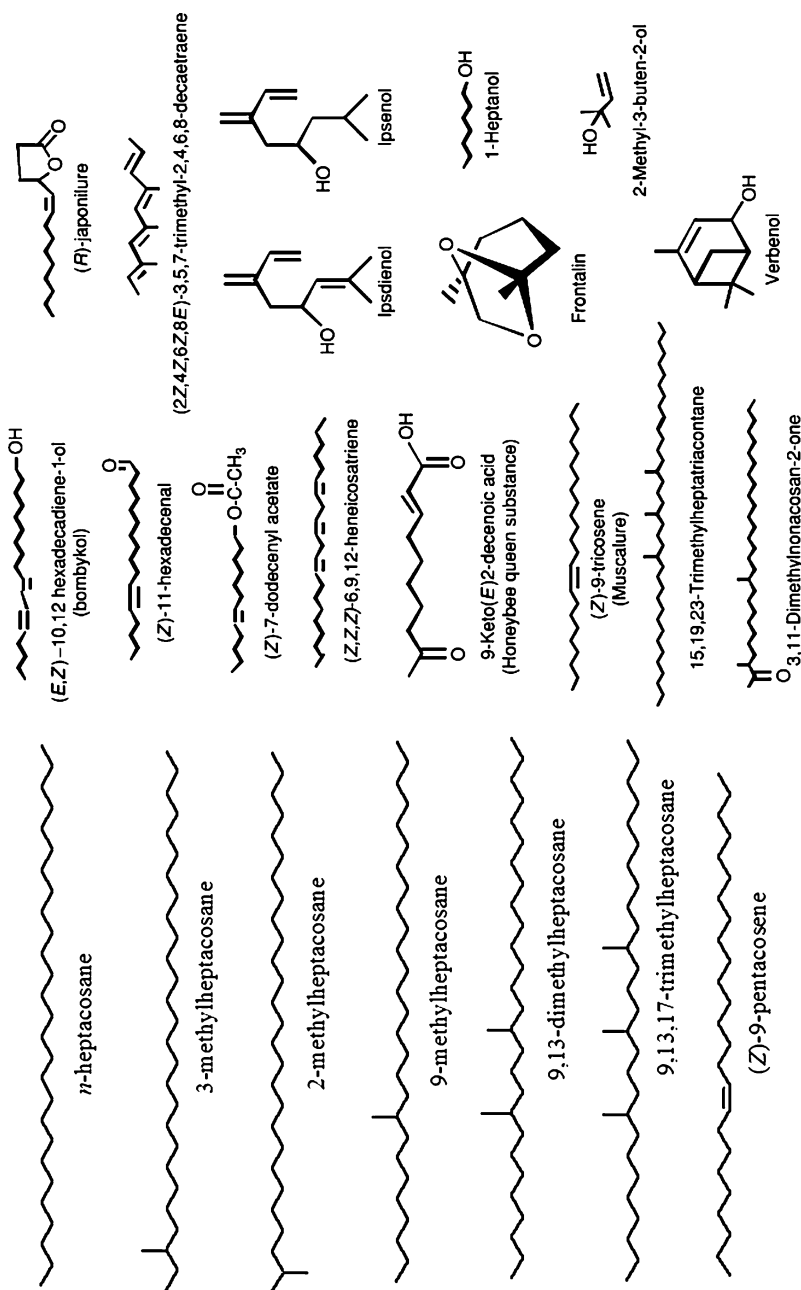


Fig. 1 Selected hydrocarbon and pheromone components representing major groups of compounds. Components were selected based on historical interest and work performed on their biosynthesis

monoterpenoid-derived pheromones ipsenol, ipsdienol, and frontalin de novo by modification of isoprenoid pathway products (Blomquist et al. 2010; Tittiger and Blomquist 2016) (Fig. 4).

2 Insect Cuticular Hydrocarbons

The hundreds of different cuticular hydrocarbon components reported in insects can be divided into three major classes: *n*-alkanes, saturated methyl-branched components, and unsaturated hydrocarbons (Fig. 1). There are examples of other types of hydrocarbons including unsaturated methyl-branched components, but these are rare and often are present in small amounts. Methyl-branched hydrocarbons have up to four methyl branches, and the alkenes have up to four double bonds (Ginzel and Blomquist 2016). Most of the alkenes have *cis* double bonds, and the positions of the double bonds, while often in the 9-position, can be found almost anywhere on the carbon chain among various insect groups.

A long standing question regarding the methyl-branched alkanes was “what is their absolute stereochemistry”? In a landmark study, the Millar laboratory (Bello et al. 2015) isolated 36 monomethylalkanes from 20 species of insects representing nine orders and, using digital polarimetry with comparisons to known standards, showed all to be “*R*.” The (*R*) configuration of the monomethylalkanes has interesting ramifications for the biosynthesis of methyl-branched hydrocarbons, indicating that the reduction of the alkene intermediate during biosynthesis is stereochemically specific. The stereochemistry of di- and trimethylalkanes has not been explored, but since they would likely be inserted by the same enzyme, the 2nd, 3rd, and 4th methyl groups would likely have the same orientation. Because of the assignment of the four groups on the chiral carbon atom, the second carbon atom on a dimethylalkane would likely have the “*S*” configuration.

The variety of chain lengths and the number and positions of the methyl branches and double bonds provides insects that use cuticular hydrocarbons in chemical communication with a large number of possible structures, the chemical equivalent of the variably colored plumage of birds. The chain lengths of insect hydrocarbons vary from about 21 up to 40 and in some rare cases even 50+ carbon atoms. There are a number of reviews of the chemistry of cuticular hydrocarbons and the use of mass spectrometry to identify components (Howard and Blomquist 2005; Blomquist 2010; Millar 2010). It is difficult to determine the positions of double bonds without first derivatizing the alkene. Dimethyldisulfide derivatives are the method of choice (Carlson et al. 1989) and methoxymercuration-demercuration has also been used (Blomquist et al. 1980).

Oxygenated components of cuticular lipids are also often associated with cuticular hydrocarbons. These include wax esters, sterols, primary and secondary alcohols, diols, ethers, epoxides, ketones, and other components that serve as semiochemicals in some cases (Buckner 2010).

For chemical communication, insects have evolved to form very complicated mixtures of *n*-, mono-, di-, tri-, and tetramethyl branched and unsaturated

components at apparently low cost, as they have modified existing components and use them both to restrict water loss and in chemical communication. A single component or a mixture of hydrocarbon components of the cuticular wax layer of many arthropods serve as a chemical signal to answer questions such as “Are you a member of my species? Are you the same sex as me?” For subsocial insects, “Are you a member of my family, cohort or group?” For eusocial insects, “Are you a member of my colony? Are you a member of my nest? To which caste do you belong? Are you a queen or perhaps brood? Are you a worker trying to convey to me the need to accomplish a certain task? Are you closely related kin?” And for many arthropods that exist asinquilines in the nest of social insects, “Can you recognize that I am alien?” (Howard and Blomquist 2005; Blomquist and Bagnères 2010; Ginzel and Blomquist 2016).

We now recognize that hydrocarbons serve critical roles as sex pheromones, kairomones, species and sex recognition cues, nestmate recognition, dominance and fertility cues, chemical mimicry, primer pheromones, task specific cues, as cues for maternal care of offspring (Blomquist and Bagnères 2010; Ginzel and Blomquist 2016), and even cues for overwintering sites of lady beetles (Wheeler and Cardé 2014). The complex mixture of hydrocarbons on the surface of insects allows them to be used in chemotaxonomy and they are gaining importance in forensic entomology (Drijfhout 2010; Braga et al. 2013). In retrospect, the diversity of hydrocarbons and hydrocarbon blends on insect cuticles might have suggested that hydrocarbons could play important roles in chemical communication. Only after the recognition of the number and variety of roles they do play in chemical communication have we come to more fully appreciate the importance of hydrocarbons in insect communication (Ginzel and Blomquist 2016).

3 Insect Pheromones

The pheromones of over 3000 insect species are now known. The website Pherobase.com is an up-to-date compilation of pheromones and other behavior-modifying chemicals found in insects and other organisms. While some of the cuticular hydrocarbons have dual functions, both restricting water loss and providing information, usually over short distances, the volatile pheromones are usually of lower molecular weight and have a singular purpose in chemical communication. Pheromones play critical roles in communication between insects and are usually species specific. Some of their roles in communication include attracting the opposite sex for mating (sex pheromones), attracting both sexes into aggregations for feeding and mating (aggregation pheromones), alerting other insects of danger (alarm pheromones), and creating feeding site paths (trail pheromones). These are all considered to be fast acting releaser pheromones while social insects utilize primer pheromones that control the long-term behavior of the receiver.

3.1 Lepidopteran Fatty Acid Derived (Type I Pheromones)

Within Lepidoptera (butterflies and moths), pheromones can be classified into two major groups, Type I and Type II, according to their chemical structures (Ando et al. 2004). Type I pheromones are the most abundant in Lepidoptera. They are comprised of straight chain acetates, aldehydes, and alcohols with chain lengths of 10–18 carbon atoms and as many as four double bonds. These compounds are usually synthesized de novo in pheromone glands. Most of these are produced from fatty acids and have carbon atom numbers from 7 to 29, with 12, 14, and 16 carbon atom components predominating. The modification of the carbonyl carbon atom of the fatty acid precursor results in acetate esters, alcohols, and aldehydes. Many of the lepidopteran pheromones have one or more double bonds with specific blends of (*Z*) and (*E*) isomers (Jurenka et al. 2017).

3.2 Polyene Hydrocarbons (Type II) Pheromones

Type II pheromones represent ~15% of known lepidopteran pheromones and are primarily restricted to the families Erebidae and Geometridae (Löfstedt et al. 2017). These polyunsaturated hydrocarbons and epoxy derivatives can be produced from diet-derived unsaturated fatty acids (i.e., linoleic and α -linolenic acid) and characterized by C₁₂–C₂₅ carbon atoms with double bonds located at carbon atom 3, 6, 9, 12, or 15 (all in the *Z*-configuration) and separated by methylene groups (Millar 2010).

In Coleoptera (beetles), volatile hydrocarbon pheromones can be found in a few species of beetles (Bartelt 2010). However, the most studied example of hydrocarbons as volatile pheromones is in the sap beetles (Coleoptera: Nitidulidae), with conjugated trienes and tetraenes serving as long-range pheromones in *Carpophilus* and *Colopterus* species (Bartelt 2010). These male-specific compounds all have alkyl branches and are on alternating carbon atoms, with double bonds in the *E*-configuration.

3.3 Terpenoid Pheromones

A number of coleopteran pheromones are isoprenoid in origin and many contain multiples of five carbon atoms (Francke et al. 1995). The shortest chain pheromone described is 2-methyl-3-buten-2-ol from *Ips typographus* (Lanne et al. 1989). Figure 1 shows a number of isoprenoid pheromone components, including ipsdienol, ipsenol, and frontalin. Frontalin contains eight carbon atoms but is clearly isoprenoid in origin (Barkawi et al. 2003; Keeling et al. 2013). In addition to isoprenoids, the pheromones from coleopterans also consist of components derived from fatty acids and components of unknown origin (Tittiger and Blomquist 2016).

3.4 Other Pheromones

Many dipteran (fly) pheromones are longer chain hydrocarbons (21 carbon atoms and longer) and function as short range or contact pheromones. The housefly sex pheromone consists of (*Z*)-9-tricosene (Fig. 1) an epoxide and ketone derived from this hydrocarbon, and methyl-branched alkanes (Blomquist 2003). Among the longest chain pheromones are the contact pheromones from the tsetse flies, which are often multimethyl branched hydrocarbons with up to 40 carbon atoms (Fig. 1) (Carlson et al. 1984, 1998). The role of long-chain hydrocarbons in chemical communication in insects has become increasingly recognized over the past two decades (Howard 1993; Howard and Blomquist 2005; Blomquist and Bagnères 2010; Ginzl and Blomquist 2016).

The honey bee queen retinue pheromone, consisting primarily of (*E*)-9-oxodec-2-enoic acid (9-ODA) and 9-hydroxy-2(*E*)-decenoic acid (9-HDA) (Callow and Johnston 1960; Barbier and Lederer 1960), is used by virgin queens to attract drones for mating. It is also used for attracting a retinue of worker bees inside the nest. It is produced by the queen mandibular gland and is one of the best understood of the social insect pheromones. Keeling et al. (2003) identified a number of additional compounds that function synergistically with 9-ODA and 9-HDA, making this a complex pheromone blend.

4 Hydrocarbon Biosynthesis

The biosynthesis of hydrocarbons occurs in specialized cells called oenocytes which are primarily found in the abdomen associated with epidermal cells or in some cases with fat body cells. The hydrocarbons produced by oenocytes are transported through the hemolymph by lipophorin to epidermal cells throughout the body for transfer to the cuticular surface. A variety of studies demonstrated this route of hydrocarbon biosynthesis and deposition; however, the mechanism of unloading and transport of hydrocarbon across the cuticle is still unknown. In the German cockroach only the abdominal sternites and tergites synthesize hydrocarbons which are then loaded onto hemolymph lipophorin for transport to sites of deposition (Gu et al. 1995). *Drosophila melanogaster* *Cyp4g1*, which encodes the cytochrome P450 catalyzing the terminal step in hydrocarbon production, is expressed predominantly in oenocytes (Qiu et al. 2012), and the fatty acid synthase (FAS) that is involved in producing 2-methylalkanes is also localized to the oenocytes (Chung et al. 2014).

The biosynthesis of insect hydrocarbons can be divided into four steps: (1) formation of the straight chain saturated, unsaturated and methyl-branched fatty acid precursors, (2) elongation of these fatty acids to very long chain fatty acyl-CoAs, (3) conversion of the very long chain fatty acyl-CoAs to aldehydes, and (4) the reductive decarbonylation of aldehydes to hydrocarbons and carbon dioxide (Fig. 2).

2-Methylalkanes arise from the elongation of the carbon skeleton of either valine (even number of carbon atoms in the chain) or isoleucine (odd number of carbon atoms in the chain) (Blailock et al. 1976). The gene that forms the *n*-2 methyl

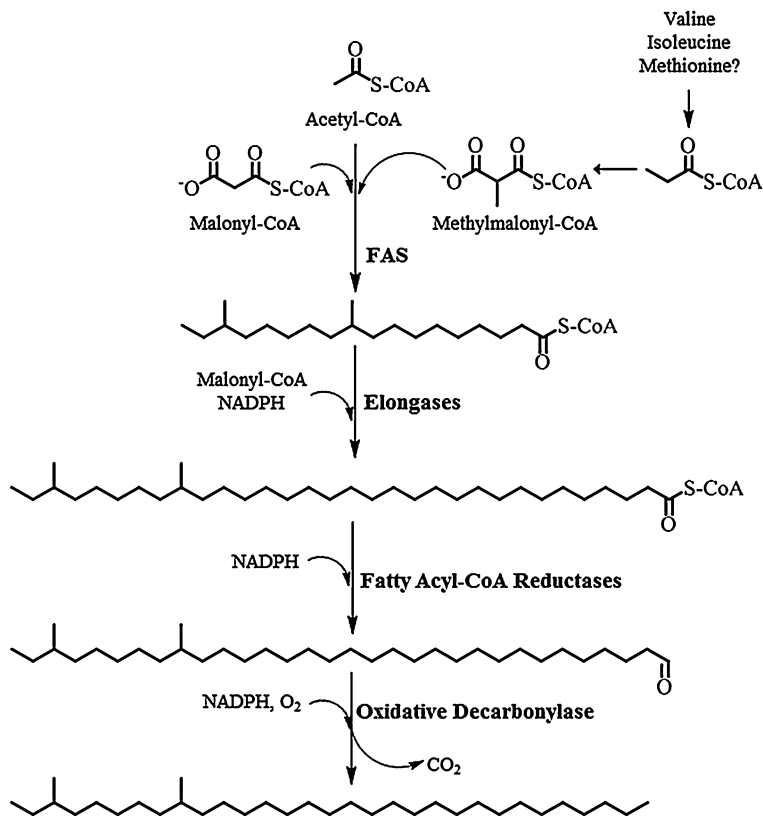


Fig. 2 Proposed biosynthetic pathways for insect cuticular hydrocarbons

branched fatty acid precursors to the 2-methylalkanes was identified in *D. melanogaster*. RNAi-mediated silencing showed that a fatty acid synthase gene (FASN^{CG3524}), one of three FAS genes in *D. melanogaster*, markedly decreased production of 2-methylalkanes but not *n*-alkanes or alkenes (Chung et al. 2014). This provides strong evidence that this FAS is required for 2-methylalkane synthesis. An alternate FAS, FASN^{CG3523}, is expressed in the fat body but not the oenocytes, suggesting that all the enzymes necessary for hydrocarbon production are localized to the oenocytes, but some fatty acids are imported to oenocytes for *n*-alkane production (Wicker-Thomas et al. 2015).

The 3-methyl- and internally branched methyl-branched hydrocarbons arise from the incorporation of propionate during chain elongation (Blomquist et al. 1975; Blomquist and Kearney 1976). The labeled carbon atom from [1-¹³C]propionate is found exclusively in the 4-position of 3-methylpentacosane as demonstrated by carbon-13 NMR in the American cockroach (Dwyer et al. 1981), indicating that it is incorporated as methylmalonyl-CoA as the second group added to the growing chain.

The internally branched methylalkanes also arise from the insertion of a propionate group, as a methylmalonyl-CoA, derived from valine, isoleucine, or methionine in place of a malonyl-CoA at specific points during chain elongation (Dillwith et al. 1982). ^{13}C -NMR studies were used to determine if the methyl branching group was inserted early or late in hydrocarbon formation and in every case the methyl branch is put on early in chain synthesis (Dwyer et al. 1981; Chase et al. 1990; Dillwith et al. 1982). An examination of the methyl-branched fatty acids from the integument of the German cockroach (Juarez et al. 1992) and the housefly (Blomquist et al. 1994) showed that small amounts of fatty acids with the appropriate methyl branching to serve as precursors to hydrocarbons were present. The presence of a unique FAS that is involved in synthesizing 2-methylalkanes was identified (Chung et al. 2014), suggesting that there may also be specific FASs that insert methylmalonyl-CoA at specific points during the formation of the methyl-branched fatty acids that are precursors to the internally branched hydrocarbons. All insect genomes studied to date appear to have two or more FASs, lending credibility to the hypothesis for a unique FAS that produces the internally methyl-branched fatty acid precursors to hydrocarbons.

Introduction of double bonds with desaturases has been investigated in *D. melanogaster*. Desaturase 1 (*desat1*) accepts both palmitic acid and stearic acid to form palmitoleic ($\Delta^9 \text{C}_{16:1}$) and oleic ($\Delta^9 \text{C}_{18:1}$) acids. This gene is expressed in both fat body and oenocytes and appears to play a role in general lipid metabolism and in hydrocarbon production (Wicker-Thomas and Chertemps 2010). A *desat2* converts myristic ($\text{C}_{14:0}$) to myristoleic ($\Delta^9 \text{C}_{14:1}$, an n-5 double bond) in flies that produce a 5,9-alkadiene (Dallerac et al. 2000). A second desaturation is required for females that produce 7,11-alkadiene, and RNA interference was used to study this gene (Chertemps et al. 2007). This desaturase is active only in females and thus is named *desatF* (Wicker-Thomas and Chertemps 2010).

The regulation of chain length to produce the specific blend of hydrocarbons often used in chemical communication appears to reside in the microsomal fatty acyl-CoA elongase reactions and the fatty acyl-CoA reductases. The American cockroach, *P. americana*, produces three major hydrocarbons: *n*-pentacosane, 3-methylpentacosane, and (*Z,Z*)-9,12-heptacosadiene (Baker et al. 1963). Studies with microsomes from integument tissue showed that stearyl-CoA was elongated up to a 26 carbon atom acyl-CoA that could serve as the precursor to *n*-pentacosane. In contrast, linoleoyl-CoA was readily elongated to 28 carbon atoms (but not longer) to serve as the precursor to the 27:2 hydrocarbon (Vaz et al. 1988).

The *D. melanogaster* genome has 19 elongases, with only two of them characterized to date (Wicker-Thomas and Chertemps 2010). Fatty acyl-CoA elongases catalyze the condensation of malonyl-CoA and a fatty acyl-CoA, and three additional steps are required to reduce the ketone to an alcohol, followed by dehydration and reduction. The elongase *eloF* from *D. melanogaster* (Chertemps et al. 2007) was expressed in yeast, and the results showed that *eloF* elongated both saturated and unsaturated fatty acids up to C_{30} . A dramatic decrease in C_{29} dienes and an increase in C_{25} dienes were observed when *eloF* was knocked down by RNAi, with a concomitant decrease in courtship and mating activities. Expression of *eloF* was

much higher in females than in males. These data support a role for *eloF* in regulating the chain length of hydrocarbon components.

Fatty acyl-CoA reductase (FAR) activity in microsomes of integument-enriched tissue from the housefly apparently produces aldehydes (Reed et al. 1994). Acyl-CoA reductases for production of primary alcohols have been described in insects for the production of pheromones in Lepidoptera (Antony et al. 2009). AmFAR1 converts C₁₄ to C₂₂ fatty acyl-CoAs to primary alcohols in the honey bee (Teerawanichpan et al. 2010). All acyl-CoA reductases described in insects to date (Lassance et al. 2013) reduce the acyl-CoA to the primary alcohol, and this raises the possibility that the acyl-CoA reductases in hydrocarbon production produce the alcohol which is then oxidized to the aldehyde by CYP4Gs as described below.

The mechanism of long-chain fatty acid derived hydrocarbon biosynthesis in insects is now coming into focus. It is now clear that very long chain fatty acyl-CoAs are reduced to aldehydes and then converted to hydrocarbons by the loss of the carbonyl carbon atom. Insects use an aerobic mechanism for oxidative decarbonylation of aldehydes, whereas plants use an anaerobic mechanism (Vioque and Kolattukudy 1997). This is consistent with plants appearing on land much earlier than insects and under oxygen levels that were much lower (Payne et al. 2009), while insects developed an aerobic mechanism for hydrocarbon production consistent with higher oxygen levels when their ancestors came to land. It is now clear that a cytochrome P450 is involved in the conversion of the aldehyde to hydrocarbon and carbon dioxide in a process that requires molecular oxygen and NADPH (Reed et al. 1994, 1995). All insects whose genomes have been studied have one or two CYP4G genes where one or both function in hydrocarbon biosynthesis (Balabanidou et al. 2016).

Full confirmation of the oxidative decarbonylation system proposed in insects was verified by the cloning, expression, and characterization of the enzymes involved. Integument-enriched cytochrome P450 cDNAs in the housefly *Musca domestica* were isolated (Qiu et al. 2012). One of these, CYP4G2, has 71.7% amino acid identity and 81.8% similarity to its ortholog, CYP4G1, from *D. melanogaster*. Numerous attempts to express CYP4G2 by itself (Blomquist et al. unpublished) led to inactive enzyme that did produce the 450 nm CO difference spectrum peak that is characteristic of all correctly folded P450s. The relatively high ratio of cytochrome P450 reductase (CPR) to P450 in oenocytes (Qiu et al. 2012) suggested the possibility that CPR was needed for CYP4G2 to properly fold. Expression of the CYP4G2-CPR fusion protein yielded an enzyme that in the presence of CO absorbed at 450 nm and converted long chain aldehydes to alkanes (Qiu et al. 2012). Similarly, production and assay of aCYP4G16-CPR fusion protein (CYP4G16 being from *Anopheles gambiae*) showed hydrocarbon production (Balabanidou et al. 2016). CYP4G16 associates with the cell membrane of oenocytes and not the endoplasmic reticulum suggesting its hydrocarbon products could be directly loaded onto lipophorin for transport (Blomquist and Bagnères 2010). Further work is needed on the subcellular location of enzymes involved in hydrocarbon synthesis.

5 Pheromone Biosynthesis

There is much variability among insects in the anatomical location of volatile pheromone production, just as there are many differences in the gross morphology and function of pheromone producing tissue. Complexity varies from simple unicellular glands distributed throughout the integument to elaborate internal cellular aggregates connected to a reservoir. Of the orders emphasized in this chapter (Lepidoptera, Coleoptera, and Diptera), the most common location for pheromone production is the abdomen. There are excellent reviews of the ultrastructure of exocrine cells in general (Percy-Cunningham and MacDonald 1987; Quennedey 1998; Ma and Ramaswamy 2003) and social insects in particular (Billen and Morgan 1998). Definitive proof that pheromone production and release occur in certain tissues comes from studies where the isolated tissue incorporates labeled precursors into pheromone components.

By the mid-1980s, studies on biosynthetic pathways of pheromones for a limited number of species were underway, and work was progressing toward the characterization of some of the unique enzymes involved (Prestwich and Blomquist 1987). It became apparent that the products and intermediates of normal metabolism, particularly those of the fatty acid and isoprenoid pathways, were modified by a few specific enzymes in pheromone gland tissue to produce the myriad of pheromone molecules. Many of the lepidopteran pheromones could be formed by the appropriate interplay of highly selective chain shortening and a unique $\Delta 11$ and other desaturases followed by modification of the carboxyl carbon atom (Bjostad et al. 1987). This work has been extended, and a clear understanding of the biosynthetic pathways for many of the lepidopteran pheromones is now known (Jurenka 2003; Jurenka et al. 2017). The $\Delta 11$ and other pheromone-specific desaturases in Lepidoptera have been characterized at the molecular level (Knipple and Roelofs 2003; Lassance et al. 2010). In some insects, fatty acid elongation followed by loss of the carboxyl carbon atom produces the hydrocarbon pheromones, and this process includes examples of lepidopterans (Jurenka 2003), dipterans (Blomquist 2003; Jallon and Wicker-Thomas 2003), the German cockroach (Schal et al. 2003), and the social insects (Blomquist and Howard 2003).

5.1 Alcohol, Aldehyde, and Acetate Ester Pheromones

A combination of acetyl-CoA carboxylase and fatty acid synthase produce saturated fatty acids. Although no direct enzymatic studies have been conducted using pheromone gland cells, these enzymes are presumably similar to enzymes found in other cell types. Labeling studies conducted with acetate indicated that pheromone glands produce 16:0 and 18:0 acid saturated products (Bjostad and Roelofs 1984; Tang et al. 1989; Jurenka et al. 1994). Indirect evidence showed that when the activity of acetyl-CoA carboxylase was inhibited by herbicides, sex pheromone biosynthesis was also inhibited in *Helicoverpa armigera* and *Plodia interpunctella* (Eliyahu et al. 2003).

Desaturases introduce a double bond into the fatty acid chain. A variety of desaturases identified so far including enzymes that act on saturated and mono-unsaturated substrates are involved in the biosynthesis of female moth sex pheromones. These include $\Delta 5$ (Foster and Roelofs 1996; Hagström et al. 2013a), $\Delta 9$ (Löfstedt and Bengtsson 1988), $\Delta 10$ (Foster and Roelofs 1988), $\Delta 11$ (Bjostad and Roelofs 1983), and $\Delta 14$ (Zhao et al. 1990) desaturases that utilize saturated substrates. The combination of these desaturases along with chain shortening can account for the majority of double bond positions in the various chain-length monounsaturated pheromones so far identified (Roelofs and Wolf 1988). Figure 3 illustrates the large number of monounsaturated compounds that can be generated through a combination of monounsaturation and chain shortening. Addition of

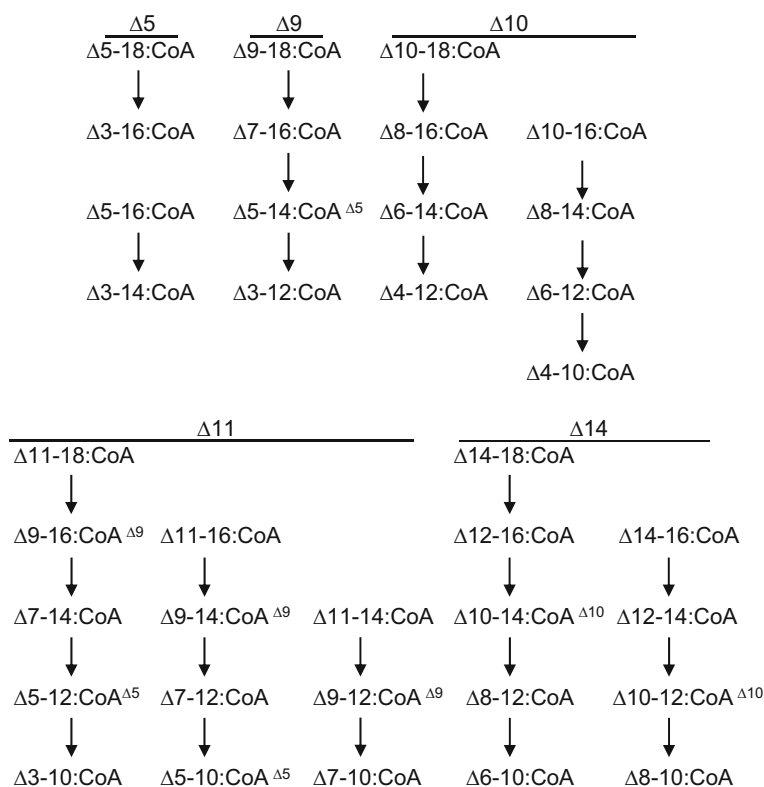


Fig. 3 Biosynthesis of lepidopteran monounsaturated pheromones. A combination of desaturation and chain shortening can produce a variety of acyl-CoA precursors that can be modified to form acetate esters, aldehydes, and alcohols. The indicated desaturase at the top of each column introduces a double bond into the first acyl-CoA, and the arrow pointing down indicates limited chain-shortening by two carbons. A superscript indicates the acyl-CoA could be produced by the desaturase without chain-shortening. Modification of all 16-, 14-, 12-, and 10-carbon acyl-CoA derivatives on the carbonyl carbon can account for the majority of monounsaturated acetate esters, aldehydes, and alcohols identified as moth sex pheromones

various functional groups, acetate esters, alcohols, and aldehydes increases the potential number of pheromone components. It is important to note that some intermediate compounds could be produced in two different ways and the order in which desaturation and chain-shortening occur must be determined experimentally.

Some pheromone components are dienes and these can be produced by either the action of two desaturases or one desaturase and isomerization around the double bond. Some dienes with a 6,9-double bond configuration are produced using dietary linoleic acid. Desaturases that utilize monounsaturated acyl-CoA substrates include $\Delta 5$ (Ono et al. 2002; Hagström et al. 2013a), $\Delta 9$ (Martinez et al. 1990), $\Delta 11$ (Foster and Roelofs 1990), $\Delta 12$ (Jurenka 1997), and $\Delta 13$ (Arsequell et al. 1990). These can act sequentially to produce the diene (Foster and Roelofs 1990; Jurenka 1997), or conjugated dienes could be produced by the action of one desaturase followed by isomerization (Ando et al. 1988; Löfstedt and Bengtsson 1988; Fang et al. 1995a). A unique $\Delta 6$ desaturase has been found in *Antheraea pernyi* that couples with a $\Delta 11$ desaturase to produce the (*E,Z*)-6,11-hexadecadienoic acid intermediate to the aldehyde and acetate ester pheromone (Wang et al. 2010a).

The biosynthesis of triene pheromone components has not been extensively investigated. Pheromones with a triene double bond system, that is, *n*-3 (3,6,9-), are produced from dietary α -linolenic acid (Choi et al. 2007; Millar 2010). This was demonstrated in the saltmarsh caterpillar, *Estigmene acrea*, and the ruby tiger moth, *Phragmatobia fuliginosa* (Rule and Roelofs 1989). Moths in the families Geometridae and Erbidae apparently utilize linoleic and α -linolenic acid as precursors for their pheromones. Most of these pheromones are produced by chain elongation and decarboxylation to form hydrocarbons. Oxygen is added across one of the double bonds in the polyunsaturated hydrocarbon to produce an epoxide (Millar 2010). A unique terminal desaturase was found to be involved in production of 1,23,26,29-nonadecatetraene, the pheromone of the winter moth, *Operophtera brumata*, via a 20 carbon atom intermediated fatty acid derived from linolenic acid (Ding et al. 2011).

A study using *Manduca sexta* identified a desaturase with Z11-desaturase/conjugase activity (Matouskova et al. 2007). Additional desaturases with Z11, Z/E14, and E13 desaturation activity were also identified (Buček et al. 2015). Site directed mutagenesis indicated that a single amino acid substitution could change the Z11-desaturase/conjugase enzyme to one that produces Z/E14 products (Buček et al. 2015).

Insects in general have the ability to shorten long-chain fatty acids to specific shorter chain lengths (Stanley-Samuelson et al. 1988). This chain-shortening pathway has not been characterized at the enzymatic level in insects. It presumably is similar to the characterized pathway as it occurs in vertebrates which is essentially a partial β -oxidation pathway located in peroxisomes (Hashimoto 1996). The evidence for limited chain-shortening enzymes in pheromone glands was originally demonstrated by Bjostad and Roelofs (1983) using the cabbage looper moth, *T. ni* in which it was shown that Z11-16:acid labeled the intermediate fatty acid Z7-12:acid. A similar study, using *Argyrotaenia velutinana*, demonstrated that deuterium-labeled

16:acid was chain-shortened to 14:acid, which was used to make *Z* and *E*11–14:acid (Bjostad and Roelofs 1984). Since then considerable evidence in a number of moths has accumulated to indicate that limited chain shortening occurs in a variety of pheromone biosynthetic pathways (Jurenka et al. 2017).

Once a specific chain-length pheromone intermediate that has the appropriate double bonds is produced, the carbonyl carbon atom is modified to form a functional group. The majority of oxygenated pheromone components are acetate esters, alcohols, and aldehydes. Production of these components requires the reduction of a fatty-acyl precursor to an alcohol that is catalyzed by a fatty acyl reductase. The fatty acyl reductase has been identified in *B. mori* for production of bombykol (Moto et al. 2003). It has been functionally characterized by expression in yeast cells and shown to preferentially reduce *E,Z*-10,12–16:acid, which thus forms bombykol (Matsumoto 2010).

Fatty acyl reductases have subsequently been identified in several other moths in which the alcohol serves as an intermediate for production of acetate esters. The reductase has been identified in the adzuki bean borer *O. scapulalis*, European corn borer *O. nubilalis*, and small ermine moths *Yponomeuta* spp. (Antony et al. 2009; Lassance et al. 2010; Liénard et al. 2010). In the European corn borer, two reductases were identified: one from each of the two strains that produce primarily Z11–14:OAc or E11–14:OAc. The reductase from each strain preferentially reduces Z11–14:acid or E11–14:acid resulting in a strain-specific pheromone blend (Lassance et al. 2010). Sequences of the two desaturases exhibited a 3.8% nucleotide divergence and corresponding 7.5% amino acid divergence. These small differences apparently change the substrate preference for the enzyme (Lassance et al. 2013). The reductases from three species of *Yponomeuta* have about 36% amino acid identity with the *Ostrinia* reductases, but they have a broad substrate specificity (Liénard et al. 2010). The pheromone gland fatty acyl reductases found in four species of heliothine moths also had a relatively broad substrate specificity (Hagström et al. 2012) as did a reductase identified from *Spodoptera littoralis* (Carot-Sans et al. 2015). Fatty acid reductases from eight species of *Ostrinia* were compared, and it was determined that amino acid changes in the enzyme active site could account for changes in reductase activity with the net result of changes in pheromone composition (Lassance et al. 2013). The subcellular location of the fatty acyl reductase found in pheromone glands is the endoplasmic reticulum (Hagström et al. 2013b). Two fatty acyl reductases were also found in the butterfly, *B. anynana*, and are used in the biosynthesis of male courtship pheromone components (Liénard et al. 2014).

Formation of aldehydes requires the oxidation of primary alcohols, and a cuticular oxidase has been characterized from pheromone glands of *Helicoverpa zea* and *Manduca sexta* that produce aldehydes as pheromones (Teal and Tumlinson 1988; Fang et al. 1995b). In those insects that utilize both an alcohol and an aldehyde as part of their pheromone, it is unclear how the production of both components occurs. Luxova and Svatos (2006) isolated a membrane-bound alcohol oxidase from *M. sexta* pheromone glands with high specificity for primary alcohols, as occurs in yeast alcohol dehydrogenase. Oxidase activity of the fall webworm, *Hyphantria*

cunea, was determined to occur in pheromone glands but had broad substrate specificity (Kiyota et al. 2011).

Production of acetate ester pheromone components utilizes acetyl-CoA:fatty alcohol acetyltransferase that converts a fatty alcohol to an acetate ester (Morse and Meighen 1987a). Therefore, alcohols could be utilized as substrates for both aldehyde and acetate ester formation. Morse and Meighen (1987a) first demonstrated its presence in the spruce budworm, *Choristoneura fumiferana*, where it is involved in producing the acetate ester that serves as a precursor to the aldehyde pheromone (Morse and Meighen 1987b). In some other tortricids, *A. velutinana*, *C. rosaceana*, and *Platynota idaeusalis*, an in vitro enzyme assay was utilized to demonstrate specificity of the acetyltransferase for the *Z* isomer of 11–14:OH (Jurenka and Roelofs 1989). This specificity contributes to the final ratio of pheromone components. These results indicate that the family Tortricidae has members that have an acetyltransferase that is specific for the *Z* isomer of monounsaturated fatty alcohols. In contrast, several studies have shown no substrate preference for the acetyltransferase in other moths (Bestmann et al. 1987; Teal and Tumlinson 1987; Jurenka and Roelofs 1989). Therefore, this unique acetyltransferase apparently evolved within the Tortricidae.

The use of RNAi has illustrated the function of many of these enzymes in *B. mori*. Injecting dsRNA to silence the Z11/Δ10,12 desaturase, fatty acyl reductase, and acyl-CoA-binding protein into pupae resulted in a reduction of gene transcripts and sex pheromone production in the adult female (Ohnishi et al. 2006; Matsumoto et al. 2007). Matsumoto (2010) reviewed the molecular mechanisms of pheromone production in moths.

More recent studies have examined the transcriptomes or sequenced genomes of insects. For example, Vogel et al. (2010) identified 8310 putative genes in the pheromone gland of *Heliothis virescens*, 6435 of which were unique to the pheromone gland (by comparison with larval tissue). Comparison with EST databases from other moth species revealed 86 candidate genes encoding enzymes that could be involved in moth sex pheromone biosynthesis, including two Δ11 and six Δ9 desaturases. Other transcriptomic studies have been conducted using pheromone glands from various moths (*Chilo suppressalis*, Xia et al. 2015; *Helicoverpa armigera* and *Helicoverpa assulta*, Li et al. 2015; *Agrotis segetum*, Strandh et al. 2008, 2009; Ding and Löfstedt 2015; *Agrotis ipsilon*, Gu et al. 2013; *Sesamia inferens*, Zhang et al. 2014a; *Grapholita molesta* and *Grapholita dimorpha*, Jung and Kim 2014; *Ephestia cautella*, Antony et al. 2015). These transcriptomic studies have revealed the presence of all the enzymes involved in pheromone biosynthesis as described above. However, the acetyltransferase and oxidase enzymes have yet to be functionally characterized, and it remains unknown as to which transcript(s) are functional in pheromone glands.

The heterologous expression of pheromone biosynthetic enzymes in various expression systems (primarily yeast cells) has aided in the characterization of desaturases and fatty-acyl-reductases as described above. Co-expression of a desaturase and fatty-acyl-reductase in yeast led to the production of a moth sex pheromone component Z11–16:OH (Hagström et al. 2013c). Transformation of plants

with moth pheromone biosynthetic enzymes could provide a source of pure pheromones that could be used in mating control strategies. Introduction of a $\Delta 11$ desaturase into the plant *Nicotiana tabacum* produced Z11–16:acid that could be extracted and chemically modified to produce sex pheromones (Nesnerova et al. 2004). Transformation of plants to produce a pheromone as a product was achieved by introducing an (*E*)- β -farnesene synthase gene into *Arabidopsis thaliana*, which produced the aphid alarm pheromone, (*E*)- β -farnesene (Beale et al. 2006). Transformation of the plant *Nicotiana benthamiana* with moth $\Delta 11$ desaturases and fatty-acyl-reductases coupled with a plant thioesterase and a diacylglycerol acetyltransferase produced E/Z-14:OAc and Z11–16:OAc products, which are sex pheromone components of a number of moths (Ding et al. 2014).

Most female moths utilize a blend of components produced in a specific ratio for pheromone attraction of conspecific males. A major question is how these species-specific ratios of components are produced. Research from several sources indicates that these ratios are produced by the inherent specificity of certain enzymes present in the biosynthetic pathways. The combination of these enzymes acting in concert produces the species-specific pheromone blend.

5.2 Polyene Hydrocarbons

Moths in the families Geometridae, Amatidae, Lyonetiidae, and Erbididae utilize hydrocarbons or epoxides of hydrocarbons as their sex pheromones. Biosynthesis of hydrocarbons occurs in oenocyte cells that are associated with either epidermal cells or fat body cells (Romer 1991). Once the hydrocarbons are biosynthesized, they are transported to the sex pheromone gland by lipophorin (Schal et al. 1998). When the transport of hydrocarbon sex pheromones in arctiid moths was investigated in detail by Schal et al. (1998), it was found that a very specific uptake was occurring at pheromone glands. Lipophorin was shown to contain both the sex pheromone and cuticular hydrocarbons; however, only the pheromone gland had the sex pheromone. Other studies have shown similar pathways in other moths (Jurenka and Subchev 2000; Subchev and Jurenka 2001; Wang et al. 2013).

A few even-chain-length hydrocarbon sex pheromones have been identified that also have 3,6,9- or 6,9-double bond configurations (Millar 2010), indicating that they are derived from linolenic or linoleic acids. A study using the winter moth, *Erannis bajaria*, which produces Z3,Z6,Z9–18:Hc, has demonstrated how these even-chained hydrocarbons are produced (Goller et al. 2007). The pathway involves chain-elongating α -linolenic acid to Z11,Z14,Z17–20:acid followed by the key step of α -oxidation to produce Z10,Z13,Z16–19:acid. The 19C acid is then converted to the hydrocarbon Z3,Z6,Z9–18:Hc. The odd-chain-length pheromone component Z3,Z6,Z9–19:Hc is formed from Z11,Z14,Z17–20:acid as usual for odd-chain-length hydrocarbons.

A study using the gypsy moth, *Lymantria dispar*, illustrates the overall pathways involved in production of epoxide pheromone components (Jurenka et al. 2003). This insect uses disparlure, 2me-18:7,8Epoxy, as a pheromone component.

Incubation of isolated abdominal epidermal tissue with deuterium-labeled valine resulted in incorporation into 2me-Z7-18:Hc. This indicates that the oenocyte cells associated with the epidermal tissues biosynthesize 2me-Z7-18:Hc using the carbon atoms of valine to initiate the chain. The double bond is probably introduced by a Δ^{12} -desaturase as determined by using specific deuterium-labeled intermediates. Hemolymph transport of 2me-Z7-18:Hc is indicated by the finding of this alkene in the hemolymph (Jurenka and Subchev 2000). Demonstration that 2me-Z7-18:Hc is converted to the epoxide in the pheromone gland was shown by using deuterium-labeled 2me-Z7-18:Hc and incubation with isolated pheromone glands. Disparlure is a stereoisomer that has the 7*R*, 8*S* or (+) configuration, and chiral chromatography indicated that only the (+)-isomer was produced by pheromone glands (Jurenka et al. 2003).

A few moths, primarily in the families Pyralidae and Crambidae, utilize a combination of hydrocarbon and fatty-acid-derived pheromone components. The navel orangeworm moth is one of these, and labeling studies supported different pathways producing the hydrocarbons and the aldehydes. The aldehydes were produced through a fatty acid biosynthetic route in pheromone glands, while the hydrocarbons were produced by oenocytes and transported to the pheromone gland for release (Wang et al. 2010b).

5.3 Terpenoid Pheromones

Pheromone biosynthesis in the Coleoptera is as diverse as the taxon involving several types of pheromone biosynthetic pathways has been demonstrated (Vanderwel and Oehlschlager 1987; Vanderwel 1994; Seybold and Vanderwel 2003; Tittiger 2003; Blomquist et al. 2010; Tittiger and Blomquist 2016). Bark beetles can generate pheromones either by modification of dietary host compounds or de novo biosynthesis, with the latter accounting for the majority of beetle pheromone components (Tittiger and Blomquist 2016).

Most of the knowledge about beetle pheromone biosynthesis and endocrine regulation comes from studies of various bark beetles, especially *Ips* and *Dendroctonus* species (Scolytidae). Some bark beetles may modify fatty acyl or amino acid precursors (Vanderwel and Oehlschlager 1987; Birgersson et al. 1990); however, the majority of pheromone components are isoprenoid (Schlyter and Birgersson 1999; Seybold et al. 2000).

Our understanding of the origin of bark beetle pheromone components underwent a paradigm shift in the 1990s. Until then, it was widely accepted that bark beetles obtained their pheromone components by simple modification of host tree dietary precursors (Bordon 1985; Vanderwel and Oehlschlager 1987; Vanderwel 1994). Key genes in pheromone production, including *HMG-R* and *HMG-CoA synthase* (*HMG-S*), have expression patterns consistent with their roles in participating in de novo isoprenoid pheromone biosynthesis (Tittiger et al. 1999; Keeling et al. 2004, 2006). A geranyl diphosphate synthase/myrcene synthase (GPPS/MS) cDNA from *Ips pini* was also isolated, functionally expressed, and modeled (Gilg et al. 2005, 2009). The

existence of this novel enzyme argues strongly for the evolution of de novo pheromone biosynthetic capacity in bark beetles. Taken together, the data emerging from *Ips* species overwhelmingly indicate the de novo production of some monoterpene pheromone components.

The capacity for de novo biosynthesis does not preclude the conversion of host precursors to pheromone components. For example, the incorporation of acetate and mevalonolactone into ipsdienol and ipsenol proceeds through the conversion of geranyl diphosphate to myrcene, which could then be directly hydroxylated to ipsdienol and *E*-myrcenol and indirectly, perhaps through a ketone intermediate, to ipsenol (Martin et al. 2003). In this scheme, host myrcene ingested during feeding would enter the de novo pathway downstream of geranyl diphosphate. Similarly, cotton plant monoterpenes (myrcene and limonene) could enter a de novo biosynthetic pathway to grandlure in *Anthonomus grandis*. The question then arises as to whether de novo biosynthesis or host precursor conversion is the preferred route to pheromone production. Male *I. pini* exposed to myrcene vapors produce a racemic mixture of ipsdienol, whereas the naturally occurring pheromone of Western *I. pini* is about 95:5 (–)/(+) ratio (Seybold et al., 1995).

A proposed biosynthetic scheme for several coleopteran isoprenoid pheromone components is presented in Fig. 4. Hemiterpene pheromone components of bark beetles are similarly synthesized de novo. Lanne et al. (1989) demonstrated the incorporation of labeled acetate, glucose, and mevalonate into 2-methyl-3-buten-2-ol in *I. typographus*. This also argues for the de novo synthesis of 3-methyl-3-buten-1-ol and 3-methyl-2-buten-1-ol. The mevalonate pathway intermediate, dimethylallyl diphosphate, likely provides the carbon skeleton for 3-methyl-2-buten-1-ol by dephosphorylation. The other five-carbon atom intermediate, isopentenyl diphosphate, could be directly converted to 3-methyl-3-buten-1-ol and, perhaps through several steps, to 2-methyl-3-buten-2-ol.

Geranyl diphosphate synthase (GPPS) catalyzes the condensation of dimethylallyl diphosphate (DMAPP) and isopentenyl diphosphate (IPP) to form geranyl diphosphate (GPP). GPP is the precursor of monoterpenes, a large family of naturally occurring C₁₀ compounds predominately found in plants. Martin et al. (2003) showed myrcene synthase activity in *I. paraconfusus*. Conclusive evidence for de novo monoterpene biosynthesis in an animal was obtained by assays of functionally expressed recombinant GPPS/MS, which showed geranyl diphosphate as its major product but can also produce myrcene (Gilg et al. 2009) and thus likely provides the myrcene synthase activity reported by Martin et al. (2003).

Cytochrome P450 monooxygenases (P450s) constitute a diverse superfamily of enzymes with crucial roles in the metabolism of a wide range of both endogenous and foreign compounds. Insect genomes have approximately 100 cytochrome P450 genes, so the preliminary identification of *I. pini* myrcene hydroxylase relied on expression profiling. CYP9T2 was the only P450 with an expression pattern consistent with pheromone biosynthesis. A functional assay using microsomes of Sf9 cells infected with baculoviral constructs encoding CYP9T2 and housefly (*M. domestica*) P450 reductase (CPR) demonstrated that CYP9T2 is a myrcene hydroxylase that converts myrcene to ipsdienol (Sandstrom et al. 2006).

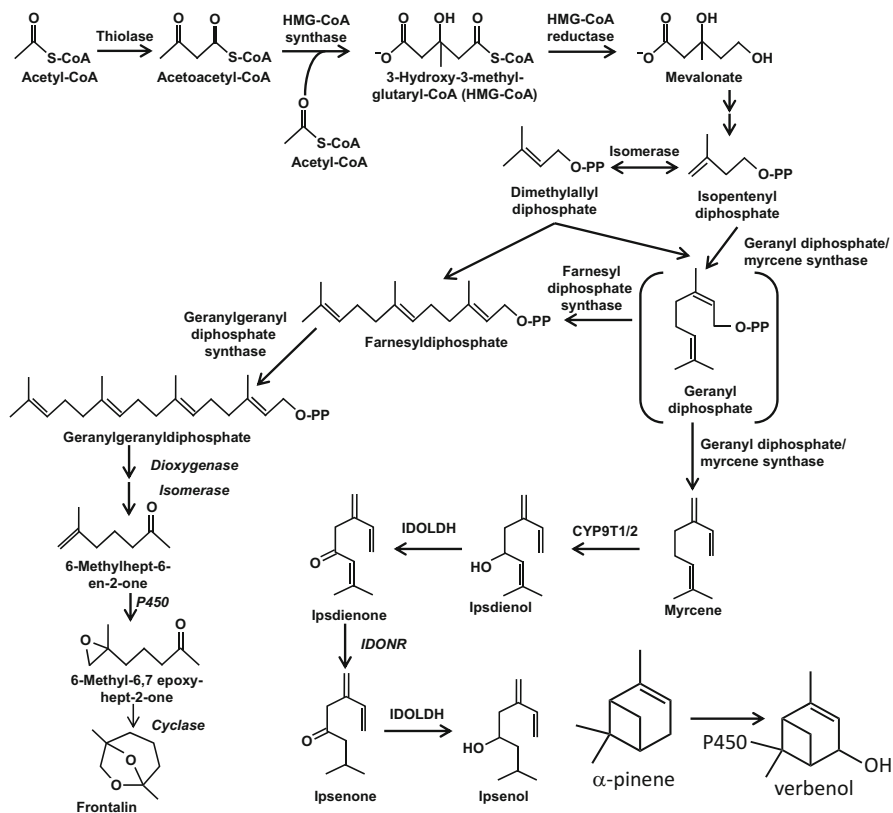


Fig. 4 Proposed biosynthetic pathways for monoterpene pheromone components in the Coleoptera. Intermediates and products are in normal font. Enzymes are in **bold**, and enzymes that have not been identified or characterized are in *bold italics*

5.4 Other Pheromones

Recombinant CYP9T2 produces 81% *R*-(−)-ipsdienol, whereas the major monoterpene aggregation pheromone component released by *I. pini* is 95% *R*-(−)-ipsdienol. Similarly, the ortholog (CYP9T1) from *Ips confusus* produces a similar ratio of 85% *R*-(−)- to *S*-(+)-ipsdienol as does CYP9T2, even though the pheromone blend from *I. confusus* is approximately a 10/90 *R*-(−)/*S*-(+) (Sandstrom et al. 2008). These data strongly suggest that enzymatic steps downstream from the hydroxylation step are required to produce the final enantiomeric blend. Candidate enzymes involved in “tuning” the enantiomeric ratio of ipsdienol were first identified from microarray and PCR data, leading to the eventual characterization of ipsdienol dehydrogenase (IDOLDH). IDOLDH is a short chain dehydrogenase/reductase (SDR) (Kavanagh et al. 2008). IDOLDH readily oxidizes *R*-(−)-ipsdienol to ipsdienone and stereo-specifically catalyzes the reverse reaction (Figuroa-Teran et al. 2012, 2016).

Dendroctonus ponderosae isoprenoid pheromone components include frontalin and (–)-*trans*-verbenol. Similar to the situation in *Ips* spp., frontalin biosynthesis requires carbon to be shunted from the mevalonate pathway at some point. Microarray data show coordinate regulation between *HMGR*, *HMGS* (both encoding enzymes acting early in the pathway), and a putative *GGPPS* (Aw et al. 2010). mRNA levels for all three genes are highest in males after they have mated with females, consistent with frontalin production. The activity of the putative *GGPPS* verified that it produced C₂₀ monoterpenes and RNAi inhibition markedly decreased frontalin production (Keeling et al. 2013). An RNA-seq study (Nadeau et al. 2017) complemented and verified many of the conclusions from RT-PCR data and pointed out several new target genes in the *D. ponderosa* pheromone biosynthetic pathway.

A second isoprenoid pheromone component in *D. ponderosae* is (–)-*trans*-verbenol, which is a hydroxylated derivative of α -pinene derivative. It is produced by females when they enter a host tree. Pierce et al. (1987) used surveys of volatiles and extracts of female *D. ponderosae* to hypothesize that (–)-*trans*-verbenol arises from a dedicated monoterpene hydroxylating activity specific to (–)- α -pinene, while a second activity hydroxylates a broad range of monoterpene resin components as a detoxification mechanism.

Numerous beetle genera use modified fatty-acyl compounds as pheromone components. Less is known about their biosynthesis compared to that of isoprenoid pheromones, but the same general strategy of modifying or combining existing biosynthetic pathways is conserved.

exo-Brevicommin (*exo*-7-Ethyl-5-methyl-6,8-dioxabicyclo[3.2.1]octane) is a bicyclic acetal that synergizes the aggregation effect of female-produced *trans*-verbenol in *D. ponderosae*. It is produced in the fat body of newly emerged males (but not females) (Song et al. 2014), and production drops when the males arrive at a new tree and mate (Pureswaran et al. 2000). While many of the steps required to convert longer chain fatty acyl-CoA precursors to *exo*-brevicommin remain uncharacterized, two enzymes have been identified: 6(*Z*)-nonen-2-one dehydrogenase (*ZnoDH*) oxidizes 6(*Z*)-nonen-2-ol to its corresponding methyl-ketone, which is then epoxidized by *Cyp6CR1* to 6,7-epoxy-nonen-2-one, the direct precursor that is then cyclized to *exo*-brevicommin (Song et al. 2014b).

For some beetles, the modifications to produce pheromones are relatively minor. For example, *Attagenus* spp. (Dermestidae) myristic acid may be desaturated at the $\Delta 5$ and $\Delta 7$ positions to produce tetradecadienoic acid pheromone components. The stereochemistries of the double bonds apparently provide specificity between species (Fukui et al. 1977). It is unclear whether the short-chain fatty acid precursors to these pheromone components are synthesized through normal fatty acid elongations or are the β -oxidation products of longer fatty acids. For other beetles, modifications can become more complex. Female *Tenebrio molitor* produce 4-methyl-1-nonanol from propionyl-, malonyl-, and methylmalonyl-precursors (Islam et al. 1999). This is an example of carbon being shunted away from fatty-acyl elongation before long fatty acids are completed. The use of methylmalonate to produce methyl-branched hydrocarbons is well established in other insect systems (Ginzel and Blomquist 2016),

though it is unknown if beetles have a secondary fatty acyl synthase which, similar to that in houseflies, incorporates methylmalonyl-CoA precursors efficiently.

The flexibility of the fatty acid biosynthetic pathway is extended in some nitidulid beetles (*Carpophilus* spp.), where males use propionate and butyrate (presumably as methylmalonate and ethylmalonate) to make methyl and ethyl-branched triene and tetraene pheromone components (Fig. 1), apparently also via the fatty acid biosynthetic pathway (Bartelt et al. 1992). The branched hydrocarbons generally have 10–12 carbon atom backbones with conjugated double bonds. In contrast to other systems, where pheromone component biosynthesis is highly specific, *Carpophilus* spp. males produce a mixture of related structures, some of which act as pheromones and some of which do not. Since di-substituted tetraenes are less abundant than mono- or unsubstituted tetraenes, it appears that nonacyl units placed in the growing hydrocarbon chains represent “mistakes” made by a synthesis machinery with a low stringency for substrate selection (Bartelt 1999). Such nonspecific hydrocarbon biosynthesis may serve speciation, since changes in antennal receptivity may accommodate preexisting compounds (Bartelt 1999). Interestingly, the desaturated nature of these hydrocarbons is not due to fatty acyl desaturases, but to the inactivity of enoyl-ACP reductase during biosynthesis so that the enoyl-ACP intermediate formed during elongation is not reduced (Petroski et al. 1994). This suggests that carbon is shunted out of the fatty acid biosynthetic pathway when the chains are of the correct length, similar to the situation in *T. molitor*.

Rather than modifying the normal biosynthetic pathway to produce pheromone components, some beetles modify normal products of the pathway. For example, lactone pheromone components of some scarab beetles are produced by the stereospecific alterations of long chain fatty acids. Female *Anomala japonica* (Scarabaeidae) are perhaps best studied among scarab beetles for the biosynthesis of japonilure and buibuilactone, which involves the successive Δ^9 desaturation, hydroxylation, two rounds of β -oxidation to shorten the chain length, and cyclization of stearic and palmitic acids (Leal et al. 1999). Of all these, only the hydroxylation step appears to be stereospecific (Leal 1998). This step is important because different enantiomers have different functions in different *Anomala* species (Leal et al. 1999).

In an elegant set of experiments, Plettner et al. (1996, 1998) elucidated the biosynthetic pathways for the honeybee queen mandibular pheromone (QMP) components 9-ODA and 9-HDA and compared their biosynthesis to that of worker produced 10-hydroxy-2(E)-decenoic acid (10-HDA) and the corresponding diacid. Plettner et al. (1996, 1998) demonstrated the de novo synthesis of stearic acid in worker mandibular glands, the hydroxylation of stearic acid at the *n*- (workers) and *n*-1 (queens) positions, chain shortening through β -oxidation to the 10- and 8-carbon atom hydroxy acids, and oxidation of *n* and *n*-1 hydroxy groups to give diacids and 9-keto-2(E)-decenoic acid, respectively. Stearic acid was shown to be the main precursor of the pheromone molecules as it was converted to C₁₀ hydroxy acids and diacids more efficiently than either 16 or 14 carbon atom fatty acids.

Hormonal regulation of pheromone production: Three hormones have been shown to regulate pheromone production in insects. Pheromone biosynthesis activating neuropeptide (PBAN) has been studied in female moths and alters enzyme

activity through second messengers at one or more steps during or subsequent to fatty acid synthesis during pheromone production (Rafaeli and Jurenka 2003). In contrast, 20-hydroxyecdysone and juvenile hormone (JH) induce or repress the synthesis of specific enzymes at the transcription level. The action of JH has been studied most thoroughly in bark beetles. Ecdysteroid regulation of pheromone production occurs in Diptera and has been most extensively studied in the housefly, *M. domestica* (Blomquist 2003).

6 Research Needs

Our increased understanding of the chemistry, biochemistry, and molecular biology of hydrocarbons and pheromone production in insects over the last four decades has been impressive. The work in Lepidoptera has moved from simply demonstrating that pheromone components were synthesized de novo to the molecular characterization of the unique $\Delta 11$ -desaturase and other desaturases that are involved in many female moths and their interplay with specific chain shortening steps. Similarly, a number of the genes involved in Coleoptera pheromone biosynthesis have been cloned, expressed, and assayed. While it is still true that in no system do we have a complete understanding of both the biochemical pathways and their endocrine regulation, we do have a much better understanding of how pheromones are made and in some systems are developing an understanding of their regulation at the molecular level. The continued application of the powerful tools of molecular biology along with studies using genomics and proteomics will only increase the rate at which we increase our understanding of pheromone and hydrocarbon production. Ultimately, just as behavioral chemicals themselves have been extended into pest control, research on pheromone production needs to be directed toward practical applications in insect control. This offers large challenges and large potential rewards.

References

- Ando T, Hase T, Arima R, Uchiyama M (1988) Biosynthetic pathway of bombykol, the sex pheromone of the female silkworm moth. *Agric Biol Chem* 52:473–478
- Ando T, Inomata S, Yamamoto M (2004) Lepidopteran sex pheromones. *Top Curr Chem* 239:51–96
- Antony B, Fujii T, Moto K, Matsumoto S, Fukuzawa M, Nakano R, Tatsuki S, Ishikawa Y (2009) Pheromone-gland-specific fatty-acyl reductase in the adzuki bean borer, *Ostrinia scapulalis* (Lepidoptera: Crambidae). *Insect Biochem Mol Biol* 39:90–95
- Antony B, Soffan A, Jakše J, Alfaifi S, Sutanto KD, Aldosari SA, Aldawood AS, Pain A (2015) Genes involved in sex pheromone biosynthesis of *Ephesthia cautella*, an important food storage pest, are determined by transcriptome sequencing. *BMC Genomics* 16:532
- Arsequell G, Fabriàs G, Camps F (1990) Sex pheromone biosynthesis in the processionary moth *Thaumetopoea pityocampa* by delta-13 desaturation. *Arch Insect Biochem Physiol* 14:47–56

- Aw T, Schlauch K, Keeling CI, Young S, Bearfield JC, Blomquist GJ, Tittiger C (2010) Functional genomics of the mountain pine beetle (*Dendroctonus ponderosae*) midguts and fat bodies. *BMC Genomics* 11:215
- Baker GL, Vroman HE, Padmore J (1963) Hydrocarbons of the American cockroach. *Biochem Biophys Res Commun* 13:360–365
- Balabanidou EA, Kampouraki MacLean M, Blomquist GJ, Tittiger C, Juarez MP, Mijailovsky SJ, Chalepakakis G, Anthousi A, Lynd A, Antoine S, Memingway J, Ranson H, Lycett G, Vontas J (2016) Cytochromes P450 associated with insecticide resistance catalyze cuticular hydrocarbon production in *Anopheles gambiae*. *Proc Natl Acad Sci U S A* 113:9268–9273
- Barbier J, Lederer E (1960) Structure chimique de la substance royale de la reine d'abeille (*Apis mellifica* L.). *C R Acad Sci Paris* 251:1131–1135
- Barkawi LS, Francke W, Blomquist GJ, Seybold SJ (2003) Frontalin: *de novo* synthesis of an aggregation pheromone component by *Dendroctonus* spp. bark beetles (Coleoptera: Scolytidae). *Insect Biochem Mol Biol* 33:773–788
- Bartelt RJ (1999) Sap beetles. In: Hardie J, Minks AK (eds) Pheromones of non-lepidopteran insects associated with agricultural plants. CAB International, Wallingford, pp 69–89
- Bartelt RJ (2010) Volatile hydrocarbon pheromones from beetles. In: Blomquist GJ, Bagnères A-G (eds) *Insect hydrocarbons biology, biochemistry and chemical ecology*. Cambridge University Press, Cambridge, pp 448–476
- Bartelt RJ, Weisleder D, Dowd PF, Plattner RD (1992) Male-specific tetraene and triene hydrocarbons of *Carpophilus hemipterus*: structure and pheromonal activity. *J Chem Ecol* 18:379–402
- Beale MH, Birkett MA, Bruce TJA, Chamberlain K, Field LM, Huttly AK, Martin JL, Parker R, Phillips AL, Pickett JA (2006) Aphid alarm pheromone produced by transgenic plants affects aphid and parasitoid behavior. *Proc Natl Acad Sci USA* 103:10509–10513
- Bello JE, McElfresh S, Millar JG (2015) Isolation and determination of absolute configurations of insect-produced methyl-branched hydrocarbons. *Proc Natl Acad Sci USA* 112:1077–1082
- Berger RS (1966) Isolation, identification, and synthesis of the sex attractant of the cabbage looper, *Trichoplusia ni*. *Ann Entomol Soc Am* 59:767–771
- Bestmann HJ, Herrig M, Attygalle AB (1987) Terminal acetylation in pheromone biosynthesis by *Mamestra brassicae* L. (Lepidoptera: Noctuidae). *Experientia* 43:1033–1034
- Billen J, Morgan ED (1998) Pheromone communication in social insects: sources and secretions. In: Vander Meer RK, Breed MD, Winston ML, Espelie KE (eds) *Pheromone communication in social insects*. Westview Press, Boulder, pp 3–33
- Birgersson G, Byers JA, Bergstrom G, Lofqvist J (1990) Production of pheromone components, chalcogran and methyl (E,Z)-2,4-decadienoate, in the spruce engraver *Pityogenes chalcographus*. *J Insect Physiol* 36:391–395
- Bjostad LB, Roelofs WL (1983) Sex pheromone biosynthesis in *Trichoplusia ni*: key steps involve delta-11 desaturation and chain-shortening. *Science* 220:1387–1389
- Bjostad LB, Roelofs WL (1984) Biosynthesis of sex pheromone components and glycerolipid precursors from sodium [1-¹⁴C]acetate in redbanded leafroller moth. *J Chem Ecol* 10:681–691
- Bjostad LB, Wolf WA, Roelofs WL (1987) Pheromone biosynthesis in lepidopterans: desaturation and chain shortening. In: Prestwich GD, Blomquist GJ (eds) *Pheromone biochemistry*. Academic Press, New York, pp 77–120
- Blailock TT, Blomquist GJ, Jackson LL (1976) Biosynthesis of 2-methylalkanes in the cricket *Nemobius fasciatus* and *Gryllus pennsylvanicus*. *Biochem Biophys Res Commun* 68:841–849
- Blomquist GJ (2003) Biosynthesis and ecdysteroid regulation of housefly sex pheromone production. In: Blomquist GJ, Vogt RG (eds) *Insect pheromone biochemistry and molecular biology*. Elsevier, San Diego, pp 131–252
- Blomquist GJ (2010) Structure and analysis of insect hydrocarbons. In: Blomquist GJ, Bagnères A-G (eds) *Insect hydrocarbons: biology biochemistry and chemical ecology*. Cambridge University Press, Cambridge, pp 19–34
- Blomquist GJ, Bagnères A-G (2010) *Insect hydrocarbons: biology, biochemistry, and chemical ecology*. Cambridge University Press, Cambridge

- Blomquist GJ, Howard RW (2003) Pheromone biosynthesis in social insects. In: Blomquist GJ, Vogt RG (eds) *Insect pheromone biochemistry and molecular biology*. Elsevier, New York, pp 323–340
- Blomquist GJ, Kearney GP (1976) Biosynthesis of the internally branched monomethylalkanes in the cockroach *Periplaneta fulliginosa*. *Arch Biochem Biophys* 173:546–553
- Blomquist GJ, Major MA, Lok JB (1975) Biosynthesis of 3-methylpentacosane in the cockroach *Periplaneta americana*. *Biochem Biophys Res Commun* 64:43–50
- Blomquist GJ, Howard RW, McDaniel CA, Remaley S, Dwyer LA, Nelson DR (1980) Application of methoxymercuration-demercuration followed by mass spectrometry as a convenient micro-analytical technique for double-bond location in insect-derived alkenes. *J Chem Ecol* 6:257–269
- Blomquist GJ, Guo L, Gu P, Blomquist C, Reitz RC, Reed JR (1994) Methyl-branched fatty acids and their biosynthesis in the housefly, *Musca domestica* L. (Diptera: Muscidae). *Insect Biochem Mol Biol* 24:803–810
- Blomquist GJ, Figueroa-Teran R, Aw M, Song M, Gorzalski A, Abbot A, Chang E, Tittiger C (2010) Pheromone production in bark beetles. *Insect Biochem Mol Biol* 40:699–712
- Blount BK, Chibnall AC, Mangouri EI (1937) The wax of the white pine chermes. *Biochem J* 31:1375–1378
- Bordon JH (1985) Aggregation pheromones. In: Kerkut GA, Gilbert LI (eds) *Comprehensive insect physiology, biochemistry, and pharmacology*, vol 9. Pergamon Press, Oxford, pp 257–285
- Braga MV, Pinto ZT, de Carvatho Queiroz MM, Matsumoto N, Blomquist GJ (2013) Cuticular hydrocarbons as a tool for the identification of insect species: puparial cases from Sarcophagidae. *Acta Trop* 128:479–485
- Buček A, Matoušková P, Vogel H, Šebesta P, Jahn U, Weissflog J, Svatos A, Pichová I (2015) Evolution of moth sex pheromone composition by a single amino acid substitution in a fatty acid desaturase. *Proc Natl Acad Sci USA* 112:12586–12591
- Buckner JS (2010) Oxygenated derivatives of hydrocarbons. In: Blomquist GJ, Bagnères A-G (eds) *Insect hydrocarbons: biology, biochemistry, and chemical ecology*. Cambridge University Press, Cambridge, pp 187–203
- Butenandt A, Beckmann R, Stamm D, Hecker E (1959) U^{ber}dem sexual-lockstoff des seidenspinners *Bombyx mori*: Reindarstellung und konstitution. *Z Naturforsch A* 14:283–284
- Callow RK, Johnston NC (1960) The chemical constitution and synthesis of queen substance of honeybees (*Apis mellifera* L.). *Bee World* 41:152–153
- Carlson DA, Nelson DR, Langley PA, Coates TW, Leegwater-Vander Linden ME (1984) Contact sex pheromone in the tsetse fly *Glossina pallidipes* (Austen): identification and synthesis. *J Chem Ecol* 10:429–450
- Carlson DA, Roan C-S, Yost RA (1989) Dimethyl disulfide derivatives of long chain alkenes, alkadienes, and alkatrienes for gas chromatography/mass spectrometry. *Anal Chem* 61:1564–1571
- Carlson DA, Offor II, El Messoussi S, Matsuyama K, Mori K, Jallon JM (1998) Sex pheromone of Glossinatachioides: isolation, identification and synthesis. *J Chem Ecol* 24:1563–1575
- Carot-Sans G, Muñoz L, Piulachs MD, Guerrero A, Rosell G (2015) Identification and characterization of a fatty acyl reductase from a *Spodoptera littoralis* female gland involved in pheromone biosynthesis. *Insect Mol Biol* 24:82–92
- Chase J, Jurenka RA, Schal C, Halarnkar PP, Blomquist GJ (1990) Biosynthesis of methyl branched hydrocarbons in the German cockroach *Blattella germanica* (L.) (Orthoptera, Blattellidae). *Insect Mol Biol* 20:149–156
- Chertemps T, Duportets L, Labeur C, Udeda R, Takahashi K, Saigo K, Wicker-Thomas C (2007) A female-biased expressed elongase involved in long-chain hydrocarbon biosynthesis and courtship behavior in *Drosophila melanogaster*. *Proc Natl Acad Sci USA* 104:4273–4278
- Chibnall AC, Piper SH, Pollard A, Willimas EF, Sahai PN (1934) The constitution of the primary alcohols, fatty acids and paraffins present in plant and insect waxes. *Biochem J* 28:2189–2208

- Choi M-Y, Lim H, Park K-C, Adlof R, Wang S, Zhang A, Jurenka R (2007) Identification and biosynthetic studies of the hydrocarbon sex pheromone in *Utetheisa ornatrix* (Lepidoptera: Arctiidae). *J Chem Ecol* 33:1336–1345
- Chung H, Loehlin DW, Dufour HD, Vaccarro K, Millar JG, Carroll SB (2014) A single gene affects both ecological divergence and mate choice in *Drosophila*. *Science* 343:148–151
- Dallerac R, Labeur C, Jallon J-M, Knipple DC, Roelofs WL, Wicker-Thomas C (2000) A 9 desaturase gene with a different substrate specificity is responsible for the cuticular diene hydrocarbon polymorphism in *Drosophila melanogaster*. *Proc Natl Acad Sci USA* 97:9449–9454
- Dillwith JW, Nelson JH, Pomonis JG, Nelson DR, Blomquist GJ (1982) A ^{13}C NMR study of methyl-branched hydrocarbon biosynthesis in the housefly. *J Biol Chem* 257:11305–11314
- Ding B-J, Löfstedt C (2015) Analysis of the *agrotis segetum* pheromone gland transcriptome in the light of sex pheromone biosynthesis. *BMC Genomics* 16:711
- Ding B-J, Liénard MA, Wang H-L, Zhao C-H, Löfstedt C (2011) Terminal fatty-acyl-CoA desaturase involved in sex pheromone biosynthesis in the winter moth (*Operophtera brumata*). *Insect Biochem Mol Biol* 41:715–722
- Ding B-J, Hofvander P, Wang H-L, Durrett TP, Stymne S, Löfstedt C (2014) A plant factory for moth pheromone production. *Nature Comm* 5:3353
- Drijfhout FK (2010) Cuticular hydrocarbons: a new tool in forensic entomology? In: Amendt J, Lee Goff M, Campobasso CP, Grassberger M (eds) *Current concepts in forensic entomology*. Springer, New York, pp 179–203
- Dwyer LA, Blomquist GJ, Nelson JH, Pomonis JG (1981) A ^{13}C -NMR study of the biosynthesis of 3-methylpentacosane in the American cockroach. *Biochim Biophys Acta* 663:536–544
- Eliyahu D, Applebaum S, Rafaëli A (2003) Moth sex-pheromone biosynthesis is inhibited by the herbicide diclofop. *Pestic Biochem Physiol* 77:75–81
- Fang N, Teal PEA, Doolittle RE, Tumlinson JH (1995a) Biosynthesis of conjugated olefinic systems in the sex pheromone gland of female tobacco hornworm moths, *Manduca sexta* (L.). *Insect Biochem Mol Biol* 25:39–48
- Fang N, Teal PEA, Tumlinson JH (1995b) Characterization of oxidase(s) associated with the sex pheromone gland in *Manduca sexta* (L.) females. *Arch Insect Biochem Physiol* 29:243–257
- Figueroa-Teran R, Welch WH, Blomquist GJ, Tittiger C (2012) Ipsdienol dehydrogenase (IDOLDH): a novel oxidoreductase important for *Ips pini* pheromone production. *Insect Biochem Mol Biol* 42:81–90
- Figueroa-Terany R, Pak H, Blomquist GJ, Tittiger C (2016) High substrate specificity of ipsdienol dehydrogenase (IDOLDH), a short-chain dehydrogenase from *Ips pini* bark beetles. *J Biochem* 160:141–151
- Foster SP, Roelofs WL (1988) Sex pheromone biosynthesis in the leafroller moth *Planotortrix excessana* by $\Delta 10$ desaturation. *Arch Insect Biochem Physiol* 8:1–9
- Foster SP, Roelofs WL (1990) Biosynthesis of a monoene and a conjugated diene sex pheromone component of the light brown apple moth by E11-desaturation. *Experientia* 46:269–273
- Foster SP, Roelofs WL (1996) Sex pheromone biosynthesis in the tortricid moth, *Ctenopseustis herana* (Felder & Rogenhofer). *Arch Insect Biochem Physiol* 33:135–147
- Francke W, Bartels J, Meyer H, Schroder F, Kohnle U, Baader E, Vite JP (1995) Semiochemicals from bark beetles: new results, remarks, and reflections. *J Chem Ecol* 21:1043–1063
- Fukui H, Matsumura F, Barak AV, Burkholder WE (1977) Isolation and identification of a major sexattracting component of *Attagenus elongatus* (Casey) (Coleoptera: Dermestidae). *J Chem Ecol* 3:539–548
- Gilg AB, Bearfield JC, Tittiger C, Welch WH, Blomquist GJ (2005) Isolation and functional expression of the first animal geranyl diphosphate synthase and its role in bark beetle pheromone biosynthesis. *Proc Natl Acad Sci USA* 102:9760–9765
- Gilg AB, Tittiger C, Blomquist GJ (2009) Unique animal prenyltransferase with monoterpene synthase activity. *Naturwissenschaften* 96:731–735

- Ginzel MD, Blomquist GJ (2016) Insect hydrocarbons: biochemistry and chemical ecology. In: Cohen E, Moussian B (eds) *Extracellular matrices in arthropods*. Springer, Switzerland, pp 221–252
- Goller S, Szöcs G, Francke W, Schulz S (2007) Biosynthesis of (3Z,6Z,9Z)-3,6,9-octadecatriene: the main component of the pheromone blend of *Erannis bajaria*. *J Chem Ecol* 33:1505–1509
- Gu X, Quilici D, Juarez P, Blomquist GJ, Schal C (1995) Biosynthesis of hydrocarbons and contact sex pheromone and their transport by lipophorin in females of the German cockroach (*Blattella germanica*). *J Insect Physiol* 41:257–267
- Gu S-H, Wu K-M, Guo Y-Y, Pickett JA, Field LM, Zhou J-J, Zhang Y-J (2013) Identification of genes expressed in the sex pheromone gland of the black cutworm *Agrotis ipsilon* with putative roles in sex pheromone biosynthesis and transport. *BMC Genomics* 14:636
- Hagström ÅK, Liénard MA, Groot AT, Hedenström E, Löfstedt C (2012) Semi-selective fatty acyl reductases from four heliothine moths influence the specific pheromone composition. *PLoS One* 7:e37230
- Hagström ÅK, Albre J, Tooman LK, Thirmawithana AH, Corcoran J, Löfstedt C, Newcomb RD (2013a) A novel fatty acyl desaturase from the pheromone glands of *Ctenopseustis obliquana* and *C. herana* with specific Z5-desaturase activity on myristic acid. *J Chem Ecol* 40:63–70
- Hagström ÅK, Walther A, Wendland J, Löfstedt C (2013b) Subcellular localization of the fatty acyl reductase involved in pheromone biosynthesis in the tobacco budworm, *Heliothis virescens* (Noctuidae: Lepidoptera). *Insect Biochem Mol Biol* 43:510–521
- Hagström ÅK, Wang H-L, Liénard MA, Lassance J-M, Johansson T, Löfstedt C (2013c) A moth pheromone brewery: production of (Z)-11-hexadecenol by heterologous co-expression of two biosynthetic genes from a noctuid moth in a yeast cell factory. *Microb Cell Factories* 12:125
- Hashimoto T (1996) Peroxisomal β -oxidation: enzymology and molecular biology. *Ann N Y Acad Sci* 804:86–98
- Howard RW (1993) Cuticular hydrocarbons and chemical communication. In: Stanley-Samuelson DW, Nelson DR (eds) *Insect lipids: chemistry, biochemistry and biology*. University of Nebraska Press, Lincoln, pp 179–226
- Howard RW, Blomquist GJ (2005) Ecological, behavioral, and biochemical aspects of insect hydrocarbons. *Annu Rev Entomol* 50:371–393
- Islam N, Bacala R, Moore A, Vanderwel D (1999) Biosynthesis of 4-methyl-1-nonanol: female-produced sex pheromone of the yellow mealworm beetle, *Tenebrio molitor* (Coleoptera: Tenebrionidae). *Insect Biochem Mol Biol* 29:201–208
- Jallon J-M, Wicker-Thomas C (2003) Genetic studies on pheromone production in *Drosophila*. In: Blomquist GJ, Vogt RG (eds) *Insect sex pheromone biochemistry and molecular biology*. Elsevier, San Diego, pp 253–281
- Juarez P, Chase J, Blomquist GJ (1992) A microsomal fatty acid synthetase from the integument of *Blattella germanica* synthesizes methyl-branched fatty acids, precursors to hydrocarbon and contact sex pheromone. *Arch Biochem Biophys* 293:333–341
- Jung CR, Kim Y (2014) Comparative transcriptome analysis of sex pheromone glands of two sympatric lepidopteran congener species. *Genomics* 103:308–315
- Jurenka RA (1997) Biosynthetic pathway for producing the sex pheromone component (Z,E)-9,12-tetradecadienyl acetate in moths involves a Δ 12 desaturase. *Cell Mol Life Sci* 53:501–505
- Jurenka RA (2003) Biochemistry of female moth sex pheromones. In: Blomquist GJ, Vogt R (eds) *Insect pheromone biochemistry and molecular biology*. Elsevier, San Diego, pp 53–80
- Jurenka RA, Roelofs WL (1989) Characterization of the acetyltransferase involved in pheromone biosynthesis in moths: specificity for the Z isomer in Tortricidae. *Insect Biochem* 19:639–644
- Jurenka RA, Subchev M (2000) Identification of cuticular hydrocarbons and the alkene precursor to the pheromone in hemolymph of the female gypsy moth *Lymantria dispar*. *Arch Insect Biochem Physiol* 43:108–115
- Jurenka RA, Haynes KF, Adlof RO, Bengtsson M, Roelofs WL (1994) Sex pheromone component ratio in the cabbage looper moth altered by a mutation affecting the fatty acid chain-shortening reactions in the pheromone biosynthetic pathway. *Insect Biochem Mol Biol* 24:373–381

- Jurenka RA, Subchev M, Abad J-L, Choi M-Y, Fabrias G (2003) Sex pheromone biosynthetic pathway for disparlure in the gypsy moth, *Lymantria dispar*. Proc Natl Acad Sci USA 100:809–814
- Jurenka RA, Blomquist GJ, Schal C, Tittiger C (2017) Biochemistry and molecular biology of pheromone production. Ref Mod Life Sci. <https://doi.org/10.1016/B978-0-12-809633-8.04037-1>
- Kavanagh K, Jornvall H, Persson B (2008) The SDR superfamily: functional and structural diversity within a family of metabolic and regulatory enzymes. Cell Mol Life Sci 65:3895–3906
- Keeling CI, Slessor KN, Higo HA, Winston ML (2003) New components of the honey bee (*Apis mellifera* L.) queen retinue pheromone. Proc Natl Acad Sci USA 100:4486–4491
- Keeling CI, Blomquist GJ, Tittiger C (2004) Coordinated gene expression for pheromone biosynthesis in the pine engraver beetle, *Ips pini* (Coleoptera: Scolytidae). Naturwissenschaften 91:324–328
- Keeling CI, Bearfield JC, Young S, Blomquist GJ, Tittiger C (2006) Effects of juvenile hormone on gene expression in the pheromone-producing midgut of the pine engraver beetle, *Ips pini*. Insect Mol Biol 15:207–216
- Keeling CI, Chiu CC, Aw T, Li M, Henderson H, Tittiger C, Weng H, Blomquist GJ, Bohlman J (2013) Frontaliln pheromone biosynthesis in the mountain pine beetle, *Dendroctonus ponderosae*, and the role of isoprenyl diphosphate synthases. Proc Natl Acad Sci USA 110:18838–18843
- Kiyota R, Arakawa M, Yamakawa R, Yasmin A, Ando T (2011) Biosynthetic pathways of the sex pheromone components and substrate selectivity of the oxidation enzymes working in pheromone glands of the fall webworm, *Hyphantria cunea*. Insect Biochem Mol Biol 41:362–369
- Knipple DC, Roelofs WL (2003) Molecular biological investigations of pheromone desaturases. In: Blomquist GJ, Vogt R (eds) Insect pheromone biochemistry and molecular biology. Elsevier, San Diego, pp 81–106
- Lanne BS, Ivansson P, Johnsson P, Bergström G, Wassgren A-B (1989) Biosynthesis of 2-methyl-3buten-2-ol, a pheromone component of *Ips typographus* (Coleoptera: Scolytidae). Insect Biochem 19:163–168
- Lassance J-M, Groot AT, Liénard MA, Antony B, Borgwardt C, Andersson F, Hedenstrom E, Heckel DG, Lofstedt C (2010) Allelic variation in a fatty-acyl reductase gene causes divergence in moth sex pheromones. Nature 466:486–489
- Lassance J-M, Liénard MA, Antonya B, Qian S, Fujii T, Tabata J, Ishikawa Y, Lofstedt C (2013) Functional consequences of sequence variation in the pheromone biosynthetic gene pgFAR for *Ostrinia* moths. Proc Natl Acad Sci USA 110:3967–3972
- Leal WS (1998) Chemical ecology of phytophagous scarab beetles. Annu Rev Entomol 43:39–61
- Leal WS, Zabin PHG, Wojtasek H, Ferreira JT (1999) Biosynthesis of scarab beetle pheromones: enantioselective 8-hydroxylation of fatty acids. Eur J Biochem 259:175–180
- Li Z-Q, Zhang S, Luo J-Y, Wang C-Y, Lv L-M, Dong S-L, Cui J-J (2015) Transcriptome comparison of the sex pheromone glands from two sibling *Helicoverpa* species with opposite sex pheromone components. Sci Rep 5:932
- Liénard MA, Hagström ÅK, Lassance J-M, Löfstedt C (2010) Evolution of multicomponent pheromone signals in small ermine moths involves a single fatty-acyl reductase gene. Proc Natl Acad Sci U S A 107:10955–10960
- Liénard MA, Wang H-L, Lassance J-M, Löfstedt C (2014) Sex pheromone biosynthetic pathways are conserved between moths and the butterfly *Bicyclus anynana*. Nat Commun 5:957
- Löfstedt C, Bengtsson M (1988) Sex pheromone biosynthesis of (*E,E*)-8,10-dodecadienol in codling moth *Cydia pomonella* involves E9 desaturation. J Chem Ecol 14:903–915
- Löfstedt C, Wahlberg N, Millar JG (2017) Evolutionary patterns of pheromone diversity in Lepidoptera. In: Allison JD, Cardé RT (eds) Pheromone communication in moths: evolution, behavior, and application. University of California Press, Oakland, pp 43–78

- Luxova A, Svatos A (2006) Substrate specificity of membrane-bound alcohol oxidase from the tobacco hornworm moth (*Manduca sexta*) female pheromone glands. *J Mol Catal B Enzym* 38:37–42
- Ma PWK, Ramaswamy SB (2003) Biology and ultrastructure of sex pheromone producing tissue. In: Blomquist GJ, Vogt R (eds) *Insect pheromone biochemistry and molecular biology*. Elsevier, San Diego, pp 19–51
- Martin D, Bohlmann J, Gershenzon J, Francke W, Seybold SJ (2003) A novel sex-specific and inducible monoterpene synthase activity associated with a pine bark beetle, the pine engraver, *Ips pini*. *Naturwissenschaften* 90:173–179
- Martinez T, Fabria's G, Camps F (1990) Sex pheromone biosynthetic pathway in *Spodoptera littoralis* and its activation by a neurohormone. *J Biol Chem* 265:1381–1387
- Matouskova P, Pichova I, Svatos A (2007) Functional characterization of a desaturase from the tobacco hornworm moth (*Manduca sexta*) with bifunctional Z11- and 10,12-desaturase activity. *Insect Biochem Mol Biol* 37:601–610
- Matsumoto S (2010) Molecular mechanisms underlying sex pheromone production in moths. *Biosci Biotechnol Biochem* 74:223–231
- Matsumoto S, Hull J, Ohnishi A, Moto KI, Fonagy A (2007) Molecular mechanisms underlying sex pheromone production in the silkworm, *Bombyx mori*: characterization of the molecular components involved in bombykol biosynthesis. *J Insect Physiol* 53:752–759
- Millar JG (2010) Polyene hydrocarbons, epoxides, and related compounds as components of lepidopteran pheromone blends. In: Blomquist GJ, Bagnères A-G (eds) *Hydrocarbon: biology biochemistry and chemical ecology*. Cambridge University Press, Cambridge, pp 390–447
- Morse D, Meighen EA (1987a) Biosynthesis of the acetate ester precursors of the spruce budworm sex pheromone by an acetyl CoA: fatty alcohol acetyltransferase. *Insect Biochem* 17:53–59
- Morse D, Meighen EA (1987b) Pheromone biosynthesis: enzymatic studies in lepidoptera. In: Prestwich G, Blomquist GJ (eds) *Pheromone biochemistry*. Academic Press, Orlando, pp 121–158
- Moto K, Yoshiga T, Yamamoto M, Takahashi S, Okano K, Ando T, Nakata T, Matsumoto S (2003) Pheromone gland specific fatty-acyl reductase of the silk moth. *Bombyx mori*. *Proc Natl Acad Sci USA* 100:9156–9161
- Nadeau J, Petereit J, Tillett RJ, Jung K, Fotoohi M, MacLean M, Young S, Schlauch K, Blomquist GJ, Tittiger C (2017) Comparative transcriptomics of mountain pine beetle heromone-biosynthetic tissues and functional analysis of CYP6DE3. *BMC Genomics* 18(1):1–15
- Nelson DR, Sukkestad DR (1970) Normal and branched aliphatic hydrocarbons from the eggs of the tobacco hornworm. *Biochemist* 9:4601–4610
- Nesnerova P, Sebek P, Macek T, Svatos A (2004) First semi-synthetic preparation of sex pheromones. *Green Chem* 6:305–307
- Ohnishi A, Hull JJ, Matsumoto S (2006) Targeted disruption of genes in the *Bombyx mori* sex pheromone biosynthetic pathway. *Proc Natl Acad Sci USA* 103:4398–4403
- Ono A, Imai T, Inomata S-I, Watanabe A, Ando T (2002) Biosynthetic pathway for production of a conjugated dienyl sex pheromone of a plusiinae moth, *Thysanoplusia intermixta*. *Insect Biochem Mol Biol* 32:701–708
- Payne JL, Boyer AG, Brown JH, Finnegan S, Kowalewski M, Krause RA, Lyons SK, McClain CR, McShea D, Navack-Gottshall PM (2009) Two phase increase in the maximum size of life over 3.5 billion years reflects biological innovation and environmental opportunity. *Proc Natl Acad Sci USA* 106:24–27
- Percy-Cunningham JE, MacDonald JA (1987) Biology and ultrastructure of sex pheromone-producing glands. In: Prestwich G, Blomquist GJ (eds) *Pheromone biochemistry*. Academic Press, Orlando, pp 27–75
- Petroski RJ, Bartelt RJ, Weisleder D (1994) Biosynthesis of (2E,4E,6E)-5 ethyl-3-methyl-2,4,6-nonatriene: the aggregation pheromone of *Carpophilus freemani* (Coleoptera: Nitidulidae). *Insect Biochem Mol Biol* 24:69–78

- Pierce HD, Conn JE, Oehlschlager AC, Borden JH (1987) Monoterpene metabolism in female mountain pine beetles, *Dendroctonus ponderosae* Hopkins, attacking ponderosa pine. *J Chem Ecol* 13:1455–1480
- Plettner E, Slessor KN, Winston ML, Oliver JE (1996) Caste-selective pheromone biosynthesis in honeybees. *Science* 271:1851–1853
- Plettner E, Slessor KN, Winston ML (1998) Biosynthesis of mandibular acids in honeybees (*Apis mellifera*): de novo synthesis, route of fatty acid hydroxylation and caste selective β -oxidation. *Insect Biochem Mol Biol* 28:31–42
- Prestwich GD, Blomquist GJ (1987) Pheromone biochemistry. Academic Press, Orlando
- Pureswaran DS, Gries R, Borden JH, Pierce HD Jr (2000) Dynamics of pheromone production and communication in the mountain pine beetle, *Dendroctonus ponderosae* Hopkins and the pine engraver, *Ips pini* (say) (Coleoptera: Scolytidae). *Chemoecology* 10:153–168
- Qiu Y, Tittiger C, Wicker-Thamas C, Le Goff G, Young S, Wajnberg E, Fricaux T, Tautet N, Blomquist GJ, Feyereisen R (2012) An insect-specific P450 oxidative decarbonylase for cuticular hydrocarbon biosynthesis. *Proc Natl Acad Sci USA* 109:14858–14863
- Quennedey A (1998) Insect epidermal gland cells: ultrastructure and morphogenesis. In: Harrison FW, Locke M (eds) *Microscopic anatomy of invertebrates*, vol 11A. Wiley-Liss, New York, pp 177–207
- Rafaeli A, Jurenka RA (2003) PBAN regulation of pheromone biosynthesis in female moths. In: Blomquist GJ, Vogt R (eds) *Insect pheromone biochemistry and molecular biology*. Elsevier, San Diego, pp 107–136
- Reed JR, Vanderwel D, Choi S, Pomonis JG, Reitz RC, Blomquist GJ (1994) Unusual mechanism of hydrocarbon formation in the housefly: cytochrome P450 converts aldehyde to the sex pheromone component (Z)-9-tricosene and CO₂. *Proc Natl Acad Sci USA* 91:10000–10004
- Reed JR, Quilici DR, Blomquist GJ, Reitz RC (1995) Proposed mechanism for the cytochrome P450-catalyzed conversion of aldehydes to hydrocarbons in the house fly, *Musca domestica*. *Biochemistry* 34:16221–16227
- Roelofs WL, Wolf WA (1988) Pheromone biosynthesis in Lepidoptera. *J Chem Ecol* 14:2019–2031
- Romer F (1991) The oenocytes of insects: differentiation, changes during molting, and their possible involvement in the secretion of moulting hormone. In: Gupta A (ed) *Morphogenetic hormones of arthropods*, vol 3. Rutgers University Press, New Brunswick, NJ, pp 542–566
- Rule GS, Roelofs WL (1989) Biosynthesis of sex pheromone components from linolenic acid in arctiid moths. *Arch Insect Biochem Physiol* 12:89–97
- Sandstrom P, Welch WH, Blomquist GJ, Tittiger C (2006) Functional expression of a bark beetle cytochrome P450 that hydroxylates myrcene to ipsdienol. *Insect Biochem Mol Biol* 36:835–845
- Sandstrom P, Ginzel MD, Bearfield JC, Welch WH, G J Blomquist GJ, Tittiger C (2008) Myrcene hydroxylases do not determine enantiomeric composition of pheromonal ipsdienol in *Ips* spp. *J Chem Ecol* 34:584–592
- Schal C, Sevala VL, Young HP, Bachmann JAS (1998) Synthesis and transport of hydrocarbons: cuticle and ovary as target tissues. *Am Zool* 38:382–393
- Schal C, Fan Y, Blomquist GJ (2003) Regulation of pheromone biosynthesis, transport and emission in cockroaches. In: Blomquist G, Vogt R (eds) *Insect pheromone biochemistry and molecular biology*. Elsevier, San Diego, pp 283–322
- Schlyter F, Birgersson GS (1999) Forest beetles. In: Hardie J, Minks AK (eds) *Pheromones of non-lepidopteran insects associated with agricultural plants*. CAB International, Wallingford, pp 113–148
- Seybold SJ, Ohtsuka T, Wood DL, Kubo I (1995) Enantiomeric composition of ipsdienol - a chemotaxonomic character for North-American populations of *Ips* spp in the pini subgenerec group (Coleoptera, Scolytidae). *J Chem Ecol* 21:995–1016
- Seybold SJ, Vanderwel D (2003) Biosynthesis and endocrine regulation of pheromone production in the Coleoptera. In: Blomquist GJ, Vogt R (eds) *Insect pheromone biochemistry and molecular biochemistry*. Elsevier, San Diego, CA, pp 137–200

- Seybold SJ, Bohlmann J, Raffa KF (2000) Biosynthesis of coniferophagous bark beetle pheromones and conifer isoprenoids: evolutionary perspective and synthesis. *Can Entomol* 132:697–753
- Silverstein RM, Rodin JO, Wood DL (1966) Sex attractants in frass produced by male *Ips confusus* in ponderosa pine. *Science* 154:509–510
- Song M, Gorzalski A, Nguyen TT, Liu X, Jeffrey C, Blomquist GJ, Tittiger C (2014) *exo-Brevicommin* biosynthesis in the fat body of the mountain pine beetle, *Dendroctonus ponderosae*. *J Chem Ecol* 40:181–189
- Stanley-Samuelson DW, Jurenka RA, Cripps C, Blomquist GJ, deRenobales M (1988) Fatty acids in insects: composition, metabolism and biological significance. *Arch Insect Biochem Physiol* 9:1–33
- Strandh M, Johansson T, Ahren D, Löfstedt C (2008) Transcriptional analysis of the pheromone gland of the turnip moth, *Agrotis segetum* (Noctuidae), reveals candidate genes involved in pheromone production. *Insect Mol Biol* 17:73–85
- Strandh M, Johansson T, Löfstedt C (2009) Global transcriptional analysis of pheromone biosynthesis-related genes in the female turnip moth, *Agrotis segetum* (Noctuidae) using a custom-made cDNA microarray. *Insect Biochem Mol Biol* 39:484–489
- Subchev M, Jurenka RA (2001) Identification of the pheromone in the hemolymph and cuticular hydrocarbons from the moth *Scoliopteryx libatrix* L. (Lepidoptera: Noctuidae). *Arch Insect Biochem Physiol* 47:35–43
- Tang JD, Charlton RE, Jurenka RA, Wolf WA, Phelan PL, Sreng L, Roelofs WL (1989) Regulation of pheromone biosynthesis by a brain hormone in two moth species. *Proc Natl Acad Sci USA* 86:1806–1810
- Teal PEA, Tumlinson JH (1987) The role of alcohols in pheromone biosynthesis by two noctuid moths that use acetate pheromone components. *Arch Insect Biochem Physiol* 4:261–269
- Teal PEA, Tumlinson JH (1988) Properties of cuticular oxidases used for sex pheromone biosynthesis by *Heliothis zea*. *J Chem Ecol* 14:2131–2145
- Teerawanichpan P, Robertson AJ, Qiu X (2010) A fatty acyl-CoA reductase highly expressed in the head of honey bee (*Apis mellifera*) involves biosynthesis of a wide range of aliphatic fatty alcohols. *Insect Biochem Mol Biol* 40:641–649
- Tillman JA, Seybold SJ, Jurenka RA, Blomquist GJ (1999) Insect pheromones: an overview of biosynthesis and endocrine regulation. *Insect Biochem Mol Biol* 29:481–514
- Tittiger C (2003) Molecular biology of bank beetle pheromone production and endocrine regulation. In: Blomquist GJ, Vogt RG (eds) *Insect biochemistry and molecular biology*. Elsevier, San Diego, pp 201–230
- Tittiger C, Blomquist GJ (2016) Pheromone production in pine bark beetles. *Adv Insect Physiol* 50:235–263
- Tittiger C, Blomquist GJ, Ivarsson P, Borgeson CE, Seybold SJ (1999) Juvenile hormone regulation of HMG-R gene expression in the bark beetle *Ips paraconfusus* (Coleoptera: Scolytidae): implications for male aggregation pheromone biosynthesis. *Cell Mol Life Sci* 55:121–127
- Vanderwel D (1994) Factors affecting pheromone production in beetles. *Arch Insect Biochem Physiol* 25:347–362
- Vanderwel D, Oehlschlager AC (1987) Biosynthesis of pheromones and endocrine regulation of pheromone production in Coleoptera. In: Prestwich GD, Blomquist GJ (eds) *Pheromone biochemistry*. Academic Press, Orlando, pp 175–215
- Vaz AH, Blomquist GJ, Reitz RC (1988) Characterization of the fatty acyl elongation reactions involved in hydrocarbon biosynthesis in the housefly, *Musca domestica* L. *Insect Biochem* 18:177–184
- Vioque J, Kolattukudy PE (1997) Resolution and purification of an aldehyde-generating and an alcohol-generating fatty acyl-CoA reductase from pea leaves (*Pisum sativum* L.). *Arch Biochem Biophys* 340:64–72
- Vogel H, Heidel A, Heckel D, Groot A (2010) Transcriptome analysis of the sex pheromone gland of the noctuid moth *Heliothis virescens*. *BMC Genomics* 11:29

- Wang H-L, Liénard MA, Zhao C-H, Wang C-Z, Löfstedt C (2010a) Neofunctionalization in an ancestral insect desaturase lineage led to rare $\Delta 6$ pheromone signals in the Chinese tussah silkworm. *Insect Biochem Mol Biol* 40:742–751
- Wang H-L, Zhao C-H, Millar J, Cardé R, Löfstedt C (2010b) Biosynthesis of unusual moth pheromone components involves two different pathways in the navel orangeworm, *Amyelois transitella*. *J Chem Ecol* 36:535–547
- Wang H-L, Zhao C-H, Szöcs G, Chinta S, Schulz S, Löfstedt C (2013) Biosynthesis and PBAN-regulated transport of pheromone polyenes in the winter moth, *Operophtera brumata*. *J Chem Ecol* 39:790–796
- Wheeler CA, Cardé RT (2014) Following in their footprints: cuticular hydrocarbons as overwintering aggregation site markers in *Hippodamia convergens*. *J Chem Ecol* 40:418–428
- Wicker-Thomas C, Cheretemps T (2010) Molecular biology and genetics of hydrocarbon production. In: Blomquist GJ, Bagnères A-G (eds) *Insect hydrocarbons: biology biochemistry and chemical ecology*. Cambridge University Press, Cambridge, pp 53–74
- Wicker-Thomas C, Garrido D, Bontonou G, Napal L, Mazuras N, Denis B, Rubin T, Parvy J-P, Montagne J (2015) Flexible origin of hydrocarbon/pheromone precursors in *Drosophila melanogaster*. *J Lipid Res* 56:2094–2101
- Xia Y-H, Zhang Y-N, Hou X-Q, Li F, Dong S-L (2015) Large number of putative chemoreception and pheromone biosynthesis genes revealed by analyzing transcriptome from ovipositor-pheromone glands of *Chilo suppressalis*. *Sci Rep* 5:7888
- Zhang Y-N, Xia Y-H, Zhu J-Y, Li S-Y, Dong S-L (2014) Putative pathway of sex pheromone biosynthesis and degradation by expression patterns of genes identified from female pheromone gland and adult antenna of *Sesamia inferens* (Walker). *J Chem Ecol* 40:439–451
- Zhao C, Löfstedt C, Wang X (1990) Sex pheromone biosynthesis in the Asian corn borer *Ostrinia furnicalis* 2. Biosynthesis of (E) and (Z)-12-tetradecenyl acetate involves $\Delta 14$ desaturation. *Arch Insect Biochem Physiol* 15:57–65

Relevant Website

Database of Pheromones and Semiochemicals. <http://www.pherobase.com/>



Tomáš Řezanka, Irena Kolouchová, Lucia Gharwalová,
Andrea Palyzová, and Karel Sigler

Contents

1	Introduction	246
2	Fatty Acids	247
3	Archaea	250
4	Bacteria	252
4.1	Plasmalogens	253
4.2	Mycobacteria	255
5	Yeast	256
6	Cyanobacteria and Algae	258
6.1	Cyanobacteria	258
6.2	Algae	258
7	Research Needs	261
	References	262

Abstract

Current lipidomics is a modern method of analysis of lipids, important cell constituents found in all microbial cells and fulfilling vital roles as structural components of cell membranes, cell energy storage sources, and in some cases as signaling compounds. In either of its current branches, i.e., shotgun lipidomics and LC-MS lipidomics, it provides a fast and reliable information on the lipids present in microorganisms such as archaea, bacteria, cyanobacteria,

T. Řezanka (✉) · A. Palyzová · K. Sigler
Institute of Microbiology, Academy of Sciences of the Czech Republic, Prague, Czech Republic
e-mail: rezanka@biomed.cas.cz; palyzova@biomed.cas.cz; sigler@biomed.cas.cz

I. Kolouchová · L. Gharwalová
Department of Biotechnology, University of Chemical Technology Prague, Prague, Czech Republic
e-mail: Irena.Kolouchova@vscht.cz; lucia.gharwalova@gmail.com

algae, and yeast, including those inhabiting unusual (psychrophilic, halophilic, thermophilic, etc.) habitats. The number of lipids and more specifically molecular species of lipids ranges from hundreds to thousands, and lipidomics is thus expected to provide a huge amount of data to be processed and evaluated. Further development of lipidomic analysis can be expected to involve the use of new ionization techniques, e.g., atmospheric pressure photoionization MS or high-resolution mass spectrometry of time-of-flight MS analysis of lipids containing unusual head groups, very-long chain saturated, or very-long chain polyunsaturated fatty acids and the application and use of chemical compounds labeled with stable isotopes in the study of dynamic changes of metabolic pathways.

1 Introduction

Lipidomics is a new research field, which has recently begun to be used in the study of lipids in biological systems based on the principles of analytical chemistry. The main tool is a mass spectrometric analysis of lipids, often implemented on devices with a high resolution, which allows determination of the molecular formula of analyzed compounds. There are two major and mutually complementary approaches in lipidomics. The first consists in the direct entry of the sample into the mass spectrometer and is called “shotgun lipidomics.” The second uses a classical connection of a chromatograph, almost exclusively liquid, with mass spectrometer.

The main advantage of shotgun lipidomics over liquid chromatography-mass spectrometry (LC-MS) is the fact that the mass spectrum of molecular ions of each molecular species of occurring lipid classes can be obtained at a constant concentration of the lipid solution during direct infusion. Another advantage is the short analysis time (several tens of seconds). Conversely, a huge drawback is the inability to separate and identify the regioisomers and enantiomers of the individual molecular species (see Table 1 for the number of triacylglycerols (TAGs)). Both approaches can of course use tandem mass spectrometry including neutral loss scans and precursor ion scans of one or more ionic reactions. An ideal way is the combination of both methods for sample analysis, see e.g., the lipidomic profile of snow algae (Rezanka et al. 2014).

Rapid development of lipidomic analysis began in essence 10 years ago with the advent of commercially available mass spectrometers using soft ionization techniques (electrospray ionization (ESI), atmospheric pressure chemical ionization

Table 1 The number of possible TAGs from algal oil

Description	Number of possible TAGs	Number of possible TAGs for $y = 11$
Without isomers	$x = (y^3 + 3y^2 + 2y)/6$	286
Without enantiomers	$x = (y^2 + y^3)/2$	726
All isomers	$x = y^3$	1331

where x is the number of TAGs, y is the number of FAs in TAGs

(APCI), matrix-assisted laser desorption/ ionization (MALDI), time-of - flight mass spectrometry (TOF)), etc.

Lipids are structurally diverse chemical compounds that perform many key biological functions, serving as structural components of cell membranes, reservoirs and sources of energy, or as signaling molecules. Lipids may be broadly defined as hydrophobic or amphipathic molecules which, at least in part, are formed by condensation of thioesters (fatty acids, polyketides, etc.) or isoprene units (prenols, sterols, etc.).

Lipids are generally divided into “simple” and “complex” ones. Simple lipids are those which on hydrolysis provide at most two types of products, whereas complex lipids yield upon hydrolysis three or more products. Examples are shown in Fig. 1.

The variability of cell lipids reaches tens of thousands of molecular species, see, e.g., Table 1 showing the number of possible TAGs.

Obviously, all theoretically predicted molecular species may not be present or even detected. Many of them are below the detection limit of the instrumentation used. Even so, several thousand molecular species of phospho- and glycolipids have, for instance, been identified in *Staphylococcus aureus* (Hewelt-Belka et al. 2014).

2 Fatty Acids

Though as such they are not a subject of lipidomic analysis, fatty acids (FAs) play an important and irreplaceable role in the analysis of lipids. Their analysis has been performed for more than 50 years and the number of analyzed microorganisms therefore exceeds several times the number of organisms that have been analyzed as to their lipidomic profile. Furthermore, analysis of FAs, whether concerning total FAs or individual classes of lipids, is far easier to implement, and at a much lower cost per analysis. With certain exceptions (see below) routine determination of FAs presents no problem. Therefore, an introduction to this chapter describes the types of fatty acids (Fig. 2) that can be encountered in different groups of organisms.

In bacteria, the situation is different and is characterized by a huge variety and diversity of FAs. Besides the common bacteria such as *Escherichia coli* (gram-negative bacteria) that contains saturated FAs, often with a cyclopropane ring in the middle of the alkyl chain, or *Bacillus subtilis* (gram-positive bacteria) which are characterized by the presence of iso- and anteiso-FAs having amino acids Val, Leu, or Ile as biosynthetic precursors, bacteria contain also less common FAs. These are mainly polyunsaturated fatty acids (PUFAs) of a structure that may be identical with those of PUFAs of eukaryotes (algae, mammals). These PUFAs were surprisingly identified primarily in extremophilic bacteria, e.g., the genus *Shewanella* and many others (Russell and Nichols 1999). Their biosynthesis is also quite different; unlike the biosynthesis of PUFAs in animals, plants, fungi, and cyanobacteria, which are biosynthesized by a combination of elongation and oxygen-dependent desaturation of existing fatty acids catalyzed by fatty acid synthetase, in these bacteria they are biosynthesized using polyketide synthases, i.e., very much like antibiotics such as tetracyclines.

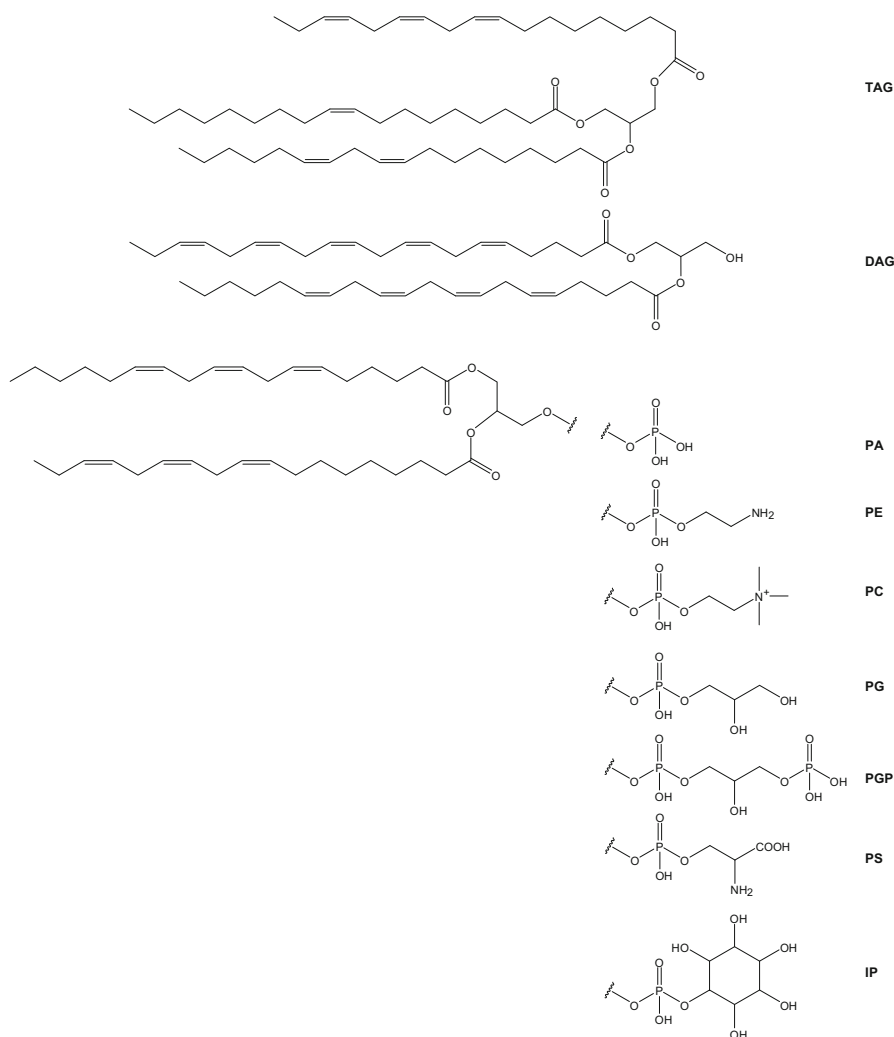


Fig. 1 Structures of “simple” and “complex” lipids (explanation of abbreviations, see below). *DAG* diacylglycerol, *TAG* triacylglycerol, *PA* phosphatidic acid, *PC* phosphatidylcholine, *PE* phosphatidylethanolamine, *PG* phosphatidylglycerol, *PGP* phosphatidylglycerolphosphate, *PI* phosphatidylinositol, *PS* phosphatidylserine

As mentioned above, bacterial FAs may contain a cyclopropane ring, with mycobacteria containing even more rings. Anaerobic ammonium oxidizing (anammox) bacteria belonging to the phylum Planctomycetes, which oxidize ammonium to N_2 with nitrite as the terminal electron acceptor, contain ladderanes, which are compounds containing cyclobutane ring(s) (see below). Cyclopentane fatty acids were identified in, e.g., *Gibberella fujikuroi* which is a fungal plant pathogen, or in the plant family Flacourtiaceae. ω -Cyclohexyl and ω -cycloheptyl FAs have

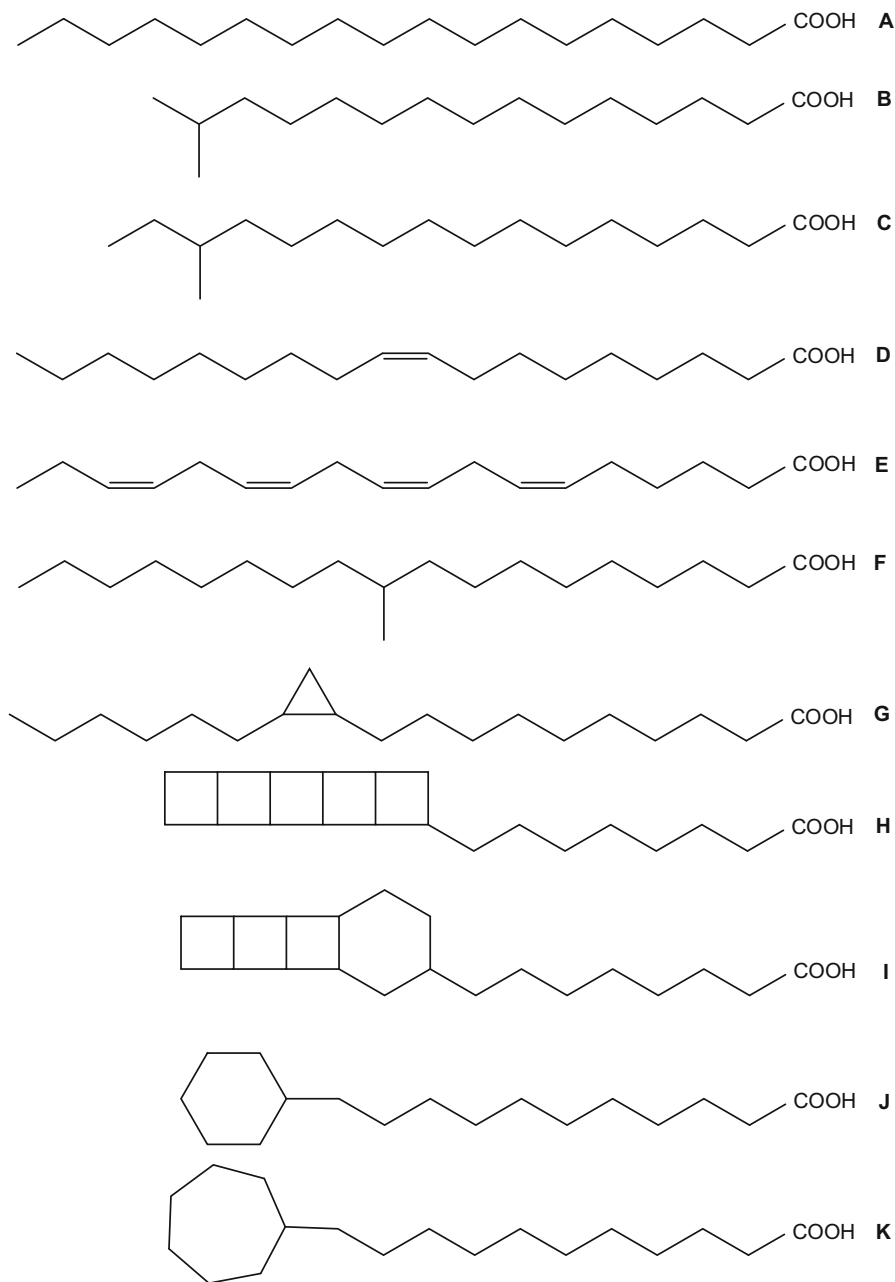


Fig. 2 Types of fatty acids (**A** – saturated, i.e., stearic acid, **B** – *iso*-branched, i.e., isopalmitic acid, **C** – anteisobranched, i.e., anteisomargaric acid, **D** – oleic acid, **E** – α -linolenic acid, **F** – tuberculostearic acid, **G** – lactobacillic acid, **H**, **I** – ladderane fatty acids, **J** – 11-cyclohexylundecanoic acid, **K** – 11-cycloheptylundecanoic acid)

been identified in thermoacidophilic bacteria of the genus *Alicyclobacillus* (Rezanka et al. 2009).

It can thus be said that bacteria contain all known types FAs with the exception of those with a cyclopentane ring.

Eukaryotic organisms from algae through lower plants (mosses, ferns, lichens) to flowering plants contain mainly straight-chain FAs, either saturated or monounsaturated, and also PUFAs. Many plants contain so-called very-long-chain fatty acids, which are considered to include FAs with a chain longer than 22 carbon atoms. Typical examples are wax esters on the surface of vascular plants, which are important biomarkers found in sediments.

By contrast, specialized tissues (organs) of mammals, e.g., sperm, brain, or eye, contain very-long-chain polyunsaturated fatty acids (VLCPUFAs) of the type of C28-C36 FAs belonging to the n-3 and n-6 families and containing 4–6 double bonds. It is surprising that similar FAs, although only up to the C₂₈, but with up to eight double bounds are found in dinoflagellates, which are a large group of flagellate protists, mostly from the marine plankton that constitute the phylum Dinoflagellata.

This brief introduction about the types of fatty acids and their presence or absence in various organisms is intended to show the enormous diversity of their structure. According to Chemical Abstracts (SciFinder database), there are reportedly around one thousand known naturally occurring FAs.

3 Archaea

Archaea are a large domain of prokaryotic unicellular organisms whose independence from bacteria and eukaryotes was recognized in 1977. First, one should note that the Archaea (formerly archaeobacteria) form a large kingdom of unicellular prokaryotic organisms that is independent of other domains of life (bacteria and eukaryotes). They differ from bacteria and eukaryotes in the structure of their cell membrane, cell wall, the genome, and certain metabolic processes. These differences include, for example, the presence of different stereochemistry of the archaeal glycerol moiety (another enantiomer) and the fact that none of the hitherto analyzed archaeal microorganisms contains fatty acids. Complex phospholipids contain isoprenoid chains with multiple side-branches coupled to the glycerol backbone by ether bond (see below). Archaea might be found in areas with extremely high temperatures, extreme pH, or high salt content.

The chemical structure of archaeal membrane is unique. As mentioned above, their lipids do not contain FAs. Archaeal phospholipids are unusual in several respects; above all, they consist of glycerol-ether lipids (De Rosa et al. 1986). The ether linkages are highly stable and this enables Archaea to inhabit extreme environments (Albers et al. 2000). Chains are not straight but mostly branched and are based on isoprene units (Damste et al. 2002) and therefore have no double bond(s) (Koga and Morii 2005). As stated above, the complex lipids contain

L-glycerol, which is the enantiomer of D-glycerol occurring in all other organisms (Koga and Morii 2005). The main problems with Archaea are the difficult analysis and their non-culturability. This problem, however, far exceeds the scope of this chapter. For more details, see, e.g., Woese et al. (1990).

The use of lipidomics for Archaea is illustrated by several studies reporting on the possibilities of lipidomic analysis. HPTLC and MALDI-TOF/MS of the archaeon *Pyrococcus furiosus*, which grows at 100 °C, were used to identify polar lipids of the type of archaeol (diethers) and caldarchaeol (tetraethers) (Lobasso et al. 2012). MALDI with 9-aminoacridine- like matrix identified the structure shown in Fig. 3.

Lipidomic analysis of two extremely haloalkaliphilic archaea, *Natronococcus occultus* and *N. amylolyticus*, combined the use of TLC and MALDI-TOF/MS analysis (Angelini et al. 2012). The major lipids were phosphatidylglycerol and phosphatidylglycerophosphate methyl ester, including cardiolipin that contained four isoprenoid chains. This lipid was also hypothesized to play a crucial part in the adaptation to high pH and high salinity.

MALDI-TOF/MS was again used in the lipidomic analysis of the halophilic archaeon *Halobacterium salinarum* (Angelini et al. 2010) which identified many glyco- and phospholipids up to a molecular weight of 2,000 Da, among them, e.g., (3'-sulfo)Galpβ1-6Manpα1-2Glcα1-1-[sn-2,3-di-O-phytanylglycerol] or (3'-sulfo)Galpβ1-6Manpα1-2Glcα1-1-[sn2,3-di-O-phytanylglycerol]-6-[phospho-sn-2,3-di-O-phytanylglycerol].

In two halophilic microorganisms, *Halorubrum trapanicum* and *Haloferax volcania* isolated from a salt lake near Malaga (Spain), Lobasso et al. (2015) identified unusual sulfated bis-diglycosyl diphytanylglyceroldiethers with m.w. around 1000 Da using a TLC-MALDI-TOF/MS and discussed their effect on the bacterial resistance to high salinity.

The frequently studied archaeon *Sulfolobus islandicus* was found to contain common archaeal lipids, i.e., dialkyl glycerol diethers and tetraethers substituted with polar phosphate groups often further substituted by, e.g., inositol, glycerol, or from one to four monosaccharides (Jensen et al. 2015a). In another study, Jensen et al. (2015b) investigated the influence of temperature on the number of cyclopentane rings in the lipid molecule.

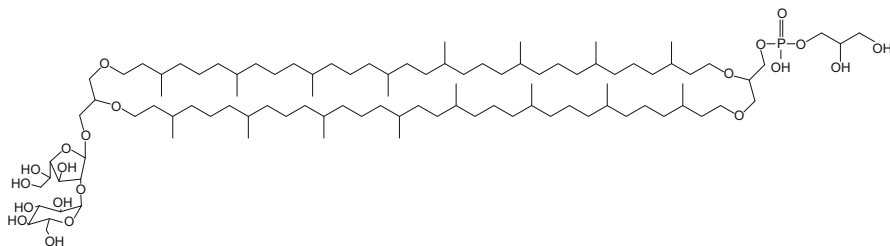


Fig. 3 The structure of diglycosyl phosphatidylglycerol tetraether (hexose2-PG-T) from marine hyperthermophilic archaeon *Pyrococcus furiosus*

Gagen et al. (2016) described a change in lipids (mainly tetraethers) in *Thermococcus kodakarensis* during cultivation; the lipids were separated by UHPLC and identified by tandem ESI/MS.

RP-HPLC with tandem QTOF-ESI-MS was used to analyze the lipids of the thaumarchaeon *Nitrosopumilus maritimus* (Elling et al. 2014). The value of the organic paleothermometer (TEX₈₆) was found to depend on membrane dibiphytanyl glycerol tetraether lipids (GDGTs).

The above examples constitute a mere fraction of published works and should allow readers to get familiar with the analysis of archaeal lipids. The main problem in the field does not seem to be the actual analysis of lipids but the collection and especially cultivation of these microorganisms (Blum 2008), or their contamination by other organisms.

A very nice example of a connection of cultivation and analysis of Archaea is given in the study performed on *T. kodakarensis* by (Gagen et al. 2016; Meador et al. 2014); it should be however noted that the research team has extensive experience with cultivation of hardly cultivable microorganisms.

4 Bacteria

Bacteria are a separate domain of unicellular prokaryotic organisms and are the most widespread living organisms. This is reflected in the large number of different classes of lipids, see Fig. 1.

It is believed that the lipids of a single bacterial cell can include many thousands of molecular lipid species (Breslow et al. 2008; Schuldiner et al. 2005; Yetukuri et al. 2008). As mentioned above, bacteria contain in addition to conventional-type straight-chain FAs (saturated, unsaturated, and polyunsaturated) (Russell and Nichols 1999) also branched (iso and anteiso) fatty acids and FAs with cycles, see Fig. 2 (Lanekoff and Karlsson 2010).

Data on the diversity of bacterial lipid structures were published in several reviews (Parsons and Rock 2013; Sohlenkamp and Geiger 2016). Lipidomic analysis of these lipid structures has also been published (Leray 2012; Řezanka et al. 2012).

Escherichia coli and *Bacillus subtilis* are two typical representatives of gram-negative and gram-positive bacteria, and it is therefore not surprising that one of the first studies dealing with lipidomic analysis of bacteria was devoted to them (Gidden et al. 2009). MALDI-TOF/tandem MS showed that both fatty acids and lipids of the two species differ widely. For instance, *B. subtilis* contains lysyl-PG and diglucosyl diglycerides that are missing in *E. coli*.

Zhang et al. (2011) analyzed lipids up to m.w. 1,000 Da in 2 gram-positive and 14 gram-negative bacteria by DESI and ESI and used principal component analysis to determine the taxonomy of the bacteria.

Analysis of *S. aureus*, one of the best known human pathogens, was performed by HPLC-QTOF-MS (Hewelt-Belka et al. 2014). The authors identified over 7000 molecular species belonging to 18 major classes and 36 subclasses of lipids.

This provided the possibility to compare strains with different phenotypic characteristics and hence different sensitivity to antibiotics.

Garrett et al. (2012) used NP-LC/ESI-MS to identify molecular species of cardiolipin in *E. coli* grown at different temperatures; the content of these lipids was found to vary depending on temperature.

Lipidomic analysis of *Pseudomonas aeruginosa*, a known pathogen that forms biofilms, showed changes in the inner and outer membrane of the cells depending on their age (Benamara et al. 2014). Kondakova et al. (2015) described lipidomic analysis of *P. fluorescens* by HPTLC-MALDI-TOF/MS, which detected PC otherwise contained in eukaryotes.

Lipids in *B. subtilis*, *Streptomyces coelicolor*, *Mycobacterium smegmatis*, and *P. aeruginosa* were determined using nanospray MS-DESI directly from Petri dishes without performing the extraction of lipids (Watrous et al. 2012).

Identification of different species of *Bacillus* was performed by MALDI-TOF/MS and the cells were found to contain phospholipids – PE, PC, PG, DGDG (Shu et al. 2012).

Hansen et al. (2015) investigated the plasma membrane of the probiotic *Lactobacillus acidophilus* La-5 using high-resolution shotgun lipidomics. They described changes in the composition of fatty acids in plasma membrane lipids, mainly in cardiolipin and monolysocardiolipin, after addition of Tween 20, a polysorbate surfactant like Tween 80, but primarily containing lauric and myristic acids as well as linoleic and alpha-linolenic acids.

4.1 Plasmalogens

One of the most interesting groups of lipids is plasmalogens. These compounds are glycerol derivatives wherein alcohol is bound to the *sn*-1 position via ether bonds and a fatty acid esterifies the *sn*-2 position. The alcohol binds as vinyl ether, the acid by an ester linkage, see Fig. 4 for the structure of plasmalogen-phosphatidyl ethanolamine (pPE).

The alcohol usually has 16 or 18 carbon atoms, whereas the acid is always characteristic for the given group of organisms, for instance, straight chain or branched chain saturated (iso or anteiso) acid in bacteria (Rezanka et al. 2012), or polyunsaturated acids in mammals.

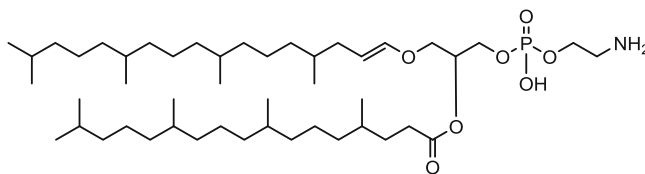


Fig. 4 The structure of plasmalogen-phosphatidyl ethanolamine (pPE)

At the 3-position of the glycerol, backbone is a phosphate group, so that plasmalogens include plasmalogen-phosphatidylserine, plasmalogen-phosphatidylglycerol, plasmalogen-phosphoethanolamine, etc.

Much more interesting than their structure is their distribution in nature. They are found only in anaerobic bacteria and in animals (Braverman and Moser 2012; Magnusson and Haraldsson 2011) and have not been found in aerobic bacteria, fungi, and plants, including algae (Felde and Spiteller 1994). Their presence in fungi is highly debatable (Horrocks and Sharma 1982).

Plasmalogens were analyzed in recent years almost exclusively by LC-MS. Other methods are time-consuming and inaccurate and usually do not provide information about native plasmalogens and their molecular species. Identification of plasmalogens is usually not complicated, see the paper of Hsu et al. (2003) which describes very well the analysis and provides excellent background information.

Lipidomic analysis can be used in industrial practice for instance in the brewing industry to identify the contamination of beer by anaerobic bacteria of the genus *Pectinatus* and *Megasphaera* (Rezanka et al. 2015). Analysis of *Pectinatus frisingensis* was performed by LC-MS, see Fig. 5, and it was found that the major plasmalogen is cyclo-plasmenyl-19:0/17:1 PE. Alanyl, lysyl-, and glucosyl-phosphatidylglycerols and CLS have been identified in thermophilic bacteria of the genus *Anoxybacillus* using HILIC-LC / ESI-MS/MS (Rezanka et al. 2012). Bacteria of genus *Clostridium* have been found to contain plasmalogens (Goldfine and Guan 2017; Kolek et al. 2015).

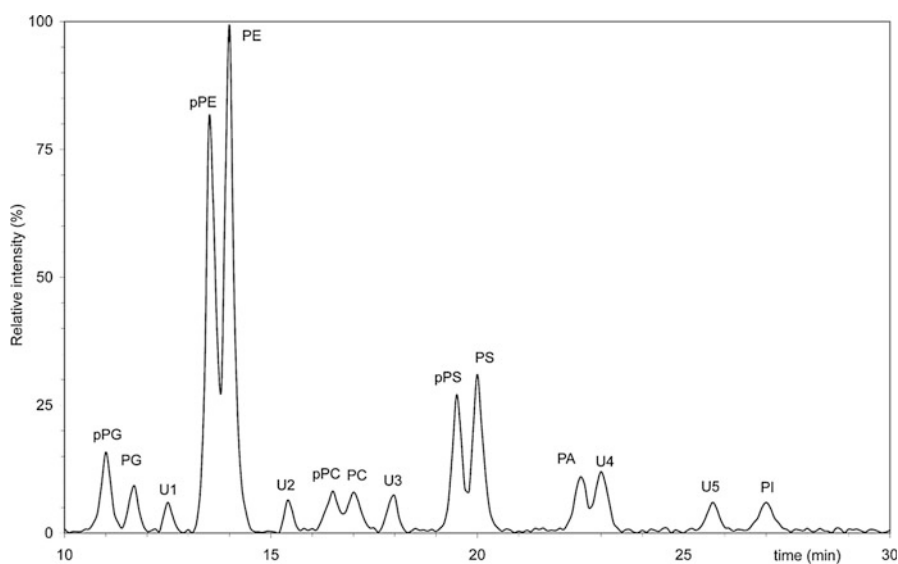


Fig. 5 HILIC/APCI-MS chromatogram of the phospholipids from *Pectinatus frisingensis* DSM 20465

Basically the same facts that were said about cultivability and/or noncultivability of Archaea also apply to bacteria. The review by Alain and Querellou (2009) stated that more than 90% of bacteria found in nature are noncultivable. Their presence can obviously be proved in substrates such as geothermal water, forest soil, active sludge from wastewater treatment, but during subsequent culture of bacteria from these substrates only some are able to multiply and grow. The overall population is thus overgrown by several fastest propagating bacteria, which reduces the species diversity of the population.

4.2 Mycobacteria

As suggested by their name, mycobacteria were for many years considered to belong to fungi, among others for the unusual structure of their lipids, particularly mycolic acids and mycolates (Fig. 6). Many of them are human pathogens (*M. tuberculosis* or *M. leprae*). The lipids of mycobacteria include both nonpolar lipids, such as phthiocerol dimycocerosates, and polar ones (phosphatidylinositol mannosides). Lipidomic analysis identified over 5000 molecular species (Layre et al. 2011).

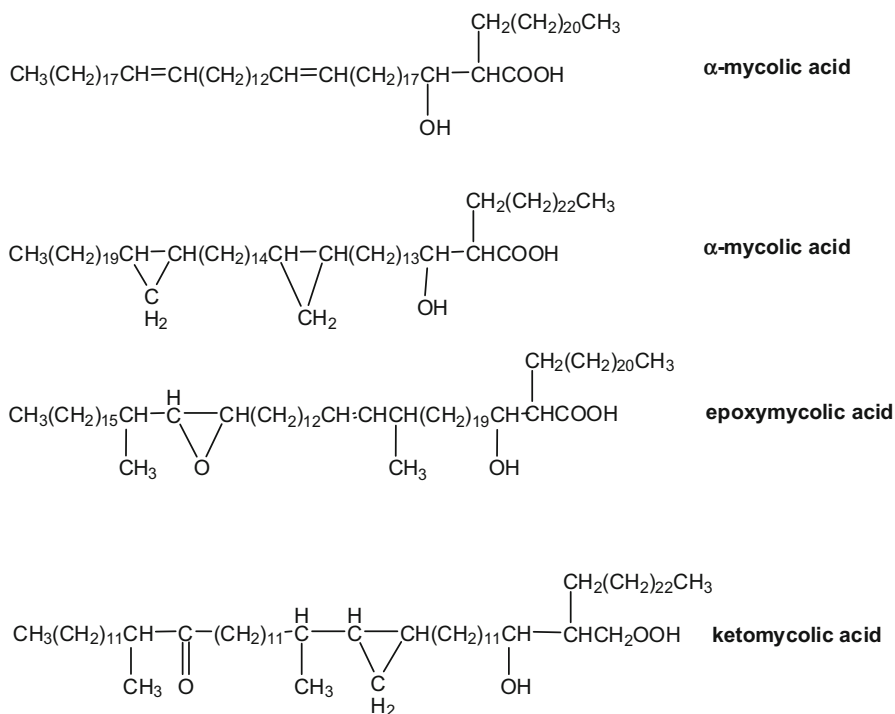


Fig. 6 Unusual structure of mycolic acids

Three databases of these lipids were created, i.e., MTB LipidDB, MycoMass, and MycoMap (Layre et al. 2011; Madigan et al. 2012; Sartain et al. 2011).

Lipids can form over half of cell mass and, in addition to the already mentioned mycolic acids, they include complex lipids and FAs such as palmitic, oleic and tuberculostearic acids. The complex lipids have not been found to include sphingolipids, PE, PC, PG, and diphosphatidylglycerol, whereas the presence of phosphatidylinositol and phosphatidylinositol mannosides is common (Hsu et al. 2007a, b).

Mycolic acids, which have a totally unique structure and have not been found in other bacteria, consist of α - and β -hydroxymycolic chains differing in length and chain branching, unsaturation, and substitution of polar groups (Guenin-Mace et al. 2009). They provide essential structure information that can be used in taxonomy (Butler and Guthertz 2001).

The use of isoniazid, an important drug which inhibits the biosynthesis of mycobacterial lipids, led to the understanding of the structure of cell membranes (Layre et al. 2014).

Lipidomic analysis of bacteria including mycobacteria revealed the great variability of complex lipids, the use of which can be seen especially in chemotaxonomy, but also in the elucidation of resistance to antibiotics including the knowledge of the behavior of bacteria in the biofilm.

5 Yeast

Yeast is one of the most important microorganisms used in biotechnology. Yeasts are basically single-celled fungi that usually reproduce by budding or fission and are used primarily for the production of beer, wine, and bread. However, some yeasts, e. g., *Candida albicans*, are pathogenic.

Lipidomics of yeast was the subject of several major studies that mostly analyzed the famous yeast species *Saccharomyces cerevisiae*. Shotgun lipidomic analysis of two million cells allowed the identification of 21 classes of lipids and more than 250 molecular species. Changes were found in the lipid content of yeast cultured at 24 °C and 37 °C (Ejsing et al. 2009).

Lipidomic studies using UHPLC-MS/MS performed on a wild and a recombinant strain of *S. cerevisiae* showed a correlation between PI metabolism of xylose and glucose (Xia et al. 2011).

A study of the dependence of the 21 classes of lipid in *S. cerevisiae* on the duration of cultivation showed a change in the contents of 34:2-PC versus 32:2-PC or 34:2-PA versus 32:2-PA (Casanovas et al. 2015).

Cultivation of two yeasts, *S. cerevisiae* and *Zygosaccharomyces bailii*, on an atypical carbon source (acetic acid) was investigated by lipidomic analysis, and it was found that the tolerance to acetic acid is related to the increase in the content of sphingolipids (Lindberg et al. 2013).

Da Silveira dos Santos et al. (2014) studied the effect of deletion of nonessential genes encoding kinases or phosphatases on lipid content. The results showed changes in some molecular species, e.g., 32: 2 and 34: 2-PC.

The absence of YBR141C and YJR015W genes, whose function is unknown, was studied in mutants of *S. cerevisiae* (Tarasov et al. 2014).

Lipidomic profile of *S. cerevisiae*, *S. bayanus*, *Kluyveromyces thermotolerans*, *Pichia angusta*, and *Yarrowia lipolytica* showed that the yeast contain 9 classes of phospholipids (mainly CL, PE, PI PC, PS, and PG) with more than 100 molecular species (Hein and Hayen 2012).

Lipidomic analysis of the wild type strain of *S. cerevisiae* and its mutants cultured at four different temperatures (15 °C, 24 °C, 30 °C, and 37 °C) was performed in order to investigate changes in phospholipids (Klose et al. 2012). The analysis showed that increased temperature enhances PI content and reduces the content of TAG and PE.

Comparison of lipidomic profiles of homogenate and microsomes in methylotrophic yeast *Pichia pastoris* showed changes in the content of TAG, PC, and PI (Klug et al. 2014).

As stated above, with a few exceptions the authors examined only *S. cerevisiae*. Further developments in this area can be seen particularly in the lipidomic analysis of less and less easily cultivable yeasts, for example, psychrophilic yeasts (Fig. 7) (Rezanka et al. 2016).

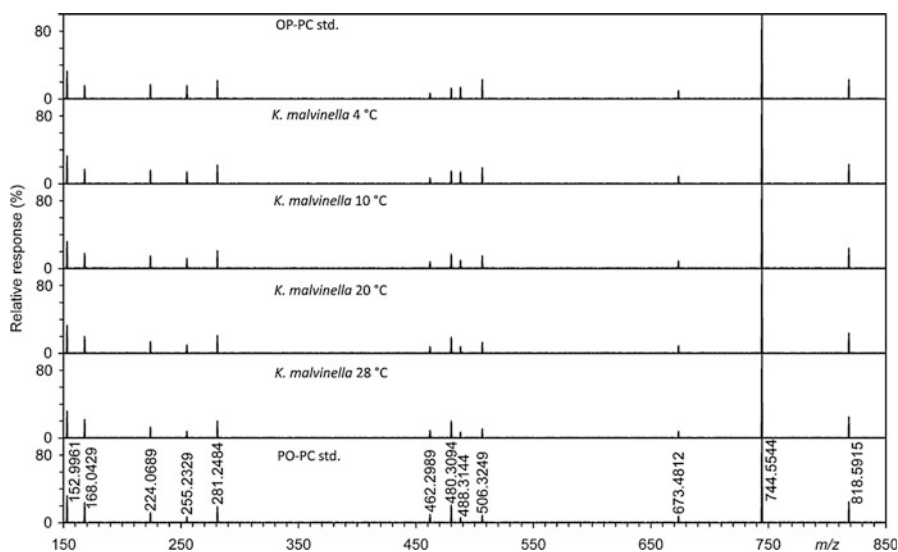


Fig. 7 Tandem mass spectrum of natural PC of *K. malvinella* cultivated at different temperatures and two commercial standards, i.e., molecular species 1-palmitoyl-2-oleylphosphatidylethanolamine and (PO-PC) and 1-oleyl-2-palmitoyl-phosphatidylethanolamine (OP-PC), respectively

6 Cyanobacteria and Algae

6.1 Cyanobacteria

Algae and cyanobacteria are taxonomically very different, but they biosynthesize basically very similar lipids. Also both their occurrence and cultivation are very much the same. That is why they are here discussed together, although algae are eukaryotes while cyanobacteria are prokaryotes.

Cyanobacteria were found to contain glycolipids (MGDG, DGDG, and SQDG) as well as phospholipids, with PG as a major lipid. In this cyanobacterial lipids resemble lipids of algae and are different from most bacteria, which are taxonomically much closer.

Marques et al. (2016) examined the effects of As (III) on the lipidomic profiles of two cyanobacterial species (*Anabaena* and *Planktothrix agardhii*) using LC-MS with simultaneous processing of the results by the multivariate curve resolution alternating least squares. They found that As (III) induced significant changes in the lipid composition of the cyanobacteria. The biggest changes occurred primarily in the content of pigments (chlorophyll *a* and its degradation product pheophytin *a*, as well as in carotene compounds such as 3-hydroxycarotene and 3-carotene-3,3'-dione) and in the content of MGDG.

6.2 Algae

Algae are lower plants, both unicellular and multicellular (see thallus). They live in fresh or salt water, or in symbiosis in lichens. Although algae are typical photosynthetic organisms, they can be cultivated exclusively heterotrophically, which is widely used in various biotechnological applications. Algae contain a variety of lipids, including the less common ones, e.g., betaine lipids or sulfolipids. Typical examples are diacylglyceryltrimethylhomoserine (DGTS), diacylglyceryl hydroxymethyl trimethylalanine (DGTA), and diacylglycerylcarboxyhydroxymethylcholine (DGCC), see Fig. 8.

Unlike bacteria and yeasts, algal dry weight often contains more than 50% PUFAs, for instance, 18:5, 20:5, and 22:6 acids that are missing in higher plants. To produce PUFAs, algae are commonly cultured in fermenters with volumes of tens of thousands liters (e.g., the commercially available preparation containing docosahexaenoic acid from different strains of algae).

Lipidomic analysis has often been performed in order to determine the behavior of algae under abnormal cultivation conditions. One of the stressful conditions is a salt content higher than that at which algae usually grow. For freshwater algae, it is, e.g., cultivation in sea water. Lu et al. (2012, 2013) studied the alga *Chlamydomonas nivalis* (snow alga that lives in the snow, which is basically almost pure water) for its content of lipid biomarkers (DGTS, MGDG, DGDG, or SQDG) using ESI

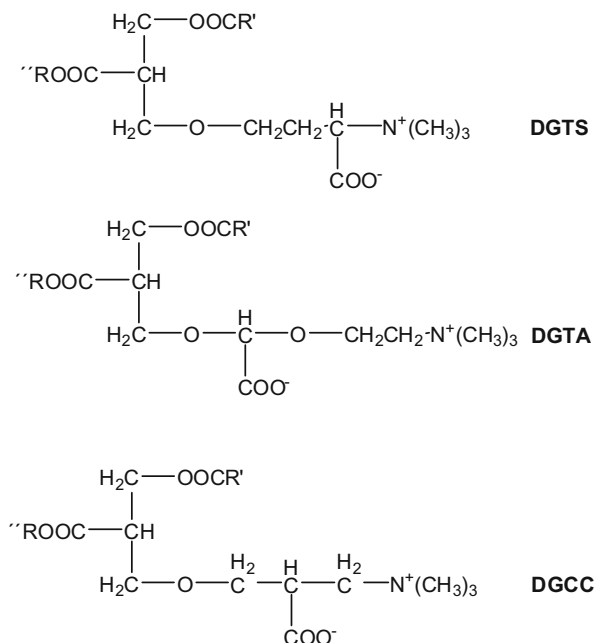


Fig. 8 Examples of structures of diacylglyceryltrimethylhomoserine (DGTS), diacylglyceryl hydroxymethyl trimethylalanine (DGTA) and diacylglycerylcarboxyhydroxymethylcholine (DGCC)

in positive- and negative-ion mode. They identified a noncommonly occurring hexadecatetraenoic acid and identified lipids in algae cultured under different conditions using multivariate statistical analysis.

Two geographic varieties of the alga *Nannochloropsis oceanica*, which are morphologically and taxonomically (via 18S rRNA) indistinguishable, showed, using UHPLC-Q-TOF-MS, a completely different taxonomically pertinent lipid profile (Li et al. 2015). As biomarkers have been identified, e.g., 20:4/20:5-DGTS, 20:5/14:0-MGDG, 20:5/16:1-DGDG, and 16:1/20:5/20:5-TAG.

Geographic varieties of the snow alga *Chloromonas pichincae* were analyzed by silver LC/APCI-MS and LC-NARP/APCI-MS (Rezanka et al. 2014), see Fig. 9, who identified uncommon molecular species of 16:4/16:4/18:4-TAGs, 16:3/16:3/18:4-TAGs or 18:4/18:4-SQDG.

The dependence of the lipidomic profile on culture conditions of the red alga *Galdieria sulphuraria* growing at low pH was determined by LC-MS (Vitova et al. 2016). Cultivation was carried out at pH 1–4 and 14 classes of lipids were identified including many tens of molecular species of lipids, including regioisomers. Low pH promotes the biosynthesis of betaine lipids and causes variation in the ratio of regioisomers.

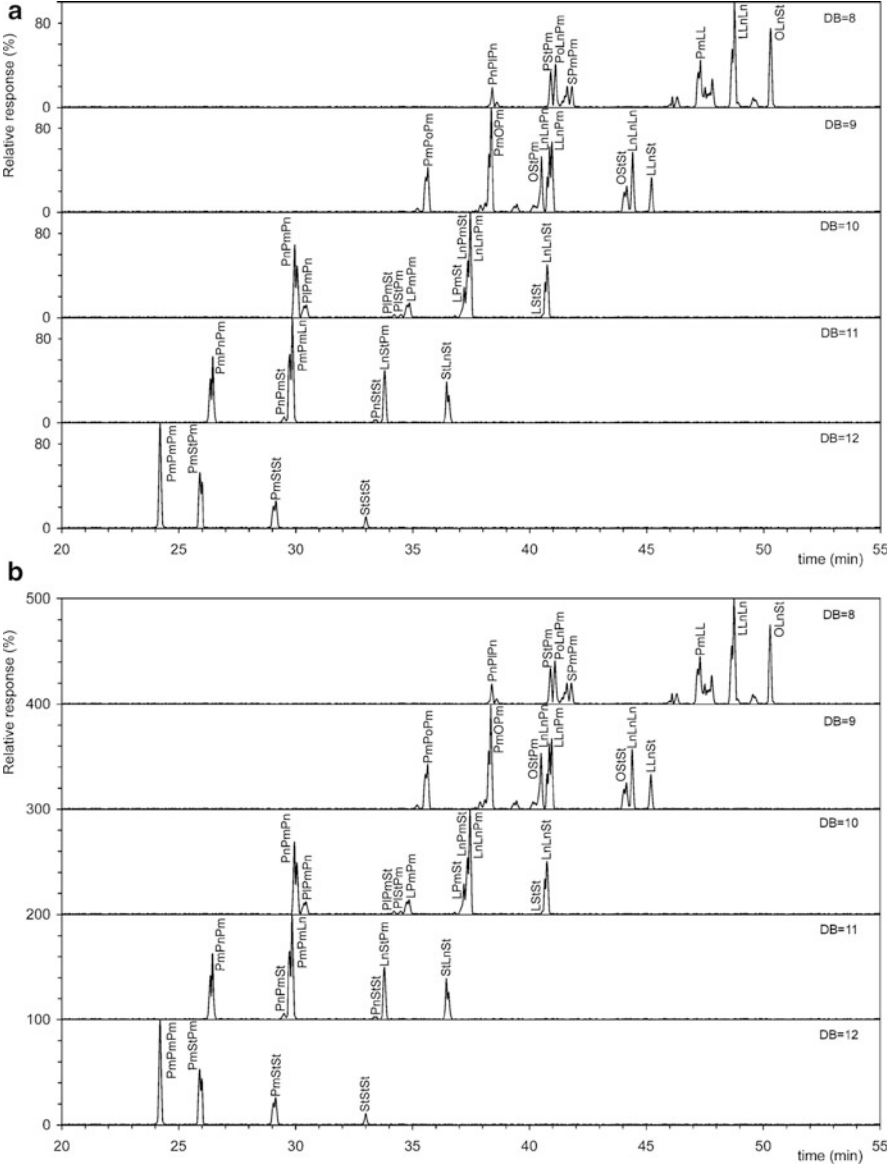


Fig. 9 (a) Silver-LC chromatograms of the TAGs mixture from snow alga *Chloromonas pichincae* with labeled double bonds groups (sample UDOLI). (b) Analysis of TAGs from snow alga *C. pichincae* by NARP-HPLC/APCI-MS (sample UDOLI)

Analysis of the psychrophilic alga *Chlamydomonas reinhardtii* (Yang et al. 2015) using positive and negative mode ESI identified polar lipids, and their molecular species, e.g., 16:0/18:4-DGTS, 16:0/18:3-SQDG, and 16:1/18:3-PG.

Danielewicz et al. (2011) studied the possibility of using lipidomic analysis for potentially oleaginous saltwater microalgae *Phaeodactylum tricornutum*, *Nannochloropsis salina*, *Nannochloropsis oculi*, and *Tetraselmis suecica*. Using MALDI and ESI-TOF profile, they detected dozens of triacylglycerols, for example, 20:5/20:5/20:4-TAG or 16:1/16:3/20:5-TAG. The method is very suitable for the rapid screening of algae for biofuel production.

The alga *Nannochloropsis salina* was investigated using several ionization techniques (ESI, APCI, APPI, and MALDI) and showed differences in the representation of individual lipid classes (Lee et al. 2013). This study pointed out how important it is to use internal standards for the quantification. It is to be regretted that not all necessary standards are commercially available.

Investigation of the influence of temperature changes on the lipidome of red alga *Pyropia haitanensis* revealed that the alga contains 39 lipids that can serve as lipid biomarkers (Chen et al. 2016).

MacDougall et al. (2011) used UHPLC-MS to identify and quantify the contents of TAGs in 6 algae of the genus *Botryococcus*, *Nannochloropsis*, *Neochloris*, *Phaeodactylum*, *Porphyridium*, and *Scenedesmus*. They detected the presence of 28:1/28:2/18:1 TAG or 28:2/28:2/18:1-TAG belonging to TAGs with the longest known chain found in nature. In addition, the alga *Scenedesmus obliquus* contains polyunsaturated TAGs, e.g., 20:5/18:3/16:3-TAG. Although the publication is 6 years old, it points to further possibilities of lipidomic analysis of algae and other organisms.

In their excellent review, da Costa et al. (2016) summarized the findings obtained by lipidomic analysis of glycolipids of many tens of microalgae.

7 Research Needs

We believe that further development of lipidomic analysis is expected in four directions.

New ionization techniques. The first is the use of new ionization techniques, e.g., atmospheric pressure photoionization MS which is connected to tandem MS, or the use of high-resolution mass spectrometry of time-of-flight MS, connected with ultra-performance liquid chromatography.

Wider range of samples. The second direction is the analysis of a much wider range of samples, particularly from the group of microorganisms not commonly found, such as extremophilic Archaea, bacteria, yeast or cyanobacteria, and algae harvested from unusual (psychrophilic, halophilic, thermophilic, etc.) habitats. Shotgun and LC-MS lipidomics has so far been rarely used for analysis of lipids containing unusual head groups, very-long chain or very-long chain polyunsaturated FAs.

Chemical compounds labeled with stable isotopes. The third direction involves the application and use of chemical compounds labeled with stable isotopes in the study of dynamic changes of metabolic pathways. This approach is at the beginning and suffers so far from the lack of suitable and commercially available precursors

and metabolites and their high price. Nevertheless, the use of labeled compounds leads to a complex analysis of lipid metabolism on the molecular level and a better understanding of the role of lipids in biotechnological applications.

Single cell lipidomics. The fourth area concerns the sensitivity of currently produced mass spectrometers, which has already reached the attomole (10^{-18}) level, i.e., the concentration of lipids in a single cell. This creates a new highly promising discipline, which we may call single cell lipidomics.

Acknowledgments The research was supported by GACR project 17-00027S and by Institutional Research Concept RVO61388971.

References

- Alain K, Querellou J (2009) Cultivating the uncultured: limits, advances and future challenges. *Extremophiles* 13:583–594. <https://doi.org/10.1007/s00792-009-0261-3>
- Albers SV, van de Vossen JL, Driessen AJ, Konings WN (2000) Adaptations of the archaeal cell membrane to heat stress. *Front Biosci* 5:813–820. <https://doi.org/10.2741/albers>
- Angelini R, Babudri F, Lobasso S, Corcelli A (2010) MALDI-TOF/MS analysis of archaeobacterial lipids in lyophilized membranes dry-mixed with 9-aminoacridine. *J Lipid Res* 51:2818–2825. <https://doi.org/10.1194/jlr.D007328>
- Angelini R, Corral P, Lopalco P, Ventosa A, Corcelli A (2012) Novel ether lipid cardiolipins in archaeal membranes of extreme haloalkaliphiles. *Biochim Biophys Acta* 1818:1365–1373. <https://doi.org/10.1016/j.bbamem.2012.02.014>
- Benamara H, Rihouey C, Abbes I et al (2014) Characterization of membrane lipidome changes in *Pseudomonas aeruginosa* during biofilm growth on glass wool. *PLoS One* 9:e108478. <https://doi.org/10.1371/journal.pone.0108478>
- Blum P (2008) *Archaea: new models for prokaryotic biology*. Horizon Scientific Press, Norfolk
- Braverman NE, Moser AB (2012) Functions of plasmalogen lipids in health and disease. *Biochim Biophys Acta* 1822:1442–1452. <https://doi.org/10.1016/j.bbadis.2012.05.008>
- Breslow DK, Cameron DM, Collins SR et al (2008) A comprehensive strategy enabling high-resolution functional analysis of the yeast genome. *Nat Methods* 5:711–718. <https://doi.org/10.1038/nmeth.1234>
- Butler WR, Guthertz LS (2001) Mycolic acid analysis by high-performance liquid chromatography for identification of *Mycobacterium* species. *Clin Microbiol Rev* 14:704–726. <https://doi.org/10.1128/CMR.14.4.704-726.2001>
- Casanovas A, Sprenger Richard R, Tarasov K et al (2015) Quantitative analysis of proteome and lipidome dynamics reveals functional regulation of global lipid metabolism. *Chem Biol* 22:412–425. <https://doi.org/10.1016/j.chembiol.2015.02.007>
- Chen J, Li M, Yang R et al (2016) Profiling lipidome changes of *Pyropia haitanensis* in short-term response to high-temperature stress. *J Appl Phycol* 28:1903–1913. <https://doi.org/10.1007/s10811-015-0733-z>
- da Costa E, Silva J, Mendonça SH, Abreu MH, Domingues MR (2016) Lipidomic approaches towards deciphering glycolipids from microalgae as a reservoir of bioactive lipids. *Mar Drugs* 14. <https://doi.org/10.3390/md14050101>
- da Silveira Dos Santos AX, Riezman I, Aguilera-Romero MA et al (2014) Systematic lipidomic analysis of yeast protein kinase and phosphatase mutants reveals novel insights into regulation of lipid homeostasis. *Mol Biol Cell* 25:3234–3246. <https://doi.org/10.1091/mbc.E14-03-0851>
- Damste JS, Schouten S, Hopmans EC, van Duin AC, Geenevasen JA (2002) Crenarchaeol: the characteristic core glycerol dibiphytanyl glycerol tetraether membrane lipid of cosmopolitan pelagic crenarchaeota. *J Lipid Res* 43:1641–1651

- Danielewicz MA, Anderson LA, Franz AK (2011) Triacylglycerol profiling of marine microalgae by mass spectrometry. *J Lipid Res* 52:2101–2108. <https://doi.org/10.1194/jlr.D018408>
- De Rosa M, Gambacorta A, Gliozzi A (1986) Structure, biosynthesis, and physicochemical properties of archaeobacterial lipids. *Microbiol Rev* 50:70–80
- Ejning CS, Sampaio JL, Surendranath V et al (2009) Global analysis of the yeast lipidome by quantitative shotgun mass spectrometry. *Proc Natl Acad Sci U S A* 106:2136–2141. <https://doi.org/10.1073/pnas.0811700106>
- Elling FJ, Könneke M, Lipp JS et al (2014) Effects of growth phase on the membrane lipid composition of the thaumarchaeon *Nitrosopumilus maritimus* and their implications for archaeal lipid distributions in the marine environment. *Geochim Cosmochim Acta* 141:579–597. <https://doi.org/10.1016/j.gca.2014.07.005>
- Felde R, Spiteller G (1994) Search for plasmalogens in plants. *Chem Phys Lipids* 71:109–113. [https://doi.org/10.1016/0009-3084\(94\)02305-0](https://doi.org/10.1016/0009-3084(94)02305-0)
- Gagen EJ, Yoshinaga MY, Garcia Prado F, Hinrichs KU, Thomm M (2016) The proteome and lipidome of *Thermococcus kodakarensis* across the stationary phase. *Archaea* 2016:5938289. <https://doi.org/10.1155/2016/5938289>
- Garrett TA, O'Neill AC, Hopson ML (2012) Quantification of cardiolipin molecular species in *Escherichia coli* lipid extracts using liquid chromatography/electrospray ionization mass spectrometry. *Rapid Commun Mass Spectrom* 26:2267–2274. <https://doi.org/10.1002/rcm.6350>
- Gidden J, Denson J, Liyanage R, Ivey DM, Lay JO (2009) Lipid compositions in *Escherichia coli* and *Bacillus subtilis* during growth as determined by MALDI-TOF and TOF/TOF mass spectrometry. *Int J Mass Spectrom* 283:178–184
- Goldfine H, Guan Z (2017) Lipidomic analysis of bacteria by thin-layer chromatography and liquid chromatography/mass spectrometry. In: McGenity TJ, Timmis KN, Nogaes B (eds) *Hydrocarbon and lipid microbiology protocols: genetic, genomic and system analyses of pure cultures*. Springer, Berlin/Heidelberg, pp 125–139. https://doi.org/10.1007/8623_2015_56
- Guenin-Mace L, Simeone R, Demangel C (2009) Lipids of pathogenic *Mycobacteria*: contributions to virulence and host immune suppression. *Transbound Emerg Dis* 56:255–268. <https://doi.org/10.1111/j.1865-1682.2009.01072.x>
- Hansen ML, Petersen MA, Risbo J, Hummer M, Clausen A (2015) Implications of modifying membrane fatty acid composition on membrane oxidation, integrity, and storage viability of freeze-dried probiotic, *Lactobacillus acidophilus* La-5. *Biotechnol Prog* 31:799–807. <https://doi.org/10.1002/btpr.2074>
- Hein EM, Hayen H (2012) Comparative lipidomic profiling of *S. cerevisiae* and four other hemiascomycetous yeasts. *Metabolites* 2:254–267. <https://doi.org/10.3390/metabo2010254>
- Hewelt-Belka W, Nakonieczna J, Belka M et al (2014) Comprehensive methodology for *Staphylococcus aureus* lipidomics by liquid chromatography and quadrupole time-of-flight mass spectrometry. *J Chromatogr A* 1362:62–74. <https://doi.org/10.1016/j.chroma.2014.08.020>
- Horrocks LA, Sharma M (1982) Chapter 2. Plasmalogens and O-alkyl glycerophospholipids. In: Hawthorne JN, Ansell GB (eds) *New comprehensive biochemistry*, vol 4. Elsevier, Amsterdam, pp 51–93. [https://doi.org/10.1016/S0167-7306\(08\)60006-X](https://doi.org/10.1016/S0167-7306(08)60006-X)
- Hsu FF, Turk J, Thukkani AK et al (2003) Characterization of alkylacyl, alk-1-enylacyl and lyso subclasses of glycerophosphocholine by tandem quadrupole mass spectrometry with electrospray ionization. *J Mass Spectrom* 38:752–763. <https://doi.org/10.1002/jms.491>
- Hsu FF, Turk J, Owens RM, Rhoades ER, Russell DG (2007a) Structural characterization of phosphatidyl-myo-inositol mannosides from *Mycobacterium bovis* *Bacillus Calmette Guérin* by multiple-stage quadrupole ion-trap mass spectrometry with electrospray ionization. I. PIMs and lyso-PIMs. *J Am Soc Mass Spectrom* 18:466–478. <https://doi.org/10.1016/j.jasms.2006.10.012>
- Hsu FF, Turk J, Owens RM, Rhoades ER, Russell DG (2007b) Structural characterization of phosphatidyl-myo-inositol mannosides from *Mycobacterium bovis* *Bacillus Calmette Guerin* by multiple-stage quadrupole ion-trap mass spectrometry with electrospray ionization. II. Monoacyl- and diacyl-PIMs. *J Am Soc Mass Spectrom* 18:479–492. <https://doi.org/10.1016/j.jasms.2006.10.020>

- Jensen SM, Brandl M, Treusch AH, Ejsing CS (2015a) Structural characterization of ether lipids from the archaeon *Sulfolobus islandicus* by high-resolution shotgun lipidomics. *J Mass Spectrom* 50:476–487. <https://doi.org/10.1002/jms.3553>
- Jensen SM, Neesgaard VL, Skjoldbjerg SL et al (2015b) The effects of temperature and growth phase on the lipidomes of *Sulfolobus islandicus* and *Sulfolobus tokodaii*. *Life* 5:1539–1566. <https://doi.org/10.3390/life5031539>
- Klose C, Surma MA, Gerl MJ et al (2012) Flexibility of a eukaryotic Lipidome – insights from yeast lipidomics. *PLoS One* 7:e35063. <https://doi.org/10.1371/journal.pone.0035063>
- Klug L, Tarazona P, Gruber C et al (2014) The lipidome and proteome of microsomes from the methylotrophic yeast *Pichia pastoris*. *Biochim Biophys Acta* 1841:215–226. <https://doi.org/10.1016/j.bbaliip.2013.11.005>
- Koga Y, Morii H (2005) Recent advances in structural research on ether lipids from archaea including comparative and physiological aspects. *Biosci Biotechnol Biochem* 69:2019–2034. <https://doi.org/10.1271/bbb.69.2019>
- Kolek J, Patakova P, Melzoch K, Sigler K, Rezanka T (2015) Changes in membrane plasmalogens of *Clostridium pasteurianum* during butanol fermentation as determined by lipidomic analysis. *PLoS One* 10:e0122058. <https://doi.org/10.1371/journal.pone.0122058>
- Kondakova T, Merlet-Machour N, Chapelle M et al (2015) A new study of the bacterial lipidome: HPTLC-MALDI-TOF imaging enlightening the presence of phosphatidylcholine in airborne *Pseudomonas fluorescens* MFAF76a. *Res Microbiol* 166:1–8. <https://doi.org/10.1016/j.resmic.2014.11.003>
- Lanekoff I, Karlsson R (2010) Analysis of intact ladderane phospholipids, originating from viable anammox bacteria, using RP-LC-ESI-MS. *Anal Bioanal Chem* 397:3543–3551. <https://doi.org/10.1007/s00216-010-3913-3>
- Layre E, Sweet L, Hong S et al (2011) A comparative lipidomics platform for chemotaxonomic analysis of *Mycobacterium tuberculosis*. *Chem Biol* 18:1537–1549. <https://doi.org/10.1016/j.chembiol.2011.10.013>
- Layre E, Al-Mubarak R, Belisle JT, Moody DB (2014) Mycobacterial lipidomics. In: Hatfull GF, Jacobs WR (eds) *Molecular genetics of Mycobacteria*. ASM Press, Washington, DC, pp 341–360
- Lee YJ, Leverence RC, Smith EA et al (2013) High-throughput analysis of algal crude oils using high resolution mass spectrometry. *Lipids* 48:297–305. <https://doi.org/10.1007/s11745-013-3757-7>
- Leray C (2012) Introduction to lipidomics: from bacteria to man. CRC Press, Boca Raton
- Li S, Xu J, Jiang Y et al (2015) Lipidomic analysis can distinguish between two morphologically similar strains of *Nannochloropsis oceanica*. *J Phycol* 51:264–276. <https://doi.org/10.1111/jpy.12271>
- Lindberg L, Santos AX, Riezman H, Olsson L, Bettiga M (2013) Lipidomic profiling of *Saccharomyces cerevisiae* and *Zygosaccharomyces bailii* reveals critical changes in lipid composition in response to acetic acid stress. *PLoS One* 8:e73936. <https://doi.org/10.1371/journal.pone.0073936>
- Lobasso S, Lopalco P, Angelini R et al (2012) Coupled TLC and MALDI-TOF/MS analyses of the lipid extract of the hyperthermophilic archaeon *Pyrococcus furiosus*. *Archaea* 2012:10. <https://doi.org/10.1155/2012/957852>
- Lobasso S, Pérez-Davó A, Vitale R, Sánchez MM, Corcelli A (2015) Deciphering archaeal glycolipids of an extremely halophilic archaeon of the genus *Halobellus* by MALDI-TOF/MS. *Chem Phys Lipids* 186:1–8. <https://doi.org/10.1016/j.chemphyslip.2014.11.002>
- Lu N, Wei D, Jiang X-L, Chen F, Yang S-T (2012) Regulation of lipid metabolism in the snow alga *Chlamydomonas nivalis* in response to NaCl stress: an integrated analysis by cytomic and lipidomic approaches. *Process Biochem* 47:1163–1170. <https://doi.org/10.1016/j.procbio.2012.04.011>
- Lu N, Wei D, Chen F, Yang S-T (2013) Lipidomic profiling reveals lipid regulation in the snow alga *Chlamydomonas nivalis* in response to nitrate or phosphate deprivation. *Process Biochem* 48:605–613. <https://doi.org/10.1016/j.procbio.2013.02.028>
- MacDougall KM, McNichol J, McGinn PJ, O’Leary SJ, Melanson JE (2011) Triacylglycerol profiling of microalgae strains for biofuel feedstock by liquid chromatography-high-resolution

- mass spectrometry. *Anal Bioanal Chem* 401:2609–2616. <https://doi.org/10.1007/s00216-011-5376-6>
- Madigan CA, Cheng TY, Layre E et al (2012) Lipidomic discovery of deoxysiderophores reveals a revised mycobactin biosynthesis pathway in *Mycobacterium tuberculosis*. *Proc Natl Acad Sci U S A* 109:1257–1262. <https://doi.org/10.1073/pnas.1109958109>
- Magnusson CD, Haraldsson GG (2011) Ether lipids. *Chem Phys Lipids* 164:315–340. <https://doi.org/10.1016/j.chemphyslip.2011.04.010>
- Marques AS, Bedia C, Lima KM, Tauler R (2016) Assessment of the effects of As(III) treatment on cyanobacteria lipidomic profiles by LC-MS and MCR-ALS. *Anal Bioanal Chem* 408:5829–5841. <https://doi.org/10.1007/s00216-016-9695-5>
- Meador TB, Gagen EJ, Loscar ME et al (2014) *Thermococcus kodakarensis* modulates its polar membrane lipids and elemental composition according to growth stage and phosphate availability. *Front Microbiol* 5. <https://doi.org/10.3389/fmicb.2014.00010>
- Parsons JB, Rock CO (2013) Bacterial lipids: metabolism and membrane homeostasis. *Prog Lipid Res* 52:249–276. <https://doi.org/10.1016/j.plipres.2013.02.002>
- Rezanka T, Siristova L, Melzoch K, Sigler K (2009) Identification of (S)-11-cycloheptyl-4-methylundecanoic acid in acylphosphatidylglycerol from *Alicyclobacillus acidoterrestris*. *Chem Phys Lipids* 159:104–113. <https://doi.org/10.1016/j.chemphyslip.2009.02.001>
- Rezanka T, Kresinova Z, Kolouchova I, Sigler K (2012) Lipidomic analysis of bacterial plasmalogens. *Folia Microbiol* 57:463–472. <https://doi.org/10.1007/s12223-012-0178-6>
- Rezanka T, Nedbalova L, Prochazkova L, Sigler K (2014) Lipidomic profiling of snow algae by ESI-MS and silver-LC/APCI-MS. *Phytochemistry* 100:34–42. <https://doi.org/10.1016/j.phytochem.2014.01.017>
- Rezanka T, Matoukova D, Benada O, Sigler K (2015) Lipidomics as an important key for the identification of beer-spoilage bacteria. *Lett Appl Microbiol* 60:536–543. <https://doi.org/10.1111/lam.12415>
- Rezanka T, Kolouchova I, Sigler K (2016) Lipidomic analysis of psychrophilic yeasts cultivated at different temperatures. *Biochim Biophys Acta* 1861:1634–1642. <https://doi.org/10.1016/j.bbaliip.2016.07.005>
- Russell NJ, Nichols DS (1999) Polyunsaturated fatty acids in marine bacteria – a dogma rewritten. *Microbiology* 145:767–779. <https://doi.org/10.1099/13500872-145-4-767>
- Sartain MJ, Dick DL, Rithner CD, Crick DC, Belisle JT (2011) Lipidomic analyses of *Mycobacterium tuberculosis* based on accurate mass measurements and the novel “Mtb LipidDB”. *J Lipid Res* 52:861–872. <https://doi.org/10.1194/jlr.M010363>
- Schuldiner M, Collins SR, Thompson NJ et al (2005) Exploration of the function and organization of the yeast early secretory pathway through an epistatic miniarray profile. *Cell* 123:507–519. <https://doi.org/10.1016/j.cell.2005.08.031>
- Shu X, Liang M, Yang B et al (2012) Lipid fingerprinting of *Bacillus* spp. using online MALDI-TOF mass spectrometry. *Anal Methods* 4:3111–3117. <https://doi.org/10.1039/C2AY25579K>
- Sohlenkamp C, Geiger O (2016) Bacterial membrane lipids: diversity in structures and pathways. *FEMS Microbiol Rev* 40:133–159. <https://doi.org/10.1093/femsre/fuv008>
- Tarasov K, Stefanko A, Casanovas A et al (2014) High-content screening of yeast mutant libraries by shotgun lipidomics. *Mol Biosyst* 10:1364–1376. <https://doi.org/10.1039/c3mb70599d>
- Vitova M, Goecke F, Sigler K, Rezanka T (2016) Lipidomic analysis of the extremophilic red alga *Galdieria sulphuraria* in response to changes in pH. *Algal Res* 13:218–226. <https://doi.org/10.1016/j.algal.2015.12.005>
- Watrous J, Roach P, Alexandrov T et al (2012) Mass spectral molecular networking of living microbial colonies. *Proc Natl Acad Sci* 109:1743–1752. <https://doi.org/10.1073/pnas.1203689109>
- Woese CR, Kandler O, Wheelis ML (1990) Towards a natural system of organisms: proposal for the domains *Archaea*, *Bacteria*, and *Eucarya*. *Proc Natl Acad Sci U S A* 87:4576–4579
- Xia J, Jones AD, Lau MW et al (2011) Comparative lipidomic profiling of xylose-metabolizing *S. cerevisiae* and its parental strain in different media reveals correlations between membrane lipids and fermentation capacity. *Biotechnol Bioeng* 108:12–21. <https://doi.org/10.1002/bit.22910>

- Yang D, Song D, Kind T et al (2015) Lipidomic analysis of *Chlamydomonas reinhardtii* under nitrogen and sulfur deprivation. PLoS One 10:e0137948. <https://doi.org/10.1371/journal.pone.0137948>
- Yetukuri L, Ekroos K, Vidal-Puig A, Oresic M (2008) Informatics and computational strategies for the study of lipids. Mol Biosyst 4:121–127. <https://doi.org/10.1039/b715468b>
- Zhang JI, Talaty N, Costa AB et al (2011) Rapid direct lipid profiling of bacteria using desorption electrospray ionization mass spectrometry. Int J Mass Spectrom 301:37–44. <https://doi.org/10.1016/j.ijms.2010.06.014>

Part III

Hydrocabons and Lipids in the Geosphere



Composition and Properties of Petroleum 11

R. Paul Philp

Contents

1	Introduction	270
2	How to Define a Crude Oil?	270
3	Characterization of Crude Oils	272
3.1	Bulk Parameters	272
3.2	Molecular Characteristics	275
4	Where Does the Oil Come From? Photosynthesis and How Things Change Over Time ...	288
5	Productivity Versus Preservation	290
6	What Are the Major Factors Involved in Determining the Composition of Crude Oils? ...	290
7	What Is the Impact of Depositional Environment?	292
8	What Is the Impact of Maturity?	295
9	How Does the Molecular Composition of an Oil Change During and After Generation?	296
10	Expulsion and Migration	300
11	Biodegradation and Preservation	301
12	Summary	305
	References	306

Abstract

Our understanding of the composition and related properties of crude oils has changed significantly over time. Many of the most significant changes have occurred in parallel with developments in analytical techniques. Until the mid-1900s, techniques available for characterizing crude oils were relatively crude by today's standards and for the most part could only determine bulk properties such as color, optical activity, API gravity, bulk isotope composition, and limited compositional analyses. The development of techniques such as gas chromatography, gas chromatography-mass spectrometry in the 1960s and 1970s, and gas

R. P. Philp (✉)

School of Geosciences, University of Oklahoma, Norman, OK, USA

e-mail: pphilp@ou.edu

© Springer Nature Switzerland AG 2020

H. Wilkes (ed.), *Hydrocarbons, Oils and Lipids: Diversity, Origin, Chemistry and Fate*,
Handbook of Hydrocarbon and Lipid Microbiology,

https://doi.org/10.1007/978-3-319-90569-3_13

269

chromatography-isotope ratio mass spectrometry in the 1980s saw a significant change in the way oils could be characterized. The molecular compositions of crude oils could be determined, and with the development of the biomarker concept, it became possible to identify individual compounds in crude oils that could be used to provide a significant amount of information on the origin and history of crude oils. Information such as source, maturity, depositional environments, migration pathways, and geological age became available. Furthermore, correlation of biomarker fingerprints from oils and source rock extracts permitted oil/source rock correlations to be undertaken to evaluate the actual source of an oil. Developments in these areas have continued up until the present, and new information is continually becoming available. With the age of shale oil and shale gas upon us, the knowledge gained on the composition of crude oils over the past five or six decades has become invaluable in the development of these resources. Analytical techniques continue to become more sophisticated and at the same time shed new light on the history of crude oils and their origin.

1 Introduction

This chapter is concerned with the composition and properties of crude oils. With such a title, there are numerous topics that could be covered, and obviously it would not be possible to cover all such topics in this chapter. Instead the chapter is broken down into a number of sections that highlight major features that impact the composition and properties of crude oils. Each of these sections will highlight major issues related to a specific topic and provide some additional references. It should be noted at the outset that for general information on crude oil compositions there are a number of excellent monographs including *Petroleum Geochemistry and Geology* by Hunt (1979, 1996), *Petroleum Formation and Occurrence* by Tissot and Welte (1978, 1984), the second edition of *The Biomarker Guide: Volume 2* by Peters and Moldowan (1992) and Peters et al. (2005), and the Holland and Turekian (2014) treatise plus extensive publications in the peer-reviewed journals in such journals as the *AAPG Bulletin* and *Organic Geochemistry*. A paper by Hunt et al. (2002) also provides a comprehensive overview of early developments in petroleum geochemistry going back to the early twentieth century.

2 How to Define a Crude Oil?

Crude oils are complex mixtures of hundreds of thousands of organic compounds along with varying concentrations of metals such as nickel and vanadium. The organic components are many and varied and include hydrocarbons and heteroatomic compounds, which are commonly defined on the basis of their PIANO or SARA composition. The PIANO composition is comprised of the relative proportions of the paraffins (P), isoalkanes (I), aromatics (A), naphthenes (N), and olefins (O). Initially this parameter was developed for use in refineries to provide

information on the composition of crude oils and the types and amounts of products that could be produced from a specific crude oil. Many years ago these values were obtained by high-resolution mass spectrometry, but today this compositional parameter is generally determined following the calibration of a gas chromatograph (GC) with a complex mixture of standards from each of the five aforementioned classes of compounds. The compounds in the standard that are present in the crude oil are quantified, and the PIANO composition determined. The SARA composition is comprised of the relative proportions of saturates (S), aromatics (A), resins or polars (R), and asphaltenes (A) as determined following the precipitation of the asphaltenes and fractionation of the remaining maltenes by column chromatography. While characterizing crude oils using these bulk approaches is very basic, it is useful to get general information on the composition of the crude oils and provide information on the range of products that may be expected to be produced from a crude oil. Both parameters can be used for correlation purposes or making comparisons between different crude oils, but it must be remembered these are bulk parameters, and there will be many oils that are totally unrelated that have similar PIANO and SARA values. Correlations based on these parameters need to be confirmed using more specific properties or parameters. Many years ago Tissot and Welte (1978) showed that in general crude oils could be divided into five different groups ranging from very heavy biodegraded to far lighter condensate like products as shown in Fig. 1.

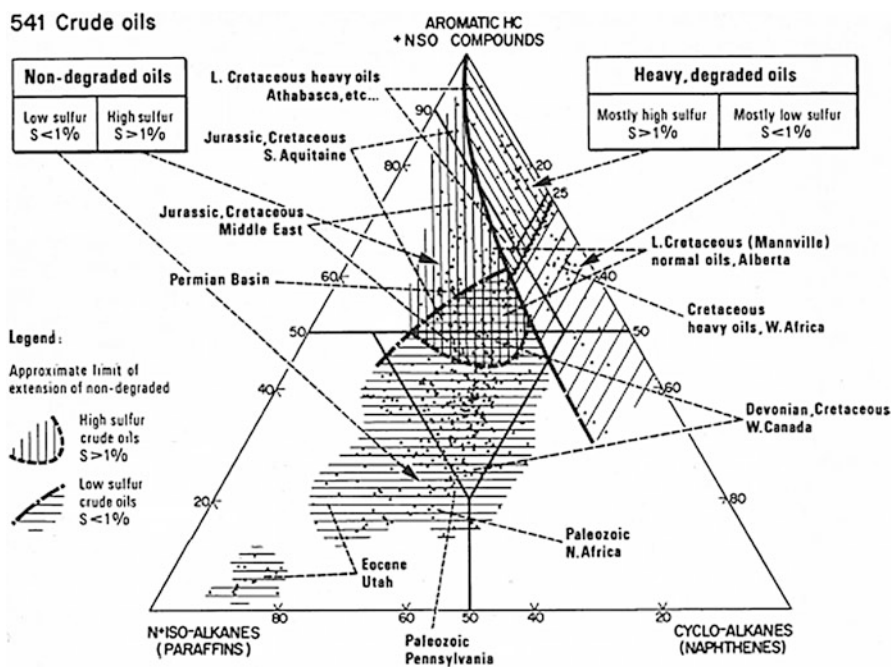


Fig. 1 Tissot and Welte (1978) showed that crude oils could, in general, be divided into five different groups ranging from very heavily biodegraded sulfur-rich oils to light condensate-type products. (Reproduced with permission from Tissot and Welte 1984)

The variations observed in these crude oils were determined from bulk fraction parameters, but ultimately these parameters are derived from the original source materials and processes that impacted the oils after generation.

3 Characterization of Crude Oils

3.1 Bulk Parameters

Crude oils can be characterized on a number of different levels using bulk characterization methods or more sophisticated techniques that characterize oils on a molecular level. The composition of crude oils can be viewed in a number of different ways depending upon the nature of the information obtained from the characterization process, but in general the information will be used either for upstream or downstream purposes. From a downstream perspective, the most important information required is a determination of the products that can be produced from that oil as it is refined, for example, how much gasoline vs. heating oil might be produced since this in turn will determine the value of the oil. Much of this information can be obtained directly from the bulk properties of the oil. Historically the most important methods for characterizing crude oils were based on distillation where different boiling point fractions were determined by conventional distillation. More recently distillation has been replaced by simulated distillation that can be undertaken by gas chromatography. In gas chromatography, one of the major properties responsible for separating compounds chromatographically is based on vapor pressure differences between individual compounds. A generic gas chromatogram showing a typical non-degraded crude oil is shown in Fig. 2 along with an indication of the range of products that can be produced from the different carbon number ranges in the crude. The separation of these individual compounds is largely determined by differences in vapor pressures of the individual compounds. Historically going back to the 1920s, the US Bureau of Mines used the so-called Hempel distillation method to differentiate or correlate crude oils (Smith 1940; Hunt et al. 2002).

Other bulk properties of crude oils were used for many years for correlation purposes prior to the advent of molecular geochemistry starting in the early 1970s. Such bulk parameters may have included simple properties such as color, optical activity, API gravity, simulated distillation curves, Hempel distillation and correlation indices, bulk carbon isotopes, relative proportions of hydrocarbon and polar fractions in the oil based on SARA and PIANO analyses, and many other properties.

One very important parameter, still used extensively today, was the API (American Petroleum Institute) gravity (Ruh et al. 1959; Hunt et al. 2002). This is a parameter related to the specific gravity (SG) of the oil through the simple formula shown below:

$$\text{API} = \frac{141.3}{\text{SG}} - 131.3$$

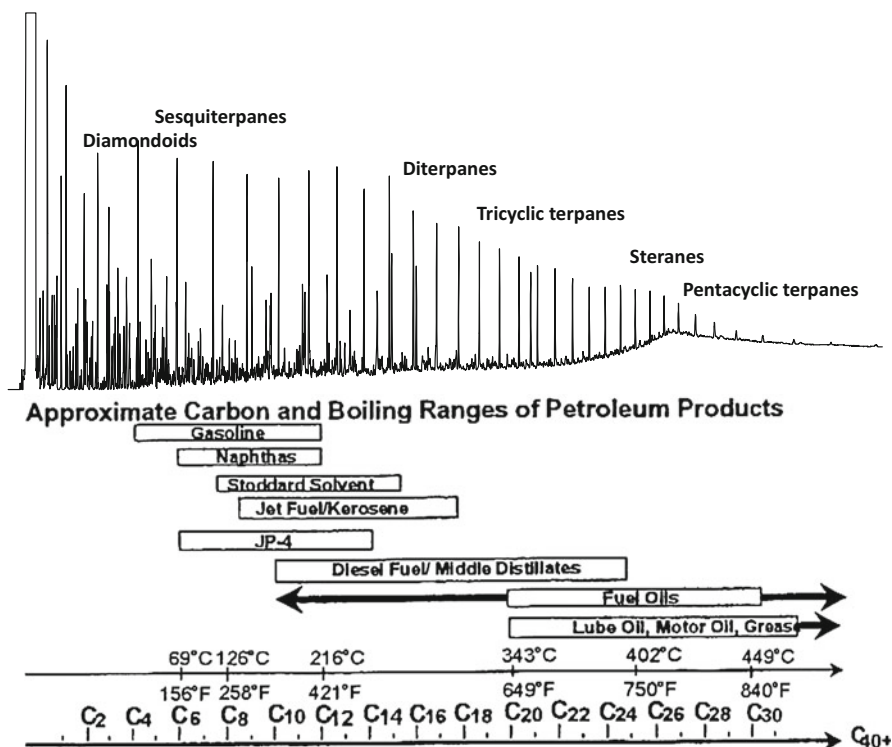


Fig. 2 A gas chromatogram for a typical non-degraded crude oil along with an indication of the boiling point range of products that can be produced from the different carbon number ranges in the crude oil. The carbon number ranges of the major families of biomarkers are also indicated on this chromatogram

The heavier the oil, the lower its API gravity; hence an oil that may be very extensively biodegraded and enriched in asphaltenes, polar and aromatic compounds, will have a very low API gravity around 10. However, a very light condensate oil will have a very high value around 50–55. Between the two extremes, there will be a wide range of oils with intermediate API values. Many years ago these values were used for correlation purposes, but there are many oils that have similar API values but are not related to each other since there cannot be an infinite range of API values. There are of course many factors that can complicate interpretation of the API gravities since you could have a very heavily degraded oil which ultimately mixes with a very light condensate, and the resulting API gravity would be somewhere between the heavy and the light values depending on the extent of mixing. However the integration of GC data can reveal the extent of such mixing. Also oils with low API values are not necessarily heavily biodegraded since oils generated at low levels of maturity from sulfur-rich kerogens will also have low API values. Heavy oils with low API gravities are worthless since they will produce less

gasoline and require specialized conditions for refining. Not only will the asphaltene fractions produce less gasoline, but heavy metals, such as nickel and vanadium, and also sulfur are concentrated in that fraction and will possibly have detrimental effects on the catalysts used in the refining process.

Even further back in history, more basic properties such as color, or optical activity, were used to differentiate or correlate crude oils (Whitehead 1971; Hunt et al. 2002). Despite what many people think, not all oils are black. There is a wide range of colors ranging from a deep black or brown through colors such as green and yellow until the very light clear condensates. However again this is not a very specific tool for correlating oils from similar sources or discriminating those from different sources and is generally not used extensively today. Most oils have the ability to rotate plane-polarized light as a result of being optically active. This results from the fact that when many molecules are being biosynthesized only one optical isomer or enantiomer is synthesized and preserved in the sediments and source rocks. However as the maturity level increases, the other enantiomer will be formed and change the optical activity of the oil. The extent of this optical activity has been used in the past to correlate or discriminate between oils from the same or different sources.

For upstream purposes the crude oil compositional data are used in a very different manner since both bulk and molecular characteristics can play important roles in the characterization of crude oils. Historically, prior to approximately the mid-1960s, as mentioned above, bulk characteristics were the major tools available for use in correlating oils with source rocks and establishing the relationship between oils within different families of oils prior to the availability of the analytical techniques in common use today such as GC, gas chromatography-mass spectrometry (GC-MS) and gas chromatography-isotope ratio mass spectrometry (GC-IRMS). Most of these bulk techniques were not very specific and in general not very useful for correlation or characterization purposes but all that was available. Early applications of bulk carbon isotope values included a study by Silverman and Epstein (1958) of several tertiary crude oils from different environments. The molecular characteristics that became routinely available from the 1970s soon replaced the use of many of the bulk parameters (Eglinton and Murphy 1969; Seifert and Moldowan 1978), although parameters such as bulk isotope values and API gravity are still commonly used.

API gravity and stable isotope values of the whole oil are generally determined at the outset of any characterization and provide useful guidelines concerning the relationship between samples and provide information that will assist in ultimately establishing relationships between groups or families of oils. There is a limited range of isotope values for crude oils covering the range of approximately -20 to -35 per mil, and therefore one can expect many oils for totally unrelated sources will have similar isotope values. The reason for this being that the primary source material present in the source rocks that generate the crude oils is derived from photosynthesis where the primary producers are incorporating CO_2 from the atmosphere and converting it into cell wall and other components (Philp 2014), since there has been a finite range of C isotope values for atmospheric CO_2 over time that will translate

into the finite range of values for the resulting crude oils as discussed in more detail below.

3.2 Molecular Characteristics

Characterization of crude oils on the molecular level developed rapidly with commercial availability of GC-MS systems in the early 1970s and followed a little later in that decade with GC-MS systems equipped with associated data systems (Hunt et al. 2002). Prior to this the only tool for molecular level of characterization was gas chromatography. This permitted a basic fingerprint showing the *n*-alkanes and major isoprenoids but showed nothing related to the complex mixture of compounds present in lower concentrations but hidden in the baseline of the chromatogram. These compounds, known as biomarkers, required the use of GC-MS for their detection, and from the 1970s until today, an ever-increasing number of these compounds have been discovered (Eglinton and Calvin 1967). By definition biomarkers are generally hydrocarbons present in oils and source rock extracts that have carbon skeletons that can be related directly to the carbon skeletons of their precursors that were present in the original source material. A significant number of these compounds are now used to provide information of the source, maturity, depositional environments, level of biodegradation, geologic age, and other parameters related to the origin and history of the oil (Eglinton and Calvin 1967; Peters et al. 2005; Philp 2014).

Before entering a discussion related to biomarkers, a brief introduction to the sophisticated analytical methods in current use to characterize crude oils will be provided. It is fair to say that the most commonly used methods to characterize crude oils are those related to determining molecular composition of crude oils, namely, GC and GC-MS. There are many additional and associated methods, such as 2D GC which provides more details on the composition of the crude oils by undertaking the chromatographic separation in two dimensions.

A generic gas chromatogram for a conventional crude oil is shown in Fig. 2, and the dominant components being a homologous series of *n*-alkanes (structures I and II; Fig. 3 – note that representative structures for compounds mentioned in the text are shown in this figure. In the following text, structures are indicated by roman numerals and can be found in this figure). There can be a tremendous variation in the distribution of the *n*-alkanes in crude oils as a result of source materials, maturity, depositional environment, and partial, or total, absence of these compounds as a result of biodegradation. The more important issue here is the boiling point range of the various products that can be produced from a crude oil as illustrated in Fig. 2. It should be evident that the composition of a crude oil will closely control the nature of the products that can be produced and their relative yields.

Routine GC analyses permit the determination of compounds present in crude oils ranging from C₁ to approximately C₄₀ as shown in Fig. 2. However it should be noted that hydrocarbons in crude oils do not stop at C₄₀ but rather can be shown to be present up to C₁₂₀ by using high-temperature GC (HTGC) as illustrated in Fig. 4

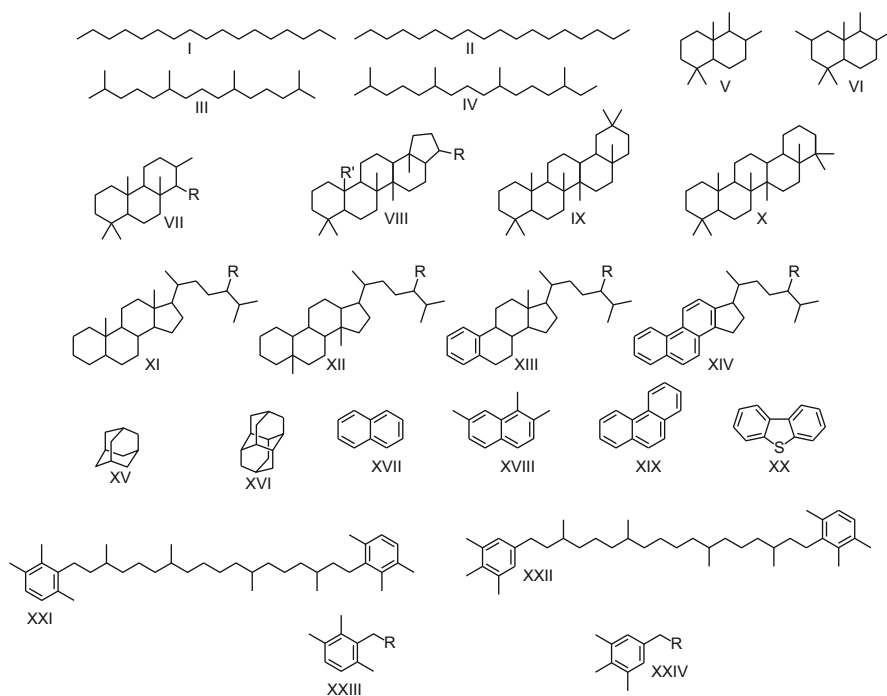


Fig. 3 Structures of key compounds mentioned in the text. R denotes different alkyl groups or eventually a hydrogen atom; I, *n*-heptadecane; II, *n*-octadecane; III, pristane (2,6,10,14-tetramethylpentadecane); IV, phytane (2,6,10,14-tetramethylhexadecane); V, drimane; VI, homodrimane; VII, tricyclic triterpanes; VIII, R' = CH₃; hopanes, R' = H; 25-norhopanes; IX, 18a(H)-oleanane; X, gammacerane; XI, regular steranes; XII, diasteranes; XIII monoaromatic steroid hydrocarbons; XIV, triaromatic steroid hydrocarbons; XV, adamantane; XVI, diamantane; XVII, naphthalene; XVIII, 1,2,7-trimethylnaphthalene; XIX, phenanthrene; XX, dibenzothiophene; XXI, isorenieratane; XXII, paleorenieratane; XXIII, 2,3,6-trimethylaryl isoprenoids; XXIV, 3,4,5-trimethylaryl isoprenoids

(Philp et al. 2004). But again hydrocarbons do not stop at C₁₂₀ and probably extend to much higher carbon numbers although there are probably limits on the migration of such really large hydrocarbons from the source to reservoir to surface collection facilities. However routine GC analyses permit significant information to be determined and related to the properties of the oils, whether biodegraded, a condensate, a mixture of oils, nature of source material, depositional environment, and then as mentioned above some indication of the nature of refined products that could be produced from a specific crude oil.

The molecular characteristics of crude oils form a very broad topic by itself, and only some of the major topics can be described and discussed in a chapter of this nature. Major uses of these compounds are related to providing information on the history and origin of crude oils. This can be broken down into information related to source, depositional environments, and maturity, possible levels of biodegradation,

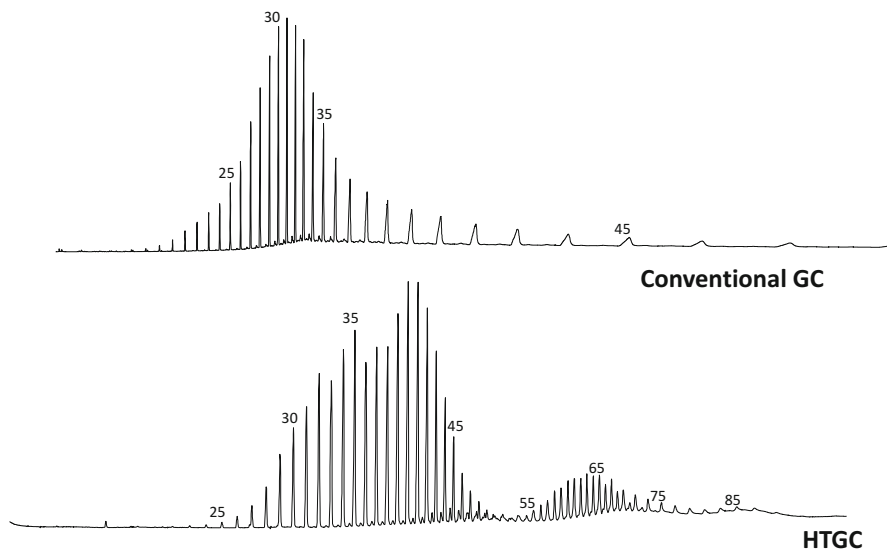


Fig. 4 Hydrocarbons in crude oils do not stop at C₄₀ but extend up to at least C₁₂₀ as revealed by high-temperature GC (HTGC). This diagram compares the same sample of ozocerite run on a conventional column and a high-temperature column to compare the differences in distributions obtained by the two methods (Philp et al. 2004)

and finally undertaking oil-to-oil and oil-to-source rock correlations. The majority, if not all, of these topics have evolved from the original concept of biomarkers, or hydrocarbons in crude oils that are derived from, and have very similar carbon skeletons, to the functionalized compounds that occur in the original source materials (Peters et al. 2005).

Biomarkers can be traced back to the work of Treibs in the 1920s and 1930s (Treibs 1934a, b, 1936) but were further refined following the efforts of Eglinton and Calvin (1967) in the late 1960s and 1970s and Seifert and co-workers at the Chevron Oil Company in Richmond, California, in the mid-1970s (Seifert and Moldowan 1978, 1981, 1986) and many others since those days have continued to develop this very important concept. The reason for this rapid development can be traced to advances in the analytical field, particularly the combined GC-MS system permitting the identification of trace amounts of individual compounds using the concept of single ion or multiple ion detection pioneered by the work of Klaus Biemann at MIT in the early 1970s (Hites and Biemann 1970). This led to the ability to obtain fingerprints of specific families of compounds present in crude oils such as the steranes and terpanes and other widely used families of biomarkers. The distributions of the biomarkers in crude oils have been used for a variety of purposes, but the major uses can be summarized as providing information on source, depositional environments, maturity, extent of crude oil biodegradation, age dating of crude oils, and possible information on migration distances (Peters et al. 2005). In addition utilization of multiple biomarker fingerprints and comparison between

oils and source rocks can be used for correlation purposes which are a very important part of any exploration effort. More recently there has been a more concerted effort into the integration of biomarker data in sequence stratigraphic models (Curiale et al. 1992) particularly with unconventional oil and gas systems, in order to demonstrate the heterogeneity of the shales and define the more productive facies within the shales that provide the more attractive horizontal drilling targets (Slatt and Rodriguez 2012).

A brief overview of some of the more important biomarkers and their important applications and interpretations is provided below. Many of the early biomarker interpretations have changed as more samples from different petroleum systems, i.e., sedimentary basins, have been characterized and novel biomarkers have also been discovered and are now in routine use. In the early days, the rate of novel biomarker discoveries increased exponentially which was not surprising as documented in a landmark paper by Mackenzie et al. (1982). All of these discoveries really stemmed from the development of the GC-MS systems and then a little later the introduction of the data systems. Later the development of the GC-MSMS systems also led to a renewed surge in the number of novel biomarkers being discovered. Today the number of novel biomarkers being discovered in crude oils and source rock extracts has slowed, but when the number of compounds in any crude oil is compared to the actual number identified, it should not surprise anyone to learn that there are still many compounds awaiting discovery.

n-Alkanes (**I** and **II**) and the isoprenoids, pristane (**III**; Pr, 2,6,10,14-tetramethylpentadecane) and phytane (**IV**; Ph, 2,6,10,14-tetramethylhexadecane), have been studied extensively since the mid-1960s primarily because their distributions can be determined by GC and GC-MS is not required (i.e., Powell and McKirdy 1973). The *n*-alkane distributions have been widely used to get some indication of possible source materials, primarily marine vs. terrigenous. *n*-Alkane distributions can also be impacted by factors such as maturity and biodegradation in particular. Increasing maturation will lead to thermal degradation of the longer-chain alkanes shifting the carbon maximum to lower carbon numbers and ultimately if the maturity level becomes high enough leading to the formation of gas. Biodegradation will preferentially remove the *n*-alkanes over all the other compounds and starting at the lower carbon-numbered alkanes.

The isoprenoids, Pr (**III**) and Ph (**IV**), have also been widely studied since the late 1960s and have produced one of the most widely used geochemical parameters, the Pr/Ph ratio. This ratio was initially proposed by Powell and McKirdy (1973), further refined by Didyk et al. (1978) in the mid-1970s, and has been discussed extensively since that time. It was initially proposed that high Pr/Ph ratios (>3) were indicative of an oxic depositional environment and a low ratio (<1) indicative of an anoxic or reducing environment. However this interpretation is based upon Pr and Ph both being derived from degradation of chlorophyll. But over the years, a number of additional sources have been proposed for both Pr and Ph, and under those circumstances, there can be problems with the interpretation of the ratio. In order to determine whether or not the Pr and Ph are derived from the same source, it is necessary to measure the stable isotope composition of both compounds. Despite

this issue, the Pr/Ph ratio is still a very useful oil/oil or oil/source rock correlation parameter which is relatively resistant to biodegradation and does not change significantly with maturation.

Other classes of biomarkers generally require GC-MS and multiple ion detection for their characterization since they are present in relatively low concentrations and generally not visible on the GC chromatograms unless the oils are biodegraded enhancing the relative concentrations of the steranes and terpanes. In the following sections, a few of the more widely used biomarkers will be discussed to provide some examples of the utility of these compounds from an exploration perspective (Philp and Lewis 1978; Peters and Fowler 2002; Peters et al. 2005).

There are four major families of biomarkers that are present in the saturate fraction of a crude oil that are extremely useful in petroleum exploration and production. The four groups of compounds are the sesquiterpanes, steranes, terpanes, and diamondoids, and below a brief summary for each of these compound classes is provided.

3.2.1 Sesquiterpanes

The family of sesquiterpanes is generally comprised of C₁₄–C₁₆ bicyclic sesquiterpanes (V and VI) which are generally present in virtually all crude oils in varying proportions (Alexander et al. 1984). Care needs to be taken such they are not lost during sample preparation since a little too much enthusiasm in evaporating the solvent during sample preparation can greatly affect the distribution of these compounds. The identity of most of these compounds can be found in *The Biomarker Guide: Volume 2* (Peters et al. 2005) or papers in the exploration literature going back to the late 1970s. Drimane and homodrimane are typically the most abundant compounds and are thought to have a microbial origin. There are variations in the distributions of these compounds between oils coming from different sources, and this provides one of the first sets of fingerprints for differentiating oils from different sources. The impact of weathering on these compounds has not been widely studied since the major weathering impact with these samples is evaporation rather than biodegradation which will remove the compounds faster than biodegradation.

The second important family of biomarkers is referred to as the terpanes (VII and VIII; Aquino Neto et al. 1983; Peters et al. 2005). This is a family of compounds widely used in exploration studies, and despite the fact that the pentacyclic compounds are derived from precursors ubiquitous in bacteria and the tricyclic compounds are thought to probably be sourced from *Tasmanites*, a tremendous amount of useful exploration information can be derived from these fingerprints. A classic terpane fingerprint is shown below (Fig. 5), and the areas where the tricyclic and pentacyclic compounds elute are clearly labeled. The identities of virtually all the compounds in the chromatogram are known.

In Fig. 6 a number of different terpane chromatograms are shown to illustrate differences that may be expected for oils derived from different source rocks. Close examination of these fingerprints reveals both relatively subtle differences and some significant differences. In general the major differences should be used initially to differentiate unrelated samples coming from different sources, and once samples that

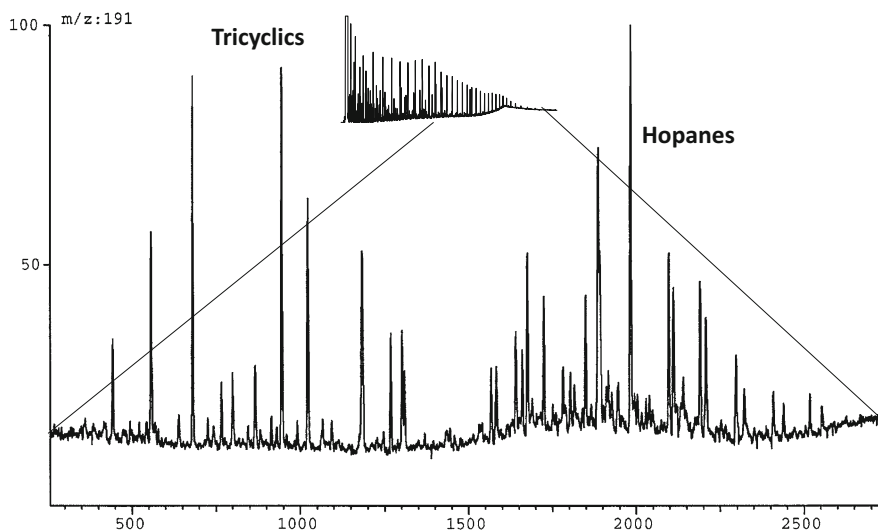


Fig. 5 One of the most commonly utilized families of biomarkers in crude oils is the terpanes which can be monitored by GC-MS and multiple ion detection monitoring the ion at m/z 191. This figure shows a typical terpane fingerprint with the areas showing the tricyclic and pentacyclic terpanes labeled on the chromatogram

have significantly different fingerprints are excluded, further differentiation can be undertaken using these more subtle differences. It should also be noted that over geological time periods terpanes can be impacted by biodegradation. Under certain reservoir conditions, compounds such as the 25-norhopane series (**VIII- R' = H**) generally provide evidence of an episode of biodegradation (Bennett et al. 2006).

An illustration of the power of individual biomarkers to differentiate samples can be shown with the use of 18 α (H)-oleanane (**IX**; Samuel et al. 2010). This compound is thought to be uniquely sourced from angiosperms or flowering plants. The presence of oleanane in one oil and not another is a very strong piece of evidence to suggest that the two oils are not related. However, as with all of these compounds, one should not depend upon one parameter alone. This piece of information is one line of evidence and can be used to build the case that the two samples are not related. Another individual terpane that can be used in this manner is a compound called gammacerane (**X**; ten Haven et al. 1988). This is generally associated with oils coming from a saline or hypersaline depositional environment and a stratified water column, but presence in one sample and absence in another would be strong evidence that the two samples are not related.

3.2.2 Steranes

There are multiple families of steranes (**XI–XIV**) in most crude oils, and these typically range in carbon number from C_{20} to C_{30} with additional minor series of steranes present extending to C_{35} . The sterane families commonly used for

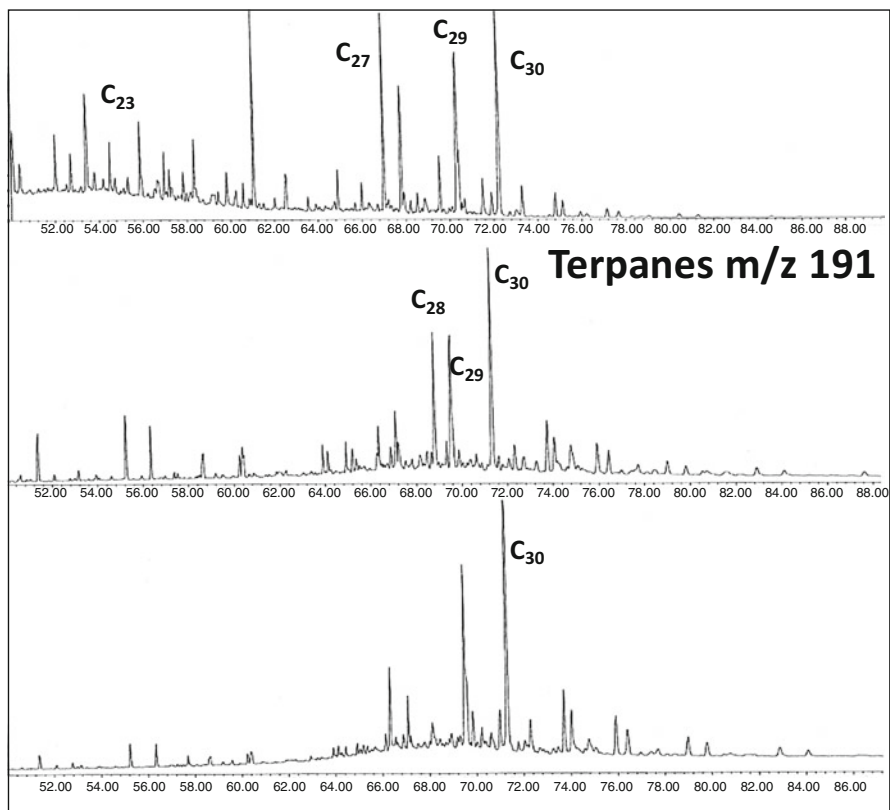


Fig. 6 Three different terpane chromatograms are illustrated in this figure to show variations that might be expected in oils coming from different sources and depositional environments

correlation purposes in exploration studies include regular steranes (**XI**), rearranged steranes (**XII**), monoaromatic steroid hydrocarbons (**XIII**), triaromatic steroid hydrocarbons (**XIV**), methylsteranes, and minor series of alkylsteranes (Mackenzie et al. 1982; Peters et al. 2005). Many of these family members also provide information on other aspects of exploration such as maturity and depositional environments. There are multiple components within each family as can be seen in the figure below that shows examples of steranes and diasteranes from two crude oils (Fig. 7). These sterane fingerprints clearly show the complexity of these mixtures although with increasing aromaticity, the number of isomers and epimers tends to decrease due to removal of hydrogen atoms (as well as methyl groups) with progress of the aromatization process (Fig. 8).

The most useful sterane source parameter is based on the relative proportions of the $C_{27}/C_{28}/C_{29}$ steranes plotted on a ternary diagram (Fig. 9). The relative proportions of steranes can be determined using either the distribution of the regular steranes (**XI**) or the monoaromatic steroid hydrocarbon (**XIII**) fingerprint that is less

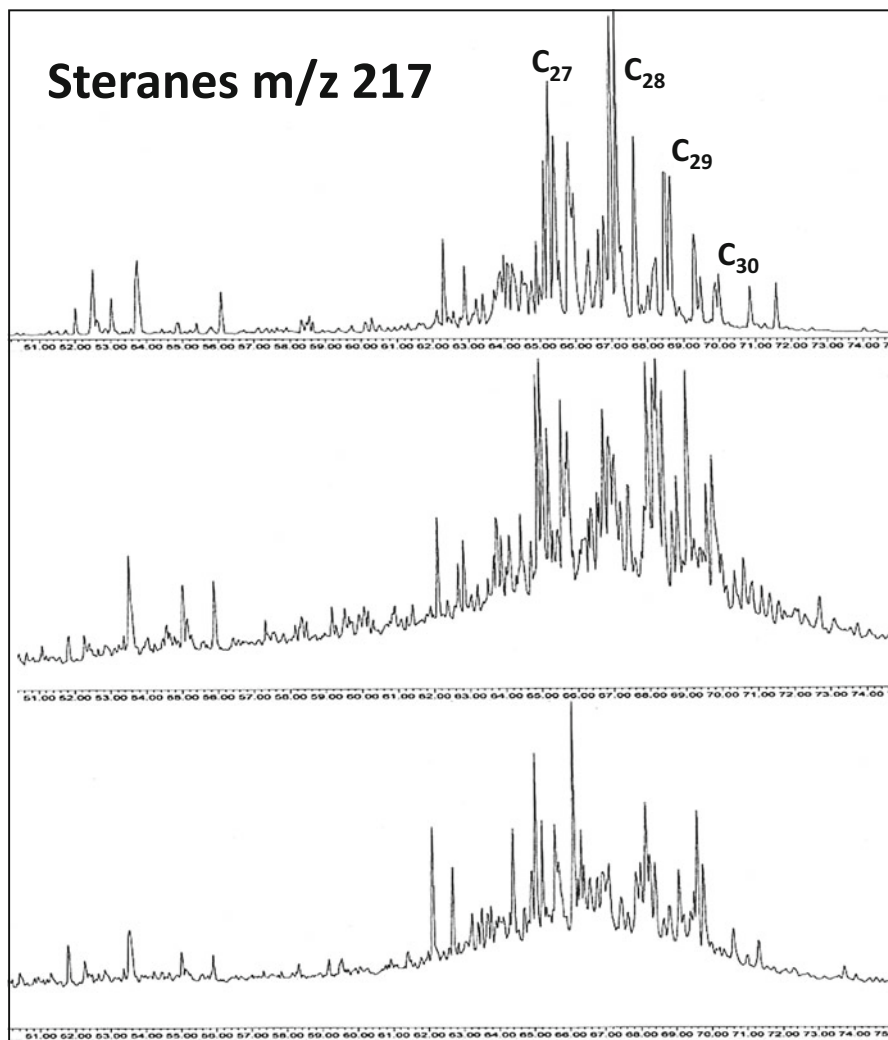


Fig. 7 The second most commonly monitored biomarkers in a crude oil are the steranes, both regular and rearranged steranes. In this figure the steranes from three unrelated sources are shown to illustrate the differences resulting from different source materials

complex making it easier to calculate the relative proportions of these individual steranes (Moldowan et al. 1985). However, the goal here is to establish the relationship between the groups of samples. Those that are related will group very close to each other, while those from a different source will show signs of separation.

A more detailed separation of the steranes can be obtained through the use of the GC-MSMS approach, as discussed above, which will introduce an additional element of separation based on mass spectral characteristics rather than

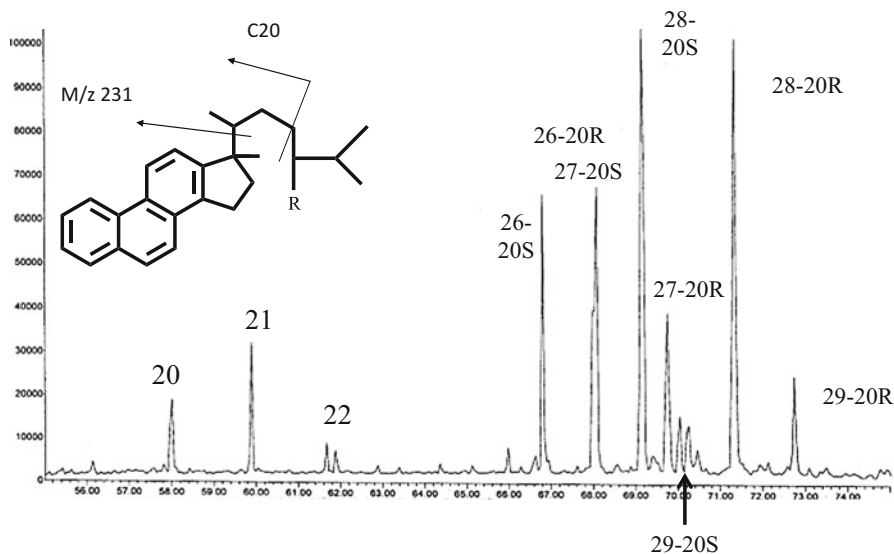


Fig. 8 Steranes become aromatized with increasing maturity which in turn reduces the complexity of the resulting mixtures greatly due to the decrease in the number of possible isomers and epimers with increasing aromatization. This figure shows the distribution of the triaromatic steroid hydrocarbons resulting from this aromatization process

chromatography. In most environmental cases, this level of investigation may not be necessary but suffice it to mention that it may provide additional pieces of information when evaluating points of release or looking for an unknown source of release. For example, components which may be present in relatively low concentrations can be very important in establishing relationships between samples. Such compounds may be the C_{30} *n*-propylsteranes or the C_{26} steranes (Moldowan et al. 1990; Holba et al. 1998). The former which are uniquely related to marine-sourced oils are clearly evident from the regular GC-MS analyses. The C_{26} steranes can only be detected through the use of GC-MSMS as illustrated below (Fig. 10). The important point to indicate here is that minor components such as these, which are relatively unique, may provide important correlation parameters and may differentiate between two samples that were previously thought to be related.

3.2.3 Diamondoids

Diamondoids (XV and XVI) are another family of compounds used in exploration studies for many years (Moldowan et al. 2015; Liu et al. 2016b). Diamondoids exist as a homologous series of structural isomers and ranging from adamantanes, diamantanes, and triamantanes and continuing into significantly higher carbon numbers. These compounds can be readily detected by GC-MS and multiple ion detection. The lower members of the adamantanes series are volatile and can easily be lost during sample preparation. If it is necessary to obtain the isotopic

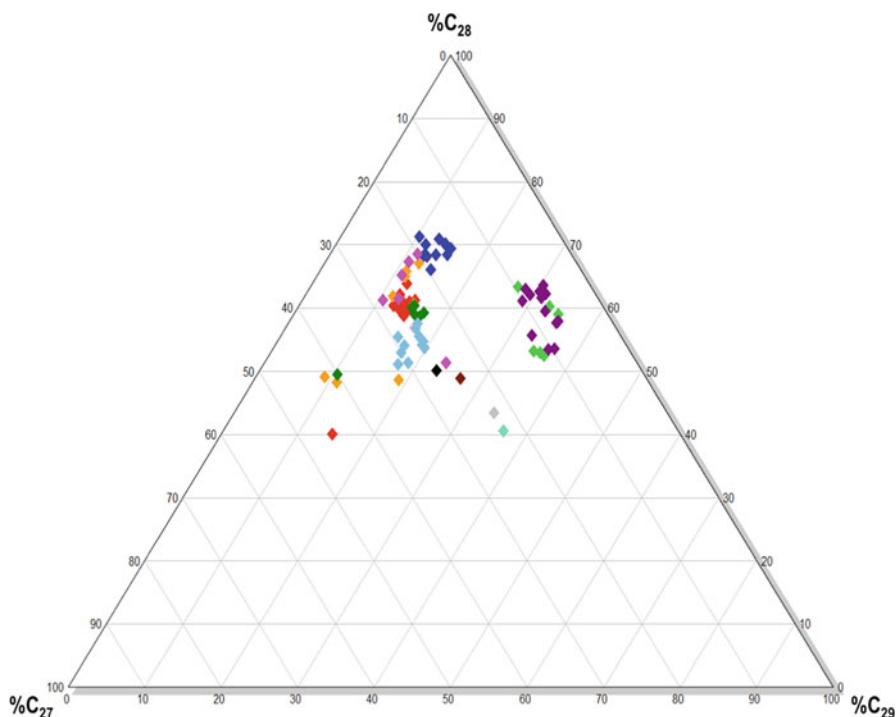


Fig. 9 Relationships between oils from the same or different sources can be determined using a ternary diagram showing the relative proportions of the $C_{27}/C_{28}/C_{29}$ steranes as illustrated in this figure. Several families of oils can be clearly seen on this diagram providing information that can be integrated with additional biomarker distributions to further confirm the relationships between these families

composition of individual diamondoids, it is necessary to isolate the diamondoids using published methods (Fig. 11; Wei et al. 2007; Moldowan et al. 2015). Unfortunately, only a few papers provide any specific details on the actual isolation of the diamondoids from crude oils (Ling et al. 2011; Nguyen and Philp 2016).

These compounds are extremely resistant to biodegradation that makes them very useful for correlating degraded and non-degraded samples. Most applications are restricted to using the adamantanes and diamantanes since these are more abundant diamondoid components. These compounds are also extremely stable and tend to increase in concentrations with increasing maturity of the source rocks responsible for their generation. Condensates have particularly high concentrations of diamondoids, and these may be the only family of compounds available for correlation purposes due to the loss of the more traditional biomarkers at these higher levels of maturity.

C_7 Compounds

The term “ C_7 compounds” can often be found in the petroleum geochemistry literature referring to those compounds with seven carbon atoms, including heptane,

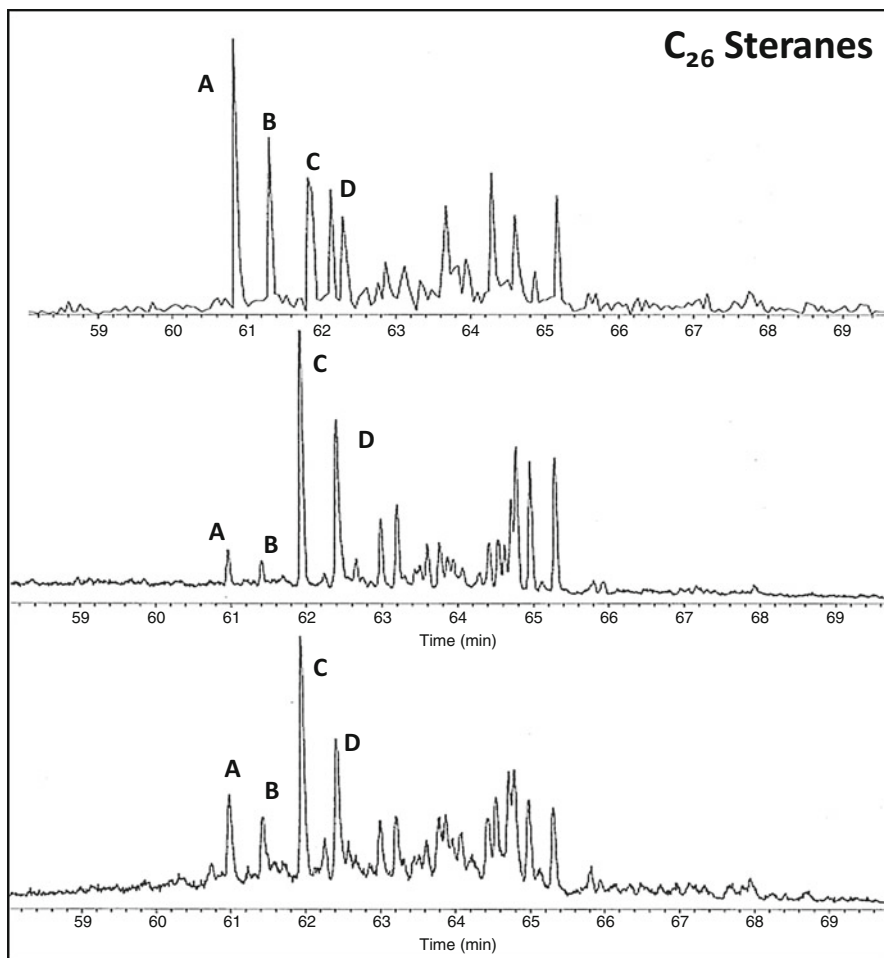


Fig. 10 GC-MSMS is an extremely useful technique for detecting compounds that may not be clearly evident in complex mixtures such as the steranes. An example of this application is shown here where the C_{26} steranes have been extracted from the total sterane chromatogram where they were not clearly evident. The C_{26} steranes are useful for age dating purposes (Peaks A and B are 24-nordiacholestanes and peaks C and D are 27-nordiacholestanes)

toluene, branched hydrocarbons, and cyclic hydrocarbons. The reason these compounds are of interest from an exploration point of view is twofold. First, they are the highest carbon number where all the isomers can be resolved chromatographically; second, from an exploration prospective, they are invaluable maturity indicators as well as have a role in correlation studies (Halpern 1995).

3.2.4 Aromatic Hydrocarbons

Aromatic hydrocarbons in crude oils and condensates are present as very complex mixtures of a wide variety of structural types (Radke and Welte 1983; Strachan et al.

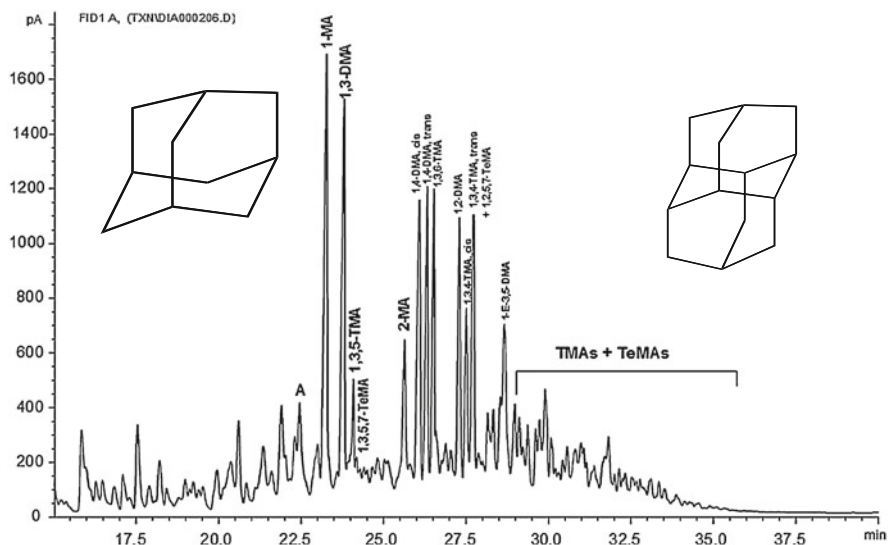


Fig. 11 Diamondoids are another useful family of compounds that can be used for correlation and maturity purposes. If the isotopic composition of individual diamondoids is required, it is initially necessary to isolate a diamondoid concentrate. There are few published methods, but the diamondoid concentrate shown here was isolated using the method reported by Nguyen and Philp (2016)

1988; van Aarssen et al. 1999). The complete distributions of the major classes of aromatic compounds such as the naphthalenes (XVII and XVIII), phenanthrenes (XIX), and dibenzothiophenes (XX) provide useful correlation parameters as well as additional source and maturity information (Fig. 12). Following that initial separation, the various alkylated members of these series can be separated using GC-MS and multiple ion detection using the characteristic ions for the various alkylated series. These chromatograms provide information on the distribution of the individual isomers at each carbon number and vary between oils derived from different source materials. In some cases these differences may be very subtle, but they are significant and reproducible. Many of these differences are indirectly related to differences in source material, and such differences, albeit small, may be sufficient to differentiate between oils that were initially thought to be related on the basis of the more commonly used biomarker parameters. For example, 1,2,7-trimethylnaphthalene (XVIII; Armstroff et al. 2006) has been proposed to be a degradation product of oleanane, a higher plant derivative. If it is present in certain samples but not in others, that will indicate that these oils are not related. Aromatic compounds are susceptible to biodegradation over geologic time, and lower carbon compounds such as benzene and toluene are more prone to weathering and will be removed relatively rapidly.

As noted above this is only a very brief summary of some commonly used biomarkers. Some additional biomarkers are discussed in various sections below.

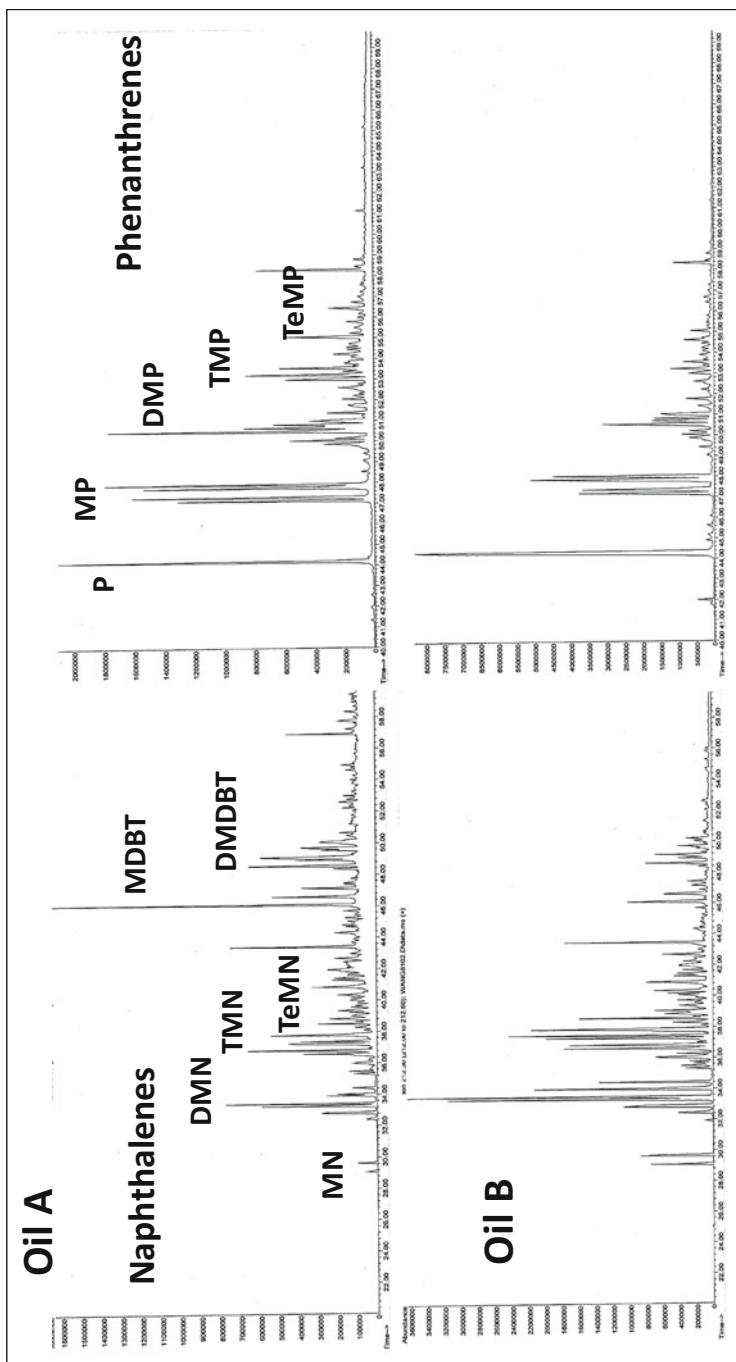


Fig. 12 Most oils contain significant quantities of aromatic compounds, and distributions of the major classes of aromatic compounds, such as the naphthalenes, phenanthrenes, and dibenzothiophenes, are shown in this figure and compared between two different oils labeled as A and B, respectively (MN=methylnaphthalene; DMN=dimethylnaphthalene; TMN=trimethylnaphthalene; TeMN=tetramethylnaphthalene; P=phenanthrene; DMP=dimethylphenanthrene; TMP=trimethylphenanthrene; MDBT=methyl/dibenzothiophene; DMDBT=dimethyl/dibenzothiophene)

4 Where Does the Oil Come From? Photosynthesis and How Things Change Over Time

The origin of crude oil or any fossil fuel begins with photosynthesis where the carbon dioxide in the atmosphere is incorporated into biomass constituents of living plants, phytoplankton, algae, and certain photosynthetic bacteria. These are the primary producers which provide carbon or energy sources for the heterotrophic organisms. CO_2 in the atmosphere is comprised primarily of $^{12}\text{CO}_2$ but also includes minor amounts of $^{13}\text{CO}_2$. During the process of photosynthesis, there is fractionation between these two isotopes as they are incorporated into the biomass components at different rates due to a kinetic isotope effect. The nature of the photosynthetic cycle operating in the plant or organism will ultimately determine the bulk isotopic composition of the plant debris and the contribution it will make to the isotopic composition of the crude oil formed from the source material. Since source rocks are derived from mixtures of different source materials, they will have different isotopic compositions determined by the extent of mixing of source materials. Ultimately the oils derived from these different source rocks will have isotopic compositions reflecting that of the rock responsible for generating the oils. However the range of isotopic values is not infinite and will be controlled by the isotopic composition of the assimilated atmospheric CO_2 and the nature of the primary producers contributing to the source material. Other factors such as maturation will play a significant role, but photosynthesis is still the starting point for any variations. A diagram taken from a paper by Andrusevich et al. (1998) shows the general trend in isotopic compositions of crude oils over time and how they have varied primarily due to variation in the CO_2 content of the atmosphere. Over time with increasing diversity of the primary producers utilizing the CO_2 in the atmosphere, the residual CO_2 has become heavier leading to the observed changes in the isotopic compositions of the oils. Ultimately these living organisms will die, and the organic debris will be deposited in a wide variety of depositional environments (Fuex 1977). The organic matter will start to degrade, and a large proportion will be degraded and converted back into CO_2 which will be released into the atmosphere and recycled. The extent of degradation will depend on the nature of the depositional environment with the major controlling factors being oxygen availability and salinity. The organic matter that survives these early stages of biodegradation and is preserved will be buried and at sufficient depths will start to be thermally degraded and converted into products that will ultimately become crude oil and/or natural gas. Tissot and Welte (1984) suggested many years ago that only about 0.01% of the organic carbon actually gets incorporated into the geological cycle with the rest being recycled. While small in relative terms, this still represents a significant amount of organic carbon in absolute terms and has led to a tremendous accumulation of organic matter in sedimentary basins over geological timescales.

Variations in crude oil composition are basically related to the combination of source materials responsible for the accumulation of organic matter in the sediments that, with time, burial and increasing temperature will become source rocks. Such variations result from differences in climate, marine vs. nonmarine or lacustrine,

evolutionary and extinction events, geological time period, and many other factors. However the relative contribution of the different types of source materials will be one of the primary controls on the composition of crude oils. For example, all other factors being equal, oils dominated by higher plant material will generally be waxy and contain higher proportions of longer-chain *n*-alkanes (nC_{25} – nC_{35}); oils derived from marine source materials will generally contain higher proportions of sulfur-containing compounds, asphaltenes and steranes. While oils derived from higher plant material may be waxy, the hydrocarbons responsible for the wax content of the oils are in the range C_{25} – C_{35} . The main role of these plant waxes is to preserve the water content of plants, and the *n*-alkanes in this carbon number range are very effective for this process. The concept that all waxy oils are derived from higher plant materials originated with the work of Hedberg (1968) who examined many oils derived from higher plant material and which indeed were waxy. However, since that paper many oils from marine sources and lacustrine sources have been analyzed and found to contain hydrocarbons extending to C_{120} and probably even higher. These compounds are probably derived from higher molecular weight components present in the cell walls of bacteria and algae that degrade after deposition and maturation.

Maturity leads to thermal degradation of the organic material in the source rocks generating hydrocarbons and other compounds, collectively thought of as bitumen, which is expelled from the source rock as a crude oil that will migrate to a trap or reservoir. With increasing maturity, increasing cracking of the organic material in the source rock along with thermal cracking of the hydrocarbons in the bitumen will lead to a shift in the distribution of the hydrocarbons to lower carbon numbers, initially forming a condensate, and at very high levels of maturity, everything will be thermally degraded to methane.

A tertiary control on crude oil composition will be related to biodegradation in the reservoir. Biodegradation of crude oils occurs in a well-defined manner. The *n*-alkanes are removed initially starting at the lower carbon numbers and then moving toward the higher carbon-numbered *n*-alkanes. This is accompanied by subsequent removal of the more complex structures such as the isoprenoids, steranes, terpanes, and aromatic compounds. However the impact of biodegradation will change the properties of a crude oil in many different ways. The removal of certain compounds will lead to the oils becoming heavier and have lower API gravities. They will also become more viscous, and this will also lower their value since they will not be as desirable to refiners due to their increasing sulfur and heavy metal content as well as being more expensive to refine.

Finally it would be remiss not to mention unconventional crude oils which differ from conventional crude oils, not as much in their composition but due to the fact that they are sourced but not expelled from their source rocks due to the low permeability of the source rocks. The oil is ultimately released and produced through hydrofracking of the source rocks. In this situation if the maturity level continues to increase, the trapped oil will be thermally degraded, and this will lead to the formation of shale gas, an unconventional source of gas, which also requires hydrofracking for production (Jarvie et al. 2007).

5 Productivity Versus Preservation

In the preceding section, variations in source material were mentioned as one factor that can impact the composition of crude oils. Another issue that comes into play in the formation of source rocks is preservation vs. productivity. Productivity is related to the amount of organic matter produced but not necessarily the type of organic matter. The issue whether preservation or productivity was more important was a major source of discussion many years ago when there were two fields of thought on this issue. Demaison and Moore (1980) were major proponents of the idea that preservation of organic matter was the most significant factor driving the formation of organic-rich source rocks, with anoxic environments preferentially preserving more oil-prone organic matter and oxic environments preserving lesser amounts and more recalcitrant forms of organic matter, which would ultimately be more gas prone than oil prone. This in turn is another factor that will contribute to determining whether a source rock will primarily generate oil or gas or a mixture of oil and gas. Anoxic and oxic environments are of course the extremes, and there is a complete spectrum of intermediate environments which in turn exercise varying degrees of preservation and variations in the generated products.

On the contrary an opposing proposal was made several years ago by Pedersen and Calvert (1990) and based on data from a couple of inlets of the West Coast of the USA, similar environments, and source matter input, but one environment was oxic and one anoxic. Data obtained from sediments in cores from the two environments showed that the oxic sediments actually had higher TOC values than those from the anoxic environments, leading them to conclude that productivity was the more important factor over preservation in the formation of the organic-rich rocks. In reality both preservation and productivity are probably equally important. If there is no production, there is nothing to preserve!

In addition to productivity and preservation, the actual type of organic matter is very important in the formation of crude oil. Different types of organic matter have different structures. Organic matter derived from algal, phytoplankton, or bacterial sources has a relatively high content of aliphatic structures, which means they have relatively high H/C ratios and will be primarily oil prone. However organic matter derived from higher plants will be more aromatic in nature and will therefore be more gas prone. Many source rocks are mixtures of various types of organic matter and will produce varying amounts of oil and gas from the source material itself, and this will be discussed in more detail in the next section.

6 What Are the Major Factors Involved in Determining the Composition of Crude Oils?

As mentioned earlier there are a large number of crude oil types ranging from very heavy, asphaltene-rich biodegraded oils to very light condensates, generally asphaltene-free. A knowledge of crude oil type is important since this will determine the nature and relative proportions of the refined products that can be produced from

a specific crude and hence the value of price of that particular crude. The types of crude oils can be defined in many different ways. As mentioned above Tissot and Welte (1978) examined 541 oils based on the relative proportions of various fractions and divided them into five different types.

Crude oils are derived from a wide variety of source materials deposited in a variety of depositional environments. After deposition, the organic material can undergo a series of complex reactions and alterations, and a significant proportion will be totally degraded and recycled back into the atmosphere as CO_2 and H_2O . The organic matter that is preserved will ultimately become part of the fraction referred to as kerogen (Durand 1980). Kerogen is the residual fraction after all the mineral matrix has been removed and all the soluble organic matter has been removed. Over the years our understanding of kerogen and its structure has changed significantly. In the 1960s and 1970s, kerogen was thought to have a well-defined molecular structure. Despite much effort no specific molecular structure for kerogen was ever identified. In retrospect that should not be a surprise since it is now clearly understood and established that kerogen is primarily comprised of macerals or residual particles of organic source material that have survived the early stages of diagenesis and become incorporated into the sedimentary matrix. While some of these macerals may be loosely bound to each other through covalent bonds, there is no well-defined structure, and instead there can be significant variation in the kerogen composition from samples collected very close to each other, simply because deposition and accumulation of organic material are not going to be constant or uniform throughout the depositional environment.

The kerogen concept was developed primarily by Tissot and Welte in the 1970s but was basically an extension of the extensive work of van Krevelen (1961) based on coal characterization. In brief van Krevelen's diagram for coals and then kerogens was based on the H/C vs. O/C ratios which enabled the kerogens to be divided into four different types (types I, II, III, IV). An example of the classic van Krevelen diagram, showing the four kerogen types introduced by Tissot and Welte is shown in Fig. 13a. The use of the elemental compositions was subsequently replaced by the hydrogen and oxygen indices as determined by the Rock-Eval analyses and is shown in Fig. 13b. However the general idea was that on the basis the characterization the four kerogen types could be divided into oil prone (types I and II), gas prone (type III), or inert and non-generative (type IV). However the problem of characterizing the kerogens in this manner was the tendency to compartmentalize kerogens into these types and hence predict the nature of products that could be generated. However this is somewhat misleading since, for example, a type II kerogen may not be a pure marine kerogen but a mixture of type I and type II kerogens, and this of course would have a direct impact on the nature of the products that will be generated. Another problem with this method of kerogen characterization is that it is impacted by maturation and therefore it only reflects the kerogen type when examining immature samples. Although this method is still used extensively for characterizing kerogens and predicting the nature of products that can be formed, an alternative approach has been developed over the years based on organofacies. In this approach the kerogens are characterized based on their petrographic properties

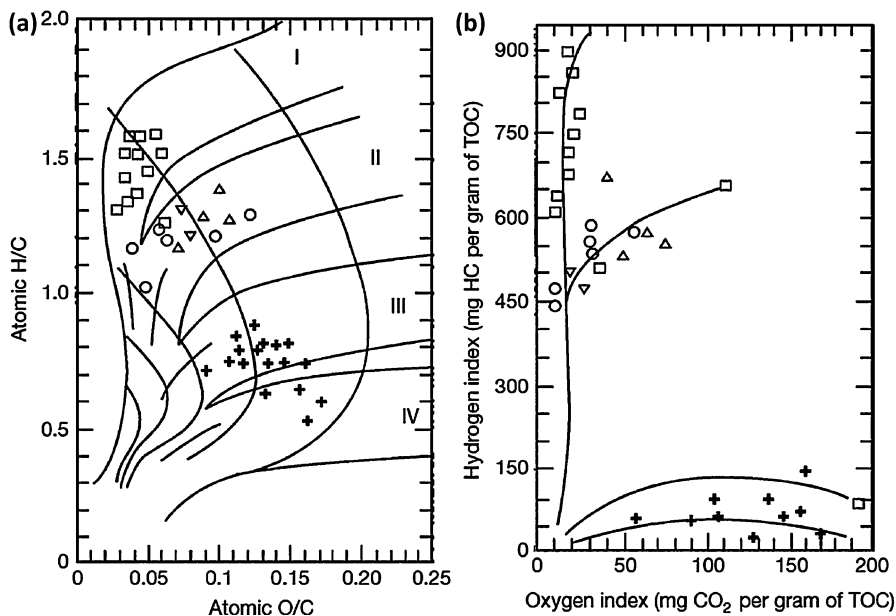


Fig. 13 (a) An early method used to characterize kerogens was based on the elemental composition of the kerogen. Initially kerogens were divided into four major types as illustrated on this diagram with well-defined boundaries. (b) With the development of the Rock Eval pyrolysis system, it was found that the HI and OI indices were directly proportional to the H/C and O/C ratios and therefore a plot of HI to OI could be used to replace the H/C and O/C values on the Tissot-Welge diagram. (Reproduced with permission from Philp 2014)

which avoid the maturity impact. This approach, although not as widely used as the method described above, was initially introduced by Jones (1987) and is based on mappable units, or organofacies, derived from similar types of organic matter which will produce similar types of hydrocarbon products at appropriate maturity levels.

7 What Is the Impact of Depositional Environment?

The major role of the depositional environment will be preservation of the organic source material. Clearly there is a complete spectrum of depositional environments varying in oxicity and salinity. The characteristics of the depositional environment will control the rate at which the organic material is degraded and also the characteristics of the residual organic material. In more oxic environments, the more susceptible organic components, which are typically the more oil-prone components, will be degraded more rapidly than the more recalcitrant components, which are generally the more gas-prone components. Hence with increasing oxicity, not only do we typically see a decrease in the organic matter content, but this is accompanied

by a decrease in the oil-producing fraction of the source rock and a relative increase in the gas-producing components.

In certain situations specific biomarkers provide a far more detailed interpretation of the depositional environment and the ability or potential to preserve organic matter. The Pr/Ph ratio mentioned above is a good example of a biomarker ratio giving useful information on environmental conditions. At certain times in the geological past, there have been episodes of oceanic anoxic events (OAE), and some of these events have been accompanied by the development of photic-zone euxinia and production of certain carotenoids, which are highly specific for these depositional conditions (see below). Photic-zone euxinia denotes a situation in which the photic zone extends into the sulfidic anoxic part of the water column. This in turn permits anoxygenic photosynthetic organisms that thrive under anoxic conditions and utilize hydrogen sulfide to produce organic matter that will be preserved under anoxic conditions with the ultimate production of organic-rich source rocks with very characteristic signatures. There are several OAE in the geological record, particularly in the Late Devonian when many prolific black shales were deposited and again in the Cretaceous. A classic example would be the Woodford Shale, OK, USA, which is a prolific source rock in the Anadarko Basin. This shale has been extensively explored since the late 1800s and has risen to prominence again during the past decade when the focus shifted to determining its potential as an unconventional source of both oil and gas. Traditionally the Woodford Shale has been divided into three members, namely, the Upper, Middle, and Lower Woodford. However it has been recognized recently that these three members are far from homogeneous and should be divided into a number of organolithofacies which can be integrated into sequence stratigraphic models and permit variations in organic matter content to be related to changes in the depositional history and sea-level changes (Miceli and Philp 2012). However the more important observation in terms of this section is that the occurrence of these episodes of photic-zone euxinia related to OAE can be recognized by the presence of a range of specific biomarkers, namely, C₄₀ carotenoids and their arylisoprenoid degradation products. These compounds provide a unique fingerprint for these specific depositional conditions and have also been observed in the Late Cretaceous black shales (French et al. 2015; Connock et al. 2018). There are four or five major C₄₀ carotenoids that are derived from different photosynthetic bacteria that grow at different depths within the water column and in turn produce different C₄₀ carotenoids; hence the presence of certain C₄₀ carotenoids (i.e., isorenieratane (XXI) and paleorenieratane (XXII)) provides information about water column depth during the growth period of these organisms and the initial production of the organic matter as summarized in Fig. 14. These compounds are relatively stable and have been observed in many samples of Woodford oils and source rock extracts. At higher levels of maturity in the late oil condensate window, these compounds will ultimately degrade.

The arylisoprenoids which are proposed to be derived from the carotenoids occur as two major series of isomers, namely, the 2,3,6-trimethylaryl isoprenoids (XXIII) and the 3,4,5-trimethylaryl isoprenoids (XXIV). These compounds have been

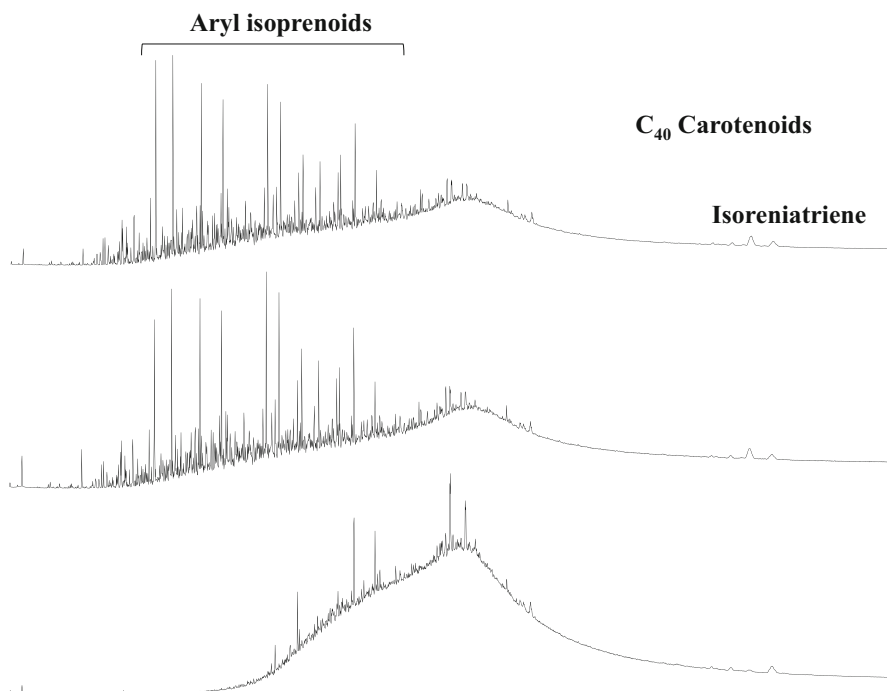


Fig. 14 Specific C_{40} carotenoids such as isorenieratane, shown here, as well as arylisoprenoids, derived from green sulfur bacteria, provide information on the occurrence of photic-zone euxinia during the deposition of organic-rich sediments

studied quite extensively, and several parameters based on these two series and how they relate to the oxicity and photic-zone anoxia of the depositional environment have been developed (Schwark and Frimmel 2004; Miceli and Philp 2012; Connock et al. 2018). The AIR or arylisoprenoid ratio is one such parameter and is based on the proportions of the short-chain (C_{13} – C_{17}) and intermediate-chain (C_{18} – C_{22}) arylisoprenoids. High AIR (3.0) is associated with episodic PZA, which leads to alteration of the long- and intermediate-chain arylisoprenoids. On the contrary, low AIR (0.5) indicates persistent PZA, which contributes to preservation of the long-chain arylisoprenoids.

Another parameter that has been widely used to characterize depositional environments is the gammacerane index. The presence of gammacerane (**X**) has long been associated with salinity, and there were many papers published in the early 1970s on the significance of gammacerane in the Green River Shale. Initially it was taken as an indicator of salinity, particularly in lacustrine environments. Increasing salinity results in significantly higher relative concentrations of gammacerane as illustrated in Fig. 15. However following those initial observations, it was also determined that elevated gammacerane concentrations could be associated with stratified water columns and consequently enhanced conditions for preservation of organic matter.

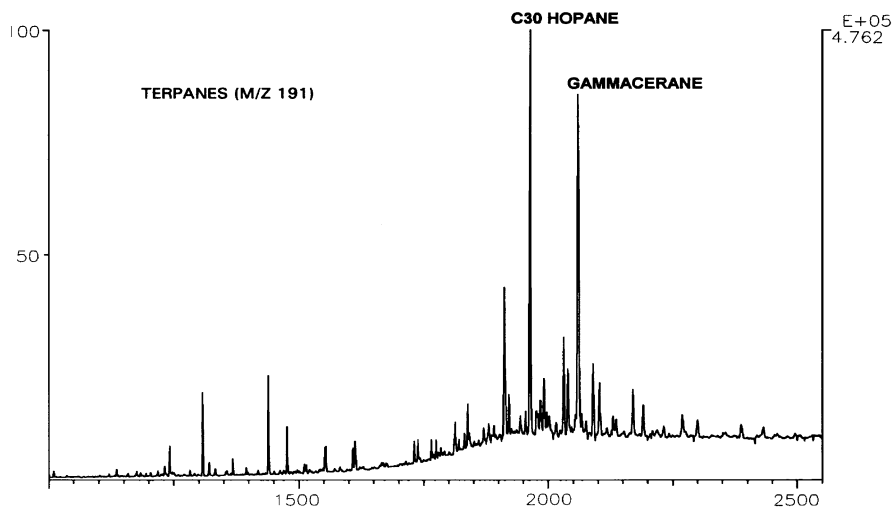


Fig. 15 Gammacerane is an indicator of a stratified water column resulting from increasing salinity and is illustrated in this chromatogram in high abundance in a lacustrine oil from China

8 What Is the Impact of Maturity?

Maturity plays an important role in determining the bulk and molecular characteristics of a crude oil. Initially maturity plays a primary role in generation of the oil through breakdown of the kerogen, and maturation of organic matter in sedimentary rocks is typically monitored through measuring vitrinite reflectance, a long established maturity parameter originally developed by coal chemists for monitoring changes in the reflectance of the vitrinite maceral. This scale was subsequently extrapolated to measuring the maturity of source rocks using the same scale. The ranges covering oil and gas generation are: <0.55% immature source rocks; 0.55–1.15% oil window; 1.15–1.40% condensate-wet gas window; > 1.40% dry gas window. These are just guidelines, and there will be variations, for example, kerogens that have a high sulfur content will start to generate oil at lower levels of maturity than those with a lower sulfur content or no sulfur.

In addition to the importance of maturity in the generation process, once the oil has been generated, maturity can play an additional role in affecting the composition of crude oils. During the early stages of generation, crude oils can contain varying proportions of hydrocarbons clearly extending to C_{40} and, in many cases, beyond but maximizing in the C_{20} – C_{30} range, depending on the nature of the source material as discussed elsewhere. After generation if these oils experience higher levels of maturity, the longer-chain hydrocarbons will undergo thermal cracking to shorter-chain hydrocarbons. As the maturity level continues to increase, the original oil will become lighter and lighter until it will become a condensate and finally be converted to methane. This is what happens in many shale gas accumulations, where many of

the source rocks were originally type II marine kerogens. Oil was generated, but as a result of low permeability, much of the oil was not expelled but trapped in the source rock. In such a situation, the shale is acting as a source and reservoir, but as the maturity increases, the trapped oil is converted into gas.

Maturity is critical in terms of generation – if the rocks remain at low maturity, no, or low quantities of, products will be generated, and generation will cease unless the source rock undergoes further burial and experiences higher levels of maturity. Maturity is a key parameter in basin modeling, and it is essential that reliable and accurate information is available on the burial, uplift, and erosion history of the formation since this provides key information on the time/temperature history and the total amount of thermal energy experienced by a specific source rock. The nature of the kerogen in the source rock is important since that determines the nature of the products being generated and also kerogens with a high sulfur content will start to generate at a lower level of maturity, but ultimately it is the time temperature history that will determine the quantity of hydrocarbons generated.

9 How Does the Molecular Composition of an Oil Change During and After Generation?

As mentioned above, crude oils are formed from organic material originally derived from living plants and organisms deposited, and preserved, in various depositional environments. With burial, or subsidence, and increasing temperature, the organic matter will start to degrade and lead to the generation of hydrocarbons and associated polar compounds. The composition of the products will be determined primarily by the composition of the original source materials which initially gets converted into the very important intermediate, kerogen, prior to thermal degradation and formation of crude oils.

At the molecular level, there is a very wide range of changes that can be reported (Philp and Lewis 1987; Peters et al. 2005; Philp 2014). For example, if we consider the *n*-alkanes, which in most cases are the most abundant class of compounds in a crude oil, it is well documented that with increasing maturity the odd/even predominance of *n*-alkanes commonly seen in immature source rocks will typically reach a value of approximately 1 by the time the oil window is reached. So in most cases, no odd/even predominance is seen for the *n*-alkanes in most oils. A more important change that is seen in the distribution of the *n*-alkane distributions is the thermal degradation of the longer-chain compounds with increasing maturity. As a result the distribution of the alkanes will change with increasing maturity with the carbon number at which the *n*-alkanes maximize decreasing, ultimately converting oils dominated by higher carbon number compounds to condensates dominated by alkanes in a much lower carbon number range. If the process continues even further, the condensate could be converted into a wet gas and then ultimately to pure methane. Another significant change associated with increasing maturity would be changes in the pristane/*n*-C₁₇ and phytane/*n*-C₁₈ ratios (Shanmugam 1985). These ratios will decrease with increasing maturity due to the formation of additional

amounts of the *n*-alkanes through the thermal cracking process. The relative amounts of pristane and phytane do not change significantly at lower levels of maturity, but Kissin (1993) reported significant cracking of pristane and phytane can occur at higher levels of maturity. The changes mentioned above are relatively easy to observe using GC. It should be noted that it is possible that pristane and phytane will undergo thermal degradation but in all probability degrade at similar rates such that changes to the Pr/Ph ratio will be relatively small with increasing maturity. In addition, there are numerous changes to the various families of biomarkers that are typically determined using GC-MS or GC-MSMS, some of which will be described below.

A chapter of this nature is not the place to discuss all biomarker maturity parameters, and a detailed discussion of such parameters can be readily found in many published papers as well as both editions of *The Biomarker Guide: Volume 2* (Peters and Moldowan 1992; Peters et al. 2005). Instead a few basic examples will be given to illustrate the value of these parameters in assessing the relative maturity of a crude oil. The majority of biomarker maturity parameters can be divided into two categories, either parameters related to changes in the distributions of isomers or parameters related to changes in relative proportions of the lower carbon members to higher carbon members of the same series of compounds.

There are many types of isomers in a crude oil, but the three that are most commonly encountered isomers are structural, stereo-, and optical isomers. For instance, the methylphenanthrene index (MPI), initially proposed by Radke and Welte (1983) for coals and subsequently type III kerogens, is based on changes in the relative proportions of the four methylphenanthrene structural isomers, shown in the figure below (Fig. 16). As a result of differences in the thermal stability of these

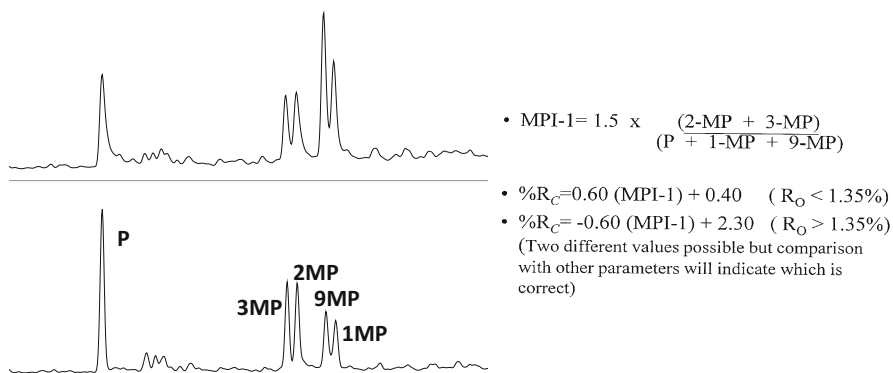


Fig. 16 The methylphenanthrene index (MPI) initially proposed by Radke and Welte (1983) for coals and subsequently type III kerogens is based on changes in the relative proportions of phenanthrene and the 4 methylphenanthrene structural isomers shown in the figure for two oils at different levels of maturity (P=phenanthrene; 3MP=3-methylphenanthrene; 2MP=2-methylphenanthrene; 9MP=9-methylphenanthrene; 1MP=1methylphenanthrene). The MPI is also shown on this figure along with the formula used to convert these values into vitrinite equivalent values (R_c)

isomers due to position of the methyl group, this ratio will change with increasing maturity, and initially the ratio was correlated with that of vitrinite reflectance for coal samples (Teichmüller 1958). This correlation has been extended to all kerogen types although there have been problems when applying it to type II and III kerogens. For oils it is a very useful tool to get a general idea of the maturity level at which the oil was generated and also for comparing relative maturities of oils known to be derived from the same source rock.

Two of the main biomarker families, steranes and terpanes, exist as a complex mixture of homologues, stereoisomers, and diastereomers. For example, Fig. 17 shows typical distribution of individual steranes in a crude oil by displaying traces for the C_{26} – C_{29} homologues which have been resolved through the use of MSMS and monitoring of the m/z 358, 372, 386, and 400 to 217 transitions, respectively (Fig. 17). Four components have been identified that show the presence of both the stereoisomers and the diastereomers. Two very commonly used maturity parameters based on these distributions have been used as far back as the late 1970s when molecular geochemistry started to evolve (Seifert and Moldowan 1978). These ratios are shown below:

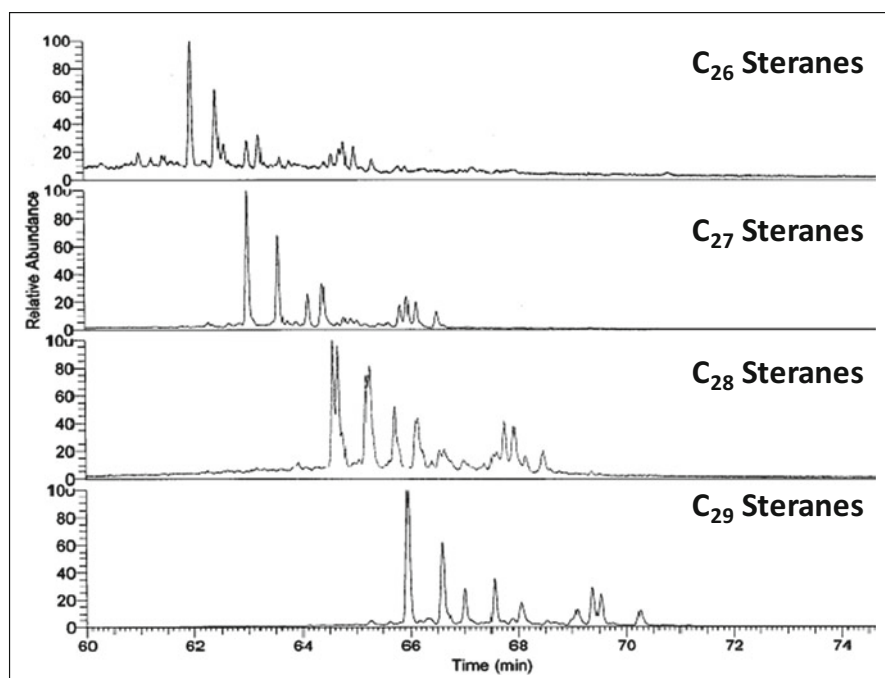


Fig. 17 As noted elsewhere, GC-MSMS can be used to separate individual compounds within a complex mixture. The data in this figure show the separation of the individual steranes from within the total sterane distribution

- (i) $\alpha\alpha C_{29}20S/(20S+20R)$
(ii) $\beta\beta C_{29}(20S+20R)/\alpha\alpha C_{29}20S/(20S+20R)+\beta\beta C_{29}(20S+20R)$

(In the above $\alpha\alpha$ and $\beta\beta$ refer to stereochemistry and C14 and C17 in the sterane molecule.)

Both increase with increasing maturity. It should be noted that in general both increase with increasing maturity but may not increase at the same rate in different basins since there are a number of factors that are also involved in these changes such as the presence or absence of clay minerals and heating or burial rates. It should also be noted that there has been much discussion as to whether these ratios increase as a result of conversion of one isomer into the other or alternatively is it a case of one isomer being transformed to another compound faster than the other compounds (Requejo 1992). This question can only be answered if an internal standard is used for quantification, but regardless of the mechanism responsible for the change, the end result is the same, the ratios increase. In the case of the hopanes, another commonly used maturity parameter is the $22S/22R + 22S$ ratio for the extended hopanes which increases with increasing maturity until it reaches an equilibrium ratio of approximately 0.64, a value commonly observed in most oils. But in immature source rocks, this ratio will be much lower since the $22R$ diastereomer is the dominant component.

The final example shows the changes that result when compounds such as the triaromatic steroid hydrocarbons are subject to increasing maturity. The triaromatic steroid hydrocarbons occur over a range of carbon numbers from C_{20} to C_{28} (Fig. 8). It is generally assumed that the lower carbon-numbered compounds in the C_{20} – C_{21} range are formed from the cleavage of the side chain of the higher carbon-numbered compounds in the C_{26} – C_{28} range with increasing maturity. Again, as with the changes in the stereoisomers, caution has to be exercised in the interpretation as it is possible either that the C_{20} – C_{21} compounds are formed directly from the C_{26} – C_{28} compounds by cleavage of the side chains or that all these compounds were initially present but with a faster degradation of the higher carbon-numbered compounds during maturation as initially proposed by Beach et al. (1989). This issue can only be resolved through the presence of an internal standard. Regardless of the mechanism, the end result is the same, i.e., the ratio of the C_{20} – C_{21} triaromatic steroid hydrocarbons to the total triaromatic steroid hydrocarbons increases with increasing maturity.

These are just a few examples of maturity parameters that are used extensively for getting information about the relative maturity of both oils and source rock extracts. It was mentioned above that increasing maturity also leads to certain changes in the n -alkane distributions, but in addition there are other families of compounds that are also impacted by maturity. For example, diamondoids are a family of compounds that cannot be defined as biomarkers in the true sense of the word but are thought to form by cyclization of steranes and terpanes. Diamondoids are present in low concentrations in conventional crude oils, but their relative concentration increases significantly with increasing maturity, primarily due to the thermal degradation of other commonly occurring compounds that are thermally less stable (Dahl et al. 1999). One of the earliest papers published on the use of these

compounds as maturity parameters was that of Chen et al. (1996) who discussed the use of two parameters based on these compounds for use as high-maturity indices in a number of Chinese basins. One of the main attractions of these parameters as proposed by Chen et al. (1996) was the claim they operate over a wide range of maturities from immature ($<0.6\% R_o$) to overmature ranges (approx. $2.0\% R_o$). A more recent paper by Li et al. (2000) suggested there was no linear correlation between these adamantane maturity parameters at the higher levels of maturity and therefore they may have a limited range just like many of the biomarker parameters. Condensates in particular contain very high relative concentrations of these compounds, and it has been shown that they are extremely useful for correlating condensates with other condensates or even potential source rocks. A number of examples have been published in the literature where the isotopic compositions of individual diamondoids have been used for correlation purposes and to determine the extent of oil cracking with increasing levels of maturity. This is not a routine tool due to difficulties in isolating the diamondoid concentrates and the very limited number of papers that actually provide the experimental method for isolating these compounds (Ling et al. 2011; Nguyen and Philp 2016).

10 Expulsion and Migration

Expulsion and migration both have the potential to change the composition of crude oils. It is a very simple concept to grasp since expulsion refers to the movement of the bitumen that is initially generated from the kerogen in the source rock that has to be expelled into the carrier beds that will transport the oil to the reservoir. However several barriers have to be overcome in order for this to occur. First bitumen has to displace any interstitial water that may be in pore spaces of the source rock and replace and saturate the pore spaces with bitumen before any expulsion may occur. Expulsion also requires sufficient pressure to push molecules through pore throats of the reservoir rock out into the carrier beds. Not surprisingly smaller molecules will be preferentially expelled. A series of classic experiments many years ago by Leythaeuser and co-workers (1984) clearly demonstrated this type of fractionation during expulsion in cores from Greenland where a comparison between the alkane distributions on extracts from a source rock and overlying sands clearly showed the preferential expulsion of the lower carbon-numbered *n*-alkanes. Prior to that observation, Hunt (1979) had noted that the composition of most source rock extracts and related crude oils differs in composition and more specifically the expelled oils typically contain lower proportions of the polar fraction which has a greater tendency to interact with the mineral matrix and be held back during expulsion.

Expulsion is often referred to as primary migration with secondary migration being the longer-distance phenomenon of movement of the oil into the reservoir, which may occur over very short distances or distances of hundreds of miles. In this process which is driven to a large degree by buoyance and pressure differences, many of the issues experienced during primary migration will be experienced on a larger scale. Pore throat pressures have to be overcome, water has to be displaced,

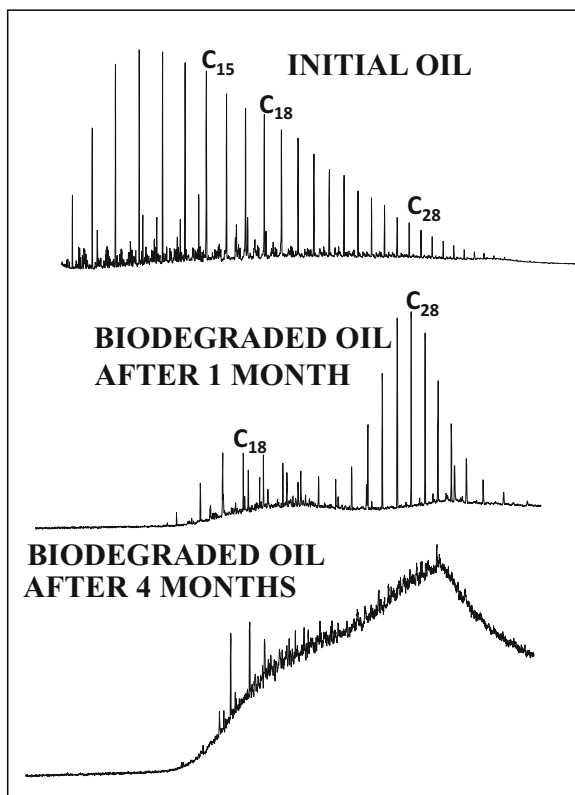
and additional interactions between the polar compounds and minerals may occur. With secondary migration additional changes to the distribution of individual compound classes have also been proposed to occur. For example, tricyclic compounds have been proposed to migrate more readily than hopanes, and thus care must be taken not to confuse such a change with maturity variations which could also have the same effect. It has also been proposed that certain sterane isomers may migrate faster than others and that formed the basis of a very early migration distance parameter proposed by Seifert and Moldowan (1978). Another migration distance parameter proposed was based on changes in relative proportions of two dibenzocarbazole isomers with increasing migration distance (Larter et al. 1996). This parameter held a great promise for many years but ultimately came under pressure when it was shown that there were other factors that could change the relative proportions of these two compounds in addition to migration.

11 Biodegradation and Preservation

Biodegradation of crude oils in a reservoir is a comprehensive topic that deserves an extensive chapter devoted to that topic alone, but only highlights are provided here. Biodegradation can be evaluated on a number of different levels ranging from the bulk properties of a crude oil to the changes in distribution of individual compounds. From the perspective of the bulk parameters, it is clear that with increasing biodegradation the API gravity will decrease; viscosity will increase; asphaltene content will increase; metal content will increase; sulfur content will increase; *n*-alkanes will be removed; and the most obvious signs of biodegradation are often the absence of *n*-alkanes and the appearance of an unresolved complex mixture as shown in the figure below (Fig. 18).

Heavily biodegraded oils are less valuable since the amount of gasoline that can be produced from a heavily biodegraded oil is much lower than from a non-degraded oil. It has been known for many years that biodegradation of crude oils occurs in reservoirs, and of course prior to that, much exploration was undertaken based on the presence of oil seeps formed when oils that have migrated to the surface are extensively biodegraded (Winters and Williams 1969). Early papers on biodegradation commonly assumed that degradation was occurring under aerobic conditions leading to a well-established order in which different compound classes were removed starting with the *n*-alkanes. In general, the *n*-alkanes are removed starting at the lower carbon numbers and then progressively moving to the higher carbon-numbered alkanes. Most chromatograms reported in the literature on showing hydrocarbons extending to around C₄₀ and indicate complete removal of all *n*-alkanes below that carbon number in a heavily degraded oil. However, if high-temperature GC is used to analyze heavily biodegraded samples, a different picture emerges. As can be seen in Fig. 19, the low molecular weight hydrocarbons are removed as would be expected, but above C₄₀ the hydrocarbons that are present are basically unaffected by increasing levels of biodegradation (Fig. 19).

Fig. 18 This figure shows the most evident impact of biodegradation, namely, removal of the lower carbon number alkanes initially followed by higher carbon-numbered alkanes with increasing biodegradation



This observation is typically overlooked since most laboratories do not use high-temperature GC to analyze their oil samples.

For many years it was generally assumed that crude oil degradation in reservoirs occurred under oxic conditions. More recently it has been shown that in many reservoirs worldwide the oil in these reservoirs is actually undergoing degradation under anoxic conditions (Head et al. 2003; Holba et al. 2004; Jones et al. 2008; ► Chap. 22, “Secondary Microbial Gas”). Larter et al. (2003 and 2006) clearly demonstrated that biodegradation occurs at the oil/water interface, and as components are degraded at that position, fresh levels of non-degraded components diffuse through the reservoir to replace those compounds being removed. Extensive studies of reservoirs in China clearly showed changes in the composition of oils in the reservoirs with increasing depth and preferential degradation of the more readily degradable compounds. It has been well established that hydrocarbons are removed during biodegradation in a systematic manner and there are several scales in the literature documenting the relative rates of removal of these compounds. Initially these scales were established assuming they were being removed under oxic conditions, but it appears that similar rates of removal occur under anoxic conditions (Head et al. 2003; Jones et al. 2008). The most widely used of these would be the one

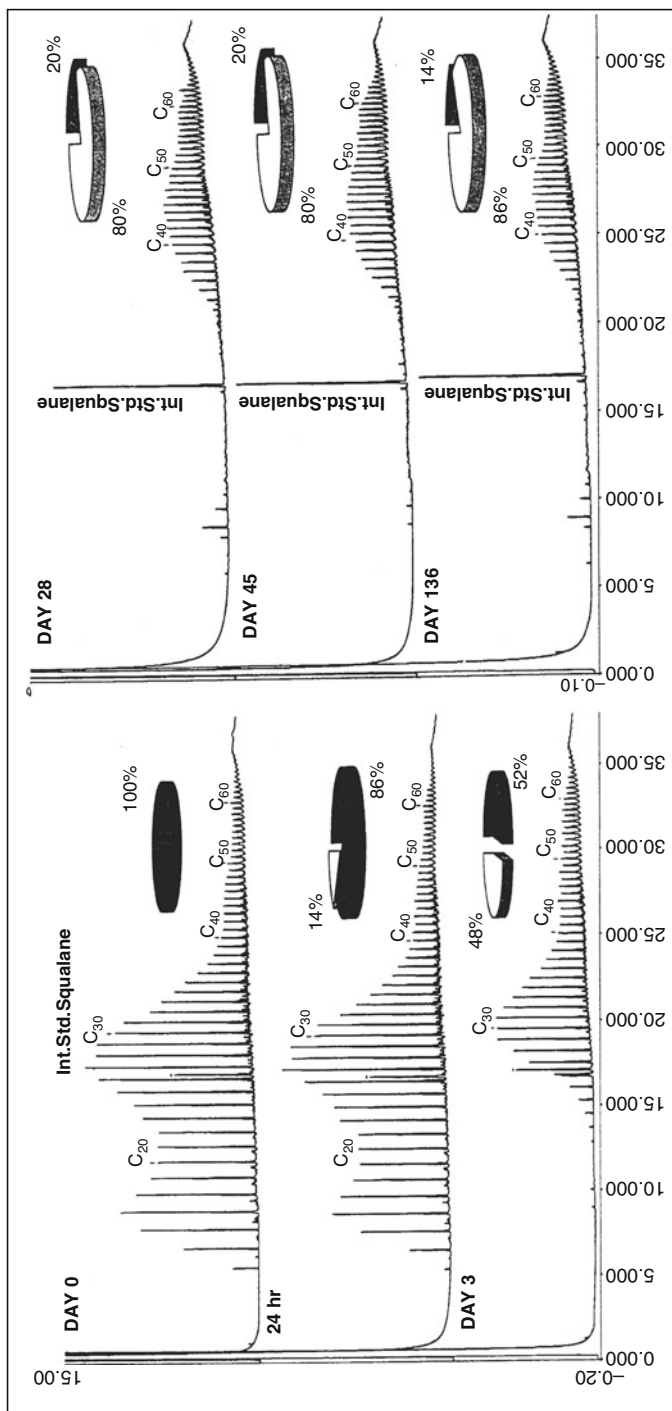


Fig. 19 Although it is well documented that lower carbon numbered *n*-alkanes are removed relatively rapidly by biodegradation, the fate of *n*-alkanes above C₄₀ is typically overlooked. The chromatograms shown here from a laboratory study show that these alkanes are relatively resistant to biodegradation. (Reproduced with permission from Heath et al. 1997)

of Peters and Moldowan (1992) which is very useful for comparing relative extents of degradation of different oils in different parts of a field. A version of this table is shown in Fig. 20, but it should be mentioned, there is criticism of this table that it is not specific enough in terms of distinguishing different levels of biodegradation. This becomes evident when looking at a large number of samples coming from similar depths within a reservoir that may have a range of API and viscosity values and be degraded to different levels, but ultimately all have the same or very similar values on the PM scale. There are a number of other biodegradation scales that have been published including one by Wenger and Isaksen (2002) which incorporates more aromatic components along with changes to gaseous components; however this scale does not seem as widely used as the PM scale. In recent years Larter and others (2012) have introduced a new scale called the Manco scale which correlates the level of biodegradation and viscosity. This again is a very important development since this scale can also be used to predict the level of biodegradation and hence viscosity with the Manco parameters that are based on changes to various aromatic components.

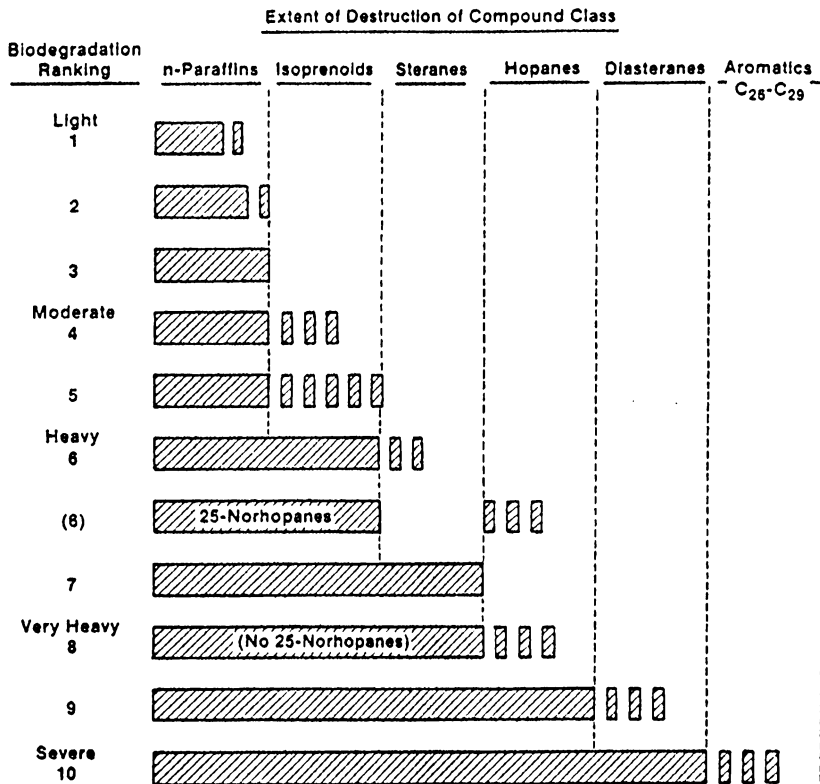


Fig. 20 A number of scales have been published in the literature illustrating the relative rate of removal of different compound classes during biodegradation. The scale shown here is probably the most widely cited such scheme and is commonly referred to as the Peters and Moldowan scale. (Reproduced with permission from Peters and Moldowan 1992)

As mentioned above for many years, it was always assumed that biodegradation in reservoirs occurred under aerobic conditions. However there is now significant evidence to show that in many of the major oil accumulations worldwide biodegradation is occurring under anaerobic conditions. Evidence for anaerobic degradation includes the presence of succinates in crude oils, indicators of early stages of anoxic biodegradation; the presence of gases from shallow petroleum accumulations and natural seeps led to the recognition that some gases previously thought to have primary microbial origin actually formed from biodegraded petroleum during secondary methanogenesis (Etiope et al. 2009; Milkov 2010); and the presence of isotopically enriched associated CO₂ provides strong evidence for secondary microbial gas formed under anoxic conditions (► Chap. 22, “Secondary Microbial Gas”). Jones et al. (2008) used a combination of laboratory microcosm experiments and isotope data from well head samples to demonstrate the degradation of crude oils under anaerobic conditions as well as noting that in general relative rates of removal of compound classes were very similar under both oxic and anoxic conditions. Holba and others (2004) showed that in oils from the N. Slope of Alaska that were undergoing anaerobic degradation, the *n*-alkanes were not removed, but the most significant change was the initial removal of the alkyltoluenes. A similar observation has been made in other basins since that time (Liu et al. 2016a).

An interesting set of observations have been made related to the presence of the 25-norhopanes and biodegradation. It has been assumed for many years that the presence of 25-norhopanes indicates biodegradation of the crude oil. These compounds are also excellent indicators of mixing occurring between degraded and non-degraded oils such that the *n*-alkanes are restored through the contribution of non-degraded oils with the presence of the 25-norhopanes indicating biodegradation. More recently it has been proposed that the presence of the 25-norhopanes is probably related to anaerobic degradation within the reservoir. Anaerobic degradation has been used to explain degradation of crude oils in a reservoir where conditions were not possibly aerobic due to the depth of the reservoir and the inability to replenish the oxygen in the reservoir or the nutrients necessary for the aerobic bacteria. It has also been clearly established that biodegradation, aerobic or anaerobic, will cease at temperatures exceeding 80 °C due to the fact that the bacteria can no longer exist above these temperatures. This in turn led to the concept of paleopasteurization which basically suggests that if a reservoir is buried and temperatures exceed the 80 °C limit and then the reservoir is uplifted or overburden eroded such that temperature declines, then no more degradation will occur due to the sterilization of the reservoir (Wilhelms et al. 2001). This has been reported in a number of reservoirs but was first reported in N. Sea reservoirs.

12 Summary

Crude oils are very complex mixtures of a wide variety of hydrocarbons, heteroatomic compounds, and metals. The distribution of these compounds provides us with a tremendous amount of information related to the origin and history of the oils and also the types of products that can be obtained upon refining the oils.

The composition of the oils also determines the value of the oil, with heavy asphaltene-rich oils being of less value than lighter hydrocarbon-rich oils, primarily because of the amounts of gasoline that can be produced from the lighter oils. Studies of the complex biomarker content of the oils provide information on source, depositional environments, maturity, and age of the source rocks responsible for the generation of the oils, information that is extremely valuable for the exploration geologist. With the advent of unconventional resources, again the composition of the oils provides much information related to whether or not the oil was actually generated in situ which has significant ramifications for production. In brief the composition of a crude oil provides a wealth of information on its origin and use, and there is still much to be learned from this information.

There have been tremendous advances in our ability to characterize crude oils due to advances in available analytical techniques that have evolved since the 1960s/1970s. In reality much of this characterization has focused on the saturate and aromatic hydrocarbons. Hydrocarbons in these fractions have proved to be very powerful when applied to exploration and production problems. However, relatively little work has been done on characterizing either the more polar heteroatomic compounds or the high molecular weight compounds. The past few years have seen a number of novel analytical techniques, such as electrospray ionization Fourier transform ion cyclotron resonance mass spectrometry, that have been developed to characterize these fractions and identify individual compounds. In addition, ^{31}P -NMR has been used to analyze the different hydroxyl groups present in crude oils and asphaltene precipitates, along with Fourier transform infrared spectroscopy. 2D gas chromatography will continue to be used in these characterization studies further increasing the number of individual compounds being identified. Liquid chromatography-mass spectrometry will also continue to be applied to characterizing polar compounds which will undoubtedly be incorporated into interpretation of the origin and history of crude oils.

References

- Alexander R, Kagi RI, Noble RA, Volkman JK (1984) Identification of some bicyclic alkanes in petroleum. In: Schenck PA, De Leeuw JW, Lijmbach GWM (eds) *Advances in organic geochemistry 1983*. Pergamon Press, Oxford
- Andrusevich VE, Engel MH, Zumberge JE, Brothers LA (1998) Secular, episodic changes in stable carbon isotope composition of crude oils. *Chem Geol* 152:59–72
- Aquino Neto FR, Trendel JM, Restle A, Connan J, Albrecht PA (1983) Occurrence and formation of tricyclic and tetracyclic terpanes in sediments and petroleums. In: Bjorøy M et al (eds) *Advances in organic geochemistry, 1981*. Wiley Chichester, New York, pp 659–667
- Armstroff A, Wilkes H, Schwarzbauer J, Littke R, Horsfield B (2006) Aromatic hydrocarbon biomarkers in terrestrial organic matter of Devonian to Permian age. *Palaeogeogr Palaeoclimatol Palaeoecol* 240(1–2):253–274
- Beach F, Peakman TM, Abbott GD, Sleeman R, Maxwell JR (1989) Laboratory thermal alteration of triaromatic steroid hydrocarbons. *Org Geochem* 14:109–111

- Bennett B, Fustic M, Farrimond P, Huang H, Larter SR (2006) 25-Norhopanes: formation during biodegradation of petroleum in the subsurface. *Org Geochem* 37(7):787–797
- Chen J, Fu J, Sheng G, Liu D, Zhang J (1996) Diamondoid hydrocarbon ratios: novel maturity indices for highly mature crude oils. *Org Geochem* 25(3/4):179–190
- Connock GT, Nguyen TX, Philp RP (2018) Elucidating environmental fluctuations concomitant with Woodford shale deposition: an integration of sequence stratigraphy and organic geochemistry. *Am Assoc Pet Geol Bull* 102(6):959–986
- Curiale JA, Cole RD, Witmer RJ (1992) Application of organic geochemistry to sequence stratigraphy analysis; Four Corners Platform area, New Mexico, U.S.A. *Org. Geochemistry* 19(1–3):53–75
- Dahl J, Moldowan M, Peters K, Claypool G, Rooney M, Michael G, Mello M, Kohnen M (1999) Diamondoid hydrocarbons as indicators of natural cracking. *Nature* 399:54–56
- Demaison GJ, Moore GT (1980) Anoxic environments and oil source bed genesis. *Am Assoc Pet Geol Bull* 64:1179–1209
- Didyk BM, Simoneit BRT, Brassell SC, Eglinton G (1978) Organic geochemical indicators of palaeoenvironmental conditions of sedimentation. *Nature* 272:216–221
- Durand B (ed) (1980) Kerogen-insoluble organic matter from sedimentary rocks. Editions Technip, Paris
- Eglinton G, Calvin M (1967) Chemical fossils. *Sci Am* 216:32–43
- Eglinton G, Murphy MTJ (eds) (1969) *Organic geochemistry: methods and results*. Springer, New York
- Etiopie G, Feyzullayev A, Milkov AV, Waseda A, Mizobe K, Sun CH (2009) Evidence of subsurface anaerobic biodegradation of hydrocarbons and potential secondary methanogenesis in terrestrial mud volcanoes. *Mar Pet Geol* 26:1692–1703
- French KL, Rocher D, Zumberge J, Summons RE (2015) Assessing the distribution of sedimentary C40 carotenoids through time. *Geobiology* 13:139–151
- Fuex A (1977) The use of stable isotopes in hydrocarbon exploration. *J Geochem Explor* 7:155–188
- Halpern HI (1995) Development and applications of light-hydrocarbon based star diagrams. *Am Assoc Pet Geol Bull* 79:801–815
- Heath DJ, Lewis CA, Rowland SJ (1997) The use of high temperature gas chromatography to study the biodegradation of high molecular weight hydrocarbons. *Org Geochem* 26:769–785
- Hedberg HD (1968) Significance of high-wax oils with respect to genesis of petroleum. *Am Assoc Pet Geol Bull* 52:736–750
- Hites RA, Biemann K (1970) Computer evaluation of continuously scanned mass spectra of gas chromatographic effluents. *Anal Chem* 42:855–860
- Holba AG, Wright L, Levinson R, Huizinga B, Scheihing M (2004) Effects and impact of early-stage anaerobic biodegradation on Kuparuk River Field, Alaska. *Geol Soc Lond, Spec Publ* 237:53–88
- Holland HD, Turekian KK (eds) (2014) *Treatise on geochemistry*, 2nd edn. Elsevier, Oxford
- Hunt JM (1979) *Petroleum geochemistry and geology*. Freeman, San Francisco
- Hunt JM (1996) *Petroleum geochemistry and geology*, 2nd edn. Freeman, New York
- Hunt JM, Philp RP, Kvenvolden K (2002) Early developments in petroleum geochemistry. *Org Geochem* 33(9):1025–1052
- Jarvie DM, Hill RJ, Ruble TE, Pollastrano RM (2007) Unconventional shale gas systems: the Mississippian Barnett Shale of north central Texas as one model for thermogenic shale-gas assessment. In: Hill RJ, Jarvie DM (eds) *Special issues Barnett Shale*. *Am Assoc Pet Geol Bull* 91. AAPG, Tulsa, Oklahoma, pp 475–499
- Jones RW (1987) Organic facies. In: Brooks J, Welte D (eds) *Advances in petroleum geochemistry*. Academic, New York, pp 1–90
- Jones DM, Head IM, Gray ND, Adams JJ, Rowan AK, Aitken CM, Bennett B, Huang H, Brown A, Bowler BFJ, Oldenburg T, Erdmann M, Larter SR (2008) Crude-oil biodegradation via methanogenesis in subsurface petroleum reservoirs. *Nature* 451:176–180

- Kissin YV (1993) Catagenesis of light acyclic isoprenoids in petroleum. *Org Geochem* 20:1077–1090
- Larter SR, Bowler BFJ, Li M, Chen M, Brincat D, Bennett B, Noke K, Donohoe P, Simmons D, Kohnen M, Allan J, Telnaes N, Horstad I (1996) Molecular indicators of secondary oil migration distances. *Nature* 383:593–597
- Larter SR, Wilhelms A, Head I, Koopmans M, Aplin A, Di PR, Zwach C, Erdmann M, Telnaes N (2003) The controls on the composition of biodegraded oils in the deep subsurface: Part I—Biodegradation rates in petroleum reservoirs. *Org Geochem* 34:601–613
- Larter S, Huang H, Adams J, Bennett B, Jokanola O, Oldenburg T, Jones M, Head I, Riediger C, Fowler M (2006) The controls on the composition of biodegraded oils in the deep subsurface: Part II—Geological controls on subsurface fluxes and constraints on reservoir fluid property prediction. *Am Assoc Pet Geol Bull* 90(6):921–938
- Larter S, Huang H, Adams J, Bennett B, Snowdon LR (2012) A practical biodegradation scale for use in reservoir geochemical studies of biodegraded oils. *Org Geochem* 45:66–76
- Leythaeuser D, Mackenzie A, Schaafeffer RG, Bjoroy M (1984) A novel approach for recognition and quantification of hydrocarbon migration effects in shale – sandstone sequences. *Am Assoc Pet Geol Bull* 68(2):196–219
- Li J, Philp RP, Cui M (2000) Methyl diamantane index (MDI) as a maturity parameter for Lower Paleozoic carbonate rocks at high maturity and over maturity. *Org Geochem* 31:267–272
- Ling H, Shuichang Z, Huitong W, Xiaofang F, Wenlong Z, Yirui X, Caiyun W (2011) A novel method for isolation of diamondoids from crude oils for compound-specific isotope analysis. *Org Geochem*. <https://doi.org/10.1016/j.orggeochem.2011.02.010>
- Liu L, Philp RP, Nguyen TX (2016a) The origin and history of the oils in the Lawton Oil Field, Southwestern Oklahoma. *Am Assoc Pet Geol Bull* 101(2):205–232
- Liu Z, Moldowan JM, Nemchenko-Rovenskaya A, Peters KE (2016b) Oil families and mixed oil of the North–Central West Siberian basin, Russia. *Am Assoc Pet Geol Bull* 100(3):319–343
- Mackenzie AS, Brassell SC, Eglinton G, Maxwell JR (1982) Chemical fossils: the geological fate of steroids. *Science* 217:491–504
- Miceli RA, Philp RP (2012) Organic geochemistry of the Woodford Shale, southeastern Oklahoma: how variable can shales be? *Am Assoc Pet Geol Bull* 93(3):493–517
- Milkov AV (2010) Methanogenic biodegradation of petroleum in the West Siberian basin (Russia): significance for formation of giant Cenomanian gas pools. *Am Assoc Pet Geol Bull* 94:1485–1541
- Moldowan JM, Seifert WK, Gallegos EJ (1985) Relationship between petroleum composition and depositional environment of petroleum source rocks. *Am Assoc Pet Geol Bull* 69:1255–1268
- Moldowan JM, Dahl J, Zinniker D, Barbanti SM (2015) Underutilized advanced geochemical technologies for oil and gas exploration and production-1. The diamondoids. *J Pet Sci Eng* 126:87–96
- Nguyen TX, Philp RP (2016) Molecular sieving to separate diamondoids in oils for compound-specific isotope analysis. *Org Geochem* 95:1–12
- Pedersen TF, Calvert SE (1990) Anoxia vs. productivity: what controls the formation of organic-carbon-rich sediments and sedimentary rocks. *Am Assoc Pet Geol Bull* 74:454–466
- Peters KE, Fowler M (2002) Applications of petroleum geochemistry to exploration and reservoir management. *Org Geochem* 33(1):5–37
- Peters KE, Moldowan JM (1992) *The biomarker guide: interpreting molecular fossils in petroleum and ancient sediments*. Prentice Hall, Englewood Cliffs
- Peters KE, Walters CC, Moldowan JM (2005) *The biomarker guide*, vol 2, 2nd edn. Cambridge University Press, Cambridge, 1155 p
- Philp RP (2014) Formation and geochemistry of oil and gas. In: Holland HD, Turekian KK (eds) *Treatise on geochemistry*, vol 9, 2nd edn. Elsevier, Oxford, pp 233–265
- Philp RP, Lewis CA (1987) Organic geochemistry of biomarkers. *Annu Rev Earth Planet Sci* 15:363–395

- Philp RP, Hsieh M, Tahira F (2004) A review of developments related to the characterization and significance of high molecular weight paraffins ($>C_{40}$) in crude oils. In: Cubitt JM, England WA, Larter S (eds) *Understanding petroleum reservoirs: towards an integrated reservoir engineering and geological approach*, vol 237. Royal Geological Society, London, pp 37–51
- Powell TG, McKirdy DM (1973) Relationship between ratio of pristane to phytane, crude oil composition and geological environment in Australia. *Nature* 243:37–39
- Radke M, Welte D (1983) The methylphenanthrene index (MPI): a maturity parameter based on aromatic hydrocarbons. *Adv Org Geochem* 1981:504–512
- Requejo AG (1992) Quantitative analysis of triterpane and sterane biomarkers: methodology and applications in molecular maturity studies. In: Moldowan JM, Albrecht P, Philp RP (eds) *Biological markers in sediments and petroleum*. Prentice Hall, Engelwood Cliffs, pp 223–240
- Ruh EL, Moran JJ, Thompson RD (1959) Measurement problems in the instrument and laboratory apparatus fields. In: Kayan CF (ed) *Systems of units. National and international aspects*, Publication no 57 of the AAAS. American Association for the Advancement of Science, Washington, DC
- Samuel OJ, Kildahl-Andersen G, Nytoft HP, Johansen JE, Jones M (2010) Novel tricyclic and tetracyclic terpanes in Tertiary deltaic oils: structural identification, origin and application to petroleum correlation. *Org Geochem* 41:1326–1337
- Schwark L, Frimmel A (2004) Chemostratigraphy of the Posidonia Black Shale, SW Germany II. Assessment of extent and persistence of photic-zone anoxia using aryl isoprenoids distributions. *Chem Geol* 206:231–248
- Seifert WK, Moldowan JM (1978) Applications of steranes, terpanes and monoaromatics to the maturation, migration and source of crude oils. *Geochim Cosmochim Acta* 42:77–95
- Seifert WK, Moldowan JM (1981) Paleoreconstruction by biological markers. *Geochim Cosmochim Acta* 45:783–794
- Seifert WK, Moldowan JM (1986) Use of biological markers in petroleum exploration. *Methods Geochem Geophys.* (ed: Johns RB) 24:261–290
- Shanmugam G (1985) Significance of coniferous rain forests and related organic matter in generating commercial quantities of oil, Gippsland Basin, Australia. *Am Assoc Pet Geol Bull* 69:1241–1254
- Silverman SR, Epstein S (1958) Carbon isotopic composition of petroleum and other sedimentary organic materials. *Am Assoc Pet Geol Bull* 42:998–1012
- Slatt RM, Rodriguez ND (2012) Comparative sequence stratigraphy and organic geochemistry of gas shales: commonality or coincidence? *J Nat Gas Sci Eng.* <https://doi.org/10.1016/j.jngse.2012.01.008>
- Smith HM (1940) Correlation index to aid in interpreting crude oil analyses. U.S. Bureau of Mines technical paper 610. U.S. Department Interior Bureau of Mines, Washington, DC, 34 pp
- Strachan MG, Alexander R, Kagi RI (1988) Trimethylnaphthalenes in crude oils and sediments: Effects of source and maturity. *Geochim Cosmochim Acta* 52:1255–1264
- Teichmüller M (1958) Metamorphism du carbon et propection du petrole. *Rev Indus Min (Special Issue)*:1–15
- ten Haven HL, de Leeuw JW, Sinninghe Damste JS, Schenck PA, Palmer SE, Zumberge JE (1988) Application of biological markers in the recognition of paleohypersaline environments. In: Kelts AJFK, Talbot MR (eds) *Lacustrine petroleum source rocks*, Geological society special publication no 40. Blackwell, Oxford, pp 123–130
- Tissot B, Welte DH (1978) *Petroleum formation and occurrence*. Springer, Heidelberg
- Tissot B, Welte DH (1984) *Petroleum formation and occurrence*, 2nd edn. Springer, Berlin
- Treibs A (1934a) Chlorophyll- und Häminderivate in bituminösen Gesteinen, Erdölen, Erdwachsen und Asphalten. *Liebigs Ann Chem* 510:42–62
- Treibs A (1934b) Über das Vorkommen von Chlorophyllderivaten in einem Ölschiefer aus der oberen Trias. *Justus Liebigs Ann Chem* 509:103–114
- Treibs A (1936) Chlorophyll- und Häminderivate in organischen Mineralstoffen. *Angew Chem* 49:682–686

- van Aarssen BGK, Bastow TP, Alexander R, Kagi RI (1999) Distributions of methylated naphthalenes in crude oils: indicators of maturity, biodegradation and mixing. *Org Geochem* 30:1213–1227
- van Krevelen DW (1961) *Coal: typology-chemistry-physics-constitution*. Elsevier Science, Amsterdam
- Wei Z, Moldowan JM, Peters KE, Wang Y, Xiang W (2007) The abundance and distribution of diamondoids in biodegraded oils from the San Joaquin Valley: implications for biodegradation of diamondoids in petroleum reservoirs. *Org Geochem* 38(11):1910–1926
- Wenger LM, Isaksen GH (2002) Controls of hydrocarbon seepage intensity on level of biodegradation in sea bottom sediments. *Org Geochem* 33(12):1277–1292
- Whitehead EV (1971) Chemical clues to petroleum origin. *Chem Ind* 27:1116–1118



Clifford C. Walters and Meytal B. Higgins

Contents

1	What Is Petroleomics?	312
2	Determining the Petroleome	314
2.1	Gas Chromatography	314
2.2	Liquid Chromatography	316
2.3	Ultrahigh-Resolution Mass Spectrometry	320
2.4	Modeling the Petroleome	324
3	Applications of Petroleomics	326
4	Limitations and Future Research	327
	References	328

Abstract

Petroleum, one of the most complex organic mixtures in nature, is derived from biochemicals deposited in sediments that are then buried and thermally altered. Petroleomics aims at a complete molecular description of petroleum, the petroleome, from which all physical properties – such as density, viscosity, phase behavior, and interfacial activity – and chemical reactivity – such as reservoir alteration and refinery upgrading processes – could be modeled. Although petroleomics has its roots in decades of petroleum chemical characterization, its modern conception is less than 20 years old. It is only through recent analytical advances, such as ultrahigh-resolution mass spectrometry, that an approximation of the petroleome is possible. The ability to use the petroleome to predict physical properties and chemical reactivity is just emerging.

C. C. Walters (✉) · M. B. Higgins
Corporate Strategic Research, ExxonMobil Research and Engineering Company, Annandale,
NJ, USA
e-mail: clifford.c.walters@exxonmobil.com; meytal.b.higgins@exxonmobil.com

© Springer Nature Switzerland AG 2020

H. Wilkes (ed.), *Hydrocarbons, Oils and Lipids: Diversity, Origin, Chemistry and Fate*,
Handbook of Hydrocarbon and Lipid Microbiology,
https://doi.org/10.1007/978-3-319-90569-3_4

311

1 What Is Petroleomics?

The inaugural symposium on *Petroleomics* held at the 2003 PittCon ushered in a new science, whose name follows a convention in vogue within the biological community, wherein the suffix “-omics” is used to refer to a totality or comprehensiveness of study. Even the organizer, Alan Marshall of the National High Magnetic Field Laboratory (NHMFL) acknowledged that “people sort of chuckle when they see the term” (Petkewich 2003). The biological “-omic” sciences originated with genomics, which is derived from the word “genome,” and have now expanded to include transcriptomics, proteomics, lipidomics, metabolomics, fluxomics, and others. Together they comprehensively describe the evolutionary relationships, genetic potential, cellular regulation, biochemical makeup, and chemical reactions of biological systems. Similarly, petroleomics aims at a complete molecular description of petroleum, the *petroleome*, from which all physical properties – such as density, viscosity, phase behavior, and interfacial activity – and chemical reactivity – such as reservoir alteration and refinery upgrading processes – could be modeled.

Petroleum, one of the most complex organic mixtures in nature, originates from biomass that has been deposited in sediments (Peters et al. 2005; Walters 2016). This biomass is altered by microbial and chemical processes to form kerogen or coal, solid organic matter that is highly cross-linked with no defined chemical structure, as well as a small amount of unbound species. If a sedimentary rock contains sufficient organic matter (total organic concentration typically >0.5%) that is not oxidized (H/C typically >1), it will generate upon further burial and heating liquid and gaseous hydrocarbons and other organic compounds containing heteroatoms (mostly nitrogen, oxygen, and sulfur). The composition of the generated species varies and is determined by the nature of the biotic input, the conditions of deposition and sedimentary preservation, and the degree of thermal exposure. The generated compounds, in turn, are selectively and partially expelled from the source rock, migrate through permeable strata, and accumulate in subsurface structures of porous rocks. Various physical (phase separation), chemical (thermal cracking, asphaltene precipitation, thermochemical sulfate reduction), and microbial (biodegradation) processes can further alter the chemical composition of oil in reservoir rocks. Not all of the kerogen is converted and not all of the generated compounds are expelled from the source rocks, leaving behind “unconventional” resources. A consequence of this origin is that oils share a general set of major and minor components in varying proportions and a near infinite variety of trace species.

When petroleum was first recognized as organic in nature is lost to antiquity. The earliest known use of the word *petroleum*, which is derived from Latin *petra* + *oleum* or *rock* + *oil*, is in the works of Constantinus Africanus (c. 1020–1087) (McDonald 2011). The first molecular study of petroleum was conducted by De la Rue and Miller (1856), who identified several aromatic hydrocarbons by forming and crystallizing barium salts of sulfonic acids. Several other hydrocarbons were identified in the second half of the nineteenth century based on distillation and wet chemical methods (Rossini and Mair 1951). In 1927, the American Petroleum Institute launched Project 6 to investigate the composition of petroleum. This

collaborative program, which ran until 1959, was able to isolate and identify 169 individual hydrocarbons using laborious procedures involving distillation, selective solvent extraction, selective absorption, and finally crystallization (Rossini and Mair 1959; Rabkin and Lafitte-Houssat 1979). Alfred Treibs (1936) used spectroscopy to establish a link between chlorophyll in living organisms and porphyrins in petroleum and provided the first molecular evidence for petroleum being derived from biomass.

Further identification of the components of petroleum followed advances in analytical methods. Gas chromatography (GC) offered the first of the modern advances in molecular characterization. Pioneering efforts by Eglinton et al. (1959) and Bray and Evans (1961) allowed for the identification of the major hydrocarbons, such as *n*-alkanes and isoprenoids, and recognition that these compounds occur as homologous series with distributions controlled by biotic input and thermal maturity. Technological improvements in hydrocarbon separation through the use of capillary columns and more thermally stable stationary phases and identification by mass spectrometry ushered in an explosion of hydrocarbon characterization (Hsu and Drinkwater 2001). Today, all major and minor hydrocarbons and many trace compounds that are amenable to gas chromatography are relatively easily characterized (Peters et al. 2005).

Gas chromatography continues to be a primary technique in petroleum characterization, but components must be in the gas phase for the analysis to occur. Large hydrocarbons and many polar heteroatomic compounds will thermally degrade before they volatilize and the vast majority of the components in petroleum that are not saturated or aromatic hydrocarbons remained uncharacterized until recently. This included most of the “heavy” fraction, the high molecular weight residue that cannot be distilled at atmospheric pressure. Pioneering work by Boduszynski (1988) characterized the heavy components by first separating crude oil into chemically related fractions using high performance liquid chromatography (HPLC) and then by field ionization mass spectroscopy (FIMS). These analyses suggested that much of the heavy material contains continuations of homologous series of lower molecular weight compounds. From this, a remarkable framework emerged for predicting chemical and physical properties and the distribution of molecular weights for the heteroatomic species (Altgelt and Boduszynski 1993).

The emergence of ultrahigh-resolution mass spectrometry opened a new window to this chemical “underworld” of petroleum (Marshall and Rodgers 2008). Initial studies conducted on a custom built Fourier transform ion cyclotron resonance mass spectrometer (FT-ICR-MS) at NHMFL at Florida State University revealed that the mass resolution was sufficient to identify the molecular formulas for several thousand individual species (Qian et al. 2001a, b; Hughey et al. 2002). For the next several years, a NHMFL team focused on FT-ICR-MS applications to petroleum, leading to a more complete description of the petroleome and developing the science of petroleomics (e.g., Hsu et al. 2011). With the availability of commercial ultrahigh-resolution mass spectrometers in the mid-2000s, petroleomics started to be practiced worldwide. The science is in its infancy and only some of the needed chemical structural-function relationships have been established, either empirically or from fundamental principles. Nevertheless, there are clear practical applications with

economic impact to both upstream and downstream operations. Increasingly finer molecular characterization offers new methods for decreasing exploration risk, improving flow assurance, maximizing refinery efficiency and profitability, and improving assessment of environmental impact.

2 Determining the Petroleome

Petroleomics requires knowledge of the *petroleome* – a complete compositional analysis of petroleum in terms of the absolute abundance and molecular description of each individual component. Presently, only ~1000 compounds can be assigned with a complete identification, and most of these are hydrocarbons with less than 35 carbon atoms. This is far short of the ~100,000 components that have partial characterization. The actual number of compounds present in petroleum is not known and, in theory, could be many, many orders of magnitude greater. The ultimate goal of petroleomics may be impractical and never achieved. However, oil is not a random assemblage of all possible organic compounds but is derived from living matter that has been geologically altered. This results in a distribution of common hydrocarbon components that can constitute a large percentage of most crudes. About 70% of the total mass of a typical crude oil, unaltered by reservoir processes, can be characterized by GC-based methods, and ~25% of the remaining components can be partially described by more advanced techniques. The completeness of a petroleum's characterization is roughly inversely proportional to its density. For light condensates with low density, GC-based methods can provide a complete molecular description of the components that make up >99% of the total weight. For a severely biodegraded, high density tar, few if any compounds can be identified by GC-based methods. More advanced techniques such as liquid chromatography and ultrahigh-resolution mass spectrometry can now provide molecular information for a majority of these components allowing for the petroleome to be defined sufficiently for petroleomic applications.

2.1 Gas Chromatography

Gas chromatography provides routine analysis of whole crude oil and oil fractions that are obtained by distillation or chemical separation (Grob and Barry 2004). Nearly all C₉ and smaller hydrocarbon isomers can be baseline resolved using a single, long capillary column. GC remains the analysis choice for low-molecular-weight hydrocarbons. The complexity of a hydrocarbon mixture increases with carbon number. Above C₁₀, the major (e.g., the *n*-alkanes and isoprenoids) and minor (e.g., monomethylalkanes, alkylaromatics) components co-elute with an increasingly complex, unresolved mixture. If the co-eluting hydrocarbons have different molecular weights, they can be resolved using a mass spectrometer. All major, most minor, and many trace hydrocarbons <C₃₅, many of which are biomarkers, can be characterized by GC-MS and GC-MS/MS (Peters et al. 2005).

Absolute quantification by MS, however, is difficult as the detector response is compound-dependent.

Two factors limit GC for petroleomic characterization: the compounds must be GC-amenable, and incomplete separation prevents easy detection and quantification. As GC separation occurs in the gas phase, the analyte must be volatilized. Typical equipment restricts the analysis to $<C_{40}$ hydrocarbons because of limitations in the thermal stability of column materials and temperature limitations of the injector, oven, transfer lines, and detector. Specialized high-temperature GC equipment can extend the analytical range for hydrocarbons to over 100 carbons, though with decreasing chromatographic resolution (Sutton and Rowland 2012). While hydrocarbons and some heteroatomic species are sufficiently thermally stable for conventional (e.g., polyaromatic thiophenes) or high-temperature-GC (e.g., porphyrins), most of the polar NSO-compounds (e.g., sulfides, naphthenic acids) will degrade before they volatilize. Derivatization of the polar functional group, such as conversion of carboxylic acids to alkyl esters (e.g., Meredith et al. 2000), is an option for only some of the polar compounds.

Chromatographic resolution can be improved using multidimensional heart-cutting (Marriott et al. 2012; Seeley and Seeley 2013). In this technique, a segment of the effluent from the first column is routed to second column with a different stationary phase. Ideally, the combined resolving power exceeds that of the individual columns and co-eluting compounds are separated. Two multidimensional heart-cutting methods are in common use. In the first, high-resolution separation is conducted on the first column, and one or more co-eluting peaks or intended intervals are routed to a second column with a different stationary phase that provides additional resolution. The second method involves chemical traps or molecular sieves, which first separate an oil into chemical groups (e.g., *n*-alkanes, *iso*-alkanes, cycloalkanes, and aromatics) that are subsequently separated into individual components by high-resolution GC. Industry standard methods (e.g., ASTM D6839; EN 14517; EN ISO 22854) that combine on-line fractionation and multiple heart-cutting techniques can provide a near complete quantitative measurement of molecular composition of $<C_{16}$ refined products (gasoline and kerosene), including oxygenates, olefins, and other compounds not found in geologic samples, and relatively complete composition of diesel fuels ($<C_{25}$).

In recent years, comprehensive two-dimensional gas chromatography, also known as GC \times GC or 2D-GC, has proven very effective for petroleomic-type analysis of crude oils and refined products (Bertoncini et al. 2013; Eiserbeck et al. 2015; Wang 2017). In this technique, small increments of effluent from a first column are repeatedly collected and routed to a short second column. Hence, GC \times GC can be viewed as a form of multidimensional heart-cutting GC. Either thermal trapping/release or mechanical valves are used to modulate the effluent on very short intervals, typically <10 s, in order to preserve the separation of the first column. Both FID and fast-acquisition MS are used commonly for petroleum GC \times GC analyses; the former offers the advantage of easy quantification, whereas the latter is suited for identification and provides an additional data dimension of separation. Chemoluminescence detectors provide selective detection of compounds

containing sulfur (Wang et al. 2003; Ruiz-Guerrero et al. 2006; Dijkmans et al. 2014) or nitrogen (Dutriez et al. 2011; Dijkmans et al. 2015).

Specialized software is required for data processing and visualization of GC \times GC results. While each modulation interval can be used as its own chromatogram, individual components are likely to cut across multiple time slices and quantification requires summation of peak areas. A common practice used to visualize the analysis is to stack the individual chromatograms by plotting the elution time from the first column on the *x*-axis and the elution time from the second column on the *y*-axis and representing signal intensity by color. Individual components are then visualized as extrapolated color-coded areas or volumes spanning multiple modulations.

Comprehensive two-dimensional gas chromatography can provide petroleomic data for the majority of $<C_{35}$ hydrocarbons and apolar NSO-compounds present in crude oils and refined fuels (Nizio et al. 2012; Bertocini et al. 2013; Eiserbeck et al. 2015; Nelson et al. 2016). Typically, the stationary phase of the first column is apolar (e.g., 100% methylsilicone), which separates components primarily through interaction with dispersal forces, and with a temperature ramp, the hydrocarbon elution order is controlled mostly by boiling point. The phase of the second column is more polar (e.g., 50%-phenyl), which promotes separation through π - π bond interaction. In this system, a modulated time slice containing hydrocarbons unresolved by the first column will be separated by their polarity in the second. Isoprenoidal hydrocarbons elute first, followed by *n*-alkanes, cycloalkanes, and then aromatic hydrocarbons by increasing ring number. This results in discrete bands of homologous series that possess similar core structures with varying degrees of alkylation (Fig. 1).

Many biomarker compounds possess stereogenic carbon centers resulting in multiple diastereomers or have similar structures with identical formulae; hence, such compounds cannot be differentiated by their mass alone and are indistinguishable if they co-elute. Targeted GC \times GC methods can provide resolution of some isomers that are difficult to separate by other chromatographic means. For example, Eiserbeck et al. (2011) were able to separate 18 α (H)-, 18 β (H)-oleanane, and lupine, and Araújo and Azevedo (2016) were able to separate and identify uncommon steranes that are produced by dinoflagellates. Mogollón et al. (2016) demonstrated that geochemical parameters determined by GC-MS, GC \times GC-MS and GC \times GC-MS/MS varied considerably in a suite of lacustrine oils. This was attributed to peak co-elutions that only were resolved by GC \times GC-MS/MS. Such separations demonstrate the power of comprehensive two-dimensional gas chromatography but also show the underlying complexity of petroleum composition.

2.2 Liquid Chromatography

Liquid chromatography (LC) has long been used to separate oils and rock extracts into chemically related groups. The most basic preparation first precipitates asphaltene by the addition of a large volume of nonpolar organic solvent (usually *n*-C₅, *n*-C₆, or *n*-C₇) and then separates the remaining fraction (maltenes) into three fractions. This is known as a SARA group-type analysis (Saturate hydrocarbons,

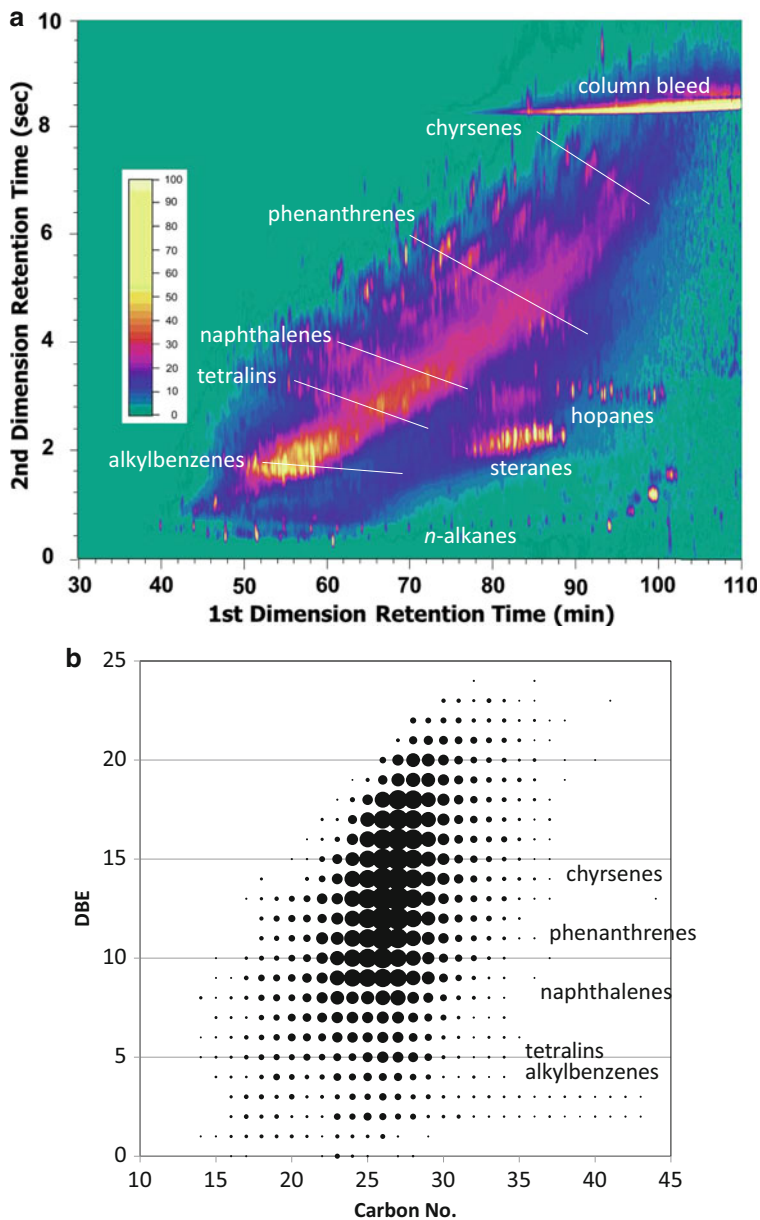


Fig. 1 Petroleomic analysis of an extract from hydrothermally altered sediment (30–33 cm) from Guaymas Basin: (a) GC x GC-FID and (b) +APPI-FT-ICR-MS. GC x GC can provide separation of isomers with the same elemental composition, but is limited to volatile compounds. +APPI ionizes compounds with double bonds and is insensitive to saturated compounds, but when combined with FT-ICR-MS, can characterize the full range of highly condensed aromatic species present. Experimental procedures and instrumental conditions are listed in Walters et al. (2015).

Aromatic hydrocarbons, Resins, and Asphaltenes). Resin is a historic term for the polar fraction containing heteroatomic (NSO) species. This separation can be done using gravimetric adsorption chromatography (ASTM D412409), a manual technique using silica gel open columns and a series of organic solvents with increasing polarity. The relative SARA proportions are determined by weighing the recovered fractions that then can be analyzed separately. Instrumented preparative LC methods provide greater reliability and throughput with the cut times established by chemical standards and monitored by refractive index and UV detectors (e.g., Grizzle and Sablotny 1986). HPLC with column switching offers finer separation of the chemical groups, such as separating sulfides from the other polars and separating aromatic hydrocarbons by ring number (Robbins 1998). Asphaltenes must be removed before LC separation as these compounds absorb tightly to the stationary phase and are difficult to recover. Schabron et al. (2010) developed the “asphaltene determinator,” an automatic method using HPLC that precipitates asphaltenes onto ground polytetrafluoroethylene from which they can be recovered with increasingly polar solvents into individual fractions. This system can be interfaced with a conventional HPLC separation to provide a fully automated SARA analysis (Boysen and Schabron 2013). Bissada et al. (2016) developed an alternative HPLC procedure for a completely automated SARA.

Analytical-scale LC determination of SARA can be done using universal detectors such as flame ionization (Pearson and Gharfeh 1986), dielectric constant (Hayes and Anderson 1988), or evaporative light scattering (Boysen and Schabron 2013; Bissada et al. 2016). Thin-layer chromatography (Iatroscan TLC-FID) offers an alternative to analytical LC. Separation of the four SARA fractions is made on rods composed of a stationary phase using a sequence of increasingly polar solvents and the developed fractions are detected by FID. The advantages of TLC-FID are that only a small quantity of sample is needed, multiple samples can be developed simultaneously, and the FID analysis is rapid. The disadvantages are that the detector response must be calibrated and variations in oil composition limit accuracy.

HPLC-MS is widely used to analyze polar lipids and other biochemical derivatives in low maturity sediments (e.g., Hopmans et al. 2000; Talbot et al. 2007; Pitcher et al. 2009; Zhu et al. 2013; Becker et al. 2013; Bataglion et al. 2015; Liu et al. 2017) (Fig. 2). However, the molecular complexity of petroleum greatly exceeds the resolution capacity of HPLC and even the improved resolution of UPLC (Ultrahigh performance LC) to separate individual petroleum polar components. Studies are restricted mostly to the polar compounds in relatively simple refined products such as jet fuels (Adams et al. 2013) and have targeted specific compounds, such as hydrocarbons (Gao et al. 2012), nitrogen-containing polycyclic aromatic (Lung and Liu 2015; da Cunha et al. 2016), or sulfur-aromatic compounds (da Silveira et al. 2016).

Porphyrins and naphthenic acids are two classes of polar petroleum compounds that have undergone petroleomic-type analysis using LC separations. Porphyrins were the first polar petroleum compounds to be characterized by HPLC-MS (Eglinton et al. 1985; Sundararaman 1985). These compounds yield diagnostic UV spectra that allow for easy detection and the development of enrichment procedures

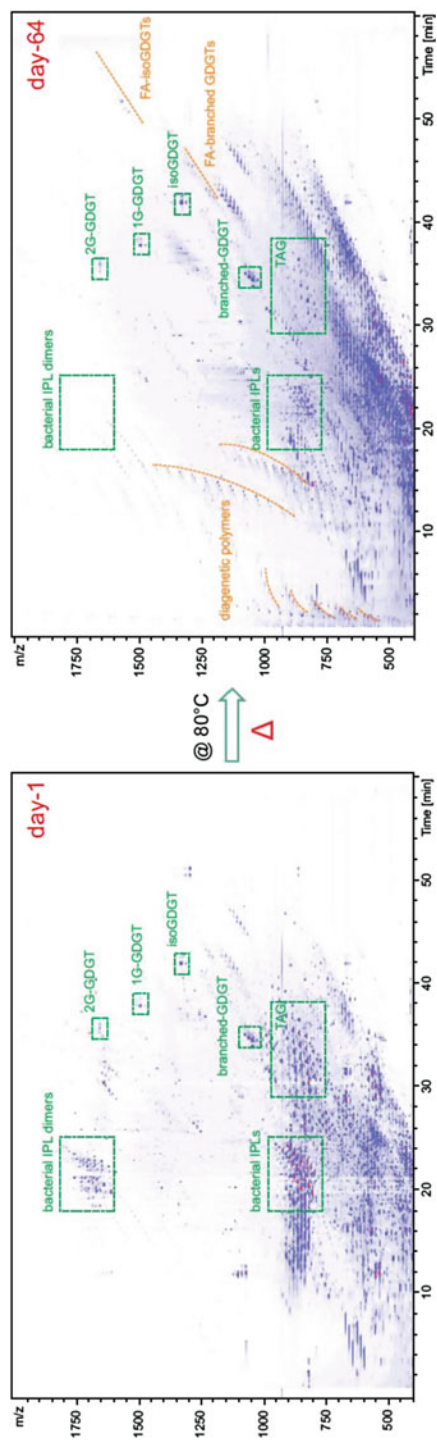


Fig. 2 HPLC-MS petroleomic analysis of extracts from artificially matured Salt Pond, MA sediments with molecular features, plotted by mass versus retention time. Many of the detected compounds are lipids that are initially seen in their biological state that have undergone a variety of diagenetic alterations into geochemical forms. (From Liu et al. 2017)

(e.g., Johnson and Freeman 1990; Magi et al. 2001). Once isolated, porphyrin fractions can be further separated and characterized by LC-MS (e.g., Rosell-Melé et al. 1996; Mawson et al. 2004; Espinosa et al. 2014; Woltering et al. 2016) or for their stable isotopic composition (e.g., Kashiyama et al. 2007; Higgins et al. 2009; Junium et al. 2015). Naphthenic acids are largely formed during the biodegradation of crude oil, and their impact on corrosion and fouling of facilities (Brocart et al. 2007; Simon et al. 2008; Smith and Rowland 2008) and on the environment around oil sand processing (Han et al. 2009; Wang et al. 2013; Huang et al. 2015) has spurred development of more advanced characterization methods using LC-MS.

Supercritical fluid chromatography (SFC) is a variant of normal phase LC where supercritical CO₂, often doped with polar solvents, is used as the mobile phase. Early applications of SFC to fossil fuels ranged from group-type separation and simulation distillation (Levy 1994; Thiebaut and Robert 1999) to molecular characterization of porphyrins (Khorassani and Taylor 1989); however, the instrumentation was difficult to maintain and operate. Recent technology advances have made SFC practical (Taylor 2010), and the technique now is routinely used in natural products and pharmaceutical research and has expanding applications in petroleum analysis (Poole 2017).

2.3 Ultrahigh-Resolution Mass Spectrometry

Advances in ultrahigh-resolution mass spectrometry ushered in the concept of petroleomics with its apparent ability to completely characterize the composition of petroleum in terms of elemental compositions. With ¹²C set exactly at 12 Daltons (Da), every other isotope of every element has a different mass defect (the difference between its exact mass and the nearest integer mass). No two mass defects are exactly alike or are integer multiples of each other. Consequently, a molecule's elemental composition may be determined directly from its exact mass. However, several combinations of the most abundant stable isotopes of CHNSO can have similar mass defects (e.g., ¹²CH₄ vs. O, $\Delta m = 36.4$ mD; ¹²CH₂ vs. N, $\Delta m = 12.6$ mDa; and ¹²C₃ vs. ³²SH₄, $\Delta m = 3.4$ Da). Consideration of rare isotope combinations (e.g., ¹H₃³²S¹³C vs. ¹²C₄ $\Delta m = 1.1$ mD) and the inclusion of other elements such as nickel (Qian et al. 2010) place additional demands on resolution. A practical minimum required mass resolution for petroleomics is ± 5 mDa, which is acceptable for assigning reasonable formulae to molecules containing only CHNSO that are <500 Da (Kim et al. 2006b). A mass resolution better than ± 100 μ Da is needed for truly unambiguous formulae assignments (Hsu 2012), about one-fifth the mass of an electron.

Commercial instruments used in petroleomic studies include systems with Time of Flight (ToF), Orbitrap, and FTICR mass spectrometers (Pomerantz et al. 2011; Xian et al. 2012; Zubarev and Makarov 2013). In general, ToF-MS systems provide high resolution spectra at fast acquisition speeds and are ideally suited for interfacing with GC and LC systems where rapid detection of eluting compounds is needed. The mass resolution of most ToF-MS is typically not sufficient to fully resolve ¹²C₃ from

$^{32}\text{SH}_4$ ($\Delta m = 3.4$ Da); however, the highest resolution ToF-MS instruments are capable of providing compositional information comparable to FT-ICR on routine samples (Klitzke et al. 2012). FT-ICR-MS systems provide the highest (ultrahigh) resolution possible but require longer acquisition time. Consequently, petroleomic samples are typically analyzed by direct infusion of whole oil or oil fractions rather than following chromatographic separation. The achievable mass resolution by FT-ICR depends on numerous factors related to instrument design. A magnetic field >7 T is required to achieve the needed resolution for petroleomics. Orbitrap MS sits in between with mass resolution that can approach FT-ICR-MS and acquisition speeds suitable for GC and LC detection. The highest performing Orbitraps are capable of providing the ultrahigh mass resolution needed for petroleomics (Zhurov et al. 2013). Further discussion of ultrahigh-resolution MS for petroleomics will be limited to FT-ICR-MS; however, continual improvements in other MS technologies offer new opportunities.

In order to be analyzed in a mass spectrometer, a molecule must be volatilized and ionized to possess a charge. No ionization technique is universally applicable to all compounds, and all have selective biases in their ionization efficiencies that can vary depending on sample matrix effects that can be modified by the selection of the solvent system. Electrospray ionization (ESI) (Qian et al. 2001a, b), atmospheric pressure chemical ionization (APCI), and atmospheric pressure photoionization (APPI) are the most commonly used ionization techniques in petroleomics (Pudenzi and Eberlin 2016). These techniques respond well to petroleum molecules containing aromatic moieties and/or heteroatoms that are <2000 Da, but are less efficient ionizing saturated hydrocarbons and large, low volatility asphaltene species. APPI is considered to be the least discriminating, while the ionization efficiency of ESI is highly dependent on chemical structure. For example, acids are particularly easy to ionize and a negative ESI mass spectrum of an oil may be dominated by their ions even though the absolute abundance of naphthenic acids is low. Various laser ionization methods also have been tested for petroleum analysis such as laser desorption (LDI) (Mennito and Qian 2013; Cho et al. 2014), atmospheric pressure laser (APLI) (Gaspar et al. 2012), matrix assisted laser desorption (MALDI) (Klein et al. 2006), and laser-induced acoustic desorption (LIAD) (Crawford et al. 2005; Pinkston et al. 2009). Many of the laser ionization studies are centered on overcoming the limitations on ionizing saturated hydrocarbons and asphaltenes. Classic techniques, such as field desorption/ionization (FD/FI) and electron ionization (EI) (Rodgers and Marshall 2007), and ambient ionization methods, such as direct analysis in real time (DART) (Romão et al. 2016) and desorption electrospray ionization (DESI) (Rummel et al. 2010; Wu et al. 2010), have also been applied in petroleum analysis.

Once the components in a whole crude oil or oil fraction are ionized, their masses may be measured. FT-ICR-MS has limited dynamic range and its performance depends on the number, relative abundance, and composition of the ions being detected (Marshall et al. 1998). Consequently, while ultrahigh-resolution petroleomic analysis may be conducted on a whole oil, the signal from minor components may be swamped. The best mass resolution and dynamic range can

be achieved using oil fractions that have been either separated by distillation and/or chromatographic preparation (e.g., Zhang et al. 2010; Oro and Lucy 2013; Podgorski et al. 2013; Sim et al. 2014), though care needs to be taken that the separation does not add contaminants (Oro et al. 2012). Another technique to improve dynamic range is spectral stitching, whereby small packets of ions spanning a limited mass range are sequentially introduced into the FT-ICR cell for individual analysis and then recombined into one mass spectrum (Gaspar and Schrader 2012).

Following detection, ion masses are assigned a chemical formula based on the mass defect. Even the best FT-ICR-MS instruments are not capable of providing unambiguous formulae above 500 Da just from accurate masses without additional information. Here, the molecular complexity of petroleum can actually help. Many compounds in petroleum are homologous series of a similar core structure and increasing degrees of alkylation. This allows for a form of “walking” internal calibration where the spectrum is divided into many adjoining segments and a separate calibration is applied to each based on ions from known homologous series (Savory et al. 2011).

Several data visualization methods are commonly used in ultrahigh-resolution MS petroleomics (Cho et al. 2015). With a list of accurate mass, molecular formula, and ion abundance for each detected ion, the composition is examined by comparing the distributions of related components. The most basic is a normalized distribution by chemical class. A chemical class is defined to include all species with an identical number of heteroatoms. Chemical classes may be comprised of species containing only varying number of one type of heteroatom (e.g., 1O, 2O, 3O, . . . , xO) or having two or more heteroatoms at fixed values (e.g., 1S1O, 1N1O, 2S1O, 2N1O, 1S2O, 1N2O, 1N1S, 4N1O1V). Pure hydrocarbons form their own chemical class with no heteroatoms.

The components within a single chemical class can be examined individually with normalized distributions of the sum of all components with identical Double Bond Equivalence (DBE). DBE is an expression of hydrogen deficiency and for molecules with the formula of $C_cH_nN_nO_oS_s$ can be calculated as: $DBE = c - \frac{h}{2} + \frac{n}{2} + 1$. An alternative to DBE is the Z-number as expressed in the molecular formula $C_cH_{2c+Z}N_nO_oS_s$. Distributions within a chemical class tend to decrease with increasing DBE, representing decreased relative abundance with an increasing degree of cyclization/aromatization and core size. The distributions are not usually smooth but exhibit increased abundances at fully aromatized core states. For example, the 1S species will be enriched at DBE = 3, 6, 9, and 12, diagnostic of thiophenes with one, two- and three-additional aromatic rings, respectively. Finally, the distribution of masses or carbon numbers within an individual chemical class for a specific DBE can be plotted. If a core structure is assumed, a distribution can be made representing the number of alkyl carbons.

The magnitude of the ultrahigh-resolution mass data makes it difficult to visualize the complete composition of a sample in a single figure. A common practice is to plot DBE versus mass and to project the abundance of individual species either by color coding or varying the symbol size. 3D graphics of these data, with abundance projected on the z-axis, are useful if the graph can be actively manipulated, but are

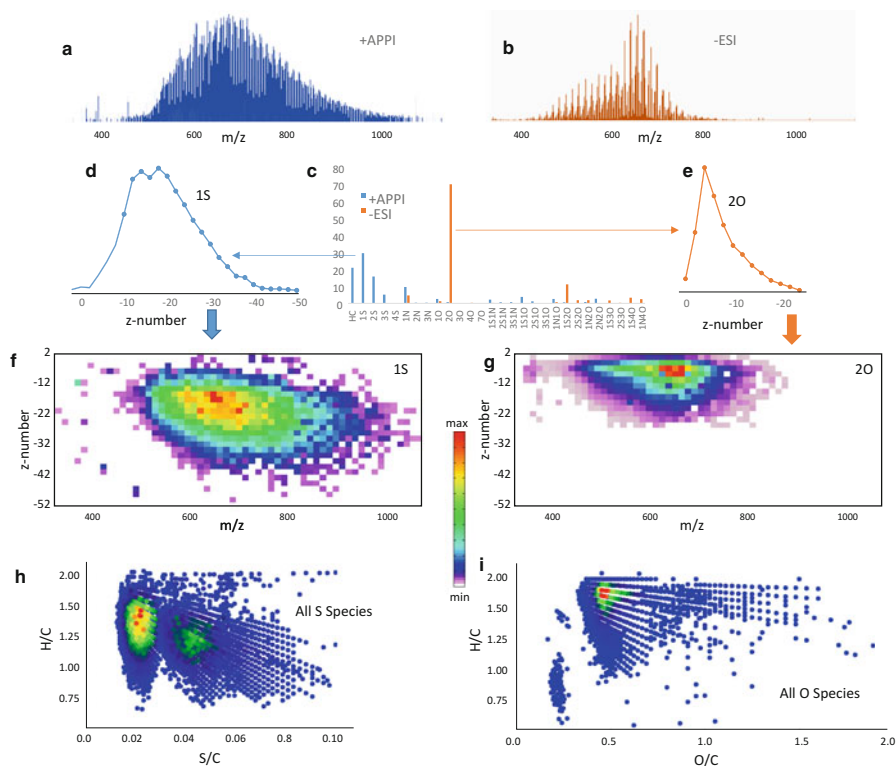


Fig. 3 Visualization of petroleomic analysis by FT-ICR-MS. Comparison of broad-band mass spectra obtained by (a) +APPI and (b) –ESI. Highly accurate mass resolution allow for the assignment of unambiguous elemental compositions. When summed by chemical class, the distributions derived from +APPI and –ESI (c) are highly influenced by ionization efficiency. The compounds within a chemical class can be visualized as summed distribution by Z-number (or DBE) (d, e), or as individual masses where the abundance is color-coded (f, g). Van Krevelen-type diagrams, plotting masses by various elemental ratios (e.g., H/C, S/C, O/C) and indicating relative abundance by color or symbol-size, are frequently used graphic displays (h, i)

of limited value as a static image. Multiple plots of mass versus DBE (with relative or absolute abundance optionally coded to color or symbol size) can be arranged in a montage (Fig. 3).

Kendrick mass defect plots also allow complete data from one or more chemical classes to be examined in a single graph (Hughes et al. 2001). The Kendrick mass defect assigns CH_2 to an integer mass of 14. Hence, a plot of the Kendrick nominal mass (x-axis) versus Kendrick mass defect (y-axis) will yield a flat line for a homologous series with the same DBE and heteroatoms that differ only by the addition of CH_2 . Increasing DBE within an individual chemical class results in greater Kendrick mass defect, producing a series of parallel lines. Again, the relative or normalized abundance can be projected using symbol color coding or size, or multiple chemical classes can be displayed on the same graph by color coding.

Van Krevelen-type plots are also used for visualizing processed FT-ICR-MS data. Originally developed to characterize coals using a plot of H/C versus O/C atomic ratios, van Krevelen-type plots provide broad insight into overall composition by plotting various permutation of H/C, O/C, N/C, S/C, and other atomic ratios (Kim et al. 2003).

Petroleomics is lagging other -omics when it comes to computational analysis of “big data,” and few tools beyond basic statistical methods, such as principle component analysis (Hur et al. 2010a), have been applied. Hur et al. (2010b) showed that Circos diagrams developed for genomics could be applied to petroleomics, but their utility is not obvious and few have adapted the method. Clearly, new methods are needed for computational analysis of postacquisition/processed ultrahigh-resolution data for use in property prediction and for the comparison of composition across multiple samples.

2.4 Modeling the Petroleome

A definitive petroleome is far beyond current analytical capabilities; however, the science has sufficiently advanced that it is now possible to construct a model of composition (MoC) using data from the techniques described above and complementary data from other analyses. The MoC is defined by a mixture of compounds of known or hypothesized molecular structures that approximates the petroleome that can then be correlated to physical properties or used as input for chemical reaction networks. Most petroleomics publications do not attempt to construct a MoC that approximates the petroleome; rather the data are discussed without molecular assignment or are assumed to be related to a molecular structure within a specific chemical class. For example, high molecular weight 2O species detected by –ESI-FT-ICR-MS have been assigned to naphthenic acids with biomarker structures based on the identified structures of low molecular weight species (e.g., Kim et al. 2005; Hughey et al. 2007) and species in the 4N1V1O, or 4N1Ni classes are assumed to be vanadyl and nickel porphyrins (e.g., Qian et al. 2008a, 2010; McKenna et al. 2009, 2014).

There are no defined procedures for constructing a MoC that approximates the petroleome. The volatile component of a crude oil is relatively easy to characterize by GC methods, and most hydrocarbons and many compounds with heteroatoms can be assigned to a specific molecular structure or to a structural family with variable positions of alkylation. Defining a MoC for the nonvolatile fraction is much more challenging. Qian et al. (2016) and Wang et al. (2018) describe one approach in defining a MoC for a vacuum resid. This procedure is very involved and requires a combination of advanced analytical practices. The procedure is:

- (a) Characterizing the volatile fraction by GC-FID, GC \times GC-FID, and/or GC \times GC-MS. Multiple methods may be used to best characterize gases (C₁-C₅), light liquid (C₃-C₁₅), and heavier liquids (C₁₀₊). Identification and quantification of all major and minor volatile hydrocarbons are possible using a GC \times GC equipped with dual FID and ToF-MS detectors (Wang et al. 2016).

- (b) Separating the resid sample into asphaltenes and deasphalted oils (DAO) using solvent precipitation.
- (c) Separating the (DAO) into chemical classes: saturates, aromatics, sulfides, and polars. The aromatic fraction is further separated into four aromatic ring class fractions that are dominated by 1-ring, 2-ring, 3-ring, and 4- and more ring aromatic hydrocarbons and neutral heteroatom species (e.g., thiophenic species).
- (d) Directly measuring bulk physical and chemical properties of the asphaltenes and individual DAO fractions. These routinely include CHNSO elemental, trace metal, ^1H - and ^{13}C -NMR, simulated distillation by high-temperature GC, and density. Supplemental analyses can include trace metals, and CNSO speciation by XPS or XANES.
- (e) Conducting ultrahigh-resolution mass spectrometry analysis of the individual asphaltenes and DAO fractions using a combination of ionization modes (ESI, APPI, APCI, and FD/FI) and scanning for positive and negative ions. This is necessary as different modes of ionization will yield different responses. For example, positive ion electrospray ionization preferentially ionizes basic nitrogen molecules, whereas negative ion electrospray ionization preferentially ionizes acidic molecules.
- (f) Determining an elemental formula for all masses based on the ions' mass defects.
- (g) Assigning molecular structures to each mass. This procedure involves separating the masses into their chemical class, determining the z-number (or DBE) distribution within a chemical class, assigning one or more core structures as representative within a specific chemical class and z-number, and finally a carbon number distribution with this subgroup.
- (h) Comparing the MoC derived from ultrahigh-resolution MS against measured bulk and molecular properties (step d). The MoC is then minimally adjusted to match the observed properties. This may involve artificially stretching the observed distribution to include higher molecular weight and/or higher z-number species that were not volatilized/ionized or issues involving dynamic range. The adjustment process is repeated until all data are reconciled.
- (i) Combining all MoCs obtained for the volatile and DOA fractions preserving mass balance.

Assignment of the distribution of the core structures relies on both indirect and direct evidence. The concept that petroleum comprises a continuum of homologous compounds allows for some core structures to be based on lower molecular weight species where the structure of individual components are more easily determined. The structure of higher molecular weight species, particularly asphaltenes, is contentious with researchers favoring models described either as "island," a single large PAH multi-ring core (e.g., Mullins et al. 2006; Mullins 2010), or "archipelago," linkages of multiple smaller PAH cores (e.g., Karimi et al. 2011; Silva et al. 2016). Insight into the nature of the distribution of "island" and "archipelago" core structures can be obtained from thermal decomposition (Alshareef et al. 2012), collision-induced dissociation (Qian et al. 2012), and NMR and other spectrometric techniques (Dutta Majumdar et al. 2016). In truth, both types of structures exist and must be included in construction of the MoCs (Borton et al. 2010; Podgorski et al. 2013).

3 Applications of Petroleomics

The goal of petroleomics is to model all physical properties and chemical reactivity from the *petroleome*, the complete molecular description. This goal is still far from being achieved. Petroleomic predictions of physical properties, such as density and boiling point distributions, can be made from a MoC as these values are known or can be modeled for each of the assigned molecular structures and combined in an additive manner. Prediction of viscosity or phase behavior is much more difficult as these properties depend on the interaction of molecules and theories for these interactions have not been developed fully within a MoC framework. Some studies have shown empirical relationships between polar/asphaltene compositions (e.g., Pomerantz et al. 2010), but these are not predictive based on a MoC.

Petroleomic predictions of many bulk chemical properties (e.g., elemental composition, carbon speciation as measured from ^{13}C -NMR, and sulfur speciation as measured by XPS or S-XANES) are inherent to a MoC. Some chemical properties, such as the total acid number (TAN), can be predicted (Qian et al. 2008b; Orrego-Ruiz et al. 2016). Typically, these and other bulk measurements are used to constrain and extrapolate data from ultrahigh-resolution MS and other molecular analyses to construct the MoC. In cases where the direct measurement of the bulk chemical composition and/or physical properties are not possible due to small sample size or the need for in situ spatial resolution, they can be predicted from a MoC derived from mass spectra obtained by LDI or DESI-MS (Wu et al. 2015).

Petroleomics has furthered our understanding of geologic processes. Hydrocarbons in crude oils and source rock extracts have been extensively studied and a well-developed biomarker toolkit has emerged for upstream applications (Peters et al. 2005). However, only a few polar species have been examined (e.g., petroporphyrins). Applications of petroleomic methods have provided new insights into thermal maturation (Hughes et al. 2004; Oldenburg et al. 2014), migration (Zhang et al. 2010; Liu et al. 2015), and reservoir alteration processes, such as biodegradation (Kim et al. 2005; Liao et al. 2012; Vaz et al. 2013) and thermochemical sulfate reduction (TSR) (Walters et al. 2011; Li et al. 2012). Most studies have correlated the petroleome of heteroatomic species with no defined or assumed molecular structure to conditions established by conventional hydrocarbon analyses. Several studies have combined GC \times GC and FT-ICR-MS analyses to characterize the complete petroleome and relate this to reservoir connectivity (Pomerantz et al. 2010) and TSR (Walters et al. 2015) or use the complete petroleome to construct models to predict reservoir oil quality (Walters et al. 2009).

In oil production, flow assurance is a major concern as both inorganic and organic precipitates can clog wellbores, top-side facilities, and pipelines, imposing significant economic impact. Petroleomic characterization of asphaltenes (Juyal et al. 2010) and calcium and sodium naphthenates (Mapolelo et al. 2009) is providing a new level of understanding that will help ameliorate these problems.

Environmental science was an early user of petroleomics (Petkewich 2003). Ultrahigh-resolution MS is readily applied toward oil spill source identification (Corilo et al. 2013; Bayona et al. 2015), investigations of natural attenuation,

photochemistry and weathering (Hegazi et al. 2012; Islam et al. 2013; McKenna et al. 2013; Chen et al. 2016; Vaughan et al. 2016), and remediation practices (Seidel et al. 2016). Waters stored in tailing ponds resulting from the processing of Athabasca oil sands are of environmental concern due to the potential toxicity of soluble naphthenic acids (Headley et al. 2016). Petroleomic methods have shown the diversity of these species (Barrow et al. 2004; Lengger et al. 2013) and have aided in tracing their detoxification (Yue et al. 2016).

Natural waters contain a complex mixture of dissolved organic matter (DOM) that has been challenging to characterize. Some of earliest ultrahigh-resolution MS studies examined the humic and fulvic acids dissolved in water (Kujawinski et al. 2002; Llewelyn et al. 2002; Kim et al. 2003). Sources of DOM (Koch et al. 2005; Sleighter and Hatcher 2008; Kujawinski et al. 2009) and their photochemical and biological transformations (Kujawinski et al. 2004; Kim et al. 2006a; Gonsior et al. 2009) can be distinguished. Petroleomic methods are now routinely used to characterize DOM in sediments (e.g., Schmidt et al. 2014; Seidel et al. 2014; McKee and Hatcher 2015) and soils (e.g., Ikeya et al. 2015; Guigue et al. 2016).

Petroleomics offers a major advance in optimizing refining processes including better characterization of product streams (Schaub et al. 2005; Wang et al. 2016), the effects of hydroprocessing (Kekäläinen et al. 2009), monitoring the effects of corrosion by organic acids (Dias et al. 2014), and the effective treatment of refinery waste waters (Li et al. 2015; Fang et al. 2016). Significant economic benefits emerge from being able model a refinery for optimal yields within specific quality limits. The efficiency of these process models is dependent on the accuracy of the petroleome of the feedstock crude and models of the thermal and catalyzed reactions involved in crude upgrading. Approximations using a limited number of compounds, groups of compounds, or pseudo-species can yield satisfactory results (e.g., Zhu et al. 2012), but petroleome-based models are now possible using an expansion of structure-oriented lumping (Jaffe et al. 2005; Alvarez-Majmutov et al. 2016).

4 Limitations and Future Research

Recent advances in analytical science have enabled the emergence of petroleomics, but the ultimate goals – the complete petroleome and the ability to predict all physical properties and chemical reactivity – are just in their embryonic state. For very light crude oils, we are confident that the petroleome can be described with sufficient detail that further detailed characterization would yield little additional value. However, for heavy crudes, a complete characterization of the petroleome falls well short of the necessary detail. Indeed, most of the nonvolatile petroleome remains uncharacterized at a molecular structural level. The level of specificity routinely conducted on pure hydrocarbons, such as biomarker analysis with full assignment of the configurations of stereogenic centers, is lacking for most non-GC amenable heteroatomic species. Improvements in LC-MS methods offer the promise of expanding such specificity to higher molecular weight species.

Asphaltenes, in particular, remain exceedingly difficult to characterize on a molecular level. These compounds may not be completely volatilized and ionized in the mass spectrometer's source and, hence, a portion, and possibly a very significant portion, of the asphaltenes may go undetected. Of those ions that are observed, the mass defect becomes increasingly uncertain with higher mass and even the best ultrahigh-resolution MS instruments cannot provide an unambiguous chemical formula. Even improving mass accuracy and resolution, the actual molecular structure of asphaltenes still would not be resolved without additional insight into the distribution and nature of the core structures. Direct visualization by atomic force microscopy (Schuler et al. 2015) may provide an avenue to resolve these issues.

Absolute quantification by mass spectrometry requires determining the response of a compound to the analytical conditions under which it is observed. There is no MS ionization or detection method that is universal and insensitive to the chemical structure of the analyte. Quantitation is possible if one has pure standards and internal standards, but careful study still is needed to minimize variable response of the compound within a changing chemical matrix as well as instrumental conditions. It is doubtful that pure standards representing the vast diversity of the petroleome will ever become available. Quantification even with pure standards will be exceedingly difficult as ionization efficiency and selectivity as well as FT-ICR-MS detector response is dependent not only on concentration of individual compounds but also on the composition and abundance of other components within the mixture. At present, the best quantitative determinations of a petroleome require ultrahigh-resolution mass spectra to be harmonized with data from ancillary analysis to yield a consistent mass. New, nonspecific ionization methods may alleviate some of these problems.

Recent developments in analytical techniques have enabled the establishment of the nascent field of petroleomics. Although petroleomics has its roots in decades of petroleum chemical characterization, its modern conception is less than 20 years old. We have now established a beachhead and are breaking out in applications. Much as genomics and other such -omics have revolutionized the biological sciences, petroleomics promises to do the same for geochemistry and petroleum chemical engineering.

References

- Adams RK, Zabarnick S, West ZJ, Striebich RC, Johnson DW (2013) Chemical analysis of jet fuel polar, heteroatomic species via high-performance liquid chromatography with electrospray ionization–mass spectrometric detection. *Energy Fuels* 27:2390–2398
- Alshareef AH, Scherer A, Tan X, Azyat K, Stryker JM, Tykwinski RR, Gray MR (2012) Effect of chemical structure on the cracking and coking of archipelago model compounds representative of asphaltenes. *Energy Fuels* 26:1828–1843
- Altgelt KH, Boduszynski MM (1993) *Composition and analysis of heavy petroleum fractions*. CRC Press, Boca Raton. 512 pp
- Alvarez-Majmutov A, Chen J, Gieleciak R (2016) Molecular-level modeling and simulation of vacuum gas oil hydrocracking. *Energy Fuels* 30:138–148
- Araújo BQ, Azevedo DA (2016) Uncommon steranes in Brazilian marginal crude oils: Dinoflagellate molecular fossils in the Sergipe-Alagoas Basin, Brazil. *Org Geochem* 99:38–52

- Barrow MP, Headley JV, Peru KM, Derrick PJ (2004) Fourier transform ion cyclotron resonance mass spectrometry of principal components in oilsands naphthenic acids. *J Chromatogr A* 1058:51–59
- Batagliion GA, Meurer E, de Albergaria-Barbosa ACR, Bicego MC, Weber RR, Eberlin MN (2015) Determination of geochemically important sterols and triterpenols in sediments using ultrahigh-performance liquid chromatography tandem mass spectrometry (UHPLC–MS/MS). *Anal Chem* 87:7771–7778
- Bayona JM, Domínguez C, Albaigés J (2015) Analytical developments for oil spill fingerprinting. *Trends Environ Anal Chem* 5:26–34
- Becker KW, Lipp JS, Zhu C, Liu X-L, Hinrichs K-U (2013) An improved method for the analysis of archaeal and bacterial ether core lipids. *Org Geochem* 61:34–44
- Bertoncini F, Courtiade-Tholance M, Thiebaut D (2013) Gas chromatography and 2D-gas chromatography for petroleum industry. The race for selectivity. Editions Technip, Paris. 368 pp
- Bissada KK, Tan J, Szymczyk E, Darnell M, Mei M (2016) Group-type characterization of crude oil and bitumen. Part I: enhanced separation and quantification of saturates, aromatics, resins and asphaltenes (SARA). *Org Geochem* 95:21–28
- Boduszynski MM (1988) Composition of heavy petroleums. 2. Molecular characterization. *Energy Fuels* 2:597–613
- Borton D, Pinkston DS, Hurt MR, Tan X, Azyat K, Tykwinski R, Gray M, Qian K, Kenttämää HI (2010) Molecular structures of asphaltenes based on the dissociation reactions of their ions in mass spectrometry. *Energy Fuels* 24:5548–5559
- Boysen RB, Schabron JF (2013) The automated asphaltene determinator coupled with saturates, aromatics, and resins separation for petroleum residua characterization. *Energy Fuels* 27:654–6661
- Bray EE, Evans ED (1961) Distribution of *n*-paraffins as a clue to recognition of source beds. *Geochim Cosmochim Acta* 22:2–15
- Brocart B, Bourrel M, Hurtevent C, Volle J-L, Escoffier B (2007) ARN-type naphthenic acids in crudes: analytical detection and physical properties. *J Dispers Sci Technol* 28:331–337
- Chen H, Hou A, Corilo YE, Lin Q, Lu J, Mendelssohn IA, Zhang R, Rodgers RP, McKenna AM (2016) 4 years after the Deepwater Horizon spill: molecular transformation of Macondo well oil in Louisiana salt marsh sediments revealed by FT-ICR mass spectrometry. *Environ Sci Technol* 50:9061–9069
- Cho Y, Witt M, Jin JM, Kim YH, Nho N-S, Kim S (2014) Evaluation of laser desorption ionization coupled to Fourier transform ion cyclotron resonance mass spectrometry to study metalloporphyrin complexes. *Energy Fuels* 28:6699–6706
- Cho Y, Ahmed A, Islam A, Kim S (2015) Developments in FT-ICR MS instrumentation, ionization techniques, and data interpretation methods for petroleomics. *Mass Spectrom Rev* 34:248–263
- Corilo YE, Podgorski DC, McKenna AM, Lemkau KL, Reddy CM, Marshall AG, Rodgers RP (2013) Oil spill source identification by principal component analysis of electrospray ionization Fourier transform ion cyclotron resonance mass spectra. *Anal Chem* 85:9064–9069
- Crawford KE, Campbell JL, Fiddler MN, Duan P, Qian K, Gorbaty ML, Kenttämää HI (2005) Laser-induced acoustic desorption/Fourier transform ion cyclotron resonance mass spectrometry for petroleum distillate analysis. *Anal Chem* 77:7916–7923
- da Cunha ALMC, Sá A, Mello SC, Vásquez-Castro YE, Luna AS, Aucelio RQ (2016) Determination of nitrogen-containing polycyclic aromatic compounds in diesel and gas oil by reverse-phase high performance liquid chromatography using introduction of sample as detergentless microemulsion. *Fuel* 176:119–129
- da Silveira GD, Faccin H, Claussen L, Goularte RB, Nascimento PC, Bohrer D, Cravo M, Leite LFM, de Carvalho LM (2016) A liquid chromatography–atmospheric pressure photoionization tandem mass spectrometric method for the determination of organosulfur compounds in petroleum asphalt cements. *J Chromatogr A* 1457:29–40
- De la Rue W, Miller H (1856) Chemical examination of Burmese naphtha or Rangoon tar. *Proc R Soc Lond* 8:221–228
- Dias HP, Pereira TMC, Vanini G, Dixini PV, Celante VG, Castro EVR, Vaz BG, Fleming FP, Gomes AO, AQUIJE GMFV, Romão W (2014) Monitoring the degradation and the corrosion of

- naphthenic acids by electrospray ionization Fourier transform ion cyclotron resonance mass spectrometry and atomic force microscopy. *Fuel* 126:85–95
- Dijkmans T, Van Geem KM, Djokic MR, Marin GB (2014) Combined comprehensive two-dimensional gas chromatography analysis of polyaromatic hydrocarbons/polyaromatic sulfur-containing hydrocarbons (PAH/PASH) in complex matrices. *Ind Eng Chem Res* 53:15436–15446
- Dijkmans T, Djokic MR, Van Geem KM, Marin GB (2015) Comprehensive compositional analysis of sulfur and nitrogen containing compounds in shale oil using GC × GC – FID/SCD/NCD/TOF-MS. *Fuel* 140:398–406
- Dutriez T, Borrás J, Courtiade M, Thiébaud D, Dulot H, Bertoincini F, Hennion M-C (2011) Challenge in the speciation of nitrogen-containing compounds in heavy petroleum fractions by high temperature comprehensive two-dimensional gas chromatography. *J Chromatogr A* 1218:3190–3199
- Dutta Majumdar R, Bake KD, Ratna Y, Pomerantz AE, Mullins OC, Gerken M, Hazendonk P (2016) Single-core PAHs in petroleum- and coal-derived asphaltene: size and distribution from solid-state NMR spectroscopy and optical absorption measurements. *Energy Fuels* 30:6892–6906
- Eglinton G, Hamilton RJ, Hodges R, Raphael RA (1959) Gas-liquid chromatography of natural products and their derivatives. *Chem Ind (Lond)* 1959: 955–957
- Eglinton G, Maxwell JR, Evershed RP, Barwise AJG (1985) Red pigments in petroleum exploration. *Interdiscip Sci Rev* 10:222–236
- Eiserbeck C, Nelson RK, Grice K, Curiale J, Reddy CM, Raiteri P (2011) Separation of 18 α (H)-, 18 β (H)-oleanane and lupane by comprehensive two-dimensional gas chromatography. *J Chromatogr A* 1218:5549–5553
- Eiserbeck C, Nelson RK, Reddy CM, Grice K (2015) Advances in comprehensive two-dimensional gas chromatography (GC × GC). In: Grice K (ed) *Principles and practice of analytical techniques in geosciences*. The Royal Society of Chemistry, Cambridge, pp 324–365
- Espinosa M, Pacheco US, Leyte F, Ocampo R (2014) Separation and identification of porphyrin biomarkers from a heavy crude oil Zaap-1 offshore well, Sonda de Campeche, México. *J Porphyrins Phthalocyanines* 18:542–551
- Fang Z, He C, Li Y, Chung KH, Xu C, Shi Q (2016) Fractionation and characterization of dissolved organic matter (DOM) in refinery wastewater by revised phase retention and ion-exchange adsorption solid phase extraction followed by ESI FT-ICR MS. *Talanta* 162:466–473
- Gao J, Owen BC, Borton DJ, Jin Z, Kenttämäa HI (2012) HPLC/APCI mass spectrometry of saturated and unsaturated hydrocarbons by using hydrocarbon solvents as the APCI reagent and HPLC mobile phase. *J Am Soc Mass Spectrom* 23:816–822
- Gaspar A, Schrader W (2012) Expanding the data depth for the analysis of complex crude oil samples by Fourier transform ion cyclotron resonance mass spectrometry using the spectral stitching method. *Rapid Commun Mass Spectrom* 26:1047–1052
- Gaspar A, Zellermann E, Lababidi S, Reece J, Schrader W (2012) Impact of different ionization methods on the molecular assignments of asphaltene by FT-ICR mass spectrometry. *Anal Chem* 84:5257–5267
- Gonsior M, Peake BM, Cooper WT, Podgorski D, D'Andrilli J, Cooper WJ (2009) Photochemically induced changes in dissolved organic matter identified by ultrahigh-resolution Fourier transform ion cyclotron resonance mass spectrometry. *Environ Sci Technol* 43:698–703
- Grizzle PL, Sablotny DM (1986) Automated liquid-chromatographic compound class group-type separation of crude oils and bitumens using chemically bonded aminosilane. *Anal Chem* 58:2389–2396
- Grob RL, Barry EF (2004) *Modern practice of gas chromatography*, 4th edn. Wiley, Hoboken. 1064 pp
- Guigue J, Harir M, Mathieu O, Lucio M, Ranjard L, Lévêque J, Schmitt-Kopplin P (2016) Ultrahigh-resolution FT-ICR mass spectrometry for molecular characterisation of pressurised hot water-extractable organic matter in soils. *Biogeochemistry* 128:307–326
- Han X, MacKinnon MD, Martin JW (2009) Estimating the in situ biodegradation of naphthenic acids in oil sands process waters by HPLC/HRMS. *Chemosphere* 76:63–70

- Hayes PC, Anderson SD (1988) Paraffins, olefins, naphthenes and aromatics analysis of selected hydrocarbon distillates using on-line column switching high-performance liquid chromatography with dielectric constant detection. *J Chromatogr A* 437:365–377
- Headley JV, Peru KM, Barrow MP (2016) Advances in mass spectrometric characterization of naphthenic acids fraction compounds in oil sands environmental samples and crude oil – a review. *Mass Spectrom Rev* 35:311–328
- Hegazi AH, Fathalla EM, Panda SK, Schrader W, Andersson JT (2012) High-molecular weight sulfur-containing aromatics refractory to weathering as determined by Fourier transform ion cyclotron resonance mass spectrometry. *Chemosphere* 89:205–212
- Higgins MB, Robinson RS, Casciotti KL, McIlvin MR, Pearson A (2009) A method for determining the nitrogen isotopic composition of porphyrins. *Anal Chem* 81:184–192
- Hopmans EC, Schouten S, Pancost RD, van der Meer MTJ, Singhe Damsté JS (2000) Analysis of intact tetraether lipids in archaeal cell material and sediments by high performance liquid chromatography/atmospheric pressure chemical ionization mass spectrometry. *Rapid Commun Mass Spectrom* 14:585–589
- Hsu CS (2012) Mass resolving power for molecular formula determination. *Energy Fuels* 26:1169–1177
- Hsu CS, Drinkwater D (2001) Chapter 3. GC/MS in the petroleum industry. In: Niessen WMA (ed) *Current practice in gas chromatography-mass spectrometry*. Dekker Marcel, New-York, pp 55–94
- Hsu CS, Hendrickson CL, Rodgers RP, McKenna AM, Marshall AG (2011) Petroleomics: advanced molecular probe for petroleum heavy ends. *J Mass Spectrom* 46:337–343
- Huang R, McPhedran KN, Gamal El-Din M (2015) Ultra performance liquid chromatography ion mobility time-of-flight mass spectrometry characterization of naphthenic acids species from oil sands process-affected water. *Environ Sci Technol* 49:11737–11745
- Hughey CA, Hendrickson CL, Rodgers RP, Marshall AG (2001) Kendrick mass defect spectrum: a compact visual analysis for ultra-high resolution broadband mass spectra. *Anal Chem* 73:4676–4681
- Hughey CA, Rodgers RP, Marshall AG (2002) Resolution of 11,000 compositionally distinct components in a single electrospray ionization Fourier transform ion cyclotron resonance mass spectrum of crude oil. *Anal Chem* 36:4145–4149
- Hughey CA, Rodgers RP, Marshall AG, Walters CC, Qian K, Mankiewicz P (2004) Acidic and neutral polar NSO compounds in Smackover oils of different thermal maturity revealed by electrospray high field Fourier transform ion cyclotron resonance mass spectrometry. *Org Geochem* 35:863–880
- Hughey CA, Galasso SA, Zumberge JE (2007) Detailed compositional comparison of acidic NSO compounds in biodegraded reservoir and surface crude oils by negative ion electrospray Fourier transform ion cyclotron resonance mass spectrometry. *Fuel* 86:758–768
- Hur M, Yeo I, Kim E, No M-h, Koh J, Cho YJ, Lee JW, Kim S (2010a) Correlation of FT-ICR mass spectra with the chemical and physical properties of associated crude oils. *Energy Fuels* 24:5524–5532
- Hur M, Yeo I, Park E, Kim YH, Yoo J, Kim E, No M-h, Koh J, Kim S (2010b) Combination of statistical methods and Fourier transform ion cyclotron resonance mass spectrometry for more comprehensive, molecular-level interpretations of petroleum samples. *Anal Chem* 82:211–218
- Ikeya K, Sleighter RL, Hatcher PG, Watanabe A (2015) Characterization of the chemical composition of soil humic acids using Fourier transform ion cyclotron resonance mass spectrometry. *Geochim Cosmochim Acta* 153:169–182
- Islam A, Cho Y, Yim UH, Shim WJ, Kim YH, Kim S (2013) The comparison of weathered oil spills at two stages and photo-degraded oil at one stage at the molecular level by a combination of SARA fractionation and FT-ICR MS. *J Hazard Mater* 263(Part 2):404–411
- Jaffe SB, Freund H, Olmstead WN (2005) Extension of structure-oriented lumping to vacuum residua. *Ind Eng Chem Res* 44:9840–9852
- Johnson AL, Freeman DH (1990) Systematic preparative methods for petroporphyrin purification. *Energy Fuels* 4:695–699

- Junium CK, Freeman KH, Arthur MA (2015) Controls on the stratigraphic distribution and nitrogen isotopic composition of zinc, vanadyl and free base porphyrins through Oceanic Anoxic Event 2 at Demerara Rise. *Org Geochem* 80:60–71
- Juyal P, Yen AT, Rodgers RP, Allenson S, Wang J, Creek J (2010) Compositional variations between precipitated and organic solid deposition control (OSDC) asphaltenes and the effect of inhibitors on deposition by electrospray ionization Fourier transform ion cyclotron resonance (FT-ICR) mass spectrometry. *Energy Fuels* 24:2320–2326
- Karimi A, Qian K, Olmstead WN, Freund H, Yung C, Gray MR (2011) Quantitative evidence for bridged structures in asphaltenes by thin film pyrolysis. *Energy Fuels* 25:3581–3589
- Kashiyama Y, Kitazato H, Ohkouchi N (2007) An improved method for isolation and purification of sedimentary porphyrins by high-performance liquid chromatography for compound-specific isotopic analysis. *J Chromatogr A* 1138:73–83
- Kekäläinen T, Pakarinen JMH, Wickström K, Vainiotalo P (2009) Compositional study of polar species in untreated and hydrotreated gas oil samples by electrospray ionization Fourier transform ion cyclotron resonance mass spectrometry (ESI FTIC-MS). *Energy Fuels* 23:6055–6061
- Khorassani MA, Taylor LT (1989) Application of sub- and supercritical fluid chromatography to vanadium and nickel porphyrins. *J Chromatogr Sci* 27:329–333
- Kim S, Kramer RW, Hatcher PG (2003) Graphical method for analysis of ultrahigh-resolution broadband mass spectra of natural organic matter, the van Krevelen diagram. *Anal Chem* 75:5336–5344
- Kim S, Stanford LA, Rodgers RP, Marshall AG, Walters CC, Qian K, Wenger LM, Mankiewicz P (2005) Microbial alteration of the acidic and neutral polar NSO compounds revealed by Fourier transform ion cyclotron resonance mass spectrometry. *Org Geochem* 36:1117–1134
- Kim S, Kaplan LA, Hatcher PG (2006a) Biodegradable dissolved organic matter in a temperate and a tropical stream determined from ultra-high resolution mass spectrometry. *Limnol Oceanogr* 51:1054–1063
- Kim S, Rodgers RP, Marshall AG (2006b) Truly “exact” mass: elemental composition can be determined uniquely from molecular mass measurement at ~0.1 mDa accuracy for molecules up to ~500 Da. *Int J Mass Spectrom* 251:260–265
- Klein GC, Angström A, Rodgers RP, Marshall AG (2006) Use of saturates/aromatics/resins/asphaltenes (SARA) fractionation to determine matrix effects in crude oil analysis by electrospray ionization Fourier transform ion cyclotron resonance mass spectrometry. *Energy Fuels* 20:668–672
- Klitzke CF, Corilo YE, Siek K, Binkley J, Patrick J, Eberlin MN (2012) Petroleomics by ultrahigh-resolution time-of-flight mass spectrometry. *Energy Fuels* 26:5787–5794
- Koch BP, Witt M, Engbrodt R, Dittmar T, Kattner G (2005) Molecular formulae of marine and terrigenous dissolved organic matter detected by electrospray ionization Fourier transform ion cyclotron resonance mass spectrometry. *Geochim Cosmochim Acta* 69:3299–3308
- Kujawinski EB, Hatcher PG, Freitas MA (2002) High-resolution Fourier transform ion cyclotron resonance mass spectrometry of humic and fulvic acids: improvements and comparisons. *Anal Chem* 74:413–419
- Kujawinski EB, Del Vecchio R, Blough NV, Klein GC, Marshall AG (2004) Probing molecular-level transformations of dissolved organic matter: insights on photochemical degradation and protozoan modification of DOM from electrospray ionization Fourier transform ion cyclotron resonance mass spectrometry. *Mar Chem* 92:23–37
- Kujawinski EB, Longnecker K, Blough NV, Del Vecchio R, Finlay L, Kitner JB, Giovannoni SJ (2009) Identification of possible source markers in marine dissolved organic matter using ultrahigh-resolution mass spectrometry. *Geochim Cosmochim Acta* 73:4384–4399
- Lenger SK, Scarlett AG, West CE, Rowland SJ (2013) Diamondoid diacids (‘O4’ species) in oil sands process-affected water. *Rapid Commun Mass Spectrom* 27:2648–2654
- Levy JM (1994) Fossil fuel applications of SFC and SFE: a review. *J High Resolut Chromatogr* 17:212–216
- Li S, Shi Q, Pang X, Zhang B, Zhang H (2012) Origin of the unusually high dibenzothiophene oils in Tazhong-4 Oilfield of Tarim Basin and its implication in deep petroleum exploration. *Org Geochem* 48:56–80

- Li Y, Xu C, Chung KH, Shi Q (2015) Molecular characterization of dissolved organic matter and its subfractions in refinery process water by Fourier transform ion cyclotron resonance mass spectrometry. *Energy Fuels* 29:2923–2930
- Liao Y, Shi Q, Hsu CS, Pan Y, Zhang Y (2012) Distribution of acids and nitrogen-containing compounds in biodegraded oils of the Liaohe Basin by negative ion ESI FT-ICR MS. *Org Geochem* 47:51–65
- Liu P, Li M, Jiang Q, Cao T, Sun Y (2015) Effect of secondary oil migration distance on composition of acidic NSO compounds in crude oils determined by negative-ion electrospray Fourier transform ion cyclotron resonance mass spectrometry. *Org Geochem* 78:23–31
- Liu X-L, Summons RE, Higgins MB, Walters CC (2017) Esterified glycerol dialkyl glycerol tetraethers derived from low temperature thermal diagenesis of microbial lipids. In: 28th international meeting on organic geochemistry, p 98
- Llewelyn JM, Landing WM, Marshall AG, Cooper WT (2002) Electrospray ionization Fourier transform ion cyclotron resonance mass spectrometry of dissolved organic phosphorus species in a treatment wetland after selective isolation and concentration. *Anal Chem* 74:600–606
- Lung S-CC, Liu C-H (2015) Fast analysis of 29 polycyclic aromatic hydrocarbons (PAHs) and nitro-PAHs with ultra-high performance liquid chromatography-atmospheric pressure photoionization-tandem mass spectrometry. *Sci Rep* 5:12992
- Magi E, Ianni C, Rivaro P, Frache R (2001) Determination of porphyrins and metalloporphyrins using liquid chromatography-diode array detection and mass spectrometry. *J Chromatogr A* 905:141–149
- Mapolelo MM, Stanford LA, Rodgers RP, Yen AT, Debord JD, Asomaning S, Marshall AG (2009) Chemical speciation of calcium and sodium naphthenate deposits by electrospray ionization FT-ICR mass spectrometry. *Energy Fuels* 23:349–355
- Marriott PJ, Chin S-T, Maikunthod B, Schmarr H-G, Bieri S (2012) Multidimensional gas chromatography. *TrAC Trends Anal Chem* 34:1–21
- Marshall AG, Rodgers RP (2008) Petroleomics: chemistry of the underworld. *Proc Natl Acad Sci* 105:18090–18095
- Marshall AG, Hendrickson CL, Jackson GS (1998) Fourier transform ion cyclotron resonance mass spectrometry: a primer. *Mass Spectrom Rev* 17:1–35
- Mawson DH, Walker JS, Keely BJ (2004) Variations in the distributions of sedimentary alkyl porphyrins in the Mulhouse basin in response to changing environmental conditions. *Org Geochem* 35:1229–1241
- McDonald GR (2011) Georgius Agricola and the invention of petroleum. *Bibl Hum Renaiss* 73:351–364
- McKee GA, Hatcher PG (2015) A new approach for molecular characterization of sediments with Fourier transform ion cyclotron resonance mass spectrometry: extraction optimisation. *Org Geochem* 85:22–31
- McKenna AM, Purcell JM, Rodgers RP, Marshall AG (2009) Identification of vanadyl porphyrins in a heavy crude oil and raw asphaltene by atmospheric pressure photoionization Fourier transform ion cyclotron resonance (FT-ICR) mass spectrometry. *Energy Fuels* 23:2122–2128
- McKenna AM, Nelson RK, Reddy CM, Savory JJ, Kaiser NK, Fitzsimmons JE, Marshall AG, Rodgers RP (2013) Expansion of the analytical window for oil spill characterization by ultrahigh-resolution mass spectrometry: beyond gas chromatography. *Environ Sci Technol* 47:7530–7539
- McKenna AM, Williams JT, Putman JC, Aeppli C, Reddy CM, Valentine DL, Lemkau KL, Kellermann MY, Savory JJ, Kaiser NK, Marshall AG, Rodgers RP (2014) Unprecedented ultrahigh-resolution FT-ICR mass spectrometry and parts-per-billion mass accuracy enable direct characterization of nickel and vanadyl porphyrins in petroleum from natural seeps. *Energy Fuels* 28:2454–2464
- Mennito AS, Qian K (2013) Characterization of heavy petroleum saturates by laser desorption silver cationization and Fourier transform ion cyclotron resonance mass spectrometry. *Energy Fuels* 27:7348–7353
- Meredith W, Kelland S-J, Jones DM (2000) Influence of biodegradation on crude oil acidity and carboxylic acid composition. *Org Geochem* 31:1059–1073

- Mogollón NGS, Prata PS, dos Reis JZ, Neto EVdS, Augusto F (2016) Characterization of crude oil biomarkers using comprehensive two-dimensional gas chromatography coupled to tandem mass spectrometry. *J Sep Sci* 39:3384–3391
- Mullins OC (2010) The modified Yen model. *Energy Fuels* 24:2179–2207
- Mullins OC, Sheu EY, Hammami A, Marshall AG (2006) *Asphaltenes, heavy oils, and petroleomics*. Springer-Verlag New York, 670 pp
- Nelson RK, Aepli C, Samuel J, Chen H, de Oliveira AHB, Eiserbeck C, Frysinger GS, Gaines RB, Grice K, Gros J, Hall GJ, Koolen HHF, Lemkau KL, McKenna AM, Reddy CM, Rodgers RP, Swarthout RF, Valentine DL, White HK (2016) Applications of comprehensive two-dimensional gas chromatography (GC × GC) in studying the source, transport, and fate of petroleum hydrocarbons in the environment. In: Stout SA, Wang Z (eds) *Standard handbook oil spill environmental forensics*, 2nd edn. Academic, Boston, pp 399–448
- Nizio KD, McGinitie TM, Harynyuk JJ (2012) Comprehensive multidimensional separations for the analysis of petroleum. *J Chromatogr A* 1255:12–23
- Oldenburg TBP, Brown M, Bennett B, Larter SR (2014) The impact of thermal maturity level on the composition of crude oils, assessed using ultra-high resolution mass spectrometry. *Org Geochem* 75:151–168
- Oro NE, Lucy CA (2013) Analysis of the nitrogen content of distillate cut gas oils and treated heavy gas oils using normal phase HPLC, fraction collection and petroleomic FT-ICR MS data. *Energy Fuels* 27:35–45
- Oro NE, Whittall RM, Lucy CA (2012) Sample handling and contamination encountered when coupling offline normal phase high performance liquid chromatography fraction collection of petroleum samples to Fourier transform ion cyclotron resonance mass spectrometry. *Anal Chim Acta* 741:70–77
- Orrego-Ruiz JA, Gomez-Escudero A, Rojas-Ruiz FA (2016) Combination of negative electrospray ionization and positive atmospheric pressure photoionization Fourier transform ion cyclotron resonance mass spectrometry as a quantitative approach of acid species in crude oils. *Energy Fuels* 30:8209–8215
- Pearson CD, Gharfeh SG (1986) Automated high-performance liquid chromatography determination of hydrocarbon types in crude oil residues using a flame ionization detector. *Anal Chem* 58:307–311
- Peters KE, Walters CC, Moldowan JM (2005) *The biomarker guide*, vol 1 & 2, 2nd edn. Cambridge University Press, New York. 1155 pp
- Petkewich R (2003) “Cracking” the structure of petroleum. Sophisticated mass spectrometry method may fingerprint crude oil. *Environ Sci Technol* 37:206A–207A
- Pinkston DS, Duan P, Gallardo VA, Habicht SC, Tan X, Qian K, Gray M, Müllen K, Kenttämäa HI (2009) Analysis of asphaltenes and asphaltene model compounds by laser-induced acoustic desorption/Fourier transform ion cyclotron resonance mass spectrometry. *Energy Fuels* 23:5564–5570
- Pitcher A, Hopmans EC, Schouten S, Sinninghe Damsté JS (2009) Separation of core and intact polar archaeal tetraether lipids using silica columns: insights into living and fossil biomass contributions. *Org Geochem* 40:12–19
- Podgorski DC, Corilo YE, Nyadong L, Lobodin VV, Bythell BJ, Robbins WK, McKenna AM, Marshall AG, Rodgers RP (2013) Heavy petroleum composition. 5. Compositional and structural continuum of petroleum revealed. *Energy Fuels* 27:1268–1276
- Pomerantz AE, Ventura GT, McKenna AM, Cañas JA, Auman J, Koerner K, Curry D, Nelson RK, Reddy CM, Rodgers RP, Marshall AG, Peters KE, Mullins OC (2010) Combining biomarker and bulk compositional gradient analysis to assess reservoir connectivity. *Org Geochem* 41:812–821
- Pomerantz AE, Mullins OC, Paul G, Ruzicka J, Sanders M (2011) Orbitrap mass spectrometry: a proposal for routine analysis of non-volatile components of petroleum. *Energy Fuels* 25:3077–3082
- Poole CF (ed) (2017) *Supercritical fluid chromatograph*. Elsevier, Amsterdam. 560 pp
- Pudenzi MA, Eberlin MN (2016) Assessing relative electrospray ionization, atmospheric pressure photoionization, atmospheric pressure chemical ionization, and atmospheric pressure photo-

- and chemical ionization efficiencies in mass spectrometry petroleomic analysis via pools and pairs of selected polar compound standards. *Energy Fuels* 30:7125–7133
- Qian K, Robbins WK, Hughey CA, Cooper HJ, Rodgers RP, Marshall AG (2001a) Resolution and identification of elemental compositions for more than 3000 crude acids in heavy petroleum by negative-ion microelectrospray high-field Fourier transform ion cyclotron resonance mass spectrometry. *Energy Fuels* 15:1505–1511
- Qian K, Rodgers RP, Hendrickson CL, Emmett MR, Marshall AG (2001b) Reading chemical fine print: resolution and identification of 3000 nitrogen-containing aromatic compounds from a single electrospray ionization Fourier transform ion cyclotron resonance mass spectrum of heavy petroleum crude oil. *Energy Fuels* 15:492–498
- Qian K, Mennito AS, Edwards KE, Ferrughelli DT (2008a) Observation of vanadyl porphyrins and sulfur-containing vanadyl porphyrins in a petroleum asphaltene by atmospheric pressure photoionization Fourier transform ion cyclotron resonance mass spectrometry. *Rapid Commun Mass Spectrom* 22:2153–2160
- Qian K, Edwards KE, Dechert GJ, Jaffe SB, Green LA, Olmstead WN (2008b) Measurement of total acid number (TAN) and TAN boiling point distribution in petroleum products by electrospray ionization mass spectrometry. *Anal Chem* 80:849–855
- Qian K, Edwards KE, Mennito AS, Walters CC, Kushnerick JD (2010) Enrichment, resolution, and identification of nickel porphyrins in petroleum asphaltene by cyclograph separation and atmospheric pressure photoionization Fourier transform ion cyclotron resonance mass spectrometry. *Anal Chem* 82:413–419
- Qian K, Edwards KE, Mennito AS, Freund H, Saeger RB, Hickey KJ, Francisco MA, Yung C, Chawla B, Wu C, Kushnerick JD, Olmstead WN (2012) Determination of structural building blocks in heavy petroleum systems by collision-induced dissociation Fourier transform ion cyclotron resonance mass spectrometry. *Anal Chem* 84:4544–4551
- Qian K, Edwards K, Mennito A, Saeger RB (2016) Generation of model of composition of petroleum by high resolution mass spectrometry and associated analytics. US Patent 9490109
- Rabkin YM, Lafitte-Houssat JJ (1979) Cooperative research in petroleum chemistry. *Scientometrics* 1:327–338
- Robbins WK (1998) Quantitative measurement of mass and aromaticity distributions for heavy distillates 1. Capabilities of the HPLC-2 system. *J Chromatogr Sci* 36:457–466
- Rodgers RP, Marshall AG (2007) Petroleomics: advanced characterization of petroleum-derived materials by Fourier transform ion cyclotron resonance mass spectrometry (FT-ICR MS). In: Mullins OC, Sheu EY, Hammami A, Marshall AG (eds) *Asphaltenes, heavy oils, and petroleomics*. Springer, New York, pp 63–93
- Romão W, Tose LV, Vaz BG, Sama SG, Lobinski R, Giusti P, Carrier H, Bouyssiere B (2016) Petroleomics by direct analysis in real time-mass spectrometry. *J Am Soc Mass Spectrom* 27:182–185
- Rosell-Melé A, Carter JF, Maxwell JR (1996) High-performance liquid chromatography–mass spectrometry of porphyrins by using an atmospheric pressure interface. *J Am Soc Mass Spectrom* 7:965–971
- Rossini FD, Mair BJ (1951) Composition of petroleum. In: *Progress in petroleum technology*, vol 5. American Chemical Society, Washington, DC, pp 334–352
- Rossini FD, Mair BJ (1959) The work of the API research project 6 on the composition of petroleum. In: *Proceedings of 5th world petroleum congress*, pp 223–245
- Ruiz-Guerrero R, Vendevure C, Thiébaud D, Bertoncini F, Espinat D (2006) Comparison of comprehensive two-dimensional gas chromatography coupled with sulfur-chemiluminescence detector to standard methods for speciation of sulfur-containing compounds in middle distillates. *J Chromatogr Sci* 44:566–573
- Rummel JL, McKenna AM, Marshall AG, Eyler JR, Powel DH (2010) The coupling of direct analysis in real time ionization to Fourier transform ion cyclotron resonance mass spectrometry for ultrahigh-resolution mass analysis. *Rapid Commun Mass Spectrom* 24:784–790
- Savory JJ, Kaiser NK, McKenna AM, Xian F, Blakney GT, Rodgers RP, Hendrickson CL, Marshall AG (2011) Parts-per-billion Fourier transform ion cyclotron resonance mass measurement accuracy with a “walking” calibration equation. *Anal Chem* 83:1732–1736

- Schabron JF, Rovani JF, Sanderson MM (2010) Asphaltene determinant method for automated on-column precipitation and redissolution of percondensed aromatic asphaltene components. *Energy Fuels* 24:5984–5996
- Schaub TM, Rodgers RP, Marshall AG, Qian K, Green LA, Olmstead WN (2005) Speciation of aromatic compounds in petroleum refinery streams by continuous flow field desorption ionization FT-ICR mass spectrometry. *Energy Fuels* 19:1566–1573
- Schmidt F, Koch BP, Witt M, Hinrichs K-U (2014) Extending the analytical window for water-soluble organic matter in sediments by aqueous Soxhlet extraction. *Geochim Cosmochim Acta* 141:83–96
- Schuler B, Meyer G, Peña D, Mullins OC, Gross L (2015) Unraveling the molecular structures of asphaltenes by atomic force microscopy. *J Am Chem Soc* 137:9870–9876
- Seeley JV, Seeley SK (2013) Multidimensional gas chromatography: fundamental advances and new applications. *Anal Chem* 85:557–578
- Seidel M, Beck M, Riedel T, Waska H, Suryaputra IGNA, Schnetger B, Niggemann J, Simon M, Dittmar T (2014) Biogeochemistry of dissolved organic matter in an anoxic intertidal creek bank. *Geochim Cosmochim Acta* 140:418–434
- Seidel M, Kleindienst S, Dittmar T, Joye SB, Medeiros PM (2016) Biodegradation of crude oil and dispersants in deep seawater from the Gulf of Mexico: insights from ultra-high resolution mass spectrometry. *Deep Sea Res Part II Top Stud Oceanogr* 129:108–118
- Silva RC, Radović JR, Ahmed F, Ehrmann U, Brown M, Carbognani Ortega L, Larter S, Pereira-Almao P, Oldenburg TBP (2016) Characterization of acid-soluble oxidized asphaltenes by Fourier transform ion cyclotron resonance mass spectrometry: insights on oxycracking processes and asphaltene structural features. *Energy Fuels* 30:171–179
- Sim A, Cho Y, Kim D, Witt M, Birdwell JE, Kim BJ, Kim S (2014) Molecular-level characterization of crude oil compounds combining reversed-phase high-performance liquid chromatography with off-line high-resolution mass spectrometry. *Fuel* 140:717–723
- Simon S, Nordgård E, Bruheim P, Sjöblom J (2008) Determination of C80 tetra-acid content in calcium naphthenate deposits. *J Chromatogr A* 1200:136–143
- Sleighter RL, Hatcher PG (2008) Molecular characterization of dissolved organic matter (DOM) along a river to ocean transect of the lower Chesapeake Bay by ultrahigh-resolution electrospray ionization Fourier transform ion cyclotron resonance mass spectrometry. *Mar Chem* 110:140–152
- Smith BE, Rowland SJ (2008) A derivatisation and liquid chromatography/electrospray ionisation multistage mass spectrometry method for the characterisation of naphthenic acids. *Rapid Commun Mass Spectrom* 22:3909–3927
- Sundaraman P (1985) High-performance liquid chromatography of vanadyl porphyrins. *Anal Chem* 57:2204–2206
- Sutton PA, Rowland SJ (2012) High temperature gas chromatography-time-of-flight-mass spectrometry (HTGC-ToF-MS) for high-boiling compounds. *J Chromatogr A* 1243:68–90
- Talbot HM, Rohmer M, Farrimond P (2007) Rapid structural elucidation of composite bacterial hopanoids by atmospheric pressure chemical ionisation liquid chromatography/ion trap mass spectrometry. *Rapid Commun Mass Spectrom* 21:880–892
- Taylor LT (2010) Supercritical fluid chromatography. *Anal Chem* 82:4925–4935
- Thiebaut DRP, Robert EC (1999) Group-type separation and simulated distillation: a niche for SFC. *Analisis* 27:681–690
- Treibs A (1936) Chlorophyll and hemin derivatives in organic mineral substances. *Angew Chem* 49:682–686
- Vaughan PP, Wilson T, Kamerman R, Hagy ME, McKenna A, Chen H, Jeffrey WH (2016) Photochemical changes in water accommodated fractions of MC252 and surrogate oil created during solar exposure as determined by FT-ICR MS. *Mar Pollut Bull* 104:262–268
- Vaz BG, Silva RC, Klitzke CF, Simas RC, Lopes Nascimento HD, Pereira RCL, Garcia DF, Eberlin MN, Azevedo DA (2013) Assessing biodegradation in the Llanos Orientales crude

- oils by electrospray ionization ultrahigh-resolution and accuracy Fourier transform mass spectrometry and chemometric analysis. *Energy Fuels* 27:1277–1284
- Walters CC (2016) The origin of petroleum. In: Hsu CS, Robinson PR (eds) Springer handbook of petroleum technology. Springer, Cham
- Walters CC, Freund H, Kelemen SR, Braun AL, Wenger LM (2009) Predicting oil quality – simulating reservoir alteration processes. In: 2009 Napa AAPG Hedberg research conference on basin and petroleum systems modeling
- Walters CC, Qian K, Wu C, Mennito AS, Wei Z (2011) Proto-solid bitumen in petroleum altered by thermochemical sulfate reduction. *Org Geochem* 42:999–1006
- Walters CC, Wang FC, Qian K, Wu C, Mennito AS, Wei Z (2015) Petroleum alteration by thermochemical sulfate reduction – a comprehensive molecular study of aromatic hydrocarbons and polar compounds. *Geochim Cosmochim Acta* 153:37–71
- Wang FC (2017) Comprehensive three-dimensional gas chromatography mass spectrometry separation of diesel. *J Chromatogr A* 1489:126–133
- Wang FC, Robbins WK, Sanzo FP, McElroy FC (2003) Speciation of sulfur-containing compounds in diesel by comprehensive two-dimensional gas chromatography. *J Chromatogr Sci* 41: 519–523
- Wang B, Wan Y, Gao Y, Yang M, Hu J (2013) Determination and characterization of oxynaphthenic acids in oilfield wastewater. *Environ Sci Technol* 47:9545–9554
- Wang W, Liu Y, Liu Z, Tian S (2016) Detailed chemical composition of straight-run vacuum gas oil and its distillates as a function of the atmospheric equivalent boiling point. *Energy Fuels* 30:968–974
- Wang FC, Qian K, Edwards KF (2018) Integrated hydrocarbon analysis. US Patent 9417220
- Woltering M, Tulipani S, Boreham CJ, Walshe J, Schwark L, Grice K (2016) Simultaneous quantitative analysis of Ni, VO, Cu, Zn and Mn geoporphyrins by liquid chromatography – high resolution multistage mass spectrometry: method development and validation. *Chem Geol* 441:81–91
- Wu C, Qian K, Neffiu M, Cooks RG (2010) Ambient analysis of saturated hydrocarbons using discharge-induced oxidation in desorption electrospray ionization. *J Am Soc Mass Spectrom* 21:261–267
- Wu C, Walters CC, Qian K (2015) Analysis of hydrocarbon liquid and solid samples. US Patent 9053296 B2
- Xian F, Hendrickson CL, Marshall AG (2012) High resolution mass spectrometry. *Anal Chem* 84:708–719
- Yue S, Ramsay BA, Wang J, Ramsay JA (2016) Biodegradation and detoxification of naphthenic acids in oil sands process affected waters. *Sci Total Environ* 572:273–279
- Zhang Y, Xu C, Shi Q, Zhao S, Chung KH, Hou D (2010) Tracking neutral nitrogen compounds in subfractions of crude oil obtained by liquid chromatography separation using negative-ion electrospray ionization Fourier transform ion cyclotron resonance mass spectrometry. *Energy Fuels* 24:6321–6326
- Zhu R, Shen B, Liu J, Chen X (2012) A kinetic model for catalytic cracking of vacuum gas oil using a structure-oriented lumping method. *Energy Sources A* 34:2066–2072
- Zhu C, Lipp JS, Wörmer L, Becker KW, Schröder J, Hinrichs K-U (2013) Comprehensive glycerol ether lipid fingerprints through a novel reversed phase liquid chromatography–mass spectrometry protocol. *Org Geochem* 65:53–62
- Zhurav KO, Kozhinov AN, Tsybin YO (2013) Evaluation of high-field Orbitrap Fourier transform mass spectrometer for petroleomics. *Energy Fuels* 27:2974–2983
- Zubarev RA, Makarov A (2013) Orbitrap mass spectrometry. *Anal Chem* 85:5288–5296



Stable Isotopes in Understanding Origin and Degradation Processes of Hydrocarbons and Petroleum

13

A. Vieth-Hillebrand and Heinz Wilkes

Contents

1	Introduction	340
2	Definitions	340
3	Stable Isotope Applications in Petroleum Geochemistry	342
3.1	Petroleum Formation in Sedimentary Basins	342
3.2	Alteration Processes in Petroleum Reservoirs	346
4	Research Needs	350
	References	350

Abstract

In this essay we provide a short introduction to some basics of stable isotope geochemistry and an overview of few common applications in petroleum geochemistry. We identify the processes that are responsible for the carbon and hydrogen isotopic compositions of biological and geological organic matter and indicate the utility of stable isotopes in oil-source rock correlations. Stable isotope analyses are also exploited in the investigation of different alteration processes within oils and petroleum reservoirs. State of the art work is presented, and future research needs are identified.

A. Vieth-Hillebrand (✉)

Organic Geochemistry, GFZ German Research Centre for Geosciences, Potsdam, Germany
e-mail: vieth@gfz-potsdam.de

H. Wilkes

Organic Geochemistry, Institute for Chemistry and Biology of the Marine Environment (ICBM),
Carl von Ossietzky University, Oldenburg, Germany
e-mail: heinz.wilkes@uni-oldenburg.de

© Springer Nature Switzerland AG 2020

H. Wilkes (ed.), *Hydrocarbons, Oils and Lipids: Diversity, Origin, Chemistry and Fate*,
Handbook of Hydrocarbon and Lipid Microbiology,
https://doi.org/10.1007/978-3-319-90569-3_36

339

1 Introduction

Processes controlling the molecular and isotopic composition of petroleum – and thus its physicochemical properties and quality – are divided into two fundamental categories. Primary processes include everything influencing petroleum composition *prior* to the accumulation in a trap (reservoir); these are, for example, the biological origin of the source organic matter, the depositional environment of the source rock, and its thermal maturity, as well as migration of petroleum fluids from the source rock to the trap. Secondary controls lead to an alteration of reservoired petroleum *after* accumulation in the trap; this includes (bio)chemical processes such as biodegradation and thermochemical sulfate reduction and physical processes such as water washing and evaporative fractionation. The evaluation of these processes is challenging as petroleum reservoirs typically have complex filling histories with, for example, alternating charging and biodegradation events.

Within this essay, some general information about stable isotopes is given (Sect. 2). Then the complex processes related to petroleum generation and their influence on the isotopic composition of crude oil and natural gas are mentioned, in conjunction with some applications (Sect. 3.1). Section 3.2 discusses the role of alteration processes within reservoirs with a main focus on microbial activity in these environments. It is not within the scope of this essay to give a comprehensive overview on the detailed factors influencing the isotopic composition of petroleum. Excellent reviews on this topic can be found in the literature (Galimov 2006; Peters et al. 2005).

2 Definitions

For a more comprehensive introduction to stable isotope geochemistry and the analytical methods for determining relative isotope ratios, the interested reader is advised to consult one of the following textbooks: Clark and Fritz (1997), Hoefs (2018), and Sharp (2007). With respect to hydrocarbons, this essay will be focused on the stable isotopes of carbon and hydrogen.

The isotopes of a given element have the same number of protons and electrons but differ from each other by the number of neutrons in the nucleus. Most elements in the periodic table have two or more naturally occurring isotopes; carbon and hydrogen both have two stable isotopes (Table 1).

Table 1 Isotopic abundances and relative atomic masses of carbon and hydrogen. (Data taken from Sharp 2007)

Symbol	Atomic number	Mass number	Abundance (%)	Atomic weight
H	1	1	99.985	1.007825
D	1	2	0.015	2.0140
C	6	12	98.89	≐12.0
C	6	13	1.11	13.00335

The mass differences, resulting from the difference in the number of neutrons, lead to differences in the chemical and physical properties of molecules with light and/or heavy isotopes. This causes partial separation of the light isotopes from the heavy isotopes during chemical reactions (isotope fractionation). Equilibrium chemical reactions (e.g., dissolution of CO₂ in water) are accompanied by equilibrium isotope effects, whereas unidirectional reactions – such as biodegradation – quite often are accompanied by significant kinetic isotope effects. In biodegradation, usually reactions with the lighter isotopes are preferred, due to the lower energy that is required to break a bond within one molecule between two light isotopes, in comparison to the higher energy that is needed to break the bond between a light and a heavy isotope.

The delta (δ) notation has been introduced to express the relative differences in isotopic compositions (McKinney et al. 1950),

$$\delta[\text{‰}] = \left(\frac{R_{\text{sample}} - R_{\text{standard}}}{R_{\text{standard}}} \right) \times 1000 \quad (1)$$

where R is the ratio of the abundance of the heavy to the light isotope (within the sample and the international standard; see Table 2).

R is given by D/H and ¹³C/¹²C, respectively. δ values are reported in per mil, or parts per thousands.

Biodegradation processes typically lead to enrichment of the molecules with the heavier isotope in the residual fraction of a substrate due to kinetic isotope effects of the first irreversible reaction in a degradation pathway. The relation between decrease in concentration and change in isotopic composition of the residual substrate can be described by the Rayleigh Equation (2) where F is the fraction of the hydrocarbon remaining (C/C_i), R is the isotopic composition of the hydrocarbon at a particular F, and R_i is the initial isotopic composition.

$$\frac{R}{R_i} = F^{(\alpha-1)} \quad (2)$$

The isotope fractionation factor (α) relates changes in the isotopic composition to changes in the concentration of the residual fraction during the transformation. It is quite common to use the enrichment factor ϵ (3) instead of α . The Rayleigh Equation provides the opportunity to quantify the extent of biodegradation based on carbon or

Table 2 Names and relative and absolute isotope ratios of international standards

Name	Description	Ratio	Accepted value	δ value
PDB	<i>Belemnitella americana</i> from Pee Dee Formation in USA	¹³ C/ ¹² C	11237.3 ± 2.9 (Craig 1957)	0.00
SMOW	Standard Mean Ocean Water	D/H	155.76 ± 0.10 (Hagemann et al. 1970)	0.00

hydrogen isotope ratios and the appropriate isotope fractionation factor independent of concentration measurements.

$$\varepsilon = (\alpha - 1) \cdot 100 \quad (3)$$

3 Stable Isotope Applications in Petroleum Geochemistry

3.1 Petroleum Formation in Sedimentary Basins

A key task of petroleum geochemistry is the correct correlation of natural gas or crude oil accumulations to their respective source rock(s) in a given exploration area. Any approach used in oil- or gas-source correlation is based on the assumption that similarities exist between the molecular and/or isotopic composition of a petroleum fluid and its source. The discussion in this subsection will focus on biochemical and geochemical processes that have to be considered when using the stable carbon or hydrogen isotopic composition of organic matter as a correlation tool, although typically multiple independent data types, both molecular and isotopic, are used in such studies.

The most important control on the carbon isotopic composition of crude oils and natural gas is the carbon isotopic composition of the source organic matter that has been deposited in the sediment later forming a petroleum source rock. The isotopic composition of biogenic organic matter depends on four key elements, namely, (1) the carbon source utilized; (2) isotope effects associated with assimilation of carbon by the producing organism; (3) isotope effects associated with metabolism and biosynthesis, and (4) cellular carbon budgets (Hayes 1993). Autotrophic organisms assimilate inorganic carbon (marine carbonate or bicarbonate, atmospheric carbon dioxide) with $\delta^{13}\text{C}$ values typically between +2 and -8% (Mook 2000) while heterotrophic organisms assimilate carbon from biogenic organic matter with $\delta^{13}\text{C}$ from -5 to -35% (Mook 2000). However, methane with $\delta^{13}\text{C}$ values in the range of ~ -35 to -60% (thermogenic) and ~ -55 to -85% (biogenic) (Schoell 1980) has to be considered as a significant and sometimes unusually light carbon source for methanotrophic organisms (Fig. 1). Typically, biomass is depleted in ^{13}C relative to the respective carbon source due to isotope fractionation processes whose magnitudes depend on the mechanism of carbon fixation. As a consequence of differences in the isotope fractionation associated with specific biosynthetic pathways, ^{12}C and ^{13}C are not equally distributed between the different carbon pools (e.g., carbohydrates, proteins, and lipids) within a single organism (Chikaraishi 2014). Furthermore, it has to be taken into account that sedimentary organic matter typically represents a complex mixture of biomass derived from different source organisms which all contribute their own specific carbon isotopic signatures. This is revealed by compound-specific isotope analysis of biomarkers which can be attributed to specific source organisms.

In general, $\delta^{13}\text{C}$ values of sedimentary organic matter are relatively similar to those of the biomass exported from the water column, indicating that even significant

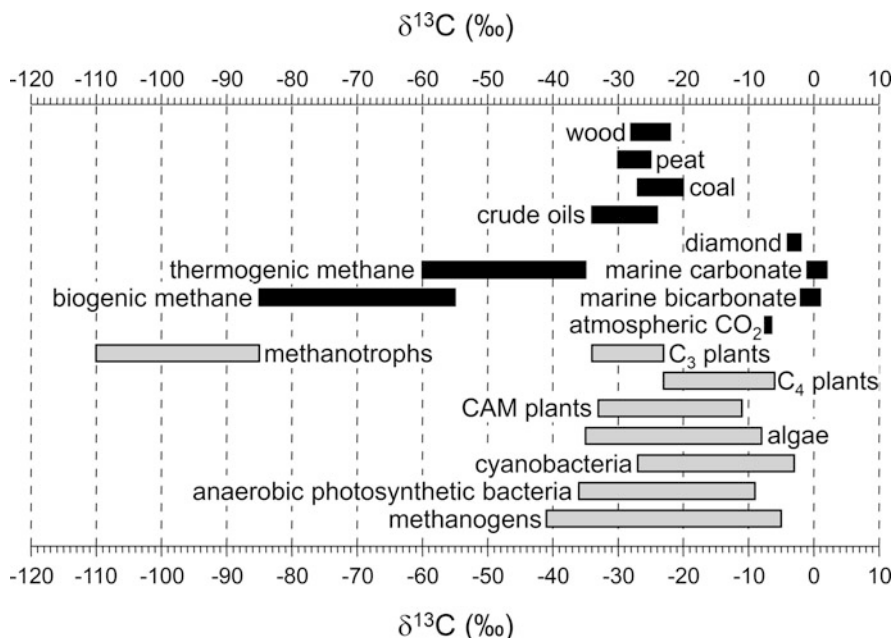


Fig. 1 Variations in stable carbon isotope ratios (VPDB standard) for different organic and inorganic natural materials. (Modified from Mook (2000) and Schidlowski and Aharon (1992), originally published by Vieth and Wilkes (2010), published with kind permission of © Springer Science+Business Media New York, 2003. All rights reserved)

changes in organic matter composition during transport through the water column and early diagenesis after deposition in the sediment (including complete recycling of about 99% of the primary production) do not strongly influence the carbon isotopic composition (for review see Galimov 2006). Likewise, only small shifts towards higher $\delta^{13}\text{C}$ values (up to 1‰) are observed in kerogens due to thermal maturation during catagenesis as a result of the release of ^{12}C -enriched oil and gas (Clayton 1991). Kinetic isotope effects related to oil-to-gas cracking may lead to ^{13}C -enrichment of the remaining oil up to 4‰ (Clayton 1991). A maturation effect is also seen in the carbon isotopic composition of individual oil constituents; however, it normally will not exceed a 2–3‰ shift towards less negative values (Clayton and Bjorøy 1994).

The carbon isotopic composition of bulk crude oils typically ranges between ~ -24 and -34 ‰ (Fig. 1). Small differences in the average isotopic compositions of the C_{15+} fractions of saturated and aromatic hydrocarbon fractions of oils sourced from terrestrial or marine organic matter are mostly insignificant (Sofer 1984). However, it is well established that different petroleum source rocks generate oils with distinct carbon isotopic signatures. This can be illustrated by a case study from the North Viking Graben, an exploration area in the Norwegian North Sea (Gormly et al. 1994). In this area, two potential source rocks, both of Upper Jurassic age, the

Heather and the Draupne Formations, may contribute to the reservoirized crude oils. Kerogen of the Draupne Fm. (-28 to -27‰) is slightly ^{13}C -depleted than that of the Heather Fm. (-27 to -25‰) which corresponds well to the isotopic signatures of the generated oils (-31 to -28‰ versus -28 to -25‰). These variations in isotopic composition are furthermore correlated to those of a molecular biomarker parameter (pristane/phytane ratio) indicating an influence of the source rock depositional environment on the $\delta^{13}\text{C}$ values of the kerogens. In many cases, reservoirized crude oils are not derived from a single source but rather represent mixtures whose isotopic compositions depend on the isotopic composition and relative amounts of the contributing sources. In the North Viking Graben, mixed oils sourced from both the Draupne and the Heather Fm. have $\delta^{13}\text{C}$ values in the range of -28.8 to -28.0‰ (Gormly et al. 1994). The isotopic composition of individual oil constituents, for example, gasoline-range hydrocarbons, may provide useful clues as to the mixed origin of oil (Rooney et al. 1998). Ideally, the carbon isotopic composition of mixed oil can be used to quantify the contributions of the individual sources (Peters et al. 1989).

The stable carbon isotopic compositions of crude oil fractions (saturated and aromatic hydrocarbon fractions) have been shown to become ^{13}C -enriched with decreasing geologic age (Andrusevich et al. 1998). The authors compared evolutionary changes in the biosphere to episodic changes in stable carbon isotopic compositions throughout the Phanerozoic and concluded that these isotopic shifts may be related to the diversity of preserved phytoplankton. Furthermore, crude oils generated from source rocks of Upper Jurassic age become increasingly ^{13}C -enriched from high to low paleolatitudes (=latitudes at which the source rocks were deposited), indicating that the $\delta^{13}\text{C}$ values of oils reflect that of the primary marine biomass, which varied as a function of spatial paleoenvironmental parameters, in particular sea-surface paleotemperature (Andrusevich et al. 2000). The stable carbon isotope compositions of the aromatic and aliphatic fractions in crude oils have been used to differentiate between oils derived from marine or terrigenous source rocks (Sofer 1984).

Stable carbon isotope ratios of individual aromatic hydrocarbons, like alkyl-naphthalenes and alkylphenanthrenes, have been successfully applied as source and age indicators in oils from western Australian basins (Maslen et al. 2011).

Stable carbon isotope ratios are extremely useful for the assessment of the origin of natural gas (for review see Whiticar 1994). This is because fractionations due to kinetic isotope effects lead to a much higher variability in the $\delta^{13}\text{C}$ values of small molecules with only one to five carbon atoms, as is the case in the natural gas hydrocarbons methane (CH_4), ethane (C_2H_6), propane (C_3H_8), *i*-butane (C_4H_{10}), *n*-butane (C_4H_{10}), *i*-pentane (C_5H_{12}), and *n*-pentane (C_5H_{12}). Methane is by far the most predominant constituent of natural gas. The C_2 - C_5 hydrocarbons occur in highly variable amounts which in general are low in biogenic gas and higher in thermogenic gas. The relative amount of the C_2 - C_5 hydrocarbons in natural gas is typically referred to as the "gas wetness" (4).

$$\text{gas wetness} = \frac{[C_2 - C_5]}{[C_1 - C_5]} \quad (4)$$

Likewise, biogenic methane is significantly more ^{13}C -depleted than thermogenic methane. Typically, $\delta^{13}\text{C}$ values of methane lower than -60% and higher than -55% are attributed to a purely biogenic or a purely thermogenic origin, respectively, while a mixed source has to be considered for intermediate $\delta^{13}\text{C}$ values. Methane isotopic composition provides clear evidence for the occurrence of biogenic methane in very deep reservoirs (at least down to 3000 m) and thus is a very important hint to the existence of a subterranean so-called deep biosphere (Schoell 1980). The isotopic compositions of ethane and propane in cold, deeply buried sediments from the southeastern Pacific were interpreted to reflect the microbial production of these hydrocarbons in situ (Hinrichs et al. 2006).

Until now, the hydrogen isotopic compositions of organic components are used to a much lesser extent in petroleum geochemistry (for review see Sessions 2016; Pedentchouk and Turich 2018). It might be expected that they show similar fractionation behavior during processes involved in the formation and destruction of petroleum as discussed here for the distribution of the carbon isotopes. However, recent progress on this topic appears to indicate significant differences, likely due to different modes in which hydrogen is involved in biogeochemical processes. A crucial aspect seems to be that hydrogen atoms in hydrocarbons (and organic matter in general) are exchangeable with external hydrogen, both organically and inorganically bound, which likely is negligible for carbon atoms (Sessions et al. 2004). In particular, water has to be considered as a relevant source of hydrogen in petroleum systems, and hydrocarbons may interact with water on the migration pathway from the source to the trap or with the formation water in a reservoir. It is true that the C–H acidity of hydrocarbons is extremely low; however, on geological timescales, i.e., many million years or even more, and at the elevated temperatures occurring in many petroleum systems, hydrogen exchange reactions may become significant, although they would not be observable on a human timescale. Numerous recent studies have investigated such exchange processes and have clearly indicated that the hydrogen isotopic signatures of geological organic matter (kerogen, bulk oils, oil fractions, individual oil, and gas constituents) become systematically ^2H -enriched with increasing levels of thermal maturity (Dawson et al. 2005; Lis et al. 2006; Mastalerz and Schimmelmann 2002; Pedentchouk et al. 2006; Radke et al. 2005; Schimmelmann et al. 2001; Sessions et al. 2004; Tang et al. 2005). The extent and rate of ^2H -enrichment has been shown to depend on the organic compound class (Schimmelmann et al. 2006).

To evaluate the equilibrium fractionation that occurs between C-bound H and H_2O , laboratory incubation experiments and ab initio molecular modeling have been performed by Wang et al. (2009a, b, 2013), establishing a computational framework, which allows the prediction of equilibrium fractionation factors in linear, branched, and cyclic aliphatic hydrocarbons (Sessions 2016).

This seems to indicate that hydrogen isotope ratios could be efficient tools in thermal history assessment where carbon isotope ratios are not very useful (see

above). Beyond this, the systematics of hydrogen isotopes in organic components of petroleum systems awaits further investigations to fully establish their potential as a tool in exploration and production of petroleum.

3.2 Alteration Processes in Petroleum Reservoirs

Biodegradation in petroleum reservoirs will preferentially take place near the oil-water interface and has been described to be of relevance in reservoirs that were not exposed to temperatures >80 °C (Connan 1984; Wilhelms et al. 2001). The oil-water contact provides conditions that are the most conducive to microbial activity. Diffusive transport of hydrocarbons through the oil column to the oil-water contact will provide electron donors, whereas inorganic nutrients required for microbial growth can be transported by water flow or diffusion in the water column to the oil-water contact (Head et al. 2003). Biodegradation processes in crude oils were described to lead to the quasi-sequential removal of compound groups as follows: *n*-alkanes $>$ branched alkanes $>$ alkylbenzenes $>$ alkyl-naphthalenes $>$ alkylcyclohexanes, alkylphenanthrenes, and alkyl-dibenzothiophenes $>$ isoprenoids (C_{15+}) $>$ regular steranes $>$ hopanes $>$ aromatic steranes (Peters and Moldowan 1993; Wenger et al. 2002). However, recent work on molecular changes in biodegraded oils indicates that the degradation patterns of light hydrocarbons and *n*-alkanes differ in different petroleum systems. This suggests that microbial communities are different and therefore generate different molecular degradation patterns which have to be evaluated individually for each system (Elias et al. 2007).

The molecular and isotopic composition of natural gas hydrocarbons (C_1 – C_5) is used traditionally for gas-gas correlations, as has been successfully demonstrated by Boreham and co-authors for Australian gases (Boreham et al. 2001). However, influences of source, maturity, and biodegradation processes on the molecular and isotopic composition of these compounds have to be evaluated carefully. The relative abundance of the wet gases (C_2 – C_5) will decrease and their $\delta^{13}C$ will shift to less negative values with biodegradation. The isotopic composition of the original methane will be influenced by additional biogenic methane with light isotopic composition ($<-60\%$). The $\delta^{13}C$ values of natural gas constituents from different Australian basins, which are influenced by biodegradation, show large isotopic separations between successive *n*-alkane homologues, and ^{13}C -enriched CO_2 (up to $+19.5\%$) (Pallasser 2000). Also in deep hot reservoirs (~ 2900 m below sea level, ~ 80 – 115 °C), the $\delta^{13}C$ values of natural gas constituents indicated that they have been overprinted by biological processes (Milkov and Dzou 2007). In addition to field studies, laboratory experiments demonstrated that the anaerobic degradation of propane and *n*-butane resulted in significant carbon isotope fractionation ($\Delta\delta^{13}C$ up to 15%) (Kniemeyer et al. 2007; Jaekel et al. 2014).

Shifts in $\delta^{13}C$ of C_5 – C_9 hydrocarbons of crude oils have been used as qualitative indicators of biodegradation processes. In the Barrow Island oilfield, Australia, that shows minor to moderate biodegradation, quite distinct patterns of changes in $\delta^{13}C$ have been observed (George et al. 2002). Here, cyclohexane, methylcyclohexane,

and the branched alkanes show isotopic shifts up to 10‰ to higher $\delta^{13}\text{C}$ values within a set of six oil samples. Whereas $n\text{C}_6$ and $n\text{C}_7$ show quite similar $\delta^{13}\text{C}$ values between -28 and -26 ‰ (George et al. 2002). This is in contrast to results from West Sak oils from the North Slope, Alaska where isotope fractionation of n -alkanes has been reported to be larger than for cyclic and branched alkanes (Masterson et al. 2001).

Biodegradation processes of hydrocarbons in oil reservoirs can be described and quantified by, for example, changes in the molecular composition (Elias et al. 2007) but also by changes in the carbon isotopic composition of the residual substrate fraction (Vieth and Wilkes 2006). The increase in the concentration ratio $i\text{C}_5/n\text{C}_5$ provides valuable information about biodegradation in oil reservoirs because it is known that the branched hydrocarbon is less susceptible to biodegradation than the n -alkane (Welte et al. 1982). The changes in the $i\text{C}_5/n\text{C}_5$ ratio in oil samples from three different petroleum systems are therefore indicative of light to moderate biodegradation (Fig. 2). The increase in the $i\text{C}_5/n\text{C}_5$ ratio is correlated to increasing $\delta^{13}\text{C}$ values of $i\text{C}_5$ and $n\text{C}_5$. It is obvious for all oil fields that the $\delta^{13}\text{C}$ values of $i\text{C}_5$ are slightly more negative than the $\delta^{13}\text{C}$ values of $n\text{C}_5$ and show a smaller ^{13}C -enrichment with increase in the $i\text{C}_5/n\text{C}_5$ ratios (Fig. 2).

Evaluation of the carbon isotope and concentration data for $i\text{C}_5$ and $n\text{C}_5$ using the Rayleigh equation (2) indicates that the Rayleigh model can be applied here. It turns out that the isotope fractionation factors for $i\text{C}_5$ are identical in Norway (Gullfaks)

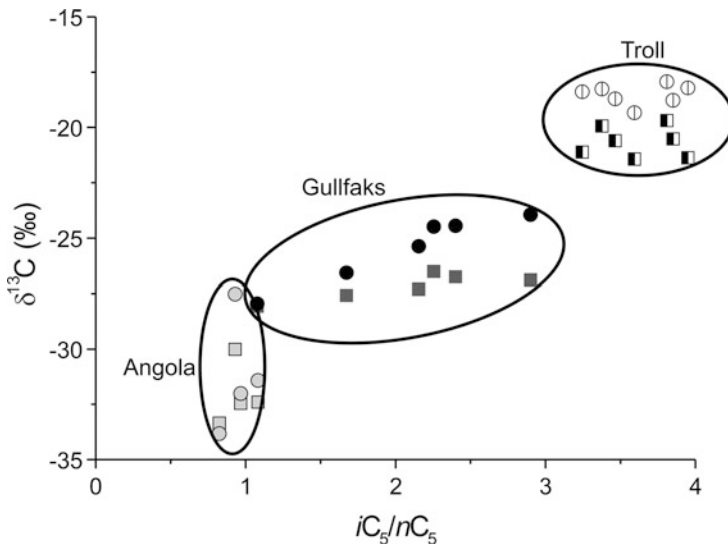


Fig. 2 $\delta^{13}\text{C}$ of $i\text{C}_5$ (squares) and $n\text{C}_5$ (circles) in oil samples from offshore Angola and offshore Norway (Gullfaks and Troll) plotted over their $i\text{C}_5/n\text{C}_5$ concentration ratio; data taken from Barman Skaare et al. (2007), Vieth and Wilkes (2006), and Wilkes et al. (2008). (Originally published in Vieth and Wilkes (2010), published with kind permission of ©Springer Science+Business Media New York, 2003. All rights reserved)

and Angola, and that the fractionation factors for nC_5 are very similar (Fig. 3) (Wilkes et al. 2008). This may indicate that the extent of isotopic fractionation of individual hydrocarbons due to biodegradation is very similar in different petroleum systems, even if the molecular patterns of alteration are different. The carbon isotope and concentration data of the Troll oil samples have not been included in the Rayleigh evaluation because all oil samples have a relatively similar extent of biodegradation (Barman Skaare et al. 2007). For an unambiguous assessment of biodegradation, a reliable nonbiodegraded (end-member) oil sample is necessary to provide the initial isotopic composition and concentration of iC_5 and nC_5 .

The application of compound-specific isotope analysis to assess in-reservoir biodegradation has certain restrictions. Carbon isotope fractionation of the residual substrate occurs in the first irreversible reaction, which mechanistically takes place at (a) certain specific carbon atom(s) of the substrate in most known cases. Therefore, the observable isotope effect will become less observable with increasing number of carbon atoms in the molecule that are not involved in the crucial transformation (Boreham et al. 1995). Dilution of the fractionation effect limits the application of the Rayleigh approach to light hydrocarbons (Morasch et al. 2004; Wilkes et al. 2008). Therefore, the compound-specific carbon isotope ratios of C_{15+} hydrocarbons will not be significantly affected by biodegradation processes and can still be used as specific indicators of the origin of the oil as well as for oil-oil and oil-source correlations (Vieth and Wilkes 2006).

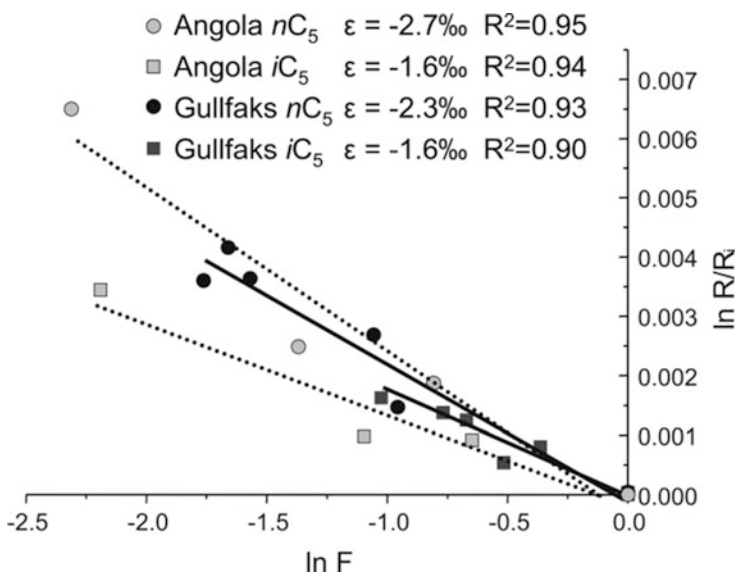


Fig. 3 Concentration and $\delta^{13}C$ of iC_5 (squares) and nC_5 (circles) for oil samples from the Gullfaks field (dark grey symbols; data taken from Vieth and Wilkes 2006) and an oil field offshore Angola (light grey symbols; data taken from Wilkes et al. 2008), plotted according to the Rayleigh equation as $\ln R/R_i$ over $\ln F$. (Originally published in Vieth and Wilkes 2010, published with kind permission of © Springer Science+Business Media New York, 2003. All rights reserved)

Based on the assumption that only light hydrocarbons show an observable carbon isotope fractionation related to biodegradation processes, it becomes clear that the carbon isotopic composition of whole oils and individual oil fractions (e.g., saturated and aromatic hydrocarbons) will not show significant changes due to biodegradation (Sofer 1984; Stahl 1980; Sun et al. 2005). Within bulk oils, the isotopic signatures of components which show a significant fractionation will be overprinted by the isotopic signatures of non-degraded oil constituents that become relatively ^{13}C -enriched. Hydrocarbons from C_{15+} saturates and C_{11+} aromatics oil fractions are generally made up of larger compounds which are not expected to show significant fractionation due to biodegradation (Wilkes et al. 2008).

For hydrogen isotope fractionation due to biodegradation, the same principal behavior would be expected. In general, hydrogen isotope fractionation tends to be one order of magnitude larger than carbon isotope fractionation due to the higher relative mass difference between the two isotopes. Therefore, the dilution effect will become relevant at a higher number of hydrogen atoms being present within the substrate molecule. This is in agreement with results of aerobic degradation experiments where the hydrogen isotopic composition of long-chain alkanes ($n\text{C}_{19}$ to $n\text{C}_{27}$) did not change significantly (Pond et al. 2002). Sun et al. (2005) studied seven oils from the lacustrine Shahejie Formation of the Liaohe Basin in NE China, showing biodegradation levels from none to heavy. The δD values of the n -alkanes increased from roughly -175‰ to -140‰ with the increase in biodegradation level. Asif et al. (2009) studied a series of oils with low extents of biodegradation from the Upper Indus Basin in Pakistan. Here, n -alkanes between $n\text{C}_{14}$ and $n\text{C}_{22}$ had quite uniform δD values in each sample, but deviated from -166 to -127‰ (average δD value for $n\text{C}_{14}$ to $n\text{C}_{22}$) with assumed increase in biodegradation. The isoprenoid hydrocarbons pristane and phytane did not change their δD values in relation to biodegradation, the variability in average δD for pristane and phytane was between -162 and -141‰ . Based on these results, the authors developed an approach that uses the difference in δD values between pristane, phytane, and the n -alkanes as indicator of biodegradation.

Additional insight into the biodegradation mechanisms related to aerobic or anaerobic biodegradation of individual saturated and aromatic hydrocarbons will be provided by combined evaluation of carbon and hydrogen isotope compositions. In the last decade, several biodegradation experiments were performed where carbon and hydrogen isotope fractionation related to aerobic as well as anaerobic degradation of selected hydrocarbons was characterized (e.g., Fischer et al. 2008; Vogt et al. 2008; Jaekel et al. 2014; review provided by Vogt et al. 2016). Here, most well-known microbial transformation reactions of hydrocarbons were investigated and it became obvious that especially the anaerobic degradation processes can be identified by combined evaluation of carbon and hydrogen isotope data (Vogt et al. 2016). In contrast to laboratory experiments, the hydrogen isotope ratios of light hydrocarbons in crude oils may not show a clear dependence on biodegradation processes. It has been suggested that in petroleum reservoirs, in addition to differences in maturity and source, the effects of hydrogen exchange between oil and formation water over geologic times have also to be considered (Sessions et al. 2004; Sessions 2016).

Thermochemical sulphate reduction (TSR) is the abiobiological reduction of sulphate by hydrocarbons in reservoirs close to anhydrite (source of sulphate) at high temperatures (range of minimum temperature between 100 °C and 140 °C) (Machel 2001). Some types of hydrocarbons are more susceptible to TSR than others, for example, C₂–C₅ gases are more reactive than methane and saturated hydrocarbons are more reactive than aromatic hydrocarbons (Peters et al. 2005). This is confirmed by the observation that larger isotopic shifts (e.g., up to 22‰) occur during TSR for the branched and *n*-alkanes, whereas relatively smaller shifts (e.g., 3–6‰) have been found for the cyclic and monoaromatic hydrocarbons (Rooney 1995). Whiticar and Snowdon reported changes during TSR in δ¹³C of individual hydrocarbons of the C₅–C₈ range by up to 10‰ (Whiticar and Snowdon 1999). In experimental studies using sealed gold tubes for pyrolysis of oil in the presence or absence of mineral phases and water, Xiao and co-authors observed that low-molecular weight cycloalkanes, *n*-alkanes, and isoalkanes are more susceptible to TSR and tend to become more ¹³C-enriched. Low-molecular weight monoaromatic hydrocarbons are the most resistant to TSR and show only small isotopic variation. Therefore, isotopic signature of saturated alkanes in TSR-altered oils cannot be used for oil-oil and oil-source correlations (Xiao et al. 2011).

4 Research Needs

In order to strengthen the application of stable carbon and hydrogen isotopes as valuable process indicators for an improved understanding of petroleum generation, reservoir filling, and secondary alteration, it is necessary to deepen the insight into the hydrogen exchange processes occurring in petroleum reservoirs over geological time scales. The role of mineralogy in catalyzing hydrogen isotopic exchange, the effect of salinity of the formation water as well as temperature on the D/H exchange have not been fully understood and quantified until now (Sessions 2016). Such research would help to evaluate compound-specific hydrogen isotope ratios of petroleum hydrocarbons. In the last decade, multi-element isotope analysis was often applied to decipher details in microbial degradation pathways in laboratory experiments but also in field studies, with focus on contaminated aquifers. However, the application of multi-element isotope analysis in petroleum reservoir studies is still missing, probably due to the problems in differentiating the main controls on the hydrogen isotope composition on petroleum hydrocarbons.

References

- Andrusevich VE, Engel MH, Zumberge JE, Brothers LA (1998) Secular, episodic changes in stable carbon isotope composition of crude oils. *Chem Geol* 152:59–72
- Andrusevich VE, Engel MH, Zumberge JE (2000) Effects of paleolatitude on the stable carbon isotope composition of crude oils. *Geology* 28:847–850

- Asif M, Grice K, Fazeelat T (2009) Assessment of petroleum biodegradation using stable hydrogen isotopes of individual saturated hydrocarbon and polycyclic aromatic hydrocarbon distributions in oils from the Upper Indus Basin, Pakistan. *Org Geochem* 40:301–311
- Barman Skaare B, Wilkes H, Vieth A, Rein E, Barth T (2007) Alteration of crude oils from the Troll area by biodegradation: analysis of oil and water samples. *Org Geochem* 38:1865–1883
- Boreham CJ, Dowling LM, Murray AP (1995) Biodegradation and maturity influences on n-alkane isotopic profiles in terrigenous sequences. In: Grimalt JO, Dorronsoro C (eds) *Organic geochemistry: developments and applications to energy, climate, environment and human history*, Selected paper of the 7th International Meeting on Organic Geochemistry, pp 539–544
- Boreham CJ, Hope JM, Hartung KB (2001) Understanding source, distribution and preservation of Australian natural gas; a geochemical perspective. In: 2001 APPEA conference Australian petroleum production and exploration association, Canberra, pp 523–547
- Chikaraishi Y (2014) $^{13}\text{C}/^{12}\text{C}$ signatures in plants and algae. In: Holland HD, Turekian KK (eds) *Treatise on geochemistry*, 2nd edn. Elsevier, Oxford, pp 95–123
- Clark ID, Fritz P (1997) *Environmental isotopes in hydrogeology*. Lewis Publishers, Boca Raton
- Clayton CJ (1991) Effect of maturity on carbon isotope ratios of oils and condensates. *Org Geochem* 17:887–899
- Clayton CJ, Bjørøy M (1994) Effect of maturity on $^{13}\text{C}/^{12}\text{C}$ ratios of individual compounds in North Sea oils. *Org Geochem* 21:737–750
- Connan J (1984) Biodegradation of crude oils in reservoirs. In: Brooks JM, Welte D (eds) *Advances in petroleum geochemistry*, vol 1. Academic, London, pp 299–355
- Craig H (1957) Isotopic standards for carbon and oxygen and correction factors for mass-spectrometric analysis of carbon dioxide. *Geochim Cosmochim Acta* 12:133–149
- Dawson D, Grice K, Alexander R (2005) Effect of maturation on the indigenous δD signatures of individual hydrocarbons in sediments and crude oils from the Perth Basin (Western Australia). *Org Geochem* 36:95–104
- Elias R, Vieth A, Riva A, Horsfield B, Wilkes H (2007) Improved assessment of biodegradation extent and prediction of petroleum quality. *Org Geochem* 38:2111–2130
- Fischer A, Herklotz I, Herrmann S, Thullner M, Weelink SAB, Stams AJM, Schlömann M, Richnow HH, Vogt C (2008) Combined carbon and hydrogen isotope fractionation investigations for elucidating benzene biodegradation pathways. *Environ Sci Technol* 42:4356–4363
- Galimov EM (2006) Isotope organic geochemistry. *Org Geochem* 37:1200–1262
- George SC, Boreham CJ, Minifie SA, Teerman SC (2002) The effect of minor to moderate biodegradation on C5 to C9 hydrocarbons in crude oils. *Org Geochem* 33:1293–1317
- Gormly JR, Buck SP, Chung HM (1994) Oil-source rock correlation in the North Viking Graben. *Org Geochem* 22:403–413
- Hagemann R, Nief G, Roth E (1970) Absolute isotopic scale for deuterium analysis of natural waters. Absolute D/H ratio for SMOW. *Tellus* 22:712–715
- Hayes JM (1993) Factors controlling ^{13}C contents of sedimentary organic compounds: principles and evidence. *Mar Geol* 113:111–125
- Head IM, Jones DM, Larter SR (2003) Biological activity in the deep subsurface and the origin of heavy oil. *Nature* 426:344–352
- Hinrichs KU, Hayes JM, Bach W, Spivack AJ, Hmelo LR, Holm NG, Johnson CG, Sylva SP (2006) Biological formation of ethane and propane in the deep marine subsurface. *Proc Natl Acad Sci U S A* 103:14684–14689
- Hoefs J (2018) *Stable isotope geochemistry*, 8th edn. Springer, Berlin
- Jaekel U, Vogt C, Fischer A, Richnow HH, Musat F (2014) Carbon and hydrogen stable isotope fractionation associated with the anaerobic degradation of propane and butane by marine sulfate-reducing bacteria. *Environ Microbiol* 16:130–140
- Kniemeyer O, Musat F, Sievert SM, Knittel K, Wilkes H, Blumenberg M, Michaelis W, Classen A, Bolm C, Joye SB, Widdel F (2007) Anaerobic oxidation of short-chain hydrocarbons by marine sulphate-reducing bacteria. *Nature* 449:898–902
- Lis GP, Schimmelmann A, Mastalerz M (2006) D/H ratios and hydrogen exchangeability of type-II kerogens with increasing thermal maturity. *Org Geochem* 37:342–353

- Machel HG (2001) Bacterial and thermochemical sulfate reduction in diagenetic settings – old and new insights. *Sediment Geol* 140:143–175
- Maslen E, Grice K, Métayer PL, Dawson D, Edwards D (2011) Stable carbon isotopic compositions of individual aromatic hydrocarbons as source and age indicators in oils from western Australian basins. *Org Geochem* 42:387–398
- Mastalerz M, Schimmelmann A (2002) Isotopically exchangeable organic hydrogen in coal relates to thermal maturity and maceral composition. *Org Geochem* 33:921–931
- Masterson WD, Dzou LIP, Holba AG, Fincannon AL, Ellis L (2001) Evidence for biodegradation and evaporative fractionation in West Sak, Kuparuk and Prudhoe Bay field areas, North Slope, Alaska. *Org Geochem* 32:411–441
- McKinney CR, McCrea JM, Epstein S, Allen HA, Urey HC (1950) Improvements in mass spectrometers for the measurement of small differences in isotope abundance ratios. *Rev Sci Instrum* 21:724–730
- Milkov AV, Dzou L (2007) Geochemical evidence of secondary microbial methane from very slight biodegradation of undersaturated oils in a deep hot reservoir. *Geology* 35:455–458
- Mook WG (2000) Environmental isotopes in the hydrological cycle – principles and applications. IAEA Publications, UNESCO, Paris
- Morasch B, Richnow HH, Vieth A, Schink B, Meckenstock RU (2004) Stable isotope fractionation caused by glycol radical enzymes during bacterial degradation of aromatic compounds. *Appl Environ Microbiol* 70:2935–2940
- Pallasser RJ (2000) Recognizing biodegradation in gas/oil accumulations through the $\delta^{13}\text{C}$ compositions of gas components. *Org Geochem* 31:1363–1373
- Pedentchouk N, Turich C (2018) Carbon and hydrogen isotopic compositions of *n*-alkanes as a tool in petroleum exploration. *Geol Soc Spec Publ* 468:105–125. London
- Pedentchouk N, Freeman KH, Harris NB (2006) Different response of δD values of *n*-alkanes, isoprenoids, and kerogen during thermal maturation. *Geochim Cosmochim Acta* 70:2063–2072
- Peters KE, Moldowan JM (1993) The biomarker guide: interpreting molecular fossils in petroleum and ancient sediments. Prentice Hall, Englewood Cliffs
- Peters KE, Moldowan JM, Driscoll AR, Demaison GJ (1989) Origin of Beatrice oil by co-sourcing from Devonian and Middle Jurassic source rocks, inner Moray Firth, United Kingdom. *AAPG Bull* 73:454–471
- Peters KE, Walters CC, Moldowan JM (2005) The biomarker guide – biomarkers and isotopes in the environment and human history. Cambridge University Press, Cambridge
- Pond KL, Huang Y, Wang Y, Kulpa CF (2002) Hydrogen isotopic composition of individual *n*-alkanes as an intrinsic tracer for bioremediation and source identification of petroleum contamination. *Environ Sci Technol* 36:724–728
- Radke J, Bechtel A, Gaupp R, Puttmann W, Schwark L, Sachse D, Gleixner G (2005) Correlation between hydrogen isotope ratios of lipid biomarkers and sediment maturity. *Geochim Cosmochim Acta* 69:5517–5530
- Rooney MA (1995) Carbon isotope ratios of light hydrocarbons as indicators of thermochemical sulfate reduction. In: Grimalt JO, Dorronsoro C (eds) *Organic geochemistry: developments and applications to energy, climate, environment and human history*, Selected paper of the 7th International Meeting on Organic Geochemistry, pp 523–525
- Rooney MA, Vuletich AK, Griffith CE (1998) Compound-specific isotope analysis as a tool for characterizing mixed oils: an example from the West of Shetlands area. *Org Geochem* 29:241–254
- Schidlowski M, Aharon P (1992) Carbon cycle and carbon isotope record: geochemical impact of life over 3.8 Ga of earth history. In: Schidlowski M (ed) *Early organic evolution: implications for mineral and energy resources*. Springer, Berlin, pp 147–175
- Schimmelmann A, Boudou JP, Lewan MD, Wintsch RP (2001) Experimental controls on D/H and $^{13}\text{C}/^{12}\text{C}$ ratios of kerogen, bitumen and oil during hydrous pyrolysis. *Org Geochem* 32:1009–1018
- Schimmelmann A, Sessions AL, Mastalerz M (2006) Hydrogen isotopic (D/H) composition of organic matter during diagenesis and thermal maturation. *Annu Rev Earth Planet Sci* 34:501–533

- Schoell M (1980) The hydrogen and carbon isotopic composition of methane from natural gases of various origins. *Geochim Cosmochim Acta* 44:649–661
- Sessions AL (2016) Factors controlling the deuterium contents of sedimentary hydrocarbons. *Org Geochem* 96:43–64
- Sessions AL, Sylva SP, Summons RE, Hayes JM (2004) Isotopic exchange of carbon-bound hydrogen over geologic timescales. *Geochim Cosmochim Acta* 68:1545–1559
- Sharp Z (2007) Principles of stable isotope geochemistry. Prentice Hall, Upper Saddle River
- Sofer Z (1984) Stable carbon isotope compositions of crude oils; application to source depositional environments and petroleum alteration. *AAPG Bull* 68:31–49
- Stahl WJ (1980) Compositional changes and $^{13}\text{C}/^{12}\text{C}$ fractionations during the degradation of hydrocarbons by bacteria. *Geochim Cosmochim Acta* 44:1903–1907
- Sun Y, Chen Z, Xu S, Cai P (2005) Stable carbon and hydrogen isotopic fractionation of individual n-alkanes accompanying biodegradation: evidence from a group of progressively biodegraded oils. *Org Geochem* 36:225–238
- Tang Y, Huang Y, Ellis GS, Wang Y, Kralert PG, Gillaizeau B, Ma Q, Hwang R (2005) A kinetic model for thermally induced hydrogen and carbon isotope fractionation of individual n-alkanes in crude oil. *Geochim Cosmochim Acta* 69:4505–4520
- Vieth A, Wilkes H (2006) Deciphering biodegradation effects on light hydrocarbons in crude oils using their stable carbon isotopic composition: a case study from the Gullfaks oil field, offshore Norway. *Geochim Cosmochim Acta* 70:651–665
- Vieth A, Wilkes H (2010) Stable isotopes in understanding origin and degradation processes of petroleum. In: Timmis KN (ed) *Handbook of hydrocarbon and lipid microbiology*. Springer, Berlin, pp 97–111
- Vogt C, Cyrus E, Herklotz I, Schlosser D, Bahr A, Herrmann S, Richnow HH, Fischer A (2008) Evaluation of toluene degradation pathways by two-dimensional stable isotope fractionation. *Environ Sci Technol* 42:7793–7800
- Vogt C, Dorer C, Musat F, Richnow HH (2016) Multi-element isotope fractionation concepts to characterize the biodegradation of hydrocarbons – from enzymes to the environment. *Curr Opin Biotechnol* 41:90–98
- Wang Y, Sessions AL, Nielsen RJ, Goddard WA III (2009a) Equilibrium 2H/1H fractionations in organic molecules: I. Experimental calibration of ab initio calculations. *Geochim Cosmochim Acta* 73:7060–7075
- Wang Y, Sessions AL, Nielsen RJ, Goddard WA III (2009b) Equilibrium 2H/1H fractionations in organic molecules. II: Linear alkanes, alkenes, ketones, carboxylic acids, esters, alcohols and ethers. *Geochim Cosmochim Acta* 73:7076–7086
- Wang Y, Sessions AL, Nielsen RJ, Goddard WA III (2013) Equilibrium 2H/1H fractionation in organic molecules: III. Cyclic ketones and hydrocarbons. *Geochim Cosmochim Acta* 107:82–95
- Welte DH, Kratochvil H, Rullkötter J, Ladwein H, Schaefer RG (1982) Organic geochemistry of crude oils from the Vienna Basin and an assessment of their origin. *Chem Geol* 35:33–68
- Wenger LM, Davis CL, Isaksen GH (2002) Multiple controls on petroleum biodegradation and impact on oil quality. *SPE Reserv Eval Eng* 5:375–383
- Whiticar MJ (1994) Correlation of natural gases with their sources. In: Magoon LB, Dow WG (eds) *The petroleum system – from source to trap*. American Association of Petroleum Geologists, pp 261–283
- Whiticar MJ, Snowdon LR (1999) Geochemical characterization of selected Western Canada oils by $\text{C}_5\text{--}\text{C}_8$ compound specific isotope correlation (CSIC). *Org Geochem* 30:1127–1161
- Wilhelms A, Larter SR, Head I, Farrimond P, Di Primio R, Zwach C (2001) Biodegradation of oil in uplifted basins prevented by deep-burial sterilization. *Nature* 411:1034–1037
- Wilkes H, Vieth A, Elias R (2008) Constraints on the quantitative assessment of in-reservoir biodegradation using compound specific stable carbon isotopes. *Org Geochem* 39:1215–1221
- Xiao Q, Sun Y, Chai P (2011) Experimental study of the effects of thermochemical sulfate reduction on low molecular weight hydrocarbons in confined systems and its geochemical implications. *Org Geochem* 42:1375–1393



The Origin of Organic Sulphur Compounds and Their Impact on the Paleoenvironmental Record

14

Ilya Kutuzov, Yoav O. Rosenberg, Andrew Bishop, and Alon Amrani

Contents

1	Introduction	356
2	Nomenclature, Methods, and Instrumentation for the Characterization of Sedimentary Organic Sulphur Compounds	357
2.1	Nomenclature and Chemical and Thermal Treatment for the Analysis of Organic S	357
2.2	Instrumentation for the Analysis of Organic S	359
2.3	Sulphur and Carbon Isotope Analysis	359
3	The Marine Sulphur Cycle and Its Impact on Organic Matter	362
3.1	The Link Between the Sulphur and Organic Carbon Cycles	362
3.2	Mechanism of Abiotic Sulphurization	366
3.3	Timing of Abiotic Sulphurization	367
3.4	Sulphurization as OM Preservation Mechanism	370
3.5	Other Possible Sources for Sedimentary Organic Sulphur	372
3.6	The Formation and Structural Modifications of Sedimentary OSC During Catagenesis	375
4	Application of Organic Sulphur Compounds in Paleoenvironmental Research	376
4.1	<i>n</i> -Alkanes	376
4.2	Long-Chain C ₃₇ –C ₃₉ Alkenes and Alkenones	380
4.3	Phytol-Derived and Phytol-Related Isoprenoids	381
4.4	Highly Branched Isoprenoids (HBIs) and Their Sulphur-Containing Derivatives ...	386

I. Kutuzov · A. Amrani (✉)

The Hebrew University of Jerusalem, Jerusalem, Israel

e-mail: ilya.kutuzov@mail.huji.ac.il; alon.amrani@mail.huji.ac.il

Y. O. Rosenberg

The Hebrew University of Jerusalem, Jerusalem, Israel

Geological Survey of Israel, Jerusalem, Israel

e-mail: yoavr@gsi.gov.il

A. Bishop

Power, Environmental and Energy Research Institute, Covina, CA, USA

e-mail: andy.bishop@peeri.org

© Springer Nature Switzerland AG 2020

H. Wilkes (ed.), *Hydrocarbons, Oils and Lipids: Diversity, Origin, Chemistry and Fate*, Handbook of Hydrocarbon and Lipid Microbiology,

https://doi.org/10.1007/978-3-319-90569-3_1

355

4.5	Steroids	387
4.6	Hopanoids	388
4.7	Carotenoids	391
4.8	Porphyryns	393
4.9	Polyprenoid Sulphides	394
4.10	Carbohydrates	394
5	Summary	395
5.1	Future Directions	396
	References	397

Abstract

Over the past three decades, significant scientific progress has been achieved in the field of sedimentary organic sulphur compounds (OSC). Advances include structural identification, formation pathways, sulphur and carbon isotopic signatures of OSC, and their significance with respect to the paleoenvironmental record. The scope of the present review covers these efforts and highlights future directions in the field.

Initially, we review the marine sulphur cycle and its coupling to the carbon cycle from modern sediments to thermally immature sedimentary rocks. Microbial sulphate reduction (MSR) is a central process in providing reduced sulphur (e.g., HS^-) which reacts abiotically with organic matter, on a very rapid (geological) timescale ($<10,000$ years), leading to its preservation. The S isotopic fractionation during MSR is significant, which subsequently leads to sedimentary OSC with very distinctive $\delta^{34}\text{S}$ signature from that of biochemical OSC. Evaluating S isotope values on bulk fractions (e.g., kerogen), as well as individual OSC, can shed light on their formation pathways, the relative contributions of biochemically derived and abiotic sulphur, and competition with inorganic S pathways (e.g., organic S incorporation versus pyrite formation). New reservoirs of OSC (volatile, dissolved, and particulate), some of which comprise biochemically sourced sulphur, have been recently identified. Their role in the S cycle with respect to sedimentary OM is an ongoing research question.

We further discuss the progress made on specific groups of OSC as paleoenvironmental indicators. For each group, we first briefly highlight their significance as biomarkers. Then, we discuss aspects related to their sulphurization sites, rates and extent of sulphurization, preservation, and biases of the geological record resulting from the sulphurization process. New frontiers, both on the analytical level and in terms of our conceptual view of the sulphur cycle, are also highlighted.

1 Introduction

Sedimentary organic sulphur compounds (OSCs) are a ubiquitous class of compounds, which directly reflect the prevailing mechanisms of organic matter (OM) preservation, thereby recording the paleoenvironmental signature (Sinninghe Damsté and De Leeuw 1990; Werne et al. 2004). Thousands of sedimentary OSC, some with assumed biomarker carbon skeletons, were identified during the 1980s

(Sinninghe Damsté and De Leeuw 1990) and in the following decades (Adam et al. 1991; Kohnen et al. 1993; Schaeffer et al. 1993, 1995, 2006; Sinninghe Damsté and Rijpstra 1993; Vairavamurthy et al. 1994; Poinsoot et al. 1997; Sinninghe Damsté et al. 1999; Squier et al. 2003; van Dongen et al. 2006; Junium et al. 2011). Some sulphurized compounds are linked to a precursor biomarker, but many are still of unknown affinity (e.g., Poinsoot et al. 1998; Pancost et al. 2001). Most of these OSCs result from secondary incorporation of sulphur into the OM during early diagenesis (“sulphurization”). This process imparts a substantial overprint on the resulting molecular signature, with consequences for paleoenvironmental interpretation (Kohnen et al. 1991a, 1992; Sinninghe Damsté et al. 1995; Koopmans et al. 1997; Köster et al. 1997; Kok et al. 2000a). Since the landmark review by Sinninghe Damsté and De Leeuw (1990), several other papers have discussed specific aspects of sedimentary OSC (Aizenshtat et al. 1995; Anderson and Pratt 1995; Aizenshtat and Amrani 2004a, b; Werne et al. 2004; Amrani 2014; Greenwood et al. 2015).

This review considers the biogeochemistry of sedimentary OSC, their formation pathways, and their effect on the biomarker distributions in young sediments and immature sedimentary rocks, focusing on advances documented since Sinninghe Damsté and De Leeuw (1990).

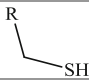
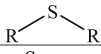
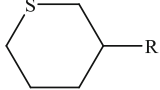
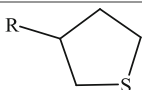
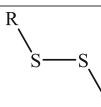
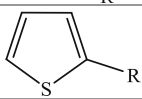
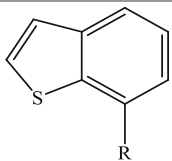
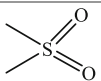
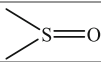
The term *sediments* is used synonymously when its age is not important for the discussion. When it is, we use the term *young sediments* for recent or modern systems (i.e., mainly not older than Holocene, 10,000 years), in which the sediments were not necessarily lithified and sulphurization processes are still active (see Sect. 3.3), and the term *immature sedimentary rocks* when dealing with older sediments that were lithified, but were not matured thermally (at least not extensively). The linkages of the marine sulphur and organic carbon cycles are discussed, which is essential to understanding the information that OSCs convey. This synthesis includes the more “traditional” view of sulphur incorporation, leading to the formation of sulphurized biomarkers, but highlights recent work suggesting possible new sources of sedimentary OSC. We then survey the progress made in identifying sulphurized biomarkers and how they affect paleoenvironmental records. Though the use of OSC as proxies for maturation and other thermochemical processes is extensive and important, it is beyond the scope of the current review and will only be discussed briefly.

2 Nomenclature, Methods, and Instrumentation for the Characterization of Sedimentary Organic Sulphur Compounds

2.1 Nomenclature and Chemical and Thermal Treatment for the Analysis of Organic S

Sedimentary OSCs comprise thousands of structures that can be found either in insoluble (e.g., protokerogen, kerogen) or soluble (polar and nonpolar) fractions of the OM. Table 1 summarizes the nomenclature and structures of the main sulphur moieties. Organic matter is often operationally divided into different fractions:

Table 1 Common sulphur moieties in sedimentary organic matter. R represents H or alkyl group

Compound class	Structure
Thiol (mercaptan)	
Sulphide (thioether)	
Thiane	
Thiolane (tetrahydrothiophene)	
Disulphide or polysulphide	
Aromatic S (thiophene)	
Fused aromatic S (benzothiophene)	
Sulphone	
Sulphoxide	

kerogen (insoluble in organic solvents) and the soluble fractions, e.g., asphaltenes (polar and macromolecular fraction), saturates (apolar), aromatics (slightly polar), and nitrogen, sulphur, and oxygen compounds (polar), with the saturate and aromatic fractions containing OSC amenable to gas chromatography (GC). These fractions might be considered to form a continuum, with decreasing size, heteroatom content, and polarity (Tissot 1984; Orr 1986). The preservation and distribution of these fractions highly depends on sulphurization at the molecular level, as well as on oxygen and nitrogen cross-linking (Koopmans et al. 1996a; Putschew et al. 1998; Farrimond et al. 2003; Amrani et al. 2007; McKee and Hatcher 2010). For example, pyrolysates of the asphaltene and kerogen fractions from an Upper Jurassic carbonate source rock exhibit striking similarities, except that the asphaltene has a lower OSC content. This suggests that the asphaltene differs from the kerogen primarily in terms of the number and nature of intermolecular linkages (van Kaam-Peters and Sinnighe Damsté 1997).

Several different analytical approaches can be used to effectively characterize sedimentary OSC constituents, including various preparative methods to make the

OSC amenable for measurement. For example, chemical or thermal degradation methods need to be applied to macromolecular and polar fractions, cleaving either C-S or S-S bonds, in order to release compounds bound by sulphur linkages. The common approaches for the study of OSC are presented in Table 2. This is not an exhaustive list, but provides a comprehensive overview of the most commonly applied approaches. Care needs to be taken as to which methods are applied, as some methods may mask original sulphur signatures.

2.2 Instrumentation for the Analysis of Organic S

Once OSCs are liberated from the macrostructure (e.g., asphaltene, kerogen), using chemical or thermal methods, their concentration, structural, and isotopic analysis requires liquid chromatography and other analytical techniques, some of which are specific for S compounds (Table 2). In young sediments and immature sedimentary rocks, many of the OSC are not thermally stable, especially those moieties with S-S bonds (Table 1). Because of their high reactivity, it is important to note that they can thermally react upon GC analysis, either in the injection port or on the column, and generate *artificial* OSC (Krein 1993; Schouten et al. 1994). Therefore, the characterization of OSC in young sediments should be performed with caution, preferably with the application of appropriate chemical degradation methods (e.g., MeLi/MeI, Table 2).

The most common separation and detection technique for sedimentary OSC is GC with a sulphur-specific detector, such as flame photometric detector (FPD) or sulphur chemiluminescence detector (SCD). Identification of the various OSCs, and quantification of lower abundance species, is typically performed by gas chromatography-mass spectrometry (GC-MS), with interrogation of the characteristic mass fragment ions for each of the major compound groups (e.g., Sinninghe Damsté and De Leeuw 1990). Other techniques and instruments (e.g., X-ray absorption near edge structure, Fourier-transform ion cyclotron resonance mass spectrometry (FT-ICR-MS)) are used for elemental analysis, determination of sulphur functionality distribution, and mass spectrometry of non-GC-amenable components, such as the kerogen, asphaltene, and polar fractions (Table 2).

2.3 Sulphur and Carbon Isotope Analysis

Since isotope chemistry is essential in understanding the geochemical processes discussed here, some basic definitions are given.

The *isotopic value* of a certain element is defined as:

$$\delta^{\text{H}}\text{X} = \left[\left(\frac{\text{H}\text{X}}{\text{L}\text{X}} \right)_{\text{sample}} / \left(\frac{\text{H}\text{X}}{\text{L}\text{X}} \right)_{\text{standard}} - 1 \right] \quad (1)$$

where X is the element (e.g., S) and the superscript H and L denote the fraction of the heavy and light isotopes, respectively (e.g., ^{34}S and ^{32}S or ^{13}C and ^{12}C). The ratio

Table 2 Summary of common approaches and methods for the characterization of sulphur-bearing OM

Approach	Chemical consideration	Method(s) or instruments	Comments	Refs ^b
Chemical cleavage^a	Selective for S-S and S-H bonds	MeLi/MeI	Cleaves S-S bonds and methylates the S attached to carbon (MeLi/MeI) or reduces it to the thiol (LiAlH ₄)	[1, 2]
		LiAlH ₄		
	Any S-S and C-S bonds for solvent-soluble OM (polar, asphaltene)	Raney nickel Nickel boride	Open cyclic structures. Hydrogenation step may be required following Raney Ni. Ni boride is better for less soluble fractions and allows deuteration	[3, 4]
Thermal cleavage^a	Any S-S and C-S bonds for non-soluble OM (kerogen)	Li/EtNH ₂	Labelling with deuterium is possible	[5–7]
		Ni(0)cene/ LiAlH ₄		
Thermal cleavage^a	Nonselective	Flash pyrolysis	High temperature (~610 °C) and short time pyrolysis (~10 s), online coupling to GC. Products do not preserve their original carbon skeleton	[8, 9]
	Nonselective	Closed system hydrous/ anhydrous pyrolysis	Medium temperatures (~160–360 °C), keeping some of the biomarkers intact for a later <i>offline</i> GC analysis A more time-consuming approach and the maximum yield of the biomarkers vary significantly with pyrolysis temperature. Useful for laboratory simulations of maturation	[10–14]

(continued)

Table 2 (continued)

Approach	Chemical consideration	Method(s) or instruments	Comments	Refs ^b
	Nonselective	Hydro (H ₂)-pyrolysis	Thermal cleavage under H ₂ pressure maximizes the fraction of GC-amenable products for offline analysis, while structural rearrangement of biomarker species is minimal The effect of the catalyst used ((NH ₄) ₂ MoO ₂ S ₂) on the compound-specific δ ³⁴ S values is not yet known	[15–18]
Isotopic analysis	Bulk OM	Isotope-ratio mass spectrometry (IRMS)	Most common is elemental analyzer coupled with IRMS. Kerogen must be isolated offline from other sulphur and mineral phases For a precise quartet sulphur isotope analysis, fluorination to SF ₆ is needed	[19, 20]
	Compound-specific isotopic analysis	GC-IRMS GC/MC-ICPMS	Measured on apolar volatile compounds. S isotope analysis is achieved by a GC coupled with multicollector inductively coupled plasma mass spectrometry (GC/MC-ICPMS). Often liquid chromatography is needed before isotope analysis	[21, 22]
Elemental analysis	High-resolution mass determination, providing molecular elemental composition	Fourier-transform ion cyclotron resonance mass spectrometry (FT-ICR MS)	Solid-phase extraction technique for water-soluble compounds (DOM) should precede the FT-ICR MS analysis	[23–25]

(continued)

Table 2 (continued)

Approach	Chemical consideration	Method(s) or instruments	Comments	Refs ^b
Nondestructive	Identification of S functionalities	X-ray absorption near edge structure (XANES)	May be applied to solid samples including kerogen. No chemical pretreatment needed. Relative crude abundance of S moieties such as thiophenes, sulphonic acids, sulphoxides, and sulphonates	[26, 27]

^aCleavage is followed by gas chromatography (GC) coupled with specific S detectors (flame photometric detector (FPD), sulphur chemiluminescence detector (SCD)) or mass spectrometer (MS, see characterized fragments in Table 1)

^bReferences: 1. Eliel et al. (1976); 2. Kohnen et al. (1991b); 3. Sinninghe Damsté et al. (1988); 4. Sinninghe Damsté et al. (1994); 5. Hofmann et al. (1992); 6. Hartgers et al. (1997); 7. Richnow et al. (1992); 8. Eglinton et al. (1992); 9. Goñi and Eglinton (1994); 10–14. Koopmans et al. (1995, 1996a, b, 1997, 1998); 15. Love et al. (1997); 16. Lockhart et al. (2008); 17. Murray et al. (1998); 18. Grotheer et al. (2017); 19. Giesemann et al. (1994); 20. Grassineau (2006); 21. Amrani et al. (2009); 22. Hayes et al. (1990); 23. Dittmar et al. (2008); 24. Ksionzek et al. (2016); 25. Pohlabein and Dittmar (2015); 26. Vairavamurthy et al. (1994); 27. Sarret et al. (2002)

between these two isotopes in a sample is normalized to an internationally accepted standard (e.g., Vienna Canyon Diablo Troilite (V-CDT) in the case of sulphur). The $\delta^{\text{H}}\text{X}$ notation is a relative scale, expressed as a per-mil (‰) deviation of the sample from that of the standard. Negative values of $\delta^{\text{H}}\text{X}$ imply that the element in the sample is “lighter” compared to the internationally defined standard, while positive values are considered to be “heavier.”

For a given reaction, the *isotopic fractionation* generated by it is defined as:

$$\varepsilon_{\text{A} \rightarrow \text{B}} = (\delta^{\text{H}}\text{X}_{\text{B}} - 1,000) / (\delta^{\text{H}}\text{X}_{\text{A}} - 1,000) - 1 \quad (2)$$

where the subscripts A and B denote the reagent (e.g., SO_4^{2-}) and product (e.g., H_2S), respectively, for a given reaction (e.g., sulphate reduction). The most common methods for sulphur ($^{34}\text{S}/^{32}\text{S}$) and carbon ($^{13}\text{C}/^{12}\text{C}$) isotope analysis are described in Table 2.

3 The Marine Sulphur Cycle and Its Impact on Organic Matter

3.1 The Link Between the Sulphur and Organic Carbon Cycles

Sulphur, with its multiple oxidation states (from -2 to $+6$), participates in many biochemical processes in conjugation with the carbon cycle, such as biosynthesis of proteins, and as electron donor/acceptor for respiration (Sievert et al. 2007). Hence,

these two elements mutually affect the fate of each other through their biogeochemical cycles. Figure 1 conceptually illustrates the coupling between sulphur and organic carbon in the marine system. Sulphate (SO_4^{2-} , oxidation state S^{6+}) is the most stable form of sulphur in the ocean today. It participates in two major biochemical processes, which eventually reduce it into H_2S , namely, *assimilatory sulphate reduction* (point # 1a, Fig. 1) and *dissimilatory sulphate reduction* (point # 2, Fig. 1).

Assimilatory sulphate reduction (ASR) is the metabolic pathway employed by organisms to incorporate SO_4^{2-} into constituents of the living cell. In this process, sulphate is enzymatically reduced first to sulphite and then to H_2S , whereupon the sulphide can be incorporated into, e.g., the amino acids cysteine and methionine (Schiff 1980). Each reaction step requires ATP, and thus it is an energy-consuming process (Takahashi et al. 2011). This is a fundamental biochemical process, given sulphur's essential requirement for life. Quantitatively, sulphur constitutes on average about 1% of the dry mass of living organisms (Shen and Buick 2004; Sievert et al. 2007), with a Redfield ratio similar to phosphorus ($\text{C}_{124}\text{N}_{16}\text{P}_1\text{S}_{1.3}\text{K}_{1.7}$) in many marine phytoplanktons (Ho et al. 2003). Because in this pathway sulphur is biologically incorporated into functional molecules needed by living organisms (e.g., as the amino acid cysteine, point #1b in Fig. 1), it is termed a *biotic sulphurization* pathway.

Dissimilatory sulphate reduction is a fundamentally different type of process. In many environments on Earth, such as below the water-sediment interface of aquatic systems, oxygen becomes depleted. Important groups of bacteria and archaea, known as *microbial sulphate reducers* (MSR), are capable of using SO_4^{2-} as the electron acceptor for respiration. This ubiquitous process of anaerobic environments is termed *dissimilatory sulphate reduction* since the reduced sulphur species (typically H_2S) is released back into the environment (point # 2 in Fig. 1; Rabus et al. 2006). The dissimilatory sulphate reduction process utilizes organic matter as the electron donor and is an energy-yielding metabolic process. It has a critical effect on both the carbon and sulphur cycles. Studies on young sediments suggest that this process can remineralize up to ~80 to 90% of initially buried organic carbon (Kasten and Jørgensen 2000 and references therein). However, the H_2S produced will rapidly react with available iron to form pyrite (point #7, Fig. 1) or be available to react with the remaining dead OM via *abiotic sulphurization* (points # 8–10, Fig. 1), thus fostering OM preservation.

Pyrite is usually the major sink for reduced sulphur species in the geological record, with sedimentary OSC being the second largest sink (Bernier and Raiswell 1983; Bernier 1984; Werne et al. 2004). In some cases (e.g., carbonate depositional environments) such as in the Ghareb Formation, limited iron availability leads to sedimentary OSC becoming the major sink (Minster et al. 1992; Alsenz et al. 2015). It has also been suggested that sulphurization of OM can even compete with pyrite formation, despite the presence of Fe (Urban et al. 1999; Filley et al. 2002; Shawar et al. 2018). Thus, understanding the interplay between organic carbon, reduced sulphur, and iron in a sedimentary sequence is essential to paleoenvironmental interpretation. Like OSC, the formation of pyrite also depends on the supply of

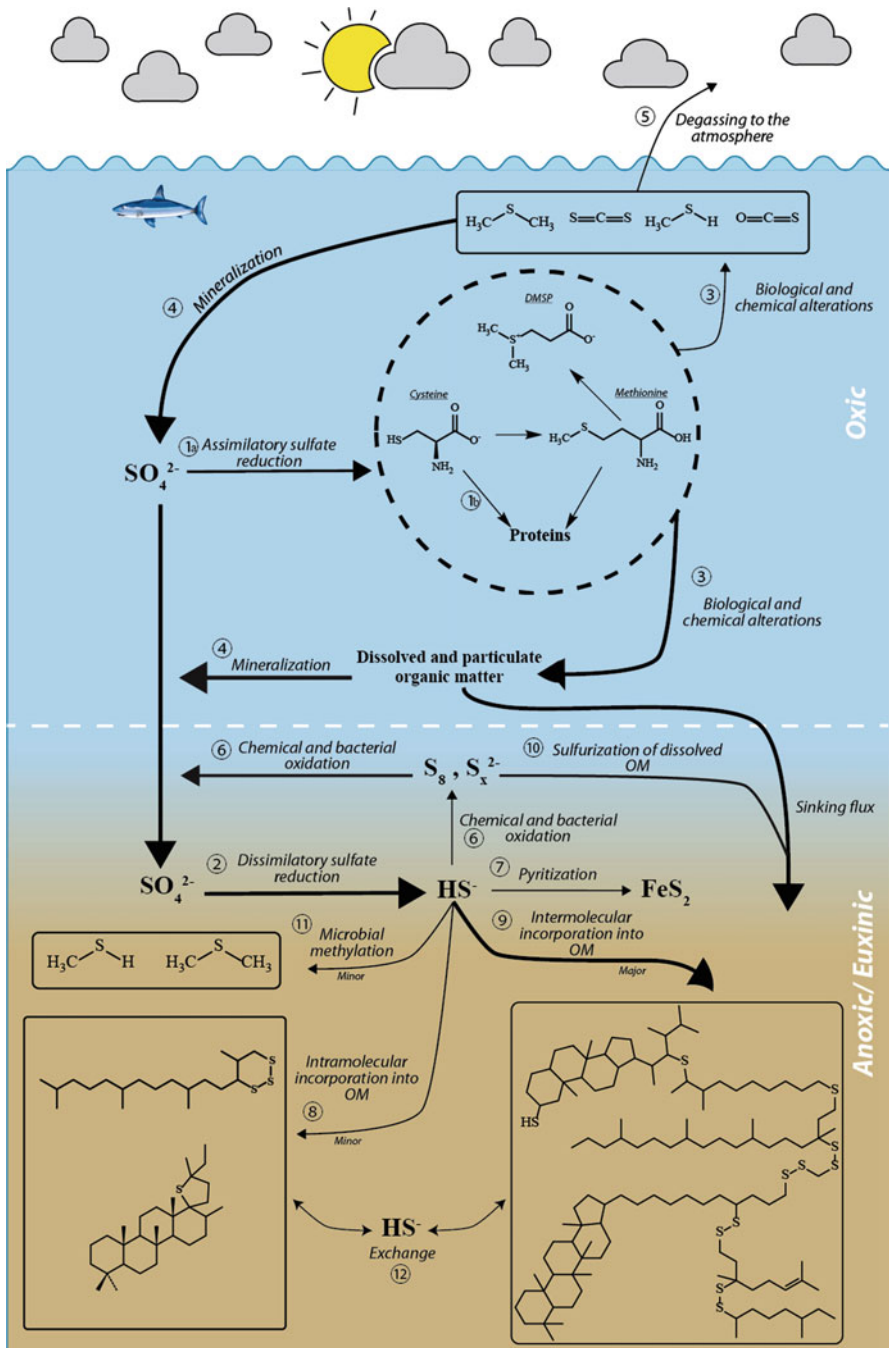


Fig. 1 (continued)

labile OM (Schoonen 2004), and clear correlations between pyritic S and total organic carbon (TOC) have been demonstrated (Berner and Raiswell 1983; Berner 1984). Accordingly, cross plots and ternary diagrams using bulk elemental concentrations (i.e., total S, Fe, and organic C) can be applied to elucidate the oxidation state of young and ancient environments (Dean and Arthur 1989; Morse and Emeis 1992; Leventhal 1995).

3.1.1 Isotopic Evidence for the Abiotic Sulphurization Pathway of Sedimentary Organic Matter

The assimilatory and dissimilatory sulphate reduction pathways have distinctive isotopic fractionations for sulphur ($\epsilon_{\text{Assimilatory}} = -1$ to -3‰ (Kaplan and Rittenberg 1964), $\epsilon_{\text{Dissimilatory}} = -20$ to -75‰ (see summary table in Brunner and Bernasconi 2005; Sim et al. 2011)). The very light $\delta^{34}\text{S}$ generated by the dissimilatory pathways recorded in pyrite was suggested as evidence that microbial sulphate reducers are one of the most ancient forms of life on Earth, dated back to 3.47 Ga (Shen and Buick 2004). Similarly, the large isotopic difference between the assimilatory and dissimilatory pathways is a powerful evidence for the significance of the abiotic sulphurization in sedimentary OM (Amrani 2014).

Abiotic sulphurization, based on isotopic mass balance consideration, is estimated to account for at least 75–90% of total sedimentary organic sulphur (Anderson and Pratt 1995; Werne et al. 2004). Biosynthetic OSCs are generally biologically and chemically labile, typically being remineralized quickly (points # 3–4, Fig. 1). In contrast, secondary OSCs from abiotic sulphurization are more stable and less accessible to microbial degradation (Sinninghe Damsté and De Leeuw 1990; Grice et al. 1998). Therefore, it is expected that in the course of diagenesis, the fraction of secondary sulphur will increase over that of primary biosynthetic, through both the degradation of biosynthetic compounds and also via the incorporation of inorganic S species (Aizenshtat et al. 1983; Mossman et al. 1991).

The pathways and the role of abiotic sulphurization on the OM are discussed in more detail below. However, new studies on sulphur of biotic origin raise new questions on the role of biotic sulphurization in the sedimentary record and are addressed in more detail in Sect. 3.5.



Fig. 1 A conceptual drawing of the marine sulphur cycle and its coupling to the organic carbon cycle. Annotated numbers showing important pathways as discussed in the text: Assimilatory sulphate reduction pathway, introducing OSC of biogenic origin (1), while dissimilatory sulphate reduction generates reduced sulphur species (2). The biotic OSC are labile and undergo biological and chemical alteration (3), some of which can be further remineralized back to SO_4^{2-} (4), degassed to the atmosphere as volatile OSC (5), or sink to the sediment. The assimilatory reduced sulphur (e.g., HS^-) can be oxidized (6) and can react with iron to precipitate pyrite (7) or with OM leading to different pathways of secondary sulphurization (7–11) and OM preservation. Exchange of S between these different fractions of OSC (free and bound) is possible during diagenesis (12)

3.2 Mechanism of Abiotic Sulphurization

Abiotic sulphurization pathway requires three main biogeochemical conditions (Werne et al. 2004; Amrani 2014): (1) presence of reduced S species, (2) low concentration of metal ions, and (3) supply of reactive organic compounds. While H_2S is supplied by the MSR, subsequent biological and chemical oxidation processes produce elemental S and S_x^{2-} (point # 6, Fig. 1). Polysulphide anions are stronger nucleophiles and thus react faster with organic compounds than $\text{H}_2\text{S}/\text{HS}^-$ (LaLonde et al. 1987; Loch et al. 2002; Amrani and Aizenshtat 2004c; Wu et al. 2006). The presence of reduced sulphur species (HS^- , S_x^{2-}) thereby facilitates sulphur incorporation into OM, while metal ions forming insoluble sulphides, especially Fe (II), compete with OM for the available sulphur. When metal ions are in low concentrations (e.g., carbonate environments) sulphur incorporation into OM is often favored. In some settings, sulphurization of OM may compete with pyrite formation despite the presence of Fe (Urban et al. 1999; Filley et al. 2002). More specifically, it was suggested that in OM-rich and Fe-poor environments, iron species can be scavenged by organic compounds to form Fe-organic complexes, thus limiting the formation of pyrite and enhancing the formation of OSC (Shawar et al. 2018). Finally, not all OM may react with the available reduced sulphur species. Rather, a supply of organic compounds with appropriate functional groups (e.g., conjugated double bonds, carbonyl groups), which can react with reduced sulphur species, is required.

The potential and rate of a given biomarker to undergo abiotic sulphurization strongly depends on the reactivity of the organic precursor, with the carbonyl functionality and conjugated double bond systems being the most reactive (Schouten et al. 1994; Adam et al. 2000; Kok et al. 2000a; Amrani and Aizenshtat 2004a). Prior to sulphurization, early diagenetic changes (point # 3, Fig. 1) can increase the sulphurization potential of some compounds by altering less reactive functionalities (e.g., isolated double bonds, alcohols) to more labile moieties, such as carbonyl groups and conjugated double bonds (Grossi et al. 1998; Rontani et al. 1999; Schaeffer et al. 2006; Blumenberg et al. 2010). Inorganic reduced S species (e.g., HS^- , S_x^{2-}) attack the functional sites of organic precursors via nucleophilic, electrophilic, or radical mechanisms, generating an initial C-S bond (Amrani 2014). Some of these initially formed C-S bonds and S-S bonds subsequently undergo continuous exchange with the surrounding inorganic reduced sulphur pool (Amrani et al. 2006). The specific chemical mechanisms for sulphurization are still a matter of debate and are beyond the scope of this review. The interested reader is referred to other reviews that summarized previous works, under variable chemical and physical conditions, that attempted to simulate sulphurization in the laboratory (Krein 1993; Werne et al. 2004; Amrani 2014).

Abiotic sulphurization can proceed via two general pathways, *intramolecular* and *intermolecular* sulphurization which lead to free OSC and bound OSC products, respectively (Sinninghe Damsté and De Leeuw 1990). An intramolecular S cyclic structure is formed if the S-bound can create another S-C bond on the same molecule (point # 8, Fig. 1). Common S moieties that form by the intramolecular pathway are

thianes, thiolanes, thiophenes, benzothiophenes, and dibenzothiophenes (Table 1, Fig. 4; Krein 1993). In this context, aromatic compounds are usually indicative of OM which is more thermally mature (Krein and Aizenshtat 1995; Rosenberg et al. 2017). Intermolecular C-S and S-S cross-linkages may occur when a second bond on the same molecule cannot be formed (e.g., the next reactive site is too far or does not exist), enabling the S functionality to react with a second molecule (point # 9, Fig. 1). These compounds can form monosulphidic (C-S-C), disulphidic (C-S-S-C), or polysulphidic (C-S_x-C) bonds (Werne et al. 2004). Successive intermolecular sulphurization cross-links more and more compounds into a macromolecules, which eventually contributes to the formation of kerogen. It is important to note that cross-linking of organic compounds is not limited to sulphur bridges. Oxygen, and possibly nitrogen, also may play a role in the cross-linking of organic compounds and thus the preservation of OM in sediments (Koopmans et al. 1996a; Putschew et al. 1998; Farrimond et al. 2003; Amrani et al. 2007; McKee and Hatcher 2010).

The intramolecular sulphurization pathway creates OSC that, if not further bound into the macromolecule, may be found in the free, apolar fraction of petroleum and bitumen. The number of suitable functional groups of a given precursor will affect its sulphurization pathway (i.e., intermolecular, intramolecular, or both) and the mode of occurrence in an immature sedimentary rock (i.e., in the macromolecules or as a free OSC) (Kohnen et al. 1992). At early stages of diagenesis, different chemical alterations can take place leading to multiple routes of S addition (Schaeffer et al. 2006; Amrani 2014). Thus the occurrence of OSC with a given carbon skeleton in different fractions of the OM (free OSC and bound OSC) does not necessarily imply that these were two distinguished biological precursors. Moreover, it is important to note that through the diagenetic process, there may be interaction between free OSC and bound OSC fractions (point # 12, Fig. 1; Amrani et al. 2006).

Following the discussion above, OM is operationally divided into three pools: (1) free (GC-amenable) hydrocarbons that were not sulphurized; (2) free (GC-amenable) OSC that derive from intramolecular sulphurization and were not further cross-linked into the macromolecular structure, hereafter termed “free OSC”; and (3) S-bound (i.e. cross-linked) – compounds that were sulphurized intermolecularly into the macrostructure of the organic matter hereafter termed “bound OSC.”

3.3 Timing of Abiotic Sulphurization

Timescales of 60–10,000 years have been reported for the sulphurization of different compounds within the sediment column (Wakeham et al. 1995; Urban et al. 1999; Kok et al. 2000a, b; Werne et al. 2000; Farrimond et al. 2003; Sinninghe Damsté et al. 2007). This reflects the fact that below the water-sediment interface, the environment becomes rapidly anoxic when burrowing macrofauna are absent (Werne et al. 2004). In extreme cases, extensive parts of the water column can be anoxic or even euxinic (e.g., Black Sea, Cariaco Basin; Wakeham et al. 2007; Raven et al. 2016), where the chemocline of O₂ is very shallow and H₂S is detected below

it. In such settings, abiotic sulphurization may occur within the water column as the organic particles sink through it, on a timescale of days (Raven et al. 2016). Such rapid sulphurization rates are supported by laboratory experiments, with reaction times ranging from minutes to weeks for different functionalities (Amrani and Aizenshtat 2004a).

When sulphurization rate is considered at the molecular level, additional complexity arises, thus affording further insight into the process and its paleoenvironmental significance. Since sulphurization depends (among other factors) on the reactivity of the precursor, different precursors will undergo sulphurization at different rates. For example, in young sediments of Ace Lake (Antarctica), Kok et al. (2000a) found that only steroid biomarkers were extensively sulphurized. Further into the diagenetic process (i.e., deeper sediments), other classes of biomarkers (e.g., isoprenoids, hopanoids) can be found primarily in a sulphurized form or even exclusively in the S-bound OSC fraction (e.g., the dinosteranes; Kohlen et al. 1992). The sulphurization process may continue deeper in the sediments, sulphurizing other, less reactive classes of organic compounds, fueled by other biogeochemical processes. For example, deeper in the sediments, where SO_4^{2-} becomes depleted, a consortium of anaerobic methane-oxidizing bacteria and sulphate-reducing bacteria (AOM-SR) can produce significant amounts of H_2S (Kasten and Jørgensen 2000). The AOM-SR microbial consortium is constrained to a narrow depth interval at the sulphate-methane transition zone, but the overall effect is that the H_2S maxima is located between the zones of MSR and AOM-SR. Recently, Quijada et al. (2016) showed in the Cariaco Basin that the maximum of OM sulphurization is associated with this maxima of H_2S concentration between the MSR and AOM-SR zones.

3.3.1 Sulphur Isotope Considerations

In most young sediments, the $\delta^{34}\text{S}$ of all bulk phases (H_2S , SO_4^{2-} , pyrite, kerogen) increases with depth (Fig. 2) as a result of the MSR process acting in a closed system for sulphate (e.g., Werne et al. 2003). Both OSC and pyrite respond to this effect, but there is a S isotope difference between them, with an average discrepancy of 10‰ globally (Anderson and Pratt 1995). Several scenarios have been suggested to explain this phenomenon (see detailed discussion in Anderson and Pratt 1995; Amrani 2014). One such scenario is the potentially different timing of sulphurization for Fe and organic compounds. Indeed, reactive iron species are likely to outcompete organic compounds for reduced S species (Gransch and Poshtuma 1974; Hartgers et al. 1997), thereby taking the most ^{34}S -depleted fraction from the MSR according to the Rayleigh distillation model. However, several studies have shown that during early diagenesis, OSC may form simultaneously with Fe sulphurization or even outcompete it (Bates et al. 1995; Brüchert and Pratt 1996; Urban et al. 1999; Filley et al. 2002; Werne et al. 2003; Riedinger et al. 2017). The variability in S isotopes as a result of the different timing of sulphurization and/or reactive S species may be recorded by specific OSC, whereas bulk S phases such as pyrite and kerogen average it out (Amrani 2014). Compound-specific sulphur isotope analysis (CSSIA) data may unravel this process (Amrani et al. 2009).

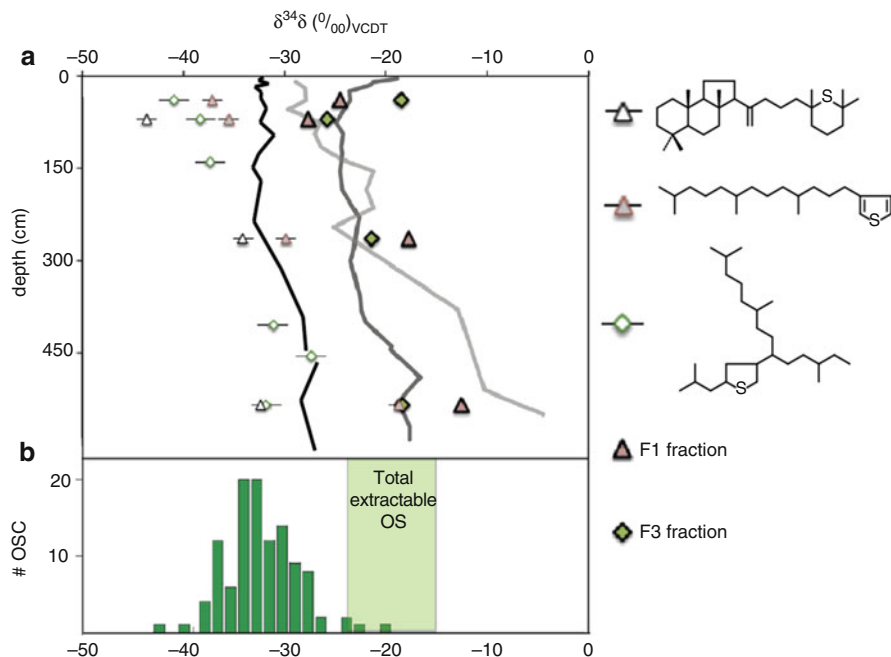


Fig. 2 Early sulphurization in the Cariaco Basin sediments. Sulphur isotopic values of inorganic compounds, extractable OM fractions, and individual OSC. (Panel a) Porewater sulphide (light gray line), residual OS (dark gray line), and pyrite S (black line). Symbols with thick outlines indicate $\delta^{34}\text{S}$ values of bulk extractable OM fractions F1 (apolar, triangles) and F3 (polar, diamonds). Open symbols indicate $\delta^{34}\text{S}$ values of individual GC-amenable compounds in these fractions – tri-terpenoid thiane in F1 (open triangles), C_{20} isoprenoid in F1 (shaded triangles), and HBI thiolanes in F3 (diamonds). (Panel b) Histogram of all compound-specific measurements from Cariaco Basin sediment extracts, including both assigned and unidentified compounds. The shaded area represents the range of $\delta^{34}\text{S}$ measured for total extractable OS. (Modified from Raven et al. (2015) and Werne et al. (2003))

Raven et al. (2015) used CSSIA in young sediments from the Cariaco Basin. Large S isotopic variability between the different OSC was observed (up to 23‰). Moreover, they have shown an intriguing phenomenon where some specific OSCs were ^{34}S -depleted relative to pyrite, while the bulk organic S was ^{34}S -enriched compared to pyrite (Fig. 2). Raven et al. (2015) explained their observations by different sulphurization mechanisms, either kinetic or equilibrium effects that are associated with ^{34}S depletion or enrichment of the OSC, respectively (Amrani and Aizenshtat 2004a; Amrani et al. 2008). They further suggested that the kerogen is ^{34}S -enriched relative to the measured individual OSC because there is a significant contribution of ^{34}S -enriched organic sulphur from the overlying water body (Raven et al. 2016).

In another recent CSSIA study on the immature Ghareb Formation, a wide range of $\delta^{34}\text{S}$ values (up to 14‰) of individual OSC has also been observed

(Shawar et al. 2015). However, all of the measured OSC were ^{34}S -enriched relative to the coexisting pyrite throughout the studied section (~350 m). The bigger variability in $\delta^{34}\text{S}$ of OSC of the young Cariaco sediments (23‰) compared to the immature Ghareb Formation (14‰, Late Cretaceous) might reflect S isotope exchange and homogenization with inorganic S species and other diagenetic processes during later stages (Amrani et al. 2006; Rosenberg et al. 2017). It is also possible that some of the most reactive organic compounds in the Cariaco Basin may react with reduced S species shallower within the sediments than the reaction of S with Fe species to form Fe sulphides (Shawar et al. 2018). The timing of sulphurization in the Rayleigh distillation sequence probably dictates the $\delta^{34}\text{S}$ of both pyrite and OSC. Formation of pyrite later than OSC may be the result of faster reaction kinetics of some organic compounds with reduced S, very high abundances of organic matter, or some hindrance to Fe sulphide formation as was suggested by Shawar et al. (2018). More detailed CSSIA studies from young sediments to mature rocks are needed to answer such questions.

3.4 Sulphurization as OM Preservation Mechanism

An important geochemical consequence of the sulphurization process is better preservation of the OM record. Because most components of living OM are chemically and biologically labile (e.g., proteins and carbohydrates), the preserved fraction in the sedimentary record is not necessarily representative of the original input. Upon diagenesis, more refractory compounds are preferentially preserved, and the initial distribution between terrestrial and marine input (see review by Arndt et al. 2013), or between plankton and heterotroph populations (Wakeham et al. 1997), can be distorted. Since sulphurization quenches reactive OM sites and binds biomolecules into macromolecules, it makes the organic matter less susceptible to microbial consumption (Kohnen et al. 1992; Werne et al. 2004). Sulphurization of biologically labile carbohydrates is another example of the important preservation role of sulphurization in euxinic environments (Kok et al. 2000b; van Dongen et al. 2006).

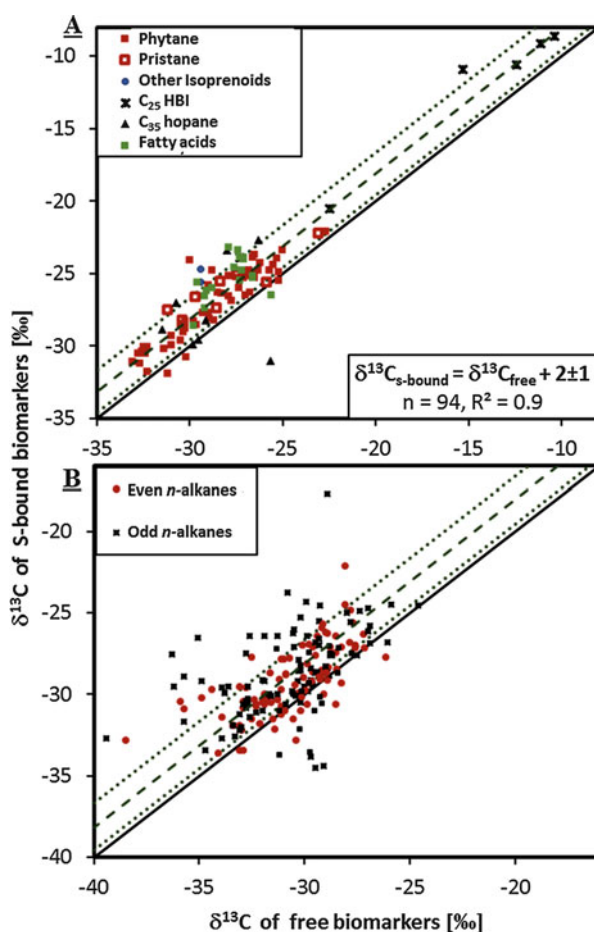
Indeed, many sedimentary rocks exhibit a strong correlation between bulk organic carbon and organic S, indicating that the fate of these elements is connected. Examples for such $\text{TOC-S}_{\text{organic}}$ correlation have been reported in the Monterey Formation (Zaback and Pratt 1992), the Kimmeridge Clay Formation (Lallier-Vergès et al. 1997), and the Ghareb Formation (Meilijson et al. 2015). Marine kerogens with atomic S-C ratios greater than ~0.04 are recognized as a unique type (type II-S, Orr 1986), reflecting the importance that S plays in preserving organic matter in such sedimentary rocks.

Another possible characteristic of preservation via sulphurization, notable at the molecular level, is suggested by compound-specific ^{13}C isotope studies. Through a compilation of literature data, Rosenberg et al. (2018) have found a consistent difference between the $\delta^{13}\text{C}$ of S-bound and free HC, where the former are heavier by $2 \pm 1\%$ on average (Fig. 3). The difference in $\delta^{13}\text{C}$ between these two fractions is rather constant, regardless of the type of the biomarkers (i.e., *n*-alkanes,

isoprenoids, HBIs, hopanes), the source of the compounds (e.g., marine vs. terrestrial, autotrophic vs. heterotrophic), the age of the rock (~235 to 5 Ma), the range of $\delta^{13}\text{C}$ (from ~ -30 to -10‰), and the prevailing paleoenvironment of each data point depicted in Fig. 3. The different mechanisms suggested to account for this difference include (A) kinetic isotope effects of the reactions involved in the sulphurization process (Schouten et al. 1995b) and (B) different sources of the original precursors of the biomarkers in the free HC and S-bound fraction having different $\delta^{13}\text{C}$ values (Kohnen et al. 1992; Grice et al. 1996).

Rosenberg et al. (2018) have suggested that a broader diagenetic process, such as the degradation of OM, may be responsible for the constant difference. As the free compound is more prone to degradation compared to its S-bound counterpart, it is possible that the $\delta^{13}\text{C}$ of the S-bound biomarker better represents the original $\delta^{13}\text{C}$ signature. Such preservation of the $\delta^{13}\text{C}$ record has significant geochemical

Fig. 3 $\delta^{13}\text{C}$ of S-bound biomarkers vs. $\delta^{13}\text{C}$ of free biomarkers for isoprenoid-based skeletons and fatty acids (a) and *n*-alkanes (b). Data was compiled from 17 different studies (e.g., Forster et al. 2008; Grice et al. 1996, 1998; Hefter et al. 1995; Kohnen et al. 1992; Putschew et al. 1995; Schouten et al. 1997, 2001, 1995b; Sinninghe Damsté et al. 2007, 2008). The complete list of references and more details can be found in Rosenberg et al. (2018). Bold black line is the 1:1 agreement line. The fine line and the two dashed lines are the best fit and the 1 stdev envelope after adjusting the slope to unity in plot A (i.e., reflecting a $2 \pm 1\%$ constant difference between the two axes)



implications, as carbon isotopes are often used for precursor identification and paleo- $p\text{CO}_2$ estimations (Sinninghe Damsté et al. 2008; Pagani 2014).

3.5 Other Possible Sources for Sedimentary Organic Sulphur

3.5.1 Volatile Organic Sulphur Compounds (VOSC) as a Possible Source to Sedimentary Organic Sulphur

In the photic zone of the ocean, some of the biogenic OSC are chemically or biologically altered and become volatile (hence, VOSC, point # 5, Fig. 1) such as methanethiol (MT), dimethyl sulphide (DMS), carbonyl sulphide (COS), and carbon disulphide (CS_2) (Liss et al. 1997). These VOSC are typically present in the surface ocean at low concentrations, in the range of 10^{-12} to 10^{-8} M (Mopper and Kieber 2002). Despite their low concentration, VOSC play a major role in the global sulphur cycle as they transfer sulphur from the ocean to the continents (Bates et al. 1992; Lomans et al. 2002; Lana et al. 2011). The most abundant oceanic VOSC is DMS that has been suggested to affect the Earth's radiative balance and cloud formation (Charlson et al. 1987; Levasseur 2013). DMS is produced by the enzymatic cleavage of dimethylsulphoniopropionate (DMSP) which is biosynthesized by phytoplankton in vast amounts as an osmoregulator as well as for several other suggested functions (Stefels et al. 2007).

At the present time, ocean-derived DMS is the primary source of sulphur to the atmosphere (Bates et al. 1992; Gondwe et al. 2003), yet only a small fraction of VOSC produced in the ocean is released to the atmosphere. A complex set of reactions in the ocean can oxidize VOSC back to sulphate (point # 5, Fig. 1), or they can be consumed as sources of sulphur and carbon by microbial populations (Kiene and Linn 2000; Simó et al. 2009). Alternatively, VOSC can react with DOM or metals to form complexes and be deposited with the sediment (Stefels et al. 2007), where they may provide another source of S that participates in the formation of sedimentary OSC. The magnitude of this flux is as yet unknown.

Under anoxic conditions (e.g., stratified water body or sediment), VOSC can also be formed in situ (as opposed to transfer from the surface water) via different formation pathways (Lomans et al. 2002; Higgins et al. 2006). For example, DMS can be formed by microbial reduction of dimethyl sulphoxide (DMSO) and sequential methylation of H_2S (evolved from MSR) by enzymatic activity carried out by a variety of microorganisms, possibly including methanogens (Stets et al. 2004; Zhuang et al. 2017 and references therein).

Several studies provide isotopic evidence for the dissimilatory sulphur source of VOSC in anoxic environments. For example, Oduro et al. (2013) have shown that VOSC in stratified freshwater of Fayetteville Green Lake (NY, USA) are ^{34}S -depleted, down to about -30% , close to the coexisting H_2S $\delta^{34}\text{S}$ value. These authors suggested a combination of biological and abiotic processes in the formation of VOSC that involved reactive sulphur species evolved from MSR and methyl groups of lignin components. In a compound-specific sulphur isotope study, DMS in the hypolimnion (during summer) of the freshwater Lake Kinneret (Israel) was ^{34}S -depleted, similar to the coexisting H_2S (Sela-Adler et al. 2016). When the lake

was mixed (winter), DMS was ^{34}S -enriched, similar to DMSP and coexisting sulphate as also observed in oxic oceanic basins (Oduro et al. 2012; Amrani et al. 2013). In the sediment of Lake Kinneret, DMS has mixed sources between dissimilatory S (^{34}S -depleted, e.g., methylation of H_2S) and assimilatory S (^{34}S -enriched) from the degradation of detrital OSC (Sela-Adler et al. 2016). Kiene (1988) was the first to identify this pool of “DMS” and suggested that the precursors could be sulphonium compounds or DMS that were absorbed to sediment particles and could only be released by a strong base treatment. This “base-hydrolyzable” DMS fraction is two to three orders of magnitude more concentrated (10–200 $\mu\text{mol}/\text{kg}$ sediment) than the dissolved DMSP and DMS. Therefore, this fraction represents a significant quantity of S that might also contribute to CH_4 formation (by demethylation) in anoxic sediments (Kiene 1996). This is a widespread phenomenon, occurring in sediments from all over the world, including diverse settings such as freshwater lakes, salt marshes, subtidal, intertidal, carbonate, and across a range of water depths (Kiene 1988, 1996; Kiene and Service 1991; Sela-Adler et al. 2016; Zhuang et al. 2017). Vairavamurthy et al. (1997) have noted a similar phenomenon in marsh sediments from Shelter Island (NY, USA), since their “base-hydrolyzable” 3-mercaptopropionate (3-MPA) is another DMSP degradation product. Since such “base-hydrolyzable” fractions of OSC are associated with the sediment, they are protected from biodegradation and can escape mineralization at the very early stages of diagenesis (Kiene 1996). Vairavamurthy et al. (1997) estimated the age of the “base-hydrolyzable” 3-MPA to be 90 years, well into the timing of abiotic sulphurization of OM. Therefore, this “base-hydrolyzable” OSC, once released from its association with sediment particles, might react with other organic compounds to form secondary sulphur compounds (i.e., part of protokerogen or humic substances) that could be preserved through diagenesis. It has been shown that compounds such as thiols act as good nucleophiles for sulphurization and formation of other OSCs (Amrani et al. 2008). Hypothetically, it is therefore conceivable that some sulphurized biomarkers might carry sulphur from this source; that is, they will have an assimilatory heavy $\delta^{34}\text{S}$ value. Combined compound-specific sulphur and carbon isotope determination for these “sediment-bound” OSC and sulphurized biomarkers in young sediment may reveal the significance of this process.

3.5.2 Refractory Biotic Organic Sulphur Compounds in the Ocean Possible Abiotic Sulphurization of Dissolved and Particulate Organic Matter

When organic compounds (e.g., DOM) enter sulphidic water, abiotic sulphurization can occur, potentially adding to the particulate sulphur that reaches the sediment. Sulphurization experiments of DOM (e.g., humic acids) with H_2S have shown incorporation into DOM, accompanied by oxidation of H_2S (Heitmann and Blodau 2006). However, these experiments were conducted at $\text{pH} = 6$ and thus may not be applicable to marine environments. In a recent study, Pohlabein et al. (2017) have carried out laboratory experiments to study the sulphurization of DOM with HS^- and S under anaerobic conditions. They found that sulphurization was nonselective for the chemical properties of the DOM precursors, such as saturation, aromaticity,

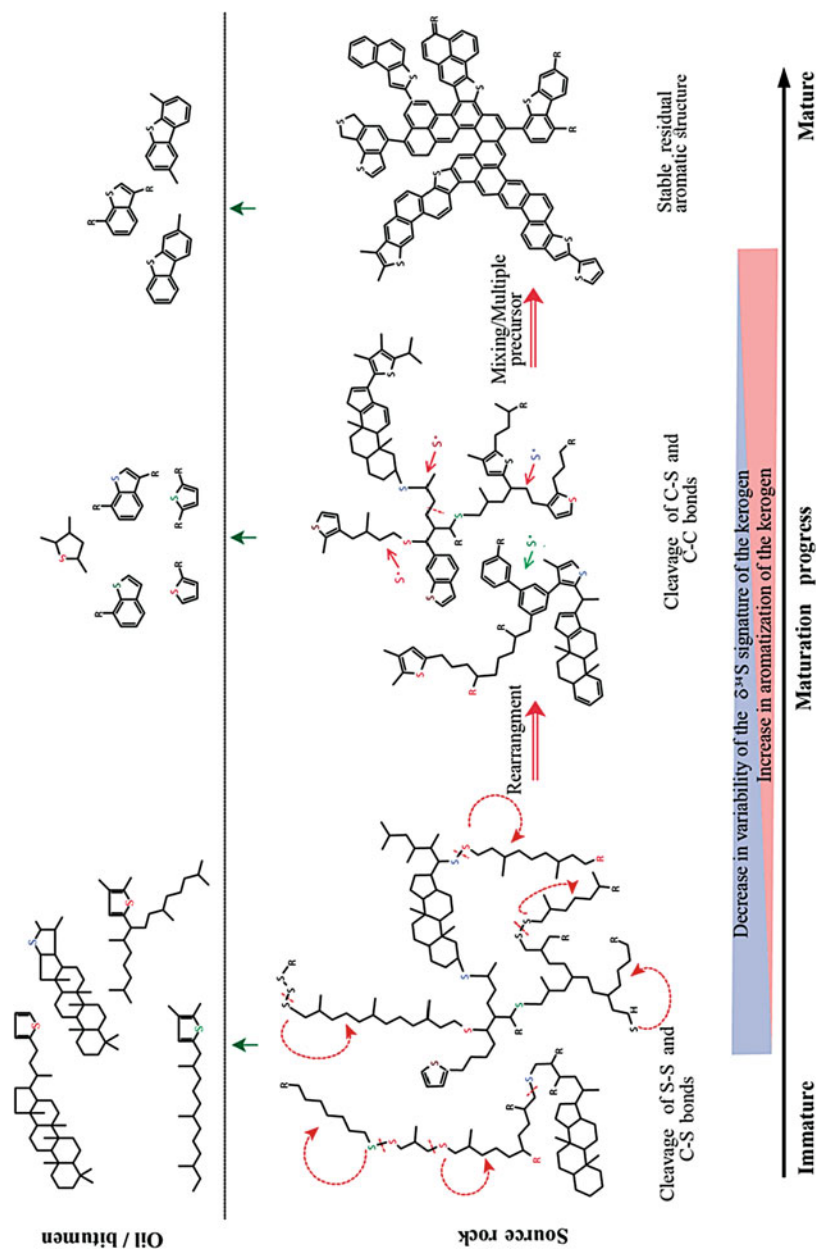


Fig. 4 (continued)

and degree of oxidation or heteroatom content (e.g., nitrogen). The authors concluded that sulphurization of DOM under anaerobic conditions is likely to be a major source of DOS in the open ocean. Using isotopic mass balance models, Raven et al. (2016) argued that abiotic sulphurization, in the water column of the Cariaco Basin, was responsible for 50% of the total organic sulphur found in the young sediment. However, rapid exchange of S isotopes between organic and reactive sulphur can commence even at moderate temperature, and thus the contribution of abiotic S from the water column may not be readily determined (point # 12, Fig. 1; Amrani et al. 2006). It is possible that refractory OSC may not participate in such organic-inorganic S isotope exchange, but further studies are needed to address this.

3.6 The Formation and Structural Modifications of Sedimentary OSC During Catagenesis

The discussion so far has dealt with the different pathways whereby OM and S are transferred from young sediments and into the geological record. With burial and increase of thermal stress on the sediments, the chemistry of OSC evolves further. Though the effects of thermal maturation (catagenesis) are beyond the scope of this review, some aspects are described here briefly to provide a more complete view of the S cycle. There is no definitive and clear line which separates diagenesis from catagenesis. Rather, they should be considered as a continuum, ranging between the realms of biochemical processes and temperature-driven reactions. The S-S and C-S bonds that were generated as a result of the sulphurization of the OM are weak relative to C-C bonds. This can lead to their further rearrangement to more stable bonds (i.e., aromatic) in the macromolecular structure, cleavage at relatively low thermal stress, and to the formation of radicals that further destabilize the OM (Tannenbaum and Aizenshtat 1985; Orr 1986; Baskin and Peters 1992; Martin 1993; Krein and Aizenshtat 1994; Koopmans et al. 1998; Lewan 1998; Aizenshtat and Amrani 2004a). Thus, apparently “thermally immature” sedimentary rocks may already have been altered to some degree by catagenetic processes (Siedenberg et al. 2018). In such cases, some of the “free” OSC may be different from those of the initial, low-temperature sulphurization products, with the formation of compounds such as alkylthiophenes rather than organic sulphides and polysulphides. With increasing maturation, the kerogen continues to rearrange into thermally more stable configurations, expressed as an increase in cyclization and aromatization of the kerogen, as well as the eventual generation of petroleum fluids (Fig. 4; Sinninghe



Fig. 4 A conceptual figure of kerogen maturation. The different colors of the S atoms represent different $\delta^{34}\text{S}$ values (i.e., high variability in $\delta^{34}\text{S}$). There is no sharp transition from the diagenetic to the catagenetic processes: they should rather be thought of as continuum, where the later becomes dominant as the transfer of organic carbon from the macromolecular structure to the free HC liquids increases. With thermal maturation, the kerogen continues to undergo rearrangement and structural changes. This is reflected by an increase in the aromatization and decrease in the variability of $\delta^{34}\text{S}$ values (represented by only black S atoms) of the OSC generated as oil and bitumen constituents

Damsté and De Leeuw 1990; Krein and Aizenshtat 1995). This gradual process is reflected by decreasing variability of $\delta^{34}\text{S}$ among the different OSC generated from the kerogen with progressive maturation (Rosenberg et al. 2017).

4 Application of Organic Sulphur Compounds in Paleoenvironmental Research

In the following sections, nine groups of biomarkers and their sulphurized derivatives are discussed. Studies in which these groups have been characterized in terms of their sulphurized fraction (free or bound OSC) are summarized in Table 3. For each group, we first briefly highlight their significance as biomarkers. Then, we discuss aspects related to their sulphurization sites, rates and extent of sulphurization, preservation, and biases of the geological record resulting from the sulphurization process. Where possible we discuss the potential benefit gained by quantifying sulphurized biomarkers in paleoenvironmental studies.

4.1 *n*-Alkanes

The distribution of *n*-alkanes is considered to be a marker of the relative input of marine vs. terrestrial organic matter into the depositional basin (Wakeham et al. 1995; Grice et al. 1996; Gelin et al. 1997; Hartgers et al. 1997; Peters et al. 2005). Their distribution and source is often represented by indices such as the carbon preference index (CPI) and odd-to-even predominance (OEP), which is occasionally used also for thermal maturity assessment (Peters et al. 2005). Under conditions where sulphurization takes place, *n*-alkanes occur as both free and S-bound compounds. However, the occurrence of *n*-alkane carbon skeletons as S-bound compounds might bear extra insight, not revealed by the free HC. The content of S-bound *n*-alkanes may greatly exceed (up to 90%) the content of their free-form counterparts (Fig. 5). Moreover, distributions of free and S-bound *n*-alkanes may be considerably different from one another (Fig. 5), leading to significant differences in the CPI and OEP indices (by a factor of 1.5–8) for a given sample (Koopmans et al. 1996a; Schouten et al. 1997, 2001; van Kaam-Peters and Sinninghe Damsté 1997; van Kaam-Peters et al. 1998). Strong even-over-odd carbon number predominance of the *n*-alkanes released by desulphurization was observed, in contrast to the OEP of the free *n*-alkanes fraction (Schaeffer et al. 1995; Koopmans et al. 1996a; van Kaam-Peters et al. 1998). Schaeffer et al. (1995) noted that the even-over-odd distribution of bound *n*-alkanes is widespread in evaporitic sediments, but did not identify the responsible mechanism. Schouten et al. (2001) suggested that different distributions of *n*-alkanes in the free and S-bound fractions of the Monterey Formation represent a predominant origin from terrestrial and marine sources in each of these fractions,

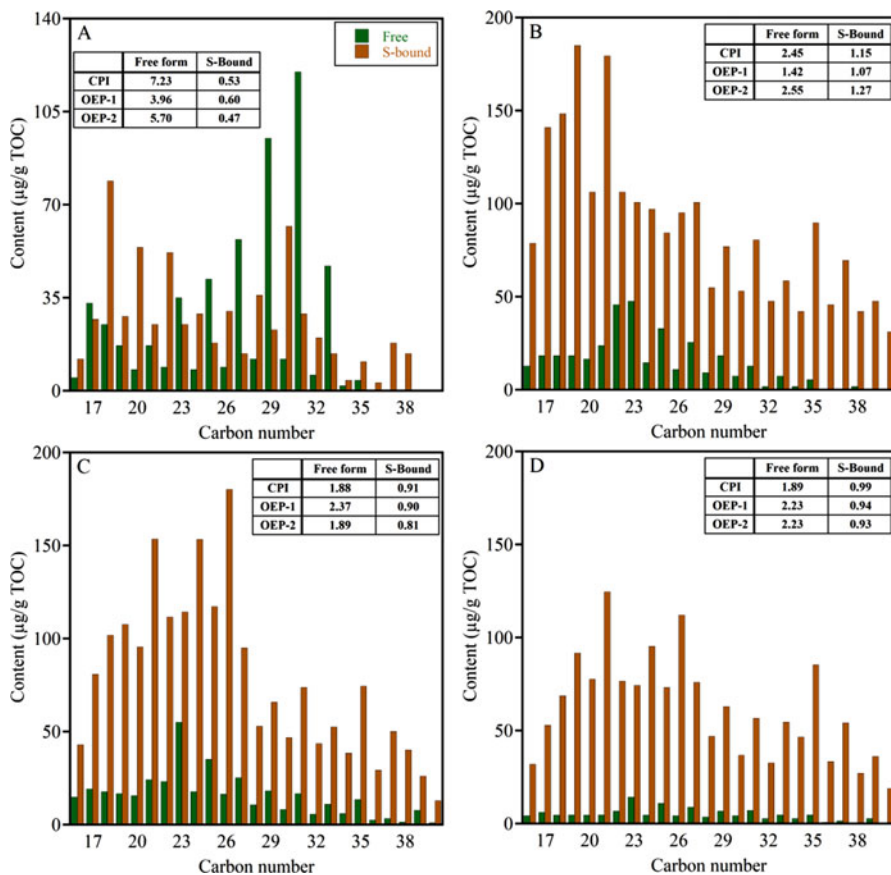


Fig. 5 Free and S-bound *n*-alkane contents ($\mu\text{g/g TOC}$) of several sulphur-rich sedimentary rocks, showing how their distribution and CPI and OEP indices differ dramatically between the two fractions. Data is from (a) Vena del Gesso marl (Koopmans et al. 1996a), (b) Calcaires en plaquettes (van Kaam-Peters and Sinninghe Damsté 1997), (c, d) Calcaires en plaquettes, layers M and DU, respectively (van Kaam-Peters et al. 1998)

respectively. No mechanism to explain the selective preservation of marine and terrestrial *n*-alkanes in the two fractions was suggested by the authors. It might be that terrestrial OM, which travels longer to the sulphurization regime, is then less reactive (Arndt et al. 2013) and therefore less prone to sulphurization.

Linear fatty acids are thought to be one of the sources of *n*-alkanes in sedimentary OM (e.g., Hartgers et al. 2000). Sulphur-bound C_{16} – C_{26} linear fatty acids predominated by C_{18} were identified in the Messinian age Tripoli Unit rocks of the Lorca Basin, SE Spain (Russell et al. 2000). The most abundant isomers were those with sulphur substitution at carbon atom 9. This points to an early sulphurization of

Table 3 Summary of main applications of the biomarker families discussed in the text and aspects of their sulphurization as revealed by different studies cited here

Biomarker group	Main applications as biomarkers and aspects of their sulphurization	References
<i>n-Alkanes</i>	<i>n</i> -Alkane distribution is a signature of OM origin. Distribution of free and S-bound may vary significantly (Fig. 5). For the application of proxies, such as CPI and OEP, both fractions should be considered	[1–4]
<i>Long-chain C₃₇–C₃₉ alkenes and alkenones</i>	C ₃₇ –C ₃₉ alkenones and their derivatives indicate input of calcareous nannoplankton material. In addition C ₃₇ unsaturated alkenones are used for reconstruction of ancient sea surface temperatures (SST) and paleo- <i>p</i> -CO ₂ . The effect of sulphurization on the SST proxy is minimal, but if all alkenones are sulphurized, SST determination is not applicable	[5–8]
<i>Phytol-derived and phytol-related isoprenoids</i>	Sulphurization of phytane and pristane can be significant. Under S-rich conditions, sulphurization of phytane seems to be favored over pristane. This selective sulphurization creates a bias which might limit the use of the Pr/Ph ratio under S-rich conditions (Fig. 6). Free OSC compounds such as the C ₂₀ isoprenoid thiophenes can be highly abundant at moderate thermal maturation. Their distribution is used as a marker for paleosalinity	[2, 4, 5, 9–20]
<i>Highly branched isoprenoids (HBIs)</i>	HBI occurrence indicates diatom OM input, with an age constrain (U. Turonian–present day). Also, they may act as a marker for nutrient abundance during deposition (i.e., upwelling conditions). HBIs are known to undergo rapid sulphurization in young sediments, both inter- and intramolecularly	[5, 12, 15, 21–30]
<i>Steroids</i>	The distribution of the sterane groups is used to determine the origin of OM. Steroids are known to undergo rapid sulphurization in the early stages of diagenesis. The sulphurized form occurs mainly as free OSC. Preferential sulphurization of C ₂₇ steroid derivatives is common and may introduce bias if only the free hydrocarbon fraction is analyzed. 4-Methylsteroids (dinosterane) can be found in large abundance in the S-bound fraction	[7, 31–36]
<i>Hopanoids</i>	Indicator of OM input from bacterial origin, redox conditions of the water column, and assessment of the extent of diagenesis in immature samples. Also, they may be applied for paleo-reconstruction of dissolved CO ₂ concentration. Sulphurization is relatively rapid and preferential for C ₃₅ hopanoids. This can introduce a bias if only the free hydrocarbon fraction is analyzed for both redox and maturity proxies	[1, 37–39]
<i>Carotenoids</i>	Isorenieratene and chlorobactane are exclusively synthesized by green sulphur bacteria and are therefore specific indicators of photic zone euxinia. They are easily degraded and	[1, 3–5, 34, 39–47]

	<p>therefore rarely observed as free compounds. They usually are present in the sulphurized forms with the majority being in the S-bound OSC fraction. Main limitation of use is because β-isoreneratane can be formed by diagenetic aromatization of β-carotene (regardless of anoxic conditions). Degradation of isoreneratene as a result of thermal maturation may result in the formation of aromatic OSCs</p>	[7, 48–51]
Porphyryns	<p>Used as a marker for the source of OM input. Their preservation is enhanced by sulphurization, with the majority being in the S-bound OSC fraction. In addition, sulphur derivatives of bacteriochlorophyll <i>c</i> and <i>d</i> are indicators of photic zone anoxia</p>	[38, 52–55]
Polyprenoid sulphides	<p>C₃₀ tetraacyclic polyprenoid sulphides are an indicator of lacustrine depositional environments. They require sulphur-rich conditions to form, under which they will mostly occur in the free OSC fraction. They have a unique source or specific path of sulphurization that is not yet known</p>	

References: 1. Grice et al. (1998); 2. Koopmans et al. (1996a); 3. van Kaam-Peters et al. (1998); 4. van Kaam-Peters and Sinnighe Damsté (1997); 5. Wakeham et al. (1995); 6. Brassell and Dumitrescu (2004); 7. Schaeffer et al. (1995); 8. Koopmans et al. (1998); 9. van Dongen et al. (2006); 10. Fukushima et al. (1992); 11. Barakat and Rullkötter (1995); 12. Hartgers et al. (1997); 13. Koopmans et al. (1995); 14. Sinnighe Damsté et al. (1989); 15. Adam et al. (2000); 16. Eglinton et al. (1994); 17. Grimalt et al. (1993); 18. Kohnen et al. (1993); 19. Naafls and Pancost (2014); 20. Putschew et al. (1996); 21. Grossi et al. (2004); 22. Schouten et al. (1995a); 23. Sinnighe Damsté et al. (2007); 24. Volkman et al. (1994); 25. Xavier et al. (1997); 26. Kohnen et al. (1990); 27. Russell et al. (2000); 28. Sinnighe Damsté and Rijpstra (1993); 29. Bechtel et al. (2013); 30. Belt et al. (2017); 31. Adam et al. (1991); 32. Schouten et al. (1998a); 33. Sinnighe Damsté et al. (1999); 34. Kok et al. (2000a); 35. Bayona et al. (2002); 36. Dellwig et al. (1998); 37. Köster et al. (1997); 38. Schaeffer et al. (2006); 39. Sinnighe Damsté et al. (1995); 40. Koopmans et al. (1996b); 41. Sinnighe Damsté and Koopmans (1997); 42. Hebbing et al. (2006); 43. French et al. (2015); 44. Kohnen et al. (1991b); 45. Kenig et al. (1995); 46. Kolonic et al. (2002); 47. Broeks et al. (2005); 48. Squier et al. (2003); 49. Squier et al. (2004); 50. Pickering and Keely (2013); 51. Junium et al. (2011); 52. Poinsoot et al. (1998); 53. Holba et al. (2003); 54. Adam et al. (2009); 55. Cabrera et al. (2002)

octadeca-9,12-dienoic acid and/or octadec-9-enoic acid, which are major lipid constituents of algae. Therefore sulphurization can preferentially preserve the unsaturated fatty acids and may cause a major bias of the original compositions of fatty acids (Russell et al. 2000).

The different abundance of specific *n*-alkanes in the free and S-bound fractions may lead to inaccurate assessments of the source of organic matter and thermal maturity, if only free HC are measured. Such bias can be overcome by measuring both free and S-bound *n*-alkane distributions in sediments deposited in a S-rich environment.

4.2 Long-Chain C₃₇–C₃₉ Alkenes and Alkenones

Long-chain C₃₇–C₃₉ alkenones are biosynthetic products of the alga *Emiliana huxleyi* and other members of the Prymnesiophyceae (Brassell 1993). The C₃₇ alkenones, mainly the di- and triunsaturated compounds, are used as valuable proxies for sea surface temperatures (SST) and paleobarometer for atmospheric *p*CO₂ (Brassell et al. 1986a; Brassell 1993; Wakeham 2002). The presence of C₃₇–C₃₉ alkenones in sediments is also used as a marker for input of calcareous nanophytoplankton material (coccolithophore), as was shown, for example, for sediment of the oceanic anoxic event 3 (87.3–84.6 Ma, Wagner et al. 2004). Long-chain C₃₇–C₃₉ alkenes and alkenones (di- and triunsaturated methyl and ethyl ketones) were observed in young sediments (<7,000 years) as those of the Black Sea (Wakeham et al. 1991, 1995) and many ancient sediments ranging in age from Pliocene to lower Aptian (~120.5 Ma) (see Table 3 for references; Brassell and Dumitrescu 2004 and references therein). Under oxic marine conditions, where sulphurization plays a minor role, the application of this SST proxy is age-limited to ~270 ky BP or younger sediments, as *Emiliana huxleyi* only evolved during that period (Thierstein et al. 1977; Volkman et al. 1995; Sawada et al. 1996). However, there is a continuous effort to extend the applicable time range of alkenones based SST proxy to ancient sediments (see a review of Brassell and Dumitrescu 2004 for the occurrence of different alkenones in the geological record).

Under anoxic-sulphidic (euxinic) conditions, both alkenes and alkenones are known to react with reduced S species and evolve into C₃₇–C₃₈ alkylthiolanes or to macromolecular S-bound forms (Schaeffer et al. 1995; Koopmans et al. 1996a, 1997). However, compared with older sedimentary rocks, in which all the C₃₇–C₃₈ alkenes and alkenones were S-bound, in the young sediments of the Black Sea, these compounds were found exclusively in the free HC fraction (Wakeham et al. 1995). These authors suggested that time spans greater than ~7,000 years may be needed for the formation of such OSC.

Koopmans et al. (1996a, 1997) found that alkenones may occur as macromolecular S-bound and O-bound components in varying proportions. Despite variations in their abundance in the macromolecular structure, the relative amounts of di- and triunsaturated ketones, which are used for the SST proxy, were unaffected. This indicates that there is no selectivity for the reactions of different alkenones with

reduced S species. Hence, if free di- and triunsaturated ketones occur in sediments from S-rich environments, they can be used for the SST proxy. When all of the long-chain C₃₇–C₃₉ alkenes and alkenones are sulphurized, the determination of SST is impossible, even after desulphurization treatment, because the original unsaturations disappear (Brassell 1993).

4.3 Phytol-Derived and Phytol-Related Isoprenoids

Sulphurized isoprenoids are one of the most abundant sedimentary OSC groups (Sinninghe Damsté and De Leeuw 1990). The most abundant carbon numbers of linear sulphurized isoprenoids are C₂₀ (phytane-derived) and C₁₉ (pristane-derived), but other examples of C₁₅ to C₄₀ carbon skeletons are known as well (Krein 1993; Pancost et al. 2001). Pristane (Pr) and phytane (Ph) are ubiquitous isoprenoids in sediments as they are diagenetic products of phytol which is part of chlorophyll *a* (Eglinton et al. 1964). Pristane and phytane carbon skeletons can also derive from pristenes (zooplankton) and archaeol (archaea species), respectively (Kuypers et al. 2001). The pristane to phytane ratio (Pr/Ph) is often used as an indicator of the redox state of the depositional environment with Pr/Ph < 1 indicating anoxia (Didyk et al. 1978). In addition, Pr/Ph ratio was suggested to be lithology related when used in conjunction with the ratio of dibenzothiophene to phenanthrene (Hughes et al. 1995).

Under S-rich conditions, the carbon skeletons of these isoprenoids can be found both as free and S-bound compounds with varying distributions among these fractions. Chemical cleavage treatment of the macromolecular fractions in young sediments and immature sedimentary rocks has shown the preferential sulphurization of phytane at carbon atoms 1–4 and 17 with 1 and 3 being the most dominant by far (Fig. 6 please note legend to the figure for details on the numbering of carbon atoms; Kohnen et al. 1993; Adam et al. 2000). Sulphurized phytane was suggested to derive mainly from phytenal or (to lesser extent) phytadiene, early diagenetic products of phytol (Krein and Aizenshtat 1994; Adam et al. 2000; Schouten et al. 2001; Amrani and Aizenshtat 2004c).

Different diagenetic processes occurring within the sediment lead to preferential preservation of phytane over pristane in the S-bound fraction (Fig. 7a; Kohnen et al. 1991a; Wakeham et al. 1995). Pristane is the diagenetic product of phytol formed under oxic conditions by loss of a carbon atom as a result of decarboxylation. Under reducing conditions, phytol is hydrogenated via a series of steps to form phytane (Didyk et al. 1978). Thus the Pr/Ph ratio is used for paleo-reconstruction of the redox conditions during deposition with Pr/Ph < 1 indicating anoxia (Didyk et al. 1978). It is logical to assume that under euxinic conditions, phytol will tend to undergo sulphurization rather than oxygenation and will thus be preserved as S-bound phytane. The selective preservation of phytane over pristane leads to a remarkable difference in the Pr/Ph ratio between the free and S-bound fractions in several basins (Fig. 8b). This difference in the Pr/Ph ratios between the free and S-bound fractions can thus give rise to contradicting interpretations as shown in Fig. 8b for the Black Sea and for

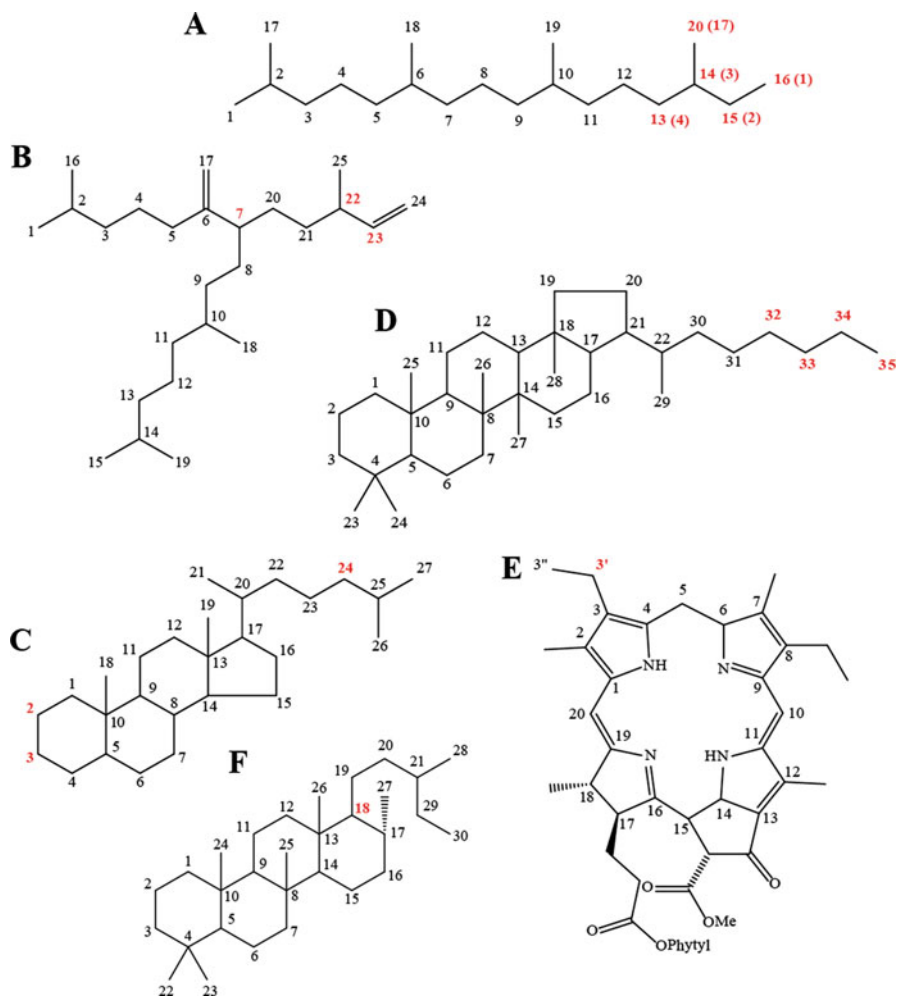


Fig. 6 Examples of carbon skeleton structure of biomarkers representing the main groups discussed in Sect. 4 with the main sulphurization sites are marked in red: (a) Phytane, sulphurization sites are after Kohnen et al. (1993) (site numbering is in respect to IUPAC numbering of phytane. For numbering in respect to phytol, the sulphurization sites are 1–4 and 17 respectively, as presented in parentheses). (b) $C_{25:2}$ HBI. Structure and sulphurization sites are after Hartgers et al. (1997) and Sinnighe Damsté et al. (2007). (c) C_{27} sterane. Structure and sulphurization sites are after Adam et al. (1991), Schouten et al. (1998), and Adam et al. (2000). (d) C_{35} hopane. Structure and sulphurization sites are after Schoell et al. (1994) and Ourisson et al. (1984). (e) Chlorophyll *a* derivative: methyl pyropheophorbide *a*. Structure and sulphurization sites are after Pickering and Keely (2008). (f) C_{30} tetracyclic terpane. Structure and sulphurization sites are after Holba et al. (2003). It is important to note the sulphurization sites are the most common ones that reported in the literature. Other sulphurization positions were identified as well, and they are usually directly related to previous locations of functional groups such as double bonds, carbonyls, and hydroxyls in specific biomarkers. See more details about the sulphurization mechanisms in Sect. 3.2 and references therein. A more specific example for sulphurization pathways is given in Fig. 7 for phytol

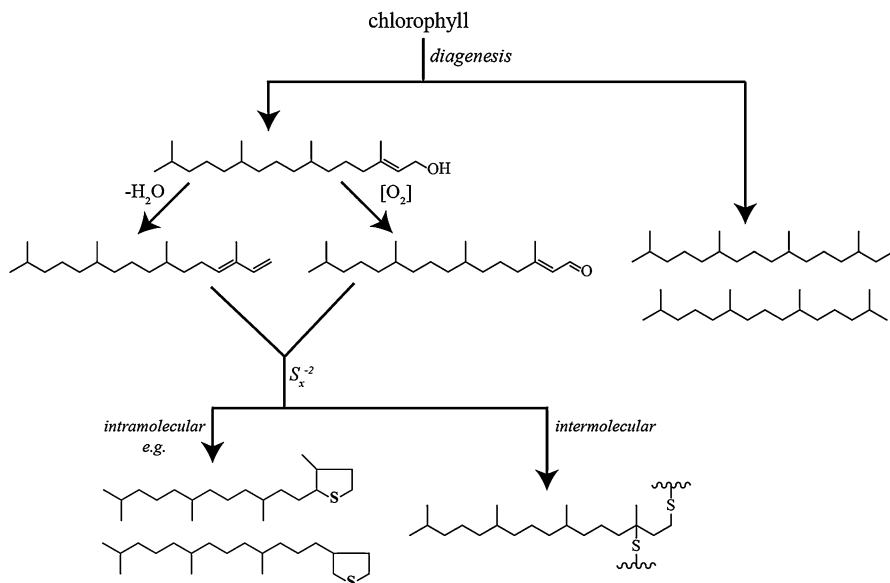


Fig. 7 General scheme for the diagenesis of the phytol side chain in sediments. Formation of OSCs with a phytol carbon skeleton is shown in the left pathway. Formation of pristane and phytane is shown in the right pathway. (Modified after Schouten et al. (2001) and Krein and Aizenshtat (1994))

Messinian sediments from Sicily. Therefore, under anoxic-sulphidic conditions, the analysis of free pristane and phytane only may be misleading, unless both free and S-bound fractions are considered. However, some very S-rich sediments still show close correspondence of Pr/Ph ratios between free and S-bound fractions, such as in Calcaires en plaquettes and the Ghareb Formations (Fig. 8). Under S-poor conditions, such as those in the Green River Formation, the extent of pristane and phytane sulphurization is still significant (Fig. 8), yet there is no apparent preferential preservation of phytane over pristane in the S-bound fraction, and Pr/Ph ratios in the free and S-bound fractions are very similar (Koopmans et al. 1999).

The most abundant group of isoprenoid thiophenes in paleoenvironmental studies has a phytane carbon skeleton (i.e., C_{20} isoprenoid thiophenes). Compounds of this group were first isolated and identified in immature sedimentary rocks recovered during the Deep Sea Drilling Project (DSDP) in the apolar fraction of organic-rich sediments (Brassell et al. 1986b). This group has seven main isomers (Fig. 9) which were observed in young sediments and immature sedimentary rocks of various depositional settings (see Table 3 for references). The most abundant ones are thiophenes I and II (Fig. 9). These thiophenes are not formed during low-temperature laboratory sulphurization experiments with phytanal or phytadienes (Krein and Aizenshtat 1994; Schouten et al. 1994; Amrani and Aizenshtat 2004c). During low-temperature thermal alteration of S cross-linked macromolecules, thiophenes I and II are formed rapidly and efficiently (Krein and Aizenshtat 1994; Schouten et al. 1994; Amrani and Aizenshtat 2004b). Therefore, it has been suggested that they

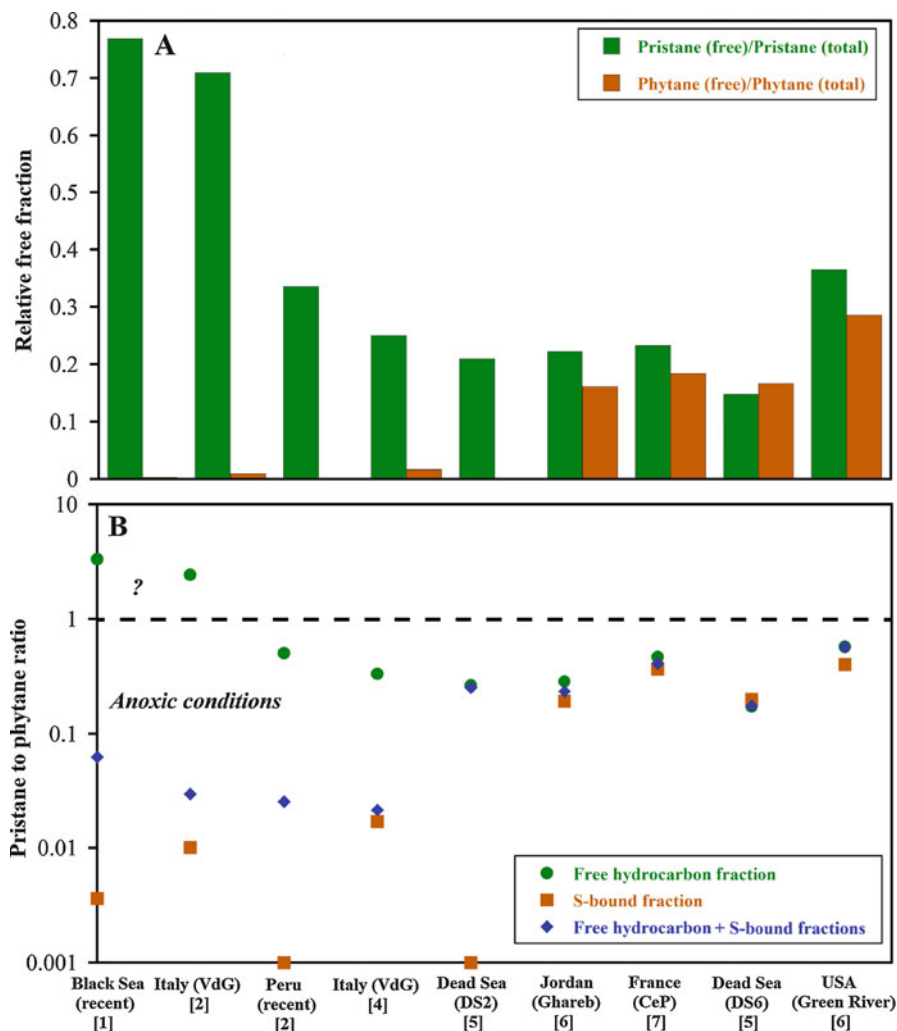


Fig. 8 (a) Relative abundance of free phytane and pristane, (b) Pr/Ph ratio calculated for the free fraction only, the S-bound fraction only, and the sum of the two fractions for different sediments. All sediments, except the Green River shale, are considered to be sulphur-rich. The dashed horizontal line in panel (b) marks the top value for anoxic conditions considered by the Pr/Ph ratio (Peters et al. 2005). Note how this ratio differs between the free and S-bound fractions (panel b) if these biomarkers have different abundance between these fractions (panel a). In some sulphur-rich environments, the relative abundance between the free and S-bound fractions is very similar, leading to very similar Pr/Ph ratios. Numbers in brackets refer to [1] Wakeham et al. (1995) (unit I 0–2.5 cm), [2] Kohnen et al. (1991a) (VgS-4a), [3] Kohnen et al. (1991b) (Peru upwelling), [4] Koopmans et al. (1996a) (VdG), [5] Grice et al. (1998) (DS-2), [6] Koopmans et al. (1999) (Ghareb and Green river Fm.), [7] van Kaam-Peters and Sinninghe Damsté (1997) (Cep fm)

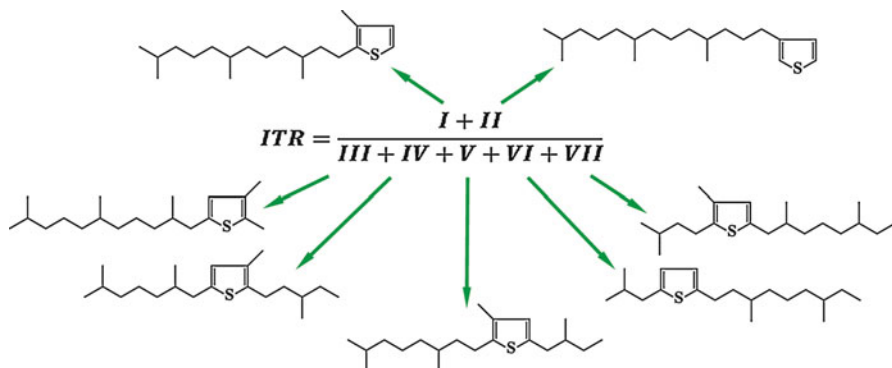


Fig. 9 The isoprenoid thiophene ratio (ITR) after Sinninghe Damsté et al. (1989) and De Leeuw and Sinninghe Damsté (1990). Structures of the various thiophenes implemented in this parameter are shown

arise primarily during early thermal maturation and not as a result of early diagenetic intramolecular sulphurization (Krein and Aizenshtat 1994; Amrani and Aizenshtat 2004b). The origin of specific thiophenic isomers is related to the C-S bonding position in the phytane carbon skeleton, which in turn depends on the functionality of the precursor molecule (Krein and Aizenshtat 1994).

The distribution of isoprenoid thiophene isomers appears to depend on the salinity of the depositional environment (Sinninghe Damsté et al. 1989; Barakat and Rullkötter 1995). Under normal, non-hypersaline conditions, the most abundant photosynthetic microbes have chlorophyll with phytol as a side chain. The sulphurization of phytol diagenetic products (e.g., phytenal), followed by thermal alteration, leads to the formation of compounds I and II (Fig. 9). Under hypersaline conditions, archaeal populations thrive, which produce polyunsaturated phytenols. Sulphurization of these compounds yields isoprenoid mid-chain thiophenes (Sinninghe Damsté et al. 1989; Barakat and Rullkötter 1995; Schwark et al. 1998; Rontani and Volkman 2003). Hence, the distribution of the C₂₀ isoprenoid thiophenes was proposed as a proxy for paleo-salinity (referred as the “Isoprenoid Thiophene Ratio,” ITR; Fig. 9), with ITR < 0.5 considered to be indicative of a hypersaline paleoenvironment (Sinninghe Damsté et al. 1989; De Leeuw and Sinninghe Damsté 1990; Barakat and Rullkötter 1995).

Several studies have noted that the ITR proxy is not always applicable. Schwark et al. (1998) studied the Solnhofen carbonates (Upper Jurassic, Germany), deposited under stratified water column conditions. They observed low ITR values (< 0.08) which were inconsistent with other markers of salinity such as the Pr/Ph ratio or the methylchromane signature (MTTC ratio). The authors suggested that the ITR might preferentially represent the salinity in deep sections of the stratified water column or it might be impacted by sedimentary diagenetic alteration.

Hartgers et al. (1997) worked on solar salt ponds of La Trinitat and observed ITR >10 despite the high salinity of the ponds ($70\text{--}100\text{ g}\cdot\text{L}^{-1}$). These authors explained the high ITR value to be a result of low abundance of compound III (Fig. 9) in their study. This isomer is abundant in immature sedimentary rocks deposited in hypersaline paleoenvironments, but probably forms only at later stages of diagenesis and therefore is not detected in young, active evaporate settings. A similar issue is observed in young hypersaline environments from Pétrola Saladar in Spain with ITR >0.5 , in which only compounds I, II, and III (Fig. 9) were observed (Schreiber et al. (2001)). The ITR value reached a hypersaline value (<0.5) only after pyrolysis of the samples ($350\text{ }^\circ\text{C}$), consistent with the observation that this ratio is not always applicable to immature organic-rich sedimentary rocks.

In immature sedimentary rocks, the C_{20} isoprenoidal thiolanes probably represent earlier diagenetic products relative to their thiophene analogues. Thus, consideration of both thiolane and thiophene C_{20} isoprenoids may give a better representation of their precursors. An improved index that contains the thiolane- C_{20} isomers (ITTR) was suggested by Barakat and Rullkötter (1995). The modified ratio provides the same classification of hypersalinity as ITR, but in one case, ITTR values suggested higher salinity in agreement with the chromane distribution (Rontani and Volkman 2003).

4.4 Highly Branched Isoprenoids (HBIs) and Their Sulphur-Containing Derivatives

Highly branched isoprenoids (HBIs) are a common group of biomarkers derived from four genera of the marine primary producers diatoms (Volkman et al. 1994; Belt et al. 2000, 2017; Grossi et al. 2004; Sinninghe Damsté et al. 2007). Therefore, HBIs are useful biomarkers indicative of high nutrient levels (upwelling systems) due to the high Si consumption of diatoms (Wagner et al. 2004). Their occurrence in marine sediments is limited to the geological period from the Upper Turonian ($\sim 90\text{ Ma}$) to the present (Wakeham et al. 1995; Köster et al. 1998; Sinninghe Damsté et al. 2004).

HBI alkenes are prone to abiotic sulphurization (Fig. 6b) and the formation of free sulphurized HBI such as HBI thiophenes as well as thiolanes and macromolecular S-bound HBI (Kenig et al. 1995; Xavier et al. 1997; Belt et al. 2000; Sinninghe Damsté et al. 2007). Sulphurization of HBI depends on the number and positions of double bonds within the alkene structure, with a minimum of two double bonds in the precursor required to promote this process (Belt et al. 2000). Higher numbers of double bonds significantly increase the reactivity and therefore the chances for sulphurization. Hartgers et al. (1997) noted that under hypersaline conditions, C_{20} HBI-derived thiophenes were formed by preferential sulphurization of C_{20} HBI dienes and polyenes, leaving behind non-sulphurized C_{20} HBI with only one double bond. This is in agreement with laboratory and theoretical work, which shows that the reactivity of alkenes to sulphurization increases with the number of conjugated double bonds (LaLonde et al. 1987).

Wakeham et al. (1995) observed high concentrations of free C_{25} HBI alkenes just below the water-sediment interface in the Black Sea, which rapidly decreased in the

upper 5 cm of the sediment column. C₂₅ HBI derivatives were only found below 25 cm in the desulphurized polar fractions. To bridge the gap between their removal from the free HC fraction at shallow depth and their appearance as S-bound HBI significantly deeper in the sediment, the authors suggested the HBI alkenes might be sequestered in fractions not analyzed such as the asphaltenes and protokerogen or alternatively that they were biodegraded. The important implication of this study is that intermolecular sulphurization of HBI alkenes occurs during very early diagenesis (<7,000 years) in the upper sediment column and leads to preservation of the HBI carbon skeletons in the S-bound OSC fraction. Similar results were reported by Werne et al. (2000) for the Cariaco Basin and Sinninghe Damsté et al. (2007) for the Ellis Fjord in Antarctica. Sinninghe Damsté et al. (2007) estimated that complete sulphurization of C₂₅ HBI diene would be achieved within 500 years, following a first-order reaction with a rate constant of $1.3 \cdot 10^{-2} \text{ years}^{-1}$.

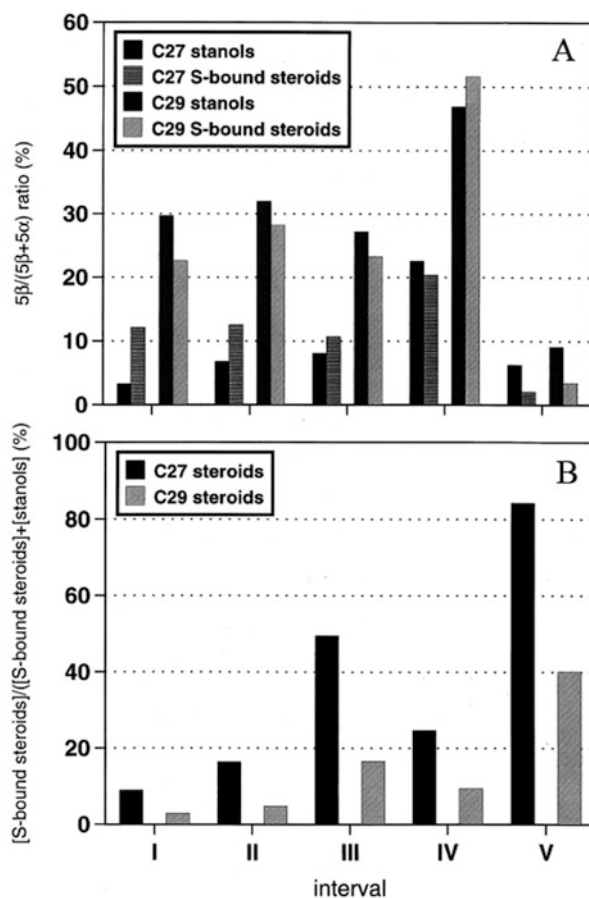
4.5 Steroids

Steroids occur widely in algae and vascular plants and thus are ubiquitous in most depositional environments (Huang and Meinschein 1979). They are commonly used as tools for oil-source rock and oil-oil correlation, as well as proxies for the origin of OM inputs. The sterane carbon number distribution, i.e., the relative amounts of C₂₇, C₂₈, and C₂₉ steranes, is the most commonly applied sterane proxy, as it reflects the origin of OM from primary production to the sediment (Huang and Meinschein 1979). During diagenesis, steroids undergo various structural modifications including removal of the hydroxyl group (Mackenzie et al. 1982), the formation of steradienes, and oxidation of sterols to stenones and stanones. Both of these diagenetic products are prone to sulphurization.

The sulphurization of steroids is a relatively rapid process which has been shown to occur within the very early stages of diagenesis (Kok et al. 2000). The C-S bond position in macromolecularly bound steroids is mainly at C₂ and C₃ in the A-ring (Fig. 10; Adam et al. 1991; Kohnen et al. 1991b, 1993; Kok et al. 2000a). In some low molecular weight S-containing steroids, the C-S bond is located at the 3-alkyl side chain of the 3-alkylsteroids (Schouten et al. 1998b) or at the D-ring and at the side chain of regular steroids (Schmid 1986; Behrens et al. 1997; Peng et al. 1998).

Kok et al. (2000a) have estimated steroid sulphurization to be completed in 1,000–3,000 years in the upper sediments of Ace Lake in Antarctica, based on assumed rates of sedimentation and age of the sediment core studied. The authors noted that C₂₇ stanols are preferentially sulphurized compared with C₂₉ stanols which remain abundant in their free form (Fig.10). The possibility of a sulphurization bias toward C₂₇ relative to C₂₉ sterols has also been mentioned by Wang et al. (2004), in a study based on young sediment cores from a salt lake. However, the authors noted that the evidence for such a bias is not conclusive. Desulphurized fractions of samples from the Messinian (Sicily) exhibit a dominance of the C₂₇ sterane homologues, while in the free fraction, no steranes were detected (Schaeffer et al. 1995). This observation indicates preferential sulphurization and preservation of C₂₇ steranes, as had been suggested by the other studies. The

Fig. 10 The preferential sulphurization of C_{27} stanols over C_{29} stanols. (Panel a) $5\beta/(\text{5}\alpha\text{15}\beta)$ ratio (in %) for C_{27} and C_{29} stanols and S-bound steroids. (Panel b) $[\text{S-bound steroid}]/([\text{S-bound steroid}] + [\text{stanol}])$ ratio (in %) for C_{27} and C_{29} steroids for five different core sections representing $\sim 1,250$ year in Ace Lake sediments (Kok et al. 2000)



mechanism behind this preferential sulphurization (and thus preservation) of C_{27} steranes is still unknown, but it may provide a bias in using the sterane carbon number distributions to assess OM source input. This can be overcome by examining both free and S-bound sterol derivatives.

A more taxon-specific biomarker steroid group are the 4-methylsteroids (dinosteranes), which are derived from certain primary producers such as dinoflagellates (Summons et al. 1987) and prymnesiophyte algae (Volkman et al. 1990). Schaeffer et al. (1995) noted that these compounds were found exclusively in the S-bound fraction of Messinian sediments from Sicily.

4.6 Hopanoids

Hopanoids are ubiquitous compounds in organic-rich sediments, where they are among the most diagnostic biomarkers for bacterial input (Ourisson et al. 1984). Homohopanes in sedimentary environments are thought to result from the

degradation, under relatively oxic conditions, of the labile side chain of C_{35} -hopanepolyols leading to smaller homologues (Peters and Moldowan 1991). Thus C_{35} homohopane is expected to be best preserved under anoxic conditions giving rise to elevated values of the ratio $C_{35}/\Sigma(C_{31}-C_{35})$ (the “ C_{35} homohopane index”) used as an indicator of anoxic depositional settings (Peters and Moldowan 1991).

Hopanoids can undergo sulphurization at carbon atom 4 in the side chain (Fig. 6d) forming S-containing products which are abundant in sedimentary rocks. In fact, a C_{35} hopane containing a thiophene ring was the first reported OSC with a carbon skeleton clearly linked to that of a biological precursor (Valisolalao et al. 1984). Since then, many other S-containing hopanoids (thiolanes, thiophenes, and S-bound) have been reported and grouped into different series (Table 3; Sinninghe Damsté et al. 1995, 2014; Schaeffer et al. 2006).

Richnow et al. (1992) investigated the macromolecular structure of a S-rich oil (resins and asphaltenes) and its presumed source kerogen (Monterey Formation, California) by sequential chemical degradation. They showed that the macromolecularly bound hopanoids were cross-linked by both S and O bonds, with a significantly different distribution of hopanoid species relative to free hydrocarbons in the extractable fraction. Farimmond et al. (2003) studied the incorporation of hopanoids into the macromolecular (bound OSC) fraction in young sediments of a freshwater lake (Priest Pot) and an anoxic-sulphidic fjord (Framvaren). They concluded that this process is very rapid (<350 years) and extensive (22–86% of the total hopanoids were incorporated). They further showed that cross-linking bonds of hopanoids by S were 15%, while S and O bonding (at the same molecule) was ~40%, and the rest were bound exclusively with O (ether bonds, ~47%). Despite this, a positive correlation was found between the bound hopanoid fraction and the total S in the sediment (Farimmond et al. 2003). Sinninghe Damsté et al. (1995) studied the C_{35} hopanepolyol derivatives in the Upper Cretaceous organic-rich limestone of Jurf ed Darawish in Jordan. The S-bound form made up 50–80% of the total hopanoids preserved in the sediment with preferential sulphurization of the C_{35} $17\alpha,21\beta(H)$ -homohopanes. Similar observation of C_{35} homohopane preferential sulphurization (Fig. 11) of both free and bound OSC forms was later described in marls and limestones of different depositional environments and ages (Köster et al. 1997; Grice et al. 1998; Schaeffer et al. 2006). Schaeffer et al. (2006) found that some thermally stable hopane derivatives (e.g., $17\alpha,21\beta$ -hopanes) can also be directly biosynthesized. This finding implies that the ratios of $\alpha\beta$ -/ $\beta\beta$ -hopanes used to evaluate the maturity of sedimentary organic matter can be biased in some settings.

The C_{35} homohopanes possess the most intact carbon skeleton derived from bacteriohopanepolyols. The predominance of sulphurized C_{35} hopanoids can therefore be explained by the reaction of reduced S species with the homohopane side chain during the earliest stages of diagenesis (Köster et al. 1997). Other sulphurized hopanoids are far less common at that diagenetic stage and therefore less represented in the S-bound fraction.

Köster et al. (1997) noted that the distribution of various sulphurized hopane derivatives may indicate the extent of diagenesis. In a study of samples from the Hauptdolomit, Calcaires en Plaquettes, and Ghareb Formations, which are traditionally defined as immature sedimentary rocks, they were able to distinguish subclasses

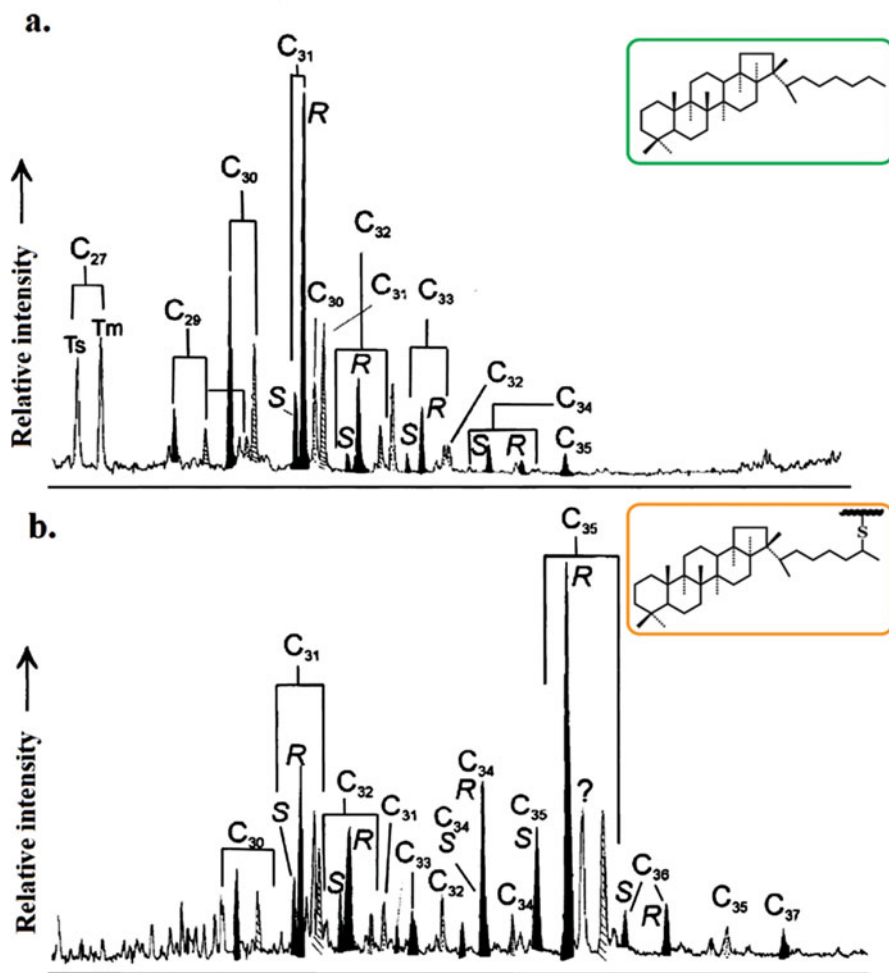


Fig. 11 The bias of C₃₅ hopane sulphurization: (a) Chromatogram of the free hopanes showing C₃₁ predominance. (b) Chromatogram of the S-bound sulphurized hopanes showing distinctive C₃₅ predominance; both are from a sample of the Permian Kupferschiefer Formation, considered to be a type II kerogen. (Modified from Grice et al. (1996))

of maturity based on the distribution of sulphurized hopane derivatives. The thermally most mature sample had the highest content of C₃₅ hopanoid thiophenes, while the least mature samples comprised mostly hopanoid sulphides (Köster et al. 1997). This finding is in accordance with the release of macromolecular S-bound C₃₅ hopanoids and its cyclization to thiophenes upon the early stages of thermal maturation (Fig. 4).

The carbon isotopic ratio of S-bound C₃₅ hopanes has been demonstrated to be useful in paleoclimate reconstructions (Schoell et al. 1994). Changes in $\delta^{13}\text{C}$ (−29.5

to -32.5‰) throughout the Middle to Late Miocene section of the Monterey Formation have been observed. It has been proposed that the distinct $\delta^{13}\text{C}$ signature of the S-bound C_{35} hopanes (compared with C_{27} sterane and bulk kerogen values) reflects changes at the base of the photic zone. This conclusion assumes that this hopane represents the photosynthetic cyanobacteria which live deeper in the photic zone compared with eukaryotic photosynthetic organisms that synthesize steroids. More specifically it has been pointed out that changing water temperature led to a change of dissolved CO_2 concentration that in turn led to a change in the $\delta^{13}\text{C}$ of the hopanes. This hypothesis was supported by the available $\delta^{18}\text{O}$ record for the Pacific Ocean in the relevant timeframe. Sulphurization and thus preservation of the C_{35} hopanes and their presumed original $\delta^{13}\text{C}$ values played a key role in the paleoenvironmental interpretation.

4.7 Carotenoids

Carotenoids are tetraterpenoid pigments (C_{40}) which are widespread in living organisms such as algae, bacteria, and higher plants. The most common members of this group are β -carotene, which is biosynthesized by marine and terrestrial plants, and fucoxanthin which often occurs in planktonic organisms such as diatoms and dinoflagellates (Hebting et al. 2006). The multiple sites of unsaturation in the carotenoids are prone to oxidation, hydrogenation, and other diagenetic reactions. Therefore a low concentration of oxygen and available inorganic S species in the water column and/or sediment are crucial for carotenoid preservation in the geological record (Sinninghe Damsté and Koopmans 1997).

Carotenoids can readily react with reduced S species (e.g., H_2S and polysulphides) at various sites of double bonds in their carbon skeletons (Hebting et al. 2006; French et al. 2015). They usually form bound OSC structures, which increases their stability and resistance to degradation in the sediment. Hebting et al. (2006) studied samples from Lake Cadagno (Switzerland) and suggested that reduced S species can reduce (hydrogenate) the double bonds of the carotenoids, leading to increased preservation in an anoxic water column (Fig. 12). However, their quantitative data indicates that this pathway is minor and sulphurization outcompetes the hydrogenation pathway. Under such conditions, most, if not all preserved carotenoids, are S-bound in the macromolecular fraction (Kohnen et al. 1992). Via cleavage of S-bonds, and release of monomeric compounds, double bonds can be reduced as has been shown in several pyrolysis experiments (Krein and Aizenshtat 1995). This thermal alteration pathway could be another route for the reduction of double bonds during the later stages of diagenesis. Note that both preservation pathways (i.e., sulphurization or double bond reduction) are mediated by reduced S species (Hebting et al. 2006).

Because of their large carbon skeleton structure and multiple C-S binding sites, carotenoids are often not GC-amenable, even after selective S-S cleavage (e.g., MeLi/MeI). This has probably limited studies on their abundance and sulphurization pathways in many young sediments. One of the rare examples of carotenoid GC

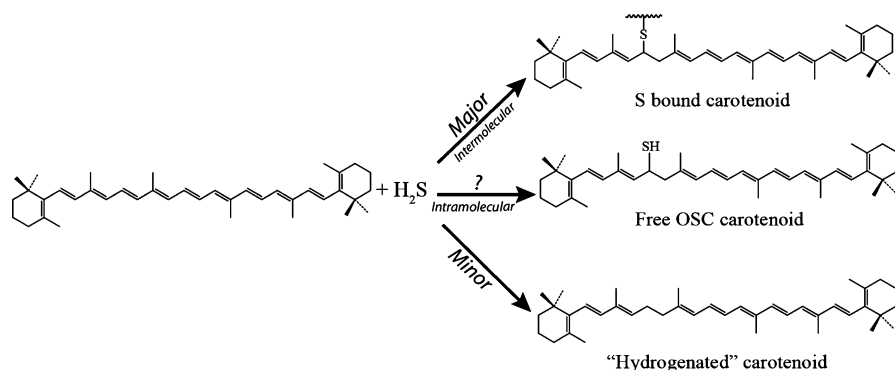


Fig. 12 Reduction (“hydrogenation”) and sulphurization products obtained by reaction of H_2S with β -carotene in aqueous medium (Modified after Hebting et al. (2006)). Other double bond positions can also be sulphurized or hydrogenated as well as multiple sulphurization/hydrogenation positions

analysis is documented by Grice et al. (1998), who identify linear thiophenes and thianes with large carbon skeletons (C_{40}) in the sediments of the Sdom Formation (Miocene, Dead Sea, Israel). The carbon skeletons and $\delta^{13}\text{C}$ values of these OSCs are similar to those of the co-occurring lycopane, which led the authors to conclude that the C_{40} OSC originated from this carotenoid.

Two important carotenoid biomarkers are isorenieratene and chlorobactene. These two carotenoids are exclusively biosynthesized by the brown and green strains of green sulphur bacteria (GSB, *Chlorobiaceae*), respectively (Ohkouchi et al. 2015). These photoautotrophic bacteria use reduced S as an electron donor in photosynthesis and require relatively low light intensities. Thus, the presence of these compounds indicates photic zone euxinia (PZE, Schaeffer et al. 1995; Grice et al. 1996; Koopmans et al. 1996b; Kolonic et al. 2002; French et al. 2015).

The use of sulphurized isorenieratene and chlorobactene derivatives to assess PZE has been exemplified by Wagner et al. (2004), who studied the S-bound profile through the oceanic anoxic event 3 (OAE-3, Coniacian-Santonian, ODP site 959). They observed short-term fluctuations in the S-bound isorenieratene and chlorobactene concentrations during OAE-3, which they attributed to penetration of the chemocline into the photic zone (Fig. 13). The increase of chlorobactene concentration was suggested as an indicator for chemocline rise to very shallow (~15 m) depths during OAE-3. The presence of S-bound chlorobactene and isorenieratene was limited to a specific nannofossil zone, indicating that PZE was confined to a restricted time interval of the OAE-3.

However, a potential concern regarding the use of isorenieratene as a PZE proxy was raised by Koopmans et al. (1996b) who demonstrated that aryl isoprenoids and β -isorenieratene can be formed by diagenetic aromatization of β -carotene. In addition, during diagenesis, sequential cyclization and sulphurization of isorenieratene may lead to formation of aromatic OSC such as benzothiophenes (Koopmans et al. 1996b). The distinct $\delta^{13}\text{C}$ values of β -isorenieratene can help verify the origin of

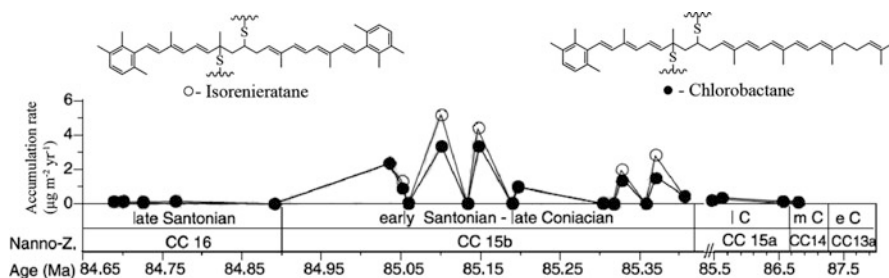


Fig. 13 Time series of accumulation rate of biomarkers indicative of PZE, isorenieratane, and chlorobactane, during the OAE-3 of Late Cretaceous (87.3–84.6 Ma) in the Deep Ivorian Basin (eastern equatorial Atlantic, ODP site 959). Both biomarkers are derived from photosynthetic green sulphur bacteria. Fluctuation in their abundance suggests variation of the chemocline position relative to the photic zone and repetitive penetration of sulphidic conditions into the lower photic zone (Modified from Wagner et al. (2004)). Location of the sulphurization sites is from Koopmans et al. (1996b), but sulphurization in other positions, as well as multiple sulphurization positions, can occur too

these compounds and allow their use as PZE indicators in cases where no genuine β -isorenieratane survived.

4.8 Porphyrins

Porphyrins are compounds of the chlorin group. Among the most common types of porphyrins are the ubiquitous chlorophylls, which occur in all green plants and photosynthetic bacteria. Their presence is a marker of the photoautotrophic primary producer community. During diagenesis, chlorophyll *a* is converted to other stable forms of porphyrins, for example, bicycloalkanoporphyrins (BiCAPs) which are often found in calcareous, OM-rich sediments that are deposited under reducing conditions (Junium et al. 2011).

Sulphur-containing porphyrins have been identified in young sediments of a coastal lake in Antarctica (Squier et al. 2003, 2004), in immature sedimentary rocks of the Messinian of Sicily (Schaeffer et al. 1995), and in laboratory experiments involving the reaction of porphyrins with reduced inorganic S species (Pickering and Keely 2008, 2011, 2013).

Porphyrins may undergo sulphurization by several mechanisms which may lead to their preservation in sediments (Squier et al. 2003; Pickering and Keely 2013). An example for such process is the enhanced preservation of BiCAP. This occurs under euxinic conditions by reduction at carbon atom 3 through reaction with S species as was demonstrated under laboratory and natural conditions (Fig. 6e; Mawson and Keely 2008; Junium et al. 2011).

In sediment extracts from the Messinian of Sicily, the amount of S-bound porphyrins was seven times larger than the amount of their free analogues (Schaeffer et al. 1995). The authors determined that the S-bound porphyrins were dominated by

BiCAPs from a diatom source. The free porphyrins were of a different type and therefore may indicate different environmental conditions in the basin during deposition and diagenesis or perhaps different sources of porphyrins.

The presence of S derivatives of bacteriochlorophyll *c* and *d* is of paleoenvironmental significance since they are a clear marker for anaerobic GSB (*Chlorobiaceae*) activity in the depositional environment and therefore indicate PZE. The detection of these S derivatives suggests that the process of sulphurization can be significant for the preservation of porphyrins (Squier et al. 2004).

4.9 Polyprenoid Sulphides

Polyprenoid sulphides are a group of OSC that possess di-, tri-, tetra-, or pentacyclic carbon skeletons (Fig. 6f shows a tetracyclic structure). Members of this group occur in sediments from a wide range of depositional environments with anoxic conditions including upwelling environments, shallow continental platforms, hypersaline environments, and lagoon sub-basins (Schaeffer et al. 2006; Adam et al. 2009). Polyprenoid sulphides are present in some sediments where no other sulphurized biomarkers (e.g., with linear, sterane, or hopane carbon skeletons) were detected (Poinsot et al. 1998). This observation suggests a unique precursor with high reactivity or a specific path of S incorporation. Moreover, the detection of polyprenoid sulphides in young sediments (<1,000 years) suggests their formation takes place during the earliest stages of diagenesis or even within the water column (Poinsot et al. 1997, 1998).

Polyprenoid sulphides may share a common and specific biological origin with that of the predominant pentacyclic C₃₀ sulphides (Poinsot et al. 1998) and are probably related to the C₃₀ tetracyclic polyprenoids (TPP, Holba et al. 2000). However, the biological lipid precursor of the TPPs is unknown, and based on carbon isotopic studies, it has been suggested that they originate from oxygenic photosynthetic organisms (algae, cyanobacteria) or heterotrophic organisms thriving on algal/cyanobacterial biomass in the oxic part of the water column (Poinsot et al. 1998). This hypothesis of nonmarine algal precursor for TPP was later supported by Holba et al. (2003) who studied a large set of oils which covers lacustrine, terrigenous, and marine source origins. The authors found the presence of high TPP occurrence in oils from fresh to brackish water, algal-rich, lacustrine depositional environments while oils from marine origin were TPP poor. Furthermore, by examining the sterane and hopane distributions in conjunction with TPP, the authors concluded the source of TPP is likely from nonmarine algae, possibly Chlorophyta.

4.10 Carbohydrates

Although carbohydrates are not considered as biomarkers, their preservation in a given environment may give rise to important paleoenvironmental information. Carbohydrates such as polysaccharides and gels comprise a large part of living

biomass. Because these compounds are very labile, they are normally biologically consumed and less preserved in the sedimentary OM record (Arndt et al. 2013). Sulphurization, however, can preserve carbohydrates as part of the macromolecular S-bound fraction as was shown by Kok et al. (2000b). One of the unique signatures of carbohydrates in sedimentary organic matter is their enrichment in ^{13}C (up to 16‰) relative to lipids of a given organism (van Dongen et al. 2006). Van Kaam-Peters et al. (1998) hypothesized that short-chain alkylthiophenes ($\text{C}_1\text{--C}_3$, Kimmeridge Clay Formation (KCF)) were the diagenetic products of S incorporation into monosaccharides based on their higher $\delta^{13}\text{C}$ values relative to *n*-alkanes from the same algal source. Similar conclusions were drawn for the origin of small amounts of $\text{C}_1\text{--C}_3$ alkylthiophenes isolated from pyrolysates of laboratory sulphurization experiments on the algae *Nannochloropsis salina* (Gelin et al. 1998). The reaction of reduced S species with polysaccharides of mucilage origin in the Northern Adriatic Sea was reported by Ciglenc̆ki et al. (2000). The authors also conducted laboratory sulphurization experiments on polysaccharides of bacterial and algal origin, all of which led to the formation of sulphurized polysaccharides. Other sulphurization experiments of algal material and glucose carried out by Kok et al. (2000b) gave rise to S-rich macromolecular material that yielded short-chain alkylthiophenes and other OSCs upon pyrolysis.

The contribution of carbohydrates preserved through sulphurization to the total organic carbon (TOC) of organic-rich sedimentary rocks may, under certain conditions, be significant. van Dongen et al. (2006) worked on the Blackstone Band of the Kimmeridge Clay Formation, where total organic carbon is enriched in ^{13}C relatively to other strata within the Formation. The authors suggested that this might be the result of preservation of sulphurized carbohydrates, which they estimate to account for up to ~90% of the OM in the section of the Blackstone Band richest in total organic carbon. Thus, S incorporation into carbohydrates may preserve a substantial amount of them under euxinic conditions as S-rich macromolecular matter with a ^{13}C -enriched isotopic signature.

5 Summary

This contribution highlights the significant advances achieved by numerous studies on several fundamental aspects of OSC and their role as paleoenvironmental indicators. Among these aspects are the following:

1. Sulphurization is a rapid process (<10,000 years), occurring during the earliest stages of diagenesis. In some cases, sulphurization in the water column can occur within days, even before deposition takes place in the sediment. It is a continuous process, with reactions ongoing deeper in the sediment following diagenetic modifications of the original precursor compounds. Accordingly, sulphurization of less reactive compounds can take place during these later stages after most reactive compounds have already been sulphurized. Sulphurization occurs at specific positions within the carbon skeleton, typically at locations of original

functional groups (i.e., hopanoids are sulphurized via the original hopane polyol side chain), resulting in distinct structural and S isotopic compositions which are different from any original biosynthetic OSC species. The major pathway for sulphurization is via intermolecular linkage, leading to the formation of S cross-linked macromolecules.

2. Recent studies suggest that in some settings, sulphurization of organic matter may compete with iron sulphide (e.g., pyrite) formation. This contrasts with the original presumed sulphur diagenesis scheme, whereby OM sulphurization does not commence until available iron is effectively exhausted. Moreover, compound-specific sulphur isotopic studies suggest that some OSC may form rapidly, resulting in their S isotope signature being lighter than that of the coexisting pyrite. This large S isotope variance between individual OSC, and between bulk fractions (e.g., kerogen), may suggest different sulphurization rates and mechanisms. The sulphur isotopic record of OSC between modern sediments and immature rocks may be changed over the course of diagenesis due to isotopic exchange processes with the reduced inorganic S pool.
3. The contribution of biosynthetic S to the sedimentary organic S pool might be larger than previously thought. Possible reservoirs may include refractory dissolved and particulate organic S, as well as volatile organic S compounds that were adsorbed to inorganic particles. Their interactions with other organic compounds and/or with other sources of reduced sulphur species (i.e., dissimilatory S) can further contribute to their preservation in the sedimentary record.
4. Sulphurization leads to notable preservation of compounds otherwise susceptible to biodegradation and mineralization. Examples include the preservation of carbohydrates, carotenoids, and porphyrins in S-rich sediments as part of the S-bound fraction. The distribution of biomarkers (e.g., Pr/Ph) between the free and S-bound fractions may bias paleoenvironmental interpretations if only the free HC fraction is analyzed. Biomarker analysis for the purpose of paleoenvironmental research should independently examine both the free and S-bound biomarker fractions, as the similarities and contrasts between these pools provide another dimension to the preserved environmental signal. Carbon isotope data may also be biased in a similar manner. A consistent difference is found between the $\delta^{13}\text{C}$ signatures of S-bound and free HC, where the former is heavier by $2 \pm 1\text{‰}$ on average. This may suggest different sources for the original precursors of the biomarkers in the free HC and S-bound fraction and/or a preservation effect of the original $\delta^{13}\text{C}$ values of the biomarkers in the S-bound fraction.

5.1 Future Directions

The analytical developments of the 1980s, primarily GC-MS, fueled the tremendous progress of sedimentary OSC research at that time. Likewise, recent analytical developments in the last decade provide new opportunities to further develop our understanding of the sulphur cycle and its significance with regard to geochemical process in recent and ancient sulphur-rich marine environments. For example, Fourier-transform ion cyclotron resonance mass spectrometry (FT-ICR MS) is

increasingly being used for the analysis of OSC fractions (e.g., O and N functionalized compounds, aqueous dissolved species and molecules with weights in excess of 1000 Daltons), which were not previously amenable to characterization. It is likely that these new data types will reveal mechanisms previously unrecognized, further developing our models of the sedimentary sulphur cycle. Already, sulphur isotope analysis of organic matter in terms of individual compounds (e.g., nonpolar, volatile), specific fractions (e.g., polar, kerogen), and with consideration of all four stable isotopes is changing the way we understand the timing of OM sulphurization and the mechanisms and relationship with other sulphurized species (e.g., pyrite). Not only will these new data enable improved S proxies and potentially provide new proxies for paleoenvironmental research, but inevitably will lead to our better understanding of the sulphur and carbon cycles.

Acknowledgments This paper is dedicated to the memory of Ronald Kiene, an inspiring scientist and mentor and a dear friend. A.A. thanks the Israel Science Foundation (ISF) grant No. 1738/16 for partial support to this study. Y. O. R. and A.A. acknowledge grant No. 15/16 from the Ministry of National Infrastructures, Energy and Water Resources of Israel.

References

- Adam P, Schmid J-C, Albercht P, Connan J (1991) 2α and 3β steroid thiols from reductive cleavage of macromolecular petroleum fraction. *Tetrahedron Lett* 32:2955–2958
- Adam P, Schneckenburger P, Schaeffer P, Albrecht P (2000) Clues to early diagenetic sulfurization processes from mild chemical cleavage of labile sulfur-rich geomacromolecules. *Geochim Cosmochim Acta* 64:3485–3503
- Adam P, Schaeffer P, Gug S, Motsch E, Albrecht P (2009) Identification of a sulfide derivative with a bicyclic hydrocarbon skeleton related to squalene. Part II: synthesis of a S-spiro-like dithiolane triterpenoid. *Org Geochem* 40:885–894
- Aizenshtat Z, Stoler A, Cohen Y, Nielsen H (1983) The geochemical sulfur enrichment of recent organic matter by polysulfides in the Solar Lake. In: Bjørøy M, Albrecht P, Cornford C, de Groot K, Eglinton G (eds) *Advances in organic geochemistry*. John Wiley & Sons, Chichester, pp 279–288
- Aizenshtat Z, Amrani A (2004a) Significance of $\delta^{34}\text{S}$ and evaluation of its imprint on sedimentary organic matter: I. The role of reduced sulfur species in the diagenetic stage: a conceptual review. In: Hill RJ, Leventhal J, Aizenshtat Z, Baedeker MJ, Claypool G, Eganhouse R, Goldhaber M, Peters K (eds) *The geochemical society special publications*, vol 9. Elsevier, Amsterdam, pp 15–33
- Aizenshtat Z, Amrani A (2004b) Significance of $\delta^{34}\text{S}$ and evaluation of its imprint on sedimentary sulfur rich organic matter II: thermal changes of kerogens type II-S catagenetic stage controlled mechanisms. A study and conceptual overview. In: Hill RJ, Leventhal J, Aizenshtat Z, Baedeker MJ, Claypool G, Eganhouse R, Goldhaber M, Peters K (eds) *The geochemical society special publications*, vol 9. Elsevier, Amsterdam, pp 35–50
- Aizenshtat Z, Krein EB, Vairavamurthy MA, Goldstein TP (1995) Role of sulfur in the transformations of sedimentary organic matter: a mechanistic overview. In: Vairavamurthy MA, Schoonen MAA (eds) *Geochemical transformations of sedimentary sulfur*, ACS Symposium Series, vol 612. American Chemical Society, Washington, DC, pp 16–37
- Alsensz H et al (2015) Geochemical evidence for the link between sulfate reduction, sulfide oxidation and phosphate accumulation in a late Cretaceous upwelling system. *Geochem Trans* 16:2

- Amrani A (2014) Organosulfur compounds: molecular and isotopic evolution from biota to oil and gas. *Annu Rev Earth Planet Sci* 42:733–768
- Amrani A, Aizenshtat Z (2004a) Mechanisms of sulfur introduction chemically controlled: $\delta^{34}\text{S}$ imprint. *Org Geochem* 35:1319–1336
- Amrani A, Aizenshtat Z (2004b) Photosensitized oxidation of naturally occurring isoprenoid allyl alcohols as a possible pathway for their transformation to thiophenes in sulfur rich depositional environments. *Org Geochem* 35:693–712
- Amrani A, Aizenshtat Z (2004c) Reaction of polysulfide anions with α,β unsaturated isoprenoid aldehydes in aquatic media: simulation of oceanic conditions. *Org Geochem* 35:909–921
- Amrani A, Said-Ahmed W, Lewan MD, Aizenshtat Z (2006) Experiments on $\delta^{34}\text{S}$ mixing between organic and inorganic sulfur species during thermal maturation. *Geochim Cosmochim Acta* 70:5146–5161
- Amrani A, Turner JW, Ma Q, Tang Y, Hatcher PG (2007) Formation of sulfur and nitrogen cross-linked macromolecules under aqueous conditions. *Geochim Cosmochim Acta* 71:4141–4160. <https://doi.org/10.1016/j.gca.2007.06.051>
- Amrani A, Ma Q, Ahmad WS, Aizenshtat Z, Tang Y (2008), Sulfur isotope fractionation during incorporation of sulfur nucleophiles into organic compounds. *Chem Commun* 1356–1358. <https://doi.org/10.1039/B717113G>
- Amrani A, Sessions AL, Adkins JF (2009) Compound-specific $\delta^{34}\text{S}$ analysis of volatile organics by coupled GC/multicollector-ICPMS. *Anal Chem* 81:9027–9034
- Amrani A, Said-Ahmad W, Shaked Y, Kiene RP (2013) Sulfur isotope homogeneity of oceanic DMSP and DMS. *Proc Natl Acad Sci* 110:18413–18418
- Anderson TF, Pratt LM (1995) Isotopic evidence for the origin of organic sulfur and elemental sulfur in marine sediments. In: Vairavamurthy MA, Schoonen MAA (eds) *Geochemical transformations of sedimentary sulfur*, vol 612. ACS Publications, Washington, DC, pp 378–396
- Arndt S, Jørgensen BB, LaRowe DE, Middelburg JJ, Pancost RD, Regnier P (2013) Quantifying the degradation of organic matter in marine sediments: a review and synthesis. *Earth Sci Rev* 123:53–86
- Barakat AO, Rullkötter J (1995) The distribution of free organic sulfur compounds in sediments from the Nördlinger Ries, Southern Germany. In: Vairavamurthy MA, Schoonen MAA (eds) *Geochemical transformations of sedimentary sulfur*. American Chemical Society, Washington, DC, pp 311–331
- Baskin DK, Peters KE (1992) Early generation characteristics of a sulfur-rich Monterey Kerogen. *AAPG Bull* 76:1–13
- Bates TS, Lamb BK, Guenther A, Dignon J, Stoiber RE (1992) Sulfur emissions to the atmosphere from natural sources. *J Atmos Chem* 14:315–337
- Bates AL, Spiker EC, Hatcher PG, Stout SA, Weintraub VC (1995) Sulfur geochemistry of organic-rich sediments from Mud Lake, Florida, U.S.A. *Chem Geol* 121:245–262
- Bayona JM, Monjonell A, Miquel JC, Fowler SW, Albaigés J (2002) Biogeochemical characterization of particulate organic matter from a coastal hydrothermal vent zone in the Aegean Sea. *Org Geochem* 33:1609–1620
- Bechtel A, Movsumova U, Strobl SAI, Sachsenhofer RF, Soliman A, Gratzner R, Püttmann W (2013) Organofacies and paleoenvironment of the Oligocene Maikop series of Angeharan (eastern Azerbaijan). *Org Geochem* 56:51–67
- Behrens A, Schaeffer P, Albrecht P (1997) $14\beta,22\text{R}$ -epithiosteranes, a novel series of fossil steroids widespread in sediments. *Tetrahedron Lett* 38:4921–4924
- Belt ST, Allard WG, Massé G, Robert J-M, Rowland SJ (2000) Highly branched isoprenoids (HBIs): identification of the most common and abundant sedimentary isomers. *Geochim Cosmochim Acta* 64:3839–3851
- Belt ST et al (2017) Identification of C₂₅ highly branched isoprenoid (HBI) alkenes in diatoms of the genus *Rhizosolenia* in polar and sub-polar marine phytoplankton. *Org Geochem* 110:65–72
- Berner RA (1984) Sedimentary pyrite formation: an update. *Geochim Cosmochim Acta* 48:605–615

- Berner RA, Raiswell R (1983) Burial of organic carbon and pyrite sulfur in sediments over phanerozoic time: a new theory. *Geochim Cosmochim Acta* 47:855–862
- Blumenberg M, Mollenhauer G, Zabel M, Reimer A, Thiel V (2010) Decoupling of bio- and geohopanoids in sediments of the Benguela Upwelling System (BUS). *Org Geochem* 41:1119–1129
- Brassell SC (1993) Applications of biomarkers for delineating marine paleoclimatic fluctuations during the Pleistocene. In: Engel MH (ed) *Organic geochemistry*. Plenum Press, New York, pp 699–738
- Brassell SC, Dumitrescu M (2004) Recognition of alkenones in a lower Aptian porcellanite from the west-central Pacific. *Org Geochem* 35:181–188
- Brassell SC, Eglinton G, Marlowe IT, Pflaumann U, Sarnthein M (1986a) Molecular stratigraphy: a new tool for climatic assessment. *Nature* 320:129
- Brassell SC, Lewis CA, de Leeuw JW, de Lange F, Sinninghe Damsté JS (1986b) Isoprenoid thiophenes: novel products of sediment diagenesis? *Nature* 320:160–162
- Brocks JJ, Love GD, Summons RE, Knoll AH, Logan GA, Bowden SA (2005) Biomarker evidence for green and purple sulphur bacteria in a stratified Palaeoproterozoic sea. *Nature* 437:866–870
- Brüchert V, Pratt LM (1996) Contemporaneous early diagenetic formation of organic and inorganic sulfur in estuarine sediments from St. Andrew Bay, Florida, USA. *Geochim Cosmochim Acta* 60:2325–2332
- Brunner B, Bernasconi SM (2005) A revised isotope fractionation model for dissimilatory sulfate reduction in sulfate reducing bacteria. *Geochim Cosmochim Acta* 69:4759–4771
- Cabrera L, Cabrera M, Gorchs R, de las Heras FXC (2002) Lacustrine basin dynamics and organosulphur compound origin in a carbonate-rich lacustrine system (Late Oligocene Mequinenza Formation, SE Ebro Basin, NE Spain). *Sediment Geol* 148:289–317
- Charlson RJ, Lovelock JE, Andreae MO, Warren SG (1987) Oceanic phytoplankton, atmospheric sulphur, cloud albedo and climate. *Nature* 326:655
- Ciglencečki I, Čosović B, Vojvodić V, Plavšić M, Furić K, Minacci A, Baldi F (2000) The role of reduced sulfur species in the coalescence of polysaccharides in the Adriatic Sea. *Mar Chem* 71:233–249
- De Leeuw JW, Sinninghe Damsté JS (1990) Organic sulfur compounds and other biomarkers as indicators of palaeosalinity. In: Orr WL, White CM (eds) *Geochemistry of sulfur in fossil fuels*. American Chemical Society, Washington, DC, pp 417–443
- Dean WE, Arthur MA (1989) Iron-sulfur-carbon relationships in organic-carbon-rich sequences I: cretaceous western interior seaway. *Am J Sci* 289:708–743
- Dellwig O et al (1998) Geochemical and microfacies characterization of a Holocene depositional sequence in northwest Germany. *Org Geochem* 29:1687–1699
- Didyk BM, Simoneit BRT, Brassell SC, Eglinton G (1978) Organic geochemical indicators of palaeoenvironmental conditions of sedimentation. *Nature* 272:216
- Dittmar T, Koch B, Hertkorn N, Kattner G (2008) A simple and efficient method for the solid-phase extraction of dissolved organic matter (SPE-DOM) from seawater. *Limnol Oceanogr Methods* 6:230–235
- van Dongen BE, Schouten S, Sinninghe Damsté JS (2006) Preservation of carbohydrates through sulfurization in a Jurassic euxinic shelf sea: examination of the Blackstone Band TOC cycle in the Kimmeridge Clay Formation, UK. *Org Geochem* 37:1052–1073
- Eglinton G, Scott P, Belsky T, Burlingame AL, Calvin M (1964) Hydrocarbons of biological origin from a one-billion-year-old sediment. *Science* 145:263–264
- Eglinton TI, Sinninghe Damsté JS, Pool W, de Leeuw JW, Eijk G, Boon JJ (1992) Organic sulphur in macromolecular sedimentary organic matter. II. Analysis of distributions of sulphur-containing pyrolysis products using multivariate techniques. *Geochim Cosmochim Acta* 56:1545–1560
- Eglinton TI, Irvine JE, Vairavamurthy A, Zhou W, Manowitz B (1994) Formation and diagenesis of macromolecular organic sulfur in Peru margin sediments. *Org Geochem* 22:781–799

- Eliel EL, Hutchins RO, Mebane R, Willer RL (1976) Endocyclic vs. exocyclic attack in nucleophilic displacement reactions on five- and six-membered cyclic onium salts. *J Org Chem* 41:1052–1057
- Farrimond P, Love GD, Bishop AN, Innes HE, Watson DF, Snape CE (2003) Evidence for the rapid incorporation of hopanoids into kerogen. *Geochim Cosmochim Acta* 67:1383–1394
- Filley TR, Freeman KH, Wilkin RT, Hatcher PG (2002) HABiogeochemical controls on reaction of sedimentary organic matter and aqueous sulfides in Holocene sediments of Mud Lake, Florida. *Geochim Cosmochim Acta* 66:937–954
- Forster A et al (2008) The Cenomanian/Turonian oceanic anoxic event in the South Atlantic: new insights from a geochemical study of DSDP Site 530A. *Palaeogeogr Palaeoclimatol Palaeoecol* 267(3–4):256–283. <https://doi.org/10.1016/j.palaeo.2008.07.006>
- French KL, Rocher D, Zumberge JE, Summons RE (2015) Assessing the distribution of sedimentary C40 carotenoids through time. *Geobiology* 13:139–151
- Fukushima K, Yasukawa M, Muto N, Uemura H, Ishiwatari R (1992) Formation of C20 isoprenoid thiophenes in modern sediments. *Org Geochem* 18:83–91
- Gelin F, Boogers I, Noordeloos AAM, Sinninghe Damsté JS, Riegman R, De Leeuw JW (1997) Resistant biomacromolecules in marine microalgae of the classes Eustigmatophyceae and Chlorophyceae: geochemical implications. *Org Geochem* 26:659–675
- Gelin F, Kok MD, de Leeuw JW, Sinninghe Damsté JS (1998) Laboratory sulfurisation of the marine microalga *Nannochloropsis salina*. *Org Geochem* 29:1837–1848
- Giesemann A, Jaeger HJ, Norman AL, Krouse HR, Brand WA (1994) Online sulfur-isotope determination using an elemental analyzer coupled to a mass spectrometer. *Anal Chem* 66:2816–2819
- Gondwe M, Krol M, Gieskes W, Klaassen W, de Baar H (2003) The contribution of ocean-leaving DMS to the global atmospheric burdens of DMS, MSA, SO₂, and NSS SO₄⁼. *Glob Biogeochem Cycles* 17:1056
- Goffi MA, Eglinton TI (1994) Analysis of kerogens and kerogen precursors by flash pyrolysis in combination with isotope-ratio-monitoring gas chromatography-mass spectrometry (irm-GC-MS). *J High Resolut Chromatogr* 17:476–488
- Gransch J, Poshtuma J (1974). On the origin of sulfur in crudes. In: Tissot B, Biernner F (eds) *Advances in organic geochemistry*, Editions Technip, Paris, pp 727–830
- Grassineau NV (2006) High-precision EA-IRMS analysis of S and C isotopes in geological materials. *Appl Geochem* 21:756–765
- Greenwood PF et al (2015) Development and initial biogeochemical applications of compound-specific sulfur isotope analysis. In: Grice K (ed) *Principles and practice of analytical techniques in geosciences*. The Royal Society of Chemistry, Cambridge, UK, pp 285–312
- Grice K, Schaeffer P, Schwark L, Maxwell JR (1996) Molecular indicators of palaeoenvironmental conditions in an immature Permian shale (Kupferschiefer, Lower Rhine Basin, north-west Germany) from free and S-bound lipids. *Org Geochem* 25:131–147
- Grice K, Schouten S, Nissenbaum A, Charrach J, Sinninghe Damsté JS (1998) A remarkable paradox: sulfurised freshwater algal (*Botryococcus braunii*) lipids in an ancient hypersaline euxinic ecosystem. *Org Geochem* 28:195–216
- Grimalt JO, Yruela I, Saiz-Jimenez C, Toja J, de Leeuw JW, Albaigés J (1991) Sedimentary lipid biogeochemistry of an hypereutrophic alkaline lagoon. *Geochim Cosmochim Acta* 55:2555–2577
- Grossi V, Hirschler A, Raphael D, Rontani J-F, De Leeuw J, Bertrand J-C (1998) Biotransformation pathways of phytol in recent anoxic sediments. *Org Geochem* 29:845–861
- Grossi V, Beker B, Geenevasen JAJ, Schouten S, Raphael D, Fontaine M-F, Sinninghe Damsté JS (2004) C25 highly branched isoprenoid alkenes from the marine benthic diatom *Pleurosigma strigosum*. *Phytochemistry* 65:3049–3055
- Grotheer H, Greenwood PF, McCulloch MT, Böttcher ME, Grice K (2017) δ34S character of organosulfur compounds in kerogen and bitumen fractions of sedimentary rocks. *Org Geochem* 110:60–64

- Hartgers WA, Lòpez JF, Sinninghe Damstè JS, Reiss C, Maxwell JR, Grimalt JO (1997) Sulfur-binding in recent environments: II. Speciation of sulfur and iron and implications for the occurrence of organo-sulfur compounds. *Geochim Cosmochim Acta* 61:4769–4788
- Hartgers WA, Schouten S, Lopez JF, Sinninghe Damstè JS, Grimalt JO (2000) ^{13}C -contents of sedimentary bacterial lipids in a shallow sulfidic monomictic lake (Lake Cisó, Spain). *Org Geochem* 31:777–786
- Hayes JM, Freeman KH, Popp BN, Hoham CH (1990) Compound-specific isotopic analyses: a novel tool for reconstruction of ancient biogeochemical processes. *Org Geochem* 16:1115–1128
- Hebting Y et al (2006) Biomarker evidence for a major preservation pathway of sedimentary organic carbon. *Science* 312:1627–1631
- Hefter J, Hauke V, Richnow HH, Michaelis W (1995) Alkanoic subunits in sulfur-rich geomacromolecules, geochemical transformations of sedimentary sulfur. *Am Chem S*, pp 93–109
- Heitmann T, Blodau C (2006) Oxidation and incorporation of hydrogen sulfide by dissolved organic matter. *Chem Geol* 235:12–20
- Higgins MJ, Chen Y-C, Yarosz DP, Murthy SN, Maas NA, Glindemann D, Novak JT (2006) Cycling of volatile organic sulfur compounds in anaerobically digested biosolids and its implications for odors. *Water Environ Res* 78:243–252
- Ho TY, Quigg A, Finkel ZV, Milligan AJ, Wyman K, Falkowski PG, Morel FMM (2003) The elemental composition of some marine phytoplankton. *J Phycol* 39:1145–1159
- Hofmann IC, Hutchison J, Robson JN, Chicarelli MI, Maxwell JR (1992) Evidence for sulphide links in a crude oil asphaltene and kerogens from reductive cleavage by lithium in ethylamine. *Org Geochem* 19:371–387
- Holba AG, Tegelaar E, Ellis L, Singletary MS, Albrecht P (2000) Tetracyclic polyprenoids: indicators of freshwater (lacustrine) algal input. *Geology* 28:251–254
- Holba AG et al (2003) Application of tetracyclic polyprenoids as indicators of input from fresh-brackish water environments. *Org Geochem* 34:441–469
- Huang W-Y, Meinschein WG (1979) Sterols as ecological indicators. *Geochim Cosmochim Acta* 43:739–745
- Hughes WB, Holba AG, Dzou LI (1995) The ratios of dibenzothiophene to phenanthrene and pristane to phytane as indicators of depositional environment and lithology of petroleum source rocks. *Geochim Cosmochim Acta* 59:3581–3598
- Junium CK, Keely BJ, Freeman KH, Arthur MA (2011) Chlorins in mid-cretaceous black shales of the demerara rise: the oldest known occurrence. *Org Geochem* 42:856–859
- van Kaam-Peters HME, Sinninghe Damstè JS (1997) Characterisation of an extremely organic sulphur-rich, 150 Ma old carbonaceous rock: palaeoenvironmental implications. *Org Geochem* 27:371–397
- van Kaam-Peters HME, Schouten S, Köster J, Sinninghe Damstè SJ (1998) Controls on the molecular and carbon isotopic composition of organic matter deposited in a Kimmeridgian euxinic shelf sea: evidence for preservation of carbohydrates through sulfurisation. *Geochim Cosmochim Acta* 62:3259–3283
- Kaplan I, Rittenberg S (1964) Microbiological fractionation of sulphur isotopes. *Microbiology* 34:195–212
- Kasten S, Jørgensen BB (2000). Sulfate reduction in marine sediments. In: Horst D. Schulz and Matthias Zabel (eds) *Marine geochemistry*. Springer, Berlin, pp 263–281
- Kenig F, Sinninghe Damstè J, Frewin N, Hayes J (1995) Molecular indicators for palaeoenvironmental change in a Messinian evaporitic sequence (Vena del Gesso, Italy) II. Stratigraphic changes in abundances and ^{13}C contents of free and sulphur-bound skeletons in a single marl bed. *Org Geochem* 23:485–526
- Kiene RP (1988) Dimethyl sulfide metabolism in salt marsh sediments. *FEMS Microbiol Lett* 53:71–78
- Kiene RP (1996) Microbial cycling of organosulfur gases in marine and freshwater environments. *Int Ver Theor Angew Limnol: Mitt* 25:137–151

- Kiene RP, Linn LJ (2000) The fate of dissolved dimethylsulfoniopropionate (DMSP) in seawater: tracer studies using ^{35}S -DMSP. *Geochim Cosmochim Acta* 64:2797–2810
- Kiene RP, Service SK (1991) Decomposition of dissolved DMSP and DMS in estuarine waters: dependence on temperature and substrate concentration. *Mar Ecol Prog Ser* 76:1–11
- Kohnen MEL, Sinninghe Damsté JS, Kock-van Dalen AC, Ten Haven HL, Rullkötter J, De Leeuw JW (1990) Origin and diagenetic transformations of C25 and C30 highly branched isoprenoid sulphur compounds: further evidence for the formation of organically bound sulphur during early diagenesis. *Geochimica et Cosmochimica Acta* 54:3053–3063
- Kohnen ME, Sinninghe Damsté JS, De Leeuw JW (1991a) Biases from natural sulphurization in palaeoenvironmental reconstruction based on hydrocarbon biomarker distributions. *Nature* 349:775
- Kohnen ME, Sinninghe Damsté JS, van Dalen KA, De Leeuw JW (1991b) Di- or polysulphide-bound biomarkers in sulphur-rich geomacromolecules as revealed by selective chemolysis. *Geochimica et Cosmochimica Acta* 55:1375–1394
- Kohnen MEL, Schouten S, Sinninghe Damsté JS, de Leeuw JW, Merritt DA, Hayes JM (1992) Recognition of paleobiochemicals by a combined molecular sulfur and isotope geochemical approach. *Science* 256:358–362
- Kohnen MEL, Sinninghe Damsté JS, Baas M, van Dalen ACK, de Leeuw JW (1993) Sulphur-bound steroid and phytane carbon skeletons in geomacromolecules: implications for the mechanism of incorporation of sulphur into organic matter. *Geochim Cosmochim Acta* 57:2515–2528
- Kok MD, Rijpstra WIC, Robertson L, Volkman JK, Sinninghe Damsté JS (2000a) Early steroid sulfuration in surface sediments of a permanently stratified lake (Ace Lake, Antarctica). *Geochim Cosmochim Acta* 64:1425–1436
- Kok MD, Schouten S, Sinninghe Damsté JS (2000b) Formation of insoluble, nonhydrolyzable, sulfur-rich macromolecules via incorporation of inorganic sulfur species into algal carbohydrates. *Geochim Cosmochim Acta* 64:2689–2699
- Kolonic S et al (2002) Geochemical characterization of Cenomanian/Turonian black shales from the Tarfaya Basin (SW Morocco). *J Pet Geol* 25:325–350
- Koopmans MP, Sinninghe Damsté JS, Lewan MD, De Leeuw JW (1995) Thermal stability of thiophene biomarkers as studied by hydrous pyrolysis. *Org Geochem* 23:583–596
- Koopmans MP, De Leeuw JW, Lewan MD, Sinninghe Damsté JS (1996a) Impact of diagenetic and catagenesis on sulphur and oxygen sequestration of biomarkers as revealed by artificial maturation of an immature sedimentary rock. *Org Geochem* 25:391–426
- Koopmans MP et al (1996b) Diagenetic and catagenetic products of isorenieratene: molecular indicators for photic zone anoxia. *Geochim Cosmochim Acta* 60:4467–4496
- Koopmans MP, Schaeffer-Reiss C, de Leeuw JW, Lewan MD, Maxwell JR, Schaeffer P, Sinninghe Damsté JS (1997) Sulphur and oxygen sequestration of n-C37 and n-C38 unsaturated ketones in an immature kerogen and the release of their carbon skeletons during early stages of thermal maturation. *Geochim Cosmochim Acta* 61:2397–2408
- Koopmans MP, Rijpstra WIC, De Leeuw JW, Lewan MD, Sinninghe Damsté JS (1998) Artificial maturation of an immature sulfur and organic matter rich limestone from the Ghareb formation, Jordan. *Org Geochem* 28:503–521
- Koopmans MP, Rijpstra WIC, Klapwijk MM, de Leeuw JW, Lewan MD, Sinninghe Damsté JS (1999) A thermal and chemical degradation approach to decipher pristane and phytane precursors in sedimentary organic matter. *Org Geochem* 30:1089–1104
- Köster J, Van Kaam-Peters HME, Koopmans MP, De Leeuw JW, Sinninghe Damsté JS (1997) Sulphurisation of homohopaneoids: effects on carbon number distribution, speciation, and 22S/22R epimer ratios. *Geochim Cosmochim Acta* 61:2431–2452
- Köster J, Rospondek M, Schouten S, Kotarba M, Zubrzycki A, Sinninghe Damsté JS (1998) Biomarker geochemistry of a foreland basin: the Oligocene Menilite Formation in the Flysch Carpathians of Southeast Poland. *Org Geochem* 29:649–669
- Krein EB (1993) Organic sulfur in the geosphere: analysis, structures and chemical processes. In: Patai S, Rappoport Z (eds) *Sulphur-containing functional groups*. Wiley, New York, pp 975–1032

- Krein EB, Aizenshtat Z (1994) The formation of isoprenoid sulfur compounds during diagenesis: simulated sulfur incorporation and thermal transformation. *Org Geochem* 21:1015–1025
- Krein EB, Aizenshtat Z (1995), Proposed thermal pathways for sulfur transformations in organic macromolecules; laboratory simulation experiments. Vairavamurthy MA, Schoonen MAA, Eglinton TI, Luther GW, III, Manowitz B. *Geochemical transformations of sedimentary sulfur*, 612. American Chemical Society, Washington, 110–137
- Ksionzek KB, Lechtenfeld OJ, McCallister SL, Schmitt-Kopplin P, Geuer JK, Geibert W, Koch BP (2016) Dissolved organic sulfur in the ocean: biogeochemistry of a petagram inventory. *Science* 354:456–459
- Kuypers MM, Blokker P, Erbacher J, Kinkel H, Pancost RD, Schouten S, Damsté JSS (2001) Massive expansion of marine archaea during a mid-Cretaceous oceanic anoxic event. *Science* 293:92–95
- Lallier-Vergès E, Hayes JM, Boussafir M, Zaback DA, Tribovillard NP, Connan J, Bertrand P (1997) Productivity-induced sulphur enrichment of hydrocarbon-rich sediments from the Kimmeridge Clay Formation. *Chem Geol* 134:277–288
- LaLonde RT, Ferrara LM, Hayes MP (1987) Low-temperature, polysulfide reactions of conjugated ene carbonyls: a reaction model for the geologic origin of S-heterocycles. *Org Geochem* 11:563–571
- Lana A et al (2011) An updated climatology of surface dimethylsulfide concentrations and emission fluxes in the global ocean. *Glob Biogeochem Cycles* 25:GB1004
- Levasseur M (2013) Impact of Arctic meltdown on the microbial cycling of sulphur. *Nat Geosci* 6:691
- Leventhal JS (1995) Carbon-sulfur plots to show diagenetic and epigenetic sulfidation in sediments. *Geochim Cosmochim Acta* 59:1207–1211
- Lewan MD (1998) Sulphur-radical control on petroleum formation rates. *Nature* 391:164–166
- Liss PS, Hatton AD, Malin G, Nightingale PD, Turner SM (1997) Marine sulphur emissions. *Philos Trans R Soc Lond B: Biol Sci* 352:159–169
- Loch A, Lippa K, Carlson D, Chin Y, Traina S, Roberts A (2002) Nucleophilic aliphatic substitution reactions of propachlor, alachlor, and metolachlor with bisulfide (HS⁻) and polysulfides (S_n²⁻). *Environ Sci Technol* 36:4065–4073
- Lockhart RS, Meredith W, Love GD, Snape CE (2008) Release of bound aliphatic biomarkers via hydrolysis from type II kerogen at high maturity. *Org Geochem* 39:1119–1124
- Lomans BP, van der Drift C, Pol A, Op den Camp HJM (2002) Microbial cycling of volatile organic sulfur compounds. *Cell Mol Life Sci CMLS* 59:575–588
- Love GD, McAulay A, Snape CE, Bishop AN (1997) Effect of process variables in catalytic hydrolysis on the release of covalently bound aliphatic hydrocarbons from sedimentary organic matter. *Energy Fuel* 11:522–531
- Mackenzie AS, Brassell SC, Eglinton G, Maxwell JR (1982) Chemical fossils: the geological fate of steroids. *Science* 217:491–504
- Martin G (1993) Pyrolysis of organosulphur compounds. In: Patai S, Rappoport Z (eds) *Sulphur-containing functional groups*. Wiley, New York, pp 395–437
- Mawson DH, Keely BJ (2008) Novel functionalised chlorins in sediments of the Messinian Vena del Gesso evaporitic sequence: evidence for a facile route to reduction for biomarkers. *Org Geochem* 39:203–209
- McKee GA, Hatcher PG (2010) Alkyl amides in two organic-rich anoxic sediments: a possible new abiotic route for N sequestration. *Geochim Cosmochim Acta* 74:6436–6450
- Meilijson A et al (2015) Evidence for specific adaptations of fossil benthic foraminifera to anoxic-dysoxic environments. *Paleobiology* 42:77–97
- Minster T, Nathan Y, Raveh A (1992) Carbon and sulfur relationships in marine Senonian organic-rich, iron-poor sediments from Israel – a case study. *Chem Geol* 97:145–161
- Mopper K, Kieber DJ (2002) Photochemistry and the cycling of carbon, sulfur, nitrogen and phosphorus. In: Carlson CA (ed) *Biogeochemistry of marine dissolved organic matter*. Academic, San Diego, pp 455–507
- Morse JW, Emeis KC (1992) Carbon/sulphur/iron relationships in upwelling sediments. In: Summerhayes CP, Prell WL, Emeis KC (eds) *Upwelling systems: evolution since the Early Miocene*, vol 64. vol 1. Geological Society Special Publications, London, 247–255

- Mossmann J-R, Aplin AC, Curtis CD, Coleman ML (1991) Geochemistry of inorganic and organic sulphur in organic-rich sediments from the Peru Margin. *Geochim Cosmochim Acta* 55:3581–3595
- Murray IP, Love GD, Snape CE, Bailey NJL (1998) Comparison of covalently-bound aliphatic biomarkers released via hydrolysis with their solvent-extractable counterparts for a suite of Kimmeridge clays. *Org Geochem* 29:1487–1505
- Naafs BDA, Pancost RD (2014) Environmental conditions in the South Atlantic (Angola Basin) during the Early Cretaceous. *Org Geochem* 76:184–193
- Oduro H, Van Alstyne KL, Farquhar J (2012) Sulfur isotope variability of oceanic DMSP generation and its contributions to marine biogenic sulfur emissions. *Proc Natl Acad Sci* 109:9012–9016
- Oduro H, Kamyshny A Jr, Zerkle AL, Li Y, Farquhar J (2013) Quadruple sulfur isotope constraints on the origin and cycling of volatile organic sulfur compounds in a stratified sulfidic lake. *Geochim Cosmochim Acta* 120:251–262
- Ohkouchi N, Kuroda J, Taira A (2015) The origin of Cretaceous black shales: a change in the surface ocean ecosystem and its triggers. *Proc Jpn Acad Ser B Phys Biol Sci* 91:273–291
- Orr WL (1986) Kerogen/asphaltene/sulfur relationships in sulfur-rich Monterey oils. *Org Geochem* 10:499–516
- Ourisson G, Albrecht P, Rohmer M (1984) The microbial origin of fossil fuels. *Sci Am* 251:44–51
- Pagani M (2014) Biomarker-based inferences of past climate: the alkenone pCO₂ Proxy. In: Turekian KK (ed) *Treatise on geochemistry*, 2nd edn. Elsevier, Oxford, pp 361–378
- Pancost RD, Telnæs N, Sinninghe Damsté JS (2001) Carbon isotopic composition of an isoprenoid-rich oil and its potential source rock. *Org Geochem* 32:87–103
- Peng P, Morales-Izquierdo A, Fu J, Sheng G, Jiang J, Hogg A, Strausz OP (1998) Lanostane sulfides in an immature crude oil. *Org Geochem* 28:125–134
- Peters KE, Moldowan JM (1991) Effects of source, thermal maturity, and biodegradation on the distribution and isomerization of homohopanes in petroleum. *Org Geochem* 17:47–61
- Peters KE, Walters CC, Moldowan MJ (2005) *The biomarker guide*, vol 1. The Press Syndicate of the University of Cambridge, Cambridge, UK
- Pickering MD, Keely BJ (2008) Alkyl sulfur chlorophyll derivatives: preparation and liquid chromatography-multistage tandem mass spectrometric characterisation of analogues of naturally occurring sedimentary species. *Org Geochem* 39:1046–1050
- Pickering MD, Keely BJ (2011) Low temperature abiotic formation of mesopyropheophorbide a from pyropheophorbide a under conditions simulating anoxic natural environments. *Geochim Cosmochim Acta* 75:533–540
- Pickering MD, Keely BJ (2013) Origins of enigmatic C-3 methyl and C-3 H porphyrins in ancient sediments revealed from formation of pyropheophorbide d in simulation experiments. *Geochim Cosmochim Acta* 104:111–122. <https://doi.org/10.1016/j.gca.2012.11.021>
- Pohlabein AM, Dittmar T (2015) Novel insights into the molecular structure of non-volatile marine dissolved organic sulfur. *Mar Chem* 168:86–94
- Pohlabein AM, Gomez-Saez GV, Noriega-Ortega BE, Dittmar T (2017) Experimental evidence for abiotic sulfuration of marine dissolved organic matter. *Front Mar Sci* 4(364):1–11
- Poinsot J, Schneckenburger P, Trendel J (1997). Novel polycyclic polyprenoid sulfides in sediments. *Chem Commun* 2191–2192. <https://doi.org/10.1039/A704649I>
- Poinsot J, Schneckenburger P, Adam P, Schaeffer P, Trendel JM, Riva A, Albrecht P (1998) Novel polycyclic sulfides derived from regular polyprenoids in sediments: characterization, distribution, and geochemical significance. *Geochim Cosmochim Acta* 62:805–814
- Putschew A, Scholz-Böttcher BM, Rullkötter J (1995) Organic geochemistry of sulfur-rich surface sediments of meromictic lake Cadagno, Swiss Alps. In M.A. Vairavamurthy, M.A.A. Schoonen, T.I. Eglinton, G.W. Luther III, B. Manowitz (eds.), *Geochemical Transformations of Sedimentary Sulfur*. American Chemical Society, pp. 59–79
- Putschew A, Scholz-Böttcher BM, Rullkötter J (1996) Early diagenesis of organic matter and related sulphur incorporation in surface sediments of meromictic Lake Cadagno in the Swiss Alps. *Org Geochem* 25:379–390

- Putschew A et al (1998) Release of sulfur- and oxygen-bound components from a sulfur-rich kerogen during simulated maturation by hydrous pyrolysis. *Org Geochem* 29:1875–1890
- Quijada M, Riboulleau A, Faure P, Michels R, Tribouvillard N (2016) Organic matter sulfurization on protracted diagenetic timescales: the possible role of anaerobic oxidation of methane. *Mar Geol* 381:54–66
- Rabus R, Hansen TA, Widdel F (2006) Dissimilatory sulfate- and sulfur-reducing prokaryotes. In: Rosenberg E, DeLong EF, Lory S, Stackebrandt E, Thompson F (eds) *The prokaryotes*. Springer, Berlin, pp 659–768
- Raven MR, Adkins JF, Werne JP, Lyons TW, Sessions AL (2015) Sulfur isotopic composition of individual organic compounds from Cariaco Basin sediments. *Org Geochem* 80:53–59
- Raven MR, Sessions AL, Adkins JF, Thunell RC (2016) Rapid organic matter sulfurization in sinking particles from the Cariaco Basin water column. *Geochim Cosmochim Acta* 190:175–190
- Richnow HH, Jenisch A, Michaelis W (1992) Structural investigations of sulphur-rich macromolecular oil fractions and a kerogen by sequential chemical degradation. *Org Geochem* 19:351–370
- Riedinger N et al (2017) Sulfur cycling in an iron oxide-dominated, dynamic marine depositional system: the argentine continental margin. *Front Earth Sci* 5(33):1–19
- Rontani JF, Volkman JK (2003) Phytol degradation products as biogeochemical tracers in aquatic environments. *Org Geochem* 34:1–35
- Rontani J-F, Bonin PC, Volkman JK (1999) Biodegradation of free phytol by bacterial communities isolated from marine sediments under aerobic and denitrifying conditions. *Appl Environ Microbiol* 65:5484–5492
- Rosenberg OY et al (2017) Study of thermal maturation processes of sulfur-rich source rock using compound specific sulfur isotope analysis. *Org Geochem* 112:59–74
- Rosenberg OY, Kutuzov I, Amrani A (2018) Sulfurization as a preservation mechanism of compound specific $\delta^{13}\text{C}$. *Org Geochem* 125:66–69
- Russell M, Hartgers WA, Grimalt JO (2000) Identification and geochemical significance of sulphurized fatty acids in sedimentary organic matter from the Lorca Basin, SE Spain. *Geochim Cosmochim Acta* 64:3711–3723
- Sarret G, Mongenot T, Connan J, Derenne S, Kasrai M, Bancroft MG, Largeau C (2002) Sulfur speciation in kerogens of the Orbagnoux deposit (Upper Kimmeridgian, Jura) by XANES spectroscopy and pyrolysis. *Org Geochem* 33:877–895
- Sawada K, Handa N, Shiraiwa Y, Danbara A, Montani S (1996) Long-chain alkenones and alkyl alkenoates in the coastal and pelagic sediments of the northwest North Pacific, with special reference to the reconstruction of *Emiliania huxleyi* and *Gephyrocapsa oceanica* ratios. *Org Geochem* 24:751–764
- Schaeffer P, Ocampo R, Callot H, Albrecht P (1993) Extraction of bound porphyrins from sulphur-rich sediments and their use for reconstruction of palaeoenvironments. *Nature* 364:133
- Schaeffer P, Reiss C, Albrecht P (1995) Geochemical study of macromolecular organic matter from sulfur-rich sediments of evaporitic origin (Messinian of Sicily) by chemical degradations. *Org Geochem* 23:567–581
- Schaeffer P et al (2006) The wide diversity of hopanoid sulfides evidenced by the structural identification of several novel hopanoid series. *Org Geochem* 37:1590–1616
- Schiff JA (1980) Pathways of assimilatory sulphate reduction in plants and microorganisms. In: Elliott K, Whelan J (eds) *Sulphur in biology*, vol 72. Excerpta Medica, Amsterdam, pp 49–64
- Schmid J-C (1986) *Marqueurs biologiques soufrés dans les pétroles*. University of Strasbourg, France
- Schoell M, Schouten S, Damst JSS, de Leeuw JW, Summons RE (1994) A molecular organic carbon isotope record of miocene climate changes. *Science* 263:1122–1125
- Schoonen MA (2004) Mechanisms of sedimentary pyrite formation. In: Amend JP, Edwards KJ, Lyons TW (eds) *Sulfur biogeochemistry—past and present*. Geological Society of America, Boulder, pp 117–134

- Schouten S, de Graaf W, Sinninghe Damsté JS, van Driel GB, de Leeuw JW (1994) Laboratory simulation of natural sulphurization: II. Reaction of multi-functionalized lipids with inorganic polysulphides at low temperatures. *Org Geochem* 22:825–834
- Schouten S, Sinninghe Damsté JS, De Leeuw JW (1995a) The occurrence and distribution of low-molecular-weight sulphoxides in polar fractions of sediment extracts and petroleum. *Org Geochem* 23:129–138
- Schouten S, Sinninghe Damsté JS, Kohnen MEL, De Leeuw JW (1995b) The effect of hydrosulphurization on stable carbon isotopic compositions of free and sulphur-bound lipids. *Geochim Cosmochim Acta* 59:1605–1609
- Schouten S, Schoell M, Rijpstra WIC, Sinninghe Damsté JS, de Leeuw JW (1997) A molecular stable carbon isotope study of organic matter in immature Miocene Monterey sediments, Pismo basin. *Geochim Cosmochim Acta* 61:2065–2082
- Schouten S et al (1998a) Biosynthetic effects on the stable carbon isotopic compositions of algal lipids: implications for deciphering the carbon isotopic biomarker record. *Geochim Cosmochim Acta* 62:1397–1406
- Schouten S, Sephton S, Baas M, Sinninghe Damsté JS (1998b) Steroid carbon skeletons with unusually branched C-3 alkyl side chains in sulphur-rich sediments. *Geochim Cosmochim Acta* 62:1127–1132
- Schouten S, De Loureiro MR, Sinninghe Damsté J, de Leeuw J (2001) Molecular biogeochemistry of Monterey sediments, Naples Beach, California: I. Distributions of hydrocarbons and organic sulfur compounds. In: Isaacs C, Rullkötter J (eds) *The Monterey formation: from rocks to molecules*. Columbia University Press, New York, pp 150–174
- Schreiber BC et al (2001) Characterisation of organic matter formed in hypersaline carbonate/evaporite environments: hydrocarbon potential and biomarkers obtained through artificial maturation studies. *J Pet Geol* 24:309–338
- Schwark L, Vliex M, Schaeffer P (1998) Geochemical characterization of Malm Zeta laminated carbonates from the Franconian Alb, SW-Germany (II). *Org Geochem* 29:1921–1952
- Sela-Adler M, Said-Ahmad W, Sivan O, Eckert W, Kiene RP, Amrani A (2016) Isotopic evidence for the origin of dimethylsulfide and dimethylsulfoniopropionate-like compounds in a warm, monomictic freshwater lake. *Environ Chem* 13:340–351
- Shawar L, Said-Ahmad W, Amrani A (2015) Compound specific sulfur isotope approach to study the redox cycling during the deposition of senonian oil shales in the late cretaceous tethyan margin, Israel. In: 27th international meeting on organic geochemistry, Prague, Czech Republic
- Shawar L, Halevy I, Said-Ahmad W, Feinstein S, Boyko V, Kamyshny A, Amrani A (2018) Dynamics of pyrite formation and organic matter sulfurization in organic-rich rocks: cretaceous chalks from the Shefela Basin, Israel. *Geochim Cosmochim Acta* 241:219–239
- Shen Y, Buick R (2004) The antiquity of microbial sulfate reduction. *Earth Sci Rev* 64:243–272
- Siedenberg K, Strauss H, Podlaha O, den Boorn SV (2018) Multiple sulfur isotopes ($\delta^{34}\text{S}$, $\Delta^{33}\text{S}$) of organic sulfur and pyrite from Late Cretaceous to Early Eocene oil shales in Jordan. *Org Geochem* 125:29–40
- Sievert SM, Kiene RP, Schulz-Vogt HN (2007) The sulfur cycle. *Oceanography* 20:117–123
- Sim MS, Bosak T, Ono S (2011) Large sulfur isotope fractionation does not require disproportionation. *Science* 333:74–77
- Simó R, Vila-Costa M, Alonso-Sáez L, Cardelús C, Guadayol Ò, Vázquez-Domínguez E, Gasol JM (2009) Annual DMSP contribution to S and C fluxes through phytoplankton and bacterioplankton in a NW Mediterranean coastal site. *Aquat Microb Ecol* 57:43–55
- Sinninghe Damsté JS, De Leeuw JW (1990) Analysis, structure and geochemical significance of organically-bound sulphur in the geosphere: state of the art and future research. *Org Geochem* 16:1077–1101
- Sinninghe Damsté JS, Koopmans MP (1997) The fate of carotenoids in sediments: an overview. *Pure Appl Chem* 69:2067–2074
- Sinninghe Damsté JS, Rijpstra WIC (1993) Identification of a novel C25 highly branched isoprenoid thiophene in sediments. *Org Geochem* 20:327–331

- Sinninghe Damsté JS, Rijpstra WIC, de Leeuw JW, Schenck PA (1988) Origin of organic sulphur compounds and sulphur-containing high molecular weight substances in sediments and immature crude oils. *Org Geochem* 13:593–606
- Sinninghe Damsté JS, Rijpstra WIC, De Leeuw JW, Schenck PA (1989) The occurrence and identification of series of organic sulphur compounds in oils and sediment extracts: II. Their presence in samples from hypersaline and non-hypersaline palaeoenvironments and possible application as source, palaeoenvironmental. *Geochim Cosmochim Acta* 53:1323–1341
- Sinninghe Damsté JS, Rijpstra WIC, De Leeuw JW, Lijmbach GWM (1994) Molecular characterization of organically-bound sulfur in crude oils. A feasibility study for the application of Raney Ni desulfurization as a new method to characterize crude oils. *J High Resolut Chromatogr* 17:489–500
- Sinninghe Damsté JS, Van Duin ACT, Hollander D, Kohnen MEL, De Leeuw JW (1995) Early diagenesis of bacteriohopanepolyol derivatives: formation of fossil homohopanooids. *Geochim Cosmochim Acta* 59:5141–5157
- Sinninghe Damsté JS, Schouten S, de Leeuw JW, van Duin ACT, Geenevasen JAJ (1999) Identification of novel sulfur-containing steroids in sediments and petroleum: probable incorporation of sulfur into $\delta 5,7$ -sterols during early diagenesis. *Geochim Cosmochim Acta* 63:31–38
- Sinninghe Damsté JS et al (2004) The rise of the rhizosolenid diatoms. *Science* 304:584–587
- Sinninghe Damsté JS, Rijpstra WIC, Coolen MJL, Schouten S, Volkman JK (2007) Rapid sulfurisation of highly branched isoprenoid (HBI) alkenes in sulfidic Holocene sediments from Ellis Fjord, Antarctica. *Org Geochem* 38:128–139
- Sinninghe Damsté JS, Kuypers MMM, Pancost RD, Schouten S (2008) The carbon isotopic response of algae, (cyano)bacteria, archaea and higher plants to the late Cenomanian perturbation of the global carbon cycle: insights from biomarkers in black shales from the Cape Verde Basin (DSDP Site 367). *Org Geochem* 39:1703–1718
- Sinninghe Damsté JS, Schouten S, Volkman JK (2014) C27–C30 neohop-13(18)-enes and their saturated and aromatic derivatives in sediments: indicators for diagenesis and water column stratification. *Geochim Cosmochim Acta* 133:402–421
- Squier AH, Hodgson DA, Keely BJ (2003) Identification of novel sulfur-containing derivatives of chlorophyll a in a recent sediment. *Chem Commun*, pp 624–625
- Squier AH, Hodgson DA, Keely BJ (2004) Structures and profiles of novel sulfur-linked chlorophyll derivatives in an Antarctic lake sediment. *Org Geochem* 35:1309–1318
- Stefels J, Steinke M, Turner S, Malin G, Belviso S (2007) Environmental constraints on the production and removal of the climatically active gas dimethylsulphide (DMS) and implications for ecosystem modelling. *Biogeochemistry* 83:245–275
- Stets EG, Hines ME, Kiene RP (2004) Thiol methylation potential in anoxic, low-pH wetland sediments and its relationship with dimethylsulfide production and organic carbon cycling. *FEMS Microbiol Ecol* 47:1–11
- Summons RE, Volkman JK, Boreham CJ (1987) Dinosterane and other steroidal hydrocarbons of dinoflagellate origin in sediments and petroleum. *Geochim Cosmochim Acta* 51:3075–3082
- Takahashi H, Kopriva S, Giordano M, Saito K, Hell R (2011) Sulfur assimilation in photosynthetic organisms: molecular functions and regulations of transporters and assimilatory enzymes. *Annu Rev Plant Biol* 62:157–184
- Tannenbaum E, Aizenshtat Z (1985) Formation of immature asphalt from organic-rich carbonate rocks. 1. Geochemical correlation. *Org Geochem* 8:181–192
- Thierstein HR, Geitsenauer KRM, Molino B (1977) Global synchronicity of late Quaternary coccolith datum levels validation by oxygen isotopes. *Geology* 5:400–404
- Tissot B (1984) Recent advances in petroleum geochemistry applied to hydrocarbon exploration. *AAPG Bull* 68:545–563
- Urban N, Ernst K, Bernasconi S (1999) Addition of sulfur to organic matter during early diagenesis of lake sediments. *Geochim Cosmochim Acta* 63:837–853

- Vairavamurthy A, Zhou W, Eglinton T, Manowitz B (1994) Sulfonates: a novel class of organic sulfur compounds in marine sediments. *Geochim Cosmochim Acta* 58:4681–4687
- Vairavamurthy MA, Manowitz B, Maletic D, Wolfe H (1997) Interactions of thiols with sedimentary particulate phase: studies of 3-mercaptopropionate in salt marsh sediments from Shelter Island, New York. *Org Geochem* 26:577–585
- Valisolalao J, Perakis N, Chappe B, Albrecht P (1984) A novel sulfur containing C35 hopanoid in sediments. *Tetrahedron Lett* 25:1183–1186
- Volkman JK, Kearney P, Jeffrey SW (1990) A new source of 4-methyl sterols and 5 α (H)-stanols in sediments: prymnesiophyte microalgae of the genus *Pavlova*. *Org Geochem* 15:489–497
- Volkman JK, Barrett SM, Dunstan GA (1994) C25 and C30 highly branched isoprenoid alkenes in laboratory cultures of two marine diatoms. *Org Geochem* 21:407–414
- Volkman JK, Barrerr SM, Blackburn SI, Sikes EL (1995) Alkenones in *Gephyrocapsa oceanica*: implications for studies of paleoclimate. *Geochim Cosmochim Acta* 59:513–520
- Wagner T, Sinninghe Damste JS, Hofmann P, Beckmann B (2004) Euxinia and primary production in Late Cretaceous eastern equatorial Atlantic surface waters fostered orbitally driven formation of marine black shales. *Paleoceanography* 19:1–13
- Wakeham S (2002) Palaeoenvironmental reconstructions using stable carbon isotopes and organic biomarkers. In: Gianguzza A, Pelizzetti E, Sammartano S (eds) *Chemistry of marine water and sediments*. Springer Berlin Heidelberg, Berlin, pp 423–443
- Wakeham SG, Beier JA, Clifford HC (1991) Organic matter sources in the Black Sea as inferred from hydrocarbon distributions. In: Ízdar E, Murray JW (eds) *Black Sea oceanography*. Springer, Dordrecht, pp 319–341
- Wakeham SG, Sinninghe Damsté JS, Kohnen MEL, De Leeuw JW (1995) Organic sulfur compounds formed during early diagenesis in Black Sea sediments. *Geochim Cosmochim Acta* 59:521–533
- Wakeham SG, Lee C, Hedges JI, Hernes PJ, Peterson MJ (1997) Molecular indicators of diagenetic status in marine organic matter. *Geochim Cosmochim Acta* 61:5363–5369
- Wakeham SG et al (2007) Microbial ecology of the stratified water column of the Black Sea as revealed by a comprehensive biomarker study. *Org Geochem* 38:2070–2097
- Wang RL, Brassell SC, Scarpitta SC, Zheng MP, Zhang SC, Hayde PR, Muench LM (2004) Steroids in sediments from Zabuye Salt Lake, western Tibet: diagenetic, ecological or climatic signals? *Org Geochem* 35:157–168
- Werne JP, Hollander DJ, Behrens A, Schaeffer P, Albrecht P, Damsté JSS (2000) Timing of early diagenetic sulfurization of organic matter: a precursor-product relationship in Holocene sediments of the anoxic Cariaco Basin, Venezuela. *Geochim Cosmochim Acta* 64:1741–1751
- Werne JP, Lyons TW, Hollander DJ, Formolo MJ, Sinninghe Damsté JS (2003) Reduced sulfur in euxinic sediments of the Cariaco Basin: sulfur isotope constraints on organic sulfur formation. *Chem Geol* 195:159–179
- Werne JP, Hollander DJ, Lyons TW, Sinninghe Damsté JS (2004) Organic sulfur biogeochemistry: recent advances and future research directions. In: Amend JP, Edwards KJ, Lyons TW (eds) *Sulfur biogeochemistry – past and present*, vol 379. Geological Society of America, Boulder, pp 135–150
- Wu B-Z, Feng T-Z, Sree U, Chiu K-H, Lo J-G (2006) Sampling and analysis of volatile organics emitted from wastewater treatment plant and drain system of an industrial science park. *Anal Chim Acta* 576:100–111
- Xavier F et al (1997) Free and sulphurized hopanoids and highly branched isoprenoids in immature lacustrine oil shales. *Org Geochem* 27:41–63
- Zaback DA, Pratt LM (1992) Isotopic composition and speciation of sulfur in the Miocene Monterey Formation: reevaluation of sulfur reactions during early diagenesis in marine environments. *Geochim Cosmochim Acta* 56:763–774
- Zhuang G-C, Lin Y-S, Bowles MW, Heuer VB, Lever MA, Elvert M, Hinrichs K-U (2017) Distribution and isotopic composition of trimethylamine, dimethylsulfide and dimethylsulfoniopropionate in marine sediments. *Mar Chem* 196:35–46



History of Life from the Hydrocarbon Fossil Record

15

Clifford C. Walters, Kenneth E. Peters, and J. Michael Moldowan

Contents

1	Introduction	410
2	Evidence for the Earliest Life on Earth	412
3	Methanogenic Archaea in the Archean	413
4	Purple Sulfur Bacteria and the Oldest Syngenetic Biomarkers	413
5	Cyanobacteria and the Great Oxidation Event	414
6	Early Eukarya and Steranes	417
7	The Diversification of Eukarya	418
8	Rise of the Animals	420
9	<i>Gloeocapsomorpha prisca</i> Dominates the Ordovician	421
10	Higher Land Plants	421
11	Biomarkers of the Great Dying	423
12	Diatoms, 23,24-Dimethylcholestanes, and HBIs	425
13	Glycerol Dialkyl Glycerol Tetraether (GDGTs)	426
14	Phytoplankton Alkenones	427
15	C ₃₀ –C ₃₇ Botryococcene Derivatives	427
16	Research Needs	428
	Appendix	428
	References	432

C. C. Walters (✉)

Corporate Strategic Research, ExxonMobil Research and Engineering Company, Annandale, NJ, USA

e-mail: clifford.c.walters@exxonmobil.com

K. E. Peters

Schlumberger, Mill Valley, CA, USA

e-mail: KPeters2@slb.com

J. M. Moldowan

Biomarker Technology, Rohnert Park, CA, USA

Department of Geological Sciences, Stanford University, Stanford, CA, USA

e-mail: jmmoldowan@biomarker-inc.com; moldowan@stanford.edu

© Springer Nature Switzerland AG 2020

H. Wilkes (ed.), *Hydrocarbons, Oils and Lipids: Diversity, Origin, Chemistry and Fate*, Handbook of Hydrocarbon and Lipid Microbiology,

https://doi.org/10.1007/978-3-319-90569-3_32

409

Abstract

Certain lipids and biopolymers retain their original carbon backbone structure through sedimentary diagenesis and catagenesis and can be assigned to a specific biological origin. These “taxon-specific biomarkers” (TSBs) can serve as chemical fossils that trace the evolution of life. TSBs in Precambrian rocks reveal the early evolution of archaea, cyanobacteria, and eukarya and the development of atmospheric free oxygen. However, improved criteria for assessing syngeneticity have questioned their proposed earliest occurrence in Archean rocks. Steroidal TSBs document the changing assemblages of marine phytoplankton from Neoproterozoic organic-walled acritarchs to present-day predominance of diatoms. Terpanoid TSBs reveal the evolution of higher land plants. TSBs used in conjunction with isotopic analysis can identify the taxa of enigmatic fossils, provide important clues to the causes of mass extinctions, and describe the global changes in biotic diversity and Earth’s conditions as the biosphere recovers from them. Biomarkers record the evolutionary history of life on Earth and, perhaps, other planets.

1 Introduction

Our understanding of the evolution of life is based on three lines of evidence: extant life, fossilized life, and molecular fossils. Living organisms reflect the cumulative evolution of biochemical pathways encoded within DNA. Fossilized life preserves the morphology and habitat of extinct lifeforms. Molecular fossils are organic compounds inherited from once-living organisms that occur in sediments and rocks.

All living organisms share biochemical features that indicate life evolved from a common ancestor. This lifeform, the *last universal common ancestor* (LUCA), already possessed an extensive set of proteins for DNA, RNA, protein synthesis, DNA repair, recombination, and control systems for regulation of genes and cell division (Penny and Poole 1999) and may have had organelles (Seufferheld et al. 2003). A recent genomic study of extant microorganisms suggests that LUCA was anaerobic, CO₂-fixing, H₂-dependent, N₂-fixing, and thermophilic with a metal dependency suggesting an association with hydrothermal vents (Weiss et al. 2016). From LUCA, the bacteria and archaea evolved along separate paths ~4000 Ma (Hedges 2002; Sheridan et al. 2003) not in a simple progression of increasing complexity but in a complex manner involving the sharing of traits via horizontal gene transfer. Eukarya evolved from the archaea after an endosymbiosis with a member of the alphaproteobacteria that became the mitochondria (Williams et al. 2013) and later with a cyanobacterium that became the chloroplast (Falcón et al. 2010).

Phylogenetic relationships based on genomic sequencing can be depicted by the *tree of life* from which the evolution of biochemical pathways can be inferred. The *tree of life* is an evolving work. Modern phylogenetic trees are based on the sequence

of the small subunit of ribosomal RNA (Woese et al. 1990), or more recently on the entire genomic sequence (Hug et al. 2016). Phylogenetic trees express the relative order of evolutionary events, but not absolute time. Because rates of genetic evolution are not constant, the fossil record needs to be examined to determine the timing of these events. Locked in the geologic record are physical and chemical fossils that, if properly deciphered, can constrain when evolutionary changes occurred. Physical fossils provide temporal benchmarks for the evolution of multicellular organisms and can signal the earliest occurrence of both extinct and extant forms. Some single cell organisms may be preserved as microfossils; however, they rarely have sufficient morphological features to determine phylogenetic affinity. Many organisms, such as all archaea, are completely missing from the fossil record.

Molecular fossils offer the promise of bridging gaps between extant biochemistry and physical fossils. Few biogenic organic compounds remain intact during burial and lithification of sediments. When buried and exposed to higher temperatures, most biochemicals undergo microbial and chemical alterations involving the loss of functional groups, hydrogenation of double bonds, cleavage of weaker heteroatomic bonds such as sulfidic, ether and ester linkages, formation of new cross-linking, condensation, and aromatization reactions (Peters et al. 2005). Nevertheless, some of these molecules still retain enough of their original structure that they can be related to biochemical precursors. These molecular fossils are commonly termed biomarkers.

The ideal biomarker for tracing life's evolution would be DNA, but DNA degrades very rapidly and typically can be recovered only in fossils that were preserved in cool, dry environments, younger than ~50,000 years old. Early studies claiming DNA older than 1 Ma were flawed by contamination (Brown and Barnes 2015); however, advanced techniques have reconstructed Neanderthal DNA from bones dated at 430 ka (Meyer et al. 2016). Some sedimentary environments promote the preservation of DNA. Frozen sediments, such as <400 ka Siberian permafrost (Willerslev et al. 2003) and ~450–850 ka Greenland ice cores (Willerslev et al. 2007), are ideal for preserving DNA that reflect the flora and fauna of warmer times. Anoxic conditions during deposition, such as ~125 ka sapropels from cored Mediterranean sediments (Boere et al. 2011), and certain microfossils, such as diatoms as great as 1.4 Ma (Kirkpatrick et al. 2016), also promote the preservation of DNA.

Proteins are more stable than DNA, but typically lose their diagnostic sequences within $\sim 10^2$ – 10^5 years (Cappellini et al. 2014). Collagen proteins are stabilized in bone (Collins et al. 2000), and fragments have been successfully sequenced from fossils older than a million years. The presence of proteins in an exceptionally well preserved, 68 million-year old *T. Rex* femur (Asara et al. 2007) remains controversial, but the detection of possible proteins in older Cretaceous dinosaur fossils suggests that some protein fragments can survive for >65 Ma (Manning et al. 2009; Schweitzer et al. 2009, 2013; Lindgren et al. 2011; Bertazzo et al. 2015; Cleland et al. 2015).

All living organisms produce membrane lipids, molecules that contain both hydrophilic and hydrophobic moieties. These compounds range from simple fatty acids to steroids or hopanoids formed by the cyclization of isoprenoids to complex

structures consisting of fatty acids linked to a carbon platform to which a phosphate or sugar is attached. Bacteria and Eukarya have lipid membranes composed of unbranched fatty acid chains attached to glycerol by ester linkages while the Archaea have membranes composed of isoprenoid chains attached to glycerol by ether linkages. Many membrane lipids are quite unstable, rapidly losing their polar head group upon cell death. Their core structures, however, are quite stable and can survive in sediments for a much longer time (Volkman 2006). As hydrocarbons they can endure exposure to higher temperatures and survive for billions of years. The inherent thermal stability of hydrocarbons allows them to be used as biomarkers to trace the evolution of life for much of Earth's history.

Many lipids are common to all of life and are generic. Others are specific to genetically related organisms (deemed taxon-specific biomarkers or TSBs, Moldowan and Jacobson 2000) and provide insight into the evolution of life. The level of specificity may encompass domains, whole kingdoms or phyla or be confined to orders/families or even can be restricted to a genus/species. Their occurrences often tend to predate fossil evidence for a class of organisms and can sometimes be used to validate certain evolutionary relationships that are suggested, but incomplete, based on fossil morphologies and occurrences (Moldowan 2000). These and other molecular fossils also are referred to as biomarkers. A comprehensive review of biomarkers is beyond the scope of this paper, and the reader is directed to several recent books that more broadly cover these topics (Peters et al. 2005; Bianchi and Canuel 2011; Schwarzbauer and Jovančićević 2016). Instead, we will examine several examples that illustrate the use and limitations of biomarkers as molecular fossils in charting the evolution of life.

2 Evidence for the Earliest Life on Earth

The Hadean Eon marks the time between Earth's accretion (~4.6 Ga) to the stabilization of its crust (~4.0 Ga) and includes the time when Earth was heavily bombarded by meteorites and comets that are thought to have contributed water and organic compounds that may have given rise to life (Sarafian et al. 2014). Evidence for the earliest life may be preserved within single crystals of zircon from Jack Hills, Australia, that contain microscopic inclusions of isotopically light graphite (Bell et al. 2015). Similar ^{12}C -rich carbon residue is found in some of the oldest Archean metasedimentary rocks (~3.7 Ga) from Isua, Greenland (Mojzsis et al. 1996; Nishizawa et al. 2005; McKeegan et al. 2007). This formation contains laminated metacarbonate structures identified as microbial stromatolites (Nutman et al. 2016) that morphologically similar to ~3.4 Ga stromatolites in Pilbara, Australia (Allwood et al. 2006, 2007), supporting the theory that life arose >4 Ga (Hedges 2002). These rocks were all metamorphosed and no hydrocarbons or other biogenic organic compounds could have survived. And, while isotopically light carbon is a signature of life (Schidlowski 2001), abiotic processes may complicate interpretation (Westall and Folk 2003). In some cases, questions have arisen whether

the carbon is syngenetic or transported into the rock at a younger time (Papineau et al. 2010).

3 Methanogenic Archaea in the Archean

Tail-to-tail linked C₂₀ (2,6,11,15-tetramethylhexadecane = crocetane) and C₂₅ (2,6,10,15,19-pentamethylcosane = PMI) isoprenoid hydrocarbons are diagnostic markers for methanogenic archaea or anaerobic methanotrophic consortia and one or both of these compounds are reported to occur in shale extracts from the ~750 Ma Chuar Group (Summons et al. 1988a) and the ~1690 Ma Barney Creek Formation (Summons et al. 1988b; Greenwood and Summons 2003). It is difficult to prove that hydrocarbons extracted from ancient rocks are syngenetic (i.e., dating from the time of sedimentation) as there is always the possibility that the hydrocarbons migrated into the rocks at a later time. Extracts from ~2.7 Ga metasedimentary rocks from Timmins, Ontario, Canada contain cyclic and acyclic biphytanes and C₃₆–C₃₉ derivatives (Ventura et al. 2007). These compounds are likely to be syngenetic because similar compounds were released by catalytic hydrogenation of extracted rock. Isotopically light carbon in kerogen (<–57‰) from rocks of similar age is interpreted to originate from methanotrophs consuming biogenic methane (Eigenbrode and Freeman 2006). Isotopically light methane (–55‰) in ~3.5 Ga fluid inclusions may be further evidence for the very early evolution of methanogens (Ueno et al. 2006). However, it is unclear if this methane is biogenic (Sherwood Lollar et al. 2006). Geochemical indicators for the early evolution of methanogenic archaea are consistent with biochemical and genomic assessments for the evolution of life (Sheridan et al. 2003; Martin and Sousa 2016).

4 Purple Sulfur Bacteria and the Oldest Syngenetic Biomarkers

Isotopic studies suggest that the earliest microbial ecosystems were based on sulfur metabolism (Shen et al. 2001; Wacey et al. 2010, 2015). Although microfossils identified as sulfur bacteria are observed in ~3.5 Ga rocks (Wacey et al. 2011), the earliest chemical fossil evidence is in much younger rocks of the Barney Creek Formation dated at 1.64 Ga. These may be the oldest hydrocarbon biomarkers that are undoubtedly syngenetic (Summons et al. 1988b). Here, abundant okenane occurs with lesser amounts of chlorobactane and isorenieratane (Brocks et al. 2005; Brocks and Schaeffer 2008). The only known precursor for okenane is okenone, a C₄₀ monoaromatic carotenoid synthesized by the Chromatiaceae family of purple sulfur bacteria. Chlorobactane and isorenieratane are other carotenoids that are characteristic of the Chlorobiaceae family of green sulfur bacteria. Curiously, okenane appears to be restricted to Proterozoic rocks, leading to a suggestion that Chromatiaceae may have acquired the genes to synthesize okenone recently or that an extinct family of bacteria synthesized okenone in the Proterozoic (Brocks and

Butterfield 2009). Since then, okenane has been reported in middle Triassic (Saito et al. 2014) and Toarcian (French et al. 2014) strata associated with shallow photic zone euxinia, reinforcing the concept that okenane is a taxon-specific biomarker for purple sulfur bacteria.

5 Cyanobacteria and the Great Oxidation Event

For its first two billion years, Earth's atmosphere contained little or no oxygen (Canfield 2005; Holland 2006). Mineralogical evidence for low oxygen is seen throughout the Archean by the lack of oxidized iron in paleosols (Rye and Holland 1998) and preservation of detrital pyrite and uraninite (Rasmussen and Buick 1999). Around 2.4–2.3 Ga, the amount of oxygen in the Archean atmosphere jumped to >0.01 PAL (present atmospheric level) and possibly >0.1 PAL. This was proven from sulfur isotopic measurements on marine pyrites that show strong mass-independent fractionation prior to ~ 2.4 Ga (Pavlov and Kasting 2002; Holland 2006; Farquhar et al. 2007). The rapid rise is attributed to free oxygen produced by photosynthetic cyanobacteria outpacing its sequestration as mineral oxides (Kump and Barley 2007) or to ozone forming a UV protective shield at $>10^{-5}$ PAL that extended the lifetime of atmospheric oxygen (Goldblatt et al. 2006). The transition is termed the Great Oxidation Event (GOE) (Holland 2002).

The GOE implies that cyanobacteria evolved before 2.4 Ga; however, how much earlier remains uncertain. Some have argued that the GOE was triggered by the late emergence of cyanobacteria (Kopp et al. 2005; Kirschvink and Kopp 2008), which was consistent with early RNA phylogenetic analyses that suggest that major diversification of eubacteria, including the cyanobacteria, took place $\sim 2.6 \pm 0.3$ Ga (Hedges 2002; Sheridan et al. 2003). Some models suggest that oxygen could have overwhelmed redox buffers less than a million years following the emergence of cyanobacteria (Ward et al. 2016) and other studies pin age for the evolution of cyanobacteria after the GOE (Tomitani et al. 2006). This requires extinct proto-cyanobacteria to evolve a progenitor bacteriochlorophyll system that produced oxygen, which was replaced by chlorophyll once molecular oxygen became available (Xiong et al. 2000; Raymond and Blankenship 2004).

Microfossils and stromatolites, however, suggest that cyanobacteria existed long before the Great Oxidation Event (Schopf 2006). Assemblages of cyanobacterium-like microorganisms were described by Schopf and Packer (1987) and Schopf (1993) in the Apex Chert of Western Australia. Frequently cited as the oldest microfossils (~ 3.465 Ga), their biogenicity was questioned by Brasier et al. (2002, 2006) who considered these microstructure to be artifacts associated with mineral growth and the associated organic matter to be amorphous graphite within multiple generations of hydrothermal chert. This triggered a debate that even with the application of the most advanced analytical techniques

(carbon isotopic analysis, Raman spectroscopy, laser induced fluorescence imaging, TEM, XANES, and nanoSIMS) failed to be reconciled (Pinti and Altermann 2011; Schopf and Kudryavtsev 2012; Brasier et al. 2015). The Apex Chert has been subjected to regional metamorphism and exposed to temperatures as high as 350 °C. Consequently, no hydrocarbon signature is expected to be preserved. The carbonaceous matter is composed of large polynuclear aromatic moieties that are disordered or organized into nanometer-size graphitic domains. Although microbial induced sedimentary structures are associated with the Apex Chert (Hickman-Lewis et al. 2016), there is no direct or conclusive microfossil or chemical evidence for life.

The earliest undisputed microfossils are from the nearby Strelley Pool Formation (~3.43 Ga). Here, kilometer-long remnants of an ancient stromatolitic carbonate platform provide compelling evidence of microbial activity (Allwood et al. 2006, 2007). Large (>40 μm) lenticular to spindle-like structures, spheroidal structures, mat-forming thread-like structures, and tubular sheath-like envelopes were trapped between sand grains and entombed within a silica cement. The presence of stromatolites and microfossil morphology strongly suggests photosynthetic bacteria, but not necessarily oxygen producing cyanobacteria. More convincing microfossil evidence for cyanobacteria exists in rocks ~3.0–2.9 Ga (Altermann and Kazmierczak 2003; Nisbet et al. 2007; Schopf et al. 2007). The oldest microfossils with definitive cyanobacterial features date no earlier than ~2100 Ma (Hofmann 1976; Tomitani et al. 2006).

2- and 3-Methylhopanes and steranes tell a similar story of possible, but not proven, evidence for cyanobacteria evolving long before the GOE. The initial discovery of these compounds in extracts from 2.7 Ga (Brocks et al. 1999) and follow up studies of 2.78 Ga Pilbara shales (Brocks et al. 2003a, b) and 2.67–2.46 Ga sediments from the Transvaal Supergroup (Waldbauer et al. 2009a, b) appeared to prove that cyanobacteria evolved significantly prior to the GOE. Precursors of the 2 α -methylhopanes were believed to be biosynthesized only by cyanobacteria (Summons et al. 1999). The co-detection of steranes and 3 β -methylhopanes (Brocks et al. 2003a, b) provided additional biomarker evidence for the presence of free oxygen as all extant eukaryotes require molecular oxygen to synthesize sterols and 3-methylhopanes were considered to be a TSB for aerobic methanotrophic bacteria. The relative abundance of the 3-methylhopanes correlated with the $\delta^{13}\text{C}$ of the kerogen suggesting syngeneity (Eigenbrode and Freeman 2006), and the 2 α -methylhopanes were found to be more abundant in shallow-water sediments than those deposited in deeper waters consistent with photic zone cyanobacteria (Knoll et al. 2007a; Eigenbrode et al. 2008).

We must be cautious with these conclusions as all aspects have come under suspicion. Although these studies were conducted using strict procedures to minimize contamination and differentiate syngenetic from migrated hydrocarbons, it is unlikely that the free biomarkers date from the time of rock deposition.

Using nanoSIMS, Rasmussen et al. (2008) examined the $\delta^{13}\text{C}$ of samples from Pilbara and other Archean rock at a μm -scale and found that the kerogen and pyrobitumen were significantly lighter (-36 to -51‰) than associated free hydrocarbons (-26 to -29‰) and concluded that the hydrocarbons must have been added after peak metamorphism (~ 2.2 Ga). Examination of 2.7 Ga core sliced at a millimeter scale found that biomarker hydrocarbons were concentrated on the rock surfaces, indicating they were contaminants (Brocks 2011). French et al. (2015) studied new Pilbara cores collected and processed to minimize drilling contamination and found that while the rock extracts and hydropyrolysates contained PAHs and diamondoids at concentrations above background, steranes and hopanes were not detected in concentrations exceeding procedural blanks. They concluded that the earlier studies resulted from contamination.

Even if the biomarkers are syngenetic, their use as proof for cyanobacteria and free oxygen is questionable as well (Newman et al. 2016). 2-Methylhopanes, 3-methylhopanes, and steranes are certainly associated with extant cyanobacteria, aerobic methanotrophic bacteria and eukaryotes, respectively. However, the taxonomic specificity of these compounds is now known to be not unique and extant organisms may not capture the full biochemical diversity of biosynthetic pathways expressed by extinct genera. The first warning that 2-methylhopanes may not be a proven biomarker for cyanobacteria came with the discovery that strains of *Rhodopseudomonas palustris*, a purple non-sulfur phototrophic α -proteobacterium, can synthesize 2-methylbacteriohopanepolyols (Rashby et al. 2007). This was thought to result from horizontal gene transfer or because *R. palustris* is related to the ancestor that gave rise to the cyanobacteria. Subsequently, genomic analyses found that only about one fifth of the cyanobacteria species actually possess the gene needed to synthesize 2-methylhopanoids while many species of alphaproteobacteria and acidobacteria possess this gene (Welander et al. 2010). This gene, *hpnP*, was found to correlate with environments that support plant–microbe interactions and in closely packed microbial communities such as stromatolites, hot springs, and hypersaline microbial mats (Ricci et al. 2014). 2-Methylhopanes are not reliable TSBs for cyanobacteria, but rather serve as indicators of low oxygen niches that are enriched in sessile microbial communities. Similarly, *hpnR*, the gene needed for the synthesis of 3-methylhopanoids, was found not be unique to aerobic methanotrophs or methylotrophs. It is expressed by acetic acid bacteria, occurs in the genomes of other bacteria, and appears to be required for cell survival in the late stationary phase (Welander and Summons 2012).

Even though the molecular evidence that was once considered proof for the early evolution of cyanobacteria is now viewed skeptically, new trace-metal evidence has emerged supporting the hypothesis that free oxygen was being produced much earlier than 2.5 Ga. Transient strong enrichments and isotopic fractionations in some trace metals are interpreted as signatures of oxic water (Anbar et al. 2007;

Duan et al. 2010; Czaja et al. 2012; Planavsky et al. 2014a). These “whiffs of oxygen” suggest that oxygen producing cyanobacteria predate the GOE by 500 Ma; however, they may have been restricted, highly localized benthic niches while atmospheric oxygen remained $<10^{-5}$ PAL (Lalonde and Konhauser 2015). Early evolution of cyanobacteria is consistent with the current genomic analysis (Schirrmeyer et al. 2015).

6 Early Eukarya and Steranes

Eukarya are believed to have evolved from an ancient archaeon that engulfed one or more bacteria as symbionts. Mitochondria and chloroplast organelles are certainly derived by the endosymbiosis of α -proteobacteria and cyanobacteria, respectively. The engulfing archaeon and the last common Eukarya ancestor are long extinct, but metagenomic sequencing of the recently discovered *Lokiarchaeota* shows that it contains a rich gene repertoire for forming complex cytoskeleton and membrane remodeling systems that would be required for the archaeon host (Spang et al. 2015). The Eukarya are now viewed as a sister group splitting off, if not part of, the Archaea (Hug et al. 2016). Genetic analyses tend to agree that major diversification of eukaryotes occurred at ~800 Ma, but the calculated age for the last common eukaryotic ancestor varies from ~2100 to 900 Ma, depending on the assumptions, statistical methods, and accuracy of microfossil constraints used to calibrate the molecular clocks (Parfrey et al. 2011; Eme et al. 2014).

Can biomarkers help define the emergence of Eukarya? All Eukarya incorporate sterols to regulate membrane fluidity and perform other critical cellular functions. As such, steroidal hydrocarbons (e.g., steranes, diasteranes, and their aromatized forms) are considered to be biomarkers for the domain and the genes responsible for sterol biosynthesis were most likely present in the last common ancestor of all Eukarya. Free oxygen is required for sterol synthesis, suggesting that the Eukarya evolved around the time of the GOE (Summons et al. 2006a). However, the amount of dissolved oxygen necessary for their synthesis in some species is only in the nanomolar range (Waldbauer et al. 2009a, b), allowing for an even older emergence when only “whiffs” were present in microenvironments.

Curiously, steranes are absent or at very low abundance in many Upper Proterozoic sediment extracts where syngeneity is not in question and Eukarya should have been present (Brocks et al. 2005; Pawlowska et al. 2013). The lack of a sterane signature, typical of later Phanerozoic rocks, is attributed to the “mat effect” where benthic microbial mats favored the preservation of heterotrophs and anaerobic bacteria living within and below the mats and the lipids of plankton and upper mat dwellers were degraded (Pawlowska et al. 2013). Older strata should show similar preservation biases, so the lack of steranes does not mean that eukaryotes had not yet evolved.

Since the steranes reported in the ~2.7 Ga Pilbara craton shales discussed above are now considered to be contaminants, the oldest known steranes are in fluid inclusions within Matinenda Formation quartz (Dutkiewicz et al. 2006; George et al. 2008). The inclusions, themselves, may be somewhat younger (>2.2 Ga) than the host rock (~2.45 Ga). Preservation of organic matter appears to be enhanced in fluid inclusions as they are closed systems with no minerals that promote oil cracking. Organic matter associated with microfossils embedded in chert is also remarkably well preserved even after exposure to temperatures exceeding ~150 °C (Alleon et al. 2016). The Matinenda inclusions contain a full range of saturated and aromatic hydrocarbons that resembles produced oil from upper Precambrian source rocks. In addition to abundant biomarkers that are consistent with cyanobacteria (e.g., 2-methylhopanes, monomethyl alkanes), there is a diverse suite of steranes including C₂₈ and C₂₉ steranes and C₂₈ diasteranes and at lower concentration C₂₇, C₃₀ 24-*n*-propyl-, C₃₀ 4 α -methyl-, and C₂₆ 24-nor- and 27-nor-cholestanes and diacholestanes. Dinosteranes and 24-isopropylcholestanes were not detected. The regular C₂₇, C₂₈, and C₂₉ diasteranes and steranes are not taxon-specific beyond being characteristic of Eukarya. C₃₀ 24-*n*-propylcholestanes are known to be produced by some chryso-phytes (Moldowan et al. 1990).

The presence of steroidal hydrocarbon in oil inclusions strongly suggests, but does not prove, that Eukarya evolved prior to ~2.45 Ga as some bacteria synthesize sterols (Volkman 2005). This is generally not an issue when interpreting the molecular fossil record of Phanerozoic strata when eukaryotic organisms was significant contributors of sedimentary organic carbon and sterol synthesis were thought to be restricted to a few bacterial strains that acquired the genes by horizontal transfer (Summons et al. 2006a). Caution now is needed for pushing the age boundary for eukaryotes to older time, as recent studies have shown that the gene needed for the initial cyclization of oxidosqualene into the sterol structure is present in numerous bacteria spanning five different phyla (Wei et al. 2016). These findings suggest that bacterial sterol synthesis has a complex evolutionary history and likely occurs in diverse organisms.

7 The Diversification of Eukarya

Following the GOE, Earth's atmosphere contained free oxygen but substantially below present levels. Estimates range from as high as 40% to as little as 0.1% of the present level (Planavsky et al. 2014b). Regardless of the actual oxygen level, there were sufficient amounts to trigger the evolutionary diversification of Eukarya. Differentiating eukaryotic from prokaryotic microfossils by morphology alone is challenging. Criteria for eukaryotes, such as size (>50 μ m), complex ultrastructure, or ornamented walls, may be mimicked by bacteria (Javaux et al. 2003; Knoll et al. 2006). The uncertainty as to whether a microfossil is a eukaryote increases with age. Javaux et al. (2010) reported on relatively large (up to ~300 μ m) acritarchs (organic-walled microfossil) in the 3.2 Ga Moodies Group that could be eukaryotic. These are

considerably older than microfossils deemed likely to be eukaryotes from ~2.1 Ga (*Grypania*, Knoll et al. 2006) and ~1.7 Ga (Pang et al. 2013) or ~1.5 Ga microfossils that are almost certainly eukaryotic (Javaux et al. 2004) and multicellular (Zhu et al. 2016). The oldest accepted “crown group” (last common ancestor to all extant members of a clade) fossil is a red alga dating from 1.2 Ga (Butterfield 2000). A claim for “crown group” fossilized green alga at 1.8 Ga (Moczyłowska et al. 2011) is disputed (Knoll 2015). Based on models of the genome of extant organisms and microfossil evidence, we confidently state only that eukaryotic organisms evolved earlier than ~1.2 Ga and likely as old as ~2.1 Ga.

There are numerous studies reporting steranes and other chemical fossils in Proterozoic bitumens (Summons and Walter 1990; McKirdy and Imbus 1992). As with Archean strata, Proterozoic biomarkers have been subjected to increased scrutiny concerning their syngeneity. Analysis of oils in fluid inclusions from the ~1.4 Ga Roper Group (Dutkiewicz et al. 2004; Volk et al. 2005; Siljeström et al. 2013) consistently show a predominance of bacterial biomarkers with minor amounts of steranes.

Fossil and chemical records become more synchronous and reliable in the Neoproterozoic. Biomarkers can reveal evolutionary events that have left no physical fossils. Collectively, the C₃₀ 4 α -methylsteranes and C₂₆ norcholestanes tell an interesting story. C₃₀ 4 α -methylsteranes can arise from multiple sources but are most commonly associated with dinoflagellates. One specific type, the dinosteranes, are produced almost exclusively by dinoflagellates. The fossil record for dinoflagellates begins in the Triassic, but because few living dinoflagellates produce cysts, this record has long been suspect. Organic-walled acritarchs believed to be related to dinoflagellates (Moldowan et al. 1996) date to the Neoproterozoic (Butterfield and Rainbird 1998). Here, the mineralized fossil record matches well with the chemical fossil observations as dinosteranes and related aromatic biomarkers have a continuous record back to the Early Cambrian (Moldowan and Talyzina 1998) and possibly the Neoproterozoic (Summons et al. 1992; Zhang et al. 2002) and even the Mesoproterozoic (Meng et al. 2005) but are most abundant in Phanerozoic sediments.

The chemical record for C₂₆ 24-norcholestanes and 24-nordiacholestanes also extends back to the Neoproterozoic (Zhang et al. 2002), although concentrations of these compounds in source rocks remain low until the Jurassic and become particularly abundant in the Tertiary (Holba et al. 1998a, b). This temporal pattern and the association of high concentrations of 24-norcholestanes with siliceous sediments containing diatom-specific biomarkers (e.g., highly branched isoprenoids) strongly suggests that these compounds are from diatoms. However, diatoms did not evolve until <100 Ma (Sorhannus 2007) and dinoflagellates were the only source of 24-norsterols known until the discovery of 24-norcholesta-5,22-dien-3 β -ol in the diatom *Thalassiosira* aff. *Antarctica* (Rampen et al. 2007a). Hence, 24-norcholestanes in post-Triassic sediments, particularly those of Tertiary age deposited at high latitude, can be attributed to diatoms, while older occurrences originate from dinoflagellates.

8 Rise of the Animals

A diverse assemblage of Ediacaran animal fossils arose after the Gaskiers glaciation (~580 Ma). The Ediacaran biota includes a mixture of stem-group animals and fossils that appear to be failed experiments in multicellular evolution (Droser and Gehling 2015). Sponges were certainly one of the earliest extant animals to emerge. Cryogenian fossils identified as sponges have been reported from 760 Ma (Brain et al. 2012) and 659 Ma (Wallace et al. 2014) strata. The biomarker record fully supports this age of emergence. McCaffrey et al. (1994) were the first to note the occurrence of 24-isopropylcholestanes throughout the geologic record (~1.8 Ga to 15 Ma) and particular enrichment in Ediacaran-Lower Cambrian strata. 24-Isopropylcholestanes were proposed to be highly taxon specific because demosponges were the only known extant organisms that synthesize 24-isopropylcholesterol, the biological precursor to C₃₀ 24-isopropylcholestane. Love et al. (2009) conducted a rigorous study of Huqf Supergroup core that spanned Cryogenian strata below the Marinoan cap carbonate (>635 Ma) through the Ediacaran and into the Early Cambrian. In addition to a rich diversity of C₂₆–C₂₉ steranes attributed to eukaryotic algae, the samples contained abundant 24-isopropylcholestane in both extractable bitumen and the hydropyrolysate of the kerogen. This study seemed to firmly position the evolution of the demosponges in the Cryogenian; however, some questioned whether the demosponges are the only source or whether 24-isopropylcholestane might originate from other extinct sponges or sister groups, such as the single-celled choanoflagellates (Brocks and Butterfield 2009). The discovery that several different pelagophyte algae are also capable of synthesizing 24-isopropylcholesterol suggested that the biomarker was not as specific as once thought (Antcliffe 2013). Genomic analyses, however, suggest that the pelagophytes and sponges independently evolved the required biosynthetic pathways at different times; the sponges in the Neoproterozoic and the pelagophytes later in the Phanerozoic (Gold et al. 2016). Hence the occurrence of 24-isopropylcholestane in the Neoproterozoic is a valid TSB for demosponges. An unusual C₂₈ sterane, 26-methylcholestane or cryostane, was recently reported in several pre-Sturtian (~800–740 Ma) successions (Brocks et al. 2016). As demosponges are the only known extant organisms that can methylate sterols in the 26-position, this biomarker pushes the emergence of metazoa prior to Snowball Earth.

The rise of complex multicellular animals may have been tied to marine planktonic algae replacing cyanobacteria as the dominant primary producers. A marked increase in steroid diversity and abundance is seen within a narrow time interval, 659–645 Ma, between the Sturtian and Marinoan “snowball Earth” glaciations (Brocks et al. 2017). This rapid change in biomarker distributions suggests that a surge in nutrients supplied by the deglaciation triggered the development of a new ecosystem that created more efficient food webs, further increasing O₂ levels, and promoting the evolution of new multicellular phyla, such as the sponges, protists (predatory rhizarians), and the subsequent radiation metazoans in the Ediacaran period.

9 *Gloeocapsomorpha prisca* Dominates the Ordovician

Normal alkanes are ubiquitous and are not typically taxon-specific. An exception is the unique hydrocarbon distribution (high C_{11} – C_{19} odd carbon preference, low abundance of C_{20+} alkanes and isoprenoids) that is characteristic of *Gloeocapsomorpha prisca*, a microorganism of uncertain affinity. This microorganism emerged in the Early Cambrian and rose to prominence in the Ordovician, where it dominated in some environments and contributed nearly all of the organic matter in oil shales that can be over 70% TOC with the kerogen being 90% of the total rock volume (Fowler 1992). Although *G. prisca* dominance is mostly restricted to the Ordovician, it is rarely reported in the Silurian and became extinct in the Late Devonian (Fowler et al. 2004).

The affinity of *G. prisca* has been debated for decades and remains uncertain. To complicate the matter, *G. prisca* had different life cycle stages where it could exist as either plankton or benthic mats (Pak et al. 2010). Low concentrations of pristane and phytane led Reed et al. (1986) to conclude that *G. prisca* was a non-photosynthetic or non-chlorophyll containing bacterium. A eukaryotic green alga, similar to extant *Botryococcus braunii*, was suggested based on similar biochemical adaptations to salinity and the composition of selectively preserved algaenan cell walls (Derenne et al. 1992; Metzger and Largeau 1994). However, the resorcinolic lipids in *G. prisca* that are suggestive of *Botryococcus* may be polymerized cyanobacterial sheath material excreted as an anti-oxidant and/or UV filter (Blokker et al. 2001). *G. prisca* as extinct cyanobacterium has been suggested in several studies (Hoffman et al. 1987; Pancost et al. 1998; Stasiuk and Osadetz 1990). The occurrence of aromatized hopanes and abundant methylhopanes in Estonia kukersite, a shale predominantly composed of *G. prisca*, strongly support a cyanobacterial affinity (Liao et al. 2015). Aromatized hopanes are believed to be derived from C_{30} diplopterol and/or diploptenes, consistent with cyanobacteria.

10 Higher Land Plants

Prior to the Devonian Period, most biomass contributed to sediments consisted of algae and bacteria with little or no higher-plant input, such as lignin, leaf cuticle, spores, or pollen. Land plants have undergone several phases of rapid diversification (Gensel and Edwards 2001). Since their apparent origin in the Ordovician (Wellman et al. 2003), an explosion of new higher plant taxa occurred in the Late Silurian–Early Devonian (Bateman et al. 1998). Major land-plant groups arose during the Devonian and Carboniferous and the flowering plants, the angiosperms, underwent rapid diversification ~90 Ma to become the dominant land plants. The transition of plants from a marine to a terrigenous environment required many molecular adaptations (Waters 2003) and each major radiation spawned novel biochemical markers that are now biomarkers. Extracts from organic-rich pre-Devonian sedimentary rocks contain only limited amounts of extended *n*-alkanes having more than ~25 carbon atoms. Waxy coatings on the leaves of higher plants contain abundant

precursors of the extended *n*-alkanes. For this reason, many Devonian or younger rocks and related crude oils may contain abundant extended alkanes as well as other higher-plant biomarkers.

Plants continually evolved isoprenoid-based polycyclics for many purposes, such as attracting pollinators with floral scents to defend against herbivores, resulting in many highly taxon-specific biomarkers. In general, tricyclic diterpenoids are characteristic of gymnosperms, specifically conifers, while pentacyclic triterpenoids are almost exclusively synthesized by angiosperms. For example, Moldowan et al. (2015) used a large shift in the distributions of the tricyclic diterpanes, rimuane, pimarane, rosane, and isopimarane to distinguish terrestrial contributions in Cretaceous and Tertiary oils on northern South America. The presence and abundance of oleanane in most of the oils was insufficient to make the distinction, while shifts in the tricyclic diterpane distributions were definitive. Tricyclic diterpanes are related to all plant types (Zinniker 2005) and the shift in their distributions could have originated from plant extinctions during the end-Cretaceous mass extinction event.

Phyllocladane and related diterpanes are structures along the gibberellin biosynthetic pathway inherent to all plants and absent from all other life kingdoms (Zinniker 2005). They are most commonly associated with gymnosperms and their occurrence in Upper Carboniferous coals is attributed to the first appearance of conifers (Schulze and Michaelis 1990). However, older occurrences into the Devonian are noteworthy (Zinniker 2005). Several aromatized arborane/fernane derivatives appear to be biomarkers for Cordaites, an important genus of extinct gymnosperms (Auras et al. 2006).

The progenitors and evolution of the angiosperms remain a topic of intense debate (Frohlich and Chase 2007). DNA phylogenetic analyses of extant plants place the divergence of the angiosperms in the Paleozoic (Peterson et al. 2007), well before the earliest known angiosperm fossils in the Late Jurassic. The association of oleanane with the radiation of the angiosperms is well documented (Moldowan et al. 1994) and its occurrence in pre-Cretaceous fossils can help unravel this paleontological conflict between genomic analysis and the macrofossil record. Cladistic analysis of living and fossil seed plants places the angiosperms with the extant Gnetales and three extinct groups, Bennettitales, *Pentoxylon*, and Caytoniales. Molecular phylogenetic analyses indicate that Gnetales are more closely related to conifers, not angiosperms. In a large, but incomplete survey, oleanane and its functionalized triterpenoid precursors proved to be widespread within living and fossil angiosperms (Taylor et al. 2006). Oleanane was absent in the pyrolyzates of living Gnetales species, Carboniferous medullosan pteridosperms, and in the conifer relatives Cordaitales (including *Mesoxylon*). Oleanane was detected in pre-Cretaceous rocks containing two classes of non-angiosperm fossils, Aptian Bennettitales and Upper Permian Gigantopterids. The relative abundance of oleanane to hopane, the Oleanane Index, correlated with the relative abundance of Gigantopterid fossil remains relative to other plant species, indicating that Gigantopterids are the source of the oleanane. The occurrence of oleanane in a

Pennsylvanian coal ball (Moldowan et al. 1994) and 1,2,7-trimethylnaphthalene, an assumed diagenetic product of oleanane type biomarkers, in Carboniferous coal and sediment samples and even one Devonian cannel coal sample (Armstroff et al. 2006) supports the hypothesis that the angiosperm lineage existed well before the Permian and that their progenitors belonged to an extinct group of seed plants from which only the angiosperms survived.

Higher-plant biomarkers can be very taxon-specific. For example, Early Eocene resin from the Paris Basin was found to contain quesnoin, a pentacyclic *ent*-diterpene (Jossang et al. 2008). This biomarker is believed to be a diagenetic product of guamaic acid, suggesting an association to *Hymenaea oblongifolia*, which is classified within the Caesalpiniaceae, one of the oldest families of angiosperms. *H. oblongifolia* is a modern tropical tree found in the Amazon Basin. Quesnoin, therefore, supports the hypothesis that the climate of the Paris Basin was tropical 55 Ma.

11 Biomarkers of the Great Dying

The diversity of life is in constant flux. Over 99% of all species that lived are now extinct. The rates of extinction are not uniform and there are periods in Earth's history when many species rapidly died out. Five large mass extinctions occurred in the Phanerozoic: end-Ordovician (~440 Ma), Late Devonian (~365 Ma), end-Permian (~252 Ma), end-Triassic (~201 Ma), and end-Cretaceous (~66 Ma). The end-Triassic extinction was the weakest with 76% of all species dying out, and the end-Permian event, termed the Great Dying, was the most severe resulting in loss of up to 96% of all marine species and ~70% of terrigenous vertebrates (Erwin 2006; Benton 2008; Bergstrom and Dugatkin 2012). The causes of these major upheavals have been long debated and biomarkers have provided clues as to key changes in the environment, such as eutrophy, euxinia, ocean acidification, changes in hydrological balance, and atmospheric CO₂ that occurred with these extinctions (Knoll et al. 2007b; Whiteside and Grice 2016).

The reasons for the P-Tr mass extinction remain unclear, but they must account for six observations (Payne and Clapham 2012): (1) the event affected both marine and terrigenous species; (2) the main extinction event occurred over a short timescale of ~200,000 years; (3) marine animals having limited ability to protect themselves from changes in the partial pressure of carbon dioxide (pCO₂), temperature, pH, and oxygen in the water were particularly prone to extinction (e.g., heavily calcified organisms); (4) sedimentary fabrics, pyrite framboid abundance, and biomarkers suggest widespread ocean anoxia that affected shallow marine settings beginning ~254 Ma and maximizing near the main extinction event; (5) stable carbon isotope compositions of carbonate and organic matter become lighter before the main extinction event and then abruptly decrease further during the mass extinction (the δ¹³C excursion); and (6) environmental and biological disruption continued through

the Early Triassic. These observations are best explained by massive eruption of the Siberian Traps, which released huge amounts of carbon dioxide and other gases from contact aureoles in carbonate and evaporite sediments within this province (Retallack and Jahren 2008; Svensen et al. 2009). These volatiles may have caused global warming, ocean acidification, and increased terrigenous weathering and nutrient runoff, which enhanced oceanic anoxia.

Biomarker analyses indicate suppressed dissolved oxygen in shallow marine settings near the P-Tr boundary. Aryl isoprenoids and isorenieratane occur in boundary rocks at Meishan in China and in the Hovea-3 core from Australia (Grice et al. 2005a; b). These biomarkers originate from isorenieratene, a photosynthetic pigment in green sulfur bacteria, which conduct photosynthesis in the marine photic zone under euxinic conditions where hydrogen sulfide is available. Isorenieratane occurs at several stratigraphic levels in Changhsingian strata at the Meishan location, suggesting that photic zone anoxia was intermittent prior to the main extinction event (Cao et al. 2009). Uranium isotope measurements support increased marine anoxia during the mass extinction (Brennecke et al. 2011). Abundant isorenieratane co-occurs with various benthic invertebrate fossils, supporting intermittent anoxia that did not significantly impact the megafauna. Seafloor microbialites in the boundary interval at Meishan (Cao and Zheng 2009) and in the Hovea-3 core (Thomas et al. 2004) suggest that these biomarkers originated from benthic photosynthetic organisms in microbial mats rather than from planktonic organisms in a euxinic water column.

The biomarker data also indicate increased input of microbial biomass to sediments through the P-Tr boundary interval. Increased 2-methylhopanes/hopanes and hopane/sterane ratios at Meishan were interpreted to indicate increased cyanobacterial contributions, primary production, and changes in the overall composition of the microbial community (Xie et al. 2005; Summons et al. 2006b; Cao et al. 2009). Based on the 2-methylhopane index, cyanobacterial blooms occurred in the western and eastern Tethys Sea after the P-Tr mass extinction (Jia et al. 2012), though caution is needed in the interpretation as other microbial groups can produce 2-methylhopanoids (Welander et al. 2010). The shallow water Bulla section in northern Italy shows evidence of synchronous blooms of cyanobacteria and prasinophytes with the C₂₈/C₂₉ sterane ratio suggesting blooms of prasinophyte algae immediately after the extinction event (Jia et al. 2012). However, at Meishan in southern China, the cyanobacteria bloom declined earlier than at Bulla. Increased 2-methylhopane index corresponds to a decrease in the nitrogen isotope ratio at Meishan, which suggests that enhanced nitrogen fixation by the cyanobacteria provided ammonium for a bloom of prasinophytes in the otherwise nutrient-limited shallow marine waters.

Geochemical data also suggest the collapse of terrigenous ecosystems. For example, dibenzofurans and other polycyclic aromatic hydrocarbons are commonly abundant in Upper Permian strata from China, Italy, and Greenland (Fenton et al. 2007; Sephton et al. 2005; Wang and Visscher 2007), possibly due to increased input

of soil organic carbon and the collapse of terrigenous plant communities (e.g., Sephton et al. 2005). However, a negative excursion in the $\delta^{13}\text{C}$ of these compounds across the P-Tr boundary in the Hovea-3 core was interpreted to indicate dominantly terrigenous input in the Permian followed by mainly marine algal input in the Triassic (Grice et al. 2007). Cao et al. (2009) argued that lithology and diagenesis exert major control on the abundance of these compounds, casting doubt on whether the geochemical record indicates collapse of the terrigenous ecosystem at the P-Tr boundary.

Triaromatic 23,24-dimethylcholesteroids (TA-DMC) originate from 23,24-dimethylcholesterols in dinoflagellates, haptophytes, and diatoms and are useful to distinguish Paleozoic from Mesozoic and younger oil and rock extracts (Barbanti et al. 2011). The relative abundance of TA-DMC in source rock extracts and crude oils from different global localities and ages help to identify the P-Tr boundary.

12 Diatoms, 23,24-Dimethylcholestanes, and HBIs

As discussed above, dinosteranes (4 α ,23,24-trimethylcholestanes) occur in sedimentary rocks from the Late Archean to the present. In contrast, with very few exceptions in a few Ordovician rocks and oils, triaromatic 23,24-dimethylcholestanes occur only in Triassic and younger marine sediments and oils (Barbanti et al. 1999; Moldowan and Jacobson 2000) indicating that these compound classes have independent origins, though likely still derived from dinoflagellates. Increasing abundance of triaromatic 23,24-dimethylcholestanes through the Cretaceous suggested the biosynthetic pathways for a precursor evolved in a different organism. Diatoms proved to be this late-evolved source. A survey of >100 diatom species found abundant 23,24-dimethylsterols in 21 species belonging to six different orders (Rampen et al. 2007b).

Several genera of diatoms are the only organisms known to synthesize C_{20} , C_{25} , or C_{30} highly-branched isoprenoids (HBIs). HBIs may have one or multiple saturated bonds, although the HBIs with one to three are most common. The function of these “T-branched” alkenes is unknown, but two groups of diatoms evolved independent pathways for their synthesis, implying that they provide a significant advantage (Massé et al. 2004). In a study that integrated 18S rRNA phylogenetic analysis with the mineral and chemical fossil record, Sinninghe Damsté et al. (2004) showed that HBIs were first biosynthesized by the rhizosolenid diatoms. The mineral fossil record for the rhizosolenids dates to ~70 Ma, while saturated HBIs are found in oils and marine sediments <90 Ma. Thus, the chemical fossil record unambiguously extends the emergence of the rhizosolenid diatoms by an additional 20 Ma. Moldowan et al. (2015) used the C_{25} HBI to help distinguish Early Cretaceous oils (HBI absent) from Late Cretaceous oils (HBI present) in the Llanos Basin.

Belt et al. (2007) proposed a specific C_{25} monounsaturated HBI (IP₂₅) is produced by diatoms living within sea ice and its presence in sediments is a

proxy for the extent of ice. IP₂₅ appears to be relatively stable and has been used in paleoclimate studies from Recent to the early Pleistocene. The presence of IP₂₅ in Arctic marine sediments appears to measure the extent of past seasonal sea ice rather than permanent or multi-year ice conditions (Belt and Müller 2013). Brown et al. (2014) confirmed that IP₂₅ originates in diatom species endemic to sea ice.

13 Glycerol Dialkyl Glycerol Tetraether (GDGTs)

Both archaea and bacteria synthesize lipids that have two polar head groups and are long enough to span across membranes: the glycerol dialkyl glycerol tetraether lipids (GDGTs). Several groups of archaea (Pearson and Ingalls 2013) synthesize isoprenoid GDGTs (isoGDGTs) that are two biphytane moieties containing 0–3 cyclopentane rings each (crenarchaeol also has one cyclohexane ring) link at both ends by ether bonds to glycerols. Branched GDGTs (brGDGTs) are composed of two *n*-alkyl chains having 2–3 methyl and 0–1 cyclopentane rings. The biological source of the brGDGTs has not yet been found but the *Acidobacteria* are believed to be likely candidates (Sinninghe Damsté et al. 2014). The intact polar lipids (IPLs) are fragile and many of the polar headgroups are quickly lost upon cell death. IPLs survive in the geologic environment for <7000 years (Lengger et al. 2014). Their core structures, however, can persist into the middle Jurassic provided the stratum has not been heated (Jenkyns et al. 2012).

In laboratory cultures of thermophilic archaea, the number of cyclopentane rings is highly dependent on growth temperature (Uda et al. 2001). Schouten et al. (2002) suggested that marine planktonic archaea, principally the ammonia-oxidizing Thaumarchaeota, functioned similarly and formulated TEX₈₆, a GDGT ratio that correlates linearly with the annual mean sea surface temperatures (SST). Considerable attention has been given to TEX₈₆ as it can function as temperature proxy in paleoclimate studies and is applicable to both marine and terrestrial sediments. The calibrations have been refined with modifications to the original TEX₈₆ to compensate for very hot (TEX₈₆^H) and very cold (TEX₈₆^L) environments (Kim et al. 2010). However, in a study of modern Mediterranean waters, Kim et al. (2015) found that TEX₈₆^H measured on suspended particulates correlated only partially to temperature was mostly dependent on water depth while the sediments collected at water depths >1000 m did correlate to SST. Somehow the ammonia-oxidizing Thaumarchaeota are able to respond to SST when they have maximum activity below the surface water mixing zone and do yield TEX₈₆ values that co-vary with their own growth temperature. Hurley et al. (2016) provide a possible solution to this conundrum by finding that a cultured thaumarchaeon yielded TEX₈₆ values inversely proportional to growth rate, which is controlled by the rate of ammonia oxidation. TEX₈₆, therefore, reflects the metabolic activity of Thaumarchaeota in the water column

and its correlation with SST is a secondary effect of nutrient dynamics and the archaeal community.

14 Phytoplankton Alkenones

Isochrysidales, phytoplankton within the class Prymnesiophyceae, biosynthesize alkenones, linear C_{34} – C_{41} methyl- and ethylketones with one to four double bonds. Since, the proportion of double bonds increases with decreasing growth temperature, it was reasonable to assume that these compounds were membrane lipids (Brassell et al. 1986). This proved not to be the case (Eltgroth et al. 2005) and alkenones are likely produced as food storage lipids. The degree of unsaturation proved to be extremely sensitive to temperature and is now widely used as a proxy for paleoclimate. The most common is the U_{37}^{KI} , the ratio of $C_{37:2}/(C_{37:2} + C_{37:3})$ alkenones, which can provide paleo sea surface temperatures with an estimated accuracy of 0.5 °C.

Alkenones have been found in sediments as old as 120 Ma (Brassell et al. 2004) and may mark the divergence of the Isochrysidales from other haptophyte algae as indicated from genomic molecular clock analysis (Medlin et al. 2008). However, the alkenones in strata older than ~62 Ma are very different from those in younger strata as they consist only of even-numbered alkadien-3-ones and odd-numbered alkadien-2-ones. In contrast, C_{37} – C_{39} alkadienones and alkatrienones constitute the principal alkenones found in younger Paleogene sediments. The occurrence of these alkenones immediately following the Early Eocene Climate Optimum couples with the occurrence of calcareous nannoplankton genera within the Noelaerhabdaceae suggesting that these compounds were responses to climate change that allow marine haptophytes to store energy during periods of high nutrient availability (Brassell 2014).

15 C_{30} – C_{37} Botryococcene Derivatives

Fossils as old as the Precambrian have been identified as members of the green algae *Botryococcus*; however, the evolution of a specific biochemical pathway that produces C_{30} – C_{37} unusually branched isoprenoid hydrocarbons referred to as botryococcenes appears to have arisen in *Botryococcus braunii* Race B in the early Eocene around 55 Ma (Volkman 2014). The biosynthesis of these compounds resulted from the duplication and subsequent alteration of the squalene synthase gene resulting in the production of both C_{30} botryococcene and squalene. These products are then methylated to higher carbon number botryococcenes and methylated squalenes. The recent evolution of these novel isoprenoidal pathways explains the lack of botryococcenes in pre-Eocene sediments.

16 Research Needs

Our view of the life's history is no longer limited to interpreting mineralized fossils but has expanded to integrating these observations within a comprehensive theory of evolution that incorporates new findings in biochemistry, molecular phylogeny, and the chemical fossil record. Hydrocarbons have existed throughout Earth's history and understanding their origin, alteration, and preservation is a key to helping reconstruct the evolutionary history of life on Earth. There are still many orphan biomarkers, hydrocarbons found in source rocks and oils that are certainly of biological origin but have no known biochemical precursors. For example, tricyclic terpanes are common throughout the geologic record and are particularly abundant in strata associated with coastal marine upwellings, but their biologic precursors remain elusive.

Many of life's fundamental biochemical pathways evolved in the Archean, but deciphering this past remains problematic as the syngenicity of extracted biomarkers is suspect. Generation of biomarkers from kerogens via hydrolysis and in situ chemical analyses of carefully selected fluid inclusions and microfossils offer the prospect of identifying hydrocarbon biomarkers from this age. Many of the lessons learned in discriminating life's signatures in ancient rocks are now being applied to planetary exploration (Simoneit 2004; Sephton et al. 2013; Georgiou and Deamer 2014).

Functionalized structures are less stable than saturated and aromatic hydrocarbons and are still considered to be largely restricted to recent or very low maturity sediments. However, later studies have shown some functionalized biomarkers to be more stable than previously thought. For example, the first appearance of alkenones was thought to be in the early Eocene but they are now known in rocks three times as old (Brassell 2014). Petroleomics provides through advances in liquid chromatography and ultra-high resolution mass spectrometry a near complete picture of the organic diversity of polar compounds in crude oils and rock extracts (Marshall and Rodgers 2008). Currently, our knowledge of these polar compounds is largely restricted to elemental compositions. Structural characterization may provide new taxon-specific biomarkers.

Genomics and metagenomics delve into the phylogeny of life by showing how genes have evolved and were transferred between organisms. New techniques in transcriptomics are able to determine what genes are active. Metabolomics and lipidomics provide comprehensive analyses of pathways and networks of cellular metabolites and lipids in biological systems. By combining these biochemical sciences with geochemistry, we may be able to address long-standing questions in the hydrocarbon fossil record (Fig. 1).

Appendix

Biomarker structures mentioned in text.

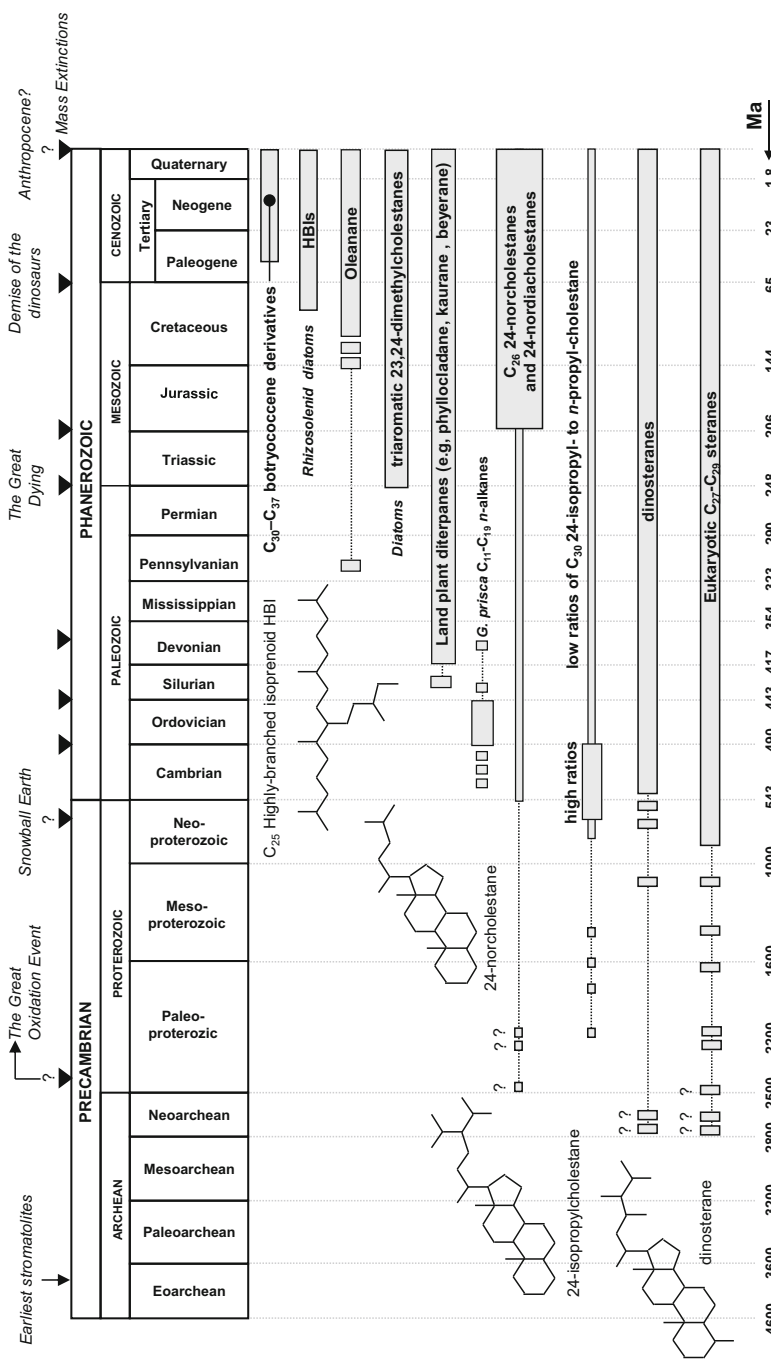
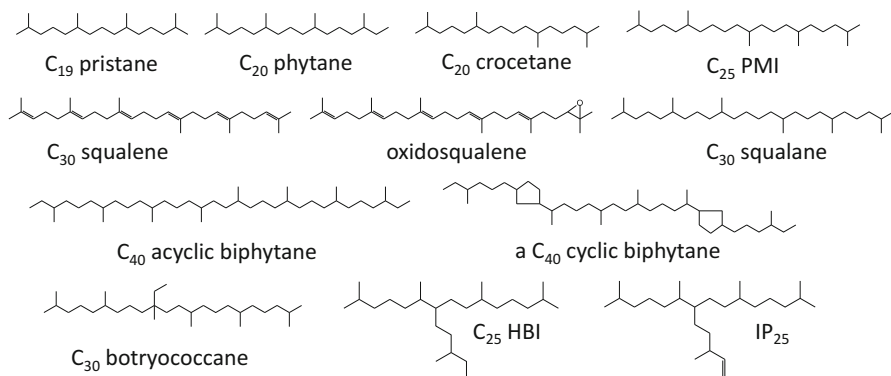
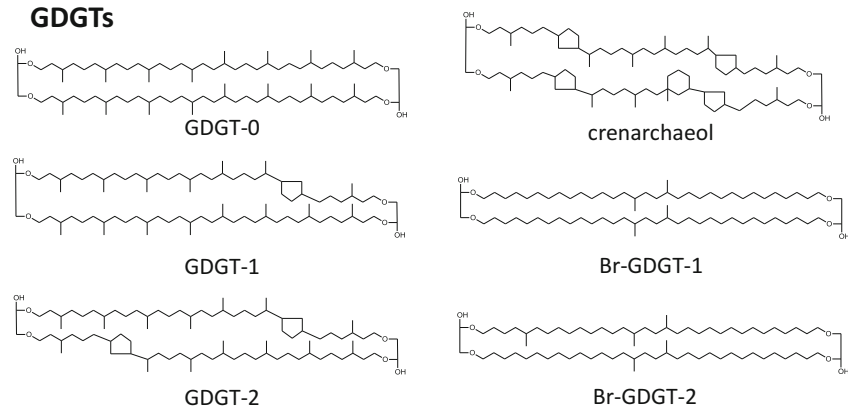


Fig. 1 Temporal distribution of several biomarkers discussed in this paper. ? = Uncertain occurrence

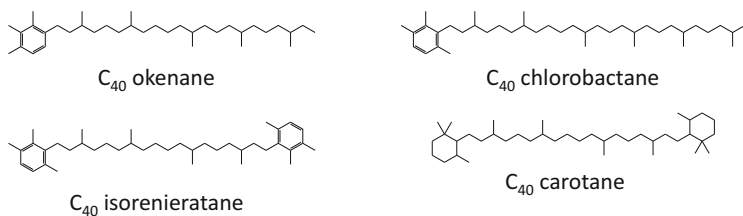
Isoprenoids



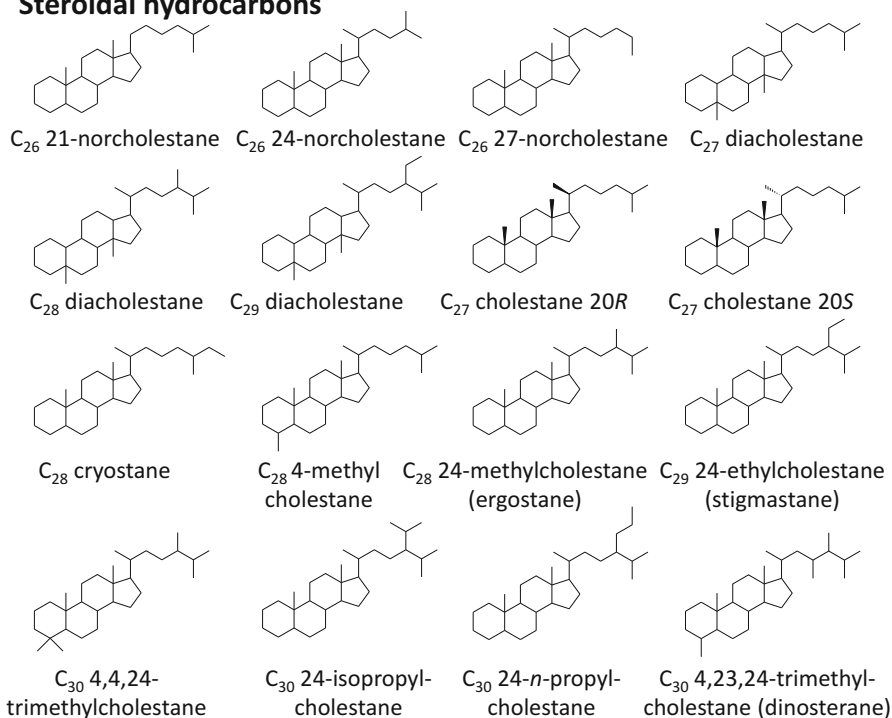
GDGTs



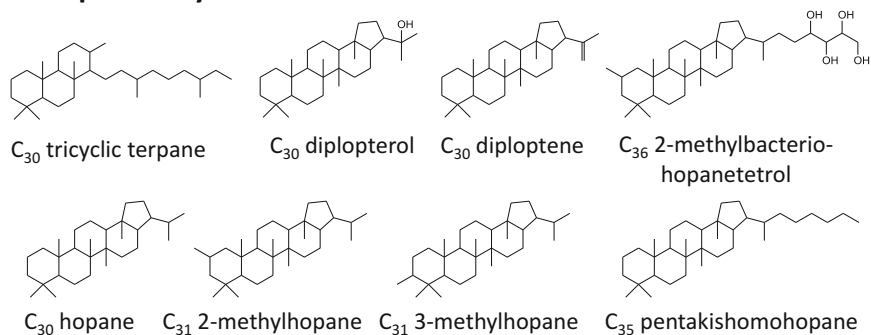
Carotenoids



Steroidal hydrocarbons

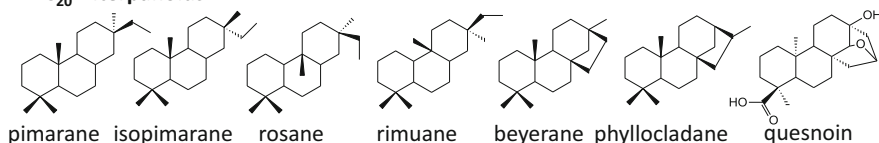


Triterpanoid hydrocarbons

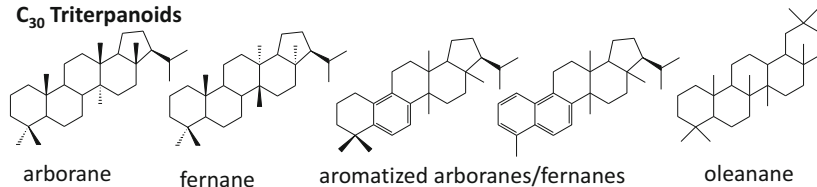


Higher Land Plant Terpanoids

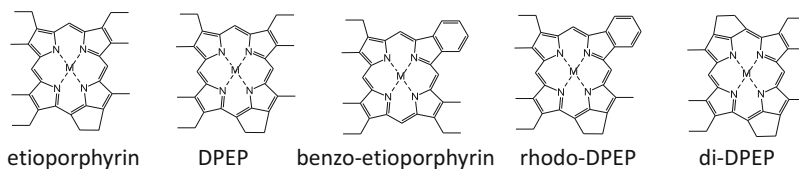
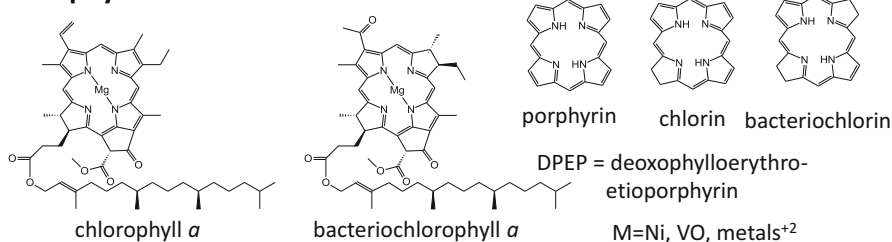
C₂₀ Diterpanoids



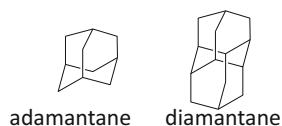
C₃₀ Triterpanoids



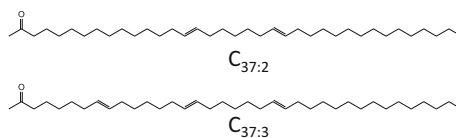
Porphyryns



Diamondoids



Alkenones



References

- Alleon J, Bernard S, Le Guillou C, Daval D, Skouri-Panet F, Pont S, Delbes L, Robert F (2016) Early entombment within silica minimizes the molecular degradation of microorganisms during advanced diagenesis. *Chem Geol* 437:98–108
- Allwood AC, Walter MR, Kamber BS, Marshall CP, Burch IW (2006) Stromatolite reef from the Early Archaean Era of Australia. *Nature* 441:714–718

- Allwood AC, Walter MR, Burch IW, Kamber BS (2007) 3.43 billion-year-old stromatolite reef from the Pilbara Craton of Western Australia: ecosystem-scale insights to early life on Earth. *Precambrian Res* 158:198–227
- Altermann W, Kazmierczak J (2003) Archean microfossils: a reappraisal of early life on Earth. *Res Microbiol* 154:611–617
- Anbar AD, Duan Y, Lyons TW, Arnold GL, Kendall B, Creaser RA, Kaufman AJ, Gordon GW, Scott C, Garvin J, Buick R (2007) A whiff of oxygen before the Great Oxidation Event? *Science* 317:1903–1906
- Antcliff JB (2013) Questioning the evidence of organic compounds called sponge biomarkers. *Palaeontology* 56:917–925
- Armstroff A, Wilkes H, Schwarzbauer J, Littke R, Horsfield B (2006) Aromatic hydrocarbon biomarkers in terrestrial organic matter of Devonian to Permian age. *Palaeogeogr Palaeoclimatol Palaeoecol* 240:253–274
- Asara JM, Schweitzer MH, Freimark LM, Phillips M, Cantley LC (2007) Protein sequences from mastodon and *Tyrannosaurus rex* revealed by mass spectrometry. *Science* 316:280–285
- Auras S, Wilde V, Hoernes S, Scheffler K, Püttmann W (2006) Biomarker composition of higher plant macrofossils from Late Palaeozoic sediments. *Palaeogeogr Palaeoclimatol Palaeoecol* 240:305–317
- Barbanti SM, Moldowan JM, Mello MR, Kolaczowski E, Watt DS, Huizinga BJ (1999) Analysis and occurrence of novel triaromatic 23,24 dimethylcholestanes in geologic time. In: Proceedings of the 19th international meeting on organic geochemistry, Istanbul, 6–10 Sept 1999, pp 159–160
- Barbanti SM, Moldowan JM, Watt DS, Kolaczowska E (2011) New triaromatic steroids distinguish Paleozoic from Mesozoic oil. *Org Geochem* 42:409–424
- Bateman RM, Crane PR, DiMichele WA, Kenrick PR, Rowe NP, Speck T, Stein WE (1998) Early evolution of land plants: phylogeny, physiology, and ecology of the primary terrestrial radiation. *Annu Rev Ecol Syst* 29:263–292
- Bell EA, Boehnke P, Harrison TM, Mao WL (2015) Potentially biogenic carbon preserved in a 4.1 billion-year-old zircon. *Proc Natl Acad Sci* 112:14518–14521
- Belt ST, Müller J (2013) The Arctic sea ice biomarker IP₂₅: a review of current understanding, recommendations for future research and applications in palaeo sea ice reconstructions. *Quat Sci Rev* 79:9–25
- Belt ST, Massé G, Rowland SJ, Poulin M, Michel C, LeBlanc B (2007) A novel chemical fossil of palaeo sea ice: IP₂₅. *Org Geochem* 38:16–27
- Benton MJ (2008) When life nearly died: the greatest mass extinction of all time, 2nd edn. Thames & Hudson, London
- Bergstrom CT, Dugatkin LA (2012) *Evolution*. Norton, New York. 786 pp
- Bertazzo S, Maidment SCR, Kallepitis C, Fearn S, Stevens MM, Xie H (2015) Fibres and cellular structures preserved in 75-million-year-old dinosaur specimens. *Nat Commun* 6:7352
- Bianchi TS, Canuel EA (2011) *Chemical biomarkers in aquatic ecosystems*. Princeton University Press, Princeton. 392 pp
- Blokker P, van Bergen P, Pancost R, Collinson ME, de Leeuw JW, Sinninghe Damsté JS (2001) The chemical structure of *Gloeocapsomorpha prisca* microfossils: implications for their origin. *Geochim Cosmochim Acta* 65:885–900
- Boere AC, Rijpstra WIC, De Lange GJ, Sinninghe Damsté JS, Coolen MJL (2011) Preservation potential of ancient plankton DNA in Pleistocene marine sediments. *Geobiology* 9:377–393
- Brain CK, Prave AR, Hoffmann K-H, Fallick AE, Botha A, Herd DA, Sturrock C, Young I, Condon DJ, Allison SG (2012) The first animals: ca. 760-million-year-old sponge-like fossils from Namibia. *S Afr J Sci* 108. <https://doi.org/10.4102/sajs.v108i1/2.658>
- Brasier MD, Green OR, Jephcoat AP, Kleppe AK, Van Kranendonk MJ, Lindsay JF, Steele A, Grassineau NV (2002) Questioning the evidence for Earth's oldest fossils. *Nature* 416:76–81
- Brasier M, McLoughlin N, Green O, Wacey D (2006) A fresh look at the fossil evidence for early Archaean cellular life. *Philos Trans R Soc B: Biol Sci* 361:887–902

- Brasier MD, Antcliffe J, Saunders M, Wacey D (2015) Changing the picture of Earth's earliest fossils (3.5–1.9 Ga) with new approaches and new discoveries. *Proc Natl Acad Sci* 112:4859–4864
- Brassell SC (2014) Climatic influences on the Paleogene evolution of alkenones. *Paleoceanography* 29:255–272
- Brassell SC, Eglinton G, Marlowe IT, Pflaumann U, Sarnthein M (1986) Molecular stratigraphy: a new tool for climatic assessment. *Nature* 320:129–133
- Brassell SC, Dumitrescu M, the ODP Leg 198 Shipboard Scientific Party (2004) Recognition of alkenones in a lower Aptian porcellanite from the west-central Pacific. *Org Geochem* 35:181–188
- Brennecke GA, Herrmann AC, Algeo TJ, Anbar AD (2011) Rapid expansion of oceanic anoxia immediately before the end-Permian mass extinction. *Proc Natl Acad Sci U S A* 108:17631–17634
- Brooks JJ (2011) Millimeter-scale concentration gradients of hydrocarbons in Archean shales: live-oil escape or fingerprint of contamination? *Geochim Cosmochim Acta* 75:3196–3213
- Brooks JJ, Butterfield NJ (2009) Biogeochemistry: early animals out in the cold. *Nature* 457:672–673
- Brooks JJ, Schaeffer P (2008) Okenane, a biomarker for purple sulfur bacteria (Chromatiaceae), and other new carotenoid derivatives from the 1640 Ma Barney Creek Formation. *Geochim Cosmochim Acta* 72:1396–1414
- Brooks JJ, Logan GA, Buick R, Summons RE (1999) Archean molecular fossils and the early rise of eukaryotes. *Science* 285:1033–1036
- Brooks JJ, Buick R, Logan GA, Summons RE (2003a) Composition and syngeneity of molecular fossils from the 2.78 to 2.45 billion-year-old Mount Bruce Supergroup, Pilbara Craton, Western Australia. *Geochim Cosmochim Acta* 67:4289–4319
- Brooks JJ, Buick R, Summons RE, Logan GA (2003b) A reconstruction of Archean biological diversity based on molecular fossils from the 2.78 to 2.45 billion-year-old Mount Bruce Supergroup, Hamersley Basin, Western Australia. *Geochim Cosmochim Acta* 67:4321–4335
- Brooks JJ, Love GD, Summons RE, Knoll AH, Logan GA, Bowden S (2005) Biomarker evidence for green and purple sulfur bacteria in an intensely stratified Paleoproterozoic ocean. *Nature* 437:866–870
- Brooks JJ, Jarrett AJM, Sirantoine E, Kenig F, Moczyłowska M, Porter S, Hope J (2016) Early sponges and toxic protists: possible sources of cryostane, an age diagnostic biomarker antedating Sturtian Snowball Earth. *Geobiology* 14:129–149
- Brooks JJ, Jarrett AJM, Sirantoine E, Hallmann C, Hoshino Y, Liyanage T (2017) The rise of algae in Cryogenian oceans and the emergence of animals. *Nature* 548:578–581
- Brown TA, Barnes IM (2015) The current and future applications of ancient DNA in Quaternary science. *J Quat Sci* 30:144–153
- Brown TA, Belt ST, Tatarek A, Mundy CJ (2014) Source identification of the Arctic sea ice proxy IP25. *Nat Commun* 5:4197
- Butterfield NJ (2000) *Bangiomorpha pubescens* n. gen., n. sp.: implications for the evolution of sex, multicellularity, and the Mesoproterozoic/Neoproterozoic radiation of eukaryotes. *Paleobiology* 26:386–404
- Butterfield NJ, Rainbird RH (1998) Diverse organic-walled fossils, including “possible dinoflagellates”, from the early Neoproterozoic of Arctic Canada. *Geology* 26:963–966
- Canfield DE (2005) The early history of atmospheric oxygen: homage to Robert M. Garrels. *Annu Rev Earth Planet Sci* 33:1–36
- Cao C, Zheng Q (2009) Geological event sequences of the Permian-Triassic transition recorded in the microfossils in Meishan section. *Sci China D* 52:1529–1536
- Cao C, Love GD, Hays LE, Wang W, Shen S, Summons RE (2009) Biogeochemical evidence for euxinic oceans and ecological disturbance presaging the end-Permian mass extinction event. *Earth Planet Sci Lett* 281:188–201
- Cappellini E, Collins MJ, Gilbert MTP (2014) Unlocking ancient protein palimpsests. *Science* 343:1320–1322

- Cleland TP, Schroeter ER, Zamdborg L, Zheng W, Lee JE, Tran JC, Bern M, Duncan MB, Lebleu VS, Ahlf DR, Thomas PM, Kalluri R, Kelleher NL, Schweitzer MH (2015) Mass spectrometry and antibody-based characterization of blood vessels from *Brachylophosaurus canadensis*. *J Proteome Res* 14:5252–5262
- Collins MJ, Germaey AM, Nielsen-Marsh CM, Vermeer C, Westbroek P (2000) Slow rates of degradation of osteocalcin: green light for fossil bone protein? *Geology* 28:1139–1142
- Czaja AD, Johnson CM, Roden EE, Beard BL, Voegelin AR, Nägler TF, Beukes NJ, Wille M (2012) Evidence for free oxygen in the Neoproterozoic ocean based on coupled iron–molybdenum isotope fractionation. *Geochim Cosmochim Acta* 86:118–137
- Derenne S, Metzger P, Largeau C (1992) Similar morphological and chemical variations of *Gloeocapsomorpha prisca* in Ordovician sediments and cultured *Botryococcus braunii* as a response to changes in salinity. *Org Geochem* 19:299–313
- Droser ML, Gehling JG (2015) The advent of animals: the view from the Ediacaran. *Proc Natl Acad Sci* 112:4865–4870
- Duan Y, Anbar AD, Arnold GL, Lyons TW, Gordon GW, Kendall B (2010) Molybdenum isotope evidence for mild environmental oxygenation before the Great Oxidation Event. *Geochim Cosmochim Acta* 74:6655–6668
- Dutkiewicz A, Volk H, Ridley J, George SC (2004) Geochemistry of oil in fluid inclusions in a middle Proterozoic igneous intrusion: implications for the source of hydrocarbons in crystalline rocks. *Org Geochem* 35:937–957
- Dutkiewicz A, Volk H, George SC, Ridley J, Buick R (2006) Biomarkers from Huronian oil-bearing fluid inclusions: an uncontaminated record of life before the Great Oxidation Event. *Geol* 34:437–440
- Eigenbrode JL, Freeman KH (2006) Late Archean rise of aerobic microbial ecosystems. *Proc Natl Acad Sci* 103:15759–15764
- Eigenbrode JL, Freeman KH, Summons RE (2008) Methylhopane biomarker hydrocarbons in Hamersley Province sediments provide evidence for Neoproterozoic aerobic biosynthesis. *Earth Planet Sci Lett* 273:323–331
- Eltgroth ML, Watwood RL, Wolfe GV (2005) Production and cellular localisation of neutral long-chain lipids in the haptophyte algae, *Isochrysis galbana* and *Emiliania huxleyi*. *J Phycol* 41:1000–1009
- Eme L, Sharpe SC, Brown MW, Roger AJ (2014) On the age of eukaryotes: evaluating evidence from fossils and molecular clocks. *Cold Spring Harb Perspect Biol* 6. <https://doi.org/10.1101/cshperspect.a016139>
- Erwin DH (2006) Extinction: how life on earth nearly ended 250 million years ago. Princeton University Press, Princeton. 306 pp
- Falcón LI, Magallón S, Castillo A (2010) Dating the cyanobacterial ancestor of the chloroplast. *ISME J* 4:777–783
- Farquhar J, Peters M, Johnston DT, Strauss H, Masterson A, Wiechert U, Kaufman AJ (2007) Isotopic evidence for Mesoarchean anoxia and changing atmospheric sulphur chemistry. *Nature* 449:706–709
- Fenton S, Grice K, Twitchett RJ, Bottcher ME, Looy CV, Nabbefeld B (2007) Changes in biomarker abundances and sulfur isotopes of pyrite across the Permian-Triassic (P/Tr) Schuchert Dal section (East Greenland). *Earth Planet Sci Lett* 262:230–239
- Fowler MG (1992) The influence of *Gloeocapsomorpha prisca* on the organic geochemistry of oils and organic-rich rocks of late Ordovician age from Canada. In: Schidlowski M, Golubic S, Kimberley MM, McKirdy DM, Trudinger PA (eds) Early organic evolution. Springer, Berlin, pp 336–348
- Fowler MG, Stasiuk LD, Hearn M, Obermajer M (2004) Evidence for *Gloeocapsomorpha prisca* in Late Devonian source rocks from Southern Alberta, Canada. *Org Geochem* 35:425–441
- French KL, Sepúlveda J, Trabucho-Alexandre J, Gröcke DR, Summons RE (2014) Organic geochemistry of the early Toarcian oceanic anoxic event in Hawsker Bottoms, Yorkshire, England. *Earth Planet Sci Lett* 390:116–127
- French KL, Hallmann C, Hope JM, Schoon PL, Zumberge JA, Hoshino Y, Peters CA, George SC, Love GD, Brocks JJ, Buick R, Summons RE (2015) Reappraisal of hydrocarbon biomarkers in Archean rocks. *Proc Natl Acad Sci* 112:5915–5920

- Frohlich MW, Chase MW (2007) After a dozen years of progress the origin of angiosperms is still a great mystery. *Nature* 450:1184–1189
- Gensel PG, Edwards D (2001) Plants invade the land: evolutionary and environmental perspectives. Columbia University Press, New York. 324 pp
- George SC, Volk H, Dutkiewicz A, Ridley J, Buick R (2008) Preservation of hydrocarbons and biomarkers in oil trapped inside fluid inclusions for >2 billion years. *Geochim Cosmochim Acta* 72:844–870
- Georgiou CD, Deamer DW (2014) Lipids as universal biomarkers of extraterrestrial life. *Astrobiology* 14:541–549
- Gold DA, Grabenstatter J, de Mendoza A, Riesgo A, Ruiz-Trillo I, Summons RE (2016) Sterol and genomic analyses validate the sponge biomarker hypothesis. *Proc Natl Acad Sci* 113:2684–2689
- Goldblatt C, Lenton TM, Watson AJ (2006) Bistability of atmospheric oxygen and the Great Oxidation. *Nature* 443:683–686
- Greenwood PF, Summons RE (2003) GC-MS detection and significance of crocetane and penta-methylcosane in sediments and crude oils. *Org Geochem* 34:1211–1222
- Grice K, Cao C, Love GD, Böttcher ME, Twitchett RJ, Grosjean E, Summons RE, Turgeon SC, Dunning W, Jin Y (2005a) Photic zone euxinia during the Permian-Triassic superanoxic event. *Science* 307:706–709
- Grice K, Twitchett RJ, Alexander R, Foster CB, Looy C (2005b) A potential biomarker for the Permian-Triassic ecological crisis. *Earth Planet Sci Lett* 236:315–321
- Grice K, Nabbefeld B, Maslen E (2007) Source and significance of selected polycyclic aromatic hydrocarbons in sediments (Hovea-3 well, Perth Basin, Western Australia) spanning the Permian-Triassic boundary. *Org Geochem* 38:1795–1803
- Hedges SB (2002) The origin and evolution of model organisms. *Nat Rev Genet* 3:838–849
- Hickman-Lewis K, Garwood RJ, Brasier MD, Goral T, Jiang H, McLoughlin N, Wacey D (2016) Carbonaceous microstructures from sedimentary laminated chert within the 3.46 Ga Apex Basalt, Chinaman Creek locality, Pilbara, Western Australia. *Precambrian Res* 278:161–178
- Hoffman CF, Foster CB, Powell TG, Summons RE (1987) Hydrocarbon biomarkers from Ordovician sediments and the fossil alga *Gloeocapsomorpha prisca* Zalesky 1917. *Geochim Cosmochim Acta* 51:2681–2697
- Hofmann HJ (1976) Precambrian microflora, Belcher Islands, Canada: significance and systematics. *J Paleontol* 50:1040–1073
- Holba AG, Dzou LIP, Masterson WD, Singletary MS, Moldowan JM, Mello MR, Tegelaar E (1998a) Application of 24-norcholestanes for constraining source age of petroleum. *Org Geochem* 29:1269–1283
- Holba AG, Tegelaar EW, Huizinga BJ, Moldowan JM, Singletary MS, McCaffrey MA, Dzou LIP (1998b) 24-norcholestanes as age-sensitive molecular fossils. *Geology* 26:783–786
- Holland HD (2002) Volcanic gases, black smokers, and the Great Oxidation Event. *Geochim Cosmochim Acta* 66:3811–3826
- Holland H (2006) The oxygenation of the atmosphere and oceans. *Philos Trans R Soc B: Biol Sci* 361:903–915
- Hug LA, Baker BJ, Anantharaman K, Brown CT, Probst AJ, Castelle CJ, Butterfield CN, HERNSDORF AW, Amano Y, Ise K, Suzuki Y, Dudek N, Relman DA, Finstad KM, Amundson R, Thomas BC, Banfield JF (2016) A new view of the tree of life. *Nat Microbiol* 1:16048
- Hurley SJ, Elling FJ, Könneke M, Buchwald C, Wankel SD, Santoro AE, Lipp JS, Hinrichs K-U, Pearson A (2016) Influence of ammonia oxidation rate on thaumarchaeal lipid composition and the TEX₈₆ temperature proxy. *Proc Natl Acad Sci* 113:7762–7767
- Javaux EJ, Knoll AH, Walter MR (2003) Recognizing and interpreting the fossils of early eukaryotes. *Orig Life Evol Biosph* 33:75–94
- Javaux EJ, Knoll AH, Walter MR (2004) TEM evidence for eukaryotic diversity in mid-Proterozoic oceans. *Geobiology* 2:121–132

- Javaux EJ, Marshall CP, Bekker A (2010) Organic-walled microfossils in 3.2-billion-year-old shallow-marine siliciclastic deposits. *Nature* 463:934–938
- Jenkyns HC, Schouten-Huibers L, Schouten S, Sinninghe Damsté JS (2012) Warm middle Jurassic–Early Cretaceous high-latitude sea-surface temperatures from the Southern Ocean. *Clim Past* 8:215–226
- Jia C, Huang J, Kershaw S, Luo G, Farabegoli E, Perri MC, Chen L, Bai X, Xie S (2012) Microbial response to limited nutrients in shallow water immediately after the end-Permian mass extinction. *Geobiology* 10:60–71
- Jossang J, Bel-Kassaoui H, Jossang A, Seuleiman M, Nel A (2008) Quesnoin, a novel pentacyclic ent-diterpene from 55 Million years old Oise amber. *J Org Chem* 73:412–417
- Kim J-H, van der Meer J, Schouten S, Helmke P, Willmott V, Sangiorgi F, Koç N, Hopmans EC, Sinninghe Damsté JS (2010) New indices and calibrations derived from the distribution of crenarchaeal isoprenoid tetraether lipids: implications for past sea surface temperature reconstructions. *Geochim Cosmochim Acta* 74:4639–4654
- Kim J-H, Schouten S, Rodrigo-Gámiz M, Rampen S, Marino G, Huguet C, Helmke P, Buscail R, Hopmans EC, Pross J, Sangiorgi F, Middelburg JBM, Sinninghe Damsté JS (2015) Influence of deep-water derived isoprenoid tetraether lipids on the paleothermometer in the Mediterranean Sea. *Geochim Cosmochim Acta* 150:125–141
- Kirkpatrick JB, Walsh EA, D’Hondt S (2016) Fossil DNA persistence and decay in marine sediment over hundred-thousand-year to million-year time scales. *Geology* 44:615–618
- Kirschvink JL, Kopp RE (2008) Paleoproterozoic icehouses and the evolution of oxygen mediating enzymes: the case for a late origin of photosystem-II. *Philos Trans R Soc B* 363:2755–2765
- Knoll AH (2015) Paleobiological perspectives on early microbial evolution. *Cold Spring Harb Perspect Biol* 7:a018093
- Knoll AH, Javaux EJ, Hewitt D, Cohen P (2006) Eukaryotic organisms in Proterozoic oceans. *Philos Trans R Soc B: Biol Sci* 361:1023–1038
- Knoll AH, Summons RE, Waldbauer JR, Zumberge JE (2007a) The geological succession of primary producers in the oceans. In: Falkowski P, Knoll AH (eds) *The evolution of primary producers in the sea*. Academic, Boston, pp 133–164
- Knoll AH, Bambach RK, Payne JL, Pruss S, Fischer WW (2007b) Paleophysiology and end-Permian mass extinction. *Earth Planet Sci Lett* 256:295–313
- Kopp RE, Kirschvink JL, Hilburn IA, Nash CZ (2005) The Paleoproterozoic snowball earth: a climate disaster triggered by the evolution of oxygenic photosynthesis. *Proc Natl Acad Sci* 102:11131–11136
- Kump LR, Barley ME (2007) Increased subaerial volcanism and the rise of atmospheric oxygen 2.5 billion years ago. *Nature* 448:1033–1036
- Lalonde SV, Konhauser KO (2015) Benthic perspective on Earth’s oldest evidence for oxygenic photosynthesis. *Proc Natl Acad Sci* 112:995–1000
- Lengger SK, Hopmans EC, Sinninghe Damsté JS, Schouten S (2014) Fossilization and degradation of archaeal intact polar tetraether lipids in deeply buried marine sediments (Peru Margin). *Geobiology* 12:212–220
- Liao J, Lu H, Sheng G, Peng P, Hsu CS (2015) Monoaromatic, diaromatic, triaromatic, and tetraaromatic hopanes in Kukersite shale and their stable carbon isotopic composition. *Energy Fuel* 29:3573–3583
- Lindgren J, Uvdal P, Engdahl A, Lee AH, Alwmark C, Bergquist K-E, Nilsson E, Ekström P, Rasmussen M, Douglas DA, Polcyn MJ, Jacobs LL (2011) Microspectroscopic evidence of Cretaceous bone proteins. *PLoS One* 6:e19445
- Love GD, Grosjean E, Stalvies C, Fike DA, Grotzinger JP, Bradley AS, Kelly AE, Bhatia M, Meredith W, Snape CE, Bowring SA, Condon DJ, Summons RE (2009) Fossil steroids record the appearance of Demospongiae during the Cryogenian Period. *Nature* 457:718–721
- Manning PL, Morris PM, McMahon A, Jones E, Gize A, Macquaker JHS, Wolff G, Thompson A, Marshall J, Taylor KG, Lyson T, Gaskell S, Reamtong O, Sellers WI, van Dongen BE,

- Buckley M, Wogelius RA (2009) Mineralized soft-tissue structure and chemistry in a mummified hadrosaur from the Hell Creek Formation, North Dakota (USA). *Proc R Soc B* 276:3429–3437
- Marshall AG, Rodgers RP (2008) Petroleomics: chemistry of the underworld. *Proc Natl Acad Sci* 105:18090–18095
- Martin WF, Sousa FL (2016) Early microbial evolution: the age of anaerobes. *Cold Spring Harb Perspect Biol* 8:a018127
- Massé G, Belt ST, Rowland SJ, Rohmer M (2004) Isoprenoid biosynthesis in the diatoms *Rhizosolenia setigera* (Brightwell) and *Haslea ostrearia* (Simonsen). *Proc Natl Acad Sci* 101:4413–4418
- McCaffrey MA, Moldowan JM, Lipton PA, Summons RE, Peters KE, Jeganathan A, Watt DS (1994) Paleoenvironmental implications of novel C₃₀ steranes in Precambrian to Cenozoic age petroleum and bitumen. *Geochim Cosmochim Acta* 58:529–532
- McKeegan KD, Kudryavtsev AB, Schopf JW (2007) Raman and ion microscopic imagery of graphitic inclusions in apatite from older than 3830 Ma Akilia supracrustal rocks, West Greenland. *Geology* 35:591–594
- McKirdy DM, Imbus SW (1992) Precambrian petroleum: a decade of changing perceptions. In: Schidlowski M, Golubic S, Kimberley MM, McKirdy DM, Trudinger PA (eds) *Early organic evolution: implications for mineral and energy resources*. Springer, Berlin, pp 176–192
- Medlin LK, Sáez AG, Young JR (2008) A molecular clock for coccolithophores and implications for selectivity of phytoplankton extinctions across the K/T boundary. *Mar Micropaleontol* 67:69–86
- Meng F, Zhou C, Yin L, Chen Z, Yuan X (2005) The oldest known dinoflagellates: morphological and molecular evidence from Mesoproterozoic rocks at Yongji, Shanxi Province. *Chin Sci Bull* 50:1230–1234
- Metzger P, Largeau C (1994) A new type of ether lipid comprising phenolic moieties in *Botryococcus braunii*. Chemical structure and abundance, and geochemical implications. *Org Geochem* 22:801–814
- Meyer M, Arsuaga J-L, de Filippo C, Nagel S, Aximu-Petri A, Nickel B, Martínez I, Gracia A, de Castro JMB, Carbonell E, Viola B, Kelso J, Prüfer K, Pääbo S (2016) Nuclear DNA sequences from the Middle Pleistocene Sima de los Huesos hominins. *Nature* 531:504–507
- Moczydłowska M, Landing E, Zang W, Palacios T (2011) Proterozoic phytoplankton and timing of chlorophyte algae origins. *Palaeontology* 54:721–733
- Mojzsis SJ, Arrhenius G, McKeegan KD, Harrison TM, Nutman AP, Friend CRL (1996) Evidence for life on Earth before 3,800 million years ago. *Nature* 384:55–59
- Moldowan JM (2000) Trails of life. *Chem Br* 36:34–37
- Moldowan JM, Jacobson SR (2000) Chemical signals for early evolution of major taxa: biosignatures and taxon-specific biomarkers. *Int Geol Rev* 42:805–812
- Moldowan JM, Talyzina NM (1998) Biogeochemical evidence for dinoflagellate ancestors in the early Cambrian. *Science* 281:1168–1170
- Moldowan JM, Fago FJ, Lee CY, Jacobson SR, Watt DS, Slougui N-E, Jeganathan A, Young DC (1990) Sedimentary 24-*n*-propylcholestanes, molecular fossils diagnostic of marine algae. *Science* 247:309–312
- Moldowan JM, Dahl J, Huizinga BJ, Fago FJ, Hickey LJ, Peakman TM, Taylor DW (1994) The molecular fossil record of oleanane and its relation to angiosperms. *Science* 265:768–771
- Moldowan JM, Dahl J, Jacobson SR, Huizinga BJ, Fago FJ, Shetty R, Watt DS, Peters KE (1996) Chemostratigraphic reconstruction of biofacies; molecular evidence linking cyst-forming dinoflagellates with pre-Triassic ancestors. *Geology* 24:159–162
- Moldowan JM, Moldowan S, Blanco-Velandia V, Blanco-Velandia Y, Orejuela-Parra C, Bott G, Dahl J (2015) Llanos Basin: unraveling its complex petroleum systems with advanced geochemical technologies. AAPG Search Discovery 10776. http://www.searchanddiscovery.com/documents/2012/40979dahl/ndx_dahl.pdf

- Newman DK, Neubauer C, Ricci JN, Wu C-H, Pearson A (2016) Cellular and molecular biological approaches to interpreting ancient biomarkers. *Annu Rev Earth Planet Sci* 44:493–522
- Nisbet EG, Grassineau NV, Howe CJ, Abell PI, Regelous M, Nisbet RER (2007) The age of Rubisco: the evolution of oxygenic photosynthesis. *Geobiology* 5:311–335
- Nishizawa M, Takahata N, Terada K, Komiya T, Ueno Y, Sano Y (2005) Rare-earth element, lead, carbon, and nitrogen geochemistry of apatite-bearing metasediments from the 3.8 Ga Isua Supracrustal Belt, West Greenland. *Int Geol Rev* 47:952–970
- Nutman AP, Bennett VC, Friend CRL, Van Kranendonk MJ, Chivas AR (2016) Rapid emergence of life shown by discovery of 3,700-million-year-old microbial structures. *Nature* 537:535–538
- Pak R, Pemberton SG, Stasiuk L (2010) Paleoenvironmental and taphonomic implications of trace fossils in Ordovician kukersites. *Bull Can Petrol Geol* 58:141–158
- Pancost RD, Freeman KH, Patzkowsky ME, Wavrek DA, Collister JW (1998) Molecular indicators of redox and marine photoautotroph composition in the late Middle Ordovician of Iowa, U.S.A. *Org Geochem* 29:1649–1662
- Pang K, Tang Q, Schiffbauer JD, Yao J, Yuan X, Wan B, Chen L, Ou Z, Xiao S (2013) The nature and origin of nucleus-like intracellular inclusions in Paleoproterozoic eukaryote microfossils. *Geobiology* 11:499–510
- Papineau D, De Gregorio BT, Cody GD, Fries MD, Mojzsis SJ, Steele A, Stroud RM, Fogel ML (2010) Ancient graphite in the Eoarchean quartz-pyroxene rocks from Akilia in southern West Greenland I: petrographic and spectroscopic characterization. *Geochim Cosmochim Acta* 74:5862–5883
- Parfrey LW, Lahr DJG, Knoll AH, Katz LA (2011) Estimating the timing of early eukaryotic diversification with multigene molecular clocks. *Proc Natl Acad Sci* 108:13624–13629
- Pavlov AA, Kasting JF (2002) Mass-independent fractionation of sulfur isotopes in Archean sediments: strong evidence for an anoxic Archean atmosphere. *Astrobiology* 2:27–41
- Pawlowska MM, Butterfield NJ, Brocks JJ (2013) Lipid taphonomy in the Proterozoic and the effect of microbial mats on biomarker preservation. *Geology* 41:103–106
- Payne JL, Clapham ME (2012) End-Permian mass extinction in the oceans: an ancient analog for the twenty-first century? *Annu Rev Earth Planet Sci* 40:89–111
- Pearson A, Ingalls AE (2013) Assessing the use of archaeal lipids as marine environmental proxies. *Annu Rev Earth Planet Sci* 41:359–384
- Penny D, Poole A (1999) The nature of the last universal common ancestor. *Curr Opin Genet Dev* 9:672–677
- Peters KE, Walters CC, Moldowan JM (2005) *The biomarker guide, vol 1 & 2*. Cambridge University Press, Cambridge. 1155 pp
- Peterson KJ, Summons RE, Donoghue PCJ (2007) Molecular paleobiology. *Palaeontology* 50:775–809
- Pinti DL, Altermann W (2011) Apex Chert, microfossils. In: Gargaud M, Amils R, Quintanilla JC, Cleaves HJ, Irvine WM, Pinti DL, Viso M (eds) *Encyclopedia of astrobiology*. Springer, Berlin, pp 48–54
- Planavsky NJ, Asael D, Hofmann A, Reinhard CT, Lalonde SV, Knudsen A, Wang X, Ossa Ossa F, Pecoits E, Smith AJB, Beukes NJ, Bekker A, Johnson TM, Konhauser KO, Lyons TW, Rouxel OJ (2014a) Evidence for oxygenic photosynthesis half a billion years before the Great Oxidation Event. *Nat Geosci* 7:283–286
- Planavsky NJ, Reinhard CT, Wang X, Thomson D, McGoldrick P, Rainbird RH, Johnson T, Fischer WW, Lyons TW (2014b) Low Mid-Proterozoic atmospheric oxygen levels and the delayed rise of animals. *Science* 346:635–638
- Rampen SW, Schouten S, Abbas B, Panoto FE, Muyzer G, Campbell CN, Fehling J, Sinninghe Damsté JS (2007a) On the origin of 24-norcholestanes and their use as age-diagnostic biomarkers. *Geology* 35:419–422
- Rampen SW, Schouten S, Sinninghe Damsté JS (2007b) Origin of 4-desmethyl-dinosteranes in sediments and oils. In: 23rd international meeting on organic geochemistry, Torquay, 9–14 Sept 2007 Abstract O43

- Rashby SE, Sessions AL, Summons RE, Newman DK (2007) Biosynthesis of 2-methylbacterioplanepolyols by an anoxygenic phototroph. *Proc Natl Acad Sci* 104: 15099–15104
- Rasmussen B, Buick R (1999) Redox state of the Archean atmosphere: evidence from detrital heavy minerals in ca. 3250–2750 Ma sandstones from the Pilbara Craton, Australia. *Geology* 27:115–118
- Rasmussen B, Fletcher IR, Brocks JJ, Kilburn MR (2008) Reassessing the first appearance of eukaryotes and cyanobacteria. *Nature* 455:1101–1104
- Raymond J, Blankenship RE (2004) Biosynthetic pathways, gene replacement and the antiquity of life. *Geobiology* 2:199–203
- Reed JD, Illich HA, Horsfield B (1986) Biochemical evolutionary significance of Ordovician oils and their sources. *Org Geochem* 10:347–358
- Retallack GJ, Jahren AH (2008) Methane release from igneous intrusion of coal during late Permian extinction events. *J Geol* 116:1–20
- Ricci JN, Coleman ML, Welander PV, Sessions AL, Summons RE, Spear JR, Newman DK (2014) Diverse capacity for 2-methylhopanoid production correlates with a specific ecological niche. *ISME J* 8:675–684
- Rye R, Holland HD (1998) Paleosols and the evolution of atmospheric oxygen: a critical review. *Am J Sci* 298:621–672
- Saito R, Oba M, Kaiho K, Schaeffer P, Adam P, Takahashi S, Nara FW, Chen Z-Q, Tong J, Tsuchiya N (2014) Extreme euxinia prior to the Middle Triassic biotic recovery from the latest Permian mass extinction. *Org Geochem* 73:113–122
- Sarafian AR, Nielsen SG, Marschall HR, McCubbin FM, Monteleone BD (2014) Early accretion of water in the inner solar system from a carbonaceous chondrite-like source. *Science* 346:623–626
- Schidlowski M (2001) Carbon isotopes as biogeochemical recorders of life over 3.8 Ga of Earth history: evolution of a concept. *Precambrian Res* 106:117–134
- Schirmeister BE, Gugger M, Donoghue PCJ (2015) Cyanobacteria and the Great Oxidation Event: evidence from genes and fossils. *Palaeontology* 58:769–785
- Schopf JW (1993) Microfossils of the Early Archean Apex Chert: new evidence of the antiquity of life. *Science* 260:640–646
- Schopf J (2006) Fossil evidence of Archaean life. *Philos Trans R Soc B: Biol Sci* 361:869–885
- Schopf JW, Kudryavtsev AB (2012) Biogenicity of Earth's earliest fossils: a resolution of the controversy. *Gondwana Res* 22:761–771
- Schopf JW, Packer BM (1987) Early Archean (3.3-billion to 3.5-billion-year-old) microfossils from Warrawoona Group, Australia. *Science* 237:70–73
- Schopf JW, Kudryavtsev AB, Czaja AD, Tripathi AB (2007) Evidence of Archean life: stromatolites and microfossils. *Precambrian Res* 158:141–155
- Schouten S, Hopmans EC, Schefuß E, Sinninghe Damsté JS (2002) Distributional variations in marine crenarchaeotal membrane lipids: a new tool for reconstructing ancient sea water temperatures? *Earth Planet Sci Lett* 204:265–274
- Schulze T, Michaelis W (1990) Structure and origin of terpenoid hydrocarbons in some German coals. *Org Geochem* 16:1051–1058
- Schwarzbauer A, Jovančević B (2016) From biomolecules to chemofossils. Springer, 160 pp
- Schweitzer MH, Zheng W, Organ CL, Avci R, Suo Z, Freimark LM, Lebleu VS, Duncan MB, Vander Heiden MG, Neveu JM, Lane WS, Cottrell JS, Horner JR, Cantley LC, Kalluri R, Asara JM (2009) Biomolecular characterization and protein sequences of the Campanian Hadrosaur *B. canadensis*. *Science* 324:626–663
- Schweitzer MH, Zheng W, Cleland TP, Bern M (2013) Molecular analyses of dinosaur osteocytes support the presence of endogenous molecules. *Bone* 52:414–423
- Sephton MA, Looy CV, Brinkhuis H, Wignall PB, de Leeuw JW, Visscher H (2005) Catastrophic soil erosion during the end-Permian biotic crisis. *Geology* 33:941–944
- Sephton MA, Sims MR, Court RW, Luong D, Cullen DC (2013) Searching for biomolecules on Mars: considerations for operation of a Life Marker Chip instrument. *Planet Space Sci* 86:66–74

- Seufferheld M, Vieira MCF, Ruiz FA, Rodrigues CO, Moreno SNJ, Docampo R (2003) Identification of organelles in bacteria similar to acidocalcisomes of unicellular eukaryotes. *J Biol Chem* 278:29971–29978
- Shen Y, Buick R, Canfield DE (2001) Isotopic evidence for microbial sulphate reduction in the early Archaean Era. *Nature* 410:77–81
- Sheridan PP, Freeman KH, Brenchley JE (2003) Estimated minimal divergence times of the major bacterial and archaeal phyla. *Geomicrobiol J* 20:1–14
- Sherwood Lollar B, Lacrampe-Couloume G, Telling J, McCollom TM, Slater GF (2006) Compound specific isotope analysis and the challenge for identifying life: the role of biosignatures and abiosignatures. *Geochim Cosmochim Acta* 70:A582
- Siljeström S, Volk H, George SC, Lausmaa J, Sjövall P, Dutkiewicz A, Hode T (2013) Analysis of single oil-bearing fluid inclusions in mid-Proterozoic sandstones (Roper Group, Australia). *Geochim Cosmochim Acta* 122:448–463
- Simoneit BRT (2004) Biomarkers (molecular fossils) as geochemical indicators of life. *Adv Space Res* 33:1255–1261
- Sinninghe Damsté JS, Muyzer G, Abbas B, Rampen SW, Massé G, Allard WG, Belt ST, Robert J-M, Rowland SJ, Moldowan JM, Barbanti SM, Fago FJ, Denisevich P, Dahl J, Trindade LAF, Schouten S (2004) The rise of the rhizosolenid diatoms. *Science* 304:584–587
- Sinninghe Damsté JS, Rijpstra WIC, Hopmans EC, Foesel BU, Wüst PK, Overmann J, Tank M, Bryant DA, Dunfield PF, Houghton K, Stott MB (2014) Ether- and ester-bound iso-diabolic acid and other lipids in members of *Acidobacteria* subdivision 4. *Appl Environ Microbiol* 80:5207–5218
- Sorhannus U (2007) A nuclear-encoded small-subunit ribosomal RNA timescale for diatom evolution. *Mar Micropaleontology* 65:1–12
- Spang A, Saw JH, Jorgensen SL, Zaremba-Niedzwiedzka K, Martijn J, Lind AE, van Eijk R, Schleper C, Guy L, Ettema TJG (2015) Complex archaea that bridge the gap between prokaryotes and eukaryotes. *Nature* 521:173–179
- Stasiuk LD, Osadetz KG (1990) Progress in the life cycle and phyletic affinity of *Gloeocapsomorpha prisca* Zalesky 1917 from Ordovician rocks in Canadian Williston Basin. *Geol Sur Canada Curr Res D*:127–137
- Summons RE, Walter MR (1990) Molecular fossils and microfossils of prokaryotes and protists from Proterozoic sediments. *Am J Sci* 290-A:212–244
- Summons RE, Brassell SC, Eglinton G, Evans E, Horodyski RJ, Robinson N, Ward DM (1988a) Distinctive hydrocarbon biomarkers from fossiliferous sediment of the late Proterozoic Walcott Member, Chuar Group, Grand Canyon, Arizona. *Geochim Cosmochim Acta* 52:2625–2637
- Summons RE, Powell TG, Boreham CJ (1988b) Petroleum geology and geochemistry of the Middle Proterozoic McArthur Basin, northern Australia: III. Composition of extractable hydrocarbons. *Geochim Cosmochim Acta* 52:1747–1763
- Summons RE, Thomas J, Maxwell JR, Boreham CJ (1992) Secular and environmental constraints on the occurrence of dinosterane in sediments. *Geochim Cosmochim Acta* 56:2437–2444
- Summons RE, Jahnke LL, Hope JM, Logan GA (1999) 2-Methylhopanoids as biomarkers for cyanobacterial oxygenic photosynthesis. *Nature* 400:554–557
- Summons RE, Bradley AS, Jahnke LL, Waldbauer JR (2006a) Steroids, triterpenoids and molecular oxygen. *Philos Trans R Soc B* 361:951–968
- Summons RE, Love GD, Hays L, Cao C, Jin Y, Shen SZ, Grice K, Foster CB (2006b) Molecular evidence for prolonged photic zone euxinia at the Meishan and East Greenland sections of the Permian Triassic Boundary. *Geochim Cosmochim Acta* 70:A625
- Svensen H, Planke S, Polozov AG, Schmidbauer N, Corfu F, Podladchikov YY, Jamtveit B (2009) Siberian gas venting and the end-Permian environmental crisis. *Earth Planet Sci Lett* 277:490–500
- Taylor DW, Li H, Dahl J, Fago FJ, Zinniker D, Moldowan JM (2006) Biogeochemical evidence for the presence of the angiosperm molecular fossil oleanane in Paleozoic and Mesozoic non-angiospermous fossils. *Paleobiology* 32:179–190

- Thomas BM, Willink RJ, Grice K, Twitchett RJ, Purcell RR, Archbold NW, George AD, Tye S, Alexander R, Foster CB, Barber CJ (2004) Unique marine Permian-Triassic boundary section from Western Australia. *Aust J Earth Sci* 51:423–430
- Tomitani A, Knoll AH, Cavanaugh CM, Ohno T (2006) The evolutionary diversification of cyanobacteria: molecular-phylogenetic and paleontological perspectives. *Proc Natl Acad Sci* 103:5442–5447
- Uda I, Sugai A, Itoh YH, Itoh T (2001) Variation on molecular species of polar lipids from *Thermoplasma acidophilum* depends on growth temperature. *Lipids* 36:103–105
- Ueno Y, Yamada K, Yoshida N, Maruyama S, Isozaki Y (2006) Evidence from fluid inclusions for microbial methanogenesis in the early Archaean era. *Nature* 440:516–519
- Ventura GT, Kenig F, Reddy CM, Schieber J, Frysinger GS, Nelson RK, Dinel E, Gaines RB, Schaeffer P (2007) Molecular evidence of Late Archean archaea and the presence of a subsurface hydrothermal biosphere. *Proc Natl Acad Sci* 104:14260–14265
- Volk H, George SC, Dutkiewicz A, Ridley J (2005) Characterisation of fluid inclusion oil in a Mid-Proterozoic sandstone and dolerite (Roper Superbasin, Australia). *Chem Geol* 223:109–135
- Volkman JK (2005) Sterols and other triterpenoids: source specificity and evolution of biosynthetic pathways. *Org Geochem* 36:139–159
- Volkman JK (2006) Lipid markers for marine organic matter. In: Volkman JK (ed) *The handbook of environmental chemistry, Vol 2: Reactions and processes, Part N, Marine organic matter: biomarkers, isotopes and DNA*. Springer, Berlin, pp 27–70
- Volkman JK (2014) Acyclic isoprenoid biomarkers and evolution of biosynthetic pathways in green microalgae of the genus *Botryococcus*. *Org Geochem* 75:36–47
- Wacey D, McLoughlin N, Whitehouse MJ, Kilburn MR (2010) Two coexisting sulfur metabolisms in a ca. 3400 Ma sandstone. *Geology* 38:1115–1118
- Wacey D, Kilburn MR, Saunders M, Cliff J, Brasier MD (2011) Microfossils of sulphur-metabolizing cells in 3.4-billion-year-old rocks of Western Australia. *Nat Geosci* 4:698–702
- Wacey D, Noffke N, Cliff J, Barley ME, Farquhar J (2015) Micro-scale quadruple sulfur isotope analysis of pyrite from the ~3480 Ma Dresser formation: new insights into sulfur cycling on the early Earth. *Precambrian Res* 258:24–35
- Waldbauer JR, Sherman LS, Summer DY, Summons RE (2009a) Late Archean molecular fossils from the Transvaal Supergroup record the antiquity of microbial diversity and aerobiosis. *Precambrian Res* 169:28–47
- Waldbauer JR, Newman DK, Summons RE (2009b) Microaerobic steroid biosynthesis and the molecular fossil record of Archean life. *Proc Natl Acad Sci* 108:13409–13414
- Wallace MW, Hood AS, Woon EMS, Hoffmann K-H, Reed CP (2014) Enigmatic chambered structures in Cryogenian reefs: the oldest sponge-grade organisms? *Precambrian Res* 255:109–123
- Wang C, Visscher H (2007) Abundance anomalies of aromatic biomarkers in the Permian-Triassic boundary section at Meishan, China – evidence of end-Permian terrestrial ecosystem collapse. *Palaeogeogr Palaeoclimatol Palaeoecol* 252:291–303
- Ward LM, Kirschvink JL, Fischer WW (2016) Timescales of oxygenation following the evolution of oxygenic photosynthesis. *Orig Life Evol Biosph* 46:51–65
- Waters ER (2003) Molecular adaptation and the origin of land plants. *Mol Phylogenet Evol* 29:456–463
- Wei JH, Yin X, Welander PV (2016) Sterol synthesis in diverse bacteria. *Front Microbiol* 7:990
- Weiss MC, Sousa FL, Mrnjavac N, Neukirchen S, Roettger M, Nelson-Sathi S, Martin WF (2016) The physiology and habitat of the last universal common ancestor. *Nat Microbiol* 1:16116
- Welander PV, Summons RE (2012) Discovery, taxonomic distribution, and phenotypic characterization of a gene required for 3-methylhopanoid production. *Proc Natl Acad Sci* 109:12905–12910

- Welander PV, Coleman ML, Sessions AL, Summons RE, Newman DK (2010) Identification of a methylase required for 2-methylhopanoid production and implications for the interpretation of sedimentary hopanes. *Proc Natl Acad Sci* 107:8537–8542
- Wellman CH, Osterloff PL, Mohiuddin U (2003) Fragments of the earliest land plants. *Nature* 425:282–285
- Westall F, Folk RL (2003) Exogenous carbonaceous microstructures in Early Archaean cherts and BIFs from the Isua Greenstone Belt: implications for the search for life in ancient rocks. *Precambrian Res* 126:313–330
- Whiteside JH, Grice K (2016) Biomarker records associated with mass extinction events. *Annu Rev Earth Planet Sci* 44:581–612
- Willerslev E, Hansen AJ, Binladen J, Brand TB, Gilbert MTP, Shapiro B, Bunce M, Wiuf C, Gilichinsky DA, Cooper A (2003) Diverse plant and animal genetic records from Holocene and Pleistocene sediments. *Science* 300:791–795
- Willerslev E, Cappellini E, Boomsma W, Nielsen R, Hebsgaard MB, Brand TB, Hofreiter M, Bunce M, Poinar HN, Dahl-Jensen D, Johnsen S, Steffensen JP, Bennike O, Schwenninger J-L, Nathan R, Armitage S, de Hoog C-J, Alfimov V, Christl M, Beer J, Muscheler R, Barker J, Sharp M, Penkman KEH, Haile J, Taberlet P, Gilbert MTP, Casoli A, Campani E, Collins MJ (2007) Ancient biomolecules from deep ice cores reveal a forested southern Greenland. *Science* 317:111–114
- Williams TA, Foster PG, Cox CJ, Embley TM (2013) An archaeal origin of eukaryotes supports only two primary domains of life. *Nature* 504:231–236
- Woese CR, Kandler O, Wheelis ML (1990) Towards a natural system of organisms: proposal for the domains Archaea, Bacteria, and Eucarya. *Proc Natl Acad Sci U S A* 87:4576–4579
- Xie SC, Pancost RD, Yin HF, Wang HM, Evershed RP (2005) Two episodes of microbial change coupled with Permo/Triassic faunal mass extinction. *Nature* 434:494–497
- Xiong J, Fischer WM, Inoue K, Nakahara M, Bauer CE (2000) Molecular evidence for the early evolution of photosynthesis. *Science* 289:1724–1730
- Zhang S, Moldowan JM, Li M, Bian L, Zhang B, Wang F (2002) The abnormal distribution of the molecular fossils in the pre-Cambrian and Cambrian: its biological significance. *Sci China Ser D* 45:193–200
- Zhu S, Zhu M, Knoll AH, Yin Z, Zhao F, Sun S, Qu Y, Shi M, Liu H (2016) Decimetre-scale multicellular eukaryotes from the 1.56-billion-year-old Gaoyuzhuang formation in North China. *Nature Commun* 7:11500
- Zinniker D (2005) New insights into molecular fossils : the fate of terpenoids and the origin of gem-dialkylalkanes in the geological environment. PhD. dissertation, Stanford Univ: 321 pp.



Phospholipids as Life Markers in Geological Habitats 16

Kai Mangelsdorf, Cornelia Karger, and Klaus-G. Zink

Contents

1	Introduction	446
2	The Life Marker Concept	447
3	Methods	451
3.1	Lipid Extraction	451
3.2	Extract Column Fractionation	451
3.3	Detection of Phospholipids Using HPLC-MS	452
3.4	Detection of Phospholipid Fatty Acids (PLFAs) and Phospholipid Ethers (PLELs) Using GC-MS	455
3.5	Determination of Phospholipid Fatty Acid Structures	455
4	Applications of Phospholipid Biomarkers in Geoscience Research	457
4.1	Presence and Abundance of Microbial Life in Natural Habitats	457
4.2	Taxonomic Information from PLFAs	460
4.3	Membrane Adaptation to Environmental Conditions	461
4.4	Monitoring of Microbial Life Over Time and Space	465
5	Research Needs	466
	References	467

Abstract

Microbial life plays a significant role not only in the biological surface but also in the geological subsurface carbon cycle as indicated by the widespread findings of microbial communities (deep biosphere) in the deep underground. Thereby, microorganisms occupy a wide range of different habitats determined by moderate to extreme environmental conditions. Suitable analytical tools are required to assess the presence, spatial distribution, abundance, and composition of microbial

K. Mangelsdorf (✉) · C. Karger · K.-G. Zink
GFZ German Research Centre for Geosciences – Helmholtz Centre Potsdam, Organic
Geochemistry, Potsdam, Germany
e-mail: K.Mangelsdorf@gfz-potsdam.de; cornelia.karger@gfz-potsdam.de; k.g.zink@gmx.de

© Springer Nature Switzerland AG 2020

H. Wilkes (ed.), *Hydrocarbons, Oils and Lipids: Diversity, Origin, Chemistry and Fate*,
Handbook of Hydrocarbon and Lipid Microbiology,
https://doi.org/10.1007/978-3-319-90569-3_12

445

life in the many different natural environments on Earth, to understand the response and survival strategies of microorganisms to various environmental living conditions, and to unravel the role of microbial communities on the global biogeochemical cycles in natural habitats. From a biogeochemical perspective, such a tool is provided by microbial biomolecules such as phospholipids (PL) representing a significant part of microbial cell membranes. With their polar head groups and long hydrophobic side chains, they form the basic module of the membrane structure. PLs and especially phospholipid esters not only indicate the occurrence of microbial biomass but also the presence of living microorganisms, since they are only stable in viable microorganisms over longer periods of time. Therefore, PLs are also named microbial life markers. PLs can be used to quantify microbial life, to illustrate its spatial distribution, to provide taxonomic information at least on a broad level, and to assess microbial adaptation and carbon transformation processes. In this chapter we will present basic information on the utilization of phospholipids as life markers, will report on analytical methods to measure these biomolecules and elucidate their structures, and will provide examples for the application of these biomarkers in a geoscientific context.

1 Introduction

Microbial life seems to exist everywhere on Earth, not only on the land surface, in soils, and in the aquatic systems but also in the deep subsurface and even in the air (Al-Dagal et al. 2009; Parkes et al. 2014; Pedersen 2000). In recent decades microbial communities have been found in many habitats thought for long to represent hostile environments such as polar and desert regions, localities with extreme pH or salinity, as well as high temperature, pressure, or radiation conditions (Rothschild and Mancinelli 2001). The findings of microbial life in those, from an anthropogenic perspective, extreme environments made Kerr (1997) to state that “it seems that wherever a source of energy exists, life is present. And although there are obvious limits to what life can endure, they are turning out to be far less restrictive than once assumed.”

Due to its ubiquity, microbial communities are an integrated part of the life cycle on Earth, and their numbers are assessed to $11.7\text{--}34.2 \times 10^{29}$ cells (Kallmeyer et al. 2012; Parkes et al. 2014; Whitman et al. 1998) with a total biomass of $54.3\text{--}247.3 \times 10^{15}$ g (Kallmeyer et al. 2012; Whitman et al. 1998) which approximately equals up to half of the remaining biosphere biomass with 560×10^{15} g. This demonstrates that microbial communities play an important role in the carbon cycling on Earth. With the widespread discovery of microbial life in the deep marine and terrestrial subsurface during the last three decades (Parkes et al. 1994, 2000; Pedersen 1997, 2000), the research on microbial communities was brought into a geological context and became a hot topic in modern geosciences (D’Hondt et al. 2007). Up to now deep microbial life has been found down to 2800 m in deep terrestrial gold mines (Lin et al. 2006), in approximately 2500 m deep lignite coal layers nowadays overlain by marine sediments (Inagaki et al. 2015) and in 1922 m deep marine sediments (Ciobanu et al. 2014). Current estimates of cell numbers for

the deep biosphere suggest $2.9\text{--}5.4 \times 10^{29}$ cells in the marine (Kallmeyer et al. 2012; Parkes et al. 2014) and $2.5\text{--}25 \times 10^{29}$ cells in the terrestrial sedimentary subsurface (Whitman et al. 1998). Thus, although microbial life significantly decreases with sedimentary depth (Parkes et al. 2014), the deep biosphere makes up the largest pool of microorganisms on our planet. To investigate microbial life in the many different environments on Earth, it became mandatory to obtain a tool to distinguish between living and fossil/ancient microbial signals. From a biogeochemical perspective, such a tool is provided by intact polar lipids (IPLs) forming an integrated part of living microbial cell membranes (Frostegard and Bååth 1996; Harvey et al. 1986; Rütters 2001; Sturt et al. 2004; White et al. 1979; Zink et al. 2003).

2 The Life Marker Concept

A microbial life marker is a biomolecule which indicates by its intact molecular structure that it derives from a living microorganism. An essential prerequisite is that appropriate biomolecules should only be stable in living microorganisms and should rapidly degrade after cell death (Harvey et al. 1986; Logemann et al. 2011; White et al. 1979). Thus, their detection is a clear evidence for the presence of living microorganisms in a given habitat. Furthermore, the respective life marker should make up an abundant part of the cell to ensure its detectability with state-of-the-art analytical methods. Such biomarkers are given by intact polar lipids from microbial cell membranes.

Especially, phospholipids (PLs) with ca 5% of cell dry weight (Madigan et al. 1999) are considered to represent living biomass (White et al. 1979). PLs consist of a glycerol backbone linked to a polar (hydrophilic) phosphatidyl head group and two long hydrophobic aliphatic side chains (Fig. 1). In *Bacteria* these side chains generally are ester-linked long chain fatty acids (diacylglycerols, DAG) (Fig. 2), although some bacteria, e.g., some sulfate reducers, can also contain two non-isoprenoid ether side chains (dietherglycerol, DEG) or combinations between ester and ether (acyletherglycerols, AEG) (Rütters et al. 2001) or enol ether side chains (plasmalogens) (Nagan and Zoeller 2001). The chain length of the fatty acid side chains is variable and mainly ranges between 12 and 20 but can be up to 26 carbon atoms with a maximum normally at C₁₆ or C₁₈. Additionally, the fatty acid side chain can contain terminal branches (*iso*- and *anteiso*-branches); mid chain branches; hydroxy and methoxy groups; cyclopropyl, cyclopentyl, cyclohexyl, and cycloheptyl rings; ladderane ring structures; and different numbers of double bonds at various positions (Kaneda 1991; Sinninghe Damsté et al. 2002). In contrast, in *Archaea* side chains are ether-linked isoprenoid alcohols. The isoprenoid side chains are usually less variable consisting of 20 carbon atoms (phytanyl side chains; Figs. 1 and 2). Thus, the archaeal core lipid (without head group) is formed by archaeol. However, archaeal side chains can also contain hydroxy groups, unsaturations, and cyclopentyl rings or can be terminally linked to form a macrocyclic archaeol moiety (Koga and Morii 2005). In certain cases, such as halophilic archaea, the isoprenoid side chains can also consist of 25 carbon atoms (sesterterpanyl side chain) (Dawson et al. 2012).

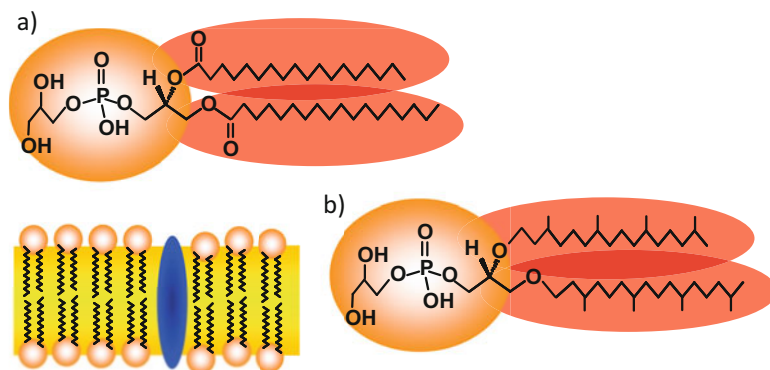


Fig. 1 Intact phospholipids: (a) phosphatidylglycerol diester and (b) diether representing life markers for bacteria and archaea, respectively, and schematic bilayer cell membrane. The blue ellipse illustrates a membrane spanning protein

The most common phospholipid head groups are phosphatidyl glycerol (PG), phosphatidyl ethanolamine (PE), phosphatidyl choline (PC), phosphatidic acid (PA), phosphatidyl serine (PS), phosphatidyl inositol (PI), diphosphatidyl glycerol (DPG), and phospho-glycolipids (Sturt et al. 2004) (Fig. 2). Phospholipid diesters or diethers form bilayers within the cell membrane, in which the hydrophobic side chains are directed to each other forming the core of the membrane and the polar head groups are directed to the interior and exterior of the cell (Fig. 1).

Archaea and some specific bacteria (Schouten et al. 2013) can also contain membrane-spanning tetraether lipids with a phosphatidyl or glycosyl head group forming a monolayer membrane (Gambacorta et al. 1995; Koga and Morii 2005). Other membrane lipids can be glycolipids with a glycosidic group directly linked to the glycerol backbone or, for instance, sphingolipids with sphingosine instead of the glycerol backbone (Olsen and Jantzen 2001). A compilation of further prokaryotic and eukaryotic membrane lipids is provided in Fig. 3. However, all these components will not be discussed here.

PLs have widely been used as life markers in geosciences in recent years (Lipp et al. 2008; Rütters 2001; Sturt et al. 2004; Zink et al. 2003). This application is mainly based on the experimental outcome that PLs rapidly degrade after cell death (Harvey et al. 1986; White et al. 1979). Harvey et al. (1986) already showed that an ester-linked phospholipid was much more rapidly degraded than a glycosidic diphytanyl glycerol diether lipid. This already suggests a higher stability of membrane lipids with ether-bound side chains. Logemann et al. (2011) confirmed this with a wider range of phospholipid esters with different head groups in comparison to different diphytanyl glycerol diethers. They also showed that diphytanyl glycerol diether lipids with phosphatidyl head groups show approximately the same degradation rates than those with a glycosidic head group directly linked to the glycerol backbone. This suggests that different head group compositions seem to have only minor effect on the lipid stability and that the side chain bonding is the crucial stability factor.

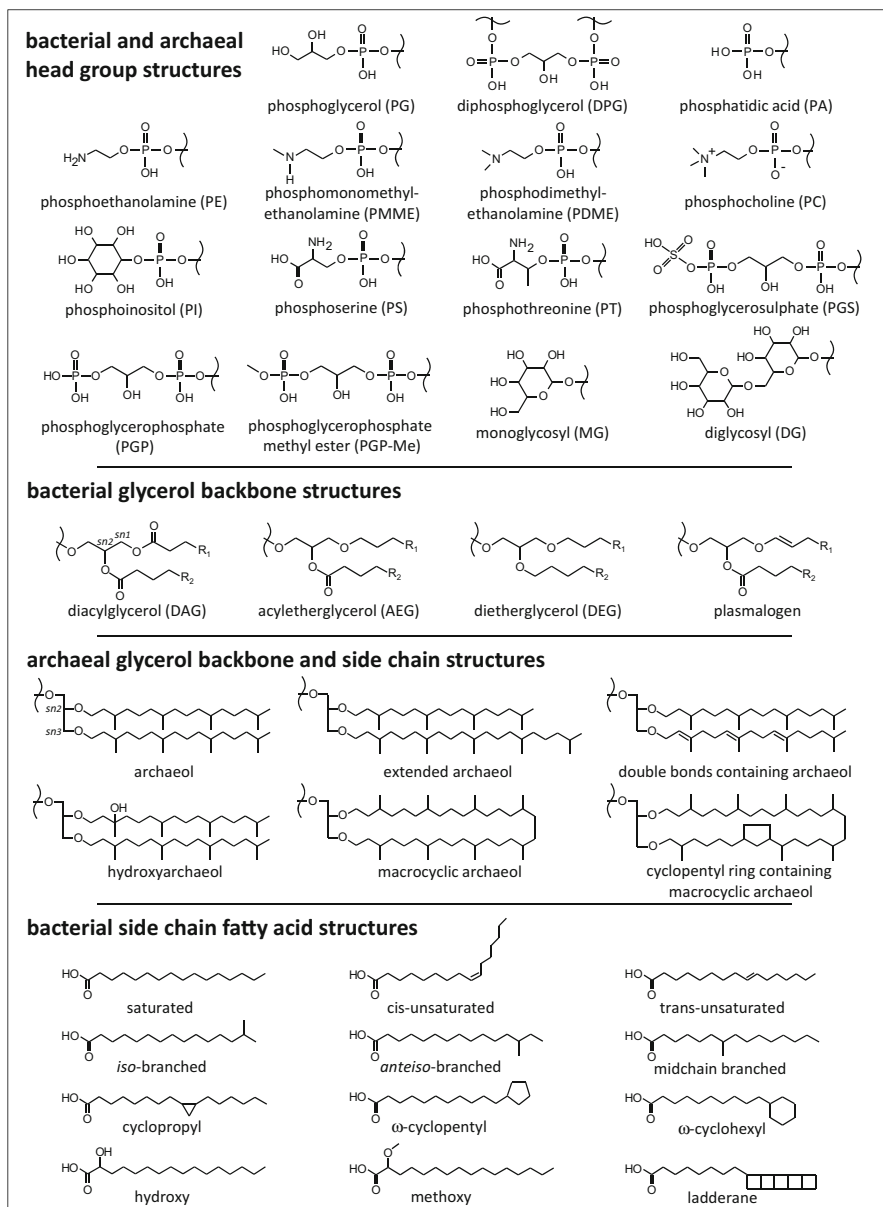


Fig. 2 Compilation of different bacterial and archaeal phospholipid head group, backbone, and side chain structures

Thus, in contrast to the bacterial ester-linked PLs, archaeal ether-linked PLs have due to their higher stability only a restricted potential to act as life markers for archaea, and their application in sedimentary succession has to be made at least with

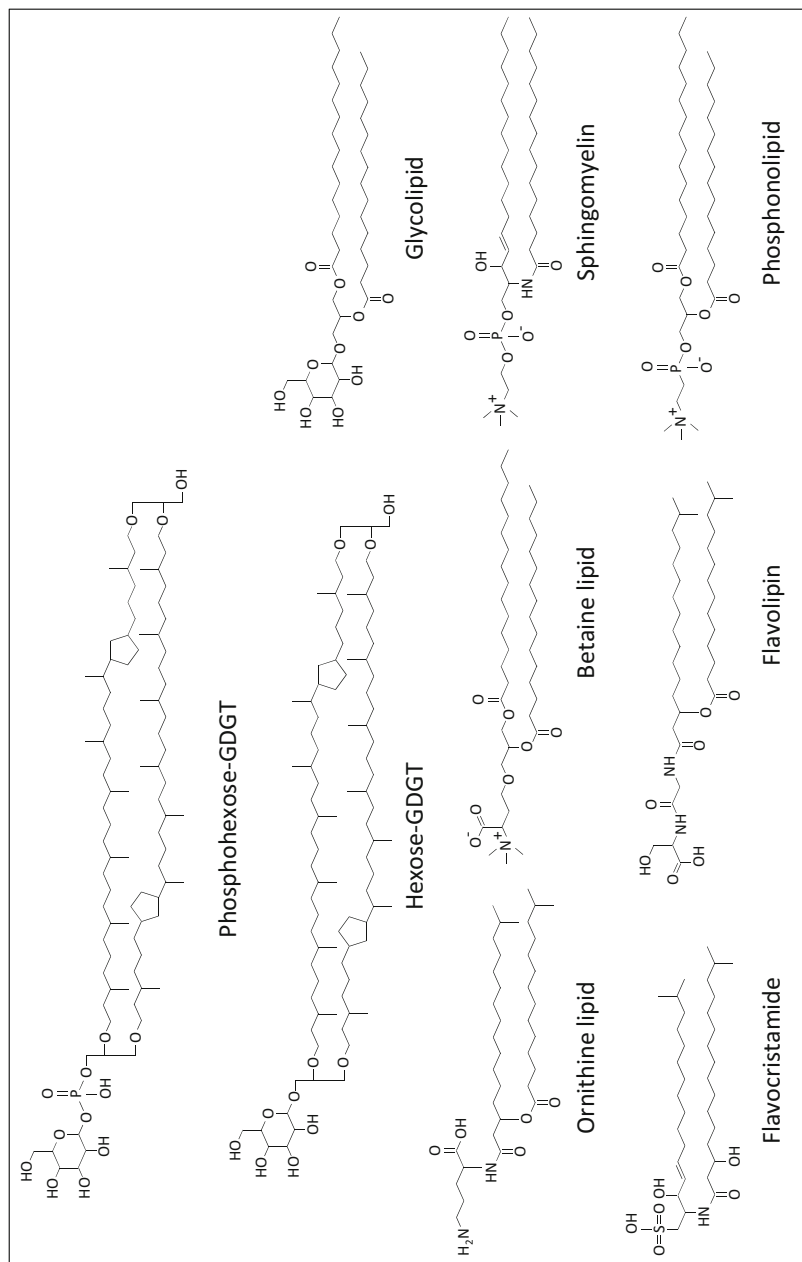


Fig. 3 Compilation of some additional membrane lipid structures

caution (Logemann et al. 2011). In addition to these structural considerations, Harvey et al. (1986) presented indications that the oxygen and organic matter content in sediments also affects the degradation of membrane lipids.

3 Methods

3.1 Lipid Extraction

In literature a series of in principal similar analytical methods are available to investigate prokaryotic cell membrane phospholipid compositions in sediments, water samples, and microbial cultures (Gruner et al. 2017; Heinzelmann et al. 2014; Ringelberg et al. 1997; Rütters et al. 2002; Sturt et al. 2004; Zink and Mangelsdorf 2004). Basically, PLs are extracted with organic solvents from the sample material. Usually, an extraction method modified after Bligh and Dyer (1959) is used. Here the sample material (sediments, cultures, or filters from water filtration) is extracted by a solvent mixture of methanol, dichloromethane, and buffer (e.g., ammonium acetate buffer, 10 mM, pH 7.4–7.6) in a ratio of 2:1:0.8 (v/v). In this ratio the three solvents form one phase, and extraction is conducted with sonication (Rütters et al. 2002; Sturt et al. 2004) or flow blending (Zink and Mangelsdorf 2004). In case of sediment extraction, the residual sample material is removed by centrifugation or filtration. For subsequent quantification of lipids, internal standards, e.g., deuterated PLs, might be added. This is also useful to consider compound losses during sample treatment. Afterwards, further dichloromethane and buffer are added to the solvent mixture to achieve a final ratio of 1:1:0.9 (v/v). In this ratio the water phase becomes separated from the organic phase. The water phase is re-extracted two times with dichloromethane, and the organic phases are combined and evaporated to dryness.

3.2 Extract Column Fractionation

To reduce the extract complexity, total extracts are usually separated into fractions of different polarity. In sediments and water samples, it is especially important to separate the free fatty acids representing dead biomass from phospholipid fatty acids (PLFAs) obtained later after saponification representing living biomass. Different column material and applied solvents can lead into different fraction cuts (Gruner et al. 2017; Heinzelmann et al. 2014; Ringelberg et al. 1997; Rütters et al. 2002; Sturt et al. 2004; Zink and Mangelsdorf 2004). However, most common methods provide (i) a neutral polar fraction including the free fatty acids, (ii) a glycolipid fraction, and (iii) a phospholipid fraction. Heinzelmann et al. (2014) claimed that glycolipids might partly also end up in the phospholipid fraction leading to the presence of glycolipid fatty acids in the PLFA inventory after saponification. Thus, if glycolipids are present in the sample, they advise to combine both fractions to obtain a polar fraction containing all intact polar lipids.

3.3 Detection of Phospholipids Using HPLC-MS

PLs cannot be transferred into the gas phase without decay. Thus, the measuring system of choice for PLs is high-performance liquid chromatography-electrospray ionization-mass spectrometry (HPLC-ESI-MS) (Fang and Barcelona 1998; Rütters et al. 2002), although also other interfaces are partly applied such as matrix-assisted laser desorption/ionization (MALDI) (Pulfer and Murphy 2003). There are many HPLC-MS methods available (Heinzelmann et al. 2014; Rütters et al. 2002; Stapel et al. 2016; Sturt et al. 2004).

Normal phase chromatography with pure and diol-modified silica gel is usually applied to detect intact phospholipids, since this allows the separation of the phospholipids by their different head groups (Rütters et al. 2002; Zink and Mangelsdorf 2004). As an example the chromatogram of a standard mixture is shown in Fig. 4. In addition to normal phase chromatography, methods using reversed phase chromatography allowing separation by different side chain structures (Lanekoff and Karlsson 2010) and hydrophilic interaction chromatography (HILIC) also separating phospholipids by their head groups are available (Wörmer et al. 2013).

The ESI interface represents a soft ionization technique. In the negative ion mode, a proton is removed from the target molecule generating a negatively charged molecular ion $(M-H)^-$. In contrast in the positive ion mode, a proton is transferred to the molecule creating a positively charged molecular ion $(M+H)^+$ (Zink and Mangelsdorf 2004). Depending on their chemical structure, most of the phospholipids are better ionized in the negative ion mode, since a proton can easily be cleaved off from the phosphate group (Fig. 4a). In contrast phosphatidylcholines forming a permanent zwitterion with a positively charged quaternary nitrogen atom and a negatively charged phosphate group (Fig. 2) are better ionized in the positive ion mode (Fig. 4b), because the phosphate group can easily be protonated (Pulfer and Murphy 2003; Zink and Mangelsdorf 2004). Due to the soft ionization technique, the HPLC-ESI-MS mass spectra usually only consist of the phospholipid molecular ions ($\pm H$).

The purpose of the HPLC system prior to the ESI-MS detection is to separate the PLs by their different head groups. However, also functional groups (e.g., hydroxy groups) attached to the side chains can lead to additional chromatographic separation (Fig. 5a). In natural samples one peak in the HPLC-MS chromatogram is composed of a series of PLs with an equal head group but different fatty acid side chain compositions (Fig. 5b). The fatty acyl groups usually can differ in chain length, number of unsaturation, rings, or branches (Rütters et al. 2002; Sturt et al. 2004; Zink and Mangelsdorf 2004).

For structural elucidation of individual PL esters concerning their linked fatty acyl side chains, collision-induced decomposition (CID) (or collision-activated dissociation, CAD) MS/MS experiments can be applied (Pulfer and Murphy 2003) using specific mass spectrometers such as a triple quadrupole and ion trap or orbitrap mass spectrometer. In the CID mode, molecular ion masses of individual phospholipids are selected and decomposed in a collision experiment with a collision gas

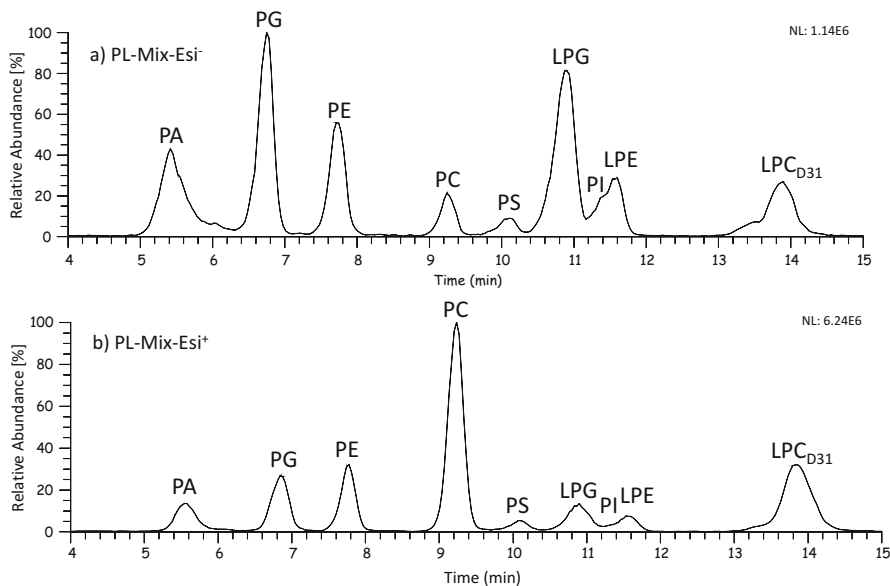


Fig. 4 Chromatograms of a standard mixture of phospholipid diesters measured (a) in negative and (b) in positive ion mode. For lipid abbreviations see head group structures in Fig. 2. Lx = lyso phospholipids (loss of side chain fatty acid in the *sn*2-position). LPC_{D31} = deuterated 1-hexadecanoyl-lyso-phosphatidylcholine

yielding the molecular ions of the linked fatty acids and to a smaller extent also head group and lyso-phospholipid (loss of one fatty acid side chain) fragments (Mangelsdorf et al. 2005b) (Fig. 5c). The CID experiments allow to link specific fatty acid combinations to individual phospholipid groups defined by their head groups (Mangelsdorf et al. 2005b) (Fig. 5b). For more structural information on the fatty acids beyond the molecular mass, a detailed analysis after phospholipid saponification is necessary (see below). With an ion trap mass spectrometer, also MSⁿ experiments can be conducted. Here a fragment from a prior CID experiment can be selected for further dissociation experiments to get deeper information on individual fragment structures (Jahn et al. 2004). The ether side chains from phospholipid ethers cannot be cleaved by MS/MS experiments; however information about the head group moieties can be obtained (Jahn et al. 2004).

Quantification of intact PLs is possible via the addition of an internal standard, e.g., deuterated PL. Deuterated PLs can also be used as internal standard for quantification of PLFAs. Intact PLs with different head groups show different response behavior during the ESI-MS detection. To overcome this problem, response factors have to be determined for the PLs with different head groups relative to the internal standard for the specific HPLC-ESI-MS system using a phospholipid standard mixture with equal and known concentrations (Mangelsdorf et al. 2005b; Zink et al. 2008). Furthermore, at low microbial abundance in sample material with relatively high organic background, the detection of intact PLs is impeded due to

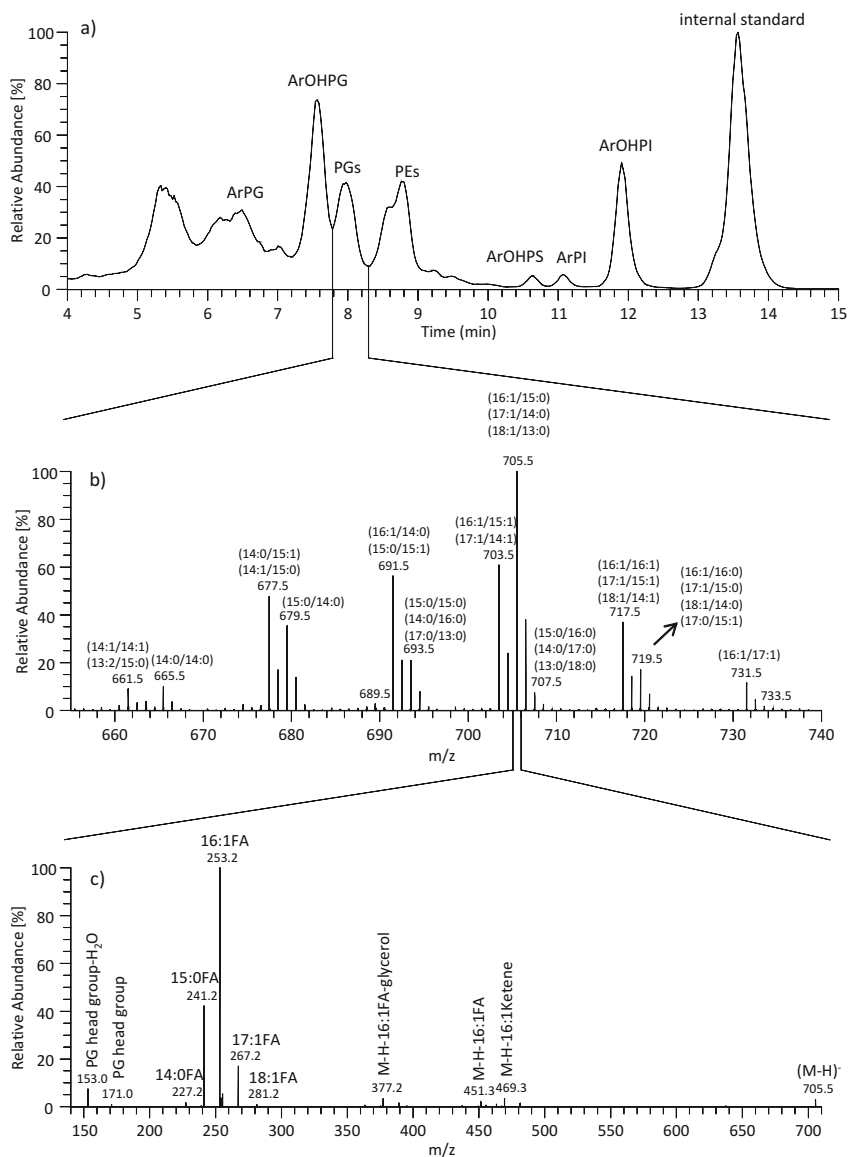


Fig. 5 (a) Chromatogram from an HPLC-ESI-MS run (negative ion mode) of a seafloor sample from the Barents Sea containing intact bacterial (PGs and PEs) and archaeal (ArPG, ArOHPG, ArOHPS, ArPI, and ArOHPI) membrane lipids. (b) Mass range of PG molecular ions ($M-H$)⁻ differing by different fatty acid chain length and number of double bonds. (c) Collision-induced decomposition (CID) MS-MS experiment of the PG molecular ion m/z 705 showing that this signal is composed of different PGs with different fatty acid side chain combinations. *PG* phosphatidyl glycerol, *PE* phosphatidyl ethanolamine, *ArPG* archaeal phosphatidyl glycerol, *ArOHPG* hydroxyarchaeal phosphatidyl glycerol, *ArOHPS* archaeal phosphatidyl serine, *ArPI* archaeal phosphatidyl inositol, *ArOHPI* hydroxyarchaeal phosphatidyl inositol, *FA* fatty acid

matrix-induced ion suppression in the ESI interface (Mallet et al. 2004). This can have severe impact on the quantification of bacterial biomass in natural samples. Thus, quantification of bacteria via the phospholipid-derived fatty acids (PLFAs) might often be a preferable procedure to assess bacterial abundance (see below).

3.4 Detection of Phospholipid Fatty Acids (PLFAs) and Phospholipid Ethers (PLELs) Using GC-MS

A common procedure to detect and quantify PLs is the measurement of their fatty acid side chains (PLFA) using gas chromatography-mass spectrometry (GC-MS). For this purpose the PLs should have been separated from the free fatty acid fraction using column fractionation before they are chemically cleaved by a saponification reaction. Mueller et al. (1990) provided an easy-to-conduct procedure for the transesterification of PLs to directly obtain the methylated formerly phospholipid-linked fatty acids. However, there are also other methods available to perform PL saponification (Mills et al. 2006; White et al. 1979). PLFAs are also used to quantify bacterial abundances relative to an internal standard (Frostegard and Bååth 1996; Mancuso et al. 1990; Zink et al. 2008). Since PLs represent an important part of the microbial cell membranes, they can provide a measure for viable cell numbers. In literature conversion factors are available, which roughly allow to transfer the amount of PLFAs per gram sediment into cell biomass. For instance, Balkwill et al. (1988) determined that 350 pmol PLFA/g sediment correspond to ca. 7×10^6 cells/g sediment, which results into 20,000 cells/pmol PLFA. A comparison of bacterial cell biomass determined from intact PLs and PLFAs is provided in Zink et al. (2008).

Analogous to the phospholipid esters, also the phospholipid ethers can be cleaved by an ether cleavage procedure to obtain the former ether side chains (PLEL). The common way is to cleave the ethers with hydriodic acid to generate the respective isoprenoid iodides. Subsequently, the halogenated isoprenoids are reduced with zinc to obtain the corresponding isoprenoid hydrocarbons, e.g., phytane (Gattinger et al. 2003).

3.5 Determination of Phospholipid Fatty Acid Structures

PLFAs can contain taxonomic information of their source organisms (Table 1). Therefore, a detailed structural elucidation of the PLFAs is crucial. Fatty acids are a well-investigated compound class with manifold information on mass spectra available (Christie 1999). Most fatty acids can be identified by their mass spectrum. Saturated straight chain or *iso*- and *anteiso*-branched fatty acids are usually easy to identify by their GC elution behavior. In contrast, the determination of double bond positions in unsaturated fatty acids is not always straightforward. Chemical experiments can be conducted to unravel double bond positions in the acyl chains (Fig. 6). Derivatization techniques such as reactions with dimethyl disulfide (DMDS)

Table 1 Phospholipid fatty acids and their potential taxonomic origin. X:Y = carbon number/number of double bonds; *iso* = methyl branch at carbon atom 2 counted from the tail end; *anteiso* = methyl branch at carbon atom 3 counted from the tail end; SFA = saturated fatty acids; MUFA = monounsaturated fatty acids; β -OH-FA = 3-hydroxy fatty acids; cy = cyclopropyl ring; ω X = double bond in position X counted from the tail end; XMe = methyl branch in position X counted from the functional group; GNB = Gram-negative bacteria; GPB = Gram-positive bacteria; SRB = sulfate-reducing bacteria; AOM = anaerobic oxidation of methane; Anammox = anaerobic ammonium oxidation

Phospholipid fatty acids	Potential origin	References
SFA (<i>n</i> -C ₁₄ -C ₂₀)	All organisms	Harwood and Russell (1984), Vestal and White (1989), Yeagle (2016)
Long-chain SFA (<i>n</i> -C ₂₀ -C ₂₆)	All organisms	Lipp and Hinrichs (2009), Yeagle (2016)
MUFA	GNB	Zelles (1997)
<i>Iso</i> - and <i>anteiso</i> C ₁₄ -C ₁₇	GPB, SRB	Harwood and Russell (1984), Parkes and Taylor (1983), Vestal and White (1989), Yeagle (2016)
β -OH-FA	GNB, occur also in other bacterial genera	Zelles (1997)
13:0	<i>Cellulomonas</i> spp.	Harwood and Russell (1984)
cy15:0	GNB (<i>Escherichia coli</i>), <i>Clostridia</i>	Vestal and White (1989), Yeagle (2016)
16:1 ω 7cis	Aerobic bacteria, barophilic bacteria	Fang et al. (2002), Parkes and Taylor (1983), Rajendran et al. (1997), Vestal and White (1989)
16:1 ω 9cis	Aerobic bacteria, SRB	Rajendran et al. (1997), Vestal and White (1989)
16:1 ω 8	Methanotrophic bacteria	Fang et al. (2000), Frostegård et al. (2011)
cy17:0	Anaerobic bacteria, certain methylotrophs (<i>Agrobacterium tumefaciens</i>), many bacterial genera	Guckert et al. (1991), Vestal and White (1989), Zelles (1997)
17:1 ω 8, iso17:1 ω 7, br17:1	SRB, anaerobic bacteria	Parkes and Taylor (1983), Rajendran et al. (1997), Vestal and White (1989)
cy17:0 ω 5,6, 16:1 ω 5cis	SRB (<i>Desulfosarcina/Desulfococcus</i> species) related to AOM	Elvert et al. (2003)
<i>Iso</i> - and <i>anteiso</i> -17:2 ω 3,7	<i>Chryseobacterium</i>	Bajerski et al. (2017), Mangelsdorf et al. (2017)
10Me18:0 and 10Me16:0	Actinomycetes	Butler et al. (2003), Vestal and White (1989), Zhang et al. (2007)
12Me16:0	<i>Rubrobacter</i>	Suzuki et al. (1988)
18:1 ω 7cis	Aerobic eubacteria, <i>Proteobacteria</i>	Guckert et al. (1991), Parkes and Taylor (1983), Zelles (1997)

(continued)

Table 1 (continued)

Phospholipid fatty acids	Potential origin	References
cy19:0	Anaerobic bacteria, eubacteria (<i>Agrobacterium tumefaciens</i>), occur in many bacterial genera	Guckert et al. (1991), Vestal and White (1989), Zelles (1997)
20:5	Marine algae, barophilic and psychrophilic bacteria	Fang et al. (2002), Vestal and White (1989), Yeagle (2016)
22:6	Marine algae, human erythrocytes, barophilic and psychrophilic bacteria	(Fang et al. 2002; Vestal and White 1989; Yeagle 2016)
Ladderane	Anammox bacteria (<i>Planctomycetales</i>)	Kuypers et al. (2003), Sinninghe Damsté et al. (2002)
ω -Cyclohexyl FA	Acidophilic thermophilic bacteria, <i>Curtobacterium pusillum</i>	Oshima and Ariga (1975), Suzuki et al. (1981)

(Dunkelblum et al. 1985) and osmium tetroxide (Rontani 1998) directly mark the double bonds (Fig. 6b and c). Subsequent GC-MS measurement leads to fragmentation directly at the former double bond location with the resulting fragments being indicative for the double bond position in the side chain. Other techniques such as 4,4-dimethyl oxazoline (DMOX) (Laurent and Richli 1991) and 3-pyridylcarbinol (Destailats and Angers 2002) derivatization lead to reaction with the PLFA functional carboxyl group (Fig. 6b and e). GC-MS of these derivatives reveals individual fragments for each carbon-carbon bond. While saturated side chain sections lead to fragment ions separated by 14 mass units, double bonds are indicated by a step of 12 mass units. Additionally, the 3-pyridylcarbinol derivatization indicates branching positions by the lack of the respective fragment ion (Mangelsdorf et al. 2017).

4 Applications of Phospholipid Biomarkers in Geoscience Research

PLs can be used to detect and quantify microbial life in natural environments, and their carbon isotopic composition can give indication on microbial metabolic processes. They can provide taxonomic information on the associated microbial communities, can be applied to investigate membrane adaptation mechanisms of microorganisms toward changing environmental conditions, and can be used to monitor changes in the presence, abundance, and distribution of microbial communities in time series and over space (Fig. 7).

4.1 Presence and Abundance of Microbial Life in Natural Habitats

PLs are used to verify the presence and to determine the abundance of microbial life not only in, from an anthropogenic perspective, moderate but also in extreme natural

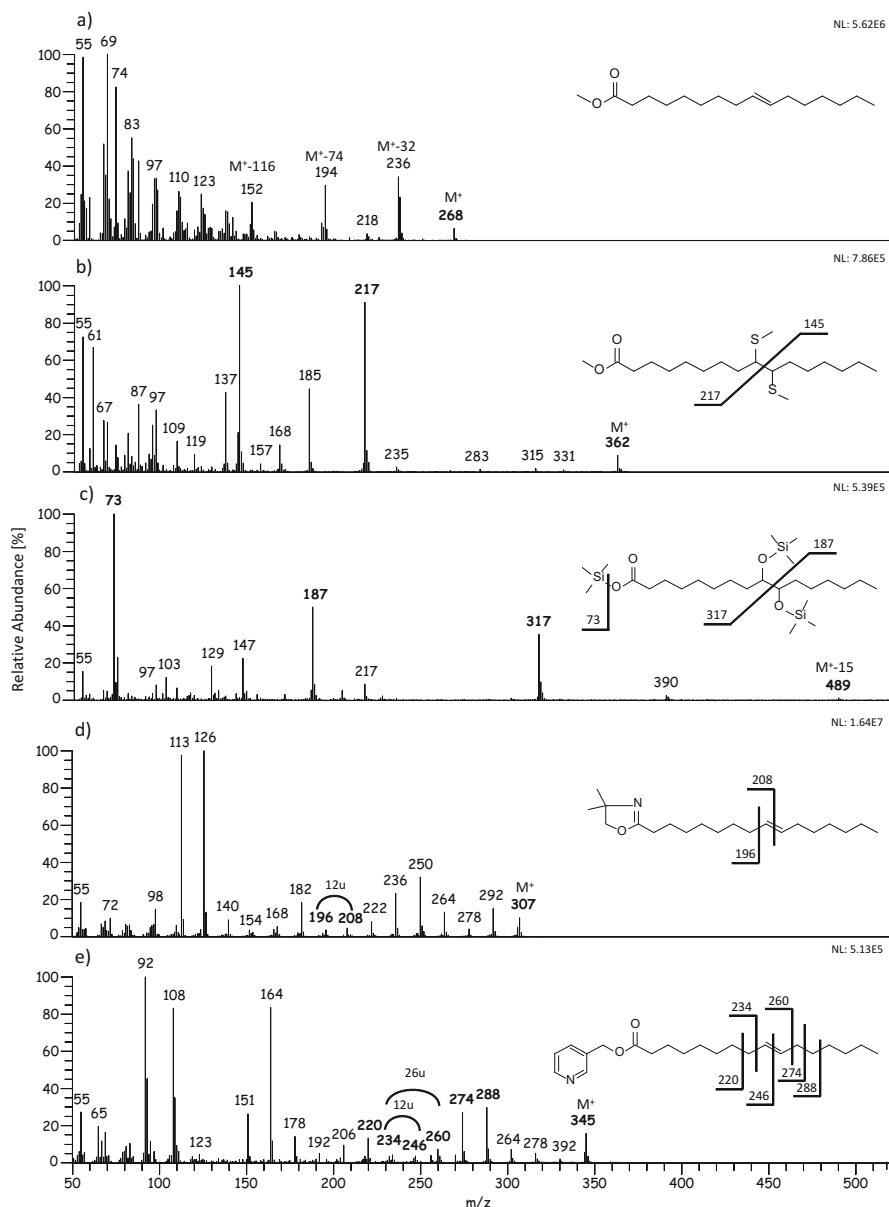


Fig. 6 Mass spectra of products formed by different derivatization techniques to determine the double bond positions of hexadec-9-enoic acid: (a) methyl ester, (b) dimethyl disulfide, (c) osmium tetroxide, (d) 4,4-dimethylloxazoline (DMOX), and (e) 3-pyridylcarbinol derivatives

habitats. Pioneering work has been conducted, for instance, by White et al. (1979) in estuarine environments, by Frostegård et al. (1993a) in soils, by Rütters et al. (2002) in Wadden Sea sediments, by Sturt et al. (2004) in surface marine sediments, and by Zink and Mangelsdorf (2004) in freshwater surface sediments, showing the

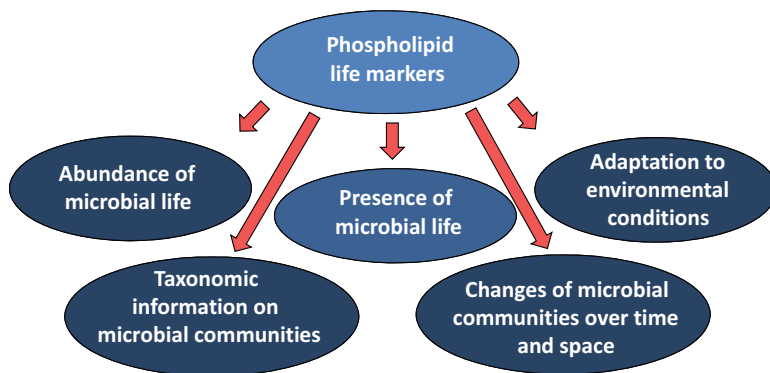


Fig. 7 Applications of the phospholipid and PLFA life marker signal in geoscientific research

applicability of phospholipid analysis to investigate microbial community structures in near surface environments. Furthermore, Zink et al. (2003) were able to indicate the presence of microbial life in deep marine sediments (deep biosphere) from the Nankai Trough offshore Japan for the first time by applying PL analysis, and Sturt et al. (2004) showed the presence of intact polar tetraether lipids in deeply buried sediments from the Peru margin. In a deep terrestrial borehole located in the Waikato Basin, New Zealand, deep microbial life associated to organic-rich lithologies was indicated by intact PLs (Fry et al. 2009; Vieth et al. 2008). Meanwhile, microbial life has been detected using intact PLs in many deep marine and terrestrial habitats (Biddle et al. 2006; Horsfield et al. 2006; Lipp and Hinrichs 2009; Lipp et al. 2008; Mangelsdorf et al. 2005a, 2011). Intact PLs were also used for quantification and characterization of bacterial and archaeal life as well as for microbial biomass assessment (Lipp and Hinrichs 2009; Lipp et al. 2008; Schubotz et al. 2009; Zink et al. 2008). However, as mentioned above due to their higher stability phospholipid, di- or tetraether lipids representing archaeal biomass have to be used with caution as life markers especially when quantitatively comparing them with the less stable bacterial phospholipid ester signal (Harvey et al. 1986; Logemann et al. 2011; Pearson 2008; Schouten et al. 2010). Life markers were also used to detect the depth distribution of microbial communities in extreme environments other than the deep biosphere. For instance, in arctic and desert environments, PL signals were used to detect the presence and depth distribution of microbial life in near-surface permafrost and salt pan deposits (Bischoff et al. 2013; Genderjahn et al. 2017; Stapel et al. 2016). PLs allow deep insight into the community structure and distribution of microbial life in those extreme and near-surface environments, and comparison with fossil microbial biomarkers provides information on past microbial communities and on associated climatic and environmental conditions (Genderjahn et al. 2018; Stapel et al. 2018). For the elucidation of the microbial community structure, it is of specific strength to combine lipid biomarker analysis with molecular microbiological methods (e.g., DNA-based approaches). Such joint research strategies allow a comprehensive evaluation of microbial communities from different scientific disciplines with their

specific analytical methods (Beulig et al. 2015; Fry et al. 2009; Orwin et al. 2018; Schulze-Makuch et al. 2018; Toffin et al. 2005).

The carbon isotope signature of PLFAs and PLELs can provide crucial information on microbial processes in a given habitat. For instance, lipid biomarkers of archaea (anaerobic methanotrophs, ANME) and bacteria (specific sulfate-reducing bacteria, SRB) associated to the anaerobic oxidation of methane (AOM) are, due to the low ^{13}C content of the methane substrate, highly depleted in ^{13}C down to $\delta^{13}\text{C}$ values less than -100% (Blumenberg et al. 2004; Boetius et al. 2000; Elvert et al. 2003; Hinrichs et al. 1999). In addition to the characterization of natural samples, lipid biomarker analysis can also be used for feeding experiments with artificially ^{13}C -labelled substrates to elucidate metabolic pathways (Boschker and Middelburg 2002).

Investigation of microbial communities in deeper sedimentary successions requires drilling of appropriate sample material. During the drilling process, the core material comes into contact with drilling fluids. Since cell numbers usually drastically decrease with increasing sediment depth (Parkes et al. 2014), core material can easily be contaminated by microbial cells from the surface brought down by the drill fluids. Although up to date contamination cannot be avoided during drilling, it can be controlled by using drill mud tracers indicating how deep the drill mud has penetrated the core material (Kallmeyer et al. 2006). Several tracers have been applied in the past such as fluorescent dyes, chemical tracers, and fluorescent microspheres (Kallmeyer 2017). The tracer allows identification of uncontaminated core material. Usually an inner coring technique is applied to remove the outer contaminated core material from the inner pristine material. However, if the tracer is also detectable in the inner core part, the whole sample has to be discarded from further analysis.

4.2 Taxonomic Information from PLFAs

Microorganisms can have specific PLFA inventories. Thus, the molecular structure of the PLFAs can provide indication on the composition of the microbial community in a given habitat (Table 1). However, since many fatty acids are shared between different microorganisms – preventing in most cases a direct link to specific microbial species – the assignment of PLFAs to microorganisms is usually on a broad taxonomic level.

For instance, saturated fatty acids are common lipids in living organisms, and they are therefore not very specific. Saturated terminally branched FAs such as *iso*- and *anteiso*-FAs with 15 and 17 carbon atoms are often discussed as markers for Gram-positive bacteria and monounsaturated FAs for Gram-negative bacteria. Specific unsaturated FAs such as 16:1 ω 7cis and 16:1 ω 9cis are reported to be markers for aerobic bacteria and 16:1 ω 8 for methanotrophic bacteria. However, with all these FAs overlaps exist. Other FAs appear to be more specific such as 10Me FAs with 16 and 18 carbon atoms showing on the order-level indication for the presence of actinomycetes. Some other FAs such as *iso*- and *ai*-17:2 ω 3,7 for *Chryseobacterium*

and 12Me16:0 for *Rubrobacter* might be quite specific even down to the genus level. Thus, PLFA analysis can be used to gain taxonomic information from the phylum sometimes down to the family and in some specific cases to the genus level (Table 1). Overall, PLFAs can provide first insights into the microbial community structure (Table 1); however, caution has to be taken while interpreting the PLFA signal, since most PLFAs provide only indication on the microbial community structure rather than a proof of the presence of specific microorganisms.

Of specific strength is to combine the taxonomic information from PLFA analysis with those from nucleic acid-based molecular microbiological approaches such as gene profiling on ribosomal ribonucleic acid (rRNA). The molecular microbiological methods provide deep and better verified information on the microbial community structure, and a complementary approach will allow to better link the PLFA signal to microbial groups or even species. With this more reliable assignment, the PLFA signals then can be used to better trace variations of microbial communities over time and space by following the occurrence, abundance, and distribution of marker PLFAs.

4.3 Membrane Adaptation to Environmental Conditions

The microbial cell membrane forms the interface of the cell to the ambient environment. Since microorganisms conduct essential metabolic processes across their membranes, it is mandatory for the cells that their membranes are always in an optimal liquid or flexible stage in response to external environmental stress factors such as temperature, pressure, pH, starvation, and salinity conditions or toxic substances (Russell 1989). A solid membrane would not allow metabolic exchange processes, and a membrane being too flexible would bear the danger of uncontrolled passing of substances or cell lysis. Microorganisms can regulate their membrane fluidity by changing the structural lipid composition. Thus, investigation of the PL inventory can be used to elucidate microbial adaptation mechanisms and can help to understand how microbial life is able to cope with variable to extreme environmental conditions.

Sinensky (1974) introduced the concept of homeoviscous adaptation, meaning that microorganisms change the cell membrane lipid inventory in order to keep the membrane fluidity and functionality despite changing ambient temperatures (see also de Mendoza 2014). Decreasing ambient temperature forces the microorganism to decrease the membrane solid to liquid phase transition temperature (melting temperature) to prevent rigidification of the membrane. To maintain the membrane melting temperature always below the ambient temperature, microorganisms are able to incorporate a higher relative proportion of *cis*-unsaturated fatty acids with usually up to two double bonds and/or fatty acids with shorter chain lengths; the melting temperature decrease is stronger upon the integration of more *cis*-unsaturated double bonds in comparison to chain shortening (Russell 1989; Suutari and Laakso 1994). In response to higher temperature, a higher proportion of saturated fatty acids and/or longer fatty acid chains are incorporated, respectively (Russell and Fukunaga 1990). For instance, Mangelsdorf et al. (2009) showed in a study in

permafrost-affected soils that microbial communities from a surface-near and a deeper permafrost-near horizon of the active layer (thawed surface interval during summer season) generally differ in the proportion of unsaturated fatty acids, with the higher proportion in the horizon close to the perennial frozen ground. However, temperature-dependent cultivation experiments with the microbial communities from these different active layer horizons showed that temperature response within the horizon was mainly regulated by the length of the fatty acid side chains. In this context, it has to be noted that when investigating complex microbial communities, it is difficult to differentiate between a direct membrane adaptation within individual microorganisms and a community shift toward better adapted species. Additional microbiological information on the microbial community structure (e.g., gene sequencing) provides improved insight into this uncertainty. In addition to the degree of unsaturation and chain length, methyl branches in the alkyl chain can also influence the melting temperature, e.g., *anteiso*-FAs show a stronger effect toward lower melting temperatures than *iso*-FAs (e.g., Kaneda 1991). Bajerski et al. (2017) showed in temperature cultivation experiments with *Chryseobacterium frigidisoli*, isolated from an Antarctic glacier forefield, a complex restructuring of the membrane lipid inventory. They observed a shift from saturated *iso*-FAs to unsaturated *iso*-FAs from 20 °C to 10 °C cultivation temperature and a shift from *iso*-FAs to more *anteiso*-FAs between 10 °C and 0 °C. Over the whole temperature range, a newly identified double unsaturated *anteiso*-FA (*ai*-17:2 ω 3,7) showed an increasing trend, becoming the most abundant FA in the 0 °C culture (Bajerski et al. 2017; Mangelsdorf et al. 2017). Furthermore, changes of the relative head group composition can have an impact (Boggs 1986), with larger and repulsive head groups (e.g., PG and PC) showing lower melting temperatures than smaller intermolecularly interacting ones (e.g., PE).

Increasing external pressure has a similar effect on the cell membrane than decreasing temperature. Higher pressure leads to a compaction and therefore rigidification of the cell membrane. As response microorganisms incorporate increasing amounts of *cis*-unsaturated fatty acids into the membrane structure, and even polyunsaturated FAs such as C_{20:5} and C_{22:6} have been observed in some piezophilic microorganisms (DeLong and Yayanos 1985; Yano et al. 1998). The reason for this is that the bended structure of the *cis*-unsaturated FAs counteracts a stronger compaction of the cell membrane. Mangelsdorf et al. (2005b) investigated the PL compositional changes during membrane adaptation of a piezosensitive bacterium from the deep biosphere (297 m below seafloor and 4791 m water depth) using cultivation experiments under different pressure conditions. Cells cultivated under high-pressure conditions showed a marked shift to more unsaturated fatty acids (Fig. 8). Furthermore, a shift from smaller PE head groups to larger and repulsive PG head groups was observed. The change toward more bulky membrane lipids represents a clear adaptation in response to increasing ambient pressure conditions.

Compared to microbial membrane adaptation in response to varying temperature and pressure conditions, adaptation mechanisms with respect to changing pH are not similarly straightforward, and literature seems to document somehow complex membrane responses (Bååth and Anderson 2003; Frostegård et al. 1993a; Männistö

et al. 2007). Bajerski et al. (2017) presented, for instance, in pH cultivation experiments with *Chryseobacterium frigidisoli*, relatively constant membrane FA compositions around neutral pH and significant changes toward the pH extremes for this microorganisms of 5.5 and 8.5. At pH 8.5 they observed a decrease of unsaturated FAs and suggested a compaction or stabilization of the cell membrane, which was partly attenuated by an additional shift to more short chain *iso*- and *anteiso*-FAs. At low pH the opposite trend was observed. Thus, they argued that pH adaptation in *Chryseobacterium frigidisoli* is a balanced interplay between membrane stabilization and enhanced flexibility to prevent or allow protons or other substances to pass the cell membrane at pH extremes.

In response to starvation phases, a shrinking of the cell volume went along with an overall loss of *cis*-monoenoic FAs and a relative increase of *trans*-monoenoic FAs as well as the occurrence of cyclopropyl-FAs. Guckert et al. (1986) proposed that the *trans/cis* ratio might be useful as a stress or starvation indicator. Similarly, Mukamolova et al. (1995), who studied biochemical changes due to starvation in cells of *Micrococcus luteus*, observed a change in membrane PL composition with an early increase of cardiolipin (DPG) to the expense of PG and a later accumulation of PA at the expense of DPG and PI. In addition, lyso-PLs occurred to 5–10% of the total PLs during the first 10 days of starvation. However, Mukamolova et al. (1995) stated that it remains open if the changed PL composition is a useful response of the bacterial cell to survive starvation or just a consequence of starvation.

Adaptation of microbial cell membranes is also relevant when conditions in the ambient environment become toxic for the respective microorganisms. Toxicity can occur due to anthropogenically induced pollutants or naturally occurring processes. This includes, for instance, enhanced petroleum hydrocarbon or heavy metal concentrations especially in soils, aquifers, or water bodies. In particular cyclic hydrocarbons such as toluene or alkylbenzenes being widespread in contaminated environments are well known for being toxic to many microorganisms as they accumulate in the cell membrane due to their lipophilic character and disturb the membrane function (Sikkema et al. 1994; Weber and de Bont 1996). On the other hand, some microbial strains are able to degrade hydrocarbons (e.g., Rabus and Widdel 1995; Widdel and Rabus 2001; Wilkes et al. 2000 and references therein), which make them particularly useful for bioremediation (Harayama et al. 1999; Pelz et al. 2001). For instance, certain microorganisms such as the denitrifying bacteria *Aromatoleum aromaticum* are able to use small aromatic hydrocarbons (e.g., toluene) as substrate or carbon source (Trautwein et al. 2008). With increasing solvent stress, *A. aromaticum* adapts its membrane phospholipid inventory by increasing the degree of PLFA saturation as well as the relative proportion of larger PL head groups as shown by cultivation experiments (Zink and Rabus 2010). Together those changes counteract the swelling and expansion of the membrane caused by the hydrocarbons and restabilize the membrane structure. Hence, cells of *A. aromaticum* manage to survive solvent stress even at semi-inhibitory conditions (ca 50% growth inhibition). The toxic impact of heavy metals on microorganisms has, to some extent, similar effects as those of hydrocarbons, but results are more complex and can sometimes be ambiguous. Vestal and White (1989) and Frostegård

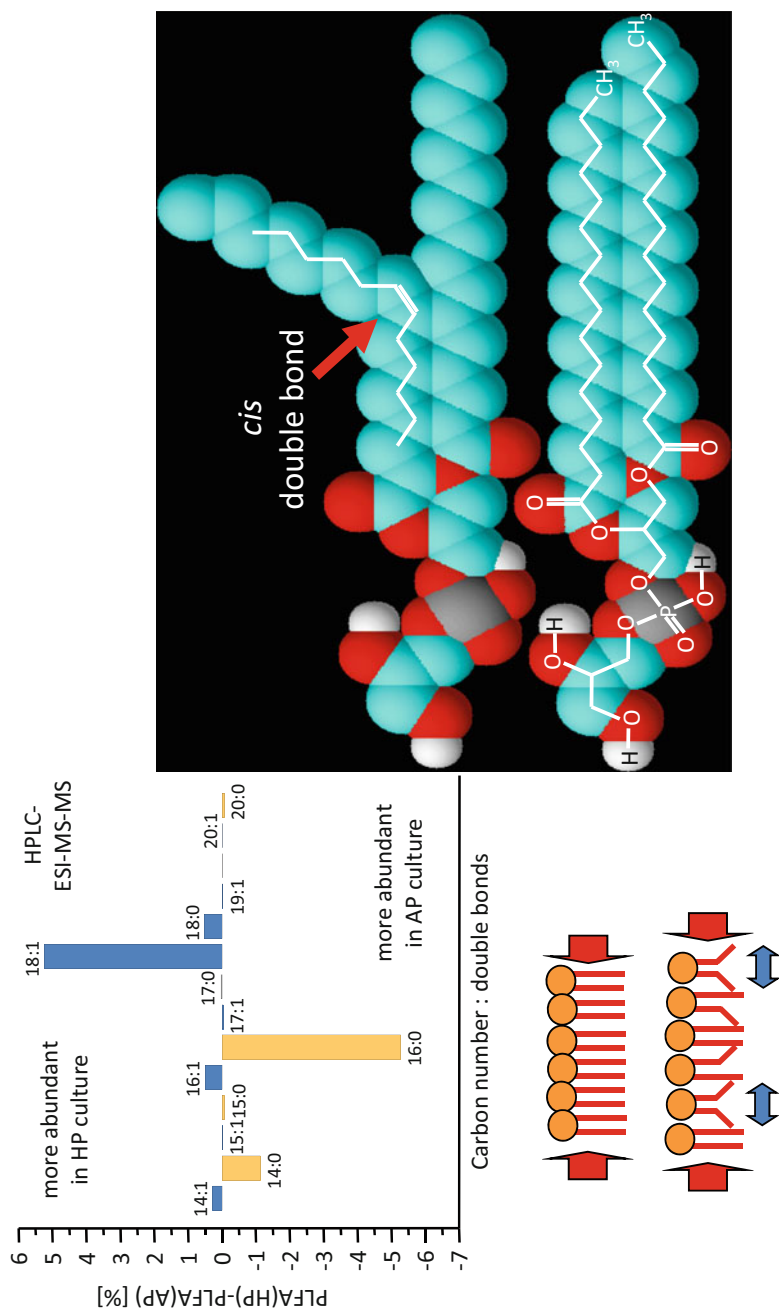


Fig. 8 Difference diagram of the PLFA inventory of a piezosensitive deep sub-seafloor bacterium cultivated at high pressure (HP) of 25 MPa subtracted by the PLFA inventory obtained at atmospheric pressure (AP) conditions indicating a shift to more unsaturated PLFAs in the high-pressure culture (modified after Mangelsdorf et al. 2005b). The bend in the side chain structure associated to the *cis* double bond prevents a closer compaction of the cell membrane

et al. (1993b) showed that heavy metals influence microbial population growth and composition depending on the type of metal and on concentrations. Overall highest toxicity was observed for Cd, but effects are increasingly complex and challenging to interpret when different soil types and with that different microbial communities, the influence on pH or oxygen or water levels is considered.

Several studies, in particular on agricultural and bioremediation aspects, have shown that high salinity, for instance, in soils or lakes, has various effects on microbial growth and community composition (e.g., Qin et al. 2012; Yuan et al. 2007). In this context, Rath et al. (2016) found in certain soils that, with respect to growth, bacteria were less resistant to high salt concentrations than fungi, which is hence also reflected in the lipid composition detected in the soils. Similar results with regard to bacterial growth inhibition and bacterial-fungal community structure have been demonstrated for soils in arid regions such as NW Iran (Barin et al. 2015). In addition, they observed changes in microbial PLFA composition as an indicator for salinity stress. Saline environments contain specific intact polar lipid inventories from halophilic archaea (Bale et al. 2019). Often occurring head groups (Fig. 2) are among others (see Bale et al. 2019) phosphatidyl glycerophosphate (PGP), phosphatidyl glycerophosphate methyl ester (PGP-Me), phosphatidyl glycerol (PG), and phosphatidic acid (PA) (Genderjahn et al. 2017). Additionally, the archaeal lipids are often composed of one or two sesterterpanyl (extended side chain of 25 carbon atoms) side chains instead of the usual phytanyl ones and can also contain double bonds and hydroxy groups (Bale et al. 2019; Genderjahn et al. 2017). Halophilic archaea from the class of *Halobacteria* are often the dominant archaeal species in saline environment. Their polar lipids exhibit archaeol and extended archaeol but usually no GDGTs. Thus, the archaeol vs GDGT ratio is used as a paleo-proxy to indicate salinity changes over geological times (Genderjahn et al. 2017; Turich and Freeman 2011).

4.4 Monitoring of Microbial Life Over Time and Space

Subsurface microbial communities can have strong impact on hydrocarbon resources, mineral deposits, geological reservoir systems, and technical production facilities (Baveye et al. 1998; Head et al. 2003). Therefore, the technical utilization of the underground requires the consideration of microbial communities as an important factor for the quality of energy, water, and material resources and for their reliable exploitation. Other technical utilization of the geological subsurface is, for example, the extraction of geothermal energy or the use of aquifers as cold and surplus heat energy storages (Vetter et al. 2012b). Subsurface microbial communities can directly interfere with the resources in the underground or with the technical below- and aboveground facilities. Thus, microbial activity is known to cause, for instance, biodegradation of petroleum, biofilm clogging of pore space in geological reservoirs and aquifers, as well as plugging and corrosion of pipes, pumps, or other technical equipment (Head et al. 2003; Vetter et al. 2012b). Thus, monitoring of

microbial life in economically used underground systems is an important issue for the reliable operation of technical production facilities.

Vetter et al. (2012b) monitored variations of the bacterial community in a cold storage aquifer system over a period of 3 years along the flow path from the discharge wells to the charge wells using PLFA analysis. They were repeatedly able to show that the PLFA inventory significantly differs between periods of normal operation and periods of reduced injectivity and claimed increased abundance of biofilm-forming Fe- and S-oxidizers during time of operation disturbance. Furthermore, Vetter et al. (2012a) showed strong temperature adaptation in a heat storage system between a warm and cold well. The PLFA inventory of the warm side was dominated by saturated FAs while that of the cold side by *iso*- and *anteiso*-FAs. During downtime of the plant and temperature equilibration of the warm and cold side, the bacterial PLFA patterns on both sides became more similar, but differences rapidly re-established after operation continued.

In another study, Gruner et al. (2017) investigated the microbial composition in a petroleum plant from the production well through the aboveground storage facilities to the injection well. The monitoring over time enabled to identify hot spots of microbial activity mainly in the aboveground facilities of the oil production plants, and also a change of the bacterial community along the flow path was indicated by the variation of the PLFA signal. Furthermore, the effect of biocide application on the microbial abundance could be monitored providing essential information on the adjustment of biocide dosing to mitigate the negative consequences of microbial activity in a petroleum production plant.

Hence, PLFA analysis provides an excellent tool to monitor variations of bacterial communities over time and space not only in natural systems but also in technical facilities.

5 Research Needs

In recent years complementary research strategies are increasingly applied to obtain a more holistic view on microbial communities in not only natural but also economically used systems. The PLFA method is used in combination with a broad set of other biogeochemical and microbiological methods (e.g., Schulze-Makuch et al. 2018). Such comprehensive approaches combine the strengths but also balance the weaknesses of the different methods. In this context it is important to improve our understanding about what the different methods actually indicate. This will help to better utilize and interpret the data sets obtained from the different analytical methods and to combine them to a consistent picture of the microbial communities in a given habitat.

For instance, Genderjahn et al. (2018) showed based on PLFA data a rapid decrease of bacterial abundance from the surface layer down to 10 cm depth in Kalahari pan sediments. In contrast microbiological data obtained by quantitative polymerase chain reaction (qPCR) indicated a decrease of bacteria not below 20 cm. Thus, both methods reveal an abundant surface-near bacterial community, but the depth intervals only partly overlap. Obviously, the two methods detect to some

extent different things. Genderjahn et al. (2018) argued that the qPCR approach might not only detect DNA from living but also from dead bacteria leading to a deeper detection of abundant bacterial biomass. A quite new approach separating between internal DNA (iDNA) indicating living microorganisms and external DNA (eDNA) representing dead microbial biomass might be useful to shed light on the observed discrepancy of the different methods (Alawi et al. 2014).

Thus, future research is needed to improve our understanding on the signals from different analytical methods and how these signals can be best integrated to a realistic image of the investigated microbial community.

References

- Alawi M, Schneider B, Kallmeyer J (2014) A procedure for separate recovery of extra- and intracellular DNA from a single marine sediment sample. *J Microbiol Methods* 104:36–42
- Al-Dagal M, Fung DY, Bennett RW (2009) Aeromicrobiology—a review. *Crit Rev Food Sci Nutr* 29:330–340
- Bååth E, Anderson TH (2003) Comparison of soil fungal/bacterial ratios in a pH gradient using physiological and PLFA-based techniques. *Soil Biol Biochem* 35:955–963
- Bajerski F, Wagner D, Mangelsdorf K (2017) Cell membrane fatty acid composition of *Chryseobacterium frigidisoli* PB4T, isolated from Antarctic glacier forefield soils, in response to changing temperature and pH conditions. *Front Microbiol* 8:677
- Bale N, Sorokin D, Hopmans EC, Koenen M, Rijpstra WIC, Villanueva L, Wienk H, Sinninghe Damsté JS (2019) New insights into the polar lipid composition of extremely halo(alkali)philic euryarchaea from hypersaline lakes. *Front Microbiol* 10:377
- Balkwill DL, Leach FR, Wilson JT, McNabb JF, White DC (1988) Equivalence of microbial biomass measures based on membrane lipid and cell wall components, adenosine triphosphate, and direct counts in subsurface aquifer sediments. *Microb Ecol* 16:73–84
- Barin M, Aliasgharzad N, Olsson PA, Rasouli-Sadaghiani M (2015) Salinity-induced differences in soil microbial communities around the hypersaline Lake Urmia. *Soil Res* 53:494–504
- Baveye P, Vandevivere P, Hoyle BL, DeLeo PC, de Lozada DS (1998) Environmental impact and mechanisms of the biological clogging of saturated soils and aquifer materials. *Crit Rev Environ Sci Technol* 28:123–191
- Beulig F, Heuer VB, Akob DM, Viehweger B, Elvert M, Herrmann M, Hinrichs K-U, Küsel K (2015) Carbon flow from volcanic CO₂ into soil microbial communities of a wetland mofette. *The ISME Journal* 9:746–759
- Biddle JF, Lipp JS, Lever MA, Lloyd KG, Sorensen KB, Anderson R, Fredricks HF, Elvert M, Kelly TJ, Schrag DP, Sogin ML, Brenchley JE, Teske A, House CH, Hinrichs K-U (2006) Heterotrophic archaea dominate sedimentary subsurface ecosystem off Peru. *Proc Natl Acad Sci* 103:3846–3851
- Bischoff J, Mangelsdorf K, Gattinger A, Schloter M, Kurchatova AN, Herzschuh U, Wagner D (2013) Response of methanogenic archaea to Late Pleistocene and Holocene climate changes in the Siberian Arctic. *Glob Biogeochem Cycles* 27:305–317
- Bligh EG, Dyer WJ (1959) A rapid method of total lipid extraction and purification. *Can J Biochem Physiol* 37:911–917
- Blumenberg M, Seifert R, Reitner J, Pape T, Michaelis W (2004) Membrane lipid patterns typify distinct anaerobic methanotrophic consortia. *Proc Natl Acad Sci* 101:11111–11116
- Boetius A, Ravensschlag K, Schubert CJ, Rickert D, Widdel F, Gieseke A, Amann R, Jørgensen BB, Witte U, Pfannkuche O (2000) A marine microbial consortium apparently mediating anaerobic oxidation of methane. *Nature* 407:623–626
- Boggs JM (1986) Effect of lipid structural modifications on their intermolecular hydrogen bonding interactions and membrane functions. *Can J Biochem Cell Biol* 64:50–57

- Boschker HTS, Middelburg JJ (2002) Stable isotopes and biomarkers in microbial ecology. *FEMS Microbiol Ecol* 40:85–95
- Butler JL, Williams MA, Bottomley PJ, Myrold DD (2003) Microbial community dynamics associated with rhizosphere carbon flow. *Appl Environ Microbiol* 69:6793–6800
- Christie WW (1999) The LipidWeb. www.lipidhome.co.uk
- Ciobanu MC, Burgaud G, Dufresne A, Breuker A, Redou V, Ben Maamar S, Gaboyer F, Vandenaabeele-Trambouze O, Lipp JS, Schippers A, Vandenkoornhuysen P, Barbier G, Jebbar M, Godfroy A, Alain K (2014) Microorganisms persist at record depths in the seafloor of the Canterbury Basin. *ISME J* 8:1370–1380
- D'Hondt SL, Inagaki F, Ferdelman TG, Jorgensen BB, Kato K, Kemp P, Sobecky P, Sogin ML, Takai K (2007) Exploring seafloor life with the Integrated Ocean Drilling Program. *Sci Drill* 5:26–37
- Dawson KS, Freeman KH, Macalady JL (2012) Molecular characterization of core lipids from halophilic archaea grown under different salinity conditions. *Org Geochem* 48:1–8
- de Mendoza D (2014) Temperature sensing by membranes. *Annu Rev Microbiol* 68:101–116
- DeLong EF, Yayanos AA (1985) Adaptation of membrane lipids of deep-sea bacterium to changes in hydrostatic pressure. *Science* 228:1101–1103
- Destailhats F, Angers P (2002) On-step methodology for the synthesis of FA picolinyl esters from intact lipids. *J Am Oil Chem Soc* 79:253–256
- Dunkelblum E, Tan SH, Silk PJ (1985) Double-bond location in monounsaturated fatty acids by dimethyl disulfide derivatization and mass spectrometry. *J Chem Ecol* 11:265–277
- Elvert M, Boetius A, Knittel K, Jorgensen BB (2003) Characterisation of specific membrane fatty acids as chemotaxonomic markers for sulfate-reducing bacteria involved in anaerobic oxidation of methane. *Geomicrobiol J* 20:403–419
- Fang J, Barcelona MJ (1998) Structural determination and quantitative analysis of bacterial phospholipids using liquid chromatography/electrospray ionization/mass spectrometry. *J Microbiol Methods* 33:23–35
- Fang J, Barcelona MJ, Semrau JD (2000) Characterization of methanotrophic bacteria on the basis of intact phospholipid profiles. *FEMS Microbiol Lett* 189:67–72
- Fang J, Barcelona MJ, Abrajano T, Nogi Y, Kato C (2002) Isotopic composition of fatty acids of extremely piezophilic bacteria from the Mariana Trench at 11,000 m. *Mar Chem* 80:1–9
- Frostegård A, Bååth E (1996) The use of phospholipid fatty acid analysis to estimate bacterial and fungal biomass in soil. *Biol Fert Soils* 22:59–65
- Frostegård Å, Bååth E, Tunlid A (1993a) Shifts in the structure of soil microbial communities in limed forests as revealed by phospholipid fatty acid analysis. *Soil Biol Biochem* 25:723–730
- Frostegård Å, Tunlid A, Bååth E (1993b) Phospholipid fatty acid composition, biomass, and activity of microbial communities from two soil types experimentally exposed to different heavy metals. *Appl Environ Microbiol* 59:3605–3617
- Frostegård Å, Tunlid A, Bååth E (2011) Use and misuse of PLFA measurements in soils. *Soil Biol Biochem* 43:1621–1625
- Fry JC, Horsfield B, Sykes R, Cragg BA, Heywood C, Kim GT, Mangelsdorf K, Mildenhall DC, Rinna J, Vieth A, Zink K-G, Sass H, Weightman AJ, Parkes RJ (2009) Prokaryotic populations and activities in an interbedded lignite/coal deposit, including a previously deeply buried section (1.6–2.3 km) and ~150 Ma basement rock. *Geomicrobiol J* 26:163–178
- Gambacorta A, Gliozzi A, De Rosa M (1995) Archaeal lipids and their biotechnological applications. *World J Microbiol Biotechnol* 11:115–131
- Gattinger A, Günthner A, Schloter M, Munch JC (2003) Characterisation of archaea in soils by polar lipid analysis. *Acta Biotechnol* 23:21–28
- Genderjahn S, Alawi M, Kallmeyer J, Belz L, Wagner D, Mangelsdorf K (2017) Present and past microbial life in continental pan sediments and its response to climate variability in the southern Kalahari. *Org Geochem* 108:30–42
- Genderjahn S, Alawi M, Wagner D, Schüller I, Wanke A, Mangelsdorf K (2018) Microbial community responses to modern environmental and past climatic conditions in Omongwa

- pan, western Kalahari: a paired 16S rRNA gene profiling and lipid biomarker approach. *J Geophys Res Biogeo* 123. <https://doi.org/10.1002/2017JG004098>
- Gruner A, Mangelsdorf K, Vieth-Hillebrand A, Horsfield B, van der Kraan GM, Köhler T, Janka C, Morris BEL, Wilkes H (2017) Membrane lipids as indicators for viable bacterial communities inhabiting petroleum systems. *Environ Microbiol* 74:373–383
- Guckert JB, Hood MA, White DC (1986) Phospholipid ester-linked fatty acid profile changes during nutrient deprivation of *Vibrio cholerae*: Increases in the trans/cis ratio and proportions of cyclopropyl fatty acids. *Appl Environ Microbiol* 52:794–801
- Guckert JB, Ringelberg D, White DC, Hanson RS, Bratina BJ (1991) Membrane fatty acids as phenotypic markers in the polyphasic taxonomy of methylotrophs within the Proteobacteria. *J Gen Microbiol* 137:2631–2641
- Harayama S, Kishira H, Kasai Y, Syutsubo K (1999) Petroleum biodegradation in marine environments. *J Mol Microbiol Biotechnol* 1:63–70
- Harvey HR, Fallon R, Patton JS (1986) The effect of organic matter and oxygen on the degradation of bacterial membrane lipids in marine sediments. *Geochem Cosmochim Acta* 50:795–804
- Harwood JL, Russell NJ (1984) Lipids in plants and microbes. George Allen & Unwin, London, p 162
- Head IM, Jones DM, Larter SR (2003) Biological activity in the deep subsurface and the origin of heavy oil. *Nature* 426:344–352
- Heinzelmann SM, Bale NJ, Hopmans E, Sinninghe Damsté JS, Schouten S, van der Meer MTJ (2014) Critical assessment of glyco- and phospholipid separation by using silica chromatography. *Appl Environ Microbiol* 80:360–365
- Hinrichs K-U, Hayes JM, Sylva SP, Brewer PG, DeLong EF (1999) Methane-consuming archaeobacteria in marine sediments. *Nature* 398:802–805
- Horsfield B, Schenk HJ, Zink K-G, Ondrak R, Dieckmann V, Kallmeyer J, Mangelsdorf K, di Primio R, Wilkes H, Parker J, Fry JC, Cragg B (2006) Living microbial ecosystems within the active zone of catagenesis: implications for feeding the deep biosphere. *Earth Planet Sci Lett* 246:55–69
- Inagaki F, Hinrichs K-U, Kubo Y, Bowles MW, Heuer VB, Hong W-L, Hoshino T, Ijiri A, Imachi H, Ito M, Kaneko M, Lever MA, Lin Y-S, Methe BA, Morita S, Morono Y, Tanikawa W, Bihan M, Bowden SA, Elvert M, Glombitza C, Gross D, Harrington GJ, Hori T, Li K, Limmer D, Liu C-H, Murayama M, Ohkouchi N, Ono S, Park Y-S, Phillips SC, Prieto-Mollar X, Purkey M, Riedinger N, Sanada Y, Sauvage J, Snyder G, Susilawati R, Takano Y, Tasumi E, Terada T, Tomaru H, Trenbath-Reichert E, Wang DT, Yamada Y (2015) Exploring deep microbial life in coal-bearing sediments down to ~2.5 km below the ocean floor. *Science* 349:420–424
- Jahn U, Summons RE, Sturt H, Grosjean E, Huber H (2004) Composition of the lipids of *Nanoarchaeum equitans* and their origin from its host *Ignicoccus* sp strain KIN4/I. *Arch Microbiol* 182:404–413
- Kallmeyer J (2017) Contamination control for scientific drilling operation. *Adv Appl Microbiol* 98:61–91
- Kallmeyer J, Mangelsdorf K, Cragg B, Horsfield B (2006) Techniques for contamination assessment during drilling for terrestrial subsurface sediments. *Geomicrobiol J* 23:227–239
- Kallmeyer J, Pockalny R, Adhikari RR, Smith DC, D'Hondt S (2012) Global distribution of microbial abundance and biomass in seafloor sediment. *Proc Natl Acad Sci* 109:16213–16216
- Kaneda T (1991) *Iso*- and *anteiso*-fatty acids in bacteria: biosynthesis, function, and taxonomic significance. *Microbiol Rev* 55:288–302
- Kerr RA (1997) Life goes to extremes in the deep earth-and elsewhere. *Science* 276:703–704
- Koga Y, Morii H (2005) Recent advances in structural research on ether lipids from archaea including comparative and physiological aspects. *Biosci Biotechnol Biochem* 69: 2019–2034

- Kuypers MMM, Sliemers AO, Lavik G, Schmid M, Jorgensen BB, Kuenen JG, Sinninghe Damsté JS, Strous M, Jetten MSM (2003) Anaerobic ammonium oxidation by anammox bacteria in the Black Sea. *Nature* 422:608–611
- Lanekoff I, Karlsson R (2010) Analysis of intact ladderane phospholipids, originating from viable anammox bacteria, using RP-LC-MS. *Anal Bioanal Chem* 397:3543–3551
- Laurent F, Richli U (1991) Location of double bonds in polysaturated fatty acids by gas chromatography-mass spectrometry after 4,4-dimethylloxazoline derivatization. *J Chromatogr* 541:89–98
- Lin L-H, Wang P-L, Rumble D, Lippmann-Pipke J, Boice E, Pratt LM, Sherwood Lollar B, Brodie EL, Hazen TC, Andersen GL, DeSantis TZ, Moser DP, Kershaw D, Onstott TC (2006) Long-term sustainability of a high-energy, low-diversity crustal biome. *Science* 314:479–482
- Lipp JS, Hinrichs K-U (2009) Structural diversity and fate of intact polar lipids in marine sediments. *Geochim Cosmochim Acta* 73:6816–6833
- Lipp JS, Morono Y, Inagaki F, Hinrichs K-U (2008) Significant contribution of Archaea to extant biomass in marine subsurface sediments. *Nature* 454:991–994
- Logemann J, Graue J, Koester J, Engelen B, Rullkoetter J, Cypionka H (2011) A laboratory experiment of intact polar lipid degradation in sandy sediments. *Biogeosciences* 8:2547–2560
- Madigan MT, Martinko JM, Parker J (1999) *Brock-biology of microorganisms*. Prentice Hall, London
- Mallet CR, Lu Z, Mazzeo JR (2004) A study of ion suppression effects in electrospray ionization from mobile phase additives and solid phase extracts. *Rapid Commun Mass Spectrom* 18:49–58
- Mancuso CA, Franzmann PD, Burton HR, Nichols PD (1990) Microbial community structure and biomass estimates of a methanogenic Antarctic lake ecosystem as determined by phospholipid analyses. *Microb Ecol* 19:73–95
- Mangelsdorf K, Haberer RM, Zink K-G, Dieckmann V, Wilkes H, Horsfield B (2005a) Molecular indicators for the occurrence of deep microbial communities at the Mallik 5L-38 gas hydrate research well. In: Dallimore SR, Collett TS (eds) *Scientific results from the Mallik 2002 gas hydrate production research well program, Mackenzie Delta, Northwest Territories, Canada*. Geological Survey of Canada, Bulletin, pp 1–11
- Mangelsdorf K, Zink K-G, Birrien J-L, Toffin L (2005b) A quantitative assessment of pressure dependent adaptive changes in the membrane lipids of a piezosensitive deep sub-seafloor bacterium. *Org Geochem* 36:1459–1479
- Mangelsdorf K, Finsel E, Liebner S, Wagner D (2009) Temperature adaptation of microbial communities in different horizons of Siberian permafrost-affected soils from the Lena-Delta. *Chem Erde* 69:169–182
- Mangelsdorf K, Zink K-G, Di Primio R, Horsfield B (2011) Microbial lipid markers within and adjacent to Challenger Mound in the Belgica carbonate mound province, Porcupine Basin, offshore Ireland (IODP Expedition 307). *Mar Geol* 282:91–101
- Mangelsdorf K, Bajerski F, Karger C, Wagner D (2017) Identification of a novel fatty acid in the cell membrane of *Chryseobacterium frigidisoli* PB4T isolated from an East Antarctic glacier forefield. *Org Geochem* 106:68–75
- Männistö MK, Tirola M, Häggblom MM (2007) Bacterial communities in Arctic fields of Finnish Lapland are stable but highly pH dependent. *FEMS Microbiol Ecol* 59:452–465
- Mills CT, Dias RF, Graham D, Mandernack KW (2006) Determination of phospholipid fatty acid structures and stable carbon isotope compositions of deep-sea sediments of the Northwest Pacific, ODP site 1179. *Mar Chem* 98:198–209
- Mueller KD, Husmann H, Nalik HP (1990) A new and rapid method for the assay of bacterial fatty acids using high resolution capillary gas chromatography and trimethylsulfonium hydroxide. *Zentralbl Bakteriol* 274:174–182
- Mukamolova GV, Yanopolskaya ND, Votyakova TV, Popov VI, Kaprelyants AS, Kell DB (1995) Biochemical changes accompanying the long-term starvation of *Micrococcus luteus* cells in spent growth medium. *Arch Microbiol* 163:373–379
- Nagan N, Zoeller RA (2001) Plasmalogens: biosynthesis and functions. *Prog Lipid Res* 40:199–229

- Olsen I, Jantzen E (2001) Sphingolipids in bacteria and fungi. *Anaerobe* 7:103–112
- Orwin KH, Dickie IA, Holdaway R, Wood JR (2018) A comparison of the ability of PLFA and 16S rRNA gene metabarcoding to resolve soil community change and predict ecosystem functions. *Soil Biol Biochem* 117:27–35
- Oshima M, Ariga T (1975) ω -Cyclohexyl fatty acids in acidophilic thermophilic bacteria. *J Biol Chem* 250:6963–6968
- Parkes RJ, Taylor J (1983) The relationship between fatty acid distributions and bacterial respiratory types in contemporary marine sediments. *Estuar Coast Shelf Sci* 16:173–189
- Parkes RJ, Cragg BA, Bale SJ, Getliff JM, Goodman K, Rochelle PA, Fry JC, Weightman AJ, Harvey SM (1994) Deep bacterial biosphere in Pacific Ocean sediments. *Nature* 371:410–413
- Parkes RJ, Cragg BA, Wellsbury P (2000) Recent studies on bacterial populations and processes in subseafloor sediments: a review. *Hydrogeol J* 8:11–28
- Parkes J, Cragg B, Roussel E, Webster G, Weightman AJ, Sass H (2014) A review of prokaryotic populations and processes in sub-seafloor sediments, including biosphere:geosphere interactions. *Mar Geol* 352:409–425
- Pearson A (2008) Who lives in the sea floor. *Nature* 454:952–953
- Pedersen K (1997) Microbial life in deep granitic rock. *FEMS Microbiol Rev* 20:399–414
- Pedersen K (2000) Exploration of deep intraterrestrial microbial life: current perspectives. *FEMS Microbiol Lett* 185:9–16
- Pelz O, Chatzinotas A, Andersen N, Bernasconi SM, Hesse C, Abraham W-R, Zeyer J (2001) Use of isotopic and molecular techniques to link toluene degradation in denitrifying aquifer microcosms to specific microbial populations. *Arch Microbiol* 175:270–281
- Pulfer M, Murphy RC (2003) Electrospray mass spectrometry of phospholipids. *Mass Spectrom Rev* 22:332–364
- Qin X, Tang JC, Li DS, Zhang QM (2012) Effect of salinity on the bioremediation of petroleum hydrocarbons in a saline-alkaline soil. *Lett Appl Microbiol* 55:210–217
- Rabus R, Widdel F (1995) Anaerobic degradation of ethylbenzene and other aromatic hydrocarbons by new denitrifying bacteria. *Arch Microbiol* 163:96–103
- Rajendran N, Matsuda O, Rajendran R, Urushigawa Y (1997) Comparative description of microbial community structure in surface sediments of eutrophic bays. *Mar Pollut Bull* 34:26–33
- Rath KM, Maheshwari A, Bengtson P, Rouska J (2016) Comparative toxicities of salts on microbial processes in soil. *Appl Environ Microbiol* 82:2012–2020
- Ringelberg DB, Sutton S, White DC (1997) Biomass, bioactivity and biodiversity: microbial ecology of the deep subsurface: analysis of ester-linked phospholipids fatty acids. *FEMS Microbiol Rev* 20:371–377
- Rontani J-F (1998) Electron ionization mass spectrometric determination of double bond position in monounsaturated α,β - and β,γ -isomeric isoprenoid acids. *Rapid Commun Mass Spectrom* 12:961–967
- Rothschild LJ, Mancinelli RL (2001) Life in extreme environments. *Nature* 409:1092–1101
- Russell NJ (1989) Functions of lipids: structural roles and membrane functions. In: Ratledge C, Wilkinson SG (eds) *Microbial lipids 2*. Academic Press, London, pp 279–365
- Russell NJ, Fukunaga N (1990) A comparison of thermal adaptation of membrane lipids in psychrophilic and thermophilic bacteria. *FEMS Microbiol Rev* 75:171–182
- Rütters H (2001) Tracing viable bacteria in Wadden Sea sediments using phospholipid analysis. PhD thesis, Department of Chemistry, University of Oldenburg, Oldenburg, p 133
- Rütters H, Sass H, Cypionka H, Rullkötter J (2001) Monoalkylether phospholipids in the sulfate-reducing bacteria *Desulfosarcina variabilis* and *Desulforhabdus amnigenus*. *Arch Microbiol* 176:435–442
- Rütters H, Sass H, Cypionka H, Rullkötter J (2002) Phospholipid analysis as a tool to study complex microbial communities in marine sediments. *J Microbiol Methods* 48:149–160
- Schouten S, Middelburg JJ, Hopmans E, Sinninghe Damsté JS (2010) Fossilization and degradation of intact polar lipids in deep subsurface sediments: a theoretical approach. *Geochim Cosmochim Acta* 74:3806–3814

- Schouten S, Hopmans EC, Sinninghe Damsté JS (2013) The organic geochemistry of glycerol dialkyl glycerol tetraether lipids: a review. *Org Geochem* 54:19–61
- Schubotz F, Wakeham SG, Lipp JS, Fredricks HF, Hinrichs K-U (2009) Detection of microbial biomass by intact polar membrane lipid analysis in the water column and surface sediments of the Black Sea. *Environ Microbiol* 11:2720–2734
- Schulze-Makuch D, Wagner D, Kounaves SP, Mangelsdorf K, Devine KG, de Vera J-P, Schmitt-Kopplin P, Grossart H-P, Parron V, Kaupenjohann M, Galy A, Schneider B, Airo A, Frösler J, Davila AF, Arens FL, Cáceres L, Solís Cornejo F, Carrizo D, Dartnell L, DiRuggiero J, Flury M, Ganzert L, Gessner MO, Grathwohl P, Guan L, Heinz J, Hess M, Keppler F, Maus D, McKay CP, Meckenstock RU, Montgomery W, Oberlin EA, Probst AJ, Sáenz JS, Sattler T, Schirmack J, Sephton MA, Schlöter M, Uhl J, Valenzuela B, Vestergaard G, Wörmer L, Zamorano P (2018) Transitory microbial habitat in the hyperarid Atacama Desert. *Proc Natl Acad Sci* 115:2670–2675
- Sikkema J, de Bont JA, Poolman B (1994) Interactions of cyclic hydrocarbons with biological membranes. *J Biol Chem* 269:8022–8028
- Sinensky M (1974) Homeoviscous adaptation – a homeostatic process that regulates the viscosity of membrane lipids in *Escherichia coli*. *Proc Natl Acad Sci* 71:522–525
- Sinninghe Damsté JS, Strous M, Rijpstra WIC, Hopmans E, Geenevasen JAJ, van Dult ACT, van Niftrik LA, Jetten MSM (2002) Linearly concatenated cyclobutane lipids form a dense membrane. *Nature* 419:708–712
- Stapel JG, Schirrmeyer L, Overduin PP, Wetterich S, Strauss J, Horsfield B, Mangelsdorf K (2016) Microbial lipid signatures and substrate potential of organic matter in permafrost deposits: implications for future greenhouse gas production. *J Geophys Res Biogeosci* 121:2652–2666
- Stapel JG, Schwamborn G, Schirrmeyer L, Horsfield B, Mangelsdorf K (2018) Substrate potential of last interglacial to Holocene permafrost organic matter for future microbial greenhouse gas production. *Biogeosciences* 15:1969–1985
- Sturt HF, Summons RE, Smith K, Elvert M, Hinrichs K-U (2004) Intact polar membrane lipids in prokaryotes and sediments deciphered by high-performance liquid chromatography/electrospray ionization multistage mass spectrometry – new biomarkers for biogeochemistry and microbial ecology. *Rapid Commun Mass Spectrom* 18:617–628
- Suutari M, Laakso S (1994) Microbial fatty acids and thermal adaptation. *Crit Rev Microbiol* 20:285–328
- Suzuki K-I, Saito K, Kawaguchi A, Okuda S, Komagata K (1981) Occurrence of ω -cyclohexyl fatty acids in *Curtobacterium Pusillum* strains. *J Gen Appl Microbiol* 27:261–266
- Suzuki K-I, Collins MD, Iijima E, Komagata K (1988) Chemotaxonomic characterization of a radiotolerant bacterium, *Arthrobacter radiotolerans*: description of *Rubrobacter radiotolerans* gen. nov., comb. nov. *FEMS Microbiol Lett* 52:33–39
- Toffin L, Zink K, Kato C, Pignet P, Bidault A, Bienvenu N, Birrien JL, Prieur D (2005) *Marinilactibacillus piezotolerans* sp. nov., a novel marine lactic acid bacterium isolated from deep seafloor sediment of the Nankai Trough. *Int J Syst Evol Microbiol* 55:345–351
- Trautwein K, Kühner S, Wöhlbrand L, Halder T, Kuchta K, Steinbüchel A, Rabus R (2008) Solvent stress response of the denitrifying bacterium “*Aromatoleum aromaticum*” strain EbN1. *Appl Environ Microbiol* 74:2267–2274
- Turch C, Freeman KH (2011) Archaeal lipids record paleosalinity in hypersaline systems. *Org Geochem* 42:1147–1157
- Vestal JR, White DC (1989) Lipid analysis in microbial ecology. *Biosci Biotechnol Biochem* 39:535–541
- Vetter A, Mangelsdorf K, Schettler G, Seibt A, Wolfgramm M, Rauppach K, Vieth-Hillebrand A (2012a) Fluid chemistry and impact of different operating modes on microbial community at Neubrandenburg heat storage. *Org Geochem* 53:8–15
- Vetter A, Mangelsdorf K, Wolfgramm M, Rauppach K, Schettler G, Vieth-Hillebrand A (2012b) Variations in fluid chemistry and membrane phospholipid fatty acid composition of bacterial

- community in a cold storage groundwater system during clogging events. *Appl Geochem* 27:1278–1290
- Vieth A, Mangelsdorf K, Sykes R, Horsfield B (2008) Water extraction of coals – potential for estimating low molecular weight organic acids as carbon feedstock for deep terrestrial biosphere. *Org Geochem* 39:985–991
- Weber FJ, de Bont JAM (1996) Adaptation mechanisms of microorganisms to the toxic effects of organic solvents on membranes. *Biochim Biophys Acta* 1286:225–245
- White DC, Davis WM, Nickels JS, King JD, Bobbie RJ (1979) Determination of the sedimentary microbial biomass by extractable liquid phosphate. *Oecologia* 40:51–62
- Whitman WB, Coleman DC, Wiebe WJ (1998) Prokaryotes: the unseen majority. *Proc Natl Acad Sci* 95:6578–6583
- Widdel F, Rabus R (2001) Anaerobic biodegradation of saturated and aromatic hydrocarbons. *Curr Opin Biotechnol* 12:259–276
- Wilkes H, Boreham C, Harms G, Zengler K, Rabus R (2000) Anaerobic degradation and carbon isotopic fractionation of alkylbenzenes in crude oil by sulphate-reducing bacteria. *Org Geochem* 31:101–115
- Wörmer L, Lipp JS, Schröder JM, Hinrichs K-U (2013) Application of two new LC-ESI-MS methods for improved detection of intact polar lipids (IPLs) in environmental samples. *Org Geochem* 59:10–21
- Yano Y, Nakayama A, Ishihara K, Saito H (1998) Adaptive changes in membrane lipids of barophilic bacteria in response to changes in growth pressure. *Appl Environ Microbiol* 64:479–485
- Yeagle PL (2016) *The membranes of cells*. Academic Press, San Diego, p 452
- Yuan B-C, Li Z-Z, Liu H, Gao M, Zhang Y-Y (2007) Microbial biomass and activity in salt affected soils under arid conditions. *Appl Soil Ecol* 35:319–328
- Zelles L (1997) Phospholipid fatty acid profiles in selected members of soil microbial communities. *Chemosphere* 35:275–294
- Zhang QC, Wang GH, Yao HY (2007) Phospholipid fatty acid patterns of microbial communities in paddy soil under different fertilizer treatments. *J Environ Sci (China)* 19:55–59
- Zink K-G, Mangelsdorf K (2004) Efficient and rapid method for extraction of intact phospholipids from sediments combined with molecular structure elucidation using LC-ESI-MS-MS analysis. *Anal Bioanal Chem* 380:798–812
- Zink K-G, Rabus R (2010) Stress-induced changes of phospholipids in betaproteobacterium *Aromatoleum aromaticum* strain EbN1 due to alkylbenzene growth substrates. *J Mol Microbiol Biotechnol* 18:92–101
- Zink K-G, Wilkes H, Disko U, Elvert M, Horsfield B (2003) Intact phospholipids – microbial “life markers” in marine deep subsurface sediments. *Org Geochem* 34:755–769
- Zink K-G, Mangelsdorf K, Granina L, Horsfield B (2008) Estimation of bacterial biomass in subsurface sediments by quantifying intact membrane phospholipids. *Anal Bioanal Chem* 390:885–896



Formation of Organic-Rich Sediments and Sedimentary Rocks

17

Ralf Littke and Laura Zieger

Contents

1	Introduction	476
2	Depositional Settings	477
2.1	The Sea	477
2.2	Lakes	480
2.3	Rivers and Peats	482
3	Geochemical Transformations in Young Sediments	484
4	Assessment of Organic Matter in Sedimentary Rocks	486
5	Research Needs	488
	References	489

Abstract

Organic matter-rich sediments are deposited in a variety of continental and marine settings. Their formation strongly depends on bioproductivity and preservation of organic material, which in turn is affected by sediment composition as well as aerobic and anaerobic microbial activity. Burial, pressure, and temperature increase leads to loss of porosity and mineral reactions, ultimately to the formation of sedimentary rocks, and to transformation of primary biomass into insoluble and soluble sedimentary organic matter, i.e., kerogen and bitumen.

R. Littke (✉) · L. Zieger

Institute of Geology and Geochemistry of Petroleum and Coal, Energy and Mineral Resources Group, RWTH Aachen University, Aachen, Germany

e-mail: ralf.littke@emr.rwth-aachen.de; laura.zieger@emr.rwth-aachen.de

© Springer Nature Switzerland AG 2020

H. Wilkes (ed.), *Hydrocarbons, Oils and Lipids: Diversity, Origin, Chemistry and Fate*, Handbook of Hydrocarbon and Lipid Microbiology,

https://doi.org/10.1007/978-3-319-90569-3_14

475

1 Introduction

For the generation of oil and natural gas, the formation of organic matter-rich sediments in different environments is of prime importance. The depositional settings determine, among others, the amount and quality of organic material, i.e., total organic carbon (TOC; C_{org}) content and kerogen types. The deposition of sediments rich in organic matter is taking place in terrestrial, lacustrine, and marine environments in which organic matter is produced faster than it can be destroyed (Tourtelot 1979). These sediments are usually fine-grained and either dominated by silicate (clays and quartz) or carbonate minerals; they usually develop under a permanent water cover with bottom waters being commonly oxygen-depleted. An important exception is peats, which usually develop in humid climates and in areas with limited run-off of surface water leading to a high water level at or above the peat surface.

Organic matter quantity and quality greatly varies even if environments favoring organic matter accumulation are compared. For example, deltaic and fluvial sediments as well as coals generally do not contain much organic matter derived from aquatic organisms. However, they often contain tissues of higher land plants in great quantity. This type of organic material (kerogen type III; Fig. 1) is usually less hydrogen-rich and less oil-prone than the aquatic type. In contrast, marine and lacustrine sediments with high organic matter contents are commonly characterized

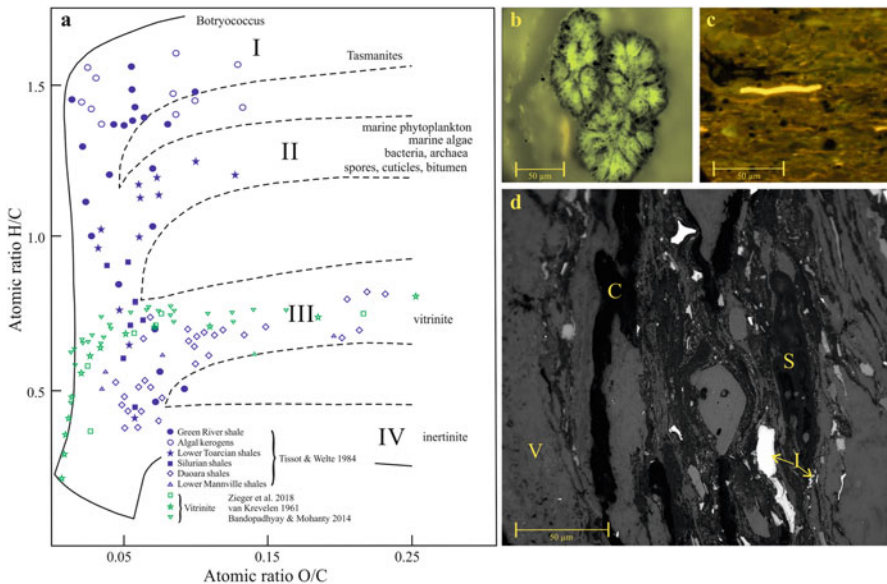


Fig. 1 Kerogen types (left) and microscopy pictures (right) showing respective organic particles (macerals). (a) van Krevelen diagram with the atomic H/C vs. O/C ratios of some organic-rich rocks and kerogens. (Modified after van Krevelen 1961), (b) Botryococcus algae (type I kerogen) under UV-light. (From Rippen et al. 2013), (c) Tasmanales algae (type I kerogen) under UV-light. (From Stock et al. 2017), (d) Carboniferous coal with *V* vitrinite, *C* cutinite, *S* sporinite, and *I* inertinite

by a predominance of aquatic organic matter, either of planktonic or benthic origin. This aquatic organic matter is usually rich in hydrogen, contains little oxygen and is classified as kerogen type I or II.

In the following, the depositional environments are presented, in which organic matter-rich sediments are deposited as well as the consequences for organic matter composition and kerogen quality and quantity. Finally, important methods for kerogen characterization are introduced.

2 Depositional Settings

2.1 The Sea

The deposition of organic matter in modern marine sediments is very complex and strongly influenced by factors such as bioproductivity, ocean currents, ocean floor morphology, and sediment composition. In general, sediments deposited near continents and sediments from marginal seas are more enriched in organic carbon as compared to the deep sea. This proximal-distal pattern reflects bioproductivity in the oceans, which is much stronger in continent-near areas and in marginal seas (Fig. 2) due to the higher availability of nutrients there. High bioproductivity exists, for example, along the northwest and southwest margin of Africa, the west coast of northern South America, and the northwestern coasts of the Indian Ocean (Arabia), where thus bioproductivity is enhanced by upwelling of deep, nutrient-rich cold ocean waters. Sediments there are often rich in organic carbon with values exceeding 1%.

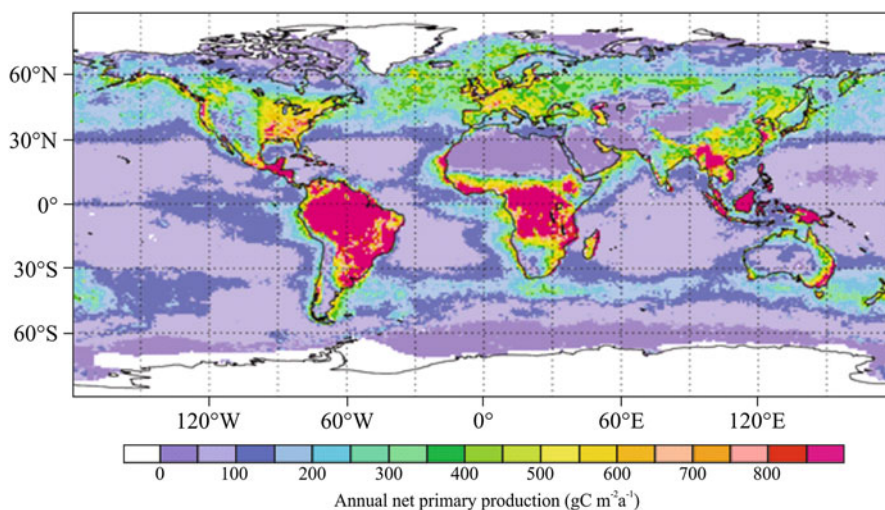


Fig. 2 Global annual net primary production ($\text{gC m}^{-2} \text{a}^{-1}$) from the biosphere. (Modified after Field et al. 1998; see also Huston and Wolverton 2009 for global chlorophyll data)

However, although bioproductivity control on organic matter deposition is obvious on a global scale, it can be disturbed significantly on a regional scale due to other factors such as sea floor topography, mineralogy, and permeability of the sediments. For the Peru sedimentary margin, for example, the areas of highest primary productivity are not exactly those of highest organic carbon content (Fig. 3). In clay-rich sediments or in rapidly deposited sediments, neither oxygen nor other oxidizing agents such as sulfate are transported in great quantity into the sediments thus decelerating organic matter decay and favoring organic matter preservation. Such conditions often occur in topographic lows (mini-basins) on the ocean floor.

Decoupling of primary bioproductivity and organic carbon content is even more pronounced in silled marginal seas with limited water exchange with the open ocean. A modern example is the Black Sea, where highest bioproductivity occurs in the northwest (Danube Inlet). However, due to water stratification and thus the presence of anoxic bottom water, the central parts of the Black Sea are much more enriched in organic carbon, in particular where clay-rich sediments occur and sedimentation rates are high (Stein 1991).

Oxygen concentration in water and at the sediment/water interface greatly influences organic matter preservation and thus the geochemical properties of organic matter in sediments. Fig. 4 shows oceanic oxygen levels at 300 m depth, i.e., within the upper part of the oxygen minimum zone (OMZ) of the oceans. This zone extends below the photic zone in the oceans from about 200 to more than 1000 m depth (Fuenzalida et al. 2009; Paulmier and Ruiz-Pino 2009). Its dimension and intensity depends on vertical exchange between deep and shallow water masses, bioproductivity, and water temperature. In warm water, less oxygen can be dissolved than in cool water. High rates of bioproductivity lead to greater oxygen consumption by decaying biomass below the photic zone. Thus, both high bioproductivity and high water temperatures are favorable for organic matter accumulation.

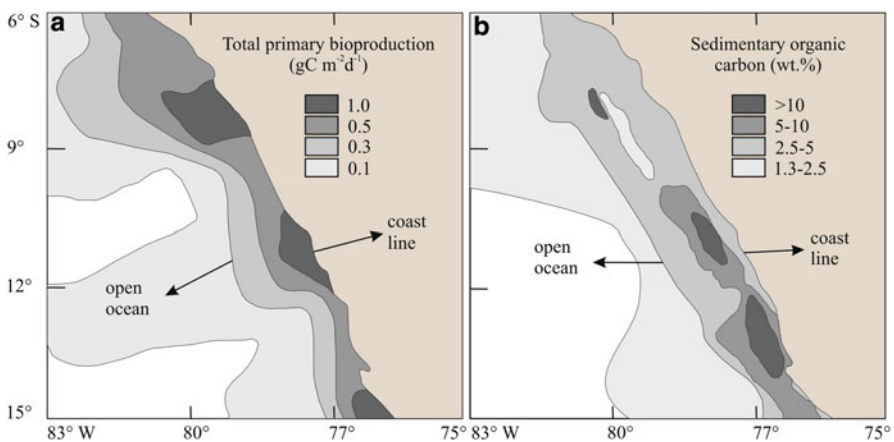


Fig. 3 (a) Total primary bioproductivity and (b) sedimentary organic carbon in surface sediments in the upwelling area off Peru. (Redrawn from Littke 1993, after Reimers and Suess 1983)

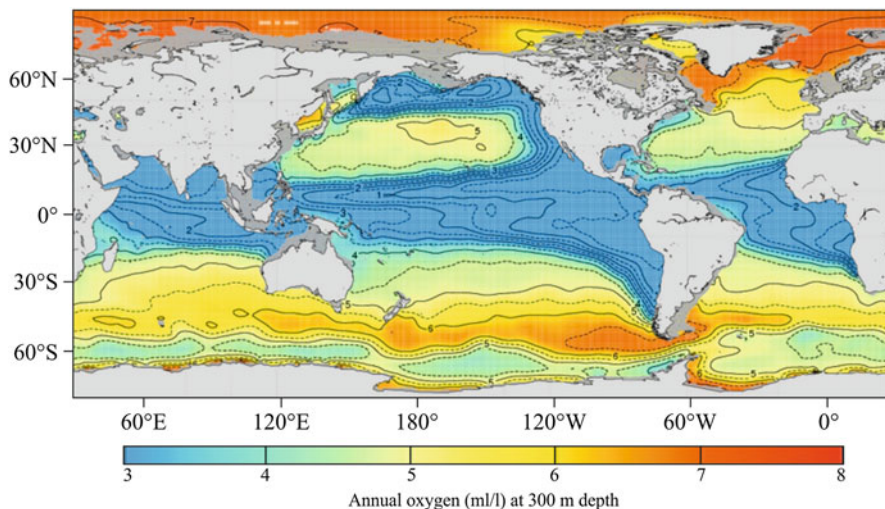


Fig. 4 Annual mean of dissolved oxygen in the oceans at 300 m depth. (Modified from NOAA 2013)

Therefore, it is not surprising that many “oceanic anoxic events” such as the Cenomanian-Turonian Boundary Event coincide with high global temperatures (Sachse et al. 2014).

Organic matter in marine sediments contains not exclusively aquatic (planktonic and benthic) organic matter but also terrestrial organic matter to a variable extent. Terrestrial organic particles (e.g., wood, spores and pollen, charcoal) have to survive a long transport from their site of bioproduction to the site of deposition. Although ocean currents can be rather fast, e.g., up to 2 m/s for the Gulf Stream, this can take several months or years, because the density contrast between organic matter and water is rather small and terrestrial particles at some distance from the coast are usually small. According to Stoke’s law, density difference between particle and water, particle size and viscosity determine the settling of particles. In addition, convective processes partly driven by wind systems can promote rapid settling of organic particles in the sea (Haake et al. 1993).

Long residence times in the sea will generally lead to a stronger physical and chemical degradation of organic matter; therefore, organic particles in central parts of the oceans are usually very rare, strongly degraded, i.e., hydrogen-poor, and small, whereas larger particles occur close to continents and islands (Littke 1993). Along continental slopes, fine dispersed marine organic matter and other sediment undergo resuspension and redeposition within benthic nepheloid layers above the sea ground, causing a proportion of the organic particles to chemically alter and to age before their final sedimentation (Inthorn et al. 2006; Bao et al. 2016).

Differentiating quantitatively terrestrial-derived and autochthonous marine organic matter is neither easy for recent nor for ancient sediments/sedimentary rocks. One possibility is point counting, because terrigenous particles (vitrinite,

inertinite, sporinite) are usually well-visible in incident light microscopy, especially if sections are studied perpendicular to bedding. Other possibilities include lipid geochemistry (Hopmans et al. 2004) and the usage of carbon/nitrogen ratios which roughly range from 15 to 35 in higher land plants and 4 to 8 in marine lower plants, zooplankton, and bacteria (Stein 1991).

In summary, different factors govern the formation of organic matter-rich sediments in marine settings including bioproductivity, organic matter type, ocean currents, sedimentation rate, mineralogy/permeability, and presence of anoxic bottom water. High bioproductivity rates, presence of anoxic bottom water, high clay contents/low permeabilities, and high sedimentation rates are favorable for organic matter deposition.

2.2 Lakes

Lakes are important settings in which organic matter-rich sediments are deposited, often with high percentages of hydrogen-rich lower plants. Deposition in lacustrine settings follows the same principles as in marine settings but has some particularities. Organic-richness of lake deposits depends on nutrient supply and bioproductivity as well as water circulation in the lake and stability of water stratification (see Meyers and Ishiwatari 1993). In comparison to marine settings, lakes are usually much smaller and thus always near to land. Therefore, deposition is strongly influenced by river inflow, lithology of surrounding rocks, and regional climate. Also, large terrestrial organic particles can be present in large quantities in lake sediments.

With respect to the geochemical characteristics, organic matter-rich lake sediments are highly diverse but tend to show an excellent preservation of primary organic matter as compared to marine organic matter-rich sediments. This is partly due to the complete absence of oxygen in the bottom waters, whereas many marine settings are characterized by oxygen-depleted but not completely anoxic conditions, e.g., due to the presence of ocean currents. Furthermore, sulfate is on average present in higher quantity (by a factor of about 5) in sea water, leading to much more intense organic matter degradation by sulfate-reducing microbes. Therefore, on average, organic matter is better preserved in lake than in marine settings, with often high organic carbon concentrations and high hydrogen over carbon ratios for lake sediments in which organic matter is dominated by phytoplankton (type I kerogen in Fig. 1). Another special feature is the high thermal stability of such hydrogen-rich kerogen derived from lakes, which is important with respect to petroleum generation (see below).

A recent example for a large stratified lake is Lake Tanganyika, which is characterized by high organic carbon contents below a stratified water column (Huc 1988). In such stratified lakes, deposition of organic carbon follows the same pattern observed in the Black Sea: organic matter-rich sediments are deposited in the deep parts of the lake, where sedimentation rates are high. Due to the fact that many lakes have a stable water stratification and anoxic bottom water, they often contain very well preserved, hydrogen-rich organic matter. Furthermore, sulfate contents are

usually much lower than in marine settings leading to an even better preservation of organic material (see ► Chap. 10, “Lipidomic Analysis of Lower Organisms”). Therefore, kerogen derived from lake sediments is often classified as type I, i.e., very rich in hydrogen. Whereas this is favorable for these rocks with respect to organic matter quantity and hydrocarbon generation capacity, lateral extension is often limited. In lakes, similar to the sea, there is also, aside from aquatic (algal) organic matter, an input of land plant material. Its quantity is strongly controlled by the vegetation surrounding the lakes and thus by climate.

A famous fossil example is the Eocene Messel Lake, Germany, studied in much detail due to well preserved fossils (early horses, primates, crocodiles, etc.). Organic matter there consists of a mixture of phytoplankton including green algae, dinoflagellates and terrestrial material, the latter partly as large fragments (Rullkötter et al. 1988). Sediments are to a large extent extremely fine laminated, indicating that no burrowing organisms could exist in the bottom waters due to bottom water anoxia. Thus, aerobic microbial activity was absent and much organic matter was deposited and preserved (Fig. 5). Like most freshwater ecosystems, Lake Messel was sulfate-poor as compared to seawater limiting microbial sulfate reduction (Berner 1984; see ► Chap. 10, “Lipidomic Analysis of Lower Organisms”). Accordingly, organic carbon over total sulfur ratios is very high, almost reaching the values of peat and coal (Fig. 5). Under these conditions, excellent preservation of organic matter

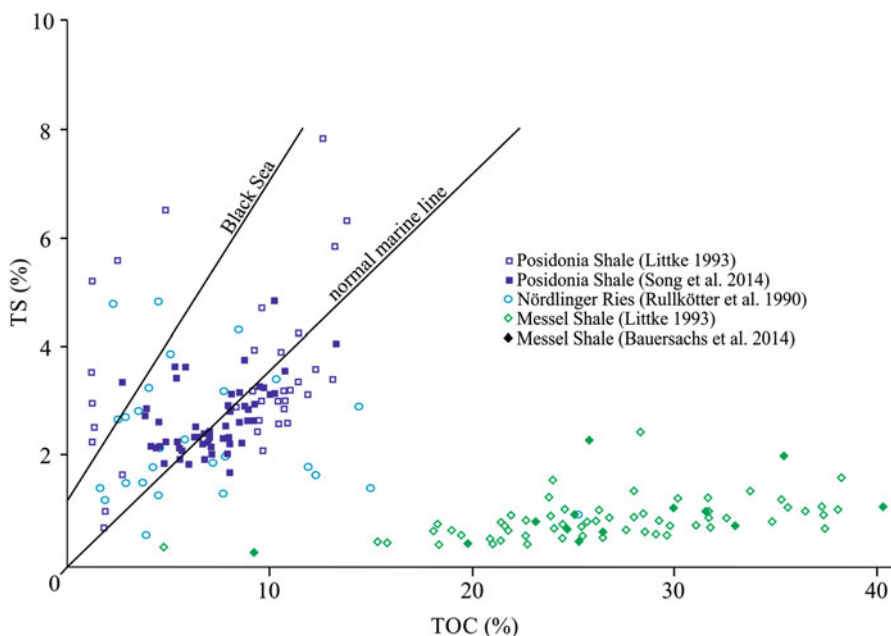


Fig. 5 Organic carbon versus total sulfur plot for the marine Posidonia Shale and the lacustrine Messel and Nördlinger Ries Shales. Lines mark the total sulfur/total organic carbon (TS/TOC) ratios of modern sediments in the Black Sea and the oceans. See also Hedges and Keil (1995)

occurs, leading also to high hydrogen/carbon ratios of the organic matter (Fig. 1). In the case of Lake Messel, oxygen/carbon ratios are also high due to the admixture of about 20% terrestrial higher land plant (woody) material (Rullkötter et al. 1990).

Another type of lake is represented by the Miocene Nördlinger Ries Lake. More than 200 m deep and covering 400 km², it was created by a major meteorite impact 15 million years ago. The resultant lake was filled within about two million years, first by lake sediments, later also by terrestrial deposits. Because the lake was situated between Jurassic limestones, it represents a carbonate lake with a water chemistry vastly different from most other freshwater lakes. Iron contents, for example, were very low and sulfate contents high leading to much higher total sulfur over organic carbon ratios as compared to the, in this respect, typical Lake Messel (Fig. 5). Due to the low iron contents, pyrite (FeS₂) formation was only possible to a limited extent. Pyrite is common in almost all organic matter-rich sediments (as long as some iron is present). Globally, by far most reduced sulfur in subaquatic sediments is present in pyrite (or in its orthorhombic twin marcasite). Exceptions to this rule are iron-poor carbonate sediments such as those of the Nördlinger Ries Lake. There, extremely high organic sulfur concentrations can occur (Barakat and Rullkötter 1993). There are several other lake sediments with this character, whereas marine examples for sulfur-rich kerogen include the Miocene, carbonate-siliceous Monterey Formation, California (Baskin and Peters 1992), or the Cenomanian-Turonian carbonates of the Tarfaya Basin, Morocco (Sachse et al. 2011).

2.3 Rivers and Peats

A major part of the terrestrial organic matter in sediments is preserved either in the form of dispersed particles in fluvial siliciclastic rocks or in peats or coal, with the latter showing the highest concentrations in TOC ($\geq 50\%$) of all organic matter-rich sediments. The formation of these sediments is restricted to regions proximate to or within areas of intense bioproductivity in humid climates with permanent freshwater and nutrient supply, where a large proportion of the produced biogenic material can be preserved under wet, oxygen-depleted conditions.

Such prerequisites are given in peatlands, which are either fed solely by rainwater (ombrotrophic mires) or by a combination of precipitation, flowing water and/or groundwater (rheotrophic mires). Ombrotrophic mires form raised, or more rarely blanked bogs, which are characterized by acidic pH values and low siliciclastic inputs, and thus have a relatively lower nutrient supply compared to mires that form under rheotrophic conditions (Moore 1995). Ombrotrophic peats and the resultant coals are characterized by low ash/mineral contents. Depending on the height of their water table, rheotrophic mires are classified into fens, swamps, and marshes. Resultant peats are usually characterized by higher ash/mineral contents including higher sulfur contents as compared to ombrotrophic peats. Processes such as peat growth, subsidence, or eustatic sea level rise can affect the hydrological conditions in a peat-mire towards ombrotrophic or rheotrophic, respectively (Moore 1995).

Most modern peatlands are situated within the temperate climate zone and are concentrated in the northern hemisphere, where the largest areas of peat formation are in Russia, Canada, Fennoscandia, and NW Europe. Bioproductivity is generally higher in tropical regions (Fig. 2) leading to thicker peat layers within tropical mires. Although tropical peats only contribute little to the total area of modern wetlands (~10%), they account for 18–25% of the global peat volume (Page et al. 2011). Different from the peatlands of the northern hemisphere, in which the vegetation is dominated by *Sphagnum* and herbaceous plants, recent mires in tropical regions are characterized by a woody, rainforest vegetation, comparable to that of many paleomires from the Carboniferous, Jurassic and Miocene that led to the formation of coal seams (Staub and Esterle 1994). Upon burial, peats grade into lignite, subbituminous and bituminous coal, anthracite, and finally graphite.

The type of vegetal material plays an important role in the deposition and preservation of organic matter in sediments. While the polysaccharides cellulose and hemicellulose have a low resistance to microbial degradation, the wood forming substance lignin is relatively stable under anaerobic conditions and is an important precursor of vitrinite (Fig. 1a, d), a typical type III kerogen and abundant constituent of coal and the organic matter in most fluvio-deltaic sediments (Hatcher et al. 1982; van Krevelen 1961). Cellulose is, however, still present in lignites (Fabbri et al. 2009; Stock et al. 2016). Lignin, on the other hand, can also be degraded substantially according to recent investigation (Waggoner et al. 2017). Other important macerals of similar resistance are sporinite, derived from spores and pollen of vascular plants, cutinite derived from waxy protective layers (cuticula) of higher land plants, and inertinite, oxidized, carbon-rich particles resulting from peat fires or fungal reduction (Fig. 1d).

Sites for deposition of dispersed organic matter on continents are, apart from lakes, lowlands flooded temporarily by rivers, but also backwaters, where conditions similar to those in lakes may exist. In humid climate zones, typical sites for the deposition of organic particles are overbank deposits and crevasse splays. Interestingly, organic matter in such fluvial systems is usually more degraded than that in peat, i.e., the petroleum generation capacity is much lower in fluvial sedimentary rocks than in the adjacent coals (Jasper et al. 2009).

Coal deposits and related plant fossils reflect very well the terrestrial plant evolution. The terrestrial plant species contributing to the organic matter preserved in sediments evolved and diversified upon geologic times. First land plants appeared during the Middle Devonian and developed to vascular plants during the early Silurian (Edwards et al. 1983), delimitating the occurrence of sediments rich in terrestrial organic matter to later dates. During the late Devonian, spore producing pteridophyte and early gymnosperm trees populated the continents, leading to an adaptive radiation of land plants and to the formation of extended tropical peat mires. During the Pennsylvanian, these mires covered large areas of present-day North America and Europe. Coal-bearing sequences derived from such tropical, humid environments can reach thicknesses of several kilometers with numerous coal seams as well as dispersed terrigenous organic matter (Scheidt and Littke 1989). The majority of Permian coals deposited on the former Gondwana continent at high

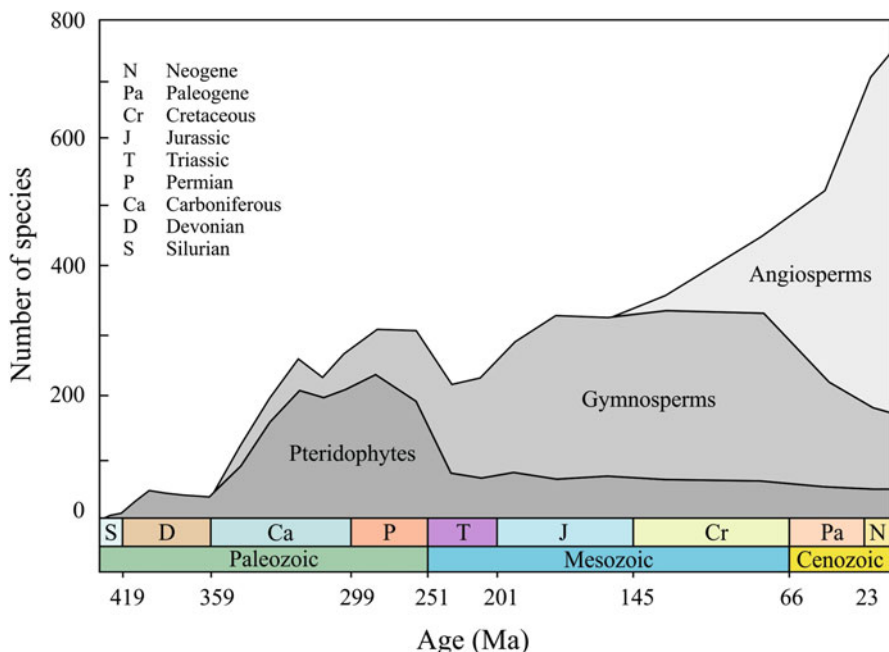


Fig. 6 Trends in plant evolution. (Modified from Robinson 1990, after Niklas 1986)

southern latitudes in humid cool-temperate climates. The higher inertinite (see Fig. 1) contents in these coals compared to coals that formed during the late Carboniferous are interpreted as indicators for seasonal changes (Taylor et al. 1989). Gymnosperms dominated the peat forming vegetation during the Triassic and Jurassic and angiosperms dominate the terrestrial vegetation since Cretaceous times (Fig. 6). The relatively young C_4 plants developed during the Oligocene (Vicentini et al. 2008; Christin et al. 2008) and expanded during Late Miocene to Pliocene times (Cerling et al. 1997). C_4 species like grasses and sedges make up the ground cover of modern fens and marshes (Rydin and Jeglum 2013) and have a 25% share in today's terrestrial net bioproductivity (Still et al. 2003). Because angiospermous lignin is more easily degraded than gymnospermous or pteridophytal lignin, (Hedges et al. 1985; Hatcher et al. 1989), vitrinite particles of coals or fluvio-deltaic deposits that formed from these species tend to be more degraded/detrital compared to vitrinite from Carboniferous coals.

3 Geochemical Transformations in Young Sediments

Organic matter-rich sediments undergo significant transformation upon burial starting in the very early phases of burial. In young and porous sediments, much of this transformation is driven by microbial activity (Jørgensen 1982). Organic

matter is oxidized in a sequence of reactions including the reduction of O_2 , NO_3^- , MnO_2 , Fe_2O_3 , SO_4^{2-} (Froelich et al. 1979), the sequence being determined by the Gibbs Free Energy Yield under the respective redox conditions. In organic matter-rich sediments, aerobic activity usually ends several centimeters to meters below the sediment/water interface, whereas the aerobic zone can reach much deeper in organic-lean sediments (Glud 2008; Fischer et al. 2009). Marine organic matter is more easily degraded as compared to terrestrial organic matter (Hedges et al. 1988) leading to a diagenetic change of the terrestrial/marine ratio.

In marine water and freshly deposited marine sediments, sulfate is usually present in high quantities (sea water has an average sulfur content of about 0.1 wt.%) and the main driver of anaerobic degradation. Almost all reduced sulfur is fixed in the sediments during this process of organic matter degradation, mainly as pyrite or organic sulfur. This leads to a strong decrease of the TOC/TS ratio below the sedimentary surface. An example is shown in Fig. 7a (Lückge et al. 1999),

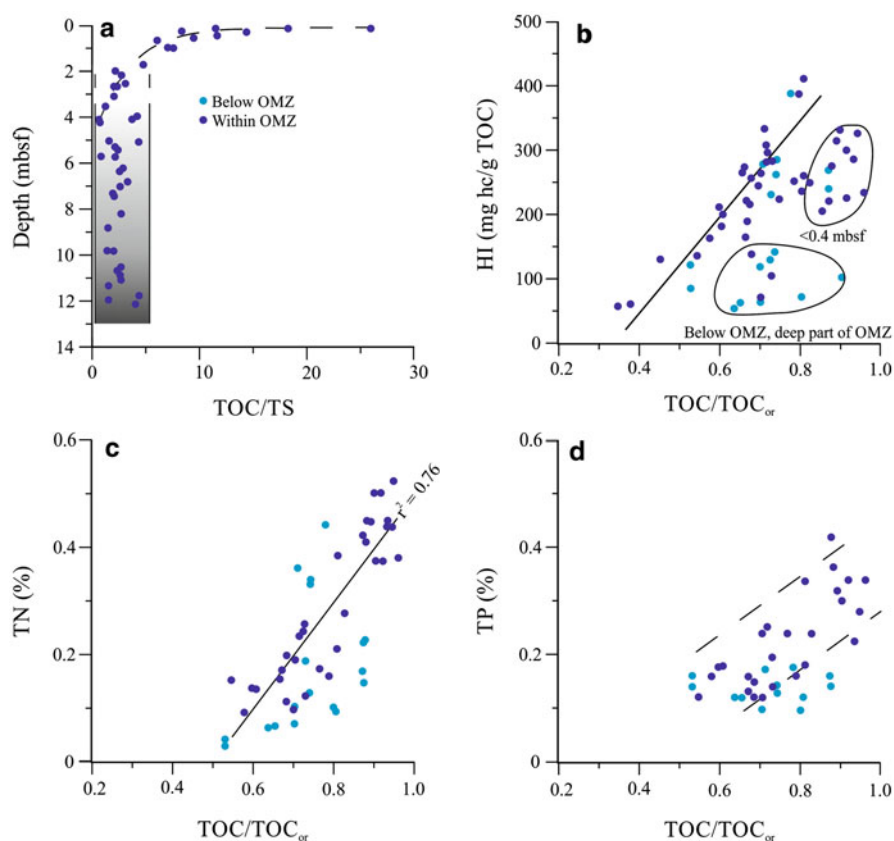


Fig. 7 (a) Depth distribution of TOC/TS ratios in sediments deposited within the OMZ off Pakistan. Ratios of TOC/TOC_{or} versus (b) HI, (c) total nitrogen (TN), and (d) total phosphorus (TP). (Redrawn after Lückge et al. 1999)

illustrating the change in composition of organic matter-rich sediments. Not only is reduced sulfur fixed in the sediments but also organic matter is also degraded. The degree of degradation can be quantified as $\text{TOC}/\text{TOC}_{\text{or}}$ (original TOC) with a ratio of 1 indicating no degradation due to sulfate reduction (Lückge et al. 1999). In the course of this process, nitrogen and phosphorous are lost from the sediments due to selective degradation of nitrogen and phosphorous rich organic matter, and the hydrocarbon generation potential (HI, see below) as a proxy for organic matter H/C ratio is also strongly affected (Fig. 7b–d).

Kerogen, the insoluble organic matter in sedimentary rocks is transformed from biomacromolecules via selective preservation of nonhydrolyzable macromolecular structures and also via restructuring of biomacromolecules into thermally more stable moieties (Tegelaar et al. 1989). Chemical changes occurring during diagenesis before the onset of thermal hydrocarbon generation, i.e., at temperatures below 80–100 °C include incorporation of sulfur into organic matter via natural vulcanization (de Leeuw and Largeau 1993), loss of oxygen from the kerogen structure, and loss of much of the organic nitrogen with transformation of a small part of it from peptide bonds into carbazolic, pyrrolic, or pyridinic structures (Boudou et al. 2008). Changes in molecular structures of specific soluble organic compounds (biomarkers) during the stage of diagenesis have been described in much detail and can be used to decipher temperature history or maximum temperatures reached during burial (Peters et al. 2005).

Sediments rich in organic matter also undergo other changes than structural and geochemical changes within the kerogen and bitumen. The rocks also experience significant compaction and are transformed from loose sediments into sedimentary rocks. Peats, for example, have water contents greater than 75%. When transformed into lignites and finally hard coals, almost all the water gets lost. Mudstones also lose most of their porosity during burial in the first 2 km of the sedimentary column, when they are transformed into solid shales. These changes have great effects on transport properties, which in turn are extremely important for petroleum migration during the stage of catagenesis, i.e., the thermal oil generation stage at temperatures of about 100–180 °C.

4 Assessment of Organic Matter in Sedimentary Rocks

There is a variety of techniques available to study sedimentary organic matter. *Elemental analysis* (C, H, N, S, O) is very time consuming due to the necessity to dissolve minerals with hydrochloric and hydrofluoric acid, before analyzing the residual mixture of organic matter and sulfides. Therefore, alternative techniques have been developed and applied in the past.

Optical microscopy is one of the most common techniques to characterize organic matter in sedimentary rocks. In organic petrography, polished sections, preferentially cut and polished perpendicular to the bedding plane, are studied at high magnification. Organic particles are grouped into numerous macerals, but only three maceral groups: inertinite, vitrinite, and liptinite (see Fig. 1). Inertinite is bright

under the microscope, rich in carbon, poor in hydrogen, and derived from, e.g., charcoal and fungi. Vitrinite is gray under the microscope, rich in oxygen, moderately rich in hydrogen, and derived from higher land plants, e.g., wood, bark, roots, parts of leaves. Liptinite, dark grey in reflected light, is derived from a variety of waxy, hydrogen-rich plants, or plant constituents such as algae, spores, pollen, cuticular layers, or resins. In most sedimentary rocks, the bulk of the organic matter is visible as particles under the microscope, but there are also sediments dominated by submicroscopic organic matter. Reflectance of organic particles changes systematically with burial temperature; this is in particular true for vitrinite reflectance. Therefore, this parameter has been widely applied to reconstruct burial and temperature histories of sedimentary rocks and to calibrate numerical models on organic matter maturation and petroleum generation. There is in addition a large number of other optical maturity parameters such as solid bitumen reflectance, graptolite reflectance, spore color, and conodont color (Hartkopf-Fröder et al. 2015). In palynological studies, rocks are pulverized and treated by hydrochloric and hydrofluoric acids; the residues are studied in transmitted light. Due to the preparation process, much of the fine liptinitic material is here grouped as AOM (amorphous organic matter), whereas terrigenous (“woody”) material can be well identified.

Pyrolysis techniques have long been used to characterize sedimentary organic matter including coal, giving access to both the soluble (bitumen) and insoluble (kerogen) parts. As an industry standard, Rock-Eval pyrolysis has been established. In an open system, powdered rocks are heated in inert atmosphere rapidly to about 300 °C to vaporize volatile “free” hydrocarbons and then at 25 °C/min to a final temperature of about 550 °C in order to pyrolyze kerogen. Also the generated CO₂ is quantified. Important parameters include the Hydrogen Index (HI, mg hydrocarbons/g TOC), the Oxygen Index (OI, mg CO₂/g TOC), and the temperature of maximum pyrolysis yield (T_{max}) which reflects maximum burial temperatures, similar to vitrinite reflectance. Kerogen is commonly classified in a “pseudo van Krevelen” plot (compare Fig. 1) of HI versus OI (Fig. 8a). Rock-Eval parameters do, however, also depend on mineral matter. Presence of low quantities of pyrolyzable organic matter can lead to retention inside the oven and thus too low HI and too high T_{max} values (Peters 1986). Rocks having sufficiently high quantities of pyrolyzable organic matter show clear trends of increasing T_{max} and decreasing HI values with maturation (Fig. 8b, c). It should be noted that there is a great number of various pyrolysis techniques available, e.g., open system, closed system with and without water, Curie-Point pyrolysis, laser-induced micropyrolysis, pyrolysis under controlled pressures. In particular, pyrolysis coupled to gas chromatography can provide much structural and chemical information on organic matter. Further information can be derived from **spectroscopic techniques** such as IR, UV, and NMR.

Bitumen, the part of sedimentary organic matter which is soluble in organic solvents, can best be studied using chromatographic techniques, in particular gas chromatography-mass spectrometry (**GC-MS**). This allows very detailed characterization on a molecular level, revealing much information on biological precursors of sedimentary organic matter (biomarkers). The concept of this approach and applications are described in detail in Peters et al. (2005).

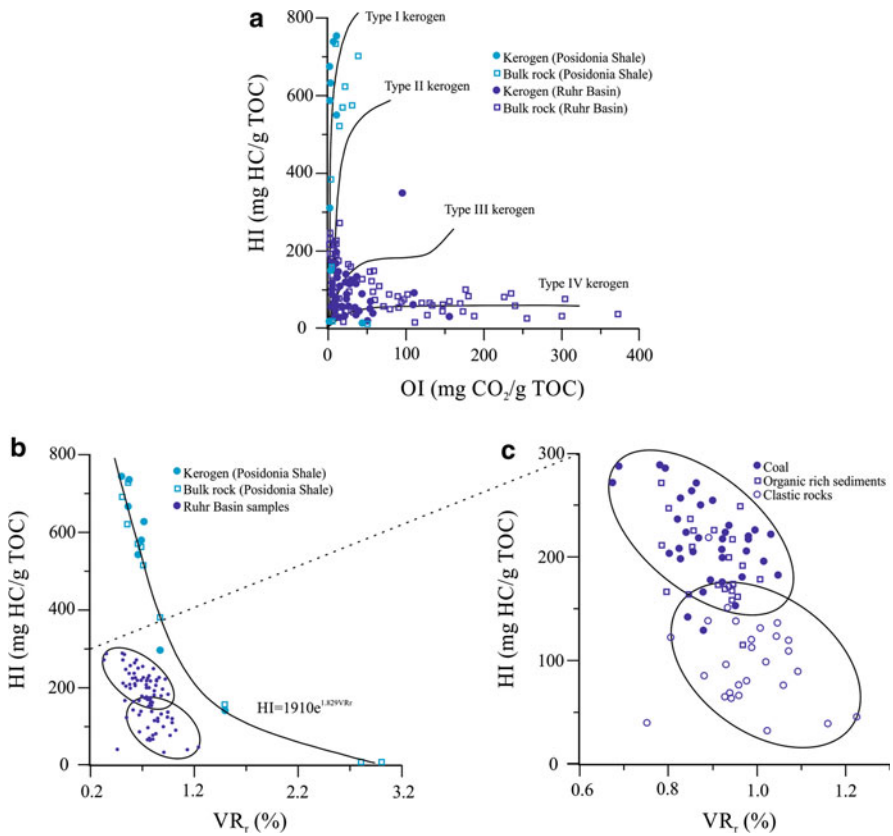


Fig. 8 (a) Pseudo van Krevelen diagram showing HI and OI values of Posidonia Shale samples (Stock et al. 2017) and sediment from within the Ruhr Basin (Jasper et al. 2009) and their concentrated kerogens, (b) development of HI values with increasing maturity (VR_r) for Posidonia Shale and Ruhr Basin samples, (c) HI/VR_r plot of coal, organic-rich sediment and clastic rocks from the Ruhr Basin

5 Research Needs

Both kerogen and bitumen are complex mixtures of organic compounds derived from organisms. Numerous studies have investigated the transformations of organic matter in very young sediments, in which biological precursors can still be identified, such as amino acids, cellulose, etc. However, a complete and quantitative understanding of transformations occurring at greater depth is still missing, e.g., with respect to the carbon, nitrogen, sulfur, hydrogen, and oxygen cycles. In particular, microbial gas generation and its impact on kerogen quality and quantity is poorly understood, although much effort has been put into studies on selected aspects. Laboratory experiments can give important insight, but their applicability to geological systems is debatable.

The same holds true for quantification of oil and gas generation from kerogen as a function of temperature. Diverse pyrolysis experiments in open or closed system, with or without water, with or without controlled pressure have been performed, each one of which giving important hints. From these experiments, kinetic parameters on petroleum generation have been developed and are widely applied in the petroleum industry. However, if kinetic parameters on petroleum generation are calculated from pyrolysis experiments, vastly different results are obtained – proving that our quantitative understanding is still poor and that extrapolation of laboratory results to geological long-time, low-temperature reactors is not possible. Therefore, comparison of pyrolysis experiments with natural maturation series, which are the products of the geological reactions, are necessary. Whereas this seems to be simple, it is complex in reality, because rocks of different thermal maturity rarely have the exact original facies, i.e., the same original organic matter quantity and quality as well as mineralogy.

References

- Bandopadhyay AK, Mohanty D (2014) Variation in hydrogen content of vitrinite concentrates with rank advance. *Fuel* 134:220–225
- Bao R, McInyre C, Zhao M, Zhu C, Kao SJ, Eglinton TI (2016) Widespread dispersal and aging of organic carbon in shallow marginal seas. *Geology* 44(10):791–794
- Barakat AO, Rullkötter J (1993) Gas-chromatographic mass-spectrometric analysis of cembrenoid diterpenes in kerogen from a lacustrine sediment. *Org Mass Spectrosc* 28(3):157–162
- Baskin DK, Peters KE (1992) Early generation characteristics of a sulfur-rich Monterey kerogen. *Pet Geol* 76(1):1–13
- Bauersachs T, Schouten S, Schwark L (2014) Characterization of the sedimentary organic matter preserved in Messel oil shale by bulk geochemistry and stable isotopes. *Palaeogeogr Palaeoclimatol Palaeoecol* 410:390–400
- Berner RA (1984) Sedimentary pyrite formation: an update. *Geochim Cosmochim Acta* 48(4): 605–615
- Boudou JP, Schimmelmann A, Ader M, Mastalerz M, Sebilo M, Gengembre L (2008) Organic nitrogen chemistry during low-grade metamorphism. *Geochim Cosmochim Acta* 72(4): 1199–1221
- Cerling TE, Harris JM, MacFadden BJ, Leakey MG, Quade J, Eisenmann V, Ehleringer JR (1997) Global vegetation change through the Miocene/Pliocene boundary. *Nature* 389(6647):153–158
- Christin PA, Besnard G, Samaritani E, Duvall MR, Hodkinson TR, Savolainen V, Salamin N (2008) Oligocene CO₂ decline promoted C₄ photosynthesis in grasses. *Curr Biol* 18(1):37–43
- De Leeuw JW, Largeau C (1993) A review of macromolecular organic compounds that comprise living organisms and their role in kerogen, coal, and petroleum formation. In: Engel MH, Macko SA (eds) *Organic geochemistry. Topics in Geobiology*, vol 11. Springer, Boston
- Edwards D, Feehan J, Smith DG (1983) A late Wenlock flora from Co. Tipperary, Ireland. *Bot J Linn Soc* 86(1–2):19–36
- Fabbri D, Torri C, Simoneit BRT, Marynowski L, Rushdi AI, Fabiańska MJ (2009) Levoglucosan and other cellulose and lignin markers in emissions from burning of Miocene lignites. *Atmos Environ* 43:2286–2295
- Field CB, Behrenfeld MJ, Randerson JT, Falkowski P (1998) Primary production of the biosphere: integrating terrestrial and oceanic components. *Science* 281:237–240
- Fischer JP, Ferdelman TG, D'Hondt S, Røy H, Wenzhöfer F (2009) Oxygen penetration deep into the sediment of the South Pacific gyre. *Biogeosciences* 6(8):1467–1478

- Froelich PN, Klinkhammer GP, Bender ML, Luedtke NA, Heath GR, Cullen D, Dauphin P, Hammond D, Hartman B, Maynard V (1979) Early oxidation of organic matter in pelagic sediments of the eastern equatorial Atlantic: suboxic diagenesis. *Geochim Cosmochim Acta* 43(7):1075–1090
- Fuenzalida R, Schneider W, Garcés-Vargas J, Bravo L, Lange C (2009) Vertical and horizontal extension of the oxygen minimum zone in the eastern South Pacific Ocean. *Deep-Sea Res II* 56:992–1003
- Glud RN (2008) Oxygen dynamics of marine sediments. *Mar Biol Res* 4(4):243–289
- Haake B, Ittekkot V, Rixen T, Ramaswamy V, Nair RR, Curry WB (1993) Seasonality and interannual variability of particle fluxes to the deep Arabian Sea. *Deep-Sea Res I* 40(7):1323–1344
- Hartkopf-Fröder C, Königshof P, Littke R, Schwarzbauer J (2015) Optical thermal maturity parameters and organic geochemical alteration at low grade diagenesis to anchimetamorphism: a review. *Int J Coal Geol* 150:74–119
- Hatcher PG, Breger IA, Szeverenyi N, Maciel GE (1982) Nuclear magnetic resonance studies of ancient buried wood: II. Observations on the origin of coal from lignite bituminous coal. *Org Geochem* 4:9–18
- Hatcher PG, Wilson MA, Vassallo AM, Lerch HE III (1989) Studies of angiospermous wood in Australian brown coal by nuclear magnetic resonance and analytic pyrolysis: new insights into the early coalification process. *Int J Coal Geol* 13:99–126
- Hedges JJ, Keil RG (1995) Sedimentary organic matter preservation: an assessment and speculative synthesis. *Mar Chem* 49(2–3):81–115
- Hedges JJ, Cowie GL, Ertel JR, Hatcher PG (1985) Degradation of carbohydrates and lignins in buried woods. *Geochim Cosmochim Acta* 49:701–711
- Hedges JJ, Clark WA, Come GL (1988) Organic matter sources to the water column and surficial sediments of a marine bay. *Limnol Oceanogr* 33(5):1116–1136
- Hopmans EC, Weijers JWH, Schefuß E, Herfort L, Sinnighe Damsté JS, Schouten S (2004) A novel proxy for terrestrial organic matter in sediments based on branched and isoprenoid tetraether lipids. *Earth Planet Sci Lett* 224(1):107–116
- Huc AY (1988) Aspects of depositional processes of organic matter in sedimentary basins. *Org Geochem* 13(1–3):263–272
- Huston MA, Wolvertson S (2009) The global distribution of net primary production: resolving the paradox. *Ecol Monogr* 79(3):343–377
- Inthorn M, Wagner T, Scheeder G, Zabel M (2006) Lateral transport controls distribution, quality, and burial of organic matter along continental slopes in high-productivity areas. *Geology* 34:205–208
- Jasper K, Krooss BM, Flajs G, Hartkopf-Fröder C, Littke R (2009) Characteristics of type III kerogen in coal-bearing strata from the Pennsylvanian (upper carboniferous) in the Ruhr Basin, Western Germany: comparison of coals, dispersed organic matter, kerogen concentrates and coal–mineral mixtures. *Int J Coal Geol* 80(1):1–19
- Jørgensen BB (1982) Mineralization of organic matter in the sea bed – the role of sulphate reduction. *Nature* 296(5858):643–645
- Littke R (1993) Deposition, diagenesis and weathering of organic matter-rich sediments. Lecture notes in earth sciences, vol 47. Springer, Berlin/Heidelberg
- Lückge A, Ercegovac M, Strauss H, Littke R (1999) Early diagenetic alteration of organic matter by sulfate reduction in quaternary sediments from the northeastern Arabian Sea. *Mar Geol* 158:1–13
- Meyers PA, Ishiwatari R (1993) Lacustrine organic geochemistry – an overview of indicators of organic matter sources and diagenesis in lake sediments. *Org Geochem* 20(7):867–900
- Moore PD (1995) Biological processes controlling the development of modern peat-forming ecosystems. *Int J Coal* 28:99–110
- National Centers for environmental information NOAA (2013) World Ocean atlas 2013 version 2. <https://www.nodc.noaa.gov/cgi-bin/OC5/woa13fv2/woa13oxnufv2.pl>

- Niklas KJ (1986) Large-scale changes in animal and plant terrestrial communities. In: Raup DM, Jablonski D (eds) Patterns and processes in the history of life. Dahlem workshop reports (Life sciences research reports), vol 36. Springer, Berlin/Heidelberg, pp 383–405
- Page SE, Rieley JO, Banks CJ (2011) Global and regional importance of the tropical peatland carbon pool. *Glob Chang Biol* 17:798–818
- Paulmier A, Ruiz-Pino D (2009) Oxygen minimum zones (OMZs) in the modern ocean. *Prog Oceanogr* 80:113–128
- Peters KE (1986) Guidelines for evaluating petroleum source rocks using programmed pyrolysis. *Amer Assoc Petr Geol Bull* 70:318–329
- Peters KE, Walters CC, Moldowan JM (2005) The biomarker guide. Cambridge University Press, Cambridge, UK
- Reimers CE, Suess E (1983) The partitioning of organic carbon fluxes and sedimentary organic matter decomposition rates in the ocean. *Mar Chem* 13:141–168
- Rippen D, Littke R, Bruns B, Mahlstedt N (2013) Organic geochemistry and petrography of lower cretaceous Wealden black shales of the Lower Saxony Basin: the transition from lacustrine oil shales to gas shales. *Org Geochem* 63:18–36
- Robinson JM (1990) Lignin, land plants, and fungi: biological evolution affecting Phanerozoic oxygen balance. *Geology* 15:607–610
- Rullkötter J, Marzi R (1988) Natural and artificial maturation of biological markers in Toarcian shale from northern Germany. *Org Geochem* 13:639–645
- Rullkötter J, Littke R, Schaefer RG (1990) Characterization of organic matter in sulfur-rich lacustrine sediments of Miocene age (Nördlinger Ries, southern Germany). In: Orr WL, White CH (eds) Geochemistry of sulfur in fossil fuels. ACS symposium series, vol 429. American Chemical Society, Washington, DC, pp 149–169
- Rullkötter J, Littke R, Hagedorn-Götz I, Jankowski B (1988) Vorläufige Ergebnisse der organisch-geochemischen und organisch-petrographischen Untersuchungen an Kernproben des Messeler Ölschiefers. In: Franzen JL, Michaelis W (eds.) Der eozäne Messelsee - Eocene Lake Messel. *Cour. Forsch.-Inst. Senckenberg* 107:37–52
- Rydin H, Jeglum JK (2013) The biology of peatlands, 2nd edn. Oxford University Press, New York
- Sachse VF, Littke R, Heim S, Kluth O, Schober J, Boutib L, Jabour H, Perssen F, Sindern S (2011) Petroleum source rocks of the Tarfaya Basin and adjacent areas, Morocco. *Org Geochem* 42:209–227
- Sachse VF, Heim S, Jabour H, Kluth O, Schumann T, Aquit M, Littke R (2014) Organic geochemical characterization of Santonian to early Campanian organic matter-rich marls (Sondage No. 1 cores) as related to OAE3 from the Tarfaya Basin, Morocco. *Mar Pet Geol* 56:290–304
- Scheidt G, Littke R (1989) Comparative organic petrology of interlayered sandstones, siltstones, mudstones and coals in the upper carboniferous Ruhr basin, Northwest Germany, and their thermal history and methane generation. *Geol Rundsch* 78(1):375–390
- Song J, Littke R, Maquil R, Weniger P (2014) Organic facies variability in the Posidonia black shale from Luxembourg: implications for thermal maturation and depositional environment. *Palaeogeogr Palaeoclimatol Palaeoecol* 410:316–336
- Staub JR, Esterle JS (1994) Peat-accumulating depositional systems of Sarawak, East Malaysia. *Sediment Geol* 89:91–106
- Stein R (1991) Accumulation of organic carbon in marine sediments. Springer, Berlin
- Still CJ, Berry JA, Collatz GJ, DeFries RS (2003) Global distribution of C₃ and C₄ vegetation: carbon cycle implications. *Glob Biogeochem Cycles* 17(1):6–1–6–14
- Stock AT, Littke R, Lücke A, Zieger L, Thielemann T (2016) Miocene depositional environment and climate in western Europe: the lignite deposits of the lower Rhine Basin, Germany. *Int J Coal Geol* 15:2–18
- Stock AT, Littke R, Schwarzbauer J, Horsfield B, Hartkopf-Fröder C (2017) Organic geochemistry and petrology of Posidonia shale (Lower Toarcian, Western Europe) – the evolution from immature oil-prone to overmature dry gas-producing kerogen. *Int J Coal Geol* 176:36–48

- Taylor GH, Liu SY, Diessel CFK (1989) The cold-climate origin of inertinite-rich Gondwana coals. *Int J Coal Geol* 11:1–22
- Tegelaar EW, De Leeuw JW, Derenne S, Largeau C (1989) A reappraisal of kerogen formation. *Geochim Cosmochim Acta* 53(11):3103–3106
- Tourtelot HA (1979) Black shale; its deposition and diagenesis. *Clay Clay Miner* 27(5):313–321
- van Krevelen DW (1961) *Coal – typology, chemistry, physics, constitution*. Elsevier, Amsterdam
- Vicentini A, Barber JC, Aliscioni SS, Giussani LM, Kellogg EA (2008) The age of the grasses and clusters of origins of C4 photosynthesis. *Glob Chang Biol* 14(12):2963–2977
- Waggoner DC, Wozniak AS, Cory RM, Hatcher PG (2017) The role of reactive oxygen species in the degradation of lignin derived dissolved organic matter. *Geochim Cosmochim Acta* 208:171–184
- Zieger L, Littke R, Schwarzbauer J (2018) Chemical and structural changes in vitrinites and megaspores from carboniferous coals during maturation. *Int J Coal Geol* 185:91. (in press)



Thermogenic Formation of Hydrocarbons in Sedimentary Basins 18

Nicolaj Mahlstedt

Contents

1	Introduction	494
2	Basic Mechanisms and Driving Forces for Thermogenic Petroleum Formation in Time and Space	495
3	Classical and Novel Analytical Methods to Investigate Thermogenic Petroleum Formation	499
3.1	Optical Microscopy	500
3.2	Elemental Analysis	501
3.3	Pyrolysis	502
4	Research Needs	513
	References	515

Abstract

A short introduction into the occurrence and bulk composition of thermogenic hydrocarbons as a fraction of natural petroleum in sedimentary basins is given. The main driving forces for the generation of thermogenic petroleum besides temperature, namely, time, pressure, and catalysts, are discussed as well as basic reaction mechanisms. The main part describes classical and novel analytical methods used to assess timing, amount, and composition of generated petroleum as a function of organic matter type and maturity. Recent work is presented and research needs are identified.

N. Mahlstedt (✉)

GFZ German Research Centre for Geosciences, Organic Geochemistry, Potsdam, Germany

e-mail: nick@gfz-potsdam.de

© Springer Nature Switzerland AG 2020

H. Wilkes (ed.), *Hydrocarbons, Oils and Lipids: Diversity, Origin, Chemistry and Fate*, Handbook of Hydrocarbon and Lipid Microbiology,

https://doi.org/10.1007/978-3-319-90569-3_15

493

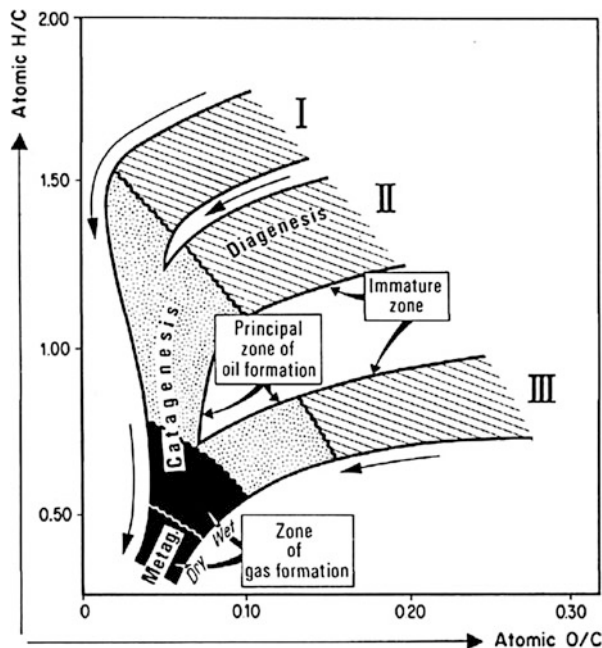
1 Introduction

Understanding thermogenic formation of hydrocarbons is key to securing mankind's need for energy resource as it is now firmly established that most recoverable oil and gas in sedimentary basins is generated by the thermal breakdown of organic matter in subsiding coals and source rocks. Thus, this topic is already comprehensively covered in a variety of textbooks related to petroleum geochemistry (e.g., Tissot and Welte 1984; Hunt 1995; Welte et al. 1997), restricting the following essay to an overview about the basic mechanisms and controls leading to thermogenic formation of hydrocarbons from organic matter and about the most important analytical approaches used to gain insights into these processes. Abiogenic hydrocarbons formed by inorganic reactions in the deeper crust or upper mantle do exist (Abrajano et al. 1988; Schoell 1988; Welhan 1988; Walters 2006) but are of no commercial relevance and therefore not discussed here.

Focus is put on thermogenic hydrocarbons as part of petroleum consisting of liquids and gaseous compounds. Hydrocarbons such as methane, ethane, propane, butane, and light hydrocarbons in so-called condensates are the major fraction in natural gas accumulations besides minor amounts of CO₂, H₂S, N₂, H₂, Ar, and He. Liquid petroleum can be divided into the so-called SARA fractions, with hydrocarbons making up the saturates and aromatics fractions and non-hydrocarbons (whose molecules contain N, S, and O besides H and C atoms) making up the resins and asphaltene fractions. Detailed petroleum composition thereby strongly depends on the biological origin of the source organic matter as well as its depositional environment, the temperature of formation, i.e., maturity zone, and fractionation and alteration processes between source and sink.

The classical maturity zones for organic matter evolution called diagenesis ($R_o < 0.5\%$, R_o = reflectance in oil, see Sect. 3.1), catagenesis ($0.5\% < R_o < 2.0\%$), and metagenesis ($2.0\% < R_o < 4.0\%$) (Tissot and Welte 1978) are used to separate the main zones of hydrocarbon formation in the Van Krevelen diagram (Fig. 1). The only thermogenic products generated during diagenesis are CO₂ and H₂O (Vandenbroucke and Largeau 2007), and biogenic methane is the only hydrocarbon formed in abundance by microbial activity through fermentation and CO₂ reduction at temperatures below 80 °C (Schoell 1988; Faber et al. 1992; Whiticar 1994). At the end of diagenesis, humic substances are no longer present, and the organic matter consists mainly of kerogen. Thermal degradation of this macromolecular kerogen, at temperatures exceeding 70 °C (Dieckmann et al. 1998; Dieckmann 2005; Horsfield et al. 2006), leads to the formation of primary petroleum, i.e., oil and wet gas during catagenesis and mainly dry gas (methane content >97%) during metagenesis (Tissot et al. 1974; Tissot and Welte 1984; Mahlstedt and Horsfield 2012). Secondary thermal cracking of petroleum in the late catagenesis and early metagenesis zones yields smaller and smaller molecules and dry gas and pyrobitumen as final products. Secondary cracking of unexpelled oil, formerly associated with lean source rocks exhibiting low oil expulsion efficiencies (Cooles et al. 1986; Pepper and Dodd 1995), recently proved to be a crucial element in the “exploration equation” for

Fig. 1 The van Krevelen diagram deploys the atomic H/C versus O/C ratios from elemental analysis to describe the evolution of three main kerogen Types (I, II, III), initially characterized by different H/C versus O/C ratios, with maturity. Generalized pathways indicate organic matter evolution with increasing burial depth/thermal stress through the classical maturity zones diagenesis, catagenesis, and metagenesis. (Modified from Tissot and Welte 1978)



defining the in-place potential of unconventional shale oil and shale gas plays (► [Chap. 19, “Oil and Gas Shales”](#)). Default temperatures for primary and secondary petroleum generation cannot be given, but factors controlling the timing of petroleum formation (organic matter lability) as well as masses and composition are discussed in the following.

2 Basic Mechanisms and Driving Forces for Thermogenic Petroleum Formation in Time and Space

After early diagenesis, where biological processes are largely involved, temperature increase associated with sediment burial is widely accepted to mainly control kerogen to petroleum transformation. Nevertheless, the prime driving force for this process is its negative Gibbs free energy (ΔG), i.e., the difference in free energy between the reactants at the initial state (immature kerogen) and products at the final state (more mature kerogen and petroleum). The Gibbs function is expressed as:

$$\Delta G = \Delta H - T\Delta S, \quad (1)$$

where ΔH and ΔS are the differences in enthalpy and entropy, respectively, of the system between these states (e.g., Atkins and de Paula 2002). As breakdown of macromolecular organic matter into smaller petroleum components increases the disorder of the system and is an overall endothermic process (Carr et al. 2009), both

ΔS and ΔH are positive. Thus, and as ΔS and ΔH usually change only subtly with temperature T , increasing temperature mainly controls whether ΔG is negative for the reaction to proceed spontaneously.

Nevertheless, petroleum system components are not in thermodynamic equilibrium but are governed by chemical reaction kinetics, i.e., both temperature and time are critical and an activation energy or potential barrier between educt (macromolecular organic matter) and product (petroleum) compounds must be overcome for oil and gas to be generated. Basic kinetic principles for modeling petroleum formation are given in Schenk et al. (1997b) or Burnham (2017b). In general, petroleum-generating reactions in nature and in the laboratory (pyrolysis) are assumed to proceed via an unknown but very large number of quasi-irreversible, parallel reactions following a first-order rate law (van Krevelen et al. 1951; Pitt 1961; Jüntgen 1964; Tissot 1969; Tissot et al. 1971). Thus, the reaction rate (dm/dt) of the “bulk” petroleum-forming reaction is proportional to the remaining amount of educt ($M - m$), where m is the mass of product generated from the initial mass M of educt at a given time t :

$$dm/dt = k (M - m). \quad (2)$$

The strong (exponential) temperature dependence of the rate constant k usually follows the semiempirical Arrhenius law:

$$k (T) = A^* e^{-E/(RT)}, \quad (3)$$

where T is the absolute temperature in Kelvin, A is termed frequency factor (s^{-1}), E is the activation energy of the reaction (J/mol; kcal/mol is used in petroleum literature), and R is the gas constant.

As the factor RT is a measure of the thermal energy of the system at a given temperature T , a rate constant k will be small, i.e., the reaction will proceed slowly, if the temperature is low and the activation energy high. Nevertheless, time as a primary (linear) control on petroleum formation can compensate for “low” temperatures to reach a certain organic matter conversion level. As a classical example, Tissot and Espitalié (1975) showed for basins exhibiting broadly similar geothermal gradients that the top of the principal zone of oil formation varies with the age of the source rock: 50 °C in the Devonian (350 Ma) of the eastern Sahara, 60 °C in the Toarcian (180 Ma) of the Paris Basin, 70 °C in the Eocene (35 Ma) of West Africa, and 115 °C in the Miocene (10 Ma) of the Los Angeles Basin (Tissot and Welte 1984).

Non-isothermal kinetic concepts take temperature changes as a function of time under geological conditions into account and are used to assign kinetic parameters to the breakdown of various organic matter types. To determine the kinetic parameters, pyrolysis experiments are performed either isothermally at different temperatures or non-isothermally at constant heating rates. Usually an activation energy distribution with a single frequency factor is used having the advantage that, analogous to kerogen conversion which proceeds according to bond strength with, e.g., weak C–S and C–O bonds breaking before strong C–C bonds, all reactions proceed in the

order of increasing activation energy with increasing temperature (Tissot and Espitalié 1975; Ungerer 1990). Kinetic parameters differ appreciably depending on the detailed organic matter composition and maturity level with main activation energies and frequency factors for petroleum generation found in the range 45–60 kcal/mol and 10^{12} – 10^{16} s⁻¹ (Ungerer 1990).

The most widely accepted concept to explain the cleavage of organic matter to smaller fragments is based on the Rice free radical theory (Rice 1933; Kossiakoff and Rice 1943; Greensfelder et al. 1949) which describes thermal cracking as a chain reaction involving free radicals. Occurrence of free radicals in kerogens and coals supports the significance of chain reactions via free radicals in natural systems, specifically the observation that free radical concentrations increase during catagenesis in the course of petroleum formation and decrease during metagenesis due to a gradual conversion of kerogen to a graphite-like structure (condensation) (Ishiwatari et al. 1976, 1977; Marchand and Conard 1980; Bakr et al. 1988, 1990, 1991). In general, the reaction chain consists of initiation, chain propagation, and termination, for which the overall activation energy can be calculated from the activation energies of the various reaction steps. For example, activation energies of initiation reactions during *n*-alkane cracking are roughly equal to the strength of a C–C bond (~82 kcal/mol). The initially formed fragments, e.g., an alpha olefin and a primary radical, are unstable and may immediately re-crack to give ethylene and another primary radical. By successive re-cracking (chain propagation reactions), the radicals ultimately are reduced to methyl or ethyl fragments, which then react with feedstock molecules to produce new free radicals and are themselves converted to methane and ethane. Termination of chain reactions works most often by radical recombination forming a stable hydrocarbon. Since termination has usually zero activation energy and most propagation reactions have lower activation energies than the strength of the C–C bond, the overall activation energy for hydrocarbon cracking is in the range of 50–60 kcal/mol (Ungerer 1990; Burnham 2017b).

Natural catalysts in the form of reactive mineral surfaces (Espitalié et al. 1980; Horsfield and Douglas 1980), clays (Kissin 1987), and trace metals (e.g., Mango 1992; Mango et al. 1994; Mango and Hightower 1997) have been proposed to drive organic matter cracking via ionic mechanisms involving positively charged carbonium ions as reaction intermediates rather than free radicals (Greensfelder et al. 1949 and references therein). Nowadays geocatalysis is ruled out to have a significant effect on natural, primary petroleum generation, “as primary cracking occurs mainly within the organic network of kerogen where minerals are absent” (Vandenbroucke and Largeau 2007; Burnham 2017b), and can only be responsible for a subsequent rearrangement of components. The main reason for taking the ionic mechanism into consideration is that it may explain some irregularities in petroleum compositional patterns. For example, main products formed during acid-catalyzed cracking of olefins are branched hydrocarbons, which can also be found in crude oils (Kissin 1987). Nevertheless, their occurrence in natural oils can more likely be tracked back to simple cracking of isoprenoid-like precursor structures in kerogen via free radical mechanisms (Ungerer 1990). Mango and co-workers discussed in various papers (e.g., Mango 1992; Mango et al. 1994; Mango and Hightower 1997; Mango and Elrod

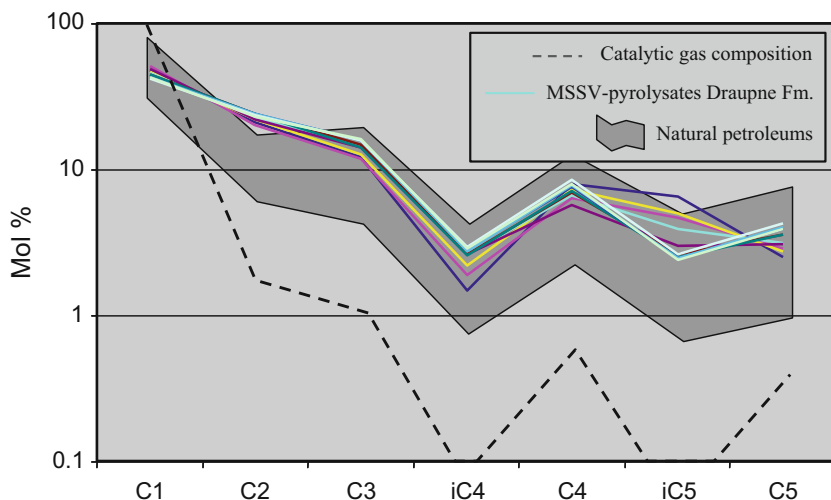


Fig. 2 Comparison of light hydrocarbon distributions for natural petroleum (shaded area) and closed-system pyrolysates (Erdmann 1999) and the compositions reflecting catalysis (Mango and Elrod 1999). MSSV (microscale sealed vessel) pyrolysate compositions of Draupne Fm source rocks clearly fall, with the exception of ethane (C2), into the range of naturally occurring petroleum compositions, whereas catalytic gas compositions do not to such an extent. (Modified after Horsfield et al. 2015)

1999) that catalytic properties of transition metal complexes can explain discrepancies observed for gas compositions of natural petroleum versus pyrolysates. Despite this claim, catalytically induced distributions in fact do not fit gas compositions associated with either natural crudes or pyrolysates (Fig. 2). The light hydrocarbons of natural crudes and pyrolysates differ only in ethane yields making pyrolysis gas wetter than petroleum gas. Catalysis changes the pyrolysate composition of a given kerogen depending on the type of minerals present; i.e., montmorillonitic sediments generate pyrolysates enriched in gaseous and aromatic hydrocarbons compared to, e.g., carbonates (Espitalié et al. 1980; Horsfield and Douglas 1980). Nevertheless, these organic-inorganic interaction effects seem to be strongly heating rate-dependent and are likely to minor under geological heating rates and much lower temperatures (Yang and Horsfield 2016), possibly also due to the effect that the presence of water under natural conditions minimizes the activity of mineral surfaces.

The exact effect of pressure on petroleum generation is very hard to define as the real pressure kerogen has experienced under natural conditions is not known for certain (Vandenbroucke and Largeau 2007) and temperature and pressure are not independent factors. Both generally increase with burial depth, with temperature being of overriding importance for kerogen-to-petroleum conversion (Philippi 1965; Tissot and Welte 1984). Thermodynamically, the effect of pressure on the Gibbs function (1) which refers to isothermal change at constant pressure (or volume) can generally be neglected, as far as the reaction is confined to condensed (solid kerogen and/or liquid petroleum) phases (Radke et al. 1997). Nevertheless, gas generation as

a strongly volume-expanding reaction pressure might shift the “oil window bottom” to greater depth/higher temperatures (Carr et al. 2009) but only in the hypothetical case that the natural system under consideration (conventional or unconventional reservoir) behaves as a true closed system. Some reaction pathways are known to be modified by pressure, which nevertheless rather leads to compositional differences than to significant differences in the timing of petroleum generation (Ungerer 1990).

3 Classical and Novel Analytical Methods to Investigate Thermogenic Petroleum Formation

As the thermal degradation of macromolecular organic matter leads to hydrogen-rich products of lower molecular weight and to hydrogen-poor residues of increasing degree of condensation (Tissot et al. 1971), two general approaches are used in concert to study petroleum formation. The first is to study naturally occurring residues and products from the sedimentary column to characterize their physiochemical properties and changes in those with increasing maturity, allowing recognition of genetic relationships and assessment of timing, masses, and composition of generated petroleum. The second approach is to simulate petroleum generation in the lab, mainly by using various pyrolysis methods, and to extrapolate masses, timing, and composition of formed products to geologic conditions. For both approaches different methods are suitable for the characterization of either precursor/residue or products. Optical microscopy and spectroscopic methods such as infrared, Raman, UV fluorescence, various X-ray methods (also coupled to electron microscopy), nuclear magnetic resonance, and electron spin resonance are nondestructive methods used for the description of optical and chemical properties of naturally and artificially matured, macromolecular organic matter. Selective chemical degradation and pyrolysis followed by chromatography and mass spectrometry are destructive methods used to also characterize macromolecules, whereas product formation specifically during pyrolysis yields important insights into natural petroleum formation (Horsfield 1984; Larter 1984; Rullkötter and Michaelis 1990). A variety of chromatography and mass spectrometry methods used to analyze extracts or produced fluids is described in Wilkes (2018). As specific biomarker compounds or stable isotope ratios of compounds found within the maltene fraction are diagnostic of input organisms and depositional conditions, they are crucial for oil-oil-source correlations and identification of certain alteration processes (Peters et al. 2005; ► Chap. 13, “Stable Isotopes in Understanding Origin and Degradation Processes of Hydrocarbons and Petroleum”). Nevertheless, in the following, the major methods which provided most insights into thermogenic petroleum generation in terms of masses, timing, composition, and reaction mechanism shall be revisited, as those form the basis for our ability to reconstruct and predict petroleum occurrence and behavior at the micrometer to kilometer scale. So much is already understood that, based on first principles, the amounts and composition of products resulting from the thermal decomposition of a given solid complex carbonaceous material can be calculated for a wide range of temperatures and rates using

mechanistic numerical models (e.g., chemical structure-chemical yield modeling published in Freund et al. 2007; Walters et al. 2007). Nevertheless, and although these models already capture a significant portion of the thermal reaction mechanisms and pathways that occur under laboratory as well as natural conditions, these models are only statistical approximations and have to be calibrated against laboratory pyrolysis data.

3.1 Optical Microscopy

One of the most used classical methods to characterize sedimentary organic matter is optical microscopy. Studying the morphology of coals, various coal-constituting maceral and maceral types were initially defined that correspond to the cells which contributed the original organic matter during deposition and which are considered to possess either gas- or oil-generating potential. In general, humic coals are primarily constituted of macerals from the vitrinites group that were derived from woody plant tissues. They are considered mainly gas prone as their major aliphatic petroleum precursor structures consist of alicyclic moieties and short alkyl chains (Given 1960). Sapropelic coals are primarily constituted of macerals from the liptinites group and are said to be oil prone at immature stages. They can be further subdivided into boghead coals, which consist of alginite macerals derived from algal remains such as aliphatic cell membranes (Cane and Albion 1973; Tegelaar et al. 1989), and cannel coals, which consist mainly of exinite macerals such as sporinite (spores and pollen), cutinite (land plant cuticles), and resinite (tree resins; amber). Inertinites make up the third big group of macerals comprising hydrogen-poor material with very low to no petroleum potential, e.g., fusain which is derived from the combustion of woody material (Scott 1989).

While all of those maceral types are also found disseminated throughout oil shales and petroleum source rocks, amorphous, i.e., structureless, organic matter might predominate in some cases. This most often oil-prone, liptinitic material is not typically observed in coals and likely either derived from marine plankton or intense microbial reworking of the originally deposited organic matter.

Reflectance, color, and fluorescence are, besides morphology, further important optical properties that can be used to discriminate organic matter types and, most importantly, maturity. In fact, vitrinite reflectance (or vitrinite reflectance equivalent where true vitrinite is not present) is the most commonly used maturity indicator. In general, reflectance increases with aromaticity of the macromolecular organic matter and therefore with maturity and for maceral types from liptinite to vitrinite to inertinite. Liptinitic organic matter fluoresces more than humic organic matter and thus is an indicator for type and oil potential. Fluorescence ceases when the petroleum potential is realized in the course of petroleum generation. The color in transmitted light is essentially a measure of carbon content of the residual organic matter and changes, for sapropelic organic matter, with maturity from yellow to yellow-brown upon onset of oil generation to progressively browner during oil

generation and to black at the end of oil generation. The thermal alteration index (TAI) uses these color changes as a measure of maturity level.

3.2 Elemental Analysis

Sedimentary organic matter can be conveniently characterized based on its C, H, O, N, and S budget using elemental analysis. The van Krevelen diagram utilizes the atomic H/C versus O/C ratio and is the best known diagram to assess organic matter type and maturity (Fig. 1). Immature to low mature kerogen in petroleum source rocks is usually classified as Type I, II, or III (Tissot et al. 1974) because the bulk kerogen composition falls roughly on the evolution pathways of the coal macerals alginite, exinite, and vitrinite as studied by van Krevelen et al. (1951) and Van Krevelen (1961) who had distinguished these macerals in the order of decreasing H/C ratios. Type III organic matter corresponds to vitrinite-rich terrestrial humic coals (Durand et al. 1977), kerogen Type I corresponds to alginite-rich boghead coals, and Type II corresponds to exinite-rich cancellite coals. Mixing of various kerogen types/coal macerals during organic matter deposition can of course lead to “intermediate” H/C – O/C ratios causing kerogen classifications such as Type I/II or Type II/III. If organic matter exhibits high organic sulfur contents, it is usually thermally less stable, i.e., more reactive, than its “normal” counterpart, and an S is added for classification (Type I-S Type II-S). Immature Type IV source rocks are inertinite-rich and show very low H/C values.

The discrimination of organic matter according to hydrogen availability helps the explorationist to determine the source rock quality, i.e., the petroleum genetic potential, in a most basic way. Concepts were established already early on (Forsman and Hunt 1958; Philippi 1965; Tissot et al. 1974) stating that the lipid-rich and therefore hydrogen-rich, sapropelic coals and kerogen Types I and II form liquid-rich, gas-poor petroleum during maturation, whereas the lignocellulosic/land plant-derived and therefore hydrogen-poor kerogens and humic coals tend to generate gas. Nevertheless, this is a rule of thumb, and many exceptions exist. For instance, and as evidenced for certain humic coals, e.g., from New Zealand, Australian, Indonesia, etc. (Smith and Cook 1984; Thompson et al. 1985; Horsfield et al. 1988; Isaksen et al. 1998; Wilkins and George 2002), Type III organic matter is not only gas prone but can expel oil. As shown by Horsfield et al. (1992a) for the Alum shale and by Muscio and Horsfield (1996) for the Bakken shale, not every Type II source rock is predominantly oil prone but may generate gas or condensate due to the presence of unusual precursor biota and/or the effects of alpha-ray bombardment (Dahl et al. 1988; Lewan and Buchardt 1989; Horsfield et al. 1992a; Yang et al. 2017). With an increasing natural maturation, first a loss of O relative to C during diagenesis and then a loss of H relative to C during catagenesis cause all organic matter types to move along distinct evolution pathways toward the point where O/C and H/C ratios are very low and kerogen types become indistinguishable (Fig. 1). This is also roughly true for the generated petroleum that becomes more and more enriched in gaseous products (Tissot and Welte 1984; England and Mackenzie 1989) because the

gas-forming precursor structures in kerogen are thermally more stable, or refractory, than oil-forming precursor structures (Mackenzie and Quigley 1988; Horsfield 1989; Krooss et al. 1995) and because secondary gas might be generated from unexpelled oil (Tissot and Welte 1984; Monin et al. 1990; Dieckmann et al. 1998, 2000; Jarvie et al. 2007).

3.3 Pyrolysis

Pyrolysis has been defined as “a chemical degradation reaction that is induced by thermal energy alone” (Ericsson and Lattimer 1989) and thereby lends itself perfectly to investigate petroleum generation during maturation, which is a technical term used to address thermally induced changes in the nature of organic matter during catagenesis (Radke et al. 1997). Geochemists use this nonselective, destructive method to break down large organic macromolecules in coals and source rocks into smaller and therefore easier to detect volatile products. In general, open-system analytical pyrolysis is conducted at high temperatures and over short heating times in a flowing stream of inert gas to gain basic information on the type, structure, and maturity of organic matter (Horsfield et al. 1983; Larter 1984; Horsfield 1989; Eglinton et al. 1990), while closed-system pyrolysis is conducted at lower temperatures and over longer heating times to simulate natural maturation and petroleum formation as good as possible. There are numerous open- and closed-system pyrolysis setups, all have their strength and weaknesses, and none is perfect. For instance, irrespective of kerogen type and pyrolysis method, natural petroleum is rich in hydrocarbons, and laboratory pyrolysates are rich in polar compounds. The reason: kerogen actually first cracks to highly polar bitumen that then cracks to yield hydrocarbon-rich oil, whereas the kerogen to bitumen reaction is rate-limiting at geologic heating rates (Braun and Rothman 1975), and the bitumen to oil reaction is rate-limiting under laboratory heating rates (Larter and Horsfield 1993; Horsfield 1997). Nevertheless, the kinetic parameters describing these two thermal degradation reactions were shown to be closely similar in most cases (Quigley et al. 1987; Ungerer and Pelet 1987; Braun and Burnham 1992; Larter and Horsfield 1993; Pepper and Corvi 1995a; Schenk and Horsfield 1998), and the application of different pyrolysis methods provides, due to loss of volatile compounds during expulsion or sampling, the only convenient way to stepwise follow the generation pathway of petroleum from organic matter in natural systems (Horsfield 1984; Espitalié et al. 1985; Lewan 1985).

3.3.1 Open-System Pyrolysis

Products generated during open-system pyrolysis can be either determined as a bulk pyrolysate, i.e., as mass or volume per mass of pyrolyzed material, or they can be resolved into boiling ranges or single compounds using gas chromatography (GC), spectroscopic methods, or both.

Bulk pyrolysis assays (e.g., Fischer, Gray-King, and USBM) were developed already in the early twentieth century mainly to determine oil shale quality (yield)

or the coking behavior of coals (Burnham 2017a). Rock-Eval pyrolysis (Espitalié et al. 1977) is nowadays the standard open-system bulk pyrolysis method to characterize petroleum source rocks in terms of type (quality) and maturity, as it uses only milligram amounts of material and can easily be run alongside drill operations (Fig. 3a). The pyrolysis yield, mainly consisting of hydrocarbon gases and oil detected by flame ionization (FID) as the S2 peak, is called the hydrogen index (HI) when normalized to the total organic carbon (TOC) content and correlates well with the H/C ratio from elemental analysis. Generated CO_2 , normalized to TOC called the oxygen index (OI), is detected as the S3 peak and acts, in analogy to the O/C ratio, as a measure for the organic oxygen content. Thus, in a “pseudo-Van Krevelen” diagram, HI replaces H/C and OI replaces O/C (Fig. 3b), and organic matter falls

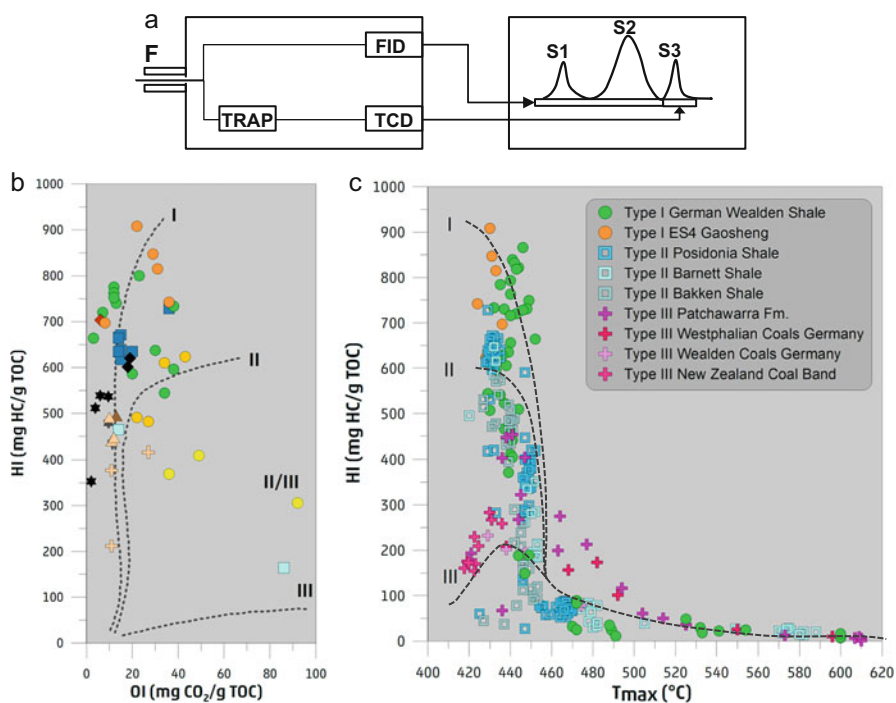


Fig. 3 (a) Schematic analytical configuration and data trace of Rock-Eval pyrolysis, with volatile and kerogen-bound hydrocarbons measured by flame ionization detector (FID) as the S1 and S2 peaks, respectively, and CO_2 measured by a thermal conductivity detector (TCD) as the S3 peak. (Modified after Horsfield et al. 1983). (b) In the Rock-Eval “pseudo-van Krevelen” diagram, the hydrogen index HI replaces the H/C ratio and the oxygen index OI replaces the O/C ratio. Here, a suite of different organic-rich, immature ($R_o \sim 0.5\%$) shales from “purely” marine (different symbol shapes) and lacustrine (circles) depositional environments is shown demonstrating natural variety. (Taken from Mahlstedt et al. 2014). (c) Schematic Rock-Eval HI versus T_{\max} value evolution pathways for the main kerogen types; T_{\max} values increase and HI values decrease with increasing maturity indicating a release of hydrocarbons by the successive cracking of kerogen. (Data taken from GFZ data base)

on the earlier described predefined kerogen-type evolution pathways that are indicative for petroleum potential (quality) and maturity. In general, a loss of O-containing functional groups during diagenesis leads first to a decrease of the OI values, and a loss of H-rich components (petroleum generation) during catagenesis leads to a decrease in HI values, causing all organic matter types to move toward the point (metagenesis) where kerogen types become indistinguishable and possess a low potential for dry gas generation only. A concomitant constant increase in T_{\max} values, the temperature of maximum generation rate, indicates that natural maturation proceeds through the release of hydrocarbons by the cracking of firstly weak and then stronger bonded labile kerogen (Fig. 3c).

Using this bulk pyrolysis Rock-Eval approach for natural maturity sequences of source rocks (uniform facies), a significant conceptual advance emerged in the mid-1980s of the twentieth century when “simple” algebraic schemes were developed for calculating not only absolute masses of petroleum generated between two maturity stages but also degrees of thermal transformation and expulsion efficiency (Larter 1984; Pelet 1985; Cooles et al. 1986). Based on the assumption that kerogen consists of a reactive and an inert part, with the inert part remaining unchanged throughout maturation and the reactive part, corresponding to the HI value, decreasing during formation of oil and gas, all that was needed for calculation was the S1, S2, and TOC (normalized per gram rock) values for any given mature source rock and the S1 and S2 (normalized per gram TOC) for its immature equivalent. It was demonstrated that the expulsion efficiency of source rocks is generally very high and that it depends on original organic richness (TOC >2% is needed for high oil expulsion efficiency) and the degree of thermal transformation, as retained oil can be potentially converted to lighter components at higher geologic temperatures and expelled in the vapor state. These concepts have been applied on a regional scale for conventional petroleum systems, as exemplified by Espitalié et al. (1987) on the Paris Basin and by Lewan et al. (1995) on the Illinois Basin, and became of great use for the assessment of unconventional petroleum plays, for example, the Barnett Shale (Jarvie et al. 2007; Han et al. 2015), for which the amount of unexpelled oil directly controls how much secondary gas or light liquids can be formed during further maturation.

Non-isothermal bulk pyrolysis (Rock-Eval, SRA, HAWK, etc.) performed at different constant heating rates to “correctly” determine the kinetic parameters of kerogen decomposition forms the basis of the main approach to assess timing and degree of petroleum generation in sedimentary basins using kinetic models. Systematic variations with organic matter type have been proposed to exist, but kinetic parameters differ appreciably also within each of the classical kerogen Types I, II, and III (di Primio and Horsfield 2006) and should therefore be determined individually for integration in petroleum basin models. The general view is that activation energy (E_a) distributions are narrow for lacustrine Type I, wider for marine Type II, and widest for fluviodelatic Type III kerogens, with increasing mean E_a values in the order Type II, Type I, and Type III (Ungerer and Pelet 1987). Mean E_a values tend to increase with increasing maturity as the weakest bonds are stripped away first. Sulfur-rich, oil-prone source rocks, e.g., Type IIS Monterey shales, are usually characterized by broad E_a distributions with appreciably lower mean values than

their sulfur-poor counterparts, because organic sulfur decreases the average bond strengths of the kerogen (Orr 1986) potentially leading to early generation of low API, sulfur- and asphaltene-rich heavy crudes (Baskin and Peters 1992). This, and generally all kinetic differences between individual source rocks, can be better illustrated using transformation rate versus temperature curves extrapolated to simplified geological heating histories (Fig. 4). Clearly, primary kerogen cracking can proceed between 70 °C and 160 °C for marine Type II source rocks, whereas sulfur-rich ones exhibit much lower petroleum generation onset temperatures than sulfur-poor ones. Nevertheless, there is no rule of thumb, and individual kinetics should be assessed, because even within a specific sulfur content group, onset temperatures can vary up to 20 °C potentially translating to a few hundred meters of burial depth.

The assumption that all of these reactions can be described by first-order kinetics is a simplification and extrapolation of petroleum formation to geologic heating conditions using laboratory-derived kinetic parameters of immature samples is not valid for all types of kerogens (Schenk and Horsfield 1998). One weakness of the parallel defunctionalization reaction model, and the same also applies to the “Cooler model” with its assumed static behavior of the inert and reactive kerogen fractions, is that besides petroleum-forming decomposition reactions, retrogressive coupling reactions as well as aromatization and polycondensation reactions are well known to occur during natural maturation of heterogeneous, humic coals or Type III kerogens (Stach et al. 1982; Solomon et al. 1988; Hatcher et al. 1992; Horsfield 1997; Schenk and Horsfield 1998; Payne and Ortoleva 2001; Wilkins and George 2002; McMillen and Malhotra 2006). This actually leads to a conversion of reactive labile kerogen into more stable reactive or inert kerogen by formation of new potentials with higher activation energies (Dieckmann et al. 2006; Erdmann and Horsfield 2006). For instance, Schenk and Horsfield (1998) demonstrated that, in contrast to generation rate curves of naturally matured marine Type II Toarcian shales, which always remained within the original envelope defined by the least mature sample, generation rate curves of a naturally matured Carboniferous coal series extended beyond the envelope defined by the least mature sample (Fig. 5). Furthermore, this extreme shift to higher temperatures could not be simulated for low-rank samples under open nor closed artificial maturation conditions clearly showing that most of these aromatization-condensation-recombination reactions are much less prominent during high-temperature short-time pyrolysis than under geological heating conditions. Nevertheless, while cases of dominating retrogressive, second-order coupling reactions during natural maturation are also described for marine Type II source rocks, e.g., the Alum shale (Horsfield et al. 1992a) or the Bakken shale (Muscio and Horsfield 1996), breakdown of organic matter within the great majority of marine source rocks can be satisfactorily described by first-order kinetics, i.e., as a unimolecular decay.

Open-system pyrolysis GC-FID is the most straightforward method to strongly refine the simple Rock-Eval bulk hydrocarbon generation potential evaluation approach (Horsfield et al. 1983). The most commonly occurring major identifiable pyrolysis products are aliphatic hydrocarbons such as normal alk-1-enes and alkanes, aromatic hydrocarbons such as alkylbenzenes and alkylnaphthalenes, and

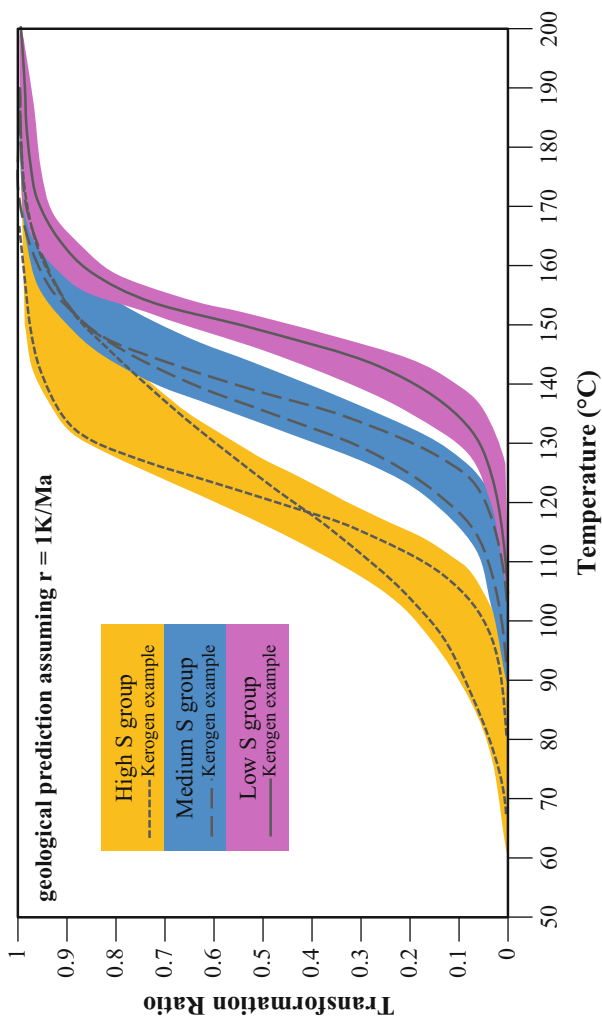


Fig. 4 Predictions for hydrocarbon generation are based on individual kinetic parameters determined using non-isothermal bulk pyrolysis and are shown in a (kerogen to petroleum) transformation ratio rate curves versus temperature cross-plot for marine kerogens with high, medium, and low organic sulfur (S) contents. Extrapolations to geological heating rates, here 1 K/Ma, make clear that low and medium S kerogens are usually more stable than high S kerogens but that significant variations also exist within specific S content groups (colored areas); individual kinetics are needed. (Modified after Tegelaar and Noble 1994)

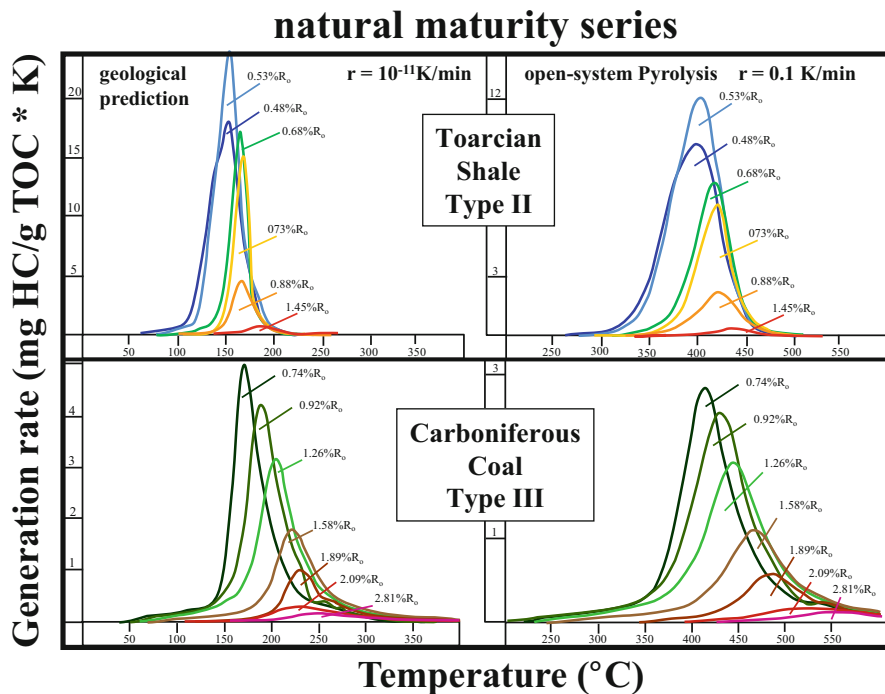


Fig. 5 Bulk hydrocarbon generation rate curves for Type II Toarcian shale (top) and Type III Westphalian coal (bottom) samples of increasing natural maturation (given in % vitrinite reflectance) for laboratory (RHS; 0.1 K/min) and geologic (LHS; 10^{-11} K/min) heating rates. Generation rate curves of all Toarcian shale samples remain within the envelope defined by the least mature sample; generation rate curves of Carboniferous Coal samples do not. Thus, kinetic parameters of immature Type III samples should only be used with care in petroleum system models. (Modified after Schenk and Horsfield 1998)

other aromatic compounds such as alkylphenols as well as alkylthiophenes. Their abundance and distribution give not only information about the bulk compositions of natural petroleum, such as paraffinicity and aromaticity that govern the physical state of the petroleum, but primarily about the parent kerogen structure that determines the amount of hydrocarbons likely to be generated and retained, recombined, or expelled under natural conditions in the first place (Horsfield 1997). Although only a small proportion of low-polarity pyrolysis products is chromatographically resolvable and readily identifiable, this proportion is representative of the petroleum precursor structural moieties in the parent kerogen as a whole (Horsfield 1989; Eglinton et al. 1990; Larter and Horsfield 1993). For instance, Horsfield (1989) has shown that aromaticity determined using relative proportions of major aromatic and aliphatic compounds in open-system pyrolysates correlates very nicely with aromaticity determined using ^{13}C NMR spectroscopy, Larter and Horsfield (1993) have shown that alkylphenol abundance in pyrolysates of Carboniferous coal is directly proportional to the hydroxyl oxygen content determined by wet chemical methods,

and Eglinton et al. (1990) have shown that the relative abundance of alkylthiophenes versus aromatic plus aliphatic hydrocarbons was proportional to the atomic S/C ratio.

These readily identifiable aliphatic, aromatic, oxygen- and sulfur-bearing pyrolysis products provide detailed insights into the major chemical building blocks of the kerogen and can, as the chemical structure of those moieties are a function of biological precursors, depositional environment, and thermal history, be used for petroleum-type organofacies classification approaches (e.g., Jones 1987). One of the most often used classifications, established by Horsfield (1989) and recalibrated by Horsfield (1997), is shown in Fig. 6a and employs the aliphatic fraction, more

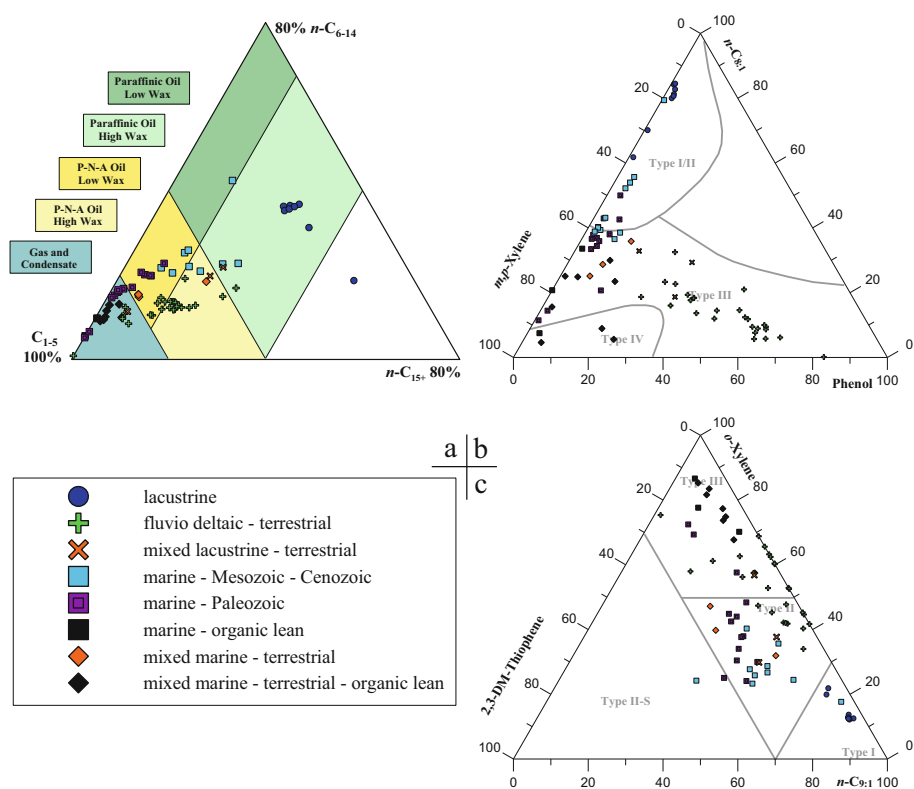


Fig. 6 Open-system pyrolysis GC-FID typing of molecular kerogen structure and petroleum-type organofacies using ternary diagrams of (a) Horsfield (1989), (b) Larter (1984), and (c) Eglinton et al. (1990) is shown for a worldwide selection of immature to early mature shales and coals deposited throughout Phanerozoic age in lacustrine, marine, terrestrial, or mixed environments. The specific pyrolysate position within the ternary diagrams (which deploy representatives of readily identifiable aliphatic, aromatic, oxygen- and sulfur-bearing pyrolysis products such as *n*-alkyl-chains, alkylxylenes, phenols, and alkylthiophenes, respectively) is a function of the kerogens' major chemical building blocks defined by the biological precursor structure, depositional environment, and thermal maturity. (Taken from Mahlstedt 2012)

specifically the *n*-alkyl chain length distribution. Based on the observation that lacustrine Type I source rocks of high-wax oils have a high proportion of long-chain *n*-alkanes and *n*-alkenes in their pyrolysates, whereas pyrolysates of Type II marine shales are characterized by intermediate chain lengths, and pyrolysates of humic coals are characterized by very short average *n*-alkyl chain lengths, organofacies fields were termed, in close relation to the nomenclature used by Tissot and Welte (1984) for classifying naturally occurring crude oils, gas and condensate, paraffinic-naphthenic-aromatic (PNA) high-wax, PNA low-wax, P high-wax, and P low-wax generating petroleum type. This also confirms that reactions leading to the formation of *n*-alkanes and *n*-alkenes under laboratory conditions are comparable to those leading to the formation of *n*-alkanes under geological conditions (Horsfield 1997; Schenk and Horsfield 1998). For further characterization of the organofacies, the abundance of phenol in comparison with *n*-octene and *m,p*-xylene in pyrolysates can be used to assess the amount of kerogen representing land plant-derived moieties (Larter 1984) (Fig. 6b), or the abundance of 2,3-dimethylthiophene in comparison with *o*-xylene and *n*-nonene can be used to discriminate high- or low-sulfur source rocks, i.e., of source rocks deposited in marine or hypersaline sedimentary environments and those deposited in freshwater lacustrine or terrestrial environments (Eglinton et al. 1990) (Fig. 6c).

3.3.2 Closed-System Pyrolysis

Closed-system pyrolysis is said to simulate maturation and petroleum formation under geological conditions better than open-system pyrolysis because, similar to natural conditions, thermally generated products are not immediately flushed away from the parent kerogen and can react with minerals or residual organic matter (Behar et al. 1995). For instance, closed-system pyrolysis products resemble natural crude oils more closely than open-system pyrolysis products in that *n*-alkenes are not major constituents, because hydrogen transfer between certain kerogen moieties and free radicals within the first-formed products leads to dominantly saturated *n*-alkyl homologues in natural fluids and closed-system pyrolysates. As cumulatively generated products stay within the reaction vessel, closed-system pyrolysis can be used to investigate step-by-step compositional changes with increasing maturity including secondary cracking processes, i.e., closed-system data can be used to not only build more realistic compositional kinetic models of primary petroleum generation from kerogen but also of secondary cracking of oil (and gas) in conventional reservoirs as well as in unconventional reservoirs (in-source unexpelled oil).

Various closed-system pyrolysis methods exist with which different potential chemical or physical influences on petroleum generation, besides thermal stress, can be investigated. Those are the presence or absence of water and the influence of elevated pressure. Nevertheless, it should be clear to everybody that neither the real pressure kerogen has experienced in its geologic source rocks environment is known for certain (Vandenbroucke and Largeau 2007) nor the water saturation, especially within the organic matter if water is present at all. In any case, significant differences in pyrolysate yields and composition may exist whether pyrolysis is conducted under hydrous or anhydrous conditions (Lewan 1993). The precise impact of water on a

specific reaction mechanism is nevertheless not easily quantifiable, as water, depending on the analytical setup, can play either a dominantly chemical, reactive role or a dominantly physical, pressurizing role or both. The term hydrous pyrolysis usually refers to setups in which a reactor contains tens or hundreds of grams of rock fragments, a water phase, and an inert gas phase, whereas heating of the system leads to the presence of both liquid and vapor phases of water and to the preferential expulsion of generated saturated over polar compounds from its source (Lewan 1985). Here, the chemical role of water on reaction mechanisms (or expulsion fractionation mechanism) dominates. Maximizing this effect, the recently developed “expulsinator” (Stockhausen et al. 2013), a semi-open hydrous system in which products are flushed away from the heated reaction zone in intervals, performs pyrolysis at pressure conditions usually prevailing during catagenesis in sedimentary basins. This more or less leads to an immediate squeeze-out of all first-formed products, which inhibits further secondary cracking reactions to take place to a significant extent and yields pyrolysate amounts even exceeding those observed under open-system conditions. In contrast, high-pressure closed-system hydrous pyrolysis setups exist in which the vessel is completely filled with source rock and water; thus, no space is left for vapor, and the water itself acts as a pressurizing medium (Carr et al. 2009; Ugana et al. 2012), strongly retarding generation, or rather expulsion, of products. Closed-system pyrolysis conducted without extra amounts of added water can be viewed as an anhydrous end-member scenario dominated by the effect of thermal stress. This kind of pyrolysis is often called confined rather than anhydrous pyrolysis as water is readily formed by organic matter conversion and therefore present within the reaction zone (Michels et al. 1995). Microscale sealed vessels (MSSV) (Horsfield et al. 1989) and sealed gold bags (Monthieux et al. 1985; Behar et al. 2010) are the best known representatives, while sealed gold bags can be pressurized by an external fluid, MSSV tubes are rigid, and the pressure inside the vessel can't be directly controlled. The pressure is generally below 10 MPa at operating temperatures (Erdmann and Horsfield 2006; Horsfield et al. 2015) and increases rather subtly in the course of volume-expanding conversion of solid organic matter into fluids whose partial pressure further increases as a direct function of increasing temperature.

Even though many authors claim that their analytical pyrolysis setup resembles natural conditions in sedimentary basins most closely, one should always keep in mind that a completely accurate simulation of molecular processes occurring under geologic conditions will never be possible using any of these pyrolysis methods as reactions taking place at temperatures from ~250 °C to 650 °C in the laboratory are extrapolated to ~100 °C to 170 °C, spanning rates that differ by ~14 orders of magnitude. Dominating reactions in both temperature regimes are known which are not identical (Walters et al. 2007), and pyrolysates are richer in polar and aromatic components than undergraded petroleum (Larter and Horsfield 1993).

Nevertheless, closed-system pyrolysis was demonstrated to be a reasonably good approximation of natural maturation processes to be used for the prediction of the phase behavior of in situ petroleum, which is directly governed by the pressure-temperature (P-T) conditions of the reservoir and bulk petroleum composition

(England et al. 1987; Düppenbecker and Horsfield 1990; di Primio et al. 1998b; di Primio 2002; di Primio and Skeie 2004a). Using MSSV pyrolysis, an excellent reconstruction of natural fluid composition was demonstrated in several case studies for various organofacies, e.g., Sonda de Campeche, Mexico (Santamaria-Orozco and Horsfield 2004); Snorre field, North Sea Viking Graben (Erdmann 1999; di Primio and Skeie 2004b); Reconcavo Basin, Brazil (di Primio and Horsfield 2006), Jeanne d'Arc Basin offshore Newfoundland (Baur et al. 2011); and the Williston Basin, USA (Kuhn et al. 2010, 2012), in that the gas-to-oil ratios of the respective source rock pyrolysates correlated very well with the natural fluid gas-to-oil ratios in the related petroleum systems at similar transformation ratios TR (see also Dueppenbecker and Horsfield 1990; Horsfield 1997) (Fig. 7). However, to correctly predict fluid-phase behavior, which is strongly governed by the gas composition (di Primio and Skeie 2004b), measured gas compositions have to be calibrated to a natural fluid database (di Primio and Skeie 2004b) or adjusted empirically (di Primio et al. 1998a; di Primio and Horsfield 2006), as pyrolysates generally exhibit too high ethane and propane contents and simultaneously rather low methane contents compared to natural fluids (Behar et al. 1991; Berner et al. 1995; Javaid 2000; Michels et al. 2002; Horsfield et al. 2015). The PhaseKinetics approach (di Primio and Horsfield 2006) combines open- and closed-system MSSV pyrolysis techniques (including gas wetness correction schemes) and has been widely used to develop compositional kinetics for the prediction of natural petroleum phase behavior for different organofacies types.

Closed-system pyrolysis is regularly used to assess secondary oil to gas cracking kinetics, which is of paramount importance in conventional petroleum systems, to

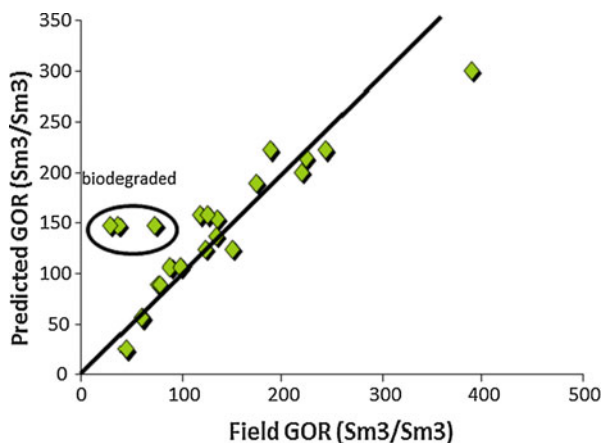


Fig. 7 A one-to-one correlation of predicted GORs using MSSV pyrolysates and measured field GORs of reservoir fluids within the Jeanne d'Arc Basin offshore Newfoundland sourced by the Jurassic (Kimmeridgian) Egret member demonstrates that closed-system pyrolysis yields a reasonably good approximation of natural maturation processes to reconstruct natural fluid compositions and physical properties. Fluids affected by biodegradation (which is not a thermogenic process) do not plot on the 1:1 line. (Modified after Baur et al. 2011)

define the oil floor or at least to predict the prevailing oil type, and in unconventional resource systems, in which secondary cracking of unexpelled oil is viewed as one of the major factors controlling gas in place or rendering heavy liquids into volatile and producible fluids.

Using MSSV pyrolysis it was demonstrated that oil in conventional siliciclastic and carbonate reservoirs is much more stable than oil in source rocks, the close contact of retained, rather polar petroleum with residual organic matter and source rock mineralogy being the most likely reasons. Horsfield et al. (1992b) and Schenk et al. (1997a) predicted for four classical crude oil types that onset of gas generation occurs around 190 °C ($R_m \sim 2\%$) under natural maturation conditions and that kinetic variability among them is minor, with high-wax oils being slightly more stable than low-wax oils (10 °C differences in onset temperature) and sulfur richness not having the destabilizing effects as observed for primary kerogen conversion. In contrast, in-source secondary cracking of unexpelled oil to gas has been determined to begin earlier at ~ 150 °C ($R_o \sim 1.2\%$) for organic-rich marine Type II source rocks (Schenk et al. 1997b; Dieckmann et al. 1998; Jarvie et al. 2004), a paleotemperature range in line with gold-bag-based pyrolysis experimental results and observations of Hill et al. (2007) for the Barnett Shale unconventional resource play.

Nevertheless, depending on depositional environments or precursor biota, type II organic matter can be highly diverse, which strongly influences not only the composition of the generated fluids but also the kinetics of primary and secondary petroleum formation. As the exact timing of the onset of the breakdown of unexpelled high-molecular-weight oils has such a big impact on the economic viability of a shale resource play, default Type II source rock kinetic models implemented in almost all petroleum system modeling software (Pepper and Corvi 1995b; Pepper and Dodd 1995) should be used with caution only. One of the most time-effective, straightforward methods to determine primary and secondary cracking kinetics for individual source rocks is the GORFit model (Mahlstedt et al. 2013, 2015; Yang et al. 2016), which utilizes both open-system and closed-system MSSV pyrolysis data to directly distinguish partly overlapping primary and secondary oil and gas evolution profiles on the basis of simple stoichiometric relationships. As in earlier approaches (Schenk et al. 1997a; Dieckmann et al. 1998, 2000) and to facilitate accurate frequency factor approximations (by the shift in T_{max} as a function of heating rate), closed-system MSSV pyrolysis is performed at 3 different heating rates but only to 13 instead of 25 end temperatures per heating rate (Fig. 8).

Metagenetic late dry gas generation (Tissot et al. 1974) by a final demethylation of aromatic moieties within spent organic matter via α -cleavage mechanisms involving condensation reactions of aromatic clusters could be shown to occur between 2.0% and 3.5% R_o using MSSV and gold-bag experiments for kinetic modeling (Lorant and Behar 2002; Erdmann and Horsfield 2006; Mahlstedt 2012; Mahlstedt and Horsfield 2012). The potential to form this additional late gas appears to evolve for every source rock type by the concentration of methyl groups via beta-cleavage mechanisms during catagenesis (Mahlstedt 2012) and is not necessarily restricted to refractory kerogen in humic source rocks (Quigley et al. 1987; Quigley and Mackenzie 1988) or heterogeneous source rocks for which the late gas potential was

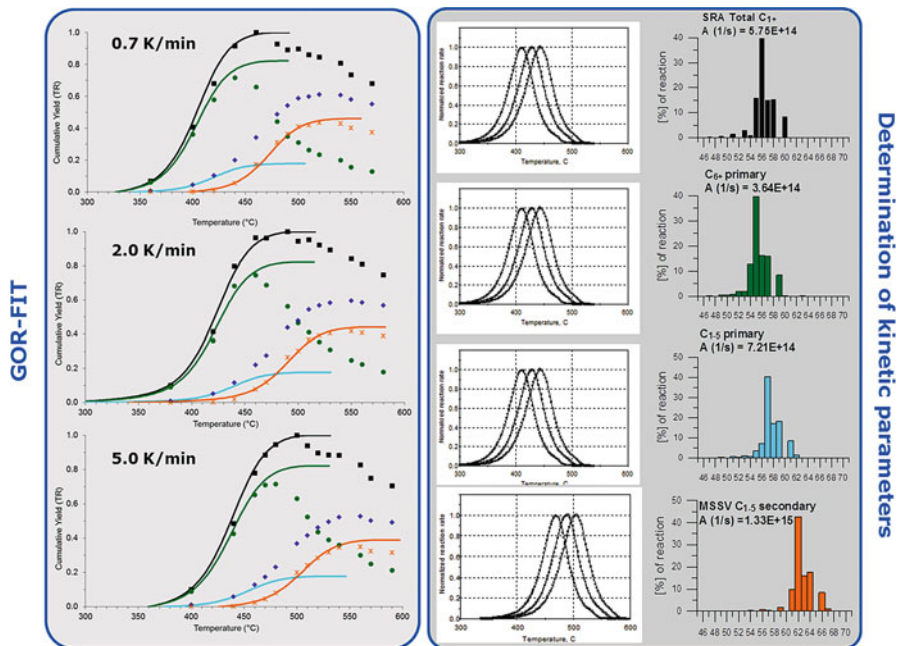


Fig. 8 The GORFit model utilizes both open-system and closed-system MSSV-pyrolysis data, derived at three different heating rates (here 0.7, 2.0 and 5.0 K/min), to determine primary and secondary cracking kinetics (LHS). Basically, the MSSV C_{1+} (black squares), C_{1-5} (dark blue diamonds), and C_{6+} (green circles) boiling fraction yields are normalized to the maximum MSSV C_{1+} yield and plotted in comparison with directly measured open-system bulk pyrolysis (SRA) transformation ratio (TR) curves (black spline curve). To approximate spline curves for the generation of primary gas C_{1-5} (bright blue spline curve) and C_{6+} (green spline curve), the C_{1+} -TR curves are directly multiplied by factors derived from a uniform open-system pyrolysis-GC-GOR and temperature shifted to fit measured MSSV C_{1-5} and C_{6+} data points until a best solution for all three heating rates is reached. Secondary gas amounts are calculated by subtracting fitted primary gas yields from measured MSSV C_{1-5} yields at corresponding temperatures (RHS). The spline curves from the LHS are directly used to calculate kinetic parameters for C_{1+} , primary C_{6+} and primary and secondary C_{1-5} formation; E_a distributions and normalized measured and calculated generation rate curves are shown. (Taken from Mahlstedt et al. 2013)

postulated to be related to a high-molecular-weight bitumen precursor structure formed during early catagenesis by back-reactions of first-formed products and residual kerogen (Dieckmann et al. 2006; Erdmann and Horsfield 2006) (Fig. 9).

4 Research Needs

The role played by source rock kerogen type and maturity in controlling the physical properties of thermogenic fluids expelled into conventional reservoirs is largely established and based on genetic relationships between kerogen moieties,

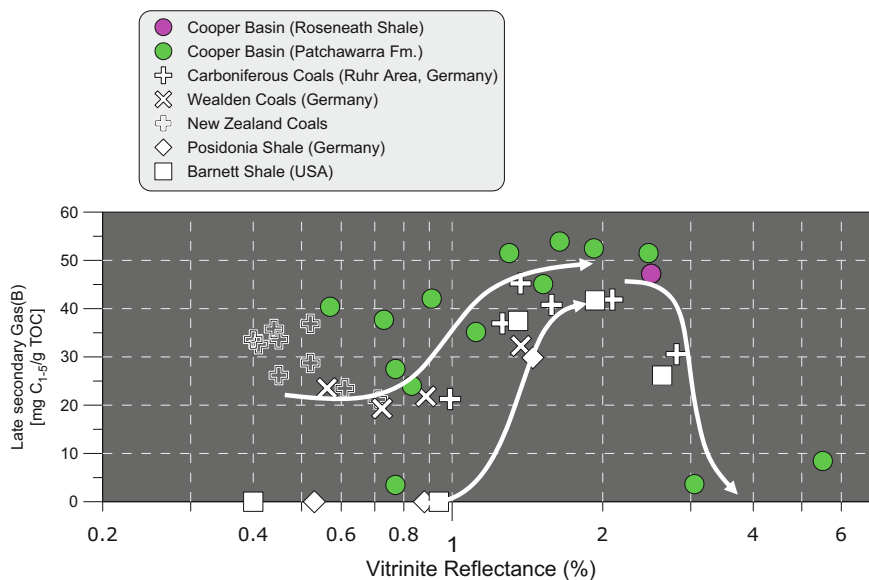


Fig. 9 High-temperature closed-system MSSV pyrolysis is used to calculate late gas potentials (“late secondary gas (B)”) which refers to a second late dry gas charge from matured organic matter subsequent to secondary cracking of oil and which goes largely unnoticed when source rock evaluation is based on open-system pyrolysis screening-methods alone. White arrows indicate how late gas potentials evolve with maturity (vitrinite reflectance) for various natural maturity series (Mahlstedt 2012; Mahlstedt et al. 2015). Late gas potentials deduced for immature samples can be underestimated and in fact increase during catagenesis up to values of at least ~40 mg/g TOC at 2.0% vitrinite reflectance for possibly any given kerogen type. Late gas potentials decrease again between 2.5% and 3.5% R_o due to the formation of late methane. (Taken from Mahlstedt et al. 2015)

deciphered by analytical and simulation pyrolysis, and hydrocarbons in petroleum. Much less can be said about the physical properties of petroleum retained in unconventional reservoirs, as in-source fluids are much more enriched in the less well-studied non-hydrocarbon fractions resins and asphaltenes than conventional oils. The chemical compositions of these fractions, which strongly govern in situ fluid behavior under various PVT conditions, e.g., the extent of fractionation during fracking leading to a preferential production of hydrocarbons over NSO compounds, are under closer investigation only since advanced analytical tools such as FT-ICR MS became available in geosciences (Mullins 2007). Thus, using various pyrolysis approaches and FT-ICR MS as the detection method is a promising research avenue to strongly improve our predictive capabilities concerning controls of kerogen type and maturity on physical properties of fluids in unconventional reservoirs. First steps are made (Mahlstedt et al. 2016), but calibration of predicted and encountered compositions in solvent extracts and produced oils is lacking for a greater variety of source rocks (Fig. 10).

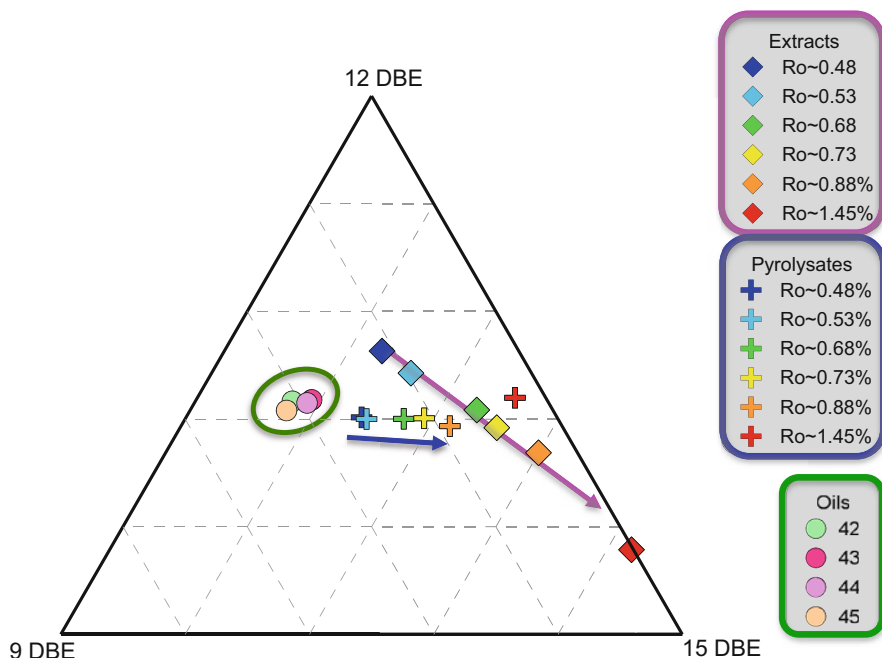


Fig. 10 Three major DBE classes of the N_1 compounds are shown in ternary diagrams for Posidonia Shale extracts and pyrolysates with increasing maturation and Posidonia Shale sourced crude oils measured using FT-ICR MS and ESI in the negative mode. As pyrolysate compounds have compositions intermediate between those of retained and expelled oil compounds, a preferential expulsion of smaller compounds in the crudes and an enhanced aromatization within retained fluids can be postulated, both mechanisms having a direct effect on the physical properties of fluids stored in unconventional versus conventional reservoirs. (Modified after Mahlstedt et al. 2016)

References

- Abrajano TA, Sturchio NC, Bohlke JK, Lyon GL, Poreda RJ, Stevens CM (1988) Methane-hydrogen gas seeps, Zambales Ophiolite, Philippines: deep or shallow origin? *Chem Geol Orig Methane Earth* 71:211–222
- Atkins P, de Paula J (2002) *Atkins' physical chemistry*, 7th edn. Oxford University Press, Oxford
- Bakr M, Akiyama M, Sanada Y, Yokono T (1988) Radical concentration of kerogen as a maturation parameter. *Org Geochem* 12:29–32
- Bakr MY, Akiyama M, Sanada Y (1990) ESR assessment of kerogen maturation and its relation with petroleum genesis. *Org Geochem* 15:595–599
- Bakr M, Akiyama M, Sanada Y (1991) In situ high temperature ESR measurements for kerogen maturation. *Org Geochem* 17:321–328
- Baskin DK, Peters KE (1992) Early generation characteristics of a sulfur-rich Monterey kerogen. *AAPG Bull* 76:1–13
- Baur F, di Primio R, Lampe C, Littke R (2011) Mass balance calculations for different models of hydrocarbon migration in the Jeanne D'Arc Basin, offshore Newfoundland. *J Pet Geol* 34:181–198

- Behar F, Kressmann S, Rudkiewicz JL, Vandenbroucke M (1991) Experimental simulation in a confined system and kinetic modelling of kerogen and oil cracking. *Org Geochem* 19:173–189
- Behar F, Vandenbroucke M, Teermann SC, Hatcher PG, Leblond C, Lerat O (1995) Experimental simulation of gas generation from coals and a marine kerogen. *Chem Geol Process Nat Gas Form* 126:247–260
- Behar F, Roy S, Jarvie D (2010) Artificial maturation of a type I kerogen in closed system: mass balance and kinetic modelling. *Org Geochem* 41:1235–1247
- Berner U, Faber E, Scheeder G, Panten D (1995) Primary cracking of algal and landplant kerogens: kinetic models of isotope variations in methane, ethane and propane. *Chem Geol Process Nat Gas Form* 126:233–245
- Braun RL, Burnham AK (1992) PMOD: a flexible model of oil and gas generation, cracking, and expulsion. *Org Geochem* 19:161–172
- Braun RL, Rothman AJ (1975) Oil-shale pyrolysis: kinetics and mechanism of oil production. *Fuel* 54:129–131
- Burnham AK (2017a) Classification and characterization. In: Burnham AK (ed) *Global chemical kinetics of fossil fuels: how to model maturation and pyrolysis*. Springer International Publishing, Cham, pp 1–24
- Burnham AK (2017b) Introduction to chemical kinetics. In: Burnham AK (ed) *Global chemical kinetics of fossil fuels: how to model maturation and pyrolysis*. Springer International Publishing, Cham, pp 25–74
- Cane RF, Albion PR (1973) The organic geochemistry of torbanite precursors. *Geochim Cosmochim Acta* 37:1543–1549
- Carr AD, Snape CE, Meredith W, Uguna C, Scotchman IC, Davis RC (2009) The effect of water pressure on hydrocarbon generation reactions: some inferences from laboratory experiments. *Pet Geosci* 15:17–26
- Coolles GP, Mackenzie AS, Quigley TM (1986) Calculation of petroleum masses generated and expelled from source rocks. *Org Geochem* 10:235–245
- Dahl J, Hallberg R, Kaplan IR (1988) The effects of radioactive decay of uranium on elemental and isotopic ratios of Alum shale kerogen. *Appl Geochem* 3:583–589
- di Primio R (2002) Unraveling secondary migration effects through the regional evaluation of PVT data: a case study from Quadrant 25, NOCS. *Org Geochem* 33:643–653
- di Primio R, Horsfield B (2006) From petroleum-type organofacies to hydrocarbon phase prediction. *AAPG Bull* 90:1031–1058
- di Primio R, Skeie JE (2004a) Development of a compositional kinetic model for hydrocarbon generation and phase equilibria modelling: a case study from Snorre Field, Norwegian North Sea. pp 157–174
- di Primio R, Skeie JE (2004b) Development of a compositional kinetic model for hydrocarbon generation and phase equilibria modelling: a case study from Snorre Field, Norwegian North Sea. In: Cubitt JM, England WA, Larter SR (eds) *Understanding petroleum reservoirs: towards an integrated reservoir engineering and geochemical approach*. Geological Society Special Publication, London, pp 157–174
- di Primio R, Dieckmann V, Mills N (1998a) PVT and phase behaviour analysis in petroleum exploration. *Organic geochemistry – advances in organic geochemistry 1997 proceedings of the 18th international meeting on organic geochemistry part I*. *Pet Geochem* 29:207–222
- di Primio R, Dieckmann V, Mills N (1998b) PVT and phase behaviour analysis in petroleum exploration. *Org Geochem* 29:207–222
- Dieckmann V (2005) Modelling petroleum formation from heterogeneous source rocks: the influence of frequency factors on activation energy distribution and geological prediction. *Mar Pet Geol* 22:375–390
- Dieckmann V, Schenk HJ, Horsfield B, Welte DH (1998) Kinetics of petroleum generation and cracking by programmed-temperature closed-system pyrolysis of Toarcian Shales. *Fuel* 77:23–31

- Dieckmann V, Schenk HJ, Horsfield B (2000) Assessing the overlap of primary and secondary reactions by closed- versus open-system pyrolysis of marine kerogens. *J Anal Appl Pyrolysis* 56:33–46
- Dieckmann V, Ondrak R, Cramer B, Horsfield B (2006) Deep basin gas: new insights from kinetic modelling and isotopic fractionation in deep-formed gas precursors. *Mar Pet Geol* 23:183–199
- Dueppenbecker S, Horsfield B (1990) Compositional information for kinetic modelling and petroleum type prediction. *Org Geochem* 16:259–266
- Düppenbecker SJ, Horsfield B (1990) Compositional information for kinetic modelling and petroleum type prediction. *Org Geochem* 16:259–266
- Durand B, Nicaise G, Roucaché J, Vandenbroucke M, Hagemann HW (1977) Etude géochimique d'une série de charbons. In: Campo R, Goñi J (eds) *Advances in organic geochemistry 1975*. ENADIMSA, Madrid, pp 601–631
- Eglinton TI, Sinninghe Damsté JS, Kohnen MEL, de Leeuw JW (1990) Rapid estimation of the organic sulphur content of kerogens, coals and asphaltenes by pyrolysis-gas chromatography. *Fuel* 69:1394–1404
- England W, Mackenzie A (1989) Some aspects of the organic geochemistry of petroleum fluids. *Geol Rundsch* 78:291–303
- England WA, Mackenzie AS, Mann DM, Quigley TM (1987) The movement and entrapment of petroleum fluids in the subsurface. *J Geol Soc* 144:327–347
- Erdmann M (1999) Gas generation from overmature Upper Jurassic source rocks, Northern Viking Graben. RWTH Aachen, Aachen, p 128
- Erdmann M, Horsfield B (2006) Enhanced late gas generation potential of petroleum source rocks via recombination reactions: evidence from the Norwegian North Sea. *Geochim Cosmochim Acta* 70:3943–3956
- Ericsson I, Lattimer R (1989) Pyrolysis nomenclature. *J Anal Appl Pyrolysis* 14:219–221
- Espitalié J, Laporte JL, Madec M, Marquis F, Leplat P, Paulet J, Boutefeu A (1977) Méthode rapide de caractérisation des roches mères, de leur potentiel pétrolier et de leur degré d'évolution. *Oil Gas Sci Technol Rev IFP* 32:23–42
- Espitalié J, Madec M, Tissot B (1980) Role of mineral matrix in kerogen pyrolysis; influence on petroleum generation and migration. *AAPG Bull* 64:59–66
- Espitalié J, Deroo G, Marquis F (1985) Rock-Eval pyrolysis and its applications. *Rev Inst Fr Petrole* 40:563–579
- Espitalié J, Marquis F, Sage L (1987) Organic geochemistry of the Paris Basin. In: Brooks J, Glennie K (eds) *Petroleum geology of North West Europe*. Graham and Trotman, London, pp 71–86
- Faber E, Stahl WJ, Whiticar MJ (1992) Distinction of bacterial and thermogenic hydrocarbons. In: Vially R (ed) *Bacterial gas*. Editions Technip, Paris
- Forsman JP, Hunt JM (1958) Insoluble organic matter (kerogen) in sedimentary rocks. *Geochim Cosmochim Acta* 15:170–182
- Freund H, Walters CC, Kelemen SR, Siskin M, Gorbaty ML, Curry DJ, Bence AE (2007) Predicting oil and gas compositional yields via chemical structure-chemical yield modeling (CS-CYM): part 1 – concepts and implementation. *Org Geochem* 38:288–305
- Given PH (1960) The distribution of hydrogen in coals and its relation to coal structure. *Fuel* 39:147–153
- Greensfelder BS, Voge HH, Good GM (1949) Catalytic and thermal cracking of pure hydrocarbons: mechanisms of reaction. *Ind Eng Chem* 41:2573–2584
- Han Y, Mahlstedt N, Horsfield B (2015) The Barnett Shale: compositional fractionation associated with intraformational petroleum migration, retention, and expulsion. *AAPG Bull* 99:2173–2202
- Hatcher PG, Faulon JL, Wenzel KA, Cody GD (1992) A structural model for lignin-derived vitrinite from high-volatile bituminous coal (coalified wood). *Energy Fuel* 6:813–820
- Hill RJ, Zhang E, Katz BJ, Tang Y (2007) Modeling of gas generation from the Barnett Shale, Fort Worth Basin, Texas. *AAPG Bull* 91:501–521

- Horsfield B (1984) Pyrolysis studies and petroleum exploration. In: Brooks J, Welte DH (eds) *Advances in petroleum geochemistry*. Academic, London, pp 47–298
- Horsfield B (1989) Practical criteria for classifying kerogens: some observations from pyrolysis-gas chromatography. *Geochim Cosmochim Acta* 53:891–901
- Horsfield B (1997) The bulk composition of first-formed petroleum in source rocks. In: Welte DH, Horsfield B, Backer DR (eds) *Petroleum and basin evolution*. Springer, Berlin, pp 335–402
- Horsfield B, Douglas AG (1980) The influence of minerals on the pyrolysis of kerogens. *Geochim Cosmochim Acta* 44:1119–1131
- Horsfield B, Dembicki H Jr, Ho TTY (1983) Some potential applications of pyrolysis to basin studies. *J Geol Soc* 140:431–443
- Horsfield B, Yordy KL, Crelling JC (1988) Determining the petroleum-generating potential of coal using organic geochemistry and organic petrology. *Org Geochem* 13:121–129
- Horsfield B, Disko U, Leistner F (1989) The micro-scale simulation of maturation: outline of a new technique and its potential applications. *Geol Rundsch* 78:361–374
- Horsfield B, Bharati S, Larter SR, Leistner F, Littke R, Schenk HJ, Dypvik H (1992a) On the atypical petroleum-generation characteristics of alginite in the Cambrian Alum Shale. In: Schidlowski M, Golubic S, Kimberly MM, McKirdy DM, Trudinger PA (eds) *Early organic evolution: implications for mineral and energy resources*. Springer-Verlag, Berlin, Heidelberg, pp 257–266
- Horsfield B, Schenk HJ, Mills N, Welte DH (1992b) An investigation of the in-reservoir conversion of oil to gas: compositional and kinetic findings from closed-system programmed-temperature pyrolysis. *Org Geochem* 19:191–204
- Horsfield B, Schenk HJ, Zink K, Ondrak R, Dieckmann V, Kallmeyer J, Mangelsdorf K, di Primio R, Wilkes H, Parkes RJ, Fry J, Cragg B (2006) Living microbial ecosystems within the active zone of catagenesis: implications for feeding the deep biosphere. *Earth Planet Sci Lett* 246:55–69
- Horsfield B, Leistner F, Hall K (2015) Microscale sealed vessel pyrolysis, Chapter 7. In: Grice K (ed) *Principles and practice of analytical techniques in geosciences*. The Royal Society of Chemistry, Cambridge, UK, pp 209–250
- Hunt JM (1995) *Petroleum geochemistry and geology*, 2nd edn. W.H. Freeman and Company, New York
- Isaksen GH, Curry DJ, Yeakel JD, Jenssen AI (1998) Controls on the oil and gas potential of humic coals. *Organic geochemistry – advances in organic geochemistry 1997 proceedings of the 18th international meeting on organic geochemistry part I*. *Pet Geochem* 29:23–44
- Ishiwatari R, Ishiwatari M, Kaplan IR, Rohrback BG (1976) Thermal alteration of young kerogen in relation to petroleum. *Genesis* 264:347–349
- Ishiwatari R, Ishiwatari M, Rohrback BG, Kaplan IR (1977) Thermal alteration experiments on organic matter from recent marine sediments in relation to petroleum genesis. *Geochim Cosmochim Acta* 41:815–828
- Jarvie DM, Hill RJ, Pollastro RM (2004) Assessment of the gas potential and yields from shales: the Barnett Shale model. In: Cardott BJ (ed) *Unconventional energy resources in the southern mid-continent, 2004 conference: Oklahoma geological survey circular 110*, Oklahoma City, p 34
- Jarvie DM, Hill RJ, Ruble TE, Pollastro RM (2007) Unconventional shale-gas systems: the Mississippian Barnett Shale of north-central Texas as one model for thermogenic shale-gas assessment. *AAPG Bull* 91:475–499
- Javaid AA (2000) PVT modelling of reservoir fluids from the Norwegian North Sea. Oslo University, Oslo
- Jones RW (1987) Organic facies. In: Brooks J, Welte DH (eds) *Advances in petroleum geochemistry*, vol 2. Academic, London, pp 1–90
- Jüntgen H (1964) Reaktionskinetische Überlegungen zur Deutung von Pyrolyse-Reaktionen. *Erdöl und Kohle-Erdgas-Petrochemie* 17:180–186
- Kissin YV (1987) Catagenesis and composition of petroleum: origin of n-alkanes and isoalkanes in petroleum crudes. *Geochim Cosmochim Acta* 51:2445–2457
- Kossiakoff A, Rice FO (1943) Thermal decomposition of hydrocarbons, resonance stabilization and isomerization of free radicals. *J Am Chem Soc* 65:590–595

- Krooss BM, Littke R, Muller B, Frielingsdorf J, Schwochau K, Idiz EF (1995) Generation of nitrogen and methane from sedimentary organic matter: implications on the dynamics of natural gas accumulations. *Chem Geol Process Nat Gas Form* 126:291–318
- Kuhn P, Di Primio R, Horsfield B (2010) Bulk composition and phase behaviour of petroleum sourced by the Bakken Formation of the Williston Basin. *Petroleum Geology Conference Proceedings*, pp 1065–1077
- Kuhn PP, di Primio R, Hill R, Lawrence JR, Horsfield B (2012) Three-dimensional modeling study of the low-permeability petroleum system of the Bakken Formation. *AAPG Bull* 96:1867–1897
- Larter SR (1984) Application of analytical pyrolysis techniques to kerogen characterisation and fossil fuel exploration/exploitation. In: Voorhees K (ed) *Analytical pyrolysis, methods and applications*. Butterworth, London, pp 212–275
- Larter SR, Horsfield B (1993) Determination of structural components of kerogens by the use of analytical pyrolysis methods. In: Engel MH, Macko SA (eds) *Organic geochemistry – principles and applications*. Plenum Press, New York, pp 271–287
- Lewan MD (1985) Evaluation of petroleum generation by hydrous pyrolysis experimentation. *Philos Trans R Soc Lond Ser A* 315:123–134
- Lewan MD (1993) Laboratory simulation of petroleum formation: hydrous pyrolysis. In: Engel MH, Macko S (eds) *Organic geochemistry principles and applications*. Plenum Press, New York, pp 419–442
- Lewan MD, Buchardt B (1989) Irradiation of organic matter by uranium decay in the Alum Shale, Sweden. *Geochim Cosmochim Acta* 53:1307–1322
- Lewan MD, Comer JB, Hamilton-Smith T, Hasenmueller NR, Guthrie JM, Hatch JR, Gautier DL, Frankie WT (1995) Feasibility study of material-balance assessment of petroleum from the New Albany shale in the Illinois basin. *U. S. Geological Survey Bulletin* 2137
- Lorant F, Behar F (2002) Late generation of methane from mature kerogens. *Energy Fuel* 16:412–427. <https://doi.org/10.1021/ef010126x>
- Mackenzie A, Quigley TM (1988) Principles of geochemical prospect appraisal. *Am Assoc Pet Geol Bull* 72:399–415
- Mahlstedt N (2012) Evaluating the late gas potential of source rocks stemming from different sedimentary environments. Dissertation. Technische Universität Berlin, Berlin, p 342
- Mahlstedt N, Horsfield B (2012) Metagenetic methane generation in gas shales I. Screening protocols using immature samples. *Mar Pet Geol Insights Shale Gas Explor Exploitation* 31:27–42
- Mahlstedt N, Horsfield B, di Primio R (2013) GORFit – from liquids to late gas: deconvoluting primary from secondary gas generation kinetics. 26th International Meeting on Organic Geochemistry (IMOG), Tenerife, Canary Islands (Spain). *Book of Abstracts*, p 193
- Mahlstedt N, Hübner A, Primio R, Horsfield B (2014) Think molecular. *Geo-Info* 11(2):74–78
- Mahlstedt N, di Primio R, Horsfield B, Boreham CJ (2015) Multi-component kinetics and late gas potential of selected Cooper Basin source rocks. *Record 2015/19 Geoscience Australia, Canberra*, p 199. <https://doi.org/10.11636/Record.12015.11019>
- Mahlstedt N, Horsfield B, Wilkes H, Poetz S (2016) Tracing the impact of fluid retention on bulk petroleum properties using nitrogen-containing compounds. *Energy Fuels* 30:6290–6305
- Mango FD (1992) Transition metal catalysis in the generation of petroleum and natural gas. *Geochim Cosmochim Acta* 56:553–555
- Mango FD, Elrod LW (1999) The carbon isotopic composition of catalytic gas: a comparative analysis with natural gas. *Geochim Cosmochim Acta* 63:1097–1106
- Mango FD, Hightower J (1997) The catalytic decomposition of petroleum into natural gas. *Geochim Cosmochim Acta* 61:5347–5350
- Mango FD, Hightower JW, James AT (1994) Role of transition-metal catalysis in the formation of natural gas. *Nature* 368:536–538
- Marchand A, Conard J (1980) Electron paramagnetic resonances in kerogen studies. In: Durand B (ed) *Kerogen: insoluble organic matter from sedimentary rocks*. Editions Technip, Paris, pp 243–270
- McMillen DF, Malhotra R (2006) Hydrogen transfer in the formation and destruction of retrograde products in coal conversion. *Chem A Eur J* 110:6757–6770

- Michels R, Landis P, Philp RP, Torkelson BE (1995) Influence of pressure and the presence of water on the evolution of the residual kerogen during confined, hydrous, and high-pressure hydrous pyrolysis of Woodford Shale. *Energy Fuel* 9:204–215
- Michels R, Enjelvin-Raoult N, Elie M, Mansuy L, Faure P, Oudin JL (2002) Understanding of reservoir gas compositions in a natural case using stepwise semi-open artificial maturation. *Mar Pet Geol* 19:589–599
- Monin JC, Connan J, Oudin JL, Durand B (1990) Quantitative and qualitative experimental approach of oil and gas generation: application to the North Sea source rocks. *Org Geochem* 16:133–142
- Monthioux M, Landais P, Monin J-C (1985) Comparison between natural and artificial maturation series of humic coals from the Mahakam delta. *Indones Org Geochem* 8:275–292
- Mullins OC (2007) Petroleomics and structure-function relations of crude oils and asphaltenes. In: Mullins OC, Sheu EY, Hammami A, Marshall AG (eds) *Asphaltenes, heavy oils, and Petroleomics*. Springer Science & Business Media, New York, pp 1–16
- Muscio GPA, Horsfield B (1996) Neof ormation of inert carbon during the natural maturation of a marine source rock: Bakken Shale, Williston Basin. *Energy Fuel* 10:10–18
- Orr WL (1986) Kerogen/asphaltene/sulfur relationships in sulfur-rich Monterey oils. *Org Geochem* 10:499–516
- Payne DF, Ortoleva PJ (2001) A model for lignin alteration – part I: a kinetic reaction-network model. *Org Geochem* 32:1073–1085
- Pelet R (1985) Évaluation quantitative des produits formés lors de l'évolution géochimique de la matière organique. *Rev Inst Fr Pétrole* 40:551–562
- Pepper AS, Corvi PJ (1995a) Simple kinetic models of petroleum formation. Part III: modelling an open system. *Mar Pet Geol* 12:417–452
- Pepper AS, Corvi PJ (1995b) Simple kinetic models of petroleum formation. Part I: oil and gas generation from kerogen. *Mar Pet Geol* 12:291–319
- Pepper AS, Dodd TA (1995) Simple kinetic models of petroleum formation. Part II: oil-gas cracking. *Mar Pet Geol* 12:321–340
- Peters KE, Walters CC, Moldowan JM (2005) *The biomarker guide*. Cambridge University Press, Cambridge, UK
- Philippi GT (1965) On the depth, time and mechanism of petroleum generation. *Geochim Cosmochim Acta* 29:1021–1049
- Pitt GJ (1961) The kinetics of the evolution of volatile products from coal. In: 4th international conference on coal science, Le Touquet
- Quigley TM, Mackenzie AS (1988) The temperatures of oil and gas formation in the sub-surface. *Nature* 333:549–552
- Quigley TM, Mackenzie AS, Gray JR (1987) Kinetic theory of petroleum generation. In: Doligez B (ed) *Migration of hydrocarbons in sedimentary basins*. Editions Technip, Paris, pp 649–666
- Radke M, Horsfield B, Littke R, Rullkötter J (1997) Maturation and petroleum generation. In: Welte DH, Horsfield B, Backer DR (eds) *Petroleum and basin evolution*. Springer, Berlin, pp 169–230
- Rice FO (1933) The thermal decomposition of organic compounds from the standpoint of free radicals. III. The calculation of the products formed from paraffin hydrocarbons. *J Am Chem Soc* 55:3035–3040
- Rullkötter J, Michaelis W (1990) The structure of kerogen and related materials. A review of recent progress and future trends. *Org Geochem Proc 14th Int Meet Org Geochem* 16:829–852
- Santamaria-Orozco D, Horsfield B (2004) Gas generation potential of Upper Jurassic (Tithonian) source rocks in the Sonda de Campeche, Mexico. In: Bartolini C, Buffler RT, Blickwede RF (eds) *The circum-Gulf of Mexico and the Caribbean: hydrocarbon habitats, basin formation and plate tectonics*, AAPG Memoir ed. American Association of Petroleum Geologists, Tulsa
- Schenk HJ, Horsfield B (1998) Using natural maturation series to evaluate the utility of parallel reaction kinetics models: an investigation of Toarcian shales and Carboniferous coals, Germany. *Org Geochem* 29:137–154

- Schenk HJ, Di Primio R, Horsfield B (1997a) The conversion of oil into gas in petroleum reservoirs. Part 1: comparative kinetic investigation of gas generation from crude oils of lacustrine, marine and fluviodeltaic origin by programmed-temperature closed-system pyrolysis. *Org Geochem* 26:467–481
- Schenk HJ, Horsfield B, Krooss B, Schaefer RG, Schwochau K (1997b) Kinetics of petroleum formation and cracking. In: Welte DH, Horsfield B, Backer DR (eds) *Petroleum and basin evolution*. Springer, Berlin, pp 231–270
- Schoell M (1988) Multiple origins of methane in the Earth. *Chem Geol Orig Methane Earth* 71:1–10
- Scott AC (1989) Observations on the nature and origin of fusain. *Int J Coal Geol* 12:443–475
- Smith GC, Cook AC (1984) Petroleum occurrence in the Gippsland Basin and its relationship to rank and organic matter type. *Aust Pet Explor Assoc J* 24:196–216
- Solomon PR, Hamblen DG, Carangelo RM, Serio MA, Deshpande GV (1988) General model of coal devolatilization. *Energy Fuel* 2:405–422
- Stach E, Mackowsky M-T, Teichmüller M, Taylor GH, Chandra D, Teichmüller R (1982) *Stach's textbook of coal petrology*, 3rd edn. Gebrüder Borntraeger, Stuttgart
- Stockhausen M, Galimberti R, Elias R, Schwark L (2013) Experimental simulation of hydrocarbon expulsion. In: 26th international meeting on organic geochemistry. Book of abstracts, Costa Adeje, Tenerife
- Tegelaar EW, Noble RA (1994) Kinetics of hydrocarbon generation as a function of the molecular structure of kerogen as revealed by pyrolysis-gas chromatography. *Org Geochem* 22:543–574
- Tegelaar EW, de Leeuw JW, Derenne S, Largeau C (1989) A reappraisal of kerogen formation. *Geochim Cosmochim Acta* 53:3103–3106
- Thompson S, Cooper BS, Morley RJ, Barnard PC (1985) Oil-generating coals. In: Thomas BM (ed) *Petroleum geochemistry in exploration of the Norwegian shelf*. Graham and Trotman, London, pp 59–73
- Tissot BP (1969) Premières données sur les mécanismes et la cinétique de la formation du pétrole dans les sédiments – Simulation d'un schéma réactionnel sur ordinateur. *Oil Gas Sci Technol Rev IFP* 24:470–501
- Tissot BP, Espitalié J (1975) L'évolution de la matière organique des sédiments: application d'une simulation mathématique. *Rev IFP* 30:743–777
- Tissot BP, Welte DH (1978) *Petroleum formation and occurrence*, 1st edn. Springer, Berlin
- Tissot BP, Welte DH (1984) *Petroleum formation and occurrence*, 2nd edn. Springer, Berlin
- Tissot B, Califet-Debyser Y, Deroo G, Oudin JL (1971) Origin and evolution of hydrocarbons in early Toarcian shales, Paris Basin, France. *Am Assoc Pet Geol Bull* 55:177–2193
- Tissot BP, Durand B, Espitalié J, Combaz A (1974) Influence of nature and diagenesis of organic matter in formation of petroleum. *AAPG Bull* 58:499–506
- Ugana CN, Snape CE, Meredith W, Carr AD, Scotchman IC, Davies RC (2012) Retardation of hydrocarbon generation and maturation by water pressure in geologic basins: an experimental investigation. In: Peters DJC KE, Kacwicz M (eds) *Basin modeling: new horizons in research and applications*. AAPG Hedberg series, no. 4. American Association of Petroleum Geologists, Tulsa, pp 19–37
- Ungerer P (1990) State of the art of research in kinetic modelling of oil formation and expulsion. *Org Geochem Proc 14th Int Meet Org Geochem* 16:1–25
- Ungerer P, Pelet R (1987) Extrapolation of the kinetics of oil and gas formation from laboratory experiments to sedimentary basins. *Nature* 327:52–54
- Van Krevelen DW (1961) *Coal: typology – chemistry – physics – constitution*, 1st edn. Elsevier, Amsterdam
- van Krevelen DW, van Heerden C, Huntjens FJ (1951) Physicochemical aspects of the pyrolysis of coal and related organic compounds. *Fuel* 30:253–259
- Vandenbroucke M, Largeau C (2007) Kerogen origin, evolution and structure. *Org Geochem* 38:719–833

- Walters CC (2006) The origin of petroleum. In: Hsu CS, Robinson PR (eds) *Practical advances in petroleum processing*, 1st edn. Springer, New York, pp 79–101
- Walters CC, Freund H, Kelemen SR, Peczak P, Curry DJ (2007) Predicting oil and gas compositional yields via chemical structure-chemical yield modeling (CS-CYM): part 2 – application under laboratory and geologic conditions. *Org Geochem* 38:306–322
- Welhan JA (1988) Origins of methane in hydrothermal systems. *Chem Geol Orig Methane Earth* 71:183–198
- Welte DH, Horsfield B, Baker DR (1997) *Petroleum and basin evolution: insights from petroleum geochemistry, geology and basin modeling*. Springer Science & Business Media, Berlin
- Whiticar MJ (1994) Correlation of natural gases with their source. In: Magoon L, Dow W (eds) *The petroleum system: from source to trap*. AAPG Memoir. The American Association of Petroleum Geologists, Tulsa, pp 261–283
- Wilkes H (2018) Methods of hydrocarbon analysis. In: Wilkes H (ed) *Hydrocarbons, oils and lipids: diversity, origin, chemistry and fate*. Handbook of hydrocarbon and lipid microbiology. Springer, Cham
- Wilkins RWT, George SC (2002) Coal as a source rock for oil: a review. *Int J Coal Geol* 50:317–361
- Yang S, Horsfield B (2016) Some predicted effects of minerals on the generation of petroleum in nature. *Energy Fuel* 30:6677–6687
- Yang S, Horsfield B, Mahlstedt N, Stephenson M, Könitzer S (2016) On the primary and secondary petroleum generating characteristics of the Bowland Shale, northern England. *J Geol Soc* 173:292–305
- Yang S, Schulz H-M, Schovsbo NH, Bojesen-Koefoed JA (2017) Oil-source rock correlation of the Lower Palaeozoic petroleum system in the Baltic Basin (northern Europe). *AAPG Bull* 101:1971–1993



Brian Horsfield, Hans-Martin Schulz, Sylvain Bernard,
Nicolaj Mahlstedt, Yuanjia Han, and Sascha Kuske

Contents

1	Introduction	524
1.1	What Is Shale Gas?	525
1.2	What Is Shale Oil?	526
1.3	The Organic Carbon Cycle	527
1.4	Investigative Tools at Our Disposal	528
1.5	Factors Governing Shale Prospectivity	528
2	Original Organic Matter in Shales	530
2.1	Depositional Environment	530
2.2	Under the Microscope	531
2.3	Building Blocks in Organic Macromolecules	532
2.4	Generating Potentials	534
3	Conversion	534
3.1	Primary Cracking of Kerogen and Bitumen	534
3.2	Secondary Cracking of Oil	535
3.3	Role of Catalysis	536
3.4	Radiolysis Effects	536
3.5	Maturity Parameters	536
3.6	Mass Balance Modelling	537
4	Retention	538
4.1	Shale Porosity and Kerogen Swelling	539
4.2	Quantification of Precursors and Retained Products	539
5	Production Characteristics	542
5.1	Recognition of Sweet Spots Within Heterogeneous Sequences	542

B. Horsfield (✉) · H.-M. Schulz · N. Mahlstedt · Y. Han · S. Kuske
GFZ German Research Centre for Geosciences, Organic Geochemistry, Potsdam, Germany
e-mail: horsf@gfz-potsdam.de; schulzhm@gfz-potsdam.de; nick@gfz-potsdam.de;
yuanjia@gfz-potsdam.de; skuske@gfz-potsdam.de

S. Bernard
Muséum National d'Histoire Naturelle, Sorbonne Université, CNRS UMR 7590, IRD, Institut de
Minéralogie, de Physique des Matériaux et de Cosmochimie, IMPMC, Paris, France
e-mail: sbernard@mnhn.fr

5.2	Rapid Insight into <i>In-Situ</i> Physical Properties of Fluids	545
5.3	Fractionation During Production: Insights from PVT Modelling	545
6	Research Needs for Unconventional Resource Assessments	547
	References	548

Abstract

Organic matter dispersed in shales and mudstones is 10,000 times more abundant than that occurring in concentrated forms such as oil, gas, coal, and gas hydrates. So-called shale plays, distributed across all continents, are fairways where shale gas and shale oil might be extracted economically from targeted volumes of what is an extremely large potential resource. Almost all shale gas and oil reservoirs currently being exploited were formerly buried to great depth during which time gas generation took place, and then geologically uplifted to depths where extraction is feasible commercially. Productive shale reservoirs are brittle rather than elastic and therefore suitable for hydraulic fracturing to be employed effectively for releasing the dispersed gas. In this chapter we provide an overview of the chemical, physical, and biological processes involved in the formation of shale gas and shale oil and outline how organic geochemistry can be applied to the exploration and production of these resources.

1 Introduction

In the short space of 10 years following the turn of the millennium, shale gas completely transformed the global energy market. This new natural gas resource, extracted in more than 30 sedimentary basins across the continental USA and others worldwide, accounted for about 1% of gas production in the USA in 2000, 10% in 2011, and may account for nearly two-thirds of total US production by 2025 (Energy Information Administration 2017). It all began in the Fort Worth Basin (Texas) where the integration of directional drilling and hydraulic fracturing (fracking) enabled natural gas to be extracted economically from the Barnett Shale (Jarvie 2012a). The technology was rapidly deployed to target other shale-bearing formations elsewhere, including the Fayetteville Shale (Arkansas), the Woodford Shale (Oklahoma), the Haynesville Shale (Louisiana and Texas), and the Marcellus Shale (Pennsylvania). A similar story rapidly unfolded for shale oil as the technology used for shale gas exploitation was modified to produce liquid petroleum from inter alia the Bakken Shale of North Dakota, the Eagle Ford and Wolfcamp Formations of Texas, and the Niobrara Formation of Colorado (Jarvie 2012b). The opening up of these new shale resource plays transformed the global oil market because the monopoly of the Organization of the Petroleum Exporting Countries (OPEC) was challenged, and the USA saw itself as becoming the world's biggest oil producer by 2020 and being energy self-sufficient by 2025 (Energy Information Administration 2017). However, the ability to rapidly (over)supply produced fluids to the world market actually played a major role in the ultimate collapse of both gas and oil prices worldwide, making the future of shale gas and shale oil uncertain.

To put shale gas and shale oil resources in perspective, there are 10^{16} tonnes of organic matter dispersed in sedimentary rocks; this is 10,000 times greater than the organic matter occurring in concentrated forms such as oil and gas (collectively termed petroleum), coal, and gas hydrates (Killops and Killops 2005). The vast bulk of this dispersed sedimentary organic matter is contained within very fine-grained rocks such as shales and mudstones whose mineral matrices vary in their relative proportions of silica and feldspars, clays, and carbonates (Aplin and Macquaker 2011; Gamero Diaz et al. 2013; Macquaker and Adams 2003; Macquaker et al. 2014; Passey et al. 2010). Thus, the *in-situ* shale gas resource potential seen globally is extremely large and distributed across all continents. A first estimation of global shale gas resources was published by Rogner (1997; $16,112 \times 10^{12}$ standard cubic feet) with North America and China as the regions with the largest potential (both around $3,000\text{--}4,000 \times 10^{12}$ standard cubic feet). According to the *World Energy Outlook 2013* published by the US Energy Information Administration, China has the largest “wet” shale gas resources of unproved technically recoverable 1,115 trillion cubic feet (Tcf), followed by Argentina (802 Tcf) and Algeria (707 Tcf). By far the largest unproven technically recoverable shale oil (tight oil) resource occurs in the USA with 78 billion barrels (BBL) and in Russia (75 BBL). Lower but still highly significant resource potentials have been calculated for China (32 BBL) and the United Arab Emirates (23 BBL). In this context, Europe has only minor shale gas and shale oil resources. While Western Canada, Argentina, and China continue to explore for and successfully produce shale gas and shale oil, the rest of the world is still at a relatively early phase of development. This is largely because of low oil and gas prices. In the case of Europe, the continuing controversy surrounding the real versus perceived impact of shale gas extraction on the environment *sensu lato* continues to block a logical and balanced evaluation of many promising stratigraphic target formations (International Energy Agency 2012; Hübner et al. 2013; Vetter and Horsfield 2014).

1.1 What Is Shale Gas?

Natural gas features prominently in all national energy portfolios. Because of its relatively low-carbon footprint and flexible utilization, natural gas is widely regarded as the most important bridge to a low-carbon energy future. In stark contrast to conventional accumulations, where the gas now occurring in coarse-grained reservoir rocks within structural or stratigraphic traps is generated in and expelled from distant source “kitchens,” unconventional shale gas is disseminated within myriads of tiny (nm sized) pores within the source rock or adsorbed on its mineral and organic particle surfaces (Fig. 1). Individual resource plays extend across tens and hundreds of kilometers laterally and tens to hundreds of meters vertically at depths ranging from 2 to 4 km. They are characterized by widespread gas saturation, subtle trapping mechanisms, and relatively short intraformational hydrocarbon migration distances (e.g., Curtis 2002; Jarvie et al. 2007; Boyer et al. 2011; Bernard and Horsfield 2014). The gas can only be released effectively using controlled hydraulic

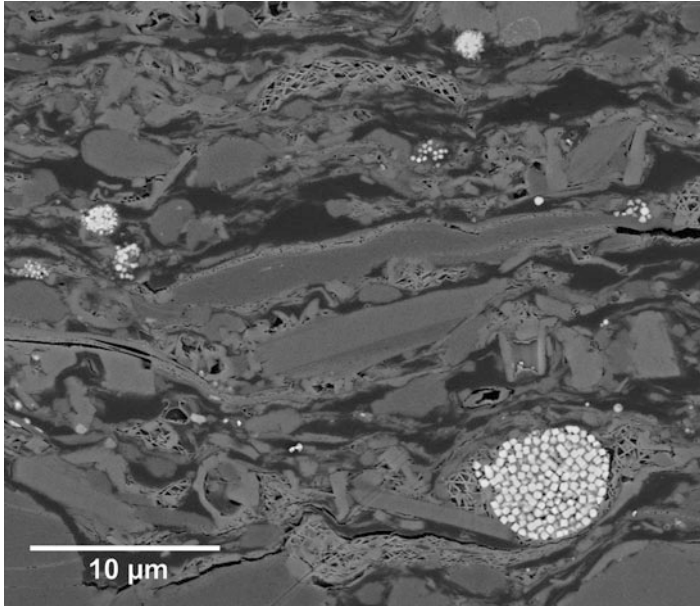


Fig. 1 FIB-SEM image of a core sample from immature Lower Toarcian Posidonia Shale (Wickensen well, 0.5% R_o ; courtesy U. Hammes, Austin). Unconventional shale gas can be stored in pores (black) or adsorbed on its mineral (white for pyrite, grey for minerals) and organic particle surfaces (dark grey)

fracturing (“fracking”). The name shale gas refers to natural gas of biogenic, thermogenic, or mixed origins contained in what is loosely termed shale but which in reality are mudstones, marls, and limestones (Fishman et al. 2011). Almost all currently producing shale gas reservoirs have been buried to great depth and hence high temperature ($>150\text{ }^{\circ}\text{C}$) and then geologically uplifted to depths where commercial extraction is possible, typically 2–4 km. They are brittle rather than elastic and therefore suitable for effective hydraulic fracturing to be employed to micro-crack the rock and release the in situ gas (e.g., Curtis 2002; Jenkins and Boyer 2008; Boyer et al. 2011). The relative content of dry gas (methane), wet gas (ethane, propane, and butanes), and non-hydrocarbon gases (CO_2 , N_2 , H_2S), and hence calorific value, varies within and between basins (Bullin and Krouskop 2008), as is also the case for conventional natural gas.

1.2 What Is Shale Oil?

The term shale oil has been used for centuries to describe the oil that is generated by retorting (pyrolyzing) oil shales (Cane 1967). Oil shales are fine-grained rocks containing indigenous and mainly macromolecular organic matter (often $>20\%$ total organic carbon (TOC)) that have not been exposed to high geological

temperatures and therefore still retain a great potential for generating oil when pyrolyzed. The name shale oil is used nowadays in a very different sense, namely, for the oil already generated naturally in the shale over geological time at elevated temperatures (>ca. 100 °C), still retained within the rock matrix and releasable by hydraulic fracturing.

Shale oil resource systems have been classified by their dominant organic and lithologic characteristics into (1) organic-rich mudstones with predominantly healed fractures, (2) organic-rich mudstones with open fractures, and (3) hybrid systems with a combination of juxtaposed organic-rich and organic-lean intervals (Jarvie 2012b). The *in-situ* oil is broadly similar in composition to that found in conventional reservoirs in that it contains all of the so-called SARA fractions (saturates, aromatics, resins, asphaltenes), but the produced fluid is strongly fractionated, being extremely enriched in light hydrocarbons, whereas the part remaining in the rock matrix is rich in heavy hydrocarbons and non-hydrocarbons (resins and asphaltenes).

1.3 The Organic Carbon Cycle

Shale gas and shale oil are formed over geological time as part of the subsurface organic carbon cycle. The starting point is the accumulation of organic residues from extant biota in fine-grained sediments. Upon burial, the organic matter undergoes progressive compositional change that is dictated initially by microbial agencies and thermodynamic instability (Arning et al. 2011, 2016) and later by mainly thermal stress. The continuum of processes is termed maturation and is divided into three consecutive stages called diagenesis *sensu stricto* ($R_o < 0.5\%$), catagenesis ($0.5\% < R_o < 2.0\%$), and metagenesis ($2.0\% < R_o < 4.0\%$) by organic geochemists (Tissot and Welte 1978). The term R_o is defined in the next section of the chapter.

Kerogen, the major precursor of shale gas, shale oil, and conventional petroleum, is insoluble in common organic solvents and consists of selectively preserved resistant cellular organic materials from algae, pollen, spores, leaf cuticle, and the like, as well as the degraded residues of microbially less resistant biopolymers (e.g., cellulose, polysaccharides) and lipids in variable proportions (Rullkötter and Michaelis 1990; de Leeuw and Largeau 1993). Kerogen formation is complete by the end of organic diagenesis. The type of kerogen and its mode of formation exert a strong influence on oil- and gas-generating characteristics, e.g., gas-oil ratio (GOR) during catagenesis. The kerogen that is found in carbonate/evaporite source rocks is enriched in organic hydrogen and organic sulfur (Type II-S; Orr 1986) and generally accompanied by high contents of heavy bitumen (sedimentary organic matter that is soluble in common organic solvents), both of which can generate oil at low levels of thermal stress. Low sulfur Type II kerogen requires more thermal energy to generate oil, and Types I and III kerogens still more (Tissot et al. 1987). A proportion of the generated fluids remains as residual shale gas or shale oil, whereas the rest is expelled into adjacent strata; retention efficiency is variable. In the late stage of catagenesis, both residual oil and kerogen generate enhanced proportions of ethane, propane, and the butanes (Dieckmann et al. 1998). Throughout metagenesis,

typically at depths of about 7 kilometers, the generated gas consists of methane (Lorant and Behar 2002; Mahlstedt and Horsfield 2012) and sometimes hydrogen sulfide (Le Tran et al. 1974) or nitrogen (Krooss et al. 1993). Periods of tectonic stress or postglacial rebound result in uplift, often on the order of several kilometers (e.g., Cavanagh et al. 2006), thus decreasing temperature and pressure and in some cases bringing about exposure to biological infiltration (Krüger et al. 2014; Schulz et al. 2015). Continued uplift leads to exposure at the Earth's surface, erosion and oxidation, thus completing the cycle.

1.4 Investigative Tools at Our Disposal

A wide range of geological and chemical tools, covering a scale from entire sedimentary basins (e.g., 10^5 m in length) all the way down to individual molecules (e.g., 10^{-9} m), is employed to study the carbon cycle in general and shale plays in particular. At the largest scale, petroleum formation histories are reconstructed using basin modelling (Poelchau et al. 1997; Hantschel and Kauerauf 2009). Going down in scale, well logs and the principles of sequence stratigraphy allow organic-rich and organic-poor lithofacies to be mapped laterally and vertically (Passey et al. 1990). With a resolution covering tens of microns down to tens of nanometers, organic petrology and scanning electron microscopy allow the habit and optical properties of organic particles, termed phytoclasts or macerals (e.g., alginite, derived from algae; sporinite, derived from spores; vitrinite, derived from wood), to be related to depositional environment and thermal maturity, as well as characterize pore dimensions and occurrence (Stasiuk 1997; Diessel 2007; Loucks et al. 2009). Thus, the reflectance under oil immersion of vitrinite (R_o) is the most widely used maturity parameter. Organic macromolecules, such as kerogen and asphaltenes (the latter being the bitumen component that is insoluble in light hydrocarbons), are characterized using pyrolysis and other degradative techniques in combination with gas chromatography and mass spectrometry (Horsfield 1984; Larter 1984; Rullkötter and Michaelis 1990). Maltenes (the bitumen component soluble in light hydrocarbons) are analyzed using a wide variety of chromatography and mass spectrometry approaches (Wilkes, *Methods of Hydrocarbon Analysis*). The techniques are deployed in three types of laboratory: the *experimental laboratory* is used to analyze individual or a combination of variables under simulated geological conditions; the *natural laboratory* is one where the effects of individual or groups of variables can be established by means of measurements on the natural system; and the *virtual laboratory* is a numerical simulation platform for integrating results in both geological time and space coordinates.

1.5 Factors Governing Shale Prospectivity

Fracking technology is highly advanced thanks to lessons learned from the drilling of 2.5 million wells in conventional petroleum systems (Montgomery and Smith 2010)

and especially in the last 15 years from the more than 40,000 wells drilled specifically into shale targets using “slickwater” and “hybrid” drilling fluids and deploying proppants. According to Jarvie et al. (2007), Slatt and O’Brien (2011), Jarvie (2012a), and Bernard and Horsfield (2014), high prospectivity and gas production rates is usually obtained from shale resource plays that:

1. Are fine-grained sedimentary rocks deposited under a variety of marine settings
2. Were originally rich in hydrogen-rich organic matter (>2% TOC)
3. Reached the liquid window (<1.2% R_o) for shale oil plays and the gas window (>1.2% R_o) for shale gas plays
4. Have low oil saturation (<5% S_o) for shale gas plays
5. Have a significant silica content (>30%) with some carbonate and non-swelling clays
6. Display less than 1,000 ηd permeability
7. Exhibit typically about 4–7% porosity, with pore sizes down to the nanoscale
8. Have a thickness exceeding 45 m and are now at a depth generally <4,000 m
9. Are slightly to highly overpressured
10. Exhibit very high first-year decline rates (>60%)
11. Allow fracking to be performed with due consideration of known principal stress fields
12. Can be drilled away from structures and faulting

In practice, all shale systems are unique in their chemical composition, physical properties, and rheology (e.g., Table 3 in Jenkins and Boyer 2008), with the result that production optimization has been based on learning-by-doing and involved the drilling of hundreds of wells, factory style (Binnion 2012). To streamline and rationalize the learning process, a simple exploration equation can be employed to address the important geochemical variables (Fig. 2). The in-place gas and/or oil potential of shale resource plays, embodied in that equation, is governed by the level

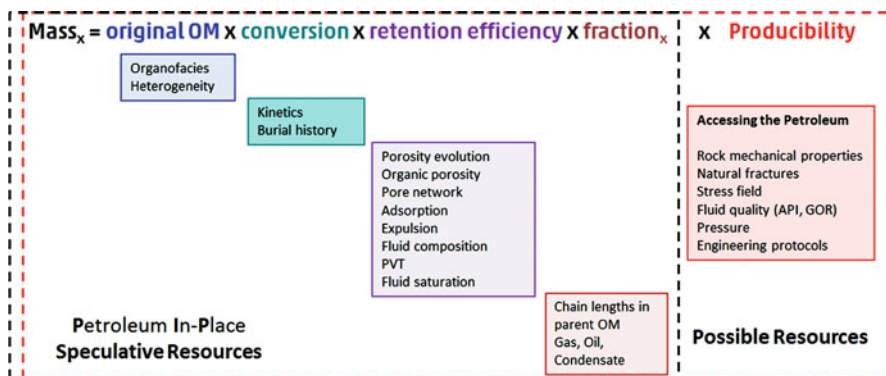


Fig. 2 Technical framework defining in-place potential (exploration equation) and technically recoverable resource potential (productivity)

of conversion of the original organic matter into hydrocarbons, the proportion of those hydrocarbons that is retained within the shale, and the fraction of the retained fraction that is gas or liquid. The boxes show the rock attributes that must be analyzed in order to address the different elements. The technically recoverable proportion of the in-place potential, hereafter termed producibility, is ultimately determined by the mechanical and petrophysical properties of the rock and the degree to which that potential can be realized using tailor-made engineering protocols. Each of these elements is considered separately in the ensuing discussion.

2 Original Organic Matter in Shales

Only shales that are rich in indigenous organic matter are targeted for gas or oil exploitation, because that organic matter is the source material from which the resource is generated. The deposition of sediments rich in organic matter is usually restricted to subaquatic sedimentary environments in which organic matter is produced faster than it can be destroyed (Tourtelot 1979). Deep-marine silled basins with haloclines, upwelling areas displaying oxygen minimum zones, marine transgressions onto continental shelves, evaporitic environments, lakes with stable thermoclines, and fluviodeltaic coal-bearing sequences are all sites of enhanced organic matter deposition (Jones 1987; Littke et al. 1997) and therefore of enhanced potential feedstock for shale gas and shale oil.

2.1 Depositional Environment

Prominent examples of shale plays occur in foreland basin settings (Mississippian Barnett and Bakken Shale, Middle Devonian Marcellus Shale), in intracratonic basins (Upper Devonian Antrim Shale), or rift basins (Upper Jurassic Haynesville Shale). The vast majority of shale resource plays were deposited in marine environments (Curtis 2002; Jarvie 2012a, b). The Lower Carboniferous Barnett Shale of the Fort Worth Basin was deposited under upwelling conditions, and has a TOC averaging 4% (Hill et al. 2007). The rhythmic stratification of chalk-marl beds is a characteristic of the Upper Cretaceous Niobrara Formation (Locklair and Sageman 2008) and brought about by the variation of siliciclastic input controlled by eustatic and climatic cycles (Pollastro 2010). TOC is in the range 1–8% (Landon et al. 2001). For the Upper Jurassic Eagle Ford Shale basin geometry played a key role in creating local depocenters of anoxic sediment deposition; TOC contents of up to 10% have been documented (Robison 1997). The marine Devonian Bakken Shale was deposited in a marine environment in the photic zone under anoxic conditions (Requejo et al. 1992) during sea level rise (Smith and Bustin 1998), and is organic-rich (TOC 3–25 wt.%; Price et al. 1984). The Upper Jurassic Haynesville Formation, whose TOC content reaches 8 wt.%, consists of shoreface clastics, carbonate shelves, and organic- and carbonate-rich mudrocks deposited in a deep, partly euxinic and anoxic basin (Hammes et al. 2011). High-salinity

conditions and water density stratification prevailed during deposition of the Upper Devonian Woodford Shale, along with manifestations of photic zone euxinia (Romero and Philp 2012); the TOC content is up to 25 wt.% (Cardott and Lambert 1985). Looking further afield, the Jurassic-Cretaceous Vaca Muerta Formation of Argentina, currently under extensive exploration, and with TOC in the range 2–12 wt.%, was deposited in a distal marine environment from outer ramp to middle ramp settings in mostly dysaerobic conditions (Kietzmann et al. 2011), and the Lower Jurassic Posidonia Shale, a potential shale gas candidate in Western Europe, was deposited in a low-energy environment under largely anoxic to euxinic marine conditions in a sea that was rich in nutrients (Schmid-Röhl et al. 2002) with short phases of more oxygenated bottom water conditions (Wignall and Hallam 1991). Its TOC, where immature, is 9–12 wt.% (Rullkötter et al. 1988). Moreover, deglaciation has led to the formation of black shales by salinity stratification, as seen for the Lower Silurian in North Africa (TOC up to 17 wt.%; Lüning et al. 2000) or after the Carboniferous glaciation of Gondwana (Lower Ecca black shales TOC up to 8 wt.%; Geel et al. 2015).

2.2 Under the Microscope

At a magnification of 600, and under blue light excitation, the organic constituents of immature marine shales mainly comprise brightly fluorescing alginite, usually derived from dinoflagellate/acritarch and prasinophyte cysts, along with lesser amounts of liptodetrinite, vitrinite, and inertinite (Littke and Rullkötter 1987; Littke et al. 1988). Mature shale oil candidates display a weaker fluorescence, and this is then entirely absent by the onset of gas generation. Finely disseminated micrinite, most likely a residue of liptinite degradation, also occurs in mature shales (Hackley and Cardott 2016). Important changes in fabric and the heterogeneity of organic chemical composition cannot be determined by this low-resolution microscopy approach. While confocal laser scanning microscopy and conventional scanning electron microscopy (SEM) cannot characterize submicrometer grains and pores if broken or mechanically polished shale samples are analyzed, argon-ion beam milling can be used to overcome this difficulty because sufficiently flat samples are produced (Loucks et al. 2009; Desbois et al. 2010; Mathia et al. 2016). Indeed, recent advances of SEM coupled with a focused ion beam (FIB-SEM) systems have offered a new alternative for investigating the three-dimensional submicrometric fabric of shales (Curtis et al. 2010, 2011a, b, 2012; Desbois et al. 2010; Sondergeld et al. 2010; Bera et al. 2011; Heath et al. 2011; Walls and Sinclair 2011; Bernard et al. 2013), so that, *inter alia*, chemical and mineralogical heterogeneities related to depositional environment have been documented (e.g., Arthur and Sageman 1994; Katsube and Williamson 1994; Ross and Bustin 2009; Loucks et al. 2009). Highly porous fossiliferous facies at low maturity have been documented alongside interparticle organic matter using FIB-SEM (Bernard et al. 2013). The FIB-SEM technique can also be used to extract ultra-thin (<100-nm-thick) sections across areas of interest, thus providing suitable samples for transmission electron microscopy, which offers a unique combination of chemical and

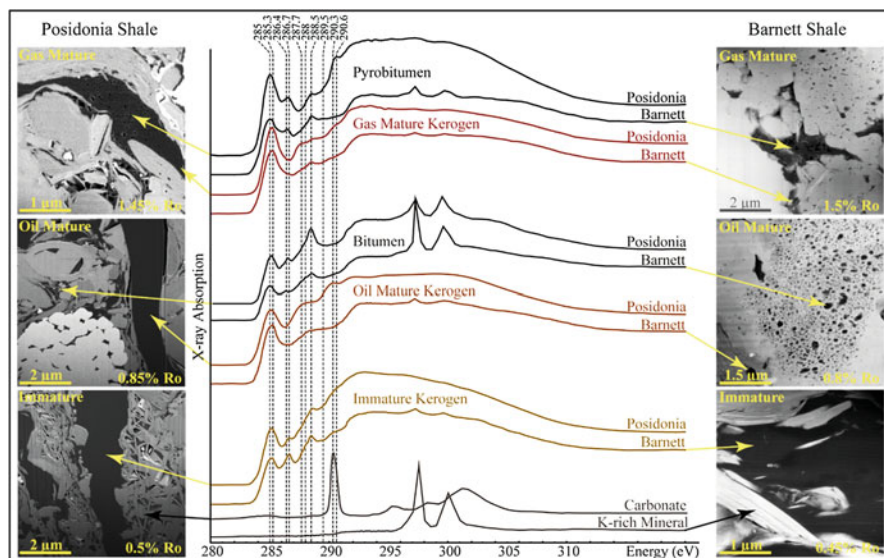


Fig. 3 Focused ion beam-scanning electron microscopy (FIB-SEM) images in backscattered electron (BSE) mode of three Posidonia Shale samples (left) and scanning transmission electron microscopy (STEM) images in high-angle annular dark-field (HAADF) mode of three Barnett Shale samples (right), showing organic matter (dark regions). These two sets of samples constitute two natural maturation series. Organic masses evolve from immature kerogen in immature samples (0.5% R_o) to bitumen and oil-mature kerogen in oil-mature samples (0.8% R_o) and to gas-mature kerogen and pyrobitumen in gas-mature samples (1.5% R_o). The scanning transmission X-ray microscopy (STXM)-based X-ray absorption near-edge structure (XANES) spectra of these different organic compounds is shown in the center. Absorption features at 285 and 285.3 eV are attributed to electronic transitions of aromatic moieties, 286.4 and 286.7 eV to ketone or phenol functionalities, 287.7 and 288 eV to aliphatic moieties, 288.5 eV to carboxyl functionalities, 289.5 eV to hydroxyl functionalities, 290.3 eV to carbonate cations, and 290.6 eV to alkyl moieties. (Modified from Bernard and Horsfield (2014))

structural information with unsurpassed spatial resolution (Chalmers et al. 2012; Bernard et al. 2012a, b), and for synchrotron-based techniques, such as scanning transmission X-ray microscopy (STXM) allowing X-ray absorption near-edge structure (XANES) spectroscopy to be performed at high spatial resolution (20 nm scale; e. g., Bernard and Horsfield 2014). For instance, recent STXM and TEM observations have elucidated the strong heterogeneous nature of gas shales down to the nanometer scale, with kerogen, bitumen, and pyrobitumen delineated within the same sample (Bernard et al. 2012a, b) (Fig. 3).

2.3 Building Blocks in Organic Macromolecules

The potential yields of gas and oil generated per unit organic matter in shales depend upon its organic hydrogen content and thence aliphaticity versus aromaticity, after

diagenesis has concluded, at the onset of catagenesis (Larter 1985; Vu et al. 2013; Sykes and Snowdon 2002). Hydrogen-rich kerogen (atomic H/C > 1.4) is usually found where anoxic lacustrine and marine shales are deposited, whereas hydrogen-poor kerogens (atomic H/C < 1.0) are found in more oxidizing, often terrestrial, settings (Tissot et al. 1974). Hydrogen-rich kerogens largely consist of algal-derived aliphatic cell membranes and lipid components (Cane and Albion 1973; Philp and Calvin 1976; Largeau et al. 1984; Tegelaar et al. 1989), whereas hydrogen-poor kerogens at low maturity often contain high proportions of altered lignocellulosic (phenolic) materials whose aliphatic constituents consist of alicyclic moieties and short alkyl chains (Mycke and Michaelis 1986). Being deposited largely under reducing conditions in marine environments, the major gas shales contain Type II kerogen and at the start of catagenesis have Hydrogen Indices in the range 300–600 mgHC/g TOC (Jarvie 2012a, b). Like the prolific source rocks in conventional petroleum systems, shale oil targets may be either marine or lacustrine and contain either Type I or II organic matter. This is illustrated in Fig. 4a for selected shales and source rocks of low maturity. The product of the TOC (%) and

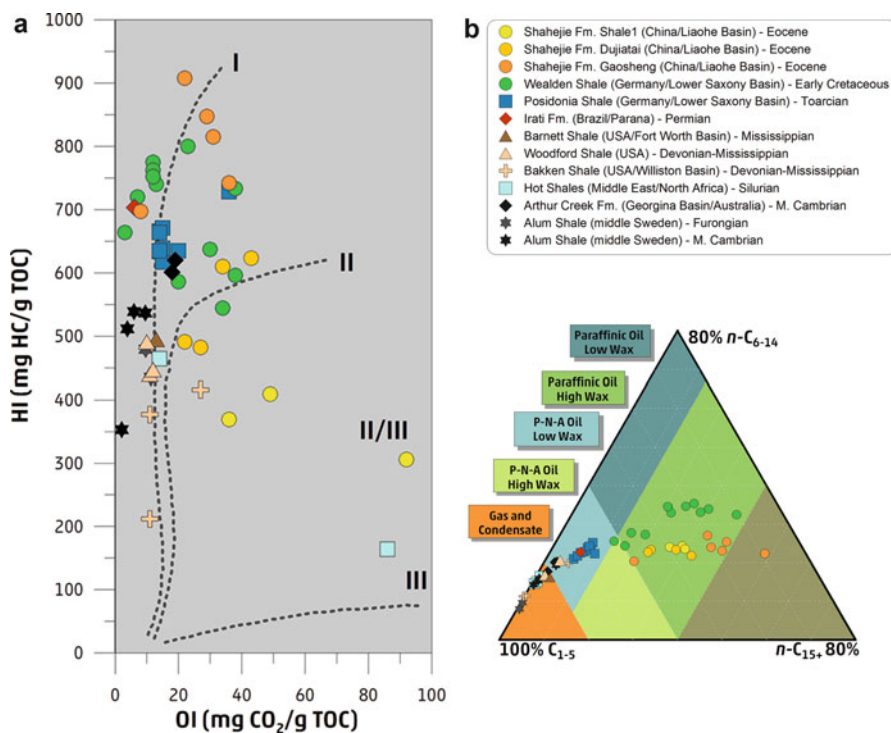


Fig. 4 (a) Kerogen typing using the Rock-Eval “pseudo-Van Krevelen” diagram for a wide variety of immature and early mature shales: the method is excellent for predicting yield, but not for predicting petroleum compositions, e.g., gas-oil ratio (GOR). (b) Petroleum-type organofacies based on analytical pyrolysis reflect the chain length distributions within labile carbon moieties that are the precursors for petroleum

Hydrogen Index (mgHC/g TOC) determines the generative potential (S₂) expressed as kg/tonne rock, or equivalent oilfield units (e.g., barrels per acre-foot).

2.4 Generating Potentials

Gas versus oil generating potential is initially governed by the relative abundance of short versus long chains in macromolecular precursors. Utilizing *n*-alkyl chain length distributions from pyrolysis gas chromatography, Mesozoic shales containing Type II kerogen, such as the Eagle Ford, Niobrara, and Posidonia (Kuske et al. 2017; Han et al. 2018; Muscio et al. 1991), mainly fall in the Paraffinic-Naphthenic-Aromatic Low-Wax petroleum-type organofacies of Horsfield (1989), whereas Type II Paleozoic shales, such as the Alum, Bakken, and Barnett (Muscio et al. 1994; Horsfield et al. 1992a; Kuhn et al. 2010, 2012; Han et al. 2015), fall in the Gas-Condensate organofacies or at the border of the two facies. Such differences in chain length distributions within the Type II elemental class reflect the variability in inherent gas- versus oil-generating potential of organic-rich shales in nature, and thus molecular typing is a key element of the exploration equation (fraction). The same is true for lacustrine shales, which are often inherently richer in long-chain alkanes and belong to the paraffinic high-wax petroleum-type organofacies. The chain length distributions for a collection of low-maturity shales and source rocks are shown in Fig. 4b.

3 Conversion

As the organic matter in shale is gradually exposed to progressively higher temperatures during burial over millions to tens of millions of years, its composition changes, driven by aromatization. Major aliphatic substituents of the kerogen structure are progressively cracked, more or less in the order of bond strength, and there is concomitant structural rearrangement of the residues (Ungerer 1990; Mao et al. 2010; Bernard et al. 2012a, b; Romero-Sarmiento et al. 2014). Assessing the thermal maturity of shales and the degree to which its in situ macromolecular organic matter has been converted into mobile products is a key element of the exploration equation. Thus, for example, in the case of the shales of the Eagle Ford Shale, gas-oil ratio (GOR) is regionally controlled by thermal maturity, with iso-maturity lines orientated NE-SW and thermal maturity levels increasing to the SE (Fan et al. 2011). Similarly, concentric iso-maturity contours occur in the Bakken Shale, linked to changing Hydrogen Index and petroleum properties (Kuhn et al. 2010).

3.1 Primary Cracking of Kerogen and Bitumen

The primary cracking of kerogen and heavy bitumen forms gaseous and liquid products at 10–90% conversion levels – this is the maturity range for shale oil,

especially the higher end of the range. The actual relationship between level of catagenesis, reflecting the thermal history of the shale, and degree of conversion into oil and gas at that maturity level is governed by their chemical kinetic parameters (activation energy distribution and frequency factor, as reviewed by Schenk et al. 1997b), and these differ appreciably from case to case, even within each of the classical kerogen Types I, II, and III (di Primio and Horsfield 2006). Very importantly as far as shale oil exploitation is concerned, bulk petroleum compositions in shales appear to reflect the most recently generated products, i.e., “instantaneously generated,” and not an accumulation of products formed since generation began, and this is because expulsion is an ongoing process during progressive maturation (Kuske et al. 2018). The GOR of instantaneous products is appreciably higher than those of cumulative products (England et al. 1987).

While the overall reaction order for petroleum generation is generally assumed to be first order (as reviewed by Schenk et al. 1997), second-order reactions between kerogen and polar bitumen components have been documented as strongly influencing bulk compositional characteristics, including gas-oil ratio (Vu et al. 2008; Mahlstedt et al. 2008). Thus, when assessing the maturation characteristics of a given shale, it is important to use samples which retain the solvent-extractable macromolecular components. Heavy bitumen makes an important yet variable contribution to the total organic matter of shales and is especially abundant in calcareous shales and marls (e.g., Powell 1984; di Primio and Horsfield 1997), even at low levels of maturation; to remove it by solvent extraction would be to take away a highly significant fraction of petroleum precursors.

3.2 Secondary Cracking of Oil

Disproportionation results in the formation of hydrogen-rich (dry and wet gases) and hydrogen-poor species (pyrobitumen) at elevated levels of maturation. In-source secondary oil-to-gas cracking begins at approximately 1.2% R_o , at a paleotemperature of about 150 °C (e.g., Dieckmann et al. 1998), this being considered a prerequisite for economically viable shale gas in the Barnett Shale of the Fort Worth Basin (Jarvie et al. 2007). By contrast, in-reservoir cracking in conventional siliciclastic reservoirs begins around 2% R_o at a paleotemperature (3 K/Ma heating rate) of approximately 200 °C (Horsfield et al. 1992b; Schenk et al. 1997a). Primary and secondary gas-forming reactions in shales overlap to variable degrees. The “GOR-Fit” model predicts the generation of primary and secondary gas from source rocks, in which overlapping liquid generation and destruction reactions occur, on the basis of simple stoichiometric relationships (Mahlstedt et al. 2015). The generation of so-called late gas from residual methyl groups in both kerogen and pyrobitumen begins at 2% R_o and appears to be complete by 3.5% R_o (Erdmann and Horsfield 2006; Mahlstedt and Horsfield 2012), this being an important prospectivity assessment parameter in plays where maturity levels are exceedingly high, e.g., the Sichuan Basin, China (Tan et al. 2013).

3.3 Role of Catalysis

Catalysis increases the gas-oil ratio when a given kerogen type is pyrolyzed in the presence of minerals, especially illite and smectite (Espitalié et al. 1980; Horsfield and Douglas 1980), and the question remains whether these organic-inorganic interactions might also occur in nature where temperatures are much lower and heating rates nine orders of magnitude slower than employed in laboratory experiments (300–650 °C). It has recently been found that gasification effects are strongly heating rate dependent and are likely to be minor under geological heating rates of, e. g., 3 K/Ma (Yang and Horsfield 2016). This means that raw data from the pyrolysis of especially relatively organic-lean ($S_2 < 10$ mgHC/g rock) and argillaceous shales should be treated with caution as predicted gas contents and bulk aromaticity might be overestimated.

3.4 Radiolysis Effects

The ionizing radiation emitted from uranium acts over the entire lifetime of a shale, beginning with deposition, to fundamentally change the chemical characteristics of organic matter in shales. This influence is significant in the case of uranium-rich shales that are Lower Paleozoic or older. While the radiation dosage resulting from the decay of uranium is linearly correlated with uranium content and exposure time, the kerogen structure changes exponentially since labile structures react early and become stabilized in later stages. The outcome is that shales which generated mainly oil during their early subsidence history, such as the Alum Shale of Scandinavia, have been altered so they appear more gas-prone than was really the case (Yang et al. 2018).

3.5 Maturity Parameters

Exact maturity assessment has been shown to be a key element in the regional exploration for sweet spots. Stable isotopes of hydrocarbon gases have been used to estimate maturity, for example, the rollover of ethane and propane $\delta^{13}\text{C}$ values ($\delta^{13}\text{C}_2$ and $\delta^{13}\text{C}_3$) and isotopic reversals among methane, ethane, and propane being correlated with the occurrence of sweet spots in the Barnett of the Fort Worth Basin (e.g., Zumberge et al. 2012; Hao and Zou 2013). Rock-Eval T_{max} or its purported “equivalent” in terms of vitrinite reflectance (Jarvie et al. 2001) is frequently deployed with the same goal. The fact that kinetic parameters of generation vary significantly within a given kerogen type (Tissot et al. 1987; di Primio and Horsfield 2006) means that there is actually no unique correlation between T_{max} and R_o for shale plays. As an example, the relationship between the two parameters for the Duvernay Shale (Devonian) of the Western Canada Sedimentary Basin differs from that of the Barnett (Wüst et al. 2013) though both have similar initial genetic potential (Type II).

Fourier transform-ion cyclotron resonance mass spectrometry (FT-ICR MS) is a powerful tool for rapidly characterizing NSO compounds in complex mixtures. Run

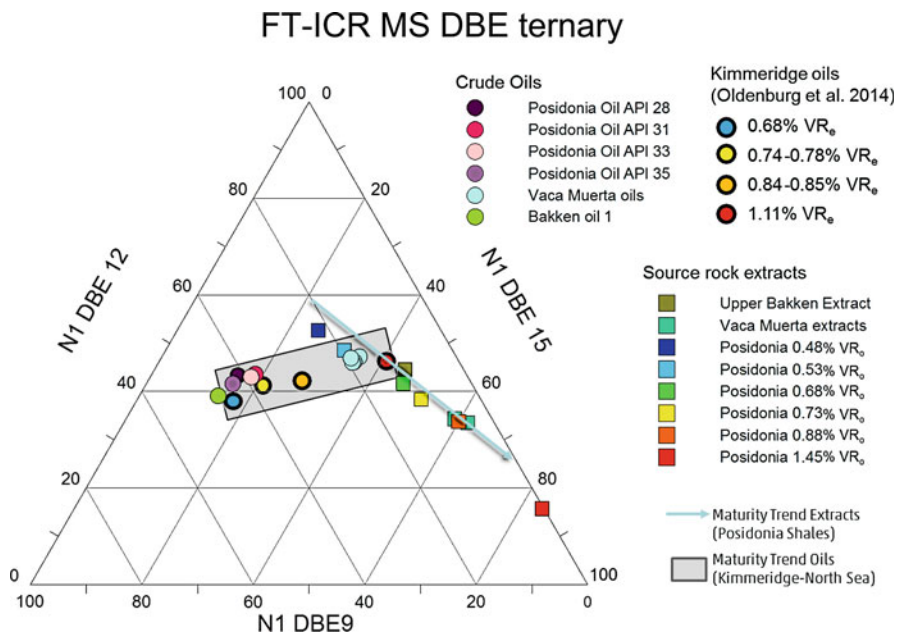


Fig. 5 Ternary plot featuring alkylcarbazoles (9 DBE (double bond equivalents)), alkybenzocarbazoles (12 DBE), and alkydibenzocarbazoles (15 DBE). The Posidonia Shale-sourced crude oils fall roughly in a position indicating oil maturities equivalent to $R_o = 0.68$ – 0.74% according to maturity assignments for North Sea crudes (Oldenburg et al. 2014), whereas Bakken Shale and Vaca Muerta oils are positioned near $R_o = 0.68\%$ and 0.9% , respectively. Related Bakken Shale and Vaca Muerta extracts from the producing wells plot close to the Posidonia Shale extracts from source rocks with R_o values of 0.68% and 0.88% , confirming that the maturity assignments are robust

in the ESI-negative ion mode, it has been used to rapidly assign maturity levels to produced oils and *in-situ* shale bitumen extracts based on the relative distribution of pyrrolic nitrogen-containing compounds (Oldenburg et al. 2014; Poetz et al. 2014; Mahlstedt et al. 2016). Specifically, as far as the alkylcarbazoles, alkybenzocarbazoles, and alkydibenzocarbazoles are concerned, there is an increase in the degree of benzannulation with increasing maturity (Fig. 5), and that is mainly due to fractionation processes, i.e., preferential expulsion (or production) of smaller compounds and enhanced cyclization and aromatization at the expense of aliphatic structures within retained fluids; the crude oils and extracts plot on different trend lines (Fig. 5).

3.6 Mass Balance Modelling

In conventional petroleum exploration, it is important to determine the timing of petroleum generation relative to trap formation as well as its level of maturation (Hantschel and Kauerauf 2009), but with the unconventional, it is simply the

final degree of alteration that is most important, because the fluids to be exploited are still *in-situ*. The inverse modelling of organic matter abundance and composition between relatively closely spaced wells is better suited to effective shale gas exploitation because it allows the determination of generative yields and generated product compositions: mass balance calculations using quantitative pyrolysis gas chromatography data (Santamaria-Orozco and Horsfield 2003) allow the generation of compound classes and individual oil and gas components to be quantified over any selected narrow or broad maturity range. For example, the generation of *n*-alkanes and alkylbenzenes in closely spaced samples within the Barnett Shale showed variability that has been linked to organofacies (Han et al. 2015). Similarly, generation profiles for these components within marls of the Niobrara Formation have been contrasted with residual hydrocarbons in reservoir facies chalks (Han 2016) as a first step in calculating retention and depletion within shales, as further explained in the section below on retention.

4 Retention

The retention of hydrocarbons in shales is governed mainly by the sorption capacity of its organic components (Baker 1962; Tissot et al. 1971; Stainforth and Reinders 1990; Pepper 1991; Han et al. 2015). Interestingly, it is the pyrolytically labile fraction (S2 of Rock-Eval) and not simply the total organic matter that has the highest selective adsorptive capacity (Mahlstedt and Horsfield 2013; Han et al. 2015; Ziegls et al. 2017). The more aromatic the labile fraction is, the higher is the adsorptive capacity. Thus, for a given level of maturity, those Type II kerogens whose S2 is inherently more aromatic, for example, the Alum, Barnett, and Bakken Shales, have a better capacity than those that are less aromatic, for example, the Posidonia and Wealden Shales (Mahlstedt and Horsfield 2013). It is important to note that the gas sorption capacity of the Alum Shale was probably less well developed during its generative period (Paleozoic times); aromaticity and thus sorption capacity have increased due to relatively recent radiolysis effects (Yang et al. 2018); thus gas generation and the development of sorptive capacity are out of step in this example.

The retentive labile fraction is contained within both bitumen and kerogen fractions (Muscio et al. 1991; Horsfield et al. 1991), and these are distributed heterogeneously within shales, this being reflected in the breadth of reflectance histograms and the variety of phytoclast types present (e.g., Bernard et al. 2010, 2012a). Figure 3 displays the evolution of this compositional variability with increasing thermal maturation of Posidonia Shale and Barnett Shale (Bernard and Horsfield 2014). While minerals play a subsidiary role in adsorption, clay minerals, especially illite (Schettler and Parmely 1991), possess microporous structures that are capable of sorbing gas (Gasparik et al. 2014).

4.1 Shale Porosity and Kerogen Swelling

Low-pressure adsorption isotherms (e.g., Bustin et al. 2008), high-pressure mercury intrusion porosimetry (e.g., Nelson 2009), solid-state nuclear magnetic resonance (e.g., Sondergeld et al. 2010), and small-angle and ultrasmall-angle neutron scattering (e.g., Ruppert et al. 2013) have shown that pore sizes within gas shales are on the order of a few nanometers to tens of nanometers. Besides sorption on particle surfaces, petroleum storage in the pores of either organic (Loucks et al. 2009) or inorganic (Bernard et al. 2013; Han et al. 2015) matrices has been documented, as have natural fractures (Lopatin et al. 2003; Pollastro 2010; Bernard et al. 2013). The occurrence of organic particles exhibiting irregular ellipsoid-shaped nanopores of approximately 1–500 nm first observed by Loucks et al. (2009) has now been reported in most gas shale systems worldwide, as reviewed by Bernard and Horsfield (2014). In high-maturity gas shales, these organic pores govern gas occurrence. Porosity in shales evolves from mostly submicrometric interparticle pores in immature samples to mostly intramineral and intraorganic pores in gas mature samples (Curtis et al. 2010, 2012; Loucks et al. 2010, 2012; Bernard et al. 2013; Mathia et al. 2016), but primary organic pores have been observed within immature and oil mature samples as reported in a recent comprehensive literature review (Han et al. 2017). For the vast bulk of the shale volume, hydrocarbon retention and porosity evolution appear to be strongly related to changes in kerogen density brought about by swelling and shrinkage as a function of thermal maturation (Kelemen et al. 2006; Han et al. 2017). Secondary organic pores form only after the maximum kerogen retention (swelling) ability is exceeded, namely, where $T_{\max} = 445\text{ }^{\circ}\text{C}$, or $0.8\% R_o$. The shrinkage of kerogen has therefore been proposed as a mechanism for forming organic nanopores, and is ostensibly a major cause of associated porosity increase, in the gas window.

4.2 Quantification of Precursors and Retained Products

The volume of gas generated within gas shales by secondary cracking directly depends on oil retention in the system, i.e., on adsorption capabilities as well as on porosity and fracture networks. The algebraic mass balance models of Larter (1985) and Cooles et al. (1986) use dead carbon for normalization, Rock-Eval S1 to define free petroleum, and S2 to define labile kerogen. They predict that organic-rich shales are excellent expellers of petroleum (approximately 90%), and thus, petroleum that is retained, and which can act as a source of secondary gas in shales, is relatively minor. According to these models, shales with lower organic richness are poorer expellers, meaning that while they are unable to source conventional petroleum, they are nevertheless potentially good gas shales. Jarvie et al. (2007) assessed expulsion to be much lower (65%) than these models predict, correctly taking into account that a high proportion of polar compounds in the retained oil actually elute in the S2 peak and not S1 (Horsfield et al. 1991). This finding is extremely important for shale oil

plays, where it is important to distinguish mobile from immobile petroleum fractions. Simple geochemical parameters from the Rock-Eval analysis of whole rock (WR) and solvent-extracted (EX) aliquots have here been formulated to describe petroleum yield and composition more rigorously:

- *Assessing in-place oil characteristics*

Volatile oil represents all FID-detectable-free hydrocarbons in the sample.

$$\text{Volatile oil} = S1_{WR} \text{ mg/g rock}$$

Total oil refers to the sum of volatile oil ($S1_{WR}$) and the macromolecular components (part of $S2$) that are soluble in the extraction solvent.

$$\text{Total oil} = S1_{WR} + (S2_{WR} - S2_{EX}) \text{ mg/g rock}$$

Oil quality refers to the ratio of volatile oil ($S1$) to total oil.

$$\text{Oil quality} = S1_{WR} / (S1_{WR} + (S2_{WR} - S2_{EX}))$$

- *Assessing kerogen and bitumen contributions*

The relative contributions of kerogen to the $S2$ signal

$$S2_K = S2_{EX} / S2_{WR}$$

is also reflected in the T_{max} shift

$$\Delta T_{max} = (T_{maxEX} - T_{maxWR}) \text{ } ^\circ\text{C}$$

Hydrogen Indices of the macromolecular kerogen and bitumen components:

$$\text{Hydrogen Index kerogen} = S2_{EX} / \text{TOC}_{EX} \text{ mg/g}$$

$$\text{Hydrogen Index bitumen} = (S2_{WR} - S2_{EX}) / (\text{TOC}_{WR} - \text{TOC}_{EX}) \text{ mg/g}$$

- *Assessing retention*

The so-called Oil Saturation Index provides a measure of the oil in place that is more readily producible (Jarvie 2012b).

$$\text{Oil saturation index} = S1_{WR} / \text{TOC}_{WR} \text{ mg/g}$$

The total oil saturation index provides a measure of the total oil in place.

$$\text{Total oil saturation index} = S1_{WR} + (S2_{WR} - S2_{EX}) / \text{TOC}_{WR} \text{ mg/g}$$

Changes in two of these parameters as a function of T_{max} are illustrated for the Vaca Muerta Formation (Argentina), the Yanchang Shale (China), the Posidonia Shale (Germany), and the Eagle Ford Shale (USA) in Fig. 6. In the simplest case, oil quality increases progressively as the proportion of polar compounds decreases, this being most clearly discernable for the Eagle Ford maturity series. The Yanchang and Posidonia show enhanced quality at lower maturity ostensibly due to infiltration by mature fluids. The Vaca Muerta Shales shown here are actually from a limited maturity range (ca. 1% R_o); low T_{max} values are most likely related to the retention of high molecular weight, in part polar, heavy oil components. The oil saturation index is said to exceed 100 mgHC/g TOC where producible oil occurs (Sandvik et al. 1992; Jarvie 2012b) and is often relatable to the presence of porous microfossils (Han et al. 2015, 2017). In the case of the Posidonia Shale, values increase and then decrease in accordance with the concepts of the oil window and kerogen swelling, and only in a few cases do values exceed 100 mgHC/g TOC. Decreasing values are seen for the Eagle Ford at high maturity levels. The Vaca Muerta displays exceedingly enriched and depleted intervals for a given maturity, consistent with intraformational migration.

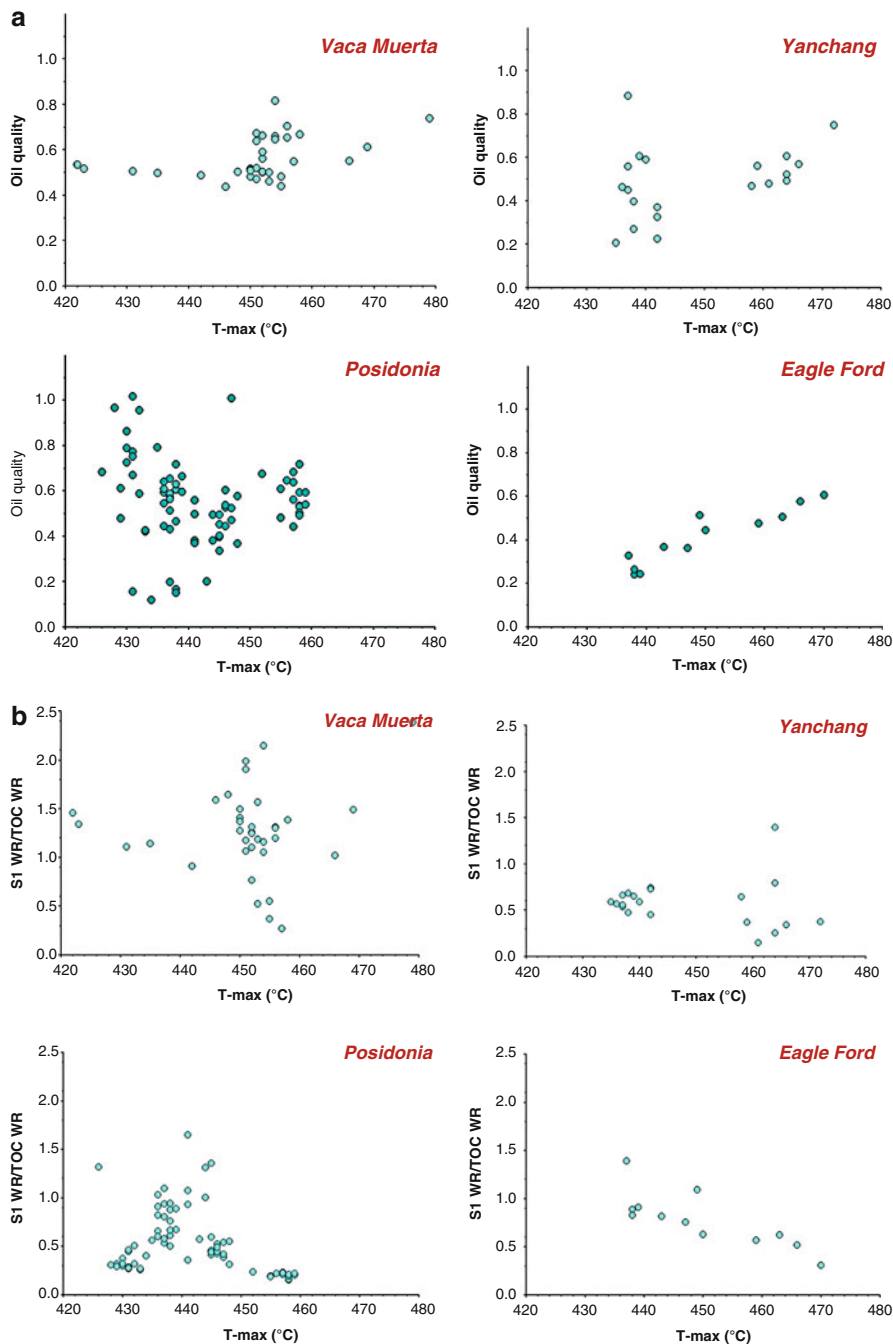


Fig. 6 The rapid assessment of bulk petroleum composition in the Vaca Muerta Formation (Argentina), Yanchang Shales (PR China), Posidonia Shale (Germany), and Eagle Ford Formation (USA) using Rock-Eval parameters. (a) Oil quality, calculated as $S1_{WR}/(S1_{WR} + S2_{WE} - S2_{EX})$. (b) Oil Saturation Index, calculated as $S1_{WR}/TOC_{WR}$

5 Production Characteristics

Prospectivity largely depends on the degree to which lithologies and compositional heterogeneities (fluids and matrix) can be recognized so that artificially stimulated fractures can be induced within selected packages (Binnion 2012). It is also noteworthy that compositional fractionations due to selective retention, and sometimes induced by phase separation, can change the ratio of gas to oil and the chemistry of the oil. Three examples are presented here to illustrate these important points.

5.1 Recognition of Sweet Spots Within Heterogeneous Sequences

This illustrative example is taken from Han et al. (2015).

The Barnett Shale sequence of the Marathon 1 Mesquite well, Hamilton County, Texas, contains Type II kerogen throughout and is at oil window maturity (1.0% R_o). It displays significant compositional heterogeneity (Fig. 7).

- Beginning at the top, the first interval is carbonate-rich and organic-lean.
- The deeper second interval consists mainly of organic-rich noncalcareous mudstones, including porous biogenic silica from sponge spicules. It behaves like a reservoir unit within the succession, exhibiting the highest Oil Saturation Index and suppressed T_{max} values.
- The third interval is argillaceous and consists mainly of organic-rich siliceous noncalcareous mudstones and phosphatic shales. It represents the best source interval.
- The fourth and fifth intervals are calcite-rich and consist mainly of siliceous calcareous mudstones.

Oil quality increases with increasing depth in the well-reflecting increasing contributions of light hydrocarbons. A preferential migration of C_{15+} aliphatic hydrocarbons from the third into the second interval, accompanied by selective retention of aromatic hydrocarbons and polar compounds in the third interval, has occurred. The migration pathway from the third to the second is via natural fractures. Carbonate-cemented fractures perpendicular to the bedding have been documented, as well as the coexistence of oil inclusion clusters within these fractures.

Whereas the retention of hydrocarbons within most intervals is primarily controlled by organic matter richness, additional storage occurs within siliceous microfossils of the second interval. Based on this enrichment and its siliceous nature, the interval represents a much more attractive target for hydrocarbon production than the clay-rich third interval.

Furthermore, at higher maturities, the horizon is expected to yield higher additional amounts of secondary gas by oil cracking. This might explain why the primary producing facies of the Barnett Shale is largely quartz dominated.

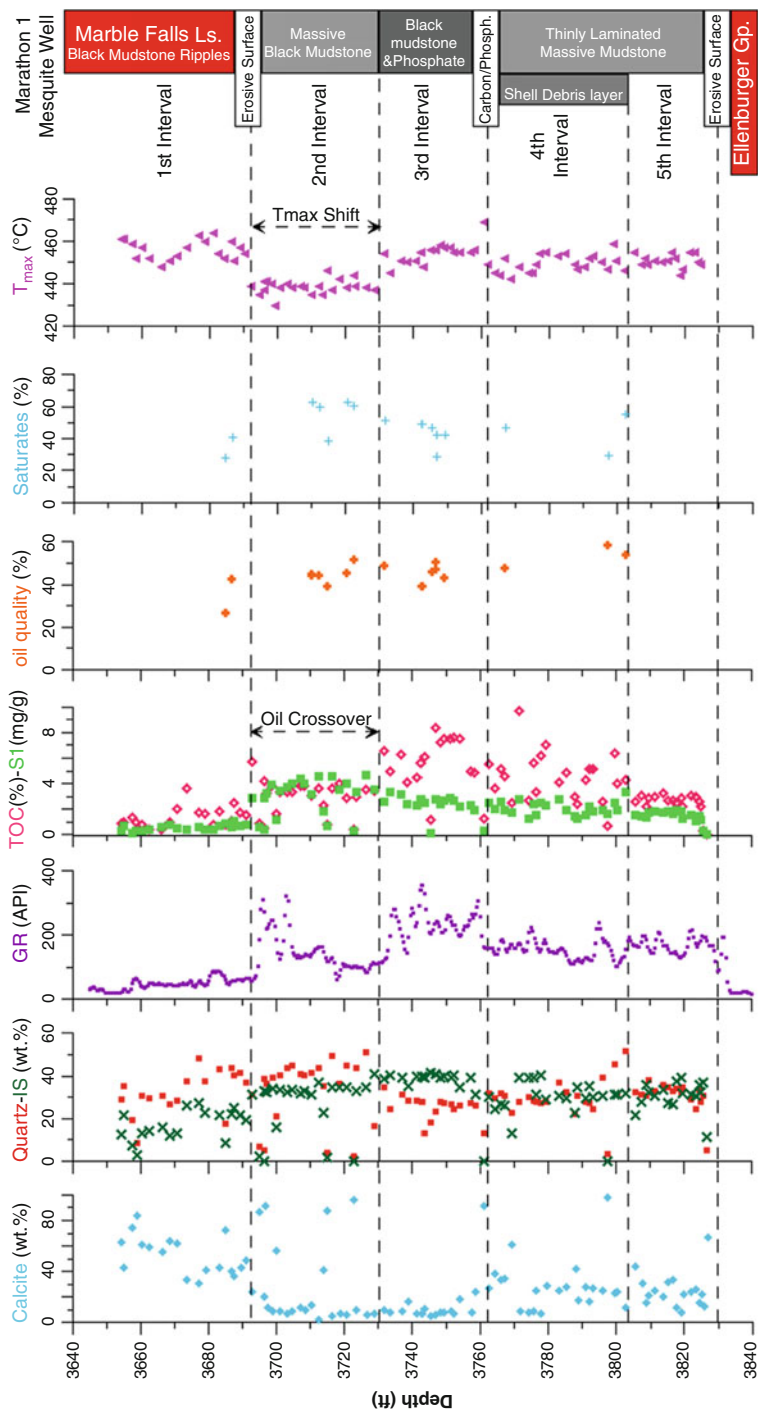


Fig. 7 Geochemical depth profile of the Marathon 1 Mesquite well. Interval subdivisions are based on (1) gamma ray (GR) log, (2) core description, (3) Rock-Eval parameters. TOC = total organic carbon (%); S1 = thermally extractable petroleum (mgHC/g rock); oil quality = $S1/(S1_{WR} + S2_{WR} - S2_{EX})$; saturates refers to C_{15+} fraction from medium pressure liquid chromatography separation; T_{max} = temperature at which S2 generation rate is at a maximum

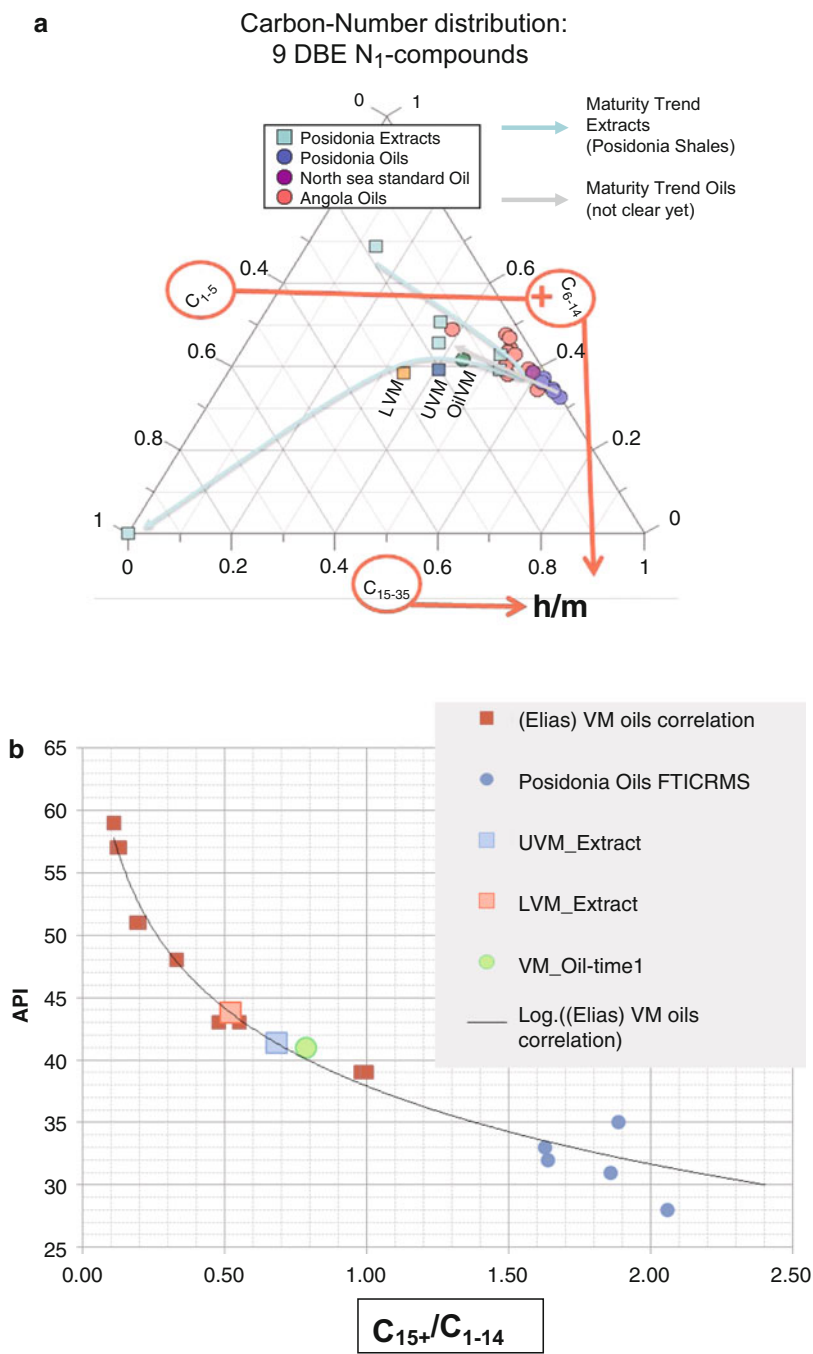


Fig. 8 (continued)

5.2 Rapid Insight into *In-Situ* Physical Properties of Fluids

Elias and Gelin (2015) used the relative proportions of heavy versus medium cuts (h/m) from GPC/UV analysis of produced oils and rock extracts to document differences in the *in-situ* API gravity of fluids within the Vaca Muerta Formation (Fig. 8b). Adopting and adapting this approach, Mahlstedt et al. (2017) used the chain lengths of alkyl substituents in N₁ carbazoles (DBE 9) from FT-ICR MS (ESI-negative mode) for the same purpose. The low and intermediate aliphatic carbon numbers (C_{1–14}) were used as the medium cut and high aliphatic carbon numbers (C₁₅₊) as the heavy cut (Fig. 8a). Plotting API gravity versus aliphatic carbon number-based h/m ratios and comparing with the GPC/UV-API° trend line resulted in a good correlation, showing that meaningful API values could already be assessed for potential resource plays, e.g., the Posidonia Shale and the Vaca Muerta Formation. The API gravity prediction for produced oil from one well in the Neuquén Basin is 40°, which is clearly within the reported range of 39–41° API for this well. API gravity predictions for source rock extracts from the producing well are 41° for the Upper Vaca Muerta and 44° for the Lower Vaca Muerta indicating that the initial oil was produced from the UVM.

5.3 Fractionation During Production: Insights from PVT Modelling

The phase behavior of in situ petroleum is governed by the pressure-temperature (P-T) conditions of the reservoir and the bulk composition of the petroleum fluid (England et al. 1987; Düppenbecker and Horsfield 1990; di Primio 2002). The petroleum phase or physical state of fluids at any given P-T condition can be described by phase envelopes whose shapes are ultimately controlled by the organofacies and thermal maturity of the source organic matter (di Primio et al. 1998). A one-phase system exists in P-T conditions that are outside of the phase envelope (undersaturated), whereas a two-phase system exists at or within the envelope (saturated), and the two meet at the saturation pressure (P_{sat}).

To date, only a few investigators have addressed prediction of petroleum quality and phase behavior within unconventional resources. Using petroleum engineering models, Whitson and Sunjerga (2012) were the first to publish that petroleum fluid



Fig. 8 FT-ICR MS N₁ aliphaticity for API prediction. (a) The aliphatic carbon number distribution of Posidonia Shale-sourced crude oils and extracts, as well as Vaca Muerta-sourced crude oils and two extracts (Upper and Lower VM), is compared in a ternary diagram displaying N₁ compounds of the 9 DBE class. Carbazoles with alkyl substituents of 1–5 carbon atoms, 6–14 carbon atoms, and ≥15 carbon atoms form the apices. The ratio of heavy (h) versus medium (m) molecular weight is determined from >C₁₅/(C₁–C₅ + C₆–C₁₄). (b) API gravity prediction using the heavy/medium cut as determined by gel permeation chromatography, as well as FT-ICR MS of N₁ compounds of the 9 DBE class, of the total extracts/oils

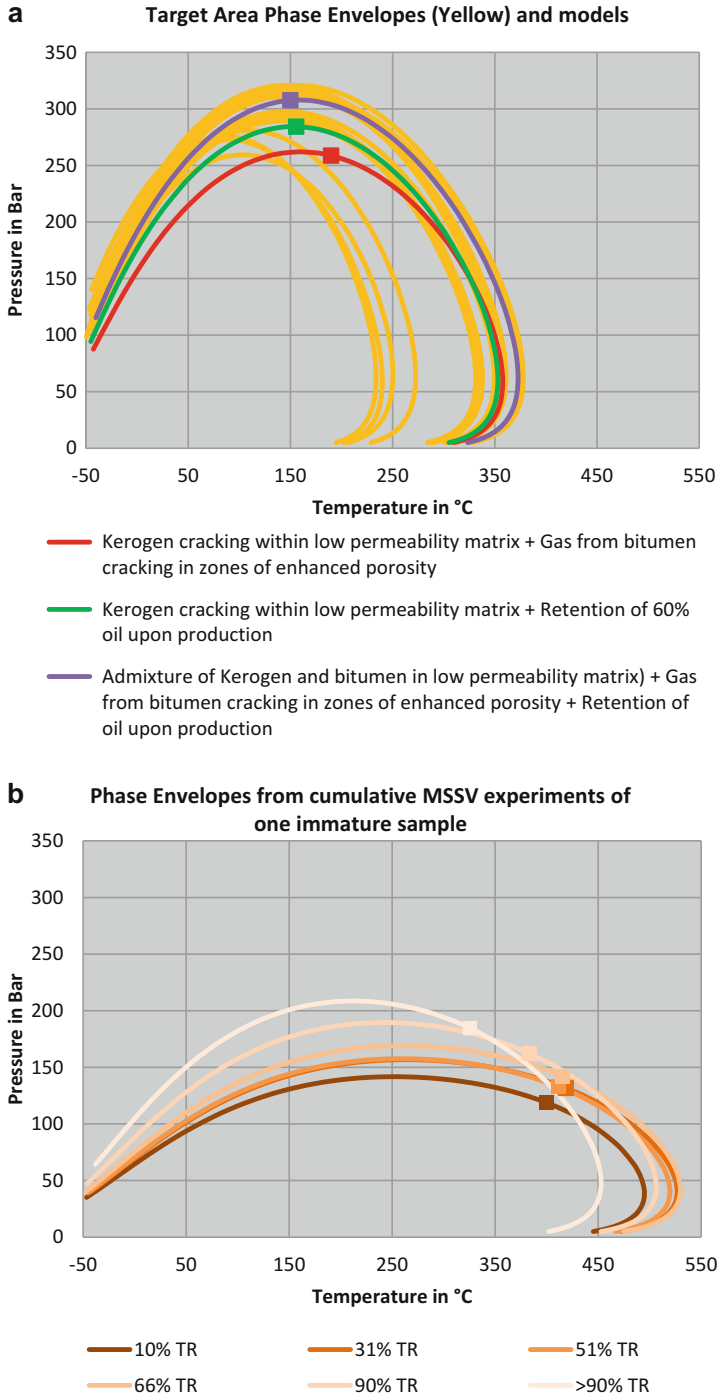


Fig. 9 (continued)

produced from surface wellhead facilities did not represent downhole fluid properties. They noted that the ultralow permeability usually found in unconventional shale plays leads to substantial amounts of oil drawdown (retention) and that the degree of oil recovery depends on whether the reservoir is initially saturated by oil or gas and whether conditions are near-saturated (greatest oil recovery loss) and to what degree.

Using microscale sealed vessel (MSSV) pyrolysis, Horsfield et al. (2015) and Kuske et al. (2017) performed artificial maturation experiments on mature Eagle Ford samples and used the results to model how the PVT properties of generated fluids would be at a slightly higher level of conversion (Fig. 9a). Phase behavior predictions from the so-called PhaseSnapShot model were compared with a regional PVT database for DeWitt County compiled from the public domain. The model that best matched the targeted PVT data was comprised of two reactive components: (1) a mixture of kerogen and bitumen that generated petroleum within the low permeability matrix and (2) bitumen that was the precursor of gas in zones of enhanced porosity within the matrix. Importantly, the enhanced generation of gas from the admixture of kerogen and bitumen and the significant retention of C_{7+} fluids in the matrix were required to enable a match between the phase behavior and geochemical compositions of fluids from the majority of wells in the study area. Cumulative compositions based on experiments using an immature sample produced gas-poor products and hence phase envelopes with consistently low P_{sat} (Fig. 9b). The overall implications were that instantaneous (most recently generated) rather than cumulatively generated fluids occur in shale reservoirs and that in situ petroleum compositions differ significantly from those at the surface, there being a major increase in gas-oil ratio because of selective retention of petroleum liquids.

6 Research Needs for Unconventional Resource Assessments

The boom in shale gas and shale oil exploration and development appears to be essentially over. However, these unconventional resources will continue to be exploited in years to come, but at a more sustainable and conservative pace than seen in the past. Looking back, we can readily see that the huge number of shale core and cutting samples principally made available for applied scientific and commercial investigation actually led to a fundamental re-think as to the workings of the deep organic carbon cycle. Shales make up the greatest global repository for sedimentary organic matter. Classically they have been viewed as containing molecular archives of paleoclimate and paleoecosystems, and as far as resources are concerned, they have been recognized as sources and/or seals for petroleum (e.g., Killops and Killops 2005). What is now clear is that transport within and throughout low permeability



Fig. 9 (a) Phase envelopes of petroleums produced from the Eagle Ford Formation of DeWitt County compared with those of instantaneous petroleums generated using MSSV SnapShot experiments, (b) phase envelopes resulting from PhaseKinetics cumulative compositional predictions based on an immature outcrop sample

shale packages is extensive. It is also clear that macromolecular organic matter in a form other than kerogen, namely, heavy bitumen, is not only abundant but plays a fundamental role in the generation and storage of hydrocarbons. Either of these fractions can develop porosity during progressive maturation, and both contain thermally labile moieties that actively adsorb hydrocarbons. Working to reveal the true chemical nature of heavy bitumen is an important research avenue that is open for development, and that means in the broadest sense unraveling the cycling of nitrogen, sulfur, and oxygen in the geosphere. Very little is actually known about the fate of these elements in the stages that fall between early diagenesis (amino acids, fatty acids, humic acids, sulfurized lipids) and metagenesis (H_2S , CO_2 , N_2). Both analytical and simulation pyrolysis methods, selective chemical degradation, and advanced analytical characterization (e.g., FT-ICR MS, STXM) provide the means to undertake the work. The role played by microbes especially in uplifted shales must also be considered. The conceptual and technological advances regarding process understanding (chemical, physical, and biological) can readily be transferred from the area of resources to that of repositories, thereby allowing the potential consequences of nuclear waste storage in shales to be better assessed.

References

- Aplin AC, Macquaker JHS (2011) Mudstone diversity: origin and implications for source, seal, and reservoir properties in petroleum systems. *AAPG Bull* 95(12):2031–2059
- Arning E, Fu Y, van Berk W, Schulz H-M (2011) Organic carbon remineralisation and complex, early diagenetic solid–aqueous solution–gas interactions: case study ODP Leg 204, Site 1246 (Hydrate Ridge). *Mar Chem* 126(1–4):120–131
- Arning ET, van Berk W, Schulz H-M (2016) Fate and behaviour of marine organic matter during burial of anoxic sediments: testing CH_2O as generalized input parameter in reaction transport models. *Mar Chem* 178:8–21
- Arthur MA, Sageman BB (1994) Marine black shales: depositional mechanisms and environments of ancient deposits. *Annu Rev Earth Planet Sci* 22:499–551
- Baker DR (1962) Organic geochemistry of Cherokee Group in southeastern Kansas and northeastern Oklahoma. *AAPG Bull* 46(9):1621–1642
- Bera B, Sushanta MK, Douglas V (2011) Understanding the micro structure of Berea Sandstone by the simultaneous use of micro-computed tomography (micro-CT) and focused ion beam-scanning electron microscopy (FIB-SEM). *Micron* 42:412–418
- Bernard S, Horsfield B (2014) Thermal maturation of gas shale systems. *Annu Rev Earth Planet Sci* 42:635–651
- Bernard S, Horsfield B, Schulz HM, Schreiber A, Wirth R, Vu TTA, Perssen F, Könitzer S, Volk H, Sherwood N, Fuentes D (2010) Multi-scale detection of organic and inorganic signatures provides insights into gas shale properties and evolution. *Chem Erde Geochem* 70:119–133
- Bernard S, Horsfield B, Schulz HM, Wirth R, Schreiber A, Sherwood N (2012a) Geochemical evolution of organic-rich shales with increasing maturity: a STXM and TEM study of the Posidonia Shale (Lower Toarcian, northern Germany). *Mar Pet Geol* 31:70–89
- Bernard S, Wirth R, Schreiber A, Schulz HM, Horsfield B (2012b) Formation of nanoporous pyrobitumen residues during maturation of the Barnett Shale (FortWorth Basin). *Int J Coal Geol* 103:3–11
- Bernard S, Wirth R, Schreiber A, Bowen L, Aplin AC, Mathia EJ, Schulz H-M, Horsfield B (2013) FIB-SEM and TEM investigations of an organic-rich shale maturation series from the lower

- Toarcian Posidonia Shale, Germany: nanoscale pore system and fluid-rock interactions. In: Camp W, Diaz E, Wawak B (eds) *Electron microscopy of shale hydrocarbon reservoirs*. AAPG Memoir, Tulsa, vol 102, pp 53–66
- Binnion M (2012) How the technical differences between shale gas and conventional gas projects lead to a new business model being required to be successful. *Mar Pet Geol* 31(1):3–7
- Boyer C, Clark B, Jochen V, Lewis R, Miller CK (2011) Shale gas: a global resource. *Oilfield Rev* 23:28–39
- Bullin K, Krouskop P (2008) Composition variety complicates processing plans for US shale gas. Presentation to the annual forum, Gas Processors Association – Houston Chapter, Houston, 7 Oct 2008
- Bustin AMM, Bustin RM, Cui X (2008) Importance of fabric on the production of gas shales. Presented at society of petroleum engineers unconventional reservoirs conference, Keystone, 10–12 Feb. <https://doi.org/10.2118/114167-MS>
- Cane RF (1967) The constitution and synthesis of oil shale. In: *Proceedings of the 7th World Petroleum Congress*, Mexico City, pp 681–689
- Cane RF, Albion PR (1973) The organic geochemistry of torbanite precursors. *Geochim Cosmochim Acta* 37(6):1543–1549
- Cardott BJ, Lambert MW (1985) Thermal maturation by vitrinite reflectance of Woodford Shale, Anadarko Basin, Oklahoma. *AAPG Bull* 69(11):1982–1998
- Cavanagh AJ, di Primio R, Scheck-Wenderoth M, Horsfield B (2006) Severity and timing of Cenozoic exhumation in the southwestern Barents Sea. *J Geol Soc London* 163(5):761–774
- Chalmers GRL, Bustin RM, Power IM (2012) Characterization of gas shale pore systems by porosimetry, pycnometry, surface area and FE-SEM/TEM image analysis: examples from the Barnett, Woodford, Haynesville, Marcellus, and Doig formations. *AAPG Bull* 96:1099–1119
- Cooles GP, Mackenzie AS, Quigley TM (1986) Calculation of petroleum masses generated and expelled from source rocks. *Org Geochem* 10:235–245
- Curtis JB (2002) Fractured shale-gas systems. *AAPG Bull* 86:1921–1938
- Curtis ME, Ambrose RJ, Sondergeld CH (2010) Structural characterization of gas shales on the micro- and nano-scales. In: *Canadian unconventional resources and international petroleum conference*. Society of Petroleum Engineers, Calgary, Alberta, Canada, pp 1–15
- Curtis ME, Ambrose RJ, Sondergeld CH, Rai CS (2011a) Investigation of the relationship between organic porosity and thermal maturity in the Marcellus Shale. Presented at N. Am. Unconv. Gas Conf. Exhib., June 14–16, The Woodlands, TX. <https://doi.org/10.2118/144370-MS>
- Curtis ME, Ambrose RJ, Sondergeld CH, Rai CS (2011b) Transmission and scanning electron microscopy investigation of pore connectivity of gas shales on the nanoscale. Presented at N. Am. Unconv. Gas Conf. Exhib., June 14–16, The Woodlands, TX. <https://doi.org/10.2118/144391-MS>
- Curtis ME, Ambrose RJ, Sondergeld CH, Rai CS (2012) Microstructural investigation of gas shales in two and three dimensions using nanometer-scale resolution imaging. *AAPG Bull* 96:665–677
- de Leeuw JW, Largeau C (1993) A review of macromolecular organic compounds that comprise living organisms and their role in kerogen, coal and petroleum formation. In: Engel MH, Macko SA (eds) *Organic geochemistry, principles and applications*. Plenum Press, New York, pp 23–72
- Desbois G, Urai JL, Houben ME, Sholokhova Y (2010) Typology, morphology and connectivity of pore space in claystones from reference site for research using BIB, FIB and cryo-SEM methods. *EPJ Web Conf* 6:22005. <https://doi.org/10.1051/epjconf/20100622005>
- di Primio R (2002) Unraveling secondary migration effects through the regional evaluation of PVT data: a case study from Quadrant 25, NOCS. *Org Geochem* 33(6):643–653
- di Primio R, Horsfield B (1997) Predicting the generation of heavy oils in carbonate/evaporitic environments using pyrolysis methods. *Org Geochem* 24(10–11):999–1016
- di Primio R, Horsfield B (2006) From petroleum-type organofacies to hydrocarbon phase prediction. *AAPG Bull* 90:1031–1058
- di Primio R, Dieckmann V, Mills N (1998) PVT and phase behaviour analysis in petroleum exploration. *Org Geochem* 29(1–3):207–222

- Dieckmann V, Schenk HJ, Horsfield B, Welte DH (1998) Kinetics of petroleum generation and cracking by programmed-temperature closed-system pyrolysis of Toarcian Shales. *Fuel* 77 (1–2):23–31
- Diessel CFK (2007) Utility of coal petrology for sequence stratigraphic analysis. *Int J Coal Geol* 70:3–34
- Düppenbecker SJ, Horsfield B (1990) Compositional information for kinetic modelling and petroleum type prediction. *Org Geochem* 16(1–3):259–266
- Elias R, Gelin F (2015) Vertical heterogeneity of kerogen and fluid compositions in the Vaca Muerta unconventional shale play and assessment of producible fluid composition and quality. In: International petroleum technology conference, Tenerife
- Energy Information Administration (EIA) (2017) Annual energy outlook 2017 with projections to 2050. Washington, DC: US Department of Energy
- England WA, Mackenzie AS, Mann DM, Quigley TM (1987) The movement and entrapment of petroleum fluids in the subsurface. *J Geol Soc* 144(2):327–347
- Erdmann M, Horsfield B (2006) Enhanced late gas generation potential of petroleum source rocks via recombination reactions: evidence from the Norwegian North Sea. *Geochim Cosmochim Acta* 70:3943–3956
- Espitalié J, Madec M, Tissot B (1980) Role of mineral matrix in kerogen pyrolysis: influence on petroleum generation and migration. *AAPG Bull* 64(1):59–66
- Fan L, Martin RB, Thompson JW, Atwood K, Robinson JR, Lindsay GF (2011) An integrated approach for understanding oil and gas reserves potential in eagle ford shale formation. Society of Petroleum Engineers. SPE Canadian Unconventional Resources Conference, Calgary, Alberta, CSUG/SPE 148751
- Fishman NS, Bereskin SR, Bowker KA, Cardott BJ, Chidsey TC, Dubiel RF, Enomoto CB, Harrison WB, Jarvie DM, Jenkins CL, LeFever JA, Li P, McCracken JN, Morgan CD, Nordeng SH, Nyahay RE, Schamel S, Sumner RL, Wray LL (2011) Gas shale/shale oil. In: Warwick PD (compiler) Unconventional energy resources – 2011 review. *Natural Resources Research* 20:288–301
- Gamero Diaz H, Lewis R, Miller CK (2013) sCore: a mineralogy based classification scheme for organic mudstones. In: SPE annual technical conference and exhibition, New Orleans, 30 Sept–2 Oct. <https://doi.org/10.2118/166284-MS>
- Gasparik M, Bertier P, Gensterblum Y, Ghanizadeh A, Krooss BM, Littke R (2014) Geological controls on the methane storage capacity in organic-rich shales. *Int J Coal Geol* 123:34–51
- Geel C, de Wit M, Booth P, Schulz H-M, Horsfield B (2015) Palaeo-environment, diagenesis and characteristics of Permian black shales in the Lower Karoo Supergroup flanking the Cape Fold Belt near Jansenville, eastern Cape, South Africa: implications for the shale gas potential of the Karoo Basin. *S Afr J Geol* 118(3):249–274
- Hackley PC, Cardott BJ (2016) Application of organic petrography in North American shale petroleum systems: a review. *Int J Coal Geol* 163:8–51
- Hammes U, Hamlin HS, Ewing TE (2011) Geological analysis of the Upper Jurassic Haynesville Shale in east Texas and west Louisiana. *AAPG Bull* 95:1643–1666
- Han Y (2016) Oil retention and migration in the Barnett, Posidonia, and Niobrara Shales. Ph.D Thesis, Technical University of Berlin. <https://doi.org/10.14279/depositonce-5815>
- Han Y, Mahlstedt N, Horsfield B (2015) The Barnett Shale: compositional fractionation associated with intraformational petroleum migration, retention, and expulsion. *AAPG Bull* 99 (12):2173–2202
- Han Y, Horsfield B, Wirth R, Mahlstedt N, Bernard S (2017) Oil retention and porosity evolution in organic-rich shales. *AAPG Bull* 101(6):807–827
- Han Y, Horsfield B, Mahlstedt N, Wirth R, Curry D, LaReau H (2018) Factors controlling source and reservoir characteristics in the Niobrara shale-oil system, Denver Basin. *AAPG Bull* (submitted)
- Hantschel T, Kauerauf AI (2009) Fundamentals of basin and petroleum systems modeling. Springer, Berlin/Heidelberg

- Hao F, Zou H (2013) Cause of shale gas geochemical anomalies and mechanisms for gas enrichment and depletion in high-maturity shales. *Mar Pet Geol* 44:1–12
- Heath JE, Dewers TA, McPherson BJOL, Petrusak R, Chidsey TC et al (2011) Pore networks in continental and marine mudstones: characteristics and controls on sealing behavior. *Geosphere* 7:429–454
- Hill RJ, Jarvie DM, Zumberge J, Henry M, Pollastro RM (2007) Oil and gas geochemistry and petroleum systems of the Fort Worth Basin. *AAPG Bull* 91:445–473
- Horsfield B (1984) Pyrolysis studies and petroleum exploration. In: Brooks J, Welte DH (eds) *Advances in petroleum geochemistry*. Academic Press, London, pp 247–298
- Horsfield B (1989) Practical criteria for classifying kerogens: some observations from pyrolysis–gas chromatography. *Geochim Cosmochim Acta* 53:891–901
- Horsfield B, Douglas A (1980) The influence of minerals on the pyrolysis of kerogens. *Geochim Cosmochim Acta* 44(8):1119–1131
- Horsfield B, Heckers J, Leythaeuser D, Littke R, Mann U (1991) A study of the Holzener Asphaltkalk, Northern Germany: observations regarding the distribution, composition and origin of organic matter in an exhumed petroleum reservoir. *Mar Pet Geol* 8:198–211
- Horsfield B, Bharati S, Larter SR, Leistner F, Littke R, Schenk HJ, Dypvik H (1992a) On the atypical petroleum-generating characteristics of alginite in the Cambrian Alum Shale. In: Schidlowski M et al (eds) *Early organic evolution: implications for mineral and energy resources*. Springer, Berlin/Heidelberg, pp 257–266
- Horsfield B, Schenk HJ, Mills N, Welte DH (1992b) An investigation of the in-reservoir conversion of oil to gas: compositional and kinetic findings from closed-system programmed-temperature pyrolysis. In: Eckardt C et al (eds) *Advances in organic geochemistry 1991*. *Organic geochemistry*, vol 19, pp 191–204
- Horsfield B, Leistner F, Hall K (2015) Microscale sealed vessel pyrolysis. In: Grice K (ed) *Principles and practice of analytical techniques in geosciences*. Royal society of chemistry detection science series no. 4. The Royal Society of Chemistry, Cambridge, pp 209–250
- Hübner A, Horsfield B, Kapp I (2013) Fact-based communication: the shale gas information Platform. *Environ Earth Sci* 70:3921–3925
- International Energy Agency (IEA) (2012) *Golden rules for a golden age of gas*. World energy outlook special report on unconventional. International Energy Agency, Paris
- Jarvie DM (2012a) Shale resource systems for oil and gas: part 1 – shale-gas resource systems. In: Breyer JA (ed) *Shale reservoirs – Giant resources for the 21st century*. AAPG memoir, vol 97, pp 69–87
- Jarvie DM (2012b) Shale resource systems for oil and gas: part 2 – shale-oil resource systems. In: Breyer JA (ed) *Shale reservoirs – Giant resources for the 21st century*. AAPG Memoir, vol 97, pp 89–119
- Jarvie DM, Claxton BL, Henk F, Breyer JT (2001) Oil and shale gas from the Barnett Shale, Fort Worth basin, Texas. AAPG National Convention, June 3–6, 2001, Denver, CO. AAPG Bull 85 (13 (Supplement)):A100
- Jarvie DM, Hill RJ, Ruble TE, Pollastro RM (2007) Unconventional shale-gas systems: the Mississippian Barnett Shale of north-central Texas as one model for thermogenic shale-gas assessment. *AAPG Bull* 91:475–499
- Jenkins CD, Boyer CM (2008) Coalbed- and shale-gas reservoirs. *J Pet Technol* 60(2):92–99
- Jones RW (1987) Organic facies. In: Brooks J, Welte DH (eds) *Advances in Petroleum Geochemistry*, vol 2. Academic Press, London, pp 1–90
- Katsube TJ, Williamson MA (1994) Effects of diagenesis on shale nano-pore structure and implications for sealing capacity. *Clay Miner* 29:451–461
- Kelemen SR, Walters CC, Ertas D, Kwiatek LM, Curry DJ (2006) Petroleum expulsion part 2. Organic matter type and maturity effects on kerogen swelling bysolvents and thermodynamic parameters for kerogen from regular solution theory. *Energy and Fuels* 20(1):301–308
- Kietzmann DA, Martín-Chivelet J, Palma RM, López-Gómez J, Lescano M, Concheyro A (2011) Evidence of precessional and eccentricity orbital cycles in a Tithonian source rock: the mid-

- outer carbonate ramp of the Vaca Muerta formation, northern Neuquén Basin, Argentina. *AAPG Bull* 95:1459–1474
- Killops S, Killops V (2005) Introduction to organic geochemistry, 2nd edn. Blackwell, Oxford
- Krooss BM, Leythaeuser D, Lillack H (1993) Nitrogen-rich natural gases. Qualitative and quantitative aspects of natural gas accumulation in reservoirs. *Erdöl Kohle Erdgas Petrochem* 46:271–276
- Krüger M, van Berk W, Arning ET, Jiménez N, Schovsbo NH, Straaten N, Schulz H-M (2014) The biogenic methane potential of European gas shale analogues: results from incubation experiments and thermodynamic modelling. *Int J Coal Geol* 136:59–74
- Kuhn P, di Primio R, Horsfield B (2010) Bulk composition and phase behaviour of petroleum sourced by the Bakken Formation of the Williston Basin. In: Vining BA, Pickering SC (eds) *Petroleum geology: from mature basins to new frontiers – proceedings of the 7th petroleum geology conference*, vol 7. Geological Society of London, London, pp 1065–1077
- Kuhn PP, di Primio R, Hill R, Lawrence JR, Horsfield B (2012) Three-dimensional modeling study of the low-permeability petroleum system of the Bakken Formation. *AAPG Bull* 96:1867–1897
- Kuske S, Horsfield B, Michael GE, Jweda J, Song Y (2017) Geochemical factors controlling the phase behavior of in-situ petroleum fluids in the eagle ford shale. *AAPG Bull* (accepted)
- Landon SM, Longman MW, Luneau BA (2001) Hydrocarbon source rock potential of the upper Cretaceous Niobrara Formation, western interior seaway of the rocky mountain region. *Mt Geol* 38(1):1–18
- Largeau C, Casadevall E, Kadouri A, Metzger P (1984) Formation of Botryococcus-derived kerogens-comparative study of immature torbanites and of the extant alga Botryococcus braunii. *Org Geochem* 6:327–332
- Larter SR (1984) Application of analytical pyrolysis techniques to kerogen characterization and fossil fuel exploration/exploitation. In: Voorhees K (ed) *Analytical pyrolysis, methods and application*. Butterworth, London, pp 212–275
- Larter SR (1985) Integrated kerogen typing in the recognition and quantitative assessment of petroleum source rocks. In: *Petroleum geochemistry in exploration of the Norwegian shelf*. Norwegian petroleum society. Graham and Trotman, London, pp 269–285
- Le Tran KJ, Connan J, van der Weide J (1974) Diagenesis of organic matter and occurrence of hydrocarbons and hydrogen sulfide in SW Aquitaine Basin (France): *bull. Cent Rech Pau-SNPA* 8:111–137
- Littke R, Rullkötter J (1987) Mikroskopische und makroskopische Unterschiede zwischen Profilen unreifen und reifen Posidonienschiefers aus der Hilsmulde. *Facies* 17(1):171–179
- Littke R, Baker D, Leythaeuser D (1988) Microscopic and sedimentologic evidence for the generation and migration of hydrocarbons in Toarcian source rocks of different maturities. *Org Geochem* 13(1–3):549–559
- Littke R, Baker DR, Rullkötter J (1997) Deposition of petroleum source rocks. In: Welte DH, Horsfield B, Baker DR (eds) *Petroleum and basin evolution*. Springer, Heidelberg, pp 271–333
- Locklair RE, Sageman BB (2008) Cyclostratigraphy of the Upper Cretaceous Niobrara Formation, Western Interior, U.S.A.: a Coniacian–Santonian orbital timescale. *Earth Planet Sci Lett* 269:540–553
- Lopatin NV, Zubairae SL, Kos IM, Emets TP, Romanov EA, Malchikhina OV (2003) Unconventional oil accumulations in the Upper Jurassic Bazhenov Black Shale Formation, West Siberian Basin: a self-sourced reservoir system. *J Pet Geol* 26(2):225–244
- Lorant F, Behar F (2002) Late generation of methane from mature kerogens. *Energy Fuel* 16:412–427
- Loucks RG, Reed RM, Ruppel SC, Jarvie DM (2009) Morphology, genesis, and distribution of nanometer-scale pores in siliceous mudstones of the Mississippian Barnett shale. *J Sediment Res* 79:848–861
- Loucks RG, Reed RM, Ruppel SC, Hammes U (2010) Preliminary classification of matrix pores in mudrocks. *Transactions* 60:435–441. Gulf Coast Association of Geological Society

- Loucks RG, Reed RM, Ruppel SC, Hammes U (2012) Spectrum of pore types and networks in mudrocks and a descriptive classification for matrix-related mudrock pores. *AAPG Bull* 96:1071–1098
- Lüning S, Craig J, Loydell DK, Štorch P, Fitches B (2000) Lower Silurian ‘hot shales’ in North Africa and Arabia: regional distribution and depositional model. *Earth Sci Rev* 49(1–4):121–200
- Macquaker JH, Adams AE (2003) Maximizing information from fine-grained sedimentary rocks: an inclusive nomenclature for mudstones. *J Sediment Res* 73:735–744
- Macquaker JHS, Taylor KG, Keller M, Polya D (2014) Compositional controls on early diagenetic pathways in fine-grained sedimentary rocks: implications for predicting unconventional reservoir attributes of mudstones. *AAPG Bull* 98:587–603
- Mahlstedt N, Horsfield B (2012) Metagenetic methane generation in gas shales. I. Screening protocols using immature samples. *Mar Pet Geol* 31:27–42
- Mahlstedt N, Horsfield B (2013) A new screening tool for the rapid evaluation of gas sorption capacity in shales. In: *AAPG Hedberg conference*, Beijing, 21–24 Apr
- Mahlstedt N, Horsfield B, Dieckmann V (2008) Second order reactions as a prelude to gas generation at high maturity. *Org Geochem* 39(8):1125–1129
- Mahlstedt N, di Primio R, Horsfield B, Boreham CJ (2015) Multi-component kinetics and late gas potential of selected Cooper Basin source rocks. *Record* 2015/19. *Geoscience Australia*, Canberra, p 199. <https://doi.org/10.11636/Record.12015.11019>
- Mahlstedt N, Horsfield B, Wilkes H, Poetz S (2016) Tracing the impact of fluid retention on bulk petroleum properties using nitrogen-containing compounds. *Energy Fuel* 30: 6290–6305
- Mahlstedt N, Noah M, Horsfield B (2017) Combining FT-ICR MS and pyrolysis to predict petroleum-type organofacies and evolving fluid physical properties. In: *28th international meeting on organic geochemistry (IMOG)*, Florence
- Mao J, Fang X, Lan Y, Schimmelmann A, Mastalerz M, Xu L, Schmidt-Rohr K (2010) Chemical and nanometer-scale structure of kerogen and its change during thermal maturation investigated by advanced solid-state ¹³C NMR spectroscopy. *Geochim Cosmochim Acta* 74:2110–2127
- Mathia EJ, Bowen L, Thomas KM, Aplin AC (2016) Evolution of porosity and pore types in organic-rich, calcareous, Lower Toarcian Posidonia Shale. *Mar Pet Geol* 75:117–139
- Montgomery CT, Smith MB (2010) Hydraulic fracturing: history of an enduring technology. *J Pet Technol* 26–32
- Muscio GPA, Horsfield B, Welte DH (1991) Compositional changes in the macromolecular organic matter (kerogens, asphaltenes and resins) of a naturally matured source rock sequence from northern Germany as revealed by pyrolysis methods. In: *DAC M (ed) Organic geochemistry advances and applications in the natural environment*. Manchester University Press, Manchester/New York, pp 447–449
- Muscio G, Horsfield B, Welte DH (1994) Occurrence of thermogenic gas in the immature zone – implications from the Bakken in-source reservoir system. In: *Telnæs N, van Graas G, Øygaard K (eds) Advances in organic geochemistry 1993*, Elsevier. *Organic geochemistry* 22(3–5): 461–476
- Mycke B, Michaelis W (1986) Lignin-derived molecular fossils from geological materials. *Naturwissenschaften* 73:731–734
- Nelson PH (2009) Pore throat sizes in sandstones, tight sandstones, and shales. *AAPG Bull* 93:1–13
- Oldenburg TBP, Brown M, Bennett B, Larter SR (2014) The impact of thermal maturity level on the composition of crude oils, assessed using ultra-high resolution mass spectrometry. *Org Geochem* 75:151–168
- Orr WL (1986) Kerogen/asphaltene/sulfur relationships in sulfur-rich Monterey oils. *Org Geochem* 10:499–516
- Passey QR, Creaney S, Kulla JB, Moretti FJ, Stroud JD (1990) A practical model for organic richness from porosity and resistivity logs. *AAPG Bull* 74(12):1777–1794

- Passey Q, Bohacs K, Esch W, Klimentidis R, Sinha S (2010) From oil-prone source rock to gas-producing shale reservoir – geologic and petrophysical characterization of unconventional shale-gas reservoirs. In: International oil and gas conference and exhibition in China. Society of Petroleum Engineers, Beijing, 8–10 June
- Pepper AS (1991) Estimating the petroleum expulsion behaviour of source rocks: a novel quantitative approach. In: England WA, Fleet AJ (eds) Petroleum migration. Geological society special publications, vol 59. Geological Society, London, pp 9–31
- Philp RP, Calvin M (1976) Possible origin for insoluble organic (kerogen) debris in sediments from insoluble cell-wall materials of algae and bacteria. *Nature* 262:134–136
- Poelchau HS, Baker DR, Hantschel T, Horsfield B, Wygrala B (1997) Basin simulation and the design of the conceptual basin model. In: Welte DH, Horsfield B, Baker DR (eds) Petroleum and basin evolution. Springer, Heidelberg, pp 3–70
- Poetz S, Horsfield B, Wilkes H (2014) Maturity-driven generation and transformation of acidic compounds in the organic-rich Posidonia shale as revealed by electrospray ionization fourier transform ion cyclotron resonance mass spectrometry. *Energy and Fuels* 28:4877–4888
- Pollastro RM (2010) Natural fractures, composition, cyclicity, and diagenesis of the Upper Cretaceous Niobrara Formation, Berthoud Field, Colorado. *The Mountain Geologist* 47(4): 135–149
- Powell TG (1984) Some aspects of the hydrocarbon geochemistry of a Middle Devonian Barrier-Reef Complex, Western Canada. In: James G. Palacas (ed) Petroleum Geochemistry and Source Rock Potential of Carbonate Rocks, 1984, AAPG Studies in Geology 18. <https://doi.org/10.1306/St18443C4>
- Price LC, Ging T, Daws TA, Love A, Pawlewicz MJ, Anders DE (1984) Organic metamorphism in the Mississippian–Devonian Bakken shale, North Dakota portion of the Williston Basin. In: Woodward J, Meissner FF, Clayton JL (eds) Hydrocarbon source rocks in the greater Rocky Mountain region: Rocky Mountain Association of Geologists, pp 83–133
- Requejo AG, Allan J, Creaney S, Gray NR, Cole KS (1992) Aryl isoprenoids and diaromatic carotenoids in Paleozoic source rocks and oils from the Western Canada and Williston basins. *Org Geochem* 19:245–264
- Robison CR (1997) Hydrocarbon source rock variability within the Austin Chalk and Eagle Ford Shale (Upper Cretaceous), East Texas, USA. *Int J Coal Geol* 34(3):287–305
- Rogner HH (1997) An assessment of world hydrocarbon resources. *Annu Rev Energy Environ* 22:217–262
- Romero AM, Philp RP (2012) Organic geochemistry of the Woodford Shale, Southeastern Oklahoma: how variable can shales be? *AAPG Bull* 96(3):493–517
- Romero-Sarmiento MF, Rouzaud JN, Bernard S, Deldicque D, Thomas M, Littke R (2014) Evolution of Barnett Shale organic carbon structure and nanostructure as a function of increasing maturation. *Org Geochem* 71:7–16
- Ross DJ, Bustin RM (2009) The importance of shale composition and pore structure upon gas storage potential of shale gas reservoirs. *Mar Pet Geol* 26:916–927
- Rullkötter J, Michaelis W (1990) The structure of kerogen and related materials. A review of recent progress and future trends. In: Durand B, Behar F (eds) Advances in organic geochemistry 1989, part II: molecular geochemistry. Pergamon Press, Oxford, pp 829–852
- Rullkötter J, Leythaeuser D, Horsfield B, Littke R, Mann U, Müller PJ, Radke M, Schaefer RG, Schenk H-J, Schwochau K, Witte EG, Welte DH (1988) Organic matter maturation under influence of a deep intrusive heat source: a natural experiment for quantification of hydrocarbon generation and expulsion from a petroleum source rock (Toarcien shale, Northern Germany). In: Mattavelli L, Novelli L (eds) Advances in organic geochemistry 1987. Organic geochemistry edn. Pergamon Press, Oxford, pp 847–856
- Ruppert L, Sakurovs R, Blach TP, He L, Melnichenko YB et al (2013) A USANS/SANS study of the accessibility of pores in the Barnett shale to methane and water. *Energy Fuel* 27:772–779
- Sandvik EI, Young WA, Curry DJ (1992) Expulsion from hydrocarbon sources: the role of organic absorption. *Org Geochem* 19(1–3):77–87

- Santamaria-Orozco D, Horsfield B (2003) Gas generation potential of Upper Jurassic (Tithonian) source rocks in the Sonda de Campeche, Mexico. In: Bartollini C, Buffler RT, Brickwede RF (eds) *The Circum-Gulf of Mexico and the Caribbean: hydrocarbons habitat, basin formation and plate tectonics*. AAPG memoir, vol 79(15). AAPG, Tulsa, pp 349–363
- Schenk HJ, di Primio R, Horsfield B (1997a) The conversion of oil into gas in petroleum reservoirs. Part 1: comparative kinetic investigation of gas generation from crude oils of lacustrine, marine and fluviodeltaic origin by programmed-temperature closed-system pyrolysis. *Org Geochem* 26:467–481
- Schenk H-J, Horsfield B, Krooß B, Schaefer RG, Schwochau K (1997b) Kinetics of petroleum formation and cracking. In: Welte DH, Horsfield B, Baker DR (eds) *Petroleum and basin evolution*. Springer, Heidelberg, pp 231–270
- Schettler PD Jr, Parmely CR (1991) Contributions to total storage capacity in Devonian shales. In: SPE Eastern Regional Meeting, Lexington, Kentucky, October 22–25, 1991, SPE-23422-MS, 12 p. <https://doi.org/10.2118/23422-MS>
- Schmid-Röhl A, Röhl H-J, Oschmann W, Frimmel A, Schwark L (2002) Palaeoenvironmental reconstruction of Lower Toarcian epicontinental black shales (Posidonia Shale, SW Germany): global versus regional control. *Geobios* 35:13–20
- Schulz H-M, Biermann S, van Berk W, Krüger M, Straaten N, Bechtel A, Wirth R, Lüders V, Schovsbo NH, Crabtree S (2015) From shale oil to biogenic shale gas: retracing organic–inorganic interactions in the Alum Shale (Furongian–Lower Ordovician) in southern Sweden. *AAPG Bull* 99(5):927–956
- Slatt RM, O’Brien NR (2011) Pore types in the Barnett and Woodford gas shales: contribution to understanding gas storage and migration pathways in fine-grained rocks. *AAPG Bull* 95:2017–2030
- Smith MG, Bustin RM (1998) Production and preservation of organic matter during deposition of the Bakken Formation (Late Devonian and early Mississippian), Williston Basin. *Paleogeogr Paleoclimatol Paléoeocol* 142(3–4):185–200
- Sondergeld CH, Ambrose RJ, Rai CS, Moncrieff J (2010) Micro-structural studies of gas shales. Presented at Society of Petroleum Engineers unconventional gas conference, Pittsburgh, 23–25 Feb. <https://doi.org/10.2118/131771-MS>
- Stainforth JG, Reinders JEA (1990) Primary migration of hydrocarbons by diffusion through organic matter networks, and its effect on oil and gas generation. *Org Geochem* 16(1–3):61–74
- Stasiuk LD (1997) The origin of pyrobitumens in Upper Devonian Leduc Formation gas reservoirs, Alberta, Canada: an optical and EDS study of oil to gas transformation. *Mar Pet Geol* 14:915–929
- Sykes R, Snowdon LR (2002) Guidelines for assessing the petroleum potential of coaly source rocks using Rock–Eval pyrolysis. *Org Geochem* 33:1441–1455
- Tan J, Horsfield B, Mahlstedt N, Zhang J, di Primio R, Vu TAT, Boreham CJ, van Graas G, Tocher BA (2013) Physical properties of petroleum formed during maturation of Lower Cambrian shale in the upper Yangtze Platform, South China, as inferred from PhaseKinetics modelling. *Mar Petrol Geol* 48:47–56
- Tegelaar EW, Matthezing RM, Jansen BH, Horsfield B, de Leeuw JW (1989) Possible origin of n-alkanes in high-wax crude oils. *Nature* 342(6249):529–531
- Tissot BP, Welte DH (1978) *Petroleum formation and occurrence*. Springer, Berlin
- Tissot BP, Califet-Debyser Y, Deroo G, Oudin JL (1971) Origin and evolution of hydrocarbons in early Toarcian shales, Paris Basin, France. *AAPG Bull* 55(12):2177–2193
- Tissot BP, Durand B, Espitalie J, Combaz A (1974) Influence of nature and diagenesis of organic matter in formation of petroleum. *AAPG Bull* 58:499–506
- Tissot BP, Pelet R, Ungerer P (1987) Thermal history of sedimentary basins, maturation indices, and kinetics of oil and gas generation. *Bull Am Assoc Pet Geol* 71:1445–1466
- Tourtlet HA (1979) Black shale – its deposition and diagenesis. *Clay Clay Miner* 27:313–321
- Ungerer P (1990) State of the art of research in kinetic modelling of oil formation and expulsion. *Org Geochem* 16(1–3):1–25

- Vetter A, Horsfield B (2014) Shale Gas Information Platform SHIP: unconventional seen from a scientific point of view. *Int Shale Gas Oil J* 2(3):6–7
- Vu TAT, Horsfield B, Sykes R (2008) Influence of in-situ bitumen on the generation of gas and oil in New Zealand coals. *Org Geochem* 39(11):1606–1619
- Vu TAT, Horsfield B, Mahlstedt N, Schenk HJ, Kelemen SR, Walters CC, Kwiatek PJ, Sykes R (2013) The structural evolution of organic matter during maturation of coals and its impact on petroleum potential and feedstock for the deep biosphere. *Org Geochem* 62:17–27
- Walls JD, Sinclair SW (2011) Eagle Ford shale reservoir properties from digital rock physics. *First Break* 29:97–101
- Whitson CH, Sunjerga S (2012) PVT in liquid-rich shale reservoirs. Society of Petroleum Engineers. <https://doi.org/10.2118/155499-MS>
- Wignall PB, Hallam A (1991) Biofacies, stratigraphic distribution and depositional models of British onshore Jurassic black shales. In: Tyson RV, Pearson TH (eds) *Modern and ancient continental shelf anoxia*, vol 58, Geological Society of London Publishing House, pp 291–309
- Wüst RAJ, Hackley PC, Nassichuk BR, Willment N, Brezovski R (2013) Vitrinite reflectance versus pyrolysis Tmax data: assessing thermal maturity in shale plays with special reference to the Duvernay shale play of the Western Canadian Sedimentary Basin, Alberta. SPE 167031. Society of Petroleum Engineers
- Yang S, Horsfield B (2016) Some predicted effects of minerals on the generation of petroleum in nature. *Energy and Fuels* 30(8):6677–6687
- Yang S, Schulz HM, Horsfield B, Schovsbo NH, Panova E, Rothe H, Hahne K (2018) On the changing petroleum generation properties of Alum Shale over geological time caused by uranium irradiation. *Geochim Cosmochim Acta* 229:20–35
- Ziegs V, Horsfield B, Skeie JE, Rinna J (2017) Petroleum retention in the Mandal Formation, Central Graben, Norway. *Mar Pet Geol* 83:195–214
- Zumberge J, Ferworn K, Brown S (2012) Isotopic reversal (“rollover”) in shale gases produced from the Mississippian Barnett and Fayetteville formations. *Mar Pet Geol* 31:43–52



Bernd R. T. Simoneit

Contents

1	Introduction	558
2	Analytical Methods	558
3	Geological Locales with Hydrothermal Petroleum	559
3.1	Sediment-Covered Marine Systems	559
3.2	Bare Rock Hydrothermal Systems	569
3.3	Continental Systems	570
4	Nature and Alteration of Organic Matter in Hydrothermal Systems	571
4.1	Organic Matter Alteration by Hydrothermal Processes	572
4.2	Composition of Hydrothermal Petroleum	575
5	Fluid Interactions	577
6	Hydrothermal Petroleum Expulsion/Extraction/Migration	579
7	Implications	580
7.1	Petroleum Resources	580
7.2	Mineral Deposits	582
7.3	Hydrothermal Organic Synthesis	582
8	Summary	583
	References	584

Abstract

Hydrothermal petroleum formation is rapid and efficient in systems associated with tectonic spreading centers and high fluid transport. In these systems the conditions driving chemical reactions are high temperatures (~60 to >400 °C) and confining pressures (>150 bar) in an aqueous open flow medium. Organic matter alteration by reductive reactions to petroleum hydrocarbons proceeds

B. R. T. Simoneit (✉)

BRT Simoneit, Department of Chemistry, College of Science, Oregon State University, Corvallis, OR, USA

e-mail: simonebe@oregonstate.edu

© Springer Nature Switzerland AG 2020

H. Wilkes (ed.), *Hydrocarbons, Oils and Lipids: Diversity, Origin, Chemistry and Fate*, Handbook of Hydrocarbon and Lipid Microbiology,

https://doi.org/10.1007/978-3-319-90569-3_16

557

generally from immature organic matter (also from entrained viable biota) instantaneously or over a brief geological time span (decades to millennia). These conditions are conducive to organic chemistry which yields concurrent products primarily from reduction (due to mineral buffering), to a lesser extent from oxidation (high thermal stress), and traces from synthesis reactions.

1 Introduction

The discovery of submarine hydrothermal vent systems (Corliss et al. 1979) with their associated chemistry and chemosynthetic biota has had great impact in the geosciences, biosciences, and chemistry and even in cosmochemistry (e.g., Holm 1992; Simoneit et al. 1998). Organic matter in sedimentary basins, usually marine, is derived from the syngenetic residues of posthumous biogenic debris (Simoneit 1982a; Tissot and Welte 1984; Hunt 1996). This material is composed of both autochthonous detritus from marine bioproductivity and allochthonous residues derived from continental sources (Simoneit 1982a). Aquatic sediments receive allochthonous organic detritus primarily by river wash-in and eolian fallout particles, with ice-rafting and sediment recycling as minor contributing processes (Simoneit 1978). The aspects of hydrothermal alteration of sedimentary organic matter, mainly contemporary, to hydrothermal petroleum are the topic discussed here. Organic matter in hydrothermal rift systems is usually marine, as in sedimentary basins, but generally of an immature recent origin (Simoneit 1982a, 1983a). Hydrothermal petroleum is defined here as the gas/bitumen product generated by rapid thermal alteration in high water flow systems (high water rock ratio) from generally immature organic matter in sediments.

2 Analytical Methods

Analyses for gasoline-range (C_4 – C_9) hydrocarbons were carried out on sealed (vials) or bagged sediment samples by the methods described (Simoneit et al. 1979, 1988; Whelan and Hunt 1982). Interstitial gases in vacutainers were analyzed for composition and stable isotope contents (Simoneit 1982b; Galimov and Simoneit 1982a, b; Simoneit and Galimov 1984). The extractable bitumen fractionations and protokerogen analyses were carried out by the well-defined organic geochemical practices (Jenden et al. 1982; Simoneit and Philp 1982; Kawka and Simoneit 1987), and hydrothermal petroleum was analyzed by the same methods after extraction from the minerals and appropriate fractionation (Kawka and Simoneit 1987; Simoneit 1994).

The various organic fractions were analyzed by capillary gas chromatography (GC) and computerized gas chromatography-mass spectrometry (GC-MS) (Kawka and Simoneit 1987; Simoneit 1994; Ventura et al. 2012). The pseudokerogens from sediments were analyzed by Curie point pyrolysis and electron spin resonance

spectrometry (ESR) and for stable isotope and elemental compositions (e.g., Jenden et al. 1982; Simoneit et al. 1984).

3 Geological Locales with Hydrothermal Petroleum

An overview of the studies of hydrothermal systems with significant petroleum is given in Table 1. The organic matter alterations in marine sediment-covered systems were studied initially, and new reports are limited. The topic presented here has been reviewed numerous times (e.g., Simoneit 1988, 1990, 1992, 1993, 1995, 2000a, b, 2003; Rokosova et al. 2001) in order to enlighten various disciplines.

3.1 Sediment-Covered Marine Systems

The locations with known hydrothermal activity and associated mineralization at seafloor spreading centers (divergent plate boundaries) number about 300 and are

Table 1 Types of hydrothermal systems

	Examples Studied	Typical discharge temperatures (°C)	References
<i>Marine</i> (recharge fluid-sea water)			
Sediment-covered spreading ridge	Guaymas Basin, Escanaba trough, Middle Valley, Red Sea	Warm up to ~400 °C	Bazylinski et al. (1988); Kvenvolden et al. (1986); Michaelis et al. (1990); Simoneit and Lonsdale (1982); Simoneit (1985a, 1994); Simoneit et al. (1987); Davis et al. (1992); Fouquet et al. (1998)
Mid-ocean ridge (no sediment)	East Pacific rise, mid-Atlantic ridge – TAG	Warm up to ~350 °C	Brault and Simoneit (1989); Brault et al. (1985, 1989)
Off-axis flanks and basins	Juan de Fuca ridge	Warm	Andersson et al. (2000)
Back-arc	Bransfield Strait	No discharge (<150 °C)	Brault and Simoneit (1988, 1990); Whiticar et al. (1985)
Hot spots	–	–	–
Subduction	Oregon margin	Ambient	Kulm et al. (1986)
<i>Continental</i> (recharge fluid-meteoric water)			
Hot spots	Yellowstone national park	<96 °C	Clifton et al. (1990)
Rift valleys	Lake Tanganyika	65–80 °C	Tiercelin et al. (1989, 1993); Simoneit et al. (2000)
Volcanism	Waiotapu, New Zealand	<100 °C	Czochanska et al. (1986)

– organic matter not yet studied

catalogued in the reviews by Rona (1984, 1988, 2003) and Rona and Scott (1993). Those discussed here, where associated organic matter alteration has been studied, are indicated on the tectonic sketch map in Fig. 1. A summary of the organic carbon content of the source sediments, total hydrocarbon yields, and carbon preference index (CPI) of *n*-alkanes is given in Table 2. Examples of two continental systems are also shown in Fig. 1. The current interests in exploration have shifted to geologically ancient hydrothermal activity and associated mineralization with regard to petroleum exploration and mining (e.g., Scott 1985; Little et al. 1997; Jin et al. 1999; Rasmussen and Buick 2000; Rona 2003, 2008; Peckmann et al. 2005; Agirrezabala 2009; Kashirtsev et al. 2010).

3.1.1 Guaymas Basin, Gulf of California

The Guaymas Basin (Fig. 1) is an actively spreading oceanic basin (2000 m water depth in the rifts), and the geology, geophysics, and physiography have been detailed elsewhere (e.g., Curray et al. 1982; Einsele et al. 1980; Einsele 1985; Lonsdale 1985). Sedimentation is rapid (1–2 m/1000 a) and covers the rift floors to a depth of at least 400 m (Curray et al. 1982). The organic matter of these recent sediments is derived primarily from diatomaceous and microbial detritus and averages about 2% organic carbon (Lanza-Espino and Soto 1999). Influx of terrigenous organic matter is low because deserts border the gulf. Thermal stress causes rapid maturation of immature organic matter with concomitant petroleum generation; the “oil window” seems to migrate upward in the sedimentary column as the magmatic heat front, and thus hot fluids invade new, shallower sediment (Simoneit 1982b, 1984; Simoneit et al. 1984).

Numerous hydrothermal mounds rise to 20–30 m above the south rift floor, and most are actively discharging vent fluids with water temperatures up to 315 °C at ~200 bars (Lonsdale 1985; Merewether et al. 1985). The mounds are composed of complex deposits of sulfide, sulfate, silicate, and carbonate minerals and colonies of tube worms, bacterial mats, and other chemosynthetic organisms (Koski et al. 1985; Jones 1985). Typical samples from these mounds are stained or saturated with petroleum and have a strong odor reminiscent of diesel fuel (Simoneit and Lonsdale 1982). Color photographs of active oil and gas discharges from vent areas in Guaymas Basin have been published (Simoneit 1993). The samples have very diverse petroleum contents and hydrocarbon distributions (one example is shown in Fig. 2a; others are found in Simoneit (1984, 1985a), Kawka and Simoneit (1987), and Simoneit and Kawka (1987)) and are analogous to those described for bitumens at depth in the Deep Sea Drilling Project (DSDP) holes (Simoneit 1983b; Simoneit et al. 1984). The *n*-alkanes range from methane to *n*-C₄₀₊, with usual maxima in the mid-C₂₀ region and no carbon number predominance (CPI = 1.0). The CPI for hydrocarbons is expressed as a summation of the odd carbon number homologs over a range divided by a summation of the even carbon number homologs over the same range (Bray and Evans 1961; Simoneit 1978); for fatty acids and alcohols, it is the same ratio only inverted to have even-to-odd homologs (Kvenvolden 1966; Simoneit 1978).

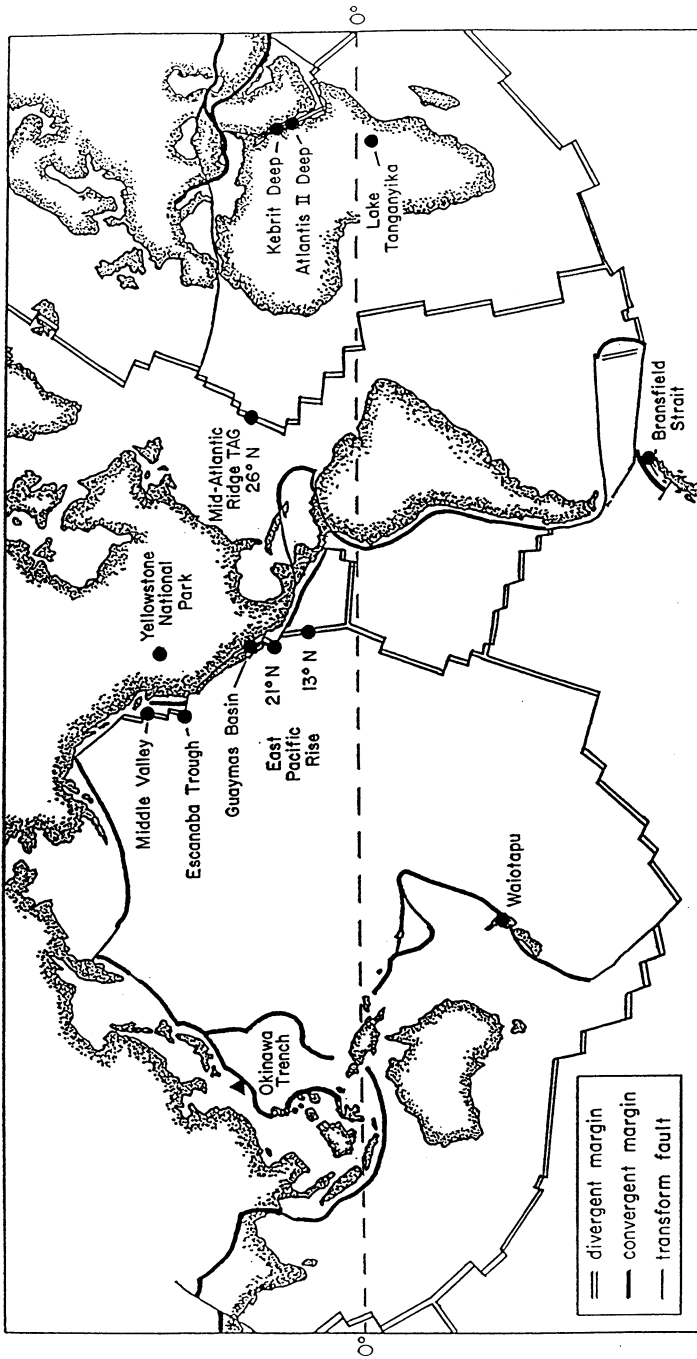


Fig. 1 General location map of the hydrothermal vent fields discussed here with the sketched global tectonics

Table 2 Summary of hydrothermal petroleum from geographic areas discussed here

Location	TOC (%)	Total hydrocarbons ($\mu\text{g/g}$)	CPI
Guaymas Basin, Gulf of CA	2	1000–550,000	1.02
Escanaba Trough, Gorda Ridge ^a	0.4–5.6	500–55,000	1.25
Kebrit Deep, Red Sea ^b	0.3–2.3	250–3800	1.5–4.2
Shaban Deep, Red Sea ^b	0.6–1.5	240–2700	1.6–3.9
Middle Valley, Juan de Fuca Ridge	0.1–0.8	0.2–500	0.5–4.1
Bransfield Straight, Antarctica	0.8	0.5–1.2	1.6–2.0
Atlantis II Deep, Red Sea	0.14	0.23	1.1
East Pacific Rise, 13°N	0.4	1	1.1
East Pacific Rise, 21°N	n.d.	0.0002–0.006	1.01
Mid-Atlantic Ridge, TAG, 26°N	n.d.	n.d.	1.01

^aKvenvolden et al. (1986)

^bMichaelis et al. (1990)

n.d. = not determined

The biomarkers, mainly the steranes and triterpanes, of the hydrothermal petroleums are generally mature. The steranes are present as complex mixtures ranging from C₂₇ to C₂₉ (e.g., Fig. 3a), and the dominant sterane in all samples is 5 α (H),14 α (H),17 α (H)-cholestane (20R). Diasteranes are also present with the 13 β (H),17 α (H)-diacholestanes (20S and 20R) as most abundant. The triterpanes consist primarily of the 17 α (H),21 β (H)-hopanes with minor amounts of 17 β (H),21 α (H)-hopanes (moretananes) and 17 β (H),21 β (H)-hopanes (biological configuration) and range from C₂₇ to C₃₄ (C₂₈ absent) (e.g., Fig. 3b). The various biomarker ratios confirm their high degree of maturity (Kawka and Simoneit 1987) and, along with the ¹⁴C age data (Peter et al. 1991), indicate that the petroleums were generated by rapid and intense heating.

An example of a GC trace of an aromatic/naphthenic fraction (F2) of an oil sample is shown in Fig. 2c. The major resolved peaks are unsubstituted polycyclic aromatic hydrocarbons (PAH), a group of compounds discussed later. The chemical compositions of the aromatic fractions suggest derivation from a combination of high-temperature pyrolysis and admixture of less mature bitumen (Kawka and Simoneit 1990; Pikovskii et al. 1996).

3.1.2 Northeastern Pacific (Escanaba Trough and Middle Valley)

The Escanaba Trough in the northeastern Pacific (Fig. 1) is the southern extension of the Gorda Ridge, an active oceanic spreading center about 300 km long and bounded on the north and south by the Blanco and Mendocino fracture zones, respectively. It is filled with up to 500 m of Quaternary turbidite sediments (Kvenvolden et al. 1986, 1990). The petroleum (tar) lenses which are interspersed in the sediments and mineral ores blanketing the ridge axis are derived from hydrothermal alteration of sedimentary organic matter (Kvenvolden et al. 1986, 1990). The organic source material for these hydrocarbons appears to be terrigenous based on the CPI, carbon number range (especially $>n$ -C₂₅), biomarker composition, and sedimentological considerations (Kvenvolden and Simoneit 1990). The *n*-alkanes of the petroleum

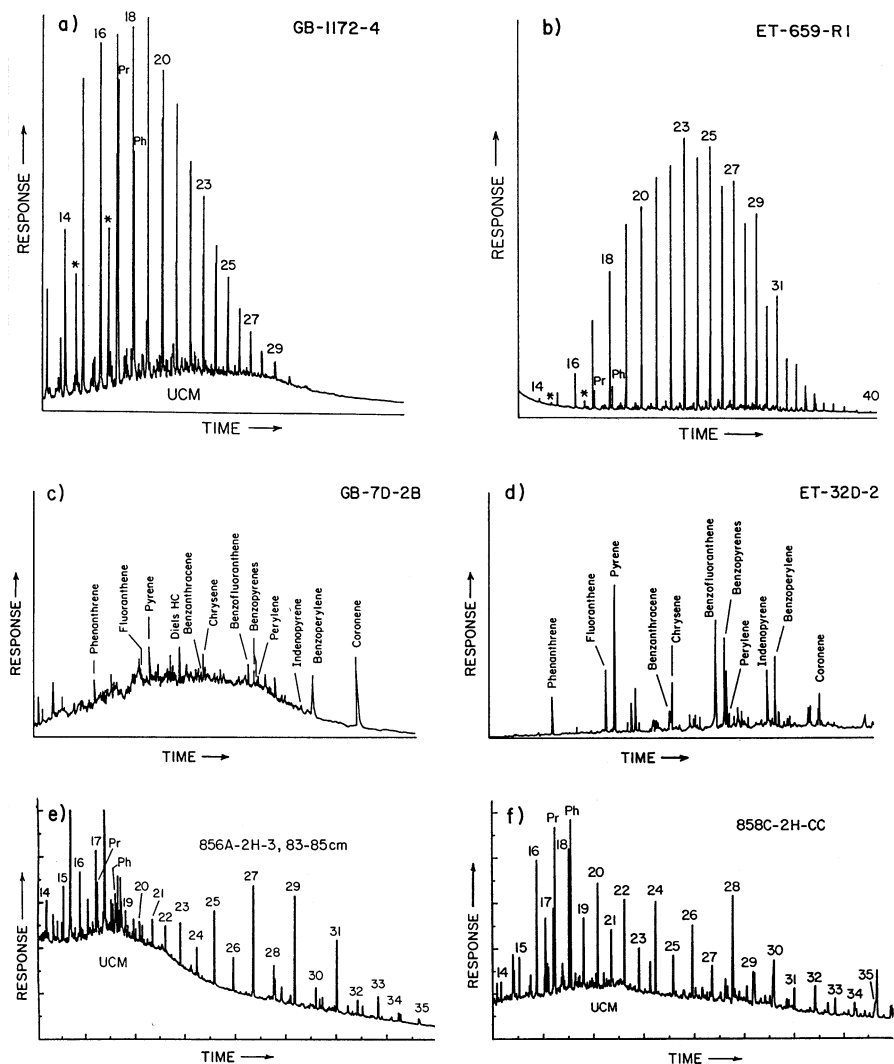


Fig. 2 Gas chromatograms of saturated (a, b), aromatic (c, d), and total (e, f) hydrocarbons in (a, c) Guaymas Basin (GB), (b, d) Escanaba Trough (ET), and (e, f) Middle Valley oils (Kvenvolden and Simoneit 1990; Davis et al. 1992; Simoneit 1994) (Numbers refer to carbon chain length of *n*-alkanes, Pr = pristane, Ph = phytane, asterisk = other isoprenoids; UCM = unresolved complex mixture; PAH are labeled)

range from C_{14} to C_{40} , with a carbon number maximum (C_{max}) $> n-C_{23}$ (Fig. 2b) and still a significant odd carbon number predominance $> n-C_{25}$ (CPI = 1.25), typical of a terrestrial organic matter origin. The CPI may also indicate admixture of bitumens with various maturities. Homologs of a marine origin ($< n-C_{25}$) are less concentrated. In general the biomarkers of these petroleum, i.e., steranes and

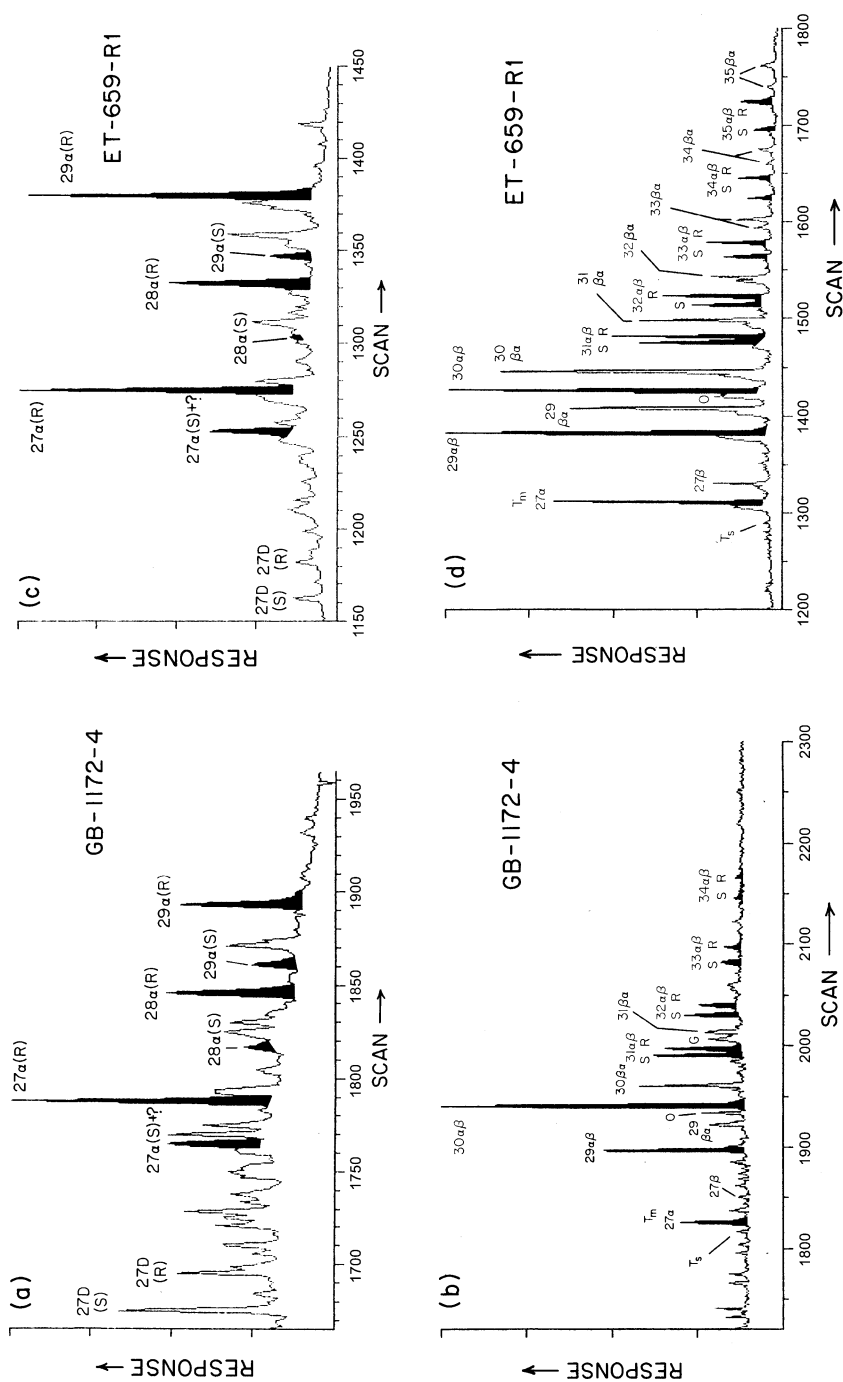


Fig. 3 Mass fragmentograms from GC-MS of biomarkers in (a, b) Guaymas Basin (GB) and (c, d) Escanaba Trough (ET) oils; (a, c) m/z 217, key ion for steranes (numbers refer to carbon skeleton; suffixes designate configuration; $\alpha = 5\alpha(H)$, $14\alpha(H)$, $17\alpha(H)$; D = diasterane [$13\beta(H)$, $17\alpha(H)$ -diacholestane]; R and S

triterpanes, are less mature than in the case of the Guaymas petroleum. The steranes range from C₂₇ to C₂₉, with 5 α (H),14 α (H),17 α (H)-cholestane (20R) slightly less concentrated than the C₂₉ homolog (Fig. 3c) (Kvenvolden and Simoneit 1990). Diasteranes are minor components. The triterpanes consist of the 17 α (H),21 β (H)-hopanes, with major amounts of the 17 β (H),21 α (H)-hopanes (Fig. 3d), and range from C₂₇ to C₃₅ (C₂₈ absent). The PAH of these oils are also dominated by the unsubstituted analogs (Fig. 2d; Kvenvolden and Simoneit 1990). The generation of this petroleum was by intense heating of short duration, as indicated by the biomarker distributions and the high concentrations of unsubstituted PAH. This was further supported by the analyses of drill cores from the region by the Ocean Drilling Program (ODP) Leg 169 (Fouquet et al. 1998; Gieskes et al. 2002b; Rushdi and Simoneit 2002b).

Middle Valley is another sediment-covered hydrothermal system in the north-eastern Pacific (Fig. 1), with associated hydrothermal organic matter alteration (Simoneit 1994; Simoneit et al. 1992a). These oils are also highly aromatic/polar in composition. This system was drilled by the ODP Legs 139 and 169 (Davis et al. 1992; Simoneit 1994; Fouquet et al. 1998), and hydrothermal petroleum was recovered in some of the upper core sections. The bitumen in the thermally unaltered sediments reflects the admixture of marine autochthonous compounds (e.g., *n*-alkanes <C₂₀) with the *n*-alkanes >C₂₃ (CPI = 2.8) from terrestrial vascular plant wax (Fig. 2f). The compositional signatures of the total hydrocarbon fractions of the hydrothermal petroleum in the various core sections were very diverse, comprised of oils consisting of either UCM, aromatics, or condensate/volatiles (C_{max} = 17), to aliphatic higher-molecular-weight mixtures (Simoneit 1994). A sample of a solid bitumen at ambient temperature from 13 m below seafloor has a CPI = 0.46, with an *n*-alkane range of ~C₁₄ to C₃₅ (Fig. 2e). The strong even carbon number predominance is intriguing and occurs in numerous hydrothermal petroleum from ODP 139 in Middle Valley (Simoneit 1994; Rushdi and Simoneit 2002a). The origins of even *n*-alkane distributions have been amply discussed in the literature as (1) microbial alteration of algal detritus, (2) reductive processes acting on acids or other lipid compounds, and (3) direct microbial lipid input. Process number (2) was proposed to occur for the Leg 139 samples (Simoneit 1994; Rushdi and Simoneit 2002a). Because maturation in these sediments commences with immature organic matter (i.e., biogenic detritus) that has not completed early diagenetic alteration, the *n*-alkanols from marine microbial sources and from terrestrial plant waxes (Simoneit 1977, 1978) appear to be the source of the even-chain alkanes.

The Escanaba Trough and Middle Valley hydrothermal systems are larger in area than the Guaymas Basin rift. Also the ¹⁴C ages of their hydrothermal petroleum are



Fig. 3 (continued) are epimer configurations at C-20); **(b, d)** *m/z* 191, key ion for triterpanes (numbers refer to carbon skeleton, $\alpha\beta$ = 17 α (H),21 β (H)-(shaded); $\beta\alpha$ = 17 β (H),21 α (H)-; $\beta\beta$ = 17 β (-H),21 β (H)-hopanes; T_s = 18 α (H)-22,29,30-trisnorhopane; T_m = 17 α (H)-22,29,30-trisnorhopane; O = oleanane; G = gammacerane. In the pairs of shaded α -hopanes, the 22S epimer is followed by the 22R epimer)

much older (Escanaba Trough ~17,090 yBP, Middle Valley ~29,000 yBP, Simoneit and Kvenvolden 1994) than those from Guaymas Basin (mean $\sim 4700 \pm 550$ yBP; Peter et al. 1991). The diverse compositions of the petroleum in drill cores from both locales reflect extensive migration reworking, deposition, remobilization, thermal searing by hot fluids, and ultimate concentrations of bitumen (heavy oils) near the seafloor (Gieskes et al. 2002a, b; Rushdi and Simoneit 2002a, b). This is illustrated by the depth profile of hydrothermal petroleum in cores from Site 858 in Middle Valley (Fig. 4, Rushdi and Simoneit 2002a). The altered bitumen is found associated with indurated minerals at shallow depths. The other low-concentration bitumens in these cores (open circles in Fig. 4) reflect the typical lower-temperature products from the primarily terrigenous organic detritus (Rushdi and Simoneit 2002a).

3.1.3 Other Sediment-Covered Systems

The Bransfield Strait, Antarctica (Fig. 1), is a typical back-arc rift, which is tectonically active with extensional features such as dip-slip faults and intrusives (Whiticar et al. 1985). Gravity cores from the eastern part of the basin have a weak petroliferous odor in the hydrothermally altered zones analogous to that described for Guaymas Basin. The lipid/bitumen compositions of two piston cores have been analyzed (Brault and Simoneit 1988, 1990). The unaltered surface samples exhibit compound distributions that can be correlated with their marine biogenic origin where the bulk of the *n*-alkanes and additional biomarkers (e.g., hop-22(29)-ene, C₂₈-steradienes, and C₂₅-polyalkenes) are derived from autochthonous marine microbial sources. This has also been reported by Venkatesan and Kaplan (1987) for other core samples from this area. The hydrocarbon patterns in the hydrothermally altered zones are dramatically different (Brault and Simoneit 1988, 1990), with a superposition of complex resolved and unresolved (UCM) thermal products on the *n*-alkane pattern. However, the hydrocarbon patterns for these hydrothermally altered samples from Bransfield Strait indicate only in situ heating and limited migration.

The Atlantis II Deep in the Red Sea (Fig. 1) contains stratified brine layers, the deepest of which is at a temperature of 62 °C (Hartmann 1980). Bulk organic matter and hydrocarbons have been analyzed in two sediment cores from the Deep (Simoneit et al. 1987). The dense brine overlying the coring areas was reported to be sterile, and sedimentary organic material derived from autochthonous marine planktonic and microbial inputs and minor terrestrial sources is present. The organic input derived from the water column above the brine is further metabolized by microorganisms, and the reworked compounds with organic detritus are apparently then incorporated into the sediments under the brine by sinking adsorbed or bound to particles of metallic oxide precipitates.

Low-temperature maturation in the sediments results in petroleum generation (Fig. 5a), even from low amounts of organic matter (average 0.14% TOC). Both steroid and triterpenoid biomarkers show that extensive acid-catalyzed reactions occur in the sediments. In comparison with other hydrothermal systems (e.g., Guaymas Basin) or intrusive systems in lithified sediments (e.g., Cape Verde

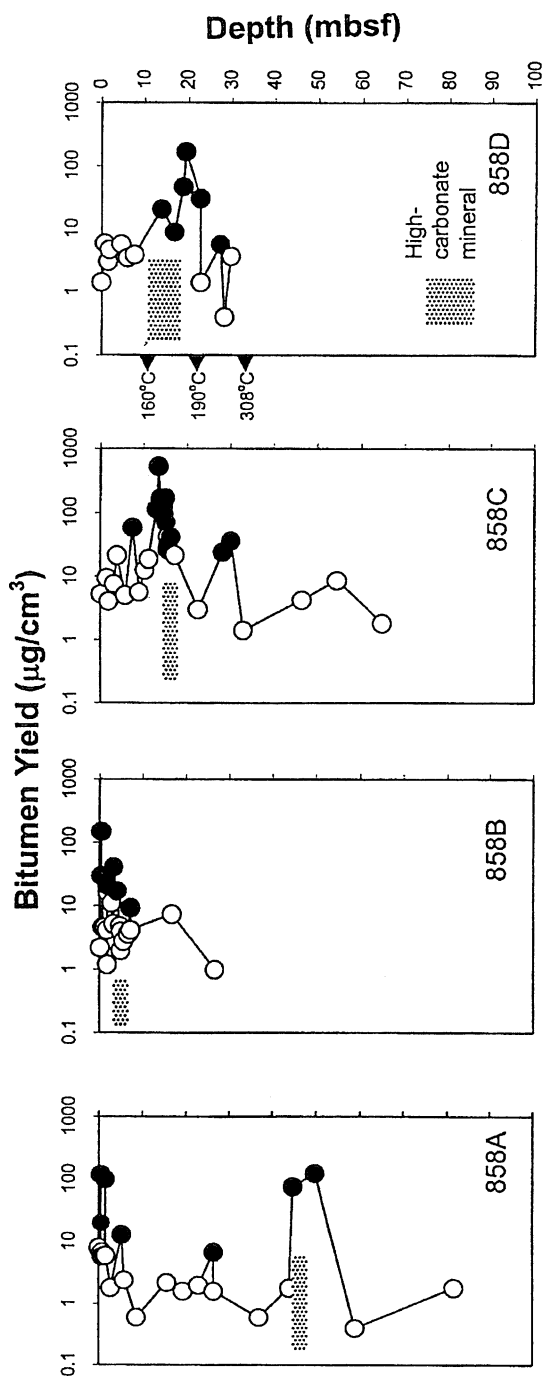


Fig. 4 Yields of bitumen extracts for sediments of Middle Valley, ODP Site 858 (solid dots are hydrothermal petroleum) (Rushdi and Simoneit 2002a)

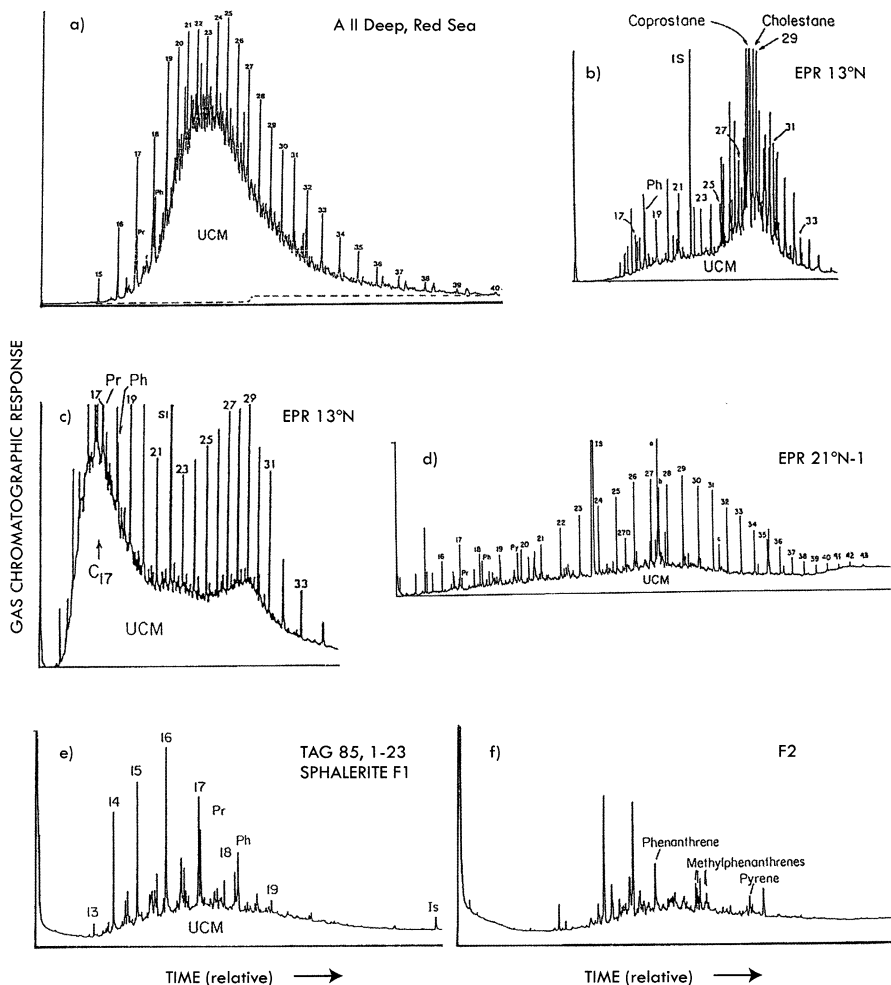


Fig. 5 Gas chromatograms of total hydrocarbons (a–e) and aromatic hydrocarbons (f) from various other hydrothermal areas: (a) Atlantis II Deep core sample 84, 443–453 cm (Simoneit et al. 1987); (b) EPR at 13°N, hydrothermal metalliferous sediment talus (Brault et al. 1985, 1988); (c) EPR at 13°N, surrounding water above active vents (Brault et al. 1989); (e, f) MAR-TAG at 26°N, sphalerite, saturates, and aromatics, respectively (Brault and Simoneit 1989)

Rise; Simoneit et al. 1978, 1981), sediments in the Atlantic II Deep exhibit a lower degree of thermal maturation, as based on the bitumen character, the elemental composition of the kerogens and the absence of pyrolytic PAH in the bitumen (Simoneit et al. 1987). The lack of a carbon number preference for the *n*-alkanes (CPI = 1.0) suggests, especially in the case of the long-chain homologs (Fig. 5a), that the organic matter has been affected by catagenesis. However, the yields of hydrocarbons with respect to sediment weight are much lower than those observed in other hydrothermal areas (Table 2), probably due to the low temperature and low

TOC of the sediments in the Deep. Related data on hydrothermal petroleum from the Kebrit and Shaban Deeps of the Red Sea have also been reported; however, these systems appear to be at higher temperatures (Michaelis et al. 1990).

3.2 Bare Rock Hydrothermal Systems

The active spreading ridges in the deep ocean without sediment cover (e.g., Mid-Atlantic Ridge) are the current areas of exploration, addressing topics such as ecology of the biota, mineral deposition, rift dynamics, and abiogenic hydrocarbon (mainly methane) formation.

3.2.1 East Pacific Rise (13°N and 21°N)

Hydrothermal activity and associated massive sulfide deposits, with abundant faunal communities, are found on the unsedimented axis of the East Pacific Rise (EPR) in the region of 13°N and 21°N (Fig. 1; Spiess et al. 1980; Ballard et al. 1981; Hékinian et al. 1983). Aliphatic hydrocarbons have been analyzed in hydrothermal plumes and in metalliferous sediments near the active vents and at the base of an inactive chimney at 13°N (Brault et al. 1985, 1988). Hydrocarbons from metalliferous sediments have distributions characteristic of immature organic matter, which was recently biosynthesized and microbiologically degraded, as indicated by the abundance of low-molecular-weight (<C₂₆) *n*-alkanes and phytane. A contribution of continental higher plant material is shown by the presence of high-molecular-weight *n*-alkanes with a slight odd carbon number predominance (Fig. 5b). The immature character of the organic matter is also suggested by the presence of steroid and terpenoid biomarkers, which are the result of low-temperature reductive alteration, as might be expected in the surrounding talus apron of a vent system. Thermally matured compounds (Fig. 5c) are also present at trace levels in waters collected within ~1 km above the hydrothermal vents. The hydrocarbon patterns of these waters are indicative in many cases of pyrolysis of bacterial matter in entrained ocean water during cooling of discharging fluids (Brault et al. 1988).

The hydrocarbon contents of massive sulfide minerals from vent chimneys at 21°N are extremely low but definitely thermogenic. The *n*-alkanes in these massive sulfides range from C₁₄ to C₄₀₊, with no carbon number predominance, and have hydrothermally altered steroid and terpenoid biomarkers from the vent biota, i.e., mainly tube worms and bacteria (Fig. 5d) (Brault et al. 1989; Simoneit et al. 1990a), whereas a sample of a pyritized tube worm from a chimney has *n*-alkanes with a slight odd carbon number predominance (CPI = 1.02). All samples contain PAH, providing further evidence for hydrothermal generation, and this coupled with the C_{max} at *n*-C₂₇ or higher indicates that the hydrocarbons were entrapped/condensed in a high-temperature regime such as an active chimney.

3.2.2 Mid-Atlantic Ridge (TAG Area 26°N)

The Trans-Atlantic Geotraverse (TAG) hydrothermal field on the Mid-Atlantic Ridge crest at 26°N (Fig. 1) is one of now numerous active vent systems known

on slow-spreading oceanic ridges (Rona et al. 1984; Thompson et al. 1988; Von Damm 1995). Hydrothermal deposits lying directly on oceanic crust were dredged from the area (TAG 1985-1). Three bulk mineral samples, consisting mainly of anhydrite, sphalerite, and chalcopyrite, respectively, contained minor amounts of the more volatile (C_{10} – C_{22}) hydrothermal petroleum (Brault and Simoneit 1989). The *n*-alkanes in the sphalerite range from C_{11} to C_{22} , with a C_{max} at *n*- C_{16} and CPI = 1.0, and a significant UCM (Fig. 5e). This pattern is analogous to that observed for samples from the EPR at 13°N. The aromatic fraction, which contains naphthalene, phenanthrene, their alkyl homologs, pyrene, and S-aromatic compounds (Fig. 5f), supports the hydrothermal origin for these trace organic components (Brault and Simoneit 1989; Simoneit et al. 1990a).

3.3 Continental Systems

Continental hydrothermal systems occur in volcanic, geothermal, or failed and dormant rift terranes, as, for example, Yellowstone National Park, Lake Tanganyika, and Waiotapu (Fig. 1). In most cases, the hydrothermal processes cause remobilization of organic matter in the form of bitumen as reported for oils from Yellowstone National Park (Clifton et al. 1990) and other areas (Venkatesan et al. 2003; Zárate del Valle and Simoneit 2005; Geptner et al. 2006; Gürgey et al. 2007; Svensen et al. 2007; Peng et al. 2011). Small amounts of hydrothermal petroleum are also formed in such areas derived from the alteration of the in situ microbiological detritus (Yamanaka et al. 2000; Simoneit et al. 2009). For example, in the Waiotapu geothermal region of New Zealand, small amounts of oil are presently being generated from volcanic sedimentary rocks of Lower Pleistocene age (Czochanska et al. 1986). The source material is terrigenous organic matter present in vitric tuff which has been rapidly buried by volcanic overburden. The associated breccias serve as regional aquifers and surround the tuff with high-temperature water. The generated oil, however, lacks the high-temperature reaction products, e.g., PAH, present in typical hydrothermal petroleum.

Massive sulfides and petroleum occur in the north Tanganyika trough of the East African Rift (Tiercelin et al. 1989, 1993). Hydrothermal fluids pass through about 2 km of organic-rich lacustrine sediments (algal detritus), mobilizing asphaltic petroleum and venting at the lake bed in a water depth of ~20 m with temperatures of 65–80 °C. The site described is in close proximity to shore; vents at higher temperatures are suspected to occur in deeper water of the lake. The vent waters also contain thermogenic hydrocarbons (Tiercelin et al. 1989). This hydrothermal petroleum contains mainly an UCM and minor amounts of *n*-alkanes (C_{15} – C_{40}), immature biomarkers, and PAHs (only chrysene and benzo[e]pyrene with monomethyl analogs) (Simoneit et al. 2000).

Hydrothermal activity can generate and migrate petroleum from continental source material in both lithified rocks and unconsolidated sediments (e.g., Jin et al. 1999; Simoneit 2000a; Kashirtsev et al. 2010). The invasion of hydrothermal fluids into mature source rocks will result in organic matter alteration and migration as

observed in the marine systems, except nearer the surface the effective temperature may be lower due to the lower confining pressure of the overburden.

4 Nature and Alteration of Organic Matter in Hydrothermal Systems

The effects of hydrothermal activity on sedimentary organic matter are elaborated here with the examples of submarine and continental systems. The major similarities and differences between hydrothermal petroleum and conventional reservoir petroleum are summarized in Table 3. The processes of maturation, i.e., catagenesis and metagenesis (Hunt 1996), and how these affect sedimentary organic matter after diagenesis are discussed elsewhere in this book series. The in situ lipids in shallow sediments of marine hydrothermal systems are overprinted by the input of hydrocarbons from the migrating fluids. However, these lipids in the unaltered sediments can be utilized to elucidate the various sources of the total organic matter (e.g., Simoneit 1978, 1982a). Thus, the lipid hydrocarbons of thermally unaltered, surface sediment in the Guaymas Basin, Gulf of California (Fig. 6a), consist of *n*-alkanes mostly $<C_{21}$ and minor homologs $>C_{23}$ with a strong odd carbon number predominance. This composition is typical of a predominantly marine planktonic and microbial origin with a minor influx of a terrigenous component ($>C_{25}$) of vascular plant wax (Simoneit et al. 1979). In contrast, the lipid hydrocarbons of a surface sediment in the Escanaba Trough (Fig. 6b) are *n*-alkanes mostly $>C_{23}$ with a strong odd carbon number predominance. This signature is derived mainly from

Table 3 Hydrothermal petroleum compared to reservoir petroleum

Similarities to conventional reservoir petroleum	
1.	Natural gas and gasoline-range hydrocarbons
2.	Full range of <i>n</i> -alkanes, no carbon number predominance (CPI = 1.0–1.2)
3.	Naphthenic components (major unresolved complex mixture of branched and cyclic hydrocarbons)
4.	Isoprenoid hydrocarbons (including significant but variable pristane and phytane)
5.	Biomarkers (e.g., mature 17 α (H)-hopanes and steranes)
6.	CH ₄ –C ₈₊ , CO ₂ , H ₂ S, benzene, toluene, etc
7.	Alkyl aromatic hydrocarbons and asphaltenes
Differences from conventional reservoir petroleum	
1.	High concentrations of parent polynuclear aromatic hydrocarbons (PAH)
2.	Residual immature biomarkers and intermediates (e.g., 17 β (H)-hopanes, hopenes, sterenes)
3.	Degraded biomarkers (e.g., Diels' hydrocarbon, porphyrins with C ₂₇ max)
4.	Significant heteroaromatic compounds (N and S)
5.	High sulfur content
6.	Alkene content in bitumen near "source sediment"
7.	Alkanone and alkylphenol content

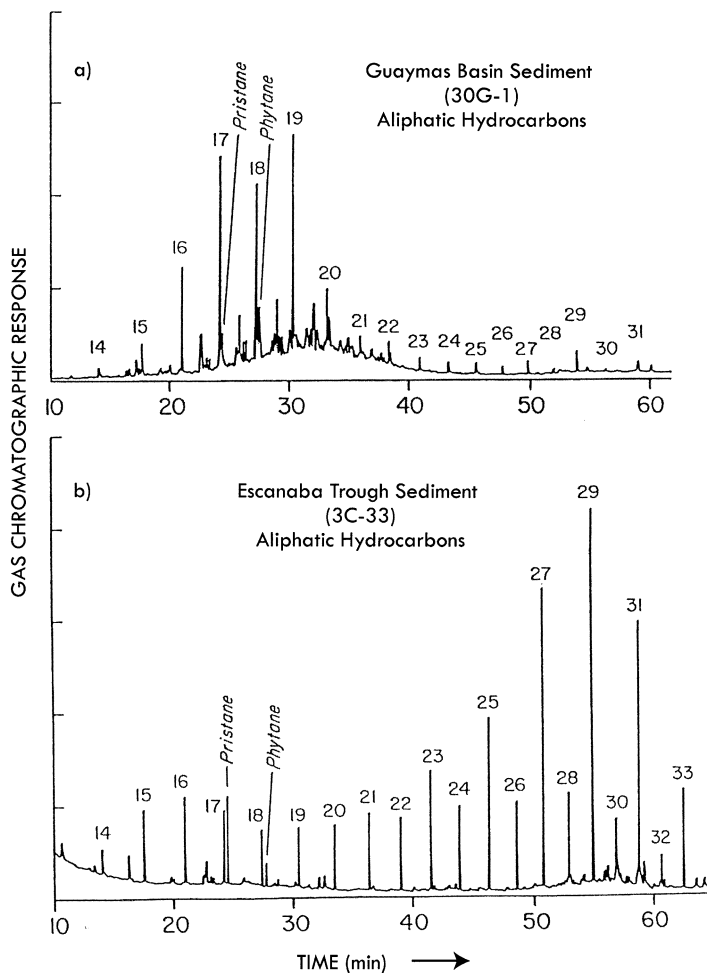


Fig. 6 Gas chromatograms of total hydrocarbons in extracts from unaltered surface sediments (a) Guaymas Basin, Site 30G (Simoneit et al. 1979), and (b) Escanaba Trough (Kvenvolden et al. 1986).

terigenous vascular plant wax, with a minor microbial component ($<C_{21}$; Kvenvolden et al. 1986).

4.1 Organic Matter Alteration by Hydrothermal Processes

An overview of the hydrothermal processes affecting organic matter alteration is presented in Table 4. Hydrothermal petroleum generated in high-temperature, high-pressure, and high-fluid-flow regimes have been defined here as such because the agent of thermal alteration and mass transfer, hot circulating water, is responsible for

Table 4 Overview of hydrothermal processes affecting organic matter alteration

Hydrothermal petroleum generation (rapid at high temperatures, 250–400 °C)		
<i>Alteration reactions (relative importance)</i>	<i>Compound type yield</i>	
(a) Reduction (primary)	Aliphatic hydrocarbons	
(b) Oxidation (minor)	PAH, alkanones, alkylphenols	
(c) Synthesis (trace)	Thioheterocyclic compounds, aliphatic lipids	
Hydrothermal petroleum composition		
<i>Source organic matter</i>	<i>Products</i>	<i>Relative concentration</i>
(a) Marine (e.g., Guaymas Basin)	Gas (CH ₄ –C ₁₀)	High
	Oil (C ₈ –C ₄₀₊)	Intermediate
	Asphalt (>C ₄₀)	Minor
(b) Terrigenous (e.g., Middle Valley)	Gas (CH ₄ –C ₁₀)	Trace
	Oil (C ₈ –C ₄₀₊)	High
	Asphalt (>C ₄₀)	Intermediate
Hydrothermal fluids as solvents		
<i>Fluid</i>	<i>Relative importance/ state</i>	<i>Effect</i>
(a) Water	Dominant/near critical	Enhanced oil solubility
(b) Methane	Minor/dissolved	Complete oil solubility
(c) Carbon dioxide	Minor/dissolved	Complete oil solubility
Hydrothermal petroleum migration		
(a) Effective in systems with high water-to-rock ratios (unlike conventional sedimentary basins)		
(b) Migration		
Bulk phase (trapped in filled veins and voids)		
Emulsion (trapped in fluid inclusions)		
Solution (precipitated as wax crystals in chimneys and fluid conduits)		
(c) Spent kerogen (amorphous C) remains in altered sediment – Possible later interaction, reducing agent		

petroleum generation and extraction from the unconsolidated sediments or source rocks (Didyk and Simoneit 1989, 1990). In contrast, conventional oils are products of basin evolution and are generated contemporaneously with sediment compaction and geothermal heating due to burial. Formation of hydrothermal oils and gases is a rapid process (e.g., days-years; Peter et al. 1991; Simoneit and Kvenvolden 1994), whereas geothermal oils are generated at a rate that is tied to basin subsidence over millions of years (Tissot and Welte 1984; Hunt 1996). Conventional petroleum formation is believed to occur in the temperature window of ~60–150 °C, and above that temperature, the organic compounds are inferred to ultimately go to CH₄ and graphite over geological time scales (Tissot and Welte 1984; Hunt 1996). Organic matter alteration in hydrothermal systems is inferred to occur over a temperature range from ~60 to >400 °C (Simoneit 1994; Kawka and Simoneit 1994). Formation of hydrothermal petroleum commences in low-temperature regions, generating products from weaker bonds in the immature organic matter, and as the temperature regime rises, products are derived from progressively more refractory organic matter and are even “reformed” (e.g., PAH). The process

progresses from reductive to more oxidative reactions as the temperature increases (Kawka and Simoneit 1994). The aqueous solubility of petroleum and individual hydrocarbons has been determined in the laboratory and increases as the temperature approaches the critical point to essentially complete miscibility (e.g., Josephson 1982; Price et al. 1983; Sanders 1986; Berkowitz and Calderon 1990; Price 1993). This enhanced solvent capacity of organic compounds and reduced solvation properties of ionic species in supercritical water are due to the loss of aqueous hydrogen bonding (Fig. 7; Connolly 1966; Tödheide 1982). Phase separation of CO₂ from water at reduced temperatures has been proposed for liquid CO₂ vents in a back-arc hydrothermal system (Sakai et al. 1990). Carbon dioxide liquid is also an excellent solvent for organic compounds. Thus, the near-critical domain of water with co-solutes like CO₂ in hydrothermal systems is expected to aid reaction rates and enhance the solvation capacity for organic matter (i.e., petroleum) in the source sediment.

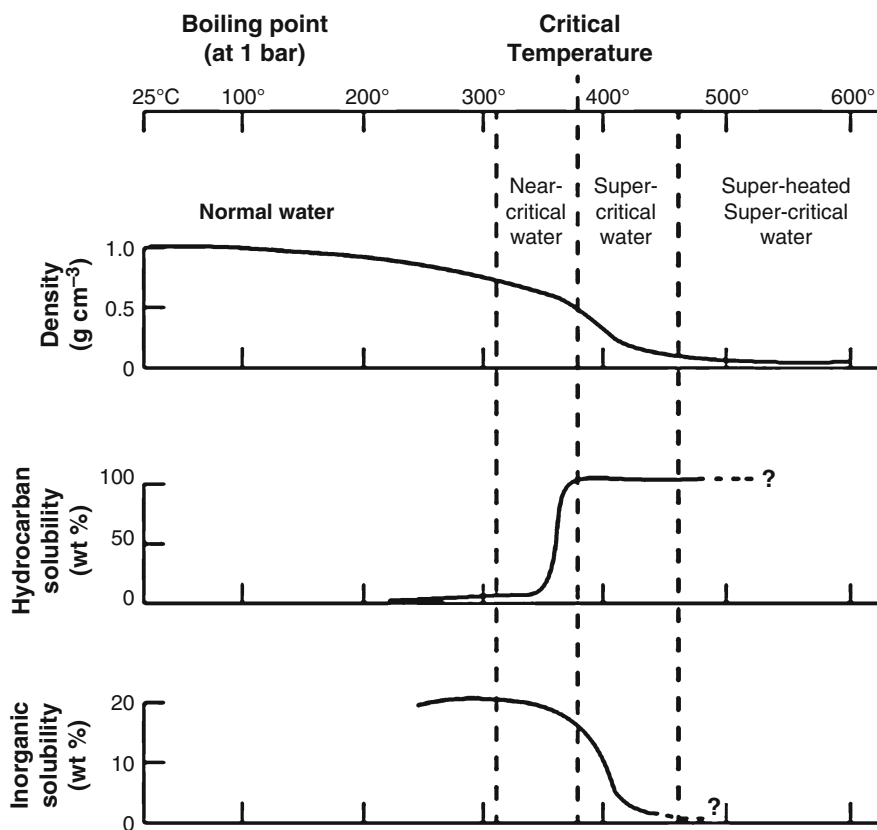


Fig. 7 Properties of water as a function of temperature at 200–300 bar pressure (Adapted from Josephson 1982)

The thermal alteration products of organic matter in hydrothermal systems have been proposed to be in a metastable equilibrium state (e.g., Shock 1990) during their brief formation and residence times at high temperatures. In this state, not all of the stable equilibrium species are present due to kinetic constraints, but theoretical evaluations of the distributions of species at metastable equilibrium are analogous to those for stable equilibrium. Thus, high-temperature vent fluids in Guaymas Basin for example, concurrently contain reduced species (e.g., hydrogen, hydrogen sulfide, and CH₄–C₄₀ hydrocarbons) and oxidized species (e.g., CO₂ acetate, alkanones, and PAH).

The reaction rates of organic matter alteration to petroleum in hydrothermal systems are rapid, and fluid extraction is highly efficient. The alteration proceeds from immature organic matter (incomplete diagenesis) to the fully mature products (Simoneit 1993, 1994). For example, carbon-14 dates have been obtained from hydrothermally derived petroleum from the southern trough of Guaymas Basin (Peter et al. 1991; Simoneit and Kvenvolden 1994). The ages range from ~3200 to 6600 yBP, mean 4690 yBP (years before present, referenced to the year A.D. 1950 and using the ¹⁴C half-life of 5570 y). These are not true ages, but rather they reflect the age of carbon within these materials. Additional ¹⁴C data on the aliphatic and aromatic hydrocarbon fractions of an oil sample from this area calculate for the same age (~4500 yBP), indicating that the PAH are generated from the same carbon pool as the saturated hydrocarbons at a subseafloor depth of 12–30 m. These results demonstrate that late-phase, high-temperature products such as PAH are derived from shallow depth just as the aliphatic material from lower-temperature alteration. Hydrothermal petroleum from the northern trough of Guaymas Basin is 7400 yBP, from Escanaba Trough 17,000 yBP, from Middle Valley 29,000 yBP, and from Lake Tanganyika 25,000 yBP (Simoneit and Kvenvolden 1994), confirming this rapid geological process.

4.2 Composition of Hydrothermal Petroleum

Most hydrothermal petroleums from Guaymas Basin and Northeastern Pacific fall outside the field of typical reservoir petroleums on the ternary composition diagram (Fig. 8; Tissot and Welte 1984; Kawka and Simoneit 1987; Kvenvolden and Simoneit 1990). This indicates that they have diverse compositions and are generally more polar than conventional petroleums. Typical hydrothermal petroleums from Guaymas Basin (Didyk and Simoneit 1990) have an intermediate content of *n*-alkanes (18%) and a relatively normal content of *iso*-, *anteiso*-, and isoprenoid and naphthenic hydrocarbons (82%), comparable to normal crude oils (e.g., Fig. 2a). The CPI of ~1 indicates complete maturation. The typical diagnostic biomarkers consist of the triterpenoid, steroid (e.g., Fig. 3), and tricyclic terpane hydrocarbons as are generally found in crude oils, and their presence is additional evidence for the strongly reductive process operating during initial organic matter alteration. The major resolved peaks in the aromatic/naphthenic fractions are unsubstituted PAH (Fig. 2), a group of compounds uncommon in petroleums but ubiquitous in high-

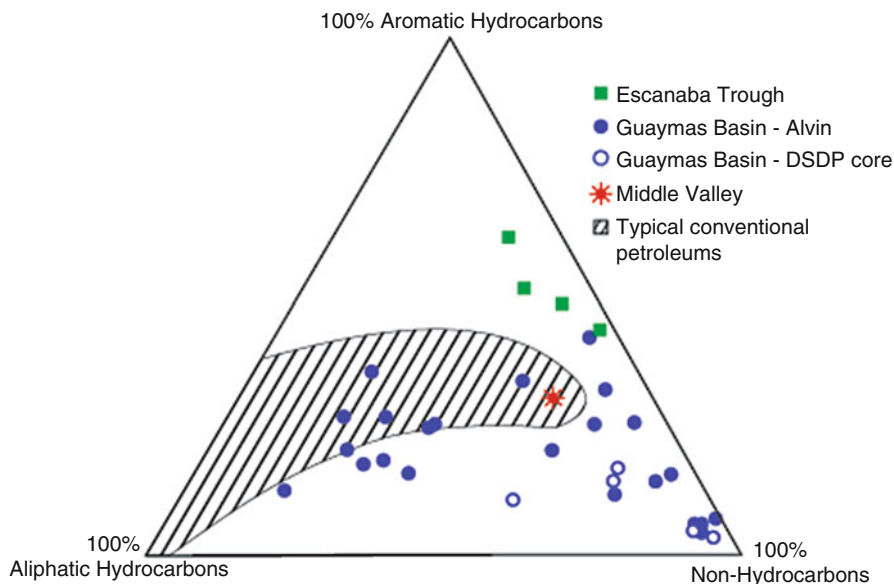


Fig. 8 Ternary diagram representing gross (C_{15+}) compositions of hydrothermal petroleum as percentages of each of three major compound classes determined gravimetrically. Guaymas Basin samples indicated by dots; Escanaba Trough samples indicated by squares; Middle Valley sample indicated by asterisk. Typical conventional petroleum falls within the hatched area (Tissot and Welte 1984)

temperature ($>250\text{ }^{\circ}\text{C}$) pyrolysates (Geissman et al. 1967; Blumer 1975, 1976; Hunt 1996). The dominant analogs are the pericondensed aromatic series (e.g., phenanthrene, pyrene, chrysene, etc.) (Kawka and Simoneit 1990), and their pyrolytic origin is further supported by the presence of PAH with five-membered alicyclic rings (e.g., fluorene, methylenephenthrene, etc.), which are found in all pyrolysates from organic matter but once formed do not easily revert to the pericondensed PAH (Blumer 1975, 1976; Scott 1982). PAH become the dominant species at very high temperatures due to their high thermal stability as well as enhanced solubility in near- and supercritical water (e.g., Sanders 1986). The aromatic/naphthenic fractions of the Guaymas oils also contain significant amounts of N, S, and O hetero-PAH (e.g., Gieskes et al. 1988) and Diels' hydrocarbon [1,2-(3'-methylcyclopenteno) phenanthrene, $C_{18}H_{16}$ M.W. 232, a dehydrogenation product from steroids as reported by Diels et al. 1927; Diels and Rickert 1935] (Simoneit et al. 1992b).

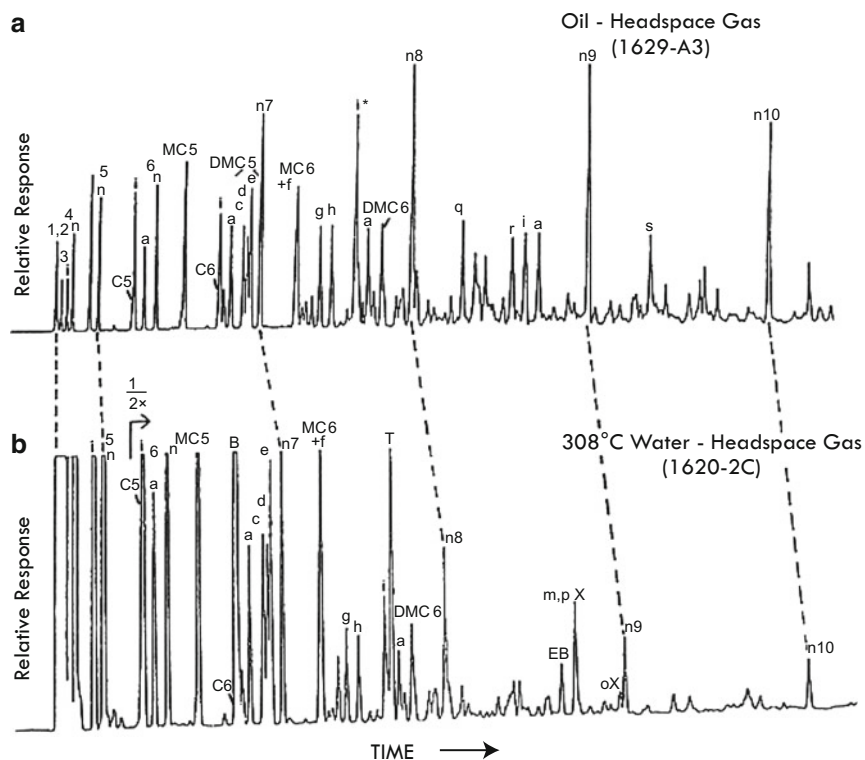
The n -alkanes of a hydrothermal petroleum from Escanaba Trough range from C_{14} to C_{40} , with a carbon number maximum at $n-C_{27}$ and a significant odd carbon number predominance $>n-C_{25}$ (CPI = 1.25), typical of a terrestrial, higher plant origin (Fig. 2b; Kvenvolden et al. 1990; Kvenvolden and Simoneit 1990). The PAH are more concentrated relative to the UCM when compared to the example from Guaymas Basin (Fig. 2c vs. 2d), although the relative yield is similar.

Volatile compounds (mainly CH₄–C₁₀ hydrocarbons) are not retained effectively with the heavy petroleum as it solidifies in the vent mounds on the seafloor of Guaymas Basin. Upon exiting at the seabed, the fluids are often saturated with a broad range of volatile hydrocarbons (CH₄ to *n*-C₁₀) as well as lower concentrations of heavy ends (>C₁₅) (e.g., Fig. 9; Simoneit et al. 1988). Interstitial gas in sediments of DSDP cores consists of biogenic methane (CH₄) overprinted by thermogenic CH₄ to C₅ hydrocarbons near the sills and, to a lesser extent, at increasing subbottom depths. These are of a similar composition as the venting volatile hydrocarbons (Simoneit et al. 1988; Whelan et al. 1988). Guaymas Basin vent water samples contain high amounts of light hydrocarbons, with CH₄ at corrected concentrations of about 150 cm³ (STP)/kg (Welhan and Lupton 1987). For comparison, the CH₄ concentration in vent fluids from the East Pacific Rise at 21°N, a sediment-starved rift system, has been reported to be 1–2 cm³ (STP)/kg (Welhan and Lupton 1987). Sedimented hydrothermal systems generate higher amounts of natural gas. The headspace gases of a Guaymas Basin mound sample (1629-A3, Fig. 9a) can be compared with the hydrocarbon content of a 308 °C vent water, which is highly enriched in the lower alkanes (<C₇, Fig. 9b; Simoneit et al. 1988). The hot water has an enhanced content of aromatic (benzene, toluene, ethylbenzene, and xylenes – i.e., more soluble) versus aliphatic hydrocarbons (Fig. 9b). Hydrogen gas is also a major component of the vent fluids in Guaymas Basin (Welhan and Lupton 1987).

5 Fluid Interactions

The interactions of hydrothermal fluids in terms of chemistry and solvent properties are not well understood. The dominant fluid component is water, and in the example locales of Guaymas Basin and Northeastern Pacific, it is at temperatures approaching 350° and 400 °C, respectively, and under pressures exceeding 200 and 300 bar, respectively. The reduced density of hydrothermal fluids due to heating results in convective circulation, which in effect makes hydrothermal systems semi-open (a flow-through system) rather than closed as in most laboratory simulation experiments. These temperature and pressure conditions are in the near-critical domain of water (Fig. 7; Chen 1981; Josephson 1982; Pitzer 1986; Bischoff and Rosenbauer 1988; Bischoff and Pitzer 1989). Supercritical water has enhanced solvent capacity for organic compounds and reduced solvation properties for ionic species due to its loss of aqueous hydrogen bonding (Fig. 7; Connolly 1966; Tödheide 1982; Shaw et al. 1991; Siskin and Katritzky 1991). Supercritical water is also a reactive medium for either reductive or oxidative reactions (Leif et al. 1992; Simoneit 1995; McCollom et al. 1999a, b). Thus, the near-critical domain of water in hydrothermal systems is expected to aid reaction rates and enhance the solvation capacity for organic matter.

Fluids in hydrothermal systems also contain large concentrations of CH₄ and CO₂ (Simoneit and Galimov 1984; Welhan and Lupton 1987; Simoneit et al. 1988; Sakai et al. 1990). These dissolved gases, as well as many other possible trace components, are expected to lower the critical point of hydrothermal water. Thus, their admixture



Numbers = carbon chain length with: n = normal i = <i>iso</i> - (2-methyl) a = <i>anteiso</i> - (3-methyl)	The DMC5 triplet contains the: c = <i>cis</i> -1,3 d = <i>trans</i> -1,3 e = <i>trans</i> -1,2-dimethyl isomers
Other acyclic compounds are: q = 2,6-dimethylheptane r = 2,3-dimethylheptane s = 2,6-dimethyloctane	Other individual alkylcyclopentanes are: f = 1,1,3-trimethyl- g = 1,2,4-trimethyl- h = 1,2,3-trimethyl-
Cyclic compounds are: C = cyclo- MC = methylcyclo- DMC = dimethylcyclo-alkanes	The aromatics are: B = benzene EB = ethylbenzene T = toluene X = xylenes
* = coeluting unknown	with: (o) = <i>ortho</i> - (m) = <i>meta</i> - (p) = <i>para</i> -isomers 1/2x = signal attenuation by a factor of 2

Fig. 9 Gas chromatograms of headspace analyses for comparison of the volatile hydrocarbons from: (a) hydrothermal mineral/oil crust, 1629-A3; (b) hot venting water, 1620-2C (T = 308 °C) (Simoneit et al. 1988)

in hydrothermal fluids may result in even more efficient solvent capacity for scavenging hydrothermally generated organic compounds (e.g., petroleum) from the source sediments and migrating them away from the high-temperature zone.

6 Hydrothermal Petroleum Expulsion/Extraction/Migration

Generally, the volatile hydrocarbon mixtures in marine hydrothermal fluids exhibit large variations in character in terms of carbon number range ($\text{CH}_4\text{--C}_{10+}$), structural diversity (relative contents of the normal, branched, and cyclic components), and polarity (aliphatic vs. aromatic components) (Simoneit et al. 1988). This character is controlled by a number of factors, primarily temperature, aqueous solubility, biodegradation, and water-washing. Migration of these volatile hydrocarbons occurs through dispersion in vent fluids and as a bulk phase in the sediments and vein systems. The more soluble and volatile hydrocarbons are released into the water column by rapidly venting fluids, rising in some cases as large plumes (Merewether et al. 1985; Simoneit et al. 1990b), and by aqueous remobilization from some exposed hydrothermal mounds.

Although direct measurement of the oil flow rate at the vent sites of the Guaymas Basin has not yet been feasible, oil globules have been collected under in situ conditions (200 bar, 2–3 °C). These samples had a gas-to-oil ratio ranging from approximately 5–155 at standard temperature and pressure (Simoneit et al. 1988). The low water temperatures at the seafloor contribute to condensation/precipitation and retention of some of the oil on inorganic substrates (Carranza-Edwards et al. 1990) and trapping volatile oil in fluid inclusions (Peter et al. 1990) of the hydrothermal vent system. In general, the low pour point (<18 °C, a consequence of the high liquefied hydrocarbon gas content; Didyk and Simoneit 1990) of the hydrothermal oil allows it to remain fluid at these bottom temperatures. The oils in Escanaba Trough and Middle Valley are emplaced as higher-temperature fluids (>80 °C, bulk phase migration) and solidify in the mineral matrix as the temperatures approach ambient.

Formation of hydrothermal petroleum is a continuous process which commences under low-temperature conditions, generating products from weaker bonds of the generally immature organic matter, and additional products are derived from more refractory organic matter and are even “reformed” (e.g., PAH) as the temperature regime rises. The products are continuously expelled/extracted and removed by fluid flow. The process progresses from reductive to more oxidative reactions of the residual organic matter as the temperature increases.

Deposition, precipitation, and/or trapping of hydrothermal petroleum occur as the migrating fluid experiences reduced temperatures. Phase separation of the oil from water is a consequence of a temperature reduction of the fluid to about 200–300 °C. The Guaymas Basin oils remain liquid at lower temperatures (Didyk and Simoneit 1990) than are those from Escanaba Trough or Middle Valley due to their high volatile hydrocarbon content ($\text{CH}_4\text{--C}_{10+}$). Thus, in the temperature window from ambient to ~300 °C, the hydrothermal oils are partitioned between bulk phase,

microdroplet emulsion, and true solution, where the predominance shifts to the former as the temperature decreases. Because these systems are semi-open, not all products are trapped. Deposition or precipitation of the heavy components of the oils ($>C_{10}$ – asphalt) occurs at the seafloor as the migrating fluid comes into contact with cold seawater ($\sim 3^\circ\text{C}$). This process happens in the mineral mounds and chimneys where the heavy petroleum deposits as a filler in voids of the mineral matrix.

7 Implications

The incorporation of hydrothermal petroleum, especially surface manifestations on the seabed, into the carbon pool of the local ecosystem has been discussed (e.g., Simoneit 1985b, 1990; Bazylinski et al. 1988). The other implications which are still of relevance and actively researched follow next.

7.1 Petroleum Resources

Hydrothermal petroleum formation is a rapid, continuous, and overlapping process consisting of rapid diagenesis of the source organic matter, petroleum generation, expulsion, and migration. In terms of tectonics, hydrothermal systems are particularly active during the early rifting of nascent ocean basins along continental margins (Lonsdale 1985). Thus, geological locales where this process should be considered in resource exploration are, for example, split rift basins, failed or dormant rifts with hemipelagic or lacustrine sediments, pull-apart basins, and rifts overridden by continental drift (Didyk and Simoneit 1989). Remobilization of petroleum by hydrothermal fluids from magmatic activity affecting conventional sedimentary basins is another aspect for consideration.

A schematic representation of the prevailing conditions existing in the Guaymas Basin vent systems is shown in Fig. 10a. Hydrothermal fluids driven by a deep heat source permeate through an open, fine-grained body of recent sediments causing organic matter alteration to petroleum and discharge directly into the water column. The oil discharged with the hydrothermal fluids partially adsorbs or condenses/precipitates on inorganic substrates cooled by seawater ($\sim 3^\circ\text{C}$) surrounding the vents. The major part of the volatile oil plume above the vent area dissipates into the water column mainly by dispersion, dissolution, and eventual biodegradation. Another scenario could be postulated, as, for example, in Fig. 10b, where a similar hydrothermally generated oil is discharged into a porous sediment body, with a finite retention time for the fluids (Didyk and Simoneit 1989, 1990). There, the hydrothermal oil-water mixtures can undergo phase separation as the temperature decreases, and petroleum can eventually accumulate if adequate sedimentary and tectonic features are available to constitute a reservoir. Such a scenario could possibly lead to a hydrothermal oil accumulation which would have a potential for exploration.

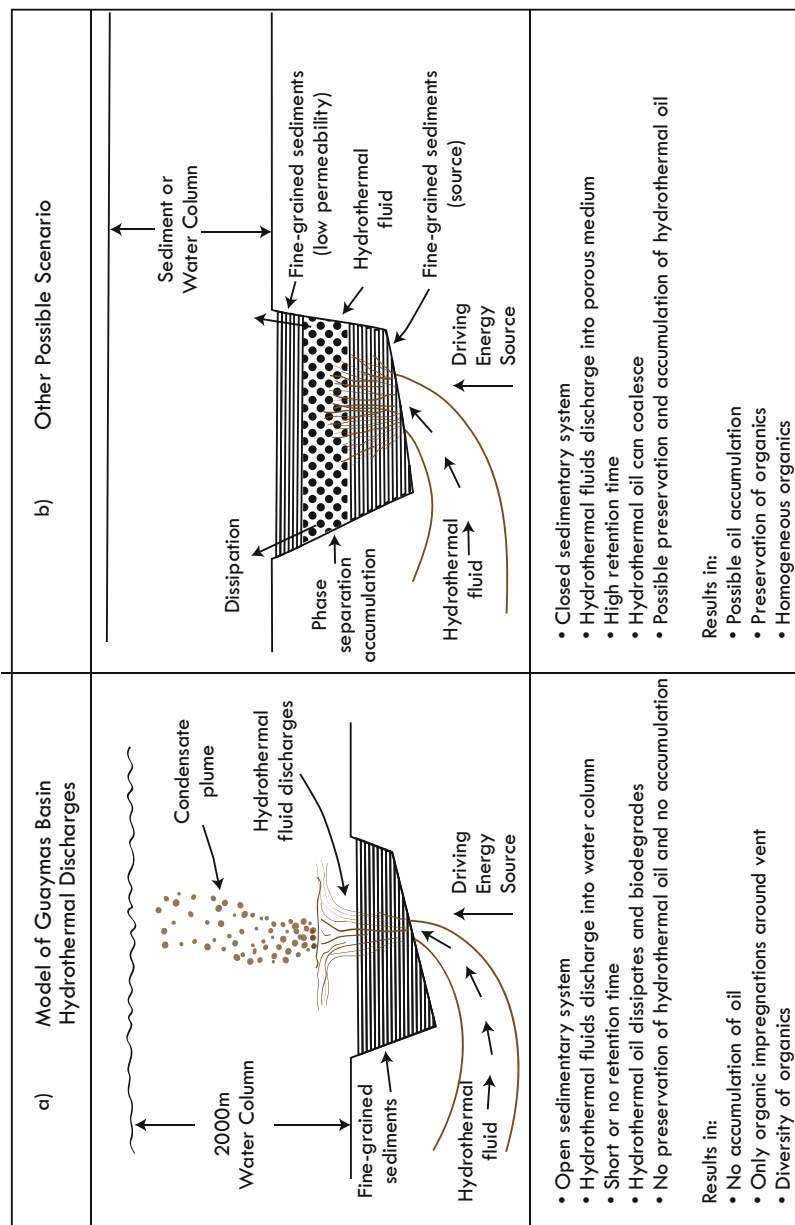


Fig. 10 Schematic models for hydrothermal petroleum generation and migration scenarios (Adapted from Didyk and Simoneit 1989, 1990): (a) Guaymas Basin open system; (b) hypothetical closed system

7.2 Mineral Deposits

The mechanisms of migration and subsequent deposition of hydrothermal petroleum are important for understanding their role in hydrothermal metallogenesis (Simoneit 2000b). Within a specific depth interval of a sedimented hydrothermal system, the aliphatic components produced at lower temperatures are transported away by the hydrothermal flow (Kawka and Simoneit 1994). With continued heating, the pyrolysate becomes more aromatic in character until a point is reached at which only the unalkylated PAH remain (Kawka and Simoneit 1994; Simoneit and Fetzer 1996). Although such an alteration sequence can occur in a geothermal system, the hydrothermal process accentuates the removal of the intermediate products away from the heat source at depth by providing a constant flow of transport medium (i.e., water). Metal transport in hydrothermal fluids is most efficient at high temperatures, which is incompatible with the aliphatic hydrothermal petroleum. Thus, the aliphatic hydrothermal petroleum is part of the reducing medium in the system and is lost or further altered during the early activity of the system. It is the high-temperature fraction (bitumen enriched in PAH), which is generated/migrated later or is deposited in the higher-temperature fluid flow channels (e.g., chimneys), which has relevance to metallogenesis. This PAH-enriched bitumen is deposited/trapped within the minerals as they precipitate or crystallize in zones of lower temperature. Hydrothermal bitumen carries complexed metals (e.g., in porphyrins – Ni, V, Cu, and possibly others, e.g., Sander and Koschinsky 2011). Later remobilization or deeper burial can generate heavy bitumen from the hydrothermal petroleum or move deposited bitumen which can then in turn act as reductant interfaces/surfaces for metal deposition (e.g., Au on bitumen; Parnell 1988, 1993).

7.3 Hydrothermal Organic Synthesis

It has been proposed that hydrothermal systems on Earth provided an appropriate setting for the abiotic formation and accumulation of organic matter (Corliss et al. 1981; Holm 1992), thus providing organic compound precursors for the evolution of life (Shock 1990; Holm 1992; Simoneit 1995). Formation of organic compounds may proceed by aqueous thermocatalytic reactions. The Fischer-Tropsch process is a well-known and analogous process in industry, which produces gas-phase hydrocarbons and oxy compounds from carbon monoxide and carbon dioxide (Fischer 1935; Anderson 1984). The Fischer-Tropsch-type (FTT) reaction has drawn the attention of geologists as a potential source of abiotic hydrocarbons and other organic compounds in various geological settings (e.g., volcanoes, marine hydrothermal systems, etc.) (Markhinin and Podkletnov 1977; Welhan and Lupton 1987; Simoneit et al. 1988; Szatmari 1989; Shock 1990; Charlou and Donval 1993; Sherwood Lollar et al. 2002; Pikoivskii et al. 2004).

Studies have shown that thermocatalytic (analogous to FTT) reactions proceed under aqueous conditions (McCollom et al. 1999a, b; Rushdi and Simoneit 2001). The synthesis products from experiments conducted at 150–400 °C were dominated

by mainly non-hydrocarbons, i.e., homologous series of straight-chain *n*-alkanols, *n*-alkanoic acids, alkyl formates, *n*-alkanals, *n*-alkan-2-ones, methyl alkanoates, and minor alkanes (Rushdi and Simoneit 2001). At temperatures above 300 °C, synthesis competed with cracking and reforming reactions.

The alkyl formates and methyl alkanoates in the aqueous thermocatalytic synthesis products indicated dehydration reactions. Thus, both condensation and reductive dehydration reactions with lipids were examined further under hydrothermal conditions. Mono- and difunctionalized alkanolic acids, alkanols, alkamines, and alkamides were heated at 300 °C in water (Rushdi and Simoneit 2004). In all cases, the dominant products consisted of reductive dehydration and condensation derivatives, confirming that these reactions occur under hydrothermal conditions to form amides, nitriles, and esters, carbon-heteroatom bonds of obvious relevance to prebiotic lipid, and biopolymer synthesis.

8 Summary

In hydrothermal systems, organic matter maturation, petroleum generation, expulsion, and migration are compressed into an “instantaneous” geological time frame. At seafloor spreading centers, hydrothermal systems active under a sedimentary cover (e.g., Guaymas Basin, Middle Valley, Escanaba Trough) generate petroleum from the generally immature organic matter in the sediments. Products rapidly migrate away from the high-temperature zone and leave behind a spent carbonaceous residue. Compositionally, for example, the Guaymas Basin petroleums (marine organic matter source) consist of the following: (1) gasoline-range hydrocarbons (C_1 – C_{12}), (2) a broad distribution of *n*-alkanes (C_{12} – C_{40+}) with essentially no carbon number predominance, (3) a naphthenic UCM of branched and cyclic hydrocarbons, (4) significant isoprenoids, (5) mature biomarkers (e.g., α -hopanes), (6) oxygenated species, and (7) major concentrations of PAH and thio-PAH. Hydrothermal petroleums exposed or present in unconsolidated surface sediments are rapidly biodegraded and leached, whereas interior samples are essentially unaltered, although some extensively reworked oils do occur. Similar compositions are observed for Middle Valley and Escanaba Trough petroleums, except volatile hydrocarbons are low in the latter and the *n*-alkanes have slight odd and in some cases even carbon number predominances ($>C_{25}$) (mainly terrestrial organic matter source). The bitumens enriched in high-molecular-weight PAH are deposited with the hydrothermal minerals.

Hydrothermal systems active in unsedimented rift areas (e.g., East Pacific Rise at 13°N and 21°N, Mid-Atlantic Ridge at 26°N and 36°N) generate trace amounts of petroleum-like material. Low amounts of bitumen are generated by hydrothermal pyrolysis of suspended and dissolved biogenic organic detritus (including bacteria and algae) entrained during the turbulent cooling of the vent fluids. Low-level maturation is also observed in the surrounding areas at vent sites, probably due to warming of ambient detritus in the hydrothermal talus. These hydrothermal bitumens are deposited and interspersed in the minerals. Hydrothermal processes also

generate, alter, and migrate, as well as remobilize, petroleum/heavy bitumen in continental systems (e.g., Yellowstone National Park, Wyoming).

In general, hydrothermal oil generation processes differ significantly from the conventionally accepted scenario for petroleum formation in sedimentary basins. In hydrothermal petroleum formation, several of the steps of oil generation, i.e., organic matter input, subsidence, geothermal maturation, oil generation, and oil migration, occur simultaneously and have been shown to complete the oil generation-migration process over brief periods of geological time. The volatile and aliphatic components provide reducing agent capacity in the system, and the heavy bitumen fractions (PAH enriched) deposit with minerals.

References

- Agirrezabala LM (2009) Mid-cretaceous hydrothermal vents and authigenic carbonates in a transform margin. Basque-Cantabrian Basin (western Pyrenees): a multidisciplinary study. *Sedimentology* 56:969–996
- Anderson RB (1984) *The Fischer-Tropsch reaction*. Academic, London
- Andersson E, Simoneit BRT, Holm NG (2000) Amino acid abundances and stereochemistry in hydrothermally altered sediments from the Juan de Fuca Ridge, Northeast Pacific Ocean. *Appl Geochem* 15:1169–1190
- Ballard RD, Francheteau J, Juteau T, Rangan C, Normark W (1981) East Pacific Rise at 21°N: the volcanic, tectonic and hydrothermal processes of the central axis. *Earth Planet Sci Lett* 55:1–10
- Bazylnski DA, Farrington JW, Jannasch HW (1988) Hydrocarbons in surface sediments from a Guaymas Basin hydrothermal vent site. *Org Geochem* 12:547–558
- Berkowitz N, Calderon J (1990) Extraction of oil sand bitumens with supercritical water. *Fuel Process Technol* 25:33–44
- Bischoff JL, Pitzer KS (1989) Liquid-vapor relations for the system NaCl- H₂O: summary of the P-T-x surface from 300° to 500°C. *Am J Sci* 289:217–248
- Bischoff JL, Rosenbauer RJ (1988) Liquid-vapor relations in the critical region of the system NaCl-H₂O from 380 to 415°C: a refined determination of the critical point and two-phase boundary of seawater. *Geochim Cosmochim Acta* 52:2121–2126
- Blumer M (1975) Curtisite, idrialite and pendletonite, polycyclic aromatic hydrocarbon minerals: their composition and origin. *Chem Geol* 16:245–256
- Blumer M (1976) Polycyclic aromatic compounds in nature. *Sci Am* 234:34–45
- Brault M, Simoneit BRT (1988) Steroid and triterpenoid distributions in Bransfield Strait sediments: hydrothermally-enhanced diagenetic transformations. *Org Geochem* 13:697–705
- Brault M, Simoneit BRT (1989) Trace petroliferous organic matter associated with hydrothermal minerals from the Mid-Atlantic Ridge at the Trans-Atlantic Geotraverse 26°N site. *J Geophys Res* 94:9791–9798
- Brault M, Simoneit BRT (1990) Mild hydrothermal alteration of immature organic matter in sediments from the Bransfield Strait, Antarctica. In: Simoneit BRT (ed) *Organic matter alteration in hydrothermal systems – petroleum generation, migration and biogeochemistry*. Applied Geochemistry, Elsevier, Amsterdam, vol 5. pp 149–158
- Brault M, Simoneit BRT, Marty JC, Saliot A (1985) Les hydrocarbures dans le système hydrothermal de la ride Est-Pacifique, à 13°N. *Comptes Rendus Academie des Sciences, Paris* 301(II): 807–812
- Brault M, Simoneit BRT, Marty JC, Saliot A (1988) Hydrocarbons in waters and particulate material from hydrothermal environments at the East Pacific Rise, 13°N. *Org Geochem* 12: 209–219

- Brault M, Simoneit BRT, Saliot A (1989) Trace petroliferous organic matter associated with massive hydrothermal sulfides from the East Pacific Rise at 13°N and 21°N. *Oceanol Acta* 12:405–415
- Bray EE, Evans ED (1961) Distribution of *n*-paraffins as a clue to recognition of source beds. *Geochim Cosmochim Acta* 22:2–15
- Carranza-Edwards A, Rosales-Hoz L, Aguayo-Camargo JE, Lozano-Santa Cruz R, Hornelas-Orozco Y (1990) Geochemical study of hydrothermal core sediments and rocks from the Guaymas Basin, Gulf of California. In: Simoneit BRT (ed) *Organic matter alteration in hydrothermal systems – petroleum generation, migration and biogeochemistry*. Applied Geochemistry, Elsevier, Amsterdam, vol 5. pp 77–82
- Charlou J, Donval J (1993) Hydrothermal methane venting between 12°N and 6°N along the Mid-Atlantic Ridge. *J Geophys Res* 98:9625–9642
- Chen C-TA (1981) Geothermal systems at 21°N. *Science* 211:298
- Clifton CG, Walters CC, Simoneit BRT (1990) Hydrothermal petroleum from Yellowstone National Park, Wyoming, U.S.A. In: Simoneit BRT (ed) *Organic matter alteration in hydrothermal systems – petroleum generation, migration and biogeochemistry*. Applied Geochemistry, Elsevier, Amsterdam, vol 5. pp 169–191
- Connolly JF (1966) Solubility of hydrocarbons in water near the critical solution temperatures. *J Chem Eng Data* 11:13–16
- Corliss JB, Dymond J, Gordon LI, Edmond JM, von Herzen RP, Ballard RD, Green K, Williams D, Bainbridge A, Crane K, van Andel TH (1979) Submarine thermal springs on the Galapagos Rift. *Science* 203:1073–1083
- Corliss JB, Baross JA, Hoffman SE (1981) An hypothesis concerning the relationship between submarine hot springs and the origin of life on Earth. *Oceanol Acta* SP:59–69
- Curry JR, Moore DG, Aguayo JE, Aubry MP, Einsele G, Fornari DJ, Gieskes J, Guerrero BC, Kastner M, Kelts K, Lyle M, Matoba Y, Molina-Cruz A, Niemitz J, Rueda J, Saunders AD, Schrader H, Simoneit BRT, Vacquier V (1982) Initial reports of the Deep Sea drilling project, vol 64, Parts I and II. U.S. Government Printing Office, Washington, DC. 1314pp
- Czochanska Z, Sheppard CM, Weston RJ, Woolhouse AD, Cook RA (1986) Organic geochemistry of sediments in New Zealand, Part I. A biomarker study of the petroleum seepage at the geothermal region of Waiotapu. *Geochim Cosmochim Acta* 50:507–515
- Davis E, Mottl M, Fisher A, Baker PA, Becker K, Boni M, Boulègue J, Brunner CA, Duckworth RC, Franklin JM, Goodfellow WD, Gröschel-Becker HM, Kinoshita M, Konyukhov BA, Körner U, Drasnov SG, Langseth M, Mao S, Marchig V, Marumo K, Oda H, Rigsby CA, BRT S, Stakes DS, Wheat CG, Whelan J, Villinger HW, Zierenberg RA, (Shipboard Scientific Party) (1992) Proceedings of the ocean drilling program, Initial reports, vol 139. Ocean Drilling Program, College Station. 1026pp
- Didyk BM, Simoneit BRT (1989) Hydrothermal oil of Guaymas Basin and implications for petroleum formation mechanisms. *Nature* 342:65–69
- Didyk BM, Simoneit BRT (1990) Petroleum characteristics of the oil in a Guaymas Basin hydrothermal chimney. In: Simoneit BRT (ed) *Organic matter alteration in hydrothermal systems – petroleum generation, migration and biogeochemistry*. Applied Geochemistry, Elsevier, Amsterdam, vol 5. pp 29–40
- Diels O, Rickert HF (1935) Über den Identitäts-Nachweis des Dehydrierungs-Kohlenwasserstoffes C₁₈H₁₆ aus Sterinen und Geninen mit γ -Methylcyclopentenophenanthen. *Ber Chem Ges* 68:267–272
- Diels O, Gädke W, Körding P (1927) Über die Dehydrierung des Cholesterins. *Liebigs Ann Chem* 459:1–26
- Einsele G (1985) Basaltic sill-sediment complexes in young spreading centers: genesis and significance. *Geology* 13:249–252
- Einsele G, Gieskes J, Curry J, Moore D, Aguayo E, Aubry MO, Fornari DJ, Guerrero JC, Kastner M, Kelts K, Lyle M, Matoba Y, Molina-Cruz A, Niemitz J, Rueda J, Saunders A, Schrader H, Simoneit BRT, Vacquier V (1980) Intrusion of basaltic sills into highly porous sediments and resulting hydrothermal activity. *Nature* 283:441–445

- Fischer F (1935) Die Synthese der Treibstoffe (Kogasin) und Schmieröle aus Kohlenoxyd und Wasserstoff bei gewöhnlichem Druck. *Brennstoff-Chem* 16:1–11
- Fouquet Y, Zierenberg RA, Miller DJ, Bahr JM, Baker PA, Bjerkgården T, Brunner CA, Duckworth RC, Gable R, Gieskes J, Goodfellow WD, Gröschel-Becker HM, Guèrin G, Ishibashi J, Iturrino G, James RH, Lackschewitz KS, Marquez LL, Nehlig P, Peter JM, Rigsby CA, Simoneit BRT, Schultheiss P, Shanks WC, Summit M, Teagle DAH, Urvat M, Zuffa GG (1998) Proceedings of the ocean drilling program, Initial reports, vol 169. Texas A & M University, College Station. 592 pp
- Galimov EM, Simoneit BRT (1982a) Geochemistry of interstitial gases in sedimentary deposits of the Gulf of California, Leg 64. In: Curray JR, Moore DG et al (eds) Initial reports of the Deep Sea drilling project, vol 64. U.S. Government Printing Office, Washington, DC, pp 781–788
- Galimov EM, Simoneit BRT (1982b) Variations in the carbon isotope compositions of CH₄ and CO₂ in the sedimentary sections of Guaymas Basin (Gulf of California). *Geokhimiya Acad Nauk SSSR* 7:1027–1034
- Geissman TA, Sim KY, Murdoch J (1967) Organic minerals. Picene and chrysene as constituents of the mineral curtisite (idrialite). *Experientia* 23:793–794
- Geptner AR, Richter B, Pikovskii YI, Chernyansky SS, Alekseeva TA (2006) Hydrothermal polycyclic aromatic hydrocarbons in marine and lagoon sediments at the intersection between Tjörnes Fracture Zone and recent rift zone (Skjálfandi and Öxarfjörður bays), Iceland. *Mar Chem* 101:153–165
- Gieskes JM, Simoneit BRT, Brown T, Shaw T, Wang YC, Magenheimer A (1988) Hydrothermal fluids and petroleum in surface sediments of Guaymas Basin, Gulf of California: a case study. *Can Mineral* 26:589–602
- Gieskes JM, Simoneit BRT, Goodfellow WD, James RH, Baker PA, Ishibashi J (2002a) Geochemistry of fluid phases and sediments: relevance to hydrothermal circulation in Middle Valley, ODP Legs 139 and 169. *Appl Geochem* 17:1381–1399
- Gieskes JM, Simoneit BRT, Goodfellow WD, Baker PA, Mahn C (2002b) Hydrothermal geochemistry of sediments and pore waters in Escanaba trough – ODP Leg 169. *Appl Geochem* 17:1435–1456
- Gürgey K, Simoneit BRT, Bati Z, Karamanderesi IH, Varol B (2007) Origin of petroliferous bitumen from the Büyük Menendes-Gediz geothermal graben system, Denizli-Sarayköy, western Turkey. *Appl Geochem* 22:1393–1415
- Hartmann M (1980) Atlantis II deep geothermal brine system. Hydrographic situation in 1977 and changes since 1965. *Deep-Sea Res* 27:161–171
- Hékinian R, Fevrier M, Avedik F, Cambon P, Charlou JL, Needham HD, Raillard J, Boulègue J, Merlivat L, Moinet A, Manganini S, Lange J (1983) East Pacific Rise near 13°N: geology of new hydrothermal fields. *Science* 219:1321–1324
- Holm NG (ed) (1992) Marine hydrothermal systems and the origin of life. *Orig Life Evol Biosp* 22:1–242
- Hunt JM (1996) Petroleum geochemistry and geology, 2nd edn. W.H. Freeman and Company, New York. 743 pp
- Jenden PD, Simoneit BRT, Philp RP (1982) Hydrothermal effects on protokerogen of unconsolidated sediments from Guaymas Basin, Gulf of California, elemental compositions, stable carbon isotope ratios and electron spin resonance spectra. In: Curray JR, Moore DG et al (eds) Initial reports of the Deep Sea drilling project, vol 64. U. S. Government Printing Office, Washington, DC, pp 905–912
- Jin Q, Xiong S-S, Lu P (1999) Catalysis and hydrogenation: volcanic activity and hydrocarbon generation in rift basins, eastern China. *Appl Geochem* 14:547–558
- Jones ML (ed) (1985) Hydrothermal vents of the eastern Pacific: an overview. *Biol Soc Wash Bull* 6:1–547
- Josephson J (1982) Supercritical fluids. *Environ Sci Technol* 16:548A–551A
- Kashirtsev VA, Kontorovich AE, Ivanov VL, Safronov AF (2010) Natural bitumen fields in the northeast of the Siberian platform (Russian Arctic sector). *Russ Geol Geophys* 51:72–82

- Kawka OE, Simoneit BRT (1987) Survey of hydrothermally-generated petroleum from the Guaymas Basin spreading center. *Org Geochem* 11:311–328
- Kawka OE, Simoneit BRT (1990) Polycyclic aromatic hydrocarbons in hydrothermal petroleum from the Guaymas Basin spreading center. In: Simoneit BRT (ed) Organic matter alteration in hydrothermal systems – petroleum generation, migration and biogeochemistry. *Applied Geochemistry*, Elsevier, Amsterdam, vol 5. pp 17–27
- Kawka OE, Simoneit BRT (1994) Hydrothermal pyrolysis of organic matter in Guaymas petroleum. *Org Geochem* 22:947–978
- Koski RA, Lonsdale PF, Shanks WC, Berndt ME, Howe SS (1985) Mineralogy and geochemistry of a sediment-hosted hydrothermal sulfide deposit from the southern trough of Guaymas Basin, Gulf of California. *J Geophys Res* 90:6695–6707
- Kulm LD, Suess E, Moore JC, Carson B, Lewis BT, Ritger ST, Kadko DC, Thornburg TM, Embley RW, Rugh WD, Massoth GJ, Langseth MG, Cochrane GR, Scamman RL (1986) Oregon subduction zone: venting, fauna and carbonates. *Science* 231:561–566
- Kvenvolden KA (1966) Molecular distributions of normal fatty acids and paraffins in some lower cretaceous sediments. *Nature* 209:573–577
- Kvenvolden KA, Simoneit BRT (1990) Hydrothermally derived petroleum: examples from Guaymas Basin, Gulf of California and Escanaba Trough, Northeast Pacific. *Am Assoc Pet Geol Bull* 74:223–237
- Kvenvolden KA, Rapp JB, Hostettler FD, Morton JL, King JD, Claypool GE (1986) Petroleum associated with polymetallic sulfide in sediment from Gorda Ridge. *Science* 234:1231–1234
- Kvenvolden KA, Rapp JB, Hostettler FD (1990) Hydrocarbon geochemistry of hydrothermally-generated petroleum from Escanaba Trough, offshore California. In: Simoneit BRT (ed) Organic matter alteration in hydrothermal systems – petroleum generation, migration and biogeochemistry. *Applied Geochemistry*, Elsevier, Amsterdam, vol 5. pp 83–91
- Lanza-Espino G, Soto LA (1999) Sedimentary geochemistry of hydrothermal vents in Guaymas Basin, Gulf of California, Mexico. *Appl Geochem* 14:499–510
- Leif RN, Simoneit BRT, Kvenvolden KA (1992) Hydrous pyrolysis of *n*-C₃₂H₆₆ in the presence and absence of inorganic components. *Am Chem Soc Div Fuel Chem 204th Nat Meet Prepr* 37(4):1748–1753
- Little CTS, Herrington RJ, Maslennikov VV, Morris NJ, Zaykov VV (1997) Silurian hydrothermal-vent community from the southern Urals, Russia. *Nature* 385:146–148
- Lonsdale P (1985) A transform continental margin rich in hydrocarbons, Gulf of California. *Am Assoc Pet Geol Bull* 69:1160–1180
- Markhinin EK, Podkletnov NE (1977) The phenomenon of formation of prebiological compounds in volcanic processes. *Orig Life* 8(3):225–235
- McCollom TM, Simoneit BRT, Shock EL (1999a) Hydrous pyrolysis of polycyclic aromatic hydrocarbons and implications for the origin of PAH in hydrothermal petroleum. *Energy Fuels* 13:401–410
- McCollom TM, Ritter G, Simoneit BRT (1999b) Lipid synthesis under hydrothermal conditions by Fischer-Tropsch-type reactions. *Orig Life Evol Biosph* 29:157–166
- Merewether R, Olsson MS, Lonsdale P (1985) Acoustically detected hydrocarbon plumes rising from 2-km depths in Guaymas Basin, Gulf of California. *J Geophys Res* 90:3075–3085
- Michaelis W, Jenisch A, Richnow HH (1990) Hydrothermal petroleum generation in Red Sea sediments from the Kebrut and Shaban Deeps. In: Simoneit BRT (ed) Organic matter alteration in hydrothermal systems – petroleum generation, migration and biogeochemistry. *Applied Geochemistry*, Elsevier, Amsterdam, vol 5. pp 103–114
- Parnell J (1988) Metal enrichments in solid bitumens: a review. *Mineral Deposita* 23:191–199
- Parnell J (1993) Paragenesis of bitumens and ore in mineral deposits. *Resour Geol Special Issue* 15:111–122
- Peckmann J, Little CTS, Gill F, Reitner J (2005) Worm tube fossils from Hollard Mound hydrocarbon-seep deposit, Middle Devonian, Morocco: Palaeozoic seep-related vestimentiferans? *Palaeogeogr, Palaeoclimatol, Palaeoecol* 227:242–257

- Peng X-T, Li J-W, Zhou H-Y, Wu Z-J, Li J-T, Chen S, Yao H-Q (2011) Characteristics and source of inorganic and organic compounds in the sediments from two hydrothermal fields in the Central Indian and Mid-Atlantic Ridges. *J Asian Earth Sci* 41:355–368
- Peter JM, Simoneit BRT, Kawka OE, Scott SD (1990) Liquid hydrocarbon-bearing inclusions in modern hydrothermal chimneys and mounds from the southern trough of Guaymas Basin. In: Simoneit BRT (ed) *Organic matter alteration in hydrothermal systems – petroleum generation, migration and biogeochemistry*. Applied Geochemistry, Elsevier, Amsterdam, vol 5. pp 51–63
- Peter JM, Peltonen P, Scott SD, Simoneit BRT, Kawka OE (1991) Carbon-14 ages of hydrothermal petroleum and carbonate in Guaymas Basin, Gulf of California – implications for oil generation, expulsion and migration. *Geology* 19:253–256
- Pikovskii YI, Chernova TG, Alekseeva TA, Kozin IS (1996) New data on the composition of polycyclic aromatic hydrocarbons in sulfides and bottom sediments of the Guaymas Basin (Gulf of California). *Geochem Int* 34:408–415
- Pikovskii YI, Chernova TG, Alekseeva TA, Verkhovskaya ZI (2004) Composition and nature of hydrocarbons in modern serpentinization areas in the ocean. *Geochem Int* 42:971–976
- Pitzer KS (1986) Large-scale fluctuations and the critical behavior of dilute NaCl in H₂O. *J Phys Chem* 90:1502–1504
- Price LC (1993) Thermal stability of hydrocarbons in nature: limits, evidence, characteristics, and possible controls. *Geochim Cosmochim Acta* 57:3261–3280
- Price LC, Wenger LM, Ging T, Bount CW (1983) Solubility of crude oil in methane as a function of pressure and temperature. *Org Geochem* 4:201–221
- Rasmussen B, Buick R (2000) Old oily ores: evidence for hydrothermal petroleum generation in an Archean volcanogenic massive sulfide deposit. *Geology* 28:731–734
- Rokosova NN, Rokosov YV, Uskov SI, Bodoev NV (2001) Composition and formation of hydrothermal petroleum (a review). *Neftekhimia* 41:3–16
- Rona PA (1984) Hydrothermal mineralization at seafloor spreading centers. *Earth-Sci Rev* 20:1–104
- Rona PA (1988) Hydrothermal mineralization at oceanic ridges. *Can Mineral* 26:431–465
- Rona PA (2003) Resources of the Sea Floor. *Science* 299:673–674
- Rona PA (2008) The changing vision of marine minerals. *Ore Geol Rev* 33:618–666
- Rona PA, Scott SD (1993) Preface to special issue on sea-floor hydrothermal mineralization: new perspectives. *Econ Geol* 88:1933–1976
- Rona PA, Thompson G, Mottl MJ, Karson JA, Jenkins WJ, Graham D, Mallette M, Von Damm K, Edmond JM (1984) Hydrothermal activity at the Trans-Atlantic Geotraverse hydrothermal field, Mid-Atlantic Ridge Crest at 26°N. *J Geophys Res* 89:11365–11377
- Rushdi AI, Simoneit BRT (2001) Lipid formation by aqueous Fischer-Tropsch-type synthesis over a temperature range of 100–400°C. *Orig Life Evol Biosph* 31:103–118
- Rushdi A, Simoneit BRT (2002a) Hydrothermal alteration of organic matter in sediments of the Northeastern Pacific Ocean: Part 1. Middle Valley, Juan de Fuca Ridge. *Appl Geochem* 17:1401–1428
- Rushdi A, Simoneit BRT (2002b) Hydrothermal alteration of organic matter in sediments of the Northeastern Pacific Ocean: Part 2. Escanaba Trough, Gorda Ridge. *Appl Geochem* 17:1467–1494
- Rushdi AI, Simoneit BRT (2004) Condensation reactions and formation of amides, esters and nitriles under hydrothermal conditions. *Astrobiology* 4:211–224
- Sakai H, Gamo T, Kim E-S, Tsutsumi M, Tanaka T, Ishibashi J, Wakita H, Yamano M, Oomori T (1990) Venting of carbon dioxide-rich fluid and hydrate formation in mid-Okinawa Trough backarc basin. *Science* 248:1093–1096
- Sander SG, Koschinsky A (2011) Metal flux from hydrothermal vents increased by organic complexation. *Nat Geosci* 4:145–150
- Sanders ND (1986) Visual observation of the solubility of heavy hydrocarbons in near-critical water. *Ind Eng Chem Fundam* 25:169–171
- Scott LT (1982) Thermal rearrangements of aromatic compounds. *Acc Chem Res* 15:52–58

- Scott SD (1985) Seafloor polymetallic sulfide deposits: modern and ancient. *Mar Min* 5:191–212
- Shaw RW, Brill TB, Clifford AA, Eckert CE, Franck EU (1991) Supercritical water, a medium for chemistry. *Chem Eng News* Dec 23:26–38
- Sherwood Lollar B, Westgate TD, Ward JA, Slater GF, Lacrampe-Couloume G (2002) Abiogenic formation of alkanes in the Earth's crust as a minor source for global hydrocarbon reservoirs. *Nature* 416:522–524
- Shock EL (1990) Chemical constraints on the origin of organic compounds in hydrothermal systems. *Orig Life Evol Biosph* 20:331–367
- Simoneit BRT (1977) Diterpenoid compounds and other lipids in deep-sea sediments and their geochemical significance. *Geochim Cosmochim Acta* 41:463–476
- Simoneit BRT (1978) The organic chemistry of marine sediments. In: Riley JP, Chester R (eds) *Chemical oceanography*, vol 7. Academic, London, pp 233–311
- Simoneit BRT (1982a) The composition, source and transport of organic matter to marine sediments – the organic geochemical approach. In: Thompson JAJ, Jamieson WD (eds) *Proceedings of the symposium marine chemistry into the eighties*. National Research Council of Canada, Victoria, B.C. pp 82–112
- Simoneit BRT (1982b) Shipboard organic geochemistry and safety monitoring, Leg 64, Gulf of California. In: Curran JR, Moore DG et al (eds) *Initial reports of the Deep Sea drilling project*, vol 64. U.S. Government Printing Office, Washington, DC, pp 723–728
- Simoneit BRT (1983a) Organic matter maturation and petroleum genesis: geothermal versus hydrothermal. In: The role of heat in the development of energy and mineral resources in the Northern Basin and Range Province, Geothermal Research Council, Davis, California, Special Report vol. 13, pp 215–241
- Simoneit BRT (1983b) Effects of hydrothermal activity on sedimentary organic matter: Guaymas Basin, Gulf of California – petroleum genesis and protokerogen degradation. In: Rona PA, Bostöm K, Laubier L, Smith KL Jr (eds) *Hydrothermal processes at seafloor spreading centers*. Plenum Press, New York, pp 451–471
- Simoneit BRT (1984) Hydrothermal effects on organic matter – high versus low temperature components. *Org Geochem* 6:857–864
- Simoneit BRT (1985a) Hydrothermal petroleum: genesis, migration and deposition in Guaymas Basin, Gulf of California. *Can J Earth Sci* 22:1919–1929
- Simoneit BRT (1985b) Hydrothermal petroleum: composition and utility as a biogenic carbon source. *Biol Soc Wash Bull* 6:49–56
- Simoneit BRT (1988) Petroleum generation in submarine hydrothermal systems – an update. *Can Mineral* 26:827–840
- Simoneit BRT (1990) Hydrothermal petroleum generation from immature organic matter – implications to the oceanic carbon cycle. In: Ittekkot V, Kemp S, Michaelis W, Spitzky A (eds) *Facets of modern biogeochemistry*. Springer, Berlin, pp 365–387
- Simoneit BRT (1992) Aqueous organic geochemistry at high temperature/high pressure, Holm NG (ed) *Orig Life Evol Biosph* 22: 43–65
- Simoneit BRT (1993) Hydrothermal alteration of organic matter in marine and terrestrial systems. In: Engel MH, Macko SA (eds) *Organic geochemistry*. Plenum Press, New York, pp 397–418
- Simoneit BRT (1994) Lipid/bitumen maturation by hydrothermal activity in sediments of Middle Valley, Leg 139. In: Mottl M, David E, Fisher A, Slack J (eds) *Proceedings of the ocean drilling program, scientific results*, vol 139. Ocean Drilling Program, College Station, pp 447–465
- Simoneit BRT (1995) Evidence for organic synthesis in high temperature aqueous media – facts and prognosis. *Orig Life Evol Biosph* 25:119–140
- Simoneit BRT (2000a) Submarine and continental hydrothermal systems – a review of organic matter alteration and migration processes, and comparison with conventional sedimentary basins. In: Giordano TH, Kettler RM, Wood SA (eds) *Ore genesis and exploration: the roles of organic matter*. *Reviews in economic geology*, vol 9. pp 193–215
- Simoneit BRT (2000b) Alteration and migration processes of organic matter in hydrothermal systems and implications for metallogenesis. In: Glikson M, Mastalerz M (eds) *Organic matter*

- and mineralization: thermal alteration, hydrocarbon generation and role in metallogenesis. Kluwer Academic Publishers, Dordrecht, pp 13–37
- Simoneit BRT (2003) Petroleum generation, extraction and migration and abiogenic synthesis in hydrothermal systems. In: Ikan R (ed) Natural and laboratory-simulated thermal geochemical processes. Kluwer Academic Publishers, Dordrecht, pp 1–30
- Simoneit BRT, Fetzer JC (1996) High molecular weight polycyclic aromatic hydrocarbons in hydrothermal petroleum from the Gulf of California and Northeast Pacific Ocean. *Org Geochem* 24:1065–1077
- Simoneit BRT, Galimov EM (1984) Geochemistry of interstitial gases in quaternary sediments of the Gulf of California. *Chem Geol* 43:151–166
- Simoneit BRT, Kawka OE (1987) Hydrothermal petroleum from diatomites in the Gulf of California. In: Brooks J, Fleet AJ (eds) Marine petroleum source rocks. Geological society of London special publication, vol 26. pp 217–228
- Simoneit BRT, Kvenvolden KA (1994) Comparison of ^{14}C ages of hydrothermal petroleum. *Org Geochem* 21:525–529
- Simoneit BRT, Lonsdale PF (1982) Hydrothermal petroleum in mineralized mounds at the seabed of Guaymas Basin. *Nature* 295:198–202
- Simoneit BRT, Philp RP (1982) Organic geochemistry of lipids and kerogen and the effects of basalt intrusions on unconsolidated oceanic sediments: sites 477, 478 and 481, Guaymas Basin, Gulf of California. In: Curray JR, Moore DG et al (eds) Initial reports of the Deep Sea drilling project, vol 64. U.S. Government Printing Office, Washington DC, pp 883–904
- Simoneit BRT, Brenner S, Peters KE, Kaplan IR (1978) Thermal alteration of cretaceous black shale by basaltic intrusions in the Eastern Atlantic. *Nature* 273:501–504
- Simoneit BRT, Mazurek MA, Brenner S, Crisp PT, Kaplan IR (1979) Organic geochemistry of recent sediments from Guaymas Basin, Gulf of California. *Deep-Sea Res* 26A:879–891
- Simoneit BRT, Brenner S, Peters KE, Kaplan IR (1981) Thermal alteration of cretaceous black shale by basaltic intrusions in the eastern Atlantic. II: effects on bitumen and kerogen. *Geochim Cosmochim Acta* 45:1581–1602
- Simoneit BRT, Philp RP, Jenden PD, Galimov EM (1984) Organic geochemistry of Deep Sea drilling project sediments from the Gulf of California – hydrothermal effects on unconsolidated diatom ooze. *Org Geochem* 7:173–205
- Simoneit BRT, Grimalt JO, Hayes JM, Hartman H (1987) Low temperature hydrothermal maturation of organic matter in sediments from the Atlantis II Deep, Red Sea. *Geochim Cosmochim Acta* 51:879–894
- Simoneit BRT, Kawka OE, Brault M (1988) Origin of gases and condensates in the Guaymas Basin hydrothermal system. In: Schoell M (ed) Origins of methane in the earth. Chemical geology, vol 71. pp 169–182
- Simoneit BRT, Brault M, Saliot A (1990a) Hydrocarbons associated with hydrothermal minerals, vent waters and talus on the East Pacific Rise and Mid-Atlantic Ridge. In: Simoneit BRT (ed) Organic matter alteration in hydrothermal systems – petroleum generation, migration and biogeochemistry. Applied Geochemistry, Elsevier, Amsterdam, vol 5. pp 115–124
- Simoneit BRT, Lonsdale PF, Edmond JM, Shanks III WC (1990b) Deep-water hydrocarbon seeps in Guaymas Basin, Gulf of California. In: Simoneit BRT (ed) Organic matter alteration in hydrothermal systems – petroleum generation, migration and biogeochemistry. Applied Geochemistry, Elsevier, Amsterdam, vol 5. pp 41–49
- Simoneit BRT, Goodfellow WD, Franklin JM (1992a) Hydrothermal petroleum at the seafloor and organic matter alteration in sediments of Middle Valley, Northern Juan de Fuca Ridge. *Appl Geochem* 7:257–264
- Simoneit BRT, Kawka OE, Wang G-M (1992b) Biomarker maturation in contemporary hydrothermal systems, alteration of immature organic matter in zero geological time. In: Moldowan J, Philp RP, Albrecht P (eds) Biological markers in sediments and petroleum. Prentice Hall, Englewood Cliffs, pp 124–141
- Simoneit BRT, Summons RE, Jahnke LL (1998) Biomarkers as tracers for life on early Earth and Mars. *Orig Life Evol Biosp* 28:475–483

- Simoneit BRT, Aboul-Kassim TAT, Tiercelin J-J (2000) Hydrothermal petroleum from lacustrine sedimentary organic matter in the East African Rift. *Appl Geochem* 15:355–368
- Simoneit BRT, Deamer DW, Kompanichenko V (2009) Characterization of hydrothermally generated oil from the Uzon Caldera, Kamchatka. *Appl Geochem* 24:303–309
- Siskin M, Katritzky AR (1991) Reactivity of organic compounds in hot water: geochemical and technological implications. *Science* 254:231–237
- Spieß FN, Macdonald KC, Atwater T, Ballard R, Carranza A, Cordoba D, Cox C, Diazgarcia VM, Francheteau J, Guerrero J, Hawkins J, Haymon R, Hessler R, Juteau T, Kastner M, Larson R, Luyendyk B, Macdougall JD, Miller S, Normark W, Orcutt J, Rangin C (1980) East Pacific Rise; hot springs and geophysical experiments. *Science* 207:1421–1433
- Svensen H, Karlsen DA, Sturz A, Backer-Owe K, Banks DA, Planke S (2007) Processes controlling water and hydrocarbon composition in seeps from the Salton Sea geothermal system, California, USA. *Geology* 35:85–88
- Szatmari P (1989) Petroleum formation by Fischer-Tropsch synthesis in plate tectonics. *Am Assoc Pet Geol Bull* 73:989–998
- Thompson G, Humphris SE, Schroeder B, Sulanowska M, Rona PA (1988) Hydrothermal mineralization on the Mid-Atlantic Ridge. *Can Mineral* 26:697–711
- Tiercelin J-J, Thourin C, Kalala T, Mondegeur A (1989) Discovery of sublacustrine hydrothermal activity and associated massive sulfides and hydrocarbons in the north Tanganyika trough, East African Rift. *Geology* 17:1053–1056
- Tiercelin J-J, Boulègue J, Simoneit BRT (1993) Hydrocarbon, sulphide and carbonate deposits related to sublacustrine hydrothermal seeps in the North Tanganyika Trough, East African Rift. In: Parnell J et al (eds) *Bitumens in Ore deposits*. Springer, Berlin, pp 96–113
- Tissot BP, Welte DH (1984) *Petroleum formation and occurrence: a new approach to oil and gas exploration*, 2nd edn. Springer, Berlin
- Tödheide K (1982) Hydrothermal solutions. *Ber Bunsenges Phys Chem* 89:1005–1016
- Venkatesan MI, Kaplan IR (1987) The lipid geochemistry of Antarctic marine sediments: Bransfield Strait. *Mar Chem* 21:347–375
- Venkatesan MI, Ruth E, Rao PS, Nath BN, Rao BR (2003) Hydrothermal petroleum in the sediments of the Andaman Backarc Basin, Indian Ocean. *Appl Geochem* 18:845–861
- Ventura GT, Simoneit BRT, Nelson RK, Reddy CM (2012) The composition, origin and fate of complex mixtures in the maltene fractions of hydrothermal petroleum assessed by comprehensive two-dimensional gas chromatography. *Org Geochem* 45:48–65
- Von Damm KL (1995) Controls on the chemistry and temporal variability of seafloor hydrothermal fluids. In: Humphris SE, Zierenberg RA, Mullineaux LS, Thomson RE (eds) *Seafloor hydrothermal systems*. Geophysical monograph, vol 91. pp 222–247
- Welhan JA, Lupton JE (1987) Light hydrocarbon gases in Guaymas Basin hydrothermal fluids: thermogenic versus abiogenic origin. *Am Assoc Pet Geol Bull* 71:215–223
- Whelan JK, Hunt JM (1982) C₁–C₈ in Leg 64 sediments, Gulf of California. In: Curran JR, Moore DG et al (eds) *Initial reports of the Deep Sea drilling project*, vol 64. U.S. Government Printing Office, Washington, DC, pp 763–779
- Whelan JK, Simoneit BRT, Tarafa M (1988) C₁–C₈ hydrocarbons in sediments from Guaymas Basin, Gulf of California – comparison to Peru Margin, Japan Trench and California Borderlands. *Org Geochem* 12:171–194
- Whiticar MJ, Suess E, Wehner H (1985) Thermogenic hydrocarbons in surface sediments of the Bransfield Strait, Antarctic Peninsula. *Nature* 314:87–90
- Yamanaka T, Ishibashi J, Hashimoto J (2000) Organic geochemistry of hydrothermal petroleum generated in the submarine Wakamiko caldera, southern Kyushu, Japan. *Org Geochem* 31:1117–1132
- Zárate PF, Simoneit BRT (2005) Hydrothermal bitumen generated from sedimentary organic matter of rift lakes – Lake Chapala, Citala Rift, western Mexico. *Appl Geochem* 20:2343–2350



Environmental and Economic Implications of the Biogeochemistry of Oil Sands Bitumen

21

H. Huang, R. C. Silva, J. R. Radović, and S. R. Larter

Contents

1	Introduction	594
2	Biodegradation Systematics	597
3	Extended Oil Sands Bitumen Compositional Analysis	600
3.1	Compositional Continuum	602
3.2	Asphaltenes	602
3.3	Other Non-hydrocarbon Compounds in Bitumens	603
4	Environmental Implications of Oil Sands Bitumen Biogeochemistry	604
5	Research Needs	608
	References	608

Abstract

Oil sands are one of the largest global resources of petroleum, which, in the future, will potentially be produced and transported on an increasing scale. The unique biogeochemistry of oil sands bitumens is the result of extensive in-reservoir biodegradation which produced very viscous and dense fluids, rich in aromatic hydrocarbons and non-hydrocarbons, containing sulfur and nitrogen and oxygen. The physicochemical properties of such species have significant implications for the economic and environmental aspects of oil sands exploitation, for example, energy and water use, residue generation (i.e., tailings ponds), fate and effects of incidental spills, etc. In this chapter we give an integrated overview of the oil sands bitumen composition, its effects on bitumen behavior, and discuss the future

H. Huang · R. C. Silva · J. R. Radović (✉) · S. R. Larter
PRG, Department of Geoscience, University of Calgary, Calgary, AB, Canada
e-mail: huah@ucalgary.ca; rcsilva@ucalgary.ca; Jagos.Radovic@ucalgary.ca; slarter@ucalgary.ca

© Springer Nature Switzerland AG 2020

593

H. Wilkes (ed.), *Hydrocarbons, Oils and Lipids: Diversity, Origin, Chemistry and Fate*,
Handbook of Hydrocarbon and Lipid Microbiology,
https://doi.org/10.1007/978-3-319-90569-3_19

research needs, in particular the integration of more advanced analytical chemical protocols and models, needed for the reliable assessment of non-hydrocarbon species, in spilled oil scenarios, which are the major component of some oil sands bitumens.

1 Introduction

The geological and biogeochemical context of oil sands have been described and reviewed in Adams et al. (2013) and Larter and Head (2014) and numerous papers referenced therein, and the following introduction is a summary of that work. Oil sands are a mixture of “bitumen,” a very viscous, heavily biodegraded crude oil, unconsolidated sand, and water, bound together by the bitumen and confining stresses. They represent an end member of a global resource consisting of oil reservoirs containing trillions of barrels of heavily biodegraded oil which are increasingly being produced as energy needs grow worldwide. Economic incentives to produce reserves from three trillion barrels of heavy oil and bitumen in the Western Canada oil sands have driven a geochemical mapping to assess fluid quality controls and improved understanding of the fundamental principles of the biodegradation of oils (Adams et al. 2012). While much of this has been for practical application, this has also presented an opportunity for fundamental advances in our understanding of subsurface biogeochemical processes and the boundaries of life in Earth. Additionally, the huge size and shallow location of oil sands, coupled with the many thousands of wells drilled, means that on a per cell basis, oil sands represent the most accessible portion of the deep biosphere in Earth. This provides a fabulous natural laboratory and also may provide new pathways for biotechnology innovation and solutions to our growing environmental and human health problems.

Output from Alberta’s oil sands bitumen reserves was expected to climb 26% from 2012 to 2.3 million barrels a day by 2015, rising to 5.2 million barrels by 2030 but economic, environmental, and political factors have reduced that estimate. Hein et al. (2013) estimate that global bitumen and heavy oil resources are around 5.6 trillion bbl, with most of that occurring in the Western Hemisphere. Much of the enabling technical developments have occurred in the largest bitumen and heavy oil fields of the Canadian oil sands, the Orinoco Heavy Oil belt of Venezuela, the heavy oil on the North Slope of Alaska and the heavy oil fields of California. Large heavy oil and bitumen occurrences are also found in Eurasia and Africa and while the detailed properties of the individual bitumens depend both on biodegradation degree and the source facies dependent initial oil composition, the general principles and observations remain common. These areas have served as development grounds for the commercial development of in situ recovery technologies (mostly thermal) that will be used to extract most of the remaining nonconventional bitumen and heavy oil resources.

Industry terminology is very inconsistent and confusing. Thus, based on the oil density-based industry standard yardstick of oil quality – API (American Petroleum Institute) gravity ([in degrees] = $[141.5/\text{specific gravity at } 60^\circ\text{F}] - 131.5$) – many of

the “extra heavy oils” of Venezuela would be considered “oil sands” in Canada or “tar sands” in the United States. Heavy oil is defined as oil with 10–20°API (oil with <10° API is denser than water) and a viscosity of more than 100 centipoise (cP; 1 cP = 1 mPa·S). Bitumen includes extra heavy oil as well as oil in oil sands, with less than 10°API and viscosity of more than 10,000 cP. The main distinction is that the high viscosity of “bitumen” prevents it from flowing to a wellbore under in situ reservoir conditions, whereas heavy oils will flow under the same conditions. Heavy oil and bitumen are part of a continuum of heavily to severely biodegraded oil (Hein et al. 2013).

Large oil sand deposits are commonly found in large foreland basins adjacent to orogenic belts, with large source rock kitchens charging large, shallow, cool, reservoirs at the basin flank, suitable for inflicting severe biodegradation on the oils (Adams et al. 2013; Larter and Head 2014), but are also found associated with lacustrine basins, in China, for example. The world’s largest oil sand deposit, located in Western Canada, is reseroired in L. Cretaceous sandstone deposits in a basin adjacent to the Canadian Rocky Mountains (foreland basin). Petroleum was derived principally from marine shale source rocks, with the petroleum migrating eastward up to several 100 km to accumulate and become biodegraded, on the northeastern margins of the basin. Oil was similarly accumulated in foreland basin settings in the Oficina Formation in Venezuela, another major heavy oil resource.

Bitumens are crude oils depleted in saturated hydrocarbons and enriched in aromatic hydrocarbons (such as alkylnaphthalenes or alkylphenanthrenes) and non-hydrocarbons containing sulfur and nitrogen and oxygen (and hydrogen and carbon). The content of non-hydrocarbon compounds in oil sands ranges from around 25%, by weight, in the western Peace River oil sands to nearly 60% in parts of the Athabasca oil sands accumulation. Not all oil floats, and Canadian bitumen, one of the most abundant petroleum resources on the planet, is predominately non-hydrocarbon in nature and in its native state sinks in water! Geochemical studies suggest the bitumen deposits of Alberta share common source rocks and similar maturities with the oil being sourced, predominantly from the Mississippian/Devonian Exshaw Formation, and the Jurassic Gordondale member source rocks locally affecting the western Peace River oil sands (Creaney et al. 1994; Adams et al. 2013).

The primary control on oil composition and viscosity is in-reservoir biodegradation (Larter et al. 2008). Oil API gravity in the Alberta Lower Cretaceous reservoirs ranges from 38°API (light oil) in the barely biodegraded oil pools west of the Peace River oil sands to 6°API (bitumen) in the severely biodegraded eastern Athabasca oil sands and to even lower values in the most extremely degraded bitumens, found in karsted Grosmont carbonate reservoirs that underlie the oil sands. Oil sulfur contents range from 1 to >10 wt%, with the western Peace River oil sands having the highest sulfur contents. This variability in fluid properties correlates roughly to levels of oil biodegradation which broadly increase from west to east and from south to north (Fig. 1c). Field observations typically record a coincidence of the lowest oil quality (highest viscosity and lowest API gravity) and strongest biological and molecular evidence for hydrocarbon biodegradation at or near oil-water transition zones

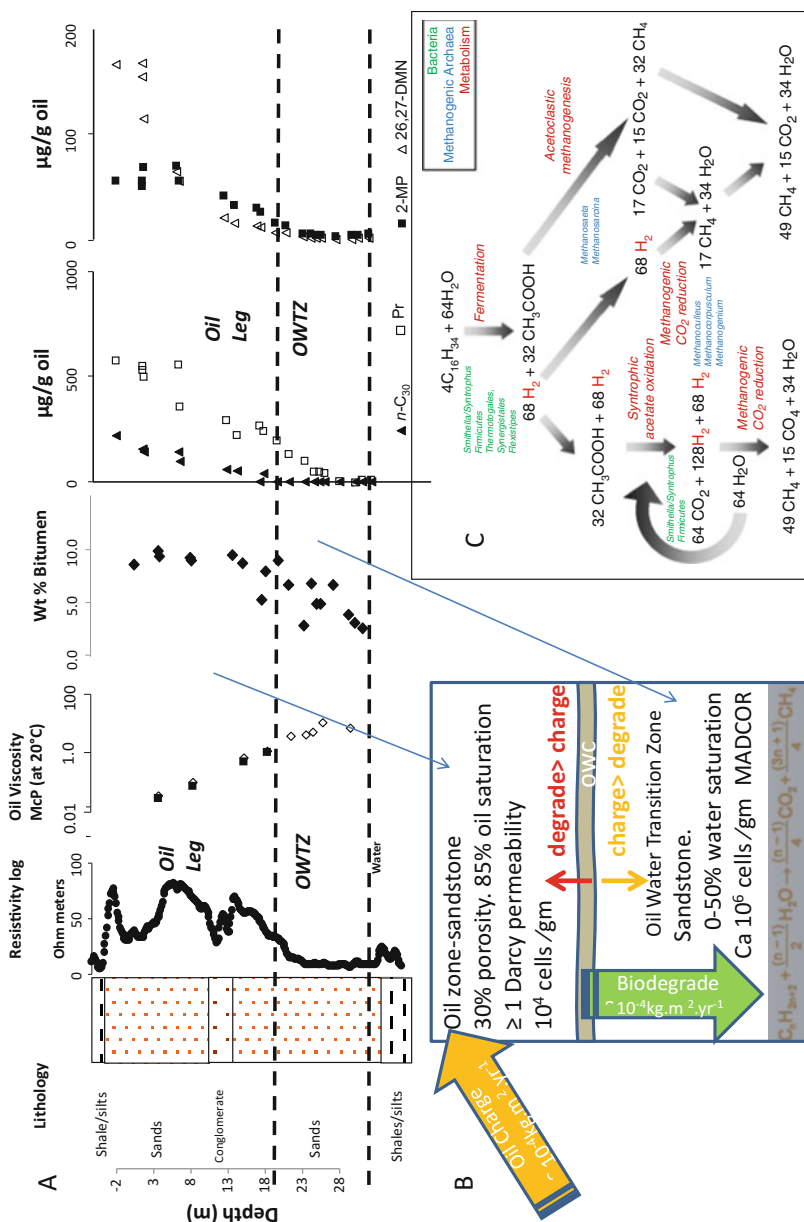


Fig. 1 Processes and bioreactors. (a) Geophysical and geochemical logs through an oil leg and oil-water transition zone (OWTZ) near 600 m depth, in a Peace River oil sand reservoir, show gradients of hydrocarbon destruction (*n*-C₃₀, alkane; Pr, pristane; 2-MP, 2-methylphenanthrene; 26,27-DMN, dimethyl/naphthalenes) and increasing oil viscosity with depth. The OWTZ has lower oil contents indicated by the resistivity log and the bitumen content

(OWTZ) in the deepest oil-filled parts of individual sandstone reservoirs, suggesting most petroleum biodegradation occurs near this interface (Bennett et al. 2013), where the biosphere meets the geosphere (Fig. 1).

2 Biodegradation Systematics

In general, biodegradation proceeds in a narrow range near the oil-water contact (OWC) of an oil field, under anaerobic conditions in any reservoir that has a water leg and has not been heated to >80 °C (Head et al. 2003) and proceeds on a similar timescale to oil charging (Larter et al. 2003). Figure 2 summarizes the factors controlling oil biodegradation and the formation of compositional gradients in a typical biodegraded oil column. The reactive compounds (hydrocarbons and non-hydrocarbons) diffuse toward the OWC, where they are degraded by microorganisms living using nutrients derived from the water-saturated zone below the oil column. Biodegradation-resistant compounds such as hopanes and non-hydrocarbons increase in concentration (relatively concentrated due to the loss of the reactive compounds) and accumulate near the OWC. Degradation produces new compounds, such as carboxylic acids, methane, and 25-norhopanes (as examples), which get distributed between oil and water phases. Compositional gradients reflect this complex charge and degradation scenario with fresh oil being charged to the top of the reservoir (Head et al. 2003; Huang et al. 2004b; Larter et al. 2006, 2008; Jones et al. 2008; Bennett et al. 2013).

Reservoir temperature is the primary control on the degree and, hence, the rates of subsurface biodegradation. Typically, net degradation fluxes for fresh petroleum in clastic reservoirs are close to zero for reservoir temperatures near 80 °C or above and increase, with decreasing reservoir temperature, to a maximum flux of 10^{-3} kg petroleum degraded/m² OWC area/year at temperatures near 40 °C (Larter et al. 2003, 2006). However, not all low temperature reservoirs contain degraded petroleum. The occurrence of non-biodegraded oils in shallow reservoirs is thought to reflect recent charging (Larter et al. 2006) or uplift of the reservoir from deeper, hotter subsurface regions where the reservoir was paleopasteurized (Wilhelms et al. 2001).



Fig. 1 (continued) log. **(b)** During filling, oil charge and biodegradation rates had similar magnitudes, and the oil-water contact (OWC) could have migrated back and forth competitively until the reservoirs filled, gas leaking through the shale caprock above. The multimeter thick OWTZ contains the main biological resource of the reservoir where the MADCOR process (methanogenic alkane degradation dominated by CO₂ reduction) takes place, reacting water and hydrocarbons to make methane and carbon dioxide, reducing bitumen content in the process. **(c)** Major processes involved in methanogenic alkane degradation. Points where molecular hydrogen is a key intermediate are highlighted in red. In oil reservoirs, acetoclastic methanogenesis is subordinate, and most degradation occurs via syntrophic acetate oxidation coupled to methanogenic CO₂ reduction (Jones et al. 2008; Bennett et al. 2013; Larter and Head 2014). (After Larter and Head 2014, with permission)

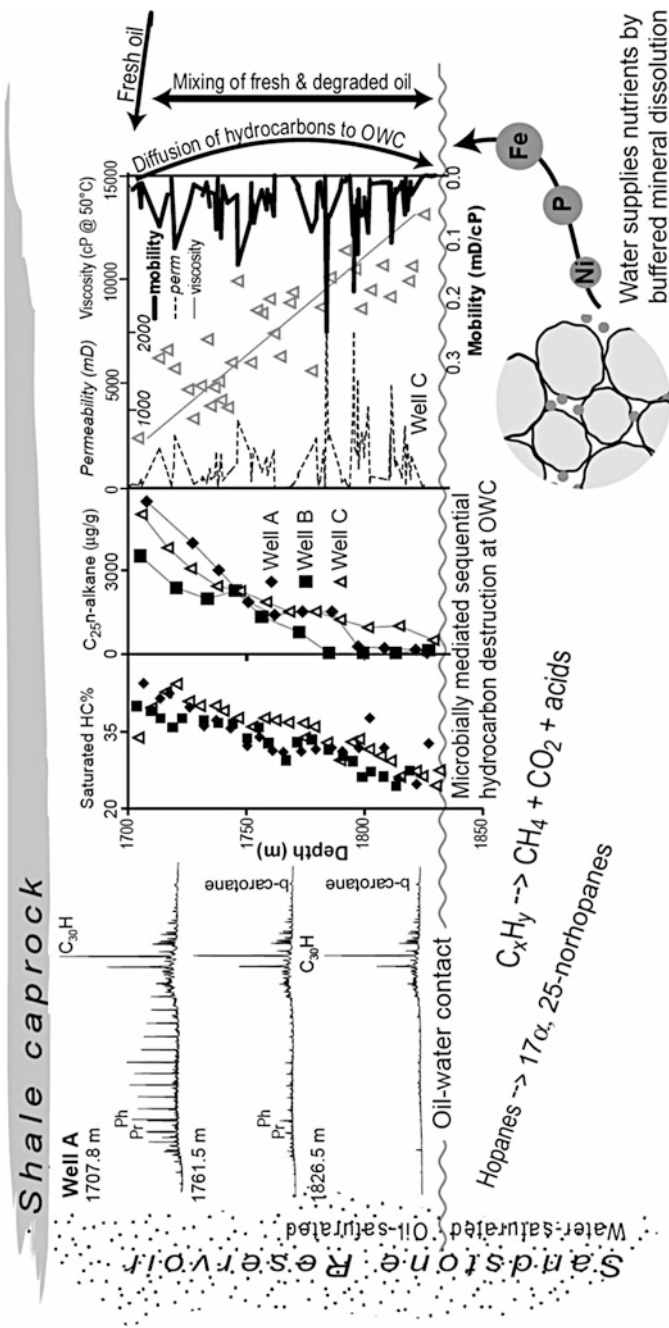


Fig. 2 Saturated hydrocarbon contents and gas chromatograms of petroleum extracted from reservoir cores show a progressive increase in biodegradation downward in three wells from a Chinese heavy oil field. On the chromatograms (left panel), Pr marks the pristane peak, Ph marks the phytane peak, and C₃₀H marks the C₃₀ hopane peak (Head et al. 2003; Huang et al. 2003, 2004a; Larter et al. 2006, 2008). (After Larter et al. 2008, with permission)

Reservoir topology or structure, in general, will be important as regards the rate and site of biodegradation. The overall extent of biodegradation will depend upon the areal extent of the biodegradation zone (at the OWC), the relative volume of the oil and water legs (determining nutrient availability) and the degree or ease of contact between them (determining nutrient accessibility). Key biological nutrients, such as phosphorus and potassium, are probably buffered by mineral dissolution reactions (Head et al. 2003; Huang et al. 2004a). Thicker water legs where the mineralogy is phosphorus enriched, for example, would be expected to promote degradation as nutrient supply by diffusion will be enhanced. The reservoir water salinity also acts as second-order controls on the process (Head et al. 2014). Very high aquifer salinities appear to slow degradation and even lower the temperature limit at which biological activity in reservoirs ceases, but the effect is currently not well quantified.

The OWC provides conditions that are the most conducive to microbial activity because, at the OWC, organisms can live in free water necessary for life and find food (oil) and reactants (water, oxidants) to generate energy and biomass. The bacterial abundances seen at the OWC of the reservoir are about two orders of magnitude higher than these within the oil leg (Bennett et al. 2013). The coincidence of high bacterial abundance and intense alteration of oil chemical and physical properties confirms that biodegradation is indeed responsible for producing gradients in oil physical and chemical properties, with most organisms residing near the base of the connected oil column (Head et al. 2003; Larter et al. 2003, 2006, 2008; Huang et al. 2004b; Bennett et al. 2013).

Geochemists have made substantial advances in their ability to describe empirically the geochemical sequences of subsurface oil degradation. The effects of biodegradation are most commonly recorded by the variations in the concentration of specific petroleum compounds throughout a reservoir, especially *n*-alkanes and isoprenoid alkanes (Connan 1984; Peters and Moldowan 1993; Wenger et al. 2002; Head et al. 2003), alkyl aromatic hydrocarbons (Volkman et al. 1984; Huang et al. 2004a), nitrogen compounds (Huang et al. 2003), and non-hydrocarbons (Liao et al. 2009; Oldenburg et al. 2017). Among the saturated hydrocarbons, the linear alkanes are depleted before polycyclic hydrocarbons. Compounds derived from natural products by substantial molecular rearrangement are usually biodegraded less rapidly than the non-rearranged hydrocarbons (Connan 1984; Peters and Moldowan 1993). Similarly, for aromatic hydrocarbons, alkylbenzenes are removed before diaromatic and triaromatic hydrocarbons, with aromatic steroid hydrocarbons being resistant until very severe levels of biodegradation are achieved. A “quasi-stepwise” process for hydrocarbon biodegradation, using artificial ranks, has been established based on laboratory experiments and field observations (Connan 1984; Volkman et al. 1984; Peters and Moldowan 1993; Wenger et al. 2002; Head et al. 2003). The widely used 10 point scale was proposed by Peters and Moldowan (1993) (PM scale) with PM1 (least altered) to PM10 (most altered). However, other studies suggested that many compound species were removed synchronously by bacterial at very different net rates rather than one after another (Larter et al. 2012; Bennett et al. 2013).

Recently, Larter et al. (2012) developed the Manco (Modular Analysis and Numerical Classification of Oils) scale, based on integrating the extent of biodegradation of various aromatic compounds and steranes. They noted a wide variation of alkyl aromatic compounds (e.g., alkyltoluenes, alkyl-naphthalenes, alkylphenanthrenes, and alkyl-dibenzothiophenes) in samples degraded to uniform levels on standard PM scales, which may show variation in local degradation systematics related to biodegradation mechanisms and extent of fresh oil recharge and mixing. The Manco scale is applicable to any crude oil system but is best defined for heavy oil and bituminous sand deposits generally relating to PM level 4–8.

Huang and Li (2017) noted that existing biodegradation scales, widely used to describe the extent of biodegradation of petroleum, have insufficient resolution at extreme biodegradation levels (PM level 8+), as the behavior of some biodegradation resistant compounds such as pregnanes, tri- and tetracyclic terpanes, and non-hopane pentacyclic terpanes had not been included. These very extreme levels of biodegradation can be further differentiated on the basis of the presence and absence of these “refractory” components, together with 25-norhopanes (NHs), 17-nortricyclic terpanes (NTTs), and C₂₃ demethylated tetracyclic terpane (C₂₃NTeT). These NHs, NTTs, and C₂₃NTeT are produced from corresponding hopanes and tri- and tetracyclic terpanes during biodegradation, but they are biodegradable as well. The norhopane system shows that both generation and destruction of such species occurs at advanced levels of biodegradation in oil sands systems (Bennett et al. 2006, 2009).

The molecular-level variations in composition are proxies for overall bitumen composition and thus fluid properties such as viscosity. However, mixing of fresh and degraded oils dominates the composition and physical properties of biodegraded oils, rendering geochemical schemes that rank the absolute level of biodegradation of oil unachievable and somewhat meaningless. All these processes complicate existing simple rankings of crude oils in terms of relative level of degradation. A more complicated filling/charge situation occurs when the first oil charge is subjected to biodegradation and is subsequently mixed with later charges to the reservoir, resulting in non-biodegraded and biodegraded oils within the same reservoir interval (Zhang et al. 2014). The nature of the primary oil charge and addition of a secondary fresh oil charge may dominate properties in settings such as in China and Western Canada (Koopmans et al. 2002; Larter et al. 2006, 2008).

3 Extended Oil Sands Bitumen Compositional Analysis

Oil sands bitumen exemplifies one of the most challenging chemical matrices, in analytical terms, given the large amounts of polar and high-molecular weight fraction material in its composition (Fig. 3). The most detailed compilation of oil sands bitumen physicochemical properties can be found in the book by Strausz et al. (2003). While a significant part of the saturated and aromatic compounds in oils has been extensively analyzed at a molecular level and studied for years (Strausz et al. 2010, 2011), the molecular description of the whole bitumen petroleome has always

COSB chemical composition (Strausz et al., 2003)

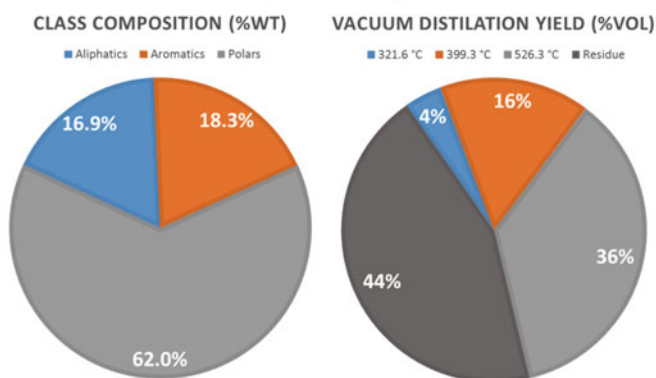


Fig. 3 Overview of Canadian oil sands bitumen (COSB) composition by chemical classes and boiling point fraction yield. Light and dark gray slices in both pie charts represent the most challenging high-molecular weight, polar compounds which have been analyzed at a molecular level after the advent of FTICR-MS technologies.

posed a challenge. Despite its geochemical and engineering significance, the assessment of the high-molecular weight polar fraction has been typically based on bulk chemical properties or spectroscopic responses. However, along the years, particularly during the early twenty-first century, new analytical technologies have allowed investigation of composition from different viewpoints. The field of study named “Petroleomics” (Marshall and Rodgers 2004), initially enabled by the development of Fourier transform ion cyclotron resonance mass spectrometers (FTICR-MS), has targeted the characterization of petroleum at the molecular level and its correlations to both up- and downstream activities within the oil industry. Not surprisingly, given oil sands bitumen strategic relevance as one of the largest fossil fuel reserves in the world, its fractions have been extensively studied by FTICR-MS and, for the first time, molecular-level insights are available.

A single petroleum FTICR-MS mass spectrum can reveal tens of thousands of peaks. As a consequence of the ultrahigh resolution and accuracy mass measurements, unique molecular formulae can be assigned to detected peaks (Marshall and Rodgers 2008). The main outcome from FTICR-MS analysis is a long list of assigned molecular formulae and intensities related to peaks found in the mass spectrum. Traditionally, compositional investigations create sequential data layers based on heteroatom content, double-bond equivalent (DBE), carbon number (C#) and elemental ratios to sort the detected molecular formulae and create plots. The chemical nature of detected ions is highly influenced by the ionization method of choice, as each technique will favor specific compound classes. In this sense, FTICR-MS analysis of bitumen sheds new light into the discussions on non-hydrocarbon petroleum components and asphaltene compositional features, with significant impact on the understanding of bitumen production and upgrading.

3.1 Compositional Continuum

McKenna et al. (2010) offered the first molecular-based evidence of the notion of a compositional continuum in a Canadian bitumen, heavy vacuum gas oil (HVGO) distillation series via FTICR-MS. An incredibly complex chemical matrix with 150,000+ elemental compositions was detected in eight different HVGO fractions. Data was useful to check the validity and accuracy of the Boduszynski model (Boduszynski 1987), which describes how compositional features of oil components progress with increasing compound boiling point. The model suggests that, in a given oil distillation fraction, the non-hydrocarbon polar compounds would have the lowest carbon numbers (compared to saturated and aromatic hydrocarbons). The abundance-weighted average carbon number measured for compound classes detected in different distillation HVGO distillation cuts, showed that species in hetero compound class S and class O₂ are generally smaller (two and three fewer carbon atoms, respectively) than the class HC. Moreover, a smooth DBE distribution of species in hetero compound class S species, showed that saturated cyclic structures are equally relevant/abundant in the polar fraction of bitumens as non-hydrocarbon species with aromatic cores.

3.2 Asphaltenes

Asphaltenes are operationally defined as the petroleum components insoluble in paraffinic solvents, such as pentane or heptane. Understanding their chemistry and solubility behavior is fundamental to avoid asphaltene precipitation during oil production, storage, transportation and refining. Oil sands bitumen asphaltene chemistry has also been extensively investigated over the years (Strausz et al. 2003). Due to limitations in analytical technologies, besides bulk (e.g., CHNSO elemental analysis) and spectroscopic analysis, one common strategy to probe asphaltene structures was via chemical modification (oxidation/reduction, thermal stress, and hydrolysis) that produced compounds amenable to the available analytical technologies of the time. Asphaltenes represent a solubility class; thus compositional differences of asphaltenes fractionated from different oils are expected. Recently, ESI-N (electrospray ionization in negative mode) FTICR-MS was used to assess bitumen asphaltene chemistry, when asphaltenes were obtained from different experimental setups (Wang et al. 2013). Not surprisingly, the separation conditions (solvent time, purity, and washing times) showed significant impact on the composition and behavior of asphaltene compound classes. FTICR-MS results have also been useful to suggest that the chemical nature of asphaltenes is different from maltenes in terms of aromaticity and heteroatom content but less so in terms of molecular weight (McKenna et al. 2013). A Canadian oil sands bitumen asphaltene feedstock was analyzed by APPI-P (atmospheric pressure photoionization in positive ion mode) FTICR-MS (Silva et al. 2016), and molecules with carbon number ranging from C₂₀ to C₆₈, DBE values of 6–33, were detected.

Silva et al. (2016) suggested the occurrence of archipelago-type asphaltene species in Canadian bitumens, after the analysis of asphaltene oxycracking products, which showed a shift to lower DBE values, compared to the parent material. Another study applied ruthenium ion-catalyzed oxidation to investigate the molecular characterization of bitumen asphaltenes by ESI-N FTICR-MS (Zhou et al. 2016). The rationale involves selectively oxidizing aromatic carbon to CO₂ and analyzing the remaining products to derive general asphaltene structural information. Alkyl groups with carbon numbers up to 60 (plus 1–5 saturated rings) could be detected in the reaction products, suggesting that even within the Canadian oil sands bitumen asphaltenes, large hydrophobic molecular portions can still be found. By fractionating five heavily biodegraded bitumens, into maltenes and asphaltenes, Pan et al. (2013) investigated the oil sands bitumen biodegradation pathways by ESI-N FTICR-MS. NO and NO₂ species compound classes were suggested to be formed from class N species via a ring-opening reaction and oxidation, while evidence of thiophenic ring opening due to oxidation was also obtained. Oldenburg et al. (2017) used FTICR-MS analysis to investigate the compositional effects of microbial alteration along an oil sand bitumen reservoir column, indicating that biodegradation primary targets, at any biodegradation level, are the most abundant species, including the heteroatomic compounds. The partial oxidation of S- and N-containing species, as detected by FTICR-MS, may have significant impacts to biodegradation mass balance as a significant fraction of the oil is transformed rather than mineralized to CO₂ and H₂O. Overall, Oldenburg et al. (2017) suggest much more complex sulfur and nitrogen species alteration routes, depending on the level of biodegradation and the oil provenance itself.

Unfractionated bitumen asphaltene analysis, by APPI-P FTICR-MS, allowed the detection of several vanadyl petroporphyrin structures all at once (McKenna et al. 2009). With a similar approach but using a petroporphyrin-rich fraction from Canadian bitumens distillation residues, Liu et al. (2015) reported both nickel and vanadyl porphyrins (40+ and 250+ different molecular formulae, respectively), including sulfur-containing porphyrins, by ESI-N FTICR-MS analysis.

3.3 Other Non-hydrocarbon Compounds in Bitumens

A sample of oil sands bitumen, heavy vacuum gas oil at 475–500 °C was used to test the ability of lithium cationization as a tool to extend the range of species able to be analyzed by ESI-P FTICR-MS (Lobodin et al. 2014). The authors showed that an enhanced detection of S_xO_y species was obtained and thus a detailed molecular characterization of such species is permitted, with implications for emulsion interface chemistry as these compounds are known to be natural surfactants. Also focused on highlighting the sulfur compounds in ESI-P (electrospray ionization in positive mode) FTICR-MS analysis, Liu et al. (2010) submitted the aliphatic fraction of oil sands bitumen to selective oxidation of sulfur compounds, followed by S-methylation reactions. While the unreacted aliphatic fraction failed to yield ions in electrospray (as expected), the compound class OS dominated the mass spectra of reaction products,

suggesting an original sulfur species class (likely sulfides) with a DBE range of 0–12 and carbon atom range from 10 to 45. When submitted to *S*-methylation reaction and analyzed by ESI-P FTICR-MS, the bitumens showed a compound class S, with an upper limit of DBE = 20 (Shi et al. 2010). On the other hand, working with Canadian bitumen vacuum residue, Purcell et al. (2007) showed that methylation, followed by ESI-P FTICR-MS, yields distinct (but somewhat complementary) class S patterns, compared to APPI-P analysis of the unreacted material. Noticeably, Purcell et al. (2007) also showed how class S species from “aromatic” and “aliphatic” fractions occupy a different compositional space in APPI-P FTICR-MS regarding DBE content, but not species carbon number distribution.

Given the omnipresence of water-oil interactions in the most used bitumen production schemes (i.e., mining and steam assisted gravity drainage, SAGD), there is a need to understand the impact of oil composition in such processes. For example, FTICR-MS has offered chemical insights of how oil sands bitumens’ asphaltenes or other naturally occurring surfactants influence production process derived from emulsion stabilization. Jarvis et al. (2015) used different methods to obtain the interfacial material from Canadian bitumen emulsion species via a wet silica partitioning chromatography approach. After FTICR-MS analyses, the isolated interfacial material was compared to the parent oil, showing higher abundances of heteroatom-containing species (O, S, and N) and lower carbon numbers for the components, indicating the importance of non-hydrocarbons to interfacial phenomena in petroleum systems.

4 Environmental Implications of Oil Sands Bitumen Biogeochemistry

The unique biogeochemistry and compositions of oil sands bitumens are a major factor which has to be considered in the environmental assessments of current and future bitumen exploitation. For example, from the production perspective, the extreme viscosity of oil sands bitumens, up to millions of centipoises at reservoir conditions (Larter et al. 2008), is one of the reasons why significant input of energy and water resources is needed in the production process (Gates and Larter 2014) (Fig. 4). Energy and water are used for extraction in both surface mining and during in situ recovery (e.g., steam assisted gravity drainage, SAGD, and cyclic steam stimulation, CSS), as well for separation of oil from the mineral phase (clays and sands) and its subsequent upgrading (Larter and Head 2014). It is estimated that 28.5 L of water are used to produce 1 L of bitumen, using surface mining (Rosa et al. 2017). In situ methods are much more water efficient, using, under ideal conditions, some 2.8 L of water per liter of bitumen produced (Rosa et al. 2017). Notwithstanding, the annual freshwater use for Canadian bitumen processing will potentially increase by approx. 40% to 2040, compared to current use (Fig. 4; Rosa et al. 2017).

Large quantities of water used in the production of bitumen generate equally large volumes of oil sands process-affected water (OSPW). OSPW is a complex, residual mixture of bitumen components, mineral fraction, and chemicals used for

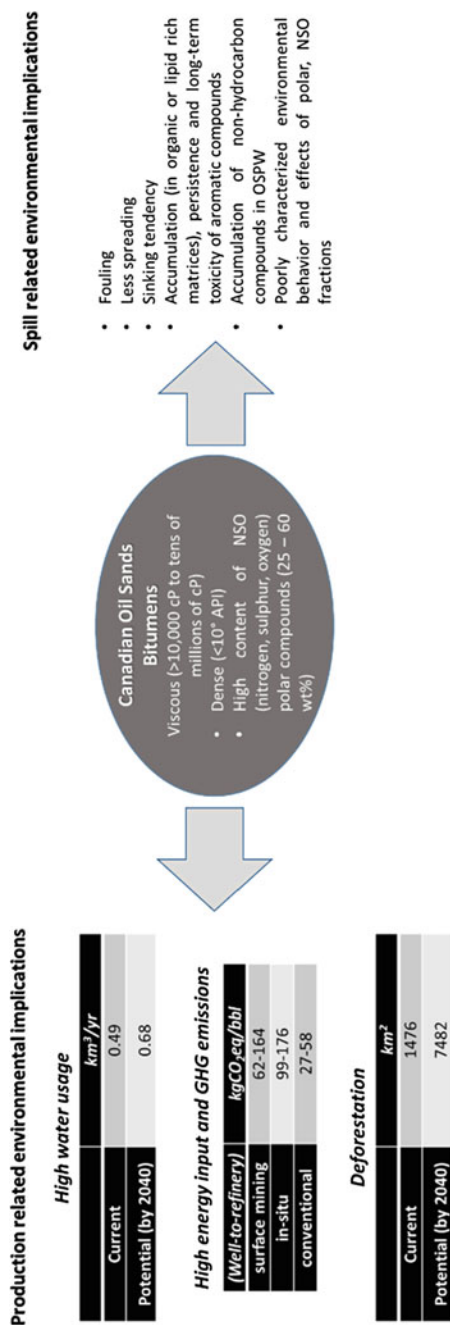


Fig. 4 Production and spill-related environmental implications of oil sands bitumen biogeochemistry. Water usage is related to current and potential freshwater use for the oil sands extraction and processing in Canada (Charpentier et al. 2009; Larter and Head 2014; Radović et al. 2018; Rosa et al. 2017)

the treatment of oil sands, which has to be stored in tailings ponds, for settling, containment, and future treatment. Currently, tailings ponds cover an area of 180 km² (Alberta Energy 2017), contributing in this way to land disruption. Deforestation is another consequence of surface oil sands mining – net forested area in Alberta has been reduced by 10% in the period from 2000 to 2014, and will potentially worsen in the future (Rosa et al. 2017; Fig. 4).

Finally, energy-intensive production process results in higher carbon emissions from the exploitation of bitumens, relative to the production emissions from conventional oil reservoirs. For example, “well-to-refinery” greenhouse gas emissions of oil sands production (both surface mining and in situ) are about three times higher than the emissions from conventional oil production (Fig. 4; Charpentier et al. 2009).

Distinct chemical compositions of oil sands bitumen are the main factor to be considered when evaluating the behavior, fate, and toxic effects of spills and leakages occurring during the oil production and transport processes or from the tailings of process water residues. In Alberta, during the 37-year long period (1975–2012), there have been, on average, close to 650 oil spills per year, releasing approx. 46,000 bbl annually (Radović et al. 2018). Of those, some of the largest releases were due to the pipeline failures, such as the Pembina pipeline spill in 1980, or from train derailments, such as the spill to Wabamun Lake in 2005.

The main compositional features that makes bitumens so different to other oils are the high content of high-molecular weight compounds, concentrated, in particular, within the non-hydrocarbon rich, polar fractions of oil (operationally defined resin and asphaltene fractions). The remaining dense and viscous fluid is dominated by highly alkylated and cyclized aromatic compounds and in particular by nitrogen, sulfur, and oxygen (NSO) containing non-hydrocarbons (Fig. 4). Such enrichment in polar species is partly the consequence of extensive in-reservoir biodegradation, which occurred over geological timescale and led to almost complete depletion of *n*-alkanes, followed by isoprenoid alkanes and cyclic and aromatic hydrocarbons (Larter and Head 2014). Additionally, in foreland basin settings, the heavily biodegraded oils on the basin margins are commonly charged from relatively low maturity, and in the case of Canada, high-organic sulfur-rich source rock systems (Adams et al. 2013).

In the case of a heavy oil or bitumen spill (often diluted with solvents to so-called dilbit), due to adverse adhesion properties and commonly high viscosity, such oils can have negative physical effects on the environment, such as the fouling of surfaces, plants, and animals. On the positive side, spills of viscous oils have limited spreading tendency, so their containment and removal in both aquatic and terrestrial media is facilitated, using response measures such as booming, in situ burning, and excavation. High densities of bitumen, on the other hand, can promote sinking when released to water. Sunken oil has negative effects to benthic biota; and, in addition, once it is in the sediments, the natural removal processes such as biodegradation and photooxidation will be significantly inhibited, extending oil's persistence in the environment. For example, a portion of heavy oil spilled on Wabamun Lake was transported to the lake floor and has been resurfacing for years after the spill (Hollebone et al. 2011). Light hydrocarbon fraction of solvents used in dilbits

would have higher environmental mobility, being preferentially lost through evaporation.

From the perspective of their environmental partitioning and toxicity in the case of a spill, the particular chemistry of the bitumen has to be considered. For example, alkylated, high ring number homologs of aromatic hydrocarbons, which are found in abundance in Canadian bitumens, are hydrophobic and have the tendency to accumulate in organic or lipid-rich matrices (e.g., sediment, fat tissues). In addition, they are more resistant to biodegradation (Overton et al. 2016) and potentially have chronic adverse effects, as demonstrated in several field and laboratory studies (deBruyn et al. 2007; Vrabie et al. 2012; Radović et al. 2014b).

Most significantly, the environmental behavior of the polar, non-hydrocarbon fractions of oil sands bitumens is still not very well understood and is often overlooked and ignored, due to the limitations of traditional analytical methods, typically based on gas chromatography, which are not capable of characterizing this nonvolatile portion of the oil. In addition to being present in native oil, heteroatom-containing compounds can also be produced from the parent hydrocarbons (typically aromatic species) during the post-spill weathering processes, such as photooxidation and/or biodegradation (Radović et al. 2014a; Ruddy et al. 2014).

Conveniently, analytical improvements in the past years, in particular the advent of novel instrumental tools, such as the Fourier transform ion cyclotron resonance mass spectrometry (FTICR-MS), have revolutionized our understanding of high-molecular weight, polar oil constituents. In a recent FTICR-MS study, it has been demonstrated that despite their high nominal mass (300–600 Da), many of the polar oil species were able to partition into water phase, if a sufficient number of heteroatoms (NSO) were present in the molecule (Liu and Kujawinski 2015). Once in water, polar oil constituents become more mobile and potentially bioavailable. Other FTICR-MS studies have confirmed that the same mechanism also occurs during bitumen production, when complex, heteroatom compound classes will preferentially partition to OSPW (Quesnel et al. 2015). For example, naphthenic acids are a group of compounds which is extensively studied in OSPW, due to their demonstrated acute and chronic toxicity (Thomas et al. 2009; Scarlett et al. 2013). Naphthenic acids are typically alkyl-substituted, alicyclic carboxylic acids, including polycarboxylic acids (i.e., with more than one acidic group), but also sulfur-containing acidic species (Quesnel et al. 2015), though aromatic components, may be also present in this fraction. Given the fact that toxic naphthenic acids can be quite persistent (Whitby 2010), there is an urgent need to find effective and feasible methods for the remediation of large volumes of OSPW currently stored in tailings ponds – almost 1,000 million m³ as of 2013 (Alberta Energy 2017).

In conclusion, from the environmental perspective, oil sands bitumen biogeochemistry needs to be better understood, in order to be able to reliably assess the effects and ultimate fate of potential future spills. In the coming years, bitumens, often diluted by solvent to facilitate transportation, will be increasingly transported via existing and planned pipelines or possibly even by tankers, thus increasing the risk of terrestrial and marine spills. Leaching, or accidental spills of contaminated waters from tailings ponds, is another troublesome risk which has to be managed.

Finally, improved knowledge of bitumen biogeochemistry and its impact on the distribution of fluid properties will help to optimize the energy and water efficiency of production processes. In all these cases, composition and behavior of polar, non-hydrocarbon fraction of oil sands bitumens is the main unknown and the main research area for investigation. Fortunately, as ever, we are in an era where new analytical tools and methods are arriving.

5 Research Needs

The principal area needing development is the holistic description and quantitation of the non-hydrocarbon species in severely biodegraded petroleum and the definition of their biogeochemical origins and fates. Relating this diverse mixtures of species to the processing behavior in a refinery, or the environmental and toxicological behavior of a complex bitumen or heavy oil, in a spill setting, is crucial and will require the integration of more advanced analytical chemical protocols, the ability to predict environmental behavior of individual chemical species from structural information, and improved laboratory techniques and computational models for the assessment of non-hydrocarbon species partition from oil into water columns under a variety of natural environments (Jaggi et al. 2017). Our understanding of the non-hydrocarbon species in petroleum today is at about the same stage of development of understanding of the hydrocarbon species and petroleum in the 1970s and 1980s. There is much to be done and many discoveries to be made!

Acknowledgments We acknowledge the support of Canada Research Chairs, Canada Foundation for Innovation, NSERC, the University of Calgary and PRG group members, past and present, for discussions.

References

- Adams J, Larter S, Bennett B, Huang H (2012) Oil charge migration in the peace river oil sands and surrounding region. In: *Geoconvention 2012: vision*. Calgary
- Adams J, Larter S, Bennett B, Westrich J, van Kruidijk C (2013) The dynamic interplay of oil mixing, charge timing, and biodegradation in forming the Alberta oil sands: insights from geologic modeling and biogeochemistry. In: *Heavy-oil and oil-sand petroleum systems in Alberta and beyond*. AAPG studies in geology, vol 64. AAPG, Canadian Heavy Oil Association and AAPG Energy Minerals Division, pp 23–102
- Alberta Energy (2017) Oil sands. <http://www.energy.alberta.ca>
- Bennett B, Fustic M, Farrimond P, Huang H, Larter SR (2006) 25-Norhopanes: formation during biodegradation of petroleum in the subsurface. *Org Geochem* 37:787–797
- Bennett B, Jiang C, Larter SR (2009) Identification and occurrence of 25-norbenzohopanes in biodegraded bitumen from Palaeozoic carbonates in northern Alberta. *Org Geochem* 40:667–670
- Bennett B, Adams JJ, Gray ND, Sherry A, Oldenburg TBP, Huang H, Larter SR, Head IM (2013) The controls on the composition of biodegraded oils in the deep subsurface-part 3. The impact of microorganism distribution on petroleum geochemical gradients in biodegraded petroleum reservoirs. *Org Geochem* 56:94–105

- Boduszynski MM (1987) Composition of heavy petroleum. 1. Molecular weight, hydrogen deficiency, and heteroatom concentration as a function of atmospheric equivalent boiling point up to 1400 °F (760 °C). *Energy Fuels* 1:2–11
- Charpentier AD, Bergerson JA, MacLean HL (2009) Understanding the Canadian oil sands industry's greenhouse gas emissions. *Environ Res Lett* 4:014005
- Connan J (1984) Biodegradation of crude oils in reservoirs. In: Brooks J, Welte DH (eds) *Advances in petroleum geochemistry*, vol 1. Academic, London, pp 299–335
- Creaney S, Allan J, Cole K, Fowler M, Brooks P, Osadetz K, Macqueen R, Snowdon L, Riediger C (1994) Petroleum generation and migration in the Western Canada Sedimentary Basin. In: *Geological atlas of the Western Canada Sedimentary Basin*. Canadian Society of Petroleum Geologists (CSPG) and the Alberta Research Council, pp 455–468
- deBruyn AM, Wernick BG, Stefura C, McDonald BG, Rudolph B-L, Patterson L, Chapman PM (2007) In situ experimental assessment of lake whitefish development following a freshwater oil spill. *Environ Sci Technol* 41:6983–6989
- Gates ID, Larter SR (2014) Energy efficiency and emissions intensity of SAGD. *Fuel* 115:706–713
- Head IM, Jones DM, Larter SR (2003) Biological activity in the deep subsurface and the origin of heavy oil. *Nature* 426:344–352
- Head IM, Gray ND, Larter SR (2014) Life in the slow lane; biogeochemistry of biodegraded petroleum containing reservoirs and implications for energy recovery and carbon management. *Front Microbiol* 5:566
- Hein FJ, Leckie D, Larter S, Suter JR (2013) Heavy oil and bitumen petroleum systems in Alberta and beyond: the future is nonconventional and the future is now. *AAPG Stud Geol* 64:1–21
- Hollebone BP, Fieldhouse B, Sergey G, Lambert P, Wang Z, Yang C, Landriault M, Owens EH, Parker HA (2011) The behaviour of heavy oil in a fresh water lake. In: *Proceedings of the 34th AMOP technical seminar on environmental contamination and response*, pp 668–709
- Huang H, Li J (2017) Molecular composition assessment of biodegradation influence at extreme levels—a case study from oilsand bitumen in the Junggar Basin, NW China. *Org Geochem* 103:31–42
- Huang H, Bowler BFJ, Zhang Z, Oldenburg TBP, Larter SR (2003) Influence of biodegradation on carbazole and benzocarbazole distributions in oil columns from the Liaohe Basin, NE China. *Org Geochem* 34:951–969
- Huang H, Bowler BFJ, Oldenburg TBP, Larter SR (2004a) The effect of biodegradation on polycyclic aromatic hydrocarbons in reservoir oils from the Liaohe Basin, NE China. *Org Geochem* 35:1619–1634
- Huang H, Larter SR, Bowler BF, Oldenburg TB (2004b) A dynamic biodegradation model suggested by petroleum compositional gradients within reservoir columns from the Liaohe Basin, NE China. *Org Geochem* 35:299–316
- Jaggi A, Snowdon RW, Stopford A, Radović JR, Oldenburg TBP, Larter SR (2017) Experimental simulation of crude oil-water partitioning behavior of BTEX compounds during a deep submarine oil spill. *Org Geochem* 108:1–8
- Jarvis JM, Robbins WK, Corilo YE, Rodgers RP (2015) Novel method to isolate interfacial material. *Energy Fuels* 29:7058–7064
- Jones DM, Head IM, Gray ND, Adams JJ, Rowan AK, Aitken CM, Bennett B, Huang H, Brown A, Bowler BFJ, Oldenburg T, Erdmann M, Larter SR (2008) Crude-oil biodegradation via methanogenesis in subsurface petroleum reservoirs. *Nature* 451:176–180
- Koopmans MP, Larter SR, Zhang C, Mei B, Wu T, Chen Y (2002) Biodegradation and mixing of crude oils in Eocene Es3 reservoirs of the Liaohe Basin, northeastern China. *AAPG Bull* 86:1833–1843
- Larter SR, Head IM (2014) Oil sands and heavy oil: origin and exploitation. *Elements* 10:277–283
- Larter S, Wilhelms A, Head I, Koopmans M, Aplin A, Di Primio R, Zwach C, Erdmann M, Telnaes N (2003) The controls on the composition of biodegraded oils in the deep subsurface – part 1: biodegradation rates in petroleum reservoirs. *Org Geochem* 34:601–613
- Larter S, Huang H, Adams J, Bennett B, Jokanola O, Oldenburg T, Jones M, Head I, Riediger C, Fowler M (2006) The controls on the composition of biodegraded oils in the deep subsurface.

- Part II: geological controls on subsurface biodegradation fluxes and constraints on reservoir-fluid property prediction. *AAPG Bull* 90:921–938
- Larter S, Adams J, Gates ID, Bennett B, Huang H (2008) The origin, prediction and impact of oil viscosity heterogeneity on the production characteristics of tar sand and heavy oil reservoirs. *J Can Pet Technol* 47:52–61
- Larter S, Huang H, Adams J, Bennett B, Snowdon LR (2012) A practical biodegradation scale for use in reservoir geochemical studies of biodegraded oils. *Org Geochem* 40:312–320
- Liao Y, Geng A, Huang H (2009) The influence of biodegradation on resins and asphaltenes in the Liaohe Basin. *Org Geochem* 40:312–320
- Liu Y, Kujawinski EB (2015) Chemical composition and potential environmental impacts of water-soluble polar crude oil components inferred from ESI FT-ICR MS. *PLoS One* 10:e0136376
- Liu P, Xu C, Shi Q, Pan N, Zhang Y, Zhao S, Chung KH (2010) Characterization of sulfide compounds in petroleum: selective oxidation followed by positive-ion electrospray Fourier transform ion cyclotron resonance mass spectrometry. *Anal Chem* 82:6601–6606
- Liu H, Mu J, Wang Z, Ji S, Shi Q, Guo A, Chen K, Lu J (2015) Characterization of vanadyl and nickel porphyrins enriched from heavy residues by positive-ion electrospray ionization FT-ICR mass spectrometry. *Energy Fuels* 29:4803–4813
- Lobodin VV, Juyal P, McKenna AM, Rodgers RP, Marshall AG (2014) Lithium cationization for petroleum analysis by positive ion electrospray ionization Fourier transform ion cyclotron resonance mass spectrometry. *Energy Fuels* 28:6841–6847
- Marshall AG, Rodgers RP (2004) *Petroleomics: the next grand challenge for chemical analysis petroleum and mass spectrometry: divergent*. *Acc Chem Res* 37:53–59
- Marshall AG, Rodgers RP (2008) *Petroleomics: chemistry of the underworld*. *Proc Natl Acad Sci USA* 105:18090–18095
- McKenna AM, Purcell JM, Rodgers RP, Marshall AG (2009) Identification of vanadyl porphyrins in a heavy crude oil and raw asphaltene by atmospheric pressure photoionization Fourier transform ion cyclotron resonance (FT-ICR) mass spectrometry. *Energy Fuels* 23:2122–2128
- McKenna AM, Purcell JM, Rodgers RP, Marshall AG (2010) Heavy petroleum composition. 1. Exhaustive compositional analysis of Athabasca bitumen HVGO distillates by Fourier transform ion cyclotron resonance mass spectrometry: a definitive test of the Boduszynski model. *Energy Fuels* 24:2929–2938
- McKenna AM, Marshall AG, Rodgers RP (2013) Heavy petroleum composition. 4. Asphaltene compositional space. *Energy Fuels* 27:1257–1267
- Oldenburg TBP, Huang H, Bennett B, Head I, Jones M, Larter SR (2017) The controls on the composition of biodegraded oils in the deep subsurface – part 4. Destruction and production of high molecular weight non-hydrocarbon species and destruction of aromatic hydrocarbons during progressive in-reservoir biodegradation. *Org Geochem* 114:57–80
- Overton EB, Wade TL, Radović JR, Meyer BM, Miles MS, Larter SR (2016) Chemical composition of macondo and other crude oils and compositional alterations during oil spills. *Oceanography* 29:50–63
- Pan Y, Liao Y, Shi Q, Hsu CS (2013) Acidic and neutral polar NSO compounds in heavily biodegraded oils characterized by negative-ion ESI FT-ICR MS. *Energy Fuels* 27:2960–2973
- Peters KE, Moldowan JM (1993) *The biomarker guide: interpreting molecular fossils in petroleum and ancient sediments*. Prentice Hall, Englewood Cliffs
- Purcell JM, Juyal P, Kim DG, Rodgers RP, Hendrickson CL, Marshall AG, April RV, Re V, Recci M, June V (2007) Sulfur speciation in petroleum: atmospheric pressure photoionization or chemical derivatization and electrospray ionization Fourier transform ion cyclotron resonance mass spectrometry. *Energy & Fuels* 77:2869–2874
- Quesnel DM, Oldenburg TBP, Larter SR, Gieg LM, Chua G (2015) Biostimulation of oil sands process-affected water with phosphate yields removal of sulfur-containing organics and detoxification. *Environ Sci Technol* 49:13012–13020
- Radović JR, Aeppli C, Nelson RK, Jimenez N, Reddy CM, Bayona JM, Albaigés J (2014a) Assessment of photochemical processes in marine oil spill fingerprinting. *Mar Pollut Bull* 79:268–277

- Radović JR, Thomas KV, Parastar H, Díez S, Tauler R, Bayona JM (2014b) Chemometrics-assisted effect-directed analysis of crude and refined oil using comprehensive two-dimensional gas chromatography–time-of-flight mass spectrometry. *Environ Sci Technol* 48:3074–3083
- Radović JR, Oldenburg TBP, Larter SR (2018) Chapter 19 – Environmental assessment of spills related to oil exploitation in Canada’s oil sands region. In: Stout SA, Wang Z (eds) *Oil spill environmental forensics case studies*. Butterworth-Heinemann, Oxford, pp 401–417.
- Rosa L, Davis KF, Rulli MC, D’Odorico P (2017) Environmental consequences of oil production from oil sands. *Earth Future* 5:158–170
- Ruddy BM, Huettel M, Kostka JE, Lobodin VV, Bythell BJ, McKenna AM, Aeppli C, Reddy CM, Nelson RK, Marshall AG, Rodgers RP (2014) Targeted petroleomics: analytical investigation of macondo well oil oxidation products from Pensacola Beach. *Energy Fuels* 28:4043–4050
- Scarlett AG, Reinardy HC, Henry TB, West CE, Frank RA, Hewitt LM, Rowland SJ (2013) Acute toxicity of aromatic and non-aromatic fractions of naphthenic acids extracted from oil sands process-affected water to larval zebrafish. *Chemosphere* 93:415–420
- Shi Q, Pan N, Liu P, Chung KH, Zhao S, Zhang Y, Xu C (2010) Characterization of sulfur compounds in oilsands bitumen by methylation followed by positive-ion electrospray ionization and Fourier transform ion cyclotron resonance mass spectrometry. *Energy Fuels* 24:3014–3019
- Silva RC, Radović JR, Ahmed F, Ehrmann U, Brown M, Carbognani Ortega L, Larter S, Pereira-Almao P, Oldenburg TBP (2016) Characterization of acid-soluble oxidized asphaltenes by Fourier transform ion cyclotron resonance mass spectrometry: insights on oxycracking processes and asphaltene structural features. *Energy Fuels* 30:171–179
- Strausz OP, Lown EM, Alberta Energy Research Institute (2003) *The chemistry of Alberta oil sands, bitumens and heavy oils*. Alberta Energy Research Institute, Calgary
- Strausz OP, Morales-Izquierdo A, Kazmi N, Montgomery DS, Payzant JD, Safarik I, Murgich J (2010) Chemical composition of Athabasca bitumen: the saturate fraction. *Energy Fuels* 24:5053–5072
- Strausz OP, Lown EM, Morales-Izquierdo A, Kazmi N, Montgomery DS, Payzant JD, Murgich J (2011) Chemical composition of Athabasca bitumen: the distillable aromatic fraction. *Energy Fuels* 25:4552–4579
- Thomas KV, Langford K, Petersen K, Smith AJ, Tollefsen KE (2009) Effect-directed identification of naphthenic acids as important in vitro xeno-estrogens and anti-androgens in North Sea offshore produced water discharges. *Environ Sci Technol* 43:8066–8071
- Volkman JK, Alexander R, Kagi RI, Rowland SJ, Sheppard PN (1984) Biodegradation of aromatic hydrocarbons in crude oils from the Barrow Sub-basin of Western Australia. *Org Geochem* 6:619–632
- Vrabie CM, Sinnige TL, Murk AJ, Jonker MTO (2012) Effect-directed assessment of the bioaccumulation potential and chemical nature of Ah receptor agonists in crude and refined oils. *Environ Sci Technol* 46:1572–1580
- Wang L, He C, Liu Y, Zhao S, Zhang Y, Xu C, Chung KH, Shi Q (2013) Effects of experimental conditions on the molecular composition of maltenes and asphaltenes derived from oilsands bitumen: characterized by negative-ion ESI FT-ICR MS. *Sci China Chem* 56:863–873
- Wenger LM, Davis CL, Isaksen GH (2002) Multiple controls on petroleum biodegradation and impact on oil quality. *SPE Reserv Eval Eng* 5:375–383
- Whitby C (2010) Microbial naphthenic acid degradation. *Adv Appl Microbiol* 70:93–125
- Wilhelms A, Larter SR, Head I, Farrimond P, di-Primio R, Zwach C (2001) Biodegradation of oil in uplifted basins prevented by deep-burial sterilization. *Nature* 411:1034–1037
- Zhang SC, Huang HP, Su J, Zhu GY, Wang XM, Larter S (2014) Geochemistry of Paleozoic marine oils from the Tarim Basin, NW China. Part 4: paleobiodegradation and oil charge mixing. *Org Geochem* 67:41–57
- Zhou X, Zhao S, Shi Q (2016) Quantitative molecular characterization of petroleum asphaltenes derived ruthenium ion catalyzed oxidation product by ESI FT-ICR MS. *Energy Fuels* 30:3758–3767



Alexei V. Milkov

Contents

1	Introduction	614
2	Formation of Secondary Microbial Gas	614
3	Recognition of Secondary Microbial Gas in Natural Environments	616
4	Global Occurrences of Secondary Microbial Gas in Petroleum Accumulations	618
5	Volumetric Significance of Secondary Microbial Gas	618
6	Research Needs	621
	References	621

Abstract

Secondary microbial gas is produced by microbes during biodegradation of petroleum. Methane is the terminal product of petroleum biodegradation and is the dominant hydrocarbon component of secondary microbial gas. Secondary microbial gas is often mixed with thermogenic gas and primary microbial gas in shallow biodegraded petroleum accumulations and in petroleum seeps, and an integrated geochemical–geological approach is needed to recognize its presence. Significant ^{13}C -enrichment of associated CO_2 ($\delta^{13}\text{C} > +2\text{‰}$) is perhaps the best geochemical indicator of secondary microbial gas. Recent assessments suggest that secondary microbial gas may be more abundant in petroleum accumulations than primary microbial gas.

A. V. Milkov (✉)

Department of Geology and Geological Engineering, Colorado School of Mines, Golden, CO, USA

e-mail: amilkov@mines.edu

© Springer Nature Switzerland AG 2020

H. Wilkes (ed.), *Hydrocarbons, Oils and Lipids: Diversity, Origin, Chemistry and Fate*,
Handbook of Hydrocarbon and Lipid Microbiology,

https://doi.org/10.1007/978-3-319-90569-3_22

613

1 Introduction

Primary microbial gas formed by microbes from dispersed organic matter in relatively shallow and cool sediments is commonly recognized in seeps, sediments, and petroleum accumulations (Strapoć 2017) and is thought to account for more than 20% of world's natural gas resources (Rice and Claypool 1981). However, the growth of geochemical database on gases and oils from shallow petroleum accumulations and from natural seeps led to the recognition that some gases previously thought to have primary microbial origin actually formed from biodegraded petroleum during secondary methanogenesis (Etiope et al. 2009; Milkov 2010). As a large portion of petroleum accumulations in the world experienced anaerobic biodegradation (Roadifer 1987; Head et al. 2003) resulting in the formation of secondary microbial gas (predominantly methane), this gas is likely a very significant component of many petroleum systems. In this chapter, I first review the main biogeochemical pathways of secondary microbial gas formation and propose how to recognize that gas in natural environments. I then describe the global occurrences of secondary microbial gas and volumetric significance of the gas in conventional petroleum accumulations.

2 Formation of Secondary Microbial Gas

Laboratory experiments demonstrate that anaerobic biodegradation of oil results in the formation of secondary microbial gas in which methane is the predominant hydrocarbon (Bokova 1953; Ekzercev 1960; Zengler et al. 1999; Jones et al. 2008). The net reaction of methanogenic hydrocarbon degradation (with hexadecane as an example) is $4C_{16}H_{34} + 64H_2O \rightarrow 49CH_4 + 15CO_2$. This reaction may proceed via several pathways. It appears that complete oxidation of alkanes to H_2 and CO_2 followed by methanogenesis from CO_2 reduction ($CO_2 + 4H_2 \rightarrow CH_4 + 2H_2O$) is the main pathway, while acetoclastic methanogenesis ($CH_3COOH \rightarrow CH_4 + CO_2$) and methylotrophic methanogenesis ($4CH_3OH \rightarrow 3CH_4 + CO_2 + 2H_2O$) are less quantitatively important (Dolfing et al. 2008; Feisthauer et al. 2010; Meslé et al. 2013). Methanogens can use other substrates such as formate, methylamines, dimethyl sulfide, ethanol, and isopropanol, but the possible relevance of these substrates for methane formation is not well documented (Colosimo et al. 2016). Although methane is the main hydrocarbon gas generated during petroleum biodegradation, limited laboratory experiments suggest that small amounts of C_2 gases ($C_1/C_{2+} \sim 2600$) also form during petroleum biodegradation, along with N_2 , CO_2 , H_2 , and H_2S (Bokova 1953).

Figure 1 describes the formation of primary and secondary microbial methane in the subsurface environments. While primary microbial methane forms from complex and commonly dispersed organic matter, secondary microbial methane forms from petroleum (commonly oil) accumulations with highly concentrated and relatively simple organic matter. As a result, secondary methanogenesis appears to be a more

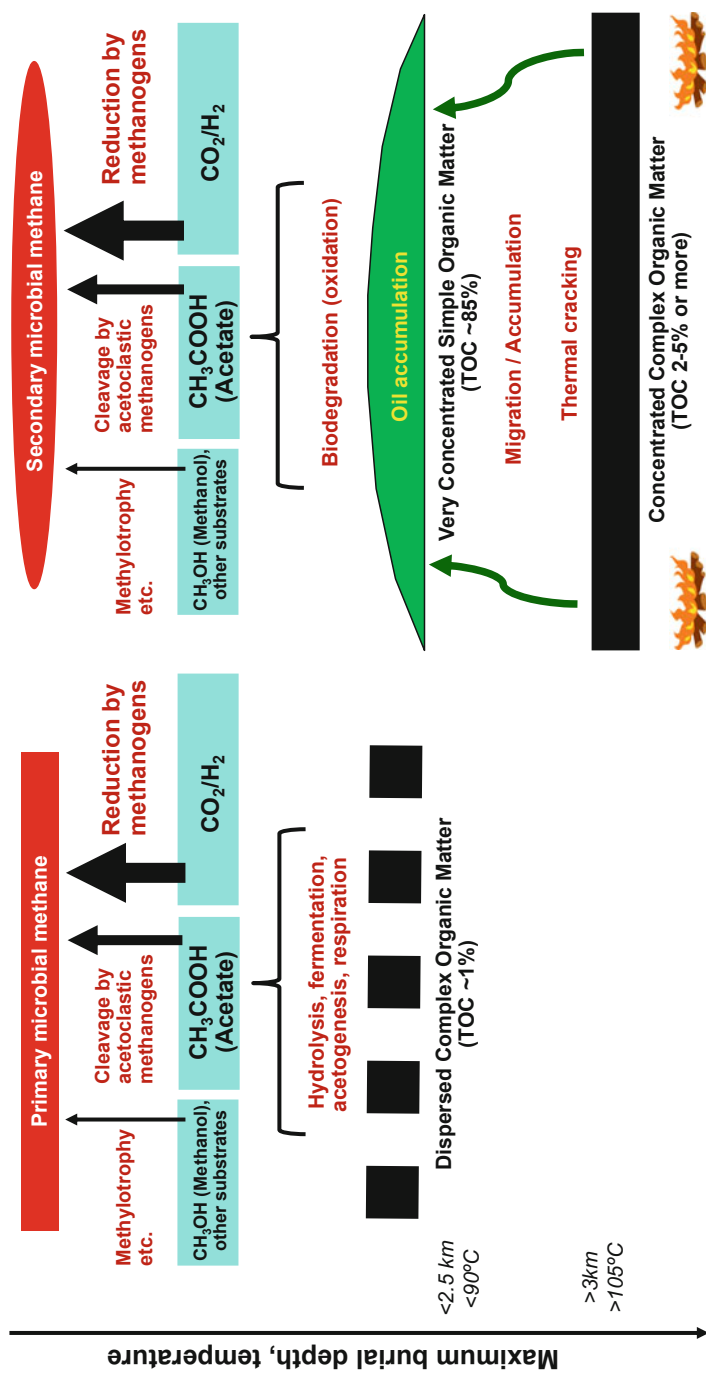


Fig. 1 Formation of primary microbial methane (left panel) and secondary microbial methane (right panel) in the subsurface. Thickness of the black arrows indicates the assumed relative significance of methanogenic pathways

efficient process and generates a larger amount of accumulated subsurface gas than primary methanogenesis as discussed below.

3 Recognition of Secondary Microbial Gas in Natural Environments

Biodegraded oils may comprise more than half of the volume of petroleum in the world's largest accumulations (Roadifer 1987). Biodegradation is also a common process in petroleum seeps (Etiopie et al. 2009). As secondary microbial methane is the terminal product of oil biodegradation (Zeikus 1977; Head et al. 2003; Larter et al. 2005), it is reasonable to expect the occurrence of secondary microbial gas in most biodegraded petroleum accumulations and in most petroleum seeps. However, natural petroleum gases are commonly mixtures. All oil accumulations have associated thermogenic gases, and many of them have an admixture of primary microbial gases (Katz et al. 2002; Milkov et al. 2007). During the biodegradation, the gas becomes more methane-dominated as some C_{2+} gases such as propane are preferentially degraded (James and Burns 1984). As the secondary microbial methane is added to the gas mixture within biodegraded petroleum accumulations, the total gas becomes even dryer, and the $C_1/(C_2 + C_3)$ ratio can increase significantly and reach values around 10,000 (Boreham et al. 2001). Based on molecular composition alone, this very dry secondary microbial gas may be confused with methane-dominated gases of primary microbial origin or thermogenic gases of high maturity.

Carbon isotopes provide means to recognize secondary microbial gas in natural environments. Milkov (2011) reviewed the geochemistry of gases within biodegraded accumulations around the world and found that methane within the global biodegradation zone is often enriched in ^{12}C relatively to methane below the biodegradation zone. Still, as biodegradation zone occurs in shallow cool sedimentary section, primary microbial methane enriched in ^{12}C may mix with biodegraded petroleum and mask the presence of secondary microbial methane. Many gases in biodegraded petroleum accumulations have CO_2 significantly enriched in ^{13}C with $\delta^{13}C$ values often exceeding +2‰ and reaching as high as +32.7‰ (Lillis et al. 2007). Petroleum seeps also often have CO_2 significantly enriched in ^{13}C (Etiopie et al. 2009) with $\delta^{13}C$ values as high as +35.6‰ (Tassi et al. 2012). Such significant enrichment of CO_2 in ^{13}C usually does not result from other petroleum systems processes and may be unique to secondary methanogenesis. As CO_2 derived from biodegraded oil is converted into secondary microbial methane, the residual CO_2 becomes more enriched in ^{13}C . Therefore, enrichment of CO_2 in ^{13}C may correlate with the degree of conversion of oil to secondary microbial gas and may be used to quantify the amount of secondary microbial gas in petroleum accumulations.

Secondary microbial gas may have wide ranges of molecular composition as well as $\delta^{13}C$ of methane and CO_2 depending on the initial oil composition, environmental conditions, microbial consortia, level of biodegradation, and extent of CO_2 conversion to methane (Milkov 2011). Still, secondary microbial gas can be recognized

based on the geochemical evidence. The most important evidence is $\delta^{13}\text{C}$ of $\text{CO}_2 > +2\text{‰}$. Gases with ratio of $\text{C}_1/(\text{C}_2 + \text{C}_3)$ exceeding 100 and having $\delta^{13}\text{C}$ of methane around -55‰ to -45‰ are also likely to have significant contribution of secondary microbial methane. Combining these geochemical evidence allows distinguishing secondary microbial gases from primary microbial gases and from thermogenic gases (Fig. 2). For more certain interpretation, these geochemical evidence should be consistent with other evidence such as the presence of biodegraded oil within the accumulation (or in deeper accumulations and/or down-dip) and the existence of geological conditions for biodegradation (relatively low temperature below 90°C , availability of nutrients, relatively low pore water salinity, relatively high porosity, proximity to oil–water contact or gas–water contact, and sufficient geological time after the reservoir filling).

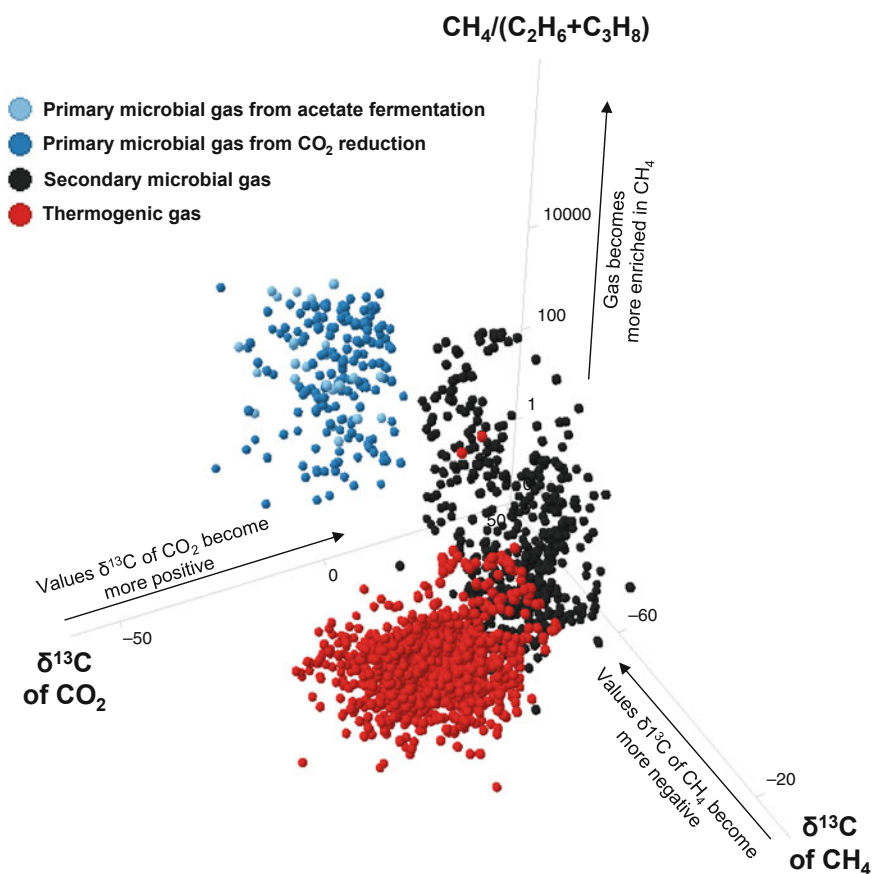


Fig. 2 The plot of $\text{C}_1/(\text{C}_2 + \text{C}_3)$, $\delta^{13}\text{C}$ of C_1 and $\delta^{13}\text{C}$ of CO_2 helps to distinguish secondary microbial gas from primary microbial gas and thermogenic gas

4 Global Occurrences of Secondary Microbial Gas in Petroleum Accumulations

Secondary microbial gases occur in petroleum seeps and mud volcanoes (Etiope et al. 2009), gas hydrates (Sassen et al. 2001) as well as in conventional (Pallasser 2000; Lillis et al. 2007; Milkov 2010; Mathur 2017), shale (McIntosh et al. 2002; Martini et al. 2003) and coalbed (Scott et al. 1994; Guo et al. 2012; Baublys et al. 2015) petroleum reservoirs.

Milkov (2011) compiled a map of secondary microbial gas occurrences in conventional petroleum accumulations, and the updated version of that map is presented in Fig. 3. To date, there are 27 basins with apparent and significant presence of secondary microbial gas, as evidenced by the presence of biodegraded petroleum and CO₂ with $\delta^{13}\text{C}$ exceeding +2‰. There are 14 basins where the presence of secondary microbial gas is probable because relatively dry gas with $\delta^{13}\text{C}$ of C₁ between -55‰ and -35‰ associates with biodegraded oil. Finally, there are six basins with possible presence of secondary microbial gas as evidenced by the high dryness of the gas associated with biodegraded oil (even though the isotope data are not available).

It is apparent that secondary methanogenesis is a global phenomenon that occurs in conventional reservoirs in numerous sedimentary basins around the world. Secondary microbial gases commonly occur in relatively shallow (<3.5 km below surface/mudline) and relatively cool (<90 °C) clastic reservoirs of mostly Cretaceous and Tertiary age.

5 Volumetric Significance of Secondary Microbial Gas

It is difficult to calculate the amount of secondary microbial gas in petroleum accumulations because this gas is always mixed with the thermogenic gas that was associated with original nondegraded petroleum and is often mixed with primary microbial gas. Geochemical mixing models need to be developed to quantify the portion of secondary microbial gas in reservoir gas mixtures. Milkov (2011) used a series of assumptions and approximations and estimated that 1461–2760 trillion cubic feet (tcf) in place (845–1644 tcf recoverable) of secondary microbial gas may be accumulated as free and oil-dissolved gas in petroleum reservoirs. This suggests that secondary microbial gas is more abundant in petroleum accumulations than primary microbial gas (Fig. 4). Although the suggestion of Rice and Claypool (1981) that more than 20% of the world's gas has primary microbial origin remains widely cited, the recent work indicates that primary microbial gas may be much less significant (3–4%), while secondary microbial gas (5–11%) and especially thermogenic gas (85–92%) dominate conventional petroleum accumulations.

A very large amount of secondary microbial gas (~65,500 tcf according to the estimation by Milkov 2011) was generated by currently existing biodegraded petroleum accumulations. Although some of that gas is present in petroleum

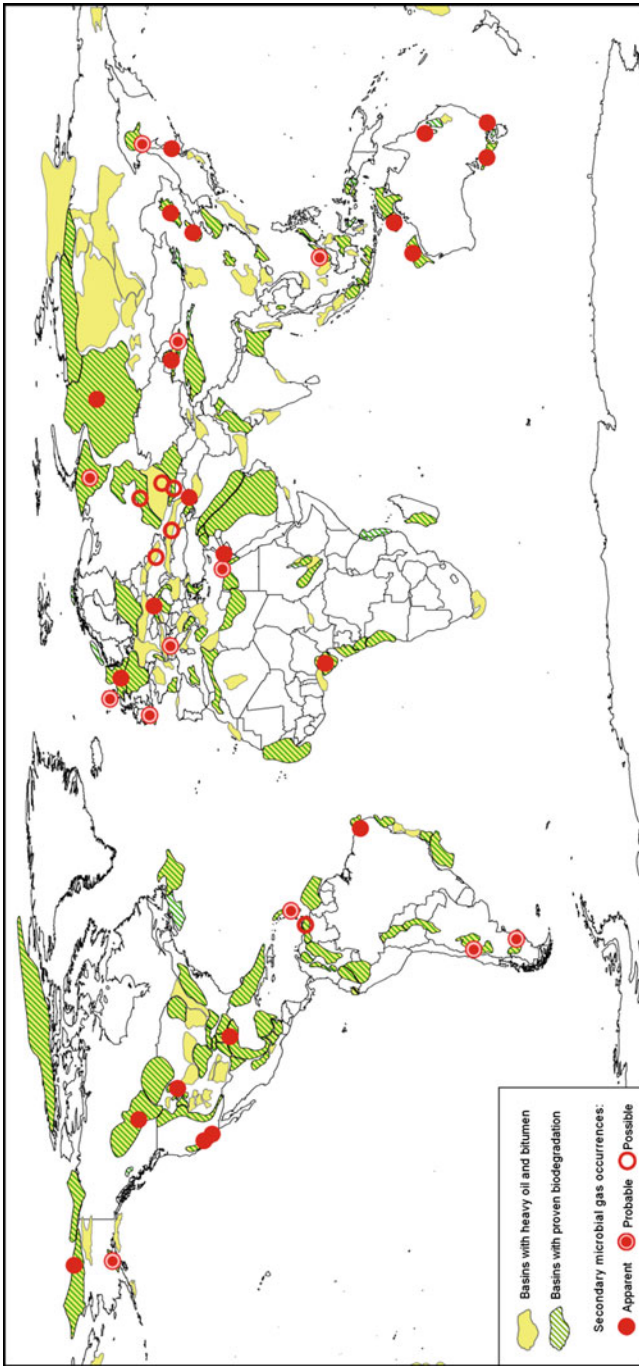


Fig. 3 Worldwide distribution of conventional petroleum reservoirs where the presence of secondary microbial gas is apparent, probable, and possible (updated from Milkov 2011)

Fig. 4 Pie chart demonstrating the relative volumetric significance of thermogenic, secondary microbial, and primary microbial gases in the global endowment of recoverable natural gas in conventional petroleum reservoirs

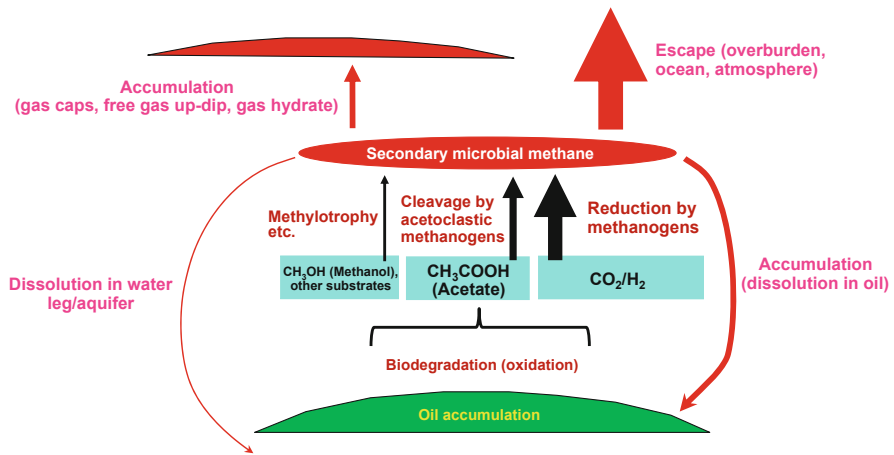
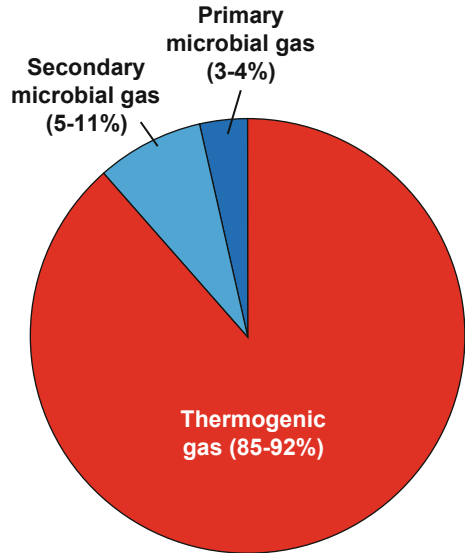


Fig. 5 The fate of secondary microbial methane. Thickness of the arrows indicates the assumed relative significance of the processes. It appears that most generated secondary microbial methane migrates to the overburden above biodegraded petroleum accumulations and escapes into the ocean and the atmosphere

accumulations, most of it likely escaped into the overburden, the ocean, and the atmosphere (Fig. 5). As secondary microbial gas is composed mostly of methane, which is a potent greenhouse gas, it likely played a significant but yet unquantified and not understood role in the past climate changes.

6 Research Needs

Although secondary microbial gas is present worldwide in conventional and unconventional petroleum accumulations as well as in petroleum seeps and mud volcanoes, relatively little research has been done to understand its volumetric significance and its role in global methane reservoir and cycle. I envision three main research needs on secondary microbial gas:

1. Creation of geochemical mixing models to quantify the portion of secondary microbial gas in reservoir gas mixtures which commonly include thermogenic gas and primary microbial gas
2. Advanced comprehensive laboratory studies of methanogenic biodegradation of petroleum to better understand molecular and isotopic properties of gas products and the relative significance of various pathways of methanogenesis
3. Assessments of secondary microbial gas flux from shallow biodegraded reservoirs into the atmosphere at present and in the past and understanding the role of this gas in carbon cycle and global climate change

References

- Baublys KA, Hamilton SK, Golding SD, Vink S, Esterle J (2015) Microbial controls on the origin and evolution of coal seam gases and production waters of the Walloon Subgroup; Surat Basin, Australia. *Int J Coal Geol* 147–148:85–104
- Bokova EN (1953) Formation of methane during microbial degradation of oil. *Polev Prom Geokh* 2:25–27. (in Russian)
- Boreham CJ, Hope JM, Hartung-Kagi B (2001) Understanding source, distribution and preservation of Australian natural gas: a geochemical perspective. *APPEA J* 41:523–547
- Colosimo F, Thomas R, Lloyd JR, Taylor KG, Boothman C, Smith AD, Lord R, Kalin RM (2016) Biogenic methane in shale gas and coal bed methane: a review of current knowledge and gaps. *Int J Coal Geol* 165:106–120
- Dolfing J, Larter SR, Head IM (2008) Thermodynamic constraints on methanogenic crude oil biodegradation. *ISME J* 2:442–452
- Ekzerceva VA (1960) Formation of methane by microorganisms in oil fields. *Geokhimiya* 1:362–370. (in Russian)
- Etiopie G, Feyzullayev A, Milkov AV, Waseda A, Mizobe K, Sun CH (2009) Evidence of subsurface anaerobic biodegradation of hydrocarbons and potential secondary methanogenesis in terrestrial mud volcanoes. *Mar Pet Geol* 26:1692–1703
- Feisthauer S, Siegert M, Seidel M, Richnow HH, Zengler K, Gründger F, Krüger M (2010) Isotopic fingerprinting of methane and CO₂ formation from aliphatic and aromatic hydrocarbons. *Org Geochem* 41:482–490
- Guo H, Yu Z, Liu R, Zhang H, Zhong Q, Xiong Z (2012) Methylotrophic methanogenesis governs the biogenic coal bed methane formation in Eastern Ordos Basin, China. *Appl Microbiol Biotechnol* 96:1587–1597
- Head IM, Jones M, Larter S (2003) Biological activity in the deep subsurface and the origin of heavy oil. *Nature* 426:344–352
- James AT, Burns BJ (1984) Microbial alteration of subsurface natural gas accumulations. *AAPG Bull* 68:957–960

- Jones DM, Head IM, Gray ND, Adams JJ, Rowan AK, Aitken CM, Bennett B, Huang H, Brown A, Bowler BFJ, Oldenburg T, Erdmann M, Larter SR (2008) Crude-oil biodegradation via methanogenesis in subsurface petroleum reservoirs. *Nature* 451:176–180
- Katz B, Narimanov A, Huseinzadeh R (2002) Significance of microbial processes in gases of the South Caspian basin. *Mar Pet Geol* 19:783–796
- Larter SR, Head IM, Huang H, Bennett B, Jones M, Aplin AC, Murray A, Erdmann M, Wilhelms A, di Primio R (2005) Biodegradation, gas destruction and methane generation in deep subsurface petroleum reservoirs: an overview. In: Dore AG, Vining B (eds) *Petroleum geology: Northwest Europe and global perspectives: proceedings of the 6th petroleum geology conference*. Geological Society, London, pp 633–640
- Lillis PG, Warden A, Claypool GE, Magoon LB (2007) Petroleum systems of the San Joaquin basin province – geochemical characteristics of gas types. In: Hosford Scheirer A (ed) *Petroleum systems and geologic assessment of oil and gas in the San Joaquin Basin Province, California*. US Geological Survey professional paper, vol 1713. Energy Resources Program, U.S. Geological Survey, Reston
- Martini AM, Walter LM, Ku TCW, Budai JM, McIntosh JC, Schoell M (2003) Microbial production and modification of gases in sedimentary basins: a geochemical case study from a Devonian shale gas play, Michigan basin. *AAPG Bull* 87:1355–1375
- Mathur N (2017) Origin, maturity and biodegradation of natural gases from Upper Assam basin, India. *J Appl Geochem* 19:1–20
- McIntosh JC, Walter LM, Martini AM (2002) Pleistocene recharge to midcontinent basins: effects on salinity structure and microbial gas generation. *Geochim Cosmochim Acta* 66:1681–1700
- Meslé M, Dromart G, Oger P (2013) Microbial methanogenesis in subsurface oil and coal. *Res Microbiol* 164:959–972
- Milkov AV (2010) Methanogenic biodegradation of petroleum in the West Siberian basin (Russia): significance for formation of giant Cenomanian gas pools. *AAPG Bull* 94:1485–1541
- Milkov AV (2011) Worldwide distribution and significance of secondary microbial methane formed during petroleum biodegradation in conventional reservoirs. *Org Geochem* 42:184–207
- Milkov AV, Goebel E, Dzou L, Fisher DA, Kutch A, McCaslin N, Bergman D (2007) Compartmentalization and time-lapse geochemical reservoir surveillance of the Horn Mountain oil field, deep-water Gulf of Mexico. *AAPG Bull* 91:847–876
- Pallasser RJ (2000) Recognising biodegradation in gas/oil accumulations through the $\delta^{13}\text{C}$ compositions of gas components. *Org Geochem* 31:1363–1373
- Rice DD, Claypool GE (1981) Generation accumulation and resource potential of biogenic gas. *AAPG Bull* 65:5–25
- Roadifer RE (1987) Size distributions of the world's largest known oil and tar accumulations. In: Meyer RF (ed) *Exploration for heavy crude oil and natural bitumen*. AAPG studies in geology, vol 25. American Association of Petroleum Geologists, Tulsa, pp 3–23
- Sassen R, Sweet ST, DeFreitas DA, Morelos JA, Milkov AV (2001) Gas hydrate and crude oil from the Mississippi Fan Foldbelt, downdip Gulf of Mexico Salt Basin: significance to petroleum system. *Org Geochem* 32:999–1008
- Scott AR, Kaiser WR, Ayers WB Jr (1994) Thermogenic and secondary biogenic gases, San Juan Basin, Colorado and New Mexico – implications for coalbed gas producibility. *AAPG Bull* 78:1186–1209
- Štrápoč D (2017) Biogenic methane. In: White WM (ed) *Encyclopedia of geochemistry: a comprehensive reference source on the chemistry of the earth*. Springer International Publishing. https://doi.org/10.1007/978-3-319-39193-9_166-1
- Tassi F, Fiebig J, Vaselli O, Nocentini M (2012) Origins of methane discharging from volcanic-hydrothermal, geothermal and cold emissions in Italy. *Chem Geol* 310–311:36–48
- Zeikus JG (1977) The biology of methanogenic bacteria. *Bacteriol Rev* 41:514–541
- Zengler K, Richnow HH, Rossello-Mora R, Michaelis W, Widdel F (1999) Methane formation from long-chain alkanes by anaerobic microorganisms. *Nature* 401:266–269



Geological, Geochemical, and Microbial Factors Affecting Coalbed Methane

23

Curtis Evans, Karen Budwill, and Michael J. Whiticar

Contents

1	Introduction	624
2	Geology of Coal and CBM	626
2.1	Characterization and Classification of Coal	627
2.2	Coal as a CBM Reservoir	628
2.3	Geochemical Factors of CBM: Stable Isotope Analysis	630
3	Microbial Ecology of Coalbeds	632
3.1	Overview of Anaerobic Degradation of Organic Matter	632
3.2	Microbial Ecology of Deep Coalbeds	633
3.3	Microbial Coal Bioconversion Pathways	637
4	Field Trial Applications of Enhanced Biogenic CBM	639
5	Future Research	641
6	Cross-References	642
	References	642

C. Evans (✉)

School of Earth and Ocean Sciences, University of Victoria, Victoria, BC, Canada
e-mail: c2evans@uvic.ca

K. Budwill

Processing Technologies, InnoTech Alberta, Edmonton, AB, Canada
e-mail: Karen.Budwill@innotechalberta.ca

M. J. Whiticar

Biogeochemistry Facility (BF-SEOS), School of Earth and Ocean Sciences, University of Victoria, Victoria, BC, Canada

Hanse-Wissenschaftskolleg, HWK (Institute for Advanced Study), Delmenhorst, Germany
e-mail: whiticar@uvic.ca

© Crown 2020

623

H. Wilkes (ed.), *Hydrocarbons, Oils and Lipids: Diversity, Origin, Chemistry and Fate*,
Handbook of Hydrocarbon and Lipid Microbiology,
https://doi.org/10.1007/978-3-319-90569-3_21

Abstract

Coalbed methane (CBM) is an unconventional resource for natural gas production. Years of research have clearly demonstrated that, in addition to thermogenically produced CBM, microorganisms indigenous to the coal seams are capable of converting some of the hydrocarbon portion of the coal to methane. CBM production is, therefore, not only dependent on the types of microbes present and their metabolic activities but also on the physicochemical properties of the coal itself, such as depositional environments and history and chemical makeup. Understanding the geological, geochemical, and microbial factors affecting CBM formation can lead to the development of effective processes to enhance methane production rates and yields.

1 Introduction

Coalbed methane (CBM, also natural gas from coal/NGC, or coal seam gas/CSG) is natural gas inherently from and dependent on coal (after Flores 1998; Golding et al. 2010). Coal is more fully characterized than CBM itself, as coal is the source substrate for both thermogenic and microbial or biological gas generation of CBM. Coal is defined as a sedimentary rock, usually black, with more than fifty percent (50%) by weight organic matter (Hatch and Affolter 2002; AER 2014a), but often with mineral matter between 5 and 15 percent (5%–15% MM). In common parlance, the simpler phrase “Coal is a usually black rock that burns and is used for fuel” is often an adequate definition of coal, but the microscopic details of coal as a hydrocarbon substrate for biological activity can be extremely complex (Van Krevelen 1961; Levine et al. 1982; Thomas 2013). The generation and release of CBM is dependent on that complexity to some degree, but it also can be simplified as the common natural processes of microbial alteration/degradation, burial/compaction, heating/coalification (the chemical and physical devolatilization of organic material by pressure, temperature, and biological processes, Tissot and Welte 1984), and flexure/cleaving, affecting organic matter to generate and release predominantly methane irrespective of the complexity of most coals. Definitions are key to understanding, and this paper, contrary to common industry use of the term biogenic (meaning sourced from “organic activity”), uses biogenic meaning “sourced from organic matter.” As all coal, except the ash component, is organic matter, all CBM is biogenic even when it is generated by heating (e.g., thermogenic subcategory that is separate from microbial).

All coals inherently have methane present to some degree, by adsorption and/or absorption – two words with very similar in spelling but very different process. The general concept is that **abs**orption has methane molecules strongly bound inside the lattice of complex hydrocarbons that forms the base structure of coal and **ad**sorption is where methane molecules are weakly bound to the surface of the hydrocarbon molecules – **ab**sorbed methane is usually not produced in commercial gas

production – the process of extracting CBM as adsorped gas is described in numerous articles (Ertekin et al. 1991; SPE 1992; Crossdale et al. 1998; Seidle 2011). Storage of natural gas in similar fashion to CBM can also be found in shaley coals and coaly shales (Lancaster 1996), but the changes to methane composition and isotopes in shales can be very different (Golding et al. 2013).

Coal is also a source for other commodities and by-products of coal extraction as discussed in a previous volume of this series (Kirby et al. 2010; Hüßers and Werner 2010; Meckenstock et al. 2010), and coal is sourced from depositional environments related to soils, wetlands, and peat deposits (Kotsyurbenko 2010), with the chemistry of the coal dependent on the peat chemistry (Spackman et al. 1988; Swaine 1990), which can be very complicated (Speight 1983). This review will include concepts that the original vegetation-derived organic matter is affected by shifting from aerobic processes to anaerobic processes with different time scales and possible reoccurrences of the different processes.

In situ coal gasification (ISCG, or underground coal gasification, UCG, Friedmann et al. 2009) and in situ coal-to-liquids (ICTL) may appear to be similar to CBM, but ISCG is a human-triggered thermal conversion process that would necessarily destroy the habitat and life patterns for microbes in coal as a partial oxidation process. ISCG is the induced pyrolysis of coal at depth in the original stratigraphic and geological structure without disturbing the strata other than by drilling injection and production wells (Bhutto et al. 2013; Klimenko 2009; Blinderman et al. 2008). Some studies have determined a new form of ISCG may be by induced microbial methanogenesis (Senthamaraiikkannan et al. 2016) as low temperature conversion of coal to liquids or gases – this has not been extensively field tested and is described below. Many jurisdictions clearly differentiate between the more passive CBM production as gas removal and the pyrolyzed coals and cavities due to ISCG (ERCB 2007; AER 2014b; Swanhills Synfuels 2017), but there has been no need to define enhanced microbial CBM or ISCG. At this time, not very much is known about the pyrolysis effects of ISCG on the microbial communities within or adjacent to the coals.

CBM has many years of production testing and analysis (Rightmire et al. 1984; Nelson et al. 2000; NEB 2007; Clarkson 2009, etc.) which is derived from analysis to determine the cause of coalmine explosion and fire events from firedamp (methane) and coal dust (Kissell et al. 1973; McCulloch et al. 1975).

The chemical analysis of coal has long history back before the 1900s, but it was usually by distillation or solvent extraction. Oxidation studies after 1925 focused on altering the benzenoid aromatic structures (Van Krevelen 1961; Speight 1983; Stranges 1997) to manufacture various synthetic drugs, dyes, plastics, solvents, etc. (Schulz 1999). Biological changes to in situ coal molecular structure have relatively little research other than recent studies described for CBM here (e.g., Stephen et al. 2014). This chapter will focus on the geological, geochemical, and microbial characteristics of coal seams that affect thermogenic versus biogenic or secondary coalbed methane production. Also, there is some description of how these characteristics can be manipulated to enhance microbial production of CBM.

2 Geology of Coal and CBM

Coal is a sedimentary rock preserved in sedimentary basins and one of the largest occurrences of hydrocarbons on this planet (Fig. 1b – WCI 2009; IEA 2012, 2016; BP 2017) with widely scattered deposits (Fig. 1a – Landis and Weaver 1993). The mechanics of excavating coal from the ground (as mining) and the chemistry of burning it for heat energy have been moderately well studied for hundreds of years (Eavenson 1939; Van Krevelen 1961; Chironis 1978; Nielsen and Richardson 1982; Peters 1991; Singh 1997; WCI 2009; IEA 2013). Even the comparatively novel and less used process of coal-to-liquids (CTL) is over 70 years old (Fischer and Tropsch 1926, 1930; Schulz 1999; Stranges 2007; SASOL 2017).

The production of CBM as natural gas from coal seams is relatively new in comparison (Rightmire et al. 1984; Dawson 1995; Law and Rice 1993) and started from degassing wells in advance of underground mining in the 1970s (Kissell et al. 1973; McCulloch et al. 1975; Rightmire et al. 1984; Ryan and Dawson 1994; Flores 1998). The development of gas production technology and resource determination separate from any plans for mining in very deep seams started as an incentive resulting from the OPEC energy crisis of the 1970s (Rightmire et al. 1984; Zuber 1998) with many programs focusing on the development of the resource, especially in the USA (Rightmire et al. 1984) and less so in other countries. Commercial production of CBM is now common in many sedimentary basins (Schraufnagel and McBane 1994).

Most sedimentary basins have coal deposits of some degree, and those are well documented as resources (WCI 2009; IEA 2012; Landis and Weaver 1993). As CBM is hosted by a sedimentary rock (coal), it is often in geological contact with other sedimentary rocks, and the coal is considered to be a possible source for methane in those strata if they have reservoir properties. Sedimentary basins have been well studied in the exploration for petroleum resources (Tissot and Welte 1984) including burial and thermal maturity (Rashid 1985; Curiale and Curtis 2016) in addition to how the basins are eroded or unroofed (Hacquebard and Donaldson 1970; Hood et al. 1975). The burial of a basin takes organic material through diagenesis for biogenic methane, catagenesis for oil, and metagenesis for

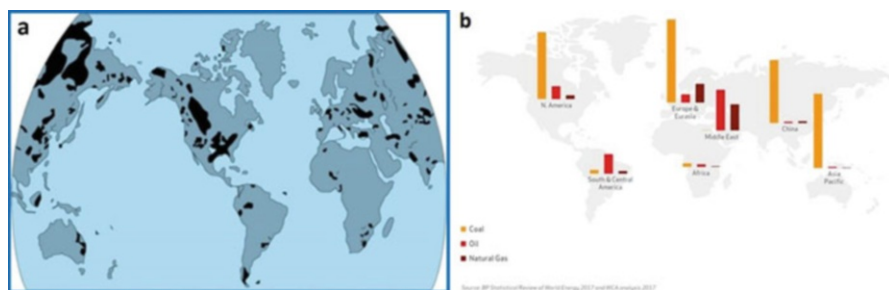


Fig. 1 (a) and (b) World coal distribution on land (Bhutto et al. 2013 figure 1) and world coal/oil/gas reserves (million tonnes oil equivalent) as framework for CBM resources (WCI <https://www.worldcoal.org/coal/where-coal-found> Last accessed August 2017)

thermogenic methane (Rashid 1985, Curiale and Curtis 2016). This history for each stratum in each basin affects the process of CBM (Mariño et al. 2015) as some basins have not been taken to a level of thermal maturity where CBM is generated by thermogenic process, thus biogenic gas is the primary form of CBM (Peck 1999; Ayers 2000; Clarkson 2009). The methane in the Powder River Basin is sourced almost completely from biological activity (Peck 1999; Formolo et al. 2008).

Other basins (IEA 2008, 2009, Johnson and Flores 1998) have had a large amount of thermogenic gas generation, but biogenic gas results may be overprinting due to a combination of flushing of the biogenic older gases and more recent biogenic influx. Depending on the basin configuration, some coals are saturated with water and form aquifers (e.g., Nelson et al. 2000; Ayers 2002; Li et al. 2015), while other coals are “dry” and do not have very much water content on a regional basis (e.g., “dry CBM” as NEB 2007, Clarkson 2009) and there is a direct effect on the coal microbiology. Some examples have later meteoric water input to the basin that change the biological activity (Riese et al. 2005), and there can be large cross-formational water exchange (Salmachi and Karacan 2017). Differences between basins have been shown as large, widespread, gently subsiding basins on the margins of stable cratons, with simple geothermal histories (e.g., Western Canada Sedimentary Basin, Gulf Coast, USA, Bowen in Australia, etc.), to isolated, structural basins that have created a dropped block of geological basement, usually in a rifting situation, that quickly fills with sediment and retains groundwater (Long 1981; Fralick and Schenk 1981; Johnson and Flores 1998). Rift environments can be subject to complex thermal histories, structural interactions, differential uplift and erosion, and volcanic or plutonic intrusions (e.g., Stellarton (Nova Scotia), Hat Creek (British Columbia), Tintina (British Columbia), Chehalis (Washington), Mount Diablo (California), Cook Inlet (Alaska), Majuba (de Oliveira and Cawthorn 1999 – South Africa), etc.). Further aspects of coal forming in sedimentary basins, other than the oceanic basins, can depend on the issues of transgression and regression of depositional environments where sequence stratigraphy analysis has coal deposition generally at maximum flooding surfaces (Catuneanu 2003, 2006). Other results indicate that coal can be preserved during extensive subaerial exposure in elevated ponding locations as sea level is dropping (Cohen et al. 1984). Sequence stratigraphy also shows that isolated parcels of terrigenous coal bearing sediments can be encapsulated in either dominantly marine environments (regression/transgression cycles – Bhattacharya 1988, Rahmani and Smith 1988) or alluvial deposits (falling stage systems tracts) either by clastic hiatus or reworking (Long 1981; Catuneanu 2003; Coe 2005).

2.1 Characterization and Classification of Coal

Coal is a “. . . variety of plant tissues in different states of preservation. . .” (Tissot and Welte 1984). To use a simpler statement: “Coal is formed by plant material that is more difficult to rot.” Just as there are different components of plants (wood, leaves, bark, resins, etc.), those components get preserved in coal as different macerals (e.g., vitrinite, exinite, tellinite, resinite, Stach et al. 1982, Thomas 2013, ICCP 1993), where macerals are to coals as minerals are to rocks (Swaine 1990). From this

concept, a complication is the varying degrees of biological or oxidizing alteration of the original plant materials before they are preserved as macerals in the coal (Speight 1983): low levels of alteration leads to preservation of the original structure of the plant material. This is opposed to high levels of alteration, where there is only a gel-like organic material remaining (biological degradation) or charcoal (oxidizing degradation) preserved (Stach et al. 1982). Also, the structure of plants has changed over geological time with more recent flowering plants in the Tertiary era having more complex structure than the early plants of the Devonian age (Fortney 1997). The spectrum of plant materials and spectrum of alteration processes result in a classification of hundreds of macerals (ICCP 1993) that can serve to identify the source plant material (in some cases) and the processes active during coal deposition (Van Krevelen 1961; Speight 1983; Swaine 1990; ICCP 1993).

Most coals are deposited in terrestrial low-productivity/stressed environments in coastal areas (Tissot and Welte 1984), lily pad marshes (Cohen et al. 1984), raised mires (Page et al. 2006), and very rarely in marine locations (Tissot and Welte 1984). By their very nature, depositional environments are highly stressed for the plants growing there, and the biodiversity is reduced in many cases (Wust and Bustin 2003). Often, the less ash in the coal and the more isolated from sediment input, the more stressed the biological environment and thus the microbial activity is low. Heavy plant growth in complex upland ecosystems is not usually associated with coal depositional environments as decomposition often occurs as quickly as growth (Tissot and Welte 1984). Coal is not preserved where an open aerobic system as a non-stressed environment is efficiently recycling the organic material by microbial activity.

As coal deposition is often in anaerobic aqueous environments, there are usually high amounts of organic acids present. There is often a strong profile of changing microbes with water depth as reflecting a shift from oxidizing to reducing conditions (Tissot and Welte 1984). This may change with groundwater recharge over time. The initial conditions usually favor one side of the redox conditions of microbial activity (Humez et al. 2016). Understanding the types of macerals present and the depositional history can provide clues as to how susceptible the coal in a given formation is to microbial biodegradation activities. Some of this will be touched in the following sections; however, much more research is required to fully understand the linkages between coal physicochemical properties, geological history and propensity for microbial CBM production, migration, or even conversion to other compounds.

2.2 Coal as a CBM Reservoir

The description of coal in the other chapters of the previous volume (Kirby et al. 2010) is further elaborated here to show the dependency of CBM on the complexity of coal. A consistent layer of coal at a scale where it can be correlated and possibly mined is called a “seam.” A coal seam can be composed of many plies of different macerals, often between a centimeter and a millimeter thick. CBM is quantified by six main factors: (1) rank, (2) composition, (3) quality, (4) thickness, (5) thermal history, and (6) depth (Dawson et al. 2000). Some of the early estimates of CBM potential completely discounted biological gas generation (Rightmire et al. 1984) or

drastically underestimated the volume produced (Dawson et al. 2000). The six factors are expanded as:

1. Rank is the degree of varying pressure and/or heat that a coal has been subjected to, ranging from low-rank peat at low temperature and shallow depths to lignite to bituminous to high-rank anthracite with major changes in composition along a consistent progression. The majority of coals have a normal correlation between pressure and temperature. The units of coal rank are often the reflectance of vitrinite particles in the coal (R_o), but other tests such as proximate analysis can indicate the rank as the degree of heating, and pressure has large effects on the volatile matter, moisture, and fixed carbon – as rank increases, the first two are reduced and the third one is increased. Those percentages are often used as a surrogate for vitrinite reflectance but can have some variation from usual assumptions. Thermal processes do not create methane until the coal is heated to bituminous rank. Microbial processes actively form methane from coal from low rank at deposition well into the bituminous rank (Strapoć et al. 2011).
2. The composition of a coal is what the primary organic compounds are after humification and is usually determined by petrology as many forms of macerals have been defined (ICCP 1993). The original plant fragments can be difficult to determine in higher-rank coals as the diagnostic fabric of the maceral can be erased. Plant material with large degrees of pre-coal alteration is often preserved only as featureless gel macerals (Tissot and Welte 1984). Macerals in the vitrain/clarain groups are generally sourced from woody/leafy plant materials and form the brighter bands or plies in coal seams with the highest amounts of volatile compounds. Macerals in the fusain/durain groups are dull and are related to oxidized/fungal/degraded material and form dull bands or plies. Macerals that have been subjected to various types of oxidation, including combustion, before, during, or after deposition of the coal often have a charcoal texture, and there is often very little volatile matter remaining.
3. Coal quality is usually measured by the specific tests used in the mining industry over hundreds of years. One indication of coal quality is the percentage and type of sulfur present in the coal. This is often a good indicator of some depositional environments and geological age of the coals. The other measure of coal quality is the ash content (usually a rough parallel to mineral matter), and it generally has very little effect on rank but can affect the type of gas storage such as clay mineral adsorption instead of hydrocarbon adsorption.
4. Thickness is a basic reservoir description to constrain the lithological limits of the coal and determine a volume of similar characteristics.
5. Thermal history is the time series of how the rank was achieved as there may have been different episodes, rates, and durations of heating due to changes in burial, intrusion, unroofing, movements of fluids, etc. Some geological settings exist where a high heat gradient and low pressure create coals of unique character and also where a low heat gradient but great depth of burial means high pressure can create very different coals.
6. Depth is related to relative permeability, in addition to rank and thermal history, as many coals have natural bidirectional fracturing called cleat, but only below certain lithostatic pressure limits. At depths greater than the equivalent to that

pressure limit, the coal tends to behave in a plastic manner with noticeable closure of the permeability and often deformation into wellbores.

All of these factors except for thickness have direct relationships to and from the microbial activity present in the strata. Examples include early aerobic microbial humification of one portion of a depositional environment having very different structure and CBM content compared to a contiguous part of the same environment where only anaerobic processes occurred. Another example is the change in fractures (known as cleats) as a coal is moved from depths greater than 1200 m to shallow depths by erosion of overlaying strata and the increased permeability of the coal allows groundwater in that either brings nutrients for dormant microbes or minerals to deposit in the cleat. Methane can also be released by fugitive emissions from coal seams during CBM dewatering (Etiopo and Klusman 2010).

2.3 Geochemical Factors of CBM: Stable Isotope Analysis

This section is included to elaborate on previous descriptions (Pearson 2010; Whiticar 2017). Stable isotopes of carbon ($^{13}\text{C}/^{12}\text{C}$) and hydrogen ($^2\text{H}/^1\text{H}$, ^2H is also known as deuterium, D) are used to estimate age, thermal history, maturity, stratigraphic correlation, depositional environment, source kerogens, biogenic limits, biodegradation, migration pathways, and mixing of natural gases (Whiticar 1996; Vlad 2010; Tilley and Muehlenbachs 2013; Golding et al. 2013). Microbial methanogenesis can complicate stable isotope results (Zumberge et al. 2009, 2012; Tilley et al. 2011), but they can also be used to determine the type of methanogenic pathways (Vinson et al. 2017 – see next section for description of the types of methanogenic pathways). Indeed, according to Niemann and Whiticar (2017), “The stable carbon isotope ratios of coalbed methane (CBM) demonstrate diagnostic changes that systematically vary with production and desorption times.” Nitrogen and oxygen isotopes are not often reported in evaluating CBM as they are minor components in the natural gas component and subject to atmospheric contamination (Golding et al. 2013).

Dissolved inorganic carbon in the ocean (DIC) is the main factor creating separation between carbonate ^{13}C isotopic ratios ($\delta^{13}\text{C}$) and organic $\delta^{13}\text{C}$ and that separation is known for different eras of geological time. The atmospheric CO_2 is also a factor as it is generally $\delta^{13}\text{C} = -8\text{‰}$ compared to DIC $\delta^{13}\text{C}$. Terrestrial plants derive carbon from the air, and further isotope fractionation occurs as the CO_2 is transferred into the plant in addition, according to Whiticar (1996), to “. . . the enzymatic fixation of carbon during photosynthesis.” As most coals are sourced from terrestrial Calvin cycle plants and not marine organic carbon, the common isotopic $\delta^{13}\text{C}$ is between -25‰ and -27‰ with very limited ranges. The procedures and detection limits are very well documented (Jochmann and Schmidt 2012).

Plant materials in the atmosphere usually decompose by aerobic biological oxidation to either 1- CO_2 in the atmosphere or 2-DIC in water. Sulfate reduction is strong in marine systems and limited in freshwater systems, so any anaerobic freshwater environments quickly accumulate organic matter. If there is biological action on the anoxic accumulation of organic matter, it is fermentation by

methanogens to methane with large isotope effects resulting in $\delta^{13}\text{C}$ of -50‰ to -112‰ (Whiticar 1999). Maceral types can have different isotope signatures (Whiticar 1996), but CBM is predominantly sourced from brighter macerals (Chalmers and Bustin 2007) such as vitrinite and liptinite.

Production of CBM affects the isotope signatures of the produced gases (Fig. 2a – Niemann and Whiticar 2017) which plot distinctly on a CD cross-plot (Fig. 3 Niemann and Whiticar 2017, after Whiticar 1990). Tests done on samples of coal as they desorb in a controlled environment showed a reversed effect (Fig. 2b – Niemann and Whiticar 2017).

Generally, radiogenic isotopes are either not present in CBM by its very nature or the half-life of the applicable isotope, ^{14}C , is far shorter than the residence of the gas in the reservoir. The only time when ^{14}C is functional in gas studies is when injected gases are spiked with a geochemical tracer to study gas pathways (e.g., Matter et al. 2011).

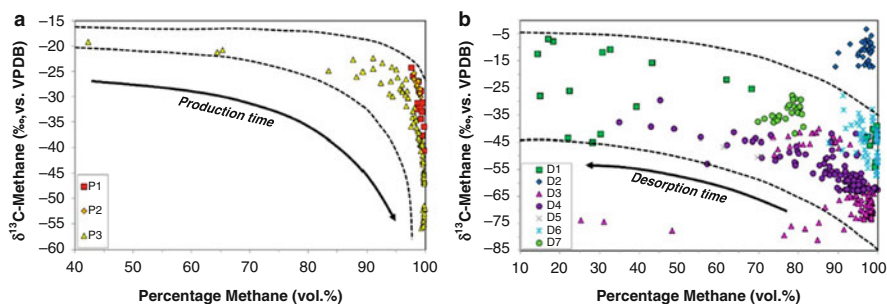
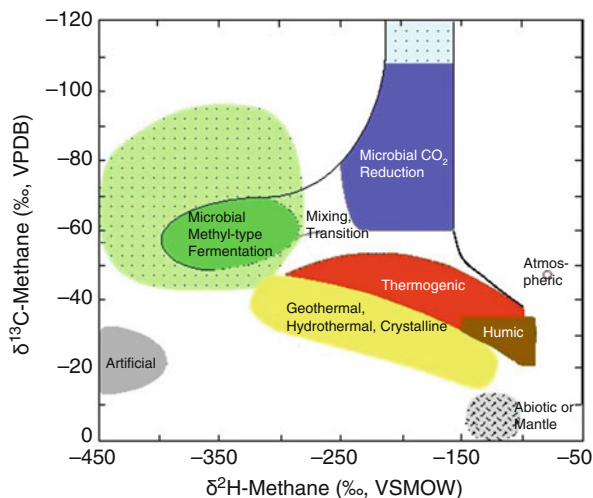


Fig. 2 (a) and (b) Time series plot of production gas composition and $\delta^{13}\text{C}$. (From Niemann and Whiticar 2017)

Fig. 3 CD (carbon/deuterium) cross-plot of methane $\delta^2\text{H}$ and $\delta^{13}\text{C}$ ratios. (After Whiticar 1993)



3 Microbial Ecology of Coalbeds

Biogenic CBM is classified as either of primary or secondary origin. Microbes involved in the initial degradation and coalification of peat and other plant precursors of coal are believed to have been sterilized during geological burial due to increased pressures and temperatures (above 80–100 °C). It is only after uplift of the coal seams and the influx of meteoric waters from shallower environments that coal seams became re-inoculated with bacterial and archaeal species (Strapóć et al. 2011; Barnhart et al. 2016). Over time and with sufficient reduction in the redox potential, as well as continued, but slow, recharge of coal seams with water, secondary biological gas generation occurred. The vast majority of the biogenic methane detected in coalbeds is of secondary production. Primary biogenic methane is being produced in only a few coal seams where insufficient burial occurred and thus the microbial community was not sterilized.

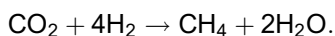
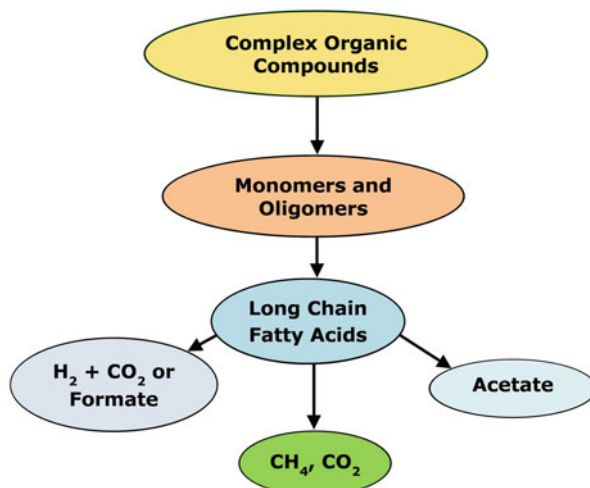
There are still unknowns about secondary biogenic CBM production, such as microbial residence time, their age (i.e., when were the coalbeds initially re-inoculated), and microbial growth rates. However, over the last decade, great strides in our understanding of the microbial ecology of deep coal seams were made and are summarized in this section.

3.1 Overview of Anaerobic Degradation of Organic Matter

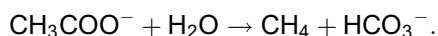
It is well established that biogenic methane is the result of complex biochemical reactions by groups of microorganisms during the decomposition of organic matter in anoxic environments (for an overview, see Formolo 2010). An often diverse and complex microbial assemblage exists consisting of different groups of microorganisms closely related trophically and co-dependent on each other (Kotsyurbenko 2005). Briefly, organic matter in the subsurface is degraded in a stepwise fashion, so that the metabolic products of some microorganisms serve as substrates for the other microorganisms (Fig. 4).

Polymers are degraded by hydrolytic microorganisms with the production of monomeric compounds, particularly carbohydrates. The latter serve as substrates for primary fermentative anaerobic bacteria, which produce hydrogen and various volatile fatty acids. The fatty acids are further utilized by syntrophic, acetogenic bacteria with the formation of acetate and hydrogen. The hydrogen is concurrently consumed by another group of microorganisms, the methanogens, to very low residual concentrations that provide for the thermodynamically favorable conditions for syntrophic reactions. Methanogens, a group of strictly anaerobic microorganisms belonging to the archaea and requiring reducing environments (redox levels $E_h < -200$ mV) for growth, produce methane as the final product during microbial methanogenesis (Zinder 1993, 1998). Methanogenic substrates are limited to CO_2 , formate, CO, methanol, acetate, and butyrate. The most common substrates are CO_2 and acetate. Hydrogenotrophic methanogens use a CO_2 reduction pathway to produce methane:

Fig. 4 Schematic flow diagram of anaerobic degradation of complex organic matter. (Adapted from Faiz and Hendry 2006; Zinder 1993, 1998)



Acetotrophic or acetoclastic methanogens cleave acetate to CO_2 plus CH_4 :



Because of their specific substrate requirements, methanogens would not grow without being trophically related to the bacteria of the previous stages. Thus, the anaerobic community represents a biological system that is balanced by the coordinated interactions of the constituent microbial groups (Kotsyurbenko 2005).

3.2 Microbial Ecology of Deep Coalbeds

With the rapid development of molecular microbiological methods over the past couple of decades, limitations to our understanding of the microbial ecology in diverse environments have been greatly reduced and a great wealth of information about the phylogenetic and functional diversity contained within microbial communities has been obtained (Hazen et al. 2013). Molecular microbiological methods typically include taxonomic sequencing (i.e., SSU rRNA sequencing), metagenomics, and metatranscriptomics. The combined application of these methods can link organism abundance and activity with physicochemical properties of their environment (Chourey et al. 2013) and, in the case for deep coal seams, can provide valuable information for the understanding of biogenic methane production mechanisms as well as for their manipulation and control in situ.

Metagenomics is the study of genetic material directly recovered from an environment (Youngblood et al. 2014). DNA is linked with genes that are associated to microbial taxonomy and function and allows the characterization of the microbial community as it exists in nature (Youngblood et al. 2014). Metagenomes are thus highly predictive of the metabolic potential within an ecosystem (Smith et al. 2013). While it provides information on the possible activities of a microbial community, metagenomics cannot reveal activities at a specific time and place or how those activities change in response to environmental forces or biotic interactions (Moran 2009).

In contrast to metagenomics, metatranscriptomics studies and correlates the transcriptome of a group of interacting organisms. Transcriptomes are the complete set of messenger RNA (mRNA) molecules (transcripts) produced in a cell or a population of cells and represent the enzymes and metabolic activities expressed by genes. Thus, metatranscriptomics analyses can allow a greater picture of microbial activities and functions that are occurring at a particular time. There are still technical challenges with extracting mRNA that can lead to low yields of expressed gene sequences which have impeded its wide-scale application to environmental samples (Moran 2009).

Despite some inherent limitations and biases with molecular microbiological methods (for review, see Hazen et al. 2013), these methods, in particular taxonomic sequencing, have been used by a number of research groups to characterize the microbial assemblage of produced water and coal samples from coal basins around the world (for review, see Colosimo et al. 2016 and for examples Shimizu et al. 2007, Green et al. 2008, Midgley et al. 2010, Singh et al. 2012, Tang et al. 2012, Guo et al. 2012, Wei et al. 2013, and Barnhart et al. 2016).

The majority of the samples that have been analyzed have been single-point samples and thus may not fully represent the entire coal seam or capture any fluctuations in microbial community structure due to perturbations to the coal seam (e.g., CBM production, groundwater recharge). However, several trends can be teased out of the taxonomic data presented in the literature.

Firstly, it is apparent that the in situ bacterial community is usually much more diverse than the archaeal community. In fact, some researchers report being unable to amplify archaeal DNA, indicating the archaea and thus methanogens were below detection limits (Barnhart et al. 2016), possibly from low population numbers.

Within the bacterial communities characterized, the most frequently occurring phyla are *Proteobacteria*, *Firmicutes*, *Bacteroidetes*, and *Actinobacteria* (Ritter et al. 2015; Colosimo et al. 2016). The *Proteobacteria* consist of a diverse group of bacteria. In general, the classes *Alphaproteobacteria*, *Betaproteobacteria*, *Gammaproteobacteria*, and *Deltaproteobacteria* have all been detected in different relative abundance in coal seams around the world. Some *Alphaproteobacteria* are capable of polyaromatic hydrocarbon (PAH) degradation, and PAHs are the main organic compound class detected in CBM-produced water samples. Several groups of *Betaproteobacteria* are aerobic or facultative bacteria that are highly versatile in their biodegradation capabilities. The *Deltaproteobacteria* contain the strictly anaerobic sulfate-reducing bacteria as well as *Geobacter* sp. which is known to syntrophically

degrade aromatics and long-chain fatty acids coupled to reduction of Fe(III) as a terminal electron acceptor. The *Gammaproteobacteria* are a large heterogeneous class, containing among others denitrifying toluene-degrading strains.

Taxonomic sequencing of coal and produced water samples has often revealed the presence of sulfate-reducing bacteria (SRB) and methanogens (Ritter et al. 2015). While SSU rRNA sequencing cannot distinguish whether the identified microbes are active or viable or non-active/nonviable, it is counterintuitive to find both SRB and methanogens present in the same sample based on previous studies on the competition between these groups of microbes for substrates (Muyzer and Stams 2008). Indeed, it was concluded from an isotopic study on the dissolved inorganic carbon in the Illinois Basin that methanogenesis occurred after sulfate reduction. Rather than geochemical zones in sediments dictating which process will occur, geological time was the main factor influencing sulfate reduction before microbial methanogenesis (Glossner et al. 2016). However, a recent study by Glossner et al. (2016) concluded that SRB and methanogens can coexist together. Their relationship and whether one dominates over the other in activity are dependent not on the sulfate concentration but on the acetate concentration supplied through the metabolic activities of fermentative bacteria. The authors concluded that sulfate reduction and microbial methanogenesis in coalbeds depend on the presence of low acetate and sulfate concentration (less than 1000 μM) together with metabolically active SRB and methanogens.

The phylum *Firmicutes* consists mainly of fermenting and acetogenic bacteria. Interestingly they are usually only minor components of the in situ microbial community but flourish in laboratory microcosm enrichment cultures, especially when nutrients are added to stimulate methane production. *Clostridia* are *Firmicutes* commonly found in coalbeds and coal enrichment cultures. These spore-forming, anaerobic bacteria are pH-neutral solvent producers, mixed acid and alcohol producers, and homoacetogenic fermenters. They can also depolymerize starch, chitin, xylan, and cellulose.

Bacteria belonging to the *Bacteroidetes* are found in sediments and are chemoorganoheterotrophs, known to degrade proteins, chitin, pectin, agar, starch, or cellulose. The *Actinobacteria* are a common phylum found in soil and sediments, involved in the decomposition of organic matter. Many members possess the ability to degrade cellulose and hydrocarbons in aerobic environments.

Of the archaeal communities detected, the dominant group has been the methanogens. In some coal basins, *Methanosarcina* (capable of acetogenic and hydrogenotrophic methanogenesis) dominated, whereas in other coal basins, those methanogens capable of strictly hydrogenotrophic methanogenesis, such as *Methanosaeta*, dominated. In one study, *Methanosaeta* was found in the coal sample, while *Methanosarcina* was found in the water sample taken from the same well site (Wei et al. 2013).

A large comparative analysis of SSU rRNA sequences from coal cuttings, coal cores, and produced water from the three main CBM plays in the Alberta Basin in Western Canada clearly showed the assembly of coal microbial communities were shaped by habitat-specific environmental conditions (Lawson et al. 2015). These

conditions included coal rank, depth-dependent physicochemical conditions (such as salinity, temperature, pH), and hydrogeological conditions. Despite different community compositions found in the three different coal plays, they all contained the right groups required for the transformation of coal into methane. For example, specific microbes previously implicated in aromatic compound degradation, fermentation, and methanogenesis affiliated with *Thauera*, *Streptococcus*, and *Methanosarcina* were found in subbituminous coals. Microbes with similar functional potentials affiliated with uncultured *Rhodobacteraceae*, *Pelobacter*, and *Methanosarcina* were detected in volatile bituminous coals (Fig. 5).

Comparative analysis of the data from the Lawson et al. (2015) study suggests successional patterns occur in coalbeds, just as it does in landfills, but on longer time scales. Vick et al. (2016) also suggest successional changes in abundance of several microbial community members during colonization of coal disks (i.e., biofilm formation) under anaerobic conditions.

An interesting, but contradictory, observation has arisen from the taxonomic studies; a prevalence of aerobic genera were detected in what has traditionally been assumed to be an anaerobic environment (An et al. 2013; Lawson et al. 2015; Barnhart et al. 2016). A metagenomic analysis of a volatile bituminous coal sample revealed the dominance of *Rhodobacteraceae*, represented by a *Celeribacter* species (Lawson et al. 2015). This species is known to exhibit both autotrophic and heterotrophic growth, as well as chemolithotrophy via oxidation reactions using CO₂ as a catalyst. The genomic analysis of this organism also revealed encoded pathways for acidogenic fermentation (products of which are primary substrates for microbial

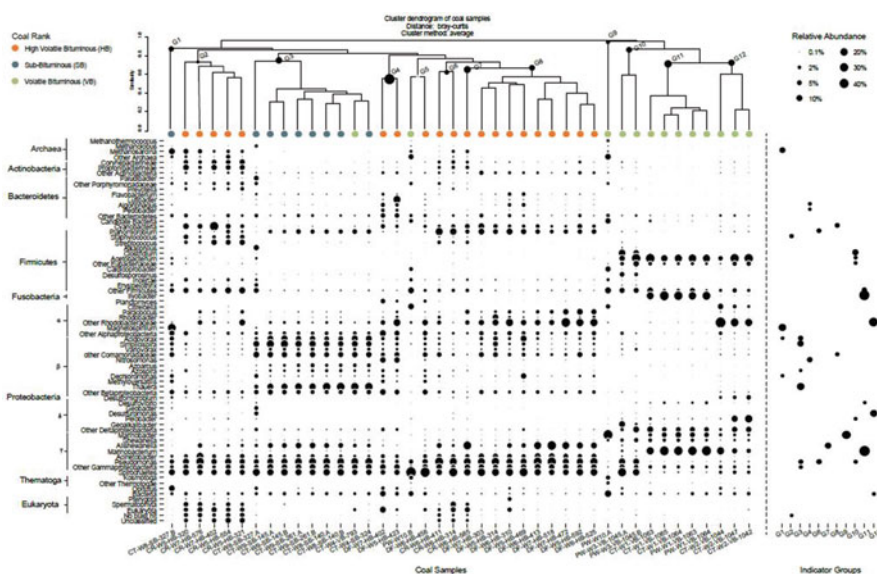


Fig. 5 Microbial community structure and indicator taxa for coalbed samples collected from three different coal zones in Alberta, Canada. For details, see Lawson et al. (2015)

methanogenesis), which would allow this organism to survive under both aerobic and anaerobic conditions. A versatile energy metabolism would be advantageous for life close to fluctuating aerobic-anaerobic interfaces that experience variable nutrient availabilities. Hydrogeological investigation of Alberta coal seams has shown the possibility of mixing of fluids from lower more saline aquifers that may carry dissolved oxygen. *Celeribacter* sp. also has the genomic potential to degrade and utilize a diverse range of aromatic compounds, such as benzoate, salicylate, and vanillate (all by-products of coal and lignin degradation).

It was proposed by Lawson et al. (2015) that exposure of *Celeribacter* sp. to aerobic-anaerobic cycling may actually promote the biodegradation of coal to methane. During aerobic conditions, *Celeribacter* sp. would degrade aromatic compounds for biomass synthesis and glycogen storage. During anaerobic conditions, the accumulated glycogen would be fermented via acidogenic fermentation pathways resulting in the formation of by-products for methanogenesis. The genomics analysis showed genes for nitrogen and carbohydrate catabolism indicating the ability to rapidly assimilate and degrade carbohydrates or organic acids that periodically become available in coalbed environments. Scavenged carbohydrate or organic acid compounds could also provide fermentation substrates for *Celeribacter* sp. under anaerobic conditions and thus stimulate methane production. Therefore, nitrogen availability and the ability to utilize diverse organic substrates may be potential drivers of selection in deep coalbeds.

In a study by Barnhart et al. (2016), coal from different depths as well as adjacent sand and silt stones were collected from a well site in the Powder River Basin, USA. *Aeribacillus*, commonly thought to be an aerobic microorganism, was found throughout the vertical sampling profile, but especially near the upper interface near the sandstone overburden. Biosurfactant-producing *Actinobacteria* were also detected in the coal at the interface near the overlying sandstone where *Aeribacillus* also dominated and methane production was the greatest. Results suggest bacteria capable of producing biosurfactants exist in coalbeds and the production of biosurfactants may play an important role in the bioavailability of coal. As well, living close to a coal:sandstone interface may allow greater exposure to aerobic conditions with the slow influx of O₂-bearing meteoric water, thus allowing growth of these bacteria (An et al. 2013).

3.3 Microbial Coal Bioconversion Pathways

Mechanisms of coal activation under anaerobic conditions are still not well understood. There have been studies that measured the chemical makeup of produced water samples from coal seams. As well, controlled microcosm studies in the laboratory have revealed some potential coal breakdown pathways that may be occurring in situ. From these studies, inferred activation sites and pathways have been proposed.

In general, the organic fraction of coalbed-produced water is a complex mixture of aromatic and aliphatic hydrocarbons, polycyclic aromatic hydrocarbons (PAHs),

as well as nitrogen-, sulfur-, and oxygen-containing – often heterocyclic – compounds (NSO compounds) (Colosimo et al. 2016). Simple alkyl-substituted aromatic hydrocarbons are more readily degraded under anaerobic conditions than unsubstituted aromatics. Biodegradation studies with unsubstituted aromatic hydrocarbons have been carried out mostly with benzene and naphthalene under sulfate-reducing conditions (Meckenstock et al. 2004). The activation of these compounds/mechanisms included the addition of a CO₂-derived carboxyl group (benzene carboxylase, naphthalene carboxylase). Aliphatics are unreactive compounds containing only apolar σ -bonds. The most common activation of aliphatics is the addition of the hydrocarbon to fumarate yielding alkylsuccinates (Rabus et al. 2016). The biodegradation of aliphatic and cyclic hydrocarbons can be a source of metabolites (fatty acids) that can be further oxidized to methanogenic substrates. The accumulation of fatty acids, however, could cause inhibition of methanogenesis due to the lowering of pH. PAHs are commonly found in coal formation waters. While PAH degradation under aerobic conditions has been well documented (Ghosal et al. 2016), many prokaryotes are capable of mineralizing PAHs under anaerobic conditions, particularly in methanogenic consortia syntrophy making biodegradation of PAHs thermodynamically favorable (Berdugo-Clavijo et al. 2012). As well, many bacteria will produce biosurfactants to solubilize PHAs (Bezza and Chirwa 2016). NSO compounds can undergo selective degradation process similar to the mechanisms of activation of hydrocarbons. NSO compounds of similar molecular weight are often more soluble in water than PAHs and therefore also more bioavailable (Colosimo et al. 2016).

In summary, microbial interactions with organic matter include biological depyritization, solubilization (by biological alkaline materials), and biological chelation, and the main pathways for coal activation are speculated to be addition to fumarate, hydroxylation, C₁ addition/carboxylation, and methylation.

An omics approach to understanding bioconversion of coal was performed by Tan et al. (2014). The metatranscriptome of coal enrichment cultures amended with the nutrient tryptone was compared to the metatranscriptome of the same cultures grown with only tryptone and no coal. Results showed similar transcripts encoding for cellulases, carboxylesterases, and thioesterases in both sets of cultures. These enzymes are involved in the modification of complex lignocelluloses and hydroxyl-, amine-, and thio-functional groups and were highly expressed in both sets. This suggests tryptone may have indirectly enhanced coal degradation by stimulating production of hydrolytic enzymes for utilization of nutrients. However, in the coal transcripts, there was strong evidence for hydroxylation (aromatic acid hydroxylases, extradiol oxygenase) and carboxylation activity (putative benzene carboxylases). These transcripts were less prominent in the nutrient-only transcriptome. Transcripts encoding methanogenesis via methanol and methylamine were enriched only in the coal transcriptome suggesting that the metabolism of coal produced substrates for methylotrophic methanogens. Taxonomic analysis showed the coal cultures were highly enriched with *Peptococcaceae* (*Firmicutes*), *Bacteroidetes*, and *Sphingobacteriales*.

The study by Tan et al. (2014) shows the power of metatranscriptomics to provide greater information about enzymes and metabolic pathways involved in the

bioconversion of coal to methane. It was used successfully on coal enrichment cultures where a large biomass could be generated to provide sufficient quantities of RNA required for the sequencing. The generally low in situ biomass of coals could be problematic in the use of metatranscriptomics directly from coal samples, unless enhancements in the extraction and amplification techniques occur.

4 Field Trial Applications of Enhanced Biogenic CBM

During the period of high natural gas prices in North America in the 2000s, interest in extending the life of CBM operations by enhancing biogenic coalbed methane was great. Indeed, several companies such as Luca Technologies, Ciris Energy, and Next Fuel (all based close to the Powder River Basin in Wyoming/Montana, USA) were formed to develop stimulated CBM methanogenesis technologies for commercial applications. These companies reportedly conducted field trials, although limited data on the trials are available in the public domain. In general, the technologies developed by different companies and researchers in the laboratory and field trialed to enhance biogenic methane production can be divided into four categories: (1) stimulating indigenous microbes (Fig. 6), (2) augmenting coal seam with non-indigenous microbes, (3) enhancing microbial access to coal through physical

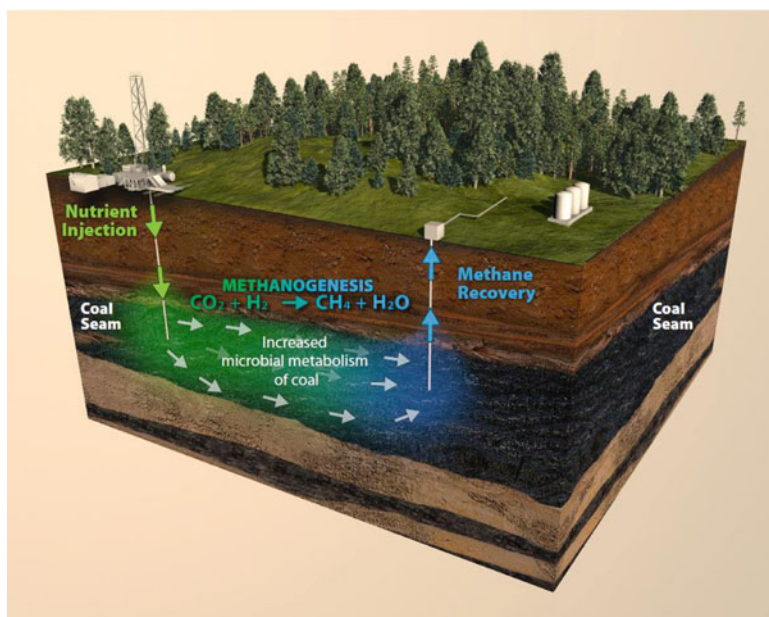


Fig. 6 Schematic diagram of stimulated biogenic coalbed methane operations with nutrient injection (diagram courtesy from InnoTech Alberta). Hydrogenotrophic methanogenesis is shown as occurring, though acetoclastic methanogenesis can also occur

means and ensuring deep distribution of amendments, and (4) increasing the bio-availability of coal organics (Ritter et al. 2015).

It should be pointed out that one must take caution in translating laboratory data to the field as laboratory cultures are in an optimum or ideal state. The experimental growth studies are often operated in batch mode. Unlike the field, there are no fluxes of water, nutrients, waste products, and microbes in and out of the growth vessel as would occur in the subsurface. In the field, reactions are much more complicated. Essentially, the enhanced biogenic CBM technology deals with the reactive transport of a reactant gas (dissolved or not), microbes, and nutrients in a subsurface environment that has multiphases and a product whose fate and transport are significantly different than its parent. In addition, that subsurface environment will be modified by the microbial activity.

Subsurface environments are often low in nutrients required by microbes for accelerated growth and division. Microbes require essential macro-elements, such as nitrogen and phosphorus; micro-elements, such as Zn, B, and Co and vitamins; and growth factors, such as amino acids, purines, and pyrimidines (Madigan et al. 2017). Buffers (e.g., carbonates) are required to maintain a pH balance within the microorganism's tolerance range. In some geological formations, microorganisms are nutrient depleted and in a dormant state (Amy 1997). Microorganisms may endure multiple nutrient deprivations and may attempt to store scavenged nutrients until such a time that they have sufficient resources to grow and divide. To ensure high activity and economical methane yields, it may be necessary, depending on the environmental conditions of the coal seam, to add nutrients such as nitrogen- and phosphorous-containing compounds, micronutrients, and vitamins. Often, undefined nutrients such as yeast extract have been used to target the organisms actually degrading the coal. If these organisms are stimulated, then by-products from their metabolic activities can be used for methanogenesis. Stimulation of indigenous microbes with nutrient amendments (Fig. 6) is by far the preferred process by commercial biogenic CBM companies (Ritter et al. 2015).

The transport of the nutrients into the coal seam as far as possible is of crucial importance to the overall success of the field trial. The target coal seam's environment, such as water content, and degree of fractures and permeability should also be taken into consideration on how best to administer the nutrients. The nutrient solution can be injected continuously for an extended period of time or pulsed. One option to introduce the nutrients is to mix the nutrient solution with a fracturing solution and fracturing the seam so that the nutrients are placed throughout the fracture length.

In some cases, however, coal seams may not harbor any microorganisms or only inactive microorganisms in unsustainable low numbers, and thus microbial augmentation is needed. Microbial augmentation is the process of adding new, nonnative microorganisms (as single strains or a consortium of different microorganisms) to the coal seam (Colosimo et al. 2016). This process has many inherent risks, the main ones being poor survivability of the introduced microorganism(s) in the new environment and poor distribution into the seam away from the injection well, causing possible fouling problems around the well. This might require further modifications

to the coal seam such as adjusting the salinity driving up costs. A major hurdle in injection of nonnative microorganisms into a coal seam is obtaining the regulatory permissions to do so.

Making sure the microbes in the coal seam get maximum access to coal surface area is another process that could increase bioconversion rates and methane yields. Often coal pore spaces are too small for microbes (Pant et al. 2015). There are different ways to increase pore space such as hydrofracturing the coal and dissolving the coal with solutions. This method is often more effective when done in conjunction with nutrient supplementation or augmentation.

The last process is to increase the bioavailability of coal organics. Coal is a complex structure containing many recalcitrant compounds. Often the rate-limiting step in the bioconversion of coal to methane is the breaking down of coal into intermediate compounds. Some researchers have used solvents, alcohols, esters of phosphoric acid, surfactants, and biosurfactants (Liu et al. 2013). Chemicals tested included potassium permanganate or hydrogen peroxide (Huang et al. 2013). The limitations to this process are the following:

Added costs to the overall technology.

Poor control over reactions.

The chemicals and solvents added may be harmful to the microbes or chemicals could migrate into the groundwater system and contaminate it.

5 Future Research

Recent reviews on microbial CBM agree that more research is required to fully understand the microbial ecology of coal seams (Ritter et al. 2015; Park and Liang 2016). As was shown in An et al. (2013) and Lawson et al. (2015), microbial community compositions are highly modified by local geochemical factors and physical properties of the coal seam. Therefore, different microorganisms undertaking the initial and critical first step of coal activation exist in different coal seams. Despite these variances in microbial diversity, similar enzymatic mechanisms and intermediate formation and utilization pathways would likely be present in the coal seams. Understanding the commonalities of microbial community structure and function during coal biodegradation, and the subsequent shifts and changes in key microbial players and metabolic pathways, would allow the development of targeted processes to enhance biogenic methane production that could also be deployed to multiple coal formations.

There is a need for greater understanding on coal availability for bioconversion as there is limited knowledge of what fraction of coal is actually bioavailable and which constituents are recalcitrant or through physical, chemical, or biological manipulation can be made more bioavailable (Furmann et al. 2013). Enhancing bioavailability and reactivity of coal would ultimately lead to greater biogenic CBM production (Huang et al. 2013). Testing any alteration or manipulation processes for environmental impacts (e.g., contamination of groundwater) is paramount.

Nutrient amendment is by far the most popular process to stimulate biological methane production (Ritter et al. 2015; Colosimo et al. 2016). A large body of research on effects of nutrient amendment on microbial growth and methane production exists; however, descriptions of methods or processes for delivering the nutrient or nutrients to the coal seam are lacking. In addition to delivery methods, injection rates, durations, and application cycles to ensure continuous microbial stimulation have only been tested for a few field trials for which the methodology and results are not always available to the public. Monitoring tools, such as stable isotope analysis, need to be optimized and validated (Vinson et al. 2017). Certainly, being able to distinguish between relic and contemporary methane is critical to measure the success of an enhanced microbial CBM field application. Conventional CBM production may have environmental impacts, and the identification of the gas sources is very relevant (Vinson et al. 2017).

There are research and development opportunities to apply the technology developed for enhanced microbial CBM to other unconventional gas resources such as shale gas (Cokar et al. 2013) or for residual oil in depleted conventional oil reservoirs (Gieg et al. 2008). A possible new application is to stimulate biological methane production in shallow legacy coal mines (PTAC 2017). Such mines would provide the large surface area conducive to microbial growth on coal and could also serve as large underground methane bioreactors with the addition of waste organic material as microbial nutrients. Finally, microbial cultures enriched from coal and produced water samples and used for laboratory studies on biogenic CBM production could be mined for novel enzymes and pathways for biotechnological applications (Strachan et al. 2014).

6 Cross-References

- ▶ Oil and Gas Shales
- ▶ The Biogeochemical Methane Cycle

References

- AER (Alberta Energy Regulator) (2014a) ST98-2014: Alberta's energy reserves 2013 and supply/demand outlook 2014–2023. <http://aer.ca/documents/sts/ST98/ST98-2014.pdf> [chapter 8]
- AER (Alberta Energy Regulator) (2014b) Swan Hills Synfuels Ltd Well Blowout October 10, 2011: AER Investigation Report. <http://www.aer.ca/documents/reports/IR-20140225-Synfuels.pdf>
- Amy PS (1997) Microbial dormancy and survival in the subsurface. In: Amy PS, Haldeman DL (eds) *The microbiology of the terrestrial deep subsurface*. CRC Lewis Publishers, pp 185–203. ISBN: 978-0849383625
- An D, Caffrey SM, Soh J, Abu Laban N, Agrawal A, Brown D, Budwill K, Dong X, Dunfield PF, Foght J, Gieg L, Hallam S, He Z, Jack T, Klassen J, Larter S, Leopatra V, Nelson W, Nesbø CL, Oldenburg T, Page A, Ramos-Padron E, Rochman F, Saidi-Mehrabad A, Sensen CW, Tamas I, Tan BF, Wilson S, Wolbring G, Wong ML, Voordouw G (2013) Metagenomic of hydrocarbon resource environments indicates aerobic taxa and genes to be unexpectedly common. *Environ Sci Technol* 47:10708–10717. <https://doi.org/10.1021/es4020184>

- Ayers WB (2000) Methane production from thermally immature coal, fort union formation, Powder River Basin. AAPG annual meeting, New Orleans. <http://www.searchanddiscovery.com/abstracts/html/2000/annual/abstracts/0032.htm>
- Ayers WB (2002) Coalbed gas systems, resources, and production and a review of contrasting cases from the San Juan and Powder River basins. AAPG Bull 86(11):1853–1890. WOS:000178870400002
- Barnhart EP, Weeks EP, Jones EJP, Ritter DJ, McIntosh JC, Clark AC, Ruppert LF, Cunningham AB, Vinson DS, Orem W, Fields MW (2016) Hydrogeochemistry and coal-associated bacterial populations from a methanogenic coal bed. Int J Coal Geol 162:14–26. <https://doi.org/10.1016/j.coal.2016.05.001>
- Berdugo-Clavijo C, Dong X, Soh J, Senson CW, Gieg LM (2012) Methanogenic biodegradation of two-ringed polycyclic aromatic hydrocarbons. FEMS Microbiol Ecol 81(1):124–133
- Bezza FA, Chirwa EM (2016) Biosurfactant-enhanced bioremediation of aged polycyclic aromatic hydrocarbons (PAHs) in creosote contaminated soil. Chemosphere 144:635–644
- Bhattacharya J (1988) Autocyclic and allocyclic sequences in river- and wave-dominated deltaic sediments of the upper cretaceous, Dunvegan formation, Alberta: core examples. In: James DP, Leckie DA (eds) Sequences, stratigraphy, sedimentology: surface and subsurface. CSPG proceedings. ISBN: 978-0-920230-60-1
- Bhutto AW, Bazmi AA, Zahedi G (2013) Underground coal gasification: from fundamentals to applications. Prog Energy Combust Sci 39(1):189–214. <https://doi.org/10.1016/j.pecs.2012.09.004>
- Blinderman MS, Saulov DN, Klimenko AY (2008) Forward and reverse combustion linking in underground coal gasification. Energy 33(3):446–454. <https://doi.org/10.1016/j.energy.2007.10.004>
- BP (British Petroleum) (2017) Statistical review of world energy. <http://www.bp.com/content/dam/bp/pdf/energy-economics/statistical-review-2016/bp-statistical-review-of-world-energy-2016-full-report.pdf> or <http://www.bp.com/en/global/corporate/energy-economics/statistical-review-of-world-energy/downloads.html> or https://en.wikipedia.org/wiki/Price_of_oil#/media/File:Crude_oil_prices_since_1861.png
- Catuneanu O (2003) Sequence stratigraphy of clastic systems. Geological Association of Canada short course notes, vol 16. ISBN: 978-0-919216-76-5
- Catuneanu O (2006) Principles of sequence stratigraphy. Elsevier. ISBN: 978-0-444-51568-1
- Chalmers GRL, Bustin RM (2007) On the effects of petrographic composition on coalbed methane sorption. Int J Coal Geol 69(4):288–304. <https://doi.org/10.1016/j.coal.2006.06.002>
- Chironis, N. P. (1978). Coal age operating handbook of coal surface mining and reclamation. ISBN: 978-0070114586
- Chourey K, Nissen S, Vishnivetskaya T, Shah M, Pfiffner S, Hettich RL, Löffler FE (2013) Environmental proteomics reveals early microbial community response to biostimulation at a uranium- and nitrate-contaminated site. Proteomics 13:2921–2930. <https://doi.org/10.1002/pmic.201300155>
- Clarkson CR (2009) Case study: production data and pressure transient analysis of horseshoe canyon CBM wells. JCPT 48(10):27–38. <https://doi.org/10.2118/114485-PA>
- Coe A (2005) The sedimentary record of sea-level change, 2nd edn. Open University. ISBN: 978-0-521-53842-8
- Cohen AD, Casagrande DJ, Andrejko MJ, Best GR (1984) The Okefenokee swamp: its natural history, geology, geochemistry. Wetland Surveys, Los Alamos
- Cokar M, Ford B, Gieg LM, Kallos MS, Gates ID (2013) Reactive reservoir simulation of biogenic shallow shale gas systems enabled by experimentally determined methane generation rates. Energy Fuels 27(5):2413–2421. <https://doi.org/10.1021/ef400616k>
- Colosimo F, Thomas R, Lloyd JR, Taylor KG, Boothman C, Smith AD, Lord R, Kalin RM (2016) Biogenic methane in shale gas and coal bed methane: a review of current knowledge and gaps. Int J Coal Geol 165:106–120. <https://doi.org/10.1016/j.coal.2016.08.011>
- Crossdale PJ, Beamish BB, Valix M (1998) Coalbed methane sorption related to coal composition. Int J Coal Geol 35:147–158. [https://doi.org/10.1016/S0166-5162\(97\)00015-3](https://doi.org/10.1016/S0166-5162(97)00015-3)
- Curiale JA, Curtis JB (2016) Organic geochemical applications to the exploration for source-rock reservoirs – a review. J Unconv Oil Gas Res 13:1–31. <https://doi.org/10.1016/j.juogr.2015.10.001>

- Dawson FM (1995) Coalbed methane: a comparison between Canada and the United States. GSC Bull 489. ISBN: 978-0-660-15753-5
- Dawson FM, Marchioni DL, Anderson TC, McDougall WJ (2000) An assessment of coalbed methane exploration projects in Canada. GSC Bull 549. ISBN: 978-0-660-17871-0
- de Oliveira DPS, Cawthorn RG (1999) Dolerite intrusion morphology at Majuba colliery, Northeast Karoo Basin, Republic of South Africa. *Int J Coal Geol* 41(4):333–349. [https://doi.org/10.1016/S0166-5162\(99\)00026-9](https://doi.org/10.1016/S0166-5162(99)00026-9)
- Eavenson HN (1939) Coal through the ages, 2nd edn. AIMME. <http://www.worldcat.org/title/coal-through-the-ages/oclc/2886601>
- EIA (US Energy Information Administration) (2016) International energy outlook. IEO2016. <https://www.eia.gov/outlooks/ieo/> [https://www.eia.gov/outlooks/ieo/pdf/0484\(2016\).pdf](https://www.eia.gov/outlooks/ieo/pdf/0484(2016).pdf)
- ERCB (Energy Resources Conservation Board) (2007) Coal conservation act <http://www.qp.alberta.ca/documents/Acts/c17.pdf> amendments for definition of ISCG/ISCL section 1(f.1), 1(f.2) and Oil and Gas Conservation Act <http://www.qp.alberta.ca/documents/Acts/O06.pdf> amendments for definition of ISCG/ISCL section 1(aa.01)
- Ertekin T, Sung W, Bilgesu HI (1991) Structural properties of coal that control Coalbed Methane Production. In: Peters DC (ed) *Geology in coal resource utilization*. ISBN:978-1-878907-22-0
- Etiopie G, Klusman RW (2010) Methane microseepage in drylands: soil is not always a CH₄ sink. *J Integr Environ Sci* 7(S1):31–38. <https://doi.org/10.1080/19438151003621359>
- Faiz M, Hendry P (2006) Significance of microbial activity in Australian coal bed methane reservoirs – a review. *BCPG* 54(3):261–272. <https://doi.org/10.2113/gscpgbull.54.3.261>
- Fischer F, Tropsch H (1926) Über die Reduktion des kohlenoxyds zu Methan am Eisenkontakt unter Druck. *Brennstoff-Chem* 7:97. <http://www.fischer-tropsch.org/>
- Fischer F, Tropsch H (1930) Über die Herstellung synthetischer Ölgemische (Synthol) durch Aufbau aus Kohlenoxyd und Wasserstoff. *Brennstoff-Chem* 11:489. <http://www.fischer-tropsch.org/>
- Flores R (1998) Coalbed methane: from hazard to resource. *Int J Coal Geol* 35:3–26. [https://doi.org/10.1016/S0166-5162\(97\)00043-8](https://doi.org/10.1016/S0166-5162(97)00043-8)
- Formolo M (2010) The microbial production of methane and other volatile hydrocarbons. In: Timmis K (ed) *Handbook of hydrocarbon and lipid microbiology*. ISBN: 978-3-540-77584-3 [chapter 6]
- Formolo M, Martini A, Petsch S (2008) Biodegradation of sedimentary organic matter associated with coalbed methane in the Powder River and San Juan basins. USA *Int J Coal Geol* 76(1–2):86–97. <https://doi.org/10.1016/j.coal.2008.03.005>
- Fortney R (1997) *Life: an unauthorized biography – a natural history of the first four billion years of life on earth*. HarperCollins. ISBN 978-0375401190
- Fralick PW, Schenk PE (1981) Molasse deposition and basin evolution in a wrench tectonic setting: the late Paleozoic, eastern Cumberland Basin, maritime Canada. In: Miall AD (ed) *Sedimentation and tectonics in alluvial basins*. GAC special paper 23. ISBN: 978-0-919216-19-6
- Friedmann SJ, Upadhye R, Kong FM (2009) Prospects for underground coal gasification in carbon-constrained world. *Energy Procedia* 1(1):4551–4557. GGCT 9. <https://doi.org/10.1016/j.egypro.2009.02.274>
- Furmann A, Schimmelmann A, Brassell SC, Mastalerz M, Picardel F (2013) Chemical compound classes supporting microbial methanogenesis in coal. *Chem Geol* 339:226–241. <https://doi.org/10.1016/j.chemgeo.2012.08.010>
- Ghosal D, Ghosh S, Dutta TK, Ahn Y (2016) Current state of knowledge in microbial degradation of p polycyclic aromatic hydrocarbons (PAHs): a review. *Front Microbiol*. <https://doi.org/10.3389/fmicb.2012.01369>
- Gieg LM, Duncan KE, Sufliata JM (2008) Bioenergy production via microbial conversion of residual oil to natural gas. *Appl Environ Microbiol* 74:3022–3029. <https://doi.org/10.1128/AEM.00119-08>
- Glossner AW, Gallagher LK, Landkamer L, Figueroa L, Munakata-Marr J, Mandernack KW (2016) Factors controlling the co-occurrence of microbial sulfate reduction and methanogenesis in coal bed reservoirs. *Int J Coal Geol* 165:121–132. <https://doi.org/10.1016/j.coal.2016.08.012>

- Golding SD, Rudolph V, Flores RM (2010) Asia Pacific coalbed methane symposium – selected papers from the 2008 Brisbane symposium on coalbed methane CO₂-enhanced coalbed methane. *Int J Coal Geol* 82(3–4):133–134. <https://doi.org/10.1016/j.coal.2010.02.003>
- Golding SD, Boreham CJ, Esterle JS (2013) Stable isotope geochemistry of coal bed and shale gas and related production waters: a review. *Int J Coal Geol* 120:24–40. <https://doi.org/10.1016/j.coal.2013.09.001>
- Green MS, Flanagan KC, Gilcrease PC (2008) Characterization of a methanogenic consortium enriched from a coalbed methane well in the Powder River Basin, U.S.A. *Int. J. Coal Geol* 76:34–45. <https://doi.org/10.1016/j.coal.2008.05.001>
- Guo H, Liu R, Yu A, Zhang H, Yun J, Li Y, Liu X, Pan J (2012) Pyrosequencing reveals the dominance of methylotrophic methanogenesis in a coal bed methane reservoir associated with Eastern Ordos Basin in China. *Int J Coal Geol* 93:56–61. <https://doi.org/10.1016/j.coal.2012.01.014>
- Hacquebard PA, Donaldson JR (1970) Coal metamorphism and hydrocarbon potential in upper Paleozoic of Atlantic provinces. *Can CJES* 7(4):1139–1163. <https://doi.org/10.1139/e70-108>
- Hatch JR, Affolter RH (2002) Resource assessment of the Springfield, Herrin, Danville, and Baker Coals in the Illinois Basin. U.S. Geological Survey Professional Paper 1625–D. <https://pubs.usgs.gov/pp/p1625d/> [chapter 3]
- Hazen TC, Rocha AM, Techtmann SM (2013) Advances in monitoring environmental microbes. *Curr Opin Biotechnol* 24:526–533. <https://doi.org/10.1016/j.copbio.2012.10.020>
- Hood A, Gutjahr CCM, Heacock RL (1975) Organic metamorphism and the generation of petroleum. *AAPG Bull* 59(6):986–996. WOS:A1975AE75400004
- Huang Z, Urynowicz MA, Colberg PJS (2013) Bioassay of chemically treated subbituminous coal derivatives using *Pseudomonas putida* F1. *Int J Coal Geol* 115:97–105. <https://doi.org/10.1016/j.coal.2013.01.012>
- Humez P, Mayer B, Nightingale M, Becker V, Kingston A, Taylor S, Bayegnak G, Millot R, Kloppmann W (2016) Redox controls on methane formation, migration and fate in shallow aquifers. *Hydrol Earth Syst Sci* 20(7):2759–2777. <https://doi.org/10.5194/hess-20-2759-2016>
- Hüser N, Werner P (2010) Coking processes and manufactured gas plants and their environmental impact on soil and groundwater. In: Timmis K (ed) *Handbook of hydrocarbon and lipid microbiology*. ISBN: 978-3-540-77584-3 [chapter 15]
- ICCP (International Committee for Coal and Organic Petrology) (1993) *The international handbook of coal petrography*. ISBN 978–84–617-5821-0. <http://www.iccop.org/?p=4212> or <http://www.iccop.org/publications/iccop-handbook/>
- IEA (International Energy Agency) (2008) *New trends in coalmine methane recovery and utilization*. International Energy Agency, Coal Industry Advisory Board Information Paper. https://www.iea.org/publications/freepublications/publication/methane_recovery.pdf
- IEA (International Energy Agency) (2009) *Coal mine methane in Russia: capturing the safety and environmental benefits*. International Energy Agency, Coal Industry Advisory Board Workshop report. https://www.iea.org/publications/freepublications/publication/cmm_russia.pdf
- IEA (International Energy Agency) (2012) *The Global Value of Coal*. International Energy Agency, Coal Industry Advisory Board report. https://www.iea.org/publications/insights/insightpublications/global_value_of_coal.pdf. See also <https://www.iea.org/publications/freepublications/publication/KeyCoalTrends.pdf> <http://www.iea.org/statistics/topics/coal/>
- IEA (International Energy Agency) (2013) *21st century coal: advanced technology and global energy solution*. International Energy Agency, Coal Industry Advisory Board report. https://www.iea.org/publications/insights/insightpublications/21stCenturyCoal_FINAL_WEB.pdf
- Jochmann MA, Schmidt TC (2012) *Compound specific stable isotope analysis*. RSC Publishing. ISBN: 978-1-84973-157-7
- Johnson RC, Flores RM (1998) Developmental geology of coalbed methane from shallow to deep in Rocky Mountain basins and in Cook Inlet Matanuska basin, Alaska. *USA Can Int J Coal Geol* 35(1–4):241–282. [https://doi.org/10.1016/S0166-5162\(97\)00016-5](https://doi.org/10.1016/S0166-5162(97)00016-5)
- Kirby BM, Vengadajellum CJ, Burton SG, Cowan DA (2010) Coal, coal mines and spoil heaps. In: Timmis K (ed) *Handbook of hydrocarbon and lipid microbiology*. ISBN: 978-3-540-77584-3 [chapter 49]

- Kissell FN, McCulloch CM, Elder CH (1973) The direct method of determining methane content of coalbeds for ventilation design. USBM Bureau of Mines Report of Investigations RI 7767. https://permanent.access.gpo.gov/lps97495/cdc_9220DS1.pdf
- Klimenko AY (2009) Early ideas in underground coal gasification and their evolution. *Energies* 2(2):456–476. <https://doi.org/10.3390/en20200456>
- Kotsyurbenko OR (2005) Trophic interactions in the methanogenic microbial community of low-temperature terrestrial ecosystems. *FEMS Microbiol Ecol* 53:3–13. <https://doi.org/10.1016/j.femsec.2004.12.009>
- Kotsyurbenko OR (2010) Soil, wetlands, peat. In: Timmis K (ed) *Handbook of hydrocarbon and lipid microbiology*. ISBN: 978-3-540-77584-3 [chapter 50]
- Lancaster DE (1996) Production from fractured shales. SPE reprint series, issue 45. ISBN: 978-1-55563-071-3. <http://store.spe.org/Production-From-Fractured-Shales-P52.aspx>
- Landis ER, Weaver TN (1993) Global coal occurrence. In: Law BE, Rice DD (eds) *Hydrocarbons from coal*. AAPG studies in geology, vol 38. <http://geoscienceworld.org/content/hydrocarbons-from-coal>
- Law BE, Rice DD (1993) Hydrocarbons from coal. *AAPG Stud Geol* 38. <http://geoscienceworld.org/content/hydrocarbons-from-coal>
- Lawson CE, Strachan CR, Williams DD, Koziel S, Hallam SJ, Budwill K (2015) Patterns of endemism and habitat selection in coalbed methane microbial communities. *Appl Environ Microbiol* 81:7924–7937. <https://doi.org/10.1128/AEM.01737-15>
- Levine DG, Schlosberg RH, Silbernagel BG (1982) Understanding the chemistry and physics of coal structure (a review). *PNAS* 79(10):3365–3370. <https://doi.org/10.1073/pnas.79.10.3365>
- Li Y, Tang D, Xu H, Elsworth D, Meng Y (2015) Geological and hydrological controls on water coproduced with coalbed methane in Liulin, eastern Ordos basin, China. *AAPG Bull* 99(2): 207–229. <https://doi.org/10.1306/07211413147>
- Liu Y, Urynowicz MA, Bagley DM (2013) Ethanol conversion to methane by a coal microbial community. *Int J Coal Geol* 115:85–91. <https://doi.org/10.1016/j.coal.2013.02.010>
- Long DGF (1981) Dextral strike slip faults in the Canadian cordillera and depositional environments of related fresh-water Intermontane coal basins. In: Miall AD (ed) *Sedimentation and tectonics in alluvial basins*. GAC special paper 23. ISBN: 978-0-919216-19-6
- Madigan MT, Martin JM, Parker J (2017) *Brock biology of microorganisms*. Prentice Hall. ISBN: 978-0134268668 [15th edition]
- Mariño J, Marshak S, Mastalerz M (2015) Evidence for stratigraphically controlled paleogeotherms in the Illinois Basin based on vitrinite-reflectance analysis: implications for interpreting coal-rank anomalies. *AAPG Bull* 99: 10: 1803–1825. <https://doi.org/10.1306/04151513001> or <http://archives.datapages.com/data/bulletns/2015/10oct/BLTN13001/BLTN13001.html>
- Matter JM, Broecker WS, Gislason SR, Gunnlaugsson E, Oelkers EH, Stute M, Sigurdardóttir H, Stefansson A, Alfreðsson HA, Aradóttir ES, Axelsson G, Sigfússon B, Wolff-Boenisch D (2011) The CarbFix pilot project – storing carbon dioxide in basalt. *Energy Procedia* 4:5579–5585. <https://doi.org/10.1016/j.egypro.2011.02.546>
- McCulloch CM, Levine JR, Kissell FN, Deul M (1975) Measuring the methane content of bituminous coalbeds. USBM Bureau of Mines Report of Investigations RI 8043. <https://permanent.access.gpo.gov/lps98148/ri8043.pdf>
- Meckenstock RU, Safinowski M, Gridder C (2004) Anaerobic degradation of polycyclic aromatic hydrocarbons. *FEMS Microbiol Ecol* 49(1):27–36
- Meckenstock RU, Lueders T, Griebler C, Selesi D (2010) Microbial hydrocarbon degradation at coal gasification plants. In: Timmis K (ed) *Handbook of hydrocarbon and lipid microbiology*. ISBN: 978-3-540-77584-3 [chapter 50]
- Midgley DJ, Hendry P, Pinetown KL, Fuentes D, Gong S, Mitchell DL, Faiz M (2010) Characterisation of a microbial community associated with a deep, coal seam methane reservoir in the Gippsland Basin. *Aust Int J Coal Geol* 82:232–239. <https://doi.org/10.1016/j.coal.2010.01.009>
- Moran MA (2009) Metatranscriptomics: eavesdropping on complex microbial communities. *Microbe Magazine* July Issue. American Society for Microbiology. <https://www.asm.org/ccLibraryFiles/FILENAME/000000005069/znw00709000329.pdf>

- Muyzer G, Stams AJM (2008) The ecology and biotechnology of sulphate-reducing bacteria. *Nat Rev Microbiol* 6:441–454. <https://doi.org/10.1038/nrmicro1892>
- NEB (National Energy Board of Canada) (2007) Overview and economics of horseshoe canyon coalbed methane development. <https://www.neb-one.gc.ca/nrg/sttstc/ntrlgs/rprtr/archive/hrsshcnynclbmdmthn2007/hrsshcnynclbmdmthn-eng.pdf>
- Nelson CR, Hill DG, Pratt TJ (2000) Properties of Paleocene fort union formation canyon seam coal at the triton Federal Coalbed Methane Well, Campbell County, Wyoming. SPE/CERI gas technology symposium, Calgary. SPE-59786-MS. <https://doi.org/10.2118/59786-MS>.
- Nielsen CV, Richardson GF (1982) Keystone coal industry manual. ISBN: 978-0076068258
- Niemann M, Whiticar MJ (2017) Stable isotope systematics of coalbed gas during desorption and production. *Geosciences* 7(43):1–21. <https://doi.org/10.3390/geosciences7020043>
- Page SE, Rieley JO, Wust R (2006) Lowland tropical peatlands of Southeast Asia. In: Martini IP, Cortizas AM, Chesworth W (eds) Peatlands: evolution and records of environmental and climate changes. *Developments in Earth surface processes*, vol 9, pp 145–172. [https://doi.org/10.1016/S0928-2025\(06\)09007-9](https://doi.org/10.1016/S0928-2025(06)09007-9)
- Pant LM, Huang H, Secanell M, Larter S, Mitra SK (2015) Multi scale characterization of coal structure for mass transport. *Fuel* 159:315–323. <https://doi.org/10.1016/j.fuel.2015.06.089>
- Park SY, Liang Y (2016) Biogenic methane production from coal: a review on recent research and development on microbially enhanced coalbed methane (MECBM). *Fuel* 166:258–267. <https://doi.org/10.1016/j.fuel.2015.10.121>
- Pearson A (2010) Pathways of carbon assimilation and their impact on organic Matter values $\delta^{13}\text{C}$. In: Timmis K (ed) *Handbook of hydrocarbon and lipid microbiology*. ISBN: 978-3-540-77584-3 [chapter 09]
- Peck C (1999) Review of coalbed methane development in the Powder River Basin of Wyoming/Montana. SPE Rocky Mountain regional meeting, Gillette. SPE-55801-MS. <https://doi.org/10.2118/55801-MS>
- Peters DC (1991) *Geology in coal resource utilization*. AAPG, EMD Techbooks. ISBN: 1-878907-22-0
- PTAC (Petroleum Technology Alliance Canada) (2017) Alternative use of legacy underground mines as energy infrastructure – Technology Roadmap Information Session. Presentation by New Paradigm Engineering, Calgary, 23 Mar 2017
- Rabus R, Boll M, Heider J, Meckenstock RU, Buckel W, Einsle O, Ermler U, Golding BT, Gunsalus RP, PMH K, Krüger M, Lueders T, Martins BM, Musat IF, Richnow HH, Schink B, Seifert J, Szalaniec M, Treude T, Ullmann M, Vogt C, von Bergen M, Wilkes H (2016) Anaerobic microbial degradation of hydrocarbons: from enzymatic reactions to the environment. *J Mol Microbiol Biotechnol* 26:5–28
- Rahmani RA, Smith DG (1988) The Cadotte member of Northwestern Alberta: a high-energy barred shoreline. In: James DP, Leckie DA (eds) *Sequences, stratigraphy, sedimentology: surface and subsurface*. CSPG proceedings. ISBN: 0-920230-60-1
- Rashid MA (1985) *Geochemistry of marine humic compounds*. Springer. ISBN:0-387-96135-6
- Riese WC, Pelzmann WL, Snyder GT (2005) New insights on the hydrocarbon system of the Fruitland Formation coal beds, northern San Juan Basin, Colorado and New Mexico, USA. In: Warwick PD (ed) *Coal systems analysis*. Geological Society of America special papers 387. ISBN: 978-0-8137-2387-7
- Rightmire CT, Eddy GE, Kirr JN (1984) Coalbed methane resources of the United States. AAPG studies in geology series, vol 17. ISBN:0-89181-023-4
- Ritter D, Vinson D, Barnhart E, Akob DM, Fields MW, Cunningham AB, Orem W, McIntosh J (2015) Enhanced microbial coalbed methane generation: a review of research, commercial activity, and remaining challenges. *Int J Coal Geol* 146:28–41. <https://doi.org/10.1016/j.coal.2015.04.013>
- Ryan BD, Dawson FM (1994) Coal and coalbed methane resource potential of the Bowser Basin, northern British-Columbia. *Energy Sources* 17(1):107–129. <https://doi.org/10.1080/00908319508946073>

- Salmachi A, Karacan CO (2017) Cross-formational flow of water into coalbed methane reservoirs: controls on relative permeability curve shape and production profile. *Environ Earth Sci* 76(5. A#: 200). <https://doi.org/10.1007/s12665-017-6505-0>
- SASOL (2017) Gas to liquids, technology. <http://www.sasol.com/innovation/gas-liquids/technology>. or <https://www.netl.doe.gov/research/coal/energy-systems/gasification/gasifiedia/sasol>. Last accessed May 2017
- Schraufnagel VA, McBane RA (1994) Coalbed methane – a decade of success. Society of Petroleum Engineers SPE-28581. <https://doi.org/10.2118/28581-MS>
- Schulz H (1999) Short history and present trends of Fischer–Tropsch synthesis. *Appl Catal A Gen* 186:3–12. [https://doi.org/10.1016/S0926-860X\(99\)00160-X](https://doi.org/10.1016/S0926-860X(99)00160-X)
- Seidle J (2011) Fundamentals of coalbed methane reservoir engineering. PennWell Books. ISBN: 978-1593700010
- Sentharamaikkannan G, Budwill K, Gates I, Mitra S, Prasad V (2016) Kinetic Modeling of the biogenic production of coalbed methane. *Energy and Fuels* 30(2):871–883. <https://doi.org/10.1021/acs.energyfuels.5b02450>
- Shimizu S, Akiyama M, Naganuma T, Fujioka M, Nako M, Ishijima Y (2007) Molecular characterization of microbial communities in deep coal seam groundwater of northern Japan. *Geobiology* 5:423–433. <https://doi.org/10.1111/j.1472-4669.2007.00123.x>
- Singh RD (1997) Principles and practices of modern coal mining. New Age Publications. ISBN: 81-224-0974-1
- Singh DN, Kumar A, Sarbhai MP, Tripathi AK (2012) Cultivation-independent analysis of archaeal and bacterial communities of the formation water in an Indian coal bed to enhance biotransformation of coal into methane. *Appl Microbiol Biotechnol* 93(3):1337–1350. <https://doi.org/10.1007/s00253-011-3778-1>
- Smith JR, Jeffries TC, Adetutu EM, Fairweather PG, Mitchell JG (2013) Determining the metabolic footprints of hydrocarbon degradation using multivariate analysis. *PLOS ONE* 8(11):e81910. <https://doi.org/10.1371/journal.pone.0081910>
- Spackman W, Ryan NJ, Rhoads CA, Given PH (1988) Studies of peat as the input to coalification II sampling sites and preliminary fractionation. *Int J Coal Geol* 9(3):253–265. [https://doi.org/10.1016/0166-5162\(88\)90016-X](https://doi.org/10.1016/0166-5162(88)90016-X)
- SPE (Society of Petroleum Engineers) (1992) Coalbed methane. SPE reprint series, Issue 35. ISBN: 978-1555630430
- Speight JG (1983) The chemistry and technology of coal. In: Heinemann H (ed) *Chemical industries*, vol 12. Marcel Dekker Inc, New York. ISBN: 0-8247-1915-8 TP325.S714
- Stach E, Mackowsky MT, Teichmüller M, Taylor GH, Chandra D, Teichmüller R, Murchison DG (1982) Stach's textbook of coal petrology, 3rd edn. <http://www.schweizerbart.de>. ISBN: 978-3-443-01018-8
- Stephen A, Adebusuyi A, Baldygin A, Shuster J, Southam G, Budwill K, Foght J, Nobes DS, Mitra SK (2014) Bioconversion of coal: new insights from a core flooding study. *RSC Adv* 4:22779–22791. <https://doi.org/10.1039/c4ra01628a>
- Strachan CR, Singh R, VanInsberghe D, Ierdokymenko K, Budwill K, Mohn WW, Eltis LD, Hallam SJ (2014) Metagenomic scaffolds enable combinatorial lignin transformation. *PNAS* 111(28): 10143–10148. <https://doi.org/10.1073/pnas.1401631111>
- Stranges AA (1997) Coal – chemistry encyclopedia. <http://www.chemistryexplained.com/Ce-Co/Coal.html>. Last accessed 17 May 2017
- Stranges AN (2007) A history of the Fischer–Tropsch synthesis in Germany 1926–45. In: Davis BH, Ocelli ML (eds) *Studies in surface science and catalysis: Fischer–Tropsch synthesis, catalysts and catalysis*. Elsevier. ISBN: 978-0-444-52221-4
- Strapoć D, Mastalerz M, Dawson K, Macalady J, Callaghan AV, Wawrik B, Turich C, Ashby M (2011) Biogeochemistry of microbial coal-bed methane. *Annu Rev Earth Planet Sci* 39:617–656. <https://doi.org/10.1146/annurev-earth-040610-133343>
- Swaine DJ (1990) Trace elements in coal. Butterworths. ISBN: 0-408-03309-6
- Swanhills Synfuels (2017) Gas manufacturing: overview. <http://swanhills-synfuels.com/gas-manufacturing/overview/>. Last accessed Aug 2017

- Tan B, Budwill K, Foght J (2014) Bioconversion and biomethanization of coal: an omics approach to bioprospecting for key microbes and genes (poster session abstracts for genomics: the power and the promise 2014). *Genome* 57:407. WOS:000345533100032
- Tang YQ, Ji P, Lai GL, Chi CQ, Liu ZS, Wu XL (2012) Diverse microbial community from the coalbeds of the Ordos Basin. *China Int J Coal Geol* 90–91:21–33. <https://doi.org/10.1016/j.coal.2011.09.009>
- Thomas L (2013) *Coal geology*, 2nd edn. Wiley. ISBN: 978-1119990444 [chapter 4]
- Tilley B, Muehlenbachs K (2013) Isotope reversals and universal stages and trends of gas maturation in sealed, self-contained petroleum systems. *Chem Geol* 339:194–204. <https://doi.org/10.1016/j.chemgeo.2012.08.002>
- Tilley B, McLellan S, Hiebert S, Quartero B, Veilleux B, Muehlenbachs K (2011) Gas isotope reversals in fractured gas reservoirs of the western Canadian foothills: mature shale gases in disguise. *AAPG Bull* 95:1399–1422. <http://archives.datapages.com/data/bulletns/2011/08aug/BLTN10103/BLTN10103.HTM>
- Tissot BP, Welte DH (1984) *Petroleum formation and occurrence*, 2nd edn. Springer, Berlin. ISBN: 0-387-13281-3
- Van Krevelen DW (1961) *Coal: typology – physics – chemistry – constitution*. Elsevier. ISBN: 978-0444406002
- Vick SHW, Tetu SG, Sherwood N, Pinetown K, Sestak S, Vallotton P, Elbourne LDH, Greenfield P, Johnson E, Barton D, Midgley DJ, Paulsen IT (2016) Revealing colonisation and biofilm formation of an adherent coal seam associated microbial community on a coal surface. *Int J Coal Geol* 160:42–50. <https://doi.org/10.1016/j.coal.2016.04.012>
- Vinson DS, Blair NE, Martini AM, Larter S, Orem WH, McIntosh JC (2017) Microbial methane from in situ biodegradation of coal and shale: a review and reevaluation of hydrogen and carbon isotope signatures. *Chem Geol* 453:128–145. <https://doi.org/10.1016/j.chemgeo.2017.01.027>
- Vlad D (2010) *Mudgases geochemistry and factors controlling their variability*. University of Alberta thesis. https://era.library.ualberta.ca/files/z890rv49v/Vlad_Daniela_Spring%202010.pdf
- WCI (World Coal Institute) (2009) *The coal resource: a comprehensive overview of coal*. [http://www.worldcoal.org/file_validate.php?file=coal_resource_overview_of_coal_report\(03_06_2009\).pdf](http://www.worldcoal.org/file_validate.php?file=coal_resource_overview_of_coal_report(03_06_2009).pdf)
- Wei M, Yu Z, Zhang H (2013) Microbial diversity and abundance in a representative small-production coal mine of Central China. *Energy Fuel* 27:3821–3829. <https://doi.org/10.1021/ef400529f>
- Whiticar MJ (1990) A geochemical perspective of natural-gas and atmospheric methane. *Org Geochem* 16(1–3):531–547. [https://doi.org/10.1016/0146-6380\(90\)90068-B](https://doi.org/10.1016/0146-6380(90)90068-B)
- Whiticar MJ (1993) Stable isotopes and global budgets. In: MAK K (ed) *Atmospheric methane: sources, sinks, and role in global change*. NATO ASI series (series I: global environmental change), vol 13. Springer, Berlin/Heidelberg. ISBN:978-3-642-84607-6. https://doi.org/10.1007/978-3-642-84605-2_8
- Whiticar MJ (1996) Stable isotope geochemistry of coals, humic kerogens and related natural gases. *Int J Coal Geol* 32(1–4):191–215. [https://doi.org/10.1016/S0166-5162\(96\)00042-0](https://doi.org/10.1016/S0166-5162(96)00042-0)
- Whiticar MJ (1999) Carbon and hydrogen isotope systematics of bacterial formation and oxidation of methane. *Chem Geol* 161(1–3):291–314. [https://doi.org/10.1016/S0009-2541\(99\)00092-3](https://doi.org/10.1016/S0009-2541(99)00092-3)
- Wust RAJ, Bustin RM (2003) Opaline and Al-Si phytoliths from a tropical mire system of West Malaysia: abundance, habit, elemental composition, preservation and significance. *Chem Geol* 200(3–4):267–292. [https://doi.org/10.1016/S0009-2541\(03\)00196-7](https://doi.org/10.1016/S0009-2541(03)00196-7)
- Youngblood J, Wallance J, Port J, Cullen A, Faustman E (2014) Metagenomic applications for environmental health surveillance: a one health case study from the Pacific Northwest ecosystem. *GRF Davos Planet@Risk Special Issue on One Health (Part II/II)* 2(4):281–285. <https://planet-risk.org/index.php/pr/article/view/106/233>
- Zinder SH (1993) Physiological ecology of methanogens. In: Ferry JG (ed) *Methanogenesis. ecology, physiology, biochemistry and genetics*. Chapman and Hall, New York, pp 128–206. <http://www.springer.com/gp/book/9780412035319>

- Zinder SH (1998) Methanogens. In: Burlage RS, Atlas RA, Stahl D, Geesey G, Saylor G (eds) *Techniques in microbial ecology*. Oxford University Press, New York, pp 113–134. ISBN: 978-0195092233
- Zuber MD (1998) Production characteristics and reservoir analysis of coalbed methane reservoirs. *Int J Coal Geol* 38:27–45. [https://doi.org/10.1016/S0166-5162\(98\)00031-7](https://doi.org/10.1016/S0166-5162(98)00031-7)
- Zumberge JE, Ferworm KA, Curtis JB (2009) Gas character anomalies found in highly productive shale gas wells. *Geochim Cosmochim Acta* 73:A1539. WOS:000267229903766
- Zumberge J, Ferworm K, Brown S (2012) Isotopic reversal ('rollover') in shale gases produced from the Mississippian Barnett and Fayetteville formations. *Mar Pet Geol* 31(1):43–52. <https://doi.org/10.1016/j.marpetgeo.2011.06.009>



Gas Hydrates as an Unconventional Hydrocarbon Resource

24

Klaus Wallmann and Judith Maria Schicks

Contents

1	Introduction	652
2	Methane Hydrate Formation in Marine Sediments	654
2.1	Thermodynamic Controls on Gas Hydrate Stability	654
2.2	Microbial Methane Formation	655
2.3	Methane Hydrate Formation in Marine Sediments	657
3	Gas Production from Hydrate-Bearing Sediments	661
4	Research Needs	664
	References	664

Abstract

Methane hydrates are formed in high-pressure and low-temperature environments such as the ocean floor and high-latitude permafrost deposits. At the molecular level, these icelike solids consist of water cages that contain methane molecules which are usually produced by the microbial decay of organic matter. The abundance of methane hydrates in sediments is controlled by temperature and pressure conditions, the rate of in situ microbial methane production, and the upward migration of dissolved and gaseous methane. The global inventory of methane-carbon in gas hydrates may be about 1000 Gt and exceeds the amount of methane in conventional gas reservoirs by about one order of magnitude. Successful field trials using different production techniques such as thermal

K. Wallmann

GEOMAR – Helmholtz Centre for Ocean Research Kiel, Kiel, Germany

e-mail: kwallmann@geomar.de

J. M. Schicks (✉)

GFZ German Research Centre for Geosciences, Potsdam, Germany

e-mail: schick@gfz-potsdam.de; judith.schicks@gfz-potsdam.de

© Springer Nature Switzerland AG 2020

H. Wilkes (ed.), *Hydrocarbons, Oils and Lipids: Diversity, Origin, Chemistry and Fate*,
Handbook of Hydrocarbon and Lipid Microbiology,

https://doi.org/10.1007/978-3-319-90569-3_20

651

stimulation, depressurization, and chemical stimulation have shown that production of natural gas from methane hydrates is technically feasible. The results so far show that high gas production rates can be achieved when methane hydrates are dissociated in the subsurface by reduction of the reservoir pressure.

1 Introduction

Gas hydrates are crystalline, icelike solids composed of water and gas molecules. They form at elevated pressures, at low temperatures, and in the presence of sufficient amounts of gas and water. These conditions are fulfilled at the seafloor and in permafrost regions and deep lakes. Therefore, gas hydrate occurs worldwide – in oceanic sediments on the continental slopes along active and passive margins and regions with similar conditions, such as the Black Sea or the Caspian Sea, and also in polar sediments and permafrost areas, such as the Canadian Arctic, Siberia, and Qilian Mountain permafrost region at the Tibet plateau (Cherskiy et al. 1985; Dallimore et al. 1999; Kvenvolden and Lorenson 2001; Liu et al. 2015). Depending on the pressure and temperature conditions as well as on the hydrate composition, gas hydrates can be found in marine sediments up to 1000 m below the seabed, while gas hydrates in permafrost regions may be found at depths between 132 m and 2000 m (Kvenvolden and Lorenson 2001; Lu et al. 2011). Gas hydrates occur finely disseminated or nodular, in veins, or as massive layers in the sediments. Figure 1 presents a sample of hydrate-bearing sediments which was recovered during the IODP Expedition 311, showing nodules of gas hydrate embedded in the sediment. Disseminated hydrates represent the large majority of marine gas hydrates likely formed from dissolved methane in the pore water and may dissociate rapidly if the pressure and temperature conditions change (Sloan and Koh 2008; Spangenberg et al. 2015). Depending on the formation conditions, hydrates exhibit an either massive or porous habitus, e.g., as demonstrated in natural gas hydrate samples from the Cascadia Margin: in the presence of free gas, a porous hydrate may grow downward toward rising gas (methane) bubbles (Suess et al. 2001).

During the last decades, more than 230 gas hydrate deposits were found worldwide (Makogon 2010). Natural gas hydrates contain predominantly methane, but also larger hydrocarbons as well as CO₂ and H₂S. The amount of additional gases varies from less than 1 mol.% (e.g., Black Sea) to more than 40 mol.% (e.g., Gulf of Mexico, Qilian Mountain) (Kvenvolden and Lorenson 2001; Lu et al. 2011). The incorporation of additional gases besides methane into the hydrate structure increases the stability fields of hydrates (see Fig. 2). This is enabling the formation of gas hydrates even below shallow permafrost (e.g., Lu et al. 2011).

Enormous amounts of gas can be stored in gas hydrate deposits: 1 m³ gas hydrate releases approximately 164 m³ gas at standard pressure and temperature conditions. The global estimates of hydrate-bound gas in marine and terrestrial sediments are highly speculative and ranged in the past from less than 1 × 10¹⁵ m³ to more than 1.5 × 10¹⁶ m³ (Milkov 2003; Makogon 2010). These variations in the calculated results are caused by the different assumptions regarding the composition of natural

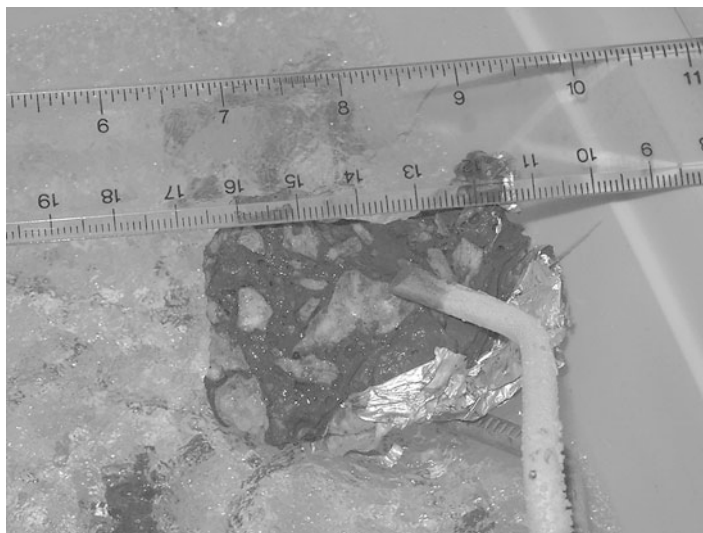
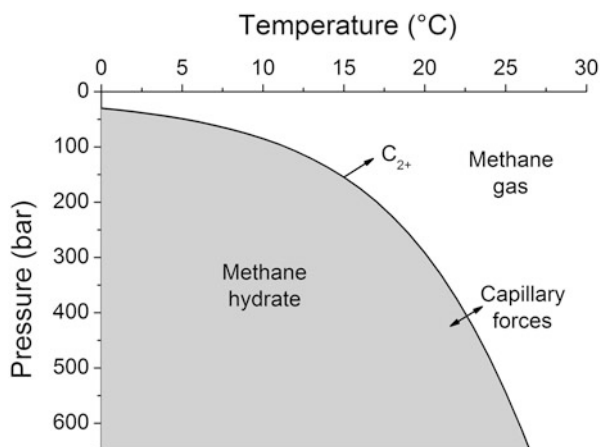


Fig. 1 Nodules of natural gas hydrate embedded in sediment. Samples were recovered during IODP Expedition 311

Fig. 2 Phase diagram for methane hydrate (structure type I) for sulfate-free seawater with a salinity of 35 (Tishchenko et al. 2005). Arrows indicate the formation of a transition zone by capillary forces and the broadening of the gas hydrate stability zone by higher hydrocarbon compounds (C_{2+})



gas hydrates and thus the stability conditions of the resulting hydrate phase as well as the hydrate saturation and morphology in the host sediment (disseminated vs. massive layers), only to name a few. A realistic estimation of the amount of hydrates and their distribution in the host sediment is crucial for the assessment of each natural hydrate deposit as a potential energy resource, in particular with regard to its production capability. It is assumed that 1–3% of the gas hydrate deposits occur on land, whereas 97–99% of natural gas hydrate have been located offshore (Sloan and Koh 2008; Moridis et al. 2009; Makogon 2010). Therefore, we will address the

formation of marine gas hydrates in Sect. 2, while in the third part of this chapter, we will present and discuss production methods for gas from hydrate-bearing sediments.

2 Methane Hydrate Formation in Marine Sediments

In the following, we will address the controls on (i) gas hydrate stability, (ii) microbial methane production, and (iii) gas hydrate saturation in marine sediments.

2.1 Thermodynamic Controls on Gas Hydrate Stability

As mentioned before, methane hydrates are only stable at low temperatures (T) and elevated pressures (P). The stability of methane hydrates is well defined (Sloan 1998), and Pitzer equations can be used to constrain the effects of seawater salinity and porewater composition on methane hydrate stability (Tishchenko et al. 2005). However, the sharp phase boundary that results from these calculations (Fig. 2) is not strictly valid for sediments and other porous media. Capillary forces acting on gas hydrates and free gas residing in sediment pores of different sizes create a broad transition area where free gas and gas hydrate coexist (Liu and Flemings 2011). Moreover, the composition of the hydrate-forming natural gas has a strong effect on the positioning of the phase boundary. Biogenic gas contains only small amounts of higher hydrocarbons (C_{2+}) and forms structure type I methane hydrate composed of more than 99.9% methane with only trace amounts of C_{2+} (Milkov 2005). However, thermogenic gas ascending from larger sediment depths contains significant amounts of C_{2+} favoring the formation of structure type II and/or the inclusion of C_{2+} components in structure type I methane hydrate. These hydrates are stable over a significantly broader P-T range (Sloan 1998).

Bottom waters filling the ocean basins are formed at high latitudes where low temperatures prevail. Therefore, water temperatures in the deep ocean typically range from about 0 °C to only 5 °C. However, temperature increases with sediment depth due to the heat ascending from the Earth's interior. At continental margins, the temperature rises to about 25–50 °C at 1 km depth below the seabed. Therefore, methane hydrate is stable only in the upper section of the sediment column (Fig. 3).

The sediment section where methane hydrate is stable is termed the gas hydrate stability zone (GHSZ). It extends from the surface down to that sediment depth where the temperature profile intersects the phase boundary (Fig. 3). Methane gas is the preferred phase below the GHSZ where it is easily detected by seismic methods. The seismic bottom simulating reflector indicates the top of the free gas occurrence zone that is located immediately below the GHSZ.

The thickness of the GHSZ in marine sediments has been calculated for the entire ocean considering global data sets for bottom water temperature, salinity, sediment thickness, and geothermal heat flow (Burwicz et al. 2011; Piñero et al. 2013; Wallmann et al. 2012). In the open ocean where sediments accumulate at a low

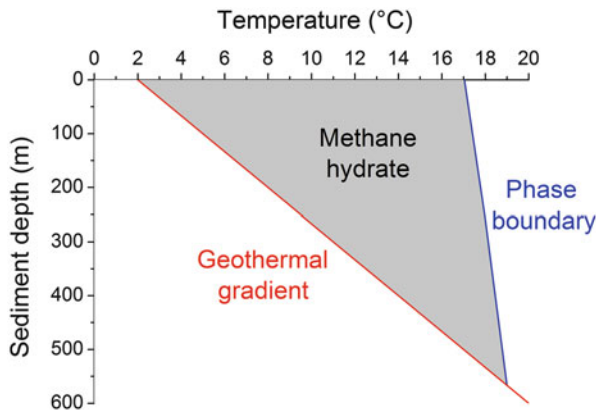


Fig. 3 Phase diagram for methane hydrate (structure type I) for sulfate-free seawater with a salinity of 35 (Tishchenko et al. 2005) in sediments deposited at 2 km water depths (corresponding to a pressure of 200 bar) at a bottom water temperature of 2 °C. The red line indicates the temperature profile in sediments at a geothermal gradient of 30 °C km⁻¹, the blue line represents the phase boundary assuming hydrostatic pressure (1 m sediment depth = 0.1 bar, Fig. 1), and the gray area delimits the region where methane hydrate is stable (0–567 m sediment depth in this case)

rate, the entire sediment column is located within the GHSZ such that the vertical extent of the GHSZ is limited by the thickness of the sediment column (Fig. 4).

Hydrates can only form within the GHSZ if sufficient methane is available to saturate the pore fluids. The solubility of methane hydrate (i.e., the concentration of dissolved methane at equilibrium with methane hydrate) has been measured experimentally and calculated using various thermodynamic approaches (Waite et al. 2009). It increases with temperature and decreases with pressure and salinity, whereas the solubility of methane gas in water is enhanced under high pressure and reduced by an increase in temperature and salinity. The down-core rise in sediment temperature thus promotes an increase in dissolved methane concentrations within the GHSZ and a decrease in dissolved methane in the underlying free gas zone (Fig. 5). Capillary forces affect the stability and solubility of gas hydrate and gas in fine-grained marine sediments. A transition zone is formed, where the solubility ranges of gas bubbles and hydrate crystals residing in sediment pores of different sizes overlap (Liu and Flemings 2011). The discontinuity at the base of the GHSZ (Fig. 5) is thus replaced by a smooth and continuous transition in methane solubility (Liu and Flemings 2011; Waite et al. 2009).

2.2 Microbial Methane Formation

Stable carbon isotope data show that hydrates are usually formed from biogenic methane produced by the anaerobic degradation of particulate organic matter (POC) in the deep marine biosphere (Wallmann et al. 2012). Scientific drilling confirmed the presence of living microorganisms in marine sediments down to the underlying

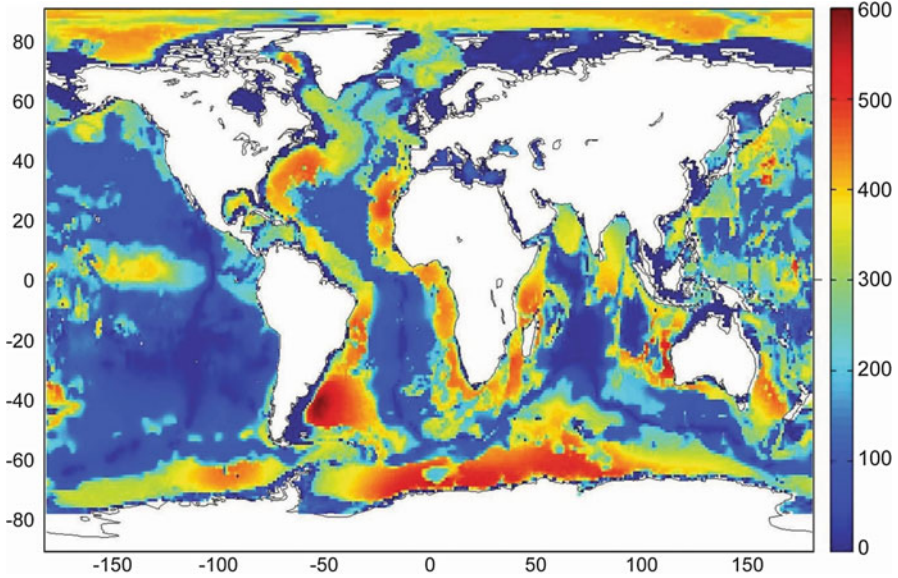


Fig. 4 Thickness of the gas hydrate stability zone (GHSZ) in marine sediments (Piñero et al. 2013). The color coding indicates the base of the GHSZ in meters below the seabed

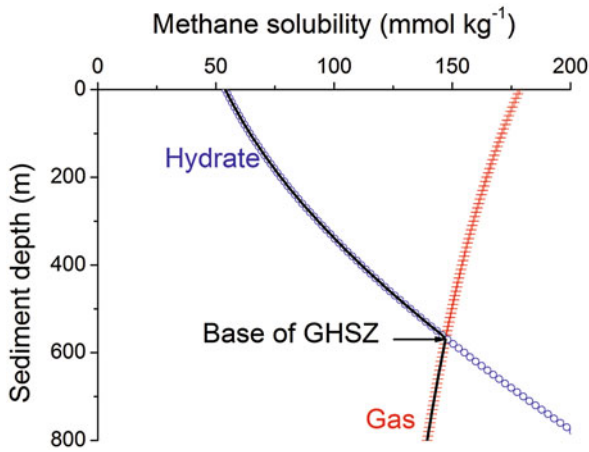


Fig. 5 Solubility of methane in marine sediments deposited at 2000 m water depth. Solubility is calculated for methane hydrate (blue circles) and methane gas (red crosses) in sulfate-free seawater with $S = 35$ assuming hydrostatic conditions, a bottom water temperature of $2\text{ }^{\circ}\text{C}$, and a linear geothermal gradient of $30\text{ }^{\circ}\text{C km}^{-1}$ (Duan et al. 1992; Tishchenko et al. 2005). The black line indicates the dissolved methane concentration attained in methane-saturated pore fluids. The base of the GHSZ is located at the intersection of the gas hydrate and free gas solubility curves

oceanic crust. The number of prokaryotic cells (bacteria and archaea) and the rates of organic matter degradation decrease exponentially with sediment depth (Jørgensen and D'Hondt 2006; Parkes et al. 2000).

Methane production kicks in only after all available oxidation agents have been consumed. Organic matter deposited at the seabed is first degraded by microorganisms using oxygen as terminal electron acceptor. The remaining organic matter is degraded employing dissolved nitrate and manganese (+IV) and iron (+III) minerals as oxidizing agents (Bernier 1980). These additional electron acceptors are usually consumed within the bioturbated surface layer (0–10 cm sediment depth) of continental margin sediments. Field data show that only a small fraction of the POC raining to the seafloor is buried below 10 cm depth (Flögel et al. 2011). The data reveal a marked contrast between fine-grained continental margin and deep-sea sediments (Burdige 2007). While at continental margins about 10% of the POC raining to the seabed is conserved and buried below 10 cm sediment depth, this fraction is reduced to about 1% at the deep-sea floor (Flögel et al. 2011). Due to the very low preservation of POC in open ocean environments, gas hydrates are usually not found in pelagic sediments but only at continental margins where a significant POC fraction is buried and therefore available for microbial methane formation in the deep subsurface. POC that is buried below the bioturbated surface layer is first degraded by microbes using dissolved sulfate as electron acceptor. Microbial methane production and accumulation starts below the depth of sulfate penetration. Several steps are needed before methane is produced as stable end product of anaerobic microbial POC degradation. In a first step, biogenic polymers are hydrolyzed and converted into monomers. These monomers (sugars, amino acids, lipids, etc.) are then fermented into CO₂, H₂, and a number of organic acids. Methane is finally formed by methanogenic microorganisms converting CO₂ and H₂ into methane (Whiticar et al. 1986).

Methane formed at depth is transported upward into the sulfate-methane transition zone via molecular diffusion and advection. Within this zone, methane is oxidized by consortia of bacteria and archaea using sulfate as terminal electron acceptor (Boetius et al. 2000). The overall stoichiometry of anaerobic oxidation of methane (AOM) is given by:



Rates and kinetics of microbial methane oxidation and production have been studied in the lab and derived from field data (Marquardt et al. 2010; Nauhaus et al. 2002; Wallmann et al. 2006).

2.3 Methane Hydrate Formation in Marine Sediments

Various models have been set up to simulate the formation of gas hydrates in marine sediments (Buffett and Archer 2004; Garg et al. 2008; Liu and Flemings 2007; Wallmann et al. 2006). These models consider microbial reactions, thermodynamic

constraints, and the relevant transport processes. In the following, we present a model simulating the reactive transport of three species dissolved in the pore water of sediments (dissolved inorganic carbon, sulfate, methane) and two solid sediment species (POC and methane hydrate). Molecular diffusion, burial, and compaction are considered as transport processes (Fig. 6). The simulated reactions include POC degradation via sulfate reduction, AOM, methanogenesis, gas hydrate formation, and gas hydrate dissolution (Wallmann et al. 2012). Fixed concentration values are applied at the upper boundary, while zero gradients are used as lower boundary conditions for all dissolved species. The model domain excludes the upper bioturbated zone of the sediment column and includes the transition zone at the base of GHSZ where the saturation concentration of dissolved methane is assumed to be constant over a depth interval of 23 m due to capillary forces (Liu and Flemings 2011). Model results are valid for steady-state conditions which were reached after a simulation time of about three million years. The model does not consider gas and fluid ascent into the GHSZ from below.

The dissolved inorganic carbon (DIC) concentrations calculated in the model show a continuous increase with sediment depth reflecting the microbial degradation of POC (Fig. 6). Dissolved methane production starts at about 8 m sediment depth

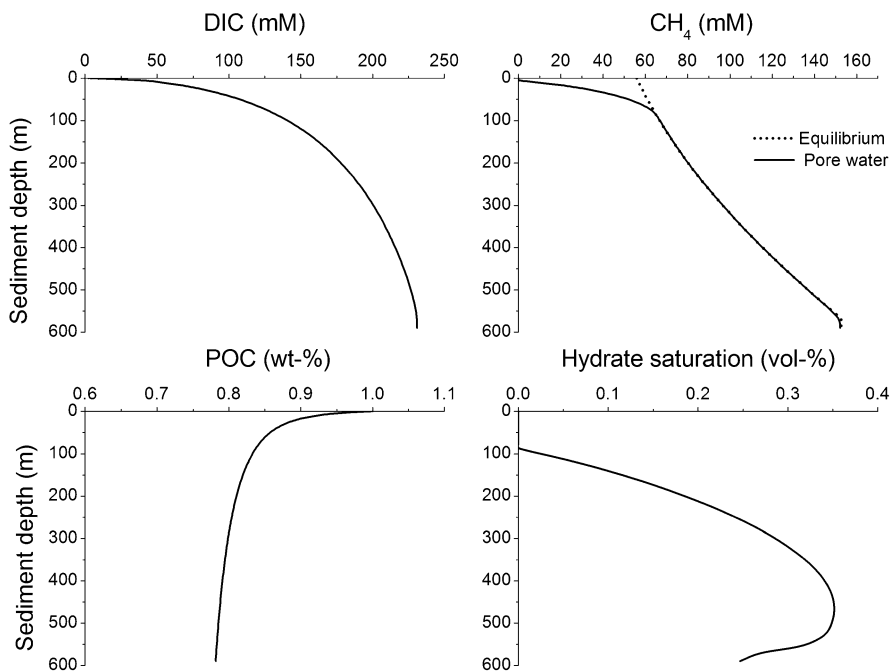
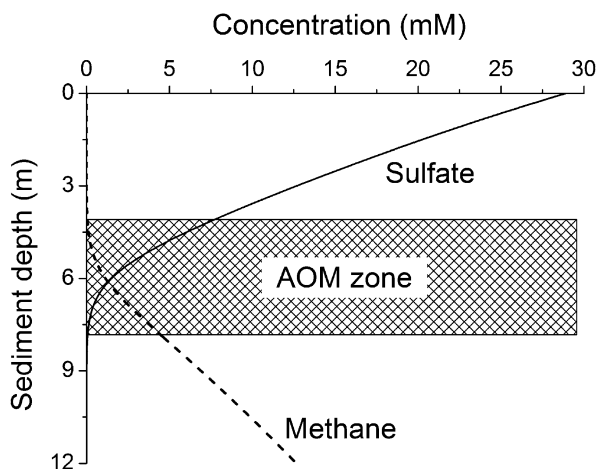


Fig. 6 Concentrations of dissolved inorganic carbon (DIC), dissolved methane (CH₄), particulate organic carbon (POC), and methane hydrate saturation (percent of pore space filled by methane hydrate). The dotted line in the upper right panel indicates the concentration of methane in equilibrium with methane hydrate (Fig. 5)

Fig. 7 Concentrations of dissolved sulfate (solid line) and dissolved methane (dotted line) in surface sediments calculated in the reference model run. The shaded bar indicates the sediment layer where methane is oxidized by microbial consortia using sulfate as terminal electron acceptor (AOM zone)



after sulfate is almost completely consumed by organic matter degradation and AOM (Fig. 7).

Dissolved methane increases down-core and reaches the saturation value with respect to methane hydrate at a sediment depth of 86 m. At this point, gas hydrate starts to form in the sediment column (Fig. 6). Methane hydrate formation continues since the microbial production of methane within the GHSZ overcompensates the down-core increase in methane hydrate solubility (Tishchenko et al. 2005). Close to the base of the GHSZ, methane hydrate dissolves since the saturation level is no longer maintained by the sluggish methane production from aging POC. The saturation level is restored by methane hydrate dissolution in the deeper portion of the GHSZ (545–567 m) and by a combination of dissolution and dissociation in the underlying transition zone (567–590 m). Methane hydrate buried below the model domain to sediment depths >590 m dissociates to form dissolved and gaseous methane. Most of the methane produced via POC degradation within the GHSZ is consumed by AOM and buried below the GHSZ. Only a small portion (9%) is permanently fixed in gas hydrates. The resulting gas hydrate saturations are very low. The maximum hydrate saturation is reached at 470 m sediment depth where 99.65% of the pore space is filled by water while only 0.35% is occupied by methane hydrate (see Wallmann et al. (2012) for further details).

Similar simulations have been performed on a global grid covering the entire ocean (Archer et al. 2008; Burwicz et al. 2011; Piñero et al. 2013; Wallmann et al. 2012). These global-scale models indicate that 400–1000 Gt methane-carbon is bound in marine gas hydrates. They predict low hydrate saturations for most continental margins (<1 vol.%) and relatively large values (1–3 vol.%) in regions where methane hydrate formation is promoted by high POC concentrations and favorable temperature and pressure conditions (Fig. 8).

However, none of these global models considers the rapid ascent of methane-charged fluids and gases through faults acting as high permeability conduits. This process may lead to very high hydrate saturations (10–100 vol.%) in the faults and

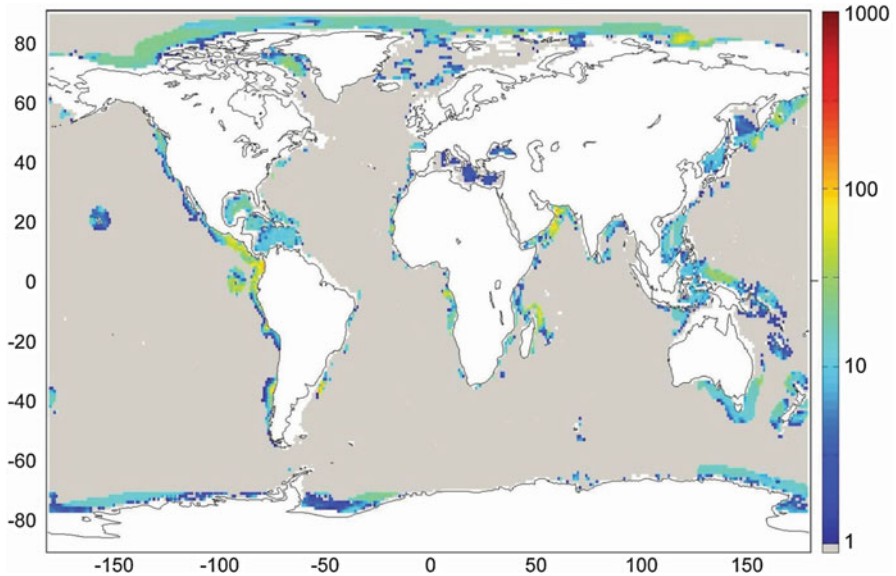


Fig. 8 Global distribution of methane hydrate in marine sediments (Wallmann et al. 2012). The color coding indicates depth-integrated hydrate inventories in kg C m^{-2}

their immediate surroundings (Chatterjee et al. 2014; Piñero et al. 2016). Another key process not considered in global models is the recycling of methane hydrate at the base of the GHSZ (Kvenvolden and Lorenson 2001). Due to continuous sedimentation, methane hydrate is ultimately buried to larger sediment depths below the GHSZ where elevated temperatures induce the dissociation of hydrate into free gas and water. The free gas produced by hydrate dissociation can migrate upward if the gas saturation is high enough to overcome the pore entry pressure. The ascending gas is trapped at the base of the GHSZ where it forms new gas hydrate. This recycling process inhibits methane burial and keeps the biogenic gas within the GHSZ. It may yield very high saturations at the base of the GHSZ if it continues over a large period of time (Burwicz et al. 2017; Wallmann et al. 2012). Sufficiently high gas contents are needed to initiate upward gas migration. In many cases, infiltration of gas from deeper layers may prime the sediment and kick-start the recycling process.

The first modeling study that considers the full complexity of the natural gas hydrate system was recently conducted to simulate the formation of gas hydrates in the Gulf of Mexico where faulting and upward gas migration are induced by salt tectonics (Burwicz et al. 2017). The model shows very high gas hydrate saturations at the base of the GHSZ induced by the recycling process discussed above. The model results are in good agreement with field observations and confirm that the study area is a very promising site for the commercial production of natural gas from methane hydrates (Fig. 9).

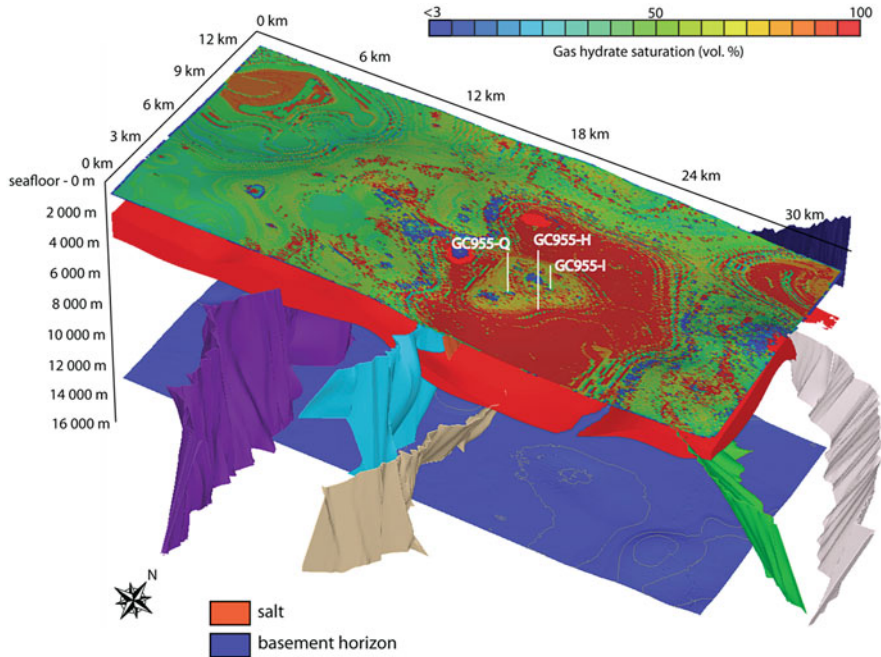


Fig. 9 Gas hydrate distribution within Pleistocene sediments of the Green Canyon province in the Gulf of Mexico (Burwicz et al. 2017). The surface of the 3-D view shows the gas hydrate saturation at the base of the GHSZ. Permeable faults indicated as irregular vertical structures connect the Pleistocene sediments to the underlying strata. Model results are consistent with observations at drill sites GC955-Q, GC955-H, and GC955-I

3 Gas Production from Hydrate-Bearing Sediments

Based on the data available for a certain natural gas hydrate deposit, an assessment of this deposit as a potential energy resource may start with a classification into four main categories (Moridis et al. 2009; Moridis and Reagan 2011):

- Class 1 hydrate deposits composed of a hydrate-bearing layer and an underlying two-phase fluid zone containing mobile gas and liquid water. The bottom of the hydrate-bearing layer defines the bottom of hydrate stability zone
- Class 2 hydrate deposits composed of a hydrate-bearing layer overlying a zone of mobile water
- Class 3 hydrate-bearing layer with an underlying layer containing no mobile fluids
- Class 4 hydrate deposits which are characterized by dispersed hydrate with low saturations ($<10\%$) and a lack of confining geologic strata.

In any case, the natural gas hydrate deposit should have the following desirable specifications to be considered for hydrate production (Moridis et al. 2009, 2011):

- Coarse porous sediments such as sands and gravels which are characterized by high porosity, accompanied by (confirmed) high hydrate saturations and intrinsic permeability of the hydrate-bearing sediment
- An ideal combination of intrinsic permeability on the one hand and hydrate saturation on the other hand, resulting in an effective permeability that is sufficiently large to ensure an adequate fluid flow
- The presence of very low permeability boundaries
- High deposit temperatures which correspond to larger sensible heat reservoirs in the vicinity of the hydrate-bearing layer to balance the endothermic dissociation reaction and potential larger pressure drops
- Pressure and temperature conditions in the reservoir close to the equilibrium conditions reducing the efforts for gas hydrate dissociation (quantified as a minimum decrease in pressure or increase in temperature)
- Access to an existing infrastructure for the transport of the produced gas.

Natural gas hydrate occurrences in sand-dominated reservoirs with high hydrate saturations could be detected, e.g., in the northern Gulf of Mexico and the eastern Nankai Trough (Boswell et al. 2012; Collett et al. 2015, and literature within Konno et al. 2017). If all the requirements listed above are met, the production of methane from natural gas hydrate deposits may become economically feasible. In general, there are three different methods which can be used to dissociate the hydrates and release the methane gas from the hydrate cavities: thermal stimulation, depressurization, and chemical stimulation. All three methods have already been tested in the field. Thermal stimulation was tested successfully in a field test in the framework of the Mallik Scientific Drilling Project in the Northwest Territories in the Canadian Arctic during the winter of 2001/2002. During the world's first gas production test, a hot fluid was circulated for 123 h into depths of 900–1100 m where the hydrate-bearing sediment occurred and the bottom-hole temperature was increased from 7.7 °C to more than 50 °C. A total of 470 m³ of methane from dissociated hydrates were produced during the thermal test (Hancock et al. 2005). This test was certainly successful in terms of a proof of principle, but the efficiency of the procedure remains questionable. The loss of heat during the hot fluid transport through hundreds of meters of permafrost and the comparatively minor radial propagation of heat in the hydrate layer indicate that this procedure is probably not efficient enough for commercial gas production. An alternative could be the generation of heat within the hydrate-bearing layer, e.g., using in situ combustion (Schicks et al. 2011, 2013). However, the efficiency of the in situ combustion technique has not been proved in the field so far. Thus, after analyzing all data from the Mallik field trial in 2002 and performing numerical simulations, it turns out that depressurization techniques may be more efficient for the production of gas from hydrate-bearing sediments (Moridis et al. 2009). In April 2007, another production test was performed at the Mallik site, this time using depressurization techniques. During 12.5 h of successful pumping operation, at least 830 m³ of methane were produced

from a hydrate-bearing formation (Yasuda and Dallimore 2007). In winter 2008, a modified pumping system with sand control devices was used for the second depressurization test. During 6 days of continuous operation, about 13,000 m³ of methane were produced (Yamamoto and Dallimore 2011). Based on these promising results, depressurization was also applied as method of choice for the first offshore production test at the eastern Nankai Trough, Japan, in 2013. The geological analyses of this area indicate that the hydrate saturation in the sandy sediments reaches up to 80%. The wellbore pressure has been decreased from 13.4 MPa to 5 MPa for 4 days and for 2 more days to 4.3 MPa. During these 6 days, a cumulative volume of about 120,000 m³ of gas and 1250 m³ of water was produced until an abrupt sand production occurred on the sixth day (Konno et al. 2017). Nevertheless, the technical feasibility of the depressurization methods for the production of methane from marine hydrate reservoirs could be partially verified with this field test.

A completely different approach, namely, the chemical stimulation via injection of a CO₂-N₂ gas mixture, was tested within the Prudhoe Bay Unit on the Alaska North Slope during 2011 and 2012 (Boswell et al. 2017). The project aimed to determine the feasibility of gas injection into hydrate-bearing sediments and the observation of the reservoir response upon subsequent flowback in order to assess the potential for the exchange of methane with CO₂ in the naturally occurring gas hydrate. The chosen area for the Ignik Sikumi field program exhibits relatively massive and homogeneous sand units with a hydrate saturation of about 60–72%. The field test was conducted in four steps (Boswell et al. 2017):

1. Injection (14 days): During this period, a total volume of about 6114 m³ gas containing 22.5% CO₂ and 77.5% N₂ was injected into the reservoir. The injection pressure was held constant at 9.8 MPa, and the temperature of the injected medium remained within 0.1 K of the formation temperature.
2. Shut-in soak (2.5 days): Operational issues associated with the changeover from injection to production resulted in a period of shut-in time before the flowback could be started. During this time, the bottom-hole pressure dropped from 9.8 MPa to 8.27 MPa.
3. Unassisted flowback (1.5 days): During the unassisted flowback, only gas was produced to the surface.
4. Jet-pumped-assisted flowback (30 days): During the first 8 days of the jet-pumped assisted flowback, the pressure was kept above the destabilization pressure of the native methane hydrate at a given temperature resulting in a relatively low and variable gas, water, and solid production. During the next 2–3 days of jet-pumped-assisted flowback, the pressure was reduced to pressures very close to the methane hydrate stability pressure at reservoir condition. An increased production of gas was observed. The bottom-hole pressure during the third phase of the jet-pumped-assisted flowback was chosen below the predicted methane hydrate stability conditions and resulted in a modest but stable and increasing gas production. A total of 24,210 m³ of methane was produced during the production period. 70% of the injected N₂ and 40% of the injected CO₂ were recovered.

The results of the field test are quite complex and not easy to interpret. However, investigation of the recovered gases indicates a preferential retention of CO₂ in the reservoir, but it is not clear how it remains. It also shows that methane was released from the reservoir, but it is not clear whether the produced methane was derived from direct exchange with CO₂ in the hydrate structures or if it was released as a result of other processes such as the dissociation of the native hydrate phase due to the chemical disequilibrium as a result of the CO₂-N₂ injection (Boswell et al. 2017). The assessment of the exchange technology as a potential economic production technology needs further investigation. It may become the preferred production method if incentives for CO₂ capture and storage are implemented to mitigate global climate change, while the depressurization technique seems to be the most promising production technology to meet the growing demand for natural gas.

4 Research Needs

Rates and mechanisms of microbial methane production in the deep biosphere and the physical conditions controlling the upward migration of gas through unconsolidated sediments and faults are still not fully understood. More field work, lab studies, and modeling is needed to characterize these key processes that control the spatial distribution of high-grade gas hydrate deposit. The various gas production methods need to be further tested to address issues such as sand production and reservoir cooling that may limit gas flow rates and the rates of hydrate dissociation. In addition to the field tests, laboratory and modeling studies are needed to improve the basic understanding of the complex multispecies chemical systems. Most notably, the geo-mechanical response of the reservoir to changes induced by different production techniques needs to be studied to minimize sand production and to investigate the possibility that the stability of the wellbore and the surrounding sediment may be affected by gas hydrate dissociation.

References

- Archer D, Buffett B, Brovkin V (2008) Ocean methane hydrates as a slow tipping point in the global carbon cycle. *Proc Natl Acad Sci* 106:20596–20601
- Berner RA (1980) *Early Diagenesis – a theoretical approach*. Princeton University Press, Princeton
- Boetius A, Ravensschlag K, Schubert CJ, Rickert D, Widdel F, Gieseke A, Amann R, Jørgensen BB, Witte U, Pfannkuche O (2000) A marine microbial consortium apparently mediating anaerobic oxidation of methane. *Nature* 407:623–626
- Boswell R Collett TS, Frye M, Shedd W, McConnell DR, Shelander D (2012) Subsurface gas hydrates in the northern Gulf of Mexico. *Mar Pet Geol* 34:4–30
- Boswell R, Schoderbek D, Collett TS, Ohtsuki S, White M, Anderson BJ (2017) The Iñiġik Sikumi field experiment, Alaska North Slope: design, operations, and implications for CO₂-CH₄ exchange in gas hydrate reservoirs. *Energy Fuels* 31:140–153
- Buffett B, Archer D (2004) Global inventory of methane clathrate: sensitivity to changes in the deep ocean. *Earth Planet Sci Lett* 227:185–199

- Burdige DA (2007) Preservation of organic matter in marine sediments: controls, mechanisms, and an imbalance in sediment organic carbon budgets? *Chem Rev* 107:467–485
- Burwicz EB, Rüpke LH, Wallmann K (2011) Estimation of the global amount of submarine gas hydrates formed via microbial methane formation based on numerical reaction-transport modeling and a novel parameterization of Holocene sedimentation. *Geochim Cosmochim Acta* 75:4562–4576
- Burwicz E, Reichel T, Wallmann K, Rottke W, Haeckel M, Hensen C (2017) 3-D basin-scale reconstruction of natural gas hydrate system of the green canyon, Gulf of Mexico. *Geochem Geophys Geosyst* 18:1959
- Chatterjee S, Bhatnagar G, Dugan B, Dickens GR, Chapman WG, Hirasaki GJ (2014) The impact of lithologic heterogeneity and focused fluid flow upon gas hydrate distribution in marine sediments. *J Geophys Res Solid Earth* 119:6705–6732
- Cherskiy NV, Tsarev VP, Nikitin SP (1985) Investigations and predictions of conditions of accumulation of gas resources in gas-hydrate pools. *Pet Geol* 21:65–89
- Collett T, Bahk J-J, Baker R, Boswell R, Divins D, Frye M, Goldberg D, Husebø J, Koh C, Malone M, Morell M, Myers G, Shipp C, Torres M (2015) Methane hydrates in nature-current knowledge and challenges. *J Chem Eng Data* 60:319–329
- Dallimore SR, Uchida T, Collett TS (1999) Scientific results from JAPAX/JNOC/GSC Mallik 2 L-38 gas hydrate research well, Mackenzie Delta, Northwest Territories, Canada. *Geol Surv Can Bull* 544:295–311
- Duan Z, Möller N, Greenberg J, Weare JH (1992) The prediction of methane solubility in natural waters to high ionic strength from 0 to 250°C and from 0 to 1600 bar. *Geochim Cosmochim Acta* 56:1451–1460
- Flögel S, Wallmann K, Poulsen CJ, Zhou J, Oschlies A, Voigt S, Kuhnt W (2011) Simulating the biogeochemical effects of volcanic CO₂ degassing on the oxygen-state of the deep ocean during the Cenomanian/Turonian anoxic event (OAE2). *Earth Planet Sci Lett* 305:371–384
- Garg SK, Pritchett JW, Katoh A, Baba K, Fujii T (2008) A mathematical model for the formation and dissociation of methane hydrates in the marine environment. *J Geophys Res Solid Earth* 113:32
- Hancock SH, Collett TS, Dallimore SR, Satoh T, Inoue T, Huenges E, Hennings J, Weatherill B (2005) Overview of thermal-stimulation production-test results for the JAPAX/JNOC/GSC Mallik 5L-38 gas hydrate production research well. In: Dallimore SR, Collett TS (eds) Scientific results from the Mallik 2002 gas hydrate production research well program, Mackenzie Delta, Northwest Territories, Canada. GSC Bulletin, vol 585. Geological Survey of Canada.
- Jørgensen BB, D'Hondt S (2006) A starving majority deep beneath the seafloor. *Science* 314:932–934
- Konno Y, Fujii T, Sato A, Akamine K, Naiki M, Masuda Y, Yamamoto K, Nagao J (2017) Key findings of the world's first offshore methane hydrate production test off the coast of Japan: towards future commercial production. *Energy Fuels* 31:2607–2616
- Kvenvolden KA, Lorenson TD (2001) The global occurrence of natural gas hydrate. *Geophys Monogr* 124:87–98
- Liu XL, Flemings PB (2007) Dynamic multiphase flow model of hydrate formation in marine sediments. *J Geophys Res Solid Earth* 112:23
- Liu X, Flemings PB (2011) Capillary effects on hydrate stability in marine sediments. *J Geophys Res* 116:B07102
- Liu CL, Meng QG, He XL, Li CF, Ye YG, Lu ZQ, Zhu YH, Li YH, Liang JQ (2015) Comparison of the characteristics for natural gas hydrate recovered from marine and terrestrial areas in China. *J Geochem Explor* 152:67–74
- Lu Z, Zhu Y, Zhang Y, Wen H, Li Y, Liu C (2011) Gas hydrate occurrences in Qilian Mountain permafrost, Qinghai Province, China. *Cold Reg Sci Technol* 66:93–104
- Makogon YF (2010) Natural gas hydrates – a promising source of energy. *J Nat Gas Sci Eng* 2:49–59
- Marquardt M, Hensen C, Pinero E, Wallmann K, Haeckel M (2010) A transfer function for the prediction of gas hydrate inventories in marine sediments. *Biogeosciences* 7:2925–2941

- Milkov AV (2003) Global estimates of hydrate-bound gas in marine sediments: how much is really out there? *Earth-Sci Rev* 66:183–197
- Milkov AV (2005) Molecular and stable isotope compositions of natural gas hydrates: a revised global dataset and basic interpretations in the context of geological settings. *Org Geochem* 36:681–702
- Moridis GJ, Reagan MT (2011) Estimating the upper limit of gas production from Class 2 hydrate accumulations in the permafrost: 1. Concepts, system description, and the production base case. *J Petrol Sci Eng* 76:194–204
- Moridis GJ, Collett TS, Boswell R, Kiruhara M, Reagan MT, Koh C, Sloan ED (2009) Towards production from gas hydrates, current status, assessment of resources, and simulation based evaluation of technology and potential. *SPE Reserv Eval Eng* 745–771
- Moridis GJ, Reagan MT, Boyle KL, Zhang K (2011) Evaluation of the gas production potential of some particularly challenging types of oceanic hydrate deposits. *Transp Porous Med* 90:269–299
- Nauhaus K, Boetius A, Krüger M, Widdel F (2002) *In vitro* demonstration of anaerobic oxidation of methane coupled to sulphate reduction in sediment from a marine gas hydrate area. *Environ Microbiol* 4:296–305
- Parkes RJ, Cragg BA, Wellsbury P (2000) Recent studies on bacterial populations and processes in subseafloor sediments: a review. *Hydrogeol J* 8:11–28
- Piñero E, Marquardt M, Hensen C, Haeckel M, Wallmann K (2013) Estimation of the global inventory of methane hydrates in marine sediments using transfer functions. *Biogeosciences* 10:959–975
- Piñero E, Hensen C, Haeckel M, Rottke W, Fuchs T, Wallmann K (2016) 3-D numerical modelling of methane hydrate accumulations using PetroMod. *Mar Pet Geol* 71:288–295
- Schicks J, Spangenberg E, Giese R, Steinhauer B, Klump J, Luzi M (2011) New approaches for the production of hydrocarbons from hydrate bearing sediments. *Energies* 4(1):151–172
- Schicks J, Spangenberg E, Giese R, Luzi-Helbing, M, Priegnitz M, Beeskow-Strauch B (2013) A counter-current heat-exchange reactor for the thermal stimulation of hydrate-bearing sediments. *Energies* 6(6):3002–3016
- Sloan ED Jr (1998) *Clathrate hydrates of natural gases*, 2nd edn. Marcel Dekker, Inc., New York
- Sloan ED Jr, Koh CA (2008) *Clathrate hydrates of natural gases*, 3rd edn. CRC Press Taylor and Francis Group, Boca Raton
- Spangenberg E, Priegnitz M, Heeschen K, Schicks JM (2015) Are laboratory-formed hydrate-bearing systems analogous to those in nature? *J Chem Eng Data* 60(2):258–268
- Suess E, Torres ME, Bohrmann G, Collier RW, Rickert D, Goldfinger C, Linke P, Heuser A, Sahling H, Heeschen K, Jung C, Nakamura K, Greinert J, Pfannkuche O, Trehu A, Klinkhammer G, Whiticar MJ, Eisenhauer A, Teichert B, Elvert M (2001) Sea floor methane hydrates at hydrate ridge, cascadia margin. In Paull CK, Dillon WP (eds) *Natural gas hydrates: occurrence, distribution, and detection*. Washington: American Geophysical Union
- Tishchenko P, Hensen C, Wallmann K, Wong CS (2005) Calculation of the stability and solubility of methane hydrate in seawater. *Chem Geol* 219:37–52
- Waite WF, Santamarina JC, Cortes DD, Dugan B, Espinoza DN, Germaine J, Jang J, Jung JW, Kneafsey TJ, Shin H, Soga K, Winters WJ, Yun T-S (2009) Physical properties of hydrate-bearing sediments. *Rev Geophys* 47:1–38
- Wallmann K, Aloisi G, Haeckel M, Obzhairov A, Pavlova G, Tishchenko P (2006) Kinetics of organic matter degradation, microbial methane generation, and gas hydrate formation in anoxic marine sediments. *Geochim Cosmochim Acta* 70:3905–3927
- Wallmann K, Pinero E, Burwicz E, Haeckel M, Hensen C, Dale A, Rüpke L (2012) The global inventory of methane hydrate in marine sediments: a theoretical approach. *Energies* 5:2449–2498
- Whiticar MJ, Faber E, Schoell M (1986) Biogenic methane formation in marine and freshwater environments: CO₂ reduction vs. acetate fermentation – isotope evidence. *Geochim Cosmochim Acta* 50:693–709
- Yasuda M, Dallimore SR (2007) Summary of the methane hydrate second Mallik production test. *J Jpn Assoc Pet Technol* 72(6):603–607

Part IV

Hydrocarbons and Lipids in the Environment



Michael J. Whiticar

Contents

1	Introduction	670
2	Biogeochemical Process of Microbial Methane Formation	673
3	Microbial Methane in Marine Environments	687
4	Microbial Methane in Freshwater and Terrestrial Environments	693
5	Microbial Methane in Special Environments	697
6	Methane Oxidation	699
6.1	Biological Methane Oxidation	700
6.2	Aerobic Methane Oxidation	700
6.3	Anaerobic Oxidation of Methane (AOM)	702
7	Atmospheric Methane	711
8	Summary	715
	References	717

Abstract

Methane, the simplest alkane, is one of the most important and abundant carbon molecules on Earth. It is a major supply of energy, a chemical feedstock, and a potent greenhouse gas. Aside from thermogenic, pyrogenic, and abiotic sources, methane is primarily formed in the Earth's surface by a variety of microbial processes, i.e., methanogenesis. These processes utilize a range of pathways that involve small carbon-bearing molecules, e.g., CO₂, acetate, etc. Methanogens are active in widely diverse anaerobic environments, e.g., rocks, soils, sediments, lakes, oceans, and animals, and cover a wide ecological habitats extending from

M. J. Whiticar (✉)

Biogeochemistry Facility (BF-SEOS), School of Earth and Ocean Sciences, University of Victoria, Victoria, BC, Canada

Hanse-Wissenschaftskolleg, HWK (Institute for Advanced Study), Delmenhorst, Germany

e-mail: whiticar@uvic.ca

© Springer Nature Switzerland AG 2020

H. Wilkes (ed.), *Hydrocarbons, Oils and Lipids: Diversity, Origin, Chemistry and Fate*, Handbook of Hydrocarbon and Lipid Microbiology,

https://doi.org/10.1007/978-3-319-90569-3_5

669

–1 °C to 122 °C, pH 5 to 11, and salinities up to 100 g/L. The biogeochemical methane cycle also includes the microbial oxidation of methane, both by aerobic and anaerobic organisms and consortia, of which some pathways remain uncertain. Together with chemical oxidation, these microbial “biofilters” of methane are critical in controlling methane distributions. A variety of tools, including biomarker molecules, stable isotopes, and molecular gene sequencing, can characterize these formation and consumption pathways. This has led to a more robust understanding of methane occurrences, abundances, reservoirs, fluxes, and budgets over the past century.

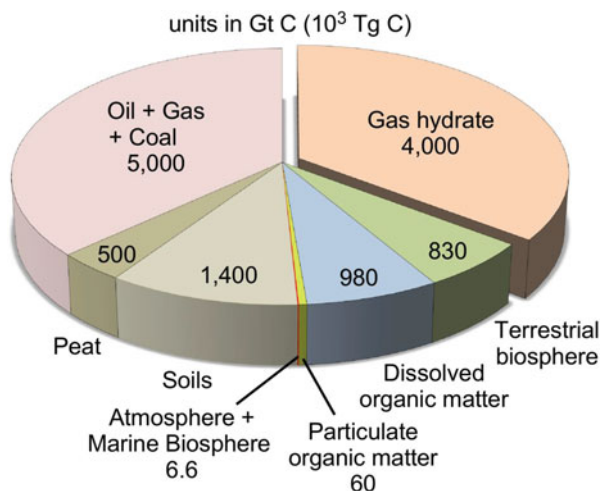
1 Introduction

Methane, named by the German chemist August Wilhelm von Hofmann (1866), is chemically the most reduced form of carbon, i.e., the antithesis of carbon dioxide (CO₂), and the most oxidized form. As a result, methane readily combusts in today’s oxygenated Earth atmosphere. Benjamin Franklin apparently reported this in 1774 (Priestley 1775; Heilbron 1976), but Alessandro Volta (1777) is generally credited with the chemical identification of CH₄ after recovering gas by stirring the sediments at Lake Maggiore, Italy (Fig. 1). Early investigators of methane formation also include MacBride (1764), who addressed fermentation reactions, and Jameson (1800), who looked at processes of anaerobic peat and torf environments. Hoppe-Seyler (1876) is one of the first to investigate methanogenesis in cultures amended with acetate, while Omelianski (1904), Söhngen (1906), Coolhass (1928), Barker (1936a, b), etc. provided the first descriptions of various methanogens.



Fig. 1 Discovery of methane gases in Italian swamps by Volta (1777)

Fig. 2 Pie diagram showing the relative sizes of the major organic carbon pools



Our interests in methane are largely driven by its energy potential and by our concern for changes to the atmospheric radiative balance and changing climate. The oxidation of CH_4 to CO_2 through biological and photochemical processes, and our combustion of methane for energy, are important contributors to the increase in the tropospheric CO_2 budget ($\sim 0.016 \text{ Wm}^{-2}$, IPCC). However, the emission of CH_4 into the troposphere of ~ 550 to $600 \text{ Tg CH}_4 \text{ year}^{-1}$ (Prather et al. 2012; Kirschke et al. 2013; Saunio et al. 2016) has resulted in $\sim 0.57 \text{ Wm}^{-2}$ total radiative forcing by CH_4 since preindustrial times (Myhre et al. 2013). The global warming potential (GWP relative to CO_2 of ~ 28 and 84 over 100- and 20-year lifetimes, respectively) emphasizes the relative impact of CH_4 compared to CO_2 .

Methane (CH_4) is the most simple and stable of the n -alkanes with the strongest C–H bond strength, i.e., dissociation energy of $+439 \text{ kJ mol}^{-1}$ (Thauer and Shima 2008). Methane is also the most abundant organic molecule on Earth, even though we actually do not know the total amount of methane present. In the lithosphere, the majority of this methane is contained in methane hydrates, in particular marine gas clathrates. Recent estimates of methane in hydrates vary, with probable values from ~ 5 – $36 \times 10^5 \text{ Tg CH}_4$ (~ 1 to $5 \times 10^{15} \text{ m}^3 \text{ CH}_4$, e.g., Milkov 2005; Boswell and Collett 2011; Wallmann et al. 2012), dropping from the earlier “consensus value” of $150 \times 10^5 \text{ Tg CH}_4$ ($21 \times 10^{15} \text{ m}^3$, Kvenvolden 1999) to the current number of $\sim 36 \times 10^5 \text{ Tg CH}_4$ ($\sim 5 \times 10^{15} \text{ m}^3$). Despite the uncertainty in the amount of methane stored in hydrates, it eclipses the global proven (recoverable) natural gas reserves of $1.4 \times 10^5 \text{ Tg CH}_4$ ($\sim 0.2 \times 10^{15} \text{ m}^3$, e.g., CIA 2017; BP 2017). In fact, the amount of carbon in methane hydrates is likely even greater than the summation of all soils, sediments, and dissolved organic carbon and is about the same as the combination of the known oil, natural gas, and coal reserves (Fig. 2). For comparison, the 2019 tropospheric methane mixing ratio of $\sim 1864 \text{ ppm}$ (Dlugokencky 2019) translates to a methane burden calculation of $0.0485 \times 10^5 \text{ Tg CH}_4$ (IPCC 2013) or ~ 740 times less than contained in methane hydrates. Methane dissolved in the ocean is estimated to

be ~ 43 Tg CH_4 (Reeburgh 2007) or 84,000 times less than the CH_4 in hydrates. Massive releases of methane from hydrates to the atmosphere have been implicated in Paleocene-Eocene Thermal Maximum, 55 mya (Dickens et al. 1995), and, questionably, the late Quaternary abrupt millennial-scale warming and climate change (Kennett et al. 2003). Destabilization of Neoproterozoic hydrates may, arguably, also have influenced both the pre- and post-snowball Earth carbon systems (Halverson et al. 2002; Kennedy et al. 2001). These catastrophic releases assume that it is predominantly microbial gas that is dissociating from massive methane hydrate deposits. This methane has a diagnostic carbon and hydrogen isotope signature (see Eq. 6), i.e., ^{13}C -depleted methane of $\delta^{13}\text{C-CH}_4 \sim -67$ ‰ versus VPDB and $\delta^2\text{H-CH}_4 \sim -190$ ‰ versus VSMOW (Figs. 3 and 4).

The majority of methane on Earth is generated from accumulated organic matter through various processes, including microbial, thermogenic, and pyrogenic mechanisms. This methane formation from organic matter is augmented by lesser amounts of abiotic methane formation (e.g., Etiope 2015). It has been estimated that approximately 0.1% of the solar radiation reaching surface of the Earth (3.4×10^6 EJ year^{-1}) is transferred into biomass (~ 150 Gt year^{-1} , Thomson 1852; Monteith 1972; Lieth 1973) and that $\sim 1\%$ of the primary productivity or about 1.5 Gt is ultimately converted to CH_4 (Thauer 1998; Reeburgh 2003). This transfer ratio does depend on the environment. For example, the conversion to CH_4 in wetlands ranges from 2% to

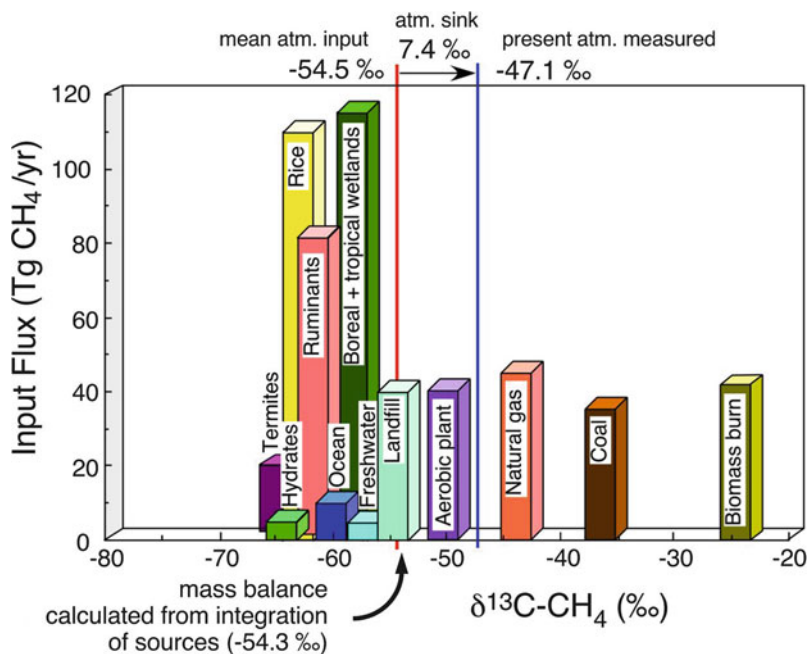


Fig. 3 Mean methane carbon stable isotope ratio of primary sources of methane flux (Tg/year) to the atmosphere. The integrated $\delta^{13}\text{C-CH}_4$ input signal from the sources and the combined isotope shift due to methane oxidation and present-day $\delta^{13}\text{C-CH}_4$ value are also shown. (From Whiticar and Schaefer 2007)

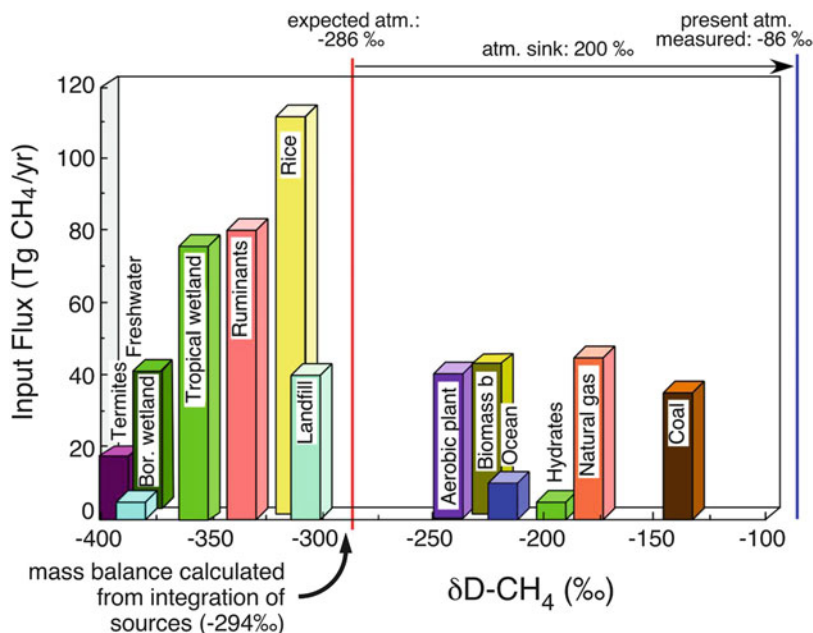


Fig. 4 Mean methane hydrogen stable isotope ratio of primary sources of methane flux (Tg/year) to the atmosphere. The integrated $\delta^2\text{H-CH}_4$ input signal from the sources and the combined isotope shift due to methane oxidation and present-day $\delta^2\text{H-CH}_4$ value are also shown. (From Whiticar and Schaefer 2007)

10% of the local primary productivity (Aselmann and Crutzen 1989; Sebacher et al. 1986; Moore and Knowles 1990; Pulliam 1993). Of this total methane generation, about 40% or 582 Tg CH₄ year⁻¹ (Denman et al. 2007) reaches the troposphere, while most of the remainder is oxidized. This microbial methane source compares with the smaller flux of geologically sourced gas (“geogas”), i.e., methane without ¹⁴C, reaching the atmosphere (~10% or ~42–64 Tg CH₄ year⁻¹, Etiope et al. 2008; Schaefer and Whiticar 2008).

Although assessing the magnitudes of the various methane reservoirs is important, it is also important to know how and how much methane moves between these reservoirs and the processes of formation and destruction of methane. A critical aspect of this is accurate characterization of the biogeochemistry of methane, the focus of this chapter.

2 Biogeochemical Process of Microbial Methane Formation

The remineralization sequence of organic matter follows distinct stages, as is shown schematically in Fig. 5. These generally occupy separate horizons or diagenetic zones as illustrated in Fig. 6. Hydrolytic microflora, which operate aerobically, anaerobically, or facultatively, break down complex organic molecules by hydrolysis

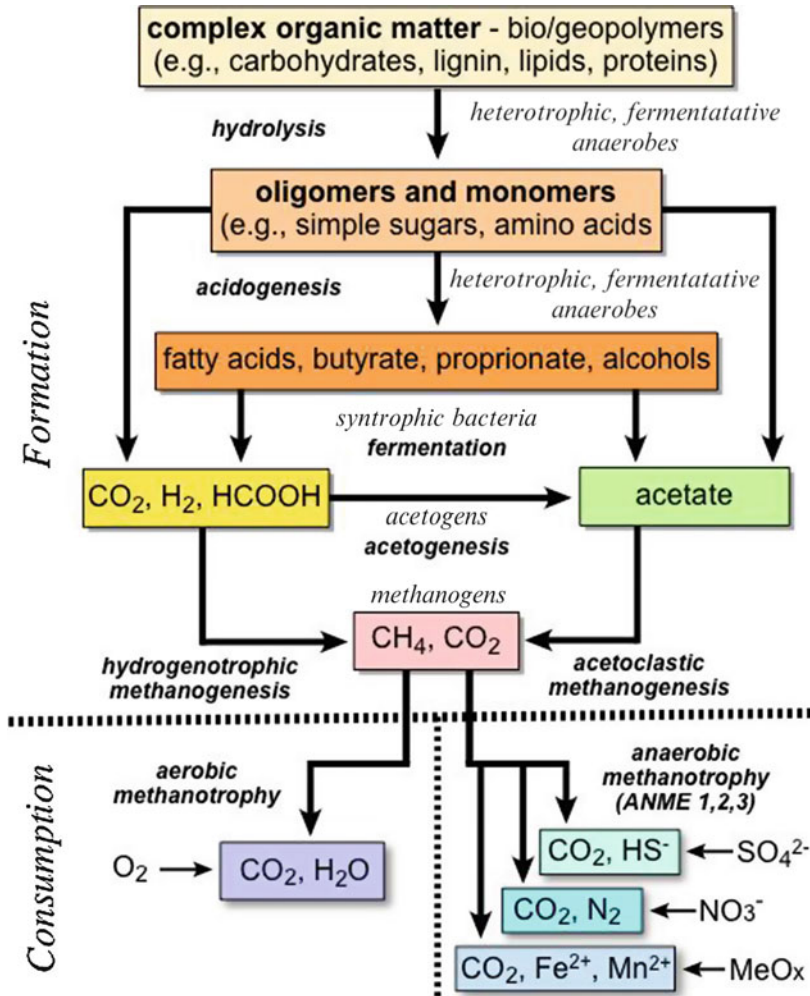


Fig. 5 Schematic of the basic remineralization sequence for organic matter as it is ultimately transformed from complex to progressively simpler organic molecules, then into methane by methanogenic processes and even consumed by aerobic or anaerobic methanotrophy. Note non-competitive substrates have not been depicted for the sake of clarity

to monomers, e.g., sugars, volatile, short-chained fatty acids, and amino acids. Acidogenesis by anaerobic or facultative fermentative microflora further degrades these monomeric and intermediate compounds to fatty acids and alcohols, etc. Subsequently, these compounds can be fermented by syntrophic or homoacetogenic bacteria to precursor substrates, such as acetate or $H_2 + CO_2$, for acetoclastic and hydrogenotrophic methanogens. Methanogenesis involves a specialized microflora that requires strict anaerobic conditions with low oxydo-reduction potentials ($Eh < -200$ mV, e.g., Thauer et al. 1977; Zinder 1993).

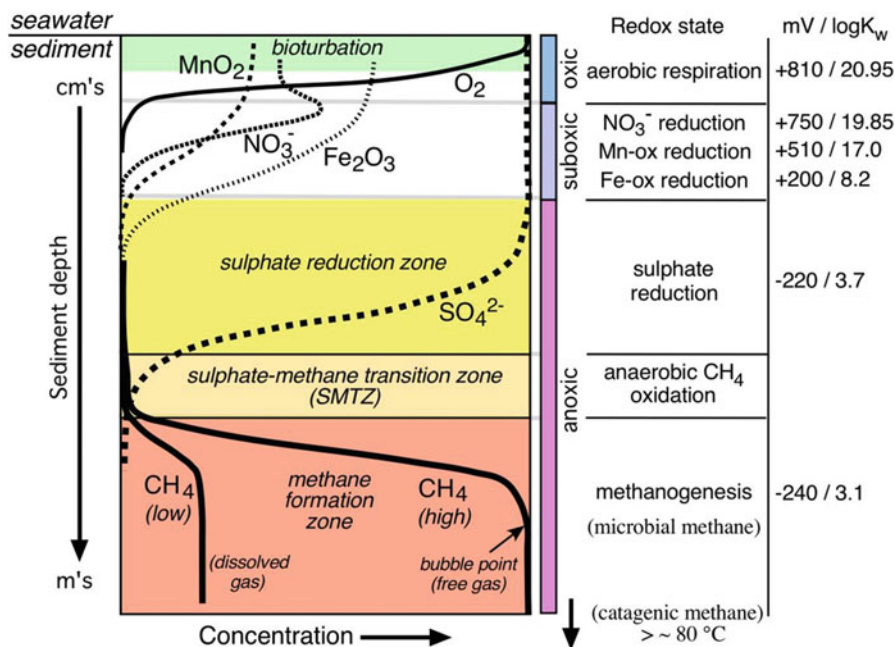


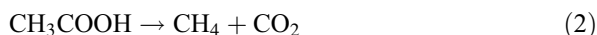
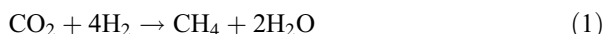
Fig. 6 Schematic representation of diagenetic depth/redox zonation in marine sediments with the corresponding compound depth distributions. Redox potentials (mV) and log K_w 's for CH_2O oxidation and TEAs along the redox ladder (standard conditions) are shown to the right (Stigliani 1988; Sikora et al. 2017). The bioturbation, sulfate reduction (SRZ), and sulfate-methane transition (SMTZ) zones are indicated in the figure

This anaerobic digestion of organic matter essentially involves heterotrophic bacteria converting larger organic bio-/geopolymers into small molecules, such as acetate, CO_2 , or substances containing a methyl group, that methanogens can utilize (e.g., Liu and Whitman 2008). This remineralization of organic matter to methane operates sympathetically with the remineralization free energy levels shown in Fig. 6.

Over the past century, since the isolation of a methanogen from mud by Stephenson and Strickland (1933) and the identification in the 1960s of archaea-specific lipids (e.g., Kates 1966), considerable progress has been made in understanding the biogeochemistry of methane. Certainly, critical was the definition of the domain Archaea as a distinct phylogenetic group using molecular biology with small rRNAs (e.g., Woese and Fox 1977). This phylogenetic system reclassified methanogens as Euryarchaeota from the original bacteria designation and also as distinct from eukaryotes (Woese et al. 1990). Currently, there are 26 methanogenic genera and over 110 known species of methanogens (NCBI 2017), and they are cosmopolitan with respect to environmental conditions, including many extremophiles (e.g., Bürgmann 2011; Plasencia et al. 2011). Initially, all methanogens were classified into the archaeal phylum Euryarchaeota. Recently, they were subdivided into the seven orders: *Methanobacteriales*, *Methanococcales*,

Methanomicrobiales, *Methanosarcinales*, *Methanocellales*, *Methanopyrales*, and *Methanomassiliicoccales* (e.g., Hedderich and Whitman 2013). Methanogens are also divided as to whether or not they have cytochromes (Thauer et al. 2008) or into the five groups based on the substrate they utilize, i.e., hydrogenotrophs, acetotrophs, methylotrophs, formatotrophs, or alcoholotrophs (Garcia et al. 2000; Le Mer and Roger 2001).

Methanogens are the microbial fermentative stage in largely, but not exclusively, anaerobic environments that convert single-carbon compounds into the catabolic end-product methane. The two most commonly described pathways are (1) hydrogenotrophic methanogenesis (Eq. 1), which involves the utilization of inorganic carbon dioxide, and (2) acetoclastic methanogenesis (Eq. 2), which uses acetate as the terminal electron acceptor (“TEA”) by dismutation (Fig. 5) (e.g., Barker and Buswell 1956; Zeikus 1977; Mah et al. 1977; Weimer and Zeikus 1978; Weiss and Thauer 1993; Demirel and Scherer 2008):



The former (also referred to in the early literature as “carbonate reduction methanogenesis”) is thought to be the ancestral methanogenic form (Baptiste et al. 2005). The relative contributions of these two pathways generally depend on the abundance of either H₂-oxidizing CO₂-reducing acetogenic species (Kotelnikova and Pedersen 1998) or acetate-oxidizing H₂-producing anaerobes (Zinder and Koch 1984), respectively.

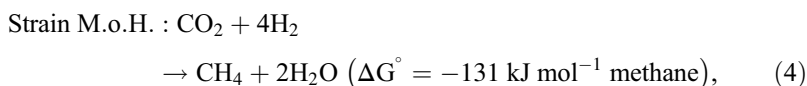
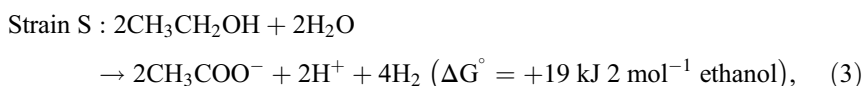
A third, general methanogenic pathway is methylotrophic methanogenesis (e.g., Thauer et al. 2008; Lang et al. 2015). In this case, simple C1-bearing compounds, such as methanol, methylamines, and methylsulfides, can serve as substrates for methanogens, often termed as “noncompetitive substrates” (e.g., King et al. 1983; Oremland 1988; Kuivila et al. 1989; Table 1). Methylotrophic methanogenesis can follow either the hydrogen-dependent or hydrogen-independent pathways, using coenzyme M or B, respectively (Keltjens and Vogels 1993; Sikora et al. 2017; Lackner et al. 2018). Some methanogens can utilize carbon monoxide, but growth is very slow (e.g., Fischer et al. 1931; Daniels et al. 1977; Rother and Metcalf 2004; Diender et al. 2015). Acetoclastic methanogenesis (sometimes in the literature referred as “methyl-type fermentation”) comprises roughly 2/3 of the microbial methane (estimated range is 50–90%) (e.g., Huser et al. 1982; Ferry 1992; Conrad and Klose 1999; Le Mer and Roger 2001; Kotsyurbenko et al. 2004; Valentine et al. 2004; Goevert and Conrad 2009).

In addition, methanogens can operate in a range of syntrophic relationships with other organisms thereby accessing a wider range of precursor compounds, such as sugars, fatty acids, ketones, and alcohols, that can result in methane formation (e.g., Barker 1936a, b); Schnellen 1947; Bryant et al. 1967; Tatton et al. 1989; Schink 1997; Hattori 2008; Wrede et al. 2012). For example, Schink (1997) described how the *Methanobacillus omelianskii* culture with strains S and M.o.H. use interspecies

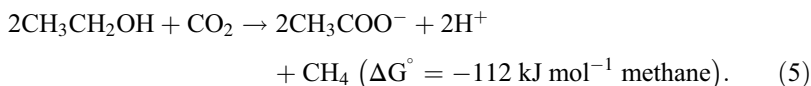
Table 1 Common methanogenic substrates (¹competitive hydrogenotrophic, ²competitive acetoclastic, ³noncompetitive substrates, ⁴involves syntrophy). Free energies (ΔG°) are at standard state and pH = 7, but ΔG° will vary in nature with actual activities of the reactants and environmental conditions. (After Rother and Metcalf 2004; Whitman et al. 2006; Liu and Whitman 2008)

Substrates	Representative reactions	ΔG° (kJ mol ⁻¹ of CH ₄)
Carbon dioxide + hydrogen gas ¹	$\text{CO}_2 + 4\text{H}_2 \rightarrow \text{CH}_4 + 2\text{H}_2\text{O}$	-131
Acetate ² (acetic acid) ¹ + proton	$\text{CH}_3\text{COO}^- + \text{H}^+ \rightarrow \text{CH}_4 + \text{CO}_2$	-36
Formate ³	$4\text{HCOO}^- \rightarrow \text{CH}_4 + 3\text{CO}_2 + 2\text{H}_2\text{O}$	-130
Methanol ³ + hydrogen gas	$\text{CH}_3\text{OH} + \text{H}_2 \rightarrow \text{CH}_4 + \text{H}_2\text{O}$	-113
Methanol ³ (hydrogen independent)	$4\text{CH}_3\text{OH} \rightarrow 3\text{CH}_4 + \text{CO}_2 + 2\text{H}_2\text{O}$	-105
Ethanol ^{3,4} /(1-propanol ^{3,4} and 1-butanol ^{2,4}) + carbon dioxide	$2\text{C}_2\text{H}_5\text{OH} + \text{CO}_2 \rightarrow \text{CH}_4 + 2\text{CH}_3\text{COO}^- + 2\text{H}^+$	-112
Carbon monoxide + water	$4\text{CO} + 5\text{H}_2\text{O} \rightarrow \text{CH}_4 + 3\text{HCO}_3^- + 3\text{H}^+$	-196
Methylamine ³ + water	$4\text{CH}_3\text{NH}_3^+ + 2\text{H}_2\text{O} \rightarrow 3\text{CH}_4 + \text{CO}_2 + 4\text{NH}_4^+$	-75
Dimethylamine ³ + water	$2(\text{CH}_3)_2\text{NH}_2^+ + 2\text{H}_2\text{O} \rightarrow 3\text{CH}_4 + \text{CO}_2 + 2\text{NH}_4^+$	-73
Trimethylamine ³ + water	$4(\text{CH}_3)_3\text{NH}^+ + 6\text{H}_2\text{O} \rightarrow 9\text{CH}_4 + 3\text{CO}_2 + 4\text{NH}_4^+$	-74
Dimethylsulfide ³ + water	$2(\text{CH}_3)_2\text{S} + 2\text{H}_2\text{O} \rightarrow 3\text{CH}_4 + \text{CO}_2 + \text{H}_2\text{S}$	-74

hydrogen transfer to syntrophically convert ethanol to methane and acetate by the following reactions (Eqs. 3, 4, and 5):



and the overall reaction



Methanogenic archaea produce organic biomarker compounds that can be used as specific molecular indicators of these organisms. When preserved in certain settings, such as sediments and soils, these archaeal biomarkers may potentially offer time records of environmental conditions. For example, archaea use irregular, acyclic isoprenoids as structural compounds for their membranes. These diagnostic compounds, including 2, 6, 10, 15, 19-pentamethylcosenes (PMIs), have been related to

methanogens (e.g., Tornabene et al. 1979; Brassell et al. 1981; Sinninghe Damsté et al. 1997) and anaerobic methanotrophs (e.g., Elvert et al. 1999; Thiel et al. 1999).

Archaea also synthesize polar membrane lipids that may in some cases be distinctive from bacteria, such as certain glycerol dialkyl diether (DGDs), such as archaeol and hydroxyarchaeol, glycerol dialkyl glycerol tetraether (GDGT), and glycerol-dialkyl-nonitol tetraether (GDNT) lipids, e.g., where isoprenoids are ether-bound to glycerol to make the lipid's hydrophobic end (Kates et al. 1963; De Rosa and Gambacorta 1988). Initially, some of these isoprenyl glycerol ethers were postulated to be related only to extremophiles, but they are now known to be commonly synthesized by other archaeal groups and occur in a broad range of environments, such as marine and lacustrine sediments (e.g., Michaelis and Albrecht 1979; Chappe et al. 1982). Subsequently, investigators identified various forms of GDGTs, including non-isoprenoid GDGTs, those with 0 to 8 cyclopentane moieties, crenarchaeol, and those with branched carbon skeletons (e.g., Sinninghe Damsté et al. 2000, 2002). GDGTs with methylated isoprenoid chains have been found in *Methanothermobacter thermautotrophicus* (Knappy 2010), but the assignment is not necessarily exclusive to this methanogen. The occurrence of GDGTs in both archaea and possibly their emerging presence in bacteria and a multitude of environments, including methanotrophy, makes the use of these compounds as biomarkers for methanogens increasingly more complicated and less specific than initially hoped (e.g., Schouten et al. 2012; Naeher et al. 2014).

The stable carbon and hydrogen isotopes of methane ($^{13}\text{C}/^{12}\text{C}$ and $^2\text{H}/^1\text{H}$ also denoted D/H) are helpful parameters to differentiate methanogenic pathways, such as hydrogenotrophic methanogenesis from those involving preformed substrates, e.g., acetate, formate, methylamines, etc. (Whiticar 1999; Hornibrook et al. 1997; Valentine et al. 2004; Londry et al. 2008). Stable isotopes are also useful to distinguish microbial methane from other sources, such as thermogenic, geothermal, and abiogenic (Lyon and Hulston 1984; Schoell 1988; Whiticar 1994; Etiope and Sherwood Lollar 2013). Stable isotope ratios in natural sciences are typically expressed for convenience in the standard delta notation (δ) as the deviation in ‰ from a standard, e.g., $\delta^{13}\text{C}-\text{CH}_4$ (sometimes shortened to $\delta^{13}\text{CH}_4$) and $\delta^2\text{H}-\text{CH}_4$ (also written as $\delta\text{D}-\text{CH}_4$), i.e., Eq. 6:

$$\delta_x(\text{‰}) = \left(\frac{R_x - R_{std}}{R_{std}} \right) \cdot 1000, \quad (6)$$

where R is the isotope ratio, for example, the $^{13}\text{C}/^{12}\text{C}$ or $^2\text{H}/^1\text{H}$ of the sample “x” and isotope reference standard “std” (generally VPDB for carbon and VSMOW for hydrogen, e.g., Verkouteren and Klinedinst 2004).

The magnitude of the isotope effect that partitions the isotopes between phases (A and B) is quantified as the fractionation factor (α_{A-B}):

$$\alpha_{A-B} = \alpha_B^A = \left(\frac{R_A}{R_B} \right), \quad (7)$$

which can be rewritten in δ notation as

$$\alpha_{A-B} = \frac{\delta_A + 1000}{\delta_B + 1000}. \quad (8)$$

For simplification, some authors prefer enrichment factors (ϵ) that recast α_{A-B} as

$$\epsilon_{A-B} \approx 10^3 \ln \alpha_{A-B} \approx 10^3 (\alpha_{A-B} - 1). \quad (9)$$

The enrichment factor (ϵ) is approximately the same as the isotope separation provided the differences are small, i.e., typically $<25\%$, so

$$\epsilon_{\text{CO}_2-\text{CH}_4} \approx \delta^{13}\text{CO}_2 - \delta^{13}\text{CH}_4. \quad (10)$$

It should be noted that methanogenesis, especially hydrogenotrophic methanogenesis, can have $\delta^{13}\text{CO}_2 - \delta^{13}\text{CH}_4 > 25\%$, so $\alpha_{\text{CO}_2 - \text{CH}_4}$ is preferred for rigorous calculations of isotope separation.

The stable C- and H-isotope signatures of the different methane sources can be shown by cross-plotting $\delta^{13}\text{C}-\text{CH}_4$ versus $\delta^2\text{H}-\text{CH}_4$ (CD plot, Fig. 7, after Whiticar 1999). In general, the combination of the C- and H isotopes give signatures for hydrogenotrophic methanogenesis (HM) that can be distinguished from acetoclastic

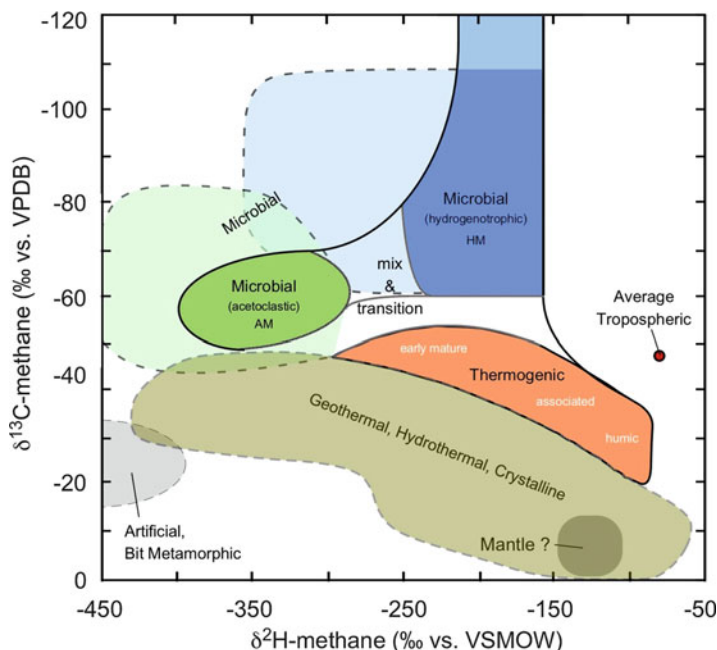


Fig. 7 Carbon and hydrogen stable isotope (CD) plot to isotopically characterize various sources of biotic and abiotic methane. (After Whiticar 1999)

methanogenesis (AM). In addition to the microbial methane, Fig. 7 also shows the typical isotope regions for thermogenic, hydrothermal, and abiogenic gases and how they also can be distinguished from microbial methane. Although other papers have reversed the axes of the CD plot (e.g., Schoell 1980; Etiope and Sherwood Lollar 2013), my historical rationale for plotting $\delta^{13}\text{C}\text{-CH}_4$ on the ordinate axis and increasing upward with ^{12}C -enriched values (e.g., Whiticar et al. 1986) is to help illustrate the typical, vertically downward depth trend of diagenesis to catagenesis observed in nature, e.g., normally encountered during drilling of a well. It should also be noted that Fig. 7 is an empirical diagram, whereby the fields are delineated by “primary gases,” i.e., those thought to be representative of the gas types and not “secondary gases,” which may have been influenced by mixing or alteration processes. Milkov and Etiope (2018) sorted the C- and H-isotope data on over 20,000 natural gases as microbial, thermogenic, and abiogenic. Their classified data on the CD plot, shown in Fig. 8, shows general agreement with the established fields in Fig. 7, although the assignments to specific gas types or whether or not the gas is “primary” remains subjective.

Several processes can shift the typical isotope signature for microbial gases in addition to the type of methanogenic pathway. These include variations in the carbon and hydrogen ratios of the precursor materials (shown by the heavy dashed box in Fig. 9). There are also secondary effects, such as mixing of methane from different

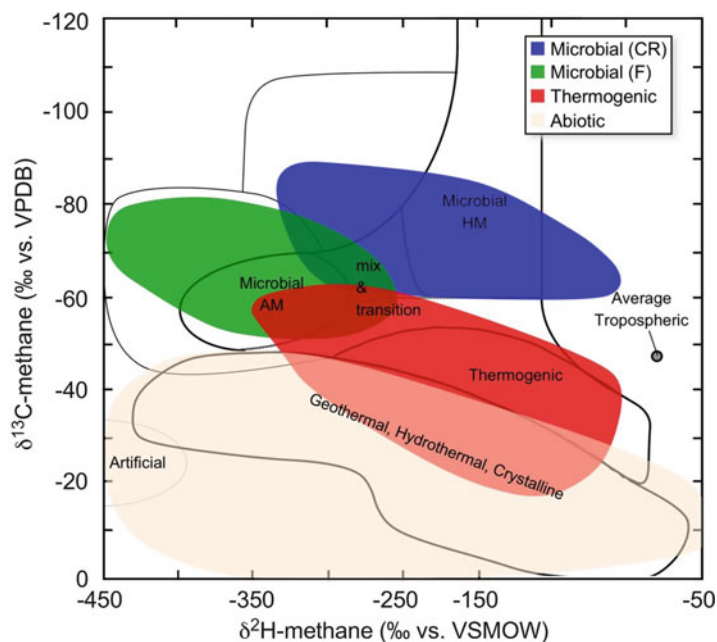


Fig. 8 Extension of carbon and hydrogen stable isotope plot of Whiticar (1999) (shown in outline) using the >20,000 data points from Milkov and Etiope (2018) to delineate biotic and abiogenic methane types

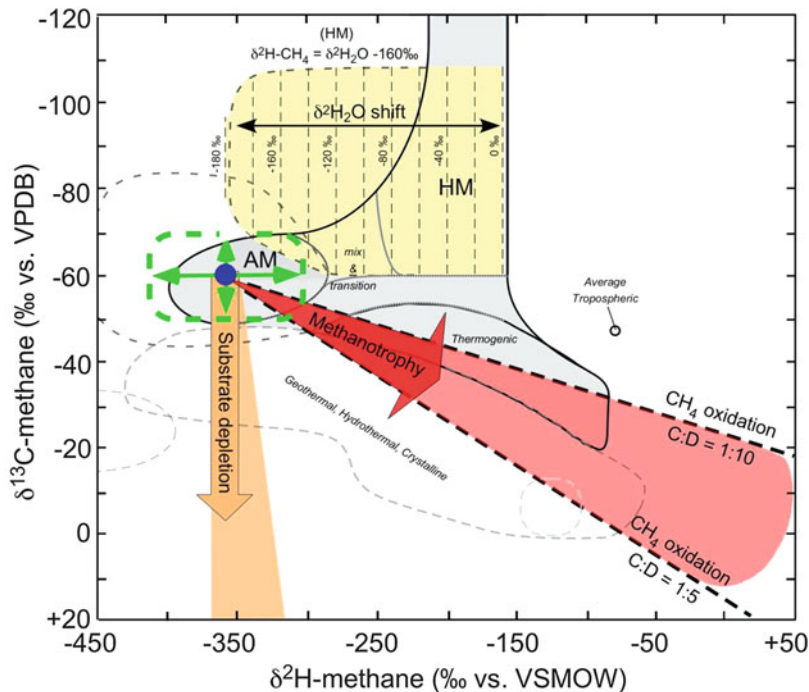
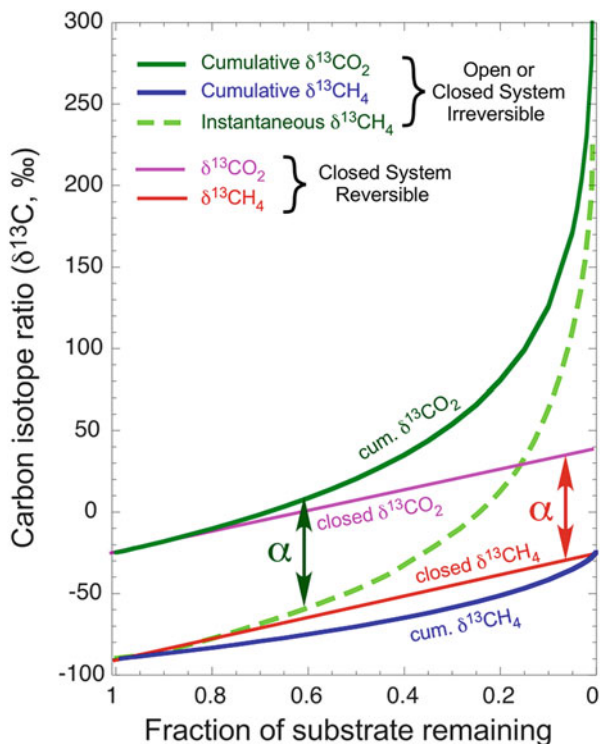


Fig. 9 Potential shifts in carbon and hydrogen stable isotope ratios for methane due to variations in precursor substrates (heavy dash and arrows), precursor $\delta^2\text{H}$ -water (grid), and due to secondary effects, such as substrate depletion and methane oxidation. (After Whiticar 1999)

microbial pathways and with nonmicrobial methane, or methane oxidation, that create diagnostic shifts in $\delta^{13}\text{C}$ - CH_4 versus $\delta^2\text{H}$ - CH_4 values from unaltered methane signatures. The utilization of the carbon substrates, e.g., CO_2 or acetate, etc., by methanogens is associated with isotope effects that usually deplete the lighter isotopologue (e.g., $^{12}\text{CO}_2$) in the substrate pool at a higher rate than the heavier isotopologue (e.g., $^{13}\text{CO}_2$). As the substrate pool is consumed, the remaining carbon becomes increasingly ^{13}C -enriched, generally following a Rayleigh relationship (Rayleigh 1896; Claypool and Kaplan 1974; Mahieu et al. 2006). This relationship depends on system conditions, such as open versus closed and reversible versus irreversible reactions as shown in Fig. 10 (e.g., Mariotti et al. 1981; Rooney et al. 1995; Hayes 2001). Because the pool of precursor hydrogen (water) is typically very much larger compared with the amount of hydrogen in methane, generally no hydrogen depletion effect is observed. The carbon shift due to substrate depletion is illustrated in CD plot in Fig. 9.

The magnitudes of kinetic isotope effects (KIE) are generally dependent on temperature, i.e., KIE decreases as temperature increases. This relationship of KIE on temperature was observed for field and culture data of methanogenesis over the temperature range of $-1.3\text{ }^\circ\text{C}$ to $110\text{ }^\circ\text{C}$ with $\epsilon_{\text{CO}_2 - \text{CH}_4}$ decreasing from 9 to ~ 3.5

Fig. 10 Rayleigh approximated shifts in carbon stable isotope ratios of reactants (CO_2) and products (CH_4 , dashed = instantaneous, solid = cumulative) for open, closed, reversible, and irreversible systems. (After Rooney et al. 1995; Hayes 2001)



(Fig. 11, Whiticar et al. 1986; Botz et al. 1996; Whiticar 1999; Fey et al. 2004). In contrast, culture experiments with various substrates by Penger et al. (2014) did not observe any change in ϵ_C over the range of 25–68 °C, so this question of temperature sensitivity is not yet fully resolved and that in some cases the influence of temperature on KIE may be masked by other factors.

The $\delta^2\text{H-H}_2\text{O}$ of the formation water from which the methanogens directly or indirectly derive their hydrogen determines the $\delta^2\text{H-CH}_4$ value along with distinguishing the methanogenic pathway (Schoell 1980; Whiticar et al. 1986; Balabane et al. 1987). Figure 12 shows the expected relationship between the formation water $\delta^2\text{H-H}_2\text{O}$ and the $\delta^2\text{H-CH}_4$ for both hydrogenotrophic methanogenesis (HM) and acetoclastic methanogenesis (AM). The relationships are defined as

$$\delta^2\text{H}_{\text{CH}_4} = m \cdot \delta^2\text{H}_{\text{H}_2\text{O}} - \beta, \quad (11)$$

where m , the slope, is 1.0 for HM and 0.25 for AM depending on the direct versus indirect (intact hydrogen transfer) (Daniels et al. 1980). The offset, β , is determined empirically from natural and culture samples to be around -160 to -180 ‰ for HM and ~ -325 ‰ for AM (Whiticar 1999). Mixtures between the HM and AM processes are commonly found, e.g., Waldron et al. (1999) reported values of

Fig. 11 Dependence of ϵ_C ($\text{CO}_2\text{-CH}_4$) on growth temperature. (After Whiticar 1999; Fey et al. 2004)

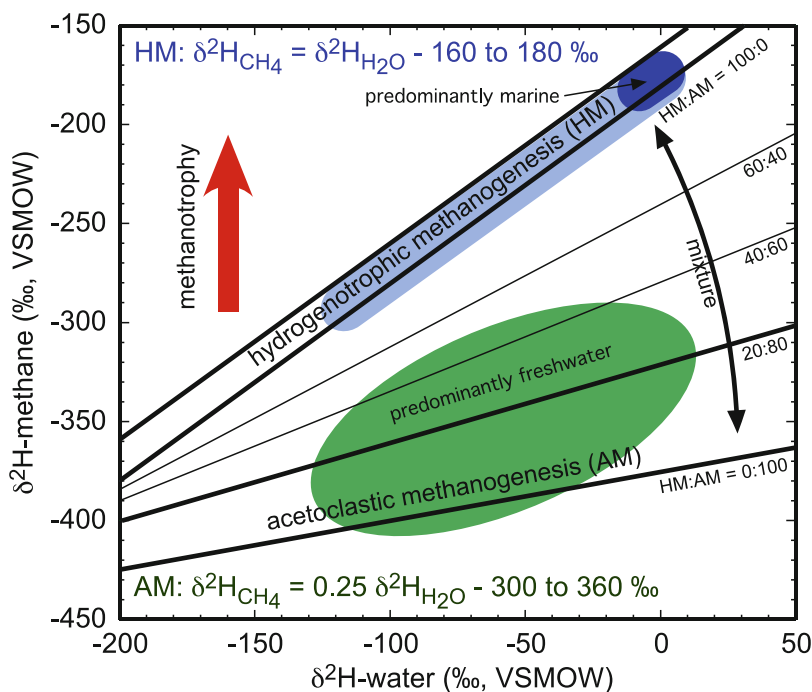
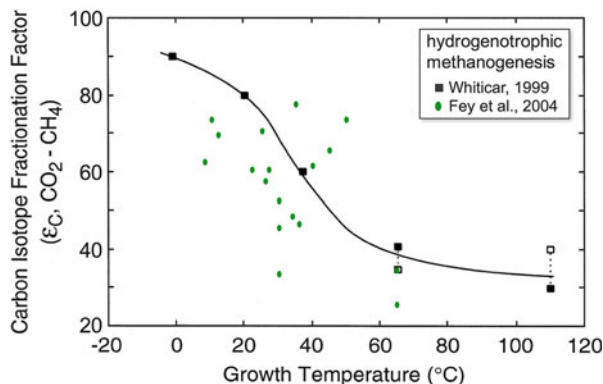
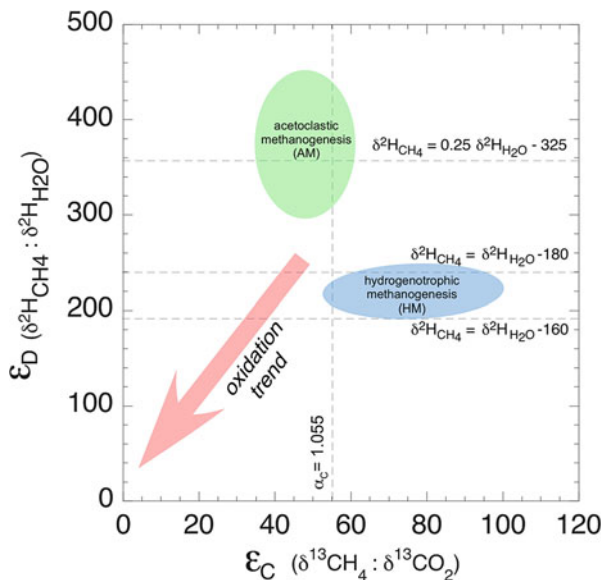


Fig. 12 Dependence of the $\delta^2\text{H-CH}_4$ for the HM and AM pathways on the associated formation water $\delta^2\text{H-H}_2\text{O}$. Mixing slopes between HM and AM and the direction for methanotrophy are shown. The wider range in the predominantly freshwater environments region is largely related to mixtures of AM and HM pathways. The approximate trajectory for methane oxidation is also indicated. (After Whiticar 1999)

0.675 for m and -284 ‰ for β (Eq. 11) from freshwater wetlands with $\delta^2\text{H-H}_2\text{O}$ values ranging from -130 ‰ to $+10$ ‰. The consequence of the dependency of $\delta^2\text{H-CH}_4$ on $\delta^2\text{H-H}_2\text{O}$ is illustrated for HM in Fig. 9. The shift in $\delta^2\text{H-CH}_4$, as

Fig. 13 Differentiation of hydrogenotrophic (HM) and acetoclastic (AM) methanogenic pathways based on carbon ($\delta^{13}\text{C}\text{-CO}_2$ and $\delta^{13}\text{C}\text{-CH}_4$) and hydrogen ($\delta^2\text{H}\text{-H}_2\text{O}$ and $\delta^2\text{H}\text{-CH}_4$) isotope separations, respectively, $\epsilon_{\text{C}(\text{CO}_2\text{-CH}_4)}$ and $\epsilon_{\text{D}(\text{H}_2\text{O}\text{-CH}_4)}$. The approximate ϵ_{C} , ϵ_{D} slope for methane oxidation is also indicated



shown, can be dramatic especially for environments with isotopically light formation water, e.g., high-latitude regions. The original HM region in Fig. 7 was largely defined for marine environments ($\delta^2\text{H}\text{-H}_2\text{O} \sim 0\%$) and must be corrected for the actual $\delta^2\text{H}\text{-H}_2\text{O}$ utilized by the methanogens. The different dependence of $\delta^2\text{H}\text{-CH}_4$ on $\delta^2\text{H}\text{-H}_2\text{O}$ for hydrogenotrophic and acetoclastic methanogenic pathways can also be expressed in terms of $\epsilon_{\text{D}(\text{H}_2\text{O}\text{-CH}_4)}$ (Eq. 9). The former (HM) typically has $\epsilon_{\text{D}(\text{H}_2\text{O}\text{-CH}_4)}$ around 160–200, while AM is larger from ~ 300 to 450 (Fig. 13).

There can also be a carbon isotope relationship between CO_2 and CH_4 , which can be exploited to further distinguish between various methane pathways and types. The delineation of HM and AM methanogenic pathways is based on their distinctive separations between $\delta^{13}\text{CO}_2$ and $\delta^{13}\text{CH}_4$ ($\epsilon_{\text{C}(\text{CO}_2\text{-CH}_4)}$). This approach is valid only if there is a direct microbial relationship between CO_2 and CH_4 (coexisting pairs) in the gas measured, i.e., the microbial processes essentially modulate the $\delta^{13}\text{CO}_2$ and $\delta^{13}\text{CH}_4$. In cases where CO_2 or CH_4 are not coupled, e.g., admixture of allochthonous CO_2 or CH_4 , such as additions of unrelated thermogenic CH_4 or inorganic CO_2 , then the use of this $\text{CO}_2\text{-CH}_4$ coexisting pair relationship can be compromised. An alternative approach is to compare the $\delta^{13}\text{C}$ of the precursor organic substrate with $\delta^{13}\text{CH}_4$ (e.g., Summons et al. 1998). Figure 14 illustrates the empirically defined regions of $\epsilon_{\text{C}(\text{CO}_2\text{-CH}_4)}$ for HM and AM pathways together with those for thermogenic gas and atmospheric methane. The general trend for CH_4 oxidation and CO_2 evolution is also depicted, although the magnitude and slope depend on degree of consumption and the TEA involved, e.g., O_2 or SO_4^{2-} (Coleman et al. 1981; Whiticar 1999). Although a $\epsilon_{\text{C}(\text{CO}_2\text{-CH}_4)}$ of ~ 55 has been used in the past to demarcate AM from HM (Fig. 14), this is not a robust measure, and there are examples where this is clearly violated. A more robust approach to demarcate AM

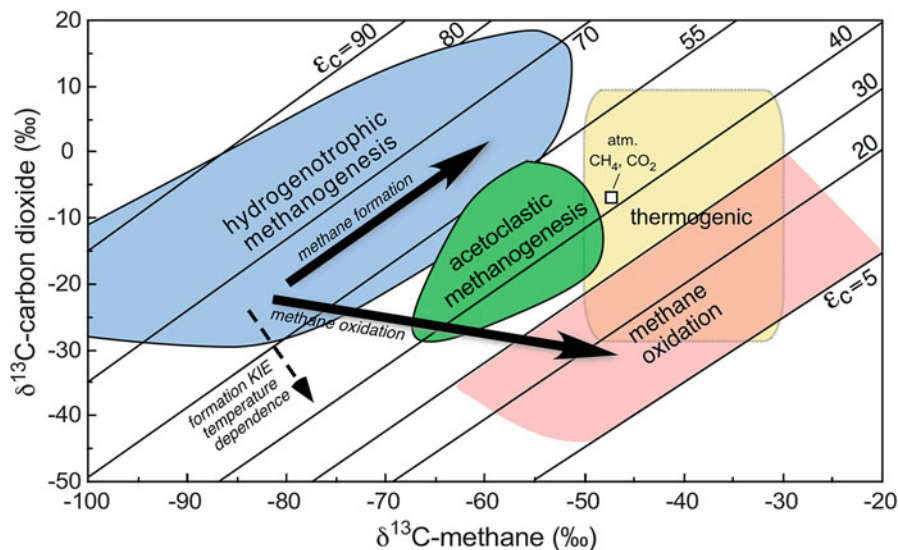


Fig. 14 Empirical differentiation of hydrogenotrophic (HM) and acetoclastic (AM) methanogenic pathways based on $\delta^{13}\text{C-CO}_2$ and $\delta^{13}\text{C-CH}_4$ of coexisting CO_2 or CH_4 . The isotope separation lines shown are given as $\epsilon_{\text{C}(\text{CO}_2\text{-CH}_4)}$ (Eq. A). For reference, the $\delta^{13}\text{C-CO}_2\text{-}\delta^{13}\text{C-CH}_4$ regions of atmospheric, thermogenic, and methane oxidation are shown, along the generalized methanogenic and methanotrophic trajectories (after Whiticar 1999). The thin dashed line shows the direction for a possible temperature dependence of the KIE during methanogenesis

from HM is the combination of $\epsilon_{\text{D}(\text{H}_2\text{O-CH}_4)}$ and $\epsilon_{\text{C}(\text{CO}_2\text{-CH}_4)}$ as shown in Fig. 13. An important feature of this plot is that the absolute isotope ratios for the gas and water are not important, rather just the magnitudes of the separation between $\delta^2\text{H-H}_2\text{O}-\delta^2\text{H-CH}_4$ and $\delta^{13}\text{CO}_2-\delta^{13}\text{CH}_4$.

Molecular ratios, such as $\text{CH}_4/\text{C}_2\text{H}_6$ or $\text{CH}_4/(\text{C}_2\text{H}_6 + \text{C}_3\text{H}_8)$ (aka Bernard parameter or $\text{C}_1/(\text{C}_2 + \text{C}_3)$, Bernard et al. 1976), are frequently used to distinguish microbial gas from thermogenic sources. The concept is based on the low amounts of microbially formed ethane and propane compared to methane, i.e., $\text{C}_1/(\text{C}_2 + \text{C}_3) > 100$ or even much higher ($\sim 10^5$). Thermogenic “wet” gases often have $\text{C}_1/(\text{C}_2 + \text{C}_3) < 50$, but high maturity or humic thermogenic gases, e.g., shale gases, coal gases, etc., can be “dry” gases with $\text{C}_1/(\text{C}_2 + \text{C}_3) \sim 10^2\text{-}10^3$. Typically to distinguish microbial from thermogenic gas, $\text{C}_1/(\text{C}_2 + \text{C}_3)$ is combined with $\delta^{13}\text{CH}_4$ to generate the Bernard diagram (Bernard et al. 1976).

Figure 15 is a rendition of this Bernard diagram that illustrates the regions occupied by the different gas types (Whiticar 1994). In addition, the trajectories of the secondary effects of mixing, migration, maturation (vitrinite reflectance or VR), and methane oxidation are shown. The magnitudes of microbial formation of ethane and propane have been long-standing issues, particularly as they can confound the signature of thermogenic gases used in petroleum exploration (Claypool 1999). In recent sediments and soils, usually there are at least trace levels of higher light

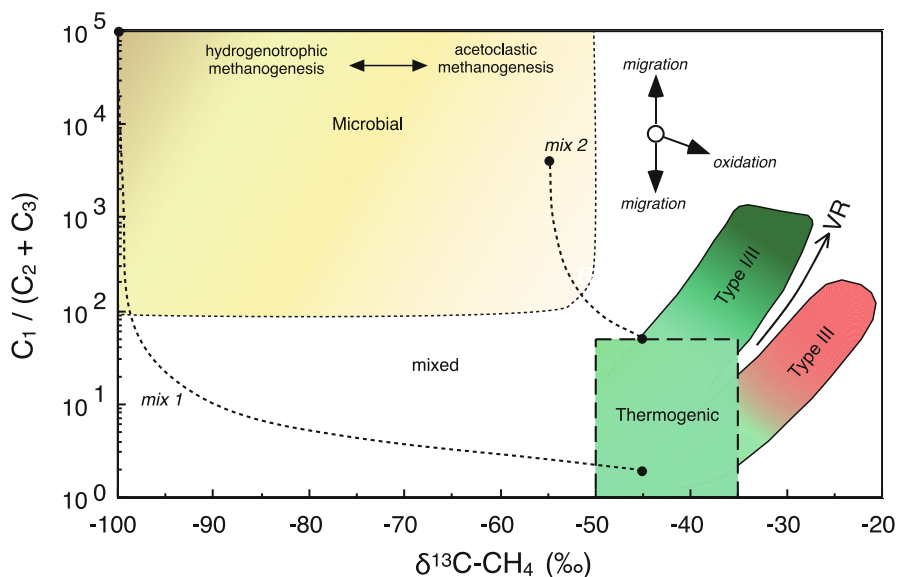


Fig. 15 Bernard diagram that combines the hydrocarbon gas molecular ratio ($C_1/[C_2 + C_3]$) and $\delta^{13}C\text{-CH}_4$ (after Bernard 1976; Whiticar 1994). The different methanogenic pathways and thermogenic types and maturities (VR), as well as the trajectories for mixing, migration, and oxidation, are shown

hydrocarbons (ethane-propane) present. Determination of the origin of these low amounts of light hydrocarbons is often challenging and potentially from a variety of microbial, thermogenic, abiotic, etc. sources and histories (Whelan et al. 1980; Vogel et al. 1982). Oremland et al. (1988) demonstrated microbial ethane formation from reduced, ethylated sulfur compounds, namely, ethanethiol (ESH) and diethylsulfide (DES), in gas samples and cultures from anoxic sediments from multiple locations. They also reported minor propanogenesis from propanethiol. The incubations required higher H_2 levels and 2-bromoethanesulfonic acid (BES), a (imperfect) methanogenesis inhibitor. Subsequently, others have reported microbial ethane in cultures (Koene-Cottaar and Schraa 1998) and surface casing vent flow from well bores (Taylor et al. 2000). Ethanogenesis and propanogenesis have also been shown by Hinrichs et al. (2006) and Xie et al. (2013) from incubation of tidal flat muds with ethanethiol, propanethiol, and BES, albeit with low H_2 levels. This suggests that the product ethylene was more important than H_2 for the ethanogenesis. Their archaeal 16S rRNA analyses also suggest that the order Methanomicrobiales (*Methanocalculus* spp.) were potentially responsible for the C_2 and C_3 formation.

Although methanogens are referred to as obligate anaerobes (Wolfe 1971), there are studies showing that they function or exist for periods of time in oxic settings as methanogenic endosymbionts in anaerobic ciliates (Schwarz and Frenzel 2005) or oxygen-limited settings (Kiener and Leisinger 1983; Kirby et al. 1981; Huser et al. 1982; Peters and Conrad 1996; Zitomer 1998) and in microniches (Field et al. 1995).

It has long been recognized due to the presence of methane oversaturation in the ocean upper water column that microbial methane formation can occur in these oxygenated surface waters (Lamontagne et al. 1973; Scranton and Brewer 1977; Burke Jr et al. 1983). This “oceanic methane paradox” (Kiene 1991) has been explained by several sources, including enteric methane production, i.e., in zooplankton and fecal pellets (e.g., Traganza et al. 1979; Sieburth 1987; Bianchi et al. 1992; Marty 1993; Karl and Tilbrook 1994), microbial methane formation in anaerobic microzones (Rusanov et al. 2004), leaching of nearshore groundwaters (Brooks 1979), or advection from shelf sources (Ward 1992).

More recently, alternative non-methanogenic explanations have been proposed, such as methane formation as a by-product of the bacterial degradation of dimethylsulfoniopropionate precursors from phytoplankton metabolism (e.g., Karl et al. 2008; Damm et al. 2010), aerobic microorganisms utilizing phosphonate esters (Kamat et al. 2013; Repeta et al. 2016), or marine algae (Lenhart et al. 2016). These non-archaeal sources are analogous to the aerobic, abiotic methane formation in plants and soils reported by, e.g., Keppler et al. (2006) and Jugold et al. (2012).

The diversity of methanogens and methanogenic pathways is controlled at a larger scale by growth environments. However, as is well illustrated by the above “oceanic methane paradox,” such traditional classifications, e.g., marine or terrestrial, provide some guidance but are generally too simplistic. Factors, including diagenetic position, availability of “competitive” versus “noncompetitive” substrates for methanogens, microbial oxidation, etc., can dramatically influence the occurrence and distribution of methane.

3 Microbial Methane in Marine Environments

The estimate for the amount of microbial methane generated in marine sediments is largely uncertain, but it comprises roughly 1/3 of the naturally generated, microbial methane (estimated range is 10–40%). This estimate is confounded by a suite of factors, including the production and consumption rates and the transport mode (e.g., diffusion, advection, seepages) in the sediments. In addition, thermogenic and abiotic sources can both contribute to the marine sediment methane budget, particularly by submarine seepages (Etiope and Klusman 2002). For marine sediment microbial methane generation, Reeburgh et al. (1993) reported ~ 80 Tg CH_4 year⁻¹, Hovland et al. 1993 suggested 8–65 Tg CH_4 year⁻¹, whereas Hinrichs and Boetius (2002) cited ~ 300 Tg CH_4 year⁻¹. Modelling by Wallmann et al. (2006) reduced these estimates to a range of 5–33 Tg CH_4 year⁻¹, with a preferred value of ~ 13 Tg CH_4 year⁻¹, similar to 26 Tg CH_4 year⁻¹ given by Boetius and Wenzhöfer (2013). Methane emissions from the marine environment (sediments and water column sources) to the atmosphere are also not well constrained and have been estimated to be 10–30 Tg CH_4 year⁻¹ (Watson et al. 1990; Kvenvolden and Rogers 2005; Boetius and Wenzhöfer 2013).

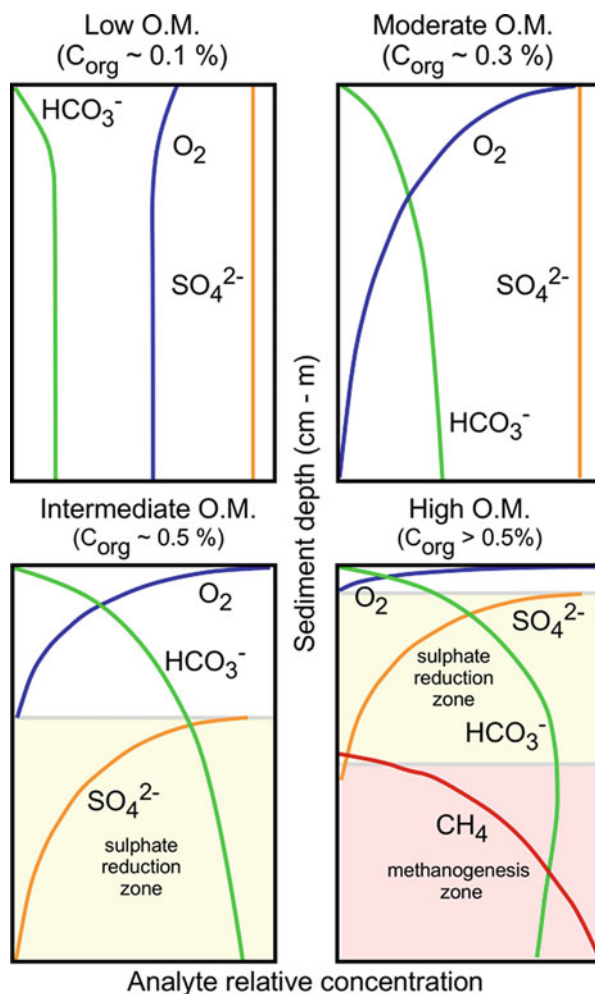
Since the 1970s (e.g., Froelich et al. 1979; Berner 1980), a diagenetic sequence for the remineralization of organic matter has been recognized for marine sediments based on redox and free energy associated with the reactions (Table 2).

Stumm and Morgan (1981) and Stigliani (1988) clearly illustrated the cascading series of oxidation-reductions or “redox ladder” associated with organic matter remineralization. As a consequence, there is a diagenetic succession with marine sediment depth for the remineralization of organic matter, as represented schematically in Fig. 6. As remarked by Jørgensen (1977), different physiological groups show a zonation similar to the chemical ones. For example, in marine sediments, the activity of SRBs typically removes acetate before it can become available for methanogens. In such cases, methanogenesis by the hydrogenotrophic pathway (Eq. 1) dominates over the acetoclastic pathway (Eq. 2).

Table 2 Energetics of selected diagenetic reactions for organic matter remineralization and methane oxidation in marine sediments. (From Zinder 1993; Schink 1997; Thauer 1998; Amend and Shock 2001; Deutzmann and Schink 2011; Ferry 2011; Whitman et al. 2006). Note: Free energies are at standard state and will vary in nature with actual temperature, pressure, and the choice and actual activities of the reactants

Diagenetic stage	Representative formula	ΔG° (kJ mol ⁻¹ , 25 °C)
Propionate metabolism/ acetogenesis	$C_2H_5COO^- + 3H_2O \rightarrow CH_3COO^- + HCO_3^- + H^+ + 3H_2$	+76
Butyrate metabolism/ acetogenesis	$C_3H_7COO^- + 2H_2O \rightarrow 2CH_3COO^- + H^+ + 2H_2$	+49
Oxic respiration	$CH_4 + 2O_2 \rightarrow CO_2 + 2H_2O$	-883
Aerobic methane oxidation	$CH_3COOH + 2O_2 \rightarrow 2CO_2 + 2H_2O$	-818
Nitrate reduction	$CH_3COOH + 8/5NO_3^- + 8/5H^+ \rightarrow 4/5 N_2 + 2CO_2 + 14/5H_2O$	-848
Iron reduction	$CH_3COOH + 8Fe^{3+} + 2H_2O \rightarrow 8Fe^{2+} + 2CO_2 + 8H^+$	-495
Sulfate reduction	$CH_3COOH + 2H^+ + SO_4^{2-} \rightarrow 2CO_2 + 2H_2S + 2H_2O$	-133
Anaerobic oxidation of methane denitrification	$CH_4 + 8NO_2^- + 8H^+ \rightarrow 3CO_2 + 4 N_2 + 10H_2O$	-928
Anaerobic oxidation of methane-sulfate reduction	$CH_4 + SO_4^{2-} + H^+ \rightarrow CO_2 + HS^- + 2H_2O$	-21
Acetoclastic methanogenesis	$CH_3COO^- + H^+ \rightarrow CO_2 + CH_4$	-36
Methanol methanogenesis	$CH_3OH + H_2 \rightarrow CH_4 + H_2O$	-113
Ethanol syntrophic co- culture acetogenesis- methanogenesis	$2CH_3CH_2OH + CO_2 \rightarrow 2CH_3COO^- + 2H^+ + CH_4$	-112
Hydrogenotrophic methanogenesis	$CO_2 + 4H_2 \rightarrow CH_4 + 2H_2O$	-131
Formate methanogenesis	$4CHOO^- + 4H^+ \rightarrow 3CO_2 + CH_4 + 2H_2O$	-130

Fig. 16 Variations in the distribution of terminal electron acceptors (TEAs) and oxidation reactions in marine environments as a function of depth and depending on organic matter contents (0.1 to >0.5% C_{org} by wt.)



The surface-most sediments are typically the most oxidized with increasing degrees of reducing conditions at greater depth (age). Bioturbation mixes and oxygenates the surface sediments, which can deepen O_2 penetration and thus depress the diagenetic zonation. Bioturbation by macrofauna can in instances of near-surface methane also promote the flux of methane to the water column (e.g., Bonaglia et al. 2014) or conversely can enhance methane consumption (e.g., Childress et al. 1986). In sediments with lower levels of labile organic matter ($C_{org} < 0.2$ wt.%), such as the mid-North Pacific, dissolved O_2 around $250 \mu M$ can be found in the surficial interstitial fluids (Fig. 16, panel 1). These sediments with mostly recalcitrant organic matter can remain aerobic for 10s of meters depth (e.g., D'Hondt et al. 2015). In such oxic settings, there may be insufficient organic matter to exhaust the dissolved O_2 or other oxidants that are co-buried or diffusing in the sediments (Table 2).

Sulfate reduction (SR) and methanogenesis are not encountered in such environments unless there are substantial amounts of organic compounds advecting up from greater depth, e.g., from petroleum or gas hydrate-related seeps. Oxygen concentrations of ~10 ppm are known to inhibit methanogenesis due to the O₂ sensitivity of enzymes and cofactors in methanogens (e.g., Schonheit et al. 1981; Ragsdale and Kumar 1996), thus restricting the methanogenic zone.

Marine sediments with higher amounts of labile organic matter (e.g., C_{org} ~0.3 wt.%, Fig. 16, panel 2), such as many shelf deposits, have rates of oxidant utilization during organic decomposition that exceed the influx of O₂ from the overlying water column (e.g., Rittenberg et al. 1955). The presence of O₂ is often restricted to the uppermost millimeter or centimeter of sediment due to the low solubility of O₂ and it being the favorite electron acceptor (e.g., Wallmann et al. 1997; Hensen and Zabel 2000).

Once O₂ is exhausted, then the microbial community switches to less energetic, suboxic oxidants, such as nitrate, nitrite and manganese (Mn(IV)), and iron (Fe(III)) oxides. The lack of free oxygen restricts the types of infauna and hence inhibits the degree and decreases the depth of bioturbation. Typically, if there is sufficient labile organic matter present to consume the interstitial O₂, e.g., C_{org} ~0.3–0.5 wt.%, then these suboxic species will also be quantitatively consumed. At that point, dissolved sulfate becomes the next oxidant utilized (Fig. 16, panel 3). Dissimilatory sulfate reduction by sulfate-reducing bacteria (SRBs) acts as the next, albeit poorer, TEA for the anaerobic respiration of organic matter (e.g., Starkey 1948, Table 2). Hydrogen sulfide is one of the reaction products that is toxic and can inhibit bioturbation at the sediment surface (e.g., Atkinson and Richards 1967). In some cases, the sulfate reduction zone (SRZ) even extends into the water column, e.g., the Black Sea (Luther III et al. 1991) or Saanich Inlet (Capelle et al. 2018). In most sediments, the H₂S is rapidly complexed and removed from the interstitial water as metallic monosulfides and eventually as pyrite. The biology of SRBs have been researched for over a century (e.g., Beijerinck 1895; Van Delden 1903), but in recent sediments, detailed distributions of SRBs were reported later by Jørgensen (1977) and others. It is interesting to note that at the base of the SRZ, sulfate concentrations are not always fully depleted, and sulfate can persist at ~100 μM levels into the methane accumulation zone (MAZ) (e.g., Neretin et al. 2004). The explanation for this is unclear, but it may be that low sulfate concentrations fall below the threshold for use by SRBs (Leloup et al. 2007) or potentially that there is a sulfur cycle below the sulfate-methane transition zone (SMTZ, e.g., Mitterer 2010) that involves sulfide reoxidation (Knab et al. 2008; 2009).

The final diagenetic link in the remineralization chain of organic matter is thought to be methanogenesis, whereby methanogens use carbon rather than oxygen as the final TEA (Table 2). Generally, organic-rich sediments (e.g., C_{org} ~0.3–0.5 wt.%, Fig. 16, panel 3) consume the oxygenated oxidants (O₂ – SO₄²⁻), enabling the formation and accumulation of higher quantities of methane. In some marine environments with high organic loading, the anaerobic diagenetic zone can extend up into the water column resulting in the presence of high methane contents

(~10 μM), e.g., Saanich Inlet (Lilley et al. 1982) or Black Sea (Reeburgh et al. 1991; Schubert et al. 2006).

There are interesting suggestions that methanogenesis may not always be the “final diagenetic link” mentioned above. Instead, under certain conditions during late-stage diagenesis, methanogenesis could transition to iron reduction, utilizing iron oxides (Crowe et al. 2011; Sivan et al. 2011). This has been shown to be biologically feasible (e.g., Lovley and Phillips 1986; Lovley 2006; Weber et al. 2006). It also appears to be more easily recognized in freshwater settings (e.g., Roden and Wetzel 1996). As discussed later, iron-coupled reactions may also play an important role in the anaerobic oxidation of methane (AOM) (e.g., Ettwig et al. 2016). However, the importance of such iron-related processes is currently uncertain, but potentially relevant, particularly in earlier Earth history.

Not shown in Fig. 5 are the noncompetitive substrates that can also be utilized by methanogens. In sulfate-bearing environments, such as marine sediments or hypersaline settings, e.g., Mono Lake (Oremland et al. 1993), methanogens are generally outcompeted by SRBs for fermentation products such as hydrogen and acetate (competitive substrates) (e.g., Lovley et al. 1982), or based on energetics (Oremland and Taylor 1978; Schönheit et al. 1982; Lovley and Klug 1983). In the SRZ, methanogens can function using the non-competitive substrates, such as methanol, dimethylsulfide, and methylated amines, that are not utilized by SRBs (e.g., Winfrey and Ward 1983; Oremland et al. 1982; Oremland and Polcin 1982; Kiene et al. 1986; Maltby et al. 2018) (Table 1). In settings with higher H_2 production, it seems that methanogens can also successfully compete with SRBs (Hoehler et al. 2001; Buckley et al. 2008). There have been some more recent suggestions that SRBs and methanogens, using substrates competitively, can coexist in the SRZ (Sela-Adler et al. 2017; Dale et al. 2008; Ozuolmez et al. 2015; Zhuang et al. 2016, 2018). Although further validation is sought, the existing studies strongly suggest that methanogenesis and sulfate reduction (SR) may coexist under particular conditions. As will be discussed, methane that is formed from non-competitive substrates or other processes in the SRZ generally does not accumulate there because of extensive AOM in the SRZ that consumes any methane produced or migrating there (e.g., Xiao et al. 2017, 2018).

Normally, in marine sediments there is a clear demarcation between the SRZ and the methane accumulation zone (MAZ), with only a short overlap between them, i.e., the SMTZ, as illustrated in Fig. 6. In settings where the methanogenesis is more intense, the accumulation of dissolved methane can reach and exceed the saturation concentration. This leads to bubble formation at depth (Fig. 17). Such free gas accumulations have long been remotely recognized in recent sediment packages as “acoustically turbid zones” or “Becken Effekt” (e.g., Schüler 1952; Busby and Richardson 1957; Edgerton et al. 1966; Werner 1968; Hinz et al. 1969; Anderson et al. 1971; Schubel 1974; Van Weering 1975; Judd and Hovland 1992). Initially, H_2S and N_2 were among the gases suggested to cause acoustic turbidity. However, the works of Claypool and Kaplan (1974), Martens and Berner (1974), and Whiticar (1978) demonstrated that the presence of methane bubbles is responsible (Fig. 17).

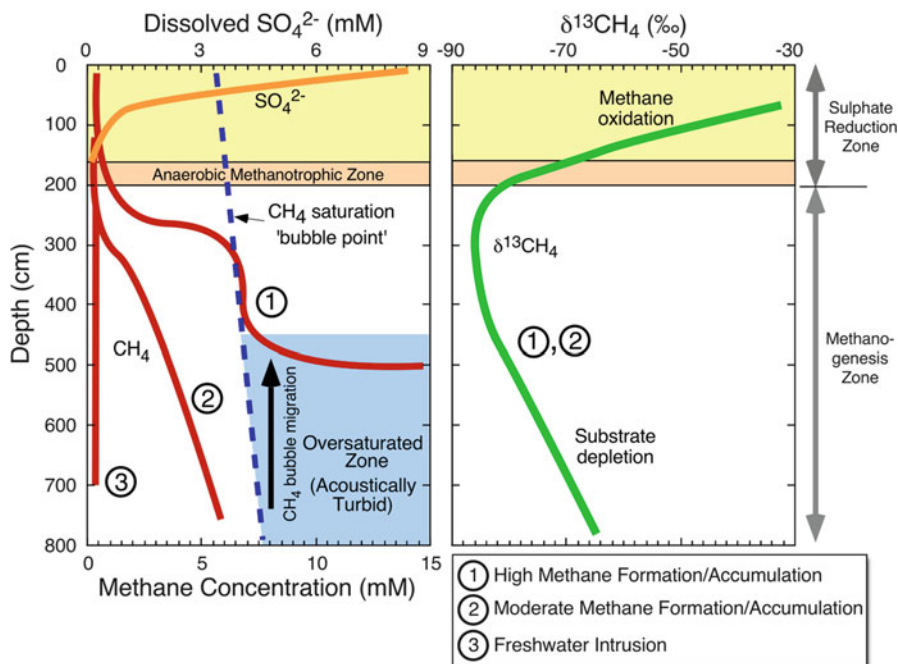
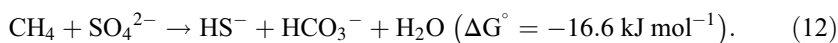


Fig. 17 Schematic sulfate, methane, and $\delta^{13}\text{C-CH}_4$ distributions in organic rich, anaerobic marine sediments. Example is from Eckernförde Bay, Germany (Whiticar 2002)

In some cases, the upward migration of, for example, thermogenic methane from greater depth can also create such acoustic turbidity (e.g., Judd and Hovland 2009).

As depicted in Figs. 6 and 16, substantial concentrations of methane are first measured once sulfate has been drawn down to less than ~ 0.5 mM. The interesting spatial interplay observed between the sulfate and methane distributions and the SMTZ in marine sediments was the subject of intense work in the 1970s (e.g., Claypool and Kaplan 1974; Martens and Berner 1974; Barnes and Goldberg 1976; Whiticar 1978). In simple terms, the concave downward shape of the depth profile of dissolved sulfate concentration in Figs. 6 and 16 is the result of the balance between the downward diffusion of sulfate, microbial uptake by SRBs, and the upward pore fluid advection. Some sulfate is consumed by the oxidation of organic matter (Table 2), but AOM is also an important, if not the dominant, sink for dissolved sulfate (e.g., Boetius et al. 2000). Although today AOM is an accepted process, this was not always the case. In fact, before the 1980s the process was highly controversial. Early geochemical studies concluded that AOM was necessary to maintain the concave upward profiles of methane observed in interstitial fluids below the SRZ (Figs. 6 and 16) (e.g., Claypool and Kaplan 1974; Martens and Berner 1974; Barnes and Goldberg 1976; Whiticar 1978). These authors surmised that diffusion and advection of methane alone could not establish the methane gradients observed.

The net equation for the generalized process of AOM was initially suggested (e.g., Reeburgh 1976) to be



Some of the more common complaints by microbial ecologists against AOM by SRBs at that time were that (a) this process could not be replicated in pure cultures (e.g., Zehnder and Brock 1979) and (b) the $\sim 16\text{--}18 \text{ kJ mol}^{-1}$ free energy yield of this exergonic reaction (Eq. 12) was below the biological energy quantum (e.g., Schink 1997; Sørensen et al. 2001). Although “obligate methane oxidizers” were discussed in freshwaters (e.g., Naguib and Overbeck 1970; Whittenbury et al. 1970) and that “. . . an association between the methane oxidizers and the sulfate reducers can be deduced” (Cappenberg 1972), the exact process remained uncertain. This was further complicated by the stark difference in sulfate concentrations between marine and freshwater systems and the possible lack of a SMTZ in the latter.

4 Microbial Methane in Freshwater and Terrestrial Environments

Low salinity and low dissolved sulfate environments, such as most terrestrial/lacustrine water columns and sediments, wetlands, soils, etc., have diagenetic remineralization stages analogous to those of marine and hypersaline settings (e.g., Capone and Kiene 1988; Roden and Wetzel 1996) (Fig. 6). Despite the obvious differences in concentrations of oxidizing agents and organic matter types between salt and freshwaters, those replete in organic carbon follow the sequential reduction of O_2 , NO_3^- , Mn(IV), Fe(III), SO_4^{2-} , and finally methanogenesis (e.g., Ponnamperna 1972; Patrick and Reddy 1978; Zehnder and Stumm 1988; Achtnich et al. 1995). The dissolved O_2 concentration thresholds are approximately $6\text{--}10 \mu\text{M}$ O_2 for denitrification, $\sim 1.5 \mu\text{M}$ O_2 for Mn(IV) reduction, and $1.5 \mu\text{M}$ O_2 for Fe(III) reduction (Tiedje 1988; Seitzinger et al. 2006; McMahon and Chapelle 2008). It was recognized in a series of papers that the presence of these oxidants leads to bacteria outcompeting the methanogens (Lovley and Phillips 1987; Lovley and Goodwin 1988; Lovley 1991).

Sulfate concentrations in freshwater environments are low compared to marine ($\sim 50\text{--}500 \mu\text{M}$ vs. $\sim 25\text{--}30 \text{ mM}$) and can be rapidly consumed, i.e., SRZ in freshwater environments is much less significant. As a consequence, the remineralization of organic matter by methanogenesis in freshwater settings is suggested to be 2–5 times greater than by SR. This remains controversial because of the potential for rapid recycling of sulfate in freshwaters (Ingvorsen and Jørgensen 1984), thereby increasing its reuse and hence proportion utilized. For comparison, methanogens in marine sediments may only remineralize 5–10% as much carbon compared to SRBs (Canfield 1993).

Due to the likely diminished role of SRBs competing for substrates and consuming methane, methanogenesis can occur much closer to the sediment surface than in

saline environments, i.e., in some cases at levels $<30 \mu\text{M}$ sulfate and within cms of the interface (e.g., Kuivila et al. 1989; Koizumi et al. 2003). At levels $>60 \mu\text{M}$ sulfate, the SRBs still outcompete the methanogens in freshwaters (Winfrey and Zeikus 1977; Ingvorsen and Brock 1982; Lovley and Klug 1986). This difference in sulfate between marine and freshwater can lead for the latter to a spatial compression of the oxic, suboxic, and methane formation zones shown in Fig. 6. The low levels of sulfate and SRBs competing for acetate in anaerobic freshwater conditions mean that acetoclastic methanogenesis (Eq. 2, Fig. 5) can be a major methanogenic pathway. Non-competitive substrates can also be utilized, but the amounts are low compared with acetoclastic and hydrogenotrophic methanogenesis (Winfrey and Zeikus 1977).

In several anoxic lakes and wetland sites, a transition with sediment depth is observed from predominantly acetoclastic methanogenesis (Eq. 2) higher in the diagenetic profile to a regime at greater depth/age increasingly dominated by hydrogenotrophic methanogenesis (Eq. 1). This methanogenic pathway transition feature has been supported by a range of methods, including stable isotope measurements, incubation and inhibitor culture experiments, 16S rRNA, and *mcrA* genes (e.g., Martens et al. 1992; Avery et al. 1999; Chan et al. 2005; Lu et al. 2005; Alstad and Whiticar 2011; Hershey et al. 2014; Lofton et al. 2015; Cadieux et al. 2016; Yang et al. 2017). This transition appears to largely reflect the exhaustion of organic substrates available for acetoclastic methanogenesis, leaving hydrogenotrophic methanogenesis to continue at depth with continued remineralization.

Common for anaerobic freshwater systems (sediments and sometimes stratified water columns) is that the concentration of dissolved methane can quickly rise above the methane saturation point, leading to bubble formation and thus ebullition of gas from the sediments and soils due to buoyancy. The importance of the spatial compression of the hypoxic and methane accumulation zones in freshwaters is that methane can more easily evade the microbial oxidation biofilter that consumes methane *in situ*. This means that a greater proportion of methane can escape by ebullition and diffusion into the troposphere from freshwater environments than from marine sources (Strayer and Tiedje 1978; Reeburgh et al. 1993; Bastviken et al. 2008). Global methane emissions from freshwaters are estimated to be $\sim 100 \text{ Tg CH}_4 \text{ year}^{-1}$ (Bastviken et al. 2011), which is substantially higher than oceanic source estimates ($10\text{--}30 \text{ Tg CH}_4 \text{ year}^{-1}$) and high-latitude emissions from tundra ($\sim 35 \text{ Tg CH}_4 \text{ year}^{-1}$, e.g., Fung et al. 1991).

The pool of nitrate ($100\text{--}200 \mu\text{M}$) in freshwaters can exceed sulfate (e.g., Mulholland et al. 2008) and thus compared with marine environments NO_3^- may be more important as a methane oxidizer (Fig. 5). Due to the short and rapid gas migration paths in soils and in freshwater columns, *in situ* methane consumption is reduced. The result is that ebullition, diffusion, and advection are major processes for the release of microbial methane from permafrost thawing, natural wetlands, and freshwaters into the atmosphere (e.g., Klapstein et al. 2014). These releases account for $\sim 20\%$ of the total tropospheric methane emissions budget compared with $\sim 5\%$ from the oceans.

Soils offer diverse environments for methanogens. These can be roughly divided into the vadose and water-saturated zones. The latter can have rapid invasion of O_2 , which maintains aerobic conditions and limits methanogenesis. In some cases, anoxic microsites can serve as a refugia for methanogenic archaea (e.g., Watanabe et al. 2007). Some studies even report CH_4 production in dry, oxic environments (e.g., Andersen et al. 1998; von Fischer 2002; Teh et al. 2005; von Fischer and Hedin 2007).

In the water-saturated zone, the 0.3 mM O_2 in fully oxygenated waters is rapidly consumed leading to anaerobic conditions and methanogenesis. This has been studied extensively for flooded soils, rice paddies, wetlands, lakes, and tundras (e.g., Holzapfel-Pschorn et al. 1985; Achtnich et al. 1995; Chanton 2005; Dalal et al. 2008; Oertel et al. 2016). In addition to soil moisture, temperature, pH, and vegetation types and gas transport mechanisms, including diffusion and plant ventilation, all play critical roles in governing the production, consumption, and emissions of methane from these settings (Zeikus and Winfrey 1976; de Bont et al. 1978; Dacey 1981; Conrad et al. 1987; Whiting and Chanton 1992; Westermann 1993; Dunfield et al. 1993). Figure 18 outlines the major processes involved with the production, consumption, and transport of methane in inundated freshwater

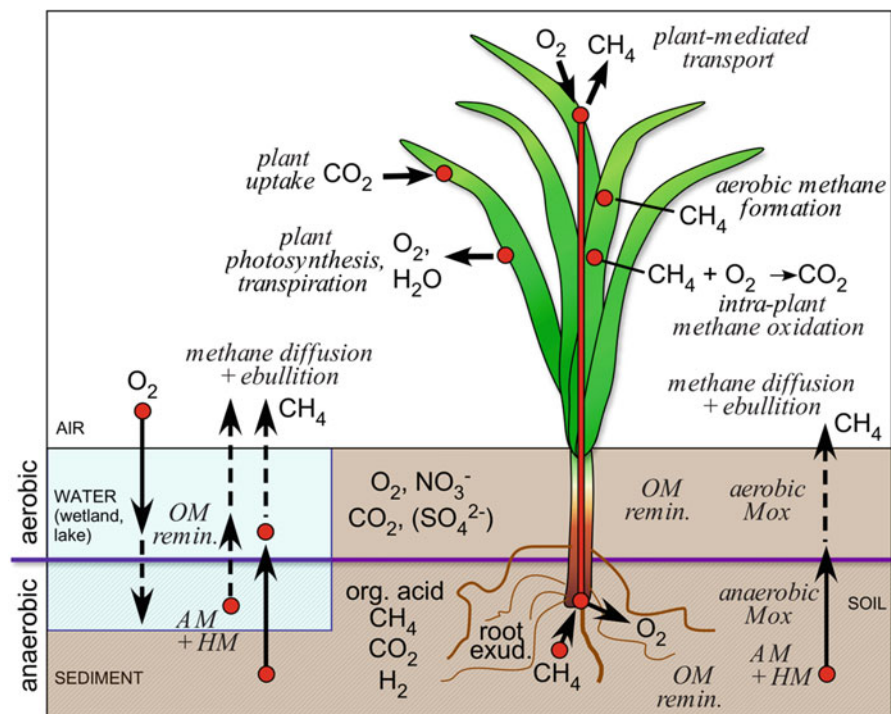


Fig. 18 Schematic of processes related to methanogenic and methanotrophic mechanisms in plants, soils, and inundated freshwater environments (wetlands, lakes, rice paddies, etc.). (Modified from Xu et al. 2016)

environments. This includes acetoclastic and hydrogenotrophic methanogenesis and methanotrophy.

The transport mechanisms include ebullition and molecular diffusion out of the soils and sediments but also plant-based aerenchyma transport in macrophytes (Colmer 2003; Chanton 2005) or in vascular plants (Shannon et al. 1996; Ström et al. 2012). Molecular diffusion in air is about 10^4 times faster than in the dissolved phase (methane diffusion coefficients at 25 °C in air $\sim 2.0 \times 10^{-1} \text{ cm}^2 \text{ s}^{-1}$, Winn 1950, and in water $\sim 2 \times 10^{-5} \text{ cm}^2 \text{ s}^{-1}$, Witherspoon and Saraf 1965). Therefore, enhanced emission from the gas phase in plants versus waterlogged soils or waters is expected. For example, Tyler et al. (1997) estimated that plants account for 98% of the CH_4 emissions from a Texas paddy field. Watanabe et al. (1999) reported that up to 60% of the methane emitted from rice fields originated from root exudates in the rice rhizosphere. Root exudates are also known to modulate methane production in peatlands and Arctic wetlands (Shannon et al. 1996; Ström et al. 2012). Similarly, Knoblauch et al. (2015) reported that plant-mediated transport accounted for 70–90% of total CH_4 fluxes from their polygonal tundra study site in Siberia. In the absence of the vascular plants, the majority of the methane was oxidized and not emitted due to the increased methane residence time.

Plants themselves are also a potential source of methane formation. Zeikus and Ward (1974) and Schink et al. (1981) reported methanogenesis related to the anaerobic degradation of wetwood and pectin in living trees. Trees have also been shown to transport methane (Rusch and Rennenberg 1998; Terazawa et al. 2007). The methanogenic potential of anaerobic mosses is not well constrained (Knoblauch et al. 2015), and mosses, especially the aerobic layers, are more likely a source of CH_4 consumption and reduced atmospheric CH_4 flux (Basiliko et al. 2004; Liebner et al. 2011; Parmentier et al. 2011). Methane consumption in emergent fen mosses in an Arctic lake during the Holocene Thermal Maximum was reported by Elvert et al. (2016) based on the presence of ^{13}C -depleted bacterial hopanoids, e.g., hop-17(21)-ene, with $\delta^{13}\text{C}$ as low as -55.9 ‰ .

In addition to production and active CH_4 transport, plants can be the site of substantial CH_4 consumption (Fig. 18). For example, Schütz et al. (1989), Frenzel (2000), Groot et al. (2003), and Zhang et al. (2014) described methane uptake by aerobic methanotrophs in rice plant rhizospheres.

Finally, there is the controversial aerobic (abiotic) formation of methane in plants, first suggested by Keppler et al. (2006) and Crutzen et al. (2006). This mechanism was disputed by Dueck et al. (2007), Beerling et al. (2008), and Kirschbaum and Walcroft (2008) but subsequently defended by processes involving ultraviolet radiation, temperature, water, cutting injuries, and reactive oxygen species by Keppler et al. (2008), Wang et al. (2008), Viganò et al. (2008, 2009), Brüggemann et al. (2009), Qaderi and Reid (2009), Bloom et al. (2010), and Bruhn et al. (2012). Interestingly, this aerobic methane production process is also suspected in ocean settings (Karl et al. 2008; del Valle and Karl 2014).

5 Microbial Methane in Special Environments

Methanogens, known as “a community of survivors” (Friedmann 1994), can exist in a wider range of environments than just the common natural and anthropogenic sources of methane, e.g., wetlands, sediments, ruminants, landfills, etc. (Fig. 3). Chaban et al. (2006) provide a comprehensive table of the various environments and genera. The diversity of environments includes high pressures, extreme temperatures, salinities, and pH range settings. These prokaryotic organisms, termed extremophiles or polyextremophiles, are typically, but not exclusively, from the domain Archaea and include some methanogens, extreme halophiles, thermophiles, hyperthermophiles, and thermoacidophiles. A detailed microbiological description of the diversity of environments can be found in several excellent review papers that cover this material (e.g., Ferry 1993; Dworkin et al. 2006; Rosenberg et al. 2014).

However, it is important here to at least briefly review the range in habitats. For example, the hyperthermophilic methanogen *Methanopyrus kandleri* strain 116 has been grown in cultures at temperatures of ~122 °C (Takai et al. 2008). This pushed the boundaries of Kashefi and Lovley (2003) who isolated the Archaea Strain 121 from the Mothra hydrothermal vent field, which grew at 85–121 °C. These are considerably higher temperatures than reported for *Pyrolobus fumarii* up to 113 °C (Blöchl et al. 1997) or the methanogens *Methanopyrus* at 110 °C (Huber et al. 1989), *Methanocaldococcus jannaschii* up to 90 °C (Miller et al. 1988), *Methanocaldococcus indicus* up to 86 °C (L’Haridon et al. 2003), and *Methanotorrus formicicus* up to 95 °C (Takai et al. 2004). Methanogenesis has also been observed in natural settings, for example, at the hydrothermal fields at the Endeavour Segment of the Juan de Fuca Ridge (Lilley et al. 1993). Although even higher growth temperatures, up to 150 °C, had been postulated (e.g., Stetter et al. 1990; Daniel 1992; Segerer et al. 1993), the deep subsurface biosphere has a general upper limit of 80–90 °C (Parkes et al. 1994; Wilhelms et al. 2001), which corresponds to subsurface depths of 1.5–3 km, depending on the geothermal gradient.

Piezophilic or barophilic hyperthermophiles have been grown under conditions up to 40 MPa (~4,100 m water depth) for the methanogen *Methanopyrus kandleri* (Takai et al. 2008) or up to 120 MPa for *Pyrococcus* CH1 (Zeng et al. 2009).

Psychrophilic or cryophilic methanogens have also been studied extensively in cold and deep lakes and in high-latitude locations (permafrost, sediments, and lakes). Nozhevnikova et al. (2003) incubated methanogens down to 1 °C, including *Methanosarcina lacustris*, from Lakes Baldegg and Soppen. Similarly, psychrophilic methanogens have been studied in the Antarctic, namely, *Methanogenium frigidum* and *Methanococcoides burtonii* by Franzmann et al. (1997) and Saunders et al. (2003). Empirical evidence, i.e., direct measurement of microbial methane, also indicates the presence of psychrophilic methanogens, e.g., in Antarctic marine sediments at –1.3 °C (Whiticar et al. 1986) and Swedish lake sediments at 4 °C (Due et al. 2010). Rivkina et al. (2002, 2004), using NaH¹⁴CO₃, demonstrated that methanogens could be successfully incubated down to –16.6 °C, albeit with

extremely low growth rates, in loamy peat permafrost soils drilled at the Kolyma Lowland (ca. 1 m, 2920 ± 40 ybp). Experiments with methanogens have also been demonstrated methanogenesis to be viable in frozen ice cores, such as the GISP2 at 3,044 m and -9 °C (Price and Sowers 2004) and the Bolivian Sajama glacier ice at 15,400 ybp, -10 °C (Campen et al. 2003). The latter observed CH_4 levels in the ice up to eight times the expected atmospheric levels, which could be best explained by *in situ* methanogenic activity of archaea living on nutrients concentrated in liquid veins at the triple junctions of ice grains (Tung et al. 2006). In contrast to permafrost with more abundant radioactive K, Th, and U in their soils, ice may provide unique, critical longer-term refugia ($>10^6$ year) for methanogen survival against DNA radiation damage from ionizing radiation (e.g., cosmic rays and α particles) (Price 2009). The disadvantage to permafrost is that nutrient abundance is lower in ice veins, which can limit methanogens.

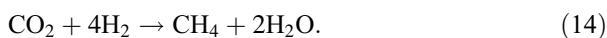
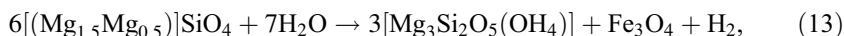
Salinity and pH also create environmental constraints for methanogens. Haloalkaliphilic methanogens have been active and isolated from the hypersaline soda lakes, e.g., in USA (Mono and Big Soda Lakes, $S = 40\text{--}95$ g/l, $\text{pH} = 10$, Oremland and Miller 1993), Egypt (Wadi al Natrun, $\text{pH} = 8.1\text{--}9.1$, Boone et al. 1986), Kenya (Lake Magadi, S up to 300 g/l, $\text{pH} = 7\text{--}8$, Kevbrin et al. 1997) India (Lonar Lake, $S = 5.6\text{--}7.6$ g/l, $\text{pH} = 9.0\text{--}10.5$, Antony et al. 2013) and Asia (Siberian soda lakes and Kulunda Lake, S up to 100 g/l, $\text{pH} = 9.5\text{--}11$, Nolla-Ardèvol et al. 2012; Sorokin et al. 2014; Sorokin et al. 2015). In concert, desiccation tolerance studies have also been conducted on a suite of methanogens, including *Methanocaldococcus jannaschii*, *Methanothermobacter thermautotrophicus*, *Methanosarcina barkeri*, and *Methanopyrus kandleri* (Martins et al. 1997; Beblo et al. 2009).

Methanogens also occupy subsurface locations, such as aquifers (Gieg et al. 2014) in oil and gas fields (Gray et al. 2009), deep geothermal aquifers, e.g., *Methanosaeta* and *Methanothermobacter* in the Pannonian aquifer, Romania (Chiriac et al. 2018), *Methanospirillum* in the Great Artesian Basin of Australia (Kimura et al. 2005), and deep sedimentary rocks of Piceance Basin, USA (Colwell et al. 1997). The degradation of oil and gas to methane by syntrophic, acetoclastic, and hydrogenotrophic methanogenesis is a common occurrence (Dolfing et al. 2008; Rowan et al. 2008; Jones et al. 2008). Deposits of coal also offer substrates for methanogenesis, albeit via complex pathways (Penner et al. 2010; Guo et al. 2014; Baublys et al. 2015; Iram et al. 2017).

Methanogenesis also operates in subsurface rocks. Pedersen (1997) and Kotelnikova and Pederson (1998) reported acetoclastic and hydrogenotrophic methanogens from boreholes into granite-granodiorites at Äspö HRL, Sweden. Methanogenesis has been reported at similar settings, e.g., Lidy Hot Springs, USA (Chapelle et al. 2002), Columbia River Basalt Group, USA (Stevens and McKinley 1995), Witwatersrand Basin mines, South Africa (Ward et al. 2004; Slater et al. 2006; Simkus et al. 2016), Snake River Plain Aquifer, USA (Newby et al. 2004), Kidd Creek and Copper Cliff South, Canada (Doig 1994), Con and Giant mines, Canada, and Enonkoski mine, Finland (Sherwood Lollar et al. 1993, 2006). Thus, it is possible for methanogens to be viable at considerable depth (pressure and both high and low temperatures) in the subsurface in rocks, soils, sediments, and ice,

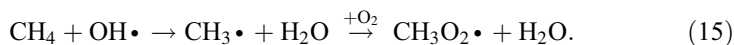
provided certain living conditions are met, including liquid water, nutrients, and pore space ($>$ few μm).

Although outside this review, it should be noted that there are also abiotic methane occurrences, including pyrogenic sources (Bousquet et al. 2006) and deep oceanic and subsurface environments, that can in some cases confound the source interpretations of methane (Etiope and Sherwood Lollar 2013). Certainly, these processes are important to characterize the occurrences of methane on Earth but also other planets and moons. The interplay between biotic and abiotic processes of methane formation and oxidation in deep earth settings, such as in the Fennoscandian Shield (Kietäväinen and Purkamo 2015), are schematically shown in Fig. 22. Abiotic methane is typically formed by gas-water-rock reactions and magmatic processes. These include carbonate methanation (Giardini et al. 1968; Yoshida et al. 1999), abiotic CO_2 reduction (Kelley and Früh-Green 1999; Seewald et al. 2006), and Fischer-Tropsch type reactions, i.e., serpentinization of ultramafic rocks/Sabatier reactions (e.g., Szatmari 1989; McCollom and Seewald 2001; Potter and Konnerup-Madsen 2003; Etiope and Ionescu 2015). Equations 13 and 14 give examples of abiotic methanation by the incongruent Fischer-Tropsch serpentinization of olivine, followed by the reduction of CO_2 with H_2 to CH_4 :



6 Methane Oxidation

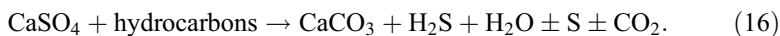
The biotic and abiotic oxidations of methane are critical mechanisms that effectively remove methane from sediments, soils, waters, and the atmosphere. In the atmosphere abiotic methane oxidation occurs via a complex chain of photochemical reactions initiated by the hydroxyl radical abstraction reaction with methyl and methylperoxy radicals, methanol, formaldehyde, and carbon monoxide as intermediate products (Levy 1972; Levine et al. 1985; Cicerone and Oremland 1988; Hein et al. 1997):



This OH radical abstraction reaction is the most important sink of tropospheric methane at ~ 420 Tg CH_4 year $^{-1}$ (Khalil and Rasmussen 1983; Crutzen 1991; Whiticar and Schaefer 2007). The other atmospheric methane sinks are (1) microbial soil uptake, ca. 25–40 Tg CH_4 year $^{-1}$ (Seller and Conrad 1987; Conrad 1996; Topp and Pattey 1997), (2) stratospheric removal, ~ 40 Tg CH_4 year $^{-1}$ (Boucher et al. 2009), and (3) chlorine sink, particularly in the Marine Boundary Layer, ~ 30 Tg CH_4 year $^{-1}$ (Wang et al. 2002; Allan et al. 2005, 2007).

The abiotic oxidation of hydrocarbons, including methane, has also been reported in geologic formations up to 100–180 °C by the reduction of anhydride via

thermochemical sulfate reduction (TSR) (e.g., Orr 1974; Krouse et al. 1988; Kiyosu and Krouse 1989; Machel 2001; Pan et al. 2006), according to general Equation 16:

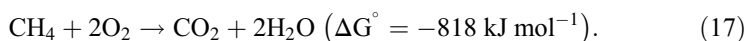


6.1 Biological Methane Oxidation

Biological oxidation or consumption of methane occurs by both aerobic and anaerobic processes. The microbiology has been treated by numerous reviews, including Hanson and Hanson (1996), Conrad (1996), Lidstrom (2007), Bowman (2011), and Zhu et al. (2016). Methanotrophy constitutes the biofilter that removes methane that could ultimately emit from sediments, soils, and waters to the troposphere (e.g., King 1992; Reeburgh 1996). Approximately 40% or 582 Tg CH₄ year⁻¹ of the methane generated annually in the biosphere reaches the atmosphere. This aerobic and anaerobic removal of methane has important global climate consequences on geologic and anthropogenic time scales, including before and after the Great Oxidation Event (2.32–2.45 Ga, e.g., Kerr and Vogel 1999; Goldblatt et al. 2006; Catling et al. 2007; Daines and Lenton 2016) and for today's changing atmospheric radiative forcing.

6.2 Aerobic Methane Oxidation

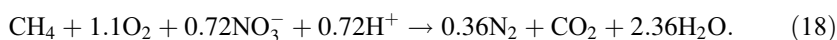
Aerobic methane oxidation with O₂ (MOx, aka AMO or AeOM) is a well-studied bacterial process (Fig. 5) (e.g., King 1992; Hanson and Hanson 1996; Lidstrom 2006; Serrano-Silva et al. 2014), including phylogenetics and ecophysiology (e.g., Knief 2015). Methanotrophic bacteria utilize CH₄ and some other C₁ compounds as their carbon source(s), ultimately converting them by transduction with dehydrogenases to CO₂ via intermediates, such as methanol, formaldehyde, and formate (Roslev and King 1995; Dedysh and Dunfield 2011; McDonald et al. 2008). Originally, the organisms were understood to be obligate methylotrophs, i.e., unable to grow on C–C compounds. However, there is evidence that some are indeed facultative methanotrophs (e.g., Im et al. 2011). The basic equation (Eq. 17) for aerobic methane consumption (e.g., Dalal and Allen 2008, Table 2) is



Aerobic methanotrophs have been known since at least the early work of Söhngen (1906), who isolated aerobic methane-oxidizing bacteria (MOB). They are a particular subgroup of methylotrophic bacteria capable of producing methane mono-oxygenases (MMO) enzymes (e.g., Bowman 2006; Blumenberg et al. 2007; Bürgmann 2011; Ménard et al. 2012). The two forms of these enzymes are a membrane-bound, particulate form with a copper active center (pMMO) and the

soluble form with non-heme iron (sMMO) (Knief 2015; Ghashghavi et al. 2017; Kallistova et al. 2017). Generally, the methanotrophic genera have the genus prefix “Methylo,” excepting *Crenothrix polyspora*. They are divided using multiple characteristics into three assemblages, namely, type I methanotrophs (RuMP pathway, e.g., *Methylobacter* and *Methylomonas*), type II methanotrophs (serine pathway, e.g., *Methylosinus*, *Methylocella*, and *Methylocystis*), and type X methanotrophs (both RuMP and serine pathways, e.g., *Methylococcus capsulatus*) (e.g., Hanson and Hanson 1996; Conrad 1996). The MMO requires O₂ and is present in (1) a soluble form (types II and X methanotrophs) and (2) membrane-bound enzyme form (type I) related to the ammonium monooxygenase (AMO) of nitrifying bacteria (Holmes et al. 1995).

Although AeOM was thought to be indirectly coupled with denitrification (Rhee and Fuhs 1978; Modin et al. 2007), aerobic methane oxidation can also be directly coupled to denitrification (AME-D) depending on the O₂ concentration (Costa et al. 2000; Kits et al. 2015). Due to the similarity of MMO with ammonia monooxygenase, many MOB may be able to perform ammonia oxidation as well. In addition, some MOB can fix N₂ at low O₂ concentrations. Zhu et al. (2016) proposed the overall stoichiometric equation for the aerobic methane oxidation with denitrification and oxygen (Eq. 18) as



In some cases, methanotrophs are extremophiles and thus inhabit a wide range of environments (Trotsenko and Khmelenina 2002; Islam et al. 2008; Pol et al. 2007), e.g., thermophiles (up to 62 °C, Bodrossy et al. 1995), psychrophiles (4 °C, Omelchenko et al. 1996; Wartiaainen et al. 2006), acidophiles (pH 5.0, Dedysh et al. 2000), alkaliphiles (pH 10.0, Sorokin et al. 2000), and halophiles (5.6% NaCl, Fuse et al. 1998; Kalyuzhnaya et al. 2008). Some methanotrophs appear to be light sensitive, with inhibition by light in lakes (Oswald et al. 2015).

Depending on methane concentrations, soil methanotrophy can be differentiated into high and low affinity (e.g., Nayak et al. 2007; Conrad 2009). Low-affinity methanotrophs are typically associated with high methane concentration environments and Michaelis-Menten kinetics with high K_m, V_{max}, and Th_a parameters (Bender and Conrad 1992). High-affinity methanotrophs have low K_m, V_{max}, and Th_a Michaelis-Menten kinetic parameters and are associated with low methane concentrations, such as atmospheric methane (1.8 ppm) diffusing into typically dry soils (<60% water-filled pore space) (Bender and Conrad 1992; Dunfield et al. 1999; Dunfield and Conrad 2000). Type II methanotrophs, e.g., *Methylocystis*, appear to dominate in such low CH₄ concentration environments. These methanotrophs are important in soils and lakes for the uptake of tropospheric methane, representing about 5–8% of the 480 Tg CH₄ year⁻¹ total tropospheric sink. This includes the methane sinks in forest and upland soils (Benstead and King 1997; Henckel et al. 2000). The uptake is strongly dependent on several factors, including CH₄ and O₂ contents, temperature, soil moisture content, and pH (e.g., Dunfield et al. 1993; Oertel et al. 2016). In freshwater lakes, AeOM is important for regulating CH₄

emissions, as aerobic methanotrophs consume 30–99% of the CH₄ produced (Bastviken et al. 2008). Global methane emissions from freshwaters are estimated to be ~100 Tg CH₄ year⁻¹ (Bastviken et al. (2011), which is substantially higher than oceanic source estimates (10–30 Tg CH₄ year⁻¹) and high-latitude emissions from tundra (~35 Tg CH₄ year⁻¹, e.g., Fung et al. 1991).

Studies have shown that temperate forest soils may consume more methane than tropical soils and that deciduous forest soils have higher rates than coniferous forest soils (e.g., Meyer et al. 1997). The degree of soil disruption can also influence the rates of consumption, with evidence of more methane consumption in pristine soils than disturbed or regrowth forest soils. Soil moisture, texture, compaction, and fertilization can also affect the rate of methane diffusion in soils and thus influence the uptake rate (Boeckx et al. 1997; Del Grosso et al. 2000; Templeton et al. 2006).

Aerobic methane oxidation also occurs in both marine and freshwater columns (e.g., Scranton and Brewer 1977; Whiticar and Faber 1986; De Angelis et al. 1993; Valentine et al. 2001). This process, albeit with generally slow rates, i.e., 10–200 pM year⁻¹ (Scranton and Brewer 1977; Rehder et al. 1999; Grant and Whiticar 2002), is also effective at reducing methane emissions from the water column to the atmosphere.

Methanotrophs can occupy and function in a variety of symbiotic situations, such as planktonic aerobic methanotrophs (Tavormina et al. 2010), marine invertebrates, such as tubeworms, provannid snails, cladorhizid sponges, and deep-sea bathymodiolin mussels (e.g., Childress et al. 1986; DeChaine and Cavanaugh 2006; Petersen and Dubilier 2009). The presence of aerobic methanotrophs in sediments and soils can sometimes be detected with specific biomarker molecules, such as specific sterols (4,4-dimethyl and 4 α -methyl sterols) and hopanoids (diploptene, diplopterol, 3 β -methyl diplopterol) (e.g., Bird et al. 1971; Bouvier et al. 1976; Zundel and Rohmer 1985; Hinrichs et al. 2000; Elvert and Niemann 2008; Berndmeyer et al. 2013; Rush et al. 2016; Spencer-Jones et al. 2015). More recently, gene sequencing, for example, using 16S rRNA, is a valuable tool to identify methanotrophs (e.g., DeChaine and Cavanaugh 2006; Duperron et al. 2006; Wendeberg et al. 2012).

6.3 Anaerobic Oxidation of Methane (AOM)

Anaerobic oxidation of methane (AOM) is operative mostly in anoxic marine sediments, equivalent to the sulfate-methane transition zone (SMTZ). However, the actual process still remains a puzzle, with various options for pathways. AOM is important as it has been estimated to consume >70 to 300 Tg CH₄ year⁻¹ methane (Reeburgh 1996; Hinrichs and Boetius 2002; Boetius and Wenzhöfer 2013). This range in consumption is comparable to the 582 Tg CH₄ year⁻¹ released to the troposphere from all sources. AOM may consume 75–95% of the methane produced in marine sediments (Valentine 2002) and exceed some estimates of current microbial methane generated in them, e.g., 5–33 Tg CH₄ year⁻¹ (Wallmann et al. 2002). This discrepancy, i.e., the excess AOM, may partly be due to the additional oxidation

of methane from geologic seeps and gas hydrates. It is estimated that 5–25% of the methane in sediments flux into the water column, where it is mostly consumed by aerobic methanotrophs. The rates of AOM are highly variable, depending on environment, ranging at various sites from ~1 to 3,000 nM year⁻¹ (up to 11 mol CH₄ m⁻² year⁻¹, e.g., Hinrichs and Boetius 2002; Luff et al. 2005; Regnier et al. 2011). Torres et al. (2002) and Joye et al. (2004) noted for the cold seeps at Hydrate Ridge and the Gulf of Mexico that the high rates of AOM and SR in active seeps appear to depend on the flux of methane and fluid advection. This is analogous to the increase in culture AOM activity with higher methane partial pressures (Nauhaus et al. 2002).

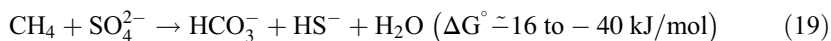
The oxidation capacity of dissolved sulfate (seawater ~29 mM) plays a central role in the consumption of methane as it is typically 50–100 times that of the other electron acceptors combined (O₂, NO₃⁻, Mn(IV), Fe(III)). Following on the early culture work of Davis and Yarbrough (1966), the process of AOM was proposed by geochemists based on interstitial fluid data (e.g., Reeburgh 1976; Claypool and Kaplan 1974; Martens and Berner 1974; Barnes and Goldberg 1976). The primary geochemical evidence for AOM was the juxtaposition of dissolved sulfate and methane in anoxic marine sediments as shown in Figs. 5 and 16, panel 4. Reeburgh (2007, Table 2) compiled an exhaustive list of similar examples.

In organic replete sediments, the dissolved sulfate in the sulfate-reduction zone (SRZ) is rapidly consumed, at a rate faster than diffusive replenishment from the overlying sediments and water column. In the SRZ, methane concentrations are low, but not necessarily zero. Beneath the SRZ, methane starts to accumulate, sometimes to levels greater than the bubble point. The depth (diagenetic) separation between the presence of dissolved sulfate and methane could potentially be explained by substrate competition between the sulfate-reducing bacteria (SRBs) and the methanogens, i.e., the latter were outcompeted and restricted in activity until the available dissolved sulfate was largely depleted. In contrast, there can be minor amounts of methanogenesis in the SRZ, e.g., by noncompetitive substrates; however, larger accumulations are generally not observed due to largely quantitative methanotrophy in the SRZ. Furthermore, Cappenberg (1975) proposed that sulfide inhibition of methanogenesis in the SRZ could prevent the production and thus buildup of methane there.

However, such interpretations are all confounded by the typical concave upward distribution of the methane concentration profile, particularly as it approaches the sulfate-methane interface (SMTZ). Simple methanogenesis with upward diffusive and advective fluxes of methane is unable to create such a profile, and there must be net consumption to maintain the observed methane gradient in Figs. 5 and 16, panel 4 (Whiticar 1978). The issue was that an organism responsible for AOM could not be found or isolated. Thorough discussions of the various microbial options and lines of evidence for AOM have been well reviewed by, e.g., Valentine and Reeburgh (2000), Hinrichs and Boetius (2002), and Valentine (2002).

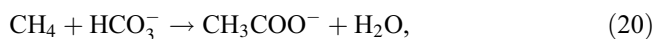
The classical view of anaerobic consumption of methane coupled to sulfate reduction (AOM-SR) involves a syntrophic relationship between methane-consuming archaea and sulfate-reducing bacteria (SRB) (Alperin and Reeburgh 1985;

Hoehler and Alperin 1996; Boetius et al. 2000; Orphan et al. 2001a; Valentine 2002; Orcutt et al. 2008) according to Eq. 19 (Table B):

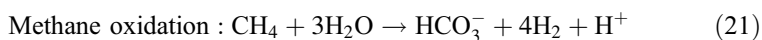


We now know that anaerobic consumption of methane is not uniquely tied to sulfate reduction (AOM-SR). Despite the varieties and uncertainties of material and energy pathways (Regnier et al. 2011; Wang et al. 2017) and the direct or indirect coupling of AOM with sulfate reduction or other terminal electron acceptors (TEAs) (Sørensen et al. 2001; Orcutt et al. 2005), AOM remains an important global CH₄ sink. This is most clearly observed in high methane flux environments, such as anaerobic sediments or waste treatment facilities.

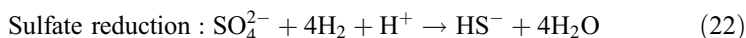
Initially, the concept of AOM by “reverse methanogenesis” was put forward by Zehnder and Brock (1979, 1980) using sulfate as the TEA. This was based on incubation experiments suggesting that methanogens are able to “. . .Oxidize a small amount of methane anaerobically.” This process helped explain the low rates of AOM demonstrated by AOM-SR inhibition studies. Reverse methanogenesis also likely involves the formation of acetate, although methanol and H₂ were also postulated as products. They showed with ¹⁴C-labelled CH₄ that the oxidation was consistently less than the concurrent methanogenesis (<1% AOM vs. methanogenesis), so net CH₄ oxidation was uncertain. This led more recently to the term “trace methane oxidation” (TMO) by Moran et al. (2005). The proposed acetate formation pathway by Zehnder and Brock (1979, 1980) (Eq. 20) is



but the authors expressed concerns about the energetics, and they included the possibility of a consortium, e.g., with sulfate reducers. Pure methanogen cultures in low H₂ and high CH₄ concentrations by Valentine et al. (2000) could not sustain H₂ production, and methane oxidation was not seen. Valentine and Reeburgh (2000) and Caldwell et al. (2008) also remarked that the many methanogens, who use acetate and methylated compounds rather than H₂ for methanogenesis, would not be good candidates for reverse methanogenesis, thus limiting the range of potential archaea. Partial support for reverse methanogenesis among other options was raised by Hoehler et al. (1994) and Harder (1997). They described a variation, also put forth by Zehnder and Brock (1979, 1980), that utilized a methanogen-sulfate reducer consortium, whereby methanogens oxidize methane with water (Eq. 21).



However, the buildup of molecular hydrogen from such a reaction would energetically inhibit the methanogens (Valentine et al. 2000). Sulfate reduction is evoked whereby SRBs scavenge the hydrogen syntrophically to allow methane oxidation to proceed exergonically, thereby maintaining the necessary lower H₂ partial pressure ($P_{\text{H}_2} \sim 1.1 \mu\text{atm}$ or 0.3 nM) (Eq. 22).



This gives rise to the frequently reported overall reaction in Eq. 16 with potentially enough energy to support ATP synthesis (e.g., Harder 1997; Valentine and Reeburgh 2000; Widdel and Rabus 2001).

Although it does address the association of SRBs with AOM, concerns were raised as to whether the sulfate reducers could account for the amount of methane oxidation required, i.e., 15–100% of the total sulfate reduced (Iversen 1984), and the energy requirements (Orcutt and Meile 2008; Regnier et al. 2011).

Hallam et al. (2004) and Timmers et al. (2017) revived this “reverse methanogenesis” hypothesis using genomic information in methane-oxidizing Archaea, whose cells contain most, but not all, of the genes typically associated with CH₄ production. The papers also suggested that a pathway of methane oxidation whereby hydrogenotrophic methanogenesis (Eq. 1) essentially runs in reverse with archaea but with assistance from bacteria, i.e., a consortium of methane-oxidizing archaea and SRBs. Associated with this is the possibility of interspecies electron carriers, for example, proposed by Hoehler et al. (1994), DeLong (2000), and Wegener et al. (2015) such that methane oxidizers directly shuttle energy to the SRBs, i.e., direct interspecies electron transfer (“DIET,” Lovley 2017). In contrast, Gao et al. (2017) pointed out that AOM is also associated with extracellular electron transfer (“EET”), especially for the reduction of solid electron acceptors.

To date, other than aerobic methane oxidation with O₂, there still has been no single microorganism identified that can oxidize methane. The suggestion that there may be a consortium of organisms that perform methane oxidation and SR was supported by phylogenetic studies but also geochemical evidence including stable isotope ratios, radiocarbon tracer experiments, and biomarker molecules. The problem of the missing isolated organisms for AOM is further complicated by the variety of possible syntrophic partners and TEAs now believed to be involved, including sulfate, iron and manganese oxides, nitrate, nitrite, and humic acids. Also uncertain is the question of the *EETing* and *DIETing* options for direct versus indirect interspecies electron transfer.

The consumption of methane by organisms is associated with predictable carbon and hydrogen kinetic isotope effects. As a consequence, AeOM and AOM consume ¹²C¹H₄ faster than the heavier isotopologues ¹³CH₄, ¹²C¹H₃²H, etc. This isotope enrichment trend due to microbial methane oxidation is shown in Fig. 9 (Whiticar 1999). The δ¹³C-CH₄-δ²H-CH₄ slope for microbial oxidation generally varies from 1:5 to 1:10 and tends to be larger for AeOM than AOM (Whiticar 1999; Kinnaman et al. 2007). The range of carbon and hydrogen enrichment for methane oxidation based on empirical measurements and incubations is 5–31 for ε_{C(CH₄)} and 37.5–320 for ε_{D(CH₄)} (Whiticar and Faber 1986; Alperin et al. 1988; Whiticar 1999; Kinnaman et al. 2007; Feisthauer et al. 2011; Wang et al. 2016; Penger et al. 2012; Rasigraf et al. 2012).

Microbial methane oxidation leads to diagnostic isotope separations between the oxidized methane and the resultant products, e.g., CO₂. Figure 13 shows the general region for δ¹³CO₂-δ¹³CH₄ pairs determined by AeOM or AOM and the

approximate trajectory of the isotope shift (after Whiticar 1999). The main difficulty in using $\delta^{13}\text{CO}_2$ – $\delta^{13}\text{CH}_4$ pairs to track methanotrophy is that there are multiple other sources of CO_2 that potentially can admix and thus confound the $\delta^{13}\text{CO}_2$ values and interpretation. Often, it is the shift in $\delta^{13}\text{CH}_4$ that is more diagnostic. The methane oxidation trend shown in Fig. 12 reflects the, perhaps obvious, fact that the trace amounts of oxidation water added by methanotrophy and thus H-isotope contribution to the formation water (e.g., Eqs. 13 and 16) essentially will not appreciably affect the isotope ratio of the formation water. Similarly, the methane oxidation trend in Fig. 13 is driven mostly by changes in $\delta^{13}\text{CH}_4$ and $\delta^2\text{H-CH}_4$, rather than by $\delta^{13}\text{CO}_2$ or $\delta^2\text{H-H}_2\text{O}$. However, in extremely dry systems, perhaps deep rock environments, the amount of water is so restricted that any H_2O involved with methanogenesis (e.g., Eqs. 1, 3, and 4), AeOM (e.g., Eqs. 18 and 19), or AOM (e.g., Eqs. 21 and 22) could conceivably have a measurable influence on the $\delta^2\text{H-H}_2\text{O}$ of the formation water.

Biomarker molecules, in combination with isotopes, are also effective tools to track AOM. Microbial and thermogenic methane is both ^{12}C -enriched (“isotopically light”) relative to normal organic matter, so when methane is consumed, the carbon in the organisms involved will grow with a distinctively ^{12}C -enriched signal. This is incorporated into their biomarker molecules, such as the putative archaeal compounds archaeol, biphytanol, crocetane, hydroxyarchaeols, 2,6,10,15,19-pentamethylcosane (PMI), glyceryl dialkyl glyceryl tetraethers (GDGTs), and acyclic and cyclic biphytanes, as well as, in the bacterial biomarkers, such as diplopterol, fatty acids, and alkyl ethers (e.g., Elvert et al. 1999, 2000; Hinrichs et al. 1999, 2000; Pancost et al. 2000; 2001; Bian et al. 2001; Orphan et al. 2001b; Schouten et al. 2001; Thiel et al. 1999, 2001; Wakeham et al. 2003; Summons 2013). In fact, the most ^{12}C -enriched naturally occurring organic compound known, the isoprenoid crocetane, has a $\delta^{13}\text{C}$ of -130‰ (Elvert et al. 2000). These ^{12}C -enriched compounds are strong evidence for the archaea-bacterial collaboration for AOM. In contrast, Biddle et al. (2006), based on $\delta^{13}\text{C}$ of archaeal cells and intact polar lipids from OPD cores off Peru, concluded that only a small fraction, if any, of the archaeal populations relied on methane as a carbon source. So there seems to be additional processes that perhaps can mask the ^{12}C -enriched compounds from oxidized methane. Part of the answer may lie in the rate of AOM, for example, methane seeps at the sediment-water interface surface have high rates compared with deep sediments with low rates.

Radioactive, ^{14}C -labelled substrates (e.g., $^{14}\text{CH}_4$ and $^{14}\text{CO}_2$) have been used successfully to elucidate the pathways of anaerobic methanotrophy (e.g., Kosiur and Warford 1979; Iversen and Jørgensen 1985, and more recently by Treude et al. 2003). It is interesting to note that although these labelled experiments showed that methanotrophs could oxidize CH_4 , the SRBs could not be shown to produce $^{14}\text{CO}_2$ from pure $^{14}\text{CH}_4$. Stable, ^{13}C -labelled methane has also been used to track the transfer of $^{13}\text{CH}_4$ to $^{13}\text{CO}_2$ and $^{13}\text{C-DIC}$ (e.g., Beal et al. 2009; Meulepas et al. 2010). The $^{13}\text{C-DIC}$ formed from $^{13}\text{CH}_4$ is a robust measure of AOM because $^{13}\text{C-DIC}$ from other natural, non- ^{13}C -enriched sources is only $\sim 1\%$.

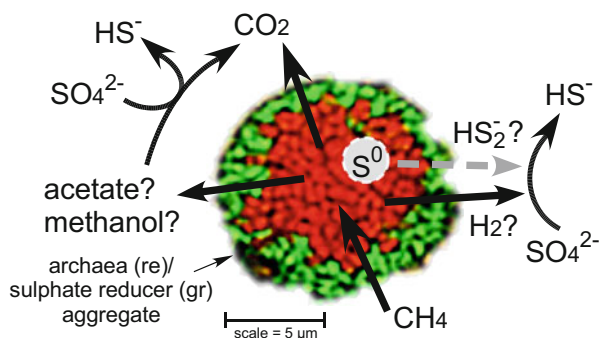
Some of the strongest evidence for the AOM pathways has come from physiologic information using molecular gene sequencing. The archaeal methanotrophs clusters, based on the archaeal 16S rRNA genes, are termed anaerobic methane-oxidizing archaea (ANaerobic MEthanotrophic archaea or ANME, e.g., Hinrichs et al. 1999; Boetius et al. 2000). In every case ANME is found to be highly intolerant of O_2 , e.g., restricted to anaerobic sediments. However, ANME are cosmopolitan and found over a range of temperatures, with thermophiles operating up to 95 °C (Schouten et al. 2003; Teske et al. 2002; Wegener et al. 2015) and at pHs ranging from 4 to 11 (Inagaki et al. 2006; Brazelton et al. 2006). Drake et al. (2015) identified AOM in granites from the Laxemar area, Sweden, with extremely ^{13}C -depleted, methane-derived secondary carbonates ($\delta^{13}C_{carb}$ of -125 ‰ VPDB) at ~ 750 m depth. Carbon-13 depleted carbonates filling fractures in the granitic rocks of the Swedish Stripa pluton were also reported by Clauer et al. (1989) to potentially have an AOM signal, further showing the ubiquitous nature of AOM in the anoxic subsurface.

Currently, three distinct, euryarchaeal, methanotrophic groups or clades, with sub-clusters, have been identified, namely, ANME-1 (subclusters a and b), ANME-2c (subclusters c and d), ANME-2a (subcluster e), and ANME-3 (subcluster f) (Niemann et al. 2006; Knittel and Boetius 2009; Bhattarai et al. 2017). ANME-1 is associated with *Methanomicrobiales* and *Methanosarcinales*, whereas ANME-2 relates to *Methanosarcinales* and ANME-3 to *Methanococoides* spp. (Timmers et al. 2017). ANME-1 and ANME-2 are both found in the SMTZ, pointing to some association with SRBs. It appears though that ANME-2 support higher AOM rates than ANME-1 (Nauhaus et al. 2005; Michaelis et al. 2002). They also distinguish themselves in that ANME-2 is associated with the diagnostic *sn*-2-hydroxyarchaeol and lipid biomarker crocetane, whereas ANME-1 is dominated by intact tetraethers (GDGT) (Blumenberg et al. 2004; Elvert et al. 2005; Niemann and Elvert 2008).

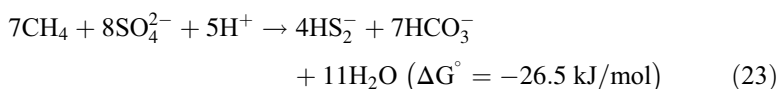
Visualization of the putative AOM aggregates of some ANME with SRBs has been made on fluorescent-labelled oligonucleotide probes with the fluorescent in situ hybridization (FISH) technique (Fig. 19). These show the syntrophic nature of the organisms (e.g., Boetius et al. 2000; Michaelis et al. 2002; Orphan et al. 2002).

On the other hand, it seems that select ANME archaea, especially certain ANME-1, appear to perform AOM alone, i.e., do not seem need a bacterial partner and thus

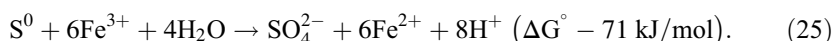
Fig. 19 Potential AOM pathways with ANME and SRBs. (Modified from Boetius et al. 2000)



may be further examples of reverse methanogenesis (Knittel et al. 2005; Orphan et al. 2002). Milucka et al. (2012) reported that ANME-2 organisms were able to reduce sulfate during AOM without SRBs (Fig. 19). Their suggestion involves the reduction of sulfate to elemental sulfur and then disulfide by ANME-2 during AOM (Eq. 23). The bisulfide is then disproportionated to sulfide and sulfate by SRBs (Eq. 24). The overall reaction is equivalent to Eq. 19:

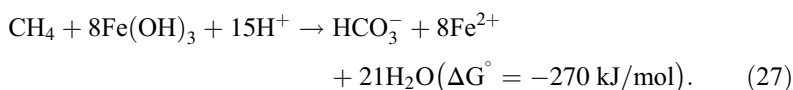
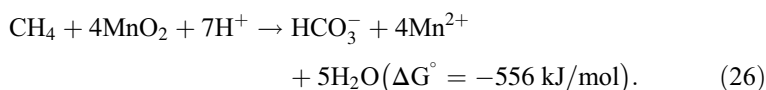


This AOM process with the intermediate to elemental sulfur could explain SR without or limited SRBs in systems such as the deep subsurface (e.g., Lollar et al. 1993; Kotelnikova 2002). Alternatively, the elemental sulfur in the AOM path could be oxidized by Mn(IV) or Fe(III) to sulfate, as put forth by Lovley and Phillips (1994), e.g., Eq. 25:



Adding to the AOM options, are the possibilities that nitrate, nitrite, iron, and manganese oxides can also act as electron accepters instead of, or in addition to, sulfate during methane oxidation. These are interesting examples of AOM, as their involvement in AOM instead of sulfate appears to violate the basic terminal electron acceptor sequence (Table 2). However, the amounts of these oxidizers in sediments are substantially less than dissolved sulfate, so unless there is recycling of N-, Mn-, and Fe oxides, they can only account for minor amounts of the total methane consumption in sediments. Sulfate is still thought to be the most significant oxidant in AOM.

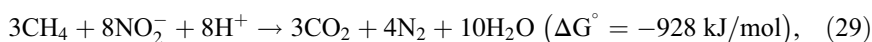
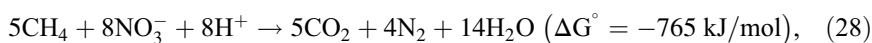
Beal et al. (2009) proposed AOM with MnO_2 and $\text{Fe}(\text{OH})_3$ reduction as shown in Eqs. 26 and 27:



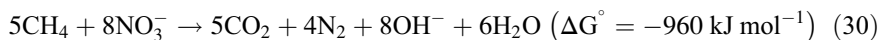
By adding the manganese and iron minerals birnessite and ferrihydrite, as TEAs, to cultures with ^{13}C -labelled methane, the authors observed enhanced AOM. The archaeal groups believed responsible belong to the Marine Benthic Group D (MBGD), as identified by 16S rRNA and methyl coenzyme M reductase (*mcrA*) gene diversity.

Beal et al. (2009), Oni and Friedrich (2017), and others make the argument that ANME-1 and ANME-2d can perform AOM independent of SRBs and that the mere proximity to SRBs does not necessarily indicate any direct electron transfer linkages between AOM and SR. Studies by Treude et al. (2014) in the Beaufort Sea sediment showed a coupling of Mn(IV) or Fe(III) reduction to AOM beneath the SMTZ, i.e., also without SR. Similar results were reported by several workers, including Biddle et al. (2006), Crowe et al. (2011), Sivan et al. (2011), Amos et al. (2012), Jorgensen et al. (2012), Wankel et al. (2012), Segarra et al. (2013), Riedinger et al. (2014, 2015), and Egger et al. (2014). Some of these studies are in marine, brackish, and transitional environments, illustrating that the amounts or fluxes of sulfate or SRBs may not always be key components in AOM. Gao et al. (2017) reported that AOM with MnO₂ as TEA ($\Delta G^\circ = -63.8 \text{ kJ/mol e}^-$) is ~15 times higher than sulfate-driven AOM ($\Delta G^\circ = -4.1 \text{ kJ/mol e}^-$). For comparison, AOM with Fe(OH)₃ ($\Delta G^\circ = -11.1 \text{ kJ/mol e}^-$) is 2.7 times higher than SR while for nitrite ($\Delta G^\circ = -116.1 \text{ kJ/mol e}^-$) is 28 times that of SR.

In addition to metals oxides, both nitrate and nitrite have also been implicated as electron acceptors for AOM, in lieu of sulfate. The bacterial denitrifying anaerobic oxidation of methane (DAMO) process is suggested by Raghoebarsing et al. (2006) to proceed according to Eqs. 28 and 29:



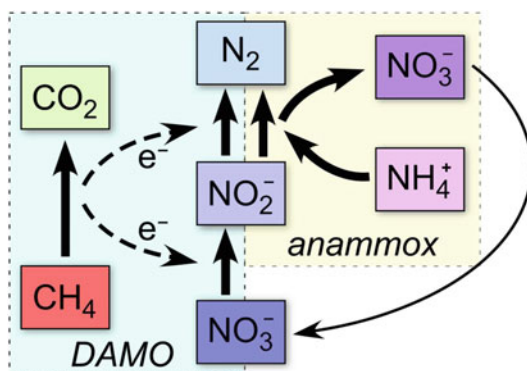
and by Islas-Lima et al. (2004) as Eq. 30:



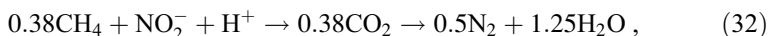
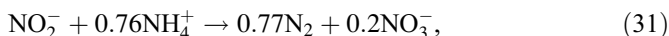
Raghoebarsing et al. (2006), using 16S rRNA gene sequence analyses, ¹³C-labelled methane, and ¹⁵N-labelled nitrate, documented that AOM was coupled to nitrite and/or nitrate reduction via an intra-aerobic methane oxidation pathway similar to the AOM-SR consortium. Their freshwater experiments ensured that oxygen was not involved, and hence AOM was performed only with denitrification. They found that the ANME-2 methanotrophic archaea was the dominant cluster in concert with the denitrifying bacteria “*Candidatus Methyloirabilis oxyfera*” (*M. oxyfera*). Similar AOM denitrification results with “*Candidatus Methanoperedens nitroreducens*” (ANME-2d) were found by Haroon et al. (2013). To complicate matters, Ettwig et al. (2008) concluded from their culture experiments with denitrifying bacteria that archaea are not required for AOM with nitrite as electron acceptor. Further, Ettwig et al. (2010) also used ¹⁵N-labelled nitrite and genomics with ¹⁸O-labelled water to show that *M. oxyfera* could reduce nitrite to nitric oxide and then using the *in situ* produced oxygen from the disproportionation of nitric oxide for methane oxidation.

Hu et al. (2015) described an analogous 3-reaction AOM process that involved the combination of anaerobic ammonium oxidation (anammox) with denitrifying

Fig. 20 Potential AOM pathways with DAMO and anammox. (After Hu et al. 2015)

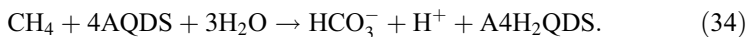


anaerobic methane oxidation DAMO (Fig. 20). Ironically, until the work on anammox by Van de Graaf et al. (1990) and Mulder et al. (1995), anaerobic ammonium oxidation, like AOM, was thought not to occur in nature. Now, it is considered to contribute critically to the ~50% of the marine N₂ production (Strous and Jetten 2004). Nitrite is reduced by anammox and then AOM with nitrite and nitrate reduction by DAMO (Eqs. 31, 32, and 33, respectively):



Initially it seemed that DAMO bacteria preferred nitrite and could utilize nitrite alone in AOM, whereas AOM decreased with nitrate (Ettwig et al. 2008). Ding et al. (2017) showed the possible decoupling of DAMO archaea from DAMO bacteria. Ultimately, DAMO culture growth depends on the mix of nitrogen utilized. He et al. (2015) required 600 days to enrich DAMO bacteria when only using nitrite, whereas a mixture of nitrite and nitrate was somewhat faster (≥ 480 days, Raghoebarsing et al. 2006). In comparison, the combination of nitrate and ammonium by Haroon et al. (2013) shortened the culturing time to 350 days. Subsequently, Fu et al. (2017) found that using nitrate, nitrite, and ammonium together could shorten growth times to ~80 days, approximately the same as AOM with SRBs (e.g., Knittel and Boetius 2009). Thus even though DAMO proceeds with the different N sources individually, it appears that combinations enhance growth and AOM.

ANME-2 archaea were shown by Scheller et al. (2016) to use external electron acceptors, such as humic acids and humic acid analogues, e.g., anthraquinone-2,6-disulfonic acid (AQDS) for AOM. These archaea are proposed to conduct AOM without syntrophic interactions, i.e., could directly transfer electrons to extracellular Fe(III) or Mn(IV) minerals without the need for SRBs. These AOM reactions with quinone-containing humic acids could be represented by Eq. 34 (Wang et al. 2017):



Wang et al. (2017) calculated that AQDS reduction coupled to ammonia oxidation was energetically viable, but not necessarily a good reaction “surrogate” for humic substances coupled with AOM. Therefore, the AOM pathway with AQDS at this point is uncertain.

The above discussion mostly pertains to marine systems replete, at least initially, in dissolved sulfate (~29 mM), supporting AOM-SR. In freshwater environments, such as oligotrophic lakes, dissolved sulfate is typically 10 to ~400 μM (Holmer and Storkholm 2001), which is thought to be too low for SR processes to be thermodynamically favorable (Smemo and Yavitt 2011). As a result of the low sulfate, it was traditionally thought that AOM, i.e., AOM-SR, was limited. There are lakes with higher sulfate, e.g., meso- and eutrophic lakes, that can have $>500 \mu\text{M SO}_4^{2-}$. Lake Cadagno, for example, has 2 mM SO_4^{2-} , and AOM-SR is suspected, although AOM-Mn/Fe could not be excluded (Schubert et al. 2011). Sulfate can be elevated in some lakes due to intense evaporation, saltwater incursions, wastewater, or drainage from mining operations, supporting AOM-SR (Martinez-Cruz et al. 2017).

Under low sulfate conditions in freshwaters, methanotrophy generally proceeds using O_2 and sometimes using NO_2^- , NO_3^- , Mn^{4+} , and Fe^{3+} as TEAs. In lakes with low $[\text{SO}_4^{2-}]$, Mn(IV), and Fe(III), reductions coupled to AOM are favorable reactions and are known to occur (Nordi et al. 2013; Sivan et al. 2011) and where aerobic methanotrophs are likely involved (Bar-Or et al. 2017; Martinez-Cruz et al. 2017). There are also observations that organic acid-mediated AOM can be an important pathway in lakes (Reed et al. 2017).

Clearly, there are multiple, possible pathways for AOM that appear to function with and without the need for sulfate or SRBs and with and without the need for direct electron transfer and utilizing various redox couples. This leads to AOM processes and sequences far more complicated than the early juxtaposition of sulfate depletion and methane accumulation zones in sediment profiles observed by geochemists in the 1970s.

7 Atmospheric Methane

Much of the current research on methane pertains to its effects in the atmosphere and on climate as, after carbon dioxide, methane is the second most important anthropogenic greenhouse gas (GHG).

The methane residence time of ~9–11 years, a perturbation lifetime of ~12.4 year, and radiative efficiency of $\sim 3.63 \times 10^{-4} \text{ Wm}^{-2} \text{ ppb}^{-1}$ (i.e., radiative forcing per molecule, Myhre et al. 2013) together with the increase in atmospheric methane since the preindustrial era (1750) of ~1,200 ppb contribute an additional 0.48 Wm^{-2} of direct radiative forcing (CH_4 , 0.33 Wm^{-2} + OH feedback, 0.11 Wm^{-2} , Schimel et al. 1996). Furthermore, the additional amount of oxidized atmospheric methane leads to an increase in tropospheric O_3 and stratospheric H_2O that contribute an additional 0.11 Wm^{-2} and 0.02 Wm^{-2} , respectively (Prather et al. 1995; Hansen and

Sato 2001; Ramaswamy et al. 2001), for a total radiative forcing of 0.57 Wm^{-2} (Ramaswamy et al. 2019). The total methane radiative forcing is $\sim 21\%$ of the long-lived GHG budget of 2.77 Wm^{-2} . This does not account for the radiative forcing of CO_2 derived from CH_4 oxidation.

The magnitudes of the various sources and sink controlling the atmospheric methane burden remain incompletely constrained. In addition to individual flux estimates, the combination of methane stable carbon and hydrogen isotope ratios of the individual major sources can help produce a bottom-up budget for the measured atmospheric values, as shown in Figs. 3 and 4 (Whiticar and Schaefer 2007). These two plots also show the respective offsets between the $\delta^{13}\text{C}\text{-CH}_4$ and $\delta^2\text{H}\text{-CH}_4$ weighted inputs and the actual atmospheric isotope values. The isotope offsets are the result of the isotope effects associated with the various removal processes of methane from the troposphere. By weighting the magnitude of the different sink fluxes and their respective isotope fractionations, we can estimate the overall enrichment factors for carbon, $\epsilon_C \sim 7.4 \%$, and hydrogen, $\epsilon_D \sim 200 \%$ (Whiticar and Schaefer 2007). The averaged values of individual methane carbon and hydrogen signatures ($\delta^{13}\text{C}\text{-CH}_4$ and $\delta^2\text{H}\text{-CH}_4$) of the major emission sources with their respective flux strengths (tg/year) can be illustrated (Fig. 22). It must be noted that the columns in Fig. 22 only illustrate the average values for the different sources and do not show the range, which is sometimes large, in methane C- and H-isotope values for any particular source. Also the groupings of source types in the budgets differ between authors and papers. The weighted input average of the sources in Fig. 22 for $\delta^{13}\text{C}\text{-CH}_4$ is -54.2% and for $\delta^2\text{H}\text{-CH}_4$ is -295% , compared with the present-day tropospheric value of $\delta^{13}\text{C}\text{-CH}_4$ of -47% and -86% , shifted due to the isotope effects of the sinks. Refinements of the methane flux source and sink terms and their representative $\delta^{13}\text{C}\text{-CH}_4$ and $\delta^2\text{H}\text{-CH}_4$ values continue to be made (e.g. Sherwood et al. 2017), which will improve our bottom-up flux source estimations and signatures. It should also be noted that there are latitudinal changes in tropospheric methane mixing ratio, $\delta^{13}\text{C}\text{-CH}_4$ and $\delta^2\text{H}\text{-CH}_4$. For example, Umezawa et al. (2012) reported North-South Pacific Ocean methane transects for the time period of 2007–2009 from 33°N to 39°S . They found for the upper troposphere a continual shift in methane mixing ratio, $\delta^{13}\text{C}\text{-CH}_4$ and $\delta^2\text{H}\text{-CH}_4$ from ~ 1810 ppb, -47% , and -87% in the north to ~ 1770 ppb, -46.9% , and -85% in the south. Similarly, in the lower troposphere, they found a continual shift in methane mixing ratio, $\delta^{13}\text{C}\text{-CH}_4$ and $\delta^2\text{H}\text{-CH}_4$ from ~ 1840 ppb, -47% , and -93% in the north to ~ 1750 , -46.8% , and -82% in the south. Considering the relatively rapid tropospheric mixing time of ~ 1 year, these interhemispheric gradients can help localize changes in fluxes.

In addition to stable isotopes, carbon-14 measurements on methane (Eisma et al. 1994; Quay et al. 1999; Petrenko et al. 2016) and ethane measurements (Helmig et al. 2016; Dalsoren et al. 2018) can also be particularly useful to indicate the inputs of fossil carbon methane (thermogenic and most abiotic methane) to the atmosphere (Wahlen et al. 1989). Based on the accepted 5,730 year half-life of ^{14}C , methane from sources $> \sim 10^5$ year, e.g., geologic sources, have diminishingly small amounts of ^{14}C and can be considered to have only “dead” carbon. In contrast, most biologic

methane is derived from recent carbon sources. Thus the abundance of $^{14}\text{CH}_4$ in the atmosphere further constrains the input flux of older sources. Owing to the recent increase in unconventional natural gas production, e.g., shale gas, there are concerns about fugitive methane emissions from wells and gas processing/transmission infrastructures to the atmosphere. The amounts and isotope signatures of these gas emissions is controversial and emphasizes the further need to refine methane sources and sinks on the underconstrained atmospheric methane budgets (Whiticar and Schaefer 2007; Schaefer et al. 2016; Schwietzke et al. 2016; Howarth 2019; Milkov et al. 2020).

As of January 2020, the mean monthly global tropospheric methane reached a high of 1873.5 ± 2 ppb (esrl.noaa.gov/gmd/ccgg/trends_ch4/), which is a $\sim 260\%$ increase over the preindustrial Holocene mixing ratio of ~ 722 ppb (WMO 2018). Since 1983, tropospheric methane has increased from 1625 ppb at rates of 2–14 ppb/year (annually 0.1–0.9%), except for a short “stabilization period” or hiatus in the rise of tropospheric methane from years 2000 to 2007 (Fig. 21, Dlugokencky et al. 1994; Dlugokencky 2019). Initially, Dlugokencky et al. (2003) offered that instead of a pause, the hiatus was simply a new steady-state condition, whereas others mentioned the curtailment of emissions from other sources, including coal, oil, and gas operations, anaerobic waste treatment plants, landfills, agricultural practices, etc. However, as tropospheric methane has been increasing again since 2007, Nisbet et al. 2014, Turner et al. (2019) and others have countered that the hiatus was only an anomalous period. This appears to be true, now 13 years post-2007, there is an

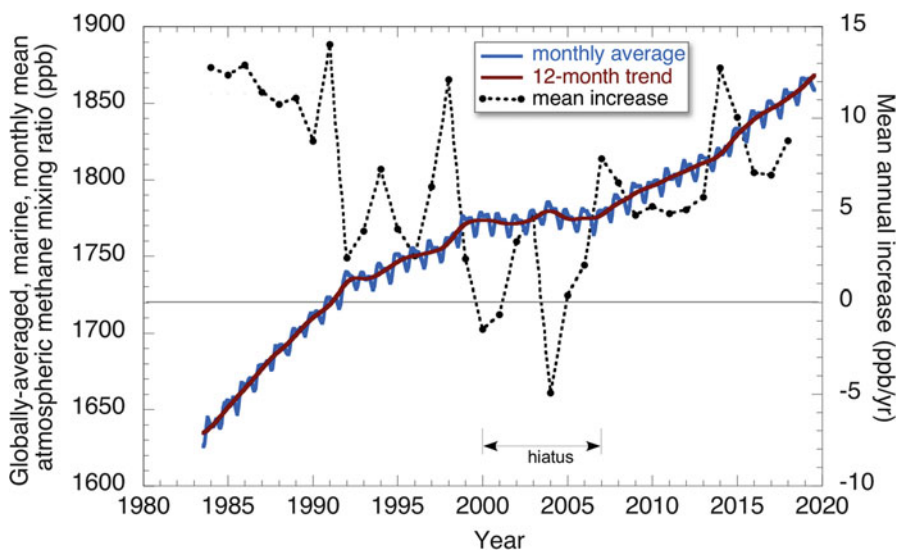


Fig. 21 Time series of NOAA/ESRL global, marine, atmospheric methane data for (1) monthly averaged mixing ratios (ppb or nmolmol^{-1} , dry air mole fraction), (2) 12-month running mean of monthly averaged mixing ratios, and (3) mean annual increase (ppb/year). The hiatus is the methane stabilization period of 2000 to 2007 (Dlugokencky et al. 1994; Dlugokencky 2019)

continual increase in methane at a growth rate of ~ 9 ppb/year, similar to pre-2000 trend.

Despite the brief pause, the NOAA/ESRL database shows a long-term increase in tropospheric methane from 1625 ppb since 1983, at an overall average annual rate of 6.4 ppb/year. It is interesting to note that the rate of increase in tropospheric methane before the hiatus (1983–2000) and after the hiatus (2007–2019) is similar (average is 8.4 ppb/year vs. 7.1 ppb/year), including maximum growth rates of 14.02 (1991) and 12.74 (2014) (Fig. 21, Dlugokencky 2019). During the hiatus the increase in tropospheric methane was only 0.48 ppb/year.

Several theories are proposed to explain the hiatus from 2000 to 2007 (e.g., Pison et al. 2013; Turner et al. 2019; Saunio et al. 2019), but there is no consensus yet. Bousquet et al. (2006) suggested that a decrease in anthropogenic emissions, such as fossil emissions in the Northern Hemisphere, caused the hiatus and that interannual variability is due to wetland and fire emissions. In contrast, Kai et al. (2011) with the combination of atmospheric CH_4 mixing ratios and $\delta^{13}\text{C}-\text{CH}_4$ state that the hiatus is consistent with long-term reductions in agricultural emissions or other microbial source(s) within the Northern Hemisphere, such as rice agriculture. They claim that the $\delta^{13}\text{C}-\text{CH}_4$ values preclude reduced fossil fuel emissions as the primary cause of the slowdown. This is juxtaposed with claims of a drop in fossil fuel emissions during that period by Schaefer et al. (2016) using $\delta^{13}\text{C}-\text{CH}_4$; by Aydin et al. (2011) and Simpson et al. (2012) using the decrease atmospheric ethane concentrations; and by Chen and Prinn (2006) using models. A decrease in biomass burning based on carbon monoxide data has also been suggested as the cause of the hiatus (Worden et al. 2017).

Kai et al. (2011) commented that the relatively constant atmospheric $\delta^2\text{H}-\text{CH}_4$ eliminates a change in the hydroxyl radical ($\text{OH}\cdot$), the largest methane sink, as the cause for the hiatus. This position contrasts with that of Rigby et al. (2008) who postulated that decreases in $\text{OH}\cdot$ concentrations were responsible. Rice et al. (2016), Turner et al. (2017), and McNorton et al. (2018) also supported changes to the hydroxyl sink.

The cause of the subsequent rise in atmospheric methane mixing ratio since 2007 (Fig. 21, Saunio et al. 2019) remains uncertain, with mismatches between top-down approaches based on atmospheric inversion models compared with bottom-up models parameterized with individual source and sink types. Increasing fossil fuel emissions and lower latitude wetlands (e.g., Northern Eurasia) and agriculture are postulated sources (Kirschke et al. 2013; Pison et al. 2013; McNorton et al. 2018). Increasing emissions of atmospheric ethane and propane support renewed emissions from oil and natural gas production (Franco et al. 2016; Hausmann et al. 2016; Helmig et al. 2016). Poulter et al. (2017) staddle this by downplaying global wetlands and suggesting a combination of fossil fuels and agriculture increases and a decrease in the photochemical sink as the cause. Nisbet et al. (2019) also suggest a possible decrease in the atmospheric sink but also noted the poorly constrained options of changes in the contributions of microbial, thermogenic, and pyrogenic methane.

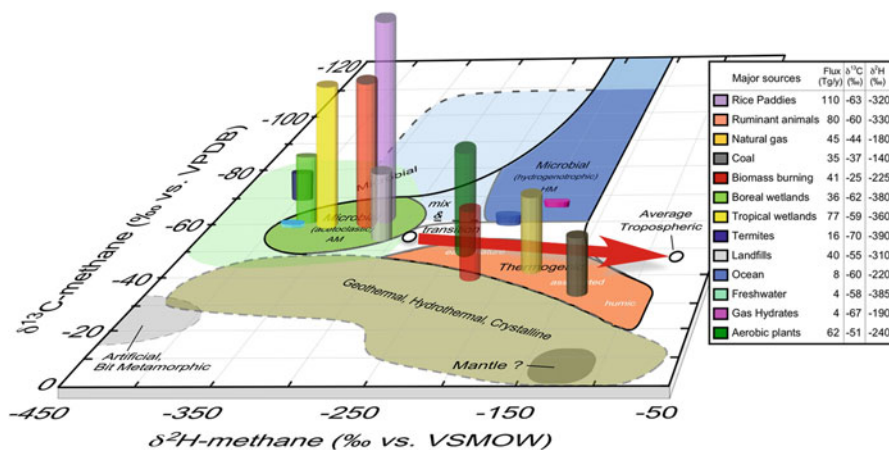


Fig. 22 3D combination CD plot of $\delta^{13}\text{C-CH}_4$ vs. $\delta^2\text{H-CH}_4$ showing the averaged values for the major methane emission source types and the magnitude (bar height) of their respective atmospheric fluxes (Tg/year). Note that the true range in isotope values for the individual sources is not depicted. The integrated input $\delta^{13}\text{C-CH}_4$ and $\delta^2\text{H-CH}_4$ signal to the troposphere from the sources and the respective C- and H-isotope fractionations by the sinks are also indicated. (Based on Whiticar and Schaefer 2007)

However, there is increasing evidence, including methane carbon isotopes and interhemispheric gradients, that high-latitude sources, such as permafrost, thermokarst lakes, wetlands, and potentially shallow gas hydrates, could be responsible (e.g., Walter et al. 2006; Dlugokencky et al. 2011; Tan and Zhuang 2015; Dimdore-Miles et al. 2018). Possible reductions in the global methane sinks, not only increases in source emissions, must also be considered in the overall budget, i.e., decreases in (1) tropospheric/stratospheric hydroxyl radical abstraction reactions (Saueressig et al. 2001; Rice et al. 2003), (2) reactions of methane with chlorine in the marine boundary layer (Allan et al. 2005), and (3) methanotrophic uptake in soils (Ridgwell et al. 1999).

The lack of consensus explaining the renewed increase in atmospheric methane is unfortunate. It is important to identify the relevant shifts in sources and sinks to determine if and how we can effect changes to reduce emissions from a climate change perspective (Fig. 22).

8 Summary

Methane is ubiquitous on Earth and contributes importantly to our energy economies, climate forcing, and carbon budgets. Under the present oxidizing atmosphere, methane cycles with carbon dioxide through a suite of biologic and abiotic pathways. Figure 23 shows a larger-scale, summary view of the methane cycle. Contributions to the methane pool come from the variety of methanogenic pathways, i.e., hydrogenotrophic (HM), acetoclastic (AM), and methylotrophic methanogenesis.

The catagenic formation of thermogenic methane from mature kerogens is also a major component. Abiotic sources, including methanation, radiolysis, and magmatic and mantle origins, also contribute unknown amounts to the methane budget, albeit substantially less than the biologic sources. Microbially mediated aerobic (AeOM) and anaerobic (AOM) methane oxidation (Fig. 23) are important biofilters that consume the majority of methane produced in sediments, soils, and lakes. Photochemical and abiotic oxidation of methane, e.g., fires, also reduce methane in the atmosphere. We are slowly establishing more reliable estimates of methane formation and oxidation rates, sizes of major methane pools (hydrates, hydrocarbon reservoirs, sediments/soils), and the magnitude of methane fluxes. Although the

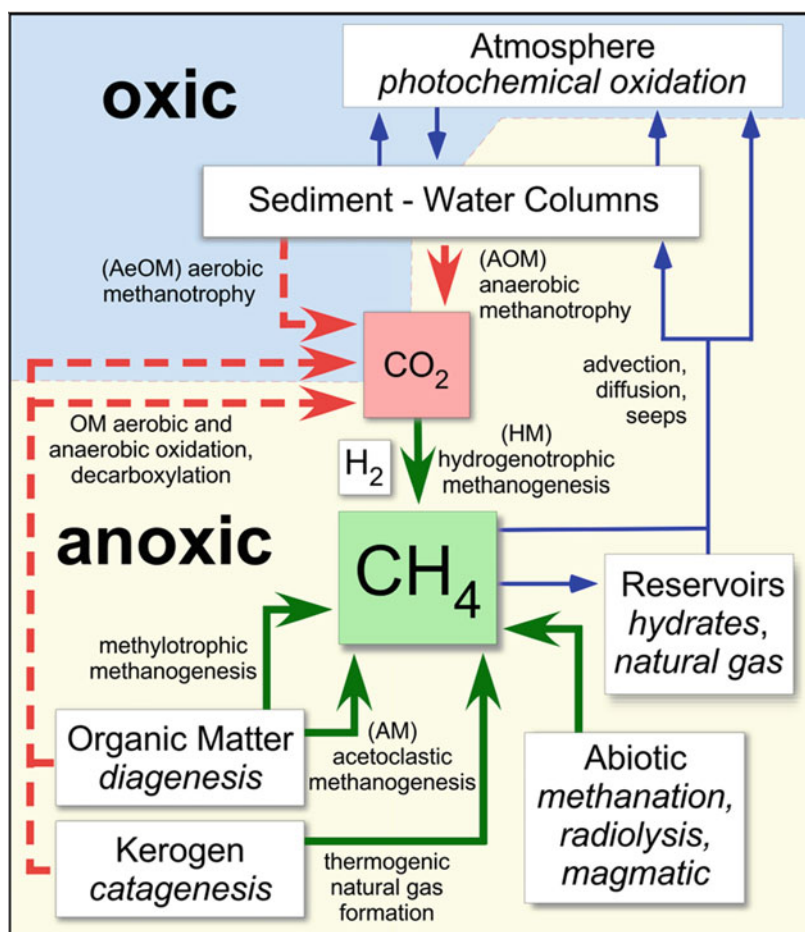


Fig. 23 Summary schematic of biotic and abiotic processes of methane formation and oxidation. The blue-shaded section is oxic, and the yellow shaded is anoxic. Methane formation processes are shown as thicker, solid, green arrow lines, while oxidation processes are dashed, red arrow lines. Transport mechanisms are shown as thin, blue arrow lines

constraints on these estimates are improving, experience demonstrates that our knowledge on this topic remains incomplete and that surprises are still possible.

Looking forward, one of the most critical aspects regarding methane biogeochemistry that needs more and immediate attention is the ongoing risk that methane poses with respect to climate change. The potential for large changes in the existing methane budget, e.g., due to shelf hydrate destabilization or permafrost sources, land-use changes, and natural gas production, requires careful attention to understanding of the mechanisms and magnitudes of the processes controlling the methane sources and sinks.

Acknowledgments The ideas and information provided in this chapter are founded on the efforts and findings of a large number of researchers, a portion of whom are in the list of references. This work and the funding for it resulted from a fellowship at the Hanse-Wissenschaftskolleg (HWK), Institute for Advanced Study, Delmenhorst, Germany. The author is very grateful for the generous support of HWK.

References

- Achtnich C, Bak F, Conrad R (1995) Competition for electron donors among nitrate reducers, ferric iron reducers, sulfate reducers, and methanogens in anoxic paddy soil. *Biol Fertil Soils* 19 (1):65–72
- Allan W, Gomez DC, Lowe AJ, Struthers H, Brailsford GW (2005) Interannual variation of ^{13}C in tropospheric methane: implications for a possible atomic chlorine sink in the marine boundary layer. *J Geophys Res* 110:D11306
- Allan W, Struthers H, Lowe DC (2007) Methane carbon isotope effects caused by atomic chlorine in the marine boundary layer: global model results compared with Southern Hemisphere measurements. *J Geophys Res Atmos* 112(D4):D04306
- Alperin MJ, Reeburgh WS (1985) Inhibition experiments on anaerobic methane oxidation. *Appl Environ Microbiol* 50(4):940–945
- Alperin MJ, Reeburgh WS, Whiticar MJ (1988) Carbon and hydrogen isotope fractionation resulting from anaerobic methane oxidation. *Glob Biogeochem Cycles* 2(3):279–288
- Alstad KP, Whiticar MJ (2011) Carbon and hydrogen isotope ratio characterization of methane dynamics for Fluxnet Peatland Ecosystems. *Org Geochem* 42(5):548–558
- Amend JP, Shock EL (2001) Energetics of overall metabolic reactions of thermophilic and hyperthermophilic Archaea and Bacteria. *FEMS Microbiol Rev* 25:175–243
- Amos RT, Bekins BA, Cozzarelli IM, Voytek MA, Kirshtein JD, Jones EJP, Blowes DW (2012) Evidence for iron-mediated anaerobic methane oxidation in a crude oil-contaminated aquifer. *Geobiology* 10:506–517
- Andersen BL, Bidoglio G, Leip A, Rembges D (1998) A new method to study simultaneous methane oxidation and methane production in soils. *Global Biogeochem Cycle* 12(4):587–594
- Anderson AL, Harwood RJ, Lovelace RT (1971) Investigation of gas in bottom sediments. Technical report 70-28 (ARL-TR-70-28), Applied Research Laboratories, University of Texas at Austin
- Antony CP, Kumaresan D, Hunger S, Drake HL, Murrell JC, Shouche YS (2013) Microbiology of Lonar Lake and other soda lakes. *ISME journal* 7(3):468–76
- Aselmann I, Crutzen DJ (1989) Global distribution of natural freshwater wetlands and rice paddies, their net primary productivity, seasonality and possible methane emissions. *J Atmos Chem* 8:307–385
- Atkinson LP, Richards FA (1967) The occurrence and distribution of methane in the marine environment. *Deep Sea Res Oceanogr Abstr* 14(6):673–684

- Avery GB, Shannon RD, White JR, Martens CS, Alperin MJ (1999) Effect of seasonal changes in the pathways of methanogenesis on the $\delta^{13}\text{C}$ values of pore water methane in a Michigan peatland. *Glob Biogeochem Cycles* 13(2):475–484
- Aydin M, Verhulst KR, Saltzman ES, Battle MO, Montzka SA, Blake DR, Tang Q, Prather MJ (2011) Recent decreases in fossil-fuel emissions of ethane and methane derived from firm air. *Nature* 476(7359):198–201
- Balabane M, Galimov E, Hermann M, Létolle R (1987) Hydrogen and carbon isotope fractionation during experimental production of bacterial methane. *Org Geochem* 11(2):115–119
- Baptiste E, Brochier E, Boucher Y (2005) Higher-level classification of the Archaea: evolution of methanogenesis and methanogens. *Archaea* 1:353–363
- Barker HA (1936a) Studies upon the methane-producing bacteria. *Arch Microbiol* 7(1):420–438
- Barker HA (1936b) On the biochemistry of the methane fermentation. *Arch Microbiol* 7(1):404–419
- Barker H, Buswell AM (1956) Biological formation of methane. *Ind Eng Chem* 48(9):1438–1443
- Barnes RO, Goldberg ED (1976) Methane production and consumption in anoxic marine sediments. *Geology* 4(5):297–300
- Bar-Or I, Elvert M, Eckert W, Kushmaro A, Vigderovich H, Zhu Q, Ben-Dov E, Sivan O (2017) Iron-coupled anaerobic oxidation of methane performed by a mixed bacterial-archaeal community based on poorly reactive minerals. *Environ Sci Technol* 51(21):12293–12301
- Basiliko N, Knowles R, Moore TR (2004) Roles of moss species and habitat in methane consumption potential in a northern peatland. *Wetlands* 24(1):178–185
- Bastviken D, Cole JJ, Pace ML, de Bogert V, Matthew C (2008) Fates of methane from different lake habitats: connecting whole-lake budgets and CH_4 emissions. *J Geophys Res Biogeosci* 113(G02024):1–13
- Bastviken D, Tranvik LJ, Downing JA, Crill PM, Enrich-Prast A (2011) Freshwater methane emissions offset the continental carbon sink. *Science* 331(6013):50
- Baublys KA, Hamilton SK, Golding SD, Vink S, Esterle J (2015) Microbial controls on the origin and evolution of coal seam gases and production waters of the wallon subgroup; surat basin, australia. *Int J Coal Geol* 147–148:85–104
- Beal EJ, House CH, Orphan VJ (2009) Manganese-and iron-dependent marine methane oxidation. *Science* 325(5937):184–187
- Beblo K, Rabbow E, Rachel R, Huber H, Rettberg P (2009) Tolerance of thermophilic and hyperthermophilic microorganisms to desiccation. *Extremophiles* 13(3):521–531
- Beerling DJ, Gardiner T, Leggett G, McLeod A, Quick WP (2008) Missing methane emissions from leaves of terrestrial plants. *Glob Chang Biol* 14:1821–1826
- Beijerinck MW (1895) Ueber *Spirillum desulfuricans* als Ursache von Sulfatreduktion. *Cent Bakt (etc.)*, Abt II 1:1,49, 104
- Bender M, Conrad R (1992) Kinetics of CH_4 oxidation in oxic soils exposed to ambient air or high CH_4 mixing ratios. *FEMS Microbiol Ecol* 101(4):261–269
- Benstead J, King GM (1997) Response of methanotrophic activity in forest soil to methane availability. *FEMS Microbiol Ecol* 23(4):333–340
- Bernard BB, Brooks JM, Sackett WM (1976) Natural gas seepage in the Gulf of Mexico. *Earth Planet Sci Lett* 31(1):48–54
- Berndmeyer C, Thiel V, Schmale O, Blumenberg M (2013) Biomarkers for aerobic methanotrophy in the water column of the stratified gotland deep (baltic sea). *Org Geochem* 55:103–111
- Berner RA (1980) Early diagenesis: a theoretical approach. Princeton University Press, Princeton, 241pp
- Bhattarai S, Cassarini C, Gonzales-Gil G, Egger M, Slomp C, Zhang Y, Lens PNL (2017) Anaerobic methane-oxidizing microbial community in a coastal marine sediment: Anaerobic methanotrophy dominated by ANME-3. *Microb Ecol* 74(3):608–622
- Bian L, Hinrichs K-U, Xie T, Brassell SC, Iversen N, Fossing H, Jørgensen BB, Hayes JM (2001) Algal and archaeal polyisoprenoids in a recent marine sediment: molecular isotopic evidence for anaerobic oxidation of methane. *Geochem Geophys Geosyst* G3, 2 2000GC000112:1–22

- Bianchi M, Marty D, Teysse J-L, Fowler SW (1992) Strictly aerobic and anaerobic bacteria associated with sinking particulate matter and zooplankton fecal pellets. *Mar Ecol Prog Ser* 88:55–60
- Biddle JF, Lipp JS, Lever MA, Lloyd KG, Sørensen KB et al (2006) Heterotrophic Archaea dominate sedimentary subsurface ecosystems off Peru. *Proc Natl Acad Sci U S A* 103: 3846–3851
- Bird CW, Lynch JM, Pirt FJ, Reid WW, Brooks CJW, Middleditch BS (1971) Steroids and squalene in *Methylococcus capsulatus* grown on methane. *Nature* 230:473–474
- Blöchl E, Rachel R, Burggraf S, Hafenbradl D, Jannasch HW, Stetter KO (1997) *Pyrolobus fumarii*, gen. and sp. nov., represents a novel group of archaea, extending the upper temperature limit for life to 113 °C. *Extremophiles* 1(1):14–21
- Bloom AA, Lee-Taylor J, Madronich S, Messenger DJ, Palmer PI, Reay DS, McLeod AR (2010) Global methane emission estimates from ultraviolet irradiation of terrestrial plant foliage. *New Phytol* 187(2):417–425
- Blumenberg M, Seifert R, Reitner J, Pape T, Michaelis W (2004) Membrane lipid patterns typify distinct anaerobic methanotrophic consortia. *Proc Natl Acad Sci* 101:11111–11116
- Blumenberg M, Seifert R, Michaelis W (2007) Aerobic methanotrophy in the oxic-anoxic transition zone of the Black Sea water column. *Org Geochem* 38(1):84–91
- Boone DR, Worakit S, Mathrani IM, Mah RA (1986) Alkaliphilic methanogens from high-pH lake sediments. *Syst Appl Microbiol* 7:230–234
- Bodrossy L, Murrell JC, Dalton H, Kalman M, Puskas LG, Kovacs KL (1995) Heat-tolerant methanotrophic bacteria from the hotwater effluent of a natural-gas field. *Appl Environ Microbiol* 61:3549–3555
- Boeckx P, Van Cleemput O, Villaralvo I (1997) Methane oxidation in soils with different textures and land use. *Nutr Cycl Agroecosyst* 49:91–95
- Boetius A, Wenzhöfer F (2013) Seafloor oxygen consumption fuelled by methane from cold seeps. *Nat Geosci* 6(9):725–734
- Boetius A, Ravensschlag K, Schubert CJ, Rickert D, Widdel F, Giesecke A, Amann R, Jørgensen BB, Witte U, Pfannkuche O (2000) A marine microbial consortium apparently mediating anaerobic oxidation of methane. *Nature* 407:623–626
- Bonaglia S, Nascimento FA, Bartoli M, Klawonn I, Brüchert V (2014) Meiofauna increases bacterial denitrification in marine sediments. *Nat Commun* 5:5133
- Boswell R, Collett TS (2011) Current perspectives on gas hydrate resources. *Energy Environ Sci* 4 (4):1206–1215
- Botz R, Pokojski HD, Schmitt M, Thomm M (1996) Carbon isotope fractionation during bacterial methanogenesis by CO₂ reduction. *Org Geochem* 25:255–262
- Boucher O, Friedlingstein P, Collins B, Shine KP (2009) The indirect global warming potential and global temperature change potential due to methane oxidation. *Environ Res Lett* 4 (4):044007
- Bousquet P, Ciais P, Miller JB, Dlugokencky EJ, Hauglustaine DA, Prigent C, Langenfelds RL (2006) Contribution of anthropogenic and natural sources to atmospheric methane variability. *Nature* 443(7110):439
- Bouvier P, Rohmer M, Benveniste P, Ourisson G (1976) D8(14)-Steroids in the bacterium *Methylococcus capsulatus*. *Biochem J* 159:267–271
- Bowman JP (2006) The methanotrophs—the families methylococcaceae and methylocystaceae. In: Dworkin M (ed) *The prokaryotes*, vol 5. Springer, New York, pp 266–289
- Bowman JP (2011) Approaches for the characterization and description of novel methanotrophic bacteria, Chapter 4. In: Rosenzweig AC, Ragsdale SW (eds) *Methods in enzymology*, vol 495. Academic, Burlington, pp 45–62
- BP Statistical Review of World Energy June 2017
- Brassell SC, Wardroper AMK, Thomson ID, Maxwell JR, Eglinton G (1981) Specific acyclic isoprenoids as biological markers of methanogenic bacteria in marine sediments. *Nature* 290 (5808):693–696

- Brazelton WJ, Schrenk MO, Kelley DS, Baross JA (2006) Methane- and sulfur-metabolizing microbial communities dominate the Lost City hydrothermal field ecosystem. *Appl Environ Microbiol* 72:6257–6270
- Brooks JM (1979) Deep methane maxima in the Northwest Caribbean Sea: possible seepage along the Jamaica ridge. *Science* 206:1069–1071
- Brüggemann N, Meier R, Steigner D, Zimmer I, Louis S, Schnitzler J (2009) Nonmicrobial aerobic methane emission from poplar shoot cultures under low-light conditions. *New Phytol* 182(4):912–918
- Bruhn D, Møller IM, Mikkelsen TN, Ambus P (2012) Terrestrial plant methane production and emission. *Physiol Plant* 144(3):201–209
- Bryant MP, Wolin EA, Wolin MJ, Wolfe RS (1967) *Methanobacillus omelianskii*, a symbiotic association of two species of bacteria. *Arch Mikrobiol* 59(1–3):20–31
- Buckley DH, Baumgartner LK, Visscher PT (2008) Vertical distribution of methane metabolism in microbial mats of the Great Sippewissett salt marsh. *Environ Microbiol* 10:967–977
- Bürgmann H (2011) Methane oxidation (aerobic). In: *Encyclopedia of geobiology*. Springer Netherlands, Dordrecht, pp 575–578
- Burke RA Jr, Rexd DF, Brooks JM, Lavom DM (1983) Upper water column methane geochemistry in the eastern tropical North Pacific. *Limnol Oceanogr* 28:19–32
- Busby J, Richardson FG (1957) The absorption of sound in sediments. *Geophysics* 22:824
- Cadioux SB, White JR, Sauer PE, Peng Y, Goldman AE, Pratt LM (2016) Large fractionations of C and H isotopes related to methane oxidation in Arctic lakes. *Geochim Cosmochim Acta* 187:141–155
- Caldwell SL, Laidler JR, Brewer EA, Eberly JO, Sandborgh SC, Colwell FS (2008) Anaerobic oxidation of methane: mechanisms, bioenergetics, and the ecology of associated microorganisms. *Environ Sci Technol* 42(18):6791–6799
- Campen RK, Sowers T, Alley RB (2003) Evidence of microbial consortia metabolizing within a low-latitude mountain glacier. *Geology* 31(3):231–234
- Canfield DE (1993) Organic matter oxidation in marine sediments. In *Interactions of C, N, P and S biogeochemical Cycles and Global Change*. Springer, Berlin, pp 333–363
- Capelle DW, Hawley AK, Hallam S, Tortell PD (2018) A multi-year time-series of N₂O dynamics in a seasonally anoxic fjord: Saanich Inlet, British Columbia. *Limnol Oceanogr* 63(2):524–539
- Capone DG, Kiene RP (1988) Comparisons of microbial dynamics in marine and freshwater sediments: contrasts in anaerobic carbon catabolism. *Limnol Oceanogr* 33:725–749
- Capenberg TE (1972) Ecological observations on Heterotrophic, methane oxidizing and sulfate reducing bacteria in Pond. *Hydrobiologia* 40(4):471–485
- Capenberg TE (1975) A study of mixed continuous cultures of sulfate-reducing and methane-producing bacteria. *Microb Ecol* 2(1):60–72
- Catling DC, Claire MW, Zahnle KJ (2007) Anaerobic methanotrophy and the rise of atmospheric oxygen. *Philos Trans R Soc A: Math Phys Eng Sci* 365(1856):1867–1888
- Chaban B, Ng SY, Jarrell KF (2006) Archaeal habitats – from the extreme to the ordinary. *Can J Microbiol* 52(2):73–116
- Chan OC, Claus P, Casper P, Ulrich A, Lueders T, Conrad R (2005) Vertical distribution of structure and function of the methanogenic archaeal community in lake dagow sediment. *Environ Microbiol* 7(8):1139–1149
- Chanton JP (2005) The effect of gas transport on the isotope signature of methane in wetlands. *Org Geochem* 36:753–768
- Chapelle FH, O'Neill K, Bradley PM, Methé BA, Ciuffo SA, Knobel LL, Lovley DR (2002) A hydrogen-based subsurface microbial community dominated by methanogens. *Nature* 415(6869):312–315
- Chappe B, Albrecht P, Michaelis W (1982) Polar lipids of archaebacteria in sediments and petroleum. *Science* 217:65–66

- Chen Y-H, Prinn RG (2006) Estimation of atmospheric methane emissions between 1996 and 2001 using a three-dimensional global chemical transport model. *J Geophys Res Atmos* 111(D10): D10307
- Childress JJ, Fisher CR, Brooks JM, Kennicutt MC, Bidigare RAAE, Anderson AE (1986) A methanotrophic marine molluscan (*Bivalvia*, Mytilidae) symbiosis: mussels fueled by gas. *Science* 233(4770):1306–1308
- Chiriac CM, Baricz A, Szekeres E, Rudi K, Dragoş N, Coman C (2018) Microbial composition and diversity patterns in deep hyperthermal aquifers from the western plain of Romania. *Microb Ecol* 75(1):38–51
- CIA The World Fact Book (2017). <https://www.cia.gov/library/publications/the-world-factbook/rankorder/2253rank.html>
- Cicerone RJ, Oremland RS (1988) Biogeochemical aspects of atmospheric methane. *Glob Biogeochem Cycles* 2:299–327
- Clauer N, Frapé SK, Fritz B (1989) Calcite veins of the stripa granite (Sweden) as records of the origin of the groundwaters and their interactions with the granitic body. *Geochim Cosmochim Acta* 53(8):1777–1781
- Claypool GE (1999) Biogenic ethane—where does it come from? Abstract. In: American Association of Petroleum Geologists Hedberg Research conference: natural gas formation and occurrence, Durango, pp 27–29
- Claypool GE, Kaplan IR (1974) The origin and distribution of methane in marine sediments. In: Kaplan IR (ed) *Natural gases in marine sediments*. Marine science, vol 3. Springer, Boston, pp 99–139
- Coleman DD, Risatti JB, Schoell M (1981) Fractionation of carbon and hydrogen isotopes by methane-oxidizing bacteria. *Geochim Cosmochim Acta* 45(7):1033–1037
- Colmer TD (2003) Long-distance transport of gases in plants: a perspective on internal aeration and radial oxygen loss from roots. *Plant Cell Environment* 26(1):17–36
- Colwell FS, Onstott TC, Delwiche ME, Chandler D, Fredrickson JK, Yao Q, Long PE (1997) Microorganisms from deep, high temperature sandstones: constraints on microbial colonization. *FEMS Microbiol Rev* 20(3):425–435
- Conrad R (1996) Soil microorganisms as controllers of atmospheric trace gases (H_2 , CO, CH_4 , OCS, N_2O , and NO). *Microbiol Rev* 60:609–640
- Conrad R (2009) The global methane cycle: recent advances in understanding the microbial processes involved. *Environmental microbiology reports* 1(5):285–292
- Conrad R, Klose M (1999) How specific is the inhibition by methyl fluoride of acetoclastic methanogenesis in anoxic rice field soil? *FEMS Microbiol Ecol* 30:47–56
- Conrad R, Schütz H, Barbbble M (1987) Temperature limitation of hydrogen turnover and methanogenesis in anoxic paddy soil. *FEMS Microbiol Ecol* 45:281–289
- Coolhaas C (1928) Zur Kenntnis der Dissimilation fettsaurer Salze und Kohlenhydrate durch thermophile Bakterien. *Zentralbl Bakteriol Parasitenkd Infektionskr Hyg Abt* 2(75):161–170
- Costa C, Dijkema C, Friedrich M, Garcia-Encina P, Fernandez-Polanco F, Stams AJM (2000) Denitrification with methane as electron donor in oxygen-limited bioreactors. *Appl Microbiol Biotechnol* 53(6):754–762
- Crowe SA, Katsev S, Leslie K, Sturm A, Magen C, Nomosatryo S, Pack MA, Kessler JD, Reebergh WS, Roberts JA, Gonzalez L, Douglas HG, Mucci A, Sundby B, Fowle DA (2011) The methane cycle in ferruginous Lake Matano. *Geobiology* 9:61–78
- Crutzen PJ (1991) Methane's sinks and sources. *Nature* 350(6317):380–381
- Crutzen PJ, Sanhueza E, Brenninkmeijer CAM (2006) Methane production from mixed tropical savanna and forest vegetation in Venezuela. *Atmos Chem Phys Discuss* 2:3093–3097
- D'Hondt S, Inagaki F, Zarikian CA, Abrams LJ, Dubois N, Engelhardt T, Hoppie BW (2015) Presence of oxygen and aerobic communities from sea floor to basement in deep-sea sediments. *Nat Geosci* 8(4):299
- Dacey JWH (1981) How aquatic plants ventilate. *Oceanus* 24:43–51

- Daines SJ, Lenton TM (2016) The effect of widespread early aerobic marine ecosystems on methane cycling and the Great Oxidation. *Earth Planet Sci Lett* 434:42–51
- Dalal RC, Allen DE (2008) Greenhouse gas fluxes from natural ecosystems. *Aust J Bot* 56(5): 369–407
- Dalal RC, Allen DE, Livesley SJ, Richards G (2008) Magnitude and biophysical regulators of methane emission and consumption in the Australian agricultural, forest, and submerged landscapes: a review. *Plant Soil* 309:43–76
- Dale AW, Regnier P, Knab N, Jørgensen BB, Van Cappellen P (2008) Anaerobic oxidation of methane (AOM) in marine sediments from the Skagerrak (Denmark): II. Reaction-transport modeling. *Geochim Cosmochim Acta* 72:2880–2894
- Dalsoren S, Myhre G, Hodnebrog O, Myhre C, Stohl A, Pisso I, Wallasch M (2018) Discrepancy between simulated and observed ethane and propane levels explained by underestimated fossil emissions. *Nat Geosci* 11(3):178–178
- Damm E, Helmke E, Thoms S, Schauer U, Nöthig E, Bakker K, Kiene RP (2010) Methane production in aerobic oligotrophic surface water in the central Arctic Ocean. *Biogeosciences* 7(3):1099–1108
- Daniel RM (1992) Modern life at high temperatures. *Orig Life Evol Biosph* 22(1–4):33–42
- Daniels L, Fuchs G, Thauer RK, Zeikus JG (1977) Carbon monoxide oxidation by methanogenic bacteria. *J Bacteriol* 132:118–126
- Daniels L, Folton G, Spencer RW, Orme-Johnson WH (1980) Origin of hydrogen in methane produced by *Methanobacterium thermoautotrophicum*. *J Bacteriol* 141:694–698
- Davis JB, Yarbrough HF (1966) Anaerobic oxidation of hydrocarbons by *Desulfovibrio desulfuricans*. *Chem Geol* 1:137–144
- De Angelis MA, Lilley MD, Baross JA (1993) Methane oxidation in deep-sea hydrothermal plumes of the Endeavour Segment of the Juan de Fuca Ridge. *Deep-Sea Res I Oceanogr Res Pap* 40 (6):1169–1186
- de Bont JAM, Lee KK, Bouldin DF (1978) Bacterial oxidation of methane in a rice paddy. *Ecol Bull* 26:91–96
- De Rosa M, Gambacorta A (1988) The lipids of archaeobacteria. *Prog Lipid Res* 27(3):153–175
- DeChaine EG, Cavanaugh CM (2006) Symbioses of methanotrophs and deep-sea mussels (mytilidae: Bathymodiolinae). In: Overmann J (ed) *Molecular basis of symbiosis*. Springer, Berlin, pp 227–249
- Dedysh SN, Dunfield PF (2011) Facultative and obligate methanotrophs: how to identify and differentiate them. In *Methods in Enzymology* 495(3):31–44
- Dedysh SN, Liesack W, Khmel'nina VN, Suzina NE, Trotsenko YA, Semrau JD, Bares AM, Panikov NS, Tiedje JM (2000) *Methylocella palustris* gen. nov., sp. nov., a new methane-oxidizing acidophilic bacterium from peat bogs, representing a novel subtype of serine-pathway methanotrophs. *Int J Syst Evol Microbiol* 50:955–969
- Del Grosso SJ, Parton WJ, Mosier AR, Ojima DS, Potter CS, Borken W, Brumme R, Butterbach-Bahl K, Crill PM, Dobbie K, Smith KA (2000) General CH₄ oxidation model and comparisons of CH₄ oxidation in natural and managed systems. *Global Biogeochem Cy* 14:999–1019
- del Valle DA, Karl DM (2014) Aerobic production of methane from dissolved water-column methylphosphonate and sinking particles in the North Pacific Subtropical Gyre. *Aquat Microb Ecol* 73(2):93–105
- DeLong EF (2000) Resolving a methane mystery. *Nature* 407:577–579
- Demirel B, Scherer P (2008) The roles of acetotrophic and hydrogenotrophic methanogens during anaerobic conversion of biomass to methane: a review. *Rev Environ Sci Biotechnol* 7(2):173–190
- Denman KL et al (2007) Couplings between changes in the climate system and biogeochemistry, chapter 7. In: Solomon S et al (eds) *Climate change 2007: the physical science basis. Contribution of working group I to the fourth assessment report of the intergovernmental panel on climate change*. Cambridge University Press, Cambridge, UK, pp 499–587

- Deutzmann JS, Schink B (2011) Anaerobic oxidation of methane in sediments of Lake Constance, an oligotrophic freshwater lake. *Appl Environ Microbiol* 77(13):4429–4436
- Dickens GR, O'Neil JR, Rea DK, Owen RM (1995) Dissociation of oceanic methane hydrate as a cause of the carbon isotope excursion at the end of the Paleocene. *Paleoceanography* 10: 965–971
- Diender M, Stams AJ, Sousa DZ (2015) Pathways and bioenergetics of anaerobic carbon monoxide fermentation. *Front Microbiol* 6:1275
- Dimdore-Miles OB, Palmer PI, Bruhwiler LP (2018) Detecting changes in Arctic methane emissions: limitations of the inter-polar difference of atmospheric mole fractions. *Atmos Chem Phys Discuss.* <https://doi.org/10.5194/acp-2017-1041>. 18p
- Ding J, Lu Y, Fu L, Ding Z, Mu Y, Cheng SH, Zeng RJ (2017) Decoupling of DAMO archaea from DAMO bacteria in a methane-driven microbial fuel cell. *Water Research* 110 112–119
- Dlugokencky EJ (2019) NOAA/ESRL. www.esrl.noaa.gov/gmd/ccgg/trends_ch4/. Accessed 7 Dec 2019
- Dlugokencky EJ, Steele LP, Lang PM, Masarie KA (1994) The growth rate and distribution of atmospheric methane. *J Geophys Res Atmos* 99(D8):17021–17043
- Dlugokencky EJ, Houweling S, Bruhwiler L, Masarie KA, Lang PM, Miller JB, Tans PP (2003) Atmospheric methane levels off: temporary pause or a new steady state? *Geophys Res Lett* 30 (19):1–4
- Dlugokencky EJ, Nisbet EG, Fisher R, Lowry D (2011) Global atmospheric methane: budget, changes and dangers. *Philos Trans: Math Phys Eng Sci* 369(1943):2058–2072
- Doig F (1994) Bacterial methanogenesis in Canadian Shield groundwaters. MSc thesis, University of Toronto, Toronto, 99pp
- Dolfing J, Larter SR, Head IM (2008) Thermodynamic constraints on methanogenic crude oil biodegradation. *ISME J* 2:442–452
- Due NT, Crill P, Bastviken D (2010) Implications of temperature and sediment characteristics on methane formation and oxidation in lake sediments. *Biogeochemistry* 100(1–3):185–196
- Dueck TA, DeVisser R, Poorter H, Persijn S, Gorissen A, DeVisser W et al (2007) No evidence for substantial aerobic methane emission by terrestrial plants: a ^{13}C -labelling approach. *New Phytol* 175:29–35
- Dunfield PF, Conrad R (2000) Starvation alters the apparent half-saturation constant for methane in the type II methanotroph *Methylocystis* strain LR1. *Appl Environ Microbiol* 66:4136–4138
- Dunfield P, Dumont R, Moore TR (1993) Methane production and consumption in temperate and subarctic peat soils: response to temperature and pH. *Soil Biol Biochem* 25(3):321–326
- Dunfield PF, Liesack W, Henckel T, Knowles R, Conrad R (1999) High-affinity methane oxidation by a soil enrichment culture containing a type II methanotroph. *Appl Environ Microbiol* 65 (3):1009–1014
- Duperron S, Bergin C, Zielinski F, Blazejak A, Pernthaler A, McKinnes ZP et al (2006) A dual symbiosis shared by two mussel species, *Bathymodiolus azoricus* and *B. puteoserpentis* (Bivalvia: Mytilidae) from hydrothermal vents along the Mid-Atlantic Ridge. *Environ Microbiol* 8:1441–1447
- Dworkin MM, Falkow S, Rosenberg E, Schleifer K, Stackebrandt E (2006) The prokaryotes: A handbook on the biology of bacteria, 3rd edition, Vol. 3 Archaea. Springer, New York, 1188 p
- Edgerton H, Seibold E, Vollbrecht K, Werner F (1966) Morphologische Untersuchungen am Mittelgrund (Eckernförder Bucht, westliche Ostsee). *Meyniana* 16:37–50
- egger M, Rasigraf O, Sapart CJ, Jilbert T, Jetten MS, Röckmann T, van der Veen C, Bändä N, Kartal B, Ettwig KF, Slomp CP (2014) Iron-mediated anaerobic oxidation of methane in brackish coastal sediments. *Environ Sci Technol* 49(1):277–283
- Eisma R, van der Borg K, de Jong AFM, Kieskamp WM, Veltkamp AC (1994) Measurements of the ^{14}C content of atmospheric methane in the Netherlands to determine the regional emissions of $^{14}\text{CH}_4$. *Nucl Instrum Methods Phys Res, Sect B* 92(1–4):410–412
- Elvert M, Niemann H (2008) Occurrence of unusual steroids and hopanoids derived from aerobic methanotrophs at an active marine mud volcano. *Org Geochem* 39(2):167–177

- Elvert M, Suess E, Whiticar MJ (1999) Anaerobic methane oxidation associated with marine gas hydrates: superlight C-isotopes from saturated and unsaturated C₂₀ and C₂₅ irregular isoprenoids. *Naturwissenschaften* 86(6):295–300
- Elvert M, Suess E, Greinert J, Whiticar MJ (2000) Archaea mediating anaerobic methane oxidation in deep-sea sediments at cold seeps of the eastern Aleutian subduction zone. *Org Geochem* 31:1175–1187
- Elvert M, Hopmans EC, Treude T, Boetius A, Suess E (2005) Spatial variations of methanotrophic consortia at cold methane seeps: implications from a high-resolution molecular and isotopic approach. *Geobiology* 3(3):195–209
- Elvert M, Pohlman JW, Becker KW, Gaglioti B, Hinrichs K, Wooller MJ (2016) Methane turnover and environmental change from holocene lipid biomarker records in a thermokarst lake in arctic Alaska. *Holocene* 26(11):1766–1777
- Etioppe G (2015) Natural gas seepage: the Earth's hydrocarbon degassing. Springer, Cham, 199p
- Etioppe G, Klusman RW (2002) Geologic emissions of methane to the atmosphere. *Chemosphere* 49(8):777–789
- Etioppe G, Ionescu A (2015) Low-temperature catalytic CO₂ hydrogenation with geological quantities of ruthenium: a possible abiotic CH₄ source in chromitite-rich serpentinized rocks. *Geofluids* 15(3):438–452
- Etioppe G, Sherwood Lollar B (2013) Abiotic methane on Earth. *Rev Geophys* 51(2):276–299
- Etioppe G, Lassey KR, Klusman RW, Boschi E (2008) Reappraisal of the fossil methane budget and related emission from geologic sources. *Geophys Res Lett* 35(L09307):1–5
- Ettwig KF, Shima S, van de Pas-Schoonen KT, Kahnt J, Medema MH, Op den Camp HJM, Jetten MSM, Strous M (2008) Denitrifying bacteria anaerobically oxidize methane in the absence of Archaea. *Environ Microbiol* 10(11):3164–3173
- Ettwig KF, Butler MK, Le Paslier D, Pelletier E, Mangenot S, Kuypers MMM, Schreiber F, Dutilh BE, Zedelius J, de Beer D, Gloerich J, Wessels HJCT, van Alen T, Luesken F, Wu ML, van de Pas-Schoonen KT, Op den Camp HJM, Janssen-Megens EM, Francoijs K-J, Stunnenberg H, Weissenbach J, Jetten MS, Strous M (2010) Nitrite-driven anaerobic methane oxidation by oxygenic bacteria. *Nature* 464:543–548
- Ettwig KF, Zhu B, Speth D, Keltjens JT, Jetten MS, Kartal B (2016) Archaea catalyze iron-dependent anaerobic oxidation of methane. *Proc Natl Acad Sci* 113(45):12792–12796
- Feisthauer S, Vogt C, Modrzynski J, Szlenkier M, Krüger M, Siebert M, Richnow HH (2011) Different types of methane monooxygenases produce similar carbon and hydrogen isotope fractionation patterns during methane oxidation. *Geochim Cosmochim Acta* 75(5):1173–1184
- Ferry JG (1992) Methane from acetate. *J Bacteriol* 174(17):5489–5495
- Ferry JG (1993) In: Ferry JG (ed) *Methanogenesis: ecology, physiology, biochemistry and genetics*. Chapman and Hall/Springer Science and Business Media, New York, 536p
- Ferry JG (2011) Fundamentals of methanogenic pathways that are key to the biomethanation of complex biomass. *Curr Opin Biotechnol* 22(3):351–357
- Fey A, Claus P, Conrad R (2004) Temporal change of ¹³C-isotope signatures and methanogenic pathways in rice field soil incubated anoxically at different temperatures. *Geochim Cosmochim Acta* 68(2):293–306
- Field JA, Stams AJM, Kato M, Schraa G (1995) Enhanced biodegradation of aromatic pollutants in cocultures of anaerobic and aerobic bacterial consortia. *Antonie Van Leeuwenhoek* 67:47–77
- Fischer F, Lieske R, Winzer K (1931) Die umsetzungen des kohlenoxyds. *Biochem Z* 236:247–267
- Franco B, Mahieu E, Emmons LK, Tzompa-Sosa ZA, Fischer EV, Sudo K, Strong K et al (2016) Evaluating ethane and methane emissions associated with the development of oil and natural gas extraction in North America. *Environ Res Lett* 11(4):044010
- Franzmann PD, Liu Y, Balkwill DL, Aldrich HC, Conway de Macario E, Boone DR (1997) *Methanogenium frigidum* sp. nov., a psychrophilic, H₂-using methanogen from Ace Lake, Antarctica. *Int J Syst Bacteriol* 47:1068–1072
- Frenzel P (2000) Plant-associated methane oxidation in rice fields and wetlands. *Adv Microb Ecol* 16:85–114

- Friedmann EI (1994) Permafrost as microbial habitat. In: Gilichinsky D (ed) Viable microorganisms in permafrost. Russian Academy of Sciences, Pushchino, pp 21–26
- Froelich PN, Klinkhammer GP, Bender ML, Luedtke GR, Heath GR, Cullen D, Dauphin P, Hammond D, Hartman B, Maynard V (1979) Early oxidation of organic matter in pelagic sediments of the eastern equatorial Atlantic: suboxic diagenesis. *Geochim Cosmochim Acta* 43:1075–1090
- Fu L, Ding J, Lu Y, Ding Z, Zeng RJ (2017) Nitrogen source effects on the denitrifying anaerobic methane oxidation culture and anaerobic ammonium oxidation bacteria enrichment process. *Applied Microbiology and Biotechnology* 101(9):3895–3906
- Fung I, John J, Lerner J, Matthews E, Prather M, Steele LP, Fraser PJ (1991) Three dimensional model synthesis of the global methane cycle. *J Geophys Res* 96:13033–13065
- Fuse H, Ohta M, Takimura O, Murakami K, Inoue H, Yamaoka Y, Oclarit JM, Omori T (1998) Oxidation of trichloroethylene and dimethyl sulfide by a marine *Methylobacterium* strain containing soluble methane monooxygenase. *Biosci Biotechnol Biochem* 62:1925–1931
- Gao Y, Lee J, Neufeld JD, Park J, Rittmann BE, Lee HS (2017) Anaerobic oxidation of methane coupled with extracellular electron transfer to electrodes. *Scientific reports* 7(1):1–9
- Garcia J-L, Patel BKC, Ollivier B (2000) Taxonomic, phylogenetic and ecological diversity of methanogenic Archaea. *Anaerobe* 6:205–226
- Ghashghavi M, Jetten MSM, Lüke C (2017) Survey of methanotrophic diversity in various ecosystems by degenerate methane monooxygenase gene primers. *AMB Express* 7(1):1–11
- Giardini AA, Salotti CA, Lakner JF (1968) Synthesis of graphite and hydrocarbons by reaction between calcite and hydrogen. *Science* 159:317–319
- Gieg LM, Fowler SJ, Berdugo-Clavijo C (2014) Syntrophic biodegradation of hydrocarbon contaminants. *Curr Opin Biotechnol* 27:21–29
- Goevert D, Conrad R (2009) Effect of substrate concentration on carbon isotope fractionation during acetoclastic methanogenesis by *Methanosarcina barkeri* and *M. acetivorans* and in rice field soil. *Appl Environ Microbiol* 75(9):2605–2612
- Goldblatt C, Lenton TM, Watson AJ (2006) Bistability of atmospheric oxygen and the Great Oxidation. *Nature* 443(7112):683
- Grant NJ, Whiticar MJ (2002) Stable carbon isotopic evidence for methane oxidation in plumes above Hydrate Ridge, Cascadia Oregon Margin. *Glob Biogeochem Cycles* 16(4):1–13
- Gray ND, Sherry A, Larter SR, Erdmann M, Leyris J, Liengen T, Head IM (2009) Biogenic methane production in formation waters from a large gas field in the North Sea. *Extremophiles* 13(3):511–519
- Groot TT, VanBodegom PM, Harren FJM, Meijer HAJ (2003) Quantification of methane oxidation in the rice rhizosphere using ¹³C-labelled methane. *Biogeochemistry* 64:355–372
- Guo H, Yu Z, Thompson IP, Zhang H (2014) A contribution of hydrogenotrophic methanogenesis to the biogenic coal bed methane reserves of southern Qinshui Basin, China. *Appl Microbiol Biotechnol* 98(21):9083–9093
- Hallam SJ, Putnam N, Preston CM, Detter JC, Rokhsar D, Richardson PM, DeLong EF (2004) Reverse methanogenesis: testing the hypothesis with environmental genomics. *Science* 305(5689):1457–1462
- Halverson GP, Hoffman PF, Schrag DP, Kaufman AJ (2002) A major perturbation of the carbon cycle before the Ghaub glaciation (Neoproterozoic) in Namibia: prelude to snowball Earth? *Geochem Geophys Geosyst* 3(6):1–24
- Hansen JE, Sato M (2001) Trends of measured climate forcing agents. *Proc Natl Acad Sci U S A* 98(26):14778–14783
- Hanson RS, Hanson TE (1996) Methanotrophic bacteria. *Microbiol Rev* 60(2):439–471
- Harder J (1997) Anaerobic methane oxidation by bacteria employing ¹⁴C-methane uncontaminated with ¹⁴C-carbon monoxide. *Mar Geol* 137(1):13–23
- Haroon MF, Hu S, Shi Y, Imelfort M, Keller J, Hugenholtz P, Yuan Z, Tyson GW (2013) Anaerobic oxidation of methane coupled to nitrate reduction in a novel archaeal lineage. *Nature* 500(7464):567–572

- Hattori S (2008) Syntrophic acetate-oxidizing microbes in methanogenic environments. *Microbes Environ* 23:118–127
- Hausmann P, Sussmann R, Smale D (2016) Contribution of oil and natural gas production to renewed increase in atmospheric methane (2007–2014): top-down estimate from ethane and methane column observations. *Atmos Chem Phys* 16:3227–3244
- Hayes J (2001) Fractionation of carbon and hydrogen isotopes in biosynthetic processes. In: *Stable isotope geochemistry. Reviews in mineralogy and geochemistry*, vol 43. Mineralogical Soc America, Washington, DC, pp 225–277
- Hedderich R, Whitman WB (2013) Physiology and biochemistry of the methane-producing archaea. In: *The prokaryotes*, vol 4 (eds: Rosenberg E et al.). Springer, Berlin, Chapter 18:635–662
- Heilbron JL (1976) Volta, Alessandro Giuseppe Antonio Anastasio. *Dict Sci Biogr* 14:69–82
- Hein R, Crutzen PJ, Heimann M (1997) An inverse modeling approach to investigate the global atmospheric methane cycle. *Glob Biogeochem Cycles* 11(1):43–76
- Helmig D, Rossabi S, Hueber J, Tans P, Montzka S, Masarie K, Pozzer A (2016) Reversal of global atmospheric ethane and propane trends largely due to US oil and natural gas production. *Nat Geosci* 9(7):490–495
- Henckel T, Jäckel U, Schnell S, Conrad R (2000) Molecular analyses of novel methanotrophic communities in forest soil that oxidize atmospheric methane. *Appl Environ Microbiol* 66(5):1801–1808
- Hensen C, Zabel M (2000) Early diagenesis at the benthic boundary layer: oxygen and nitrate in marine sediments. In: Schulz HD, Zabel M (eds) *Marine geochemistry*. Springer, Berlin, pp 209–231
- Hershey AE, Northington RM, Whalen SC (2014) Substrate limitation of sediment methane flux, methane oxidation and use of stable isotopes for assessing methanogenesis pathways in a small arctic lake. *Biogeochemistry* 117(2):325–336
- Hinrichs K-U, Boetius A (2002) The anaerobic oxidation of methane: new insights in microbial ecology and biogeochemistry. In: Wefer G, Billett D, Hebbeln D, Jorgensen BB, Schlüter M, Weering TV (eds) *Ocean margin systems*. Springer, Berlin, pp 457–477
- Hinrichs KU, Hayes JM, Sylva SP, Brewer PG, DeLong EF (1999) Methane-consuming archaeobacteria in marine sediments. *Nature* 398(6730):802–805
- Hinrichs K-U, Summons RE, Orphan V, Sylva SP, Hayes JM (2000) Molecular and isotopic analysis of anaerobic methane oxidizing communities in marine sediments. *Org Geochem* 31:1685–1701
- Hinrichs KU, Hayes JM, Bach W, Spivack AJ, Hmelo LR, Holm NG, Sylva SP (2006) Biological formation of ethane and propane in the deep marine subsurface. *Proc Natl Acad Sci* 103(40):14684–14689
- Hinz K, Kögler FC, Seibold E (1969) Reflexions-seismische Untersuchungen mit einer pneumatischen Schallquelle und einem Sedimentecholot in der westliche Ostsee. Teil 1 and 2. *Untersuchungsergebnisse und Geologische Deutung*. *Meyniana* 21:17–24
- Hoehler TM, Alperin MJ (1996) Anaerobic methane oxidation by a methanogen-sulfate reducer consortium: geochemical evidence and biochemical considerations. In *Microbial Growth on C1 Compounds* (pp 326–333) Springer, Dordrecht
- Hoehler TM, Alperin MJ, Albert DB, Martens CS (1994) Field and laboratory studies of methane oxidation in an anoxic marine sediment: evidence for a methane-sulfate reducer consortium. *Glob Biogeochem Cycles* 8:451–463
- Hoehler TM, Bebout BM, Des Marais DJ (2001) The role of microbial mats in the production of reduced gases on the early Earth. *Nature* 412:324–327
- Holmer M, Storkholm P (2001) Sulphate reduction and sulphur cycling in lake sediments: a review. *Freshw Biol* 46(4):431–451
- Holmes AJ, Costello A, Lidstrom ME, Murrell JC (1995) Evidence that particulate methane monooxygenase and ammonia monooxygenase may be evolutionarily related. *FEMS Microbiol Lett* 132:203–208

- Holzappel-Pschorn A, Conrad R, Seiler W (1985) Production, oxidation and emission of methane in rice paddies. *FEMS Microbiol Lett* 31:343–351
- Hoppe-Seyley F (1876) Ueber die Prozesse der Gährungen und ihre Beziehung zum Leben der Organismen: Erste Abhandlung. *Arch gesammte Physiol Menschen Thiere* 12:1–17. <https://www.esrl.noaa.gov/gmd/ccgg/d13C-src-inv/>
- Hornibrook ER, Longstaffe FJ, Fyfe WS (1997) Spatial distribution of microbial methane production pathways in temperate zone wetland soils: stable carbon and hydrogen isotope evidence. *Geochim Cosmochim Acta* 61(4):745–753
- Hovland M, Judd AG, Burke RA (1993) The global flux of methane from shallow submarine sediments. *Chemosphere* 26(1):559–578
- Howarth RW (2019) Ideas and perspectives: Is shale gas a major driver of recent increases in global atmospheric methane? *Biogeosciences* 16(15):3033–3046
- Hu S, Zeng RJ, Haroon MF, Keller J, Lant PA, Tyson GW, Yuan Z (2015) A laboratory investigation of interactions between denitrifying anaerobic methane oxidation (DAMO) and anammox processes in anoxic environments. *Sci Rep* 5:8706
- Huber R, Kurr M, Jannasch HW, Stetter KO (1989) A novel group of abyssal methanogenic archaeobacteria (*Methanopyrus*) growing at 110°C. *Nature* 342:833–834
- Huser BA, Wuhmann K, Zehnder AJB (1982) *Methanothrix soehngenii* gen. nov. sp. nov., a new acetotrophic non-hydrogen-oxidizing methane bacterium. *Arch Microbiol* 132:1–9
- Im J, Lee SW, Yoon S, DiSpirito AA, Semrau JD (2011) Characterization of a novel facultative *Methylocystis* species capable of growth on methane, acetate and ethanol. *Environ Microbiol Rep* 3(2):174–181
- Inagaki F, Kuypers MMM, Tsunogai U, Ishibashi J, Nakamura K et al (2006) Microbial community in a sediment-hosted CO₂ lake of the southern Okinawa Trough hydrothermal system. *Proc Natl Acad Sci U S A* 103:14164–14169
- Ingvorsen K, Brock TD (1982) Electron flow via sulfate reduction and methanogenesis in the anaerobic hypolimnion of Lake Mendota. *Limnol Oceanogr* 27:559–564
- Ingvorsen K, Jørgensen BB (1984) Kinetics of sulfate uptake by freshwater and marine species of *Desulfovibrio*. *Arch Microbiol* 139:61–66
- IPCC (2013) Climate change 2013: the physical science basis. Contribution of working group I to the fifth assessment report of the intergovernmental panel on climate change (ed: Stocker TF, Qin D, Plattner G-K, Tignor M, Allen SK, Boschung J, Nauels A, Xia Y, Bex V, Midgley PM). Cambridge University Press, Cambridge, UK/New York, 1535pp
- Iram A, Akhtar K, Ghauri MA (2017) Coal methanogenesis: a review of the need of complex microbial consortia and culture conditions for the effective bioconversion of coal into methane. *Ann Microbiol* 67(3):275–286
- Islam T, Sigmund J, Reigstad LJ, Larsen O, Birkeland NK (2008) Methane oxidation at 55°C and pH 2 by a thermoacidophilic bacterium belonging to the *Verrucomicrobia* phylum. *Proc Natl Acad Sci U S A* 105:300–304
- Islas-Lima S, Thalasso F, Gomez-Hernandez J (2004) Evidence of anoxic methane oxidation coupled to denitrification. *Water Research* 38(1):13–16
- Iversen N (1984) Interaktioner mellem fermenterings-processer og de terrinale processer. PhD thesis, Institut for Genetik og Økologi, Aarhus University, Aarhus
- Iversen N, Jørgensen BB (1985) Anaerobic methane oxidation rates at the sulfate methane transition in marine sediments from Kattegat and Skagerrak (Denmark). *Limnol Oceanogr* 30(5):944–955
- Jameson R (1800) On peat or turf, theory of the formation of peat. Extracted from Jameson's mineralogy of the Shetland Islands *Transactions of the Dublin Society*, Number 1, 1–10
- Jones DM, Head IM, Gray ND, Adams JJ, Rowan AK, Aitken CM, Oldenburg T (2008) Crude-oil biodegradation via methanogenesis in subsurface petroleum reservoirs. *Nature* 451(7175):176
- Jørgensen BB (1977) Bacterial sulfate reduction within reduced microniches of oxidized marine sediments. *Mar Biol* 41(1):7–17

- Jorgensen SL, Hannisdal B, Lanzén A, Baumberger T, Flesland K et al (2012) Correlating microbial community profiles with geochemical data in highly stratified sediments from the Arctic Mid-Ocean Ridge. *Proc Natl Acad Sci U S A* 109:2846–2855
- Joye SB, Boetius A, Orcutt BN, Montoya JP, Schulz HN, Erickson MJ, Lugo SK (2004) The anaerobic oxidation of methane and sulfate reduction in sediments from Gulf of Mexico cold seeps. *Chem Geol* 205(3):219–238
- Judd AG, Hovland M (1992) The evidence of shallow gas in marine sediments. *Cont Shelf Res* 12 (10):1081–1095
- Judd A, Hovland M (2009) *Seabed fluid flow: the impact on geology, biology and the marine environment*. Cambridge University Press, Cambridge, p 475
- Jugold A, Althoff F, Hurkuck M, Greule M, Lenhart K, Lelieveld J, Keppler F (2012) Non-microbial methane formation in oxic soils. *Biogeosciences* 9(12):5291–5301
- Kai FM, Tyler SC, Randerson JT, Blake DR (2011) Reduced methane growth rate explained by decreased Northern Hemisphere microbial sources. *Nature* 476(7359):194
- Kallistova AY, Merkel AY, Tarnovetskii IY, Pimenov NV (2017) Methane formation and oxidation by prokaryotes. *Microbiology* 86(6):671–691
- Kalyuzhnaya MG, Khmelena V, Eshinimaev B, Sorokin D, Fuse H, Lidstrom M, Trotsenko Y (2008) Classification of halo(alkali)philic and halo(alkali)tolerant methanotrophs provisionally assigned to the genera *Methylomicrobium* and *Methylobacter* and emended description of the genus *Methylomicrobium*. *Int J Syst Evol Microbiol* 58:591–596
- Kamat SS, Williams HJ, Dangott LJ, Chakrabarti M, Raushel FM (2013) The catalytic mechanism for aerobic formation of methane by bacteria. *Nature* 497:132–136
- Karl DM, Tilbrook BD (1994) Production and transport of methane in oceanic particulate organic-matter. *Nature* 368:732
- Karl DM, Beversdorf L, Björkman KM, Church MJ, Martinez A, Delong EF (2008) Aerobic production of methane in the sea. *Nat Geosci* 1(7):473–478
- Kashefi K, Lovley DR (2003) Extending the upper temperature limit for life. *Science* 301 (5635):934–934
- Kates M (1966) Biosynthesis of lipids in microorganisms. *Annu Rev Microbiol* 20(1):13–44
- Kates M, Sastry PS, Yengoyan LS (1963) Isolation and characterization of a diether analog of phosphatidylglycerophosphate from *Halobacterium cutirubrum*. *Biochim Biophys Acta* 70:705–707
- Kelley DS, Früh-Green GL (1999) Abiogenic methane in deep-seated mid-ocean ridge environments: insights from stable isotope analyses. *J Geophys Res Solid Earth* 104(B5):10439–10460
- Keltjens JT, Vogels GD (1993) Conversion of methanol and methylamines to methane and carbon dioxide. In: Ferry JG (ed) *Methanogenesis- ecology, physiology, biochemistry and genetics*. Springer, Boston, pp 253–303
- Kennedy MJ, Christie-Blick N, Sohl LE (2001) Are proterozoic cap carbonates and isotopic excursions a record of gas hydrate destabilization following earth's coldest intervals? *Geology* 29(5):443–446
- Kennett JP, Cannariato KG, Hendy IL, Behl RJ (2003) *Methane hydrates in quaternary climate change: the clathrate gun hypothesis*. AGU, Washington, DC, 216pp
- Keppler F, Hamilton JTG, Brass M, Röckmann T (2006) Methane emissions from terrestrial plants under aerobic conditions. *Nature* 439:187–191
- Keppler F, Hamilton JTG, McRoberts WC, Vigano I, Braß M, Röckmann T (2008) Methoxyl groups of plant pectin as a precursor of atmospheric methane: evidence from deuterium labelling studies. *New Phytol* 178(4):808–814
- Kerr RA, Vogel G (1999) Early life thrived despite earthly travails. *Science* 284(5423):2111–2113
- Kevbrin VV, Lysenko AM, Zhilina TN (1997) Physiology of alkaliphilic methanogen Z-7936, a new strain of *Methanosalsus zhilinae* isolated from Lake Magadi. *Microbiology (English translation of Mikrobiologija)* 66:261–266
- Khalil MAK, Rasmussen RA (1983) Sources, sinks, and seasonal cycles of atmospheric methane. *J Geophys Res Oceans* 88(C9):5131–5144

- Kiene RP (1991) Production and consumption of methane in aquatic systems. In: Rogers JE, Whitman WB (eds) *Microbial production and consumption of greenhouse gases: methane, nitrogen oxides, and halomethanes*. American Society for Microbiology, Washington, DC, pp 111–146
- Kiene RP, Oremland RS, Catena A, Miller LG, Capone DG (1986) Metabolism of reduced methylated sulfur compounds in anaerobic sediments and by a pure culture of an estuarine methanogen. *Appl Environ Microbiol* 52:1037–1045
- Kiener A, Leisinger T (1983) Oxygen sensitivity of methanogenic bacteria. *Syst Appl Microbiol* 4:305–312
- Kietäväinen R, Purkamo L (2015) The origin, source, and cycling of methane in deep crystalline rock biosphere. *Front Microbiol* 6:725
- Kimura H, Sugihara M, Yamamoto H, Patel BK, Kato K, Hanada S (2005) Microbial community in a geothermal aquifer associated with the subsurface of the Great Artesian Basin, Australia. *Extremophiles* 9(5):407–414
- King GM (1992) Ecological aspects of methane oxidation, a key determinant of global methane dynamics. *Adv Microb Ecol* 12:431–468
- King GM, Klug MJ, Lovley DR (1983) Metabolism of acetate, methanol, and methylated amines in intertidal sediments of Lowes Cove, Maine. *Appl Environ Microbiol* 45:1848–1853
- Kinnaman FS, Valentine DL, Tyler SC (2007) Carbon and hydrogen isotope fractionation associated with the aerobic microbial oxidation of methane, ethane, propane and butane. *Geochimica et Cosmochimica Acta* 71(2):271–283
- Kirby TB, Lancaster JR, Fridovich I (1981) Isolation and characterization of the iron-containing superoxide dismutase of *Methano- bacterium bryantii*. *Arch Biochem Biophys* 210:140–148
- Kirschbaum MUF, Walcroft A (2008) No detectable aerobic methane efflux from plant material, nor from adsorption/desorption processes. *Biogeosciences* 5(6):1551–1558
- Kirschke S, Bousquet P, Ciais P, Saunois M, Canadell JG, Dlugokencky EJ, Bergamaschi P, Bergmann D, Blake DR, Bruhwiler L, Cameron-Smith P (2013) Three decades of global methane sources and sinks. *Nat Geosci* 6(10):813–823
- Kits KD, Klotz MG, Stein LY (2015) Methane oxidation coupled to nitrate reduction under hypoxia by the gammaproteobacterium *Methylomonas denitrificans*, sp. nov. type strain FJG1. *Environ Microbiol* 17(9):3219–3232
- Kiyosu Y, Krouse HR (1989) Carbon isotope effect during abiogenic oxidation of methane. *Earth Planet Sci Lett* 95(3–4):302–306
- Klapstein SJ, Turetsky MR, McGuire AD, Harden JW, Czimeczik CI, Xu X, Chanton JP, Waddington JM (2014) Controls on methane released through ebullition in peatlands affected by permafrost degradation. *J Geophys Res Biogeosci* 119:418–431
- Knoblauch C, Spott O, Evgrafova S, Kutzbach L, Pfeiffer EM (2015) Regulation of methane production, oxidation, and emission by vascular plants and bryophytes in ponds of the northeast Siberian polygonal tundra. *Journal of Geophysical Research: Biogeosciences* 120(12):2525–2541
- Knab NJ, Dale AW, Lettmann K, Fossing H, Jørgensen BB (2008) Thermodynamic and kinetic control on anaerobic oxidation of methane in marine sediments. *Geochim Cosmochim Acta* 72:3746–3757
- Knab NJ, Cragg BA, Hornibrook ERC, Holmkvist L, Pancost RD, Borowski C et al (2009) Regulation of anaerobic methane oxidation in sediments of the Black Sea. *Biogeosciences* 6:1505–1518
- Knappy CS (2010) Mass spectrometric studies of ether lipids in archaea and sediments. PhD thesis, University of York, 406pp
- Knief C (2015) Diversity and habitat preferences of cultivated and uncultivated aerobic methanotrophic bacteria evaluated based on *pmoA* as molecular marker. *Front Microbiol* 6:1346
- Knittel K, Boetius A (2009) Anaerobic oxidation of methane: progress with an unknown process. *Annu Rev Microbiol* 63:311–334

- Knittel K, Lösekann T, Boetius A, Kort R, Amann R (2005) Diversity and distribution of methanotrophic archaea at cold seeps. *Appl Environ Microbiol* 71:467–479
- Koene-Cottaar FHM, Schraa G (1998) Anaerobic reduction of ethene to ethane in an enrichment culture. *FEMS Microbiol Ecol* 25(3):251–256
- Koizumi Y, Takii S, Nishino M, Nakajima T (2003) Vertical distributions of sulfate-reducing bacteria and methane-producing archaea quantified by oligonucleotide probe hybridization in the profundal sediment of a mesotrophic lake. *FEMS Microbiol Ecol* 44:101–108
- Kosior DR, Warford AL (1979) Methane production and oxidation in Santa Barbara Basin sediments. *Estuar Coast Mar Sci* 8(4):379–385
- Kotelnikova S (2002) Microbial production and oxidation of methane in deep subsurface. *Earth-Sci Rev* 58(3):367–395
- Kotelnikova S, Pedersen K (1998) Distribution and activity of methanogens and homoacetogens in deep granitic aquifers at Äspö Hard Rock Laboratory, Sweden. *FEMS Microbiol Ecol* 26(2):121–134
- Kotsyurbenko OR, Chin KJ, Glagolev MV, Stubner S, Simankova MV, Nozhevnikova AN, Conrad R (2004) Acetoclastic and hydrogenotrophic methane production and methanogenic populations in an acidic West Siberian peat bog. *Environ Microbiol* 6:1159–1173
- Krouse HR, Viau CA, Eliuk LS, Ueda A, Halas S (1988) Chemical and isotopic evidence of thermochemical sulphate reduction by light hydrocarbon gases in deep carbonate reservoirs. *Nature* 333(6172):415
- Kuivila KM, Murray JW, Devol AH, Novelli PC (1989) Methane production, sulfate reduction and competition for substrates in the sediments of Lake Washington. *Geochim Cosmochim Acta* 53:409–416
- Kvenvolden KA (1999) Potential effects of gas hydrate on human welfare. *Proceedings of the National Academy of Sciences USA*, 96(7):3420–3426
- Kvenvolden KA, Rogers BW (2005) Gaia's breath – global methane exhalations. *Mar Pet Geol* 22(4):579–590
- L'Haridon S, Reysenbach A-L, Banta A, Messner P, Schumann P, Stackebrandt E, Jeanthon C (2003) *Methanocaldococcus indicus* sp. nov., a novel hyperthermophilic methanogen isolated from the Central Indian Ridge. *Int J Syst Evol Microbiol* 53:1931–1935
- Lackner N, Hintersonleitner A, Wagner AO, Illmer P (2018) Hydrogenotrophic methanogenesis and autotrophic growth of *Methanosarcina thermophila*. *Archaea* 2018:Article ID 4712608, 7p
- Lamontagne RA, Swinnerton JW, Linnebom VJ, Smith WD (1973) Methane concentrations in various marine environments. *J Geophys Res* 78:5317–5324
- Lang K et al (2015) New mode of energy metabolism in the seventh order of methanogens as revealed by comparative genome analysis of 'Candidatus Methanoplasma termitum'. *Appl Environ Microbiol* 81:1338–1352
- Le Mer JL, Roger P (2001) Production, oxidation, emission and consumption of methane by soils: a review. *Eur J Soil Biol* 37:25–50
- Leloup J, Loy A, Knab NJ, Borowski C, Wagner M, Jørgensen BB (2007) Diversity and abundance of sulfate-reducing microorganisms in the sulfate and methane zones of a marine sediment, Black Sea. *Environ Microbiol* 9(1):131–142
- Lenhart K, Klintzsch T, Langer G, Nehrke G, Bunge M, Schnell S, Keppler F (2016) Evidence for methane production by the marine algae *Emiliana huxleyi*. *Biogeosciences* 13(10):3163–3174
- Levine JS, Rinsland CP, Tennille GM (1985) The photochemistry of methane and carbon monoxide in the troposphere in 1950 and 1985. *Nature* 318(6043):254
- Levy H (1972) Photochemistry of the lower troposphere. *Planet Space Sci* 20(6):919–935
- Lidstrom ME (2006) Aerobic methylotrophic prokaryotes. In: Dworkin M (ed) *The prokaryotes*, vol 2. Springer, New York, pp 618–634
- Liebner S, Zeyer J, Wagner D, Schubert C, Pfeiffer E-M, Knoblauch C (2011) Methane oxidation associated with submerged brown mosses reduces methane emissions from Siberian polygonal tundra. *J Ecol* 99(4):914–922
- Lieth H (1973) Primary production: Terrestrial ecosystems. *Hum Ecol* 1(4):303–332
- Lilley MD, Baross JA, Gordon LI (1982) Dissolved hydrogen and methane in Saanich Inlet, British Columbia. *Deep Sea Res Part A Oceanogr Res Pap* 29(12):1471–1484

- Lilley MD, Butterfield DA, Olson EJ, Lupton JE, Macko SA, McDuff RE (1993) Anomalous CH₄ and NH₄⁺ concentrations at an unsedimented mid-ocean-ridge hydrothermal system. *Nature* 364(6432):45–47
- Liu Y, Whitman WB (2008) Metabolic, phylogenetic, and ecological diversity of the methanogenic archaea. *Ann N Y Acad Sci* 1125(1):171–189
- Lofton DD, Whalen SC, Hershey AE (2015) Vertical sediment distribution of methanogenic pathways in two shallow arctic alaskan lakes. *Polar Biol* 38(6):815–827
- Lollar BS, Frappe SK, Fritz P, Macko SA, Welhan JA, Blomqvist R, Lahermo PW (1993) Evidence for bacterially generated hydrocarbon gas in Canadian Shield and Fennoscandian Shield rocks. *Geochim Cosmochim Acta* 57(23–24):5073–5085
- Londry KL, Dawson KG, Grover HD, Summons RE, Bradley AS (2008) Stable carbon isotope fractionation between substrates and products of *methanosarcina barkeri*. *Org Geochem* 39(5):608–621
- Lovley DR (1991) Dissimilatory Fe(III) and Mn(IV) reduction. *Microbiol Rev* 55:259–287
- Lovley DR (2006) Chapter 1.21: Dissimilatory Fe(III)- and Mn (IV)-reducing prokaryotes. In: Prokaryotes (ed: Dworkin M, Falkow S, Rosenberg E, Schleifer KH, Stacke-brandt E). Springer, New York, pp 635–658
- Lovley DR (2017) Happy together: microbial communities that hook up to swap electrons. *ISME J* 11(2):327–336
- Lovley DR, Goodwin S (1988) Hydrogen concentrations as an indicator of the predominant terminal electron-accepting reactions in aquatic sediments. *Geochim Cosmochim Acta* 52:2993–3003
- Lovley DR, Klug MJ (1983) Sulfate reducers can outcompete methanogens at freshwater sulfate concentrations. *Appl Environ Microbiol* 45:187–192
- Lovley DR, Klug MJ (1986) Model for the distribution of sulfate reduction and methanogenesis in freshwater sediments. *Geochim Cosmochim Acta* 50(1):11–18
- Lovley DR, Phillips EJ (1986) Organic matter mineralization with reduction of ferric iron in anaerobic sediments. *Appl Environ Microbiol* 51:683–689
- Lovley DR, Phillips EJP (1987) Competitive mechanisms for inhibition of sulfate reduction and methane production in the zone of ferric iron reduction sediments. *Appl Environ Microbiol* 53:2636–2641
- Lovley DR, Phillips EJP (1994) Novel processes for anaerobic sulfate production from elemental sulfur by sulfate-reducing bacteria. *Appl Environ Microbiol* 60(7):2394–2399
- Lovley DR, Dwyer DF, Klug MJ (1982) Kinetic analysis of competition between sulfate reducers and methanogens for hydrogen in sediments. *Appl Environ Microbiol* 45:187–192
- Lu Y, Lueders T, Friedrich MW, Conrad R (2005) Detecting active methanogenic populations on rice roots using stable isotope probing. *Environ Microbiol* 7(3):326–336
- Luff R, Greinert J, Wallmann K, Klauke I, Suess E (2005) Simulation of long-term feedbacks from authigenic carbonate crust formation at cold vent sites. *Chem Geol* 216:157–174
- Luther GW III, Church TM, Powell D (1991) Sulfur speciation and sulfide oxidation in the water column of the Black Sea. *Deep Sea Res Part A Oceanogr Res Pap* 38:S1121–S1137
- Lyon GL, Hulston JR (1984) Carbon and hydrogen isotopic compositions of New Zealand geothermal gases. *Geochim Cosmochim Acta* 48(6):1161–1171
- Machbride D (1764) Experimental essays on the following subjects: I. On the fermentation of alimentary mixtures. A. Millar, London, pp 1–12
- Machel HG (2001) Bacterial and thermochemical sulfate reduction in diagenetic settings — old and new insights. *Sediment Geol* 140(1):143–175
- Mah RA, Ward DM, Baresi L, Glass TL (1977) Biogenesis of methane. *Annu Rev Microbiol* 31:309–341
- Mahieu K, Visscher AD, Vanrolleghem PA, Cleemput OV (2006) Carbon and hydrogen isotope fractionation by microbial methane oxidation: improved determination. *Waste Manag* 26(4):389–398
- Maltby J, Steinle L, Löscher CR, Bange HW, Fischer MA, Schmidt M, Treude T (2018) Microbial methanogenesis in the sulfate-reducing zone of sediments in the Eckernförde Bay, SW Baltic Sea. *Biogeosciences* 15(1):137–157

- Mariotti A, Germon JC, Hubert P, Kaiser P, Letolle R, Tardieux A, Tardieux P (1981) Experimental determination of nitrogen kinetic isotope fractionation: some principles; illustration for the denitrification and nitrification processes. *Plant Soil* 62(3):413–430
- Martens CS, Berner RA (1974) Methane production in the interstitial waters of sulfate-depleted marine sediments. *Science* 185(4157):1167–1169
- Martens CS, Kelley CA, Chanton JP (1992) Carbon and hydrogen isotopic characterization of methane from wetlands and lakes of the Yukon-Kuskokwim Delta, Western Alaska. *J Geophys Res* 97:16689–16701
- Martinez-Cruz K, Leewis MC, Herriott IC, Sepulveda-Jauregui A, Anthony KW, Thalasso F, Leigh MB (2017) Anaerobic oxidation of methane by aerobic methanotrophs in sub-Arctic lake sediments. *Sci Total Environ* 607:23–31
- Martins LO, Huber R, Huber H, Stetter KO, da Costa MS, Santos H (1997) Organic solutes in hyperthermophilic archaea. *Appl Environ Microbiol* 63:896–902
- Marty DG (1993) Methanogenic bacteria in seawater. *Limnol Oceanogr* 38:452–456
- McCollom TM, Seewald JS (2001) A reassessment of the potential for reduction of dissolved CO₂ to hydrocarbons during serpentinization of olivine. *Geochim Cosmochim Acta* 65:3769–3778
- McDonald IR, Bodrossy L, Chen Y, Murrell JC (2008) Molecular ecology techniques for the study of aerobic methanotrophs. *Appl Environ Microbiol* 74(5):1305–1315
- McMahon PB, Chapelle FH (2008) Redox processes and water quality of selected principal aquifer systems. *Groundwater* 46(2):259–271
- McNorton J, Wilson C, Gloor M, Parker RJ, Boesch H, Feng W, Hossaini R, Chipperfield MP (2018) Attribution of recent increases in atmospheric methane through 3-D inverse modelling. *Atmos Chem Phys* 18(24):18149–18168
- Ménard C, Ramirez AA, Nikiema J, Heitz M (2012) Biofiltration of methane and trace gases from landfills: a review. *Environ Rev* 20(1):40–53
- Meulepas RJ, Jagersma CG, Khadem AF, Stams AJ, Lens PN (2010) Effect of methanogenic substrates on anaerobic oxidation of methane and sulfate reduction by an anaerobic methanotrophic enrichment. *Appl Microbiol Biotechnol* 87(4):1499–1506
- Meyer CP, Galbally IE, Wang YP, Weeks IA, Tolhurst KG, Tomkins IB (1997) The enhanced emission of greenhouse gases from soil following prescribed burning in a southern eucalyptus forest. Final report to the National Greenhouse Gas Inventory Committee, CSIRO, Division of Atmospheric Research, Aspendale, pp 1–66
- Michaelis W, Albrecht P (1979) Molecular fossils of Archaeobacteria in kerogen. *Naturwissenschaften* 66:402–421
- Michaelis W, Seifert R, Nauhaus K, Treude T, Thiel V, Blumenberg M, Knittel K, Gieseke A, Peterknecht K, Pape T, Boetius A, Amann R, Jørgensen BB, Widdel F, Peckmann J, Pimenov NV, Gulin MB (2002) Microbial reefs in the Black sea fueled by anaerobic oxidation of methane. *Science* 297:1014–1015
- Milkov AV (2005) Molecular and stable isotope compositions of natural gas hydrates: a revised global dataset and basic interpretations in the context of geological settings. *Org Geochem* 36(5):681–702
- Milkov AV, Etiope G (2018) Revised genetic diagrams for natural gases based on a global dataset of >20,000 samples. *Org Geochem* 125:109–120
- Milkov AV, Schwietzke S, Allen G, Sherwood OA, Etiope G (2020) Using global isotopic data to constrain the role of shale gas production in recent increases in atmospheric methane. *Scientific Reports* 10(4119):1–7
- Miller JF, Shah NN, Nelson CM, Ludlow JM, Clark DS (1988) Pressure and temperature effects on growth and methane production of the extreme thermophile methanococcus jannaschii. *Appl Environ Microbiol* 54(12):3039–3042
- Milucka J, Ferdelman T, Polerecky L, Franzke D, Wegener G, Schmid M, Lieberwirth I, Wagner M, Widdel F, Kuypers MMM (2012) Zero-valent sulphur is a key intermediate in marine methane oxidation. *Nature* 491:541–546

- Mitterer RM (2010) Methanogenesis and sulfate reduction in marine sediments: a new model. *Earth Planet Sci Lett* 295:358–366
- Modin O, Fukushi K, Yamamoto K (2007) Denitrification with methane as external carbon source. *Water Res* 41(12):2726–2738
- Monteith JL (1972) Solar radiation and productivity in tropical ecosystems. *J Appl Ecol* 9(3): 747–766
- Moore TR, Knowles R (1990) Methane emission from fen, bog, and swamp peatlands in Quebec. *Biogeochemistry* 11:45–61
- Moran JJ, House CH, Freeman KH, Ferry JG (2005) Trace methane oxidation studied in several euryarchaeota under diverse conditions. *Archaea (Vancouver, B.C.)* 1(5):303–309
- Mulder A, Van de Graaf AA, Robertson LA, Kuenen JG (1995) Anaerobic ammonium oxidation discovered in a denitrifying fluidized bed reactor. *FEMS Microbiol Ecol* 16(3):177–183
- Myhre G, Shindell D, Bréon F-M, Collins W, Fuglestedt J, Huang J, Koch D, Lamarque J-F, Lee D, Mendoza B, Nakajima T, Robock A, Stephens G, Takemura T, Zhang H (2013) Anthropogenic and natural radiative forcing. In: *Climate change 2013: the physical science basis. Contribution of working group I to the fifth assessment report of the intergovernmental panel on climate change* (ed: Stocker TF, Qin D, Plattner G-K, Tignor M, Allen SK, Boschung J, Nauels A, Xia Y, Bex V, Midgley PM). Cambridge University Press, Cambridge
- Naeher S, Niemann H, Peterse F, Smittenberg RH, Ziegler PK, Schubert CJ (2014) Tracing the methane cycle with lipid biomarkers in Lake Rotsee (Switzerland). *Org Geochem* 66:174–181
- Naguib M, Overbeck J (1970) On methane oxidizing bacteria in freshwaters. I. Introduction to the problem and investigations on the presence of obligate methane oxidizers. *Z Allg Mikrobiol* 10:17–36
- Nauhaus K, Boetius A, Krüger M, Widdel F (2002) In vitro demonstration of anaerobic oxidation of methane coupled to sulphate reduction in sediment from a marine gas hydrate area. *Environ Microbiol* 4(5):296–305
- Nauhaus K, Treude T, Boetius A, Krüger M (2005) Environmental regulation of the anaerobic oxidation of methane: a comparison of ANME-I and ANME-II communities. *Environ Microbiol* 7:98–106
- Nayak DR, Babu YJ, Datta A, Adhya TK (2007) Methane oxidation in an intensively cropped tropical rice field soil under long-term application of organic and mineral fertilizers. *J Environ Qual* 36(6):1577–1584
- NCBI (2017) The National Center for Biotechnology Information <https://www.ncbi.nlm.nih.gov/>
- Neretin LN, Bottcher ME, Jørgensen BB, Volkov I, Luschen H, Hilgenfeldt K (2004) Pyritization processes and greigite formation in the advancing sulfidization front in the Upper Pleistocene sediments of the Black Sea. *Geochim Cosmochim Acta* 68(9):2081–2093
- Newby DT, Reed DW, Petzke LM, Igoe AL, Delwiche ME et al (2004) Diversity of methanotroph communities in a basalt aquifer. *FEMS Microbiol Ecol* 48:333–344
- Niemann H, Elvert M (2008) Diagnostic lipid biomarker and stable carbon isotope signatures of microbial communities mediating the anaerobic oxidation of methane with sulphate. *Organic Geochemistry* 39(12):1668–1677
- Niemann H, Lösekann T, de Beer D, Elvert M, Nadalig T, Knittel K, Amann R, Sauter EJ, Schlüter M, Klages M, Foucher JP, Boetius A (2006) Novel microbial communities of the Haakon Mosby mud volcano and their role as a methane sink. *Nature* 443:854–858
- Nisbet EG, Dlugokencky EJ, Bousquet P (2014) Methane on the rise – again. *Science* 343 (6170):493–495
- Nisbet EG, Manning MR, Dlugokencky EJ, Fisher RE, Lowry D, Michel SE, Brownlow R et al (2019) Very strong atmospheric methane growth in the 4 years 2014–2017: implications for the Paris Agreement. *Glob Biogeochem Cycles* 33(3):318–342
- Nolla-Ardévol V, Strous M, Sorokin DY, Merkel AY, Tegetmeyer HE (2012) Activity and diversity of haloalkaliphilic methanogens in Central Asian soda lakes. *J Biotechnol* 161:167–173
- Nordi KA, Thamdrup B, Schubert CJ (2013) Anaerobic oxidation of methane in an iron rich Danish freshwater lake sediment. *Limnol Oceanogr* 58:546–554

- Nozhevnikova AN, Zepp K, Vazquez F, Zehnder AJB, Holliger C (2003) Evidence for the existence of psychrophilic methanogenic communities in anoxic sediments of deep lakes. *Appl Environ Microbiol* 69(3):1832–1835
- Oba M, Sakata S, Tsunogai U (2006) Polar and neutral isopranyl glycerol ether lipids as biomarkers of archaea in near-surface sediments from the Nankai Trough. *Organic Geochemistry* 37 (12):1643–1654
- Oertel C, Matschullat J, Zurba K, Zimmermann F, Erasmí S (2016) Greenhouse gas emissions from soils – a review. *Chem Erde–Geochem* 76(3):327–352
- Omelchenko MB, Vasilieva LV, Zavarzin GA, Savelieva ND, Lysenko AM, Mityushina LL, Khmelenina VN, Trotsenko YA (1996) A novel psychrophilic methanotroph of the genus *Methylobacter*. *Mikrobiologiya* (English translation) 65:339–343
- Omeliński W (1904) Ueber die Trennung der Wasserstoff und Methangärung der Cellulose. *Centralt f. Bakt* 2(11):369–377
- Oni OE, Friedrich MW (2017) Metal oxide reduction linked to anaerobic methane oxidation. *Trends Microbiol* 25(2):88–90
- Orcutt B, Meile C (2008) Constraints on mechanisms and rates of anaerobic oxidation of methane by microbial consortia: process-based modeling of ANME-2 archaea and sulfate reducing bacteria interactions. *Biogeosci Discuss* 5(3):1933–1967
- Orcutt B, Boetius A, Elvert M, Samarkin V, Joye SB (2005) Molecular biogeochemistry of sulfate reduction, methanogenesis and the anaerobic oxidation of methane at Gulf of Mexico cold seeps. *Geochim Cosmochim Acta* 69(17):4267–4281
- Orcutt B, Samarkin V, Boetius A, Joye S (2008) On the relationship between methane production and oxidation by anaerobic methanotrophic communities from cold seeps of the Gulf of Mexico. *Environ Microbiol* 10:1108–1117
- Oremland RS (1988) Biogeochemistry of methanogenic bacteria. In: Zehnder AJB (ed) *Biology of anaerobic microorganisms*. Wiley, New York, pp 641–705
- Oremland RS, Polcin S (1982) Methanogenesis and sulfate reduction: competitive and non-competitive substrates in estuarine sediments. *Appl Environ Microbiol* 44:1270–1276
- Oremland RS, Taylor BF (1978) Sulfate reduction and methanogenesis in marine sediments. *Geochim Cosmochim Acta* 42:209–214
- Oremland RS, Miller LG (1993) Biogeochemistry of natural gases in three alkaline, permanently stratified (meromictic) lakes. *US Geol Surv Prof Pap* 1570:439–452
- Oremland RS, Marsh LM, Polcin S (1982) Methane production and simultaneous sulphate reduction in anoxic, salt marsh sediments. *Nature* 296:143–145
- Oremland RS, Whiticar MJ, Strohmaier FE, Kiene RP (1988) Bacterial ethane formation from reduced, ethylated sulfur compounds in anoxic sediments. *Geochim Cosmochim Acta* 52 (7):1895–1904
- Oremland RS, Miller LG, Colbertson CW, Robinson SW, Smith RL, Lovley D, Sargent M (1993) Aspects of the biogeochemistry of methane in Mono Lake and the Mono Basin of California. In: *Biogeochemistry of global change*. Springer, Boston, MA, pp 704–741
- Orphan VJ, Hinrichs K-U, Ussler W III, Paull CK, Taylor LT, Sylva SP et al (2001a) Comparative analysis of methane-oxidizing archaea and sulfate-reducing bacteria in anoxic marine sediments. *Appl Environ Microbiol* 67:1922–1934
- Orphan VJ, House CH, Hinrichs K-U, McKeegan KD, DeLong EF (2001b) Methane-consuming archaea revealed by directly coupled isotopic and phylogenetic analysis. *Science* 293:484–487
- Orphan VJ, House CH, Hinrichs K-U, McKeegan KD, DeLong EF (2002) Multiple archaeal groups mediate methane oxidation in anoxic cold seep sediments. *Proc Natl Acad Sci U S A* 99:7663–7668
- Orr WL (1974) Changes in sulfur content and isotopic ratios of sulfur during petroleum maturation – study of Big Horn Basin Paleozoic oils. *AAPG Bull* 58:2295–2318
- Oswald K, Milucka J, Brand A, Littmann S, Wehrli B, Kuypers MMM, Schubert CJ (2015) Light-dependent aerobic methane oxidation reduces methane emissions from seasonally stratified lakes. *PLoS One* 10(7):e0132574

- Ozuolmez D, Na H, Lever MA, Kjeldsen KU, Jørgensen BB, Plugge CM (2015) Methanogenic archaea and sulfate reducing bacteria co-cultured on acetate: teamwork or coexistence? *Front Microbiol* 6:492
- Pan C, Yu L, Liu J, Fu J (2006) Chemical and carbon isotopic fractionations of gaseous hydrocarbons during abiogenic oxidation. *Earth Planet Sci Lett* 246(1):70–89
- Pancost RD, Damsté JSS, de Lint S, van der Maarel MJ, Gottschal JC (2000) Biomarker evidence for widespread anaerobic methane oxidation in Mediterranean sediments by a consortium of methanogenic archaea and bacteria. *Appl Environ Microbiol* 66(3):1126–1132
- Pancost RD, Hopmans EC, Sinninghe Damsté JS, the Medinaut Shipboard Scientific Party (2001) Archaeal lipids in Mediterranean cold seeps: molecular proxies for anaerobic methane oxidation. *Geochim Cosmochim Acta* 65:1611–1627
- Parkes RJ, Cragg BA, Bale SJ, Getliff JM, Goodman K, Rochelle PA, Harvey SM (1994) Deep bacterial biosphere in Pacific Ocean sediments. *Nature* 371(6496):410–413
- Parmentier FJW, van Huissteden J, Kip N, Op den Camp HJM, Jetten MSM, Maximov TC, Dolman AJ (2011) The role of endophytic methane-oxidizing bacteria in submerged Sphagnum in determining methane emissions of Northeastern Siberian tundra. *Biogeosciences* 8(5):1267–1278
- Patrick WH Jr, Reddy CN (1978) Chemical changes in rice soils. In: International Rice Research Institute (ed) *Soils and rice*. IRRI, Los Baños, pp 361–379
- Pedersen K (1997) Microbial life in deep granitic rock. *FEMS Microbiol Rev* 20(3–4):399–414
- Penger J, Conrad R, Blaser M (2012) Stable carbon isotope fractionation by methylotrophic methanogenic archaea. *Appl Environ Microbiol* 78(21):7596–7602
- Penger J, Conrad R, Blaser M (2014) Stable carbon isotope fractionation of six strongly fractionating microorganisms is not affected by growth temperature under laboratory conditions. *Geochim Cosmochim Acta* 140:95–105
- Penner TJ, Foght JM, Budwill K (2010) Microbial diversity of western Canadian subsurface coal beds and methanogenic coal enrichment cultures. *Int J Coal Geol* 82(1):81–93
- Peters V, Conrad R (1996) Sequential reduction processes and initiation of CH₄ production upon flooding of oxic upland soils. *Soil Biology and Biochemistry* 28(3):371–382
- Petersen JM, Dubilier N (2009) Methanotrophic symbioses in marine invertebrates. *Environ Microbiol Rep* 1(5):319–335
- Petrenko VV, Severinghaus JP, Schaefer H, Smith AM, Kuhl T, Baggenstos D, Weiss RF (2016) Measurements of ¹⁴C in ancient ice from Taylor Glacier, Antarctica constrain in situ cosmogenic ¹⁴CH₄ and ¹⁴CO production rates. *Geochim Cosmochim Acta* 177:62–77
- Pison I, Ringeval B, Bousquet P, Prigent C, Papa F (2013) Stable atmospheric methane in the 2000s: key-role of emissions from natural wetlands. *Atmos Chem Phys* 13(23):11609–11623
- Pol A, Heijmans K, Harhangi HR, Tedesco D, Jetten MSM, Op den Camp HJM (2007) Methanotrophy below pH1 by a new *Verrucomicrobia* species. *Nature* 450:874–878
- Ponnamperuma FN (1972) The chemistry of submerged soils. *Adv Agron* 24:29–96
- Potter J, Konnerup-Madsen J (2003) A review of the occurrence and origin of abiogenic hydrocarbons in igneous rocks. Geological Society, London, Special Publications 214(1):151–173
- Poulter B, Bousquet P, Canadell JG, Ciais P, Peregón A, Saunois M (2017) Global wetland contribution to 2000–2012 atmospheric methane growth rate dynamics. *Environ Res Lett* 12(9):94013
- Prather MJ, Derwent RG, Ehhalt D, Fraser PJ, Sanhueza E, Zhou X (1995) Other trace gases and atmospheric chemistry. In: *Climate change 1994: radiative forcing of climate change and an evaluation of the IPCC IS92 emission scenarios* (ed: Houghton JT, Meira Filho LG, Bruce J, Lee H, Callander BA, Haites E, Harris N, Maskell K). Cambridge University Press, Cambridge, UK, pp 77–126
- Prather MJ, Holmes CD, Hsu J (2012) Reactive greenhouse gas scenarios: systematic exploration of uncertainties and the role of atmospheric chemistry. *Geophys Res Lett* 39(9):L09803, 5p
- Price PB (2009) Microbial genesis, life and death in glacial ice. *Can J Microbiol* 55(1):1–11

- Price PB, Sowers T (2004) Temperature dependence of metabolic rates for microbial growth, maintenance, and survival. *Proc Natl Acad Sci U S A* 101(13):4631–4636
- Priestley J (1775) Experiments and Observations on Different Kinds of Air. In: Bowyer W, Nichols J, 1774. Experiments and Observations on Different Kinds of Air, vol. 2. J Johnson Pub, London, 399p
- Pulliam WM (1993) Carbon dioxide and methane exports from a southeastern floodplain swamp. *Ecol Monogr* 63:29–53
- Qaderi MM, Reid DM (2009) Methane emissions from six crop species exposed to three components of global climate change: temperature, ultraviolet-B radiation and water stress. *Physiol Plant* 137(2):139–147
- Quay P, Stutsman J, Wilbur D, Snover A, Dlugokencky E, Brown T (1999) The isotopic composition of atmospheric methane. *Glob Biogeochem Cycles* 13(2):445–461
- Raghoebarsing AA, Pol A, Van de Pas-Schoonen KT, Smolders AJP, Ettwig KF, Rijpman I, Schouten S, Sinnige Damste JS, Op den Camp HJM, Jetten MSM, Strous M (2006) A microbial consortium couples anaerobic methane oxidation to denitrification. *Nature* 440:918–921
- Ragsdale SW, Kumar M (1996) Nickel-containing carbon monoxide dehydrogenase/acetyl-CoA synthase. *Chem Rev* 96:2515–2539
- Ramaswamy V, Boucher O, Haigh J, Hauglustaine D, Haywood JM, Myhre G, Nakajima T, Shi GY, Solomon S (2001) Radiative forcing of climate change, Chapter 6. In: Climate change: the scientific basis. Contribution of working group I to the third assessment report of the intergovernmental panel on climate change (ed: Houghton JT, Ding Y, Griggs DJ, Noguer M, van der Linden PJ, Dai X, Maskell K, Johnson CA). Cambridge University Press, Cambridge, UK, pp 349–416
- Ramaswamy V, Collins W, Haywood J, Lean J, Mahowald N, Myhre G, Storelvmo T (2019) Radiative forcing of climate: the historical evolution of the radiative forcing concept, the forcing agents and their quantification, and applications. *Meteorological monographs*. American Meteorological Society, 367p. <https://doi.org/10.1175/AMSMONOGRAPHS-D-19-0001.1>
- Rasigraf O, Vogt C, Richnow HH, Jetten MS, Ettwig KF (2012) Carbon and hydrogen isotope fractionation during nitrite-dependent anaerobic methane oxidation by *Methylomirabilis oxyfera*. *Geochimica et Cosmochimica Acta* 89:256–264
- Rayleigh L (1896) Theoretical considerations respecting the separation of gases by diffusion and similar processes. *The London, Edinburgh, and Dublin Philosophical Magazine and Journal of Science* 42(259):493–498
- Reeburgh WS (1976) Methane consumption in Cariaco trench waters and sediments. *Earth Planet Res Lett* 28:337–344
- Reeburgh WS (1996) Soft spots in the global methane budget. In: *Microbial growth on C1 compounds* (ed: Lidstrom ME, Tabita FR). Kluwer, Dordrecht, pp 334–342
- Reeburgh WS (2003) In the atmosphere (ed: Keeling RF), vol 4 of *Treatise on geochemistry*; Holland HD, Turekian KK (eds) Elsevier-Pergamon, Oxford, pp 65–89
- Reeburgh WS (2007) Oceanic methane biogeochemistry. *Chem Rev* 107(2):486–513
- Reeburgh WS, Ward BB, Whalen SC, Sandbeck KA, Kilpatrick KA, Kerkhof LJ (1991) Black Sea methane geochemistry. *Deep Sea Research Part A. Oceanogr Res Pap* 38:S1189–S1210
- Reeburgh WS, Whalen SC, Alperin MJ (1993) The role of methylophily in the global methane budget. In: *Microbial growth on C-1 compounds* (ed: Murrell JC, Kelly DP). Intercept Press, Andover, pp 1–14
- Reed DC, Deemer BR, van Grinsven S, Harrison JA (2017) Are elusive anaerobic pathways key methane sinks in eutrophic lakes and reservoirs? *Biogeochemistry* 134(1):29–39
- Regnier P, Dale AW, Arndt S, LaRowe DE, Mogollón J, Van Cappellen P (2011) Quantitative analysis of anaerobic oxidation of methane (AOM) in marine sediments: a modeling perspective. *Earth Sci Rev* 106(1–2):105–130
- Rehder G, Keir RS, Suess E, Rhein M (1999) Methane in the northern Atlantic controlled by microbial oxidation and atmospheric history. *Geophys Res Lett* 26(5):587–590

- Repeta DJ, Ferrón S, Sosa OA, Johnson CG, Repeta LD, Acker M, Karl DM (2016) Marine methane paradox explained by bacterial degradation of dissolved organic matter. *Nat Geosci* 9 (12):884–887
- Rhee GY, Fuhs GW (1978) Wastewater denitrification with one-carbon compounds as energy-source. *J Water Pollut Control Fed* 50(9):2111–2119
- Rice AL, Tyler SC, McCarthy MC, Boering KA, Atlas E (2003) Carbon and hydrogen isotopic compositions of stratospheric methane: 1. High-precision observations from the NASA ER-2 aircraft. *J Geophys Res* 108:4460
- Rice AL, Butenhoff CL, Teama DG, Röger FH, Khalil MAK, Rasmussen RA (2016) Atmospheric methane isotopic record favors fossil sources flat in 1980s and 1990s with recent increase. *Proc Natl Acad Sci* 113(39):10791–10796
- Ridgwell AJ, Marshall SJ, Gregson K (1999) Consumption of atmospheric methane by soils: a process-based model. *Glob Biogeochem Cycles* 13:59–70
- Riedinger N, Formolo MJ, Lyons TW, Henkel S, Beck A, Kasten S (2014) An inorganic geochemical argument for coupled anaerobic oxidation of methane and iron reduction in marine sediments. *Geobiology* 12(2):172–181
- Rigby M, Prinn RG, Fraser PJ, Simmonds PG, Langenfelds RL, Huang J, Cunnold DM, Steele LP, Krummel PB, Weiss RF, O'Doherty S, Salameh PK, Wang HJ, Harth CM, Mühle J, Porter LW (2008) Renewed growth of atmospheric methane. *Geophys Res Lett* 35(22):L22805
- Rittenberg S, Emery KO, Orr WL (1955) Regeneration of nutrients in sediments of marine basins. *Deep Sea Res* (1953) 3(1):23–45
- Rivkina EM, Laurinavichus KS, Gilichinsky DA, Shcherbakova VA (2002) Methane generation in permafrost sediments. *Dokl Biol Sci* 383(1–6):179–181
- Rivkina E, Laurinavichus K, McGrath J, Tiedje J, Shcherbakova V, Gilichinsky D (2004) Microbial life in permafrost. *Adv Space Res* 33(8):1215–1221
- Roden EE, Wetzel RG (1996) Organic carbon oxidation and suppression of methane production by microbial Fe (III) oxide reduction in vegetated and unvegetated freshwater wetland sediments. *Limnol Oceanogr* 41(8):1733–1748
- Rooney M, Claypool G, Chung H (1995) Modeling thermogenic gas generation using carbon isotope ratios of natural gas hydrocarbons. *Chem Geol* 126(3–4):219–232
- Rosenberg E, DeLong EF, Lory S, Stackebrandt E, Thompson F (eds) (2014) *The prokaryotes: other major lineages of bacteria and the archaea*. Springer, Berlin, 1028p
- Roslev P, King GM (1995) Aerobic and anaerobic starvation metabolism in methanotrophic bacteria. *Appl Environ Microbiol* 61(4):1563–1570
- Rother M, Metcalf WW (2004) Anaerobic growth of *Methanosarcina acetivorans* C2A on carbon monoxide: an unusual way of life for a methanogenic archaeon. *Proc Natl Acad Sci U S A* 101 (48):16929–16934
- Rowan AK, Brown A, Bennett B, Gray ND, Erdmann M, Aitken CM, Larter SR (2008) Crude-oil biodegradation via methanogenesis in subsurface petroleum reservoirs. *Nature* 451(7175): 176–180
- Rusanov II, Yusupov SK, Savvichev AS, Lein AY, Pimenov NV, Ivanov MV (2004) Microbial production of methane in the aerobic water layer of the Black Sea. *Doklady Biol Sci* 399 (1):493–495
- Rusch H, Rennenberg H (1998) Black alder [*Alnus glutinosa* (L.) Gaertn.] trees mediate methane and nitrous oxide emission from the soil to the atmosphere. *Plant Soil* 201:1–7
- Rush D, Osborne K, Birgel D, Kappler A, Hirayama H, Peckmann J, Talbot H (2016) The bacteriohopanepolyol inventory of novel aerobic methane oxidising bacteria reveals new biomarker signatures of aerobic methanotrophy in marine systems. *PLoS One* 11(11): e0165635
- Saueressig G, Crowley JN, Bergamaschi P, Bruehl C, Brenninkmeijer CA, Fischer H (2001) Carbon 13 and D kinetic isotope effects in the reactions of CH₄ with O(1D) and OH: new laboratory measurements and their implications for the isotopic composition of stratospheric methane. *J Geophys Res* 106:23127–23138

- Saunders NF, Thomas T, Curmi PM, Mattick JS, Kuczek E, Slade R, Davis J, Franzmann PD, Boone D, Rusterholtz K, Feldman R (2003) Mechanisms of thermal adaptation revealed from the genomes of the Antarctic Archaea *Methanogenium frigidum* and *Methanococoides burtonii*. *Genome Res* 13(7):1580–1588
- Saunio M, Bousquet P, Poulter B, Peregon A, Ciais P, Canadell JG, Dlugokencky EJ, Etiope G, Bastviken D, Houweling S, Janssens-Maenhout G, Tubiello FN, Castaldi S, Jackson RB, Alexe M, Arora VK, Beerling DJ, Bergamaschi P, Blake DR, Brailsford G, Brovkin V, Bruhwiler L, Crevoisier C, Crill P, Covey K, Curry C, Frankenberg C, Gedney N, Höglund-Isaksson L, Ishizawa M, Ito A, Joos F, Kim HS, Kleinen T, Krummel P, Lamarque JF, Langenfelds R, Locatelli R, Machida T, Maksyutov S, McDonald KC, Marshall J, Melton JR, Morino I, Naik V, O'Doherty S, Parmentier FJW, Patra PK, Peng C, Peng S, Peters GP, Pison I, Prigent C, Prinn R, Ramonet M, Riley WJ, Saito M, Santini M, Schroeder R, Simpson IJ, Spahni R, Steele P, Takizawa A, Thornton BF, Tian H, Tohjima Y, Viovy N, Voulgarakis A, van Weele M, van der Werf GR, Weiss R, Wiedinmyer C, Wilton DJ, Wiltshire A, Worthy D, Wunch D, Xu X, Yoshida Y, Zhang B, Zhang Z, Zhu Q (2016) The global methane budget 2000–2012. *Earth Syst Sci Data* 8:697–751. <https://doi.org/10.5194/essd-8-697-2016>
- Saunio M, Stavert AR, Poulter B, Bousquet P, Josep G, Jackson RB, Bastviken D et al (2019) The global methane budget 2000–2017. *Earth System Science Data*. 136p
- Schaefer H, Whiticar MJ (2008) Potential glacial-interglacial changes in stable carbon isotope ratios of methane sources and sink fractionation. *Glob Biogeochem Cycles* 22 (1):GB1001, 18p
- Schaefer H, Fletcher SEM, Veidt C, Lassey KR, Brailsford GW, Bromley TM, Lowe DC (2016) A 21st-century shift from fossil-fuel to biogenic methane emissions indicated by $^{13}\text{C}_4$. *Science* 352(6281):80–84
- Scheller S, Yu H, Chadwick GL, McGlynn SE, Orphan VJ (2016) Artificial electron acceptors decouple archaeal methane oxidation from sulfate reduction. *Science* 351(6274):703–707
- Schimel D, Alves D, Enting I, Heimann M, Joos F, Raynaud D, Fraser P (1996) Radiative forcing of climate change. *Climate change 1995: the science of climate change*, 65–131
- Schink B (1997) Energetics of syntrophic cooperation in methanogenic degradation. *Microbiol Mol Biol Rev* 61(2):262–280
- Schink B, Ward JC, Zeikus JG (1981) Microbiology of wetwood: importance of pectin degradation and *Clostridium* species in living trees. *Appl Environ Microbiol* 42:526–532
- Schnellen CGTP (1947) Onderzoekingen over de methaangisting. Doctoral dissertation, Thesis Delft University of Technology De Maasstad, Rotterdam
- Schoell M (1980) The hydrogen and carbon isotopic composition of methane from natural gases of various origins. *Geochim Cosmochim Acta* 44(5):649–661
- Schoell M (1988) Multiple origins of methane in the Earth. *Chem Geol* 71(1–3):1–10
- Schonheit P, Keweloh H, Thauer RK (1981) Factor F420 degradation in *Methanobacterium thermoautotrophicum* during exposure to oxygen. *FEMS Microbiol Lett* 12:347–349
- Schönheit P, Kristjansson JK, Thauer RK (1982) Kinetic mechanism for the ability of sulfate reducers to out-compete methanogens for acetate. *Arch Microbiol* 132:285–288
- Schouten S, Wakeham SG, Sinninghe Damsté JS (2001) Evidence for anaerobic methane oxidation by archaea in euxinic waters of the Black Sea. *Org Geochem* 32:1277–1281
- Schouten S, Wakeham SG, Hopmans EC, Sinninghe Damsté JS (2003) Biogeochemical evidence that thermophilic archaea mediate the anaerobic oxidation of methane. *Appl Environ Microbiol* 69:1680–1686
- Schouten S, Pitcher A, Hopmans EC, Villanueva L, van Bleijswijk J, Damsté JSS (2012) Intact polar and core glycerol dibiphytanyl glycerol tetraether lipids in the Arabian Sea oxygen minimum zone: I. Selective preservation and degradation in the water column and consequences for the TEX86. *Geochimica et Cosmochimica Acta* 98:228–243
- Schubel JR (1974) Gas bubbles and the acoustically impenetrable, or turbid, character of some estuarine sediments. In IR Kaplan (ed) *Natural gases in marine sediments* Springer, Boston, 275–298

- Schubert CJ, Durisch-Kaiser E, Holzner CP, Klauser L, Wehrli B, Schmale O, Greinert J, McGinnis DF, De Batist M, Kipfer R (2006) Methanotrophic microbial communities associated with bubble plumes above gas seeps in the Black Sea. *Geochem Geophys Geosyst* 7:Q04002
- Schubert CJ, Vazquez F, Losekann-Behrens T, Knittel K, Tonolla M, Boetius A (2011) Evidence for anaerobic oxidation of methane in sediments of a freshwater system (Lago di Cadagno). *FEMS Microbiol Ecol* 76:26–38
- Schüler F (1952) Untersuchungen über die Mächtigkeit von Schlickschichten mit Hilfe des Echograms. *Dtsch Hydrogr Z* 5:220–231
- Schütz H, Seiler W, Conrad R (1989) Processes involved in formation and emission of methane in rice paddies. *Biogeochemistry* 7(1):33–53
- Schwarz MJ, Frenzel P (2005) Methanogenic symbionts of anaerobic ciliates and their contribution to methanogenesis in an anoxic rice field soil. *FEMS Microbiol Ecol* 52(1):93–99
- Schwietzke S, Sherwood OA, Bruhwiler LM, Miller JB, Etiope G, Dlugokencky EJ, Michel SE, Arling VA, Vaughn BH, White JW, Tans PP (2016) Upward revision of global fossil fuel methane emissions based on isotope database. *Nature* 538(7623):88–91
- Scranton MI, Brewer PG (1977) Occurrence of methane in the near surface waters of the western subtropical North-Atlantic. *Deep-Sea Res* 24:127–138
- Sebacher DI, Harriss RC, Bartlett KB, Sebacher SM (1986) Atmospheric methane sources: Alaskan tundra bogs, an alpine fen and a subarctic boreal marsh. *Tellus* 38B:1–10
- Segarra KEA, Comerford C, Slaughter J, Joye SB (2013) Impact of electron acceptor availability on the anaerobic oxidation of methane in coastal freshwater and brackish wetland sediments. *Geochim Cosmochim Acta* 115:15–30
- Segerer AH, Burggraf S, Fiala G, Huber G, Huber R, Pley U, Stetter KO (1993) Life in hot springs and hydrothermal vents. *Orig Life Evol Biosph* 23(1):77–90
- Seitzinger S, Harrison JA, Böhlke JK, Bouwman AF, Lowrance R, Peterson B, Tobias C, Van Drecht G (2006) Denitrification across landscapes and waterscapes: a synthesis. *Ecol Appl* 16(6):2064–2090
- Sela-Adler M, Ronen Z, Herut B, Antler G, Vigderovich H, Eckert W, Sivan O (2017) Co-existence of Methanogenesis and Sulfate reduction with common substrates in sulfate-rich estuarine sediments. *Front Microbiol* 8:766
- Seller W, Conrad R (1987) Contribution of tropical ecosystems to the global budget of trace gases, especially CH₄, H₂, CO and N₂O. In: *The Geophysiology of Amazonia*. R Dickenson (ed) John Wiley, New York, pp133–160
- Serrano-Silva N, Sarria-Guzmán Y, Dendooven L, Luna-Guido M (2014) Methanogenesis and methanotrophy in soil: a review. *Pedosphere* 24(3):291–307
- Shannon RD, White JR, Lawson JE, Gilmour BS (1996) Methane efflux from emergent vegetation in peatlands. *J Ecol* 84(2):239–246
- Sherwood Lollar B, Lacrampe-Couloume G, Slater GF, Ward J, Moser DP, Gihring TM, Onstott TC (2006) Unravelling abiogenic and biogenic sources of methane in the earth's deep subsurface. *Chem Geol* 226(3):328–339
- Sherwood OA, Schwietzke S, Arling VA, Etiope G (2017) Global inventory of gas geochemistry data from fossil fuel, microbial and burning sources, version 2017. *Earth Syst Sci Data* 9: 639–656
- Sieburth JM (1987) Contrary habitats for redox-specific processes: methanogenesis in oxic waters and oxidation in anoxic waters. In: Sleigh MA (ed) *Microbes in the sea*. Ellis Horwood, Chichester, pp 11–38
- Sikora A, Detman A, Chojnacka A, Błaszczuk MK (2017) Anaerobic digestion: I. A common process ensuring energy flow and the circulation of matter in ecosystems. II. A tool for the production of gaseous biofuels. In: (ed.) Jozala AF, *Fermentation processes*. InTech Rijeka, Croatia, Chapter 14, pp 271–301
- Simkus DN, Slater GF, Lollar BS, Wilkie K, Kieft TL, Magnabosco C, Sakowski EG (2016) Variations in microbial carbon sources and cycling in the deep continental subsurface. *Geochim Cosmochim Acta* 173:264–283

- Simpson IJ, Sulbaek Andersen MP, Meinardi S, Bruhwiler L, Blake NJ, Helmig D, Rowland FS, Blake DR (2012) Long-term decline of global atmospheric ethane concentrations and implications for methane. *Nature* 488(7412):490–494
- Sinninghe Damsté JS, Schouten S, van Vliet NH, Huber R, Geenevasen JA (1997) A polyunsaturated irregular acyclic C₂₅ isoprenoid in a methanogenic archaeon. *Tetrahedron Lett* 38(39):6881–6884
- Sinninghe Damsté JS, Hopmans EC, Pancost RD, Schouten S, Geenevasen JAJ (2000) Newly discovered non-isoprenoid dialkyl diglycerol tetraether lipids in sediments. *J Chem Soc Chem Commun* 23:1683–1684
- Sinninghe Damsté JS, Hopmans EC, Schouten S, van Duin ACT, Geenevasen JAJ (2002) Crenarchaeol: the characteristic core glycerol dibiphytanyl glycerol tetraether membrane lipid of cosmopolitan pelagic crenarchaeota. *J Lipid Res* 43:1641–1651
- Sivan O, Adler M, Pearson A, Gelman F, Bar-Or I, John SG, Eckert W (2011) Geochemical evidence for iron-mediated anaerobic oxidation of methane. *Limnol Oceanogr* 56:1536–1544
- Slater GF, Lippmann-Pipke J, Moser DP, Reddy CM, Onstott TC, Lacrampe-Couloume G, Lollar BS (2006) ¹⁴C in methane and DIC in the deep terrestrial subsurface: implications for microbial methanogenesis. *Geomicrobiol J* 23(6):453–462
- Smemo KA, Yavitt JB (2011) Anaerobic oxidation of methane: an underappreciated aspect of methane cycling in peatland ecosystems? *Biogeosciences* 8:779–793
- Söhngen NL (1906) Über bakterien, welche methan als kohlenstoffnahrung und energiequelle gebrauchen. *Zentralbl Bakteriol Parasitenk Infektionskr* 15:513–517
- Sørensen KB, Finster K, Ramsing NB (2001) Thermodynamic and kinetic requirements in anaerobic methane oxidizing consortia exclude hydrogen, acetate, and methanol as possible electron shuttles. *Microb Ecol* 42:1–10
- Sorokin DY, Jones BE, Kuenen JG (2000) A novel obligately methylotrophic, methane-oxidizing Methylophile species from a highly alkaline environment. *Extremophiles* 4:145–155
- Sorokin DY, Berben T, Melton ED, Overmars L, Vavourakis CD, Muyzer G (2014) Microbial diversity and biogeochemical cycling in soda lakes. *Extremophiles* 18(5):791–809
- Sorokin DY, Abbas B, Merkel AY, Rijpstra WIC, Damsté JS, Sukhacheva MV, van Loosdrecht MC (2015) *Methanosalsum natronophilum* sp. nov., and *Methanocalculus alkaliphilus* sp. nov., haloalkaliphilic methanogens from hypersaline soda lakes. *Int J Syst Evol Microbiol* 65(10):3739–3745
- Spencer-Jones CL, Wagner T, Dinga BJ, Schefuß E, Mann PJ, Poulsen JR, Talbot HM (2015) Bacteriohopanepolyols in tropical soils and sediments from the Congo river catchment area. *Org Geochem* 89–90:1–13
- Starkey RL (1948) Characteristics and cultivation of sulfate-reducing bacteria. *J Am Water Works Assoc* 40(12):1291–1298
- Stephenson M, Stickland LH (1933) Hydrogenase: the bacterial formation of methane by the reduction of one-carbon compounds by molecular hydrogen. *Biochem J* 27(5):1517–1527
- Stetter KO, Fiala G, Huber G, Huber R, Seegerer A (1990) Hyperthermophilic microorganisms. *FEMS Microbiol Rev* 75:117–124
- Stevens TO, McKinley JP (1995) Lithoautotrophic microbial ecosystems in deep basalt aquifers. *Science* 270(5235):450–455
- Stigliani WM (1988) Changes in valued “capacities” of soils and sediments as indicators of nonlinear and time-delayed environmental effects. *Environ Monit Assess* 10(3):245–307
- Strayer RF, Tiedje JM (1978) In situ methane production in a small, hypereutrophic, hard-water lake: loss of methane from sediments by vertical diffusion and ebullition. *Limnol Oceanogr* 23:1201–1206
- Ström L, Tagesson T, Mastepanov M, Christensen TR (2012) Presence of *Eriophorum scheuchzeri* enhances substrate availability and methane emission in an Arctic wetland. *Soil Biol. Biochemist* 45:61–70
- Strous M, Jetten MSM (2004) Anaerobic oxidation of methane and ammonium. *Annu Rev Microbiol* 58(1):99–117

- Stumm WS, Morgan JJ (1981) Aquatic chemistry. Wiley, New York, p 460
- Summons RE (2013) Biogeochemical cycles a review of fundamental aspects of organic matter. In Engel MH; Macko SA (ed) Organic Geochemistry: Principles and Applications Springer, pp3–17
- Summons RE, Franzmann PD, Nichols PD (1998) Carbon isotopic fractionation associated with methylophilic methanogenesis. *Org Geochem* 28:465–475
- Szatmari P (1989) Petroleum formation by Fischer-Tropsch synthesis in plate tectonics. *Am Assoc Pet Geol Bull* 73:989–998
- Takai K, Nealon KH, Horikoshi K (2004) *Methanotorris formicicus* sp. nov., a novel extremely thermophilic, methane-producing archaeon isolated from a black smoker chimney in the Central Indian Ridge. *Int J Syst Evol Microbiol* 54:1095–1100
- Takai K, Nakamura K, Toki T, Tsunogai U, Miyazaki M, Miyazaki J, Horikoshi K (2008) Cell proliferation at 122 degrees C and isotopically heavy CH₄ production by a hyperthermophilic methanogen under high-pressure cultivation. *Proc Natl Acad Sci U S A* 105(31):10949
- Tan Z, Zhuang Q (2015) Methane emissions from pan-Arctic lakes during the 21st century: an analysis with process-based models of lake evolution and biogeochemistry. *J Geophys Res Biogeosci* 120(12):2641–2653
- Tatton MJ, Archer DB, Powell GE, Parker ML (1989) Methanogenesis from ethanol by defined mixed continuous cultures. *Appl Environ Microbiol* 55(2):440–445
- Tavormina PL, Ussler W III, Joye SB, Harrison BK, Orphan VJ (2010) Distributions of putative aerobic methanotrophs in diverse pelagic marine environments. *ISME J* 4(5):700
- Taylor SW, Sherwood Lollar B, Wassenaar I (2000) Bacteriogenic ethane in near-surface aquifers: Implications for leaking hydrocarbon well bores. *Environ Sci Technol* 34(22):4727–4732
- Teh YA, Silver WL, Conrad ME (2005) Oxygen effects on methane production and oxidation in humid tropical forest soils. *Glob Chang Biol* 11:1283–1297
- Templeton AS, Chu KH, Alvarez-Cohen L, Conrad ME (2006) Variable carbon isotope fractionation expressed by aerobic CH₄-oxidizing bacteria. *Geochim Cosmochim Acta* 70:1739–1752
- Terazawa K, Ishizuka S, Sakatac T, Yamada K, Takahashi M (2007) Methane emissions from stems of *Fraxinus mandshurica* var. *japonica* trees in a floodplain forest. *Soil Biol Biochem* 39: 2689–2692
- Teske A, Hinrichs K-U, Edgcomb V, de Vera Gomez A, Kysela D et al (2002) Microbial diversity of hydrothermal sediments in the Guaymas Basin: evidence for anaerobic methanotrophic communities. *Appl Environ Microbiol* 68:1994–2007
- Thauer RK (1998) Biochemistry of methanogenesis: a tribute to Marjory Stephenson:1998 Marjory Stephenson prize lecture. *Microbiology* 144(9):2377
- Thauer RK, Shima S (2008) Methane as fuel for anaerobic organisms. *Ann N Y Acad Sci* 1125: 158–170
- Thauer RK, Jungermann K, Decker K (1977) Energy conservation in chemotrophic anaerobic bacteria. *Bacteriol Rev* 41:100–180
- Thauer RK, Kaster A-K, Seedorf H, Buckel W, Hedderich R (2008) Methanogenic archaea: ecologically relevant differences in energy conservation. *Nat Rev Microbiol* 6:579–591
- Thiel V, Peckmann J, Seifert R, Wehrung P, Reitner J, Michaelis W (1999) Highly isotopically depleted isoprenoids: molecular markers for ancient methane venting. *Geochim Cosmochim Acta* 63:3959–3966
- Thiel V, Peckmann J, Richnow HH, Luth U, Reitner J, Michaelis W (2001) Molecular signals for anaerobic methane oxidation in Black Sea seep carbonates and a microbial mat. *Mar Chem* 73:97–112
- Thomson W (1852) On the mechanical action of radiant heat on light. *Proc R Soc Edinb* 3:108–114
- Tiedje JM (1988) Ecology of denitrification and dissimilatory nitrate reduction to ammonium. In: *Biology of anaerobic microorganisms* (ed: Zehnder AJB). Wiley, New York, pp 179–244
- Timmers PH, Welte CU, Koehorst JJ, Plugge CM, Jetten MS, Stams AJ (2017) Reverse methanogenesis and respiration in methanotrophic archaea. *Hindawi Archaea* 5:1–22

- Topp E, Pattey E (1997) Soils as sources and sinks for atmospheric methane. *Can J Soil Sci* 77 (2):167–177
- Tornabene TG, Langworthy TA, Holzer G, Oro J (1979) Squalenes, phytanes and other isoprenoids as major neutral lipids of methanogenic and thermoacidophilic “archaeobacteria”. *J Mol Evol* 13 (1):73–83
- Torres ME, McManus J, Hammond DE, de Angelis MA, Heeschen KU, Colbert SL, Tyron MD, Brown KM, Suess E (2002) Fluid and chemical fluxes in and out of sediments hosting methane hydrate deposits on hydrate ridge, OR I: hydrological provinces. *Earth Planet Sci Lett* 201:525–540
- Traganza ED, Swinnerton JW, Cheek CH (1979) Methane supersaturation and ATP-zooplankton blooms in near-surface waters of the Western Mediterranean and the subtropical North Atlantic Ocean Deep Sea Research Part A. *Oceanogr Res Pap* 26(11):1237–1245
- Treude T, Boetius A, Knittel K, Wallmann K, Jørgensen BB (2003) Anaerobic oxidation of methane above gas hydrates at hydrate ridge, NE Pacific Ocean. *Mar Ecol Prog Ser* 264:1–14
- Treude T, Krause S, Maltby J, Dale AW, Coffin R, Hamdan LJ (2014) Sulfate reduction and methane oxidation activity below the sulfate-methane transition zone in alaskan beaufort sea continental margin sediments: implications for deep sulfur cycling. *Geochim Cosmochim Acta* 144:217–237
- Trotsenko YA, Khmelenina VN (2002) Biology of extremophilic and extremotolerant methanotrophs. *Arch Microbiol* 177(2):123–131
- Tung HC, Price PB, Bramall NE, Vrdoljak G (2006) Microorganisms metabolizing on clay grains in 3-km-deep greenland basal ice. *Astrobiology* 6(1):69–86
- Turner AJ, Frankenberg C, Wennberg PO, Jacob DJ (2017) Ambiguity in the causes for decadal trends in atmospheric methane and hydroxyl. *Proc Natl Acad Sci* 114:5367–5372
- Turner AJ, Frankenberg C, Kort EA (2019) Interpreting contemporary trends in atmospheric methane. *Proceedings of the National Academy of Sciences USA* 116(8):2805–2813
- Tyler SC, Bilek RS, Sass RL, Fisher FM (1997) Methane oxidation and pathways of production in a Texas paddy field deduced from measurements of flux, $\delta^{13}\text{C}$, and δD of CH_4 . *Glob Biogeochem Cycles* 11(3):323–348
- Umezawa T, Machida T, Ishijima K, Matsueda H, Sawa Y, Patra PK, Nakazawa T (2012) Carbon and hydrogen isotopic ratios of atmospheric methane in the upper troposphere over the Western Pacific. *Atmos Chem Phys* 12(17):8095–8113
- Valentine DL (2002) Biogeochemistry and microbial ecology of methane oxidation in anoxic environments. *Antonie Van Leeuwenhoek* 81:271–282
- Valentine DL, Reeburgh WS (2000) New perspectives on anaerobic methane oxidation. *Environ Microbiol* 2:477–484
- Valentine DL, Blanton DC, Reeburgh WS (2000) Hydrogen production by methanogens under low-hydrogen conditions. *Arch Microbiol* 174(6):415–421
- Valentine DL, Blanton DC, Reeburgh WS, Kastner M (2001) Water column methane oxidation adjacent to an area of active hydrate dissociation. *Eel River Basin Geochim Cosmochim Acta* 65:2633–2640
- Valentine DL, Chidthaisong A, Rice A, Reeburgh WS, Tyler SC (2004) Carbon and hydrogen isotope fractionation by moderately thermophilic methanogens. *Geochim Cosmochim Acta* 68:1571–1590
- Van de Graaf AA, Mulder A, Slijkhuys H, Robertson LA, Kuenen JG (1990) Anoxic ammonium oxidation. In: Christiansen C, Munck L, Villadsen J (eds) *Proceedings of the 5th European Congress on biotechnology*. Munksgaard International Publisher, Copenhagen, pp 338–391
- Van Delden A (1903) Beitrag zur Kenntnis der Sulfatreduktion durch Bakterien. *Cent Bakt ete Abt II* 11(81):113
- Van Weering T (1975) Late Quaternary history of the Skagerrak; an interpretation of acoustic profiles. *Geol Mijnb* 54:130–145
- Verkouteren RM, Klinedinst D (2004) Value assignment and uncertainty estimation of selected light stable isotope reference materials: RMs 8543-8545, RMs 8562-8564, and RM 8566 (NIST. Special publication (NIST SP)-260-149), 59p

- Vigano I, Van Weelden H, Holzinger R, Keppler F, Röckmann T (2008) Effect of UV radiation and temperature on the emission of methane from plant biomass and structural components. *Biogeosci Discuss* 5(1):243–270
- Vigano I, Röckmann T, Holzinger R, Van Dijk A, Keppler F, Greule M, Van Weelden H (2009) The stable isotope signature of methane emitted from plant material under UV irradiation. *Atmos Environ* 43(35):5637–5646
- Vogel TM, Oremland RS, Kvenvolden KA (1982) Low-temperature formation of hydrocarbon gases in San Francisco Bay sediment (California, USA). *Chem Geol* 37(3–4):289–298
- Volta A (1777) Volta letters on flammable Air of Marshes (Milan, 1777). First letter on flammable Air of Marshes (Milan, 1777). http://www.encyclopedia.com/topic/Alessandro_Volta.aspx
- von Fischer JC (2002) Gross methane transformations and methanogenic microsites along natural soil moisture gradients. PhD thesis, Cornell University, Ithaca, 195p
- von Fischer JC, Hedin LO (2007) Controls on soil methane fluxes: tests of biophysical mechanisms using stable isotope tracers. *Glob Biogeochem Cycles* 21(2):GB2007
- von Hofmann AW (1866) Introduction to modern chemistry, experimental and theoretic; embodying twelve lectures delivered in the Royal College of Chemistry. Walton and Maberly, London, p 268
- Wahlen M, Tanaka N, Henry R, Deck B, Zeglen J, Vogel JS, Broecker W (1989) Carbon-14 in methane sources and in atmospheric methane: the contribution from fossil carbon. *Science* 245(4915):286–290
- Wakeham SG, Lewis CM, Hopmans EC, Schouten S, Damsté JSS (2003) Archaea mediate anaerobic oxidation of methane in deep euxinic waters of the Black Sea. *Geochimica et Cosmochimica Acta* 67(7):1359–1374
- Waldron S, Lansdown JM, Scott EM, Fallick AE, Hall AJ (1999) The global influence of the hydrogen isotope composition of water on that of bacteriogenic methane from shallow freshwater environments. *Geochim Cosmochim Acta* 63:2237–2245
- Wallmann K, Linke P, Suess E, Bohrmann G, Sahling H, Schlüter M, Dählmann A, Lammers S, Greinert J, Von Mirbach N (1997) Quantifying fluid flow, solute mixing, and biogeochemical turnover at cold vents of the eastern Aleutian subduction zone. *Geochim Cosmochim Acta* 61:5209–5219
- Wallmann K, Aloisi G, Haeckel M, Obzhairov A, Pavlova G, Tishchenko P (2006) Kinetics of organic matter degradation, microbial methane generation, and gas hydrate formation in anoxic marine sediments. *Geochimica Et Cosmochimica Acta* 70(15):3905–3927
- Wallmann K, Pinero E, Burwicz E, Haeckel M, Hensen C, Dale A, Ruepke L (2012) The global inventory of methane hydrate in marine sediments: a theoretical approach. *Energies* 5(12):2449–2498
- Walter KM, Zimov SA, Chanton JP, Verbyla D, Chapin Iii FS (2006) Methane bubbling from Siberian thaw lakes as a positive feedback to climate warming. *Nature* 443(7107):71–75
- Wang JS, McElroy MB, Spivakovsky CM, Jones DB (2002) On the contribution of anthropogenic Cl to the increase in $\delta^{13}\text{C}$ of atmospheric methane. *Global Biogeochem Cycles* 16(3):1047
- Wang ZP, Han XG, Wang GG, Song Y, Gullledge J (2008) Aerobic methane emission from plants in the Inner Mongolia steppe. *Environ Sci Technol* 42(1):62–68
- Wang DT, Welander PV, Ono S (2016) Fractionation of the methane isotopologues $^{13}\text{CH}_4$, $^{12}\text{CH}_3\text{D}$, and $^{13}\text{CH}_2\text{D}_2$ during aerobic oxidation of methane by *Methylococcus capsulatus* (Bath). *Geochimica et Cosmochimica Acta* 192:186–202
- Wang X, Sun G, Zhu Y (2017) Thermodynamic energy of anaerobic microbial redox reactions couples elemental biogeochemical cycles. *J Soils Sediments* 17(12):2831–2846
- Wankel SD, Adams MM, Johnston DT, Hansel CM, Joye SB, Girguis PR (2012) Anaerobic methane oxidation in metalliferous hydrothermal sediments: influence on carbon flux and decoupling from sulfate reduction. *Environ Microbiol* 14:2726–2740
- Ward BB (1992) The subsurface methane maximum in the Southern California Bight. *Continental Shelf Research* 12(5–6):735–752
- Ward JA, Slater GF, Moser DP, Lin L, Lacrampe-Couloume G, Bonin AS, Sherwood Lollar B (2004) Microbial hydrocarbon gases in the Witwatersrand Basin, South Africa: implications for the deep biosphere. *Geochim Cosmochim Acta* 68(15):3239–3250

- Wartiainen I, Hestnes AG, McDonald I, Svenning MM (2006) *Methylocystis rosea* sp. nov., a novel methanotrophic bacterium from Arctic wetland soil, Svalbard, Norway (78°N). *Int J Syst Evol Microbiol* 56:541–547
- Watanabe A, Takeda T, Kimura M (1999) Evaluation of origins of CH₄ carbon emitted from rice paddies. *Journal of Geophysical Research: Atmospheres* 104(D19):23623–23629
- Watanabe T, Kimura M, Asakawa S (2007) Dynamics of methanogenic archaeal communities based on rRNA analysis and their relation to methanogenic activity in Japanese paddy field soils. *Soil Biol Biochem* 39:2877–2887
- Watson RT, Rodhe H, Oeschger H, Siegenthaler U (1990) Greenhouse gases and aerosols. Climate change: the intergovernmental panel on climate change scientific assessment (ed: Houghton JT, Jenkins GJ, Ephraum JJ). Cambridge University Press, Cambridge, pp 1–40
- Weber K, Urrutia MM, Churchill PF, Kukkadapu RK, Roden EE (2006) Anaerobic redox cycling of iron by freshwater sediment microorganisms. *Environ Microbiol* 8:100–113
- Wegener G, Krukenberg V, Riedel D, Tegetmeyer HE, Boetius A (2015) Intercellular wiring enables electron transfer between methanotrophic archaea and bacteria. *Nature* 526(7574):587–590
- Weimer PJ, Zeikus JG (1978) Acetate metabolism in *Methanosarcina barkeri*. *Arch Microbiol* 119:175–182
- Weiss DS, Thauer RK (1993) Methanogenesis and the unity of biochemistry. *Cell* 72(6):819–822
- Wendeberg A, Zielinski FU, Borowski C, Dubilier N (2012) Expression patterns of mRNAs for methanotrophy and thiotrophy in symbionts of the hydrothermal vent mussel *Bathymodiolus puteoserpentis*. *ISME J* 6(1):104–112
- Werner F (1968) Gefügeanalyse feingeschichteter Schlicksedimente der Eckernförder Bucht (westliche Ostsee). *Meyniana* 18:79–105
- Westermann P (1993) Temperature regulation of methanogenesis in wetlands. *Chemosphere* 26(1–4):321–328
- Whelan JK, Hunt JM, Berman J (1980) Volatile C1-C7 organic compounds in surface sediments from Walvis Bay. *Geochim Cosmochim Acta* 44(11):1767–1785
- Whiticar MJ (1978) Relationships of gases and fluids during early diagenesis in some marine sediments. In: Sonderforschungsbereiche 95 Wechselwirkung Meer-Meeressboden Report 137, Universität Kiel 152p
- Whiticar MJ (1994) Correlation of natural gases with their sources, Chapter 16: Part IV. In: Magoon LB, Dow WG (eds) *Memoir-M60: the petroleum system—from source to trap*. American Association of Petroleum Geologists, Tulsa, pp 261–283
- Whiticar MJ (1999) Carbon and hydrogen isotope systematics of bacterial formation and oxidation of methane. *Chem Geol* 161(1–3):291–314
- Whiticar MJ (2002) Diagenetic relationships of methanogenesis, nutrients, acoustic turbidity, pockmarks and freshwater seepages in Eckernförde Bay. *Mar Geol* 182(1–2):29–53
- Whiticar MJ, Faber E (1986) Methane oxidation in sediment and water column environments – isotope evidence. *Org Geochem* 10(4–6):759–768
- Whiticar MJ, Schaefer H (2007) Constraining past global tropospheric methane budgets with carbon and hydrogen isotope ratios in ice. *Philos Trans R Soc Lond A: Math Phys Eng Sci* 365(1856):1793–1828
- Whiticar MJ, Faber E, Schoell M (1986) Biogenic methane formation in marine and freshwater environments: CO₂ reduction vs. acetate fermentation – isotope evidence. *Geochim Cosmochim Acta* 50:693–709
- Whiting GJ, Chanton JP (1992) Plant-dependent CH₄ emissions in a subarctic Canadian Fen. *Glob Biogeochem Cycles* 6:225–231
- Whittentbury R, Phillips KC, Wilkinson JF (1970) Enrichment, isolation and some properties of methane-utilizing bacteria. *Gen Microbiol* 61:205–218
- Whitman WB, Bowen TL, Boone DR (2006) The methanogenic bacteria. In *The Prokaryotes: Vol. 3: Archaea Bacteria: Firmicutes, Actinomycetes* (ed) S Falkow, E Rosenberg, K-H Schleifer, E Stackebrandt, Springer, Berlin, Chapter 9:165–207

- Widdel F, Rabus R (2001) Anaerobic biodegradation of saturated and aromatic hydrocarbons. *Curr Opin Biotechnol* 12(3):259–276
- Wilhelms A, Larter S, Head I, Farrimond P, di-Primo R, Zwach C (2001) Biodegradation of oil in uplifted basins prevented by deep-burial sterilization. *Nature* 414(6859):85–85
- Winfrey MR, Ward DM (1983) Substrates for sulphate reduction and methane production in hypersaline sediments. *Appl Environ Microbiol* 45:193–199
- Winfrey MR, Zeikus JG (1977) Effect of sulfate on carbon and electron flow during microbial methanogenesis in freshwater sediments. *Appl Environ Microbiol* 33:275–281
- Winn EB (1950) The temperature dependence of the self-diffusion coefficients of argon, neon, nitrogen, oxygen, carbon dioxide, and methane. *PhysRev* 80:1024–1027
- Witherspoon PA, Saraf DN (1965) Diffusion of methane, ethane, propane, and n-butane in water from 25 to 43. *J Phys Chem* 69(11):3752–3755
- Woese CR, Fox GE (1977) Phylogenetic structure of the prokaryotic domain: the primary kingdoms. *Proc Natl Acad Sci U S A* 74(11):5088–5090
- Woese CR, Kandler O, Wheelis ML (1990) Towards a natural system of organisms: proposal for the domains Archaea, Bacteria, and Eucarya. *PNAS* 87:4576–4579
- Wolfe RS (1971) Microbial formation of methane. *Adv Microb Physiol* 6:107–146
- World Meteorological Organization (2018) The state of greenhouse gases in the atmosphere based on global observations through 2017. WMO GHG bulletin 14(22):1–8
- Worden JR, Bloom AA, Pandey S, Jiang Z, Worden HM, Walker TW, Houweling S, Röckmann T (2017) Reduced biomass burning emissions reconcile conflicting estimates of the post-2006 atmospheric methane budget. *Nat Commun* 8(1):2227–2211
- Wrede C, Dreier A, Kokoschka S, Hoppert M (2012) Archaea in symbioses. *Archaea* 2012:596846
- Xiao K, Beulig F, Kjeldsen K, Jørgensen B, Risgaard-Petersen N (2017) Concurrent methane production and oxidation in surface sediment from Aarhus Bay, Denmark. *Front Microbiol* 8:1198
- Xiao K, Beulig F, Røy H, Jørgensen BB, Risgaard-Petersen N (2018) Methylotrophic methanogenesis fuels cryptic methane cycling in marine surface sediment. *Limnol Oceanogr* 63(4):1519–1527
- Xie S, Lazar CS, Lin YS, Teske A, Hinrichs KU (2013) Ethane-and propane-producing potential and molecular characterization of an ethanogenic enrichment in an anoxic estuarine sediment. *Org Geochem* 59:37–48
- Yang Y, Li N, Wang W, Li B, Xie S, Liu Y (2017) Vertical profiles of sediment methanogenic potential and communities in two plateau freshwater lakes. *Biogeosciences* 14(2):341–351
- Yoshida N, Hattori T, Komai E, Wada T (1999) Methane formation by metal-catalyzed hydrogenation of solid calcium carbonate. *Catal Lett* 58:119–122
- Zehnder AJ, Brock TD (1979) Methane formation and methane oxidation by methanogenic bacteria. *J Bacteriol* 137(1):420–432
- Zehnder AJ, Brock TD (1980) Anaerobic methane oxidation: occurrence and ecology. *Appl Environ Microbiol* 39(1):194–204
- Zehnder AJB, Stumm W (1988) Geochemistry and biogeochemistry of anaerobic habitats. In: Zehnder AJB (ed) *Biology of anaerobic microorganisms*. Wiley, New York, pp 1–38
- Zeikus JG (1977) The biology of methanogenic bacteria. *Bacteriol Rev* 41:514–541
- Zeikus JG, Ward JC (1974) Methane formation in living trees: a microbial origin. *Science* 184:1181–1183
- Zeikus JG, Winfrey M (1976) Temperature limitation of methanogenesis in aquatic sediments. *Appl Environ Microbiol* 31:99–107
- Zeng X, Birrien J, Fouquet Y, Cherkashov G, Jebbar M, Querellou J, Prieur D (2009) *Pyrococcus* CH1, an obligate piezophilic hyperthermophile: Extending the upper pressure-temperature limits for life. *ISME J* 3(7):873–874
- Zhang G, Zhang W, Yu H, Ma J, Xu H, Yagi K (2014) Fraction of CH₄ oxidized in paddy field measured by stable carbon isotopes. *Plant Soil* 389(1–2):349–359

- Zhu J, Wang Q, Yuan M, Tan GYA, Sun F, Wang C, Wu W, Lee PH (2016) Microbiology and potential applications of aerobic methane oxidation coupled to denitrification (AME-D) process: a review. *Water Res* 90:203–215
- Zhuang G, Elling FJ, Nigro LM, Samarkin V, Joye SB, Teske A, Hinrichs K (2016) Multiple evidence for methylotrophic methanogenesis as the dominant methanogenic pathway in hypersaline sediments from the orca basin, Gulf of Mexico. *Geochim Cosmochim Acta* 187:1–20
- Zhuang G, Heuer VB, Lazar CS, Goldhammer T, Wendt J, Samarkin VA, Hinrichs K (2018) Relative importance of methylotrophic methanogenesis in sediments of the western mediterranean sea. *Geochim Cosmochim Acta* 224:171–186
- Zinder SH (1993) Physiological ecology of methanogens. In: Ferry JG (ed) *Methanogenesis. Ecology, physiology, biochemistry and genetics*. Chapman and Hall, New York, pp 128–206
- Zinder SH, Koch M (1984) Non-aceticlastic methanogenesis from acetate: acetate oxidation by a thermophilic syntrophic coculture. *Arch Microbiol* 138(3):263–272
- Zitomer DH (1998) Stoichiometry of combined aerobic and methanogenic COD transformation. *Water Res* 32(3):669–676
- Zundel M, Rohmer M (1985) Prokaryotic triterpenoids. 1. 3 β methylhopanoids from *Acetobacter* species and *Methylococcus capsulatus*. *Eur J Biochem* 150:23–27



Marine Cold Seeps: Background and Recent Advances

26

Erwin Suess

Contents

1	Introduction	748
2	Seeps at Active Plate Margins	750
2.1	Oceanic Plate: Continental Plate Convergence	750
2.2	Oceanic Plate: Oceanic Plate Convergence	751
2.3	Strike-Slip Faults, Transform Plate Margins, and Shear Zones	752
3	Seeps at Passive Continental Margins	753
4	Seep Footprints	754
4.1	Imaging by Hydro- and Geo-acoustic Tools	754
4.2	Hydrocarbon-Metazoan-Microbe-Mineral Association	755
4.3	Authigenic Carbonates	757
4.4	Fluid-Sediment Interaction	758
5	Unique Seep Settings	760
5.1	Gulf of Mexico	761
5.2	Mediterranean Sea	761
5.3	Black Sea	761
6	Research Needs	762
6.1	Budgets of Volatile Emissions from Seeps and Retention of Carbon as Authigenic Carbonates	762
6.2	Fossilization of Microbial Structures Involved in AOM	762
6.3	Elusive Carbonates from Serpentinization at Subducting Margins	763
	References	763

E. Suess (✉)

Marine Biogeochemistry, GEOMAR Helmholtz Centre for Ocean Research Kiel, Kiel, Germany

College of Earth, Ocean, and Atmospheric Sciences, Oregon State University, Corvallis, OR, USA

e-mail: esuess@geomar.de; suess@onid.orst.edu

© Springer Nature Switzerland AG 2020

747

H. Wilkes (ed.), *Hydrocarbons, Oils and Lipids: Diversity, Origin, Chemistry and Fate*,

Handbook of Hydrocarbon and Lipid Microbiology,

https://doi.org/10.1007/978-3-319-90569-3_27

Abstract

Marine cold seeps are windows into different depth levels of the submerged geosphere. Subduction zones and organic-rich passive margins host most of the world's cold seeps. The source of seep fluids ranges from 10s of meters (ground-water aquifers) to 10s of km (subducted oceanic plates) below the seafloor. Seeps transport dissolved and gaseous compounds upward and sustain oasis-type ecosystems at the seafloor. Hereby the single most important reaction is anoxic oxidation of methane (AOM) by Archaea. Subsequent reactions involve sulfur biogeochemistry and carbonate mineral precipitation generating an association of methane, metazoans, microbes, and minerals – a biogeochemical footprint. Currently 100s of cold seeps are known globally. Elucidating function, structure, and composition of the characteristic association are high-priority topics of cold seep research. Ancient seep sites are identified with increasing frequency as the libraries of biomarkers and fossilized microbial bodies grow aided by their fortuitous preservation as they become encased in carbonate precipitates. Seep footprints provide clues as to source depth, fluid-sediment/rock interaction during ascent, lifetime, and cyclicity of seepage events. The Gulf of Mexico, the Black Sea, and the Eastern Mediterranean Sea are sites of classic and ongoing seep studies.

1 Introduction

Transfer from the geosphere to the exosphere (biosphere, hydrosphere, atmosphere) is a fundamental process of the Earth's material cycling. Many sub-cycles and pathways are active on different timescales, at different depth levels transferring different magnitudes of material. Tectonic plate boundaries, volcanic arcs, and passive continental margins are the geologic settings that largely determine this transfer process. Marine cold seeps provide windows into different depth levels of the geosphere where transfer processes and reactions are active. Cold seeps emit material back into the ocean and leave characteristic footprints on the seafloor. Normally they flow more slowly than hydrothermal vents and thereby adjust to ambient temperatures, but more vigorously flowing cold seeps do have elevated temperatures. Most aspects of recent cold seeps are covered in great detail in special issues (Vanreusel et al. 2009; Fouchet et al. 2009; Bohrmann and Jørgensen 2010; Greinert et al. 2010; Roberts 2010; de Batist and Khlystov 2012; Pierre et al. 2014; Kastner et al. 2014; Suess 2014), whereas this contribution provides a general background and highlights recent advances.

Seeps occur globally along active margins driven by plate convergence and strike-slip faulting and along passive margins by sediment loading and differential compaction (Fig. 1). Seep characteristics and processes at these settings are the subject of this contribution. Beyond documenting new seep systems, recent advances relate to footprints of seeps, characterization of microbe-driven methane oxidation via metal oxide reduction, life span, use as environmental archive, source

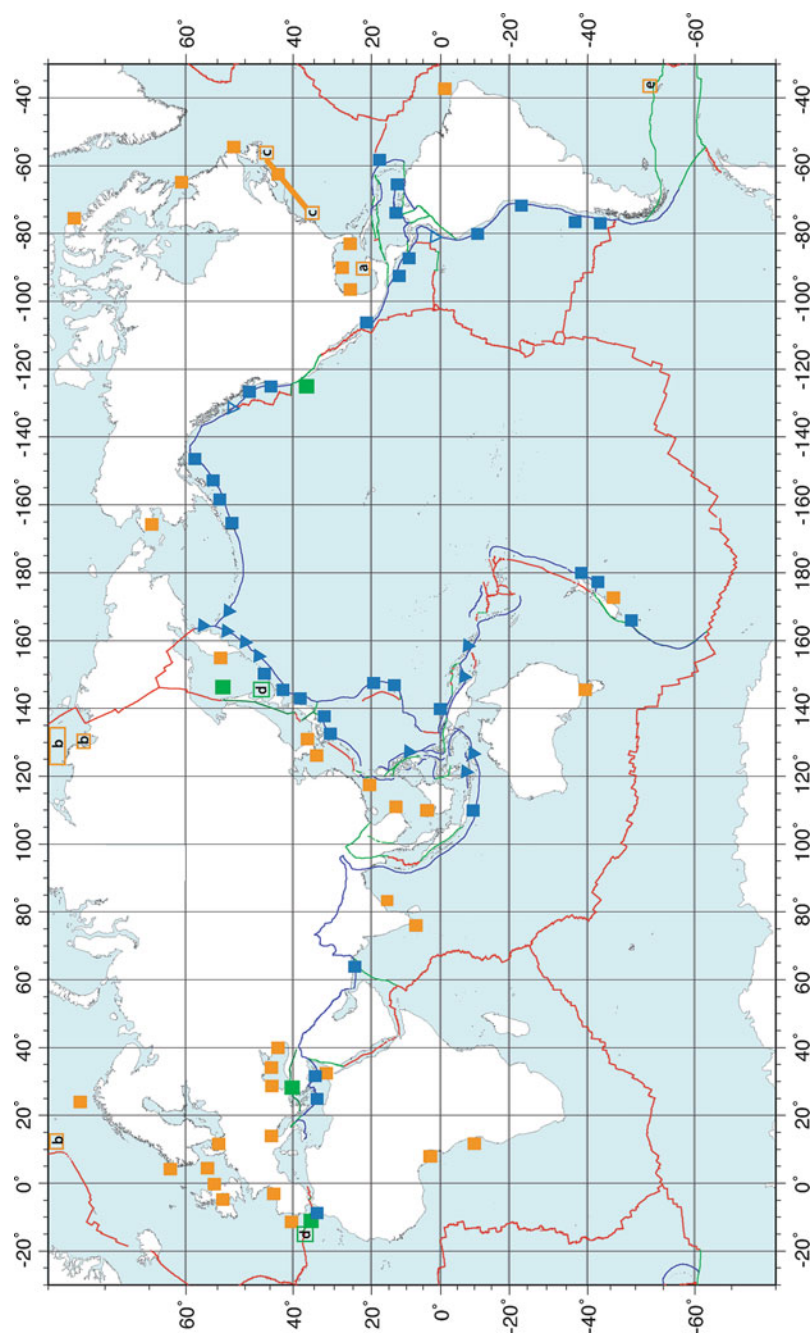


Fig. 1 Global seep distribution; locations with hydrocarbon-metazoan-microbe-carbonate associations at active margins (= blue squares); same at passive margins incl. Groundwater seeps (= orange squares), sites at transform and strike-slip faults (= green squares). Data with complete site references in Campbell (2006) and Suess (2010, 2014). New sites (= open squares, lettered): (a) asphalt seeps (Sahling et al. 2016); (b) East Siberian Shelf (Shakova et al. 2016) and Svalbard margin; (c) Atlantic margin (Skarke 2014); (d) Sakhalin strike-slip (Derkachev et al. 2015) and Africa-Eurasia strike-slip (Hensen et al. 2015); (e) South Georgia Island fjords (Römer et al. 2014)

depths, and impact of host sediments. Geologic settings, biogeochemical reactions, and biologic activities are uniquely interconnected to generate seep footprints. The magnitude of material cycled through seeps on a global scale is poorly known despite easily recognizable seep products. Considerable progress is provided on this issue by in-depth analysis and synthesis of H₂O and volatile cycling at major subduction zones that had been extensively drilled (Kastner et al. 2014). How to further improve such estimates and other research needs concludes this contribution.

2 Seeps at Active Plate Margins

2.1 Oceanic Plate: Continental Plate Convergence

By far the most frequent seeps worldwide occur at the convergence between oceanic and continental plates and extend from upper continental slopes to deep trenches. Indeed, research at global convergent margins first revealed cold seeps and their products as resulting from tectonic fluid expulsion by dewatering of sediments; for background, see Suess (2014). Dewatering occurs in response to lateral compression by plate movement whereby sediment-laden oceanic plates move underneath less dense continental plates. In the process, sediments are either scraped off and accreted onto the edge of the overriding plate or are bypassed at its base. Off-scraping and bypassing result in accretionary and erosive margins, respectively, along the global deep-sea trench system generating seep fluids and products from different depths (Schoell and von Huene 2007).

Accretionary margins consist of a series of thrust ridges oriented parallel to the trench axis that contain largely compressed, folded, and faulted turbidites and trench-fill deposits (Fig. 2). In landward troughs between the ridges, hemipelagic sediments are deposited in slope basins. The ridges as well as the basins are the source of seep fluids. Over long periods of accretion, the ridges are increasingly deformed into structural packages separated by thrust faults. These faults are pathways for extruded material. The combined thrust packages constitute the accretionary prism. Farther landward they abut against the continental framework rock (backstop or margin wedge) that comprises the upper continental plate. The surface of the accretionary wedge and framework rock continues to accumulate unconformably seaward prograding sediments.

Where the subduction angle is shallow as off Southern Chile, Cascadia, or Japan, convergence causes splay faults to develop in the framework rock that drain the upper plate (Moore et al. 2007). Where the subduction angle is steep or the surface of the descending oceanic plate is studded with volcanoes – as off Costa Rica – the base of the upper plate is eroded and/or experiences underplating of sediments that escaped being scraped off (Ranero and von Huene 2000; Meschede 2003). The underplated sediments constitute the subduction channel an increasingly recognized site for deep-seated reactions between trapped seawater-derived fluids and seawater-altered oceanic host rocks (van der Straaten et al. 2012).

Most of the global subduction zones are erosive (75% according to Schoell and von Huene (2007)). Plate edges of erosive margins subside, fracture, and eventually

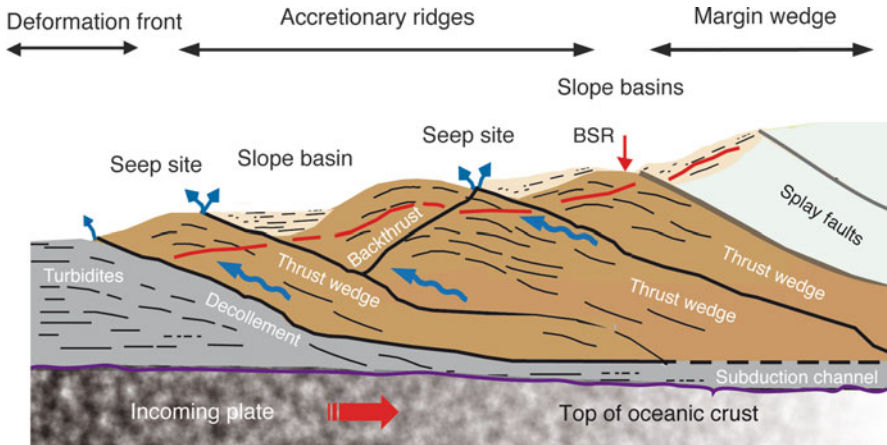


Fig. 2 Accretionary margin; seep sites at convergent tectonic settings with strongly developed accretionary prism (multiple thrust wedges), trench turbidites, slope basins, continental framework rock (backstop), hemipelagic sediment cover, and subduction channel between top of oceanic crust and accretionary and framework rocks. Fluid escape pathways are thrust faults separating accretionary ridges, along backthrusts, sometimes with slope basins between them. Well-developed bottom-simulating reflector (BSR) in sediments of thrust wedges and hemipelagic cover; schematic based on Cascadia margin, South Chile margin, and Nankai margin (Schoell and von Huene 2007)

are destroyed (Fig. 3). Destruction is severe where volcanic seamounts are subducted. These elevated basaltic features, riding on the oceanic crust, arrive at the trench and plough into the continent leaving scars and scarps. Ensuing slope failures, faulting, and bulging of the sediment strata greatly facilitate fluid escape and seepage (Liebetrau et al. 2014). It is near the front where seeps initially form. Farther under the overriding plate, increasing temperatures and higher pressures release mineral-bound water, forcing fluids, and fluidized sediments upward. Extruded material is preferentially aligned above subsurface isotherms consistent with clay mineral dehydration temperatures (Ranero et al. 2008; Buerk et al. 2010).

A significant input of water is through hydration (serpentinization) of the oceanic plate during subduction. Although this had been suspected for some time but not until it was shown that bend-faulting facilitates deep penetration of seawater into the oceanic lithosphere – which significantly alters seismic velocities – did it become possible to quantify the degree of serpentinization and hence water input (Rüpke et al. 2004). Bend-faulting results from flexure of a cold and rigid oceanic plate causing fractures that reach into the upper mantle.

2.2 Oceanic Plate: Oceanic Plate Convergence

When one oceanic plate is subducted under another, exothermic serpentinization reactions in the downgoing plate provide heat to drive fluid movement that generates a special type of seeps. At the Mariana Fore-Arc, deep-sourced high-alkaline fluids containing abiogenic methane and hydrogen mixed with serpentinite muds are emitted

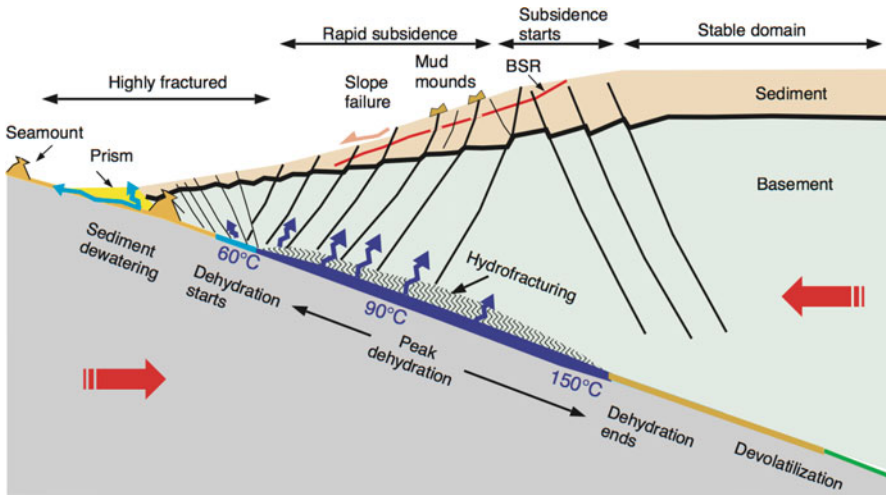


Fig. 3 Erosive margin; seep sites and mud volcanoes at convergent tectonic setting with poorly developed accretionary prisms, highly fractured edge of continental plate, region of pronounced subsidence due to removal (erosion) of material from plate underside, and continental framework rock; seaward prograding hemipelagic sediment cover with well-developed bottom-simulating reflector (BSR). Mud volcanoes situated above temperature-pressure regime of mineral dehydration from top of downgoing plate. Fluids and muds are forced upward through hydro-fractures; schematic based on Costa Rica margin (Originally published in Suess (2010), published with kind permission of ©Springer Science+Business Media New York, 2003. All rights reserved)

(Mottl et al. 2004). Here the downgoing plate contains little sediment leaving its top to undergo hydration by reacting with seawater at shallow depth to form serpentine minerals. As temperature and pressure increase at greater depth (up to 30 km), its top is dehydrated again (de-serpentinization). The liberated fluids ascend and compound hydration of the overthrust oceanic plate. At Prony Bay, North New Caledonia Basin, where one oceanic plate is abducted over another (Monnin et al. 2014), similar high-alkaline fluids are emitted.

Understanding serpentinization reactions has been advanced by experimental work (Palandri and Reed 2004) and by investigating the Lost City site at the Mid-Atlantic Ridge (Kelley et al. 2005) that is characterized by prominent carbonate chimneys populated by highly diverse biota (Brazelton et al. 2010). Whereas, the Prony Bay site shows unique gas chemistry and high microbial diversity (Postec et al. 2015).

2.3 Strike-Slip Faults, Transform Plate Margins, and Shear Zones

Seepage is active at tectonic settings where either well-defined plates or portions of fractured plates slide past each horizontally. Here fault planes are steep and often reach basement that facilitate fluid escape upward. When faults crosscut overlying

sequences, fluids are subjected to intense interaction with sediments at elevated pressure and temperature. Seeps at such settings had not previously been considered in their own right, but recently more active seep sites are identified at strike-slip settings. Transform faults at plate boundaries – a subset of strike-slip faults – pose earthquake hazards; hence, research on gas and fluid seepage and their products has recently focused on these settings (Crémière et al. 2013; Hensen et al. 2015; Derkachev et al. 2015; Dupré et al. 2015).

3 Seeps at Passive Continental Margins

On passive margins, the variety of geologic settings, the mechanisms of fluid expulsion, and the worldwide occurrence of cold seeps are immense (Fig. 4). Pockmarks on shelves and slopes are expressions of seeps fed from submerged aquifers, overpressured formations emitting volatiles, liquid and solid hydrocarbons and brines, and rapidly deposited water-rich sediments, as in deltas. Hydrocarbon seeps have long guided offshore exploration for oil and gas deposits (Judd and Hovland 2007).

Groundwater seepage from sub-seafloor extensions of aquifers has been known since the early days of seafarers. Today groundwater seepage carries pesticides, herbicides, and fertilizer residues into shelf waters off coastal areas. Pumping for drinking water depletes groundwater reservoirs and allows seawater to enter aquifers, or high tidal ranges force it back as does rising sea level. The result is

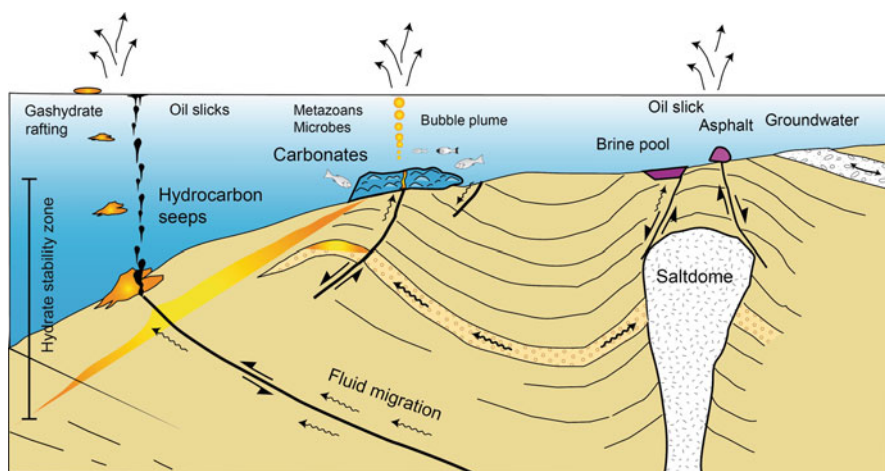


Fig. 4 Passive margin; geologic settings and forces of fluid expulsion generate different types of cold seeps; pockmarks on shelves and slopes caused by outflow from submerged aquifers, overpressured formations containing hydrocarbons and brines, and rapidly accumulating water-rich sediments in deltas or drift deposits. Carbonate chimneys, asphalt seeps, methane hydrate mounds, seep fauna, and methane plumes in the water column are ubiquitous manifestations as are infrequently observed methane hydrate rafts (Modified from Suess (2014))

widespread salt invasion of groundwater in coastal areas and other problems adversely affecting drinking water reservoirs (Gallardo and Marui 2006). Submarine groundwater discharge may be estimated from distribution patterns of Rn nuclides (Rodellas et al. 2017).

The driving mechanism for fluid expulsion at passive margins is by sediment loading, differential compaction, overpressure, and facies changes. Hence, rapidly accumulating water-rich sediments generate seeps and mud volcanoes in deltas and in deep-sea fans. Any changes involving permeabilities of fluid-rich strata such as ash layers, turbidites, sands and silts, drift sediments, and even buried reefs where intersected by faults open up pathways for fluid migration. Other driving forces for seepage are free gas movement, hydrological and tidal pumping, and thermally driven circulation.

Permafrost thawing causes widespread methane seepage and large-scale venting from Arctic shelves with concern that this greenhouse gas would reach the atmosphere (Shakhova et al. 2015). A review of the effect on climate change by methane emission concludes that anaerobic and aerobic oxidation, bubble transport, and the effects of ice cover and circulation constitute an as yet not fully known climate feedback (James et al. 2016).

Methane release from gas hydrate destabilization receives equally much attention as a key process either currently initiated by global warming or ongoing since postglacial times along the North American Atlantic margin (Phrampus and Hornbach 2012; Skarke 2014) or the Svalbard slope (Wallmann et al. 2018). Whereas emissions on the Arctic shelf appear to be initiated recently, at the other sites, “old” seep carbonates point to past emissions. Seeps are also active on the shelves off South Georgia Island (Römer et al. 2014); here the source of methane appears to be organic-rich sediments in drowned fjords.

4 Seep Footprints

4.1 Imaging by Hydro- and Geo-acoustic Tools

Free gas in the water column, pockmarks, and mud volcanoes on the seafloor and biota-carbonate associations indicate current and past cold seep activity. Detecting and mapping the spatial extent of 100s of seeps in regional geologically defined settings have been facilitated by advanced hydroacoustic technologies. Distribution of gas flares or gas plumes allows pinpointing seep sites on the seafloor and tracing methane bubble trains through the water column. Imaging bubbles depend on the impedance of acoustic waves traveling through media with different densities, in case of seep densities of seawater and free methane. Hence, multi-beam echo sounding – the use of which in mapping seep areas has significantly increased – allows individual flares, flare clusters, and entire fields to be imaged (Schneider von Deimling et al. 2011; Skarke 2014; Weber et al. 2014; Dupré et al. 2015). Commonly stationary flares originate from pockmarks, gas-doming on the seafloor, or acoustic turbidity below the seafloor (seismic chimneys). Depending on water depths and

intensity of seepage, flares may reach several 100s of meters into the water column even breach the sea surface (Shakirov et al. 2005). Rising bubble velocity, rate of gas dissolution, and shrinkage of bubble size eventually determine the maximum height of ascent. Methane bubbles originating at water depths below the gas hydrate stability zone (500–700 m) “survive longer” as hydrate skins form an armor against dissolution (Rehder et al. 2009).

Geo-acoustic tools (side-scan sonar, sub-bottom profiler, Parasound) combined with high-resolution multi-beam bathymetry identify seep sites and are indispensable for quantifying seep fluxes. Geo-acoustic seep signatures characterize smooth areas of the seafloor with elevated backscatter intensity that result from subsurface gas accumulations and doming of the seafloor (Koch et al. 2015) and rough areas with patches of carbonates (Buerk et al. 2010; Klauke et al. 2012).

4.2 Hydrocarbon-Metazoan-Microbe-Mineral Association

4.2.1 Biota Sustained by Anoxic Oxidation of Methane (AOM)

The association of biota and authigenic carbonates forms massive caps and pavements on the seafloor and is by far the most widely encountered footprint. Seep communities are highly visible, persistent, and universal indicators for seep activity past and present (Suess 2010, 2014). The dominant symbiotic taxa are tube worms, clams, and mussels, whereby different microbial consortia – mostly visible as brightly colored mats – provide carbon and energy via anaerobic oxidation of methane (AOM) (Boetius et al. 2000). Methane, either from subsurface gas hydrate, from ascending bubbles, or from dissolved gas, drives AOM and the resulting interaction between macrobiota and formation of carbonate and sulfide minerals (Fig. 5).

The AOM-consortia aggregate at different sub-seafloor depths is commonly referred to as the sulfate-methane transition (SMT). In reducing sulfate (Fig. 5; Reaction 1a), they generate hydrogen sulfide that is oxidized either in microbial mats at the sediment surface or by symbionts within macroorganism, using oxygen or nitrate (Fig. 5; Reaction 2). When mobile iron is present, hydrogen sulfide may be fixed as iron sulfide. Bivalves pump oxygen downward whereas tubeworms extract hydrogen sulfide through their roots. As a consequence of the AOM activity, calcium carbonate phases precipitate (Fig. 5; Reaction 3). Earlier views favored accidental reaction from the by-product of AOM; now it is thought plausible that the microbial community may actively promote precipitation even of select mineral phases (Krause et al. 2012). A proxy for sulfate-driven AOM based on $\delta^{18}\text{O}$ and $\delta^{34}\text{S}$ criteria appears to be preserved in calcite- and aragonite-associated sulfur of modern and ancient seep carbonates (Feng et al. 2016).

4.2.2 AOM Stimulated by Metal Oxide Reduction

Metal-AOM has become one of the hottest topics in biogeochemistry (Beal et al. 2009; Sivan et al. 2014; Riedinger et al. 2014). It involves methane oxidation by reduction of Fe oxyhydroxide and Mn oxide via microbes (Fig. 5; Reactions 1b and

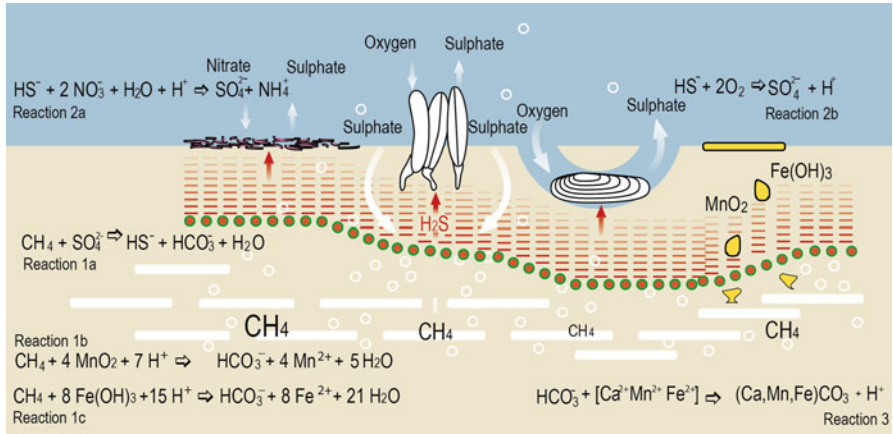


Fig. 5 Anaerobic oxidation of methane; buried gas hydrates (white slabs) and free gas (bubbles) supply methane to AOM-consortia (red-green circles) concentrated at the sulfate-methane transition (SMT) below the seafloor. Consortia consume seawater sulfate as in Reaction 1a to produce hydrogen sulfide and bicarbonate; hydrogen sulfide is oxidized by microbial mats as in Reaction 2a or by macrofauna symbionts as in Reaction 2b using nitrate and oxygen, respectively. Additionally, AOM-consortia are able to reduce metal oxides as in Reactions 1b and 1c (Beal et al. 2009; Egger et al. 2015); sulfate-AOM and metal-AOM result in mixed Ca-Mn-Fe-carbonate formation (Reaction 3) (Figure updated from Suess (2010))

1c). Implications are that this process exerts significant control on the marine methane cycle (“benthic filter”) in current and past oceans and by extension on climate. Large amounts of Fe and Mn are delivered to the ocean from multiple sources that emphasize the importance of this process. It was first reported from a cold seep setting (Beal et al. 2009) and since documented from lake sediments and brackish coastal environments (Egger et al. 2015). The importance of metal-AOM is not surprising – in hindsight – as it provides larger energy gains than sulfate-AOM does. From incubation experiments with seep sediments (Sivan et al. 2014), the research emphasizes the coexistence of sulfate reduction, iron reduction, AOM, and methanogenesis in marine seep sediments in which the presence of iron oxides vastly stimulates rates of bacterial sulfate reduction. Current research is centered on rates and microbial systematics but less so on minerals supposedly forming. Mixed Mn and Fe carbonate phases and phosphates from anoxic, methane-rich environments are very likely products from Me-AOM (Dijkstra et al. 2016).

4.2.3 Biomarkers

Function, structure, and composition of seep biota and AOM-consortia in concert with biomarkers are currently a major topic of seep research as well. Biomarkers are greatly depleted in ^{13}C relative to their carbon source and are linked to metabolism by methanotrophic Archaea. The nearly inexhaustible reservoir of methane carbon available to AOM-consortia in seep environments maximizes the kinetic carbon isotope fractionation. Biomarkers are identified from sediments and authigenic carbonates of

recent seep sites and increasingly from deposits of ancient seeps (Peckmann and Geodert 2005). Based on lipid analyses, three distinct AOM-consortia of ANaerobic MEthanotrophic (ANME-1, -2, and -3) archaea and their sulfate reducing bacterial partners were tentatively identified as environmental indicators that respond to temperature, oxygen, and sulfate availability (Rossel et al. 2011).

4.3 Authigenic Carbonates

4.3.1 Stable Isotopes and Mineralogy

A direct consequence of anaerobic oxidation of methane is the precipitation of carbonate minerals. Edifices, chimneys, or buildups (chemoherms) reach a couple of meters to as much as 50 m above the seafloor and are believed to form in contact with bottom water (Teichert et al. 2005; Han et al. 2008; Crémière et al. 2013; Liebetau et al. 2014). Other morphologies exist below the seafloor or are uplifted, exhumed, and eroded. Typically, chemoherms incorporate shell fragments and have a network of open or cemented fluid channels that can be traced throughout the structure. Many other shapes and sizes of seep carbonates have been observed, too numerous to detail here (Feng and Chen 2015; Tong et al. 2013). The seafloor around seeps is often covered by blocky carbonates and fragments; irregular doughnut-shaped, tabular, and tubular slabs; and concretions with open or cemented central channels. Some appear to be molds of burrows or linings of fluid channels that formed in the sediment. They resemble small chimneys after becoming exhumed by bottom currents. Generally, carbonate conduits facilitate fluid escape (Capozzi et al. 2015).

The dominant mineral phases are aragonite, Mg-calcite, and (proto)-dolomite; Fe and Mn carbonates occur infrequently. Their $\delta^{13}\text{C}$ and $\delta^{18}\text{O}$ signatures range from -60 to -30‰ PDB and $+6$ to $\pm 0\text{‰}$ PDB, respectively, depending on the C and O source, temperature of formation, and specific mineral phases being formed (Bohrmann et al. 1998; Teichert et al. 2005; Han et al. 2014). Alteration by meteoric water significantly lowers the O-isotope signature (Tong et al. 2016), whereas clay dehydration water, gas hydrate water, and glacial seawater cause shifts to higher values. Biogenic, thermogenic, and abiotic methane with very significantly differing carbon isotope signatures is strongly fractionated during AOM which determines the eventual C-isotope signal. Stable isotopes and carbonate mineralogies provide robust criteria to characterize recent and ancient seeps including biomarkers, trace elements, and radionuclide to constrain absolute and relative ages, redox conditions, and source and type of fluid-sediment/rock interactions.

4.3.2 Age Determination

Foremost among seep research is age determination of authigenic carbonates. The first published U-Th ages from chemoherm samples of the Cascadia subduction zone showed that methane release events largely occurred during low sea-level stands (Teichert et al. 2003). This mechanism is essentially confirmed as more ages become available. Most ages (back to 65 kya) of seep carbonates from the Japan Sea coincide

with low sea-level stands (Watanabe et al. 2008). A compilation of all available U-Th ages (Feng et al. 2010) of Quaternary seeps from the Gulf of Mexico, the Black Sea, and the Congo fan shows most dates fall around the Last Glacial Maximum (LGM). From passive margins of the South China Sea, 18 sets of U-Th ages have been published (Tong et al. 2013; Han et al. 2014) of which 16 samples coincide with low sea-level stands. Ages of seep carbonates along the Atlantic margin off North America show increased sediment delivery during low sea-level stands that results in overpressure and venting from sediment compaction (Prouty et al. 2016). During Quaternary times, eustatic sea-level fluctuations are currently favored to control the activity of most seeps.

Tales of Two Chimneys

Intercalated seep carbonates and volcanic ash layers on the flank of a mud mound on the Costa Rica margin (Kutterolf et al. 2008) revealed at first sight contradictory ages. Several active volcanic phases with ash layers provided time markers (6, 17, 25, 69, and 84 kya) as did the U-Th ages of the carbonate core (5–65 kya). Carbonate-derived ages showed downward and inward progression instead of upward as the ash-derived ages did. Both trends are readily explained by self-plugging of fluid conduits over time as illustrated (Fig. 5 left panel). A carbonate chimney (Fig. 5 right panel) from the seafloor of the oxygen minimum zone of the Northern Arabian Sea revealed fine-scale seep carbonate laminae alternating with laminae of pelagic particles (Himmler et al. 2016). The finely laminated and highly porous structure consists of AOM-derived pure aragonite alternating with biofilm-covered layers. The authors suggest a cyclicity controlled by fluctuating particle flux from the sea surface possibly related to Indian monsoonal and tidal forcing (Fig. 6).

4.4 Fluid-Sediment Interaction

The type of fluids expelled back into the ocean at accretionary, erosive, and transform margins or from shelves, slopes, and deltas at passive margins – whether from deep or shallow sources – depends on the thickness and provenance of the sediment column, the rate of sedimentation, and the age, cooling history, composition, and morphology of the underlying moving or stationary plates. Organic-rich and evaporite-containing strata are extremes of that spectrum in determining the final seep fluid composition. Seep fluids contain remineralized nutrients (silica, phosphate, ammonia, and alkalinity) and hydrogen sulfide, as well as dissolved and free methane from microbial degradation of sedimentary organic matter. Thick sediments often are deposited along continental margins associated with coastal upwelling or otherwise high primary productivity in response to nutrient loading from nearby continents. Rich in organic matter and biogenic silica, these sediments accumulate rapidly and thus greatly favor sulfate reduction and methanogenesis. Hence, most sedimented margin sites generate enough biogenic methane that, when moving upward, exits as dissolved or free gas into the bottom water. Alternatively when reaching the gas hydrate stability zone, methane is retained in layers of gas hydrate.

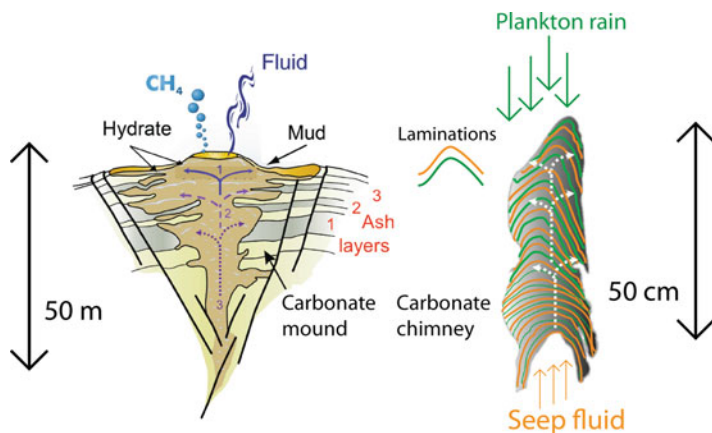


Fig. 6 (Left panel) Carbonate mound (off Costa Rica) forms AOM-derived carbonate interlayered with ash layers (3 = youngest, 1 = oldest ash) recording lifetime of seep activity (Kutterolf et al. 2008). Reverse order of U-Th ages of carbonates formed in fluid pathways (1 = oldest, 3 = youngest) implies top-down blockage of pathways over time (Published in Suess (2014), published with kind permission of ©Springer Science+Business Media New York, 2003. All rights reserved). (Right panel) Carbonate chimney (oxygen minimum zone of Northern Arabian Sea) forms AOM-derived carbonate laminae that alternates with organic-rich detrital rain from the sea surface, thereby implying a record of monsoon-driven cyclicality (Redrawn from Himmler et al. (2016))

4.4.1 Gas Hydrate Water

Much attention has been focused on Cl anomalies from the release of methane hydrate water. The anomaly is an artefact of sampling as removal of drill cores from in situ temperature and pressures destabilizes gas hydrates in the sediment. Coupled with O- and D/H-isotopes of H_2O , the resulting anomalies may be linked to gas hydrates and indeed are widely used to estimate the hydrate saturation of deposits (Matsumoto and Borowski 2000; and many others). Release of hydrate water is restricted to layers at and above the bottom-simulating reflector (BSR) diluting the Cl concentration and increasing the $\delta^{18}O_{H_2O}$ of pore fluids.

Seep carbonates being precipitated during AOM are another sink of ^{18}O from hydrate water. This was first shown in an aragonite-calcite intergrowth retrieved from seeps at the Cascadia convergent margin (Bohrmann et al. 1998). The C-isotope ratio ($\delta^{13}C = -40$ to -54% PDB) of this intergrowth identifies both mineral phases as being derived from biogenic methane. The younger aragonite layer had formed in equilibrium with ambient bottom-water temperatures, whereas the older Mg-calcite later – increased in $\delta^{18}O$ by about $+1\%$ PDB – had formed from gas hydrate water in the precipitating fluid. Hydrate water may be enriched in ^{18}O of up to 3.5% PDB. The term “clathrate” was proposed for this type of rock, invoking “clathrate” the family of water-caged gases, methane hydrate. The term did not stick, but what stuck is the interpretation of “heavy” $\delta^{18}O$ values of seep carbonates as sourced by methane hydrate. Currently, numerous reports of “heavy” $\delta^{18}O$ values of seep carbonates are linked to release of methane hydrate water in the subsurface (Tong et al. 2013; Lu et al. 2015; and many others), but alternative sources of “heavy” water need be seriously evaluated first.

4.4.2 Clay Dehydration

Trioctahedral clays (smectite group) lose interlayer water in three steps to form illite responding to temperatures and pressures that prevail at the plate interface in subduction zones (80–120 °C). This was shown experimentally some time ago and has been refined since (Hüpers and Kopf 2012). Depending on the percentage of smectites, dehydration generates considerable amounts of fresh water, affecting interstitial chloride contents. Incomplete dehydration from 18 Å- to 15 Å-smectite also releases water but without forming illite. The expression of clay dehydration either at complete or incomplete conversion to illite is evident on a large scale in Cl dilution of pore fluids of accretionary margins (Kastner et al. 2014). Temperature and compaction at different margins are the first-order control on Cl dilution (Saffer and Kopf 2016).

The δD (–32‰ SMOW) and $\delta^{18}O$ (+10‰ SMOW) of interlayer water differ significantly from seawater as determined from deeply buried strata of mud volcanos (Dählmann and de Lange 2003). Upon dehydration, these isotope characteristics affect δD and $\delta^{18}O$ of pore waters. Sorbed trace elements in interlayer space or on external clay surfaces are also affected by dehydration, exemplary shown by boron.

Significant boron enrichment with diluted Cl contents in pore fluids from seep sites (mud volcanos) and the δD and $\delta^{18}O$ isotope ratios of seep water is attributed to clay dehydration (Hensen et al. 2015). The desorption of boron from smectites is temperature dependent (complete at 100 °C and higher), and thus fluids originate 1000s of meters below the seafloor preserve a signal of high-temperature sediment-fluid interaction while moving through backstop rocks to the seafloor (Fig. 3). Temperature history and degree of compaction during subduction differentially affect clay dehydration and hence Cl and B signals such that – according to Saffer and Kopf (2016) – upon subduction of a cold sediment slab pore water freshening is maximized because clay-bound water is released into low porosity sediments but boron signature is less pronounced as B-desorption is poor at low temperatures. Whereas upon subduction of a warm sediment slab pore water freshening is less pronounced as dehydration occurs early and releases claybound water into high porosity sediments but boron signature is more pronounced. Fluids that originate from the oceanic crust and are emitted at mud volcanoes along the strike-slip fault between Africa and Eurasia show the entire spectrum of sediment-fluid interaction (Hensen et al. 2015). On the ascent to the surface, fluid composition is impacted by recrystallization of carbonates (Sr/Cl and $^{87}Sr/^{86}Sr/Cl$), clay mineral dehydration (B/Cl, $\delta^{18}O/\delta D$), and salt dissolution (Cl).

5 Unique Seep Settings

Geologic settings that generate prolific seepage are those that accumulate organic-rich sediments in basins, in deltas, and those that are underlain by evaporites and hydrocarbon reservoirs. They provide unique characteristics expressed by mud volcanoes, pockmarks, brine lakes, asphalt, and – as with all seep settings –

authigenic carbonates. The Gulf of Mexico, the Eastern Mediterranean Sea, and the Black Sea host unique and expansive seep settings that have been extensively investigated.

5.1 Gulf of Mexico

Passive margin seeps of the Gulf of Mexico are generated from underlying salt strata where loading by sediments causes salt to flow forming salt domes and salt ridges. Hereby low-density and low-viscosity salts escape the pressure of overburden by flowing upward. Salt domes push through the overlying strata, dragging them upward thereby developing faults along their flanks. This facilitates migration of fluids and liquid hydrocarbons. The tops of salt domes, when reaching the seafloor, mostly are dissolved away by circulating seawater and then collapse. Some pockmarks contain brine pools and significant amounts of non-methane hydrocarbons. The shelves and slopes surrounding the Western and Northern Gulf of Mexico host such seeps, biota, and pockmarks related to salt tectonics as does the seafloor off Yucatan (Sassen et al. 2004; Roberts 2010; Weber et al. 2014; Sahling et al. 2016). Asphalt volcanism off the Yucatan Peninsula has now been established as a distinct type of seepage. Heavy hydrocarbons extrude and flow over large areas of the seafloor developing lava-like surface structures. Abundant biota – representing most known seep organisms – colonize the flows; authigenic carbonates are present but less abundant than at gaseous-dominated hydrocarbon seeps.

5.2 Mediterranean Sea

The Messinian salt underlying the Mediterranean Sea affects seep manifestations. Here the driving mechanism for seepage is the convergence of the African and Eurasian plates (Westbrook and Reston 2002). Along the subduction zone – the Mediterranean Ridge – and at its intersection with Hellenic and Cyprus arcs mud volcanoes, gas hydrates, brine lakes, and biota-carbonate associations have been extensively studied (Olu-Le et al. 2004; Shank et al. 2011). Brine pools at the seafloor (2000–3000 m) are at or close to saturation with respect to Na, Mg, and K salts. The composition varies significantly between adjacent pools and depends on the depths within the salt sequence from which the fluid is generated (Westbrook et al. 1995).

5.3 Black Sea

The Black Sea is accorded a special role in seep studies for its anoxic, methane-rich water column below about 100 m and its thick – up to 16 km – organic-rich sedimentary cover. Over 2000 seeps were mapped off Romania and the Ukraine (Naudts et al. 2006). The sites are concentrated at the shelf-slope break extending to

725 m water depth. In the sub-seafloor below that water depth, the stability limit of methane hydrates has been projected from the bottom-water temperature and the geothermal gradient implying that above that depths gaseous methane escapes into the bottom water and below methane is retained as hydrate. The seep province continues off the Crimean Peninsula into the eastern basin with gas hydrates, methane plumes in the water column, and mud volcanos at 1000–2300 m depth. Still farther east at the margin off Georgia, extensive methane seepage occurs in the Batumi area with state-of-the-art pressure coring technology used to quantify methane emissions and subsurface gas hydrates (Pape et al. 2008; Heeschen et al. 2011). Throughout the Black Sea, authigenic carbonates of many morphologies and compositions are associated with the seep provinces although seep macrofauna appears to be scarce.

6 Research Needs

6.1 Budgets of Volatile Emissions from Seeps and Retention of Carbon as Authigenic Carbonates

Water output from the subducting sediment packages at convergent margins is by porosity reduction coupled to plate subduction rates (Kastner et al. 2014) and by upscaling of direct flow measurements (Freundt et al. 2014). Large discrepancies exist between these approaches. To improve the situation, modeled flow rates from pore water profiles, direct measurements of bubble and fluid escape, and the degree of biological methane oxidation (benthic filter) need to be quantified. Deep-sea landers equipped with flux meters deployed at single sites have recorded flow rates between $<10^{-3}$ and $>10^2$ $\text{cm} \cdot \text{y}^{-1}$. GasQuant, a tool based on backscatter intensity of bubbles, integrates bubble spectra for total gas fluxes. Large-scale acoustic mapping techniques may help to increase the database for global upscaling.

When biota at the seafloor and in the water column consume methane aerobically, the carbon is largely added as CO_2 to the seawater. If they consume methane anaerobically (AOM), the carbon is retained in carbonates. Partitioning the methane-C sink from biological oxidation between seawater bicarbonate and mineral carbonate is a scientific challenge that has not been addressed as of today.

6.2 Fossilization of Microbial Structures Involved in AOM

Geologic time for seepage based on AOM is steadily being pushed back, with ancient plate boundaries and passive margins being recognized as characteristic settings. Sediment fabric and organics isolated from geological material will continue to yield data on ancient seeps. The concern over contamination of geological samples is not as serious as with recent material since fossil microbial bodies are fully encased in a carbonate matrix. Structures of suspected fossilized microbes await identification including fossilized bodies, resembling microbial morphologies

that consist wholly of AOM-carbonates; their biomarkers will provide considerable new knowledge. Preparatory work in isolating biomarkers from such bodies requires contamination-free samples such as the miniaturized biosignature extraction procedure recently introduced (Leefmann 2008).

6.3 Elusive Carbonates from Serpentinization at Subducting Margins

Fluids released from serpentinization of the subducted oceanic plate directly into bottom waters instead through thick sediments may maintain their high pH values and Mg, Ca, and aqueous SiO₂ contents. Mixing these fluids with slightly more acidic seawater containing DIC would result in carbonates analogous to those precipitated on serpentinized oceanic crust at hydrothermal sites. Most likely sites for emission of such fluids and precipitates are at trench-outer rise with bend-faulting, usually quite deep (>4000 m). Carbonate chimneys might have escaped detection so far. Offshore Nicaragua is underlain by serpentinized and highly fractured oceanic plate. A search here for subduction zone chimneys along with molecular hydrogen emissions would be a scientific objective for future seep research. Its relevance is seen in that the hypothetical carbonates could represent a hitherto unrecognized global CO₂ sink. Studies would complement estimates of CO₂ sequestered in onshore ophiolite massifs and ultramafic intrusions as well as offshore slow-spreading ridge segments and magmatic fore-arcs as currently debated (Kelemen 2011).

Acknowledgments This contribution is an expanded and updated version of earlier publications (Suess 2010, 2014) by Springer Science+Business Media New York, 2003. I thank editors and publication staff for permission to use these previously published materials from which all illustrations are updated and/or redrawn to accommodate major advances in marine cold seep research. One last time, many thanks to Zona Bolton-Suess who helped – not just with the intricacies of the English language – but provided encouragement, genuine interest, and sustained support in my scientific pursuits. I acknowledge the College of Earth, Ocean, and Atmospheric Sciences, Oregon State University, for the courtesy appointment extended to me and the associated use of facilities.

References

- Beal EJ, House CH, Orphan VJ (2009) Manganese- and iron-dependent marine methane oxidation. *Science* 325:184–187
- Boetius A et al (2000) A marine consortium apparently mediating anaerobic oxidation of methane. *Nature* 407:623–626
- Bohrmann G, Jørgensen BB (eds) (2010) Proceeding of the 9th international conferences on gas in marine sediments. *Geo-Mar Lett* 30(3/4)
- Bohrmann G, Greinert J, Suess E, Torres ME (1998) Authigenic carbonates from the Cascadia subduction zone and their relation to gas hydrate stability. *Geology* 26:647–650
- Brazelton et al (2010) Archaea and bacteria with surprising micro-diversity show shifts in dominance over 1,000-year time scales in hydrothermal chimneys. *Proc Natl Acad Sci* 107(4):1612–1617

- Buerk D, Klaucke I, Sahling H, Weinrebe W (2010) Morpho-acoustic variability of cold seeps on the continental slope offshore Nicaragua: result of fluid flow interaction with sedimentary processes. *Mar Geol* 275:53–65
- Campbell KA (2006) Hydrocarbon seep and hydrothermal vent palaeo-environments: past developments and future research directions. *Palaeogeogr Palaeoclimatol Palaeoecol* 232:362–407
- Capozzi R, Negri A, Reitner J, Taviani M (eds) (2015) Carbonate conduits linked to hydrocarbon-enriched fluid escape. *Mar Pet Geol* 66(3):497–652
- Crémière A, Bayon G, Ponzevera E, Pierre C (2013) Paleo-environmental controls on cold seep carbonate authigenesis in the sea of Marmara. *Earth Planet Sci Lett* 376:200–211
- Crémière A et al (2016) Timescales of methane seepage on the Norwegian margin following collapse of the Scandinavian ice sheet. *Nat Commun* 7:11509. <https://doi.org/10.1038/ncomms11509>
- Dählmann A, de Lange G (2003) Fluid-sediment interactions at eastern Mediterranean mud volcanoes: a stable isotope study from ODP leg 160. *Earth Planet Sci Lett* 212:377–391
- De Batist M, Khlystov O (eds) (2012) Proceedings of the 10th international conference on gas in marine sediments. Listvyanka. *Geo-Mar Lett* SI 32(5/6)
- Derkachev AN et al (2015) Manifestation of carbonate–barite mineralization around methane seeps in the sea of Okhotsk (western slope of Kuril Basin). *Oceanology* 55(3):390–399
- Dijkstra N, Slomp CP, Behrends T (2016) Vivianite is a key sink for phosphorus in sediments of the landsort deep, an intermittently anoxic deep basin in the Baltic Sea. *Chem Geol* 438:58–72
- Dupré S et al (2015) Tectonic and sedimentary controls on widespread gas emissions in the sea of Marmara: results from systematic, shipborne multibeam echo sounder water column imaging. *J Geophys Res Solid Earth*. <https://doi.org/10.1002/2014JB011617>
- Egger M et al (2015) Iron-mediated anaerobic oxidation of methane in brackish coastal sediments. *Environ Sci Technol* 49:277–283
- Feng D, Chen D (2015) Authigenic carbonates from an active cold seep of the northern South China Sea: new insights into fluid sources and past seepage activity. *Deep-Sea Res II* 122:74–83
- Feng D et al (2010) U–Th dating of cold-seep carbonates: an initial comparison. *Deep Sea Res II* 57:2055–2060
- Feng D et al (2016) A carbonate-based proxy for sulfate-driven anaerobic oxidation of methane. *Geology* 44:999–1002
- Fouchet et al (2009) Structure and diversity of cold seep ecosystems. *Oceanography* 22:92–109
- Freundt A et al (2014) Volatile (H₂O, CO₂, Cl, S) budget of the central American subduction zone. *Int J Earth Sci* 103:2101–2127
- Gallardo AH, Marui A (2006) Submarine groundwater discharge: an outlook of recent advances and current knowledge. *Geo-Mar Lett* 26:102–113
- Greinert J, Bialas J, Lewis K, Suess E (eds) (2010) Methane seeps at the Hikurangi margin, New Zealand. *Mar Geol* 272. <https://doi.org/10.1016/j.margeo.2010.02.018>
- Han X et al (2008) Jiulong methane reef: microbial mediation of seep carbonates in the South China Sea. *Mar Geol* 249:243–256
- Han X et al (2014) Methane release events and environmental conditions at the upper continental slope of the South China Sea: constraints from seep carbonates. *Int J Earth Sci* 103:1873–1887
- Heeschen KU et al (2011) Quantifying in-situ gas hydrates at active seep sites in the eastern Black Sea using pressure coring technique. *Biogeosciences* 8:3555–3565
- Hensen C et al (2015) Strike-slip faults mediate the rise of crustal-derived fluids and mud volcanism in the deep sea. *Geology* 43:339–342
- Himmeler T et al (2016) Seep-carbonate lamination controlled by cyclic particle flux. *Nature Sci Rpt* 6:37439. <https://doi.org/10.1038/srep37439>
- Hüpers A, Kopf AJ (2012) Effect of smectite dehydration on pore water geochemistry in the shallow subduction zone: an experimental approach. *Geochem Geophys Geosyst* 13. <https://doi.org/10.1029/2012GC004212>. ISSN: 1525-2027
- James RH et al (2016) Effects of climate change on methane emissions from seafloor sediments in the Arctic Ocean: a review. *Limnol Oceanogr* 61:S283–S299

- Judd AG, Hovland M (2007) Submarine fluid flow, the impact on geology, biology, and the marine environment. Cambridge University Press, Cambridge UK, pp 475
- Kastner M et al (2014) Fluid origins, thermal regimes, and fluid and solute fluxes in the fore-arc of subduction zones. In: Stein R et al (eds) *Developments in Marine Geology*, vol 7. Elsevier, Amsterdam, pp 671–733
- Kelemen PB (2011) Rates and mechanisms of mineral carbonation in peridotite: natural processes and recipes for enhanced, in situ CO₂ capture and storage. *Annu Rev Earth Planet Sci* 39:545–576
- Kelley DS et al (2005) A serpentinite-hosted ecosystem: the Lost City hydrothermal field. *Science* 307:1428–1434
- Klaucke I et al (2012) Sidescan sonar imagery of widespread fossil and active cold seeps along the central Chilean continental margin. *Geo-Mar Lett* 32:489–499
- Koch S et al (2015) Gas-controlled seafloor doming. *Geology* 43(7):571–574
- Krause S et al (2012) Microbial nucleation of Mg-rich dolomite in exopolymeric substances under anoxic modern seawater salinity: new insight into an old enigma. *Geology* 40(7):587–590
- Kutterolf S et al (2008) Lifetime and cyclicity of fluid venting at forearc mound structures determined by tephrostratigraphy and radiometric dating of authigenic carbonates. *Geology* 36:707–710
- Leefmann T (2008) Miniaturized biosignature analysis reveals implications for the formation of cold seep carbonates at hydrate ridge (off Oregon USA). *Biogeosciences* 5:731–738
- Liebetrau V et al (2014) Authigenic carbonate archives of mound and slide related fluid venting at the central American Forearc: geochemical and mineralogical insights. *Int J Earth Sci* 103:1845–1872
- Lu Y et al (2015) Cold seep status archived in authigenic carbonates: mineralogical and isotopic evidence from northern South China Sea. *Deep Sea Res II* 122:95–105
- Matsumoto R, Borowski WS (2000) Gas hydrate estimates from newly determined oxygen isotopic fractionation α_{GH-IW} and $\delta^{18}O$ anomalies of the interstitial waters: leg 164, Blake Ridge. In: Paull CK, Matsumoto R, Wallace PJ, Dillon WP (eds) *Proceedings of the Ocean Drilling Program, vol 164 Scientific Results*, Texas A&M University, College Station TX, pp 59–66
- Meschede M (2003) The Costa Rica convergent margin: a textbook example for the process of subduction erosion. *N Jb Geol Paläont Abh* 230:409–428
- Monnin C et al (2014) Fluid chemistry of the low temperature hyper-alkaline hydrothermal system of Prony Bay (New Caledonia). *Biogeosciences* 11:5687–5706. <https://doi.org/10.5194/bg-11-5687-2014>
- Moore GF et al (2007) Three-dimensional splay fault geometry and implications for tsunami generation. *Science* 318:1128–1131
- Mottl MJ et al (2004) Chemistry of springs across the Mariana forearc shows progressive devolatilization of the subducting plate. *Geochim Cosmochim Acta* 68:4915–4933
- Naudts L et al (2006) Geological and morphological setting of 2778 methane seeps in the Dnepr paleo-delta, northwestern Black Sea. *Mar Geol* 227:177–199
- Olu-Le et al (2004) Cold seep communities in the deep eastern Mediterranean Sea: composition, symbiosis and spatial distribution on mud volcanoes. *Deep Sea Res I* 51:1915–1936
- Palandri JL, Reed MD (2004) Geochemical models of metasomatism in ultramafic systems: Serpentinization, rodingitization, and sea floor carbonate chimney precipitation. *Geochim Cosmochim Acta* 68(5):1115–1133
- Pape T et al (2008) Marine methane biogeochemistry of the Black Sea: a review. In: Dilek Y, Fumes H, Muehlenbachs K (eds) *Links between geological processes, microbial activities and evolution of life*, vol 4. Springer, Berlin. Heidelberg New York, pp 281–311. ISBN: 978-1-4020-8305-1 (Print) 978-1-4020-8306-8 (Online)
- Peckmann J, Geodert JL (eds) (2005) *Geobiology of ancient and modern methane-seeps*. *Palaeogeogr Palaeoclimat Palaeoecol* 227 (special issue)
- Phrampus BJ, Hornbach MJ (2012) Recent changes to the Gulf stream causing widespread gas hydrate destabilization. *Nature* 290:527–530

- Pierre C, Mascle J, Imbert P (eds) (2014) Contributions from the 11th international conferences on gas in marine sediments. Nice 2011, *Geo-Mar Lett* 34 (2/3)
- Postec A et al (2015) Microbial diversity in a submarine carbonate edifice from the serpentinizing hydrothermal system of the Prony Bay (New Caledonia) over a 6-year period. *Front Microbiol* 6:857–876. <https://doi.org/10.3389/fmicb.2015.00857>
- Prouty NG et al (2016) Insights into methane dynamics from analysis of authigenic carbonates and chemosynthetic mussels at newly-discovered Atlantic Margin seeps. *Earth Planet Sci Lett* 449:332–344
- Ranero CR, von Huene R (2000) Subduction erosion along the middle America convergent margin. *Nature* 404:748–752
- Ranero CR et al (2008) Hydrogeological system of erosional convergent margins and its influence on tectonics and interplate seismogenesis. *Geochem Geophys Geosyst* 9(3). <https://doi.org/10.1029/2007GC001679>
- Rehder G et al. (2009) Controls on methane bubble dissolution inside and outside the hydrate stability field from open ocean field experiments and numerical modeling. *Mar Chem.* <https://doi.org/10.1016/j.marchem.2009.03.004>
- Riedinger N et al (2014) An inorganic geochemical argument for coupled anaerobic oxidation of methane and iron reduction in marine sediments. *Geobiology.* <https://doi.org/10.1111/gbi.12077>
- Roberts HR (ed) (2010) Gulf of Mexico cold seeps. *Deep Sea Res II* 57(21/23):1835–2060
- Rodellas V et al (2017) Using the radium quartet to quantify submarine groundwater discharge and pore water exchange. *Geochim Cosmochim Acta* 196:58–73
- Römer M et al (2014) First evidence of widespread active methane seepage in the Southern Ocean, off the sub-Antarctic island of South Georgia. *Earth Planet Sci Lett* 403:166–177
- Rossel PE et al (2011) Factors controlling the distribution of anaerobic methanotrophic communities in marine environments: evidence from intact polar membrane lipids. *Geochim Cosmochim Acta* 75:164–184
- Rüpke LH, Phipps-Morgan J, Hort M, Connolly JAD (2004) Serpentine and the subduction zone water cycle. *Earth Planet Sci Lett* 223:17–34
- Saffer DM, Kopf AJ (2016) Boron desorption and fractionation in subduction zone Fore Arcs: implications for the sources and transport of deep fluids. *Geochem Geophys Geosyst* 17:4992–5008
- Sahling H et al (2016) Massive asphalt deposits, oil seepage, and gas venting support abundant chemosynthetic communities at the Campeche Knolls, southern Gulf of Mexico. *Biogeosciences* 13:4491–4512
- Sassen R et al (2004) Free hydrocarbon gas, gas hydrate and authigenic minerals in chemosynthetic communities of the northern Gulf of Mexico continental slope: relation to microbial process. *Chem Geol* 205:195–217
- Schneider von Deimling J et al (2011) Quantification of seep-related methane gas emissions at Tommeliten, North Sea. *Cont Shelf Res* 31:867–878
- Schoell DW, von Huene R (2007) Crustal recycling at modern subduction zones applied to the past -issues of growth and preservation of continental basement crust, mantle geochemistry, and supercontinent reconstruction. *Geol Soc America Mem* 200:9–32
- Shakhova N et al (2015) The East Siberian Arctic Shelf: towards further assessment of permafrost-related methane fluxes and role of sea ice. *Phil Trans R Soc A* 373:2014.0451. <https://doi.org/10.1098/rsta.2014.0451>
- Shakirov RB et al (2005) Classification of anomalous methane fields in the Sea of Okhotsk. *Polar Meteorol Glaciol* 90:50–56
- Shank TM et al (2011) Exploration of the Anaximander mud volcanoes. In: Bell KLC, Fuller A (eds) *New frontiers in ocean exploration.* *Oceanography* 24:22–23
- Sivan O et al (2014) Iron oxides stimulate sulfate-driven anaerobic methane oxidation in seeps. *Proc Natl Acad Sci* 111:4139–4147
- Skarke A (2014) Widespread methane leakage from the sea floor on the northern US Atlantic margin. *Nature Geosci* 7:657–661

- van der Straaten F et al (2012) Tracing the effects of high-pressure metasomatic fluids and seawater alteration in blueschist-facies overprinted eclogites: implications for subduction channel processes. *Chem Geol* 292/293:69–87
- Suess E (2010) Marine cold seeps. In: Timmis KN (ed) Handbook of hydrocarbon and lipid microbiology, vol 1(Part 3). Springer, pp 187–203. https://doi.org/10.1007/978-3-540-77587-4_12
- Suess E (2014) Marine cold seeps and their manifestations: geological control, biogeochemical criteria and environmental conditions. *Intl J Earth Sci* 103:1889–1916
- Teichert BMA et al (2003) U-Th systematics and ages of authigenic carbonates from hydrate ridge, Cascadia margin: recorders of fluid flow variations. *Geochim Cosmochim Acta* 67:3845–3857
- Teichert BMA, Bohrmann G, Suess E (2005) Chemoherms on hydrate ridge – unique microbially-mediated carbonate build-ups growing into the water column. *Palaeogeogr Palaeoclimatol Palaeoecol* 227:67–85
- Tong HP et al (2013) Authigenic carbonates from seeps on the northern continental slope of the South China Sea: new insights into fluid sources and geochronology. *Mar Petrol Geol* 43:260–271
- Tong HP et al (2016) Diagenetic alteration affecting $\delta^{18}\text{O}$, $\delta^{13}\text{C}$ and $^{87}\text{Sr}/^{86}\text{Sr}$ signatures of carbonates: a case study on cretaceous seep deposits from Yarlung-Zangbo Suture Zone, Tibet, China. *Chem Geol* 444:71–82
- Vanreusel A et al (2009) Biodiversity of cold seep ecosystems along the European margins. *Oceanography* 22:110–127
- Wallmann K et al (2018) Gas hydrate dissociation off Svalbard induced by isostatic rebound rather than global warming. *Nat. Commu* 9:83. <https://doi.org/10.1038/s41467-017-02550-9>
- Watanabe Y et al (2008) U-Th dating of carbonate nodules from methane seeps off Joetsu, eastern margin of Japan Sea. *Earth Planet Sci Lett* 272:89–96
- Weber TC et al (2014) Acoustic estimates of methane gas flux from the seabed in a 6000 km² region in the Northern Gulf of Mexico. *Geochem Geophys Geosyst* 15:1911–1925. <https://doi.org/10.1002/2014GC005271>
- Westbrook GK, Reston TJ (2002) The accretionary complex of the Mediterranean ridge: tectonics, fluid flow and the formation of brine lakes – an introduction. *Mar Geol* 186:1–8
- Westbrook GK et al (1995) Three brine lakes discovered in the seafloor of the eastern Mediterranean. *EOS Trans Am Geophys Union* 76:313–318



Helge Niemann

Contents

1	Introduction	770
2	Hydrocarbon Emissions	772
3	Geochemical Forcing	773
4	Research Needs	776
	References	777

Abstract

Mud volcanoes are frequently encountered geo-structures at active and passive continental margins. In contrast to magmatic volcanoes, mud volcanoes are marine or terrestrial, topographic elevation built from vertically rising fluidized mud or mud breccia. Commonly, these structures have a crater, hummocky rim, and caldera. Mud volcanism is triggered by various geological processes which lead to a high pore fluid pressure at great depth, sediment instabilities, and a subsequent discharge of mud, fluids, and gases such as hydrocarbons (mostly the greenhouse gas methane). Although global estimates of methane emissions from mud volcanoes vary over two orders of magnitude, mud volcanism could be an important source for atmospheric methane. However, a substantial fraction of the hydrocarbons are retained in the mud volcanoes surface sediments or, in the particular case of marine mud volcanoes, are consumed by microbes in the water

H. Niemann (✉)

Department of Marine Microbiology and Biogeochemistry, and Utrecht University, NIOZ Royal Netherlands Institute for Sea Research, 't Horntje, the Netherlands

CAGE – Centre for Arctic Gas Hydrate, Environment and Climate, Department of Geology, UiT the Arctic University of Norway, Tromsø, Norway

e-mail: helge.niemann@nioz.nl

© Springer Nature Switzerland AG 2020

769

H. Wilkes (ed.), *Hydrocarbons, Oils and Lipids: Diversity, Origin, Chemistry and Fate*, Handbook of Hydrocarbon and Lipid Microbiology,

https://doi.org/10.1007/978-3-319-90569-3_28

column. In sediments, the upwelled hydrocarbons fuel a variety of free-living and symbiotic, chemosynthetic communities that oxidize these with electron acceptors such as oxygen or sulfate from the water column or the atmosphere. The activity of the chemosynthetic communities is regulated by the availability of either electron donors (hydrocarbons) or acceptors which, in return, is determined by mass transport processes. Most important in this context are the magnitudes of upward advection of electron donors and the influx of electron acceptors due to diffusion and bioirrigation.

1 Introduction

Mud volcanoes are geological structures bearing only little morphological resemblances to magmatic volcanoes. In contrast to true volcanoes which expel magmatic material at plate boundaries and mantle plumes (Schmincke 2004), mud volcanoes are formed by vigorous mud discharge that is often accompanied by fluid and gas emissions commonly originating from a deep subsurface sedimentary sequence (Brown 1990; Milkov 2000; Kopf 2002). Mud volcanoes have a long tradition of scientific investigation and references were already made in historical documents (e.g., “Naturalis Historia” by Pliny the Elder, first century AD). Nevertheless, the diversity of mud volcano shapes as well geological causes responsible for their formation leads to a variety of definitions and synonymous terms such as mud volcano, mud pie, mud mound, and gryphon (among others). Hereafter, a mud volcano is defined as a marine or terrestrial, topographic elevation built from vertically rising fluidized mud or mud breccia (a mud matrix containing clasts and, sometimes, rock fragments or evaporites originating from the geological section through which the mud ascends; Norton 1917; Cita et al. 1981; Maignien et al. 2013; Mazzini and Etiope 2017). Mud volcanism is caused by various geological processes such as tectonic accretion and faulting, rapid burial of sediments due to slope failures (olistostromes) or high sedimentation rates, and fluid emissions from mineral dehydration as well as (true) volcanic and earth quake activities (Brown 1990; Milkov 2000; Kopf et al. 2001; Dimitrov 2002; Kopf 2002; Mellors et al. 2007; Manga et al. 2009). These processes can lead to an abnormally high pore fluid pressure and sediment instabilities and consequently lead to the extrusion of mud, fluids, and gases (usually through a central conduit) to the seafloor or earth surface (Fig. 1). A crater or active center, hummocky rim, and surrounding caldera are common features of mud volcanoes. However, the shape of the structure can range from amorphous mud pies to conical formations, and their size varies from a few meters to kilometers in circumference and a few decimeters to hundreds of meters in height. The viscosity and density of the extruded material as well as the duration of eruption events and the development stage of the edifice were identified as major factors determining the shape of mud volcanoes (Lance et al. 1998; Murton and Biggs 2003; Stewart and Davies 2006). In general, flat structures are composed of comparably liquid mud matrixes, while high- and cone-shaped edifices are built of successively,

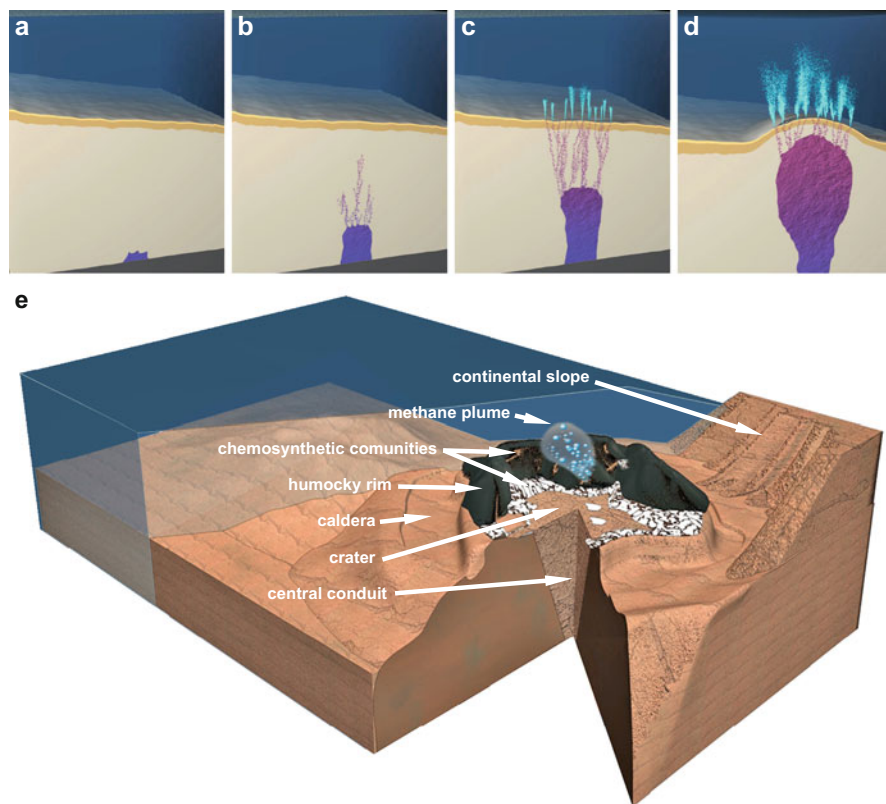


Fig. 1 Potential genesis of a gas emitting (marine) mud volcano. (a) High pore fluid pressure leads to the formation of mud breccia at great depth where also gases (mainly methane) are produced. (b) Overpressurized mud breccia and gases migrate along sediment instabilities to the seafloor (c) which is eventually breached (d) and upheaved. (e) Scheme of the Haakon Mosby Mud Volcano. At a “typical” mud volcano, mud and gases are transported through a central conduit and extruded in a crater region. The crater is surrounded by a hummocky rim of displaced sediment material. After an initial outburst and deflation of source material, a caldera (collapse structure) surrounds the mud volcano. Surface sediments of mud volcanoes can support a wide range of free-living and symbiotic, chemosynthetic organisms which oxidize the upwelled hydrocarbons and hydrogen sulfide with oxidants such as oxygen, nitrate, or sulfate from the water column. Giant sulfide-oxidizing bacteria forming white mats on the seafloor and symbiotic tube worms colonizing the seafloor in meadow- or bush-like aggregations are prominent examples of chemosynthetic communities, which are visible for the naked eye. **a–d** source: ARCHIMEDIX, e Sabine Lüdeling, MedienIngenieure Bremen

superimposed flows of more viscous material. Mud volcanoes may thus erupt in regular or irregular time intervals or emit mud, fluids, and gases continuously. In addition, they may also become inactive when the source of gas expansion and fluid flow stops (Planke et al. 2003; Mazzini et al. 2009), but also new structures evolve such as the terrestrial LUSI mud volcano in 2006 (Mazzini et al. 2007; Karyono et al.

2017). Three types of mud volcano activity are distinguished (Dimitrov 2003 and references therein):

1. Lokbatan-type: This type of mud volcanism was named after the Lokbatan Mud volcano, Azerbaijan. Lokbatan-type mud volcanoes are characterized by violent outbreaks and long phases of dormancy.
2. Chikishlyar-type: Calm, relatively weak, and continuous venting of gas, water, and mud are typical for this type of mud volcano.
3. Shugin-type: This type of mud volcanism is transitional between the other types, characterized by long periods of weak activity interrupted by eruptive events. Dimitrov (2003) suggested that this type of mud volcanism is the most common.

This distinction is based on terrestrial mud volcanism, which has been investigated for a comparably long time. In some cases, also historical documents can be used to infer the mode of activity (Aliyev et al. 2002). In contrast, most oceanic mud volcanoes were discovered and investigated in the last decade, when appropriate high-resolution geophysical tools became available to science which can resolve a few m of difference in height above- or belowground. However, from the bathymetry and sub-bottom structure, it cannot be resolved what activity type a particular mud volcano may represent because eruptive events could be separated by (longer) periods of dormancy (Feseker et al. 2009, 2014). In addition to the temporal heterogeneity of activity, visual investigation of submarine mud volcanoes by towed video cameras, submersibles, or remotely operating vehicles showed that mud volcanism is also spatially diverse (Niemann et al. 2006b; Sauter et al. 2006, Sahling et al. 2009). In general, a mud volcano has an active center above a central conduit which is usually marked by steep temperature gradients, and seepage rates decrease toward the periphery. However, the active center may not always be the geographical center, and the activity may not follow a concentric arrangement. Our knowledge about mud volcanoes in general and specific structures in particular is therefore very sketchy.

2 Hydrocarbon Emissions

The processes leading to mud volcanism on the continents as well as at active and passive continental margins are generally related to fluid and gas flow. Subsurface muds and shales in mud volcano-hosting regions often contain high amounts of methane and other hydrocarbons of thermogenic and/or microbial origin. Consequently, mud flows can be accompanied by vigorous gas expulsions, which may even ignite in contact with the atmosphere in terrestrial systems (Milkov 2000; Kopf 2002; Charlou et al. 2003; Somoza et al. 2003). Good examples for violent gas emissions from such structures are the terrestrial Lokbatan and the deepwater Haakon Mosby Mud Volcano. Since the early nineteenth century, the Lokbatan Mud Volcano has erupted more than 20 times, sometimes very violently with flames reaching more than 500 m height (Aliyev et al. 2002; Mukhtarov et al. 2003).

At Haakon Mosby, a gigantic methane plume of about 600 m was visible on echo sounder systems during several cruises, and jets of methane emitted from the seafloor were observed during submersible dives (Vogt et al. 1997; Sauter et al. 2006). The annual methane discharge from Haakon Mosby was estimated with 8–35 Mmol (0.1–0.5 Gg) of which free gas accounted for 60–90% (Niemann et al. 2006b; Sauter et al. 2006). About 650 to 900 terrestrial mud volcanoes are known (Kopf 2003), but global estimates for marine mud volcanoes range between 800 and 100,000 (Milkov 2000; Dimitrov 2002, 2003; Kopf 2003; Milkov et al. 2003). For submarine mud volcanoes, it is often not known if and when these structures emit methane. As a result, global assessments of methane emissions from mud volcanoes vary considerably. It has been suggested that terrestrial and shallow-water mud volcanoes contribute between 2.2 and 6 Tg year⁻¹ of methane to the atmosphere (Dimitrov 2003; Milkov et al. 2003) and that 27 Tg year⁻¹ of methane may escape from deepwater mud volcanoes (Milkov et al. 2003). Revised estimates of the total methane emission from mud volcanoes range between 35–45 Tg year⁻¹ (Etiope and Milkov 2004) and 30–70 Tg year⁻¹ (Etiope and Klusman 2002) and – when using only known structures and correcting for the size of the edifice – between 0.3 Tg year⁻¹ (Kopf 2003) and 1.4 Tg year⁻¹ (Kopf 2002). In comparison to the annual methane emissions to the atmosphere (526–852 Tg year⁻¹, Kirschke et al. 2013), mud volcanism may consequently be an important source for atmospheric methane. Nevertheless, a substantial fraction of methane released from marine mud volcanoes is probably consumed by aerobic methanotrophic bacteria (see Chapters on aerobic methane oxidation in Vol. ▶ “Aerobic Utilization of Hydrocarbons, Oils, and Lipids”, edited by Rojo 2019) in the water column (Reeburgh 2007), though their activity can be very low (Damm and Budéus 2003). This might be related to current dynamics and/or water column stratification regimes, which were found to cause spatiotemporal heterogeneity of aerobic methane oxidation at other methane seeps (Steinle et al. 2015, 2016).

3 Geochemical Forcing

In surface sediments of mud volcanoes, potential electron donors such as hydrocarbons and hydrogen sulfide from deeper sediment layers meet electron acceptors such as oxygen, nitrate/nitrite, oxidized metals, and sulfate, which are formed in surface sediments or originate from the water column or atmosphere. In such redox transition zones, mud volcanoes were found to support a wide range of free-living and symbiotic chemosynthetic organisms utilizing the subsurface energy sources (also known as “geofuels”) (Fig. 1). Thereby, chemosynthetic organisms reduce the efflux of reduced molecules to the hydro- and atmosphere (see Chapters on hydrocarbon and sulphur oxidising microbes in Vol. ▶ “Aerobic Utilization of Hydrocarbons, Oils, and Lipids”, edited by Rojo 2019) (Olu et al. 1997; Joye et al. 2005; Alain et al. 2006; Niemann et al. 2006a, b; Jørgensen and Boetius 2007; Knittel and Boetius 2009). Furthermore, chemosynthetic communities can also serve as an important food source for other marine organisms (Niemann et al. 2013). The most important

metabolic pathways are methanotrophy (anaerobic oxidation of methane, AOM; and aerobic oxidation of methane, MOx), anaerobic and aerobic degradation of hydrocarbons, thiotrophy (sulfide oxidation), and in some systems also iron oxidation (Omorgie et al. 2008). The distribution of chemosynthetic communities strongly depends on the availability of electron donors and acceptors, which in return is regulated by physical mass transport processes and biological activities (de Beer et al. 2006; Niemann et al. 2006b; Lösekann et al. 2007, Soetaert et al. 2012). Advection accounts for the majority of upward transport of electron donors from deeper sediment layers, while diffusion and bioirrigation are responsible for most of the influx of electron acceptors from the atmosphere or the water column into the mud volcano sediments.

Advective transport at mud volcanoes is in the form of mud, fluid, and free gas flow (see Sect. 1) (Fig. 1). Direct measurements of advection are scarce (Linke et al. 1994; Brown et al. 2005; Sauter et al. 2006; Mazzini et al. 2007, Feseker et al. 2009, 2014). In particular, rates of free gas and mud flow are poorly resolved. For gas flow, this may improve in the future as a result of new echo sounder tools allowing to quantify gas bubbles in the water column (Schneider von Deimling et al. 2007; Ostrovsky et al. 2008; Nikolovska et al. 2008; Muyakshin and Sauter 2010; Veloso et al. 2015) Also, the effect of mud and free gas flow on the distribution of chemosynthetic communities is mostly unknown. Fluid flow rates, on the other hand, can be modelled from geochemical pore water gradients and heat flow measurements, which allows for a comparably high temporal and spatial resolution. Recorded values for fluid flow at active mud volcanoes are typically a few centimeters to several meters per year (Table 1). Except for the spatial and temporal heterogeneity of mud volcano activity, advective pore water transport is a linear process, and the advective flux (J_a), i.e., the amount of pore water solute crossing a given area per time, is determined by the flow velocity (v_a) and the concentration (C) of the solute:

$$J_a = v_a C \quad (1)$$

(note that C has to be corrected for porosity $-\phi$).

The underlying mechanism of diffusion is Brownian motion (Einstein 1905), which, for biogeochemical reactions, can be simplified to the heat-induced, non-directional movement of atoms/molecules in water. Diffusive transport can be

Table 1 Fluid flow velocities (v_a ; in cm year^{-1}) at selected submarine mud volcanoes

Structure	Location	v_a	Ref.
Haakon Mosby	Barents Sea	40–600	de Beer et al. 2006, Kaul et al. 2006
Dvurechenski	Black Sea	8–25	Aloisi et al. 2004
Capt. Arutyunov	Gulf of Cadiz	10–15	Hensen et al. 2007
Mound 12	East Pacific	10	Linke et al. 2005
Atlante	West Atlantic	<1–10	Henry et al. 1996, Olu et al. 1997
Kazan	Mediterranean	4	Haese et al. 2006

illustrated by assuming two spatially separated entities in sediments or the water column with high and low concentrations of a given solute. The dissolved atoms/molecules will move randomly between both units. But more atoms/molecules will move from the unit of high concentration than from the unit of low concentration. This consequently leads to a net transport to the unit of low concentration until both units are equal in concentration. From this simple example, it is apparent that the concentration difference is an important factor determining diffusive flux. The second important factor is the net velocity of the movement. However, in contrast to the linear mode of advective flow, diffusion is random. A diffusing atom/molecule will not move in one direction but, in a simplified manner, forward and backward. As a result and when considering a large number of atoms/molecules, the mean travelled net distance (L) increases only by the square root of time (t):

$$L = \sqrt{2Dt}; \quad (2)$$

where D , the diffusion coefficient, is a compound-specific constant usually expressed in $\text{cm}^2 \text{ year}^{-1}$ (note that D has to be corrected for temperature (T) and ϕ), e.g., Boudreau 1997). Equation (2) has the rather counterintuitive implication that the net velocity of diffusion (v_d) decreases with increasing diffusion distance:

$$v_d = L/t = \sqrt{2D}/\sqrt{t} \quad (3)$$

Important electron donors and acceptors at mud volcanoes only need about a ms to travel a distance of 1 μm but already a day for 1 cm and some month for 10 cm (Table 2)! The diffusive flux (J_d) is hence determined by the concentration difference (dC), the diffusion distance (dx), and D . Assuming steady-state conditions, i.e., none of the factors determining the flux changes over the time period of measurement, J_d can be calculated according to Fick's first law of diffusion (Fick 1855; Berner 1980; Boudreau 1997):

$$J_d = D \times dC/dx \quad (4)$$

For short distances and high concentration differences (i.e., a steep concentration gradient – dC/dx), diffusion is hence an efficient transport mechanism.

The transport of electron acceptors due to bioirrigation activities is a known but poorly quantified phenomenon at marine mud volcanoes (Haese et al. 2006; Niemann et al. 2006b; Soetaert et al. 2012) and other types of cold seeps (Haese 2002; Treude et al. 2003; Cordes et al. 2005, Fischer et al. 2012). Many mud volcanoes host large populations of chemosynthetic megafauna such as tube worms and bivalves mining for sulfide and methane. Thereby, oxygenated and sulfate-rich sea water is flushed through, e.g., burrows into deeper sediment layers where it becomes available for free-living chemosynthetic microbes. Furthermore, some thiotrophic tube worms are known to secrete sulfate actively through posterior body parts to fuel sulfate reduction in the sediment. The flux via bioirrigation (J_b) is solely dependent on the faunal (pumping) activity as well as their extension into the

Table 2 Diffusion distance (L) in relation to diffusion time (t) and velocity (vd) of methane, sulphate and oxygen in sediments at a “typical” submarine mud volcano ($T \sim 3^\circ\text{C}$; $\sim 80\%$)

L	methane		sulphate		oxygen	
	t	v_d	t	v_d	t	v_d
1 μm	0.8 ms	40 km year ⁻¹	1.3 ms	24 km year ⁻¹	0.7 ms	48 km year ⁻¹
1 mm	13.2 min	40 m year ⁻¹	22 min	24 m year ⁻¹	11 min	48 m year ⁻¹
1 cm	22 h	4 m year ⁻¹	36 h	2.4 m year ⁻¹	18 h	4.8 m year ⁻¹
10 cm	92 d	0.4 m year ⁻¹	150 d	0.24 m year ⁻¹	76 d	0.48 m year ⁻¹
1 m	25 year	4 cm year ⁻¹	41 year	2.4 cm year ⁻¹	21 year	4.8 cm year ⁻¹
10 m	2.5 kyear	4 mm year ⁻¹	4.1 kyear	2.4 mm year ⁻¹	2.1 kyear	4.8 mm year ⁻¹
100 m	250 kyear	0.4 mm year ⁻¹	413 kyear	0.24 mm year ⁻¹	209 kyear	0.48 mm year ⁻¹
1 km	25 Myear	40 μm year ⁻¹	41 Myear	24 μm year ⁻¹	209 Myear	48 μm year ⁻¹

sediment. J_b can be calculated from the concentration differences of nonreactive tracers such, as e.g., silica or bromide (Wallmann et al. 1997; Haese 2002; Haese et al. 2006):

$$J_a = \alpha h(C_0 - C_x) \quad (5)$$

where α is the nonlocal exchange coefficient (in year⁻¹, dependent of faunal community composition and density) which has to be modelled from pore water concentration profiles. h is the thickness of the zone in which the transport occurs, and C_0 and C_x are the concentrations of the tracer in the bottom water and at depth, respectively. The few estimates available to date indicate that fluid flow due to bioirrigation may be 2–3 orders of magnitude higher than the purely physical transport (Wallmann et al. 1997; Haese et al. 2006). Because of the different modes and magnitudes of transport, the redox transition zones are found at various depths in mud volcano sediments ranging from the sediment surface to meters below sediment surface. For sediments devoid of burrowing megafauna, the depth is determined by the velocity of upward fluid flow (de Beer et al. 2006).

4 Research Needs

Due to the high spatial and temporal variability of fluid flow at mud volcanoes, and the many questions remaining to the functioning and interaction of geophysical forces as drivers of mud volcanism, there are still many open questions as to the trigger, sources, and change of their activity and longevity. For submarine mud volcanoes, an important issue is the relation between gas and fluid flow, heat transport, and the formation/dissociation of gas hydrates as well as its consequences

for the distribution and activity of faunal communities. Furthermore, the magnitude and spatial heterogeneity of hydrocarbon emission from marine mud volcanoes are not well constrained, and we know very little about the dynamics of microbial degradation of hydrocarbons in the water column above active mud volcanoes. One of the best studied mud volcanoes in this regard is the Haakon Mosby Mud Volcano, which has been chosen as a site for long-term observation of geophysical and biogeochemical processes of mud volcanism. Specifically for terrestrial mud volcanoes, very little is known about the occurrence, phylogeny, ecology, and activity of chemosynthetic communities.

References

- Alain K, Holler T, Musat F, Elvert M, Treude T, Kruger M (2006) Microbiological investigation of methane- and hydrocarbon-discharging mud volcanoes in the Carpathian Mountains, Romania. *Environ Microbiol* 8(4):574–590
- Aliyev AA, Guliyev IS, Belov IS (2002) Catalogue of recorded eruption of mud volcanoes of Azerbaijan (for period of years 1810–2001). Nafta Press, Baker
- Aloisi G, Drews M, Wallmann K, Bohrmann G (2004) Fluid expulsion from the Dvurechenskii mud volcano (Black Sea) – part I. Fluid sources and relevance to Li, B, Sr, I and dissolved inorganic nitrogen cycles. *Earth Planet Sci Lett* 225(3–4):347–363
- Berner RA (1980) Early diagenesis – a theoretical approach. Princeton University Press, Princeton
- Boudreau BP (1997) Diagenetic models and their implementation: modelling transport and reactions in aquatic sediments. Springer, Berlin
- Brown KM (1990) The nature and hydrogeologic significance of mud diapirs and diatremes for accretionary systems. *J Geophys Res Solid Earth Planets* 95(B6):8969–8982
- Brown KM, Tryon MD, DeShon HR, Dorman LM, Schwartz SY (2005) Correlated transient fluid pulsing and seismic tremor in the Costa Rica subduction zone. *Earth Planet Sci Lett* 238 (1–2):189–203
- Charlou JL, Donval JP, Zitter T, Roy N, Jean-Baptiste P, Foucher JP, Woodside J (2003) Evidence of methane venting and geochemistry of brines on mud volcanoes of the eastern Mediterranean Sea. *Deep-Sea Res I-Oceanogr Res Pap* 50(8):941–958
- Cita MB, Ryan WBF, Paggi L (1981) Prometheus mud breccia: an example of shale diapirism in the western Mediterranean Ridge. *Ann Géol Pays Hellén* 30:543–570
- Cordes EE, Arthur MA, Shea K, Arvidson RS, Fisher CR (2005) Modeling the mutualistic interactions between tubeworms and microbial consortia. *PLoS Biol* 3(3):497–506
- Damm E, Budéus G (2003) Fate of vent-derived methane in seawater above the Hakon Mosby mud volcano (Norwegian Sea). *Mar Chem* 82:1–11
- de Beer D, Sauter E, Niemann H, Kaul N, Foucher JP, Witte U, Schluter M, Boetius A (2006) In situ fluxes and zonation of microbial activity in surface sediments of the Hakon Mosby Mud Volcano. *Limnol Oceanogr* 51(3):1315–1331
- Dimitrov LI (2002) Mud volcanoes – the most important pathway for degassing deeply buried sediments. *Earth Sci Rev* 59(1–4):49–76
- Dimitrov LI (2003) Mud volcanoes – a significant source of atmospheric methane. *Geo-Mar Lett* 23(3–4):155–161
- Einstein A (1905) The motion of elements suspended in static liquids as claimed in the molecular kinetic theory of heat. *Ann Phys* 17(8):549–560
- Etiopie G, Klusman RW (2002) Geologic emissions of methane to the atmosphere. *Chemosphere* 49(8):777–789
- Etiopie G, Milkov AV (2004) A new estimate of global methane flux from onshore and shallow submarine mud volcanoes to the atmosphere. *Environ Geol* 46(8):997–1002

- Feseker T, Dählmann A, Foucher J-P, Harnegnies F (2009) In-situ sediment temperature measurements and geochemical porewater data suggest highly dynamic fluid flow at Isis mud volcano, eastern Mediterranean Sea. *Mar Geol* 261:128–137
- Feseker T, Boetius A, Wenzhöfer F, Blandin J, Olu K, Yoerger DR, Camilli R, German CR, de Beer D (2014) Eruption of a deep-sea mud volcano triggers rapid sediment movement. *Nat Commun* 5:5385
- Fick A (1855) Über diffusion. *Poggendorff's Annalen der Physik und Chemie* 94:59–86
- Fischer D, Sahling H, Nöthen K, Bohrmann G, Zabel M, Kasten S (2012) Interaction between hydrocarbon seepage, chemosynthetic communities, and bottom water redox at cold seeps of the Makran accretionary prism: insights from habitat-specific pore water sampling and modeling. *Biogeosciences* 9:2013
- Haese RR (2002) Macrobenthic activity and its effects on biogeochemical reactions and fluxes. In: Wefer G, Billet D, Hebbeln D, Jørgensen BB, Schlüter M, Van Weering TCE (ed) *Ocean margin systems*. Springer, pp. 219–234, Springer, Berlin-Heidelberg
- Haese RR, Hensen C, de Lange GJ (2006) Pore water geochemistry of eastern Mediterranean mud volcanoes: implications for fluid transport and fluid origin. *Mar Geol* 225(1–4):191–208
- Henry P, LePichon X, Lallemand S, Lance S, Martin JB, Foucher JP, FialaMedioni A, Rostek F, Guilhaumou N, Pranal V, Castrec M (1996) Fluid flow in and around a mud volcano field seaward of the Barbados accretionary wedge: results from Manon cruise. *J Geophys Res-Solid Earth* 101(B9):20297–20323
- Hensen C, Nuzzo M, Hornibrook E, Pinheiro LM, Bock B, Magalhaes VH, Bruckmann W (2007) Sources of mud volcano fluids in the Gulf of Cadiz – indications for hydrothermal imprint. *Geochim Cosmochim Acta* 71(5):1232–1248
- Jørgensen BB, Boetius A (2007) Feast and famine – microbial life in the deep-sea bed. *Nat Rev Microbiol* 5(10):770–781
- Joye SB, MacDonald IR, Montoya JP, Peccini M (2005) Geophysical and geochemical signatures of Gulf of Mexico seafloor brines. *Biogeosciences* 2(3):295–309
- Karyono K, Obermann A, Lupi M, Masturyono M, Hadi S, Syafri I, Abdurrokhim A, Mazzini A (2017) Lusi, a clastic-dominated geysering system in Indonesia recently explored by surface and subsurface observations. *Terra Nova* 29:13–19
- Kaul N, Foucher JP, Heesemann M (2006) Estimating mud expulsion rates from temperature measurements on Hakon Mosby Mud Volcano, SW Barents Sea. *Mar Geol* 229(1–2):1–14
- Kirschke S, Bousquet P, Ciais P, Saunoy M, Canadell JG, Dlugokencky EJ, Bergamaschi P, Bergmann D, Blake DR, Bruhwiler L, Cameron-Smith P, Castaldi S, Chevallier F, Feng L, Fraser A, Heimann M, Hodson EL, Houweling S, Josse B, Fraser PJ, Krummel PB, Lamarque JF, Langenfelds RL, Le Quere C, Naik V, O'Doherty S, Palmer PI, Pison I, Plummer D, Poulter B, Prinn RG, Rigby M, Ringeval B, Santini M, Schmidt M, Shindell DT, Simpson IJ, Spahn R, Steele LP, Strode SA, Sudo K, Szopa S, van der Werf GR, Voulgarakis A, van Weele M, Weiss RF, Williams JE, Zeng G (2013) Three decades of global methane sources and sinks. *Nature Geoscience*, 6(10):813–823
- Knittel K, Boetius A (2009) Anaerobic oxidation of methane: progress with an unknown process. *Annu Rev Microbiol* 63(1):311–334. <https://doi.org/10.1146/annurev.micro.61.080706.093130>
- Kopf AJ (2002) Significance of mud volcanism. *Rev Geophys* 40(2):B-1–B-49
- Kopf AJ (2003) Global methane emission through mud volcanoes and its past and present impact on the Earth's climate. *Int J Earth Sci* 92(5):806–816
- Kopf A, Klaeschen D, Mascle J (2001) Extreme efficiency of mud volcanism in dewatering accretionary prisms. *Earth Planet Sci Lett* 189(3–4):295–313
- Lance S, Henry P, Le Pichon X, Lallemand S, Chamley H, Rostek F, Faugeres JC, Gonthier E, Olu K (1998) Submersible study of mud volcanoes seaward of the Barbados accretionary wedge: sedimentology, structure and rheology. *Mar Geol* 145(3–4):255–292
- Linke P, Suess E, Torres M, Martens V, Rugh WD, Ziebis W, Kulm LD (1994) In situ measurement of fluid flow from cold seeps at active continental margins. *Deep-Sea Res I* 41(4):721–739
- Linke P, Wallmann K, Suess E, Hensen C, Rehder G (2005) In situ benthic fluxes from an intermittently active mud volcano at the Costa Rica convergent margin. *Earth Planet Sci Lett* 235(1–2):79–95

- Lösekan T, Knittel K, Nadalig T, Fuchs B, Niemann H, Boetius A, Amann R (2007) Diversity and abundance of aerobic and anaerobic methane oxidizers at the Haakon Mosby Mud Volcano, Barents Sea. *Appl Environ Microbiol* 73(10):3348–3362
- Maignien L, Parkes RJ, Cragg B, Niemann H, Knittel K, Coulon S, Akhmetzhanov A, Boon N (2013) Anaerobic oxidation of methane in hypersaline cold seep sediments. *FEMS Microbiol Ecol* 83:214–231
- Manga M, Brumm M, Rudolph ML (2009) Earthquake triggering of mud volcanoes. *Mar Pet Geol* 26:1785–1798
- Mazzini A, Etiope G (2017) Mud volcanism: An updated review, *Earth-Science Reviews*, 168, 81–112, <https://doi.org/10.1016/j.earscirev.2017.03.001>
- Mazzini A, Svensen H, Akhmanov GG, Aloisi G, Planke S, Malthe-Sorensen A, Istadi B (2007) Triggering and dynamic evolution of the LUSI mud volcano, Indonesia. *Earth Planet Sci Lett* 261(3–4):375–388
- Mazzini A, Svensen H, Planke S, Guliyev I, Akhmanov GG, Fallik T, Banks D (2009) When mud volcanoes sleep: insight from seep geochemistry at the Dashgil mud volcano, Azerbaijan. *Mar Pet Geol* 26:1704–1715
- Mellors R, Kilb D, Aliyev A, Gasanov A, Yetirmishli G (2007) Correlations between earthquakes and large mud volcano eruptions. *J Geophys Res-Solid Earth* 112(B4):B04304
- Milkov AV (2000) Worldwide distribution of submarine mud volcanoes and associated gas hydrates. *Mar Geol* 167(1–2):29–42
- Milkov AV, Sassen R, Apanasovich TV, Dadashev FG (2003) Global gas flux from mud volcanoes: a significant source of fossil methane in the atmosphere and the ocean. *Geophys Res Lett* 30(2):9
- Mukhtarov AS, Kadirov FA, Guliyev IS, Feyzullayev A, Lerche I (2003) Temperature evolution in the Lokbatan mud volcano crater (Azerbaijan) after the eruption of 25 October 2001. *Energy Explor Exploit* 21(3):187–207
- Murton BJ, Biggs J (2003) Numerical modelling of mud volcanoes and their flows using constraints from the Gulf of Cadiz. *Mar Geol* 195(1–4):223–236
- Muyakshin SI, Sauter E (2010) The hydroacoustic method for the quantification of the gas flux from a submersed bubble plume. *Oceanology* 50:995–1001
- Niemann H, Duarte J, Hensen C, Omoregie E, Magalhaes VH, Elvert M, Pinheiro LM, Kopf A, Boetius A (2006a) Microbial methane turnover at mud volcanoes of the Gulf of Cadiz. *Geochim Cosmochim Acta* 70(21):5336–5355
- Niemann H, Lösekann T, de Beer D, Elvert M, Nadalig T, Knittel K, Amann R, Sauter EJ, Schlüter M, Klages M, Foucher JP, Boetius A (2006b) Novel microbial communities of the Haakon Mosby mud volcano and their role as a methane sink. *Nature* 443:854–858
- Niemann H, Linke P, Knittel K, MacPherson E, Boetius A, Brückmann W, Larvik G, Wallmann K, Schacht U, Omoregie E, Hilton D, Brown K, Rehder G (2013) Methane-carbon flow into the benthic food web at cold seeps – a case study from the Costa Rica subduction zone. *PLoS One* 8: e74894–e74894
- Nikolovska A, Sahling H, Bohrmann G (2008) Hydroacoustic methodology for detection, localization, and quantification of gas bubbles rising from the seafloor at gas seeps from the eastern Black Sea, *Geochemistry Geophysics Geosystems*, 9(10)
- Norton WH (1917) A classification of breccias. *J Geol* 25:160–194
- Olu K, Lance S, Sibuet M, Henry P, FialaMedioni A, Dinat A (1997) Cold seep communities as indicators of fluid expulsion patterns through mud volcanoes seaward of the Barbados accretionary prism. *Deep-Sea Res I-Oceanogr Res Pap* 44(5):811–841
- Omoregie EO, Mastalerz V, de Lange G, Straub KL, Kappler A, Roy H, Stadnitskaia A, Foucher JP, Boetius A (2008) Biogeochemistry and community composition of iron- and sulfur-precipitating microbial mats at the Chefren mud volcano (Nile Deep Sea fan, Eastern Mediterranean). *Appl Environ Microbiol* 74:3198–3215
- Ostrovsky I, McGinnis DF, Lapidus L, Eckert W (2008) Quantifying gas ebullition with echosounder: the role of methane transport by bubbles in a medium-sized lake, *Limnology and Oceanography: Methods*, 6, 105–118
- Planke S, Svensen H, Hovland M, Banks DA, Jamtveit B (2003) Mud and fluid migration in active mud volcanoes in Azerbaijan. *Geo-Mar Lett* 23(3–4):258–268

- Reeburgh WS (2007) Oceanic methane biogeochemistry. *Chem Rev* 107:486–513
- Rojo F (2019) Aerobic Utilization of Hydrocarbons, Oils, and Lipids. *Handbook of Hydrocarbon and Lipid Microbiology*. Springer, Cham.
- Sahling H, Bohrmann G, Artemov YG, Bahr A, Bruning M, Klapp SA, Klaucke I, Kozlova E, Nikolovska A, Pape T, Reitz A, Wallmann K (2009) Vodyanitskii mud volcano, Sorokin trough, Black Sea: geological characterization and quantification of gas bubble streams. *Mar Pet Geol* 26:1799–1811
- Sauter EJ, Muyakshin SI, Charlou JL, Schluter M, Boetius A, Jerosch K, Damm E, Foucher JP, Klages M (2006) Methane discharge from a deep-sea submarine mud volcano into the upper water column by gas hydrate-coated methane bubbles. *Earth Planet Sci Lett* 243(3–4):354–365
- Schmincke H-U (2004) *Volcanism*, 2nd ed., Springer, Berlin
- Schneider von Deimling J, Brockhoff J, Greinert J (2007) Flare imaging with multibeam systems: Data processing for bubble detection at seeps, *Geochemistry Geophysics Geosystems*, 8(6), <https://doi.org/10.1029/2007GC001577>
- Soetaert K, Van Oevelen D, Sommer S (2012) Modelling the impact of Siboglinids on the biogeochemistry of the Captain Arutyunov mud volcano (Gulf of Cadiz). *Biogeosciences (BG)* 9:5341–5352
- Somoza L, Diaz-del-Rio V, Leon R, Ivanov M, Fernandez-Puga MC, Gardner JM, Hernandez-Molina FJ, Pinheiro LM, Rodero J, Lobato A, Maestro A, Vazquez JT, Medialdea T, Fernandez-Salas LM (2003) Seabed morphology and hydrocarbon seepage in the Gulf of Cadiz mud volcano area: acoustic imagery, multibeam and ultra-high resolution seismic data. *Mar Geol* 195 (1–4):153–176
- Steinle L, Graves CA, Treude T, Ferre B, Biastoch A, Bussmann I, Berndt C, Krastel S, James RH, Behrens E, Boning CW, Greinert J, Sapart C-J, Scheinert M, Sommer S, Lehmann MF, Niemann H (2015) Water column methanotrophy controlled by a rapid oceanographic switch. *Nat Geosci* 8:378–382
- Steinle L, Schmidt M, Bryant L, Haeckel M, Linke P, Sommer S, Zopf J, Lehmann MF, Treude T, Niemann H (2016) Linked sediment and water-column methanotrophy at a man-made gas blowout in the North Sea: implications for methane budgeting in seasonally stratified shallow seas. *Limnol Oceanogr* 61:367–386
- Stewart SA, Davies RJ (2006) Structure and emplacement of mud volcano systems in the South Caspian Basin. *AAPG Bull* 90(5):771–786
- Treude T, Boetius A, Knittel K, Wallmann K, Jorgensen BB (2003) Anaerobic oxidation of methane above gas hydrates at Hydrate Ridge, NE Pacific Ocean. *Mar Ecol-Prog Ser* 264:1–14
- Veloso M, Greinert J, Mienert J, De Batist M (2015) A new methodology for quantifying bubble flow rates in deep water using splitbeam echosounders: examples from the Arctic offshore NW-Svalbard. *Limnol Oceanogr Methods* 13:267–287
- Vogt PR, Cherkashev A, Ginsburg GD, Ivanov GI, Crane K, Lein AY, Sundvor E, Pimenov NV, Egorov A (1997) Haakon Mosby mud volcano: a warm methane seep with seafloor hydrates and chemosynthesis-based ecosystem in late Quaternary Slide Valley, Bear Island Fan, Barents Sea passive margin. *EOS Trans Am Geophys Union Suppl* 78(17):187–189
- Wallmann K, Linke P, Suess E, Bohrmann G, Sahling H, Schlüter M, Dähmann A, Lammers S, Greinert J, von Mirbach N (1997) Quantifying fluid flow, solute mixing, and biogeochemical turnover at cold vents of the eastern Aleutian subduction zone. *Geochim Cosmochim Acta* 61 (24):5209–5219



Methane Carbon Cycling in the Past: Insights from Hydrocarbon and Lipid Biomarkers

28

Volker Thiel

Contents

1	Introduction: Methane Sources and Sinks	782
1.1	Methane Sources	782
1.2	Abiotic Methane Sources	783
2	Methane Sinks	784
2.1	Aerobic Oxidation of Methane	785
2.2	Anaerobic Oxidation of Methane	785
2.3	Major Abiotic Methane Sinks	788
3	Lipid Biomarkers for the Aerobic Oxidation of Methane	789
3.1	Biomarkers for Organisms Involved in Aerobic Methanotrophy	789
3.2	Tracing Aerobic Methanotrophy in Ancient Environments	791
4	Lipid Biomarkers for the Anaerobic Oxidation of Methane (AOM)	794
4.1	Biomarkers for Organisms Involved in AOM	794
4.2	Tracing AOM in Ancient Environments	798
5	Research Needs	803
	References	804

Abstract

Methane produced by thermal decomposition of organic matter, biological methanogenesis, and abiotic reactions plays a prominent role in biogeochemical cycles and climate forcing. There are, however, microbiological processes that efficiently mitigate its release into Earth's surface environments. Lipid biomarkers are powerful tracers for methanotrophic (methane-consuming) organisms and their metabolisms. The particular strength of the biomarker concept, as

V. Thiel (✉)

Geobiology, Geoscience Centre, Georg-August University of Göttingen, Göttingen, Germany

e-mail: vthiel@gwdg.de

© Springer Nature Switzerland AG 2020

H. Wilkes (ed.), *Hydrocarbons, Oils and Lipids: Diversity, Origin, Chemistry and Fate*,
Handbook of Hydrocarbon and Lipid Microbiology,

https://doi.org/10.1007/978-3-319-90569-3_6

781

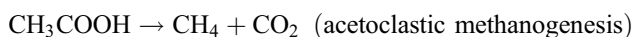
compared to DNA- or RNA-based techniques, lies in its potential to track the methane-derived processes not only in modern settings but also on a geological time scale. In the past two decades, numerous studies have provided information on the lipid inventories of the key methanotrophic biota. In addition, compound-specific isotopic measurements have become an important tool for the recognition of tracer compounds for the turnover of methane in environmental samples. After a brief introduction about methane sources and sinks, I will provide an overview about the relevant lipid biomarkers that have been reported from aerobic and anaerobic methanotrophs and their habitats. Furthermore, the occurrence and utility of their diagenetic products as molecular fossils for methane carbon cycling in ancient environments will be illustrated.

1 Introduction: Methane Sources and Sinks

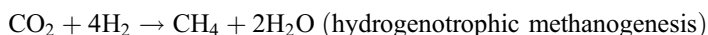
1.1 Methane Sources

1.1.1 Methanogenesis

Most methane on Earth, 85–300 Tg year⁻¹, is produced by certain anaerobic microorganisms belonging to the phylum Euryarchaeota within the domain Archaea. These prokaryotes are commonly referred to as “methanogens” and constitute the largest and most diverse group within the Archaea. Methanogens are able to grow at temperatures between 4 °C and 122 °C, at pH values from 3 to 9, and at salinities ranging from brines to freshwater. Their enormous ecological range notwithstanding, the substrates that can be used by methanogens are rather limited. In a process called fermentation, some methanogens degrade simple organic compounds, such as formate, acetate, methanol, and methylamine (Whiticar 1996; see ► Chap. 25, “The Biogeochemical Methane Cycle,” this volume), whereby methane is being formed as a metabolic end product, e.g.,



Most methanogens (>70%), however, thrive on completely inorganic substrates, namely, hydrogen and CO₂, which are energetically most favorable.



Methanogenesis ultimately converts some 10–20% of the reactive organic material buried in soils and sediments to methane (Knittel and Boetius 2009). Typical environments with a high abundance of methanogens are anoxic marine and lacustrine sediments, wetlands, waterlogged soils, and animal guts (termites, ruminants). Methanogens are strict anaerobes, but apart from that they are rather versatile in respect to environmental conditions. The current record for growth temperatures (122 °C), for instance, is held by a hyperthermophilic methanogen, *Methanopyrus kandleri* (Takai et al. 2008).

1.1.2 Other Biologically Influenced Methane Sources

The breakdown of sedimentary organic matter due to heat and pressure during burial in the Earth's crust is another significant factor that leads to major formation of "thermogenic" methane (and other gases) in the subsurface (see ► Chap. 18, "Thermogenic Formation of Hydrocarbons in Sedimentary Basins," this volume). It is, however, poorly constrained how much of the thermogenic methane actually enters the critical zone, and the atmosphere, through localized seeps (see ► Chap. 26, "Marine Cold Seeps: Background and Recent Advances," this volume), diffusive flows, and/or after having been temporarily fixed as gas hydrates (Saunois et al. 2016; see ► Chap. 24, "Gas Hydrates as an Unconventional Hydrocarbon Resource," this volume).

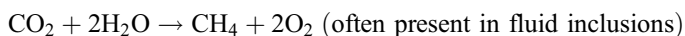
Some further biologically influenced methane sources exist, but their overall contributions have not yet been reliably integrated into global methane budgets (Xu et al. 2016). These contributions are likely to be small as compared to methanogenesis (~20%; Schubert 2011) but may be substantial in confined modern environments and/or may have been widespread in the geological past.

- Aerobic methane production within terrestrial **plant tissue** may (Keppler et al. 2006), or may not (Dueck et al. 2007), release considerable amounts of methane into the atmosphere.
- **Fungi** have recently been identified as methane sources in terrestrial habitats, with the methane being possibly produced from a methionine precursor during aerobic degradation of plant matter, e.g., wood or grass (Lenhart et al. 2012).
- **Marine algae**, namely, the widespread coccolithophorid *Emiliania huxleyi*, have been recognized as an aerobic methane source, but the underlying mechanism is as yet unknown (Lenhart et al. 2016).
- In oxygenated waters, the microbially mediated cleavage of the algal metabolite **methylphosphonate** has been identified as a source of methane (Karl et al. 2008). This mechanism may occur in marine as well as in lacustrine (Yao et al. 2016) environments and may relate to the so-called oceanic methane paradox, i.e., the local oversaturation of methane in certain depths of the upper, oxygenated water column (Repeta et al. 2016).

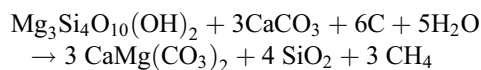
1.2 Abiotic Methane Sources

Methane can also be produced fully abiotically, either by high-temperature magmatic processes in volcanic and geothermal areas or via low-temperature (<100 °C) gas–water–rock reactions even at shallow depths. At least nine different pathways of abiogenic methane formation in the Earth's crust and mantle have been proposed (see Etiope and Sherwood Lollar 2013, for a review); selected examples are:

Late magmatic methane formed by re-speciation of C–O–H fluids during magma cooling (<600 °C);

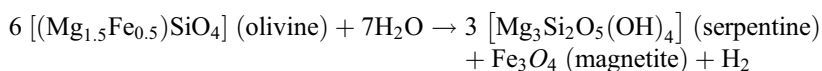


Metamorphism of carbonate and graphite bearing rocks – Below 400 °C, graphite in contact with CO₂ bearing fluids leads to methane production during retrograde metamorphism.

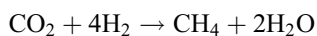


Talc + calcite + graphite → dolomite + quartz + methane

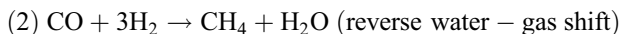
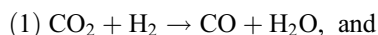
Fischer–Tropsch-type (FTT) reactions are thought to be linked to serpentinization reactions occurring in the subsurface within fractured ultramafic rocks (Proskurowski et al. 2008). Oxidation of Fe(II) in olivine to Fe(III) in magnetite produces hydrogen, which reacts with CO₂ in the presence of an iron or iron oxide catalyst.



The hydrogen so produced may react with CO or CO₂ in the actual Fischer–Tropsch reaction to form methane either in a one-step reaction



or a two-step reaction



It is interesting to note that FTT reactions can form not only methane but also higher *n*-alkane homologues, *n*-fatty acids, and *n*-alcohols (Fischer and Tropsch 1923). This may occur over a temperature range of 100 to 400 °C and at water-saturated conditions resembling those prevailing in hydrothermal systems (McCollom et al. 1999; Rushdi and Simoneit 2001; see ► Chap. 20, “Hydrothermal Petroleum,” this volume). FTT reactions have often been invoked as pathways for the abiotic formation of hydrocarbons in ancient (e.g., Lindsay et al. 2005; McCollom 2013) and modern (Proskurowski et al. 2008) environments.

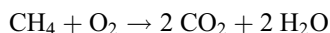
2 Methane Sinks

In soils, sediments, and waters, methane can be oxidized by microorganisms which efficiently reduce the amount of methane released into the atmosphere, and thus, climate forcing. In marine settings, microbial oxidation reduces methane to low nanomolar levels, which is why ocean water is typically undersaturated with respect to the atmosphere (Reeburgh 2007). Biological consumption of methane involves

two major pathways and functional groups of microorganisms, depending on the environmental (redox-)setting.

2.1 Aerobic Oxidation of Methane

In the presence of molecular oxygen, methane can be oxidized to CO₂ by strictly aerobic methanotrophic bacteria (*methane-oxidizing bacteria*, MOB; Hanson and Hanson 1996; Bürgmann 2011).



Most MOB fall into two well-defined phylogenetic groups within the phylum *Proteobacteria*, “Type I” (members of the *Gammaproteobacteria*) and “Type II” (members of the *Alphaproteobacteria*). Both groups possess an extensive intracytoplasmic membrane, which is the site of methane oxidation to methanol (Fig. 1), but differ in their modes of carbon assimilation. Type I methanotrophs use the ribulose monophosphate pathway and obtain all their carbon from methane. Type II methanotrophs use the serine pathway, which further involves fixation of CO₂ and is energetically less favorable (Bowman 2014; Bürgmann 2011; Madigan et al. 2003). Additionally, it has been found that some bacteria of the phylum *Verrucomicrobiaceae* also have the ability to aerobically oxidize methane (Dunfield et al. 2007; van Teeseling et al. 2014), but these are thermoacidophilic bacteria that can be expected to play a major role only in some extreme environments.

2.2 Anaerobic Oxidation of Methane

In the absence of oxygen, methane can be processed through the *anaerobic oxidation of methane* (AOM), using alternative electron acceptors. In fact, AOM is the determining process of methane consumption in sediments. It removes more than 90% of the annually produced methane, before it can reach the open water column or the atmosphere (Knittel and Boetius 2009). In modern marine environments, AOM is largely performed by three cosmopolitan clades of *anaerobic methanotrophic archaea* (commonly referred to as ANME-1, -2, and -3, plus various subgroups (Fig. 2; Hinrichs et al. 1999; Boetius et al. 2000; Niemann et al. 2006; Knittel and Boetius 2009).

Typically, marine ANME thrive as obligate methane-oxidizing, autotrophic organisms, which physically associate with specific partners that are obligate autotrophic sulfate-reducing bacteria (SRB; Wegener et al. 2016). These bacteria belong either to the *Desulfosarcina–Desulfococcus* (ANME-1/DSS and ANME-2/DSS) and the *Desulfobulbus* spp. (ANME-3/DBB) branches (Hinrichs et al. 1999; Boetius et al. 2000; Michaelis et al. 2002; Knittel et al. 2003; Niemann et al. 2006).

The consortia gain energy from AOM, and with sulfate as the final electron acceptor, according to the net reaction

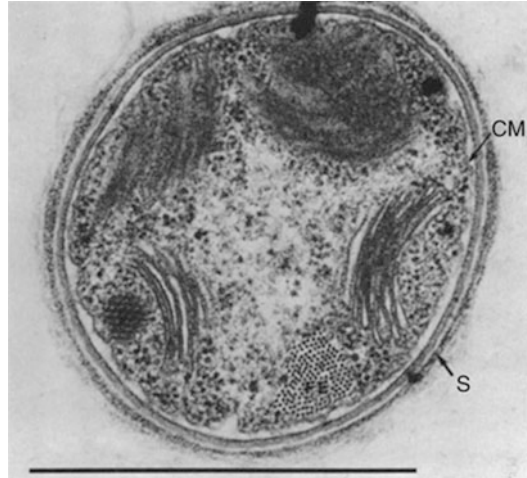


Fig. 1 Thin section through a filament of the Type I methanotroph *Crenothrix polyspora*, one of the major freshwater MOB. Note the typical lamellar stacks of intracytoplasmic membrane, the cytoplasmic membrane (CM), and the sheath layer (S). Scale bar: 1 μm . (Originally published in Bowman (2014, Fig. 21.5.d), published with kind permission of ©Springer Science+Business Media New York. All rights reserved)

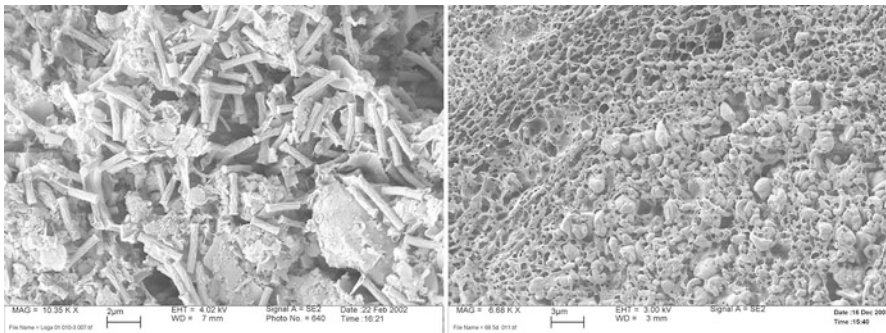


Fig. 2 Field emission scanning electron microscope images of ANME-1 (left)- and ANME-2 (right)-dominated microbial mats from the Black Sea. ANME-1 are cylindrical cells (often forming filaments up to 50 μm in length). ANME-2 have a flat morphology and are surrounded by vibrioform cells of syntrophic sulfate-reducing bacteria (see text). (Image credit: J. Reitner)

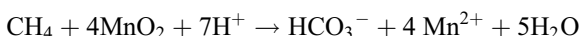


Sulfate-dependent AOM results in an energy yield of only -20 to -40 kJ mol^{-1} of methane oxidized under environmental conditions. The process obviously depends on a transfer of reducing equivalents from methane to sulfate, but the underlying mechanisms are still not fully known (Wegener et al. 2015). Interestingly,

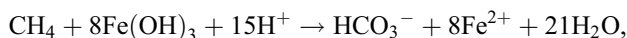
a direct transfer of electrons from ANME-1 to the associated SRB via intercellular nanowire-like structures was recently shown to occur in these consortia (Wegener et al. 2015). Moreover, some ANME seem to be metabolically versatile. Lab experiments with isotopically labeled substrates indicated that ANME-1 do not necessarily thrive on methane and have the potential of additional autotrophic metabolisms (Bertram et al. 2013). This corresponds with observations of ANME-1 as monospecific aggregates or even single cells in environmental samples (Fig. 2; Orphan et al. 2002; Reitner et al. 2005).

Different ANME clades may thrive in the same environment, but typically show distinct zone formation which could be related to localized concentrations of methane, sulfate, sulfide, bottom water oxygen, and temperature (Nauhaus et al. 2005; Rossel et al. 2011; Timmers et al. 2015). For instance, ANME-1/DSS-consortia seem to prefer higher temperatures and lower oxygen concentrations in overlying bottom waters as compared to ANME-2/DSS. Recent work showed that ANME-1 archaea, with bacterial partners other than DSS, are thriving even in geothermally heated environments as hot as 70 °C (Holler et al. 2011, see also Schouten et al. 2003). High sulfate concentrations, often associated with strong, advective methane seepage, particularly favor the ANME-2/DSS. That consortium also showed highest cell-specific AOM rates in the lab (Nauhaus et al. 2005) and is obviously associated with precipitation of abundant carbonate cements at methane seeps (Leefmann et al. 2008; Peckmann et al. 2009; see also below).

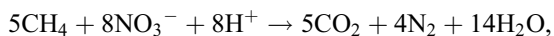
Whereas sulfate-dependent AOM is certainly prevalent in marine settings, it has earlier been argued that AOM may be coupled to a larger variety of oxidants (Peckmann and Thiel 2004). Recent studies revealed microorganisms capable of using iron and manganese to oxidize methane (Beal et al. 2009), according to



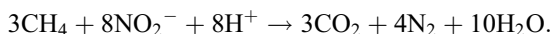
and



respectively (for implications on ancient environments, see Riedinger et al. 2014). Further possible oxidants are nitrate, according to



and nitrite, according to



Whereas the former reaction is performed by a distinctive ANME-2 subcluster (ANME-2d in association with *anaerobic ammonium-oxidizing* (anammox-)

bacteria; Raghoebarsing et al. 2006; Haroon et al. 2013), the latter is conducted by “*Candidatus Methyloirabilis oxyfera*”, an anaerobic, denitrifying bacterium that, notably, produces molecular oxygen as an intermediate during the methane-oxidizing reaction (Ettwig et al. 2010).

Recently it has also been shown that humic organic matter may be used as an oxidant of methane by AOM-performing archaea, which are obviously different from the known ANME groups (Valenzuela et al. 2017).

2.3 Major Abiotic Methane Sinks

Atmospheric decomposition – After being formed by biotic or abiotic processes, methane may escape to, and decompose in, the atmosphere. The atmospheric residence time of methane is about 12 years, before it is photochemically oxidized, mainly by OH-radicals in the troposphere, to H₂O, CO, and CO₂ (IPCC 2013; Badr et al. 1992). During that time, methane acts as a potent greenhouse gas, due to its ability to absorb on the infrared band. Its “global warming potential” is deemed 15–34 times that of CO₂ on a 100 year timescale (refs. in Malyan et al. 2016, Table 1). Methane emissions caused by industrial activity, biomass and fossil fuel burning, cattle farming, and rice cultivation, currently contribute ~70% of the total atmospheric methane input and ~16% to the anthropogenic greenhouse warming of the Earth (in 2010; IPCC 2013).

There are considerable interannual and interdecadal variations in atmospheric methane concentrations that are still not well understood (Kirschke et al. 2013; Turner et al. 2017). It is commonly accepted, however, that major emissions of methane may have a striking impact on the Earth’s climate. One example of a putatively methane-driven global temperature excursion (by about 5 °C) is the Paleocene/Eocene temperature maximum, where large amounts of isotopically light carbon entered the atmosphere, possibly due to rapid melting of sedimentary gas hydrates (Dickens 2003; Zachos et al. 2008).

Storage in sediments – Methane may migrate into sedimentary reservoirs and accumulate either as free natural gas, dissolved in fluids, or, under certain low-temperature/high-pressure conditions, frozen as solid gas hydrates. If buried and trapped in suitable structures, both biogenic and “thermogenic” methane may thus contribute to fossil natural gas reservoirs that still play a crucial role as an energy resource for man. Apart from conventional and unconventional gas trapped in reservoir rocks, shallow sedimentary gas hydrates comprise a giant, semi-stable capacitor for the storage of methane over extended time scales (see ► Chap. 3, “Gas Hydrates: Formation, Structures, and Properties,” this volume). According to the latest estimates (Ruppel and Kessler 2017), sedimentary gas hydrates amount to ~1800 Gt, which is ~15% of the global mobile carbon pool. For a detailed overview, see ► Chap. 24, “Gas Hydrates as an Unconventional Hydrocarbon Resource” of this volume.

3 Lipid Biomarkers for the Aerobic Oxidation of Methane

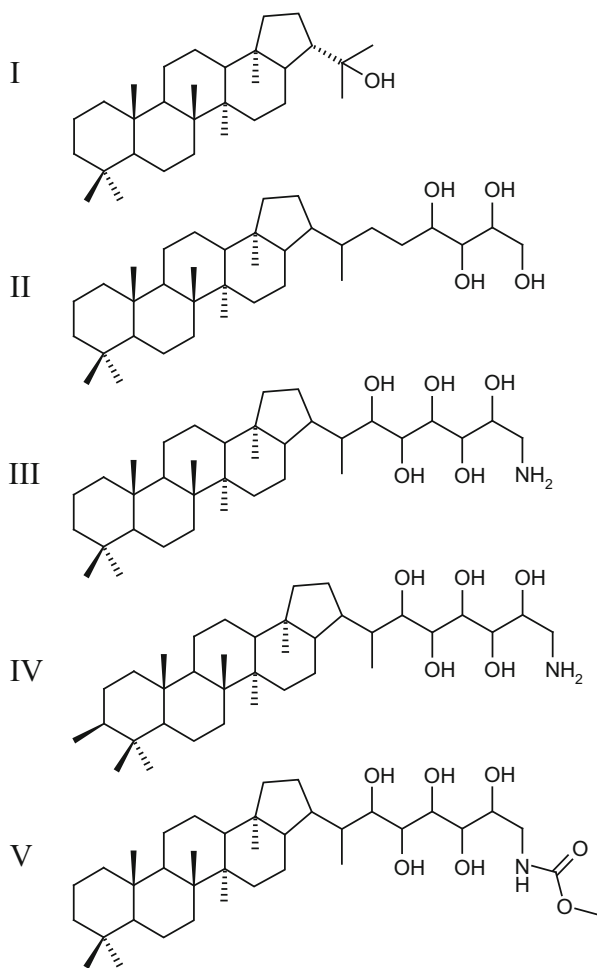
3.1 Biomarkers for Organisms Involved in Aerobic Methanotrophy

Aerobic MOB produce a number of potential diagnostic lipids, including hopanoids, steroids, and fatty acids, as will be described below. The selectivity of these biomarkers for methanotrophy can further be enhanced by compound-specific $\delta^{13}\text{C}$ -measurements. This is because the substrate (i.e., methane) is isotopically light as compared to other carbon sources. Whereas thermogenic methane largely inherits the $\delta^{13}\text{C}$ of the organic matter source (typically -25 to -40%), biogenic methane has even lower $\delta^{13}\text{C}$ values (-50 to -80%), with methane originating from archaeal CO_2 reduction at the lower end and fermentation at the higher end (Whiticar 1996). Moreover, assimilation of methane for lipid biosynthesis by MOB is accompanied by a strong isotopic fractionation (more than -30% under methane non-limited conditions; Summons et al. 1994). Hence, biomarkers derived from MOB (and other methanotrophs) usually display $\delta^{13}\text{C}$ values in the range of -60 to -120% . In ancient sediments, such strongly ^{13}C -depleted compounds can testify to the biological assimilation of methane carbon and help to differentiate indigenous substances from allochthonous compounds and contaminants.

Hopanoids are known to occur in many MOB and range from the simple C_{30} compounds diploptene and diplopterol to highly functionalized bacteriohopanepolyols (BHPs; Rohmer et al. 1984; Sahn et al. 1993; Summons et al. 1994). BHPs with a broad distribution in methanotrophs are aminobacteriohopanetriol (aminotriol), aminotetrol, and aminopentol, along with the more ubiquitous bacteriohopanetetrol. Particularly, the aminopentol appears to be a reasonably specific, though not unique, biomarker for Type I methanotrophs (Talbot and Farrimond 2007 and refs therein; Blumenberg et al. 2012). However, marked differences between the relative abundances of amino-BHPs in methanotrophs exist, and not all Type I methanotrophs synthesize aminopentol (Rush et al. 2016).

In addition to compounds showing the regular hopane skeleton, some widespread MOB (Methylococcaceae) synthesize hopanoids methylated at the C-3 position (Fig. 3 IV; Summons et al. 1994). An attractive feature of these compounds is that the methylation may readily persist in the sedimentary record while the functional groups attached to the carbon skeletons of the BHP precursors get degraded during diagenesis. However, 3β -methyl-BHPs have been observed not only in methanotrophs but also in acetic acid bacteria (Zundel and Rohmer 1985). Recent studies also revealed that the taxonomic distribution of the gene responsible for the 3β -methylation may extend even further into the bacteria and suggested a physiological role for 3β -methyl-BHPs in supporting bacterial cell survival in the late stationary phase (Welander and Summons 2012) and/or during substrate limitation (Summons et al. 1994; Burhan et al. 2002). Thus, the selectivity of sedimentary

Fig. 3 Chemical structures of some biohopanoids that are frequently found in MOB. I, diplopterol; II, bacteriohopanetetrol; III, aminopentol; IV, 3-methylaminopentol; V, methylcarbamate-aminopentol. Of these structures, only III–V have good specificity for MOB (see text)



3 β -methylhopanoids for MOB may be limited, and should ideally be corroborated by compound-specific $\delta^{13}\text{C}$ analyses.

An interesting new group of potential BHP biomarkers for bacterial methanotrophs are amino-BHPs with methylcarbamate (MC) terminal groups (Fig. 3, V). Recently, these compounds have been consistently detected in a number of cultured Type I methanotrophs and were also found in modern marine sediments influenced by methane (Rush et al. 2016). Future studies will reveal whether MC-BHPs represent selective tracers of aerobic methane oxidation in modern environments.

Sterols – A somewhat outstanding trait of the widespread Type I MOB family Methylococcaceae is the capability to synthesize 4-methylsterols (Bird et al. 1971; Summons et al. 1994; Schouten et al. 2000). Steroids are commonly regarded as an attribute of the eukaryotic domain, although recent studies suggest that the

biosynthesis of sterols from squalene may be more common among the bacteria as previously thought (Wei et al. 2016). The sterols of methanotrophs encompass lanosterol (4 α -methylcholesta-8(14),24-dien-3 β -ol) and a number of derivatives, all showing 4 α - or 4,4-methylation, a double bond located at C-8(14), but no side-chain alkylation. These compounds might be considered as “primitive” because their biosynthesis from squalene requires less enzymatic steps as needed for the more evolved 4-desmethylsterols typically found in eukaryotes. Whatsoever, 4-methylsterols are not unique to MOB, and even animals do contain lanosterols, though mostly as biosynthetic intermediates present at low steady-state concentrations. Summarizing, the occurrence of 4-methylsterols without side-chain alkylation in ancient sediments could well be related to aerobic (Type I) methanotrophs but should be corroborated by additional indicators.

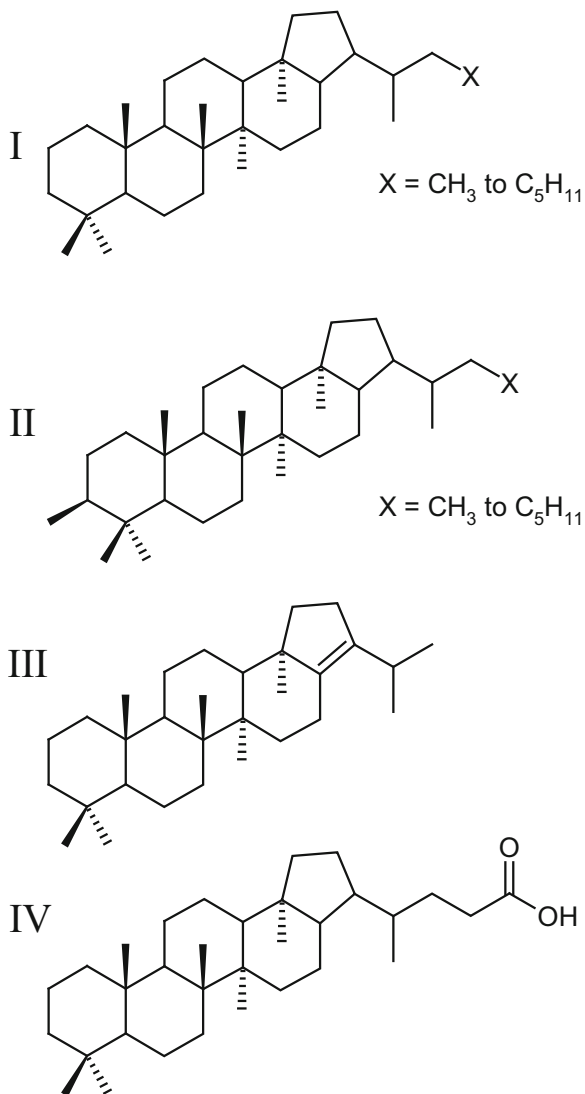
Fatty acids – A further distinctive feature of MOB is the presence of unusual phospholipid ester-linked fatty acids in their cell membranes that differentiate them from each other and also from many other organisms. Generally, Type I MOB have more C₁₄- and C₁₆ fatty acids, whereas Type II MOB contain mainly C₁₈ fatty acids. Among these, fairly diagnostic biomarkers are 16:1 ω 6c, 16:1 ω 5t, and C16:1 ω 8c for Type I and C18:1 ω 8c, 18:1 ω 6c, and 18:1 ω 5c for Type II MOB, as well as some other exotic fatty acids (Bowman et al. 1991; Bodelier et al. 2009; Taipale et al. 2016). In ecological studies, these compounds proved valuable to estimate the abundance of MOB, and thus the extent of aerobic methanotrophy in diverse modern environments such as stratified marine waters of the Baltic Sea (Berndmeyer et al. 2013) and Lake Kivu (Zigah et al. 2015), or microbial mats at methane seeps (Paul et al. 2017).

3.2 Tracing Aerobic Methanotrophy in Ancient Environments

Hopanoids – The hopanoid fingerprint of aerobic methanotrophy may be readily preserved in the sedimentary record, and there are numerous studies reporting findings of fossil hopanoids with a putative origin from MOB. It makes sense to separate here between the primary C₃₀ compounds, namely, diploptene/diplopterol, and the extended and/or functionalized diagenetic products of BHPs (Fig. 4).

Isotopically light diploptene/diplopterol have been reported from modern methane seeps (e.g., Elvert and Niemann 2008) as well as many contemporary aquatic sediments (Spooner et al. 1994; Elvert et al. 2001; Davies et al. 2016; Petrišič et al. 2017). Several studies reveal the preservation of these primary C₃₀ hopanoids, and their isotopic signatures, in Quaternary sediments. For instance, diplopterol with a $\delta^{13}\text{C}$ value of -61‰ in Santa Barbara Basin sediments was interpreted to reflect aerobic methanotrophy induced by the decay of gas hydrates during Late Pleistocene warming at around 40 kyrs b.p. (Hinrichs et al. 2003). Here, high diplopterol concentrations correlated with $^{13}\text{C}_{\text{carbonate}}$ depletions of foraminifera and were associated with laminated sediments indicative of low oxygen concentrations in bottom waters. Similar observations were made for Last Glacial marginal sediments in the western North Pacific (Uchida et al. 2004) and the Marmara Sea (Ménot and Bard 2010). Looking further back into the geological past, it seems that the

Fig. 4 Chemical structures of selected geohopanoids that may derive from the biohopanoids of MOB (Fig. 3); I, extended hopanes; II, extended 3 β -methylhopanes; III, hop-17(21)-ene; IV, dihomohopanoic acid. Of these structures, only II has some specificity for MOB (see text)



sedimentary record of diploptene/diplopterol begins to fade out in the ~ 10 kyr range. However, a plausible early diagenetic product of the primary C₃₀ hopanoids is hop-17(21)-ene, and this compound has also been observed in much older methane-derived carbonates, such as the Miocene Marmorito limestone, Italy ($\delta^{13}\text{C} = -83\%$; Thiel et al. 1999), and the Oligocene Lincoln Creek formation, USA ($\delta^{13}\text{C} = -52\%$, Thiel et al. 2001a).

Methanotroph-derived BHPs have been observed in stratified marine water columns (Berndmeyer et al. 2013), cold seep deposits (Birgel et al. 2011), peat (van Winden et al. 2012), and soil (Höfle et al. 2015). However, these highly

functionalized compounds are prone to rapid diagenetic degradation or alteration, just like BHPs from other sources. Consequently, fossil methanotroph-derived BHPs have mostly been reported from Holocene and Pleistocene sediments (Burhan et al. 2002; van Winden et al. 2012; Blumenberg et al. 2013). Recent work, however, revealed MOB-derived aminotriol, -tetrol-, and even -pentol in 115 m below sea floor in Congo fan sediments that have an estimated age of ca. 1.2 Ma (Talbot et al. 2014).

Functionalized degradation products of these BHPs occur in much older, thermally immature methane seep deposits ranging back in time to the Late Cretaceous (Birgel and Peckmann 2008). In these deposits, dihomohopanoic acids (Fig. 4, IV) and 32,35-anhydro-BHPs, together with their 3-methyl counterparts still testify to the lipids of MOB that once thrived in these environments (Burhan et al. 2002; Birgel and Peckmann 2008). In more altered ancient sediments, ^{13}C -depleted hopane-type hydrocarbons become increasingly important as markers for methanotrophy. Strongly ^{13}C -depleted hopanes/hopenes ($\delta^{13}\text{C} = -50$ to -90%) were e.g., reported from fossil microbial mats preserved in the Pleistocene Be'eri sulfur deposit (Israel, Burhan et al. 2002), from the Eocene Green River oil shale (USA, Collister et al. 1992), and from the Eocene Huadian oil shale (China, Volkman et al. 2015). These compounds have also been reported from several Mesozoic to Cenozoic seep carbonates, such as the Miocene Marmorito and Pietralunga deposits (Italy) and Late Jurassic to Early Cretaceous forearc strata in California (Thiel et al. 1999, 2001b; Birgel et al. 2006a).

Isotopic depletions and 3β -methylation in MOB-derived geohopanoids may also persist in thermally more mature deposits. An example is the Upper Cretaceous Teepee Buttes deposit which still shows abundant 8,14-secohexahydrobenzohopanes at -110% (Birgel and Peckmann 2008). The oldest setting with a well-constrained and commonly accepted 3β -methylhopane indication for ancient methanotrophy is the 1.640-Gyr-old Barney Creek Formation of the McArthur Group, northern Australia (Brocks et al. 2005). Although no $\delta^{13}\text{C}$ values could be obtained for these compounds, they co-occur together with predominant aromatic 4-methylsteranes (whereas other steranes are missing), and an origin from MOB rather than eukaryotes appears the most plausible interpretation for these biomarkers.

One pitfall when using regular geohopanoids with ^{13}C depletions as biomarkers for aerobic methanotrophs is that these compounds may also derive from bacteria associated with AOM, particularly sulfate reducers. Another problem is that methane-derived carbon may cause isotopic depletions not only in the lipids of methanotrophs and/or their symbionts but also of organisms that are further downstream in the microbial food chain. Likewise, MOB-derived hopanoids with ubiquitous structures (e.g., diplopterol and its derivatives) may mix with the same compounds from other microbial sources, thus successively diluting the isotopic depletion. Last, but not least, recent studies indicate that hopanoids from MOB do not always show a distinct depleted ^{13}C isotopic signature, specifically when methane carbon is used only for catabolism but not for lipid synthesis (Kool et al. 2014). Care has therefore to be exercised in the interpretation of hopanoids in methane-rich environments.

Steroids – Several findings of lanostane derivatives were reported from the geological record, such as in Cenozoic lacustrine sediments (Peng et al. 1998) and crude oils (Lu et al. 2011) from China, and in Lower Cambrian deposits of the Eastern Siberian platform (Parfenova 2011). However, there are surprisingly few reports where an origin of C-4 methylated steroid hydrocarbons from MOB was plausibly supported by compound specific $\delta^{13}\text{C}$ data and/or parallel detection of 3 β -methylhopanes. Examples are nor-lanostane, lanostane, and methyl lanostane with $\delta^{13}\text{C}$ -values from -92 to -75% in the Miocene Pietralunga seep limestone (Peckmann et al. 2004). Likewise, aromatic 4-methyl steranes lacking side-chain alkylation occur along with 3 β -methylhopanes in the 1.640-Gyr-old Barney Creek Formation (Brocks et al. 2005). Currently, this latter study reported the oldest commonly accepted occurrence of MOB biomarkers, and of steroids in general (see also ► Chap. 15, “History of Life from the Hydrocarbon Fossil Record,” this volume).

It should be noted that biomarkers from aerobic methanotrophs often co-occur with lipids derived from anaerobic methanotrophs (e.g., Thiel et al. 1999; Birgel et al., 2006b). This is, inter alia, due to the fact that authigenic carbonates formed by AOM tend to encase the lipids of the active microbial communities before they can be degraded by heterotrophs. As a result, ancient methane seep deposits often show an excellently preserved biomarker content allowing to reconstruct facets of the methane cycling biota in great detail (see discussion on “Preservation Aspects” in Sect. 4.2). Lipid biomarkers for anaerobic methane-oxidizing communities are outlined in the following chapter.

4 Lipid Biomarkers for the Anaerobic Oxidation of Methane (AOM)

4.1 Biomarkers for Organisms Involved in AOM

Strong variations in the biomarker patterns from anoxic methane-rich settings indicate considerable diversity of the microbial taxa involved in, or associated with, AOM. However, the classical biomarkers most commonly reported from these environments are well constrained and can be narrowed down into a few categories, according to their chemical structures and most likely biological sources (Peckmann and Thiel 2004).

Archaeal biomarkers – The following lipid biomarkers found in methane-rich environments are sourced predominantly by ANME. Selected structures are shown in Fig. 5.

- Tail-to-tail linked (irregular) isoprenoid hydrocarbons, namely, crocetane and 2,6,10,15,19-pentamethylcosane (PMI; Fig. 5, I, II), which may occur either as saturated hydrocarbons or with as much as two (crocetenes) or five double bonds (PMIA; e.g., Elvert et al. 1999; Thiel et al. 1999; Fig. 6a). Analysts should note

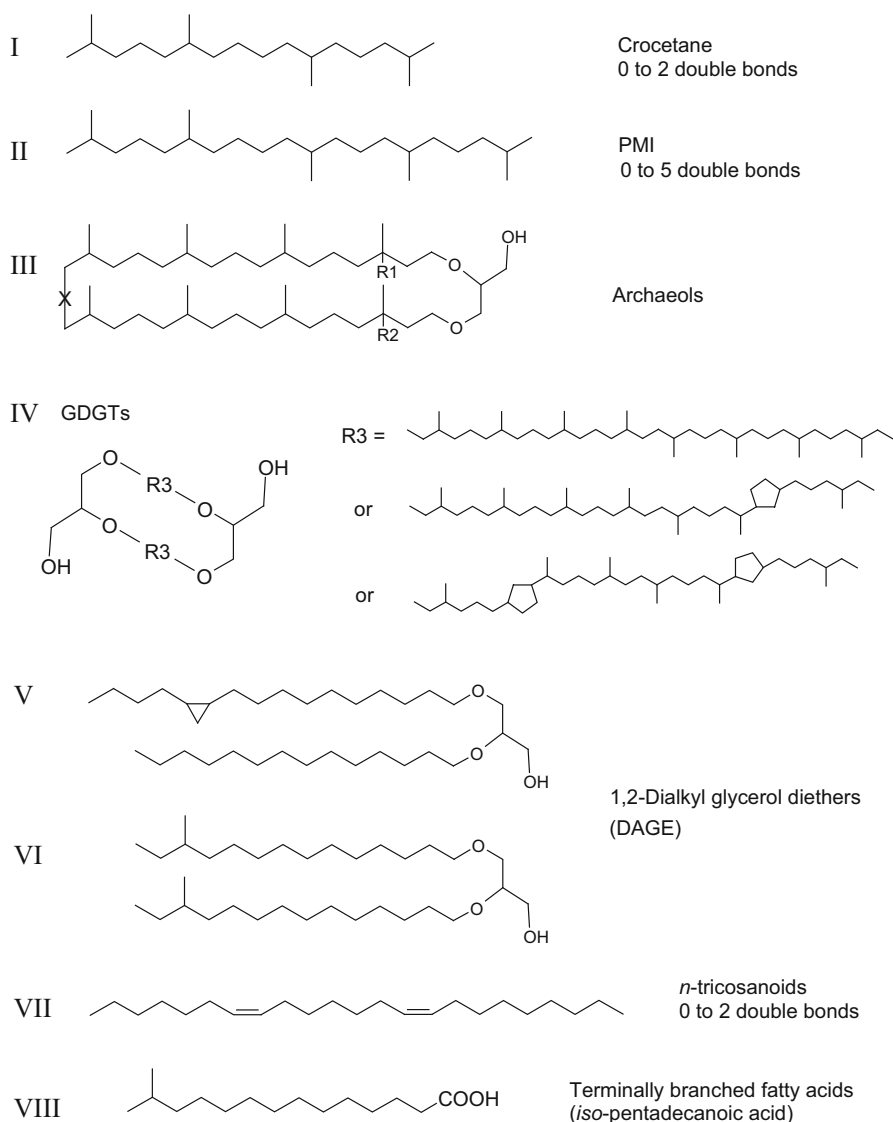


Fig. 5 Chemical structures of selected archaeal (I–IV) and bacterial (V–VIII) biomarkers found in AOM environments. I, crocetane (2,6,11,15-tetramethylhexadecane); II, PMI (2,6,10,15,19-pentamethylcosane); III, archaeols (R1 = H, R2 = H, archaeol; R1 = OH, R2 = H, *sn*-2-hydroxyarchaeol; R1 = H, R2 = OH, *sn*-3-hydroxyarchaeol; the “X”-bond is present only in macrocyclic archaeols); GDGTs (glycerol dialkyl glycerol tetraethers) with acyclic, monocyclic, or dicyclic isoprenoid chains; V, VI, non-isoprenoid *sn*-1,2 dialkyl glycerol (examples: 11,12-methylenhexadecyl-/*n*-tetradecyl-, and anteiso-pentadecyl-/anteiso-pentadecyl moieties); VII, *n*-tricosanoids (example: *n*-tricoso-7,14-diene); VIII, terminally branched fatty acids (example: 14-methyltetradecanoic acid = *iso*-pentadecanoic acid)

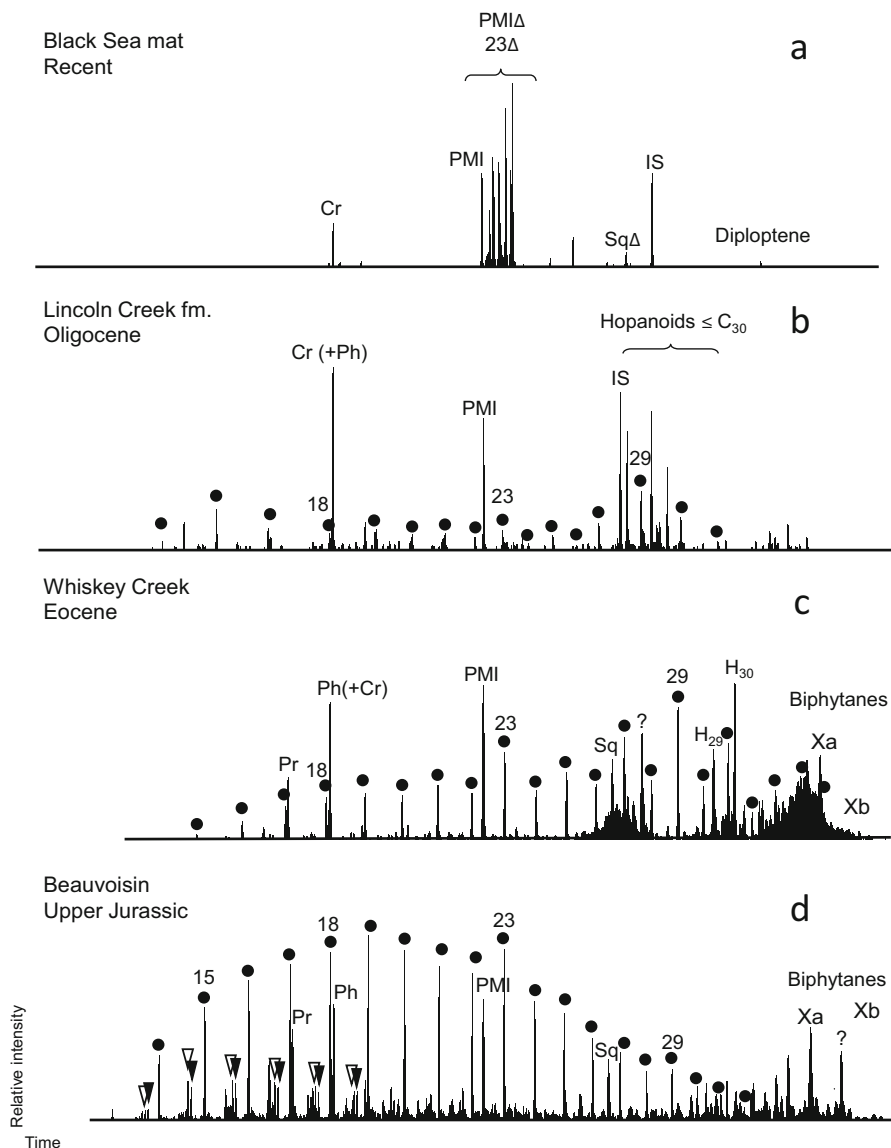


Fig. 6 Total ion current chromatograms (subtracted for background) of hydrocarbons (C₁₅+) extracted from selected seep deposits of modern to Late Jurassic age. Age and thermal maturity increase from (a) to (d) and illustrate the compositional changes the biomarker distributions experience during burial. Filled circles/numbers indicate *n*-alkanes of the respective carbon chain length. Pr = pristane (IV); Cr = crocetane; Ph = phytane (partly coeluting with Cr); 23 = *n*-tricosane; PMI = 2,6,10,15,19-pentamethylcosane; Sq = squalane; Δ = unsaturated derivatives; H₂₉, H₃₀ = 17α(H),21β(H)-30-norhopane, 17α(H),21β(H)-hopane, respectively; open and filled triangles = 2-methyl- (iso-) alkanes and 3-methyl- (anteiso-) alkanes. IS = internal standard. (Originally published in Peckmann and Thiel (2004), published with kind permission of Elsevier B.V. All rights reserved)

that crocetane coelutes with the leading edge of the phytane peak on conventional GC columns and both compounds may be difficult to separate (Robson and Rowland 1993; Thiel et al. 1999; Greenwood and Summons 2003). Recent studies also showed the presence at seeps of longer tail-to-tail isoprenoids with squalane (C₃₀) and C₃₅ carbon skeletons and up to 7 double bonds. The biological function of these hydrocarbons is not known as yet but it has been plausibly suggested that they may serve as an intracellular reversible hydrogen sink (Bertram et al. 2013).

- Glycerol dialkyl ethers with regular head-to-tail linked C₂₀ isopranyl (phytanyl) moieties, namely, archaeol, *sn*-2-, *sn*-3-hydroxyarchaeol (e.g., Hinrichs et al. 1999; Pancost et al. 2000, 2001), extended hydroxyarchaeols (i.e., with one regular C₂₅ isoprenoid chain) and, occasionally, macrocyclic diphytanyl glycerol diethers (MDGDs) with 0, 1, and 2 five-membered rings (Stadnitskaia et al. 2003). These lipids have glycosidic and phospho- or only phospho-headgroups (Rossel et al. 2011).
- Glycerol dialkyl glycerol tetraethers (GDGTs) carrying head-to-head linked acyclic and cyclic phytane dimers (biphytanes, C₄₀). Individual isopranyl units may be acyclic or contain up to two C₅ rings. The biphytanyl chains may contain and 0–6 double bonds (Zhu et al. 2014). The GDGT core lipids carry glycosidic, phospho- and phosphoglycosyl-headgroups (Rossel et al. 2011).
- Phytanol, phytanic acid, α,ω -biphytanediols, and α,ω -diacids are often found in modern AOM settings and can be regarded as early degradation products of archaeols and GDGTs (e.g., Pancost et al. 2000; Birgel et al. 2008b; Liu et al. 2016).

Available data suggest that ANME-1 preferentially produce GDGTs and archaeol, along with PMI (particularly PMI pentaene, PMI:5), squalane, and C₃₅ hydrocarbons. ANME-2 and ANME-3 are a source of archaeol, hydroxyarchaeol, crocetane, and PMI derivatives (Blumenberg et al. 2004; Thiel et al. 2007; Rossel et al. 2011; Bertram et al. 2013). However, a problem with the use of these compounds as biomarkers even in modern settings is that they may be produced not only by ANME but also by other archaea, e.g., methanogens that may thrive together with the methanotrophs. For instance, detailed biomarker surveys revealed considerable contributions from archaea other than ANME to the lipid pools at recent methane seeps (Chevalier et al. 2014; Yoshinaga et al. 2015). Again, compound-specific ¹³C data are useful to more confidently constrain the contribution of ANME, particularly in more heterogeneous samples where relative abundances of individual biomarkers are low. The $\delta^{13}\text{C}$ values of the archaeal biomarkers listed above typically range between -60‰ and -130‰ .

Bacterial biomarkers – In AOM environments, ¹³C-depleted lipids carrying non-isoprenoid carbon chains always co-occur with the archaeal isoprenoid lipids and are usually regarded as biomarkers for the bacterial partners in AOM consortia, particularly SRB. Some of these structures are shown in Fig. 5, V-VIII. The most abundant compounds are various ester-bound C₁₄ to C₁₈fatty acids, namely, saturated and monoenoic (C16:1 ω 7c, C16:1 ω 7t, and C16:1 ω 5c; C16:1 ω 7c.), terminally

branched (particularly iso- and anteiso- C_{15}), and, to a lesser extent, cyclic carbon chains (10,11-cyclopropyl and ω -cyclohexyl). The fatty acids are typically accompanied by non-isoprenoid alcohols, monoalkyl glycerol ethers (MAGE), and 1,2-dialkyl glycerol ethers (DAGE) with corresponding carbon chains (Fig. 5, V, VI; e.g., Elvert et al. 2003; Pancost et al. 2000, 2001). Another group of ^{13}C -depleted straight-chain hydrocarbon biomarkers that are often enhanced in seep environments are the n - C_{23} compounds n -tricos-10-ene and n -tricos-7,14-diene (Thiel et al. 2001b; Chevalier et al. 2014; Fig. 5, VII). The biological source of the n -tricosanoids is still unknown but circumstantial evidence suggests that they derive from bacteria associated with AOM, possibly from the uncultured bacterial “Candidate Division JS1” (Chevalier et al. 2014). The structures of selected bacterial biomarkers are shown in Fig. 5, V-VIII.

In addition to these acetate-based bacterial lipids, a number of hopanoids have been reported from AOM environments. These compounds encompass the C_{30} compounds diplopterol (Fig. 3, I) and diploptene which have been reported along with functionalized pseudohomologues with extended side chains, such as dihomohopanol and dihomohopanoic acid (Fig. 3, IV) that obviously derive from BHPs. As mentioned above, however, these compounds may originate not only from bacteria associated with AOM (i.e., SRB) but also from aerobic methanotrophs, and the exact sources of these more unspecific hopanoids are often difficult to determine (see discussion in Sect. 3.2).

4.2 Tracing AOM in Ancient Environments

Ancient seep carbonates as a matrix for biomarkers – AOM is a widespread process in the marine realm and typically occurs in the sediment at the depth of the sulfate–methane transition zone. However, the biomarker traces of this process are difficult to recognize in normal marine sediments, due to dilution with the same compounds derived from water column or sedimentary biota not related to AOM. In methane-rich environments, on the other hand, AOM leads to the formation of calcium carbonate ($CaCO_3$) deposits, i.e., methane-derived carbonates (Fig. 7). These precipitates, termed seep carbonates, or methane-derived carbonates, have frequently been reported from the geological record and often provide an excellent archive of methane-derived biomarkers (e.g., Goedert et al. 2003; Campbell 2006; Peckmann and Thiel 2004; Birgel et al. 2006b).

The classical mineralization process at seeps is driven by an increase in alkalinity due to AOM, and results in the precipitation of $CaCO_3$ as massive reef-like bodies, irregular crusts, or regular concretions (Fig. 7). These “seep carbonates” often carry not only their inherent AOM signature but also capture detritus, aerobic seep fauna (including MOB), as well as organic matter from background sources during their ongoing precipitation.

Initially, most methane-derived carbonates are typically comprised either of microcrystalline calcite (micrite) or fibrous, often botryoidal aragonite (e.g., Teichert et al. 2005). These two phases are immediately related to the microbial activity of



Fig. 7 Examples of modern and ancient methane-derived carbonates. Top, outcrop of Late Triassic seep deposits at Graylock Butte, Oregon, U.S.A (Peckmann et al. 2011); bottom left, block of a heavily brecciated Miocene seep carbonate showing multiple generations of (now silicified) aragonite-cements (near Knappton Site, Oregon, U.S.A.); bottom right, massive modern seep carbonate block from Hydrate Ridge (SE-Knoll vent site, Cascadia, off Oregon, U.S.A.). (Image credit: J. Peckmann (a), V.E. Hoffmann (b), V. Liebetrau (c))

AOM consortia and contain most of the biomarker signal by far (Leefmann et al. 2008). Later processes encompass re-crystallization of aragonite to calcite, or precipitation of sparry calcite cements and, sometimes, siliceous phases that may replace earlier carbonate phases to some degree (Kuechler et al. 2012; Hagemann et al. 2013). Specific carbonate fabrics include, in order of decreasing significance for seep-dominated environments, (i) inverted stromatactoid cavities, (ii) upside-down stromatolites, (iii) globular fabrics, (iv) botryoidal aragonite, (v) micritic nodules, (vi) fractures, (vii) clotted micrites, and (viii) constructive seams representing fossilized biofilms (for details, see Peckmann and Thiel 2004).

Due to the incorporation of oxidized methane carbon, seep carbonates are isotopically light, with $\delta^{13}\text{C}_{\text{carbonate}}$ values often dropping below -30% . However, values

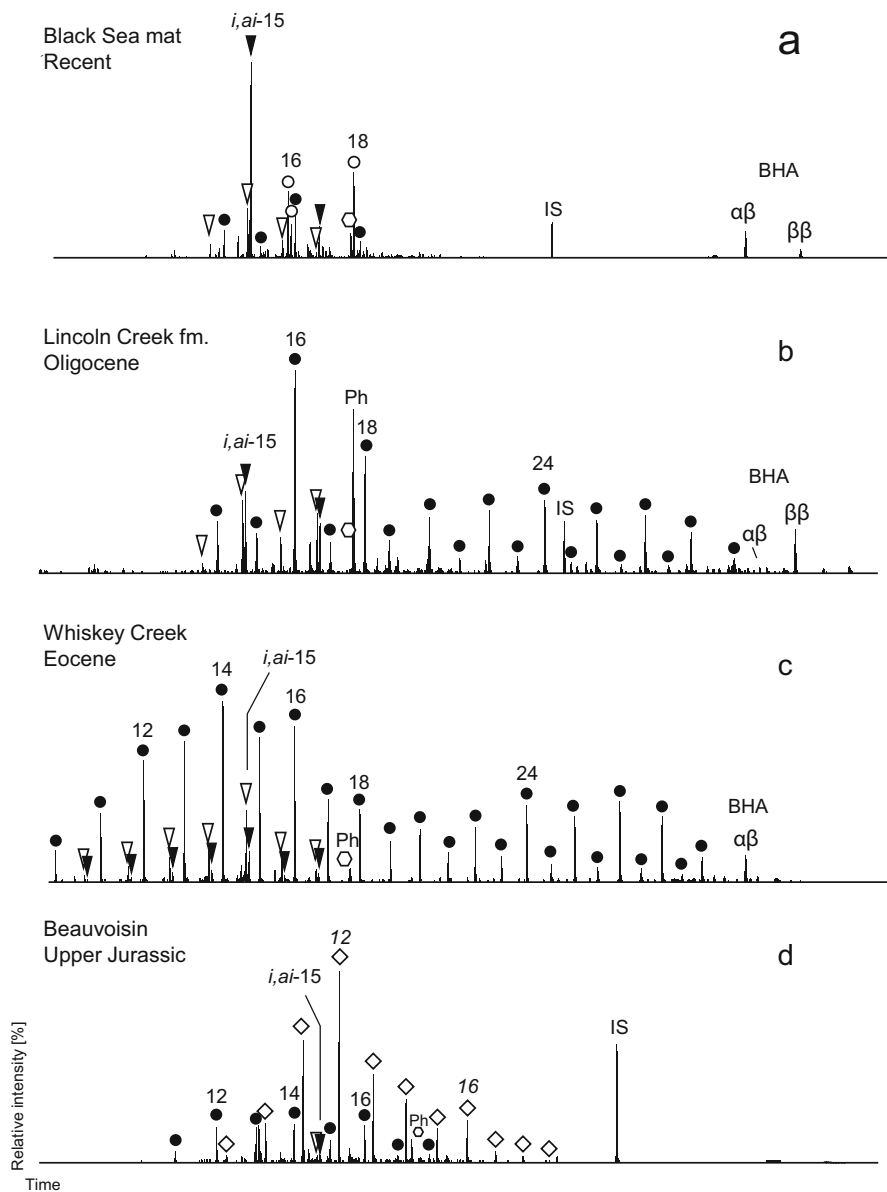


Fig. 8 Total ion current chromatograms (subtracted for background) of carboxylic acids (methyl esters) extracted from selected seep deposits. Age and thermal maturity increase from (a) to (d) and illustrate the compositional changes in the biomarker distributions during burial. Filled circles/numbers indicate *n*-alkanoic acids of the respective carbon chain length. Open circles = monoenoic C_{16} - and C_{18} -acids, respectively; open and filled triangles = ω -2- (*i*-) and ω -3- (*ai*-) methylated alkanoids; Ph = phytanic acid (VII); hexagon = ω -cyclohexylundecanoic acid (partly coeluting with Ph); BHA $\alpha\beta$, $\beta\beta$ = 17 α (H),21 β (H)-bis-homohopanoic acid (syn. dihomohopanoic acid, Fig. 4, IV; geological configuration) and 17 β (H),21 β (H)-bis-homohopanoic acid (ditto, biological

even higher than +5% may occur in some individual carbonate phases, typically from those forming later in the diagenetic sequence (Peckmann and Thiel 2004). Such heavy signatures reflect methane formation rather than oxidation, if carbonate is precipitated from a residual, ^{13}C -enriched CO_2 pool utilized by archaeal methanogenesis (Campbell 2006). It should also be noted that ancient petroleum seeps may likewise be associated with isotopically light carbonates and are sometimes difficult to distinguish from actual methane seep deposits. Recent work suggested the combined, phase-specific distribution of Rare Earth elements, Mo, and U as a means to discern ancient oil seeps from actual methane seeps (Smrzka et al. 2016).

Preservation aspects – Like for all other paleoenvironments, limitations on the use of lipid biomarkers from seep deposits arise from early biodegradation, thermal overprint, and introduction of petroleum-like compounds from other rocks via secondary migration. However, methane seep carbonates can be regarded as “biomarker-friendly” environments that often show a remarkable preservation of their indigenous compound inventory. This is due to their rapid authigenic “self-lithification” in microbial carbonate phases which provides an early sealing of organic compounds from microbial turnover (cf. Thiel et al. 1999; Leefmann et al. 2008; Peckmann et al. 2009). Another important factor may be that AOM consumes sulfate (and/or other electron acceptors) which is then no longer available for the remineralization of organic matter (Hinrichs et al. 2000). A further beneficial aspect when studying biomarkers in ancient seep deposits is the feasibility to differentiate in-situ biomarkers from allochthonous compounds not only by their structures but also by their $\delta^{13}\text{C}$ values, as outlined above. Last, but not least, seep carbonates are, unlike reef carbonates, commonly embedded in fine-grained, hemipelagic sediments, which may provide an effective sealing against diagenetic fluids (Peckmann and Thiel 2004).

Sooner or later during burial, however, methane-derived biomarkers will inevitably become influenced by thermal overprint and secondary migration which tend to erase and/or dilute the primary signal. Hence, many thermally mature seep limestones in pre-mesozoic rocks failed to provide useful biomarkers. Currently, the oldest robust biomarker evidence for AOM is from the Late Pennsylvanian of Namibia. These deposits revealed hydrocarbon biomarkers that still clearly relate to present-day lipid distributions at seeps (Birgel et al. 2008a). A number of organic geochemical studies on ancient seeps exist that allow to re-construct quite exactly the alterations that the relevant biomarkers undergo during burial (see also Figs. 6 and 8).

Archaeal biomarkers – Crocetenes, $\text{PMI}\Delta$ and higher unsaturated isoprenoids rapidly disappear during diagenesis, possibly because of enhanced microbial turnover, binding to macromolecules or reductive conversion to the saturated



Fig. 8 (continued) configuration), respectively; open squares = α,ω -dicarboxylic acids of the respective carbon chain length; IS = internal standard. (Originally published in Peckmann and Thiel (2004), published with kind permission of Elsevier B.V. All rights reserved)

hydrocarbon counterparts. As a result, the saturated isoprenoids, most prominently crocetane and PMI, typically show enhanced relative concentrations in ancient seep deposits (Fig. 6, compare a vs. b–d). ^{13}C -depleted crocetane, probably sourced by ANME-2, is a fairly specific biomarker for AOM. However, compared to PMI, crocetane shows a more scattered distribution at seeps, and its absence has been reported in several cases. Even worse, additional sources such as thermal breakdown of higher irregular isoprenoids, carotenoids, or direct synthesis by methanogenic archaea have been suggested for crocetane (Barber et al. 2001; Greenwood and Summons 2003; Orphan et al. 2008; for a detailed discussion, see Schinteie and Brocks 2017), making the compound-specific $\delta^{13}\text{C}$ information even more inevitable for a sound interpretation.

ANME-2-derived archaeol-type diethers first lose their headgroups and subsequently hydrolyze to phytanol which will further defunctionalize to form the hydrocarbons phytane (2,6,10,14-methylhexadecane) and, to a minor extent, pristane (2,6,10,14-tetramethylpentadecane, C_{19}), and even shorter isoprenoids. This conversion has not been fully completed in many Cenozoic deposits, where archaeol and even hydroxyarchaeol have been found still intact (e.g., Peckmann and Thiel 2004; Birgel et al. 2008a; Hagemann et al. 2013). Exceptionally, the rare MDGDs containing 0, 1, or 2 cyclopentane rings have been found at high abundance in Eocene seep carbonates from the Balkanides foreland (De Boever et al. 2009).

GDGTs with 0–2 cyclopentyl rings probably decompose to form α,ω -biphytanedioles and/or the respective diacids (e.g., Birgel et al. 2008b). It has been discussed in the literature whether particularly the acids could have a direct biosynthetic origin (Schouten et al. 1998, Birgel et al. 2006a; Smrzka et al. 2017), but the most parsimonious interpretation is to consider them as degradation products of GDGT (Liu et al. 2016). In thermally more mature sediments, these compounds further defunctionalize to form preferentially the corresponding C_{40} and C_{39} head-to-head linked isoprenoid hydrocarbons, and possibly shorter homologues, with the acyclic biphytane derivatives showing a greater diagenetic stability as the cyclic varieties (Peckmann and Thiel 2004; Peckmann et al. 2009). These observations are in good agreement with earlier results from experimental pyrolysis of archaeal biomass (Rowland 1990).

Bacterial biomarkers – Bacteria-derived neutral lipids and fatty acids can be expected to rapidly degrade within the uppermost part of unlithified sediments at methane seeps (Teske et al. 2002). However, ancient methane-seep deposits with pronounced carbonate formation apparently sustained the persistence of SRB-derived fatty acids and alcohols, and even intact DAGE within the carbonate lattice (Peckmann and Thiel 2004). Unsaturated carbon chains which are prominent at modern seeps (Elvert et al. 2003; Fig. 6a) are missing in even the most immature rocks, indicating that these lipids have been rapidly reduced and/or degraded upon early diagenesis. *n*-Tricosenes, biomarkers for unknown bacteria associated with AOM (see above), are obviously reduced in part to *n*-tricosane, similar to the unsaturated isoprenoid hydrocarbons discussed above. As a result, the hydrocarbon fractions of many ancient seep deposits show a peak of isotopically light *n*-tricosane sticking out from the adjacent *n*-alkanes, which provides a fairly stable and specific

hydrocarbon fingerprint for the anaerobic cycling of methane carbon (see Fig. 6d; Thiel et al. 2001b).

Fatty acids found in immature Cenozoic seep deposits encompass saturated, ^{13}C -depleted, even-numbered *n*-fatty acids, iso- and anteiso-branched, and ω -cyclohexylundecanoic acids, with similar carbon skeletons as they are found in modern settings (Peckmann and Thiel 2004; Birgel et al. 2006b; 2008b; Fig. 8b). With increasing thermal overprint, bacterial fatty acids are modified such that *n*-alkanoic acids show a much lower even-over-odd carbon number preference and an increase in saturated homologues (Fig. 8c).

Likewise, the more SRB-specific, terminally branched iso- and anteiso-isomers decrease in abundance and approach more random patterns with carbon chains shorter than in the putative precursor lipids (Fig. 8b, c). Along with these changes, the extent of $\delta^{13}\text{C}$ depletions in fatty acids typically decreases so that fatty acids in thermally mature, methane-derived rocks older than Jurassic are not likely to carry much information on methane-derived processes any more (Fig. 8d). Obviously, some of these compounds are partly transformed to *i*- and *ai*-alkanes that may still show isotopic depletions when compared to the adjacent *n*-alkanes (Fig. 6d; Peckmann and Thiel 2004; Birgel et al 2006b).

5 Research Needs

Research over the last two decades has provided an enormous wealth on information about the processes prevailing in modern methane-rich environments, and the major biomarker constraints on seepage activity are well established. Yet, the use of refined techniques, particularly focusing on the study of intact polar lipids and their headgroups continue to improve our understanding of the methane-consuming processes, and reveal an ever more complex picture of the biota involved (e.g., Yoshinaga et al. 2015). Whereas the findings from modern environments are useful for the interpretation of modern and sub-recent (Quaternary) environments, they have a limited outreach for older rocks where only the reduced carbon skeletons remain which tend to be more and more erased by thermal overprint. Here, the smart combination of biomarker, petrographic, isotopic, and inorganic geochemical traits should be further established and improved to reveal better constraints on methane carbon sources, biogeochemical pathways, and the intensity of seepage (e.g., Peckmann et al. 2009; Lin et al. 2018).

Presently, the oldest biomarker record for AOM is from a 300 Ma old Late Pennsylvanian seep. It was convincingly shown that AOM involved the same consortia of ANME and SRB as in modern environments (Birgel et al. 2008a). Apart from this, the Paleozoic record of methane-derived biomarkers remains scarce and awaits to be enhanced (and pushed back) by further studies. In even older, i.e., Precambrian settings, the 1.64-Ga-old Barney Creek Formation sticks out as a notable exception, because it provides biomarkers that enable a unique look to the methane-derived biogeochemical processes in the Proterozoic (Brocks et al. 2005). However, biomarker evidence obtained from even earlier periods of Earth's history

turned out to be elusive due to postdepositional processes, and compromised by contamination (French et al. 2015). As the contamination issues are particularly virulent for the bitumen fractions of ancient rocks, the study of kerogen-bound biomarkers could probably provide an alternative avenue for biomarker research on methane carbon cycling in very ancient rocks.

References

- Badr O, Probert SD, O'Callaghan PW (1992) Sinks for atmospheric methane. *Appl Energy* 41:137–147
- Barber CJ, Grice K, Bastow TP, Alexander R, Kagi RI (2001) The identification of crocetane in Australian crude oils. *Org Geochem* 32:943–947
- Beal EJ, House CH, Orphan VJ (2009) Manganese- and iron-dependent marine methane oxidation. *Science* 325:184–187
- Berndmeyer C, Thiel V, Schmale O, Blumenberg M (2013) Biomarkers for aerobic methanotrophy in the water column of the stratified Gotland deep (Baltic Sea). *Org Geochem* 55:103–111
- Bertram S, Blumenberg M, Michaelis W, Siegert M, Krüger M, Seifert R (2013) Methanogenic capabilities of ANME-archaea deduced from ^{13}C -labelling approaches. *Environ Microbiol* 15:2384–2393
- Bird CW, Lynch JM, Pirt FJ, Reid WW (1971) Steroids and squalene in *Methylococcus capsulatus* grown on methane. *Nature* 230:473–474
- Birgel D, Peckmann J (2008) Aerobic methanotrophy at ancient marine methane seeps: a synthesis. *Org Geochem* 39:1659–1667
- Birgel D, Thiel V, Hinrichs K-U, Elvert M, Campbell KA, Reitner J, Farmer JD, Peckmann J (2006a) Lipid biomarker patterns of methane-seep microbialites from the Mesozoic convergent margin of California. *Org Geochem* 37:1289–1302
- Birgel D, Peckmann J, Klautzsch S, Thiel V, Reitner J (2006b) Anaerobic and aerobic oxidation of methane at late cretaceous seeps in the western interior seaway. *Geomicrobiol J* 23:565–577
- Birgel D, Himmeler T, Freiwald A, Peckmann J (2008a) A new constraint on the antiquity of anaerobic oxidation of methane: late Pennsylvanian seep limestones from southern Namibia. *Geology* 36:543–546
- Birgel D, Elvert M, Han X, Peckmann J (2008b) ^{13}C -depleted biphytanic diacids as tracers of past anaerobic oxidation of methane. *Org Geochem* 39:152–156
- Birgel D, Feng D, Roberts HH, Peckmann J (2011) Changing redox conditions at cold seeps as revealed by authigenic carbonates from Alaminos Canyon, northern Gulf of Mexico. *Chem Geol* 285:82–96
- Blumenberg M, Seifert R, Reitner J, Pape T, Michaelis W (2004) Membrane lipid patterns typify distinct anaerobic methanotrophic consortia. *Proc Natl Acad Sci U S A* 101:11111–11116
- Blumenberg M, Hoppert M, Krüger M, Dreier A, Thiel V (2012) Novel findings on hopanoid occurrences among sulfate reducing bacteria: is there a direct link to nitrogen fixation? *Org Geochem* 49:1–5
- Blumenberg M, Berndmeyer C, Moros M, Muschalla M, Schmale O, Thiel V (2013) Bacteriohopanepolyols record stratification, nitrogen fixation and other biogeochemical perturbations in Holocene sediments of the Central Baltic Sea. *Biogeosciences* 10:2725–2735
- Boetius A, Ravensschlag K, Schubert CJ, Rickert D, Widdel F, Gieseke A, Amann R, Jørgensen BB, Witte U, Pfannkuche O (2000) A marine microbial consortium apparently mediating anaerobic oxidation of methane. *Nature* 407:623–626
- Bodelier PL, Gillisen MJB, Hordijk K, Damsté JSS, Rijpstra WIC, Geenevasen JA, Dunfield PF (2009) A reanalysis of phospholipid fatty acids as ecological biomarkers for methanotrophic bacteria. *ISME J* 3:606–617
- Bowman JP, Skerratt JH, Nichols PD, Sly LI (1991) Phospholipid fatty acid and lipopolysaccharide fatty acid signature lipids in methane-utilizing bacteria. *FEMS Microbiol Ecol* 85:15–22

- Bowman JP (2014) The family *Methylococcaceae*. In: Rosenberg E, DeLong EF, Lory S, Stackebrandt E, Thompson F (eds) The prokaryotes. Gammaproteobacteria. Springer, Berlin/Heidelberg, pp 411–440
- Brooks JJ, Love GD, Summons RE, Knoll AH, Logan GA, Bowden SA (2005) Biomarker evidence for green and purple Sulphur bacteria in a stratified Palaeoproterozoic Sea. *Nature* 437:866–870
- Bürgmann H (2011) Methane oxidation (aerobic). In: Encyclopedia of geobiology. Springer, Dordrecht, pp 575–578
- Burhan RYP, Trendel JM, Adam P, Wehrung P, Albrecht P, Nissenbaum A (2002) Fossil bacterial ecosystem at methane seeps: origin of organic matter from Be’eri sulfur deposit, Israel. *Geochim Cosmochim Acta* 66(23):4085–4101
- Campbell KA (2006) Hydrocarbon seep and hydrothermal vent paleoenvironments and paleontology: past developments and future research directions. *Palaeogeogr Palaeoclimatol Palaeoecol* 232:362–407
- Chevalier N, Bouloubassi I, Stadnitskaia A, Taphanel MH, Damsté JSS (2014) Lipid biomarkers for anaerobic oxidation of methane and sulphate reduction in cold seep sediments of Nyegga pockmarks (Norwegian margin): discrepancies in contents and carbon isotope signatures. *Geo-Mar Lett* 34:269–280
- Collister JW, Summons RE, Lichtfouse E, Hayes JM (1992) An isotopic biogeochemical study of the Green River oil shale. *Org Geochem* 19:265–276
- Davies KL, Pancost RD, Edwards ME, Anthony KMW, Langdon PG (2016) Diploptene $\delta^{13}\text{C}$ values from contemporary thermokarst lake sediments show complex spatial variation. *Biogeosciences* 13:2611–2621
- De Boever E, Birgel D, Thiel V, Muchez P, Peckmann J, Dimitrov L, Swennen R (2009) The formation of giant tubular concretions triggered by anaerobic oxidation of methane as revealed by archaeal molecular fossils (lower Eocene, Varna, Bulgaria). *Palaeogeogr Palaeoclimatol Palaeoecol* 280:23–36
- Dickens GR (2003) Rethinking the global carbon cycle with a large, dynamic and microbially mediated gas hydrate capacitor. *Biotechnol Bioeng* 213:169–183
- Dueck TA, De Visser R, Poorter H, Persijn S, Gorissen A, De Visser W, Schapendonk A, Verhagen J, Snel J, Harren FJ (2007) No evidence for substantial aerobic methane emission by terrestrial plants: a ^{13}C labelling approach. *New Phytol* 175:29–35
- Dunfield PF, Yuryev A, Senin P, Smirnova AV, Stott MB, Hou S et al (2007) Methane oxidation by an extremely acidophilic bacterium of the phylum *Verrucomicrobia*. *Nature* 450:879–882
- Elvert M, Suess E, Whiticar MJ (1999) Anaerobic methane oxidation associated with marine gas hydrates: superlight C-isotopes from saturated and unsaturated C_{20} and C_{25} irregular isoprenoids. *Naturwissenschaften* 86:295–300
- Elvert M, Whiticar MJ, Suess E (2001) Diploptene in varved sediments of Saanich inlet: indicator of increasing bacterial activity under anaerobic conditions during the Holocene. *Mar Geol* 174:371–383
- Elvert M, Boetius A, Knittel K, Jørgensen BB (2003) Characterization of specific membrane fatty acids as chemotaxonomic markers for sulfate-reducing bacteria involved in anaerobic oxidation of methane. *Geomicrobiol J* 20:403–419
- Elvert M, Niemann H (2008) Occurrence of unusual steroids and hopanoids derived from aerobic methanotrophs at an active marine mud volcano. *Org Geochem* 39:167–177
- Etiopie G, Sherwood Lollar B (2013) Abiotic methane on earth. *Rev Geophys* 51:276–299
- Ettwig KF, Butler MK, Le Paslier D, Pelletier E, Mangenot S, Kuypers MM et al (2010) Nitrite-driven anaerobic methane oxidation by oxygenic bacteria. *Nature* 464:543–548
- Fischer F, Tropsch H (1923) Ueber die Herstellung synthetischer Ölgemische (Synthol) durch Aufbau aus Kohlenoxyd und Wasserstoff. *Brennst Chem* 4:276–285
- French KL, Hallmann C, Hope JM, Schoon PL, Zumberge JA, Hoshino Y et al (2015) Reappraisal of hydrocarbon biomarkers in Archean rocks. *Proc Natl Acad Sci U S A* 112:5915–5920
- Goedert JL, Thiel V, Schmale O, Rau WW, Michaelis W, Peckmann J (2003) The late Eocene ‘Whiskey Creek’ methane-seep deposit (western Washington state). Part I: geology, palaeontology, and molecular geobiology. *Facies* 48:223–240

- Greenwood PF, Summons RE (2003) GC–MS detection and significance of crocetane and penta-methylcosane in sediments and crude oils. *Org Geochem* 34:1211–1222
- Hagemann A, Leefmann T, Peckmann J, Hoffmann VE, Thiel V (2013) Biomarkers from individual carbonate phases of an Oligocene cold-seep deposit, Washington state, USA. *Lethaia* 46:7–18
- Xu X, Yuan F, Hanson PJ, Wullschlegler SD, Thornton PE, Riley WJ, Song X, Graham DE, Song C, Tian H (2016) Reviews and syntheses: four decades of modeling methane cycling in terrestrial ecosystems. *Biogeosciences* 13:3735–3755
- Hanson RS, Hanson TE (1996) Methanotrophic bacteria. *Microbiol Rev* 60:439–471
- Haroon MF, Hu S, Shi Y, Imelfort M, Keller J, Hugenholtz P et al (2013) Anaerobic oxidation of methane coupled to nitrate reduction in a novel archaeal lineage. *Nature* 500:567–570
- Hinrichs KU, Hayes JM, Sylva SP, Brewer PG, EF DL (1999) Methane-consuming archaeobacteria in marine sediments. *Nature* 398:802–805
- Hinrichs K-U, Summons RE, Orphan V, Sylva SP, Hayes JM (2000) Molecular and isotopic analysis of anaerobic methane-oxidizing communities in marine sediments. *Org Geochem* 31:1685–1701
- Hinrichs KU, Hmelo LR, Sylva SP (2003) Molecular fossil record of elevated methane levels in late Pleistocene coastal waters. *Science* 299:1214–1217
- Höfle ST, Kusch S, Talbot HM, Mollenhauer G, Zubrzycki S, Burghardt S, Rethemeyer J (2015) Characterisation of bacterial populations in Arctic permafrost soils using bacteriohopanepolyols. *Org Geochem* 88:1–16
- Holler T, Widdel F, Knittel K, Amann R, Kellermann MY, Hinrichs KU et al (2011) Thermophilic anaerobic oxidation of methane by marine microbial consortia. *ISME J* 5:1946–1956
- Intergovernmental Panel on Climate Change (IPCC) (2013) Climate change 2013: the physical science basis. Contribution of working group I to the fifth assessment report of the intergovernmental panel on climate change. Cambridge University Press, Cambridge, UK/New York
- Karl DM, Beversdorf L, Björkman KM, Church MJ, Martinez A, Delong EF (2008) Aerobic production of methane in the sea. *Nat Geosci* 1:473–478
- Keppler F, Hamilton JTG, Brass M, Rockmann T (2006) Methane emissions from terrestrial plants under aerobic conditions. *Nature* 439:187–191
- Kirschke S, Bousquet P, Ciais P, Saunois M, Canadell JG, Dlugokencky EJ et al (2013) Three decades of global methane sources and sinks. *Nat Geosci* 6:813–823
- Knittel K, Boetius A (2009) Anaerobic oxidation of methane: progress with an unknown process. *Annu Rev Microbiol* 63:311–334
- Knittel K, Boetius A, Lemke A, Eilers H, Lochte K, Pfannkuche O, Linke P, Amann R (2003) Activity, distribution, and diversity of sulfate reducers and other bacteria in sediments above gas hydrate (Cascadia Margin, Oregon). *Geomicrobiol J* 20(4):269–294
- Kool DM, Talbot HM, Rush D, Ettwig K, Damsté JSS (2014) Rare bacteriohopanepolyols as markers for an autotrophic, intra-aerobic methanotroph. *Geochim Cosmochim Acta* 136:114–125
- Kuechler RR, Birgel D, Kiel S, Freiwald A, Goedert JL, Thiel V, Peckmann J (2012) Miocene methane-derived carbonates from southwestern Washington, USA, and a model for silicification at seeps. *Lethaia* 45:259–273
- Leefmann T, Bauermeister J, Kronz A, Liebetrau V, Reitner J, Thiel V (2008) Miniaturized biosignature analysis reveals implications for the formation of cold seep carbonates at hydrate ridge (off Oregon, USA). *Biogeosciences* 5:731–738
- Lenhart K, Bunge M, Ratering S, New TR, Schuttman I, Greule M, Kammann C, Schnell S, Muller C, Zorn H, Keppler F (2012) Evidence for methane production by saprotrophic fungi. *Nat Commun* 3:1046
- Lenhart K, Klintzsch T, Langer G, Nehrke G, Bunge M, Schnell S, Keppler F (2016) Evidence for methane production by the marine algae *Emiliana huxleyi*. *Biogeosciences* 13:3163–3174
- Lin Z, Sun X, Strauss H, Lu Y, Böttcher ME, Teichert BM, Gong J, Xu L, Liang J, Lu H, Peckmann, J (2018) Multiple sulfur isotopic evidence for the origin of elemental sulfur in an iron-dominated gas hydrate-bearing sedimentary environment. *Marine Geology* 403:271–284

- Liu XL, Birgel D, Elling FJ, Sutton PA, Lipp JS, Zhu R et al (2016) From ether to acid: a plausible degradation pathway of glycerol dialkyl glycerol tetraethers. *Geochim Cosmochim Acta* 183:138–152
- Lu H, Sheng G, Peng PA, Ma Q, Lu Z (2011) Identification of C₂₄ and C₂₅ lanostanes in tertiary sulfur rich crude oils from the Jinxian sag, Bohai Bay basin, northern China. *Org Geochem* 42:146–155
- Madigan MT, Martinko JM, Parker J (2003) *Brock biology of microorganisms*. Prentice Hall/Pearson Education, Upper Saddle River
- Malyan SK, Bhatia A, Kumar A, Gupta DK, Singh R, Kumar SS et al (2016) Methane production, oxidation and mitigation: a mechanistic understanding and comprehensive evaluation of influencing factors. *Sci Total Environ* 572:874–896
- McCollom TM (2013) Laboratory simulations of abiotic hydrocarbon formation in Earth's deep subsurface. *Rev Mineral Geochem* 75:467–494
- McCollom TM, Ritter G, Simoneit BRT (1999) Lipid synthesis under hydrothermal conditions by Fischer-Tropsch-type reactions. *Orig Life Evol Biosph* 29:153–166
- Ménot G, Bard E (2010) Geochemical evidence for a large methane release during the last deglaciation from Marmara Sea sediments. *Geochim Cosmochim Acta* 74:1537–1550
- Michaelis W, Seifert R, Nauhaus K, Treude T, Thiel V, Blumenberg M et al (2002) Microbial reefs in the Black Sea fueled by anaerobic oxidation of methane. *Science* 297:1013–1015
- Nauhaus K, Treude T, Boetius A, Krüger M (2005) Environmental regulation of the anaerobic oxidation of methane: a comparison of ANME-I and ANME-II communities. *Environ Microbiol* 7:98–106
- Niemann H, Lösekann T, de Beer D, Elvert M, Nadalig T, Knittel K, Amann R, Sauter EJ, Schlüter M, Klages M, Foucher JP, Boetius A (2006) Novel microbial communities of the Haakon Mosby mud volcano and their role as a methane sink. *Nature* 443:854–858
- Orphan VJ, House CH, Hinrichs KU, McKeegan KD and DeLong EF (2002) Multiple archaeal groups mediate methane oxidation in anoxic cold seep sediments. *Proc Natl Acad Sci U S A* 99:7663–7668
- Orphan VJ, Jahnke LL, Embaye T, Turk KA, Pernthaler A, Summons RE, Des Marais DJ (2008) Characterization and spatial distribution of methanogens and methanogenic biosignatures in hypersaline microbial mats of Baja California. *Geobiology* 6:376–393
- Parfenova TM (2011) Hydrocarbons of the lanostane homologous series in the Phanerozoic organic matter and their probable biologic sources. *Russ Geol Geophys* 52:773–780
- Pancost RD, Damsté JSS, de Lint S, van der Maarel MJ, Gottschal JC (2000) Biomarker evidence for widespread anaerobic methane oxidation in Mediterranean sediments by a consortium of methanogenic archaea and bacteria. *Appl Environ Microbiol* 66:1126–1132
- Pancost RD, Bouloubassi I, Aloisi G, Damsté JSS (2001) Three series of non-isoprenoidal dialkyl glycerol diethers in cold-seep carbonate crusts. *Org Geochem* 32:695–707
- Paul BG, Ding H, Bagby SC, Kellermann MY, Redmond MC, Andersen GL, Valentine DL (2017) Methane-oxidizing Bacteria shunt carbon to microbial Mats at a marine hydrocarbon seep. *Front Microbiol* 8:186
- Peckmann J, Thiel V (2004) Carbon cycling at ancient methane-seeps. *Chem Geol* 205:443–467
- Peckmann J, Thiel V, Reitner J, Taviani M, Aharon P, Michaelis W (2004) A microbial mat of a large sulfur bacterium preserved in a Miocene methane-seep limestone. *Geomicrobiol J* 21:247–255
- Peckmann J, Birgel D, Kiel S (2009) Molecular fossils reveal fluid composition and flow intensity at a cretaceous seep. *Geology* 37:847–850
- Peckmann J, Kiel S, Sandy MR, Taylor DG, Goedert JL (2011) Mass occurrences of the brachiopod *Halorella* in late Triassic methane-seep deposits, eastern Oregon. *J Geol* 119:207–220
- Peng PA, Morales-Izquierdo A, Fu J, Sheng G, Hogg A, Strausz OP (1998) Lanostane sulfides in an immature crude oil. *Org Geochem* 28(1–2):125–134
- Petrišič MG, Heath E, Ogrinc N (2017) Lipid biomarkers and their stable carbon isotopes in oxic and anoxic sediments of lake bled (NW Slovenia). *Geomicrobiol J* 34(7):606–617

- Proskurowski G, Lilley MD, Seewald JS, Früh-Green GL, Olson EJ, Lupton JE, Sylva SP, Kelley DS (2008) Abiogenic hydrocarbon production at lost City hydrothermal field. *Science* 319:604–607
- Raghoebarsing AA, Pol A, Van de Pas-Schoonen KT, Smolders AJ, Ettwig KF, Rijpstra WIC, Schouten S, Damsté JS, Op den Camp HJM, Jetten MS, Strous M (2006) A microbial consortium couples anaerobic methane oxidation to denitrification. *Nature* 440:918–921
- Reeburgh WS (2007) Oceanic methane biogeochemistry. *Chem Rev* 107:486–513
- Reitner J, Peckmann J, Reimer A, Schumann G, Thiel V (2005) Methane-derived carbonate build-ups and associated microbial communities at cold seeps on the lower Crimean shelf (Black Sea). *Facies* 51:66–79
- Repeta DJ, Ferron S, Sosa OA, Johnson CG, Repeta LD, Acker M, DeLong EF, Karl DM (2016) Marine methane paradox explained by bacterial degradation of dissolved organic matter. *Nat Geosci* 9:884–887
- Riedinger N, Formolo MJ, Lyons TW, Henkel S, Beck A, Kasten S (2014) An inorganic geochemical argument for coupled anaerobic oxidation of methane and iron reduction in marine sediments. *Geobiology* 12:172–181
- Robson JN, Rowland SJ (1993) Synthesis, chromatographic and spectral characterisation of 2,6,11,15-tetramethylhexadecane (crocetane) and 2,6,9,13-tetramethyltetradecane: reference acyclic isoprenoids for geochemical studies. *Organic Geochemistry* 20:1093–1098
- Rohmer M, Bouvier-Navé P, Ourisson G (1984) Distribution of hopanoid triterpenes in prokaryotes. *J Gen Microbiol* 130:1137–1150
- Rossel PE, Elvert M, Ramette A, Boetius A, Hinrichs KU (2011) Factors controlling the distribution of anaerobic methanotrophic communities in marine environments: evidence from intact polar membrane lipids. *Geochim Cosmochim Acta* 75:164–184
- Rowland SJ (1990) Production of acyclic isoprenoid hydrocarbons by laboratory maturation of methanogenic bacteria. *Org Geochem* 15:9–16
- Rush D, Osborne KA, Birgel D, Kappler A, Hirayama H, Peckmann J et al (2016) The Bacterio-hopanepolyol inventory of novel aerobic methane oxidising Bacteria reveals new biomarker signatures of aerobic Methanotrophy in marine systems. *PLoS One* 11:Art e0165635
- Rushdi AI, Simoneit BRT (2001) Lipid formation by aqueous Fischer-Tropsch type synthesis over a temperature range of 100 to 400°C. *Orig Life Evol Biosph* 31:103–118
- Ruppel CD, Kessler JD (2017) The interaction of climate change and methane hydrates. *Rev Geophys* 55:126–168
- Sahm H, Rohmer M, Bringer-Meyer S, Sprenger GA, Welle R (1993) Biochemistry and physiology of hopanoids in bacteria. *Adv Microb Physiol* 35:247–273
- Saunio M, Bousquet P, Poulter B, Peregon A, Ciais P, Canadell JG et al (2016) The global methane budget 2000–2012. *Earth Syst Sci Data* 8:697
- Schinteie R, Brocks JJ (2017) Paleoeology of Neoproterozoic hypersaline environments: biomarker evidence for haloarchaea, methanogens, and cyanobacteria. *Geobiology* 15:641–663
- Schouten S, Bowman JP, Rijpstra WIC, Sinninghe Damsté JS (2000) Sterols in a psychrophilic methanotroph *Methylosphaera hansonii*. *FEMS Microbiol Lett* 186:193–195
- Schouten S, Hoefs MJ, Koopmans MP, Bosch HJ, Damsté JSS (1998) Structural characterization, occurrence and fate of archaeal ether-bound acyclic and cyclic biphytanes and corresponding diols in sediments. *Org Geochem* 29:1305–1319
- Schouten S, Wakeham SG, Hopmans EC, Damsté JSS (2003) Biogeochemical evidence that thermophilic archaea mediate the anaerobic oxidation of methane. *Appl Environ Microbiol* 69:1680–1686
- Schubert CJ (2011) Methane, origin. In: *Encyclopedia of geobiology*. Springer, Dordrecht, pp 578–586
- Smrzka D, Zwicker J, Klügel A, Monien P, Bach W, Bohrmann G, Peckmann J (2016) Establishing criteria to distinguish oil-seep from methane-seep carbonates. *Geology* 44:667–670

- Smrzka D, Zwicker J, Kolonic S, Birgel D, Little CT, Marzouk AM et al (2017) Methane seepage in a cretaceous greenhouse world recorded by an unusual carbonate deposit from the Tarfaya Basin, Morocco. *Depositional Rec* 3:4–37
- Spooner N, Rieley G, Collister JW, Lander M, Cranwell PA, Maxwell JR (1994) Stable carbon isotopic correlation of individual biolipids in aquatic organisms and a lake bottom sediment. *Org Geochem* 21:823–827
- Stadnitskaia A, Baas M, Ivanov MK, Van Weering TC, Sinninghe Damsté JS (2003) Novel archaeal macrocyclic diether core membrane lipids in a methane-derived carbonate crust from a mud volcano in the Sorokin trough, NE Black sea. *Archaea* 1:165–173
- Summons RE, Jahnke LL, Roksandic Z (1994) Carbon isotopic fractionation in lipids from methanotrophic bacteria: relevance for interpretation of the geochemical record of biomarkers. *Geochim Cosmochim Acta* 58:2853–2863
- Taipale SJ, Hiltunen M, Vuorio K, Peltomaa E (2016) Suitability of phytosterols alongside fatty acids as chemotaxonomic biomarkers for phytoplankton. *Front Plant Sci* 7:212
- Takai K, Nakamura K, Toki T, Tsunogai U, Miyazaki M, Miyazaki J, Hirayama H, Nakagawa S, Nunoura T, Horikoshi K (2008) Cell proliferation at 122°C and isotopically heavy CH₄ production by a hyperthermophilic methanogen under high-pressure cultivation. *Proc Natl Acad Sci U S A* 105:10949–10954
- Talbot HM, Farrimond P (2007) Bacterial populations recorded in diverse sedimentary biohopanoid distributions. *Org Geochem* 38:1212–1225
- Talbot HM, Watson DF, Murrel JC, Carter JF, Farrimond P (2001) Analysis of intact bacteriohopanepolyols from methanotrophic bacteria by reversed-phase high-performance liquid chromatography–atmospheric pressure chemical ionisation mass spectrometry. *J Chromatogr A* 921:175–185
- Talbot HM, Handley L, Spencer-Jones CL, Dinga BJ, Schefuß E, Mann PJ et al (2014) Variability in aerobic methane oxidation over the past 1.2 Myrs recorded in microbial biomarker signatures from Congo fan sediments. *Geochim Cosmochim Acta* 133:387–401
- Teichert BM, Bohrmann G, Suess E (2005) Chemoherms on Hydrate Ridge—Unique microbially-mediated carbonate build-ups growing into the water column. *Palaeogeography, Palaeoclimatology, Palaeoecology* 227:67–85
- Teske A, Hinrichs KU, Edgcomb V, de Vera GA, Kysela D, Sylva SP et al (2002) Microbial diversity of hydrothermal sediments in the Guaymas Basin: evidence for anaerobic methanotrophic communities. *Appl Environ Microbiol* 68:1994–2007
- Thiel V, Heim C, Arp G, Hahmann U, Sjövall P, Lausmaa J (2007) Biomarkers at the microscopic range: ToF-SIMS molecular imaging of archaea-derived lipids in a microbial mat. *Geobiology* 5:413–421
- Thiel V, Peckmann J, Seifert R, Wehrung P, Reitner J, Michaelis W (1999) Highly isotopically depleted isoprenoids: molecular markers for ancient methane venting. *Geochim Cosmochim Acta* 63:3959–3966
- Thiel V, Peckmann J, Richnow HH, Luth U, Reitner J, Michaelis W (2001a) Molecular signals for anaerobic methane oxidation in Black Sea seep carbonates and a microbial mat. *Mar Chem* 73:97–112
- Thiel V, Peckmann J, Schmale O, Reitner J, Michaelis W (2001b) A new straight-chain hydrocarbon biomarker associated with anaerobic methane cycling. *Org Geochem* 32:1019–1023
- Timmers PH, Widjaja-Greefkes HA, Ramiro-Garcia J, Plugge CM, Stams AJ (2015) Growth and activity of ANME clades with different sulfate and sulfide concentrations in the presence of methane. *Front Microbiol* 6:988
- Turner AJ, Frankenberg C, Wennberg PO, Jacob DJ (2017) Ambiguity in the causes for decadal trends in atmospheric methane and hydroxyl. *Proc Natl Acad Sci U S A* 114:5367–5372
- Uchida M, Shibata Y, Ohkushi KI, Ahagon N, Hoshiba M (2004) Episodic methane release events from last glacial marginal sediments in the western North Pacific. *Geochim Geophys Geosyst* 5: Q08005

- Valenzuela EI, Prieto-Davó A, López-Lozano NE, Hernández-Eligio A, Vega-Alvarado L, Juárez K et al (2017) Anaerobic methane oxidation driven by microbial reduction of natural organic matter in a tropical wetland. *Appl Environ Microbiol* 83:e00645–e00617
- Van Teeseling MCF, Pol A, Harhangi HR, van der Zwart S, Jetten MSM, Op den Camp HJM (2014) Expanding the verrucomicrobial methanotrophic world: description of three novel species of *Methylacidimicrobium* gen. Nov. *Appl Environ Microbiol* 80:6782–6791
- Van Winden JF, Talbot HM, Kip N, Reichart GJ, Pol A, McNamara NP et al (2012) Bacteriohopanepolyol signatures as markers for methanotrophic bacteria in peat moss. *Geochim Cosmochim Acta* 77:52–61
- Volkman JK, Zhang Z, Xie X, Qin J, Borjigin T (2015) Biomarker evidence for *Botryococcus* and a methane cycle in the Eocene Huadian oil shale, NE China. *Org Geochem* 78:121–134
- Wegener G, Krukenberg V, Ruff SE, Kellermann MY, Knittel K (2016) Metabolic capabilities of microorganisms involved in and associated with the anaerobic oxidation of methane. *Front Microbiol* 7:46
- Wegener G, Krukenberg V, Riedel D, Tegetmeyer HE, Boetius A (2015) Intercellular wiring enables electron transfer between methanotrophic archaea and bacteria. *Nature* 526:587–590
- Wei JH, Yin X, Welander PV (2016) Sterol synthesis in diverse Bacteria. *Front Microbiol* 7:990
- Welander PV, Summons RE (2012) Discovery taxonomic distribution, and phenotypic characterization of a gene required for 3-methylhopanoid production. *Proc Natl Acad Sci U S A* 109:12905–12910
- Whiticar MJ (1996) Stable isotope geochemistry of coals, humic kerogens and related natural gases. *Int J Coal Geol* 32:191–215
- Yao M, Henny C, Maresca JA (2016) Freshwater Bacteria release methane as a by-product of phosphorus acquisition. *Appl Environ Microbiol* 82:6994–7003
- Yoshinaga MY, Lazar CS, Elvert M, Lin YS, Zhu C, Heuer VB et al (2015) Possible roles of uncultured archaea in carbon cycling in methane-seep sediments. *Geochim Cosmochim Acta* 164:35–52
- Zachos JC, Dickens GR, Zeebe RE (2008) An early Cenozoic perspective on greenhouse warming and carbon-cycle dynamics. *Nature* 451:279–283
- Zhu C, Yoshinaga MY, Peters CA, Liu XL, Elvert M, Hinrichs KU (2014) Identification and significance of unsaturated archaeal tetraether lipids in marine sediments. *Rapid Comm Mass Spec* 28:1144–1152
- Zigah PK, Oswald K, Brand A, Dinkel C, Wehrli B, Schubert CJ (2015) Methane oxidation pathways and associated methanotrophic communities in the water column of a tropical lake. *Limnol Oceanogr* 60:553–572
- Zundel M, Rohmer M (1985) Prokaryotic triterpenoids. 1. 3 β -Methylhopanoids from *Acetobacter* species and *Methylococcus capsulatus*. *Eur J Biochem* 150:23–27



Chemistry of Volatile Organic Compounds in the Atmosphere

29

Ralf Koppmann

Contents

1	Sources of VOCs in the Atmosphere	812
2	Sinks of VOCs in the Atmosphere	814
2.1	Degradation of Atmospheric Alkanes	816
2.2	Degradation of Atmospheric Alkenes	819
2.3	Degradation of Atmospheric Aromatic VOCs	820
2.4	Degradation of Atmospheric OVOCs	820
3	Research Needs	821
	References	822

Abstract

Volatile organic compounds (VOCs) in the atmosphere include saturated, unsaturated, aromatic, and a variety of other substituted hydrocarbons. They are emitted from anthropogenic and natural sources mainly as gaseous, often nonpolar, compounds of high vapor pressure. Photochemical oxidation reactions involving hydroxyl (OH) and nitrate (NO₃) radicals, but also ozone and in some cases chlorine atoms, transform these compounds into mainly polar, water-soluble compounds of low vapor pressure. These products are finally removed from the atmosphere by dry or wet deposition. At the very end of the reaction chains, the final products are water vapor and carbon dioxide. While most of the VOCs themselves, especially at the relatively low concentrations, are harmless, the products formed during the oxidation of VOCs in the atmosphere such as photooxidants like ozone or peroxyacetyl nitrate (PAN) have a significant impact on air quality and can be harmful to human health. VOCs also are a source of secondary organic aerosol (SOA), which influences the solar radiation budget

R. Koppmann (✉)

Institute for Atmospheric and Environmental Research, University of Wuppertal,
Wuppertal, Germany

e-mail: koppmann@uni-wuppertal.de

© Springer Nature Switzerland AG 2020

H. Wilkes (ed.), *Hydrocarbons, Oils and Lipids: Diversity, Origin, Chemistry and Fate*,
Handbook of Hydrocarbon and Lipid Microbiology,

https://doi.org/10.1007/978-3-319-90569-3_24

811

and acts as cloud condensation nuclei. Through all these complex reactions, VOCs play an important role in atmospheric chemistry, air quality, and climate.

1 Sources of VOCs in the Atmosphere

Every day, large quantities of VOCs are emitted into the atmosphere from both human activities and natural sources. The term VOC comprises a sheer limitless number of compounds. The major classes of compounds from anthropogenic sources are saturated hydrocarbons (alkanes), unsaturated hydrocarbons (alkenes and aromatic compounds such as benzene, toluene, and xylenes), and oxygenated compounds such as aldehydes, ketones, alcohols, esters, etc. Biogenic sources, mainly terrestrial vegetation, emit unsaturated compounds, preferably isoprene, but also monoterpenes and sesquiterpenes. Almost in the same amount, also aldehydes, alcohols, and esters are emitted from vegetation. The spectrum of VOC ranges from simple hydrocarbons with 2 carbon atoms (ethane, ethene, ethyne) to complex compounds with 15 carbon atoms or more. Table 1 gives an overview of sources and amounts of emitted VOC.

Table 1 Annual global emission rates of VOC from different anthropogenic and natural sources. All data are given in Tg C per year

	Emission rates	Uncertainty range
	Fossil fuel use	
Alkanes	28	15–60
Alkenes	12	5–25
Aromatic compounds	20	10–30
	Biomass burning	
Alkanes	15	7–30
Alkenes	20	10–30
Aromatic compounds	5	2–10
	Terrestrial plants	
Isoprene	590	200–1800
Sum of monoterpenes	95	50–400
Sum of other VOC	580	150–2400
	Oceans	
Alkanes	1	0–2
Alkenes	6	3–12
	Sum of anthropogenic emissions	
	100	
	Sum of biogenic emissions (incl. oceans)	
	1272	

Table taken from Williams J, Koppmann R (2007). Chapter 1 in Koppmann R (ed.) Volatile Organic Compounds in the Atmosphere. Oxford: Blackwell Publishing.; biogenic emissions updated with a more recent global data set (Sindelarova et al., Atmos. Chem. Phys., 14, 9317–9341, 2014)

The anthropogenic contribution to VOC emissions in the atmosphere is dominated by the production, handling, and use of fossil fuels (coal, oil, gas). Additionally, about 90% of all biomass burning events are attributed to human activities. Taken together, VOC emissions from both source types are estimated to be in the range of 100–150 Tg C per year (Müller 1992). On a global scale, terrestrial vegetation is the most important source of VOC with an estimated total emission of 1200–1300 Tg C per year (Guenther 2002). The ocean is a relatively small source of VOC with about 5 Tg C per year. The relative importance of VOC emissions and their immediate impact are determined by the geographic location and season. Anthropogenic emissions dominate in the northern hemisphere, especially in mid-latitudes with a maximum in northern hemispheric winter. Biogenic emissions dominate in the tropics with only small seasonal effects. Biomass burning emissions in South America, Africa, and Asia show a strong correlation with dry and rainy seasons and move from north to south over the continents in the course of the year.

Hydrocarbons or VOCs are present in the global atmosphere at mixing ratios of some 10 ppbv (parts per billion, 10^{-9} , or nmol/mol) down to some ppt (parts per trillion, 10^{-12} , or pmol/mol). Despite these low concentrations, VOCs have profound effects in the atmosphere. They are the “fuel” which keeps atmospheric photochemistry running. Therefore, their sources, sinks, residence times, and (photo)chemical reaction pathways were subject of research in the last three decades and still are an important objective of current research. They influence photochemistry on a local, regional, and even global scale. Some compounds have a potential impact on climate, both due to their properties as greenhouse gases and also through their ability to form SOA particles on oxidation.

Methane is the simplest and most abundant hydrocarbon in the atmosphere. Its mean tropospheric mixing ratio is 1.9 ppm (parts per million, 10^{-6}). In atmospheric chemistry typically mixing ratios are used. They are mostly related to a volume, i.e., a volume of trace gases compared to a volume of air. This is sometimes written as ppmV, but in most cases, the V (for volume) is omitted. The mixing ratio can also be related to the number of carbon atoms (ppmC). This is the volume mixing ratio multiplied with the number of carbon atoms of the particular compound.

In contrast to methane, all other organic compounds are referred to as “non-methane hydrocarbons” (NMHC). Some additional abbreviations for different subgroups can be found in the literature. These are, for example, ORVOCs (other reactive VOCs) or OVOCs (oxygenated VOCs). Sometimes individual groups of compounds are mentioned and studied separately, e.g., isoprene or monoterpenes, if biogenic emissions are analyzed. The abbreviation VOCs usually covers all organic compounds, except methane.

The mixing ratios of volatile organic compounds are significantly lower than the mixing ratios of methane. However, the reactivity of most of these compounds is orders of magnitude higher than the reactivity of methane. Thus, they play an important role in atmospheric chemistry. In some situations the VOC can have a much stronger influence than methane despite its significantly higher mixing ratio, e.g., near biomass burning or above tropical rainforests.

2 Sinks of VOCs in the Atmosphere

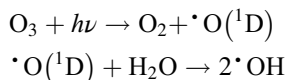
The most important sink for VOCs in the atmosphere is chemical oxidation in the gas phase by the hydroxyl radical. Some compounds can absorb sunlight and thereby photolyze to smaller fragments. Some compounds can be removed from the atmosphere by dry or wet deposition to surfaces such as soil, vegetation, or aerosol particles. The chemical and photochemical reactions are influenced and controlled by three important factors:

- Energy (in the form of solar UV radiation, mainly through photolysis and radical formation)
- “Fuel” (carbon monoxide and organic compounds)
- Catalyst (nitrogen oxides)

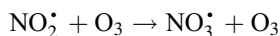
The chemical decomposition of VOCs has a significant influence on atmospheric chemistry:

- In the presence of nitrogen oxides, oxidation leads to the formation of so-called photooxidants on both regional and global scales. The most important representative of photooxidants is ozone.
- VOCs are an important source for carbon monoxide, aldehydes, and ketones in the atmosphere.
- VOCs are furthermore a source for organic nitrogen oxides which are a temporary reservoir for nitrogen oxides. Thus, they enable a wide and under some circumstances global distribution of nitrogen oxides.

The degradation of VOCs in the atmosphere is initiated mainly by the reaction with the OH radical, which itself is formed by the reaction of an O(¹D) atom with a water molecule following the photolysis of an ozone molecule at wavelengths of $\lambda < 340$ nm:



The OH radical has an average global abundance of about 10^6 radicals/cm³. Despite this low concentration, OH is the most important cleansing agent in the troposphere. In addition to OH, also ozone and the nitrate radical (NO₃) contribute to the degradation of VOCs, mainly unsaturated compounds. The nitrate radical, NO₃, is formed by the reaction



and is only present in the nighttime atmosphere due to its fast removal by photolysis during daytime. In addition, NO₃ also reacts with NO₂, forming dinitrogen pentoxide in a reversible equilibrium reaction:



Therefore, the mixing ratios of NO_3 at night are low, typically between a few ppt and a few 100 ppt. In contrast to OH and NO_3 radicals, ozone is ubiquitous in the troposphere at mixing ratios of some 10 ppb in clean environments and peak values of >100 ppb during photochemical smog episodes. Under specific circumstances such as in the marine boundary layer, also the reaction with chlorine atoms may play a role in the degradation of VOCs. However, if chlorine atoms are available, their concentrations are very low, typically a few 1000 atoms per cm^3 . Therefore, regarding atmospheric chemistry in the troposphere on a global scale, chlorine atoms are of minor importance and usually not considered in global atmospheric chemistry models. The loss rate of any VOC is determined by the concentrations of the VOCs and the corresponding oxidants and can be calculated by

$$\frac{d[\text{VOC}]}{dt} = -k_{\text{Oxidant}}[\text{Oxidant}][\text{VOC}]$$

where $[\text{X}]$ is the concentration of the oxidant and the compound of interest and k the rate coefficient (i.e., the velocity) of the corresponding reaction.

The atmospheric residence times of VOCs are determined by the concentration of the oxidant and the corresponding rate coefficient:

$$\tau_{\text{VOC}} = \frac{1}{k_{\text{Oxidant}} \cdot [\text{Oxidant}]}$$

The lifetime of alkanes reacting only with OH is:

$$\tau_{\text{alkane}} = \frac{1}{k_{\text{OH}} \cdot [\text{OH}]}$$

The lifetime of alkenes reacting with OH and O_3 is:

$$\tau_{\text{alkane}} = \frac{1}{k_{\text{OH}} \cdot [\text{OH}] + k_{\text{O}_3} \cdot [\text{O}_3]}$$

In case other reactants are involved such as NO_3 or Cl, the corresponding rate coefficients and concentrations have to be added accordingly. Average lifetimes of VOCs in the atmosphere range from about 8 years for methane to a few minutes for some sesquiterpenes. Table 2 gives an overview of the average atmospheric lifetimes of some compound groups and a number of selected VOCs.

Table 2 Overview of average tropospheric lifetimes of VOC compound groups and some selected VOCs as examples. Lifetimes are given for an average OH concentration of $6 \cdot 10^5/\text{cm}^3$ and an average ozone concentration of $7 \cdot 10^{11}/\text{cm}^3$ (about 30 ppb)

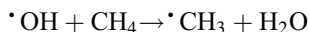
Compound	Average lifetime
Alkanes	Months – days
Ethane	2 months
Propane	2 weeks
n-Pentane	4 days
Alkenes	Days – hours
Ethene	1.5 days
Propene	11 hours
1-Butene	10 hours
Cyclic compounds	Days – hours
Cyclopentane	4 days
Methylcyclohexane	2 days
Cyclohexane	3 hours
Aromatic compounds	Weeks – hours
Benzene	2 weeks
Toluene	2 days
1,3,5-Trimethylbenzene	2.5 hours
Biogenic compounds	Hours – minutes
Isoprene	3 hours
α -Pinene	4 hours
Limonene	30 minutes

Table taken from Williams J, Koppmann R (2007). Chapter 1 in Koppmann R (ed.) Volatile Organic Compounds in the Atmosphere. Oxford: Blackwell Publishing

A schematic of the oxidation of atmospheric VOCs is shown in Fig. 1. For further details see Atkinson and Arey (2003). In the following the atmospheric degradation of different VOC groups is discussed in more detail.

2.1 Degradation of Atmospheric Alkanes

The reaction of saturated hydrocarbons with OH radicals proceeds by the abstraction of an H-atom and the formation of a water molecule and an alkyl radical. The typical reaction pathway is shown for methane as an example:



The resulting alkyl radical, a methyl radical in this case, reacts very fast in a three-body reaction with O_2 to form a methyl peroxy radical (M denotes any other molecule, because of their abundance typically NO_2 or O_2 molecules):

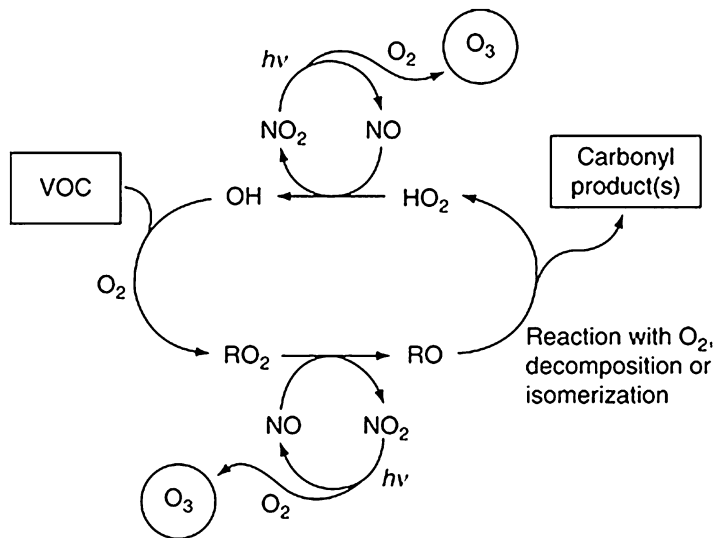
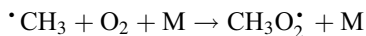
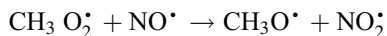


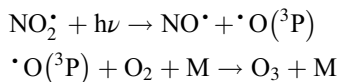
Fig. 1 Schematic of the oxidation of atmospheric VOCs into the first stable carbonyl products in the presence of NOx and the formation of ozone. (Figure taken from Le Bras G (2002) Gas Phase Reactions, Encyclopedia of Atmospheric Science. In JR Holton (ed.). Amsterdam: Elsevier, pp. 352–359)



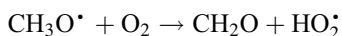
In the presence of NO (>10 ppt), oxygen is abstracted to form a methoxy radical:



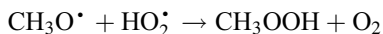
The NO₂ molecule formed in this reaction is photolyzed, leading to a ground state oxygen atom, which reacts almost immediately with an oxygen molecule to form ozone:



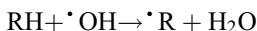
In this way, the oxidation of VOCs in the presence of NO is the main process responsible for the production of ozone in the troposphere. Especially during smog events in summer, urban air masses contain high concentrations of both VOC and NO. Intensive photochemistry during the transport of these air masses leads to the extremely high ozone levels which are often observed in rural areas downwind from urban sources. The methoxy radical reacts with O₂ to form formaldehyde as the first stable product from this reaction chain:



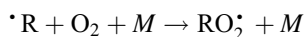
In very clean environments, the methoxy radical can also react with other peroxy radicals, (i.e., HO₂ or organic peroxy radicals). Reaction with HO₂ results in the formation of more stable methyl hydroperoxides:



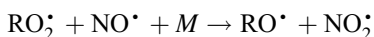
In the same way, higher molecular weight alkanes are attacked by OH radicals via hydrogen abstraction, as illustrated in the following using R as a symbol for an organic rest such as CH₃ – CH₂– in case of ethane, for instance:



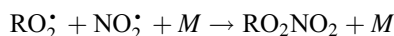
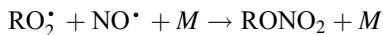
For longer-chained alkanes with different types of hydrogen-carbon bonds, reaction rates for the H-abstraction are decreasing with the number of hydrogen atoms attached to the same carbon atom. Therefore, the abstraction is favored as follows: =CH– > –CH₂– > –CH₃. The resulting alkyl radical reacts fast with O₂ to form an alkyl peroxy radical:



In the presence of NO (>10–30 ppt), oxygen is abstracted to form an alkoxy radical:

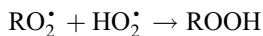


Again, NO₂ is produced, leading to tropospheric ozone formation, whereas the alkoxy radical, depending on the molecule, can thermally decompose, isomerize, or react with molecular oxygen. Breaking of the carbon chain leads to the formation of a stable aldehyde and a smaller peroxy radical, which again can react as described above. Isomerization occurs by internal hydrogen abstraction and eventually leads to a hydroxycarbonyl molecule. The reaction with O₂ leads to the formation of a stable ketone via the abstraction of a hydrogen atom, which is attached to the same carbon atom as the oxygen radical. Furthermore, alkyl peroxy radicals can also attach to an NO or an NO₂ molecule. In the case of NO, this leads to the formation of relatively stable organic nitrates, whereas with NO₂ peroxy nitrates are produced:

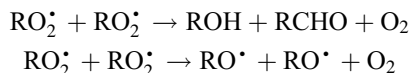


The yields of the organic nitrates increase with the chain lengths of the alkanes. Peroxyacetyl nitrate or PAN (CH₃CO(O₂)NO₂) is the most important peroxy nitrate. Since this compound is not directly emitted by human activities, it is an excellent measure for photochemical processing of an air mass and an important component of photochemical smog. PAN and organic nitrates are important in relation to long-range transport in the atmosphere, because they act as reservoirs for reactive nitrogen as they are fairly stable at low temperatures. In very clean environments, the peroxy

radicals can also react with other peroxy radicals (i.e., HO₂ or organic peroxy radicals). Reaction with HO₂ results in the formation of more stable organic peroxides:

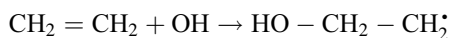


The combination with another peroxy radical is either a sink for the radicals and produces alcohols, ketones, and organic acids or leads to alkoxy radicals, which react as described above:

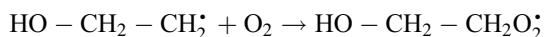


2.2 Degradation of Atmospheric Alkenes

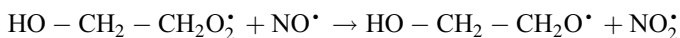
In the case of alkenes, OH radicals preferably react by addition to the C=C double bond as illustrated for ethene:



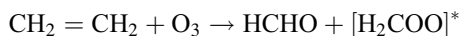
This hydroxyalkyl radical reacts with an oxygen molecule to form a hydroxyalkyl peroxy radical:



which is converted to a hydroxyalkoxy radical following the reaction with NO:



The hydroxyalkoxy radical can then either react with O₂ via H-abstraction to form a glycolaldehyde or by cleavage to form an aldehyde and a hydroxyalkyl radical, which can react again as described above. Furthermore, larger-chained molecules have the possibility to undergo isomerization. The second major pathway for the degradation of alkenes is their reaction by addition of an ozone molecule (O₃) to the C=C double bond leading to an unstable so-called ozonide, which then decomposes to a carbonyl compound and a Criegee intermediate, as shown for ethene:



Criegee intermediates can either stabilize by collision with other molecules or decompose further. After stabilization, a possible pathway leads via reaction with water vapor to the formation of organic acids. The reaction of alkenes with the nitrate radical also proceeds through the addition of the radical to the double bond. This reaction leads to formation of carbonyls and nitro-oxy carbonyls. These compounds

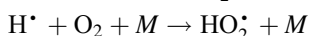
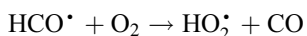
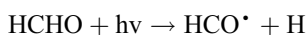
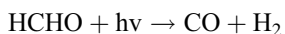
react further to finally form intermediate and stable products, which then are oxidized as described above. For further details see Calvert et al. (2000).

2.3 Degradation of Atmospheric Aromatic VOCs

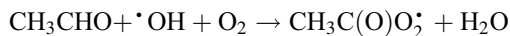
The degradation of aromatic VOCs proceeds by two different pathways, the abstraction of a hydrogen atom from one of the alkyl substitute groups or by OH-radical addition to the aromatic ring. In the first case, the stable product is an aromatic aldehyde (e.g., toluene leading to benzaldehyde). However, the OH addition is the predominant pathway for the degradation of aromatic VOCs. Following the addition of an OH radical to the aromatic ring, molecular oxygen is added to build a cyclic hydroxy peroxy radical. In the following the ring structure is opened, and epoxy compounds, saturated and unsaturated dicarbonyl radicals, and finally methylglyoxal are formed. In the last years, a large number of laboratory studies improved our knowledge of the atmospheric oxidation of aromatic hydrocarbons. However, for most of these compounds, the detailed reaction pathways in the atmosphere, especially the process of ring opening, as well as the formation of intermediate and final reaction products are still speculative. Also, their potential to form secondary organic aerosols is far from being understood and an important objective of current research.

2.4 Degradation of Atmospheric OVOCs

OVOCs are on the one hand directly emitted by anthropogenic or biogenic sources. For example, they account for the largest part of organic compounds emitted from biomass burning. On the other hand, they are also formed during the oxidation of VOCs. Again, the predominant reaction is the abstraction of a hydrogen atom from the carbon chain by an OH radical. In the case C=C double bonds are present, the addition of O₃ is also a possible initial step. The resulting peroxy radicals then react as described above. OVOCs that have UV-absorbing groups (e.g., aldehydes, ketones, organic peroxides, and organic nitrates) can also be photodissociated. Whereas formaldehyde is degraded primarily by photolysis, higher aldehydes react mainly with OH radicals. As shown for formaldehyde, products of the photolysis provide an additional source of HO₂, which can then be a source for OH radicals:



The initial steps of the aldehyde degradation by OH radicals are shown for the example of acetaldehyde:



The produced peroxy radical is a precursor for the PAN formation, if enough NO_2 is available (see above). At high NO levels, however, the peroxy radical of a C_n -aldehyde reacts dominantly with NO , leading to a C_{n-1} -aldehyde and CO_2 . For the OH -radical-initiated oxidation of ketones, the reaction proceeds by H-atom abstraction and subsequent formation of alkoxy radicals. Also the oxidation of alcohols in the atmosphere is mainly initiated by the reaction with OH radicals. The H-atom is abstracted from the C-H bond of the CHOH or CH_2OH group. The following reaction of O_2 with the hydroxyl radical leads to the formation of a ketone for secondary alcohols or of an aldehyde for primary alcohols. Furthermore, OH can abstract H-atoms from other C-H bonds, which leads to reactions analogous to those for alkanes.

3 Research Needs

VOCs' mixing ratios are measured by a number of continuous global monitoring sites within the Global Atmosphere Watch (GAW) program of the World Meteorological Organization (WMO); the Atmospheric Baseline Observatories of the National Oceanic and Atmospheric Administration's (NOAA) Earth System Research Laboratory (ESRL) in Boulder, Colorado, USA; and the Network for the Detection of Atmospheric Composition Change (NDACC). Between the 1980s and early 2000s, a statistically significant downward trend of the mixing ratios of many anthropogenic VOCs in the background atmosphere was observed. This was attributed to improved emission controls and stricter emission limits. However, in the last years, mixing ratios of some compounds are increasing again for reasons that can only be speculated about. This effect is especially reported for ethane and propane, the main sources of which are oil and natural gas production and handling, fossil fuel use, and biomass burning.

Almost all human activities (even breathing) lead to the emission of organic compounds into the atmosphere. Additionally, the terrestrial vegetation releases huge amounts of organic compounds into the air. If climate changes, as it is predicted to do, temperatures will increase, and convection systems and vegetation patterns will alter significantly and with it most likely the distribution and the composition of organic compounds in the atmosphere. At the same time, the increasing population with a steady growth of urban areas and an increasing number of megacities demand a basic necessity to assess and control air quality in order to maintain human health. In addition, in recent years the increasing demand for energy has led to rising emissions of some VOCs (Helmig et al., 2016). All this requires a still better understanding of the sources, sinks, and the chemistry of organic compounds in order to improve models for the prediction of future global change and develop appropriate abatement strategies. This calls unconditionally for a continuation of the monitoring programs, an identification of yet unknown and obviously missing

compounds, an improvement of emission inventories, and a further investigation of the atmospheric chemistry of VOCs.

References

- Atkinson R, Arey J (2003) Atmospheric degradation of volatile organic compounds. *Chem Rev* 103:4605–4438
- Calvert JG et al (2000) The mechanisms of the atmospheric oxidation of alkenes. Oxford University Press, New York
- Guenther A (2002) The contribution of reactive carbon emissions from vegetation to the carbon balance of terrestrial ecosystems. *Chemosphere* 49:837–844
- Helmig D et al (2016) Reversal of global atmospheric ethane and propane trends largely due to US oil and natural gas production. *Nat Geosci* 9:490. <https://doi.org/10.1038/ngeo2721>
- Müller JF (1992) Geographical distribution and seasonal variation of surface emissions and deposition velocities of atmospheric trace gases. *J Geophys Res, Bd. 97(D4):S. 3787–3804*
- Sinderlarova K et al (2014) Global data set of biogenic VOC emissions calculated by the MEGAN model over the last 30 years. *Atmos Chem Phys* 14:9317–9341

Further Reading

- Finlayson-Pitts BJ, Pitts JN (2000) Chemistry of the upper and lower atmosphere. Academic Press, San Diego
- Koppmann R (ed) (2007) Volatile organic compounds in the atmosphere. Blackwell Publishing, Oxford
- Seinfeld JH, Pandis SN (2000) Atmospheric chemistry and physics. Wiley, New York
- Zellner R (ed) (1999) Global aspects of atmospheric chemistry. Steinkopf, Darmstadt



Jan Schwarzbauer

Contents

1	Introduction	824
2	Terrestrial Surface Water Systems	824
2.1	Transfer and Transport Processes Affecting the Residence of Organic Matter in Rivers and Lakes	824
2.2	Natural Organic Substances	826
2.3	Anthropogenic Organic Contamination	828
3	Groundwater	832
3.1	Influence of Redox Conditions on Organic Matter Quality in Groundwater	832
3.2	Natural Organic Substances	833
3.3	Anthropogenic Organic Contamination	833
4	Marine Environment	834
4.1	Occurrence and Fate of Organic Compounds in the Marine Environment	834
4.2	Natural Organic Substances	836
4.3	Anthropogenic Organic Contamination	836
5	Research Needs	838
	References	839

Abstract

Organic matter appears in all compartments of the hydrosphere of both natural and more and more anthropogenic origin. Aquatic organic matter exhibits a high structural diversity and corresponding physicochemical properties. Marine and terrestrial surface water bodies including their corresponding sediments as well as groundwater are affected by natural compounds of autochthonous origin from aquatic species, in particular from phyto- and zooplankton, and allochthonous material from terrestrial biota. Anthropogenic pollutants are released to aquatic ecosystems mainly as the

J. Schwarzbauer (✉)

Institute of Geology and Geochemistry of Petroleum and Coal, Energy and Mineral Resources Group (EMR), School of Geosciences, RWTH Aachen University, Aachen, Germany
e-mail: jan.schwarzbauer@emr.rwth-aachen.de

© Springer Nature Switzerland AG 2020

H. Wilkes (ed.), *Hydrocarbons, Oils and Lipids: Diversity, Origin, Chemistry and Fate*, Handbook of Hydrocarbon and Lipid Microbiology,
https://doi.org/10.1007/978-3-319-90569-3_26

823

result of municipal, industrial, and agricultural emissions as well as shipping activities. Dominant factors controlling the fate and distribution of organic compounds in the hydrosphere are partition processes between water phase and particulate matter separating more hydrophilic from more lipophilic substances. With respect to hydrocarbon chemistry, an enhanced geoaccumulation of non-functionalized aliphatic and aromatic hydrocarbons in the benthic systems has to be stated.

1 Introduction

Organic matter plays an important role in aquatic ecosystems comprising surface water systems as well as groundwater reservoirs. The high diversity of organic compounds with respect to their structure and the related physicochemical properties causes a widespread and highly diverse occurrence of a multitude of organic compounds in aquatic systems. A clearly arranged and systematic description of the occurrence of organic substances in the hydrosphere is impeded by the variety of different aspects provoking the transport, transfer, and transformation of organic matter. Multiple parameters affect the singular fate of each individual organic compound in each individual aquatic compartment comprising (i) the superimposition of vertical and horizontal fluxes within most aqueous systems, (ii) different oxygen availability under anaerobic and aerobic ambiances, (iii) the different conditions in marine and terrestrial aquatic systems, (iv) transfer processes between the more lipophilic particulate matter and the polar water phase depending on the individual chemical nature of the substances, (v) the molecular size of contaminants, (vi) their different emission sources (anthropogenic vs. natural as well as autochthonous vs. allochthonous), and (vii) the huge variety of abiotic and biotic transformation in the different compartments of the hydrosphere effect a singular fate of each individual organic compound in each individual aquatic compartment.

However, this chapter represents the attempt to give a brief overview on principals regarding the occurrence and the molecular characterization of organic matter in the aquatic environment of both natural and anthropogenic origin. Microbially assisted or initiated transformation processes, affecting dominantly the molecular composition and therefore the compound spectra in the hydrosphere, are subject of many following, very detailed chapters, and, therefore, these aspects have been neglected here.

2 Terrestrial Surface Water Systems

2.1 Transfer and Transport Processes Affecting the Residence of Organic Matter in Rivers and Lakes

The most important process affecting the fate of organic compounds in the aquatic environment are the principal partition processes between the polar water phase and the more lipophilic particulate matter. These processes, dominantly adsorption and desorption, depend mainly on the polarity of the compounds

as the result of their chemical structure and the resulting physicochemical properties (see ► Chap. 1, “Hydrocarbons and Lipids: An Introduction to Structure, Physicochemical Properties, and Natural Occurrence”), Wilkes et al., and, consequently, most of the organic substances accumulate either in the water phase or in the particulate matter. A quantitative estimation of the environmental behavior of organic compounds is given by the K_{OW} -values describing the partition behavior under steady-state conditions between water and 1-octanol as representative for the lipophilicity of particulate matter. This partition determines the principal transport processes and, consequently, the distribution of the organic contaminants.

The separation of dissolved organic matter (DOM) from particulate organic matter (POM) is defined operationally by a filtration pore size of 0.45 μm . Partially, the dissolved fraction is subdivided by introduction of a third phase (see Table 1), the so-called colloidal organic matter (COM), which is also analytically defined, e.g., with an upper particle size of 0.45 μm and a lowest compound mass of 1 kDa (Guo et al. 2003; Kerner et al. 2003). Anymore, a further sub-compartment, the so-called biofilms, consisting dominantly of microbes and extracellular organic matter has been taken into account for interpreting the environmental behavior of organic substances (Headley et al. 1998).

In lakes transport processes are not as complex as in riverine systems. The distribution of dissolved organic compounds is controlled by diffusive processes superimposed by an inlet and outlet flow. Particle-associated transport is dominated by aggregation and horizontal sedimentation (e.g., Berdie et al. 1995). On the contrary river systems are characterized by a much higher dynamic of the flow regime affecting also the mobility and appearance of organic compounds. The partially very high vertical water flow determines the transport of dissolved organic matter as well as the distribution of particle-associated organic substances. Their vertical transport in rivers is linked with the transportation of the suspended particulate matter (SPM), where the corresponding organic load is referred to particulate organic carbon (POC). Additionally, saltation and reptation of heavier particles near the ground level have to be considered for matter transport in flow direction of riverine systems.

Since the polarity of non-functionalized hydrocarbons is generally low, these compounds appear dominantly particle-associated, and their horizontal and vertical transport is linked with the mobility of particulate matter. On the contrary, highly functionalized compounds exhibit enhanced dipole moments inducing an elevated water solubility and, consequently, an environmental behavior closely related to the water transport. They contribute to the dissolved organic carbon (DOC) or dissolved

Table 1 Size distribution of organic carbon and nitrogen in the Chena River water. (Data from Guo et al. 2003)

	Organic carbon	Organic nitrogen
Dissolved	28% (DOC)	27% (DON)
Colloidal	66% (COC)	57% (CON)
Particulate	6% (POC)	16% (PON)

organic matter (DOM). However, the partition between solid and aqueous phases is not strict but a dynamic exchange process as described in many studies, e.g., for amino acids or carbohydrates (Hedges et al. 1994).

Interestingly, this partition causes also a further important environmental aspect regarding the fate of organic substances. The water phase including the suspended particulate matter represents an aerobic environment, whereas the sedimentary matter is dominantly more anaerobic. Hence, it results in quite different transformation or degradation pathways in the distinct compartments for most of the organic compounds as the result of dissimilar microbial communities.

Noteworthy, a comprehensive review on the environmental behavior of anthropogenic contaminants in the sedimentary matter of freshwater systems has been published recently (Warren et al. 2003).

2.2 Natural Organic Substances

Natural organic matter (NOM) in surface water is composed of autochthonous material as the result of biological activity within the aquatic system (e.g., fresh water algae lipids) and of allochthonous substances derived from the surrounding biosphere (e.g., higher plant-derived lipids). For many compounds a clear attribution to these two pools of riverine and lacustrine organic matter can be effected, although also various substances are emitted to surface water systems by both aquatic and terrestrial biota. For instance, Countway et al. (2007) used structural differences of certain sterols to differentiate plankton-derived autochthonous contributions (represented, e.g., by cholesta-5,22-dien-3 β -ol, cholest-5-en-3 β -ol (cholesterol), 24-methylcholesta-5,22-dien-3 β -ol) from allochthonous, higher land plant-derived material (indicated by 24-methylcholest-5-en-3 β -ol (campostero), 24-ethylcholesta-5,22-dien-3 β -ol (stigmasterol), and 24-ethylcholest-5-en-3 β -ol; see Fig. 1).

An important fraction of natural organic matter is the so-called refractory material which occurs with average organic carbon content of 0.5–100 mg C/L (Frimmel 1998). In contrast to the labile or metabolizable fraction that is subject to a more or less rapid transformation and degradation, the refractory matter exhibits a prolonged residence time in lakes and rivers and, consequently, contributes in particular to the terrigenous matter entering the marine environment (see Sect. 1.3). Based on chemical analysis, the relative global proportion of the labile fraction in the major river systems has been estimated to be around 35% (Ittekkot 1988).

As mentioned before, more functionalized substances appear dominantly in the polar water phase. Non-altered biochemicals exhibit widely functional groups and, consequently, elevated water solubility. Hence, with respect to NOM, the water phase exhibits huge amounts of biological molecules derived from aquatic organisms or their excretion as well as intact biomolecules from terrestrial species. Examples include macromolecular compounds like polysaccharides or fulvic acids (Repeta et al. 2002) as well as low molecular weight substances as short-chain carboxylic acids or amino acids. In contrast the organic matter accumulating in the

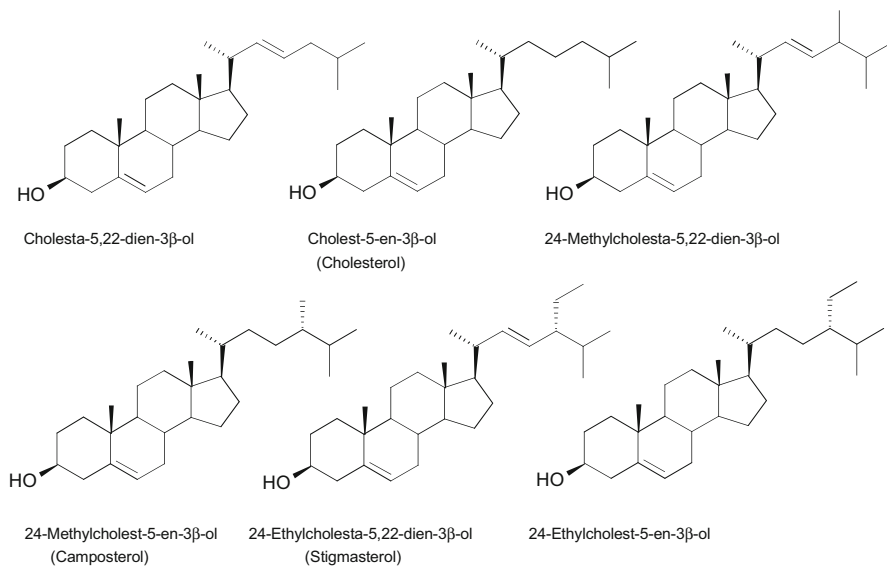


Fig. 1 Molecular structures of certain sterols differentiating autochthonous contributions (upper part) from allochthonous material (lower part)

sedimentary system constitutes by more lipophilic biochemicals (e.g., sterols, fatty acids and alcohols, long-chain *n*-aldehydes, functionalized terpenoids, cyclic di- and triterpenes, phytol, squalene) superimposed by huge amounts of defunctionalized degradation products of biogenic precursors. Well-known examples of the latter group of compounds are loliolide and actinidiolide, ionenes, different isomers of phytene and the saturated phytane, steranes and unsaturated derivatives, pheophorbide and related porphyrins, as well as 4,8,12,16-tetramethylheptadecan-4-olide. They correspond to the biogenic precursors chlorophyll, carotenoids, sterols, and tocopherols (see also Cranwell 1981; Cranwell et al. 1987; Prahl and Pinto 1987; Ittekkot 1988; Riley et al. 1991; Hedges et al. 1994; Schwarzbauer et al. 2000).

Similar to the water phase, the major proportion of the sedimentary natural organic matter in rivers belongs to the humic substances that are proposed to be generated by abiotically mediated “geopolymerization” reactions. The resulting structurally complex macromolecules represent an organic pool that is not only objective of extensive structure analysis or structural discussions (e.g., Schulten and Leinweber 1996; Kumke et al. 1999; Esteves and Duarte 2000; Sutton and Sposito 2005) but appears to be also an important reagent for the interaction with naturally occurring or anthropogenic low molecular weight substances and metal ions (e.g., Klaus et al. 1998; Zwiener et al. 1999; Northcott and Jones 2000).

An overall calculation of the individual groups of main DOC constituents has been performed, e.g., for the White Clay Creek (Pennsylvania, USA). The composition was pointed out to be 75% humic substances, 13% polysaccharides, 2% amino

acids (dominantly as peptides), and 18% compounds with a molecular weight less than 100 kDa (Volk et al. 1997).

However, the composition of biogenic organic material in surface water systems including its sediments is subject to temporal variations and dynamic partition effects. For example, Hedges et al. (1994) demonstrated for the Amazon River the usefulness of studying the partition of amino acids and carbohydrates between the liquid and the solid phase in order to differentiate biogenic sources and to determine degradation processes. Studies on organic matter transported by suspended particulate material (SPM) of the Godavari River or the York River, VA, exemplified the annual fluctuations as well as varying POM sources (Gupta et al. 1997; Countway et al. 2007).

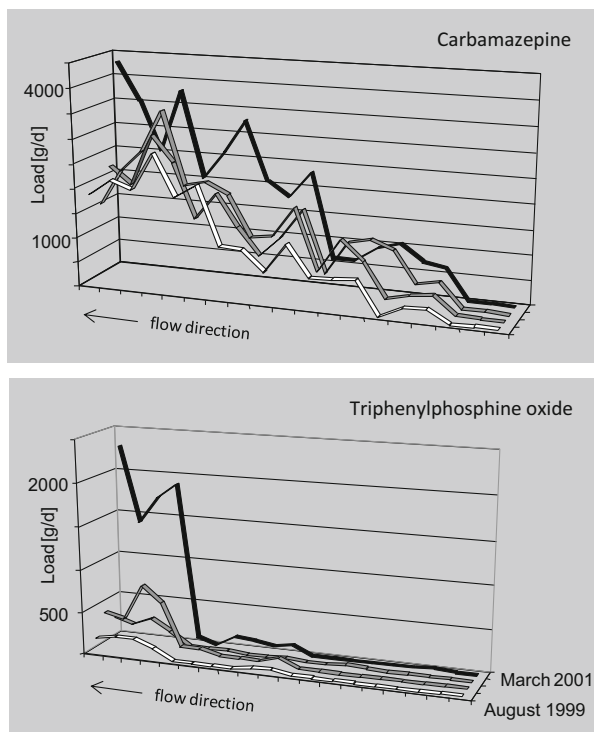
As additional remark, it has to be stated that the terms describing natural organic matter are not clearly defined. A recent review summarized the aspects on the nomenclature of “natural organic matter” (Filella 2008).

2.3 Anthropogenic Organic Contamination

Major parts of surface water systems are influenced by human activities resulting inter alia in contamination by organic pollutants. The spectrum of contaminants reflects the broad usage and application of synthetic chemicals in the anthroposphere and, therefore, varies depending on numerous aspects related to the catchment area like population density, level of industrialization, extension of agriculture, and effectiveness of waste water treatment.

Most important emission sources in highly industrialized and densely populated regions are municipal waste water and industrial effluents. As a result of insufficient waste water treatment, pharmaceuticals and bactericides (e.g., carbamazepine, clofibric acid, triclosan); personal care products comprising fragrances, repellents, and UV-protectors (*N,N*-diethyltoluamide DEET, galaxolide or tonalide, 4-methoxycinnamic acid 2-ethylhexyl ester); biocides (e.g., triclosan, thiabendazole, cyproconazole); plasticizers and further technical additives (e.g., phthalates, *N*-butylbenzenesulfonamide NBBS, 2,4,4-trimethylpentane-1,3-dioldi-*iso*-butyrate TPDB, hexa(methoxymethyl)melamine HMMS), flame retardants (e.g., tris(chloroethyl)phosphate TCEP); or detergent-related products (non-ylphenolpolyethoxylates, ethylenediaminetetraacetic acid EDTA) have been detected in river and lake water (see Fig. 2) and partially also in the corresponding sediments (Balmer et al. 2005; Schwarzbauer and Heim 2005; Dsikowitzky et al. 2004; Dsikowitzky and Schwarzbauer 2015; Wluka et al. 2016). The knowledge on indicative substances reflecting the contamination by industrial point source emissions is much more restricted due to the high chemical diversity of the individual effluents (see also Dsikowitzky and Schwarzbauer 2014). Few information on typical industrial contaminants discharged to the surface water systems have been described, e.g., for the leather, paper, chemical, pharmaceutical, rubber, dye, and petrochemical industry (e.g., Rao et al. 1994; Reemtsma et al. 1995; Castillo et al. 1999; Czaplicka 2003; Brigden et al. 2004; Pinheiro et al. 2004;

Fig. 2 Load profiles of two contaminants of the Lippe River (Germany) emitted by nonpoint sources (carbamazepine) and a point source (triphenylphosphine oxide). (Adapted from Dsikowitzky et al. 2004)



Bilgi and Demir 2005; Lopez-Grimau et al. 2006; Dsikowitzky et al. 2015). The corresponding substances belonged among others to the substance classes of benzothiazoles, nitro compounds, chlorinated benzofuranones, volatile organic compounds (VOCs), substituted anilines and amines, alkyl phosphates, and chlorinated arenes.

Although semipolar water pollutants also appear in sedimentary systems (e.g., Kronimus et al. 2004), riverine and lacustrine sediments are contaminated dominantly by less functionalized compounds. Typical sedimentary pollutants belong to the group of halogenated compounds of both aliphatic and aromatic constitution. Examples of halogenated aromatics include chlorinated benzenes and naphthalenes, polychlorinated biphenyls (PCB), polychlorinated dibenzo-*p*-dioxins and dibenzofurans (PCDD/PCDF), and polybrominated diphenyl ethers. Most of these congeneric mixtures appear as the result of technical or commercial application such as technical additives, flame retardants, or lubricants. Further on, they are partially also generated as by-products in industrial synthesis and are, consequently, discharged via industrial emissions as well. Many of these compounds are of high environmental relevance due to their ecotoxicological and toxicological properties combined with a high stability under natural conditions leading to potential geo- and bioaccumulation. Hence, a number of them are classified as priority pollutants.

Aliphatic substances with a higher degree of halogenation have to be regarded also as sedimentary pollutants. Examples include hexachlorobutadiene of potentially industrial origin as well as polychlorinated long-chain *n*-alkanes the so-called chlorinated paraffins widely used as technical additives.

In a less specific manner unfunctionalized aliphatic hydrocarbons as well as aromatic hydrocarbons can contribute to sedimentary pollution. Natural aliphatic compounds (like several *n*-alkanes, phytenes, etc.) can be superimposed by thermally generated petrogenic aliphatics which are characterized, e.g., by a different distribution pattern of the *n*-alkane homologues. For pollution source apportionment also petroleum-specific tricyclic aliphatics, the hopanes, have been used by differentiating their thermodynamically stable isomers from the biogenic ones (e.g., Yunker and Macdonald 2003; Faure et al. 2007).

Sedimentary aromatic compounds originate dominantly as the result of petrogenic contaminations but also from pyrogenic emissions (Stout et al. 2001; Srogi 2007). In particular polycyclic aromatic hydrocarbons (PAHs) and their alkylated derivatives are common constituents of oil and petroleum-related products but are also synthesis products during incomplete combustion of organic material, e.g., as the result of vehicular traffic. Based on these different sources, petrogenic compounds are characterized generally as primary contaminants, whereas pyrogenic hydrocarbons are entering the aquatic environment indirectly as the result of deposition of airborne particles or soil erosion. Hence, the latter ones referred to secondary contaminants. In order to discriminate both emission sources and the related pollution pathways, several indicative ratios using source-specific isomers have been introduced and applied to environmental studies on rivers and lakes as well as on marine systems (Barra et al. 2009; Grigoriadou et al. 2008). Common ratios are comparing individual isomers (e.g., anthracene-phenanthrene, fluoranthene-pyrene, chrysene-benz(*a*)anthracene or 1,7-2,6-dimethylphenanthrene) or the relationship between parent PAHs and alkylated homologues (phenanthrene or fluoranthene and pyrene contrasted to their methylated derivatives) (e.g., Yunker et al. 2002; Geršlova and Schwarzbauer 2014).

As a new aspect related to the contamination by fossil fuels, the contribution of coaly material and its ingredients to the riverine environment is discussed currently (e.g., Curran et al. 2000; Yang et al. 2008). Also for this material, its environmental impact has been suggested to be trackable by specific PAHs (Stout and Emsbo-Mattingly 2008).

Intensive agricultural activities in rural regions lead to the discharge of agrochemicals like herbicides, insecticides, or fertilizers into rivers and lakes (Venkatesan et al. 1999; Zhang et al. 1999; Schwarzbauer et al. 2001). These effluents are to be characterized as diffuse emissions entering the aquatic environment either by soil surface runoff or by the interaction of the surface waters with corresponding agriculturally contaminated groundwater. In particular, the environmental occurrence and fate of pesticides in the hydrosphere have been given major attention. With respect to the type of pollutant, these contaminations can be roughly

divided into generations of pesticide classes, on the one hand the older generation, which includes more persistent compounds (e.g., chlorinated pesticides such as DDT, γ -HCH or lindane, hexachlorobenzene HCB, etc.). These compounds are characterized by an elevated tendency to geo- and bioaccumulation, which led to a more or less global ban of these substances. On the other hand, a new generation of more modern pesticides is characterized by higher microbial degradation rates, lower lipophilicity, and less toxicity (for comprehensive information on the toxicity of pesticides to aquatic organisms, see DeLorenzo et al. 2001). Representatives of such pesticides are based on molecular moieties comprising carbamates and thiocarbamates (e.g., carbendazim, EPTC), phosphates (e.g., malathion, dichlorvos), sulfonylureas (e.g., cinosulfuron), triazines (e.g., simazine, atrazine), and further nitrogen-, sulfur-, and phosphorous-containing moieties. Noteworthy, these pesticides are objectives of numerous investigations on abiotic transformation processes in surface water areas, e.g., by photooxidation or hydrolysis (e.g., Lartiges and Garrigues 1995; Abu-Qare and Duncan 2002). Comprehensive studies on the environmental appearance and distribution of pesticides in rivers and lakes have been performed worldwide on many river systems (for an overview see Schwarzbauer 2005).

Beside all typical pollutants described so far, also specific but not necessarily toxic or ecotoxic compounds have been analyzed to differentiate emission sources and to trace the spatial and time-related anthropogenic impact on the aquatic environment. This approach using the so-called anthropogenic markers has been applied to riverine as well as estuarine systems and has reflected the anthropogenic burden by fecal steroids (e.g., coprostanol – indicating fecal discharge), detergents and their by-products (e.g., linear alkylbenzenes and their sulfonated derivatives LAB and LAS – reflecting municipal sewage effluents), or rubber additives (e.g., 2-morpholinylthiazol – related to urban surface runoff). A comprehensive overview on the anthropogenic marker approach has been published by Takada and Eganhouse (1998).

Such marker compounds, but also other indicative substances or pollutants, have been used to describe not only the spatial distribution and lateral dynamics (temporary deposition and subsequent erosion) of contaminated particulate matter but also to obtain a retrospective insight into the long-term storage of particle-associated pollution. These were performed on accumulated sediment deposits as received by undisturbed aquatic sedimentation in estuaries as the final sedimentation area of riverine particulate matter as well as in lacustrine systems. Investigations on the terrestrial sedimentation of fluvial matter on flood plains and wetlands have been performed to a minor extent. However, all these deposits can act as ecological archives (see Fig. 3), since radiological dating of the sediment layers in combination with quantitative chemical analyses reveals a detailed record of the riverine and lacustrine pollution histories for preserved particle-bound contaminants (e.g., Gevaio et al. 2000; Fox et al. 2001; Heim et al. 2006). A corresponding review has been recently published (Heim and Schwarzbauer 2013).

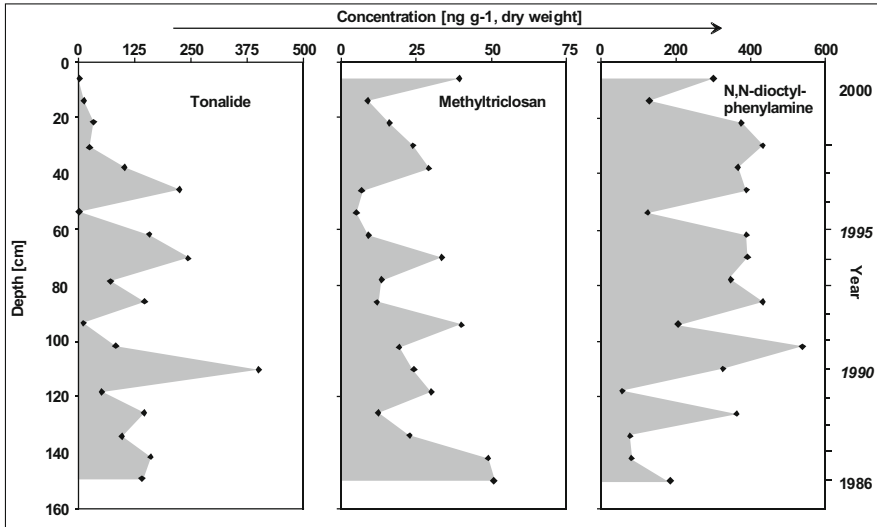


Fig. 3 Vertical distribution of environmental contaminants determined in a dated sediment core of the Rhine River (Germany). (Adapted from Heim et al. 2006)

3 Groundwater

3.1 Influence of Redox Conditions on Organic Matter Quality in Groundwater

Organic compounds introduced to the terrestrial underground can undergo various types of transport or modification/degradation processes. In groundwater systems, a vertical flux in the water-unsaturated zone as well as a horizontal flux in the water-saturated zone has to be stated, and, consequently, an associated transport of dissolved and particle-bound substances can be observed. Concurrently, corresponding aerobic and anaerobic zones have to be differentiated with respect to the microbially assisted degradation processes of organic compounds. Since the unsaturated zone belongs more to the pedosphere, the focus of this chapter lies on the saturated aquifers. However, the composition of organic matter in aquifers is dominantly controlled by soil-derived material, which is valid for natural as well as anthropogenic contaminations. Further on, since water flow rates in aquifers are typically low as compared to rivers and the partition between water phase and particulate matter has already occurred mainly in the soil zone, the quality of organic substances in groundwater is dominated by transformation processes. Groundwater systems respond very sensitively to variations of oxygen availability. Continuous changes of the redox conditions with depth as a result of ongoing oxygen-consuming processes (in particular organic matter degradation) influence the constitution of the microbial community and, consequently, the transformation processes affecting

organic compounds. The variety of microbially mediated reaction pathways covers, e.g., nitrate reduction, iron reduction, sulfate reduction, and methanogenesis. These processes have high implications in particular for the stability of organic matter in aquifers. Depending on these environmental conditions as well as on the chemical properties of the contaminants, either significant microbial degradation or stability over long periods of time (years, decades) may be observed.

3.2 Natural Organic Substances

The knowledge on natural substances in groundwater is very restricted. Similar to surface water systems, a huge proportion of humic substances is proposed to occur (e.g., Alborzfar et al. 1998). Quantitative calculations revealed, e.g., amounts of approx. 5–20 mg C/L of humic acids in shallow aquifers. However, information on low molecular weight substances is rarely reported. It is known that carboxylic acids contribute to DOC in selected aquifers (McMahon and Chapelle 1991). Furthermore, some indications for the presence of terpenoid compounds in groundwater and their possible role as humic precursors have been reported (Leenheer et al. 2003).

3.3 Anthropogenic Organic Contamination

Anthropogenic pollution is a major concern in particular with respect to shallow aquifers, which frequently represent important drinking water reservoirs. Principally, three major emission sources release organic pollutants into the groundwater systems. Firstly, a direct application of chemicals to soils and their subsequent relocation toward the aquifers contaminates groundwater resources in particular by agrochemicals like pesticides and fertilizers (e.g., Kolpin et al. 2001). Further on, two other types of emission sources are dominating the groundwater contaminations that unintentionally release pollutants toward aquifers, sometimes for decades. On the one hand, industrial facilities handling with gasoline or petroleum-related products, gas production plants, and dry-cleaning services are known to have frequently emitted huge amounts of specific pollutants in the past as the result of careless handling or leakages. Typical groundwater-relevant contaminants related to fossil fuels are monoaromatic compounds especially the BTEX (benzene, toluene, ethylbenzene, xylenes) but also naphthalene and tricyclic aromatic hydrocarbons (e.g., Cozzarelli et al. 1995; Ohlenbusch et al. 2002; Zamfirescu and Grathwohl 2001; Vinzelberg et al. 2005). Further on, much attention has been given to the gasoline additive methyl *tert*-butyl ether MTBE, which exhibits a high water solubility and a high environmental stability in groundwater (e.g., Squillace et al. 1996; Gelmann and Binstock 2008). Dry-cleaning facilities have partially emitted high amounts of the drying agent tetrachloroethylene (PER), what resulted in groundwater contaminations by this compound and its dechlorinated metabolites (e.g., Bradley 2000; Vieth et al. 2003). In particular the metabolites exhibit extended persistence under anaerobic conditions.

Beside industrial facilities or services, a last emission source of groundwater contamination can be attributed to leakages of waste deposit landfills. Continuous discharge as a result of insufficient bottom sealings has frequently released a wide spectrum of contaminants to the aquifers, because seepage water of deposit landfills is characterized by very complex mixtures in particular of organic contaminants (e.g., Öman and Hynning 1993; Paxeus 1999; Schwarzbauer et al. 2002). Several environmental studies on landfill-derived groundwater contamination focused on the distribution and fate of specific organic compounds derived from landfill leachates in the underground (e.g., Albaiges et al. 1986; Rügge et al. 1995; Heim et al. 2004).

Intensive activities are related with the remediation of contaminated groundwater either by technical measures or by the so-called *natural attenuation* approach (e.g., Lerner et al. 2005; Baun et al. 2003; Eganhouse et al. 2005). With respect to the latter remediation approach, information on occurrence and rate of microbial degradation is of fundamental importance (Sturchio et al. 1998). Principally two different approaches are used to figure out transformation processes, on the one hand the identification and quantification of metabolites and on the other hand the monitoring of degradation by compound-specific isotope analysis. Examples for characteristic transformations in anaerobic aquifers include the carboxylation of aromatic compounds under sulfate-reducing conditions (Vinzelberg et al. 2005; Meckenstock et al. 2000; Griebler et al. 2004; Coates et al. 2002) or the hydroxylation of chlorinated and non-chlorinated aromatics by methanotrophic microbes forming phenolic compounds (e.g., Adriaens and Grbic-Galic 1994; Coates et al. 2002). Investigations applying isotope analyses have focused mainly on the quantification of degradation processes as a key parameter for natural attenuation approaches. Compound specific analyses have used dominantly stable carbon but to a minor extend also hydrogen isotopes. A detailed summary of isotope analysis applied to groundwater has been recently published (Schmidt et al. 2004); for principles of isotope analysis, see Vieth-Hillebrand and Wilkes (► Chap. 13, “Stable Isotopes in Understanding Origin and Degradation Processes of Hydrocarbons and Petroleum”, this volume).

4 Marine Environment

4.1 Occurrence and Fate of Organic Compounds in the Marine Environment

Major attention has been attributed to the occurrence and behavior of organic matter in marine systems since processes causing the natural synthesis as well as degradation or preservation of organic matter in these ecosystems are the initial steps in the generation of kerogen, petroleum, and related matter. Hence, the knowledge on the zones of preferential primary production of organic matter by photosynthesis of marine organisms as well as the factors affecting the preservation especially in the benthic environment is a main topic in the scientific field of organic geochemistry (Tissot and Welte 1984; Killops and Killops 2005).

Beside the vertical distribution as the result of global ocean currents the dominant process affecting the occurrence of organic matter in the marine environment is its vertical flux within the water column. Thereby, key aspects on the corresponding fate of organic substances are the interaction of dissolved and particle-associated matter in combination with the biological uptake and excretion, e.g., by the planktonic food web (Wakeham and Lee 1989). Principally, organic substances involved in the biological loop (including the bioavailable DOC) are affected by high turn-around times, high dynamics, and intensive transformation or degradation. However, the adsorption on particulate matter reduces its bioavailability and, therefore, implies an initial step for enhanced preservation. The importance of adsorption phenomena as stabilization processes for labile organic matter was pointed out by Keil et al. (1994) as well as Mayer (1994). Since the reversible adsorption and desorption processes depend among other parameters on the polarity or lipophilicity of the substances to be sorbed, dominantly less polar compounds tend to be more enriched in the solid phase and more effectively stabilized by particle association. This particulate matter is partially deposited by sedimentation, and the associated, more lipophilic compounds are transferred into the sediments. During sedimentation, comprising a dynamic exchange between POC and DOC by adsorption and desorption, the organic matter undergoes many diagenetic alterations. After its transport through the water column, the more anaerobic ambience in the benthic compartment provides further conditions supporting an enhanced environmental stability for many organic compounds accumulated in and incorporated into sediment deposits. The persistence or stability in the benthic and later on in the sedimentary systems over geological times and the biotic and abiotic transformation processes affecting the individual molecular structures in these systems are covered by the wide field of organic geochemistry and, therefore, are not subject of this chapter.

Noteworthy, terrigenous discharge contributes significantly to marine organic matter, in particular at the intersection of marine and terrestrial ecosystems, the estuaries, and deltas (Hedges et al. 1997). Huge amounts of organic material are discharged from rivers to the coastal regions as dissolved (DOC) but also as particulate organic carbon (POC). Calculation of terrestrial budgets is based either on carbon isotope analysis (e.g., Goni et al. 1997; Raymond and Bauer 2001; Shi et al. 2001; Countway et al. 2007) or determination of indicative chemical marker compounds reflecting unambiguously terrigenous origin, e.g., lignin (e.g., Opsahl et al. 1999; Cannuel 2001; Harvey and Mannino 2001; Jaffe et al. 2001). However, calculated budget data vary depending on the approach as well as on the aquatic systems. For the arctic environment, a riverine discharge of terrigenous matter to the Arctic Ocean of roughly $25 \text{ Tg C year}^{-1}$ has been calculated, of which 10–40% may reach the Northern Atlantic Ocean (Opsahl et al. 1999). The riverine contribution to the Arctic Ocean is subdivided into approx. 80% of DOC and approx. 20% of POC (Dittmar and Kattner 2003). Global budget calculation on the basis of lignin analysis suggested an overall contribution of terrigenous material of approx. 0.7–2.4% to the total DOC in the oceans with a predicted shorter oceanic residence time of 20–130 years for this fraction (Opsahl and Benner 2003).

4.2 Natural Organic Substances

Organic matter in the marine ecosystems originates dominantly from the aquatic organisms and, therefore, exhibits partially high similarity to the contributions of biotic organic matter discharged to the terrestrial aquatic systems (see Sect. 1.2). Beside natural macromolecules like peptides, proteins, and polysaccharides (e.g., Khodse et al. 2008), in particular, cell membrane lipids and pigments from marine phyto- and zooplankton, contribute to the pools of DOC and POC. Well-known components comprise *n*-alkan-1-ols, saturated and unsaturated fatty acids, long-chain alkenones (e.g., 37:2 and 37:3 alkenones), di- and tetraphytyl ethers, steroids (e.g., cholesterol, dinosterol, desmosterol), carotenoids (e.g., lycopene, isorenieratene, diatoxanthin, fucoxanthin, peridinin), and chlorophyll-related pigments.

According to the general partition behavior of low molecular weight organic substances as described in Sect. 1.1, the less polar substances accumulate first in the particulate matter within the water body and, later on, in the sedimentary environment. However, during the passage through the water body, strong alterations due to biotic and abiotic transformation occur. Examples are autoxidation processes, photooxidation, or microbial decomposition (e.g., Sun et al. 2004; Rontani et al. 2006).

Further on, marine humic substances contribute dominantly to the DOC but exhibit structural differences as compared to terrigenous material. A major difference is the degree of aromaticity, which has been already used to discriminate terrestrial and marine humics. Aromatic carbon content has been calculated to be 20–50% in soil humics, 20–35% in peat humics, but less than 15% in marine humics. Further on, the H/C atomic ratios vary between 1.0 to 1.5 in marine humics and 0.5 to 1.0 in soil humics (Killops and Killops 2005).

Interestingly, the relative amount of biogenic halogenated compounds is enriched in the marine ecosystems as compared to terrestrial surface water systems probably due to the elevated chloride and bromide concentrations in seawater. These substances cover a wide range of structural diversity including simple molecules like halogenated methanes and ethanes but also more complex substances like brominated and chlorinated terpenoids, heterocycles, acetogenins, macrolides, and to a higher extent aromatic compounds (Gribbles 2000; Ballschmiter 2003).

Further compounds, which are still unnoticed so far but are obviously specific marine substances, are derived from biomethylation reactions of metal ions. One example of such organometallic substances is dimethylthallium, detected in surface water samples from the Atlantic Ocean accompanied by methylated cadmium and lead species (Schedlbauer and Heumann 2000).

4.3 Anthropogenic Organic Contamination

Many of the environmental aspects of terrestrial contaminants account also for the marine ecosystems due to the discharge of terrestrial matter in coastal areas. Hence,

in addition to specific natural compounds serving as terrestrial indicators, also anthropogenic contaminants are appropriate markers to monitor the riverine impact on the marine environment (Schwarzbauer et al. 2000; Grigoriadou et al. 2008; Dsikowitzky et al. 2017). Beside river discharge, also the aeolian long-range transport of particle-associated pollutants contributes to marine contamination. Beside these allochthonous emissions, the autochthonous emissions are of major interest for the state of pollution of the marine environment. A first aspect is related with shipping activities, which release pollutants during routine operation or as a result of accidents. A common example for the former type of contamination is tin organic compounds, which have been intensively used over a prolonged time as active components in antifouling paints. Noteworthy, not only the marine environment but also rivers, lakes, and, in particular, harbors are contaminated by these substances. Most prominent example is tributyltin, an ionic molecule with lipophilic butyl moieties. As a result of its amphoteric character with respect to its lipo-/hydrophilicity, it is accumulated on the one hand in sediments but is also present in high amounts in the water phase. Since tributyltin exhibits elevated ecotoxicological effects, it has been substituted recently by other antifouling agents.

Shipping activities also result in contamination by petroleum-derived substances, in particular, hydrocarbons. As introduced in Sect. 1.3, aromatic hydrocarbons can act as indicative substances to characterize petroleum discharge and to differentiate it from combustion-derived pollution, which are entering the marine environment via aeolian particles (e.g., Ding et al. 2007). Hence, PAHs have been frequently used (partially together with further petroleum-related hydrocarbons like hopanes) to assess the petroleum-derived impact on the marine ecosystems, in particular the coastal areas (e.g., Yunker and Macdonald 2003; Grigoriadou et al. 2008). Beside its marker properties, it is also obvious that PAHs harm the marine environment, e.g., by bioaccumulation in marine organisms (Meador et al. 1995, Ohwada et al. 2003; Hylland 2006). However, PAHs and further petroleum hydrocarbons are constituents of marine sediments not only as the result of shipping activities but also derived from offshore oil production. For example, drill cuttings have been reported to contribute significantly to sedimentary hydrocarbon pollution (Scholz-Böttcher et al. 2008; Skaare et al. 2008).

A further major source of petroleum-related contamination has to be attributed to oil spills. Many accidents of oil tankers have had an enormous impact on the marine ecosystems. The behavior of oil after release to seawater depends on various parameters comprising, e.g., wind drift with subsequent emulsification and dispersion, the chemical nature of individual oil fractions, sunlight intensity, water temperature, and the benthic microbial community. Individual fractions of crude oil undergo different degradation or transformation pathways as well as transport processes. The light components remain over a prolonged time on the water surface and can be subject to abiotic photolysis or photooxidation as well as evaporation. On the contrary, heavier fractions sink to the seafloor. Generally, after oil spills the principal components of oil, the linear alkanes, branched aliphatics, aromatic compounds, and functionalized substances, exhibit different residence times on water or in sediments as well as underlie varying weathering processes due to their different

potentials to be microbially degraded (e.g., Ezra et al. 2000; Gallego et al. 2006; Farias et al. 2008). The diverse fate of compound classes has been used to fingerprint oil spills and related sources by biomarkers (e.g., Wang et al. 2006). A high environmental impact has to be associated to the residual fraction of oil remaining in the benthic ecosystems or the beach sediments of the affected coasts over a prolonged time (e.g., Short et al. 2007a). Further long-term effects are attributed to the generation of more toxic biotic metabolites or the release of toxic constituents to the seawater after alteration, e.g., of the asphaltene fraction (DiToro et al. 2007). Oil spills that have been intensively investigated in terms of long-term effects and the distribution and fate of oil-derived hydrocarbons are, for example, the accidents of the *Exxon Valdez* in the Gulf of Alaska and the *Prestige* near the Spanish coast (Bence et al. 1996; Gallego et al. 2006). However, it should be also mentioned that a very small proportion of marine petroleum contamination arose from natural seeps discharging oil in particular from coastal regions to the sea (e.g., Short et al. 2007b).

In recent years, an interesting aspect arose concerning a so far neglected fraction of anthropogenic contaminants, the plastics. Huge amounts of plastic (polypropylene, polystyrene, etc.) in different forms (as pellets, foams, or foil) have been released to the oceans for decades, although their enormous environmental stability is well-known. The ingestion of plastic debris by marine birds and the related harmful effects have been reported since the 1980s, whereas the information on ingestion by fishes or filter-feeding organisms increased in the last years (e.g., Eriksson and Burton 2003). Also the accumulation of plastic debris in defined regions, e.g., of the Pacific Ocean, has been elucidated (Moore et al. 2001). Recently, the attention turned to very small plastic particles, the so-called microplastics. Not only the direct harmful impacts but also the effects of plastic resin pellets as transport medium for pollutants have been discussed and reported (Mato et al. 2001; Endo et al. 2005; Frias et al. 2010). Current knowledge on plastics including microplastics in the aquatic environment has been summarized in various reviews (e.g., Andrady 2011; Browne et al. 2011; Ivar do Sul and Costa 2014; Eerkes-Medrano et al. 2015).

5 Research Needs

Although the knowledge on organic matter in the hydrosphere has been expanded intensively in the last two decades there is still an enormous need to clarify further on the fate of organic substances in water. Interesting aspects of future research are comprehensive structural elucidation of more complex compounds as well as investigations on the environmental behavior of natural and anthropogenic substances. In particular, our knowledge on natural organic matter in groundwater remains on a more or less bulk characterization. Hence, intensive investigations on the characterization of dissolved groundwater constituents of low molecular as well as macromolecular weight are desirable for the future. Further on, the activities in characterization of the microbially assisted interaction of metals and organic matter resulting in organometallic compounds have to be expanded.

Further examples for future needful research activities are the investigations on the overall life cycle of natural as well as anthropogenic compounds in the marine systems or the detection and monitoring of disperse and especially dissolved xenobiotic polymers in river systems.

References

- Abu-Qare AW, Duncan HJ (2002) Photodegradation of the herbicide EPTC and the safener dichlormid, alone and in combination. *Chemosphere* 46:1183–1189
- Adriaens P, Grbic-Galic D (1994) Cometabolic transformation of mono- and dichlorobiphenyls and chlorohydroxybiphenyls by methanotrophic groundwater isolates. *Environ Sci Technol* 28:1325–1330
- Albaiges J, Casado F, Ventura F (1986) Organic indicators of groundwater pollution by a sanitary landfill. *Water Res* 20:1153–1159
- Alborzfar M, Jonsson G, Gron C (1998) Removal of natural organic matter from two types of humic ground waters by nanofiltration. *Water Res* 32:2983–2994
- Andrady A (2011) Microplastics in the marine environment. *Mar Pollut Bull* 62:1596–1605
- Ballschmitter K (2003) Pattern and sources of naturally produced organohalogens in the marine environment: biogenic formation of organohalogens. *Chemosphere* 52:313–324
- Balmer ME, Buser HR, Müller MD, Poiger T (2005) Occurrence of some organic UV filters in waste water, in surface waters, and in fish from Swiss lakes. *Environ Sci Technol* 39:953–962
- Barra R, Quiroz R, Saez K, Araneda A, Urrutia R, Popp P (2009) Sources of polycyclic aromatic hydrocarbons (PAHs) in sediments of the Biobio River in south central Chile. *Environ Chem Lett* 7:133–139
- Baun A, Reitzel LA, Ledin A, Christensen TH, Bjerg PL (2003) Natural attenuation of xenobiotic organic compounds in a landfill Leachate plume (Vejen, Denmark). *J Contam Hydrol* 65:269–291
- Bence AE, Kvenvolden KA, Kennicutt MC (1996) Organic geochemistry applied to environmental assessments of Prince William Sound, Alaska, after the Exxon Valdez oil spill – as review. *Org Geochem* 24:7–42
- Berdie L, Grimalt JO, Gjessing ET (1995) Combined fatty acids and amino acids in the dissolved and colloidal and particulate fractions of the waters from a dystrophic lake. *Org Geochem* 23:343–353
- Bilgi S, Demir C (2005) Identification of photooxidation degradation products of C.I. Reactive Orange 16 dye by gas chromatography-mass spectrometry. *Dyes Pigments* 66:69–76
- Bradley PM (2000) Microbial degradation of chlorethenes in groundwater systems. *Hydrogeol J* 8:104–111
- Brigden K, Labunska I, Santillo D (2004) Toxic chemical pollutants released from the Thai Plastic & Chemicals PVC facility to the Chao-Phraya River, Samut Prakan, Thailand. Greenpeace Research Laboratories, Technical note 05/2005, 31 p
- Browne MA, Crump P, Niven SJ, Teuten E, Tonkin A, Galloway T, Thompson R (2011) Accumulation of microplastics on shorelines worldwide: sources and sinks. *Environ Sci Technol* 45:9175–9179
- Cannuel EA (2001) Relations between river flow, primary production and fatty acid composition of particulate organic matter in San Francisco and Chesapeake Bays: a multivariate approach. *Org Geochem* 32:563–584
- Castillo M, Barcelo D, Pereira AS, Neto FRA (1999) Characterization of organic pollutants in industrial effluents by high-temperature gas chromatography-mass spectrometry. *Trends Anal Chem* 18:26–36
- Coates JD, Chakraborty R, McInerney MJ (2002) Anaerobic benzene biodegradation – a new era. *Res Microbiol* 153:621–628

- Countway RE, Canuel EA, Dickhut RM (2007) Sources of particulate organic matter in surface waters of the York River, VA estuary. *Org Geochem* 38:365–379
- Cozzarelli IM, Herman JS, Baedecker MJ (1995) Fate of microbial metabolites of hydrocarbons in a coastal plain aquifer: the role of electron acceptors. *Environ Sci Technol* 29:458–469
- Cranwell PA (1981) Diagenesis of free and bound lipids in terrestrial detritus deposited in a lacustrine sediment. *Org Geochem* 3:79–89
- Cranwell PA, Eglinton G, Robinson N (1987) Lipids of aquatic organism as potential contributors to lacustrine sediments – II. *Org Geochem* 11:513–527
- Curran KJ, Irvine KN, Droppo IG, Murphy TP (2000) Suspended solids, trace metals and PAH concentrations and loading from coal pile runoff to Hamilton harbour, Ontario. *J Great Lakes Res* 16:18–30
- Czaplicka M (2003) Qualitative and quantitative determination of halogenated derivatives in wastewater from coking plant. *J Sep Sci* 26:1067–1071
- DeLorenzo ME, Scott GI, Ross PE (2001) Toxicity of pesticides to aquatic microorganism: a review. *Environ Toxicol Chem* 20:84–98
- Di Toro DM, McGrath JA, Stubblefield WA (2007) Predicting the toxicity of heat and weathered crude oil: Toxic potential and the toxicity of saturated mixtures. *Environ Toxicol Chem* 26:24–36
- Ding X, Wang XM, Xie ZQ, Xiang CH, Mai BX, Sun LG, Zheng M, Sheng GY, Fu JM, Pöschl U (2007) Atmospheric polycyclic aromatic hydrocarbons observed over the North Pacific Ocean and the Arctic Sea: spatial distribution and source identification. *Atmos Environ* 41:2061–2072
- Dittmar T, Kattner G (2003) The biogeochemistry of the river and shelf ecosystem of the Arctic Ocean: a review. *Mar Chem* 83:103–120
- Dsikowitzky L, Schwarzbauer J (2014) Industrial organic contaminants: Identification, toxicity and fate in the environment. *Environ Chem Lett* 12:371–386
- Dsikowitzky L, Schwarzbauer J (2015) Hexa(methoxymethyl)melamine (HMMM), an emerging contaminant in German Rivers. *Water Environ Res* 87:461–469
- Dsikowitzky L, Schwarzbauer J, Kronimus A, Littke R (2004) The anthropogenic contribution to the organic load of the Lippe River (Germany). Part I: qualitative characterization of low-molecular weight organic compounds. *Chemosphere* 57:1275–1288
- Dsikowitzky L, Botalova O, Illgut S, Bosowski S, Schwarzbauer J (2015) Identification of characteristic organic contaminants in wastewaters from modern paper production sites and subsequent tracing in a river. *Hazard Mater* 300:254–262
- Dsikowitzky L, Schäfer L, Dwiytino, Ariyani F, Irianto HE, Schwarzbauer J (2017) Evidence of massive river pollution in the tropical megacity Jakarta as indicated by faecal steroid occurrence and the seasonal flushing out into the coastal ecosystem. *Environ Chem Lett*. <https://doi.org/10.1007/s10311-017-0641-3>. Published online
- Eerkes-Medrano D, Thompson RC, Aldridge DC (2015) Microplastics in freshwater systems: a review of the emerging threats, identification of knowledge gaps and prioritization of research needs. *Water Res* 75:63–82
- Eganhouse RP, Cozzarelli IM, Scholl MA, Matthews LL (2005) Natural attenuation of volatile organic compounds (VOCs) in the leachate plume of a municipal landfill: using alkylbenzenes as process probes. *Natl Groundw Assoc* 39(2):192–202
- Endo S, Takizawa R, Okuda K, Takada H (2005) Concentrations of polychlorinated biphenyls (PCBs) in beaches resin pellets: variability among individual particles and regional differences. *Mar Pollut Bull* 50:1103–1114
- Eriksson C, Burton H (2003) Origins and biological accumulation of small plastic particles in fur seals from Macquarie Island, Tasmania, Australia. *AMBIO J Hum Environ* 32:380–384
- Esteves VI, Duarte AC (2000) Differences between Humic substances from riverine, estuarine, and marine environments observed by fluorescence spectroscopy. *Acta Hydrochim Hydrobiol* 28:359–363
- Ezra S, Feinstein S, Pelly I, Bauman D, Miloslavsky I (2000) Weathering of fuel oil spill on the east Mediterranean coast, Ashdod, Israel. *Org Geochem* 31:1733–1741

- Farias CO, Hamacher C, Wagener ALR, Scofield AL (2008) Origin and degradation of hydrocarbons in mangrove sediments (Rio de Janeiro, Brazil) contaminated by an oil spill. *Org Geochem* 39:289–307
- Faure P, Mansuy-Hunalt L, Su X (2007) Alkanes and hopanes for pollution source apportionment in coking plant soils. *Environ Chem Lett* 5:41–46
- Filella M (2008) Freshwater: which NOM matters? *Environ Chem Lett*. <https://doi.org/10.1007/s10311-008-0158-x>. Published online first
- Fox WM, Copplestone CD, Johnson MS, Leah RT (2001) The organochlorine contamination history of Mersey estuary, UK, revealed by analysis of sediment cores from salt marshes. *Mar Environ Res* 51:213–227
- Frias J, Sobral P, Ferreira A (2010) Organic pollutants in microplastics from two beaches of the Portuguese coast. Lisboa, Portugal: *Mar Pollut Bull* 60:1988–1992
- Frimmel FH (1998) Characterization of natural organic matter as major constituents in aquatic systems. *J Contam Hydrol* 35:201–216
- Gallego JR, Gonzalez-Rojas E, Pelaez AI, Sanchez J, Garcia-Martinez MJ, Ortiz JE, Torres T, Llamas JF (2006) Natural attenuation and bioremediation of *Prestige* fuel oil along the Atlantic coast of Galicia (Spain). *Org Geochem* 37:1869–1884
- Gelmann F, Binstock R (2008) Natural attenuation of MTBE and BTEX compounds in a petroleum contaminated shallow coastal aquifer. *Environ Chem Lett*. <https://doi.org/10.1007/s10311-007-121-2>. Published online first
- Geršlova E, Schwarzbauer J (2014) Hydrocarbon based indicators for characterizing potential sources of coal derived pollution in the vicinity of the Ostrava city. *Environ Earth Sci* 71:3211–3222
- Gevao B, Hamer T, Jones KC (2000) Sedimentary record of poly-chlorinated naphthalene concentrations and deposition fluxes in a dated lake core. *Environ Sci Technol* 34:33–38
- Goni MA, Ruttenger KC, Eglinton TL (1997) Sources and contribution of terrigenous organic carbon to surface sediments in the Gulf of Mexico. *Nature* 389:275–278
- Gribbles GW (2000) The natural production of organobromine compounds. *Environ Sci Pollut Res* 7:37–49
- Griebler C, Safinowski M, Vieth A, Richnow HH, Meckenstock RU (2004) Combined application of stable carbon isotope analysis and specific metabolites determination for assessing in situ degradation of aromatic hydrocarbons in a tar oil-contaminated aquifer. *Environ Sci Technol* 38:617–631
- Grigoriadou A, Schwarzbauer J, Georgakopoulos A (2008) Organic geochemical parameters for estimation of petrogenic inputs in the coastal area of Kavala city, Greece. *J Soils Sediments* 8:253–262
- Guo L, Lehner JK, White DM, Garland DS (2003) Heterogeneity of natural organic matter from the Chena River, Alaska. *Water Res* 37:1015–1022
- Gupta LP, Subramanian V, Ittekkot V (1997) Biogeochemistry of particulate organic matter transport by the Godavari River, India. *Biogeochemistry* 38:103–128
- Harvey HR, Mannino A (2001) The chemical composition and cycling of particulate and macromolecular dissolved organic matter in temperate estuaries as revealed by molecular organic tracers. *Org Geochem* 32:527–542
- Headley JV, Gandrass J, Kuballa J, Peru KM, Gong Y (1998) Rates of absorption and partition of contaminants in river biofilms. *Environ Sci Technol* 32:3968–3973
- Hedges JI, Cowie GL, Richey JE, Quay PD, Benner R, Strom M, Forsberg BR (1994) Origins and processing of organic matter in the Amazon River as indicated by carbohydrates and amino acids. *Limnol Oceanogr* 39:743–761
- Hedges JI, Keil RG, Brenner R (1997) What happens to terrestrial organic matter in the ocean? *Org Geochem* 27:195–212
- Heim S, Schwarzbauer J (2013) Reconstructing pollution history by geochronology of anthropogenic contaminants in aquatic sediment archives – a review. *Environ Chem Lett* 11:255–270

- Heim S, Schwarzbauer J, Littke R (2004) Monitoring of waste deposit derived groundwater contaminations by organic tracers. *Environ Chem Lett* 2:21–25
- Heim S, Hucke A, Schwarzbauer J, Littke R (2006) Geochronology of anthropogenic contaminants in a dated sediment core of the Rhine river (Germany): emission sources and risk assessment. *Acta Hydrochim Hydrobiol* 34:34–52
- Hylland K (2006) Polycyclic aromatic hydrocarbon (PAH) ecotoxicology in marine ecosystems. *J Toxicol Environ Health A* 69:109–123
- Ittekkot V (1988) Global trends in the nature of organic matter in river suspensions. *Nature* 332:436–438
- Ivar do Sul JA, Costa MF (2014) The present and future of microplastic pollution in the marine environment. *Environ Pollut* 185:352–364
- Jaffe R, Mead R, Hernandez ME, Peralba MC, DiGuida OA (2001) Origin and transport of sedimentary organic matter in two subtropical estuaries: a comparative, biomarker-based study. *Org Geochem* 32:507–526
- Keil RG, Montlucon DB, Prah FG, Hedges JI (1994) Sorptive preservation of labile organic matter in marine sediments. *Nature* 370:549–552
- Kerner M, Hohenberg H, Ertl S, Reckermann M, Spitz A (2003) Self-organization of dissolved organic matter to micelle-like microparticles in river water. *Nature* 422:150–154
- Khodse VB, Fernandes L, Bhosle NB, Sardesai S (2008) Carbohydrates, uronic acids and alkali extractable carbohydrates in contrasting marine and estuarine sediments: distribution, size fractionation and partial chemical characterization. *Org Geochem* 39:265–283
- Killops S, Killops V (2005) Introduction to organic geochemistry, 2nd edn. Oxford, Blackwell
- Klaus U, Mohamed S, Volk M, Spiteller M (1998) Interaction of aquatic humic substances with anilazine and its derivatives: the nature of the bound residues. *Chemosphere* 37:341–361
- Kolpin DW, Thurman EM, Linhart SM (2001) Occurrence of cyanazine compounds in groundwater: degradates more prevalent than the parent compound. *Environ Sci Technol* 35:1217–1222
- Kronimus A, Schwarzbauer J, Dsikowitzky L, Heim S, Littke R (2004) Anthropogenic contaminants in sediments of the Lippe River, Germany. *Water Res* 38:3473–3484
- Kumke U, Zwiener C, Abbt-Braun G, Frimmel FH (1999) Spectroscopic characterization of fulvic acid fractions of a contaminated groundwater. *Acta Hydrochim Hydrobiol* 27:409–415
- Lartiges SB, Garrigues PP (1995) Degradation kinetics of organophosphorus and organonitrogen pesticides in different waters under various environmental conditions. *Environ Sci Technol* 29:1246–1254
- Leenheer JA, Nanny MA, McIntyre C (2003) Terpenoids as major precursors of dissolved organic matter in landfill leachates, surface water and groundwater. *Environ Sci Technol* 37:2323–2331
- Lerner DN, Thornton SF, Spence MJ, Banwart SA, Bottrell SH, Higgs JJ, Mallinson HEH, Pickup RW, Williams GM (2005) Ineffective natural attenuation of degradable organic compounds in a phenol-contaminated aquifer. *Natl Groundw Assoc* 38:922–928
- Lopez-Grimau V, Guadayol JM, Grier JA, Gutierrez MC (2006) Determination of non halogenated solvents in industrial wastewater using solid phase microextraction (SPME) and GC-MS. *Lat Am Appl Res* 36:12
- Mato Y, Isobe T, Takada H, Kanehiro H, Ohtake C, Kaminuma T (2001) Plastic resin pellets as a transport medium for toxic chemicals in the marine environment. *Environ Sci Technol* 35:318–324
- Mayer LM (1994) Surface area control of organic carbon accumulation in continental shelf sediments. *Geochim Cosmochim Acta* 58:1271–1284
- McMahon PB, Chapelle FH (1991) Microbial production of organic acids in aquitard sediments and its role in aquifer geochemistry. *Nature* 349:233–235
- Meador JP, Stein JE, Reichert WL, Varanasi U (1995) Bioaccumulation of polycyclic aromatic hydrocarbons by marine organisms. *Rev Environ Contam Toxicol* 143:79–165
- Meckenstock RU, Anweiler E, Michaelis W, Richnow HH, Schink B (2000) Anaerobic naphthalene degradation by a sulfate-reducing enrichment culture. *Appl Environ Microbiol* 66:2743–2747

- Moore CJ, Moore SL, Leecaster MK, Weisberg SB (2001) A comparison of plastic and plankton in the North Pacific central gyre. *Mar Pollut Bull* 42:1297–1300
- Northcott GL, Jones KC (2000) Experimental approaches and analytical techniques for determining organic compounds bound residues in soil and sediment. *Environ Pollut* 108:19–43
- Ohlenbusch G, Zwiener C, Meckenstock RU, Frimmel FH (2002) Identification and quantification of polar naphthalene derivatives in contaminated groundwater of a former gas plant site by liquid chromatography-electrospray ionization tandem mass spectrometry. *J Chromatogr* 967:201–207
- Ohwada K, Nishimura M, Wada M, Nomura H, Shibata A, Okamoto K, Toyoda K, Yoshida A, Takada H, Yamada M (2003) Study of the effect of water-soluble fractions of heavy-oil on coastal marine organisms using enclosed ecosystems, mesocosms. *Mar Pollut Bull* 47:78–84
- Öman C, Hynning P-A (1993) Identification of organic compounds in municipal landfill leachates. *Environ Pollut* 80:265–271
- Opsahl S, Benner R (2003) Distribution and cycling of terrigenous dissolved organic matter in the ocean. *Nature* 386:480–482
- Opsahl S, Benner R, Amon RMW (1999) Major flux of terrigenous dissolved organic matter through the Arctic Ocean. *Limnol Oceanogr* 44:2017–2023
- Paxeus N (1999) Organic compounds in municipal landfill leachates. *Water Sci Technol* 42:323–333
- Pinheiro HM, Touraud E, Thomas O (2004) Aromatic amines from azo dye reduction: status review with emphasis on direct UV spectrophotometric detection in textile industry wastewaters. *Dyes Pigments* 61:121–139
- Prahl FG, Pinto LA (1987) A geochemical study of long-chain n-aldehydes in Washington coastal sediments. *Geochim Cosmochim Acta* 51:1573–1582
- Rao SS, Burnison BK, Rokosh DA, Taylor CM (1994) Mutagenicity and toxicity assessment of pulp mill effluent. *Chemosphere* 28:1859–1870
- Raymond PA, Bauer JE (2001) Use of ^{14}C and ^{13}C natural abundances for evaluating riverine, estuarine, and coastal DOC and POC sources and cycling: a review and synthesis. *Org Geochem* 32:469–486
- Reemtsma T, Fiehn O, Kalnowski G, Jekel M (1995) Microbial transformations and biological effects of fungicide – derived benzothiazoles determined in industrial wastewater. *Environ Sci Technol* 29:478–485
- Repeta DJ, Quan TM, Aluwihare LI, Accardi AM (2002) Chemical characterization of high molecular weight dissolved organic matter in fresh and marine waters. *Geochim Cosmochim Acta* 66:955–962
- Riley G, Collier RJ, Jones DM, Eglinton G (1991) The biogeochemistry of Ellemser Lake U.K. – I: source correlation of leaf wax inputs to the sedimentary lipid record. *Org Geochem* 17:901–912
- Rontani JF, Marty JC, Miquel JC, Volkman JK (2006) Free radical oxidation (autoxidation) of alkenones and other microalgal lipids in seawater. *Org Geochem* 27:354–368
- Rügge K, Bjerg PL, Christensen TH (1995) Distribution of organic compounds from municipal solid waste in the groundwater downgradient of a landfill. *Environ Sci Technol* 29:1395–1400
- Schedlbauer OF, Heumann KG (2000) Biomethylation of thallium by bacteria and first determination of biogenic dimethylthallium in the ocean. *Appl Organomet Chem* 14:330–340
- Schmidt TC, Zwank L, Elsner M, Berg M, Meckenstock RU, Haderlein SB (2004) Compound-specific stable isotope analysis of organic contaminants in natural environments: a critical review of the state of art, prospects, and future challenges. *Anal Bioanal Chem* 378:283–300
- Scholz-Böttcher BM, Ahlf S, Vazquez-Gutierrez F, Rullkötter J (2008) Sources of hydrocarbon pollution in surface sediments of the Campeche Sound, Gulf of Mexico, revealed by biomarker analysis. *Org Geochem* 39:1104–1108
- Schulten HR, Leinweber P (1996) Characterisation of humic and soil particles by analytical pyrolysis and computer modelling. *J Anal Appl Pyrolysis* 38:1–53
- Schwarzbauer J (2005) Organic contaminants in riverine and groundwater systems – aspects of the anthropogenic contribution. Springer, Berlin/Heidelberg

- Schwarzbauer J, Heim S (2005) Lipophilic organic contaminants in the Rhine River, Germany. *Water Res* 39:4735–4748
- Schwarzbauer J, Littke R, Weigelt V (2000) Identification of specific organic contaminants for estimating the contribution of the Elbe River to the pollution of the German Bight. *Org Geochem* 31:1713–1731
- Schwarzbauer J, Ricking M, Franke S, Francke W (2001) Halogenated organic contaminants in sediments of the Havel and Spree Rivers (Germany). Part 5 of Organic compounds as contaminants of the Elbe River and its tributaries. *Environ Sci Technol* 35:4015–4025
- Schwarzbauer J, Heim S, Brinker S, Littke R (2002) Occurrence and alteration of organic contaminants in seepage and leakage water from a waste deposit landfill. *Water Res* 36:2275–2287
- Shi W, Sun MY, Molina M, Hodson RE (2001) Variability in the distribution of lipid biomarker and their molecular isotopic composition in Altamaha estuarine sediments: implications for the relative contribution of organic matter from various sources. *Org Geochem* 32:453–468
- Short JW, Irvine GV, Mann DH, Maselko JM, Pella JJ, Lindeberg MR, Payne JR, Driskell WB, Rice SD (2007a) Slightly weathered Exxon Valdez oil persists in Gulf of Alaska beach sediments after 16 years. *Environ Sci Technol* 41:1245–1250
- Short JW, Kolak JJ, Payne JR, van Kooten GK (2007b) An evaluation of petrogenic hydrocarbons in northern Gulf of Alaska continental shelf sediments – the role of coastal oil seep inputs. *Org Geochem* 38:643–670
- Skaare BB, Schaanning M, Morkved PT (2008) Source identification for oil-based drill cuttings on the seabed based on stable carbon isotopes. *Environ Chem Lett*. <https://doi.org/10.1007/s10311-008-0165-y>. Online first published
- Squillace PJ, Zogorski JS, Wilber WG, Price CV (1996) Preliminary assessment of the occurrence and possible sources of MTBE in groundwater in the United States, 1993–1994. *Environ Sci Technol* 30:1721–1730
- Srogi K (2007) Monitoring of environmental exposure to polycyclic aromatic hydrocarbons: a review. *Environ Chem Lett* 5:169–195
- Stout SA, Emsbo-Mattingly SD (2008) Concentration and character of PAHs and other hydrocarbons in coals of varying rank – Implications for environmental studies of soils and sediments containing particulate coal. *Org Geochem* 39:801–819
- Stout SA, Magar VS, Uhler RM, Ickes J, Abbott J, Brenner R (2001) Characterization of naturally-occurring and anthropogenic PAHs in urban sediments – wycoff/eagle harbor superfund site. *Environ Forensic* 2:287–300
- Sturchio NC, Clausen JL, Heraty LJ, Huang L, Holt BD, Abrajano TA (1998) Chlorine isotope investigation on natural attenuation of trichloroethylene in an aerobic aquifer. *Environ Sci Technol* 32:3037–3042
- Sun MY, Zou L, Dai J, Ding H, Culp RA, Scranton MI (2004) Molecular carbon isotopic fractionation of algal lipids during decomposition in natural oxic and anoxic seawaters. *Org Geochem* 35:895–908
- Sutton R, Sposito G (2005) Molecular structure in soil humic substances: the new view. *Environ Sci Technol* 39:9009–9015
- Takada H, Eganhouse RP (1998) Molecular markers of anthropogenic waste. In: Meyers RA (ed) *Encyclopedia of environmental analyses and remediation*. Wiley, New York, pp 2883–2940
- Tissot B, Welte DH (1984) *Petroleum formation and occurrence*. Springer, Berlin
- Venkatesan MI, de Leon RP, van Geen A, Luoma SN (1999) Chlorinated hydrocarbon pesticides and polychlorinated biphenyls in sediment cores from San Francisco Bay. *Mar Chem* 64:85–89
- Vieth A, Müller J, Strauch G, Kästner M, Gehre M, Meckenstock RU, Richnow HH (2003) In-situ biodegradation of tetrachloroethene and trichloroethene in contaminated aquifers monitored by stable isotope fractionation. *Isot Environ Health Stud* 39:113–124
- Vinzelberg G, Schwarzbauer J, Littke R (2005) Groundwater contamination by chlorinated naphthalenes and related substances caused by activities of a former military base. *Chemosphere* 61:770–782

- Volk CJ, Volk CB, Kaplan LA (1997) Chemical composition of biodegradable dissolved organic matter in streamwater. *Limnol Oceanogr* 42:39–44
- Wakeham SG, Lee C (1989) Organic geochemistry of particulate matter in the ocean. The role of particles in oceanic sedimentary cycles. *Org Geochem* 14:83–96
- Wang Z, Stout S, Fingas M (2006) Forensic fingerprinting of biomarkers for oil spill characterization and source identification. *Environ Forensic* 7:105–146
- Warren N, Allan IJ, Carter JE, House WA, Parker A (2003) Pesticides and other micro-organic contaminants in freshwater sedimentary environments – a review. *Appl Geochem* 18:159–194
- Wluka AK, Rüdell H, Pohl K, Schwarzbauer J (2016) Analytical method development for the determination of eight biocides in various environmental compartments and application for monitoring purposes. *Environ Sci Pollut Res* 23:21894–21907
- Yang Y, Ligouis B, Pies C, Achten C, Hofmann T (2008) Identification of carbonaceous geosorbents for PAHS by petrography in river floodplain soils. *Chemosphere* 71:2158–2167
- Yunker MB, Macdonald RW (2003) Petroleum biomarker sources in suspended particulate matter and sediments from the Fraser River basin and Strait of Georgia, Canada. *Org Geochem* 34:1525–1541
- Yunker MB, MacDonal RW, Vingarzan R, Mitchel RH, Goyette D, Sylvestre S (2002) PAHs in the Fraser River basin: a critical appraisal of PAH ratios as indicators of PAH source and composition. *Org Geochem* 33:489–515
- Zamfirescu D, Grathwohl P (2001) Occurrence and attenuation of specific organic compounds in the groundwater plume at a former gasworks site. *J Contam Hydrol* 35:407–427
- Zhang G, Min YS, Min BX, Sheng GY, Fu JM, Wang ZS (1999) Time trend of BHCs and DDTs in a sedimentary core in Macao estuary, Southern China. *Mar Pollut Bull* 39:326–330
- Zwiener C, Kumke MU, Abbt-Braun G, Frimmel FH (1999) Absorbed and bound residues in fulvic acid fractions of a contaminated groundwater – isolation, chromatographic and spectroscopic characterization. *Acta Hydrochim Hydrobiol* 27:208–213



Lessons from the 2010 *Deepwater Horizon* Accident in the Gulf of Mexico

31

Terry C. Hazen

Contents

1	Introduction	848
2	Lesson 1. Marine Oil Biodegradation Like All Politics Is Local and <i>DWH</i> Had Many Unique Aspects	848
3	Lesson 2. Oil in the Water Column and in Coastal Sediments Biodegraded Faster Than Expected	851
4	Lesson 3. Long-Term Adaption to Natural Seeps Played an Important Role in <i>DWH</i> Oil Biodegradation	853
5	Lesson 4. Jetting and Dispersants at the Well Head Increased Oil Biodegradation	853
6	Lesson 5. Comparisons of <i>DWH</i> with <i>Exxon Valdez</i> Oil Spill for Oil Biodegradation Were Not Appropriate	855
7	Lesson 6. Models for <i>DWH</i> Were Inappropriate at First	856
8	Lesson 7. Cometabolic Oil Biodegradation May Be Important in Deep Marine Basins	856
9	Lesson 8. Blooms of Oil Degraders in the Deep Led to a Temporal Succession of Other Bacterial Communities with Unknown Effects on Trophic Levels	857
10	Lesson 9. Molecular Techniques Led to a More Thorough Understanding of <i>DWH</i> Oil Biodegradation	858
11	Lesson 10. Hydrostatic Pressure Had Little Effect on <i>DWH</i> Oil Biodegradation	858
12	Research Needs	859
	References	861

T. C. Hazen (✉)

Department of Civil and Environmental Engineering, Department of Earth and Planetary Sciences, Department of Microbiology, Institute for Secure and Sustainable Environment, Methane Center, University of Tennessee, Knoxville, TN, USA

Biosciences Division, Oak Ridge National Laboratory, Oak Ridge, TN, USA

e-mail: tc hazen@utk.edu

© Springer Nature Switzerland AG 2020

H. Wilkes (ed.), *Hydrocarbons, Oils and Lipids: Diversity, Origin, Chemistry and Fate*, Handbook of Hydrocarbon and Lipid Microbiology,

https://doi.org/10.1007/978-3-319-90569-3_31

847

Abstract

The 2010 *Deepwater Horizon* (DWH) accident in the Gulf of Mexico had many unique aspects to it not seen in previous marine spills. Indeed, research related to the DWH response phase, Natural Resource Damage Assessment, Gulf of Mexico Research Initiative (GoMRI), National Academy of Sciences, US agencies: NOAA, EPA, Fish & Wildlife, DOE, and Coast Guard have made this the most studied marine oil spill in the world. There are many oil biodegradation lessons learned from this experience and these will undoubtedly continue for many years.

1 Introduction

On April 20, 2010, the *Deepwater Horizon* (DWH) an ultra-deepwater, dynamically positioned, semi-submersible, mobile offshore drilling rig owned by Transocean caught fire while drilling at the *Macondo* prospect in the Mississippi Canyon Block 252 lease and exploded 77 km off the coast of Louisiana in the Gulf of Mexico with the loss of 11 lives. Several attempts to activate the blowout prevention device and the blind shear ram failed. Two days later on April 22, 2010, the *DWH* sank to the seafloor at 1500 m, with the 53 cm riser pipe detaching from the rig it collapsed into a convoluted heap on the seafloor and began leaking oil in at least 3 sections. This caused the largest marine oil spill in United States history and the second largest marine oil spill in the world (Fig. 1). On June 3, 2010, the riser was cut off at the top of the blowout prevention device. After several attempts to stem the flow of oil failed, the well was successfully capped on July 15, 2010, and declared dead by the National Incident Commander on September 19, 2010. The government estimate of the amount of oil that came from the *Macondo* well directly into the environment was 4.1 million barrels with an additional 820,000 barrels captured via siphon tubes (Fig. 2) (FISG 2010). The cleanup effort was the largest ever in the world with more than 31,800 people involved (Fig. 2) (*Deepwater Horizon* Unified Command, 2010).

The *DWH* accident had many unique aspects to it not seen in previous marine spills. Indeed, research related to the *DWH* response phase, Natural Resource Damage Assessment, Gulf of Mexico Research Initiative (GoMRI), National Academy of Sciences, US agencies: NOAA, EPA, Fish & Wildlife, DOE, and Coast Guard have made this the most studied marine oil spill in the world. There are many oil biodegradation lessons learned from this experience and these will undoubtedly continue for many years.

2 Lesson 1. Marine Oil Biodegradation Like All Politics Is Local and *DWH* Had Many Unique Aspects

Marine oil biodegradation is affected by a large number of parameters, e.g., oil type, currents, weather, temperature, pressure, limiting nutrients, water depth, input of oil (leak, spill, failure of blowout prevention device), season, risk receptors, and ability

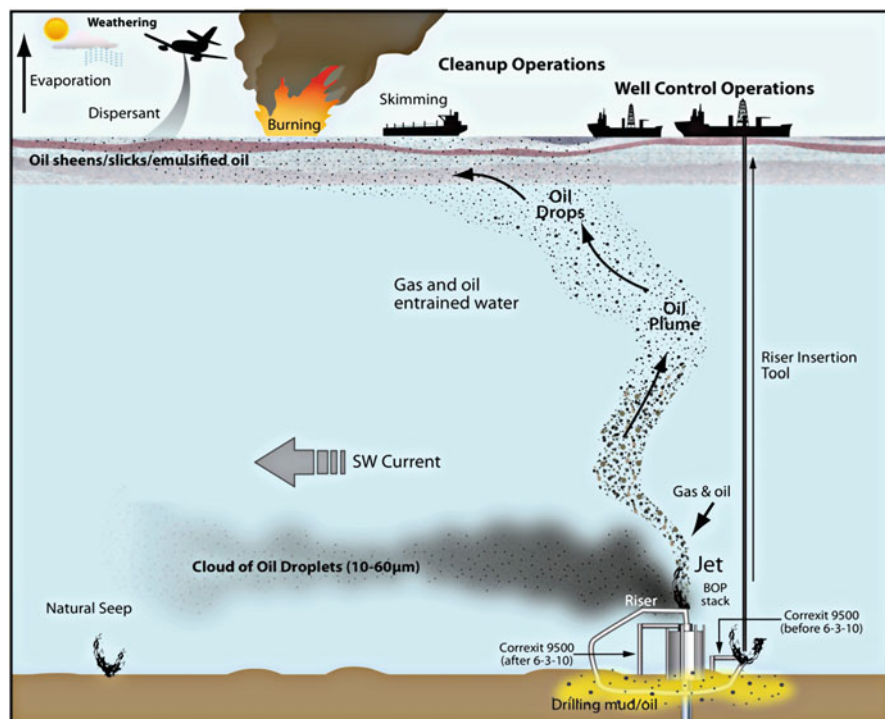


Fig. 1 Graphic depiction of Deepwater Horizon spill and cleanup, showing oil droplets rising to the surface and small droplet forming a deepwater cloud, oil sheens, and slicks the surface, with burning skimming, weathering, and blowout prevention (BOP) device that failed and injection of dispersant in the deep and at the surface. (After Atlas and Hazen (2011))

to apply remediation (dispersants, siphon tubes, booms, skimmers, burns). Many of these can work synergistically to impact oil biodegradation: (1) chemical dispersants + mineral fines can enhance formation and transfer of oil from the surface into the water column (Li et al. 2007), (2) autoinoculation from gyres + “memory response” of oil degraders leads to an increase in microbial abundance and accelerated oil biodegradation (Valentine et al. 2012), (3) oil droplet size + dispersion + biodegradation rates + dissolution enhances biodegradation, dissolution and dispersion rated oil hydrocarbons (Brakstad et al. 2015a), (4) cometabolic biodegradation + dispersion + secondary electron donors enhances biodegradation, dissolution, and dispersion rates of oil hydrocarbons even when the oil itself cannot be a suitable electron donor (Hazan et al. 2016), and (5) biosurfactants from multiple microorganisms can enhance bioavailability of poorly soluble hydrocarbons in the oil (Singh et al. 2007; McGenity et al. 2012).

DWH had many unique aspects, it was the deepest oil well blowout that has ever occurred, and it was the first time that dispersants were applied at the well head. It was not controlled for 84 days. It had deep water temperatures of 4 °C and simultaneous surface water temperatures of over 30 °C (Hazan et al. 2010).

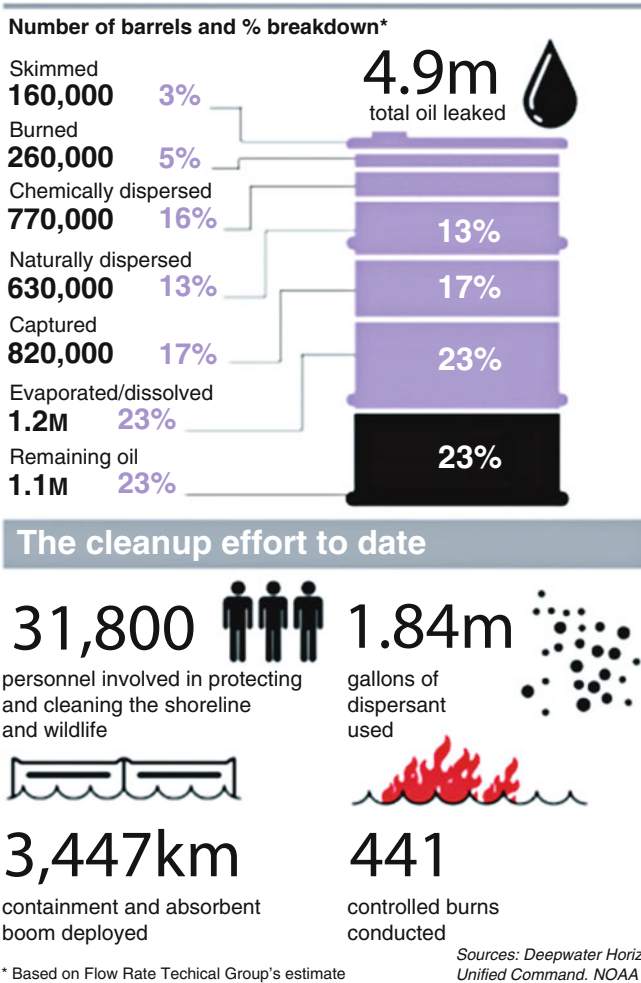


Fig. 2 Where the oil went? The Federal Interagency Solutions Group, Oil Budget Calculator Science and Engineering Team (November, 2010)

It occurred during the hurricane season, but only two major storms occurred during the period. There was a deepwater gyre at 1100 m that went from the *Macondo* well head out 15 km to the SW before turning back (Valentine et al. 2012). Deep water plumes occurred at four depths: 25, 265, 865, 1175 m, oil at the surface was moving to the North East while oil in the 1100 m plume was moving to the South West, the other three water column plumes moved to the SE, and NW (Spier et al. 2013). The Gulf of Mexico has more natural seeps than any other deepwater basin being considered for deepwater oil production (NAS 2003). *Macondo* oil is a very light crude, the *Macondo* well was jetting oil at high temperature (200 °C) and high pressure (676 bars) at the well head (pressure of the ocean at 1500 m was 152 bars).

The *Macondo* well was also one of the deepest wells; thus, the hydrostatic pressure may have had an effect on oil degraders like we have not seen before (Marietou et al. 2018). The *Macondo* oil had a high proportion of methane (Kessler et al. 2011). Nutrients from the Mississippi River made the overall nutrients higher near the spill (Hazen et al. 2010), and many hydrocarbons found in the *Macondo* oil and in the CORREXIT dispersant used were also found in Mississippi River and drainage into the Gulf of Mexico from non DWH sources (Kujawinski et al. 2011; King et al. 2014a).

3 Lesson 2. Oil in the Water Column and in Coastal Sediments Biodegraded Faster Than Expected

One of the first studies on oil biodegradation reported that the *Macondo* oil average half-life of alkanes in the deep water (1100) plume was 1.2–6.1 days (Table 1) (Hazen et al. 2010). The deepwater plume contained more than 80% alkanes, and four different techniques were used to make these calculations using microcosms with water and fresh *Macondo* oil at 5 °C, mixed consortia (Venosa and Holder 2007) incubations with fresh *Macondo* oil at 5 °C, and changes in alkane concentration from in the plume from the source to 10 km down gradient with split sample analyses done by two different labs and considering whether it took 2 days or 5 days to traverse that 10 km gradient (Hazen et al. 2010; Valentine et al. 2012). This surprised a lot of people. Rapid biodegradation also occurred initially of propane and ethane (Valentine et al. 2010). A more recent study again verified these findings (Thessen and North 2017). Considering that below 700 m the temperature in the Gulf of Mexico is always 5 °C or less and it has been that way for millions of years, it should not be surprising that there are true psychrophiles that can degrade oil faster at 5 °C than at 20 °C and given their potentially long period of adaptation degrade it faster than in previous studies at the surface (Baelum et al. 2012; Chakraborty et al. 2012; Dubinsky et al. 2013; Brakstad et al. 2015a; Hazen et al. 2016).

Macondo oil was also deposited in the sediments especially around the well head and in some other parts closer to shore as marine snow etc. (Rahsepar et al. 2017). Numerous studies also found that the sediment microbial community was degrading the *Macondo* oil faster than initially expected (Kimes et al. 2013, 2014; King et al. 2014a; Mason et al. 2014). Studies showed that a very active microbial community in the sediment was enriched in anaerobes (*Deltaproteobacteria*) in the deeper sediment and aerobes (*Gammaproteobacteria*) at the sediment surface that was very actively degrading a variety of *Macondo* well hydrocarbons including aromatic hydrocarbons (Kimes et al. 2013; Mason et al. 2014). Key hydrocarbon degradation pathways were determined by ¹⁴C-labeled substrates in order: propylene, glycol, dodecane, toluene, and phenanthrene (Mason et al. 2014).

Many studies along the coast where emulsified and weathered *Macondo* oil washed ashore also found that degradation rates of the *Macondo* oil were faster than previous studies at other sites around the world had shown (King et al. 2012, 2014a, b). Beach samples collected during the response phase and after showed a

Table 1 MC-252 alkane half-life (days) from field and laboratory with currents of 2–5 days to move 10 km from source. (After Hazen et al. (2010))

		Plume samples	Plume samples	BP data	BP data	Mixed Consortia 5 °C	Microcosm water, 5 °C
	Average	2.4	6.1	1.2	2.9	3.5	2.2
n-Tridecane	C13alk	1.6	4.0	1.4	3.5	3.1	2.1
n-Tetradecane	C14alk	1.5	3.8	1.4	3.4	3.5	2.3
Pentadecane	C15alk	1.5	3.8	1.0	2.4	3.6	2.1
n-hexadecane	C16alk	1.6	4.0	2.0	5.0	3.6	2.2
n-heptadecane	C17alk	1.7	4.3	1.1	2.8	3.6	2.3
Pristane	C19teralk	1.6	4.1	1.3	3.2	3.0	2.3
n-octadecane	C18alk	2.1	5.2	1.0	2.6	4.2	2.3
Phytane	C20teralk	1.8	4.6	1.4	3.4	3.6	2.3
n-Nonadecane	C19alk	2.1	5.4	1.0	2.6	3.6	2.3
eicosane	C20alk	3.2	7.9	1.0	2.5	3.7	2.3
Heneicosane	C21alk	3.7	9.3	1.9	4.7	3.5	2.6
n-Docosane	C22alk	3.8	9.5	1.0	2.5	3.7	2.2
Tricosane	C23alk	3.7	9.2	1.0	2.5	3.6	2.2
tetracosane	C24alk	3.2	8.0	0.9	2.2	3.5	2.3
n-Pentacosane	C25alk	2.8	7.0	0.8	1.9	3.6	2.0
n-hexacosane	C26alk	3.1	7.8	0.6	1.6	3.1	1.7

dominance of *Alphaproteobacteria* and *Gammaproteobacteria* (Kostka et al. 2011; Lamendella et al. 2014). Taxonomic diversity decreased in the sands for first few months but rebounded 1 year after the oil came ashore and much of the oil had been degraded (King et al. 2014a). Initially Pensacola Beach sands oil-degraders increased two orders of magnitude within the first week, while diversity decreased 50% (Huettel et al. 2018). Half-lives of the aliphatic and aromatic hydrocarbons were less than 25 days. Aerobic oil degradation was significantly promoted by tidal pumping. In the coastal salt marsh (Mobile Bay), the oil degrading community increased in richness and abundance especially among the *Proteobacteria*, *Bacteroidetes*, and *Actinobacteria* (Beazley et al. 2012). This study also suggested that marsh rhizosphere microbial communities could be contributing to the hydrocarbon degradation since there was a greater decrease in Macondo oil in marsh grass sediments than in inlet sediments that lacked marsh grass (King et al. 2014a). Studies in marshes in Barataria Bay, Louisiana, also showed increases in the bacteria *Rhodobacterales* and *Sphingomonadales* and the fungi *Dothideomycetes* (Mahmoudi et al. 2013). Another study that included 11 sites in southern Louisiana found that all studied marshes had increased abundance in *Proteobacteria*, *Firmicutes*, *Bacteroidetes*, and *Actinobacteria* during the first 4 months, but after 2 years with barely detectable hydrocarbon levels the bacteria communities were more diverse and dominated by *Alphaproteobacteria* (*Rhizobiales*), *Chloroflexi* (*Dehalococcoidia*), and *Planctomycetes* (Engel et al. 2017).

4 Lesson 3. Long-Term Adaption to Natural Seeps Played an Important Role in DWH Oil Biodegradation

Natural seeps in the Gulf of Mexico are the most abundant of any deepwater marine basin being considered for petroleum exploration and production (Fig. 3) (NAS 2003). A 10-year average showed that 400,000–1,000,000 barrels oil go into the Gulf of Mexico every year from natural seeps. These seeps are episodic and are primarily due to the major salt domes in the Gulf of Mexico which allow leakage from deeper petroleum reservoirs intersected by the salt domes. Recent use of satellite imagery and Fourier transform-ion cyclotron resonance-mass spectrometry may enable an even more detailed quantification of natural seeps in the Gulf of Mexico (Krajewski et al. 2018). Natural seeps in North America are estimated to exceed 160,000 tons and 600,000 tons globally each year. Over 60% of the petroleum entering North American waters comes from natural seeps, but only 45% of the petroleum entering the marine environment worldwide is from natural seeps (NAS 2003) See “Oil Biodegradation in Deep Marine Basin” by Hazen and Techtmann (2018).

It is not surprising then that microbes have become very well adapted to oil biodegradation in the Gulf of Mexico since it is the major long-term carbon and energy source that has been episodically released over millions of years (Kimes et al. 2013; Hazen et al. 2016). This long-term adaption to episodic release of oil provided a “memory” response that allowed oil-biodegraders to respond rapidly whenever oil was being seeped. Indeed, a significant increase in *Oceanospirillaceae* was seen only 1 km from the well head, and calculations suggest that it would only take the prevailing several hours to reach this area (Fig. 4) (Hazen et al. 2010).

5 Lesson 4. Jetting and Dispersants at the Well Head Increased Oil Biodegradation

The pressure of the *Macondo* well at the well head was 676 bars at >200 °C while the ambient pressure in the water around the well head was 152 bars at <5 °C. This would cause jetting a well-known phenomenon for oil well blowouts (Agbaglah et al. 2011). This would form oil droplets that would increase biodegradation primarily because of the change in the ratio of surface/volume (Fig. 4). Microbes can biodegrade oil hydrocarbons dissolved in water or are present at the oil/water interface. During *DWH* it was decided that even though jetting was occurring, there was too much oil coming to the surface close to the well control operations. This presented a major safety concern since the high methane content and relative flammability of the oil increased the risk of a fire and or explosion. So, for the first time ever permission to inject Corexit 9500 at the well head was given. It was also hoped that this would increase dispersion and biodegradation of oil so that less would reach the surface. Within 4 h after subsurface injection of dispersant was started, the oil coming to the surface was much farther away from the well control operations and every time that dispersant injection was stopped within 4 h the surface slick would move closer to the well control operations. Corexit 9500 was

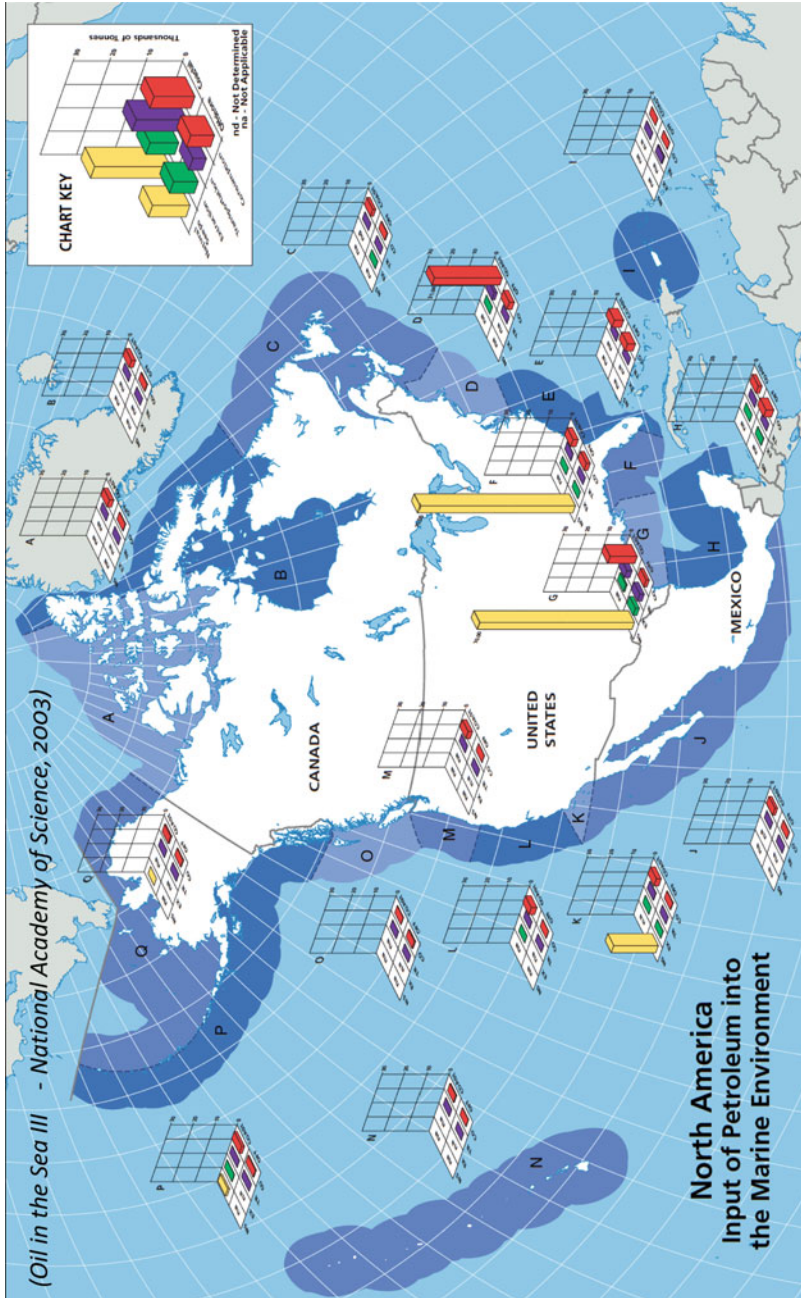


Fig. 3 Input of Oil in North America showing natural seeps, extraction, transportation, and consumption in deep water and the coast. (After NAS (2003))

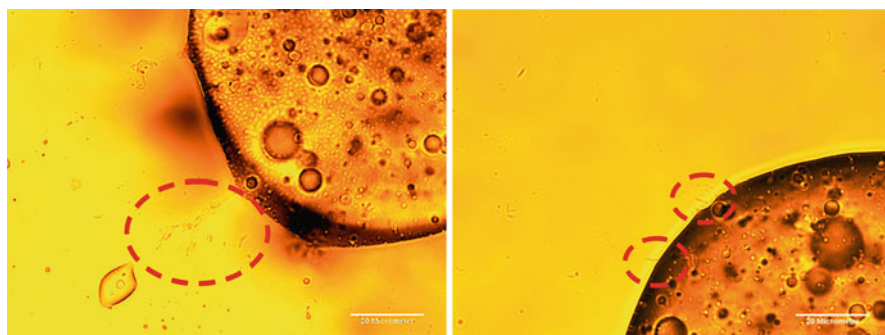


Fig. 4 Oil-degrading bacteria from 1100 m plume attached to a droplet of *Macondo* Oil. (Bright-field, 100X)

also used at the surface by spraying on surface slicks via ships and planes. It was also used on surface slicks during the Ixtoc I blowout in the Gulf of Mexico in 1979 (Hooper and NOAA Hazardous Materials Response Project (U.S.) 1982). Corexit 9500 or analogs had been used as an oil dispersant for more than 30 years. Any droplets that were formed by jetting or dispersant that were 10–60 μm in diameter were neutrally buoyant and were entrained in the current at 1100 m. Droplets that were 300 μm or larger were positively buoyant and rose to the surface.

Several studies on the *Macondo* oil have clearly demonstrated that smaller droplets degrade faster (Baelum et al. 2012; Adams et al. 2013; Vilcaez et al. 2013; Brakstad et al. 2014, 2015a, b; King et al. 2014a). Some studies have suggested that Corexit 9500 may be directly inhibitory to some oil biodegraders (Kleindienst et al. 2015). However, the vast majority of papers has found no inhibition by Corexit 9500 (Baelum et al. 2012; Prince and Butler 2014; Brakstad et al. 2015a; Prince 2015; Hazen et al. 2016; Techtmann et al. 2017b).

6 Lesson 5. Comparisons of *DWH* with *Exxon Valdez* Oil Spill for Oil Biodegradation Were Not Appropriate

It was appalling that during the *DWH* spill the media and many scientists were comparing *DWH* to the *Exxon Valdez* oil spill. While the *Exxon Valdez* oil spill was the largest oil spill in US marine waters up until *DWH* it was in no ways similar (Atlas and Hazen 2011). Unlike the *DWH*, the *Exxon Valdez* oil spill in *Prince William Sound* was a tanker spill that was close to shore and was “dead” oil, i.e., it did not have any of the methane or volatile organic carbon that the *Macondo* oil had. The *Prudhoe Bay* oil was heavier than *Macondo* oil and inherently less biodegradable. Natural attenuation was less of an option for the *Exxon Valdez* oil spill since the oil accumulated on shore near risk receptors for birds, fish, and mammals so several biostimulation techniques were tried. Since *DWH* was nearly 50 miles off shore and was degrading rapidly in the water column, no oil could be detected only 2 weeks after the well was finally capped.

Since Prince William Sound had no natural seeps and no exposure to oil prior to completion the Trans Alaskan pipeline it was not surprising that Prudhoe Bay oil biodegraded much more slowly than the Macondo oil. For a thorough comparison of *DVH* with the *Exxon Valdez* oil spills, see Atlas and Hazen (2011).

7 Lesson 6. Models for *DWH* Were Inappropriate at First

Because of the uniqueness of the *DWH* oil spill few, if any, models were prepared to simulate what happened especially in terms of oil biodegradation. The SINTEF OSCAR model was tried initially but failed to predict the oil biodegradation rates in the deep plume, primarily because it used a Q(10) algorithm that assumed that for every 10 °C change in temperature, there would be a proportional change in biodegradation rate (Bagi et al. 2013). This did not take into consideration that the dominant bacteria in the deep were psychrophiles (Hazen et al. 2010, 2016; Baelum et al. 2012; Chakraborty et al. 2012). Droplet break-up models include Equilibrium correlations (Johansen et al. 2013; Li et al. 2016) and Dynamic models (Zhao et al. 2017). SINTEF since 2010 has developed several updates to the original Oil Spill Contingency and Response (OSCAR) model. The Structured Learning in Microbial Ecology (SLiME) model was found to predict the concentration of oil in *DWH* deep plume almost perfectly from the microbial community structure (Smith et al. 2015).

8 Lesson 7. Cometabolic Oil Biodegradation May Be Important in Deep Marine Basins

The aerobic cometabolic biodegraders are dependent upon oxygenases, e.g., methane monooxygenase, toluene dioxygenase, toluene monooxygenase, and ammonia monooxygenase. These enzymes are extremely strong oxidizers, e.g., methane monooxygenase is known to transform over 1000 different compounds. However, like any bioremediation process, the proper biogeochemical conditions are necessary to maximize and maintain biodegradation, e.g., maintaining oxygen levels or other terminal electron acceptors that the cometabolic biodegrader is dependent (Hazen 1997, Hazen and Saylor 2016), and chapter on “Cometabolic Bioremediation” by Hazen 2018. In addition, co-metabolic biostimulation may require pulsing of electron donor or electron acceptor to reduce competitive inhibition between the substrate the microbe can use and the contaminant. Pulsing of methane was found to significantly improve biodegradation of trichloroethylene rates by methanotrophs (Hazen 2018). Indeed, during the *DWH* leak (Hazen et al. 2010), there was evidence that in the Gulf of Mexico where episodic releases of methane have occurred for millions of years from natural seeps this pulsing of methane may be removing oil and other organics via cometabolic biodegradation. The methane oxidizers bloomed during the *DWH* leaked above 400 m once the well was capped (Reddy et al. 2012; Redmond and Valentine 2012; Dubinsky et al. 2013). This suggests that intrinsic cometabolic bioremediation or cometabolic natural attenuation may be a

serious phenomenon in the ocean (Stackhouse et al. 2017). Methanotrophs, methane-oxidizing bacteria, oxidize methane via a series of enzymes that are unique to this group. The primary enzyme in this oxidation chain is methane monooxygenase. Methane monooxygenase is an extremely powerful oxidizer, thus giving it the capability of oxidizing a wide variety of normally recalcitrant compounds including oil constituents (Cardy et al. 1991). See chapter on “Cometabolic Bioremediation” by Hazen 2018.

9 Lesson 8. Blooms of Oil Degraders in the Deep Led to a Temporal Succession of Other Bacterial Communities with Unknown Effects on Trophic Levels

Once the oil was undetectable in the water column, many thought that the total biomass that would drastically decrease immediately and the microbial community diversity would increase to prespill levels (Hazen et al. 2010). However, once the oil degraders lost their competitive edge in using oil as a carbon and energy source, they began to die back, but there was a succession of bacteria that could use daughter products from direct oil degraders, i.e., “cheaters” bacteria that could not use the oil directly but could use some daughter product (Techtmann et al. 2016). As time progressed, even the “cheaters” could not compete so bacteria that could use the dead bacteria as a nutrient flourished (Fig. 5) (Dubinsky et al. 2013). So, the total microbial biomass slowly subsided over several months. The diversity of the microbial biomass also changed dramatically with the oil with the prespill having 951 subfamilies in 62 bacterial phyla (Fig. 6). The *DWH* deep oil plume had only 16 subfamilies in the Gammaproteobacteria (Hazen et al. 2010). Though bacteria do not sequester oil hydrocarbons like some organisms they basically convert oil hydrocarbons to bacterial compounds, this change in diversity could have had dramatic effects on the subsequent trophic levels since the size, shape, and compound composition of the food source had changed. This could also have a long-term effect even though the oil was gone! To date only a few studies have been published

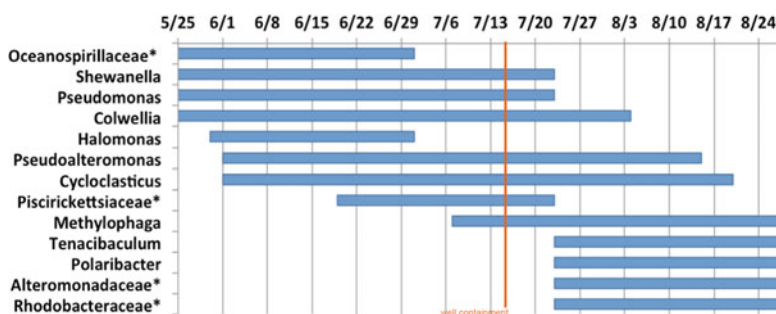


Fig. 5 Temporal Community Structure Changes showing sustained alterations in subsurface microbial communities and impacted the deep ocean for at least months after well containment. (After Dubinsky et al. (2013))

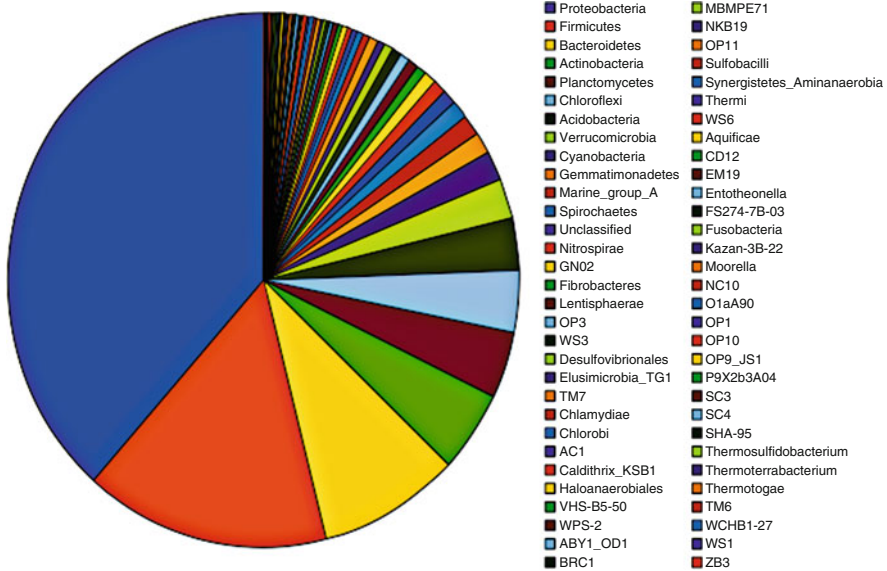


Fig. 6 951 subfamilies were detected in 62 bacterial phyla. Only 16 subfamilies in gammaproteobacteria significantly enriched in plume. (After Hazen et al. (2010))

considering this (Graham et al. 2010; Abbriano et al. 2011; Chanton et al. 2012; Jung et al. 2012; Carassou et al. 2014; Walsh et al. 2015).

10 Lesson 9. Molecular Techniques Led to a More Thorough Understanding of *DWH* Oil Biodegradation

Unlike previous major oil spills molecular techniques, especially sequencing had advanced significantly allowing a near real-time assessment of oil biodegradation microbial community structure and function, in the water column, surface, sediment and coastal areas (Hazen et al. 2010, 2013, 2016; Kostka et al. 2011; Baelum et al. 2012; Beazley et al. 2012; Dubinsky et al. 2012, 2013; Lu et al. 2012; Mason et al. 2012, 2014; King et al. 2014a). It also allowed storing of samples shipboard by freezing allowing the safe transport and subsequent analysis and archiving of critical samples (Fig. 7).

11 Lesson 10. Hydrostatic Pressure Had Little Effect on *DWH* Oil Biodegradation

Because of the depth of the *Macondo* well (1500 m), it was thought by many that the hydrostatic pressure might reduce biodegradation and/or promote biodegradation by piezophiles. Recent studies used water collected at depth during the response phase of *DWH* and preserved hydrostatic pressure as much as possible for simulations in the

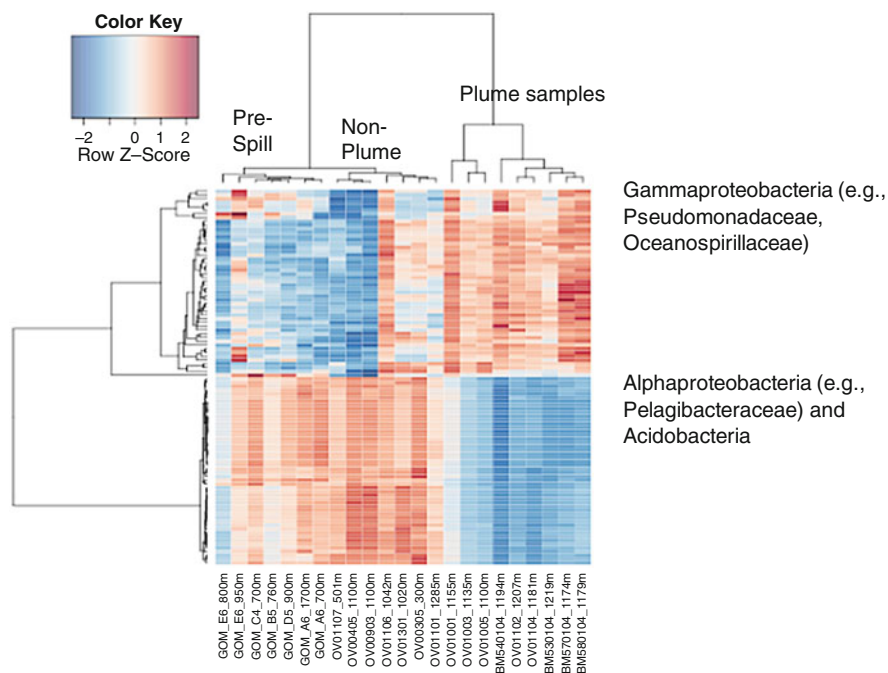


Fig. 7 The microbial community in the deep-water plume was distinct from the microbial community in uncontaminated waters at the same depth. Hierarchical clustering identified similarities between microbial communities. Uncontaminated deep-water samples showed a higher relative abundance of *Alphaproteobacteria* and *Acidobacteria*, while the deep-water oil plume had lower abundance of *Alphaproteobacteria* and *Pelagibacteraceae* and much higher abundance of *Gammaproteobacteria* including *Oceanospirillaceae* and *Pseudomonadaceae*. (After Hazen et al. (2010))

laboratory. In the laboratory simulations, these samples were exposed to 0.1, 15, and 30 Megapascals (MPa) pressure (the Macondo well was at 15 Megapascals) (Marietou et al. 2018). Their results suggest that pressure acts synergistically with low temperature to slow microbial growth and change microbial community structure and thus oil degradation in deep-sea environments. This only happened with *DWH* when the water collected was exposed to 30 MPa, since *DWH* was actually at 15 MPa and there was little effect of pressure. However, if deep basin oil exploration continues, it is bound to get deeper and more attention should be paid to getting samples collected in situ at pressure from these deeper strata to determine the effect that pressure is having on the oil degrading microbiome (Hazen et al. 2016; Hazen and Techtmann 2018).

12 Research Needs

Because of all the new techniques that were demonstrated with *DWH*, Standard Operating Procedures (SOP) were in dire need during the response phase, during the subsequent investigations for National Resource and Damage Assessment (NRDA),

and during long-term investigations of effects of the *DWH* accident. We need a dynamic set of SOPs that are put together and peer reviewed by a multidisciplinary group of experts that can be used by the scientific community for oil biodegradation research.

In Situ Sampling and Characterization. During the response phase of the *DWH* accident, it was difficult to find many in situ sampling and characterization devices that were useful for taking critical samples. A lot of SOPs were developed on the fly many of the response phase ships used standard CTD sampling rosettes out fitted with 2 UV fluorometers which used fluorescence to detect hydrocarbons and captured water at depth with Niskin bottles. The UV fluorometers (Quantech/Thermo Scientific) were employed in tandem to determine fluorescence intensity ratios (FIRs). One fluorometer was equipped with a pair of wavelength filters allowing excitation at 280 nm and emission at 340 nm. The second fluorometer was equipped with the same 280 nm excitation filter and a longer (445 nm) wavelength. The Niskin bottles were cleaned internally with distilled water and detergents between samplings. The sampling crews were sensitive to the problem of contamination from surface oil and used physical methods to disperse the surface slick before initiating sampling by the CTD, e.g., prop wash at the back of the ship before deployment and recovery, and detergent if prop wash was insufficient. For side deployments, the surface of the water was sprayed with freshwater to disperse surface oil; if this was insufficient, detergent was applied to the surface of the water then sprayed with freshwater to disperse surface oil. From each sample 800–2000 ml of water was filtered through sterile filter units containing 47 mm diameter polyethylenesulfone membranes with 0.22 μm pore size (MO BIO Laboratories, Inc., Carlsbad, CA) and then immediately frozen and stored at -20°C for the remainder of the cruise. Filters were shipped on dry ice to Lawrence Berkeley National Laboratory and stored at -80°C until DNA and PLFA extraction (Hazen et al. 2010). We also saw deployment of new in situ physical/chemical characterization devices like a subsurface hydrocarbon survey using an autonomous underwater vehicle and a ship-cabled sampler (Camilli et al. 2010). Recently it has also been demonstrated that oil seeps and spills can be linked to their origin by Fourier Transform Ion Cyclotron Resonance Mass Spectrometry (Krajewski et al. 2018). For sampling microbiomes in situ we need more development of devices that can be triggered remotely to filter and/or sample at depth like the large volume Stand Alone Particle Sampler (SAPS, Challenger Oceanic, UK, with controller, battery, and pump upgrades by Oceanlab, University of Aberdeen, Scotland) which can filter 62 and 123 L of seawater at depth through a 292 mm diameter nylon filter with a pore size of 0.2 μm (Techtmann et al. 2015) and the commercially available McLane Pump Large Volume water sampler (McLane Labs, Falmouth MA) which can filter 10.3 and 27 L of water per sample (Techtmann et al. 2017a).

Mesocosms/Microcosms. Bottle effects are real, as are sampling with consideration of ambient temperature and pressure and travel time of the sampling device (Marietou et al. 2018). It has been found that on-board ship microcosms/mesocosms start with different community structures and give different results in terms of function and diversity than water samples taken back over some days of travel for laboratory mesocosms (Liu et al. 2017). Too many times during *DWH* the media

interviewed scientists that did not have data or did not have data tied to rigorous SOPs and peer review, which gave the public the wrong impression of what was going on during the *DWH* accident.

References

- Abbriano RM, Carranza MM, Hogle SL, Levin RA, Netburn AN, Seto KL, Snyder SM, Franks PJS (2011) Deepwater Horizon oil spill a review of the planktonic response. *Oceanography* 24:294–301
- Adams EE, Socolofsky SA, Boufadel M (2013) Comment on “evolution of the Macondo well blowout: simulating the effects of the circulation and synthetic dispersants on the subsea oil transport”. *Environ Sci Technol* 47:11905–11905
- Agbaglah G, Delaux S, Fuster D, Hoepffner J, Jossierand C, Popinet S, Ray P, Scardovelli R, Zaleski S (2011) Parallel simulation of multiphase flows using octree adaptivity and the volume-of-fluid method. *Comptes Rendus Mecanique* 339:194–207
- Atlas RM, Hazen TC (2011) Oil biodegradation and bioremediation: a tale of the two worst spills in US history. *Environ Sci Technol* 45:6709–6715
- Baelum J, Borglin S, Chakraborty R, Fortney JL, Lamendella R, Mason OU, Auer M, Zemla M, Bill M, Conrad ME, Malfatti SA, Tringe SG, Holman HY, Hazen TC, Jansson JK (2012) Deep-sea bacteria enriched by oil and dispersant from the Deepwater Horizon spill. *Environ Microbiol* 14:2405–2416
- Bagi A, Pampanin DM, Brakstad OG, Kommedal R (2013) Estimation of hydrocarbon biodegradation rates in marine environments: a critical review of the Q(10) approach. *Mar Environ Res* 89:83–90
- Beazley MJ, Martinez RJ, Rajan S, Powell J, Piceno YM, Tom LM, Andersen GL, Hazen TC, Van Nostrand JD, Zhou JZ, Mortazavi B, Sobecky PA (2012) Microbial community analysis of a coastal salt marsh affected by the Deepwater Horizon oil spill. *PLoS One* 7:13
- Brakstad OG, Daling PS, Faksness L-G, Almas IK, Vang S-H, Syslak L, Leirvik F (2014) Depletion and biodegradation of hydrocarbons in dispersions and emulsions of the Macondo 252 oil generated in an oil-on-seawater mesocosm flume basin. *Mar Pollut Bull* 84:125–134
- Brakstad OG, Nordtug T, Throne-Hoist M (2015a) Biodegradation of dispersed Macondo oil in seawater at low temperature and different oil droplet sizes. *Mar Pollut Bull* 93:144–152
- Brakstad OG, Throne-Hoist M, Netzer R, Stoeckel DM, Atlas RM (2015b) Microbial communities related to biodegradation of dispersed Macondo oil at low seawater temperature with Norwegian coastal seawater. *Microb Biotechnol* 8:989–998
- Camilli R, Reddy CM, Yoerger DR, Van Mooy BAS, Jakuba MV, Kinsey JC, McIntyre CP, Sylva SP, Maloney JV (2010) Tracking hydrocarbon plume transport and biodegradation at Deepwater Horizon. *Science* 330:201–204
- Carassou L, Hernandez FJ, Graham WM (2014) Change and recovery of coastal mesozooplankton community structure during the Deepwater Horizon oil spill. *Environ Res Lett* 9:12
- Cardy DLN, Laidler V, Salmond GPC, Murrell JC (1991) Molecular analysis of the methane monoxygenase (MMO) gene cluster of *Methylosinus trichosporium* OB3b. *Mol Microbiol* 5:335–342
- Chakraborty R, Borglin SE, Dubinsky EA, Andersen GL, Hazen TC (2012) Microbial response to the MC-252 oil and Corexit 9500 in the Gulf of Mexico. *Front Microbiol* 3:357–357
- Chanton JP, Cherrier J, Wilson RM, Sarkodee-Adoo J, Bosman S, Mickle A, Graham WM (2012) Radiocarbon evidence that carbon from the Deepwater Horizon spill entered the planktonic food web of the Gulf of Mexico. *Environ Res Lett* 7:4
- Dubinsky, EA, Tom LM, Reid F, Borglin S, Chavarria K, Fortney J, Joyner D, Kuehl J, Lamendella R, Lim HC, Mackelprang R, Mason OU, Piceno Y, Wetmore K, Wu C, Hazen TC, Anderson GL (2012) Microbial community composition as a highly sensitive biosensor for oil spills in the deep ocean. Abstracts of Papers of the American Chemical Society 243

- Dubinsky EA, Conrad ME, Chakraborty R, Bill M, Borglin SE, Hollibaugh JT, Mason OU, M Piceno Y, Reid FC, Stringfellow WT, Tom LM, Hazen TC, Andersen GL (2013) Succession of hydrocarbon-degrading bacteria in the aftermath of the Deepwater Horizon oil spill in the gulf of Mexico. *Environ Sci Technol* 47:10860–10867
- Engel AS, Liu C, Paterson AT, Anderson LC, Turner RE, Overton EB (2017) Salt marsh bacterial communities before and after the Deepwater Horizon oil spill. *Appl Environ Microbiol* 83:22
- FISG (2010) Oil budget calculator technical documentation. http://www.restorethegulf.gov/sites/default/files/documents/pdf/OilBudgetCalc_Full_HQ-Print_111110.pdf. Accessed 6 July 2011. The Federal Interagency Solutions Group: Oil Budget Calculator Science and Engineering Team
- Graham WM, Condon RH, Carmichael RH, D'Ambra I, Patterson HK, Linn LJ, Hernandez FJ (2010) Oil carbon entered the coastal planktonic food web during the Deepwater Horizon oil spill. *Environ Res Lett* 5:6
- Hazen TC (1997) Bioremediation. In: Amy P, Haldeman D (eds) *Microbiology of the terrestrial subsurface*. CRC Press, Boca Raton, pp 247–266
- Hazen TC (2018) Cometabolic bioremediation. In: Steffan R (eds) *Consequences of microbial interactions with hydrocarbons, oils, and lipids: Biodegradation and bioremediation. Handbook of hydrocarbon and lipid microbiology*. Springer, Cham, pp 1–15. https://doi.org/10.1007/978-3-319-44535-9_5-1
- Hazen TC, Saylor GS (2016) Environmental systems microbiology of contaminated environments. In: Yates M, Nakatsu C, Miller R, Pillai SD (eds) *Manual of environmental microbiology*, 4th edn. ASM Press, Washington, DC, 5.1.6-1-5.1.6-10
- Hazen TC, Techtmann SM (2018) Oil biodegradation in deep marine basins. In: Steffan R (ed) *Handbook of hydrocarbon and lipid microbiology. Consequences of microbial interactions with hydrocarbons, oils, and lipids: biodegradation and bioremediation*. Springer, Cham
- Hazen TC, Dubinsky EA, DeSantis TZ, Andersen GL, Piceno YM, Singh N, Jansson JK, Probst A, Borglin SE, Fortney JL, Stringfellow WT, Bill M, Conrad ME, Tom LM, Chavarría KL, Alusi TR, Lamendella R, Joyner DC, Spier C, Baelum J, Auer M, Zemla ML, Chakraborty R, Sonnenthal EL, D'Haeseleer P, Holman HYN, Osman S, Lu ZM, Van Nostrand JD, Deng Y, Zhou JZ, Mason OU (2010) Deep-sea oil plume enriches indigenous oil-degrading bacteria. *Science* 330:204–208
- Hazen TC, Rocha AM, Techtmann SM (2013) Advances in monitoring environmental microbes. *Curr Opin Biotechnol* 24:526–533
- Hazen TC, Prince RC, Mahmoudi N (2016) Marine oil biodegradation. *Environ Sci Technol* 50:2121–2129
- Hooper CH, NOAA Hazardous Materials Response Project (U.S.) (1982) The IXTOC I oil spill: the federal scientific response. U.S. Dept. of Commerce, National Oceanic and Atmospheric Administration, Office of Marine Pollution Assessment, Boulder
- Huettel M, Overholt WA, Kostka JE, Hagan C, Kaba J, Wells WB, Dudley S (2018) Degradation of Deepwater Horizon oil buried in a Florida beach influenced by tidal pumping. *Mar Pollut Bull* 126:488–500
- Johansen O, Brandvik PJ, Farooq U (2013) Droplet breakup in subsea oil releases – part 2: predictions of droplet size distributions with and without injection of chemical dispersants. *Mar Pollut Bull* 73:327–335
- Jung SW, Kwon OY, Joo CK, Kang JH, Kim M, Shim WJ, Kim YO (2012) Stronger impact of dispersant plus crude oil on natural plankton assemblages in short-term marine mesocosms. *J Hazard Mater* 217:338–349
- Kessler JD, Valentine DL, Redmond MC, Du MR, Chan EW, Mendes SD, Quiroz EW, Villanueva CJ, Shusta SS, Werra LM, Yvon-Lewis SA, Weber TC (2011) A persistent oxygen anomaly reveals the fate of spilled methane in the deep Gulf of Mexico. *Science* 331:312–315
- Kimes NE, Callaghan AV, Aktas DF, Smith WL, Sunner J, Golding BT, Drozdowska M, Hazen TC, Sufliita JM, Morris PJ (2013) Metagenomic analysis and metabolite profiling of deep-sea sediments from the Gulf of Mexico following the Deepwater Horizon oil spill. *Front Microbiol* 4:50. <https://doi.org/10.3389/fmicb.2013.00050>
- Kimes NE, Callaghan AV, Sufliita JM, Morris PJ (2014) Microbial transformation of the Deepwater Horizon oil spill – past, present, and future perspectives. *Front Microbiol* 5:11

- King GM, Smith CB, Tolar B, Hollibaugh JT (2012) Analysis of composition and structure of coastal to mesopelagic bacterioplankton communities in the northern gulf of Mexico. *Front Microbiol* 3:438
- King GM, Kostka JE, Hazen TC, Sobecky PA (2014a) Microbial responses to the Deepwater Horizon oil spill: from coastal wetlands to the deep sea. *Annu Rev Mar Sci* 7:377–401. <https://doi.org/10.1146/annurev-marine-010814-015543>
- King SM, Leaf PA, Olson AC, Ray PZ, Tarr MA (2014b) Photolytic and photocatalytic degradation of surface oil from the Deepwater Horizon spill. *Chemosphere* 95:415–422
- Kleindienst S, Seidel M, Ziervogel K, Grim S, Loftis K, Harrison S, Malkin SY, Perkins MJ, Field J, Sogin ML, Dittmar T, Passow U, Medeiros PM, SB J (2015) Chemical dispersants can suppress the activity of natural oil-degrading microorganisms. *Proc Natl Acad Sci U S A* 112:14900–14905
- Kostka JE, Prakash O, Overholt WA, Green SJ, Freyer G, Canion A, Delgardio J, Norton N, Hazen TC, Huettel M (2011) Hydrocarbon-degrading bacteria and the bacterial community response in Gulf of Mexico beach sands impacted by the Deepwater Horizon oil spill. *Appl Environ Microbiol* 77:7962
- Krajewski LC, Lobodin VV, Johansen C, Bartges TE, Maksimova EV, MacDonald IR, Marshall AG (2018) Linking natural oil seeps from the Gulf of Mexico to their origin by use of fourier transform ion cyclotron resonance mass spectrometry. *Environ Sci Technol* 52:1365–1374
- Kujawinski EB, Soule MCK, Valentine DL, Boysen AK, Longnecker K, Redmond MC (2011) Fate of dispersants associated with the Deepwater Horizon oil spill. *Environ Sci Technol* 45:1298–1306
- Lamendella R, Strutt S, Borglin SE, Chakraborty R, Tas N, Mason OU, Hultman J, Prestat E, Hazen TC, Jansson J (2014) Assessment of the Deepwater Horizon oil spill impact on Gulf coast microbial communities. *Front Microbiol* 5:130
- Li Z, Kepkay P, Lee K, King T, Boufadel MC, Venosa AD (2007) Effects of chemical dispersants and mineral fines on crude oil dispersion in a wave tank under breaking waves. *Mar Pollut Bull* 54:983–993
- Li P, Weng LL, Niu HB, Robinson B, King T, Conmy R, Lee K, Liu L (2016) Reynolds number scaling to predict droplet size distribution in dispersed and undispersed subsurface oil releases. *Mar Pollut Bull* 113:332–342
- Liu J, Techtman SM, Woo HL, Ning DL, Fortney JL, Hazen TC (2017) Rapid response of eastern Mediterranean deep sea microbial communities to oil. *Sci Rep* 7:11
- Lu ZM, Deng Y, Van Nostrand JD, He ZL, Voordeckers J, Zhou AF, Lee YJ, Mason OU, Dubinsky EA, Chavarria KL, Tom LM, Fortney JL, Lamendella R, Jansson JK, D’Haeseleer P, Hazen TC, Zhou JZ (2012) Microbial gene functions enriched in the Deepwater Horizon deep-sea oil plume. *ISME J* 6:451–460
- Mahmoudi N, Porter TM, Zimmerman AR, Fulthorpe RR, Kasozi GN, Silliman BR, Slater GF (2013) Rapid degradation of Deepwater Horizon spilled oil by indigenous microbial communities in Louisiana saltmarsh sediments. *Environ Sci Technol* 47:13303–13312
- Marietou A, Chastain R, Beulig F, Scoma A, Hazen TC, Bartlett DH (2018) The effect of hydrostatic pressure on enrichments of hydrocarbon degrading microbes from the Gulf of Mexico following the Deepwater Horizon oil spill. *Front Microbiol* 9:11
- Mason, OU, Hazen TC, Woyke T, Jansson JK (2012) “Omics” analyses of the deep sea microbial community response to the Deepwater Horizon oil spill. Abstracts of Papers of the American Chemical Society 243
- Mason OU, Scott NM, Gonzalez A, Robbins-Pianka A, Baelum J, Kimbrel J, Bouskill NJ, Prestat E, Borglin S, Joyner DC, Fortney JL, Jurelevicius D, Stringfellow WT, Alvarez-Cohen L, Hazen TC, Knight R, Gilbert JA, Jansson JK (2014) Metagenomics reveals sediment microbial community response to Deepwater Horizon oil spill. *ISME J* 8:1464–1475
- McGenity TJ, Folwell BD, McKew BA, Sanni GO (2012) Marine crude-oil biodegradation: a central role for interspecies interactions. *Aquat Biosyst* 8:10
- NAS (2003) Oil in the sea III: inputs, fates, and effects. The National Academies Press, Washington, DC
- Prince RC (2015) Oil spill dispersants: boon or bane? *Environ Sci Technol* 49:6376–6384

- Prince RC, Butler JD (2014) A protocol for assessing the effectiveness of oil spill dispersants in stimulating the biodegradation of oil. *Environ Sci Pollut Res* 21:9506–9510
- Rahsepar S, Langenhoff AAM, Smit MPJ, Van Eenennaam JS, Murk AJ, Rijnaarts HHM (2017) Oil biodegradation: interactions of artificial marine snow, clay particles, oil and Corexit. *Mar Pollut Bull* 125:186–191
- Reddy CM, Arey JS, Seewald JS, Sylva SP, Lemkau KL, Nelson RK, Carmichael CA, McIntyre CP, Fenwick J, Ventura GT, Van Mooy BAS, Camilli R (2012) Composition and fate of gas and oil released to the water column during the Deepwater Horizon oil spill. *Proc Natl Acad Sci U S A* 109:20229–20234
- Redmond MC, Valentine DL (2012) Natural gas and temperature structured a microbial community response to the Deepwater Horizon oil spill. *Proc Natl Acad Sci U S A* 109:20292–20297
- Singh A, Van Hamme JD, Ward OP (2007) Surfactants in microbiology and biotechnology: part 2. Application aspects. *Biotechnol Adv* 25:99–121
- Smith MB, Rocha AM, Smillie CS, Olesen SW, Paradis C, Wu L, Campbell JH, Fortney JL, Mehlhorn TL, Lowe KA, Earles JE, Phillips J, Techtmann SM, Joyner DC, Elias DA, Bailey KL, Hurt RA Jr, Preheim SP, Sanders MC, Yang J, Mueller MA, Brooks S, Watson DB, Zhang P, He Z, Dubinsky EA, Adams PD, Arkin AP, Fields MW, Zhou J, Alm EJ, Hazen TC (2015) Natural bacterial communities serve as quantitative geochemical biosensors. *MBio* 6: e00326–e00315
- Spier C, Stringfellow WT, Hazen TC, Conrad M (2013) Distribution of hydrocarbons released during the 2010 MC252 oil spill in deep offshore waters. *Environ Pollut* 173:224–230
- Stackhouse B, Lau MCY, Vishnivetskaya T, Burton N, Wang R, Southworth A, Whyte L, Onstott TC (2017) Atmospheric CH₄ oxidation by Arctic permafrost and mineral cryosols as a function of water saturation and temperature. *Geobiology* 15:94–111
- Techtmann SM, Fortney JL, Ayers KA, Joyner DC, Linley TD, Pfiffner SM, Hazen TC (2015) The unique chemistry of eastern Mediterranean water masses selects for distinct microbial communities by depth. *PLoS One* 10:22
- Techtmann SM, Fitzgerald KS, Stelling SC, Joyner DC, Uttukar SM, Harris AP, Alshibli NK, Brown SD, Hazen TC (2016) *Colwellia psychrerythraea* strains from distant deep sea basins show adaptation to local conditions. *Front Environ Sci* 4:33
- Techtmann SM, Mahmoudi N, Whitt KT, Campa MF, Fortney JL, Joyner DC, Hazen TC (2017a) Comparison of Thaumarchaeotal populations from four deep sea basins. *FEMS Microbiol Ecol* 93:10
- Techtmann SM, Zhuang MB, Campo P, Holder E, Elk M, Hazen TC, Conmy R, Domingo JWS (2017b) Corexit 9500 enhances oil biodegradation and changes active bacterial community structure of oil-enriched microcosms. *Appl Environ Microbiol* 83:14
- Thessen AE, North EW (2017) Calculating in situ degradation rates of hydrocarbon compounds in deep waters of the Gulf of Mexico. *Mar Pollut Bull* 122:77–84
- Valentine DL, Kessler JD, Redmond MC, Mendes SD, Heintz MB, Farwell C, Hu L, Kinnaman FS, Yvon-Lewis S, Du MR, Chan EW, Tigreros FG, Villanueva CJ (2010) Propane respiration jump-starts microbial response to a deep oil spill. *Science* 330:208–211
- Valentine DL, Mezić I, Macesic S, Crnjarić-Zic N, Ivic S, Hogan PJ, Fonoberov VA, Loire S (2012) Dynamic autoinoculation and the microbial ecology of a deep water hydrocarbon irruption. *Proc Natl Acad Sci U S A* 109:20286–20291
- Venosa AD, Holder EL (2007) Biodegradability of dispersed crude oil at two different temperatures. *Mar Pollut Bull* 54:545–553
- Vilcaez J, Li L, Hubbard SS (2013) A new model for the biodegradation kinetics of oil droplets: application to the Deepwater Horizon oil spill in the Gulf of Mexico. *Geochem Trans* 14:4
- Walsh JJ, Lenes JM, Darrow BP, Parks AA, Weisberg RH, Zheng L, Hu C, Barnes BB, Daly KL, Shin SI, Brooks GR, Jeffrey WI, Snyder RA, Hollander D (2015) A simulation analysis of the plankton fate of the Deepwater Horizon oil spills. *Cont Shelf Res* 107:50–68
- Zhao L, Boufadel MC, King T, Robinson B, Gao F, Socolofsky SA, Lee K (2017) Droplet and bubble formation of combined oil and gas releases in subsea blowouts. *Mar Pollut Bull* 120:203–216

Index

A

- ABC transporters, 151
- Abiogenic hydrocarbons, 494
- Abiotic degradation, 194, 208
- Abiotic formation, 582
- Abiotic methane sinks
 - atmospheric decomposition, 788
 - storage in sediments, 788
- Abiotic methane sources, 783
- Abiotic sulphurization pathway, 363
 - isotopic evidence, 365
 - mechanism, 366–367
 - timing, 367–368
- Abiotic transformation, 4
- Accretionary margins, 750
- Accretionary prism, 750
- Accretionary wedge, 750
- Acetate ester pheromone, 228
- Acetoclastic methanogenesis, 676, 682, 694, 698
- Acetogenic lipid, 105
- Acid hydrolysis, 168
- Acidogenesis, 674
- Acoustically turbid zones, 691
- Actinobacteria*, 852
- Activation energy, 496, 504
- Active margins, 748
- Acyl-coenzyme A (acyl-CoAs), 143, 146, 149
- Acyltransferases, 143, 144, 147
- Advective transport, 774
- Aerobic methane oxidation, 700–702, 773
- Aerobic methanotrophic bacteria, 773
- Aerobic oxidation of methane, 774, 785
 - in ancient environments
 - hopanoids, 791
 - steroids, 794
 - in modern environments
 - fatty acids, 791
 - hopanoids, 789
 - sterols, 790
- Age determination, 757
- Alberta's oil sands, 594
- Alcohol(s), 141, 145, 149, 150
- Alcohol-forming pathway, 145, 147
- Aldehyde(s), 141, 145, 147, 148, 150
 - decarbonylase, 149
- Algae, 258–262
 - algal lipids, 103–104
 - carbon isotopes in algal lipids, 104–107
 - hydrogen isotopes in algal lipids, 107–109
 - unsaturated lipid components
 - (see Unsaturated lipid components)
- Algaenan, 168, 175
- Algebraic schemes, 504
- Alkane-forming pathway, 145, 148–150
- Alkanes, 53, 104, 141, 148, 150, 418
- n*-Alkanes, 7–8, 161, 278, 376, 560, 562, 563, 565, 566, 568, 571, 575, 576, 583
- Alkanoic acids, 105
- n*-Alkanol, 169
- Alkenes, 12, 14, 40, 163, 199
 - See also Olefins
- n*-Alkenes, 161, 194, 199
- Alkenoates, 173
- Alkenones, 104, 169, 202, 380, 427
- Alkoxy/peroxy radicals, 196
- Alkyl alkenoates, 169
- Alkylbenzenes, 16
- n*-Alkyl compounds, 109
- Alkylcycloalkanes, 10
- Alkyl diols, 173
- n*-Alkyl diols, 173

- Alkyl esters, 141, 145, 147
 Allylic hydroperoxides, 200, 207
 Z Allylic hydroperoxyacids, 205
 Allylic hydroperoxyalkenones, 203
Alphaproteobacteria, 852
 Alum Shale, 501, 505, 534, 536, 538
 Ambient pressure conditions, 462
 Ambient temperature, 860
 American Petroleum Institute (API) gravity, 76, 272
 Amines, 26
 Amino acids, 180
 Aminopentol, in methanotrophs, 789
 Ammonium monooxygenase (AMO), 701
 Amorphous clathrate hydrate nucleus, 86
 Amorphous hydrate phase, 86
 Amorphous organic matter (AOM), 487
 Anaerobic ammonium oxidation, 709
 Anaerobic bacteria, 417
 Anaerobic biodegradation, 614
 Anaerobic conditions, 597
 Anaerobic degradation, 485, 632–633
 Anaerobic methane oxidizing bacteria, 368
 Anaerobic methanotrophic (ANME) archaea, 707, 785, 787, 803
 Anaerobic oxidation of methane (AOM), 82, 460, 657, 659, 691, 702–711, 774, 785–788
 in ancient environments
 archaeal biomarkers, 801
 bacterial biomarkers, 802
 preservation aspects, 801
 seep carbonates, 798
 electron acceptors, 785
 in modern environments
 archaeal biomarkers, 794–797
 bacterial biomarkers, 797
 Analytical methods, 499
 Ancient seep(s), 757, 762
 carbonates, 755
 Angiosperms, 421, 484
 Anhydrous pyrolysis, 510
 Anoxic bottom water, 478, 480
 Anoxic conditions, 480
 Anoxic environments, 290
 Antarctica, 171
 Anthropogenic markers, 831
 Anticline cell walls, 128, 131, 135
 Antrim Shale, 530
 AOM-consortia, 755
Apedinella, 174
 Aquatic ecosystems, 824
 Aquatic organic matter, 477
 Aquatic organisms, 100
 Aqueous conditions, 582
 Aqueous solubility vs. carbon number, 36
 Arabian Sea, 174
Arabidopsis thaliana, 141, 145
 Archaea, 250–252, 410, 448, 449, 460, 465
 Archaeol, 251, 795, 797, 802
Argyrotaenia velutinana, 226
 Aromatic, 577
 compounds, 55–66
 steroid, 599
 Aromatic hydrocarbons, 285–286
 aromaticity, 15
 benzene, 16
 PAHs, 16, 18
 reactions, 42–44
 structures, 17
 Aromaticity, 15, 25, 507
 Aromatisation, 505
 Arrhenius law, 496
 Arylisoprenoid degradation, 293
 Arylisoprenoid ratio, 294
 Aryl isoprenoids, 424
 Asphalt, 580
 Asphaltenes, 73–74, 271, 290, 318, 328
 Asphaltic petroleum, 570
 Assimilatory sulphate reduction (ASR), 363
 Atlantis II Deep, 562, 566, 568
 Atmosphere, 620, 621
 Atmospheric methane, 711–715
 concentrations, 788
 Atmospheric pressure chemical ionization (APCI), 247, 321
 Atmospheric pressure photoionization (APPI), 321
 Atmospheric pressure photoionization in positive mode (APPI-P), 602–604
 Autoinoculation from gyres, 849
 Autonomous underwater vehicle, 860
 Autoxidation, unsaturated lipid components, *see* Unsaturated lipid components
 Autoxidative damages, 197
- B**
Bacillus subtilis, 252
 Backscatter intensity, 755
 Bacteria, 177, 252–253, 410, 447, 448, 455, 460, 463, 465–467
 Bactericides, 828
 Bacterioplanepolyols (BHPs), 789, 791, 792, 798
Bacteroidetes, 852

- Bakken Shale, 501, 505, 524, 530, 534, 537, 538
- Bark beetle pheromone, 230
- Barnett Shale, 504, 512, 514, 524, 530, 532, 534, 535, 536, 538, 542
- Barney Creek Formation, 793
- Barophilic hyperthermophiles, 697
- Bend-faulting, 751, 763
- Benzene, 15, 16, 577
- Benzene, toluene, ethylbenzene, and xylenes (BTEX) compounds, 55, 833
- Bernard diagram, 685
- Bioavailability, 9
- Biochemical precursors, 114
- Biochemistry, 7, 160, 161, 357
- Biodegradation, 289, 301–305, 340, 341, 346, 349, 465, 579, 580, 595, 597–600, 603, 606, 616
- anaerobic, 614
 - geological conditions for, 617
 - methanogenic, 621
 - petroleum, 614
- Biodegraded oil, 616, 618
- Biofilm clogging, 465
- Biogenic gas, 344, 627
- Biogenic lipids, 24
- Biogenic methane, 494
- Biogeochemistry of oil sands bitumens, *see* Oil sands
- Biohopanoids, 790
- Bioirrigation, 774, 776
- Biological gas generation, 632
- Biological methane oxidation, 700
- Biomarkers, 11, 160, 177, 275, 413–414, 423–425, 486, 487, 562, 565, 566, 569, 570, 575, 583, 756–757, 763
- Biomarkers, methanotrophs (ancient)
- aerobic oxidation of methane hopanoids, 791–793
 - steroids, 794
 - anaerobic oxidation of methane
 - archaeal biomarkers, 801–802
 - bacterial biomarkers, 802–803
 - preservation aspects, 801
 - seep carbonates, 798–801
- Biomarkers, methanotrophs (modern)
- aerobic oxidation of methane, 789
 - fatty acids, 791
 - hopanoids, 789–790
 - sterols, 790–791 - anaerobic oxidation of methane
 - archaeal biomarkers, 794
 - bacterial biomarkers, 797–798
- Bioproductivity, 477, 478, 480, 482, 484
- Bioremediation, 463, 465
- Biosphere, 4
- Biosurfactants, 129, 131–135
- Biosynthates, 108
- Biosynthesis, 101, 170
- of cuticular wax, 126
 - pathway, 177
- Biotic organic sulphur compounds, ocean, 373–375
- Biotic sulphurization, 363
- α,ω -Biphytanediols, 797, 802
- Biphytanes, 413, 797, 802
- Birch reduction, 44
- bis*-allylic position, 200, 209
- Bitumen, 486, 488, 534, 547
- oil sands (*see* Oil sands)
- Black Sea, 848
- Blowout prevention device, 848
- Boduszynski model, 602
- Boiling points, 33
- Bond dissociation energy, 6
- Boron, 760
- Botryococenes, 163
- Botryococcus*, 162, 261, 421
- Bottle effects, 860
- Bottom water anoxia, 481
- Branched alkanes, 9
- Branched GDGTs (brGDGTs), 426
- Bransfield Strait, Antarctica, 566
- Brine(s), 753
- lakes, 761
 - pools, 761
- Bromoethanesulfonic acid, 686
- Bubbles, 754, 755
- Budgets, 762
- Bulk compositions, 507
- Bulk isotope values, 274
- Bulk pyrolysis, 502–503
- C**
- ^{14}C age data, 562
- Cage occupancies, 89
- Caldarchaeol, 251
- Canadian oil sands, 594
- Canadian oil sands bitumen (COSB), 601
- “*Candidatus*” *Methylomirabilis oxyfera*, 709, 788
- Capillary columns, 173
- Capillary forces, 653, 655, 658
- Carbohydrates, 395

- Carbon, 124, 130, 131, 135
 assimilation, 111
 dioxide, 110
 isotope fractionation, 346, 348, 349
 isotopes, 616
- Carbonate reduction methanogenesis, 676
- Carbonium ions, 497
- Carbon-nitrogen bonds, 28
- Carbon number (C#), 601
- Carbon preference index (CPI), 560, 562, 565, 570, 575
- Carboxylic acids, 597, 607
- Cardiolipin, 253
- Cariaco Basin, 370
- Carotenoids, 14, 391, 827, 836
- Catagenesis, 343, 375, 486, 494, 527
- Catalysis, 536
- Cavities, 82–88, 90
- C₄₀ carotenoids, 293
- C₇ compounds, 284
- Cellulose, 483, 488
- C₄ grasses, 113
- CH₄, 577
- Chain elongation, 167, 168
- Chain reaction, 497
- Cheaters, 857
- Chemical composition of epicuticular waxes, 125
- Chemical dispersants, 849
- Chemical fossils, 411, 413, 419, 425
- Chemical reaction kinetics, 496
- Chemical stimulation, 662, 663
- Chemosynthetic organisms, 771, 773
- Chimneys, 758, 763
- Chiral/stereogenic centers, 9
- Chlamydomonas reinhardtii*, 260
- Chlorella*, 169
- Chlorobactene, 392
- Chloromonas pichincha*, 259
- Chlorophyceae, 162
- Chlorophyll, 180, 194, 195, 827
 photodegradation %, 197
 phytyl side-chain, 197
- Chlorophyll phytyl side-chain photodegradation index (CPPI), 197
- Chlorophytes, 161, 162, 169, 179
- Cholesterol, 179
- C₃₅ homohopane index, 389
- Choristoneura fumiferana*, 228
- Chrysotila*, 162, 170
- C₂₀ isoprenoid thiophenes, 383
- Clathrate hydrates, *see* Gas hydrates
- Clay dehydration, 757, 760
- Clay mineral dehydration, 751
- Climate changes, 620, 621
- Closed-system pyrolysis, 502, 509
- C₃₀ *n*-propylsteranes, 283
- CO₂, 574
 capture and storage, 664
 reduction, 614
- CO₂-N₂-injection, 664
- Coal, 298
 CBM reservoir, 628
 deposition, 628
 enrichment cultures, 638, 639
- Coalbed, 618
- Coalbed methane (CBM), 624
 bioavailability, 641
 biological gas generation, 624, 628
 coal bioconversion pathways, 637–639
 coal enrichment cultures, 635
 genomics, 636
 geochemical factors, 630–631
 microbial augmentation, 640
 microbial ecology, 632
 microbial methanogenesis, 635
 natural gas, 624, 626
 secondary, 625
- Coal seam gas (CSG), 624
- Coexistence, 84, 91, 92
- Coexisting phases, 83
- Coleopteran isoprenoid pheromone, 231
- Collision-activated dissociation (CAD), *see* Collision-induced decomposition (CID)
- Collision-induced decomposition (CID), 452
- Colloidal organic matter, 825
- Colonization by microorganisms, 129
- Color, 500
- Cometabolic biodegradation, 849
- Competitive, 687
- Complexed metals, 582
- Compositional kinetic models, 509
- Compound-specific δ¹³C-measurements, 789
- Compound-specific isotope analysis, 342, 348, 834
- Compound specific sulphur isotope analysis (CSSIA) data, 368
- Concentration gradient, 87
- Concentration of atmospheric CO₂, 110
- Concerted 'ene' addition, 205
- Condensate, 289
- Condensation, 583
- Confined, 510
- Contact angles, 127, 129
- Contact pheromones, 220

- Continental hydrothermal systems, 570
Continental slopes, 652
Continental systems, 570
Continuous cultures, 181
Convective circulation, 577
Conventional, 618
Coordination number, 86
Corexit 9500, 853, 855
Covalent bonding, 5–7
C₃ plants, 110
C₄ plants, 484
Crocetane, 794–797, 802
Crude oil(s), 50, 271, 340, 342, 344, 346, 349
 aromatic hydrocarbons in, 285–286
 biodegradation and preservation, 301–305
 biodegradation processes in, 346
 biomarkers, 282
 bulk parameters, 272–275
 change in molecular composition, 296–300
 definition, 270–272
 diamondoids, 283–285
 expulsion and migration, 300–301
 factors for determination of composition, 290–292
 fractions, 344
 hydrocarbons in, 277
 impact of depositional environments, 292–294
 impact of maturity, 295–296
 molecular characteristics, 275–286
 photosynthesis, 288–289
 productivity vs. preservation, 290
 sesquiterpanes, 279–280
 steranes, 280–283
C-24 stereochemistry, 177
C₃₀ tetracyclic polyprenoids, 394
Cuticle
 cutin monomers and wax compounds, export of, 150–151
 cutin monomer synthesis, 142–144
 cutin polymerization, 144
 development of, 140
 wax biosynthesis (*see* Wax biosynthesis)
Cuticular hydrocarbons
 biosynthesis, 220
 components, 217
Cuticular permeability, 127, 129, 133, 135
Cuticular waxes, plant, *see* Plant cuticular waxes
Cutin, 140
 compounds, 151
 monomer synthesis, 142
 polymerization, 144
 synthase, 144
 $\delta^{13}\text{C}$ values, 616
C₄ vegetation, 110
Cyanobacteria, 258, 391, 414–417
Cyclic hydrocarbons, 166
Cyclic steam stimulation (CSS), 604
Cycloalkanes, 10–12, 53–55
Cycloalkylalkanes, 10
 ω -Cycloheptyl fatty acids, 248
Cyclohexanes, 11
Cyclopentane fatty acids, 248
Cytochrome *b*₅, 149
Cytochrome P450, 143, 148, 150, 152
D
Decarboxylation, 161
Decomposition reactions, 505
Deep biosphere, 447, 459, 462
Deep Sea Drilling Project (DSDP), 560, 577
Deforestation, 606
Degradation products, 166
Degree of unsaturation, 203
Delphineus, 179
Deltas, 760
Demosponges, 420
Dendroctonus ponderosae, 233
Denitrification, 709
Denitrifying anaerobic oxidation of methane (DAMO) process, 709
Density, 75
 vs. carbon number, 34
Depositional environment, 530
Depressurization, 662, 664
Derivatization techniques, 455, 458
Desaturation, 167
Desulfococcus, 785
Desulfosarcina, 785
Detergents, 828, 831
Dewatering, 750
Diacylglycerylcarboxyhydroxymethylcholine (DGCC), 258
Diacylglyceryl hydroxymethyl trimethylalanine (DGTA), 258, 259
Diacylglyceryltrimethylhomoserine (DGTS), 258, 259
Diagenesis, 367, 486, 494, 527
Diagenetic alteration, 565
Diamondoids, 12, 283–286
Diasteranes, 281, 417
Diatoms, 104, 160, 161, 163, 166–168, 174, 177, 179, 181, 425–426

- Dibenzocarbazole, 301
 Dibenzothiophenes, 60, 286
 Dicarboxylic acids (DCA), 142, 144
 Diels' hydrocarbon, 576
 Diethers, 802
 Diffusion, 128, 131, 133–135, 694, 774, 775
 coefficients, 128
 layer, 87
 Dihomohopanoic acid, 792, 798
 β -Diketones, 150
 Dilbit, 606
 Dimethylsulphoniopropionate (DMSP), 372
 Dimethylthallium, 836
 Dinoflagellates, 103, 161, 167, 175,
 177–179, 419
 Dinosteranes, 388, 418
 Dinosterol, 103, 161, 178, 179
 Diploptene, 789, 791, 798
 Diplopterol, 789–791, 793, 798
 Dipole moments, 31, 32
 Dipteran pheromones, 220
 Direct interspecies electron transfer
 (DIET), 705
 Dispersed sedimentary organic matter, 525
 Dispersion and biodegradation, 853
 Dissimilatory sulfate reduction, 363, 690
 Dissociation, 659
 Dissolution, 658, 849
 Dissolved inorganic carbon (DIC), 658
 Dissolved organic matter, 825, 826
 Distillation, 272
 fractions, 77
 Diterpanes, 422
 Diterpenoids, 109
 Diversity in wax chemistry, 135
 DMDS adducts, 162, 169, 173
 DNA, 163, 411
 Dodecane, 851
 Double-bond equivalent (DBE), 601–604
 Double bond positions, 167, 169, 172, 173
 Draupne Fm., 344, 498
 Drimane, 279
 Driving forces, 495–499
 Droplet break-up models, 856
 Duvernay Shale, 536
 Dynamic models, 856
- E**
- Eagle Ford Shale, 524, 530, 534, 540, 541, 547
 Early diagenesis, 343
 Earthquake hazards, 753
 East African Rift, 570
 East Pacific Rise (EPR), 569
 Ebullition, 694
 Economic production technology, 664
 Electron acceptors, 773, 775
 Electron donors, 773, 775
 Electronegativity, 6
 Electrophilic aromatic substitution, 43
 Electrospray ionization (ESI), 74, 246, 321
 Electrospray ionization Fourier-transform ion
 cyclotron resonance spectroscopy
 (ESI-FT-ICR), 74
 Electrospray ionization in negative mode
 (ESI-N), 602, 603
 Electrospray ionization in positive mode
 (ESI-P), 603, 604
 Elemental analysis, 501
Emiliana huxleyi, 21, 108, 162, 170, 171,
 199, 203, 380
 Energy resource, 661
 Energy sources, 130, 131, 135
 Enoyl-CoA reductase (ECR), 145, 147
 Enrichment factor, 341
 Environment(s), 476, 483
 conditions, 167, 171, 175, 181
 gradients, 112
 34 EPA priority PAHs, 56
 Epi-brassicasterol, 161, 177, 178
 Epicuticular wax, 124–127, 131, 132,
 134, 135
 Epiphyllic microorganisms, 128, 131, 133–135
 Episodic release of oil, 853
 Epoxidation of olefins, 200
 Equilibrium, 856
 fractionation, 345
 isotope effects, 341
 state, 92
Erannis bajoria, 229
 Erosive margins, 750
Escherichia coli, 252
 Ethane, 851
 Ethylbenzene, 577
 Eukarya, 410, 412, 417–419
 Eustigmatophytes, 162, 169
 Euxinia, 293, 367
 Evaporites, 760
 Evapotranspiration, 111
 Evolutionary changes, 177
 Exploration equation, 494, 529, 534
 Expulsinator, 510
 Expulsion/extraction/migration, 579
 Expulsion efficiency, 504
 External environmental stress factors, 461
 Extracellular matrix, 129

- Extracellular microbial enzymes, 132
Extreme environments, 446, 459, 461
Extremophiles, 697
Exxon Valdez oil spill, 855
- F**
- Fatty acid(s), 108, 140, 151, 161, 166,
247–250, 447, 451, 453,
455, 456, 460–462
 elongation, VLCFAs, 145
 epoxyhydroxy-fatty acids, 140
 ω -hydroxy-fatty acids, 143, 144
 in methanotrophs, 791, 797, 802
 polyhydroxy-fatty acids, 142
 synthase gene, 221
 VLCFAs, 150
 See also specific types of fatty acids
- Fatty acyl-CoA reductase (FAR) activity, 147,
223
- Fatty alcohols, 168
- Fayetteville Shale, 524
- Fecal steroids, 831
- Feed gas, 82, 83, 89
- Fenton's reagent, 44
- Field ionization mass spectroscopy (FIMS), 313
- Firmicutes*, 852
- First-order rate law, 496
- Fischer-Tropsch Type (FTT) reactions, 784
- Flash point, 76
- Flash pyrolysis, 175
- Fluid flow, 771, 774, 776
- Fluorescence, 500
- Fluorescent in situ hybridization (FISH), 707
- Fluorometers, 860
- Flux, 774, 775
 advective, 774
 diffusive, 775
- Fourier transform ion cyclotron resonance mass
 spectrometry (FTICR-MS), 313,
 514, 536, 545, 601–604, 607
- Fracking, 524, 526, 528
- Fractionation during production, 545
- Fractures, 542
- Free radical(s), 497
 oxidation, 196
- Free radical-mediated processes, 194, 208
- Frequency factor, 496
- Freshwater microalgae, 174
- Fossilized microbes, 762
- Fully mature products, 575
- Fulvic acids, 826
- Functionalized organic compounds
 and lipids, 18–30
 reactions, 45, 46
- G**
- Galactolipid profiles, 166
- Gammacerane, 280, 295
- Gammaproteobacteria*, 852
- Gas(es), 614, 616, 618, 655
 emissions, 770, 772
 flux, 621
- Gas chromatography (GC), 272, 274, 313, 314
- Gas chromatography-isotope ratio mass
 spectrometry (GC-IRMS), 274
- Gas chromatography-mass spectrometry
 (GC-MS), 162, 169, 181, 274, 275,
 487, 558, 564
 phospholipid fatty acids and phospholipid
 ethers, 455
- Gas hydrate(s), 82, 652, 757, 761
 deposits, 652
 destabilization, 754
 gas hydrate stability, thermodynamic
 controls on, 654–655
 gas production, hydrate bearing sediments,
 660–664
 hydrate growth, 87–89
 interface hypothesis, nucleation at, 85
 labile cluster nucleation hypothesis, 85–87
 local structuring nucleation hypothesis, 87
 marine sediments, methane hydrate
 formation in, 657–660
 microbial methane formation, 655–657
 natural, 653
 sediments, effects of, 89–90
 stability, 654
 structure and composition, 83–85
 thermodynamic properties, 90–92
 water, 759
- Gas hydrate stability zone (GHSZ), 654, 656,
658, 661
- Gas-oil ratio (GOR), 534–536
- Gas plumes, 754
- GC-MSMS, 282, 285, 298
- Gel permeation chromatography (GPC), 74
- Gene-profiling, 461
- Genomics, 637
- Geocatalysis, 497
- Geochemical evidence, 617
- Geochemical mixing models, 618, 621
- Geologic age, 275
- Geological conditions, 617

- Geological subsurface, 465
Geothermal gradient, 655, 656
Geranyl diphosphate synthase (GPPS), 231
Geranylgeranyl unit, 166
Ghareb formation, 369
Gibbs free energy, 495
Gibbs function, 495
Global energy market, 524
Gloeocapsomorpha prisca, 421
Glucosyl-phosphatidylglycerols, 254
Glycerol dialkyl ethers, 797
Glycerol dialkyl glycerol tetraether (GDGTs), 426–427, 678, 797, 802
Glycerol-ether lipids, 250
Glycerophospholipids, 23
Glycol, 851
Glycolipids, 448, 451
GORFit model, 512
Gorgosterol, 179
Graminoids, 113
Great Oxidation Event (GOE), 414
Greenland, 171
Grosmont carbonate reservoirs, 595
Groundwater, 753, 832
Growth conditions, 163
Growth stage, 181
Guard cells, 125, 127, 128, 131, 134, 135
Guaymas Basin, Gulf of California, 560
Gulf of Mexico, 761
Gymnosperms, 422, 483, 484
- H**
- Haakon Mosby Mud Volcano, 771, 772, 777
Halogenated organic compounds, 4
Halogens, 28, 30, 31
Haptophytes, 108, 161–163, 167, 169–173, 177, 179, 181
Hard coals, 486
Haslea, 164
Haslenes, 164
Haynesville Shale, 524, 530
Heat flow, 654
Heather Fm, 344
Heat transfer, 87, 89
Heavy vacuum gas oil (HVGO), 602
Hempel distillation, 272
Hetero-PAH, 576
Heterotrophs, 417
Hexakaidecahedrons, 83, 84
Higher land plants, 421–423
Higher plant(s)
 carbon isotopes in plant lipids, 110
 hydrogen isotopes in lipids, 112–114
 lipids, 110–112
 materials, 289
High fluid flow, 572
Highly branched isoprenoids (HBI), 386, 425
 alkenes, 104, 163, 194, 201, 202
High performance liquid chromatography (HPLC), 313
High performance liquid chromatography-electrospray ionization-mass spectrometry (HPLC-ESI-MS), 452–454
High performance liquid chromatography-mass spectrometry (HPLC-MS), 181
 phospholipids, detection of, 451–455
High pressure, 572
High-pressure closed-system hydrous-pyrolysis, 510
High-resolution shotgun lipidomics, 253
High temperature, 275, 562, 569, 570, 572, 575, 576, 579, 582, 583
Homeoviscous adaptation, 461
Homodrimane, 279
Homolytic bond dissociation energy, 38, 39
Homolytic cleavage, 196, 197, 200, 205
Honey bee queen retinue pheromone, 220
Hopane(s), 299, 416, 562, 565, 793, 830, 837
Hopanepolyols
 in ancient sediments, 792
 in methanotrophs, 789
Hopanoids, 388, 411, 789, 791, 798
Housefly sex pheromone, 220
Humic substances, 827, 836
Hydrate growth, 85, 87
Hydrate nucleation
 interface hypothesis, nucleation at, 85
 labile cluster nucleation hypothesis, 85
 local structuring nucleation hypothesis, 87
Hydrate saturations, 658, 663
Hydrate structures, 83
Hydration, 752
Hydrocarbon(s), 270, 558, 569, 652, 654
 abiotic, 582
 aliphatic, 569, 575
 n-alkanes and *n*-alkenes, 161–163
 aromatic, 15–18
 compound classes, 4
 covalent bonding, 5–7
 cyclic, 166
 Diels' hydrocarbon, 576
 distributions, 560
 emissions, 772, 777

- energy resources, 4
 - functionalized organic compounds and lipids, 18–30
 - HBI alkenes in diatoms, 163–166
 - isoprenoid alkanes and alkenes, 163
 - light, 577
 - lipid, 571
 - microorganisms, 4
 - PAH, 562, 565, 569, 575, 582, 583
 - patterns, 566, 569
 - physical properties, 31–38
 - reactions, 38–46
 - saturated, 7–12
 - structures, 6
 - total, 560, 565
 - unsaturated, 12–15
 - volatile, 577, 579
 - Hydrocarbon-metazoan-microbe-mineral association, 755–757
 - Hydrofracking, 289
 - Hydrogenation, 14, 391
 - Hydrogen atom abstraction, 199, 200, 203–206
 - Hydrogen exchange reactions, 345
 - Hydrogen gas, 577
 - Hydrogen index (HI), 486, 488, 503
 - Hydrogen isotope composition, 173
 - Hydrogen isotope fractionation, 349
 - Hydrogenotrophic methanogenesis, 676, 679, 682, 694, 698
 - Hydrolytic microflora, 673
 - Hydroperoxides, 196
 - allylic, 200, 207
 - content, 197
 - formation of, 205
 - Δ^6 -5 α -hydroperoxides, 205
 - Δ^4 -6 α /6 β -hydroperoxides, 205
 - 7 β -hydroperoxides, 206
 - instability of, 205
 - labile, 205
 - Hydrophobic cuticle, 124, 127–130
 - Hydrosphere, 824, 830
 - ground water systems, organic matter in, 832
 - marine environment, organic matter in, 834–838
 - terrestrial surface water systems, organic matter in, 824–832
 - Hydrostatic pressure, 655
 - Hydrothermal metallogenesis, 582
 - Hydrothermal organic synthesis, 582
 - Hydrothermal petroleum
 - analytical methods, 558–559
 - composition of, 575–577
 - continental systems, 570–571
 - definition, 558
 - East Pacific Rise, 569
 - expulsion/extraction/migration, 579–580
 - fluid interactions, 577–579
 - Guaymas Basin, Gulf of California, 560–562
 - hydrothermal organic synthesis, 582–583
 - Mid Atlantic Ridge, 569
 - mineral deposits, 582
 - northeastern Pacific (Escanaba Trough and Middle Valley), 562–566
 - organic matter alteration, 572–575
 - resources, 580
 - Hydrothermal vent systems, 558, 579
 - Hydrous pyrolysis, 510
 - β -Hydroxyacyl-CoA dehydratase (HCD), 145, 147
 - Hydroxyarchaeol, 795, 797, 802
 - Hydroxy fatty acids, 167–168
 - ω -Hydroxy-fatty acids, 143, 144
 - Hydroxy ketones, 169
 - Hyperconjugation, 7
 - Hypersaline lakes, 172
 - Hypersaline paleoenvironment, 385
- I**
- Icosahedron, 83
 - Illite, 760
 - Immature organic matter, 558, 560, 565, 569, 573, 575, 579, 583
 - Fluid inclusions, 413, 418, 573, 579, 583
 - Inertinite(s), 480, 483, 484, 486, 500
 - Insects, 214
 - cuticular hydrocarbons, 217–218, 220–223
 - pheromones (*see* Pheromones)
 - In situ combustion, 662
 - In-situ physical properties of fluids, 545
 - In-source secondary cracking, 512
 - Intact polar lipids (IPLs), 447
 - International Union of Pure and Applied Chemistry (IUPAC), 5
 - Intracuticular wax, 125, 127
 - Ionic mechanisms, 497
 - IP₂₅, 164, 200
 - IPSO₂₅, 165
 - Iron-coupled reactions, 691
 - Irregular dodecahedrons, 83
 - Iso-/anteiso fatty acids, 798, 803
 - Isochrysidaceae, 171
 - Isochrysidales, 171
 - Isorenieratene, 12, 18, 378, 379, 412, 424, 836

- Isochrysis*, 162, 170–172
 Isomeric hydroperoxyacids, 205
 Isomerization, 166
 Isoprenoid, 411, 794, 795, 797, 802
 alkanes, 163
 lipids, 112
 thiophene ratio, 385
 24-Isopropylcholestanes, 418
 Isoerenieratane, 424
 Isothermal, 496
 Isotope fractionation, 101, 630
 factor, 341, 342, 347
 Isotopic composition of natural gas
 hydrocarbons, 346
- K**
 Kebrit and Shaban Deeps, 569
 Kerogen, 291, 359, 486, 487, 527, 534, 547
 and bitumen, 488
 classifications, 501
 sulfur-rich, 482
 type I, 476, 477, 480
 type II, 477
 type III, 476, 483
 types, 291
 β -Ketoacyl-CoA reductase (KCR), 145, 147
 β -Ketoacyl-CoA synthase (KCS), 145, 146, 152
 Keto-enol-tautomerism, 21
 Ketones, 141, 145, 148, 150
 Killed phytoplanktonic cells, 205
 Kimmeridge Clay Formation (KCF), 395
 Kinetic(s), 657
 non-isothermal, 496
 isotope effects, 341, 343, 344, 681
 parameters, 489, 496, 504
Kluyveromyces thermotolerans, 257
 K_{OW} -values, 825
- L**
 Labile cluster nucleation hypothesis, 85
 Labile hydroperoxides, 205
 Laboratory studies, 621
 Lactones, 23
 Lacustrine, 476, 481
 sediments, 169
 settings, 480
 Lake Messel, 481, 482
 Lake sediments, 171
 Lake Tanganyika, 570
 Lanostane, 794
 Lanosterol, 791
- Last universal common ancestor (LUCA), 410
 Late gas, 535
 potential, 512
 Lateral heterogeneity, 131
 Leaching, 133
 Leaf flush, 113
 Leaf surface(s), 124–129, 131–135
 wettability, 128, 129
 Leaf transpiration, 115
 Leaf wax lipids, 112
 Leaf wax synthesis, 113
 Lepidopteran fatty acid derived pheromones,
 219
 Life cycle, 166
 Life marker, 447–451, 459
 Light hydrocarbons, 577
 Light intensity, 108
 Lignin, 483, 484, 835
 Lignites, 483, 486
 Lindane, 831
 Lipid(s), 100, 247, 412
 biomarker analysis, 459, 460
 biosynthesis, 180
 extraction, 451
 in microalgae (*see* Microalgae)
 Lipidomics, 246
 Lipid transfer proteins (LTPs), 151
 Liptinite(s), 487, 500
 Liquid chromatography, 316
 Localization, 199
 Local structuring nucleation hypothesis, 87
 Lokbatan mud volcano, 772
 Lokiarchaeota, 417
 Long chain C_{37} – C_{39} alkenones, 380
 Lotus effect, 127
 Lycopadiene, 163
Lymantria dispar, 229
- M**
 Maceral(s), 291
 groups, 486
 type, 500
 Macrocyclic diethers, 797, 802
 Macrocyclic diphytanyl glycerol diethers
 (MDGDs), 797, 802
 Maltenes, 271, 528
 Manco (Modular Analysis and Numerical
 Classification of Oils)
 scale, 304, 600
Manduca sexta, 226
 Marcellus Shale, 524, 530
 Marine, 476, 480, 482
 biogenic origin, 566

- environments, 476
- oil spill in United States history, 848
- organic matter, 479, 485
- sediments, 477, 479
- sulphur cycle, 362–365
- Marine Benthic Group D (MBGD), 708
- Markownikow rule, 41
- Mass balance, 539
 - modelling, 537–538
- Mass extinction, 423
- Massive sulfide deposits, 569
- Mass spectrometry, ultrahigh-resolution, 320
- Mass transfer, 87
- Matrix-assisted laser desorption/ionization (MALDI), 247, 452
- Maturation, 527, 535, 560, 565, 566, 571, 575, 583
- Maturity, 289, 295–296, 501
 - parameters, 536
- Mean annual precipitation, 113
- Mediterranean Sea, 761
- Membrane adaptation, 457, 461–465
- Membrane fluidity and functionality, 461
- Membrane lipids, 165, 448, 451, 461, 462
- Membrane solid to liquid phase transition temperature, 461
- Mercaptans, 60
- Mesocosms/Microcosms, 860
- Messinian, 377, 383, 387, 388, 393, 761
- Metagenesis, 494, 527
- Metagenetic late dry gas generation, 512
- Metagenomics, 634
- Metal(s), 70–73
- Metal-AOM, 756
- Metastable equilibrium, 575
- Metastable states, 90
- Meteoritic precipitation, 112
- Methane, 82–86, 90, 289, 597, 614, 616, 620, 652, 655, 771, 773, 775
 - aerobic oxidation, 700–702
 - anaerobic oxidation, 702–711
 - atmospheric, 711–715
 - biological oxidation, 700
 - cage occupancies with, 89
 - discovery, 670
 - emissions, 788
 - formation from organic matter, 672
 - isotopic composition, 345
 - microbial, 82 (*see* Microbial methane)
 - monoxygenase, 857
 - plumes, 762
- Methane-derived carbonates, 798
 - fabrics, 799
- Methane hydrate(s), 762
 - formation, in marine sediments, 654–660
- Methane-oxidizing bacteria (MOB), 700, 785, 789, 791, 793, 857
- Methane sources
 - abiotic, 783–784
 - methanogenesis, 782–783
- Methanobacillus omelianskii*, 676
- Methanococcoides burtonii*, 697
- Methanogenesis, 614, 616, 618, 621, 658, 782
- Methanogenic microorganisms, 657
- Methanogenic pathways, 630
- Methanogenium frigidum*, 697
- Methanogens, 413
 - Methanopyrus kandleri*, 697
 - Methanosarcina lacustris*, 697
 - Methanothermobacter thermoautotrophicus*, 678
- Methanotrophs, 413
- 2-Methylalkanes, 220
- Methyl-branched alkanes, 217
- Methylcarbamate hopanoids, 790
- Methylhopanes, 415
- 3 β -Methylhopanes, 792–794
- 3 β -Methylhopanoids, 789
- Methyl ketones, 169
- Methylococcaceae, 789
- Methylotrophic methanogenesis, 676
- Methylphenanthrene index, 297
- Methylphosphonate, 783
- 4 α -Methylsteranes, 419
- 4-Methyl steranes, 793, 794
- 4-Methylsterols, 178
 - in methanotrophs, 790–791
- Methyl-type fermentation, 676
- Mevalonic acid pathway, 105
- MGDG and DGDG, 166
- Michaelis-Menten kinetics, 701
- Microalgae, 160
 - algaenan, 175–177
 - alkenones and alkyl alkenoates, 169–173
 - alkyl diols, 173–175
 - biochemical constituents, 180
 - fatty acids, 166–168
 - fatty alcohols, 168–169
 - hydrocarbons (*see* Hydrocarbons)
 - phyla in, 160
 - sterols, 177–180
- Microbial activity, 465, 466, 481, 484
- Microbial biodegradation, 628
- Microbial biomass, 857
- Microbial communities, 446, 457, 459–462, 465–467

- Microbial degradation, 172
Microbial diversity, 124
Microbial humification, 630
Microbial methane, 82
 biogeochemical process of formation, 673–687
 in freshwater and terrestrial environments, 693–696
 in marine environment, 687–693
 oxidation, 705
 in special environments, 697–699
Microbial methanogenesis, 625, 630, 632, 635, 637
Microbial sulphate reducers (MSR), 363
Microfossils, 411
Microorganisms, 655
Microplastics, 838
Microscale sealed vessel (MSSV), 510
 pyrolysis, 511, 547
Microscopy, 531
Mid Atlantic Ridge, 569
Mineralization, 559
Model of composition (MoC), 324
phytyldiol/phytol ratio, 197
Molecular biology, 180
Molecular clock, 177
Molecular fossils, 410
Monoaromatic steroid hydrocarbon, 281
Mono-unsaturated fatty acids (MUFAs), 205, 209
Mud breccia, 770, 771
Mud volcanoes, 618, 770
 advective transport, 774
 Chikishlyar-type, 772
 electron donors and acceptors, 775
 hydrocarbon emissions, 772–773
 Lokbatan-type, 772
 redox transition zones, 773
 Shugin-type, 772
 spatial and temporal variability of fluid flow, 776
 submarine, 776
Multi-element isotope analysis, 350
Multiple ion detection, 277
Mycobacteria, 255–256
Mycolic acids, 255
- N**
NaBH₄ reduction, 169
Nannochloropsis, 162, 168, 173–175, 179
 N. oceanica, 259
Nanopores, 539
Naphthalenes, 286
Naphthenes, *see* Cycloalkanes
Naphthenic acids, 607
Naphthenoaromatic compounds, 58
Natural attenuation, 834
Natural catalysts, 497
Natural gas, 340, 342, 344, 346
 hydrates occurrences, 662
Natural maturation series, 489
Natural organic matter, 826–828
Natural seeps, 850
 in North America, 853
Navicula, 165
Near-critical, 574, 577
Neoproterozoic hydrates, 672
New Zealand, 570
Nickel, 270
Niobrara Fm., 524, 530, 534, 538
Nitrogen, 26–29
 compounds, 69–70
Noëlaerhabdaceae, 170
Noncompetitive substrates, 674, 676, 687, 691, 703
Non-hydrocarbons, 583, 595, 597, 599, 601–604, 606–608
Norcholestanes, 419
Nördlinger Ries Lake, 482
25-Norhopanes (NHs), 305, 597, 600
Normal phase chromatography, 452
Northeastern Pacific (Escanaba Trough and Middle Valley), 562
Nucleophile, 44
Nutrients, Mississippi River, 851
- O**
Obligate anaerobes, 686
Ocean, 620
Ocean Drilling Program (ODP), 565
Oceanic anoxic events, 293, 479
Oceanic methane paradox, 687, 783
Oceanic plate, 750–752
Oceanospirillaceae, 853
Ochromonas, 174
Octanol-water partition coefficients *vs.* carbon number, 37, 38
Odd/even predominance of *n*-alkanes, 296
Oenocytes, 220
Oficina Formation, 595
Oil(s), 614, 616, 618
 droplet size, 849
 quality, 540, 542
 reservoirs, 347
 saturation index, 540
 secondary cracking of, 535
 seeps, 301

- solubility, 76
- spills, 606, 838
- Oil composition, 50–51
 - alkanes, 53
 - aromatic compounds, 55–66
 - asphaltenes, 73–74
 - cycloalkanes, 53–55
 - metals, 70–73
 - naphthenoaromatic compounds, 58
 - nitrogen compounds, 69–70
 - olefins, 55
 - oxygen compounds, 66–69
 - resins, 73
 - sulfur compounds, 58–60
- Oil-dissolved gas, 618
- Oil properties
 - API gravity, 76
 - density, 75
 - distillation fractions, 77
 - flash point, 76
 - oil solubility, 76
 - oil-water interfacial tension, 77
 - pour point, 76
 - research needs, 77
 - specific gravity, 76
 - vapor pressure, 77
 - viscosity, 74
- Oil sands
 - Alberta, 594
 - asphaltenes, 602–603
 - biodegradation systematics, 597
 - Canadian, 594
 - compositional continuum, 602
 - deposits, 595
 - environmental implications of, 604–608
 - non-hydrocarbon compounds, 603
 - Peace River, 595
- Oil sands process-affected water (OSPW), 604, 607
- Oil–water contact (OWC), 346, 597, 599
- Oil-water interfacial tension, 77
- Oil-water transition zones (OWTZ), 596, 597
- Okenane, 413
- 18 α H-oleanane, 280
- Oleanane, 422
- Olefins, 12, 14, 55
- Oleic acid, 206
- Oligomeric compounds, 200
- Open-system analytical pyrolysis, 502
- Open-system pyrolysis, 502–509
- Optical activity, 274
- Optical microscopy, 500
- Orbital hybridization, 5
- Orbitrap mass spectrometry, 321
- Order of photoreactivity, 199, 208
- Organic carbon, 477, 478, 480, 481, 560
 - cycle, 527
- Organic macromolecules, 528, 532
- Organic matter, 160, 166, 180, 357, 558, 582
 - accumulation of, 582
 - alteration, 572
 - immature, 558, 560, 565, 569, 579, 583
 - maturation, 583
 - preservation, 478
 - remineralization, 688
 - sedimentary, 558, 562
 - solvation capacity, 577
 - terrigenous, 560, 570
 - type, 501
- Organic petrology, 528
- Organic richness, 504
- Organic-rich sediments and sedimentary rocks
 - elemental analysis, 486
 - geochemical transformations, 484–486
 - lakes, 480–482
 - optical microscopy, 486
 - pyrolysis techniques, 487
 - rivers and peats, 482–484
 - sea, 477–480
 - spectroscopic techniques, 487
- Organic sulphur compounds (OSC)
 - biomarker, 357
 - carotenoids, 391
 - carbohydrates, 370, 395
 - C₃₅ hopanoids, 389
 - ¹³C isotope, 370
 - C₃₀ tetracyclic polyprenoids, 394
 - desulphurization, 376
 - diagenesis, 367
 - dimethylsulfide (DMS), 372, 373
 - double bonds, 386
 - fatty acids, 377
 - isotopic fractionations, 365
 - intermolecular sulphurization, 366
 - intramolecular sulphurization, 366
 - isotope chemistry, 359
 - polyprenoid sulphides, 394
 - porphyrins, 393
 - preservation of OM, 370
 - reduced sulphur species, 366
 - short chain alkylthiophenes, 395
 - S isotope exchange, 375
 - steroids, 387
 - thiolane-C₂₀ isomers, 386
 - timing of sulphurization, 368
 - volatile organic sulphur, 372–373

- Organofacies, 291
 Organolithofacies, 293
 Original organic matter, shales, 530
 Orinoco Heavy Oil belt, 594
 Oxidative decarbonylation system, 223
 Oxidosqualene, 418
 Oxycracking, 603
 Oxygen compounds, 66–69
 Oxygen index (OI), 487, 503
 Oxygen minimum zone (OMZ), 478, 485
 Oxygen/sulfur
 acetals and hemiacetals, 22
 aliphatic alcohols, 19
 alkylated phenols, 19
 carbonyl groups, 21
 carboxylic acids, 23
 chalcogens, 18
 epoxidation, 20
 esters, 23
 ethers, 20
 hydroxyl/sulfanyl group, 18, 19
 thioethers, 20, 25
 thiols, 25
- P**
- Palaeoproxies, 161, 181
 Paleocene/Eocene temperature maximum, 788
 Paleoclimatic investigation, 100
 Paleohydrological studies, 107
 Paleohydrology proxy, 115
 Paleopasteurization, 305, 597
 Paleotemperature estimation, 203
 Paleotemperature reconstruction, 203
 Palmitic acid, 107
 Paraffin(s), 38, 53
 Paraffinic, 507
 Parallel reactions, 496
 Particulate organic matter (POC), 194, 208,
 655, 657, 659, 825, 828
 Passive margins, 748
Pavlova, 167, 179
 Pavlovols, 179
 Peace River oil sands, 595, 596
 Peats, 482–484
 Pentagonal dodecahedrons, 83, 84, 86, 87
 2,6,10,15,19-Pentamethylcosane (PMI), 794–
 797, 802
Periplaneta americana, 214
 Permafrost regions, 652
 Permafrost-thawing, 754
 Permeability, 127, 129, 130, 133–135, 662
 Petroleome, 600
 Petroleomics, 312–314, 601
 applications, 326–327
 determination, 314
 gas chromatography, 314–316
 liquid chromatography, 316–320
 ultrahigh-resolution mass spectrometry,
 320–324
 limitation, 327–328
 modeling, 324–325
 prediction, 326
 Petroleum, 284, 305, 312, 313, 614
 accumulations, 614, 616, 618
 biodegradation, 614
 genetic potential, 501
 geochemistry, stable isotope applications in
 (see Stable isotopes)
 hydrocarbons, 837
 seeps, 616, 618
 source rocks, 342, 343
 type organofacies, 508, 534
 See also Crude oils
 Petroporphyrin, 603
 pH adaptation, 463
 Phaeopigments, 180
 Pharmaceuticals, 828
 Phase behavior, 90, 510, 545
 Phase diagram, 653, 655
 PhaseKinetics, 511, 547
 Phase separation of CO₂, 574
 Phenanthrene, 286, 851
 Pheromones
 biosynthesis, 224–235
 contact, 220
 honey bee queen retinue, 220
 housefly sex, 220
 lepidopteran, 215
 lepidopteran fatty acid derived, 219
 polyene hydrocarbons, 219, 229
 roles, 218
 terpenoid, 219, 230–235
 Phosphatidylinositol mannosides, 255
 Photic Zone Euxinia (PZE), 293, 294, 378, 392,
 393, 394
 Phospholipid(s) (PLs), 447
 analysis, 459
 esters, 448, 455, 459
 ethers, 455
 column fractionation, 451
 HPLC-MS, 452–455
 intact PLs, 459
 lipid extraction, 451
 membrane adaptation to environmental
 conditions, 461–465

- taxonomic information, 457–460
- Phospholipid fatty acids (PLFAs), 451, 453
 - GC-MS, 455
 - inventories, 460, 466
 - structures, 455–457
 - taxonomic information, 457–460
- Phosphosphingolipids, 23
- Photic zone, 478
 - anoxia, 294
- Photodynamic effect, 195
- Photooxidation, 606, 607
 - unsaturated lipid components
 - (see Unsaturated lipid components)
- Photoreactivity, 199, 200, 203, 208
- Photosensitized oxidation, 196, 199, 201, 205
- Photosynthesis, 112, 288–289
- Photosynthetically active radiation (PAR), 194
- Phthiocerol dimycoserates, 255
- Phyllosphere, 124, 129–131, 133–135
- Phylogenetic relationships, 114, 171
- Phylotypes, 171
- Physicochemical properties of leaf
 - surface, 128
- Phytane, 278, 381, 421, 796, 797, 802
- Phytanic acid, 797, 800
- Phytanol, 797, 802
- Phytodetritus, 194, 195, 197, 199
- Phytol, 113, 168, 173, 381
- Phytoplankton, 480, 481
- Phytyldiol, 197
- PIANO (paraffins, isoalkanes, aromatics, naphthenes, olefins), 270, 271
- Piezophilic hyperthermophiles, 697
- Piezophilic microorganisms, 462
- Plant cuticle, biosynthesis, *see* Cuticle
- Plant cuticular waxes
 - composition of, 125–126
 - function of, 126–128
 - interactions of microorganisms, 128–134
- Plasmalogen-phosphatidyl ethanolamine (pPE), 253
- Plasmalogen-phosphatidylglycerol, 254
- Plasmalogen-phosphatidylserine, 254
- Plasmalogen-phosphoethanolamine, 254
- Plasmalogens, 253–255
- Plastic, 838
- Plasticizers, 133, 828
- Plasticizing effect, 134
- Plate boundaries, 748
- Plate convergence, 748
- Pleurosigma*, 165
- PM scale, 599
- Polar compounds, 128, 131, 135
- Polar lipids, 166
- Polar organic solutes, 131
- Polar paths of transport, 128
- Polybrominated diphenyl ethers, 30
- Polychlorinated biphenyls (PCBs), 30, 829
- Polychlorinated dibenzo-*p*-dioxins, 829
- Polycondensation, 505
- Polycyclic aromatic hydrocarbons (PAH), 16, 18, 55, 416, 562, 565, 568, 570, 575, 576, 582, 583, 637, 830
- Polyene hydrocarbons, 219, 229–230
- Polyextremophiles, 697
- Polymer, 140, 142, 144–145
- Polyprenoid sulphides, 394
- Polyunsaturated fatty acids (PUFAs), 200, 205, 208, 209, 247
- Porewater, 654, 658
- Porosity, 662
- Porphyridium*, 180
- Porphyrins, 318, 393
- Posidonia Shale, 481, 488, 514, 515, 526, 531, 532, 534, 537, 538, 540, 541, 544, 545
- Positional isomers, 174
- Pour point, 76
- Prasinophytes, 160, 179
- Pressure, 498, 662, 860
- Primary alcohols, 141, 145, 147
- Primary and secondary cracking
 - kinetics, 512
- Primary cracking, 534
- Prince William Sound*, 855
- Priority PAHs, 56
- Pristane, 278, 381, 421, 796, 802
- Pristane/*n*-C₁₇ and phytane/*n*-C₁₈ ratios, 296
- Proboscia*, 174
- Propane, 851
- Propylene, 851
- Prospectivity, 529
- Proteins, 411
- Proteobacteria*, 852
- Proteogenomics, 134
- Proxy, 200
- Prudhoe Bay oil, 855
- Pseudo van Krevelen diagram, 503
- Pteridophyte, 483
- Pyrethrins, 11
- Pyrite, 366, 482, 485
- Pyrolysate, 576, 582
- Pyrolysis, 496, 499, 502
 - Confined, 510
 - experiments, 489
 - gas chromatography, 534, 538

Q

Quesnoin, 423

R

Radical halogenation, 39
 Radical recombination, 497
 Radiolysis effects, 536
 Raman spectroscopy, 84, 87
 Rayleigh equation, 341, 347, 348
 Real-time assessment, 858
 Recognition, 134
 Redox ladder, 688
 Redox transition zones, 773, 776
 Red Sea, 566, 569
 Reductive dehydration reactions, 583
 Reflectance, 500
 Refractory biotic organic sulphur compounds, 373–375
 Resins, 73
 Resource exploration, 580
 Retention, 527, 538, 542
 Retrogressive coupling reactions, 505
 Reverse methanogenesis, 704, 705
 Rhizenes, 164
Rhizosolenia, 161
 Rhodophyta, 180
 Ribosomal RNA, 411
 Ribulose-1,5-bisphosphate carboxylase/oxygenase (RuBisCO), 105
 Rock-Eval, 504
 analyses, 291
 pyrolysis, 487, 503
 Root exudates, 696

S

Saccharomyces cerevisiae, 256
 Saline lakes, 171
 Salinity, 446, 461, 465, 653, 655
 Saponification, 168, 451, 453, 455
 Saturate(s), 50, 53, 75
 Saturated fatty acids, 460, 461
 Saturated hydrocarbons
 n-alkanes, 7–8
 branched alkanes, 9
 cycloalkanes, 10–12
 reactions, 38–40
 structures, 8
 Saturates, aromatics, resins and asphaltene (SARA), 51, 53, 55, 271, 272
 Scanning electron microscopy (SEM), 528, 531
 Scanning transmission X-ray microscopy, 532

Scenedesmus, 161
 Seafloor, 652, 657
 Sealed gold bags, 510
 Sea level changes, 293
 Sea-level stands, 758
 Sea surface temperatures (SST), 203
 8,14-Secohexahydrobenzohopanes, 793
 Secondary alcohols, 141, 145, 148, 150
 Secondary cracking, 509
 Secondary gas, 542
 Secondary microbial gas
 formation of, 614, 616
 in natural environments, 616, 617
 petroleum accumulations, global occurrences in, 618
 volumetric significance of, 618, 620
 Secondary oil to gas cracking, 511
 Sediment(s), 89, 160, 164, 166, 167, 169–172, 174, 177, 180, 654
 Sedimentary organic matter, 558, 562, 571
 Sedimentary organic sulphur compounds (OSC), *see* Organic sulphur compounds (OSC)
 Sedimentation rates, 478, 480
 Seep carbonate(s), 757, 798
 laminae, 758
 Seep footprints, 750, 754–760
 Senescence of haptophytes, 203
 Senescence of phytoplankton, unsaturated lipid components, *see* Unsaturated lipid components
 Sequence stratigraphic models, 278
 Serpentinization, 751, 763
 Sesquiterpanes, 279–280
 Shale, 618
 oil, 526, 527
 porosity and kerogen swelling, 539
 prospectivity, 528
 resource plays, 529
 Shale gas, 527
 definition, 525
 resource potential, 525
 and shale oil resources, 525
 Ships and planes, 855
 Signals, 135
 Singlet oxygen, 194, 205
 Smectites, 760
 Soil moisture, 111
 Solubility, 655, 656, 659
 Solvation capacity, 574, 577
 Solvent extraction, 181
 Source rock quality, 501
 Sources of nutrients, 130

- Specific gravity, 76
Specific tracers of autoxidation, 199
Sphingolipids, 448
Spontaneous nucleation, 86
Squalene, 163
16S rRNA, 708
18S rRNA, 175
Stability conditions, 90, 92
Stability field, 90, 91
Stable isotopes, 630
 - alteration processes, in petroleum reservoirs, 346–350
 - of carbon and hydrogen, 340
 - of hydrocarbon gases, 536
 - sedimentary basins, petroleum formation in, 342–346Stand Alone Particle Sampler (SAPS), 860
Standard operating procedures (SOP), 859
5 α (H)-stanols, 179
Steady state conditions, 658
Steam assisted gravity drainage (SAGD), 604
Stepwise pyrolysis, 181
Steranes, 177, 277, 280–283, 416, 562, 564
Stereoisomers, 298
Steric repulsion, 7
Steroids, 387, 411
Sterol(s), 177, 826
 - autoxidation %, 208
 - biosynthesis, 177
 - in methanotrophs, 790
 - photooxidation proportion estimates, 206 Δ^5 -Sterols, 205
Stimulated biogenic coalbed methane, 639
Stimulation of indigenous microbes, 640
Stoke's law, 479
Stomata, 113
Storage aquifer system, 466
Strike-slip, 748
Stromatolites, 412
Structured Learning in Microbial Ecology (SLiME) model, 856
Subduction channel, 750
Subduction zones, 750
Sugars, 180
Sulfate, 478, 480, 485, 657
Sulfate reduction, 481, 486, 658
 - microbes, 480Sulfur, 295
 - and carbon isotope analysis, 359–362
 - compounds, 58–60
 - isotope considerations, 368, 369
 - vs. organic carbon cycles, 362–365Sulphate reducing bacteria, 368, 690–694
Sulphides, 60
Sulphurization, characteristic of preservation via, 370
Sulphurized isoprenoids, 381
Supercritical fluid chromatography, 320
Supercritical water, 574, 576, 577
Superhydrophobic, 127
Surfactants, 129, 134
Suspended particulate matter, 825
Sweet spots recognition, 542
Syngenetic, 415
Synthesis products, 582
- T**
Tailings ponds, 606, 607
Tar sands, *see* Oil sands
Taxonomic information, 455, 457
 - PLFAs, 460–461Taxonomy, 164
Taxon-specific biomarkers (TSBs), 412, 415, 416, 420
Tectonic plate boundaries, 748
Temperature, 446, 461, 462, 466, 662
 - calibrations, 172
 - vs. viscosity, 35Terminal electron acceptor, 657, 676
Ternary composition diagram, 575
Terpanes, 277, 279
Terpenoid(s), 109, 827
 - pheromones, 219, 230Terrestrial, 476, 480, 481, 483, 484
 - biota, 101
 - ecosystems, 835
 - organic matter, 479, 482, 483, 485Terrigenous material, 835
Terrigenous organic matter, 560, 570
Tetracyclic triterpenoids, 177
Tetraether lipids, 797
Tetraikadecahedrons, 83, 87, 88
Thermal alteration, 558, 572, 575
Thermal cracking, 497
Thermal hydrocarbon generation, 486
Thermal maturation, 343
Thermal maturity, 489
Thermal transformation, 504
Thermocatalytic reactions, 582
Thermochemical sulfate reduction (TSR), 340, 350
Thermococcus kodakarensis, 252
Thermodynamic properties, 90
Thermogenic gas(es), 344, 616, 618, 621

- Thermogenic gas(es) (*cont.*)
 origin, 82
Thermogenic hydrocarbons, 494
Thermogenic petroleum, 495
 formation, 499
Thermogenic wet gases, 685
Thermophilic bacteria, 254
Thin-layer chromatography (TLC), 318
Thioesterase, 150
Thiophenes, 60
Tidal pumping, 754
Time-of-flight mass spectrometry
 (TOF), 247
Time-resolved fluorescence depolarization
 (TRFD), 74
 T_{\max} -values, 487, 504
Tocopherols, 180
Toluene, 577, 851
Tomato, 144
Total hydrocarbon, 560, 565, 568
Total organic carbon (TOC), 395
 total sulfur (TOC/TS) ratio, 485
Trace methane oxidation (TMO), 704
Trans-Atlantic Geotraverse
 (TAG), 569–570
Trans-esterification, 455
Transformation process, 90
Trebouxiophytes, 179
Tree(s), 696
 of life, 410
Triaromatic steroid hydrocarbons, 299
Tributyl tin, 837
Trichomes, 125, 128, 131, 135
n-Tricosane, 796, 802
Tricosanoids, 795, 798
3 β ,5 α ,6 β -Trihydroxysterols, 206
Trilaminar structure, 175
1,2,7-Trimethylnaphthalene, 286
Trisubstituted double bond, 200, 208
Triterpanes, 562, 565
Triterpenoids, 109, 126
Turbidites, 750
Type II photosensitized oxidation, 196, 199,
 201, 205
Type II processes, 194
- U**
Ultra-high-resolution mass spectrometry, 320
Unconventional crude oils, 289
Unconventional resources, 547
Underplating, 750
Unresolved complex mixture (UCM), 10
Unsaturated fatty acids, 455, 462
Unsaturated hydrocarbons
 alkenes, 14
 cis- and *trans*-isomers, 12
 conjugated double bond, 12
 olefins, 14
 reactions, 40–42
 structures, 13
Unsaturated lipid components, 194, 195
 alkenes, 199
 alkenones, 202
 chlorophyll phytyl side-chain, 197
 Δ^2 -sterols, 205
 unsaturated fatty acids, 205
Upwelling, 174, 477, 478
- V**
Vaca Muerta Fm., 531, 537, 540, 541, 545
Vanadium, 270
van Krevelen diagram, 494, 501
Vapor pressure, 77
Vapor pressure osmometry (VPO), 74
Very-long-chain fatty acids (VLCFAs), 145,
 148, 150, 152
Very-long-chain polyunsaturated fatty acids
 (VLCPUFAs), 250
Viscosity, 34, 74, 301
Visible light-induced, 194, 208
Vitrinite, 479, 483, 484, 486, 500
 reflectance, 295, 487, 500, 685
Volatile hydrocarbon pheromones, 219
Volatile oil, 540
Volatile organic compounds (VOCs), in
 atmosphere
 annual global emission rates, 812
 anthropogenic contribution, 813
 anthropogenic emissions, 813
 aromatic VOCs, 820
 atmospheric alkanes, degradation of,
 816–819
 atmospheric alkenes, degradation of,
 819–820
 biogenic sources, 812
 biomass burning emissions, 813
 methane, 813
 mixing ratios of, 813
 OVOCs, 820

- oxygenated compounds, 812
 - saturated hydrocarbons, 812
 - terrestrial vegetation, 821
 - unsaturated hydrocarbons, 812
 - Volatile organic sulphur, sedimentary organic sulphur compounds, 372–373
- W**
- Wabamun Lake, 606
 - Waiotapu, 570
 - Waste deposit landfills, 834
 - Water, 558, 560, 566, 569, 570, 577
 - molecules, 82, 83, 85–87
 - near-critical domain of, 577
 - supercritical, 574, 576, 577
 - temperatures, 654, 656
 - washing, 340, 579
 - Wax, 289
 - coverage, 126
 - crystallites, 127
 - crystals, 124
 - layer, 126, 128, 134
 - melting, 131
 - platelets, 131, 132
 - Wax biosynthesis, 150
 - alcohol-forming pathway, 147
 - alkane-forming pathway, 148
 - fatty acid elongases, VLCFAs, 145–147
 - Wax synthase (WS), 147
 - Weathering, 607
 - Wetting, 128, 129, 131, 133, 135
 - Wolfcamp Fm., 524
 - Woodford Shale, 293, 524, 531
- X**
- Xenobiotics, 5
 - X-ray diffraction, 84, 91
 - Xylenes, 577
- Y**
- Yanchang, 540
 - Yarrowia lipolytica*, 257
 - Yeast, 256–257
 - Yellowstone National Park, 570